

this document downloaded from

**vulcanhammer.net**

Since 1997, your complete online resource for information geotechnical engineering and deep foundations:

The Wave Equation Page for Piling

*Online books on all aspects of soil mechanics, foundations and marine construction*

Free general engineering and geotechnical software

*And much more...*

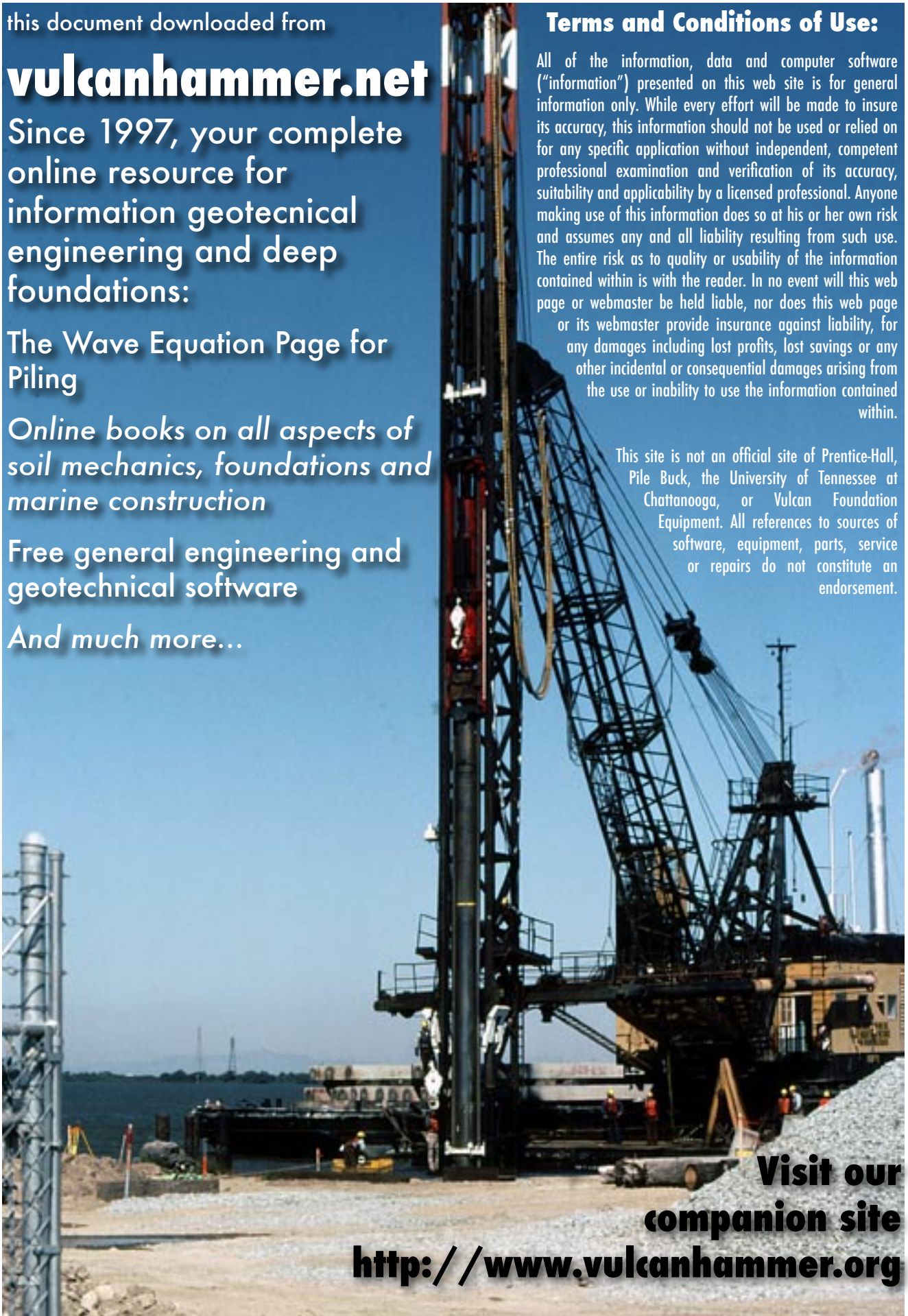
## Terms and Conditions of Use:

All of the information, data and computer software ("information") presented on this web site is for general information only. While every effort will be made to insure its accuracy, this information should not be used or relied on for any specific application without independent, competent professional examination and verification of its accuracy, suitability and applicability by a licensed professional. Anyone making use of this information does so at his or her own risk and assumes any and all liability resulting from such use. The entire risk as to quality or usability of the information contained within is with the reader. In no event will this web page or webmaster be held liable, nor does this web page or its webmaster provide insurance against liability, for any damages including lost profits, lost savings or any other incidental or consequential damages arising from the use or inability to use the information contained within.

This site is not an official site of Prentice-Hall, Pile Buck, the University of Tennessee at Chattanooga, or Vulcan Foundation Equipment. All references to sources of software, equipment, parts, service or repairs do not constitute an endorsement.

**Visit our  
companion site**

**<http://www.vulcanhammer.org>**





U.S. Department of Transportation  
Federal Highway Administration

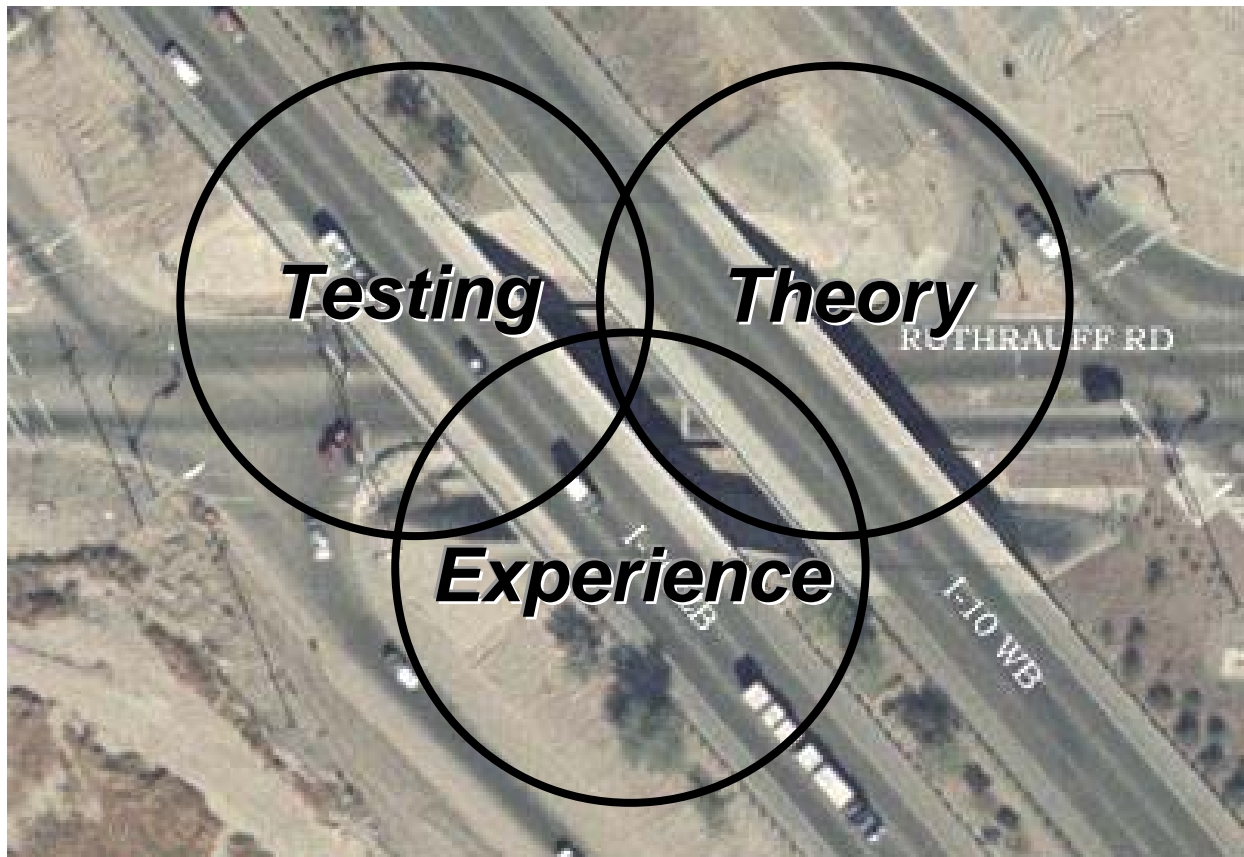
Publication No. FHWA NHI-06-088  
December 2006

**NHI Course No. 132012**

---

# **SOILS AND FOUNDATIONS**

**Reference Manual – Volume I**



*National Highway Institute*

## **NOTICE**

The contents of this report reflect the views of the authors, who are responsible for the facts and the accuracy of the data presented herein. The contents do not necessarily reflect policy of the Department of Transportation. This report does not constitute a standard, specification, or regulation. The United States Government does not endorse products or manufacturers. Trade or manufacturer's names appear herein only because they are considered essential to the objective of this document.

**Technical Report Documentation Page**

1. Report No. FHWA-NHI-06-088	2. Government Accession No.	3. Recipient's Catalog No.	
4. Title and Subtitle  SOILS AND FOUNDATIONS REFERENCE MANUAL – Volume I		5. Report Date December 2006	
		6. Performing Organization Code	
7. Author(s) Naresh C. Samtani*, PE, PhD and Edward A. Nowatzki*, PE, PhD		8. Performing Organization Report No.	
9. Performing Organization Name and Address Ryan R. Berg and Associates, Inc. 2190 Leyland Alcove, Woodbury, MN 55125 * NCS GeoResources, LLC 640 W Paseo Rio Grande, Tucson, AZ 85737		10. Work Unit No. (TRAIS)	
		11. Contract or Grant No. DTFH-61-02-T-63016	
12. Sponsoring Agency Name and Address National Highway Institute U.S. Department of Transportation Federal Highway Administration, Washington, D.C. 20590		13. Type of Report and Period Covered	
		14. Sponsoring Agency Code	
15. Supplementary Notes FHWA COTR – Larry Jones FHWA Technical Review – Jerry A. DiMaggio, PE; Silas Nichols, PE; Richard Cheney, PE; Benjamin Rivers, PE; Justin Henwood, PE. Contractor Technical Review – Ryan R. Berg, PE; Robert C. Bachus, PhD, PE; Barry R. Christopher, PhD, PE <i>This manual is an update of the 3<sup>rd</sup> Edition prepared by Parsons Brinckerhoff Quade &amp; Douglas, Inc, in 2000. Author: Richard Cheney, PE. The authors of the 1<sup>st</sup> and 2<sup>nd</sup> editions prepared by the FHWA in 1982 and 1993, respectively, were Richard Cheney, PE and Ronald Chassie, PE.</i>			
16. Abstract  The Reference Manual for Soils and Foundations course is intended for design and construction professionals involved with the selection, design and construction of geotechnical features for surface transportation facilities. The manual is geared towards practitioners who routinely deal with soils and foundations issues but who may have little theoretical background in soil mechanics or foundation engineering. The manual's content follows a project-oriented approach where the geotechnical aspects of a project are traced from preparation of the boring request through design computation of settlement, allowable footing pressure, etc., to the construction of approach embankments and foundations. Appendix A includes an example bridge project where such an approach is demonstrated. Recommendations are presented on how to layout borings efficiently, how to minimize approach embankment settlement, how to design the most cost-effective pier and abutment foundations, and how to transmit design information properly through plans, specifications, and/or contact with the project engineer so that the project can be constructed efficiently.  The objective of this manual is to present recommended methods for the safe, cost-effective design and construction of geotechnical features. Coordination between geotechnical specialists and project team members at all phases of a project is stressed. Readers are encouraged to develop an appreciation of geotechnical activities in all project phases that influence or are influenced by their work.			
17. Key Words		18. Distribution Statement	
Subsurface exploration, testing, slope stability, embankments, cut slopes, shallow foundations, driven piles, drilled shafts, earth retaining structures, construction.		No restrictions.	
19. Security Classif. (of this report)	20. Security Classif. (of this page)	21. No. of Pages	22. Price
UNCLASSIFIED	UNCLASSIFIED	462	

[THIS PAGE INTENTIONALLY BLANK]

## **PREFACE**

This update to the Reference Manual for the Soils and Foundations course was developed to incorporate the guidance available from the FHWA in various recent manuals and Geotechnical Engineering Circulars (GECs). The update has evolved from its first two versions prepared by Richard Cheney and Ronald Chassie in 1982 and 1993, and the third version prepared by Richard Cheney in 2000.

The updated edition of the FHWA Soils and Foundations manual contains an enormous amount of information ranging from methods for theoretically based analyses to “rules of thumb” solutions for a wide range of geotechnical and foundation design and construction issues. It is likely that this manual will be used nationwide for years to come by civil engineering generalists, geotechnical and foundation specialists, and others involved in transportation facilities. That being the case, the authors wish to caution against indiscriminate use of the manual’s guidance and recommendations. The manual should be considered to represent the minimum standard of practice. The user must realize that there is no possible way to cover all the intricate aspects of any given project. Even though the material presented is theoretically correct and represents the current state-of-the-practice, engineering judgment based on local conditions and knowledge must be applied. This is true of most engineering disciplines, but it is especially true in the area of soils and foundation engineering and construction. For example, the theoretical and empirical concepts in the manual relating to the analysis and design of deep foundations apply to piles installed in the glacial tills of the northeast as well as to drilled shafts installed in the cemented soils of the southwest. The most important thing in both applications is that the values for the parameters to be used in the analysis and design be selected by a geotechnical specialist who is intimately familiar with the type of soil in that region and intimately knowledgeable about the regional construction procedures that are required for the proper installation of such foundations in local soils.

### **General conventions used in the manual**

This manual addresses topics ranging from fundamental concepts in soil mechanics to the practical design of various geotechnical features ranging from earthworks (e.g., slopes) to foundations (e.g., spread footings, driven piles, drilled shafts and earth retaining structures). In the literature each of these topics has developed its own identity in terms of the terminology and symbols. Since most of the information presented in this manual appears in other FHWA publications, textbooks and publications, the authors faced a dilemma on the regarding terminology and symbols as well as other issues. Following is a brief discussion on such issues.

- **Pressure versus Stress**

The terms “pressure” and “stress” both have units of force per unit area (e.g., pounds per square foot). In soil mechanics “pressure” generally refers to an applied load distributed over an area or to the pressure due to the self-weight of the soil mass. “Stress,” on the other hand, generally refers to the condition induced at a point within the soil mass by the application of an external load or pressure. For example, “overburden pressure,” which is due to the self weight of the soil, induces “geostatic stresses” within the soil mass. Induced stresses cause strains which ultimately result in measurable deformations that may affect the behavior of the structural element that is applying the load or pressure. For example, in the case of a shallow foundation, depending upon the magnitude and direction of the applied loading and the geometry of the footing, the pressure distribution at the base of the footing can be uniform, linearly varying, or non-linearly varying. In order to avoid confusion, the terms “pressure” and “stress” will be used interchangeably in this manual. In cases where the distinction is important, clarification will be provided by use of the terms “applied” or “induced.”

- **Symbols**

Some symbols represent more than one geotechnical parameter. For example, the symbol  $C_c$  is commonly used to identify the coefficient of curvature of a grain size distribution curve as well as the compression index derived from consolidation test results. Alternative symbols may be chosen, but then there is a risk of confusion and possible mistakes. To avoid the potential for confusion or mistakes, the Table of Contents contains a list of symbols for each chapter.

- **Units**

English units are the primary units in this manual. SI units are included in parenthesis in the text, except for equations whose constants have values based on a specific set of units, English or SI. In a few cases, where measurements are conventionally reported in SI units (e.g., aperture sizes in rock mapping), only SI units are reported. English units are used in example problems. Except where the units are related to equipment sizes (e.g., drill rods), all unit conversions are “soft,” i.e., approximate. Thus, 10 ft is converted to 3 m rather than 3.05 m. The soft conversion for length in feet is rounded to the nearest 0.5 m. Thus, 15 ft is converted to 4.5 m not 4.57 m.

- **Theoretical Details**

Since the primary purpose of this manual is to provide a concise treatment of the fundamental concepts in soil mechanics and an introduction to the practical design of various geotechnical features related to highway construction, the details of the theory underlying the methods of analysis have been largely omitted in favor of discussions on the application of those theories to geotechnical problems. Some exceptions to this general approach were made. For example, the concepts of lateral earth pressure and bearing capacity rely too heavily on a basic understanding of the Mohr's circle for stress for a detailed presentation of the Mohr's circle theory to be omitted. However, so as not to encumber the text, the basic theory of the Mohr's circle is presented in Appendix B for the reader's convenience and as an aid for the deeper understanding of the concepts of earth pressure and bearing capacity.

- **Standard Penetration Test (SPT) N-values**

The SPT is described in Chapter 3 of this manual. The geotechnical engineering literature is replete with correlations based on SPT N-values. Many of the published correlations were developed based on SPT N-values obtained with cathead and drop hammer methods. The SPT N-values used in these correlations do not take in account the effect of equipment features that might influence the actual amount of energy imparted during the SPT. The cathead and drop hammer systems typically deliver energy at an estimated average efficiency of 60%. Today's automatic hammers deliver energy at a significantly higher efficiency (up to 90%). When published correlations based on SPT N-values are presented in this manual, they are noted as  $N_{60}$ -values and the measured SPT N-values should be corrected for energy before using the correlations.

Some researchers developed correction factors for use with their SPT N-value correlations to address the effects of overburden pressure. When published correlations presented in this manual are based upon values corrected for overburden they are noted as  $N_{160}$ . Guidelines are provided as to when the  $N_{60}$ -values should be corrected for overburden.

- **Allowable Stress Design (ASD) and Load and Resistance Factor Design (LRFD) Methods**

The design methods to be used in the transportation industry are currently (2006) in a state of transition from ASD to LRFD. The FHWA recognizes this transition and has developed separate comprehensive training courses for this purpose. Regardless of whether the ASD or LRFD is used, it is important to realize that the fundamentals of soil mechanics, such as the

determination of the strength and deformation of geomaterials do not change. The only difference between the two methods is the way in which the uncertainties in loads and resistances are accounted for in design. Since this manual is geared towards the fundamental understanding of the behavior of soils and the design of foundations, ASD has been used because at this time most practitioners are familiar with that method of design. However, for those readers who are interested in the nuances of both design methods Appendix C provides a brief discussion on the background and application of the ASD and LRFD methods.

## ACKNOWLEDGEMENTS

The authors would like to acknowledge the following events and people that were instrumental in the development of this manual.

- Permission by the FHWA to adapt the August 2000 version of the Soils and Foundations Workshop Manual.
- Provision by the FHWA of the electronic files of the August 2000 manual as well as other FHWA publications.
- The support of Ryan R. Berg of Ryan R. Berg and Associates, Inc. (RRBA) in facilitating the preparation of this manual and coordinating reviews with the key players.
- The support provided by the staff of NCS Consultants, LLC, (NCS) - Wolfgang Fritz, Juan Lopez and Randy Post (listed in alphabetical order of last names). They prepared some graphics, some example problems, reviewed selected data for accuracy with respect to original sources of information, compiled the Table of Contents, performed library searches for reference materials, and checked internal consistency in the numbering of chapter headings, figures, equations and tables.
- Discussions with Jim Scott (URS-Denver) on various topics and his willingness to share reference material are truly appreciated. Dov Leshchinsky of ADAMA Engineering provided copies of the ReSSA and FoSSA programs which were used to generate several figures in the manual as well as presentation slides associated with the course presentation. Robert Bachus of Geosyntec Consultants prepared Appendices D and E. Allen Marr of GeoComp Corporation provided photographs of some laboratory testing equipment. Pat Hannigan of GRL Engineers, Inc. reviewed the driven pile portion of Chapter 9. Shawn Steiner of ConeTec, Inc. and Salvatore Caronna of gINT Software prepared the Cone Penetration Test (CPT) and boring logs, respectively, shown in Chapter 3 and Appendix A. Robert (Bob) Meyers (NMDOT), Ted Buell (HDR-Tucson) and Randy Simpson (URS-Phoenix) provided comments on some sections (particularly Section 8.9).
- Finally, the technical reviews and recommendations provided by Jerry DiMaggio, Silas Nichols, Benjamin Rivers, Richard Cheney (retired) and Justin Henwood of the FHWA, Ryan Berg of RRBA, Robert Bachus of Geosyntec Consultants, Jim Scott of URS, and Barry Christopher of Christopher Consultants, Inc., are gratefully acknowledged.

## **SPECIAL ACKNOWLEDGEMENTS**

A special acknowledgement is due of the efforts of Richard Cheney and Ronald Chassie for their work in the preparation of the previous versions of this manual. It is their work that made this course one of the most popular FHWA courses. Their work in developing this course over the past 25 years is acknowledged.

With respect to this manual, the authors wish to especially acknowledge the in-depth review performed by Jerry DiMaggio and time he spent in direct discussions with the authors and other reviewers. Such discussions led to clarification of some existing guidance in other FHWA manuals as well as the introduction of new guidance in some chapters of this manual.

<b>SI CONVERSION FACTORS</b>				
<b>APPROXIMATE CONVERSIONS FROM SI UNITS</b>				
<b>Symbol</b>	<b>When You Know</b>	<b>Multiply By</b>	<b>To Find</b>	<b>Symbol</b>
<b>LENGTH</b>				
mm	millimeters	0.039	inches	in
m	meters	3.28	feet	ft
m	meters	1.09	yards	yd
km	kilometers	0.621	miles	mi
<b>AREA</b>				
mm <sup>2</sup>	square millimeters	0.0015	square inches	in <sup>2</sup>
m <sup>2</sup>	square meters	10.758	square feet	ft <sup>2</sup>
m <sup>2</sup>	square meters	1.188	square yards	yd <sup>2</sup>
ha	hectares	2.47	acres	ac
km <sup>2</sup>	square kilometers	0.386	square miles	mi <sup>2</sup>
<b>VOLUME</b>				
ml	milliliters	0.034	fluid ounces	fl oz
l	liters	0.264	gallons	gal
m <sup>3</sup>	cubic meters	35.29	cubic feet	ft <sup>3</sup>
m <sup>3</sup>	cubic meters	1.295	cubic yards	yd <sup>3</sup>
<b>MASS</b>				
g	grams	0.035	ounces	oz
kg	kilograms	2.205	pounds	lb
tonnes	tonnes	1.103	US short tons	tons
<b>TEMPERATURE</b>				
°C	Celsius	1.8°C + 32	Fahrenheit	°F
<b>WEIGHT DENSITY</b>				
kN/m <sup>3</sup>	kilonewtons / cubic meter	6.36	Pound force / cubic foot	pcf
<b>FORCE and PRESSURE or STRESS</b>				
N	newtons	0.225	pound force	lbf
kN	kilonewtons	225	pound force	lbf
kPa	kilopascals	0.145	pound force / square inch	psi
kPa	kilopascals	20.88	pound force / square foot	psf
<b>PERMEABILITY (VELOCITY)</b>				
cm/sec	centimeter/second	1.9685	feet/minute	ft/min

[THIS PAGE INTENTIONALLY BLANK]

**SOILS AND FOUNDATIONS  
VOLUME I**

**TABLE OF CONTENTS**

	Page
<b>LIST OF FIGURES</b> .....	ix
<b>LIST OF TABLES</b> .....	xv
<b>LIST OF SYMBOLS</b> .....	xviii
<b>1.0 INTRODUCTION</b> .....	1-1
1.1 PURPOSE AND SCOPE .....	1-1
1.2 SOILS AND FOUNDATIONS FOR HIGHWAY FACILITIES.....	1-5
1.3 ORGANIZATION OF MANUAL .....	1-10
1.4 REFERENCES .....	1-12
1.4.1 Primary FHWA References .....	1-12
1.4.2 Other Primary References .....	1-13
<b>2.0 STRESS AND STRAIN IN SOILS</b> .....	2-1
2.1 BASIC WEIGHT-VOLUME RELATIONSHIPS.....	2-3
2.1.1 Volume Ratios .....	2-3
2.1.2 Weight Ratios .....	2-4
2.1.3 Weight-Volume Ratios (Unit Weights) and Specific Gravity .....	2-5
2.1.4 Determination and Use of Basic Weight-Volume Relations .....	2-7
2.1.5 Size of Grains in the Solid Phase.....	2-9
2.1.6 Shape of Grains in Solid Phase.....	2-13
2.1.6.1 Bulky Shape.....	2-13
2.1.6.2 Platy Shape .....	2-15
2.1.7 Effect of Water on Physical States of Soils .....	2-15
2.2 PRINCIPLE OF EFFECTIVE STRESS.....	2-19
2.3 OVERBURDEN PRESSURE.....	2-19
2.4 VERTICAL STRESS DISTRIBUTION IN SOIL DUE TO EXTERNAL LOADINGS .....	2-22
2.4.1 Uniformly Loaded Continuous (Strip) and Square Footings .....	2-24
2.4.2 Approximate (2:1) Stress Distribution Concept .....	2-26
2.5 REPRESENTATION OF IMPOSED PRESSURES ON THE $p_o$ DIAGRAM .....	2-26
2.6 LOAD-DEFORMATION PROCESS IN SOILS .....	2-30
2.6.1 Time Dependent Load-Deformation (Consolidation) Process .....	2-31
2.6.2 Comparison of Drainage Rates between Coarse-Grained and Fine- Grained Soil .....	2-34
2.7 LATERAL STRESSES IN FOUNDATION SOILS.....	2-34
2.7.1 Effect of Shear Strength of Soils on Lateral Pressures.....	2-36

2.8	STRENGTH OF SOILS TO RESIST IMPOSED STRESSES .....	2-38
2.8.1	Basic Concept of Shearing Resistance and Shearing Strength .....	2-38
2.9	STRENGTH OF SOILS RELATED TO LATERAL EARTH PRESSURES .....	2-42
2.9.1	Distribution of Lateral Earth and Water Pressures .....	2-45
2.9.2	Deformations Associated with Lateral Pressures .....	2-47
2.10	UNSATURATED SOIL MECHANICS.....	2-47
<b>3.0</b>	<b>SUBSURFACE EXPLORATIONS.....</b>	<b>3-1</b>
3.01	Primary References.....	3-3
3.1	PREPARING FOR SUBSURFACE EXPLORATION .....	3-3
3.1.1	Soil Formations and Landforms.....	3-6
3.1.1.1	Residual Soils .....	3-7
3.1.1.2	Transported Soils .....	3-9
3.1.1.3	Area Concept of Explorations Based on Landforms .....	3-9
3.2	FIELD RECONNAISSANCE .....	3-13
3.3	SUBSURFACE EXPLORATION PROGRAM .....	3-15
3.4	SAMPLING TECHNIQUES AND TOOLS.....	3-17
3.5	BORING METHODS.....	3-20
3.5.1	Auger Borings.....	3-20
3.5.2	Wash-type Borings.....	3-26
3.5.3	Coring in Rocks .....	3-26
3.6	SAMPLING METHODS.....	3-28
3.6.1	Disturbed Sampling of Soil.....	3-28
3.6.2	Undisturbed Sampling of Soil.....	3-28
3.6.3	Thin-Walled (Shelby) Tube Sampling.....	3-35
3.6.4	Undisturbed Sampling of Rock (Rock Coring) .....	3-38
3.6.4.1	Core Barrels .....	3-38
3.6.4.2	Coring Bits.....	3-40
3.6.4.3	Drilling Fluid .....	3-43
3.6.5	Observations During Rock Core Drilling.....	3-43
3.6.5.1	Drilling Rate/Time .....	3-43
3.6.5.2	Core Photographs.....	3-43
3.6.5.3	Rock Classification .....	3-44
3.6.5.4	Recovery .....	3-44
3.6.5.5	Rock Quality Designation (RQD).....	3-44
3.6.5.6	Drilling Fluid Recovery .....	3-47
3.6.5.7	Core Handling and Labeling.....	3-48
3.6.5.8	Care and Preservation of Rock Samples.....	3-50
3.6.6	Geologic Mapping .....	3-50
3.7	STANDARD PENETRATION TEST (SPT) .....	3-51
3.7.1	Energy Efficiency of Hammers .....	3-54
3.7.2	Effect of Overburden Stress on N-values .....	3-56
3.7.3	Correlation of SPT N-Values with Basic Soil Characteristics.....	3-58
3.7.3.1	Applicability of SPTs in Gravelly Soils .....	3-58
3.7.4	SPT Test Errors .....	3-59

3.8	LOG OF BOREHOLE INFORMATION (“BORING LOGS”).....	3-62
3.8.1	Boring Log Format .....	3-62
3.8.2	Duties of the Logger .....	3-62
3.9	CONE PENETRATION TESTING (CPT).....	3-67
3.9.1	Equipment Description and Operation .....	3-68
3.9.2	The Standard Cone Penetration Test (CPT) .....	3-69
3.9.3	The Piezo-cone Penetration Test (CPTu) .....	3-71
3.9.4	The Seismic Piezocone Penetration Test (SCPTu).....	3-71
3.9.5	Test Procedures.....	3-71
3.9.6	CPT Profiles.....	3-72
3.9.7	CPT Profile Interpretation .....	3-72
3.10	DILATOMETER TEST (DMT).....	3-75
3.11	PRESSUREMETER TEST (PMT).....	3-76
3.12	VANE SHEAR TEST (VST).....	3-77
3.13	GROUNDWATER MEASUREMENTS.....	3-78
3.13.1	Information on Existing Wells.....	3-78
3.13.2	Open Borings .....	3-79
3.13.3	Observation Wells.....	3-79
3.13.4	Water Level Measurements .....	3-81
3.13.4.1	Chalked Tape .....	3-81
3.13.4.2	Tape with a Float .....	3-82
3.13.4.3	Electric Water-Level Indicator .....	3-82
3.13.4.4	Data Loggers.....	3-82
3.14	GUIDELINES FOR MINIMUM SUBSURFACE EXPLORATION .....	3-83
3.14.1	Recommendations for Sampling Depth Intervals in Soils.....	3-87
3.14.2	Recommendations for Sampling Depth Intervals in Rocks.....	3-89
3.14.3	Recommendations for Water Level Monitoring in Borings .....	3-89
3.15	GEOPHYSICAL TESTS .....	3-90
3.15.1	Types of Geophysical Tests.....	3-90
3.15.2	Advantages and Disadvantages of Geophysical Tests.....	3-94
3.15.2.1	Advantages of Geophysical Tests.....	3-94
3.15.2.2	Disadvantages of Geophysical Tests .....	3-95
3.15.3	Examples of Uses of Geophysical Tests.....	3-95

<b>4.0</b>	<b>ENGINEERING DESCRIPTION, CLASSIFICATION AND CHARACTERISTICS OF SOILS AND ROCKS .....</b>	<b>4-1</b>
4.01	Primary References.....	4-3
4.1	SOIL DESCRIPTION.....	4-3
4.1.1	Consistency and Apparent Density.....	4-4
4.1.2	Water Content (Moisture) .....	4-6
4.1.3	Color .....	4-6
4.1.4	Type of Soil.....	4-6
4.1.4.1	Coarse-Grained Soils (Gravel and Sand).....	4-7
4.1.4.2	Fine-Grained Soils .....	4-9
4.1.4.3	Highly Organic Soils .....	4-10
4.1.4.4	Minor Soil Type(s).....	4-11

	4.1.4.5 Inclusions .....	4-12
	4.1.4.6 Other Descriptors .....	4-12
	4.1.4.7 Layered Soils .....	4-12
	4.1.4.8 Geological Name .....	4-13
4.2	SOIL CLASSIFICATION .....	4-14
	4.2.1 Unified Soil Classification System (USCS) .....	4-14
	4.2.1.1 Classification of Coarse-Grained Soils.....	4-18
	4.2.1.2 Classification of Fine-Grained Soils.....	4-21
	4.2.2 AASHTO Soil Classification System.....	4-26
4.3	ENGINEERING CHARACTERISTICS OF SOILS.....	4-31
	4.3.1 Engineering Characteristics of Coarse-Grained Soils (Sands and Gravels).....	4-31
	4.3.2 Engineering Characteristics of Fine-Grained Soils (Inorganic Clays) .....	4-31
	4.3.3 Engineering Characteristics of Fine-Grained Soils (Inorganic Silts) .....	4-31
	4.3.4 Engineering Characteristics of Organic Soils .....	4-32
4.4	PRACTICAL ASPECTS OF ENGINEERING CHARACTERISTICS OF COARSE-GRAINED SOILS .....	4-32
4.5	PRACTICAL ASPECTS OF ENGINEERING CHARACTERISTICS OF FINE-GRAINED SOILS .....	4-33
4.6	DESCRIPTION OF ROCK .....	4-34
	4.6.1 Rock Type.....	4-34
	4.6.2 Color .....	4-36
	4.6.3 Grain Size and Shape .....	4-36
	4.6.4 Stratification/Foliation.....	4-37
	4.6.5 Mineral Composition .....	4-37
	4.6.6 Weathering and Alteration.....	4-37
	4.6.7 Strength.....	4-37
	4.6.8 Hardness.....	4-39
	4.6.9 Rock Discontinuity .....	4-39
	4.6.10 Fracture Description .....	4-41
	4.6.11 Rock Mass Classification.....	4-42
4.7	SUBSURFACE PROFILE DEVELOPMENT .....	4-45
	4.7.1 Use of Historical Data in Development of Subsurface Profile.....	4-48

<b>5.0</b>	<b>LABORATORY TESTING FOR GEOTECHNICAL DESIGN AND CONSTRUCTION .....</b>	<b>5-1</b>
5.01	Primary References.....	5-1
5.1	QUALITY ASSURANCE FOR LABORATORY TESTING .....	5-2
	5.1.1 Sample Tracking.....	5-2
	5.1.2 Sample Storage .....	5-2
	5.1.3 Sample Handling.....	5-4
	5.1.4 Effects of Sample Disturbance.....	5-4
	5.1.5 Specimen Selection.....	5-4
5.2	LABORATORY TESTING FOR SOILS .....	5-5

5.3	LABORATORY INDEX TESTS FOR SOILS .....	5-10
5.3.1	General.....	5-10
5.3.2	Moisture Content .....	5-10
5.3.3	Unit Weight.....	5-11
5.3.4	Particle Size Distribution.....	5-12
5.3.4.1	Sand Equivalent .....	5-16
5.3.5	Atterberg Limits.....	5-16
5.3.5.1	Significance of the “A-line” and “U-line” on Plasticity Chart.....	5-19
5.3.6	Specific Gravity .....	5-19
5.3.7	Organic Content.....	5-20
5.3.8	Electro Chemical Classification Tests .....	5-21
5.3.9	Laboratory Classification.....	5-21
5.4	CONSOLIDATION TESTING .....	5-22
5.4.1	Process of Consolidation .....	5-22
5.4.2	Consolidation Testing.....	5-23
5.4.3	Procedures.....	5-24
5.4.4	Presentation and Understanding the Consolidation Test Results ....	5-26
5.4.5	Comments on the Consolidation Tests .....	5-31
5.4.6	Useful Correlations between Consolidation Parameters and Index Values .....	5-33
5.4.6.1	Compression Index, $C_c$ .....	5-33
5.4.6.2	Recompression Index, $C_r$ .....	5-35
5.4.6.3	Coefficient of Vertical Consolidation, $c_v$ .....	5-35
5.4.6.4	Coefficient of Secondary Compression, $C_\alpha$ .....	5-37
5.5	SHEAR STRENGTH OF SOILS .....	5-38
5.5.1	Concept of Frictional and Cohesive Strengths .....	5-38
5.5.1.1	Strength Due to Friction .....	5-38
5.5.1.2	Strength Due to Cohesion.....	5-40
5.5.1.3	Simplified Expression for Shear Strength of Soils .....	5-42
5.5.2	Strength Testing of Soils in the Laboratory.....	5-42
5.5.2.1	Unconfined Compression (UC) Tests .....	5-44
5.5.2.2	Triaxial Tests .....	5-45
5.5.2.3	Direct Shear Tests .....	5-49
5.5.3	Factors Affecting Strength Testing Results.....	5-51
5.5.4	Comparison of Laboratory and Field Strengths.....	5-52
5.5.5	Selection of Design Shear Strength .....	5-53
5.5.6	Correlations of Shear Strength Parameters with Index Parameters. ....	5-53
5.5.6.1	Undrained Shear Strength of Cohesive Soils.....	5-53
5.5.6.2	Drained and Effective Shear Strength of Cohesive Soils ....	5-55
5.5.6.3	Shear Strength of Cohesionless Soils .....	5-56
5.6	PERMEABILITY .....	5-58
5.6.1	General.....	5-58
5.6.2	Equipment.....	5-58
5.6.3	Procedures.....	5-61
5.6.4	Useful Correlations of Permeability with Index Values.....	5-62

5.7	VOLUME CHANGE PHENOMENA DUE TO LOADING AND MOISTURE .....	5-65
5.7.1	Swell Potential of Clays .....	5-65
5.7.1.1	Evaluation of Expansion (Swell) Potential .....	5-67
5.7.2	Collapse Potential of Soils .....	5-68
5.7.3	Expansion of Soils due to Frost Action .....	5-70
5.8	COMPACTION CHARACTERISTICS OF SOIL .....	5-72
5.8.1	Concept of Compaction .....	5-72
5.8.2	Test Procedures .....	5-73
5.8.3	Implication of Laboratory Tests on Field Compaction Specifications .....	5-76
5.8.4	Engineering Characteristics of Compacted Soils.....	5-81
5.8.4.1	Effect of Increase in Moisture Content on Shear Strength of Compacted Soils.....	5-83
5.9	ELASTIC PROPERTIES OF SOILS .....	5-83
5.10	COMMON SENSE GUIDELINES FOR LABORATORY TESTING OF SOILS .....	5-84
5.11	LABORATORY TESTS FOR ROCK.....	5-87
5.11.1	Introduction .....	5-87
5.11.2	Point-Load Strength Test.....	5-89
5.11.3	Unconfined Compressive Strength of Intact Rock Core .....	5-91
5.11.4	Elastic Modulus of Intact Rock Core .....	5-91
5.11.5	Laboratory Direct Shear Test .....	5-92
5.12	ELASTIC PROPERTIES OF ROCKS .....	5-94
5.12.1	Elastic Modulus of Rock Mass .....	5-95
5.13	COMMON SENSE GUIDELINES FOR LABORATORY TESTING OF ROCKS .....	5-96
5.14	PRACTICAL ASPECTS FOR LABORATORY TESTING.....	5-98
5.15	VARIABILITY OF MEASURED PROPERTIES .....	5-99
<b>6.0</b>	<b>SLOPE STABILITY.....</b>	<b>6-1</b>
6.01	Primary Reference .....	6-1
6.1	EFFECTS OF WATER ON SLOPE STABILITY .....	6-3
6.2	DESIGN FACTOR OF SAFETY .....	6-5
6.3	INFINITE SLOPE ANALYSIS.....	6-5
6.3.1	Infinite Slopes in Dry Cohesionless Soils.....	6-5
6.3.2	Infinite Slopes in $c-\phi$ Soils with Parallel Seepage.....	6-6
6.4	CIRCULAR ARC FAILURE .....	6-9
6.4.1	Simple Rule of Thumb for Factor of Safety .....	6-10
6.4.2	Stability Analysis Methods (General).....	6-11
6.4.3	Ordinary Method of Slices – Step-By-Step Computation Procedure .....	6-13
6.4.4	Recommended Stability Methods.....	6-20
6.4.5	Remarks on Safety Factor.....	6-22
6.5	CRITICAL FAILURE SURFACE .....	6-22
6.6	DESIGN (STABILITY) CHARTS.....	6-24

6.6.1	Historical Background .....	6-25
6.6.2	Taylor's Stability Charts .....	6-25
	6.6.2.1 Determination of the Factor of Safety for a Slope .....	6-30
6.6.3	Janbu's Stability Charts .....	6-33
6.7	SLIDING BLOCK FAILURE .....	6-43
	6.7.1 Sliding Block – Hand Method of Analysis .....	6-44
	6.7.1.1 Computation of Forces - Simple Sliding Block Analysis .....	6-45
	6.7.2 Computation of Forces - Complicated Sliding Block Analysis .....	6-47
6.8	SLOPE STABILITY ANALYSIS USING COMPUTER PROGRAMS .....	6-48
6.9	IMPROVING THE STABILITY OF EMBANKMENTS .....	6-50
	6.9.1 Embankment Stability Design Solutions .....	6-50
	6.9.2 Design Approach for Reinforced Soil Slopes .....	6-50
	6.9.2.1 Preliminary Feasibility Design of RSS .....	6-53
6.10	IMPROVING THE STABILITY OF CUT SLOPES .....	6-57
	6.10.1 Deep Seated Failure .....	6-57
	6.10.2 Shallow Surface Failures .....	6-58
	6.10.3 Factor of Safety - Cut Slopes .....	6-59
<b>7.0</b>	<b>APPROACH ROADWAY DEFORMATIONS .....</b>	<b>7-1</b>
7.1	TYPICAL APPROACH ROADWAY DEFORMATION PROBLEMS .....	7-1
7.2	INTERNAL DERFROMTION WITHIN EMBANKMENTS .....	7-6
	7.2.1 General Considerations for Select Structural Backfill .....	7-6
	7.2.2 General Considerations for Drainage Aggregate .....	7-6
	7.2.3 Use of Geosynthetics to Control Internal Deformations .....	7-10
7.3	EXTERNAL DEFORMATION IN FOUNDATION SOILS BELOW EMBANKMENTS .....	7-10
	7.3.1 Procedure for Estimating Stress Distribution in Foundation Soils under Fills .....	7-11
7.4	COMPUTATION OF IMMEDIATE SETTLEMENT .....	7-15
	7.4.1 Modified Hough's Method for Estimating Immediate Settlements .....	7-16
	7.4.1.1 Comments on the Computed Settlement of Embankments .....	7-19
7.5	COMPUTATION OF CONSOLIDATION (LONG-TERM) SETTLEMENTS .....	7-19
	7.5.1 Correction of Laboratory One-Dimensional Consolidation Curves .....	7-21
	7.5.2 Computation of Primary Consolidation Settlements .....	7-24
	7.5.2.1 Normally Consolidated Soils .....	7-24
	7.5.2.2 Overconsolidated (Preconsolidated) Soils .....	7-26
	7.5.2.3 Underconsolidated Soils .....	7-27
	7.5.3 Consolidation Rates (Time Rate of Consolidation Settlement) .....	7-28
	7.5.3.1 Percent Consolidation .....	7-30
	7.5.3.2 Step-by-step Procedure to Determine Amount and Time for Consolidation .....	7-33
	7.5.4 Secondary Compression of Cohesive Soils .....	7-38
7.6	LATERAL SQUEEZE OF FOUNDATION SOILS .....	7-40
	7.6.1 Threshold Condition for Lateral Squeeze .....	7-41
	7.6.2 Calculation of the Safety Factor against Lateral Squeeze .....	7-42

	7.6.3	Estimation of Horizontal Movement of Abutments.....	7-43
7.7		DESIGN SOLUTIONS - DEFORMATION PROBLEMS .....	7-43
	7.7.1	Reducing the Amount of Settlement.....	7-44
		7.7.1.1 Category 1 - Increasing the Resistance.....	7-44
		7.7.1.2 Category 2 - Reducing the Load .....	7-44
	7.7.2	Reducing Settlement Time.....	7-44
		7.7.2.1 Surcharge Treatment.....	7-45
		7.7.2.2 Vertical Drains .....	7-46
	7.7.3	Design Solutions to Prevent Abutment Tilting.....	7-47
7.8		PRACTICAL ASPECTS OF EMBANKMENT SETTLEMENT .....	7-48
7.9		CONSTRUCTION MONITORING AND QUALITY ASSURANCE .....	7-48
	7.9.1	Embankment Construction Monitoring by Instrumentation.....	7-49
		7.9.1.1 Inspector's Visual Observation.....	7-49
		7.9.1.2 Types of Instrumentation .....	7-50
		7.9.1.3 Typical Locations for Instruments.....	7-51

## LIST OF FIGURES

<u>Figure</u>	<u>Caption</u>	<u>Page</u>
1-1	Aerial view of a pair of 3-span Interstate 10 (I-10) bridges over local roadway in Tucson, Arizona.....	1-1
1-2	Example of 3-span roadway bridges over another roadway.....	1-2
1-3	The “BIG I” stack interchange at the intersection of I-40 and I-25 in Albuquerque, New Mexico (Photo: Courtesy of Bob Meyers, NMDOT) (Note: A stack interchange is a free-flowing junction between two or more roadways that allows turning in all directions).....	1-2
1-4	A major multi-span bridge structure over water (George P. Coleman Bridge over the York River in Yorktown, Virginia) .....	1-3
1-5	Example of a roadway bounded by cut slopes and wet lands in an environmentally sensitive area.....	1-3
1-6	Combinations of sources of information required to solve geotechnical engineering issues .....	1-5
1-7	Geotechnical activity flow chart for a typical project using design-bid-build procurement process .....	1-8
2-1	A unit of soil mass and its idealization .....	2-2
2-2	Example of laboratory sieves for mechanical analysis for grain size distributions .....	2-11
2-3	Sample grain size distribution curves .....	2-12
2-4	Terminology used to describe shape of coarse-grained soils (Mitchell, 1976) .	2-14
2-5	Conceptual changes in soil phases as a function of water content .....	2-16
2-6	Plasticity chart and significance of Atterberg Limits .....	2-18
2-7	Example calculation of a $p_0$ -diagram.....	2-21
2-8	Schematic of vertical stress distribution under embankment loading. Graphic generated by FoSSA (2003) program. ....	2-22
2-9	Vertical stress contours (isobars) by Boussinesq’s theory for continuous and square footings (modified after Sowers, 1979; AASHTO, 2002) .....	2-25
2-10	Distribution of vertical stress by the 2:1 method (after Perloff and Baron, 1976).....	2-27
2-11	Combined plot of overburden pressures (total and effective) and pressure due to imposed loads .....	2-28
2-12	Example calculation of $p_f$ with stress increments from strip load on $p_0$ -diagram.....	2-29
2-13	Spring-piston analogy for the consolidation process of fine-grained soils.....	2-32
2-14	Comparison of excess pore water pressure dissipation in coarse-grained and fine-grained soils.....	2-34
2-15	Schematic of effect of lateral stresses.....	2-35
2-16	Schematic of lateral stress increases beneath an embankment. Graphic generated by FoSSA (2003) .....	2-37
2-17	Basic concept of shearing resistance and strength (after Murthy, 1989).....	2-39
2-18	Graphical representation of shearing strength .....	2-41

2-19	Stress states on a soil element subjected only to body stresses: (a) In-situ geostatic effective vertical and horizontal stresses, (b) Insertion of hypothetical infinitely rigid, infinitely thin frictionless wall and removal of soil to left of wall, (c) Active condition of wall movement away from retained soil, (d) Passive condition of wall movement into retained soil .....	2-43
2-20	Development of Rankine active and passive failure zones for a smooth retaining wall .....	2-45
2-21	Failure surface, pressure distribution and forces (a) active case, (b) passive case .....	2-46
2-22	General distribution of combined active earth pressure and water pressure .....	2-46
3-1	Recommended process for developing subsurface model for engineering design (FHWA, 2002a) .....	3-2
3-2	Typical weathering profile for metamorphic and igneous rocks (Deere and Patton, 1971) .....	3-8
3-3	Typical field reconnaissance form .....	3-14
3-4	Common in-situ tests for geotechnical site characterization of soils (FHWA, 2002b) .....	3-18
3-5	(a) Large diameter auger, (b) Small diameter continuous flight auger .....	3-21
3-6	(a) Solid stem auger and hollow stem auger (FHWA, 2002b), (b) Hollow stem auger components (ASTM D 4700), (c) Sizes of hollow stem auger flights (FHWA, 2002b), (d) Outer and inner assembly of hollow stem auger (FHWA, 2002b) .....	3-25
3-7	(a) Schematic of drilling rig for rotary wash methods (after Hvorslev, 1948), (b) Typical drilling configuration, (c) Settling basin (mud tank) .....	3-27
3-8	Split barrel sampler .....	3-28
3-9	Schematic of thin-walled (Shelby) tube (after ASTM D 4700) and photo of tube with end caps (FHWA, 2002b) .....	3-31
3-10	Stationary piston sampler schematic (after ASTM D 4700) and photo (FHWA 2002b) .....	3-33
3-11	Denison sampler (FHWA, 1997) .....	3-33
3-12	Pitcher sampler (FHWA, 1997, 2002b) .....	3-34
3-13	Shelby tube sealing methods: (a) Microcrystalline Wax, (b) O-Ring packer. (FHWA, 2002b) .....	3-38
3-14	(a) Single, (b) and (c) Double tube rock core barrels (FHWA, 1997) .....	3-39
3-15	Double tube core barrel. (a) Outer barrel assembly (b) Inner barrel assembly (FHWA, 2002b) .....	3-40
3-16	Coring bits: Diamond (top left), Carbide (top right), and Sawtooth (bottom center) (FHWA, 2001) .....	3-41
3-17	Modified core recovery as an index of rock mass quality (FHWA, 1997) .....	3-45
3-18	Length measurements for core RQD determination (FHWA, 1997) .....	3-46
3-19	Core box for storage of recovered rock and labeling .....	3-49
3-20	Sequence of driving split-barrel sampler during the Standard Penetration Test (modified after FHWA, 2002b) .....	3-52
3-21	(a) Stainless steel and brass liners, (b) Sample catchers (FHWA, 2002b) .....	3-53
3-22	SPT hammer types, (a) Donut, (b) Safety, and (c) Automatic (FHWA, 2006) .....	3-54

3-23	SPT N-values from (a) Uncorrected data, and (b) Corrected to 60% efficiency (Data modified after Robertson, <i>et al.</i> 1983).....	3-56
3-24	Variation of overburden correction factor, $C_N$ , as a function of vertical effective stress.....	3-57
3-25a	Example subsurface exploration log (0 - 35 ft depth) .....	3-63
3-25b	Example subsurface exploration log (35 - 60 ft depth) .....	3-64
3-26	Procedures and components of the Cone Penetration Test (FHWA, 2002b) ....	3-68
3-27	Cone penetrometer terminology (from Robertson and Campanella, 1989).....	3-69
3-28	Cone and piezocone penetrometers (Note the Quarter for Scale) (FHWA, 2002b) .....	3-70
3-29	Cone penetration testing from cone truck.....	3-71
3-30	Piezo-cone results for Apple Freeway Bridge.....	3-73
3-31	A commonly used simplified soil classification chart for standard electronic friction cone (after Robertson, <i>et al.</i> , 1986) .....	3-74
3-32	Dilatometer test equipment and procedure (FHWA, 2002b).....	3-75
3-33	Pressuremeter test schematic (FHWA, 2002b).....	3-76
3-34	Vane shear test equipment and procedure (after FHWA, 2002b).....	3-77
3-35	Representative details of observation well installations. (a) Drilled-in place stand-pipe piezometer, (b) Driven well point (FHWA, 1997).....	3-80
4-1	Flow chart to determine the group symbol and group name for coarse-grained soils (ASTM D 2488) .....	4-17
4-2	Evaluation of type of gradation for coarse-grained soils.....	4-20
4-3	Plasticity chart for Unified Soil Classification System (ASTM D 2488).....	4-22
4-4a	Flow chart to determine the group symbol and group name for fine-grained soils (ASTM D 2488) .....	4-23
4-4b	Flow chart to determine the group symbol and group name for organic soils (ASTM D 2488).....	4-24
4-5	Range of liquid limit and plasticity index for soils in groups A-2, A-4, A-5, A-6 and A-7 per AASHTO M 145 (or ASTM D 3282) .....	4-28
4-6	Comparison of the USCS with the AASHTO Soil Classification System (after Utah DOT – Pavement Design and Management Manual, 2005).....	4-29
4-7	Comparison of soil groups in the USCS with the AASHTO Soil Classification Systems (Holtz and Kovacs, 1981).....	4-30
4-8	Example boring location plan (FHWA, 2002a).....	4-47
4-9	Example interpreted subsurface profile (FHWA, 2002a).....	4-48
5-1	Sample laboratory test request form (Note: Only some tests are included in this sample form) .....	5-3
5-2	Example grain size distribution based on sieve analysis (Jumikis, 1962) .....	5-14
5-3	Grain size distribution curve based on data in Figure 5-2 .....	5-14
5-4	Some of the equipment used for Atterberg Limits testing of soil.....	5-17
5-5	Location of clay minerals on the Casagrande Plasticity Chart and Activity Index values (after Skempton, 1953, Mitchell, 1976, Holtz and Kovacs, 1981) .....	5-18
5-6	Schematic of a consolidation test.....	5-24

5-7	(a) Components of consolidation test equipment, (b) Weighted lever arm – incremental load consolidation apparatus, (c) Automatic load frame and computerized consolidation apparatus (Photo courtesy of GeoComp Corporation).....	5-25
5-8	Consolidation test relationships (after NAVFAC, 1986a).....	5-27
5-9	Empirical correlation between Compression Index and natural (in-situ) water content (from Terzaghi, <i>et al.</i> ,1996).....	5-34
5-10	Approximate correlations between $c_v$ and LL (NAVFAC, 1986a).....	5-36
5-11	Correlation between $C_{ae}$ and natural water content (NAVFAC, 1986a).....	5-37
5-12	Potential contributions of various bonding mechanisms to cohesive strength (Ingles, 1962).....	5-41
5-13	Schematic of an unconfined compression test.....	5-44
5-14	Schematic of a triaxial compression test (Lambe and Whitman, 1979).....	5-45
5-15	(a) Failure of a loose sand specimen in a triaxial cell; and (b) Load frame, pressure panel, and computerized data acquisition system (Photograph courtesy of GeoComp Corporation).....	5-46
5-16	Typical stress-strain curves from CU test.....	5-48
5-17	Schematic of the Direct Shear Test.....	5-49
5-18	Direct shear testing box (Photograph courtesy of GeoComp Corporation).....	5-50
5-19	Soil sample mounted in direct shear testing apparatus (Photograph courtesy of GeoComp Corporation).....	5-50
5-20	Relationship between the ratio of undrained shear strength to effective overburden pressure and plasticity index for normally-consolidated and overconsolidated clays (after Holtz and Kovacs, 1981).....	5-54
5-21	Relationships between $\phi$ and PI (after Terzaghi, <i>et al.</i> , 1996).....	5-56
5-22	Correlation between relative density, material classification and angle of internal friction for coarse-grained soils (NAVFAC, 1986a).....	5-57
5-23	Correlation between relative density and SPT resistance (NAVFAC, 1986a).....	5-57
5-24	Rigid wall permeameter (Photograph courtesy of GeoComp Corporation).....	5-59
5-25	Flexible wall permeameter (Photograph courtesy of GeoComp Corporation).....	5-60
5-26	The permeability of sands and gravels (after NAVFAC, 1986a).....	5-64
5-27	Classification of swell potential for soils (after Seed, <i>et al.</i> , 1962).....	5-66
5-28	Chart for evaluation of collapsible soils (after Holtz and Hilf, 1961).....	5-68
5-29	Approximate frost depth map for United States (Bowles, 1996).....	5-71
5-30	Hammer and mold for laboratory compaction test (tape measure is for scale purpose only).....	5-73
5-31	Compaction curves (after Holtz and Kovacs, 1981).....	5-74
5-32	Compactors recommended for various types of soil and rock (Schroeder, 1980).....	5-77
5-33	Relative density, relative compaction and void ratio concepts.....	5-78
5-34	Example evaluation of economical field compaction conditions (after Bowles, 1979).....	5-81
5-35	Point load strength test equipment (Wyllie, 1999).....	5-89
5-36	(a) Unconfined compression test on intact rock core, (b) Use of strain gage	

	on intact rock core sample for measurement of stress-strain characteristics (Geomechanical Laboratory, University of Arizona).....	5-92
5-37	Laboratory direct shear testing equipment for rock (Wyllie, 1999).....	5-93
6-1	Embankment failures: (a) Infinite slope failure in embankment fill, (b) Circular arc failure in embankment fill and foundation soil, (c) Sliding block failure in embankment fill and foundation soil, and (d) Lateral squeeze of foundation soil .....	6-2
6-2	Effect of water content on cohesive strength of clay .....	6-4
6-3	Infinite slope failure in dry sand .....	6-6
6-4	Infinite slope failure in a $c-\phi$ soil with parallel seepage .....	6-7
6-5	Typical circular arc failure mechanism .....	6-9
6-6	Example proposed embankment .....	6-10
6-7	Geometry of Ordinary Method of Slices .....	6-12
6-8	Example of dividing the failure mass in slices .....	6-13
6-9	Forces on a slice without water effect .....	6-15
6-10	Forces on a slice with water effect.....	6-15
6-11a	Tabular form for computing weights of slices.....	6-18
6-11b	Tabular form for calculating factor of safety by Ordinary Method of Slices ....	6-19
6-12	Typical static forces acting on a slice of sliding mass without seepage.....	6-20
6-13	Location of critical circle by plotting contours of minimum safety factors for various trial circles .....	6-23
6-14	Taylor's chart for soils with friction angle (after Taylor, 1948).....	6-27
6-15	Taylor's chart for $\phi'=0$ conditions for slope angles ( $\beta$ ) less than $54^\circ$ (after Taylor, 1948) .....	6-28
6-16	Stability charts for $\phi = 0$ soils (Janbu, 1968).....	6-34
6-17	Reduction factors to account for tension cracks to be used with stability charts for $\phi=0$ and $\phi > 0$ soils (Janbu, 1968) .....	6-36
6-18	Reduction factors to account for surcharge (upper) and submergence and/or seepage (lower) to be used with stability charts for $\phi=0$ and $\phi > 0$ soils (Janbu, 1968) .....	6-37
6-19	Stability charts for $\phi > 0$ (Janbu, 1968) .....	6-39
6-20	Data for Example 6-2.....	6-41
6-21	Sliding block failure mechanism .....	6-43
6-22	Geometry and force components for sliding block analysis.....	6-44
6-23	Example Simple Sliding Block Method using Rankine Pressure Coefficients .	6-46
6-24	Reduction of grade line to improve slope stability .....	6-52
6-25	Use of counterweight berm to improve slope stability .....	6-52
6-26	Use of shear key to improve slope stability .....	6-52
6-27	Failure modes for Reinforced Soil Slopes .....	6-53
6-28	Chart solution for determining the reinforcement strength requirements (Schmertmann, <i>et al.</i> , 1987). ©The Tensar Corporation. ....	6-55
6-29	Deep seated slope failure (left) and bench slope design (right) to prevent slope failure.....	6-57
6-30	Typical cut slope failure mechanism in clay soils .....	6-58

7-1	(a) Elements of a bridge approach system, (b) Plan view of an approach system (modified after NCHRP, 1997).....	7-2
7-2	Types of abutments (modified after NCHRP, 1990) .....	7-3
7-3	Problems leading to the existence of a bump (modified after NCHRP, 1997)....	7-4
7-4	Suggested approach embankment details .....	7-7
7-5	Structural backfill placement limits for porous drainage aggregate.....	7-8
7-6	Pressure coefficients beneath the end of a fill (NYSDOT, 1970) .....	7-12
7-7	Bearing capacity index (C') values used in Modified Hough method for computing immediate settlements of embankments (AASHTO, 2004 with 2006 Interims; modified after Hough, 1959).....	7-17
7-8	Effect of sample disturbance on the shape of the one-dimensional consolidation curve (Reese, <i>et al.</i> , 2006).....	7-21
7-9	Construction of field virgin consolidation relationships (adapted from USACE, 1994) .....	7-22
7-10	Typical consolidation curve for normally consolidated soil – (a) Void ratio versus vertical effective stress and (b) Vertical strain versus vertical effective stress.....	7-25
7-11	Typical consolidation curve for overconsolidated soil – (a) Void ratio versus vertical effective stress and (b) Vertical strain versus vertical effective stress .	7-26
7-12	Typical consolidation curve for under-consolidated soil – (a) Void ratio versus vertical effective stress and (b) Vertical strain versus vertical effective stress.....	7-27
7-13	Diagram illustrating consolidation of a layer of clay between two pervious layers (modified after Terzaghi, <i>et al.</i> , 1996) .....	7-28
7-14	Typical settlement-time curve for clay under an embankment loading.....	7-32
7-15	Logarithm-of-time method for determination of $c_v$ .....	7-34
7-16	Square-root-of-time method for determination of $c_v$ .....	7-35
7-17	Example time plot from one-dimensional consolidometer test for determination of secondary compression (USACE, 1994).....	7-39
7-18	Schematic of lateral squeeze phenomenon .....	7-40
7-19	Examples of abutment tilting due to lateral squeeze (FHWA, 2006a) .....	7-41
7-20	Definitions for calculating safety factor against later squeeze (after Silvestri, 1983) .....	7-42
7-21	Determination of surcharge time required to achieve desired settlement.....	7-45
7-22	Use of vertical drains to accelerate settlement.....	7-46
7-23	Typical locations for various types of monitoring instruments for an embankment constructed over soft ground.....	7-51

## LIST OF TABLES

<u>No.</u>	<u>Caption</u>	<u>Page</u>
1-1	Geotechnical involvement in project phases .....	1-9
2-1	Summary of index properties and their application.....	2-8
2-2	Weight-volume relations (after Das, 1990) .....	2-8
2-3	U.S. standard sieve sizes and corresponding opening dimension.....	2-10
2-4	Concept of soil phase, soil strength and soil deformation based on Liquidity Index .....	2-17
3-1	Sources of historical site data (after FHWA, 2002a).....	3-4
3-2	Common landforms of transported soils and their engineering significance ....	3-10
3-3	Reference publications on in-situ testing (FHWA, 2002b) .....	3-19
3-4a	Soil and soft rock boring methods (FHWA, 2002a).....	3-22
3-4b	Rock core drilling methods (FHWA, 2002a).....	3-23
3-4c	Other exploratory techniques (FHWA, 2002a).....	3-24
3-5a	Common samplers to retrieve disturbed soil samples (modified after NAVFAC, 1986a).....	3-29
3-5b	Common samplers to retrieve disturbed soil samples (modified after NAVFAC, 1986a).....	3-30
3-6	Nominally undisturbed soil samplers (modified after NAVFAC, 1986a).....	3-32
3-7	Dimensions of core sizes (FHWA, 1997).....	3-41
3-8	Advantages and disadvantages of the Standard Penetration Test (SPT) .....	3-51
3-9	Soil properties correlated with Standard Penetration Test values (after Peck, <i>et al.</i> , 1974).....	3-58
3-10	Factors affecting the SPT and SPT results (after Kulhawy and Mayne, 1990) .	3-61
3-11	Advantages and disadvantages of the Cone Penetration Test (CPT) (FHWA, 2002b) .....	3-67
3-12	Classification of Sensitivity Values (Mitchell, 1976).....	3-78
3-13	Guidelines for minimum number of exploration points and depth of exploration (modified after FHWA, 2002a) .....	3-84
3-14	Geophysical testing techniques (modified after FHWA, 2002a).....	3-91
4-1	Evaluation of the apparent density of coarse-grained soils (after Peck, <i>et al.</i> , 1974).....	4-5
4-2	Evaluation of the consistency of fine-grained soils (after Peck, <i>et al.</i> , 1974) .....	4-5
4-3	Adjectives to describe water content of soils (ASTM D 2488).....	4-6
4-4	Particle size definition for gravels and sands (after ASTM D 2488).....	4-7
4-5	Adjectives for describing size distribution for sands and gravels (after ASTM D 2488) .....	4-8
4-6	Field methods to describe plasticity (FHWA, 2002b) .....	4-10
4-7	Descriptive terms for layered soils (NAVFAC, 1986a) .....	4-13
4-8	Basic USCS soil designations based on percents passing No. 200 (0.075mm) Sieve (after ASTM D 2487; Holtz and Kovacs, 1981) .....	4-14

4-9	Soil classification chart (laboratory method) (after ASTM D 2487).....	4-15
4-10	Gradation based on $C_u$ and $C_c$ parameters .....	4-19
4-11	Soil plasticity descriptors (based on Figures 4-3, 4-4a and 4-4b) .....	4-25
4-12	Examples of description of fine-grained soils (based on Figures 4-3, 4-4a and 4-4b).....	4-25
4-13	AASHTO soil classification system based on AASHTO M 145 (or ASTM D 3282) .....	4-27
4-14	Example gradation limits of well-graded granular material (see Curve A in Figure 4-2) .....	4-33
4-15	Example gradation limits of drainage materials (see Curve C in Figure 4-2) ...	4-33
4-16	Rock groups and types (FHWA, 1997).....	4-35
4-17	Terms to describe grain size (typically for sedimentary rocks).....	4-36
4-18	Terms to describe grain shape (for sedimentary rocks).....	4-36
4-19	Terms to describe stratum thickness .....	4-37
4-20	Terms to describe rock weathering and alteration (ISRM, 1981).....	4-38
4-21	Terms to describe rock strength (ISRM, 1981) .....	4-38
4-22	Terms to describe rock hardness (FHWA, 2002b) .....	4-39
4-23	Terms to describe discontinuities (after ISRM, 1981).....	4-40
4-24	Terms to classify discontinuities based on aperture size (ISRM, 1981).....	4-40
4-25	Geomechanics classification of rock masses (AASHTO 2004 with 2006 Interims).....	4-43
4-26	Geomechanics rating adjustment for joint orientations (after AASHTO 2004 with 2006 Interims).....	4-44
4-27	Geomechanics rock mass classes determined from total ratings (AASHTO 2004 with 2006 Interims).....	4-44
5-1	Commonly performed laboratory tests on soils (after FHWA, 2002a) .....	5-6
5-2	Methods for index testing of soils (after FHWA, 2002a) .....	5-7
5-3	Methods for performance testing of soils (after FHWA, 2002a).....	5-8
5-4	Typical particle sizes, uniformity coefficients, void ratios and unit weights (from Kulhawy and Mayne, 1990).....	5-13
5-5	Correlations for $C_c$ (modified after Holtz and Kovacs, 1981) .....	5-33
5-6	Typical values of coefficient of vertical consolidation, $c_v$ (after Carter and Bentley, 1991).....	5-36
5-7	Typical values of $C_{ae}/C_c$ (Terzaghi, <i>et al.</i> , 1996).....	5-37
5-8	Summary of issues relevant to shear strength evaluation in support of the design of typical geotechnical features (after FHWA, 2002a) .....	5-39
5-9	Recommended maximum hydraulic gradient for permeability testing.....	5-61
5-10	Typical permeability values in soils (after Carter and Bentley, 1991).....	5-63
5-11	Typical permeability values for highway materials (after Krebs and Walker, 1971) .....	5-63
5-12	Qualitative assessment of collapse potential (after ASTM D 5333) .....	5-69
5-13	Characteristics of laboratory compaction tests .....	5-73
5-14	Some values of $D_r$ as a function of RC based on Modified and Standard Proctor Compaction Test .....	5-79
5-15	Average engineering properties of compacted inorganic soils	

	(after USBR, 1960).....	5-82
5-16	Elastic constants of various soils (after AASHTO 2004 with 2006 Interims)...	5-85
5-17	Rate of increase of soil modulus with depth $n_h$ (tsf/ft) for sand (AASHTO 2004 with 2006 Interims) .....	5-85
5-18	Common sense guidelines for laboratory testing of soils .....	5-86
5-19	Common rock tests performed in the laboratory .....	5-87
5-20	Summary information on rock laboratory test methods (FHWA, 2002a) .....	5-88
5-21	Summary of elastic moduli for intact rock (AASHTO 2004 with 2006 Interims) .....	5-94
5-22	Summary of Poisson's Ratio for intact rock (AASHTO 2004 with 2006 Interims) .....	5-95
5-23	Estimation of $E_m$ based on RQD (AASHTO 2004 with 2006 Interims).....	5-96
5-24	Common sense guidelines for laboratory testing of rocks.....	5-97
5-25	Values of coefficient of variation, $V$ , for geotechnical properties and in-situ tests (after Duncan, 2000).....	5-100
6-1	Slope stability guidelines for design.....	6-21
6-2	Practical design solutions to mitigate embankment stability problems.....	6-51
6-3	Typical design solutions to mitigate cut slope stability problems.....	6-57
7-1	General considerations for specification of select structural backfill.....	7-9
7-2	Suggested gradation for drainage aggregate.....	7-9
7-3	Reconstruction of virgin field consolidation (modified from USACE, 1994) ..	7-23
7-4	Average degree of consolidation, $U$ , versus time factor, $T_v$ , for uniform initial increase in pore water pressure .....	7-32
7-5	Summary of abutment movements (Nicu, <i>et al.</i> , 1971).....	7-43

## LIST OF SYMBOLS

### Chapter 1

AASHTO	American Association of State Highway and Transportation Officials
AC	Asphaltic concrete
CMAR	Construction manager at risk
D-B	Design-build
FHWA	Federal Highway Administration
MSE	Mechanically stabilized earth
NHI	National Highway Institute
NMDOT	New Mexico Department of Transportation
PCC	Portland cement concrete
RCC	Reinforced cement concrete
RSS	Reinforced soil slope(s)
USDA	United States Department of Agriculture
USGS	United States Geological Survey

### Chapter 2

A	Overall contact area
AASHTO	American Association of State Highway and Transportation Officials
B	Width
c	Cohesion
c'	Effective cohesion
D <sub>r</sub>	Relative density
D <sub>s</sub> , DOSI	Depth of significant influence
e	Void ratio
e <sub>max</sub>	Maximum void ratio
e <sub>min</sub>	Minimum void ratio
F <sub>a</sub>	Tangential force
F <sub>r</sub>	Shearing resistance
G	Specific gravity
G <sub>s</sub>	Specific gravity of the solid phase
h	Embankment height
h <sub>w</sub>	Depth to water table
K	Value of proportionality constant; coefficient of lateral earth pressure
K <sub>a</sub>	Coefficient of active earth pressure
K <sub>o</sub>	Coefficient of lateral earth pressure “at rest”
K <sub>p</sub>	Coefficient of passive earth pressure
K <sub>w</sub>	Coefficient of lateral earth pressure for water
L	Length
LI	Liquidity index
LL	Liquid limit
n	Porosity
P	Load applied
p <sub>a</sub>	Active lateral pressure

$p_f$	Final stress = effective overburden pressure + pressure increment due to external loads
$p_h$	Lateral stress
PI	Plasticity index
PL	Plastic limit
$P_n$	Normal force
$p_o$	Effective overburden pressure
$p_p$	Passive lateral pressure
$p_t$	Total overburden pressure
Q	Load
$q, q_o$	Unit load of embankment
S	Degree of saturation
SI	Shrinking index
SL	Shrinkage limit
t	time
u	Porewater pressure
USCS	Unified Soil Classification System
V	Volume of the total soils mass
$V_a$	Volume of air phase
$V_s$	Volume of solid phase
$V_v$	Volume of total voids
$V_w$	Volume of water phase
w	Gravimetric water or moisture content
W	Weight of the total soil mass
$W_a$	Weight of air phase
$W_s$	Weight of solid phase
$W_v$	Weight of total voids
$W_w$	Weight of water phase
z	Depth
$z_w$	Depth below water table
$\delta$	Angle of interface friction
$\delta_a$	active translation
$\delta_b$	passive translation
$\Delta p$	Pressure due to external loads
$\Delta u$	Excess pore water pressure
$\gamma$	Total unit weight
$\gamma'$	Effective unit weight
$\gamma_b$	Buoyant unit weight (same as effective unit weight)
$\gamma_d$	Dry unit weight
$\gamma_s$	Unit weight of the solid phase
$\gamma_{sat}$	Saturated unit weight
$\gamma_T$ or $\gamma_t$	Total unit weight
$\gamma_w$	Unit weight of water
$\phi$	Angle of friction
$\phi'$	Effective angle of internal friction

$\nu$	Poisson's ratio
$\theta$	Angle of obliquity
$\theta_m$	Maximum angle of obliquity
$\sigma$	Total stress
$\sigma'$	Effective stress
$\sigma_n$	Normal stress
$\sigma_n'$	Effective normal stress
$\tau$	Shearing strength
$\tau'$	Effective shear stress (strength)

### Chapter 3

AASHTO	American Association of State Highway and Transportation Officials
AR	Area ratio
ASTM	American Society for Testing and Materials
BPT	Becker (Hammer) penetration test
$C_N$	Overburden correction factor or stress normalization parameter
CPT	Cone penetration test
CPTu, PCPT	Piezocone penetration test
d	Displacement
DC	Direct current
$D_e$	Diameter of sampler cutting tip
$D_i$	Inside diameter of the sampling tube
DMT	Flat plate dilatometer
$D_o$	Outside diameter of the sampling tube
DOT	Department of Transportation
$E_f$	Energy efficiency
ER	Energy ratio
F	Force
FEMA	Federal Emergency Management Agency
FHWA	Federal Highway Administration
$f_s$	Sleeve friction
g	Gravitational constant
GPR	Ground penetrating radar
h	Drop height
i	Inclination
ICR	Inside clearance ratio
ID	Inside Diameter
ISRM	International Society of Rock Mechanics
KE	Kinetic energy
LPT	Large penetration test
m	Mass
N	SPT blows per foot
$N_{160}$	Overburden-normalized energy-corrected blowcount
$N_{60}$	Energy-corrected SPT-N value adjusted to 60% efficiency
NAVFAC	Naval Facilities Engineering Command
NCR	No core recovery

$N_{\text{meas}}$	N-Value measured in the field
OD	Outside diameter
PE	Potential energy
PMT	Pressuremeter test
$p_o$	Vertical effective pressure at the depth where the SPT is performed
PVC	Polyvinyl chloride
$q_c$	Cone tip resistance
$q_t$	Tip resistance
$R_f$	Friction ratio
RQD	Rock quality designation
$S_t$	Sensitivity
SASW	Spectral analysis of surface waves
SBT	Soil behavioral type
SCPTu	Seismic cone piezocone penetration test
SPT	Standard Penetration Test
SWPPP	Storm Water Pollution Prevention Plan
$t_s$	Shear wave time
$u_m$	Pore water pressure
USCS	Unified Soil Classification System
USEPA	United States Environmental Protection Agency
USGS	United States Geological Survey
$v$	Impact velocity
VST	Vane shear test
W	Work

#### Chapter 4

AASHTO	American Association of State Highway and Transportation Officials
ASTM	American Society for Testing and Materials
$C_c$	Coefficient of curvature
$C_u$	Coefficient of uniformity
$D_{10}$	Diameter of soil particles of which 10% of the soil is finer
$D_{30}$	Diameter of soil particles of which 30% of the soil is finer
$D_{60}$	Diameter of soil particles of which 60% of the soil is finer
DOT	Department of Transportation
EGS	Effective grain size
F	Percent passing No. 200 sieve
FHWA	Federal Highway Administration
GI	Group index
GIS	Geographic information system
GSD	Grain size distribution
IGM	Intermediate geomaterial
$I_s$	Point load index
ISRM	International Society of Rock Mechanics
LI	Liquid index
LL	Liquid limit
N	SPT blows per foot

$N_{60}$	Energy-corrected SPT-N value adjusted to 60% efficiency
NAVFAC	Naval Facilities Engineering Command
PI	Plasticity index
PL	Plastic limit
RMR	Rock mass rating
RQD	Rock quality designation
SPT	Standard penetration test
U.S.	United States
USCS	Unified Soil Classification System
USDA	United States Department of Agriculture

## Chapter 5

A	Activity index
A	Area
AASHTO	American Association of State Highway and Transportation Officials
ASTM	American Society for Testing and Materials
B	Bulk modulus
$c$	Cohesion
C	Permeability coefficient
$C_{\alpha}$	Coefficient of secondary compression
$c'$	Effective stress cohesion intercept
$c'_{cu}$	Effective stress cohesion from CU test
CBR	California Bearing Ratio
$C_c$	Compression index
$C_{ce}$	Modified compression index
CD	Consolidated drained triaxial test
CF	Clay fraction
$c_h$	Coefficient of horizontal consolidation
$c_o$	Compacted cohesion
CP	Collapse potential
$C_r$	Recompression index
$C_{re}$	Modified recompression index
$c_{sat}$	Saturated cohesion
CU	Consolidated undrained triaxial test
$c_u$	Apparent cohesion
$c_v$	Coefficient of consolidation
$c_v$	Coefficient of vertical consolidation
$C_{\alpha}$	Secondary compression index
$C_{\alpha e}$	Modified secondary compression index
D	Distance between contact points of platens
D	Vane diameter
$D_{10}$	Diameter of soil particles of which 10% of the soil is finer
$D_{60}$	Diameter of soil particles of which 60% of the soil is finer
$D_e$	Equivalent core diameter
$D_{max}$	Maximum diameter of soil particle
$D_{min}$	Minimum diameter soil particles

$D_r$	Relative density
$d_s$	Equivalent diameter
$e$	Void ratio
$e_{max}$	Maximum void ratio
$e_{min}$	Minimum void ratio
$E$	Young modulus
$E_i$	Elastic modulus of intact rock
$E_m$	Elastic modulus of rock mass
$e_{max}$	Maximum void ratio
$e_{min}$	Minimum void ratio
$e_o$	Initial void ratio
$E$ or $E_s$	Elastic modulus
FHWA	Federal Highway Administration
$g$	Gravitational constant
$G$	Shear modulus
$G_s$	Specific gravity
$H$	Height of vane
$H$	Soil layer thickness
$H/D$	Height to diameter ratio
$H_o$	Initial height of specimen
$i_B$	Angle of taper at the bottom of the vane
IL	Incremental load
$I_s$	Point load strength index
$I_{s(50)}$	Size-corrected point load strength index
$i_T$	Angle of taper at the top of the vane
$k$	Hydraulic conductivity
$k_{PLT}$	Size correction factor
LI	Liquid index
LIR	Load increment ratio
LL	Liquid limit
LVDT	Linear variable differential transducer
md	Man-days
MPC	Modified Proctor compaction
$M_s$	Mass of solid component of sample
$M_t$	Total mass
$N$	Normal stress
$N$	SPT blows per foot
$N_{160}$	Overburden-normalized energy-corrected blowcount
$N_{60}$	Energy-corrected SPT-N value adjusted to 60% efficiency
NAVFAC	Naval Facilities Engineering Command
NC	Normally consolidated
$n_h$	Rate of increase of soil modulus with depth
OC	Over consolidated
OCR	Overconsolidation ratio
OMC	Optimum moisture content
$P$	Breaking load

$p_c$	Maximum past effective stress
$p_c$	Preconsolidation pressure
PI	Plasticity index
PL	Plastic limit
$p_o$	Effective overburden pressure
$p_t$	Total vertical stress
$q_c$	Cone tip resistance
$q_u$	Unconfined compression stress
RC	Relative compaction
RMR	Rock mass rating
RQD	Rock quality designation
S	Degree of saturation
S, $S_t$	Sensitivity
$s_{collapse}$	Collapse settlement
SL	Shrinkage limit
SPC	Standard Proctor compaction
SPT	Standard penetration test
$s_r, VST$	Remolded undrained shear strength (obtained by using VST data)
$s_t, VST$	Sensitivity (obtained by using VST data)
$s_u$	Undrained shear strength
$s_u, VST$	Undrained shear strength (obtained by using VST data)
$s_u/p_o$	Undrained strength ratio
T	Tangential (shear) force
T	Torque (related to VST)
t	Vane edge thickness
$t_{100}$	Time corresponding to 100% of primary consolidation
$T_{max}$	Maximum torque (related to VST)
$T_{net}$	Difference between $T_{max}$ and $T_{rod}$
$T_{rod}$	Rod friction (related to VST)
u	Pore water pressure
UC	Unconfined compression test
U.S.	United States
USBR	United States Bureau of Reclamation
USCS	Unified Soil Classification System
UU	Unconsolidated undrained triaxial test
V	Coefficient of variation
$V_s$	Volume of soil solids
VST	Vane shear test
$V_t$	Total volume
W	Specimen width
w	Water content
$w_n$	Natural moisture content
$w_{opt}$	Optimum moisture content
$W_s$	Weight of solid component of soil
$W_t$	Total weight
Z	Depth below ground surface

$\Delta e$	Change in void ratio
$\Delta H_c$	Change in height upon wetting
$\Delta \sigma$	Incremental stress
$\varepsilon$	Strain
$\gamma$	Unit weight
$\gamma'$	Effective unit weight
$\gamma_b$	Buoyant unit weight (same as effective unit weight)
$\gamma_{d \text{ field}}$	Field dry unit weight
$\gamma_d$ or $\gamma_{dry}$	Dry unit weight
$\gamma_{d-max}$	Maximum dry unit weight
$\gamma_s$	Unit weight of solid particles in the soil mass
$\gamma_{sat}$	Saturated unit weight
$\gamma_t$ or $\gamma_{tot}$	Total unit weight
$\gamma_t$	Moist unit weight of compacted soil
$\gamma_w$	Unit weight of water
$\phi$	Angle of internal friction
$\phi'$	Effective friction angle
$\phi$	Friction
$\phi'$	Peak effective stress friction angle
$\phi'_{cu}$	Effective friction angle from CU test
$\phi'_r$	Residual effective stress friction angle
$\mu$	Coefficient of friction
$\nu$	Poisson ratio
$\rho$	Density
$\rho_d$ or $\rho_{dry}$	Dry mass density
$\rho_t$ or $\rho_{tot}$	Total mass density
$\rho_t$	Moist (total) mass density
$\sigma'$	Effective normal stress
$\sigma_c$	Uniaxial compressive strength
$\sigma_n$	Normal stress
$\sigma'_p$	Preconsolidation stress
$\sigma_{vo}$	Total vertical stress
$\tau$	Shear stress
%C	Percent collapse

## Chapter 6

AASHTO	American Association of State Highway and Transportation Officials
b	Unit width
b	Width of slice
c	Cohesion
c	Cohesion component of shear strength
c	Unit cohesion
c'	Effective cohesion
CD	Consolidated drained triaxial test
c <sub>d</sub>	Developed cohesion
CU	Consolidated undrained triaxial test
d	Depth factor
D	Depth ratio
F <sub>c</sub>	Average factor of safety with respect to cohesion
FHWA	Federal Highway Administration
FS or FOS	Factor of safety
F <sub>φ</sub>	Average factor of safety with respect to friction angle
h	Depth less than or equal to the depth of saturation
H	Height
H	Height of soil layer in active wedge
h	Slope depth
H	Slope height
H' <sub>w</sub>	Height of water within the slope
H <sub>Fill</sub>	Fill height
h <sub>i</sub>	Height of layer at center of slice
H <sub>t</sub>	Tension crack height
h <sub>w</sub>	Depth from groundwater surface to the centroid point on the circle
H <sub>w</sub>	Depth of water outside the slope
H <sub>zone</sub>	Height of zone
I <sub>N</sub>	Interslice normal (horizontal) force
I <sub>S</sub>	Interslice shear (vertical) force
K <sub>a</sub>	Coefficient of active earth pressure
K <sub>p</sub>	Coefficient of passive earth pressure
l	Arc length of slice base
L <sub>s</sub>	Radius of circle
L <sub>w</sub>	Level arm distance to the center of rotation
N	Normal force component or total normal force
N	Number of reinforcement layers
N'	Effective normal force component
N <sub>cf</sub>	Critical stability number
N <sub>o</sub>	Stability number
N <sub>s</sub>	Stability number
P <sub>a</sub>	Active force (driving)
p <sub>o</sub>	In-situ vertical effective overburden pressure
P <sub>p</sub>	Passive force (resisting)
q	Surcharge load

R	Moment arm
$R_c$	Coverage ratio of the reinforcement
RSS	Reinforced soil slope
S	Frictional force along failure plane
S	Shear strength along failure plane
SPT	Standard penetration test
$S_v$	Vertical spacing of reinforcement
T	Tangential force component
$T_a$	Sum of available tensile force per width of reinforcement for all reinforcement layers
$\tan \phi$	Coefficient of friction along failure surface
$T_{MAX}$	Maximum design tension
$T_{S-MAX}$	Maximum tensile force
$T_{zone}$	Maximum reinforced tension required for each zone
U	Pore water force
u	Water pressure on slice base
u	Water uplift pressure against failure surface
UU	Unconsolidated undrained triaxial test
W	Weight of slice
$W_i$	Partial weight
$W_T$	Total slice weight
$\alpha$	Angle between vertical and line drawn from circle center to midpoint of slice base
$\alpha_w$	Slope of water table from horizontal
$\gamma_{Fill}$	Fill soil unit weight
$\mu'_w$	Seepage correction factor
$\mu_q$	Surcharge correction factor
$\mu_t$	Tension crack correction factor
$\mu_w$	Submergence correction factor
$\sigma$	The total normal stress against the failure surface slice base due to the weight of soil and water above the failure surface
$\Sigma W_i$	Total weight of slice
$\beta$	Angle of slope
$\beta$	Inclination of the slope
$\phi$	Angle of internal friction
$\phi'$	Effective angle of internal friction
$\phi_d$	Developed angle of internal friction
$\gamma$	Unit weight of soil
$\gamma$	Unit weight of soil in the active wedge
$\gamma_i$	Unit weight of layer i
$\gamma$	Effective unit weight
$\gamma_m$	Moist unit weight
$\gamma_{sat}$	Saturated unit weight
$\gamma_t$	Total soil unit weight
$\gamma_w$	Unit weight of water

$\sigma'_n$	Effective stress between soil grains
$\tau$	Frictional shearing resistance
$\tau$	Total shear strength
$\tau_d$	Developed shear strength

## Chapter 7

AASHTO	American Association of State Highway and Transportation Officials
$C'$	Bearing capacity index
$C_c$	Compression index
$C_{ce}$	Modified compression index
$C_r$	Mean slope of the rebound laboratory curve
$C_{re}$	Modified recompression index
$c_v$	Coefficient of consolidation
$C_\alpha$	Coefficient of secondary consolidation (determined from lab consolidation test)
$C_{\alpha\varepsilon}$	Modified secondary compression index
$D_s$	Depth of soft soil beneath the toe of the end slope of the embankment
$e$	Void ratio
$e_o$	Initial void ratio at $p_o$
FHWA	Federal Highway Administration
$FS_{SQ}$	Safety factor against failure by squeezing
$H$	Height of the fill
$H$	Thickness of soil layer considered
$H_d$	Distance to the drainage boundary
$h_f$	Fill height
$H_o$	Layer thickness
ID	Inner Diameter
$N_{160}$	Number of blows per foot corrected for overburden and hammer efficiency
NCHRP	National Cooperative of Highway Research Program
OCR	Over consolidation ratio
$p_c$	Maximum past effective stress
$p_c$	Maximum past vertical pressure (preconsolidation)
$p_f$	Final effective vertical stress at the center of layer n
$p_f$	Final pressure applied to the foundation subsoil
$p_f$	Final stress
$p_f$	Total embankment pressure
PI	Plasticity index
$p_o$	Effective overburden pressure
$p_o$	Existing effective overburden pressure
$p_o$	Initial effective vertical stress at the center of layer n
RSS	Reinforced soil slope
$S$	Degree of saturation
$S$	Settlement
$S_c$	Settlement due to primary consolidation
SPT N	Number of blows per foot (blow/0.3m)
SPT	Standard penetration test

$S_s$	Settlement due to secondary compression
$S_t$	Settlement at time $t$
$s_u$	Undrained shear strength of soft soil beneath embankment
$S_{ultimate}$	Settlement at end of primary consolidation
$t$	Time
$t_{1\ lab}$	Time when secondary compression begins
$t_1$	Time when approximately 90% of primary compression has occurred
$t_{100}$	Time for 100% of primary consolidation
$t_{2\ lab}$	Arbitrary time on the curve
$t_2$	The service life of the structure or any time of interest
$t_{90}$	Time for 90% of primary consolidation
$T_v$	Time factor
$U$	Average degree of consolidation
$u_s$	Hydrostatic pore water pressure at any depth
$u_s$	Initial hydrostatic pore water pressure
USACE	United States Army Corps of Engineers
$u_{sb}$	Hydrostatic pore water pressure at bottom of layer
$u_{st}$	Hydrostatic pore water pressure at top of layer
$u_t$	Total pore water pressure at any depth after time $t$
$Z_I$	Zone of influence
$\Delta e$	Change in void ratio
$\Delta H$	Settlement
$\Delta p$	Distributed embankment pressure
$\Delta p$	Load increment
$\Delta p$	Stress increase
$\Delta p_o$	Effective vertical stress increment
$\Delta p_t$	Applied vertical stress increment
$\Delta u$	Excess pore water pressure at any depth after time $t$
$\Delta u_i$	Initial excess pore water pressure
$\epsilon_v$	Vertical strain
$\gamma$	Unit weight of fill
$\gamma'$	Effective unit weight
$\gamma_b$	Buoyant unit weight (same as effective unit weight)
$\gamma_f$	Fill unit weight
$\theta$	Angle of slope

[THIS PAGE INTENTIONALLY BLANK]

## CHAPTER 1.0 INTRODUCTION

### 1.1 PURPOSE AND SCOPE

The Soils and Foundations course is sponsored by the National Highway Institute (NHI) to provide practical knowledge in geotechnical and foundation engineering for both civil engineering generalists and geotechnical and foundation specialists. The course is developed around the design and construction aspects of a highway project that includes bridges, earthworks and earth retaining structures. Bridges can range from single span bridges to multi-span bridges as part of a stack interchange. Bridges may be constructed over land, in which case they are known as viaducts, or over water. Examples of transportation facilities that include bridge structures are shown in Figures 1-1 to 1-4. Not all highway projects include bridge structures. Figure 1-5 shows an example of a highway corridor without bridges and in an environmentally sensitive area.



**Figure 1-1. Aerial view of a pair of 3-span Interstate 10 (I-10) bridges over a local roadway in Tucson, Arizona.**



**Figure 1-2. Example of 3-span roadway bridges over another roadway.**

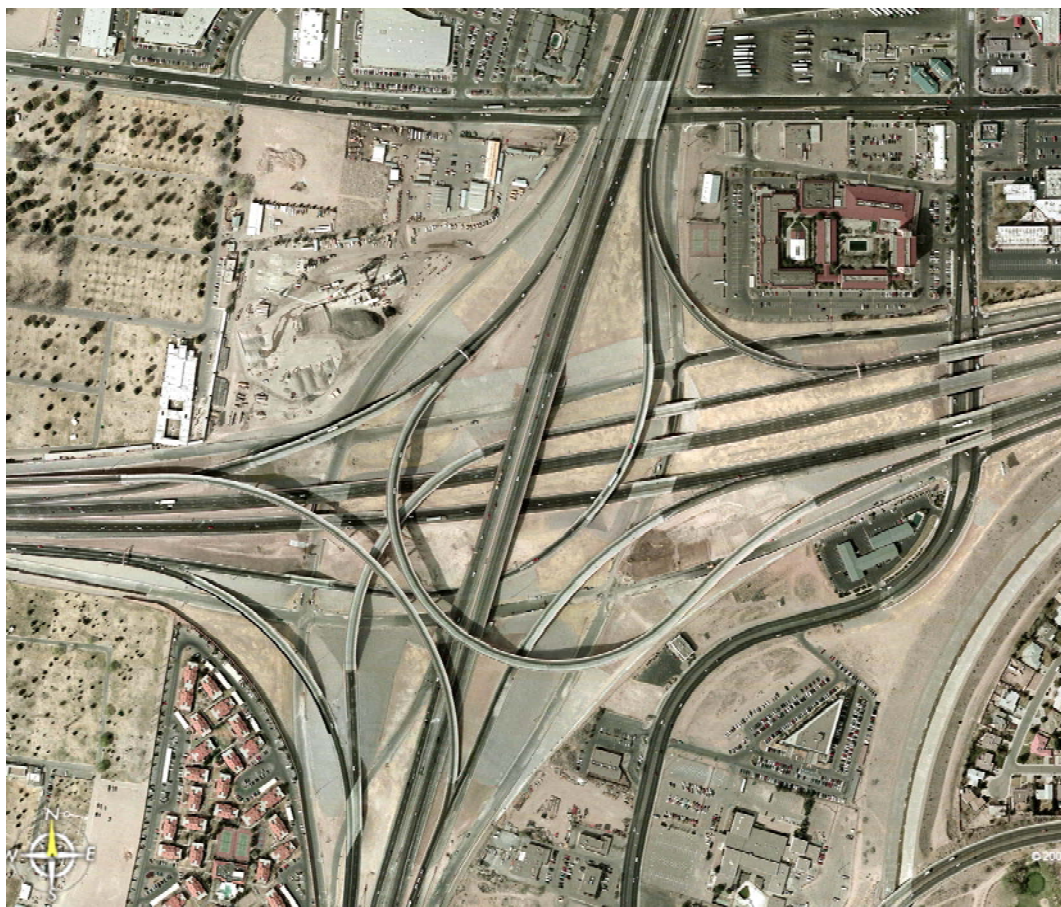


**Figure 1-3. The “BIG I” stack interchange at the intersection of I-40 and I-25 in Albuquerque, New Mexico (Photo: Courtesy of Bob Meyers, NMDOT) (Note: A stack interchange is a free-flowing junction between two or more roadways that allows turning in all directions).**



**Figure 1-4. A major multi-span bridge structure over water (George P. Coleman Bridge over the York River in Yorktown, Virginia).**

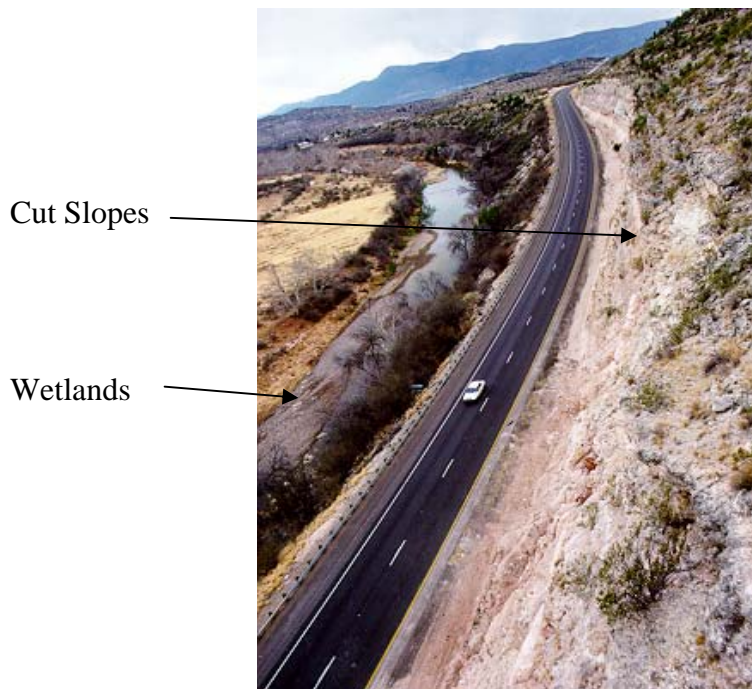


**Figure 1-5. Example of a roadway bounded by cut slopes and wetlands in an environmentally sensitive area.**

Highway projects can involve a full range of geotechnical engineering assessments and alternatives depending on the complexity of the project. For example, the foundations for the bridge piers and abutments may be shallow foundations, or deep foundations such as driven piles and/or drilled shafts. The approach embankments may be unreinforced slopes or reinforced soil slopes (RSS). Cut slopes may be in rocks and/or soils. Retaining walls may be used at abutments and/or along approaches and may consist of cantilevered walls or mechanically stabilized earth (MSE) walls. The ground under the bridge may be soft and require improvement. Similarly, the transportation corridor may traverse wetlands and special ground improvement measures may be required. Pavements seen in Figures 1-1 to 1-3 and 1-5 may be constructed of asphaltic concrete (AC), Portland cement concrete (PCC) or reinforced cement concrete (RCC) on a variety of subgrade materials<sup>1</sup>.

Recognizing the need for consistent guidance for practitioners involved in the planning, design and construction of transportation facilities that include bridges and associated structures, the Federal Highway Administration (FHWA) developed the first version of this manual in 1982. Subsequently, the manual was revised in 1993 and in 2000. The present reference manual, which is the fourth edition, represents a significant update and supersedes earlier editions of the manual. In particular, this manual has been updated to reflect the current standard of geotechnical practice in the planning, design and construction of transportation facilities. As part of this effort, this edition provides guidance consistent with that found in the latest FHWA manuals and courses.

This edition of the manual, like the earlier editions, is geared towards the practicing engineer who routinely deals with soils and foundations problems on highway projects but who may not have a thorough theoretical background of soil mechanics or foundation engineering. The overall goals of this manual are: (i) to explain geotechnical engineering principles, and (ii) to provide sound methods and recommendations related to safe, cost-effective design and construction of geotechnical features. The reader is encouraged to develop an appreciation for the design and construction of geotechnical features in all phases of a project that may influence or could be influenced by his/her work (cost, quality, time, and performance). Coordination among generalists and specialists in all project phases is stressed.

The manual contains an appendix (Appendix A) wherein the geotechnical engineering input to a bridge project is traced from conception (scoping) to completion (post construction) in a serialized illustrative problem that incorporates many of the technical concepts presented in the course. The bridge project used in Appendix A is based on an actual project in the State of New York.

---

<sup>1</sup> Pavement structures are not addressed in this manual.

## 1.2 SOILS AND FOUNDATIONS FOR HIGHWAY FACILITIES

Civilization's earliest attempts at construction probably involved soil; however, the understanding of the role of soil as a foundation or building material developed by trial and error. Since the early 20<sup>th</sup> century, an improved understanding of soil behavior has been achieved by applying the principles of physics, solid mechanics, fluid mechanics, strength of materials, and structural engineering to define soil behavior. The body of knowledge developed by analyzing soil behavior on a theoretically sound basis is called "**soil mechanics**" and its application to solution of actual problems is called "**geotechnical engineering**." Soil is a complex three-phase medium that contains various amounts of water and/or air surrounding the solid particles. It is not a solid mass, i.e., a continuum, as many of the theories of solid mechanics require. Therefore, an entirely theoretical solution of the most commonly encountered soil problems is not practical. The most practical solution to soil problems can be reached by a combination of the sources of information as illustrated in Figure 1-6.

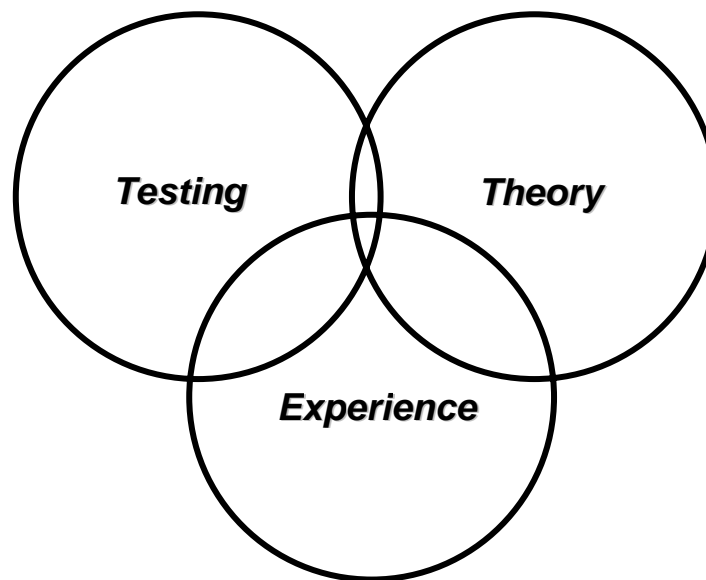


**Figure 1-6. Combinations of sources of information required to solve geotechnical engineering issues.**

1. **Experience** obtained from previous projects can be developed into the empirical or "rule of thumb" procedures followed by some engineers/specialists today. Often some geotechnical designers rely almost exclusively on experience. The weakness of using this approach exclusively is that experience does not always recognize the factors that cause differences in the engineering properties of soils. What works well at one location may not succeed with the same type of soil at another location because of a change in conditions, such as water content. The current state of the practice

requires the geotechnical specialist to rely on testing and theory in addition to experience or rules of thumb.

2. **Testing** of representative samples of soil in the field and laboratory is required to obtain information on the engineering properties and the characteristics of soils. The results of subsequent engineering analyses will be only as good as the soils data used as input.
3. **Theory** based on principles from various fields of engineering and science tempered by assumptions to fit reality is used to explain or predict the behavior of soils under various conditions.

The engineering analysis of soils is often more complex than the analysis of other construction materials because soil is not a continuum. Therefore, soil typically does not strictly meet the assumptions of the theories of solid mechanics and strength of materials. By contrast, steel and concrete are relatively uniform solids that have predictable properties. For example, the strength of steel is predictable within the elastic range of loading. Even though the strength of steel and concrete may be "ordered," that strength will be essentially constant under a wide range of climatic conditions. Structures can then be built of these materials with a high degree of confidence regarding the material strength.

The engineering properties of the soils, on the other hand, can vary widely over time and space so that their physical properties cannot be defined accurately at all locations for all conditions. Since soils are composed of a mixture of three dissimilar materials - soil solids, liquid fluids (usually water), and gaseous fluids (usually air) - their properties are influenced by the interaction of these three phases in the soil mass. Some of the factors that influence the behavior of soil are:

1. size, shape, and distribution of soil particles,
2. mineralogy,
3. degree of packing of soil particles,
4. amount of water in the soil,
5. climatic conditions, and
6. degree of confinement (i.e., depth).

In short, engineers should understand that the engineering properties of soils can be significantly influenced by many factors.

The success or failure of a geotechnical feature is often decided in the early stages of a project. Geotechnical engineering is a specialized field. Therefore, to assure success of a

project, the input of a qualified and experienced geotechnical specialist should begin at project inception and continue until completion of construction. Geotechnical designs are based upon soil properties that are generally defined from a subsurface exploration and laboratory testing of a very minute physical sampling of the soils. The volume of site soils excavated and exposed during construction is many orders of magnitude greater than that from the subsurface explorations. Thus, a great deal of geotechnical information can and should be gathered during the construction phase of a project to validate or revise the geotechnical design parameters. **A geotechnical design should not be considered complete until construction has been successfully completed.** A geotechnical specialist should also be involved during post-construction activities such as instrumentation monitoring, participating in resolution of contractor disputes and claims activities, and documenting lessons learnt on the project.

Based on the above considerations, early interactions at a project's scoping phase among the geotechnical specialist, other engineers/specialists, the project manager and the contractor will prevent the design of a project element, or even worse the construction of an element, such as alignment or grade, that may require costly foundation treatment later. **It is imperative that good communication and interaction exist among the geotechnical specialist, structural specialist, construction specialist, project manager and contractor throughout the design and the construction process.** Such interactions and involvement are required to insure a cost-effective design and to minimize change orders and contract disputes resulting from design deficiencies and/or misunderstandings during construction. **The importance of communication and interaction is stressed throughout this manual and cannot be overemphasized.**

The flow chart in Figure 1-7 and the six phases identified in Table 1-1 describe the details of geotechnical involvement in a typical project using the design-bid-build (D-B-B) procurement process where the geotechnical specialist interacts with the owner to provide information to the contractor. There are several other procurement processes such as the design-build (D-B) process and the Construction Manager at Risk (CMAR) process. In each such alternative process, the geotechnical specialist is concurrently dealing with both the owners and the contractors, with the geotechnical specialist's direct client being the contractor. Even though the geotechnical involvement is somewhat different in each of these types of procurement processes, it is important to realize that all the items listed in Figure 1-7 as well as in Table 1-1 must be addressed to achieve a successful project.

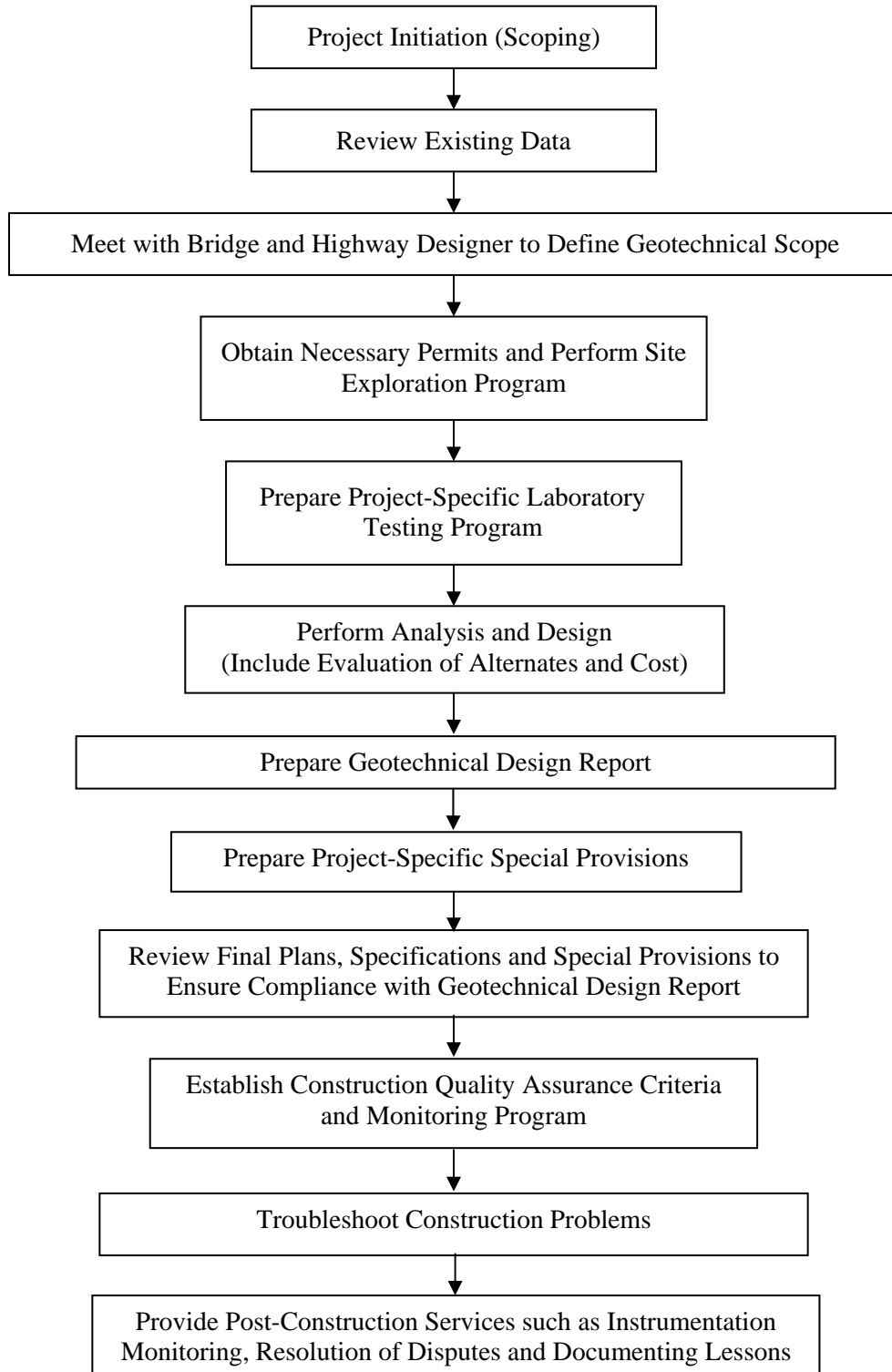


**Figure 1-7. Geotechnical activity flow chart for a typical project using design-bid-build procurement process.**

**Table 1-1  
Geotechnical involvement in project phases**

<b>Phase</b>	<b>Function</b>
<b><u>PHASE 1</u></b> Planning	<ol style="list-style-type: none"> <li>1. Study project information, scope and existing data. (a) USGS topographic sheets. (b) USDA soil maps. (c) groundwater bulletins. (d) air photos.</li> <li>2. Conduct site inspection with project manager. (a) inspect nearby structures for settlement, scour, etc. (b) assess site conditions.</li> <li>3. Prepare terrain reconnaissance report for planning engineer. Include: (a) anticipated soil, rock and water conditions. (b) major problems or costs that will hinder or preclude construction of the facility. (c) right-of-way required for possible special geotechnical treatment. (d) beneficial shifts in alignment.</li> </ol>
<b><u>PHASE 2</u></b> Design Alternatives	<ol style="list-style-type: none"> <li>1. Assess facility locations with regard to major soil issues.</li> <li>2. Provide input for specific uses, e.g., soil/rock scour.</li> <li>3. Implement subsurface exploration and laboratory testing programs after design approval.</li> </ol>
<b><u>PHASE 3</u></b> Prepare Detail Plans	<ol style="list-style-type: none"> <li>1. Review and interpret subsurface information from field and laboratory work.</li> <li>2. Provide preliminary input to bridge/roadway engineer.</li> <li>3. Submit report to bridge and roadway engineer summarizing the investigations along with recommendations. Include: (a) coordination with roadway construction. (b) alternate foundation design. (c) subsurface profile. (d) special provisions and specifications.</li> </ol>
<b><u>PHASE 4</u></b> Final Design	<ol style="list-style-type: none"> <li>1. Review final plans</li> <li>2. Make appropriate adjustments to geotechnical information if necessary</li> </ol>
<b><u>PHASE 5</u></b> Construction	<ol style="list-style-type: none"> <li>1. Provide geotechnical support to the resident engineer during construction. Examples are as follows:  (A) <i>Driven Piles</i>: (a) submit wave equation analysis to bridge engineer. (b) hammer approval. (c) stress analysis. (d) required blow count. (e) special effects, etc.  (B) <i>Drilled Shafts</i>: (a) shaft excavation information, e.g., need for casing or slurry. (b) steel placement tolerances. (c) tube placement for integrity testing. (d) concreting requirements. (e) post-installation integrity tests, etc.  (C) <i>Spread footings</i>: (a) evaluation criteria of stiffness of soils at base of footing excavation, etc.  (D) <i>Retaining Walls</i>: (a) construction process based on whether wall is top-down or bottom-up construction. (b) backfill compaction requirements, etc.  (E) <i>Slopes/Embankments</i>: (a) backfill compaction requirements. (b) final grading of a slope, etc. </li> <li>2. Attend preconstruction meeting with resident engineer and foundation inspector. Explain various important geotechnical issues: (a) general geologic profile. (b) design basis. (c) wave equation analysis for driven piles. (d) end and skin resistance values taking into account strain compatibility for drilled shafts. (e) possible geotechnical problems.</li> <li>3. Troubleshoot soils-related problems as required.</li> <li>4. Assist with structural foundation load tests as required.</li> </ol>
<b><u>PHASE 6</u></b> Post Construction	<ol style="list-style-type: none"> <li>1. Review actual pile results versus predicted. Include: (a) blow count for driven piles. (b) installation methods for drilled shafts. (c) length. (d) field problems. (e) load test capacity.</li> <li>2. Participate in contractor disputes and claims activities.</li> </ol>

### 1.3 ORGANIZATION OF MANUAL

The organization of this manual follows a project-oriented approach whereby a typical bridge project is traced from scoping stage through design computation of settlement, allowable footing pressure, selection of earth retaining structure, to the construction of approach embankments, pile driving or shaft drilling operations, etc. Recommendations are presented on how to layout borings efficiently, how to minimize approach embankment settlement and eliminate the bump at the end of-the bridge, how to design the most cost-effective deep foundation, and how to transmit design information properly to contractors directly through plans, specifications, and special provisions and/or indirectly through contact with the project engineer.

The concepts presented in various chapters are concise and specifically directed at a particular operation in the geotechnical design and construction process. Basic example problems are included in several sections to illustrate how concepts are used and for hands-on knowledge. Continuity between chapters is achieved by sequencing the information in the normal progression of a geotechnical project. In addition, the manual contains an appendix (Appendix A) with the solution to geotechnical issues, in a serialized format, for a highway project involving a bridge and approach embankment over soft ground. In each phase of the fictitious project the geotechnical concepts are developed into specific designs or recommendations for that segment of the problem.

The organization of the manual and a summary of the material presented in each chapter follow.

- Chapter 1 – this chapter (Introduction) presents the purpose and scope of NHI's Soils and Foundation course and provides introductory material about geotechnical activities related to the design and construction aspects of a highway project.
- Chapter 2 (Stress and Strain in Soils) presents basic phase (weight-volume) relationships, effective stress principles, computation of overburden pressures, estimating vertical and horizontal stresses in soils due to external (superimposed) loads on geomaterials.
- Chapter 3 (Subsurface Explorations) presents basic information on subsurface exploration procedures including terrain reconnaissance, subsurface investigation methods, standard penetration test procedures, undisturbed soil sampling, and guidelines for the geotechnical investigation of both roadway and structure sites.

- Chapter 4 (Engineering Description, Classification and Characteristics of Soils and Rocks) discusses the basic engineering characteristics of the main soil and rock groups, and presents procedures for describing and classifying soils and rocks, and for developing a subsurface profile.
- Chapter 5 (Laboratory Testing for Geotechnical Design and Construction) presents several commonly used laboratory tests for soils and rocks including soil classification, basic consolidation and strength testing concepts. This chapter also includes guidelines for laboratory testing on a typical highway project, and a procedure for summarizing and choosing design values from laboratory tests.
- Chapter 6 (Slope Stability) presents the general procedures for the stability analysis of embankments and cut slopes. Basic methods of analysis are shown and explained with emphasis on practical application to highway embankments. Stability charts are presented for a rapid preliminary evaluation of slope stability. Remedial methods are discussed for stability problems.
- Chapter 7 (Approach Roadway Deformations) distinguishes between internal and external settlement within and below embankment fills. Recommendations are provided for select fill and compaction control for soils placed near abutments. Immediate (i.e., short-term) and consolidation (i.e., long-term) settlement, and lateral squeeze are discussed and methods of analysis are presented.
- Chapter 8 (Shallow Foundations) presents the FHWA-recommended foundation design procedure for shallow foundations in soils and rocks. The analysis for both bearing capacity and settlement are discussed and the application of results is presented. Economic considerations of shallow versus deep foundations are discussed.
- Chapter 9 (Deep Foundations) discusses basic concepts in the selection and design of both driven piles and drilled shafts in soils and rocks. Analyses for skin friction and end bearing are addressed for cohesive soil, cohesionless soils and rocks. Foundation installation effects on design are discussed as well as group effects, negative skin friction and deep foundation settlement. The components of pile driving equipment are presented. The use of driving formulae and the wave equation analysis in construction is introduced monitoring. Generic information is presented on the use of load testing. Construction considerations for drilled shafts are also presented.

- Chapter 10 (Earth Retaining Structures) presents the basic lateral earth pressure theories, briefly introduces various wall types, presents a wall classification system, and presents the external stability analysis for a typical fill wall.
- Chapter 11 (Geotechnical Reports) presents outlines for various types of geotechnical reports, discussions on subsurface profiles, guidelines on the use of disclaimers, and suggestions for how to incorporate geotechnical information into contract documents.

## 1.4 REFERENCES

A detailed list of references is provided in Chapter 12. However, certain primary references were used to develop materials for many sections in this document. In addition, FHWA has either developed or is in the process of developing detailed guidance in the topic areas covered in this document. Most of those documents are reference manuals for geotechnical courses developed for the National Highway Institute. Both the FHWA and other primary references are listed below. The reader is directed to the web site for the FHWA National Geotechnical Team (NGT), <http://www.fhwa.dot.gov/engineering/geotech/index.cfm>, to obtain information on all geotechnical publications and software that have been developed by FHWA. The NAVFAC manuals and many other public domain manuals can be downloaded from <http://www.geotechlinks.com>.

### 1.4.1 Primary FHWA References

FHWA (1988). *Checklist and Guidelines for Review of Geotechnical Reports and Preliminary Plans and Specifications*. Report No. FHWA ED-88-053, Federal Highway Administration, U.S. Department of Transportation. Revised 2003.

FHWA (1999). *Drilled Shafts: Construction Procedures and Design Methods*. Report No. FHWA-IF-99-025, Authors: O'Neill, M. W. and Reese, L. C. Federal Highway Administration, U.S. Department of Transportation.

FHWA (2001a). *Soil Slopes and Embankment Design Reference Manual*. Report No. FHWA-NHI-01-026. Authors: Collin, J.G., Hung, J.C., Lee, W.S., and Munfakh, G., Federal Highway Administration, U.S. Department of Transportation.

FHWA (2002a). *Geotechnical Engineering Circular 5 (GEC5) - Evaluation of Soil and Rock Properties*. Report No FHWA-IF-02-034. Authors: Sabatini, P.J, Bachus, R.C,

- Mayne, P.W., Schneider, J.A., Zettler, T.E., Federal Highway Administration, U.S. Department of Transportation.
- FHWA (2002b). *Subsurface Investigations (Geotechnical Site Characterization)*. Report No. FHWA NHI-01-031, Authors: Mayne, P. W., Christopher, B. R., and DeJong, J., Federal Highway Administration, U.S. Department of Transportation.
- FHWA (2002c). *Geotechnical Engineering Circular 6 (GEC6), Shallow Foundations*. Report No. FHWA-SA-02-054, Author: Kimmerling, R.E. 2002, Federal Highway Administration, U.S. Department of Transportation.
- FHWA (2006a). *Design and Construction of Driven Pile Foundations - Vol. I and II*, Report No. FHWA-NHI-05-042 and FHWA-NHI-05-043, Authors: Hannigan, P.J., G.G. Goble, G. Thendean, G.E. Likins and F. Rausche., Federal Highway Administration, U.S. Department of Transportation.
- Geotechnical Engineering Notebook. *FHWA Geotechnical Guidelines GT1 –GT16*.  
<http://www.fhwa.dot.gov/engineering/geotech/index.cfm>.

#### **1.4.2 Other Primary References**

- AASHTO (1988). *Manual on Foundations Investigations, Standard Specifications for Highway Bridges*, American Association of State Highway and Transportation Officials, Washington, D.C.
- AASHTO (2002). *Standard Specifications for Highway Bridges*. 17<sup>th</sup> Edition, American Association of State Highway and Transportation Officials, Washington, D.C.
- AASHTO (2004 with 2006 Interims). *AASHTO LRFD Bridge Design Specifications*, 3rd Edition, American Association of State Highway and Transportation Officials, Washington, D.C.
- AASHTO (2006). *Standard Specifications for Transportation Materials and Methods of Sampling and Testing*, Parts I and II. American Association of State Highway and Transportation Officials, Washington, D.C.
- ASTM (2006). *Annual Book of ASTM Standards – Sections 4.02, 4.08, 4.09 and 4.13*. ASTM International, West Conshohocken, PA.

Holtz, R. D. and Kovacs, W. D. (1981). *An Introduction to Geotechnical Engineering*, Prentice Hall, Englewood Cliffs, NJ.

Lambe, T. W., and Whitman, R. V. (1979). *Soil Mechanics: SI Version*, John Wiley & Sons, Inc., New York, NY.

NAVFAC (1986a). *Design Manual 7.01 - Soil Mechanics*, Department of the Navy, Naval Facilities Engineering Command, Alexandria, VA. (can be downloaded from <http://www.geotechlinks.com>).

NAVFAC (1986b). *Design Manual 7.02 - Foundations & Earth Structures*, Department of the Navy, Naval Facilities Engineering Command, Alexandria, VA. (can be downloaded from <http://www.geotechlinks.com>).

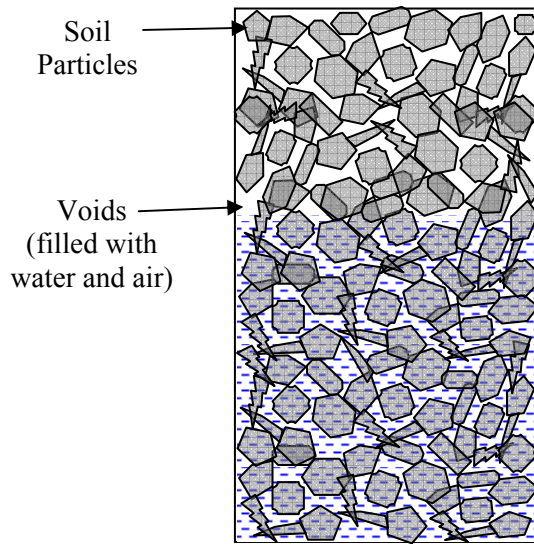
## CHAPTER 2.0 STRESS AND STRAIN IN SOILS

Soil mass is generally a three phase system that consists of solid particles, liquid and gas. The liquid and gas phases occupy the voids between the solid particles as shown in Figure 2-1a. For practical purposes, the liquid may be considered to be water (although in some cases the water may contain some dissolved salts or pollutants) and the gas as air. Soil behavior is controlled by the interaction of these three phases. Due to the three phase composition of soils, complex states of stresses and strains may exist in a soil mass. Proper quantification of these states of stress, and their corresponding strains, is a key factor in the design and construction of transportation facilities.

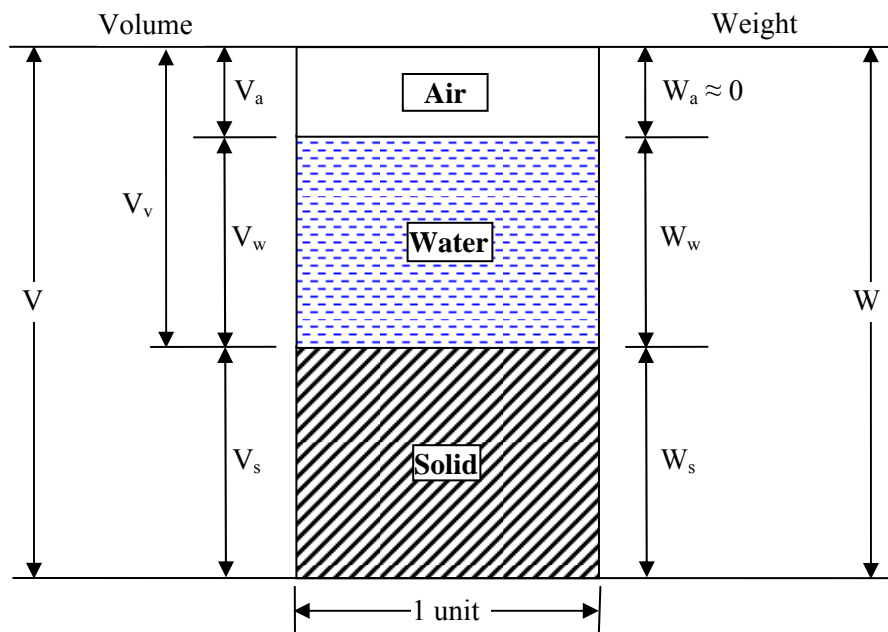
The first step in quantification of the stresses and strains in soils is to characterize the distribution of the three phases of the soil mass and determine their inter-relationships. The inter-relationships of the weights and volumes of the different phases are important since they not only help define the physical make-up of a soil but also help determine the in-situ geostatic stresses, i.e., the states of stress in the soil mass due only to the soil's self-weight. The volumes and weights of the different phases of matter in a soil mass shown in Figure 2-1a can be represented by the block diagram shown in Figure 2-1b. Such a diagram is also known as a phase diagram. A block of unit cross sectional area is considered. The symbols for the volumes and weights of the different phases are shown on the left and right sides of the block, respectively. The symbols for the volumes and weights of the three phases are defined as follows:

- $V_a, W_a$  : volume, weight of air phase. For practical purposes,  $W_a = 0$ .
- $V_w, W_w$  : volume, weight of water phase.
- $V_v, W_v$  : volume, weight of total voids. For practical purposes,  $W_v = W_w$  as  $W_a = 0$ .
- $V_s, W_s$  : volume, weight of solid phase.
- $V, W$  : volume, weight of the total soil mass .

Although  $W_a = 0$  so that  $W_v = W_w$ ,  $V_a$  is generally  $> 0$  and must always be taken into account. Since the relationship between  $V_a$  and  $V_w$  usually changes with groundwater conditions as well as under imposed loads, it is convenient to designate all the volume not occupied by the solid phase as void space,  $V_v$ . Thus,  $V_v = V_a + V_w$ . Use of the terms illustrated in Figure 2-1b, allows a number of basic phase relationships to be defined and/or derived as discussed next.



(a)



(b)

**Figure 2-1. A unit of soil mass and its idealization.**

## 2.1 BASIC WEIGHT-VOLUME RELATIONSHIPS

Various volume change phenomena encountered in geotechnical engineering, e.g., compression, consolidation, collapse, compaction, expansion, etc. can be described by expressing the various volumes illustrated in Figure 2-1b as a function of each other. Similarly, the in-situ stress in a soil mass is a function of depth and the weights of the different soil elements within that depth. This in-situ stress, also known as overburden stress (see Section 2.3), can be computed by expressing the various weights illustrated in Figure 2-1b as a function of each other. This section describes the basic inter-relationships among the various quantities shown in Figure 2-1b.

### 2.1.1 Volume Ratios

A parameter used to express of the volume of the voids in a given soil mass can be obtained from the ratio of the volume of voids,  $V_v$ , to the total volume,  $V$ . This ratio is referred to as **porosity,  $n$** , and is expressed as a percentage as follows:

$$n = \frac{V_v}{V} \times 100 \quad 2-1$$

Obviously, the porosity can never be greater than 100%. As a soil mass is compressed, the volume of voids,  $V_v$ , and the total volume,  $V$ , decrease. Thus, the value of the porosity changes. Since both the numerator and denominator in Equation 2-1 change at the same time, it is difficult to quantify soil compression, e.g., settlement or consolidation, as a function of porosity. Therefore, in soil mechanics the volume of voids,  $V_v$ , is expressed in relation to a quantity, such as the volume of solids,  $V_s$ , that remains unchanging during consolidation or compression. This is done by the introduction of a quantity known as **void ratio,  $e$** , which is expressed in decimal form as follows:

$$e = \frac{V_v}{V_s} \quad 2-2$$

Unlike the porosity, the void ratio can have values greater than 1. That would mean that the soil has more void volume than solids volume, which would suggest that the soil is “loose” or “soft.” Therefore, in general, the smaller the value of the void ratio, the denser the soil. As a practicality, for a given type of coarse-grained soil, such as sand, there is a minimum and maximum void ratio. These values can be used to evaluate the **relative density,  $D_r$  (%)**, of that soil at any intermediate void ratio as follows:

$$D_r = \frac{(e_{\max} - e)}{(e_{\max} - e_{\min})} \times 100 \quad 2-2a$$

At  $e = e_{\max}$  the soil is as loose as it can get and the relative density equals zero. At  $e = e_{\min}$  the soil is as dense as it can get and the relative density equals 100%. Relative density and void ratio are particularly useful index properties since they are general indicators of the relative strength and compressibility of the soil sample, i.e., high relative densities and low void ratios generally indicate strong or incompressible soils; low relative densities and high void ratios may indicate weak or compressible soils.

While the expressions for porosity and void ratio indicate the relative volume of voids, they do not indicate how much of the void space,  $V_v$ , is occupied by air or water. In the case of a saturated soil, all the voids (i.e., soil pore spaces) are filled with water,  $V_v = V_w$ . While this condition is true for many soils below the ground water table or below standing bodies of water such as rivers, lakes, or oceans, and for some fine-grained soils above the ground water table due to capillary action, the condition of most soils above the ground water table is better represented by consideration of all three phases where voids are occupied by both air and water. To express the amount of void space occupied by water as a percentage of the total volume of voids, the term **degree of saturation, S**, is used as follows:

$$S = \frac{V_w}{V_v} \times 100 \quad 2-3$$

Obviously, the degree of saturation can never be greater than 100%. When  $S = 100\%$ , all the void space is filled with water and the soil is considered to be **saturated**. When  $S = 0\%$ , there is no water in the voids and the soil is considered to be **dry**.

### 2.1.2 Weight Ratios

While the expressions of the distribution of voids in terms of volumes are convenient for theoretical expressions, it is difficult to measure these volumes accurately on a routine basis. Therefore, in soil mechanics it is convenient to express the void space in gravimetric, i.e., weight, terms. Since, for practical purposes, the weight of air,  $W_a$ , is zero, a measure of the void space in a soil mass occupied by water can be obtained through an index property known as the **gravimetric water or moisture content, w**, expressed as a percentage as follows:

$$w = \frac{W_w}{W_s} \times 100 \quad 2-4$$

The word “gravimetric” denotes the use of weight as the basis of the ratio to compute water content as opposed to volume, which is often used in hydrology and the environmental sciences to express water content. Since water content is understood to be a weight ratio in geotechnical engineering practice, the word “gravimetric” is generally omitted. Obviously, the water content can be greater than 100%. This occurs when the weight of the water in the soil mass is greater than the weight of the solids. In such cases the void ratio of the soil is generally greater than 1 since there must be enough void volume available for the water so that its weight is greater than the weight of the solids. However, even if the water content is greater than 100%, the degree of saturation may not be 100% because the water content is a weight ratio while saturation is a volume ratio.

For a given amount of soil, the total weight of soil,  $W$ , is equal to  $W_s + W_w$ , since the weight of air,  $W_a$ , is practically zero. The water content,  $w$ , can be easily measured by oven-drying a given quantity of soil to a high enough temperature so that the amount of water evaporates and only the solids remain. By measuring the weight of a soil sample before and after it has been oven dried, both  $W$  and  $W_s$ , can be determined. The water content,  $w$ , can be determined as follows since  $W_a = 0$ :

$$w = \frac{W - W_s}{W_s} = \frac{W_w}{W_s} \times 100 \quad 2-4a$$

Most soil moisture is released at a temperature between 220 and 230°F (105 and 110°C). Therefore, to compare reported water contents on an equal basis between various soils and projects, this range of temperature is considered to be a standard range.

### 2.1.3 Weight-Volume Ratios (Unit Weights) and Specific Gravity

The simplest relationship between the weight and volume of a soil mass (refer to Figure 2-1b) is known as the **total unit weight,  $\gamma_t$** , and is expressed as follows:

$$\gamma_t = \frac{W}{V} = \frac{W_w + W_s}{V} \quad 2-5$$

The total unit weight of a soil mass is a useful quantity for computations of vertical in-situ stresses. For a constant volume of soil, the total unit weight can vary since it does not

account for the distribution of the three phases in the soil mass. Therefore the value of the total unit weight for a given soil can vary from its maximum value when all of the voids are filled with water (S=100%) to its minimum value when there is no water in the voids (S=0%). The former value is called the **saturated unit weight**,  $\gamma_{\text{sat}}$ ; the latter value is referred to as the **dry unit weight**,  $\gamma_{\text{d}}$ . In terms of the basic quantities shown in Figure 2-1b and with reference to Equation 2-5, when  $W_w = 0$  the **dry unit weight**,  $\gamma_{\text{d}}$ , can be expressed as follows:

$$\gamma_{\text{d}} = \frac{W_{\text{s}}}{V} \quad 2-6$$

For computations involving soils below the water table, the buoyant unit weight is frequently used where:

$$\gamma_{\text{b}} = \gamma_{\text{sat}} - \gamma_{\text{w}} \quad 2-7$$

where,  $\gamma_{\text{w}}$  equals the unit weight of water and is defined as follows:

$$\gamma_{\text{w}} = \frac{W_{\text{w}}}{V_{\text{w}}} \quad 2-8$$

In the geotechnical literature, the buoyant unit weight,  $\gamma_{\text{b}}$ , is also known as the effective unit weight,  $\gamma'$ , or submerged unit weight,  $\gamma_{\text{sub}}$ . Unless there is a high concentration of dissolved salts, e.g., in sea water, the unit weight of water,  $\gamma_{\text{w}}$ , can be reasonably assumed to be 62.4 lb/ft<sup>3</sup> (9.81 kN/m<sup>3</sup>).

To compare the properties of various soils, it is often instructive and preferable to index the various weights and volumes to unchanging quantities, which are the volume of solids,  $V_{\text{s}}$ , and the weight of solids,  $W_{\text{s}}$ . A ratio of  $W_{\text{s}}$  to  $V_{\text{s}}$ , is known as the unit weight of the solid phase,  $\gamma_{\text{s}}$ , and is expressed as follows:

$$\gamma_{\text{s}} = \frac{W_{\text{s}}}{V_{\text{s}}} \quad 2-9$$

The unit weight of the solid phase,  $\gamma_{\text{s}}$ , should not be confused with the dry unit weight of the soil mass,  $\gamma_{\text{d}}$ , which is defined in Equation 2-6 as the total unit weight of the soil mass when there is no water in the voids, i.e., at S = 0%. The distinction between  $\gamma_{\text{s}}$  and  $\gamma_{\text{d}}$  is very subtle,

but it is very important and should not be overlooked. For example, for a solid piece of rock (i.e., no voids) the total unit weight is  $\gamma_s$  while the total unit weight of a soil whose voids are dry is  $\gamma_d$ . In geotechnical engineering,  $\gamma_d$  is more commonly of interest than  $\gamma_s$ .

Since the value of  $\gamma_w$  is reasonably well known, the unit weight of solids,  $\gamma_s$ , can be expressed in terms of  $\gamma_w$ . The concept of **Specific Gravity, G**, is used to achieve this goal. In physics textbooks, G is defined as the ratio between the mass density of a substance and the mass density of some reference substance. Since unit weight is equal to mass density times the gravitational constant, G can also be expressed as the ratio between the unit weight of a substance and the unit weight of some reference substance. In the case of soils, the most convenient reference substance is water since it is one of the three phases of the soil and its unit weight is reasonably constant. Using this logic, the **specific gravity of the soil solids**,  $G_s$ , can be expressed as follows:

$$G_s = \frac{\gamma_s}{\gamma_w} \quad 2-10$$

The **bulk specific gravity of a soil** is equal to  $\gamma_t / \gamma_w$ . The “bulk specific gravity” is not the same as  $G_s$  and is not very useful in practice since the  $\gamma_t$  of a soil can change easily with changes in void ratio and/or degree of saturation. Therefore, the bulk specific gravity is almost never used in geotechnical engineering computations.

The value of  $G_s$  can be determined in the laboratory, but it can usually be estimated with sufficient accuracy for various types of soil solids. For routine computations, the value of  $G_s$  for sands composed primarily of quartz particles may be taken as 2.65. Tests on a large number of clay soils indicate that the value of  $G_s$  for clays usually ranges from 2.5 to 2.9 with an average value of 2.7.

#### 2.1.4 Determination and Use of Basic Weight-Volume Relations

The five relationships,  $n$ ,  $e$ ,  $w$ ,  $\gamma_t$  and  $G_s$ , represent the basic weight-volume properties of soils and are used in the classification of soils and for the development of other soil properties. These properties and how they are obtained and applied in geotechnical engineering are summarized in Table 2-1. A summary of commonly used weight-volume (unit weight) relations that incorporate these terms is presented in Table 2-2.

**Table 2-1**  
**Summary of index properties and their application**

Property	Symbol	Units <sup>1</sup>	How Obtained (AASHTO/ASTM)	Comments and Direct Applications
Porosity	n	Dim	From weight-volume relations	Defines relative volume of voids to total volume of soil
Void Ratio	e	Dim	From weight-volume relations	Volume change computations
Moisture Content	w	Dim	By measurement (T 265/ D 4959)	Classification and in weight-volume relations
Total unit weight <sup>2</sup>	$\gamma_t$	FL <sup>-3</sup>	By measurement or from weight-volume relations	Classification and for pressure computations
Specific Gravity	$G_s$	Dim	By measurement (T 100/D 854)	Volume computations

NOTES:

1 F=Force or weight; L = Length; Dim = Dimensionless. Although by definition, moisture content is a dimensionless decimal (ratio of weight of water to weight of solids) and used as such in most geotechnical computations, it is commonly reported in percent by multiplying the decimal by 100.

2 Total unit weight for the same soil can vary from “saturated” (S=100%) to “dry” (S=0%).

**Table 2-2**  
**Weight-volume relations (after Das, 1990)**

Unit-Weight Relationship	Dry Unit Weight (No Water)	Saturated Unit Weight (No Air)
$\gamma_t = \frac{(1+w)G_s\gamma_w}{1+e}$	$\gamma_d = \frac{\gamma_t}{1+w}$	$\gamma_{sat} = \frac{(G_s+e)\gamma_w}{1+e}$
$\gamma_t = \frac{(G_s+Se)\gamma_w}{1+e}$	$\gamma_d = \frac{G_s\gamma_w}{1+e}$	$\gamma_{sat} = [(1-n)G_s+n]\gamma_w$
$\gamma_t = \frac{(1+w)G_s\gamma_w}{1+\frac{wG_s}{S}}$	$\gamma_d = G_s\gamma_w(1-n)$	$\gamma_{sat} = \left(\frac{1+w}{1+wG_s}\right)G_s\gamma_w$
$\gamma_t = G_s\gamma_w(1-n)(1+w)$	$\gamma_d = \frac{G_s\gamma_w}{1+\frac{wG_s}{S}}$	$\gamma_{sat} = \left(\frac{e}{w}\right)\left(\frac{1+w}{1+e}\right)\gamma_w$
	$\gamma_d = \frac{eS\gamma_w}{(1+e)w}$	$\gamma_{sat} = \gamma_d + n\gamma_w$
	$\gamma_d = \gamma_{sat} - n\gamma_w$	$\gamma_{sat} = \gamma_d + \left(\frac{e}{1+e}\right)\gamma_w$
	$\gamma_d = \gamma_{sat} - \left(\frac{e}{1+e}\right)\gamma_w$	

In above relations,  $\gamma_w$  refers to the unit weight of water, 62.4 pcf (=9.81 kN/m<sup>3</sup>).

### 2.1.5 Size of Grains in the Solid Phase

As indicated in Figure 2-1a, the solid phase is composed of soil grains. One of the major factors that affect the behavior of the soil mass is the size of the grains. The size of the grains may range from the coarsest (e.g., boulders, which can be 12- or more inches [300 mm] in diameter) to the finest (e.g., colloids, which can be smaller than 0.0002–inches [0.005 mm]). Since soil particles come in a variety of different shapes, the size of the grains is defined in terms of an effective grain diameter. The distribution of grain sizes in a soil mass is determined by shaking air-dried material through a stack of sieves having decreasing opening sizes. Table 2-3 shows U.S. standard sieve sizes and associated opening sizes. **Sieves with opening size 0.25 in (6.35 mm) or less are identified by a sieve number which corresponds to the approximate number of square openings per linear inch of the sieve (ASTM E 11).**

To determine the grain size distribution, the soil is sieved through a stack of sieves with each successive screen in the stack from top to bottom having a smaller (approximately half of the upper sieve) opening to capture progressively smaller particles. Figure 2-2 shows a selection of some sieves and starting from right to left soil particles retained on each sieve, except for the powdery particles shown on the far left, which are those that passed through the last sieve on the stack. The amount retained on each sieve is collected, dried and weighed to determine the amount of material passing that sieve size as a percentage of the total sample being sieved. Since electro-static forces impede the passage of finer-grained particles through sieves, testing of such particles is accomplished by suspending the chemically dispersed particles in a water column and measuring the change in specific gravity of the liquid as the particles fall from suspension. The change in specific gravity is related to the fall velocities of specific particle sizes in the liquid. This part of the test is commonly referred to as a hydrometer analysis. Because of the strong influence of electro-chemical forces on their behavior, colloidal sized particles may remain in suspension indefinitely (particles with sizes from  $10^{-3}$  mm to  $10^{-6}$  mm are termed “**colloidal**.”) Sample grain size distribution curves are shown in Figure 2-3. The nomenclature associated with various grain sizes (cobble, gravel, sand, silt or clay) is also shown in Figure 2-3. Particles having sizes larger than the No. 200 sieve (0.075 mm) are termed “**coarse-grained**” while those with sizes finer than the No. 200 sieve are termed “**fine-grained**.”

The results of the sieve and hydrometer tests are represented graphically on a grain size distribution curve or gradation curve. As shown in Figure 2-3, an arithmetic scale is used on the ordinate (Y-axis) to plot the percent finer by weight and a logarithmic scale is used on the abscissa (X-axis) for plotting particle (grain) size, which is typically expressed in millimeters.

**Table 2-3**

**U.S. standard sieve sizes and corresponding opening dimension**

U.S. Standard Sieve No. <sup>1</sup>	Sieve Opening (in)	Sieve Opening (mm)	Comment (Based on the Unified Soil Classification System (USCS) discussed in Chapter 4)
3	0.2500	6.35	
4	0.1870	4.75	<ul style="list-style-type: none"> <li>• Breakpoint between fine gravels and coarse sands</li> <li>• Soil passing this sieve is used for compaction test</li> </ul>
6	0.1320	3.35	
8	0.0937	2.36	
10	0.0787	2.00	<ul style="list-style-type: none"> <li>• Breakpoint between coarse and medium sands</li> </ul>
12	0.0661	1.70	
16	0.0469	1.18	
20	0.0331	0.850	
30	0.0234	0.600	
40	0.0165	0.425	<ul style="list-style-type: none"> <li>• Breakpoint between medium and fine sands</li> <li>• Soil passing this sieve is used for Atterberg limits</li> </ul>
50	0.0117	0.300	
60	0.0098	0.250	
70	0.0083	0.212	
100	0.0059	0.150	
140	0.0041	0.106	
200	0.0029	0.075	<ul style="list-style-type: none"> <li>• Breakpoint between fine sand and silt or clay</li> </ul>
270	0.0021	0.053	
400	0.0015	0.038	

**Note:**

- The sieve opening sizes for various sieve numbers listed above are based on Table 1 from ASTM E 11. Sieves with opening size greater than No. 3 are identified by their opening size. Some of these sieves are as follows:

4.0 in (101.6 mm)	1-1/2 in (38.1 mm)	1/2 in (12.7 mm)
3.0 in (76.1 mm)*	1-1/4 in (32.0 mm)	3/8 in (9.5 mm)
2-1/2 in (64.0 mm)	1.0 in (25.4 mm)	5/16 in (8.0 mm)
2.0 in (50.8 mm)	3/4 in (19.0 mm)**	
1-3/4 in (45.3 mm)	5/8 in (16.0 mm)	

\* The 3 in (76.1 mm) sieve size differentiates between cobbles and coarse gravels.

\*\*The 3/4 in (19 mm) sieve differentiates between coarse and fine gravels.



**Figure 2-2. Example of laboratory sieves for mechanical analysis for grain size distributions.** Shown (right to left) are sieve nos. 3/8-in (9.5-mm), No. 10 (2.0-mm), No. 40 (0.425 mm) and No. 200 (0.075 mm). Example soil particle sizes shown at the bottom of the photo include (right to left): medium gravel, fine gravel, medium-coarse sand, silt, and clay (kaolin) (FHWA, 2002b).

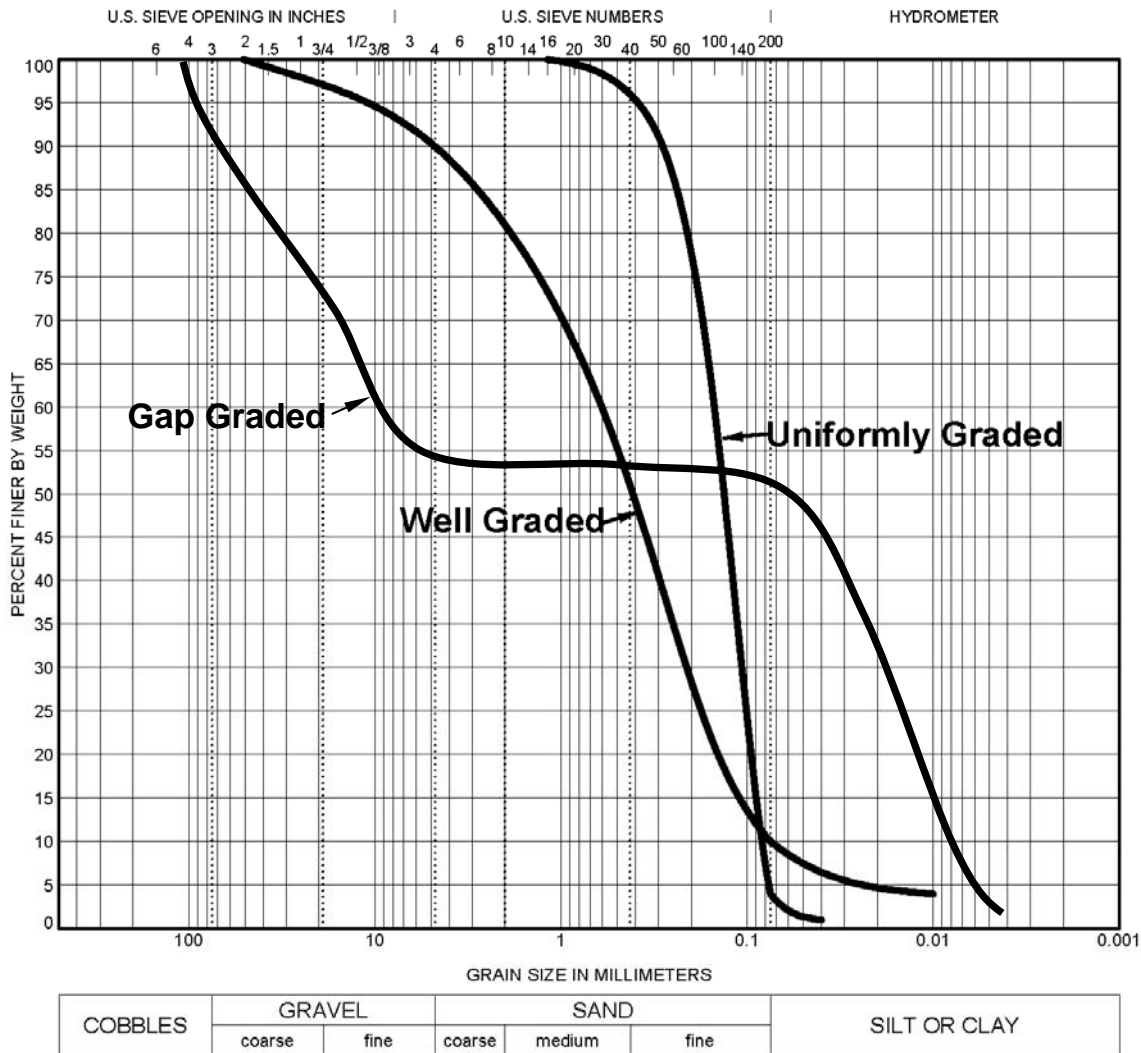


**Figure 2-3. Sample grain size distribution curves.**

The logarithmic scale permits a wide range of particle sizes to be shown on a single plot. More importantly it extends the scale, thus giving all the grains sizes an approximately equal amount of separation on the X-axis. For example, a grain-size range of 4.75 mm (No.4 sieve) to 0.075 mm (No. 200 sieve) when plotted on an arithmetic scale, will have the 0.075 mm (No. 200 sieve), 0.105 mm (No. 140 sieve), and 0.150 mm (No. 100) particle size plot very close to each other. The logarithmic scale permits separation of grain sizes that makes it easier to compare the grain size distribution of various soils.

The shape of the grain size distribution curve is somewhat indicative of the particle size distribution as shown in Figure 2-3. For example,

- A smooth curve covering a wide range of sizes represents a *well-graded* or *non-uniform* soil.
- A vertical or near vertical slope over a relatively narrow range of particle sizes indicates that the soil consists predominantly of the particle sizes within that range of particle sizes. A soil consisting of particles having only a few sizes is called a *poorly-graded* or *uniform* soil.
- A curve that contains a horizontal or nearly horizontal portion indicates that the soil is deficient in the grain sizes in the region of the horizontal slope. Such a soil is called a *gap-graded* soil.

Well-graded soils are generally produced by bulk transport processes (e.g., glacial till). Poorly graded soils are usually sorted by the transporting medium e.g., beach sands by water; loess by wind. Gap-graded soils are also generally sorted by water, but certain sizes were not transported.

### **2.1.6 Shape of Grains in Solid Phase**

The shape of individual grains in a soil mass plays an important role in the engineering characteristics (strength and stability) of the soil. Two general shapes are normally recognized, bulky and platy.

#### **2.1.6.1 Bulky Shape**

Cobbles, gravel, sand and some silt particles cover a large range of sizes as shown in Figure 2-2; however, they are all bulky in shape. The term bulky is confined to particles that are relatively large in all three dimensions, as contrasted to platy particles, in which one dimension is small as compared to the other two, see Figure 2-4. The bulky shape has five subdivisions listed in descending order of desirability for construction

- *Angular* particles are those that have been freshly broken up and are characterized by jagged projections, sharp ridges, and flat surfaces. Angular gravels and sands are generally the best materials for construction because of their interlocking characteristics. Such particles are seldom found in nature, however, because physical and chemical weathering processes usually wear off the sharp ridges in a relatively short period time. Angular material is usually produced artificially, by crushing.

- *Subangular* particles are those that have been weathered to the extent that the sharper points and ridges have been worn off.
- *Subrounded* particles are those that have been weathered to a further degree than subangular particles. They are still somewhat irregular in shape but have no sharp corners and few flat areas. Materials with this shape are frequently found in stream beds. If composed of hard, durable particles, subrounded material is adequate for most construction needs.
- *Rounded* particles are those on which all projections have been removed, with few irregularities in shape remaining. The particles resemble spheres and are of varying sizes. Rounded particles are usually found in or near stream beds or beaches.
- *Well rounded* particles are rounded particles in which the few remaining irregularities have been removed. Like rounded particles, well rounded particles are also usually found in or near stream beds or beaches.

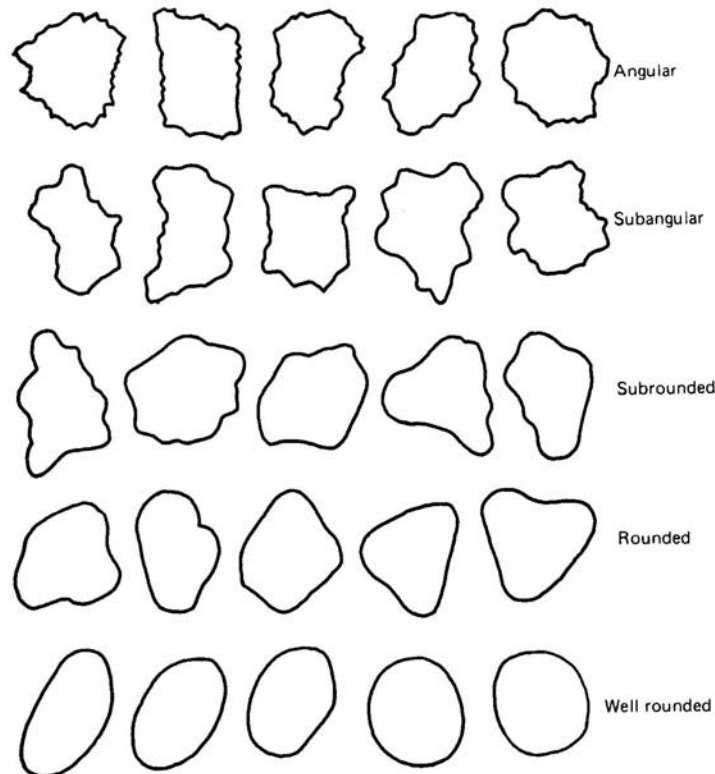


**Figure 2-4. Terminology used to describe shape of coarse-grained soils (Mitchell, 1976).**

### 2.1.6.2 Platy Shape

Platy, or flaky, particles are those that have flat, plate like grains. Clay and some silts are common examples. Because of their shape, flaky particles have a greater surface area than bulky particles, assuming that the weights and volumes of the two are the same. For example, 1 gram of bentonite (commercial name for montmorillonite clay) has a surface area of approximately 950 yd<sup>2</sup> (800 m<sup>2</sup>) compared to a surface area of approximately 0.035 yd<sup>2</sup> (0.03 m<sup>2</sup>) of 1 gram of sand. Because of their mineralogical composition and greater specific surface area, most flaky particles also have a greater affinity for water than bulky particles. Due to the high affinity of such soils for water, the physical states of such fine-grained soils change with the amount of water in these soils. The effect of water on the physical states of fine grained soils is discussed next.

### 2.1.7 Effect of Water on Physical States of Soils

For practical purposes, the two most dominant phases are the solid phase and the water phase. It is intuitive that as the water content increases, the contacts between the particles comprising the solid phase will be “lubricated.” If the solid phase is comprised of coarse particles, e.g. coarse sand or gravels, then water will start flowing between the particles of the solid phase. If the solid phase is comprised of fine-grained particles, e.g., clay or silt, then water cannot flow as freely as in the coarse-grained solid phase because pore spaces are smaller and solids react with water. However, as the water content increases even the fine-grained solid phase will conduct water and under certain conditions the solid phase itself will start deforming like a viscous fluid, e.g., like a milk shake or a lava flow. The mechanical transformation of the fine-grained soils from a solid phase into a viscous phase is a very important concept in geotechnical engineering since it is directly related to the load carrying capacity of soils. It is obvious that the load carrying capacity of a solid is greater than that of water. Since water is contained in the void space, the effect of water on the physical states of fine-grained soils is important. Some of the basic index properties related to the effect of water are described next.

The physical and mechanical behavior of fine-grained-soils is linked to four distinct states: solid, semi-solid, plastic and viscous liquid in order of increasing water content. Consider a soil initially in a viscous liquid state that is allowed to dry uniformly. This state is shown as Point A in Figure 2-5, which shows a plot of total volume versus water content. As the soil dries, its water content reduces and consequently so does its total volume as the solid particles move closer to each other. As the water content reduces, the soil can no longer flow like a viscous liquid. Let us identify this state by Point B in Figure 2-5. The water content at Point B is known as the “Liquid Limit” in geotechnical engineering and is denoted by LL.

As the water content continues to reduce due to drying, there is a range of water content at which the soil can be molded into any desired shape without rupture. In this range of water content, the soil is considered to be “plastic.”

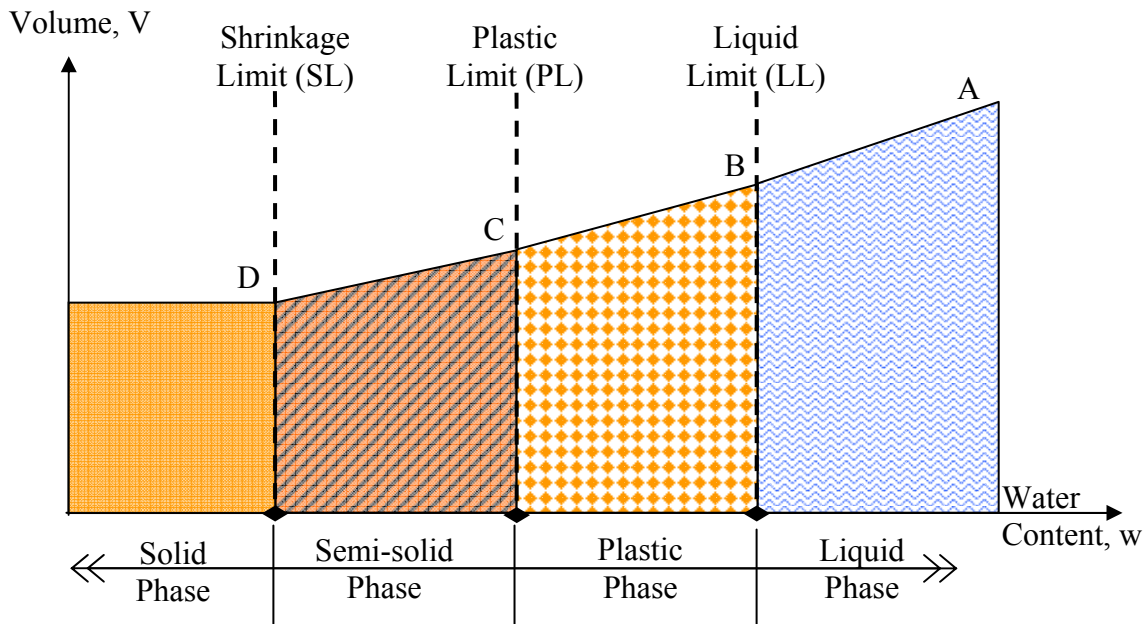


**Figure 2-5. Conceptual changes in soil phases as a function of water content.**

If the soil is allowed to dry beyond the plastic state, the soil cannot be molded into any shape without showing cracks, i.e., signs of rupture. The soil is then in a semi-solid state. The water content at which cracks start appearing when the soil is molded is known as the “Plastic Limit.” This moisture content is shown at Point C in Figure 2-5 and is denoted by PL. The difference in water content between the Liquid Limit and Plastic Limit, is known as the **Plasticity Index**, PI, and is expressed as follows:

$$PI = LL - PL \quad 2-11$$

Since PI is the difference between the LL and PL, it denotes the range in water content over which the soil acts as a plastic material as shown in Figure 2-5.

As the soil continues to dry, it will be reduced to its basic solid phase. The water content at which the soil changes from a semi-solid state to a solid state is called the **Shrinkage Limit**, SL. No significant change in volume will occur with additional drying below the shrinkage limit. The shrinkage limit is useful for the determination of the swelling and shrinkage characteristics of soils.

The liquid limit, plastic limit and shrinkage limit are called Atterberg limits after A. Atterberg (1911), the Swedish soil scientist who first proposed them for agricultural applications.

For foundation design, engineers are most interested in the load carrying capacity, i.e., strength, of the soil and its associated deformation. The soil has virtually no strength at the LL, while at water contents lower than the PL (and certainly below the SL) the soil may have considerable strength. Correspondingly, soil strength increases and soil deformation decreases as the water content of the soil reduces from the LL to the SL. Since the Atterberg limits are determined for a soil that is remolded, a connection needs to be made between these limits and the in-situ moisture content,  $w$ , of the soil for the limits to be useful in practical applications in foundation design. One way to quantify this connection is through the **Liquidity Index**, LI, that is given by:

$$LI = \frac{w - PL}{PI} \quad 2-12$$

The liquidity index is the ratio of the difference between the soil's in-situ water content and plastic limit to the soil's plasticity index. The various phases shown in Figure 2-5 and anticipated deformation behavior can now be conveniently expressed in terms of LI as shown in Table 2-4.

**Table 2-4**  
**Concept of soil phase, soil strength and soil deformation based on Liquidity Index**

<b>Liquidity Index, LI</b>	<b>Soil Phase</b>	<b>Soil Strength (Soil Deformation)</b>
$LI \geq 1$	Liquid	Low strength (Soil deforms like a viscous fluid)
$0 < LI < 1$	Plastic	Intermediate strength <ul style="list-style-type: none"> <li>• at <math>w \approx LL</math>, the soil is considered soft and very compressible</li> <li>• at <math>w \approx PL</math>, the soil is considered stiff</li> </ul> (Soil deforms like a plastic material)
$LI \leq 0$	Semi-solid to Solid	High strength (Soil deforms as a brittle material, i.e., sudden, fracture of material)

Another valuable tool in assessing the characteristics of a fine-grained soil is to compare the LL and PI of various soils. Each fine-grained soil has a relatively unique value of LL and PI. A plot of PI versus LL is known as the **Plasticity Chart** (see Figure 2-6). Arthur Casagrande, who developed the concept of the Plasticity Chart, had noted the following during the First Pan American Conference on Soil Mechanics and Foundation Engineering (Casagrande, 1959).

*I consider it essential that an experienced soils engineer should be able to judge the position of soils, from his territory, on a plasticity chart merely on the basis of his visual and manual examination of the soils. And more than that, the plasticity chart should be for him like a map of the world. At least for certain areas of the chart, that are significant for his activities, he should be well familiar. The position of soils within these areas should quickly convey to him a picture of the significant engineering properties that he should expect.*

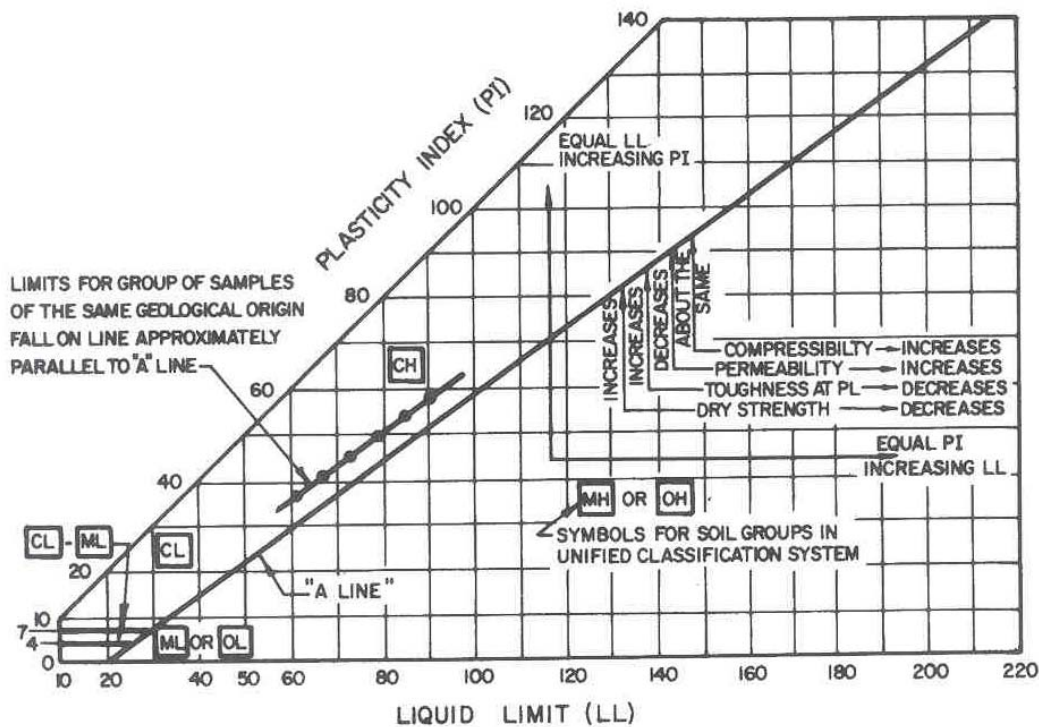


**Figure 2-6. Plasticity chart and significance of Atterberg Limits (NAVFAC, 1986a).**

Casagrande proposed the inclusion of the A-line on the plasticity chart as a boundary between clay (above the A-line) and silt (below the A-line) to help assess the engineering characteristics of fine-grained soils. Once PI and LL are determined for a fine-grained soil at a specific site, a point can be plotted on the plasticity chart that will allow the engineer to develop a feel for the general engineering characteristics of that particular soil. The plasticity

chart also permits the engineer to compare different soils across the project site and even between different project sites. (The symbols for soil groups such as CL and CH are discussed later in this manual.) The plasticity chart, including the laboratory determination of the various limits (LL, PL and SL), are discussed further in Chapters 4 and 5. Additional useful terms such as “Activity Ratio” that relate the PI to clay fraction are also introduced in Chapter 5.

## 2.2 PRINCIPLE OF EFFECTIVE STRESS

The contacts between soil grains are effective in resisting applied stresses in a soil mass. Under an applied load, the total stress in a saturated soil sample is composed of the intergranular stress and the pore water pressure. When pore water drains from a soil, the contact between the soil grains increases, which increases the level of intergranular stress. This intergranular contact stress is called the **effective stress**. **The effective stress,  $p_o$ , within a soil mass is the difference between the total stress,  $p_t$ , and pore water pressure,  $u$ .** The **principle of effective stress** is a fundamental aspect of geotechnical engineering and is written as follows:

$$p_o = p_t - u \qquad 2-13$$

In general, soil deposits below the ground water table will be considered saturated and the ambient pore water pressure at any depth may be computed by multiplying the unit weight of water,  $\gamma_w$ , by the height of water above that depth. The total stress at that depth may be found by multiplying the total unit weight of the soil by the depth. The effective stress is the total stress minus the pore water pressure. This concept is used to construct the profile of pressure in the ground as a function of depth and is discussed next.

## 2.3 OVERBURDEN PRESSURE

Soils existing at a distance below ground are affected by the weight of the soil above that depth. The influence of this weight, known generally as **overburden**, causes a state of stress to exist, which is unique at that depth, for that soil. This state of stress is commonly referred to as the **overburden** or **in-situ** or **geostatic state of stress**. When a soil sample is removed from the ground, as during the field exploration phase of a project, that in-situ state of stress is relieved as all confinement of the sample has been removed. In laboratory testing, it is important to reestablish the in-situ stress conditions and to study changes in soil properties when additional stresses representing the expected design loading are applied. The stresses

to be used during laboratory testing of soil samples are estimated from either the total or effective overburden pressure. The engineer's first task is determining the total and effective overburden pressure variation with depth. This relatively simple task involves estimating the average total unit weight for each soil layer in the soil profile, and determining the depth of the water table. Unit weight may be reasonably well estimated from tests on undisturbed samples or from standard penetration N-values and visual soil identification. The water table depth, which is typically recorded on boring logs, can be used to compute the hydrostatic pore water pressure at any depth. The **total overburden pressure,  $p_t$** , is found by multiplying the total unit weight of each soil layer by the corresponding layer thickness and continuously summing the results with depth. The **effective overburden pressure,  $p_o$** , at any depth is determined by accumulating the weights of all layers above that depth with consideration of the water level conditions at the site as follows:

#### Soils above the water table

- Multiply the total unit weight by the thickness of each respective soil layer above the desired depth, i.e.,  $p_o = p_t$ .

#### Soils below the ground water table

- Compute pore water pressure  $u$  as  $z_w \gamma_w$  where  $z_w$  is the depth below ground water table and  $\gamma_w$  is the unit weight of water
- To obtain effective overburden pressure,  $p_o$ , subtract pore water pressure,  $u$ , from  $p_t$
- For soils below the ground water table,  $p_t$  is generally assumed to be equal to  $p_{sat}$

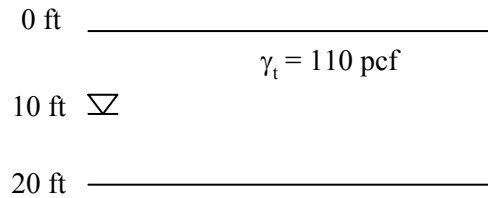
Alternatively, the following approach can be used:

- Reduce the total unit weights of soils below the ground water table by the unit weight of water (62.4 pcf (9.8 kN/m<sup>3</sup>)), i.e., use effective unit weights,  $\gamma'$ , and multiply by the thickness of each respective soil layer between the water table and the desired depth below the ground water table, i.e.,  $p_o = (\gamma_t - \gamma_w) (\text{depth})$ , or  $\gamma' (\text{depth})$ .

In the geotechnical literature, the effective unit weight,  $\gamma'$ , is also known as the buoyant unit weight or submerged unit weight and symbols,  $\gamma_b$  or  $\gamma_{sub}$ , respectively are used.

An example is solved in Figure 2-7.

**Example 2-1:** Find  $p_o$  at 20 ft below ground in a sand deposit with a total unit weight of 110 pcf and the water table 10 ft below ground. Assume  $\gamma_t = \gamma_{sat}$ . Plot  $p_t$  and  $p_o$  versus depth from 0 ft – 20 ft.



**Solution:**

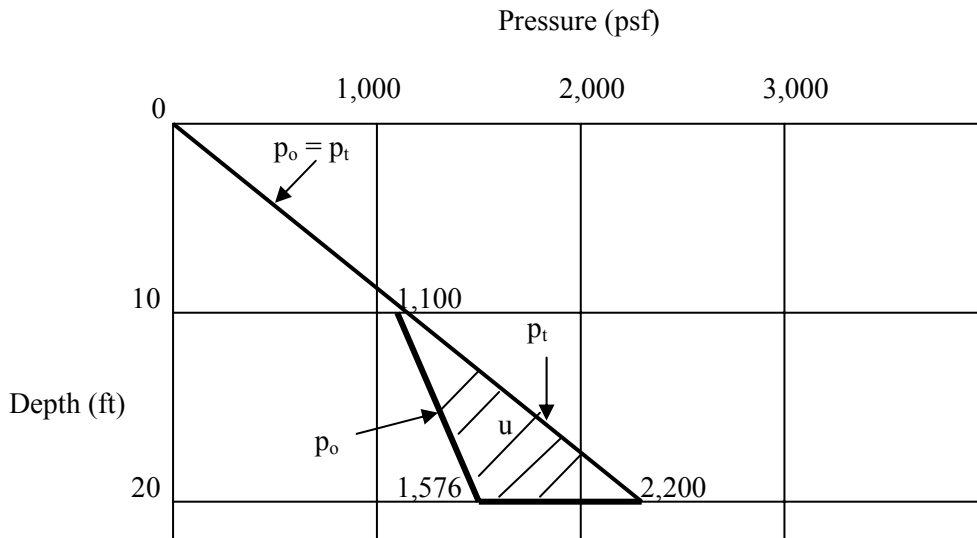
From Equation 2-13,  $p_o = p_t - u$

$$p_t @ 10 \text{ ft} = p_o @ 10 \text{ ft} = 10 \text{ ft} \times 110 \text{ pcf} = 1,100 \text{ psf}$$

$$p_t @ 20 \text{ ft} = p_t @ 10 \text{ ft} + (10 \text{ ft} \times 110 \text{ pcf}) = 2,200 \text{ psf}$$

$$u @ 20 \text{ ft} = 10 \text{ ft} \times 62.4 \text{ pcf} = 624 \text{ psf}$$

$$p_o @ 20 \text{ ft} = p_t @ 20 \text{ ft} - u @ 20 \text{ ft} = 2,200 \text{ psf} - 624 \text{ psf} = 1,576 \text{ psf}$$



**Pressure Diagram**

A plot of effective overburden pressure versus depth is called a “ $p_o$  – diagram” and is used throughout all aspects of geotechnical testing and analysis.

**Figure 2-7. Example calculation of a  $p_o$ -diagram.**

## 2.4 VERTICAL STRESS DISTRIBUTION IN SOIL DUE TO EXTERNAL LOADINGS

When a load is applied to the soil surface, it increases the vertical and lateral stresses within the soil mass. The increased stresses are greatest directly under the loaded area and dissipate within the soil mass as a function of distance away from the loaded area. This is commonly called spatial attenuation of applied loads. A schematic of the vertical stress distribution with depth along the centerline under an embankment of height,  $h$ , constructed with a soil having total unit weight,  $\gamma_t$ , is shown in Figure 2-8.

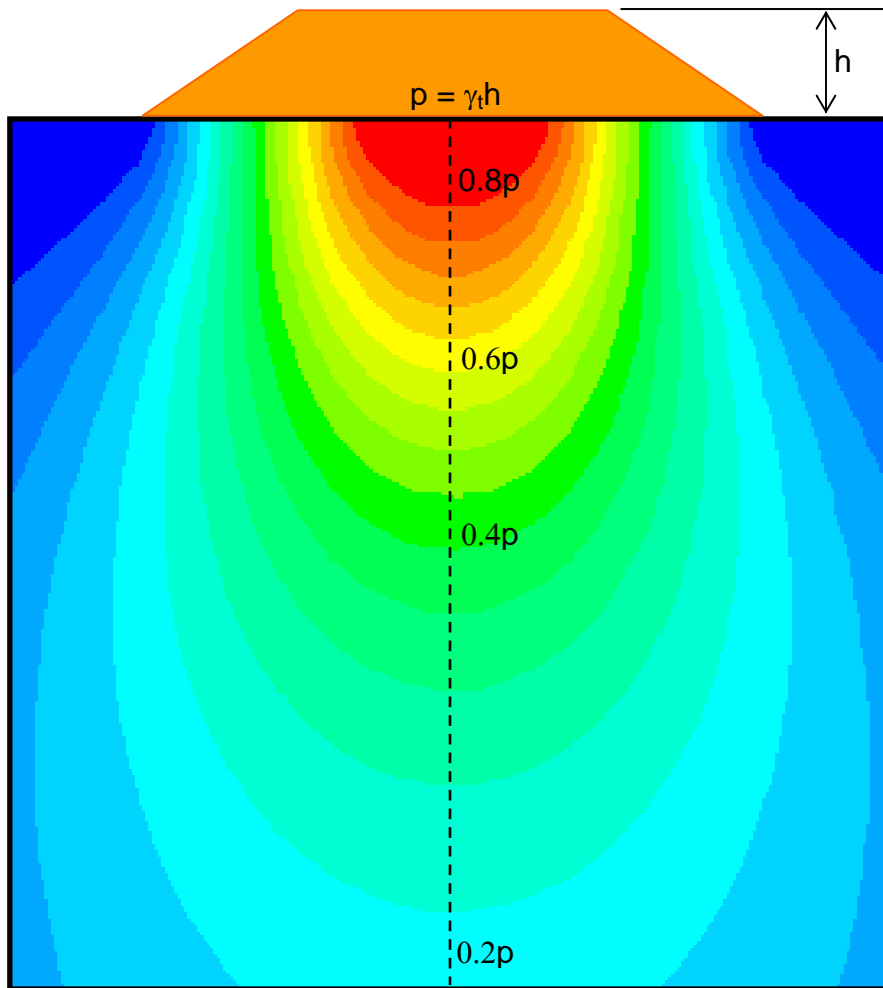


**Figure 2-8. Schematic of vertical stress distribution under embankment loading.  
Graphic generated by FoSSA (2003) program.**

**(Note: Version 1.0 of FoSSA program is licensed to FHWA. See Appendix E for a brief overview of the FoSSA program).**

Estimation of vertical stresses at any point in a soil mass due to external loadings are of great significance in the prediction of volume change of soils (e.g., settlement) under buildings, bridges, embankments and many other structures. The computation of the total vertical stress change induced by an external loading will depend on the configuration of the external loads. Common examples of the external loads are as follows:

- Uniform strip loads such as the load on a long wall footing of sufficient width,
- Uniformly loaded square, rectangular or circular footings such as column footings of buildings, pier footings, footings for water tanks, mats, etc., and
- Triangular and/or trapezoidal strip loads such as the loads of long earth embankments.

The theory of elasticity is often used to compute the stresses induced within a soil mass by external loadings. The most widely used elastic formulae were first developed by Boussinesq (1885) for point loads acting at the surface of a semi-infinite elastic half-space. These formulae, often known as **Boussinesq solutions**, can be integrated to give stresses below external loadings acting on a finite area. The basic assumptions in these formulae are (a) the stress is proportional to strain, (b) the soil is homogeneous (i.e., the properties are constant throughout the soil mass), and (c) the soil is isotropic (i.e., the properties are the same in all directions through a point). Westergaard (1938) modified the Boussinesq solutions by assuming that the semi-infinite elastic half-space is interspersed with infinitely thin but perfectly rigid layers that allow vertical movement but no lateral movement. In reality, a soil mass never fulfills the assumptions of either of these idealized solutions. Nevertheless, these elastic solutions, with appropriate modifications and judgment, have been found to yield acceptable approximate estimates of stresses in the soil mass and are widely used in geotechnical engineering practice. The Boussinesq solutions are generally used in most situations, even those where layered soils are encountered provided the thickness of the layers is on the order of a few feet or more. On the other hand, the Westergaard solutions are usually used for varved clays where the predominant soil mass is clay interspersed with thin layers of sand whose thickness is on the order of inches.

The derivations of the equations for various common loadings cited above are tedious. They are omitted in this manual so that the reader can concentrate on the use of published solutions, generally in the form of charts. The following sections contain the chart solutions for some of the loadings most commonly encountered in practice. Caution in the use of these charts is advised since they all pertain to **stress increments** at very well-defined points within the soil mass due to the applied pressures indicated. **The total stress acting at a point of interest is equal to the stress increment at that point due to the newly applied**

**load plus existing stresses at that point due to the geostatic stress and stresses due to other external loads applied previously.**

#### **2.4.1 Uniformly Loaded Continuous (Strip) and Square Footings**

A loaded area is considered to be infinitely long when its length,  $L$ , to width,  $B$ , ratio is greater than or equal to 10, i.e.,  $L/B \geq 10$ . The load on such an area is commonly known as a strip load. Figure 2-9 presents vertical pressure isobars under strip and square footings based on Boussinesq's theory. An **isobar** is a line that connects all points of equal stress increment below the ground surface. In other words, an isobar is a stress increment contour.

Each isobar represents a fraction of the stress applied at the surface and delineates the zone of influence of the footing such that the area contained within two adjacent isobars experiences stresses greater than the lower isobar and less than the upper isobar. Since these isobars form closed figures that resemble the form of a bulb, they are also termed **bulbs of pressure** or simply the **pressure bulbs**. The pressure bulb concept gives the user a feel for the spread of the stresses through a soil mass.

According to linear elastic theory, the size of the pressure bulb is proportional to the size of the loaded area. This is a key concept in geotechnical engineering that is used to evaluate the **depth of significant influence, DOSI**, denoted by  $D_s$  of an applied surface load. The depth  $D_s$  is a finite depth below which there are no significant strains in the soil mass due to the loads imposed at the surface. Typically, strains are not significant once the stresses have attenuated to a value of 10 to 15% of those at the surface. For example, Figure 2-9a shows that for "infinitely long" strip footings,  $D_s = 4$  to  $6B$ , while for square footings, Figure 2-9b shows that  $D_s = 1.5$  to  $2B$ . The depths corresponding to this 10 to 15% criterion can be used to determine the minimum depth of field exploration for proposed strip or square footings to ensure that the anticipated significant depth is explored.

It may be seen from Figure 2-9 that the effect of the vertical stresses extends laterally beyond the width of the loaded area,  $B$ . This observation is very useful in assessing the influence of one loaded area on the other. Alternatively, this observation can be used to determine an adequate spacing between adjacent loaded areas. It also indicates that the effect of construction activities may be felt beyond a specific site. Such effects should be evaluated before construction so that mitigation measures can be taken to avoid legal implications.

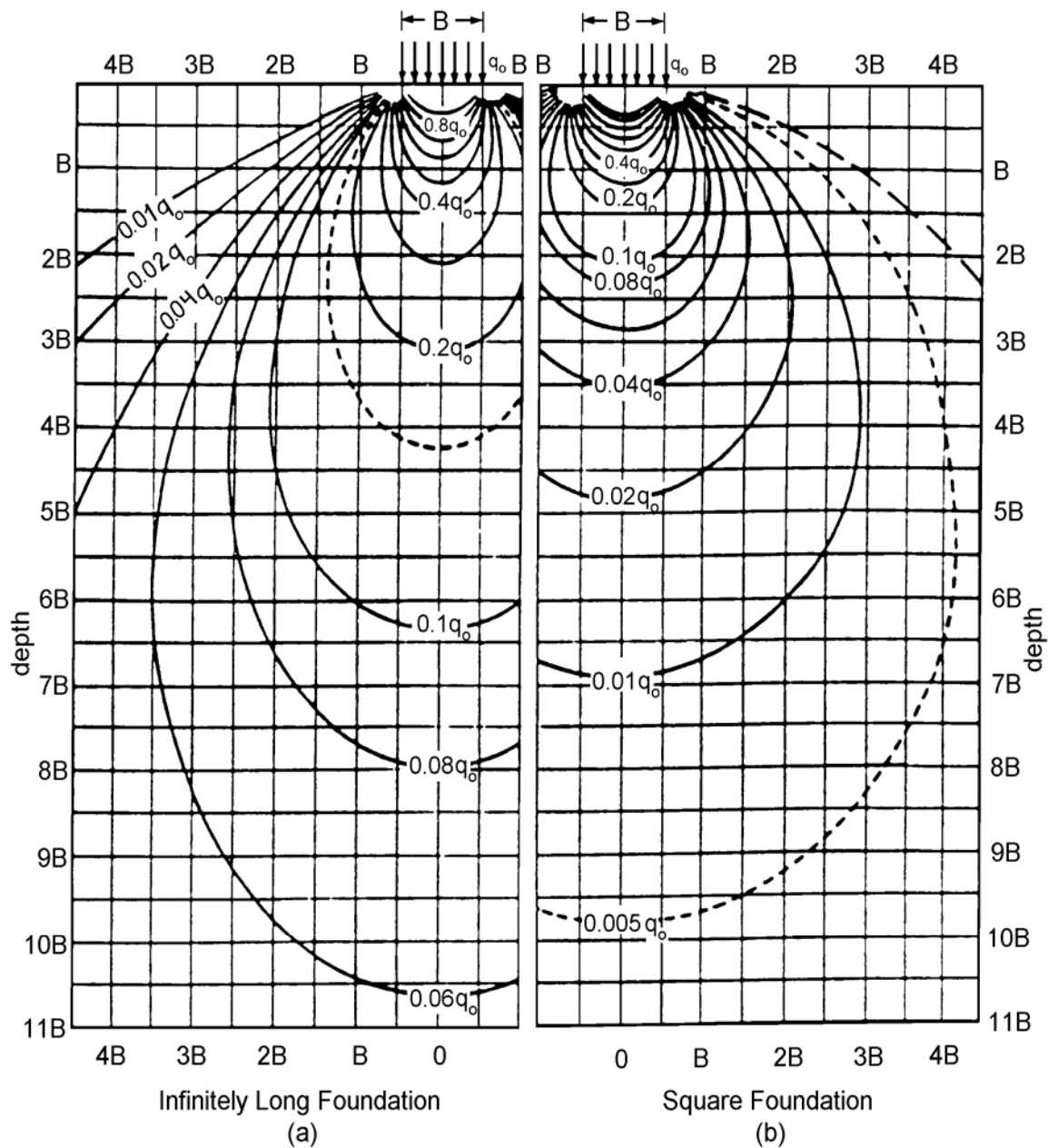


**Figure 2-9. Vertical stress contours (isobars) based on Boussinesq's theory for continuous and square footings (modified after Sowers, 1979; AASHTO, 2002).**

## 2.4.2 Approximate (2:1) Stress Distribution Concept

As an approximation to the exact solution given by the Boussinesq charts, the total load at the surface of the soil mass may be distributed over an area of the same shape as the loaded area on the surface, but with dimensions that increase with depth at a rate of one horizontal unit for every two vertical units. This is illustrated in Figure 2-10, which shows a rectangular area of dimensions  $B \times L$  at the surface. At a depth,  $z$ , the total load is assumed to be uniformly distributed over an area  $(B+z)$  by  $(L+z)$ . Since the stress is distributed at the rate of 2:1 (vertical:horizontal), this approximation method is commonly known as the “**2:1 stress distribution**” method.

The relationship between the approximate distribution of stress determined by this method and the exact distribution is illustrated in Figure 2-10. In this figure, the vertical stress distribution at a depth  $B$  below a uniformly loaded square area of width  $B$  is shown along a horizontal line that passes beneath the center of the area and extends beyond the edges of the loaded area. Also shown is the approximate uniform distribution at depth  $B$  determined by the 2:1 stress distribution method described above. The discrepancy between the two methods decreases as the ratio of the depth considered to the size of the loaded area increases (Perloff and Baron, 1976).

## 2.5 REPRESENTATION OF IMPOSED PRESSURES ON THE $p_o$ DIAGRAM

The pressure distributions computed by using the charts in Section 2.4, can be shown superimposed on the  $p_o$  diagram as shown in Figure 2-7. As discussed in the previous sections, an applied pressure at the surface causes stress increments within the soil mass that decrease with depth due to spatial attenuation. This is shown in Figure 2-11 where  $\Delta p$  is plotted with respect to the  $p_o$  line that represents the existing geostatic stress distribution. As can be seen in Figure 2-11,  $\Delta p$  approaches the  $p_o$  line, which indicates that at a sufficient depth the effect of the externally imposed loads reduces significantly. In other words, this means that most of the strain due to the increased stress from the applied load will be experienced at relatively shallow depths below the load. As noted earlier, this depth is known as the **depth of significant influence (DOSI)**,  $D_s$ . Also, as indicated previously,  $D_s$  depends on the load and load configuration as demonstrated by the pressure distribution charts in Section 2.4. Figure 2-11 also shows that the **final stress,  $p_f$ , in the soil mass at any depth is equal to  $p_o + \Delta p$ .**

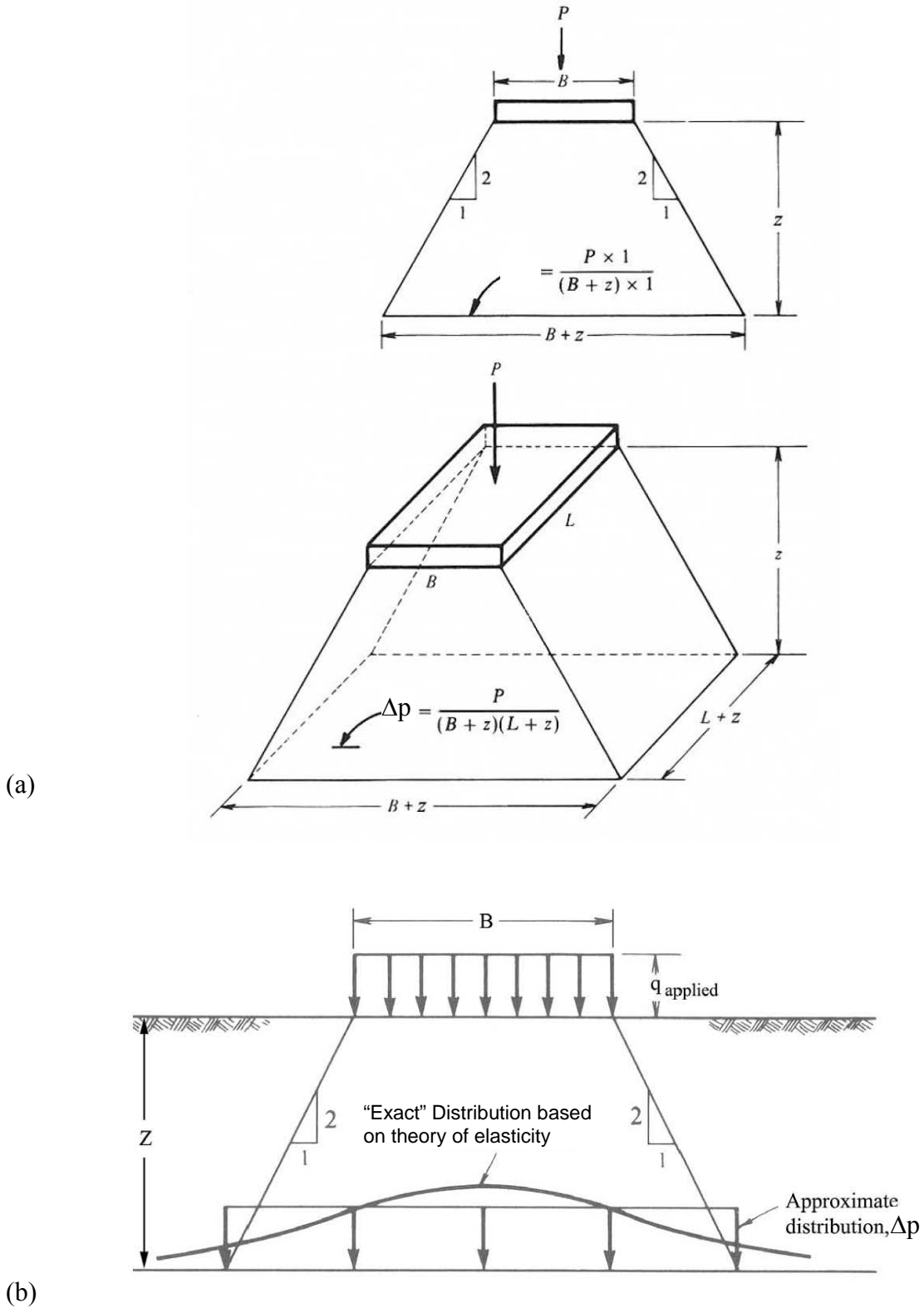


**Figure 2-10. Distribution of vertical stress by the 2:1 method (after Perloff and Baron, 1976).**

A chart such as that shown in Figure 2-11 is even more useful when the soil stratigraphy is plotted on it. Then the stress levels in various layers will be clearly identified, which can help the engineer determine depth of borings to collect subsurface information within DOSI as well as perform proper analysis.

Example 2-2 illustrates these concepts by providing calculations of  $p_f$  with depth due to stress increments from a strip load and presenting the results of the calculations on a  $p_o$ -diagram.

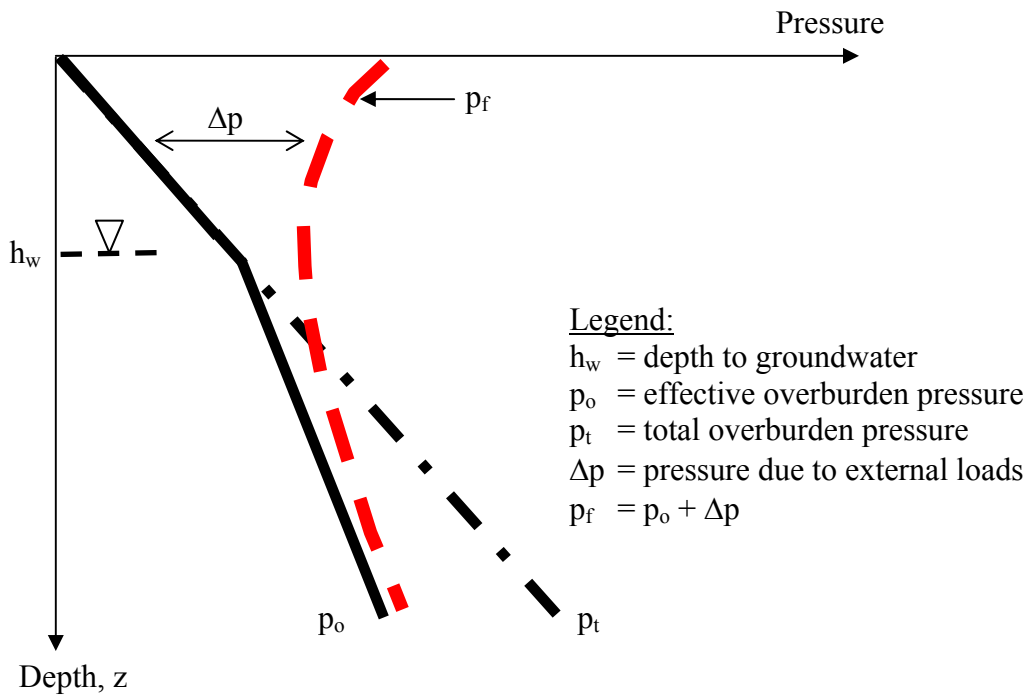


**Figure 2-11. Combined plot of overburden pressures (total and effective) and pressure due to imposed loads.**



## 2.6 LOAD-DEFORMATION PROCESS IN SOILS

When subjected to static and/or dynamic loads, soils deform mainly because of a change in void volume rather than through deformation of the soil solids. When the void volume decreases the soil is said to compress, consolidate, collapse or compact. There is an important distinction between these four mechanisms although conceptually they appear to be the same since each pertains to a reduction in volume.

- **Compression:** Compression is defined as a relatively rapid decrease in void volume that partially saturated (unsaturated) soils undergo as air is expelled from the voids during loading.
- **Consolidation:** Consolidation is generally defined as a time-dependent decrease in void volume that saturated and near-saturated soils undergo as water is expelled from the voids during loading. The conceptual process of consolidation is discussed in Section 2.6.1.
- **Collapse:** Collapse is primarily related to soil structure and its response to an increase in water content that results in a rapid decrease in void volume. Collapse-susceptible soils characteristically have dry densities less than approximately 100 pcf (16 kN/m<sup>3</sup>) that suggest high void ratios. Their structure is like a honeycomb with fine-grained “bridges” connecting coarser-grained particles. When dry, these soils are able to sustain externally applied loads with very little deformation. However, upon being wetted they tend to undergo a rapid decrease in void volume as the fine-grained “bridges” lose strength and the entire structure collapses. The magnitude of the potential collapse increases with increasing load. One of the important things to note is that full saturation (S=100%) is not required for these types of soils to collapse. Often collapse occurs at a degree of saturation of 50 to 70%. Collapse-susceptible soils are very common in the southwest and midwest of the United States and in many other parts of the world.
- **Compaction:** Compaction is the name given to the compression that takes place generally under an impact-type loading (e.g., modified and standard Proctor), a static loading (e.g., rubber-tired or steel drum rollers) or kneading-type loading (e.g., sheepfoot roller). Most commonly, the compaction processes are deliberate and intended to achieve a dense packing of soil particles. Regardless of the type of loading, the moisture content of the soil being compacted is far enough below the saturation moisture content that the compaction mechanism is considered to be related to compression (i.e., expulsion of air) rather than consolidation (i.e., expulsion

of water) from the voids. Typically, the desired moisture content in the case of compaction is slightly above or below the PL. If the moisture content of the soil being compacted gets to be too close to the saturation moisture content then “pumping” will occur, i.e. water in addition to air will be forced out of the soil.

These distinctions in load-deformation processes should be kept in mind during the discussions that follow in subsequent sections of this chapter.

Finally, in contrast to the above processes that involve void volume decrease, there are conditions under which soils may actually increase in volume. When the void volume increases under static and/or dynamic load, the soil is said to **dilate**. **Dilation** can occur in either saturated or partially saturated soils. It is a function of the initial void ratio, confinement stress, and the magnitude and direction of the loading/unloading imposed on the soil. **Expansion**, on the other hand, is generally considered to be due to the presence of expansive clay minerals, such as montmorillonite (commercially known as “bentonite”), in the soil and the response of these minerals to the introduction of water into the void spaces. The physico-chemical properties of expansive clay minerals cause inter-particle repulsions to take place in the presence of water so that even under considerable externally applied loads these soils will undergo an increase in void volume that leads to swelling. A variation of the expansion is **heave** which can occur due to various factors such as frost action or reduction in overburden pressure due to excavation.

### 2.6.1 Time Dependent Load-Deformation (Consolidation) Process

Deformation of a saturated soil is more complicated than that of a dry soil since water, which fills the voids, must be squeezed out of the soil before readjustment of the soil grains can occur. The more permeable a soil is, the faster the deformation under load will occur. However, when the load on a saturated soil is quickly increased, the increase is initially carried by the pore water resulting in the buildup of an **excess pore water pressure,  $\Delta u$** . **Excess pore water pressure is water pressure greater than the hydrostatic pressure.** As drainage of the water takes place more and more load is gradually transferred from the pore water to the soil grains until the excess pore water pressure has dissipated completely and the soil grains readjust to a denser configuration under the applied load. This time dependent process is called **consolidation** and results in a decreased void ratio and greater unit weight relative to conditions before the load was applied. To illustrate this concept, one-dimensional (vertical) drainage of the water will be considered here. The process is analogous to loading a spring-supported piston in a cylinder filled with water. The spring-piston analogy is shown schematically in Figure 2-13 and is briefly discussed below.

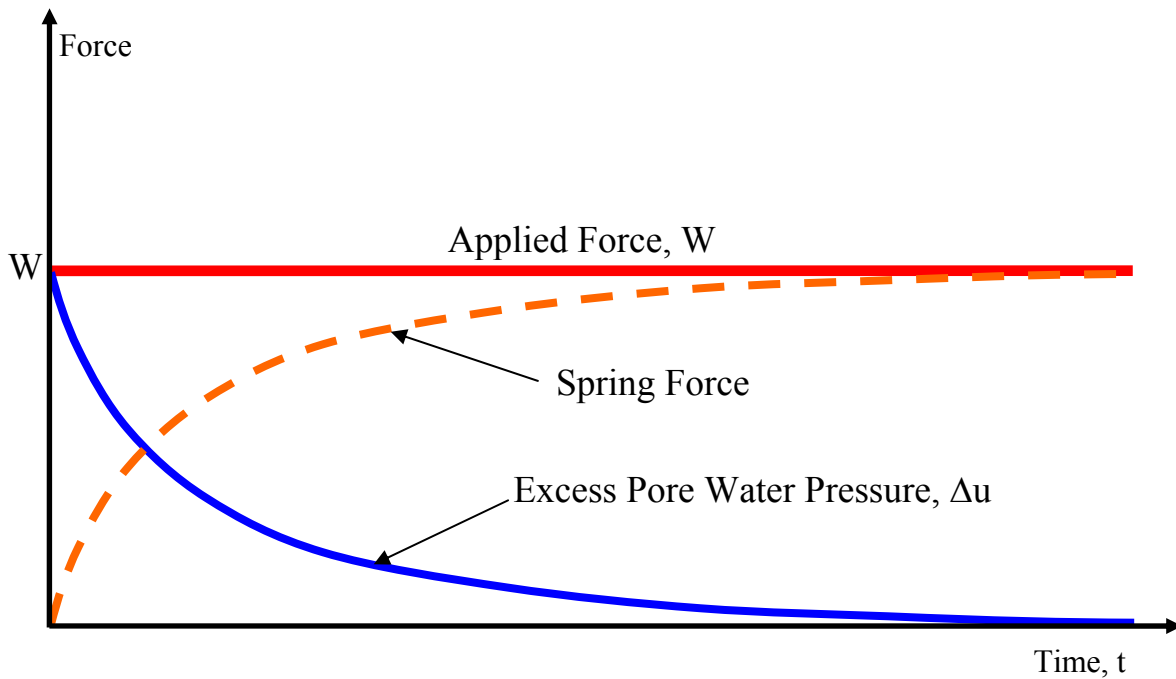
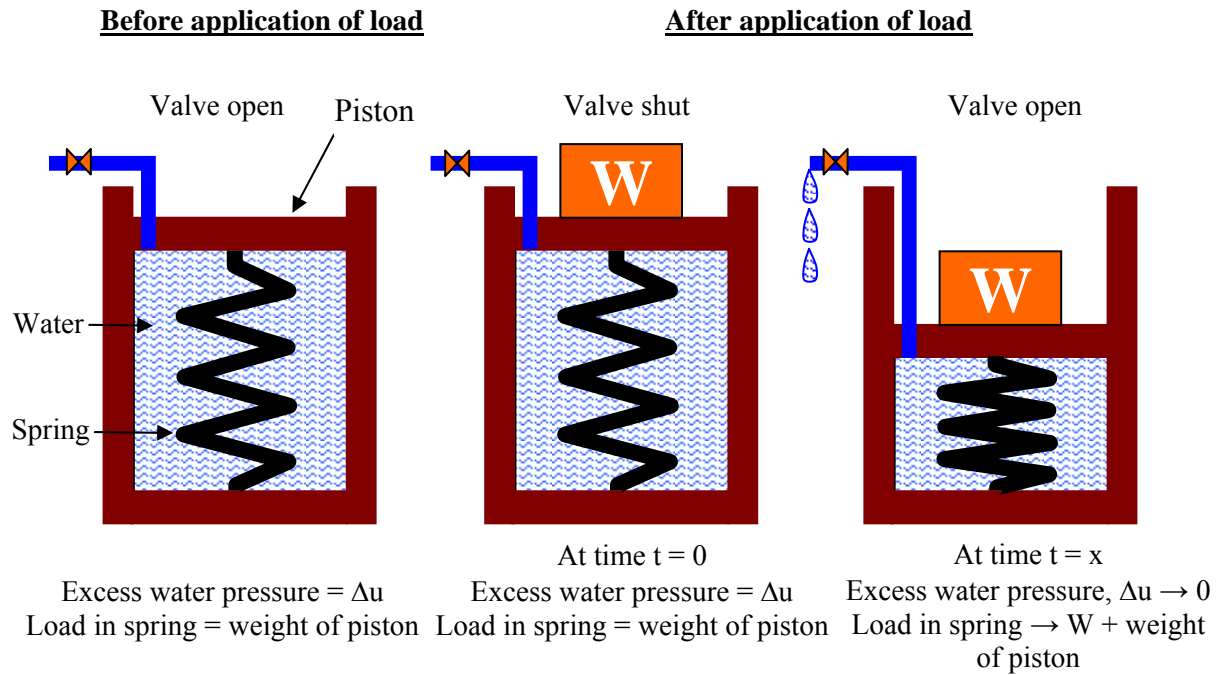


**Figure 2-13. Spring-piston analogy for the consolidation process in fine-grained soils.**

In the spring-piston model, the spring represents the solid phase of the soil and the water below the piston is the pore water under saturated condition in the soil mass. Before a new load,  $W$ , is applied to the piston, the system is assumed to be in equilibrium, i.e., the drainage valve is open and there is no excess pore water pressure,  $\Delta u = 0$ . The spring alone is carrying any previously applied loads, such as the weight of the piston itself. The drainage valve is closed just before the new load is applied. If the valve is completely shut-off and the piston is leak-proof, then, there is no chance for water to escape. Such a condition represents a clay-water system in which the clay is very impermeable so that there is significant resistance to drainage of water in any direction. When the new load,  $W$ , is placed on the piston (this is called the initial or “time = 0” condition), the total applied pressure immediately below the piston,  $p_t$ , which equals the load,  $W$ , divided by the area of the piston, is immediately transferred to the water. Since the drainage valve is closed and water is virtually incompressible, the water pressure increases to a value equal to the total applied pressure, i.e., the excess water pressure  $\Delta u = p_t$ .

At “time = 0,” the spring does not carry any of the applied load  $W$ . The excess water pressure is analogous to the pore water pressure that would be developed in a clay-water system under externally applied loads, e.g., loads due to construction of an embankment on soft saturated clay. If the valve is now opened, the water will drain to relieve the excess pressure in it. With the escape of the water, a part of the pressure carried by the water is transferred to the spring where it induces a stress increase analogous to an effective increase in the inter-particle stresses,  $p_o$ , in a soil mass. The transfer of pressure from the water to the spring occurs over a period of time as shown on the bottom part of Figure 2-13, however, at any time during the process, the increased stress in the spring,  $p_o$ , plus the excess pressure in the water,  $\Delta u$ , must equal the applied pressure,  $p_t$ . This transfer of pressure from the water to the spring goes on until the flow stops. At that time all of the applied pressure,  $p_t$ , will be carried by the spring,  $p_o$ , and none by the water, i.e.,  $\Delta u = 0$ , and the system will have come into equilibrium under the applied load. The time required to attain equilibrium depends on the avenue provided to the water to escape, i.e., the longest drainage path the water has to take to leave the system. In Figure 2-13 the longest drainage path is the length of the cylinder. Obviously, the system would drain quicker if there were another standpipe-type drain at the bottom of the cylinder.

Regardless of the number of avenues provided for drainage, the rate of excess water pressure drop generally decreases with time as shown in the lower half of Figure 2-13. After the spring water system attains an equilibrium condition under the imposed load, the compression of the piston is analogous to the settlement of the clay-water system under an externally applied load. This process is called **consolidation**.

## 2.6.2 Comparison of Drainage Rates between Coarse-Grained and Fine-Grained Soils

Figure 2-14 shows a comparison of excess pore water pressure dissipation in coarse-grained and fine-grained soils. The relatively large pore spaces in coarse-grained soils permit the water to drain quicker in comparison to fine-grained soils. This leads to a quick transfer of applied loads to the soil solids with an associated decrease in void space. This quick load transfer results in a displacement that is commonly termed “rapid” in contrast to the “long-term” displacement that is associated with the consolidation process in fine-grained soils.

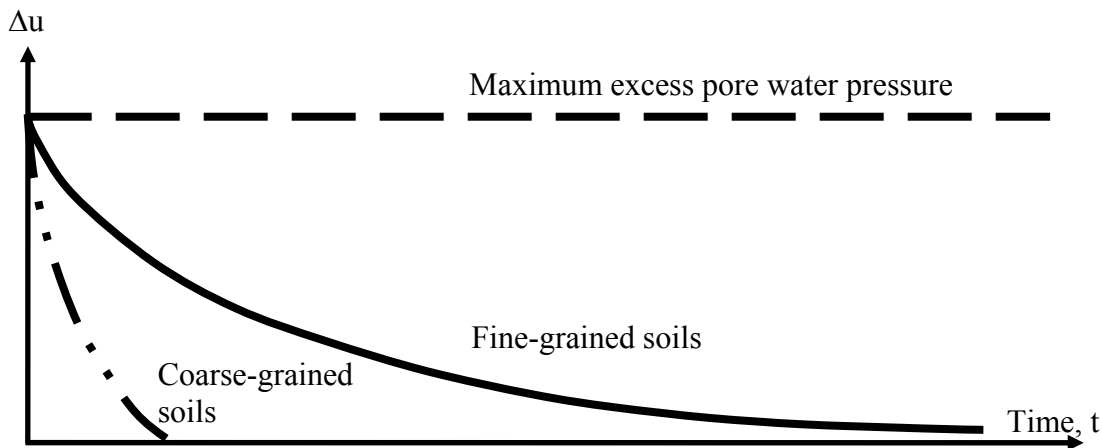


**Figure 2-14. Comparison of excess pore water pressure dissipation in coarse-grained and fine-grained soils.**

## 2.7 LATERAL STRESSES IN FOUNDATION SOILS

In most cases, the vertical stress at any depth in a soil mass due to its self weight is the summation of the simple products of the unit weight of each soil layer and its corresponding thickness down to the depth of interest. This vertical stress was denoted by  $p_t$  and the effective component of this pressure was denoted by  $p_o$ . Due a variety of factors, including depositional patterns, the lateral stress,  $p_h$ , in a soil mass is usually not the same as the vertical stress,  $p_o$ . Since the vertical stress is known with reasonable certainty for practical purposes, the lateral stress can be assumed to be a certain percentage of the vertical stress and can be expressed as follows:

$$p_h = K p_o \quad 2-14$$

For an elastic solid, the value of the proportionality constant,  $K$ , can be expressed in terms of Poisson’s ratio,  $\nu$ , as follows:

$$K = \frac{\nu}{1 - \nu} \quad 2-15$$

Poisson's ratio,  $\nu$ , is defined as a ratio of lateral to vertical strains. The value of Poisson's ratio is a function of the type of material, e.g.,  $\nu$  is practically zero for cork (hence its suitability as a bottle stopper), for concrete  $\nu$  is between 0.1 and 0.2, and for steel  $\nu$  is between 0.27 and 0.30. A theoretical upper limit of Poisson's ratio is 0.5 (rubber comes close to this limiting value). In the case of soils,  $\nu$  will have a different value depending upon the type of soil and its moisture condition. For example, for free-draining soils a reasonable value of  $\nu$  would be in the range of 0.25 to 0.35, while for very soft saturated clays under rapid loading conditions the value of  $\nu$  would be close to 0.5. Thus, for free-draining soils, the value of  $K$  based on elasticity theory will range from 33% to 54% corresponding to  $\nu=0.25$  and  $\nu=0.35$ , respectively, while for soft clays the value of  $K \approx 1$  since  $\nu \approx 0.5$ .

Even though a soil mass is not an elastic body, the point to be noted here is that at any point within the soil mass both vertical and horizontal (or lateral) stresses exist. When external forces are imposed on a soil mass, they will result in an increase in vertical stresses as discussed in Sections 2.5 and 2.6. Equation 2-14 indicates that an increase in vertical stresses will in turn lead to an increase in lateral stresses. While the increase in vertical stresses is important in assessing vertical settlements, change in lateral stresses may affect the load acting, for example, against piles supporting a bridge abutment, see Figure 2-15. In this figure, it can be seen that the increase in vertical stress imposed by the embankment leads to an increase in the lateral stress in the ground that causes lateral deformation ("squeeze") of the soft soil. As the soft soil spreads laterally it will have an effect on foundations. Therefore, it is important to evaluate the increase in lateral stresses due to vertical loadings.

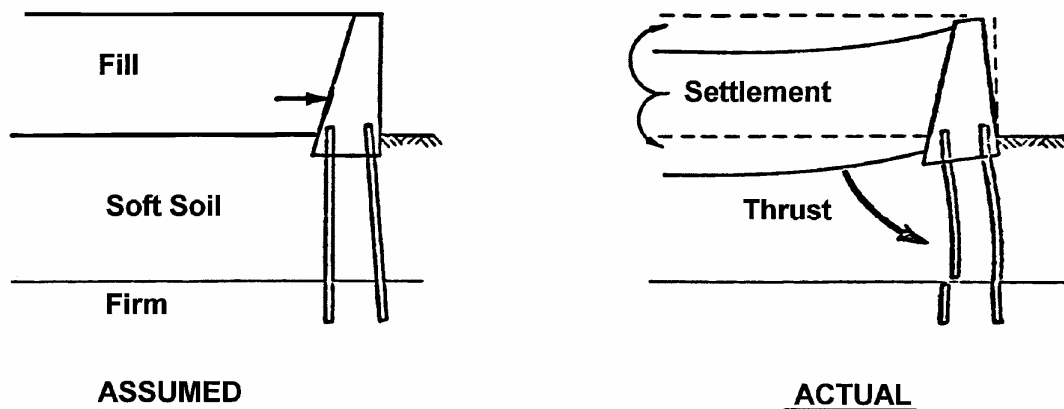


**Figure 2-15. Schematic of effect of lateral stresses.**

A two-dimensional (2-D) representation of the lateral stresses transverse to an embankment centerline is shown in Figure 2-16. This schematic was developed with a soft layer of soil under the embankment. It can be seen that significant lateral stresses are generated in the soil below the embankment load. Note that the vertical stresses due to the embankment can cause zones of tensile stresses to develop near the toes of the embankment as shown by the hatched zones in Figure 2-16. This means that tensile cracks are likely to develop near the toes of the embankments for this particular case. This knowledge can help the geotechnical specialist to select proper ground improvement measures rationally and to develop and implement an instrumentation program. The key point to understand based on the schematics shown in Figures 2-15 and 2-16 is that lateral deformations can be three-dimensional and can affect a number of facilities such as buried utilities, embankment slopes and bridge foundations. Lateral deformations can also affect off-site structures very easily leading to potential legal actions. The three-dimensional (3-D) lateral deformations coupled with vertical deformations due to vertical stresses can create a complex state of deformation that needs to be carefully considered in the design of geotechnical features.

Similar to the estimation of vertical stresses, the theory of linear elasticity yields equations for lateral stress distribution. However, in these equations Poisson's ratio is assumed to be a constant. Hence, the use of chart solutions in these cases is not as simple as for the vertical stress case since complicated equations have to be evaluated (Poulos and Davis, 1974). One can prepare spreadsheet solutions based on the equations or use commercially available computer programs that have already programmed the equations. Program FoSSA (2003) by ADAMA Engineering (Version 1.0 was licensed to FHWA) is an example of a program capable of computing the vertical and lateral stresses due to surface loading, including embankment and multiple footings. Figures 2-10 and 2-16 were generated using the FoSSA program.

### **2.7.1 Effect of Shear Strength of Soils on Lateral Pressures**

Up to now the stresses in soils have been explained by using unit weights and the theory of elasticity. Elastic theory, when suitably modified to reflect observed phenomena in soils, provides a tool to obtain a reasonable first approximation to a solution for many problems in geotechnical engineering. However, elastic theory does not recognize the role of shear strength of soil in the development of lateral pressures. For example, soils have an ability to stand vertically or at a certain slope. The reason for this observed ability is that soil has shear strength and to some degree can support itself. This shear strength may come from friction and/or cohesion between the soil particles. It is intuitive that these components of shear strength should also somehow affect the lateral pressures in soils computed by use of the theory of elasticity. The shear strength of soils and its representation for analytical purposes

is discussed in the Section 2.8 followed in Section 2.9 by a demonstration of how the shear strength parameters can be used to express lateral pressures. Readers are referred to Lambe and Whitman (1979) or Holtz and Kovacs (1981) for detailed discussions.

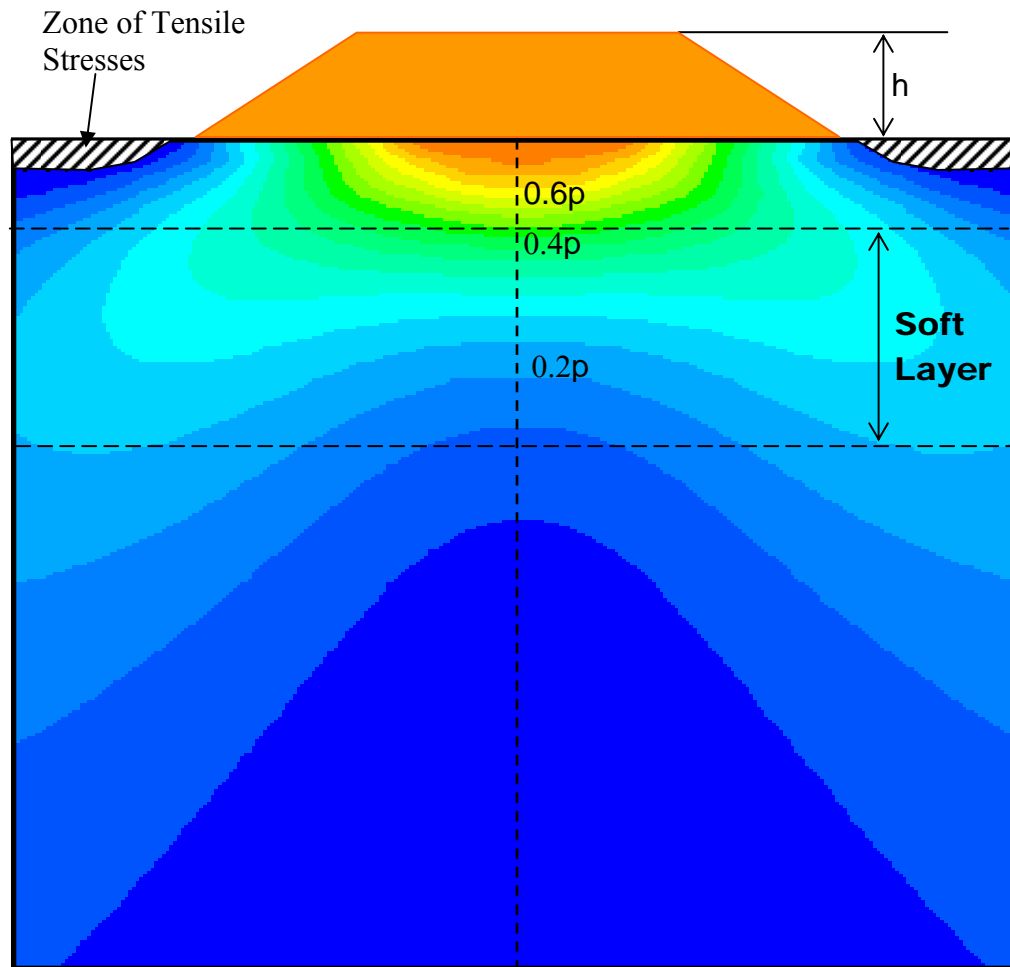


**Figure 2-16. Schematic of vertical stress distribution under embankment loading.  
Graphic generated by FoSSA (2003) program.**

**(Note: Version 1.0 of FoSSA program is licensed to FHWA. See Appendix E for a brief overview of the FoSSA program).**

## 2.8 STRENGTH OF SOILS TO RESIST IMPOSED STRESSES

If the imposed stress in a soil mass is increased until the deformations (movements) become unacceptably large, a “failure” is considered to have taken place. In this case, the strength of the soil is considered to be insufficient to withstand the applied stress.

The strength of geologic materials is a variable property that is dependent on many factors, including material properties, magnitude and direction of the applied forces and their rate of application, drainage conditions of the mass, and the magnitude of confining pressure. Unlike steel whose strength is usually discussed in terms of either tension or compression and concrete whose strength is generally discussed in terms of compressive strength only, the strength of soil is generally discussed in terms of shear strength. Typical geotechnical failures occur when the shear stresses induced by applied loads exceed the soil’s shear strength somewhere within the soil mass.

### 2.8.1 Basic Concept of Shearing Resistance and Shearing Strength

The basic concept of shearing resistance and shearing strength can be understood by first studying the principle of friction between solid bodies. Consider a prismatic block B resting on a plane surface XY as shown in Figure 2-17. The block B is subjected to two forces:

- A normal force,  $P_n$ , that acts perpendicular to the plane XY, and
- A tangential force,  $F_a$ , that acts parallel to the plane XY.

Assume that the normal force,  $P_n$ , is constant and that the tangential force,  $F_a$ , is gradually increased. At small values of  $F_a$ , the block B will not move since the applied force,  $F_a$ , will be balanced by an equal and opposite force,  $F_r$ , on the plane of contact XY. The resisting force,  $F_r$ , is developed as a result of surface roughness on the bottom of the block B and the plane surface XY. The angle,  $\theta$ , formed by the resultant R of the two forces  $F_r$  and  $P_n$  with the normal to the plane XY is known as the **angle of obliquity**.

If the applied horizontal force,  $F_a$ , is gradually increased, the resisting force,  $F_r$ , will likewise increase, always being equal in magnitude and opposite in direction to the applied force. When the force  $F_a$  reaches a value that increases the angle of obliquity to a certain maximum value  $\theta_m$ , the block B will start sliding along the plane. Recall that during this entire process the normal force,  $P_n$ , remains constant. The following terminology can now be developed:

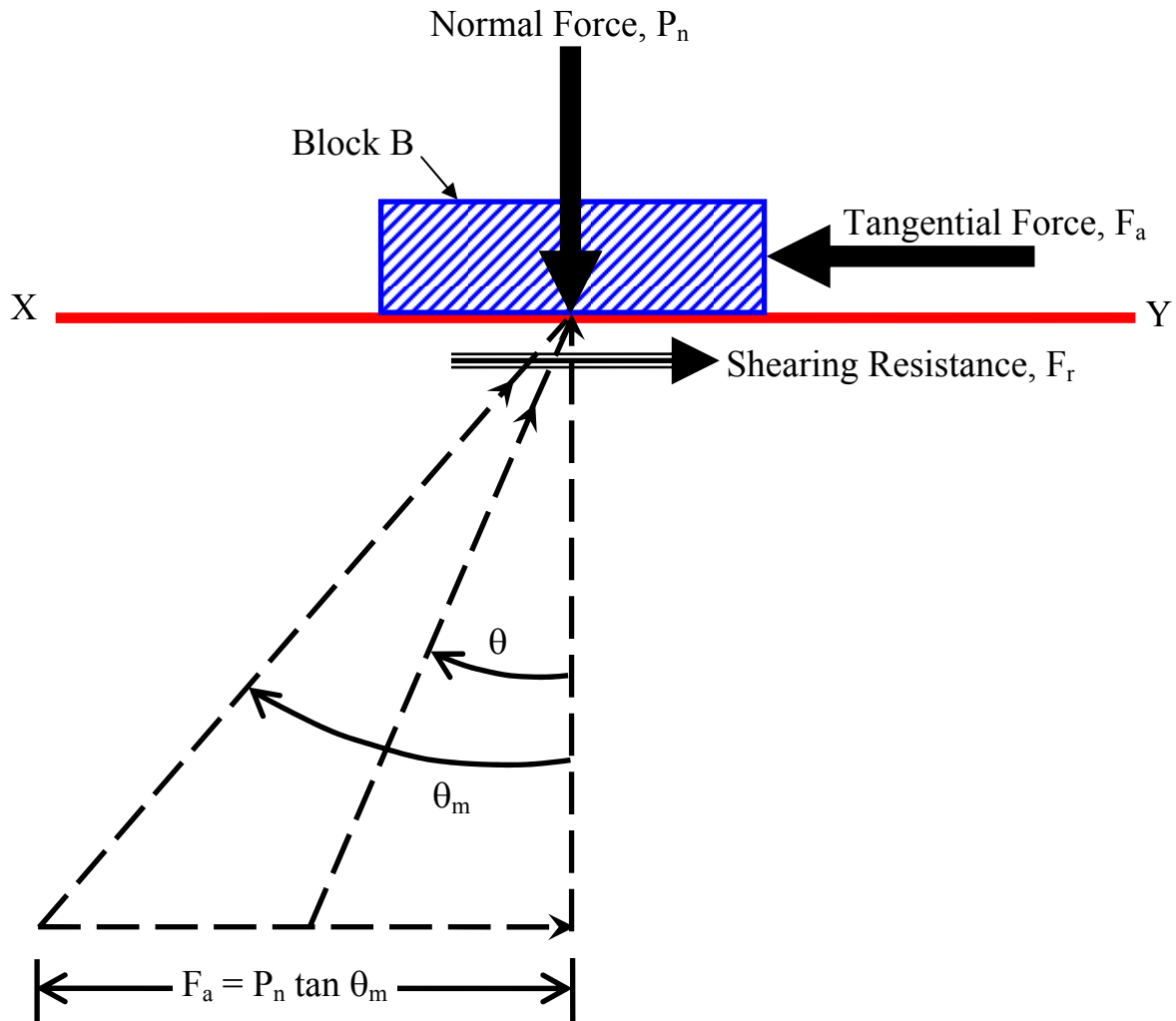


**Figure 2-17. Basic concept of shearing resistance and strength (after Murthy, 1989).**

- If the block B and the plane surface XY are made of the same material, the angle  $\theta_m$  is equal to  $\phi$ , which is termed the **angle of friction** of the material. The value  $\tan \phi$  is called the **coefficient of friction**.
- If the block B and the plane surface XY are made of dissimilar materials, the angle  $\theta_m$  is equal to  $\delta$ , which is termed the **angle of interface friction** between the bottom of the block and the plane surface XY. The value  $\tan \delta$  is called the **coefficient of interface friction**.
- The applied horizontal force,  $F_a$ , on the block B is a shearing force and the developed force is called **frictional resistance** or **shearing resistance**. The maximum frictional or

shearing resistance that the materials are capable of developing on the interface is  $(F_a)_{\max}$ .

If the same experiment is conducted with a greater normal force,  $P_n$ , the maximum frictional or shearing resistance  $(F_a)_{\max}$ , will be correspondingly greater. A series of such experiments would show that for the case where the block and surface are made of the same material, the maximum frictional or shearing resistance is approximately proportional to the normal load  $P_n$  as follows:

$$(F_a)_{\max} = P_n \tan \phi \quad 2-16$$

If  $A$  is the overall contact area of the block  $B$  on the plane surface  $XY$ , the relationship in Equation 2-16 may be written as follows to obtain stresses on surface  $XY$ :

$$\frac{(F_a)_{\max}}{A} = \left( \frac{P_n}{A} \right) \tan \phi \quad 2-17$$

or

$$\tau = \sigma_n \tan \phi \quad 2-18$$

The term  $\sigma_n$  is called the **normal stress** and the term  $\tau$  is called the **shear strength**. A graphical representation of Equation 2-18 is shown in Figure 2-18a. In reality, the relationship is curved, but since most geotechnical problems involve a relatively narrow range of pressures, the relationship is assumed to be linear as represented by Equation 2-18 over that range.

The concept of frictional resistance explained above applies to soils that possess only the frictional component of shear strength, i.e., generally coarse-grained granular soils. But soils that are not purely frictional exhibit an additional strength component due to some kind of internal electro-chemical bonding between the particles. This bonding between the particles is typically found in fine-grained soils and is termed **cohesion, c**. Simplistically, the shear strength,  $\tau$ , of such soils is expressed by two additive components as follows and can be graphically represented as shown in Figure 2-18(b):

$$\tau = c + \sigma_n \tan \phi \quad 2-19$$

Again, in reality, the relationship is curved. But, as noted above, since most geotechnical problems involve a relatively narrow range of pressures, the relationship is assumed to be linear as represented by Equation 2-19 over that range.

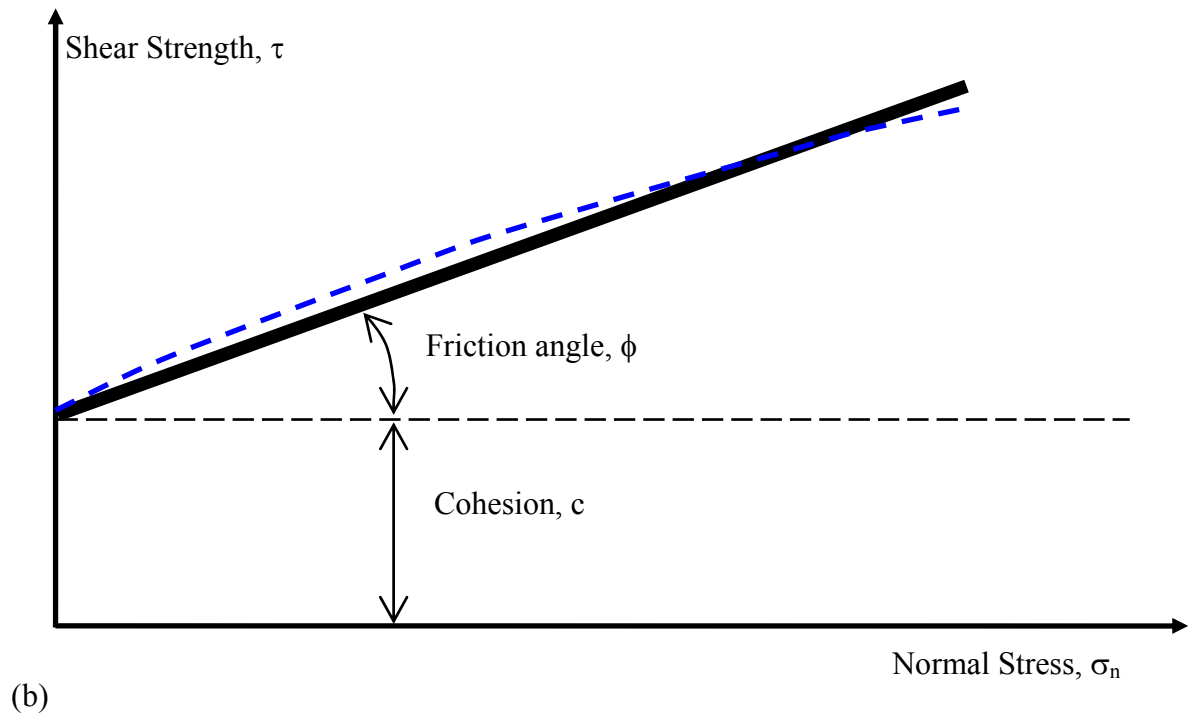
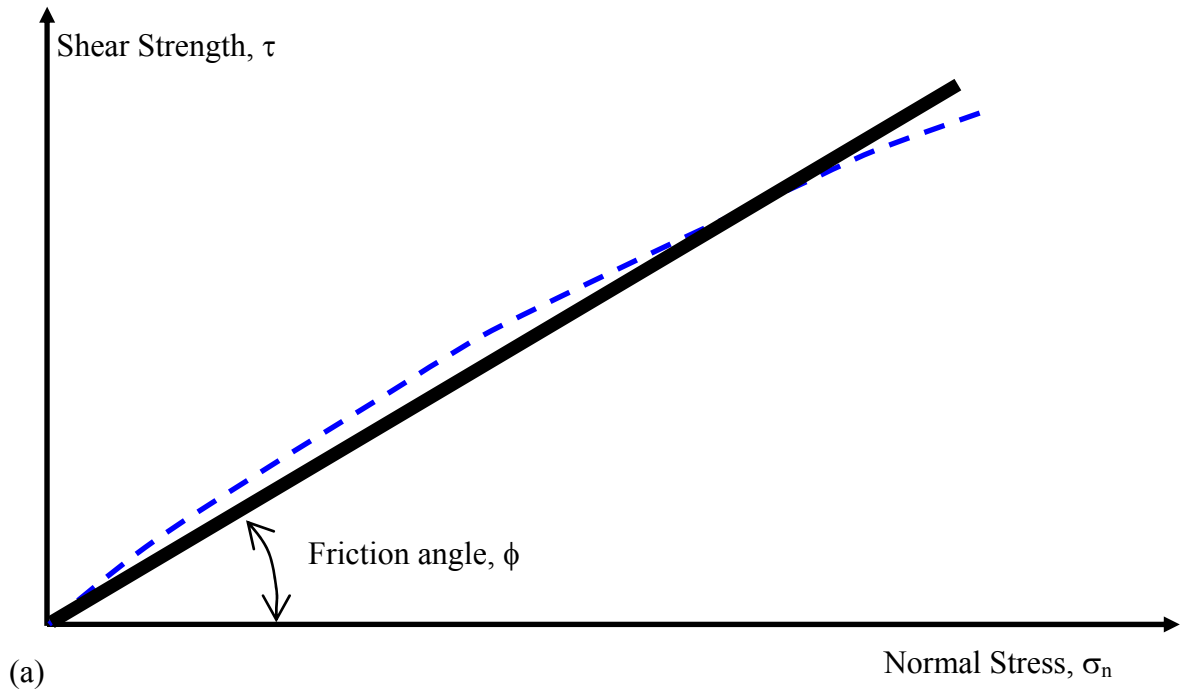


**Figure 2-18. Graphical representation of shearing strength.**

Equation 2-19 was first proposed by French engineer Coulomb and is used to express shear strength of soils. When plotted on arithmetic axes the resulting straight line is conventionally known as the Mohr-Coulomb (M-C) failure envelope. “Mohr” is included in “Mohr-Coulomb” because Equation 2-19 can also be derived based on concept of Mohr’s circle. The development of the Mohr-Coulomb failure envelope based on the application of Mohr’s circle is presented in Appendix B.

As indicated previously, the deformation of soils occurs under effective stresses. In terms of effective stresses, Equation 2-19 can be re-written as follows:

$$\tau' = c' + (\sigma_n - u) \tan \phi' = c' + \sigma' \tan \phi' \quad 2-20$$

where  $c'$  = effective cohesion,  $\sigma'$  is the effective normal stress and  $\phi'$  is the effective friction angle. Further discussion on the cohesion and friction angle is presented in Chapter 4.

In geotechnical engineering, the normal stresses are commonly expressed using the overburden pressure concept introduced in Section 2.3. In terms of overburden pressure, the term  $\sigma_n$  in above equations is the same as  $p_t$  and the term  $\sigma'$  is the same as  $p_o$ . Thus, Equations 2-19 and 2-20 can be expressed in terms of overburden stresses as follows:

$$\tau = c + p_t \tan \phi \quad 2-21$$

$$\tau' = c' + (p_t - u) \tan \phi' = c' + p_o \tan \phi' \quad 2-22$$

Since this manual relates to geotechnical engineering, Equations 2-21 and 2-22 will be used to express the M-C failure envelope. The physical meaning of the M-C failure envelope shown in Figure 2-18(a) and Figure 2-18(b) may be explained as follows:

- Every point on the M-C failure envelope represents a combination of normal and shear stress that results in failure of the soil, i.e., the Mohr failure envelope essentially defines the strength of the soil. In other words, **any point along the M-C envelope defines the limiting state of stress for equilibrium.**
- If the state of stress is represented by a point below the M-C failure envelope then the soil will be stable for that state of stress.
- States of stress beyond the M-C failure envelope cannot exist since failure would have occurred before that point could be reached.

## 2.9 STRENGTH OF SOILS RELATED TO LATERAL EARTH PRESSURES

The concept of shear strength described in the previous section can now be used to understand the phenomenon of lateral earth pressure in a soil mass, which is related to problems of slope stability and earth retention. From a theoretical viewpoint, problems in these three areas (earth pressures, slope stability, and retaining structures) fall into a class of problems involving plasticity theory and are best solved by some form of equilibrium solution. Many geotechnical engineering text books (e.g., Lambe and Whitman, 1979; Holtz and Kovacs, 1981) deal with these solutions extensively. From a practical viewpoint, values of earth pressure are needed either directly or indirectly to determine:

- a) If an unrestrained slope is stable and
- b) If not, what kind of retaining structure will be required to stabilize the slope.

The simplest consideration of earth pressure theory starts with the assessment of the vertical geostatic effective stress,  $p_o$ , at some depth in the ground (effective overburden pressure) as considered in Section 2.3. The lateral geostatic effective stress,  $p_h$ , at this depth is given in general terms by Equation 2-14 where, for an ideally elastic solid, the value of the lateral earth pressure coefficient,  $K$ , is given by Equation 2-15. However, the behavior of real soils under loads is not always ideally elastic. To simplify the discussion of this topic, consider only dry coarse-grained cohesionless soils. The geostatic effective stress condition on a soil element at any depth,  $z$ , is shown in Figure 2-19a. Since the ground is “at-rest” without any external disturbance, this condition is commonly referred to as the “**at-rest**” condition with zero deformation. The coefficient of lateral earth pressure for this condition is labeled  $K_o$ .

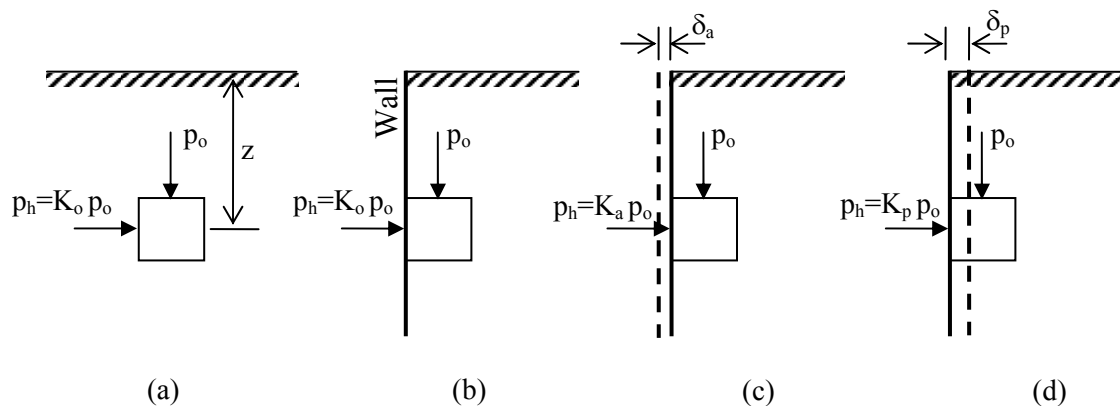


**Figure 2-19. Stress states on a soil element subjected only to body stresses: (a) In-situ geostatic effective vertical and horizontal stresses, (b) Insertion of hypothetical infinitely rigid, infinitely thin frictionless wall and removal of soil to left of wall, (c) Active condition of wall movement away from retained soil, (d) Passive condition of wall movement into retained soil.**

To relate to the lateral earth pressures acting on retaining structures, assume that a hypothetical, infinitely thin, infinitely rigid “wall” is inserted into the soil without changing the “at rest” stress condition in the soil. For the sake of discussion, assume that the hypothetical wall maintains the “at rest” stress condition in the soil to the right of the wall when the soil to the left of the wall is removed. This condition is shown in Figure 2-19b. Now suppose that the “at rest” condition is removed by allowing the hypothetical vertical wall to move slightly to the left, i.e., away from the soil element as shown in Figure 2-19c. In this condition, the vertical stress would remain unchanged. However, since the soil is cohesionless and cannot stand vertically on its own, it actively follows the wall. In this event, the horizontal stress decreases, which implies that the lateral earth pressure coefficient is less than  $K_0$  since the vertical stress remains unchanged. When this occurs the soil is said to be in the “**active**” state. The lateral earth pressure coefficient at this condition is called the “**coefficient of active earth pressure,**”  $K_a$ , and its value at failure is expressed in terms of effective friction angle,  $\phi'$ , as follows:

$$K_a = \frac{1 - \sin \phi'}{1 + \sin \phi'} \quad 2-23$$

Returning to the condition shown in Figure 2-19b, now suppose that the “at rest” condition is removed by moving the hypothetical vertical wall to the right, i.e., into the soil element as shown in Figure 2-19d. Again, the vertical stress would remain unchanged. However, the soil behind the wall passively resists the tendency for it to move, i.e., the horizontal stress would increase, which implies that the lateral earth pressure coefficient would become greater than  $K_0$  since the vertical stress remains unchanged. When this occurs the soil is said to be in the “**passive**” state. The lateral earth pressure coefficient at this condition is called the “**coefficient of passive earth pressure,**”  $K_p$ , and its value at failure is expressed in terms of effective friction angle,  $\phi'$ , as follows:

$$K_p = \frac{1 + \sin \phi'}{1 - \sin \phi'} \quad 2-24$$

When failure occurs during either of the two processes described above, “**Rankine**” failure zones form within the soil mass. The details of how the failure zones develop are described in most geotechnical engineering textbooks and will not be treated here. The so-called “Rankine” failure zones and their angles from the horizontal are shown in Figure 2-20.

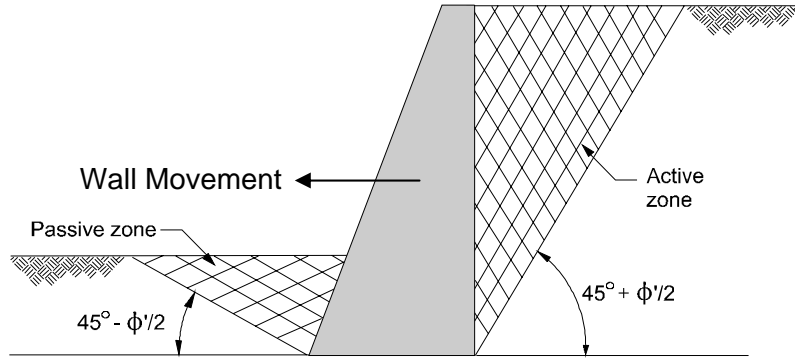


**Figure 2-20. Development of Rankine active and passive failure zones for a smooth retaining wall.**

### 2.9.1 Distribution of Lateral Earth and Water Pressures

The earth pressure coefficients,  $K_a$  and  $K_p$ , can be substituted into Equation 2-14 to obtain equations for active and passive lateral earth pressures, respectively as follows:

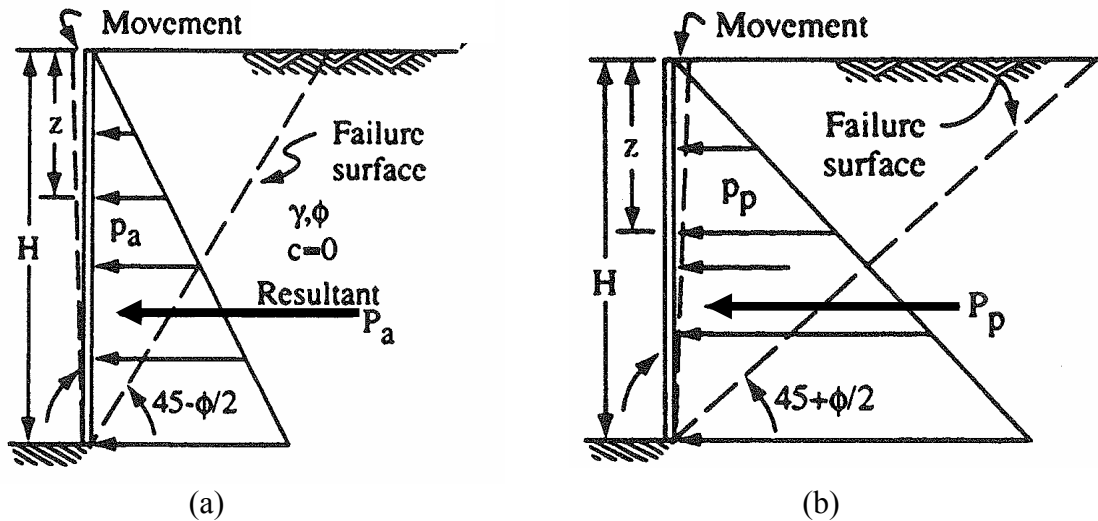
$$p_a = K_a p_o \quad 2-25a$$

$$p_p = K_p p_o \quad 2-25b$$

It can be seen from Equations 2-25a and 2-25b that the lateral pressures  $p_a$  and  $p_p$  are a certain fraction of the vertical effective overburden pressure  $p_o$ . Thus, active and passive lateral earth pressures are effective pressures and their distribution will be same as that for  $p_o$ . The overburden pressure increases in proportion to the unit weight and is typically triangular for a given geomaterial. The general distribution of the active and passive pressures along with the configuration of active and passive failure surfaces is shown in Figure 2-21a and 2-21b, respectively.

In cases where ground water exists, the lateral pressure due to the water at any depth below the ground water level is equal to the hydrostatic pressure at that point since the friction angle of water is zero and use of either Equation 2-23 or 2-24 leads to a coefficient of lateral pressure for water,  $K_w$  equal to 1.0. The computation of the vertical water pressure was demonstrated previously in Example 2-1. Since  $K_w=1$ , the same computation applies for the lateral pressure as well. The lateral earth pressure is computed by using the vertical effective overburden pressure  $p_o$  at any depth and applying Equations 2-25a and 2-25b. The lateral earth pressure is added to the hydrostatic water pressure to obtain the total lateral pressure acting on the wall at any point below the ground water level. For a typical soil friction angle of 30 degrees,  $K_a = 1/3$ . Since  $K_w = 1$ , it can be seen that the **lateral pressure due to water**

is approximately 3 times that due to the active lateral earth pressure. A general case for the distribution of combined active lateral earth pressure and lateral water pressure is shown in Figure 2-22. As will be discussed in Chapter 10 (Earth Retaining Structures), this disparity in lateral pressures has serious consequences when the stability of walls is considered and is the reason why drainage behind walls is so important.



Active pressure at depth  $z$ :  $p_a = K_a \gamma z$       Passive pressure at depth  $z$ :  $p_p = K_p \gamma z$   
 Active force within depth  $z$ :  $P_a = K_a \gamma z^2 / 2$       Passive force within depth  $z$ :  $P_p = K_p \gamma z^2 / 2$

**Figure 2-21. Failure surfaces, pressure distribution and forces (a) active case, (b) passive case.**

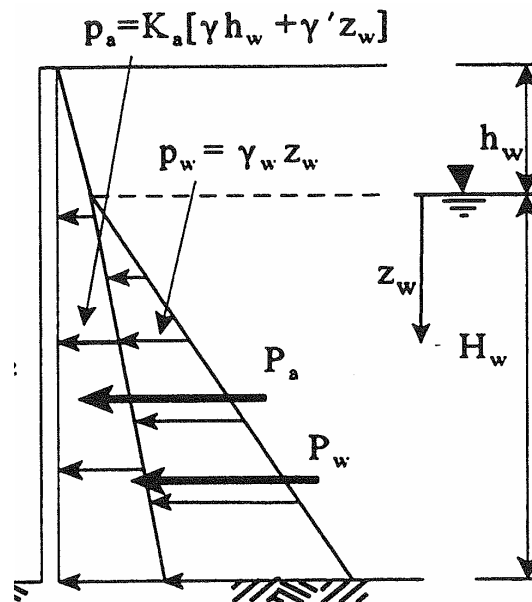


**Figure 2-22. General distribution of combined active earth pressure and water pressure.**

### **2.9.2 Deformations Associated with Lateral Pressures**

The active and passive pressures are predicated on the development of a certain amount of lateral deformation in the soil. The magnitudes of these lateral deformations and their effect on the development of earth pressures at failure are discussed in Chapter 10 (Earth Retaining Structures).

## **2.10 UNSATURATED SOIL MECHANICS**

As discussed in this Chapter, soil is three phase system that consists of solid particles, liquid and gas. Classical soil mechanics concentrates primarily on the behavior of saturated or dry soils, i.e., a two phase system. For soils in a saturated state, the principle of effective stress is invoked to quantify stress and strain in the soil mass. For soils in a dry state, pore water pressure does not exist and the total stress and effective stress are the same. In reality, all the pore space in soil within the depth of significant influence of geotechnical features is rarely occupied by liquid or gas alone. This is particularly true for soils above the ground water table and soils that are mechanically compacted as in the case of earthworks. In such soils the degree of saturation is generally intermediate between 0% (dry soil) and 100% (saturated soil). Under these conditions, negative pore pressures, i.e., suction, may exist within the soil mass depending upon the type of soil and its grain size distribution. An example of the presence of negative pore pressures is the capillary rise often encountered above the water table. Such negative pore pressures affect all aspects of soil behavior ranging from volume change and shear strength to seepage. Consequently, unsaturated soil behavior impacts a broad array of engineering issues ranging from foundation design and performance to flow through earth embankments and the engineering of facilities on or in expansive, collapsible and compacted soils (ASCE 1993, 1997).

To date the tendency in engineering practice has often been to apply a total stress approach where the effects of negative pore pressures are not properly simulated. In the last couple of decades significant progress has been made to model such negative pore pressures and that field of study is often called “unsaturated soil mechanics.” Discussion of the engineering behavior of unsaturated soils is beyond the scope of this manual. At this stage, it is important simply to realize that advanced studies beyond those discussed in this manual may be required on projects where unsaturated state can significantly affect the engineering behavior of soils. The interested readers are directed to the work by Fredlund and Rahardjo (1993), who provide a comprehensive treatment of unsaturated soils.

[THIS PAGE INTENTIONALLY BLANK]

## **CHAPTER 3.0**

### **SUBSURFACE EXPLORATIONS**

To perform properly, a structure must interact favorably with the soil on which it rests. The modern geotechnical specialist, who often must build in areas that were considered too poor to build upon a few years ago, must be well versed in the fundamentals of soil mechanics. This knowledge will be used in the design of structural foundations and earthworks to answer the following questions. Will settlements be excessive? Can the structure tolerate settlements? Will the proposed foundation type perform better than another type? Can the foundation soils safely support the imposed embankment or footing loads? Will the proposed cut or fill slopes have adequate stability? Are the foundation and earthwork designs cost-effective?

The engineer should have adequate knowledge of the subsurface conditions at a site before attempting to answer these questions. A site- and project-specific subsurface model must be developed for the cost-effective engineering design of a facility. Figure 3-1 shows a flow chart that identifies a recommended process for developing a subsurface model for engineering design. The investment of a few tens of thousands of dollars in a systematic approach as outlined in Figure 3-1 could result in design and construction savings of hundreds of thousands of dollars by preventing costly failures or overly conservative designs.

The process shown in Figure 3-1 is logical and is generally followed on many projects. In many cases, however, old “rules-of-thumb” and “status quo” approaches can result in an unconscious “by-passing” of critical steps. In particular, selection of the correct tests to determine the relevant engineering properties, the interpretation of the results of those tests, and summarization of data are often poorly performed. Rigorous attention to the rational process in Figure 3-1 is required to assure efficient and thorough exploration and testing programs, especially since many projects are fragmented to the extent that drilling, testing, and design are performed by different parties. This document provides guidance on all the items presented in Figure 3-1. The three major steps in the flow chart in Figure 3-1 and the applicable chapters in this document are as follows:

Step 1: Subsurface Exploration and Field Testing (this Chapter)

Step 2: Laboratory Testing and Test Interpretation (Chapters 4 and 5)

Step 3: Engineering Design (Chapters 6 to 10 and Appendix A)

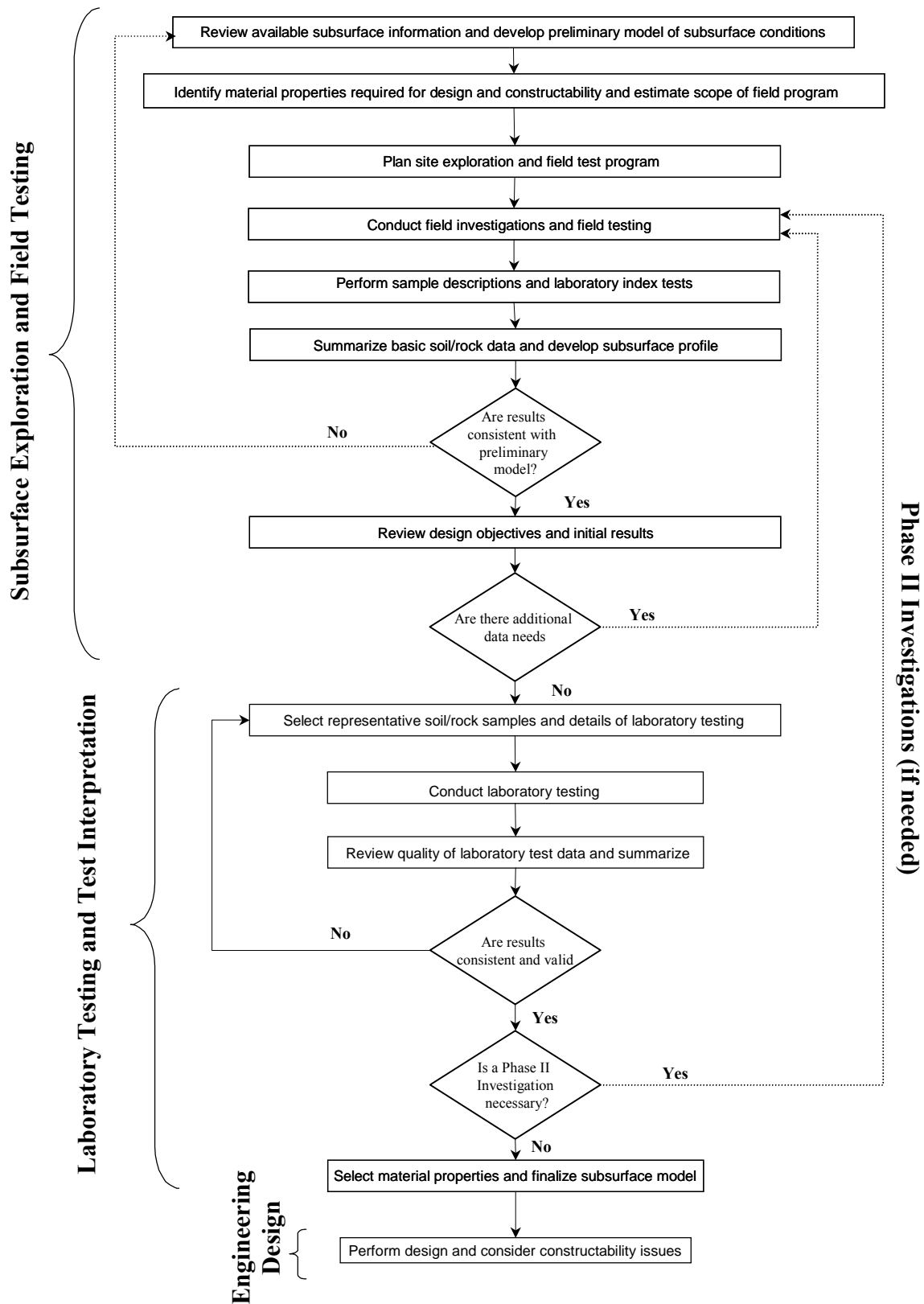


**Figure 3-1. Recommended process for developing subsurface model for engineering design (FHWA, 2002a).**

### 3.01 Primary References

The primary references for this Chapter as well as Chapters 4 and 5 are as follows:

FHWA (2002a). *Geotechnical Engineering Circular 5 (GEC5) - Evaluation of Soil and Rock Properties*. Report No FHWA-IF-02-034. Authors: Sabatini, P.J, Bachus, R.C, Mayne, P.W., Schneider, J.A., Zettler, T.E., Federal Highway Administration, U.S. Department of Transportation.

FHWA (2002b). *Subsurface Investigations (Geotechnical Site Characterization)*. Report No. FHWA NHI-01-031, Authors: Mayne, P. W., Christopher, B. R., and DeJong, J., Federal Highway Administration, U.S. Department of Transportation.

AASHTO (2006). *Standard Specifications for Transportation Materials and Methods of Sampling and Testing*, Parts I and II, American Association of State Highway and Transportation Officials, Washington, D.C.

ASTM (2006). *Annual Book of ASTM Standards – Sections 4.02, 4.08, 4.09 and 4.13*. ASTM International, West Conshohocken, PA.

### 3.1 PREPARING FOR SUBSURFACE EXPLORATION

The initial step in any highway project must include consideration of the soil or rock on which the highway embankment and structures are to be supported. The extent of the site exploration will depend on many factors, not the least of which will be the project scheduling, general subsurface conditions, and the nature of the loads to be supported. In any event, certain basic steps should be followed before exploration equipment is mobilized to the project site. The first step in the exploration is to collect and analyze all existing data. A review of available information prior to the field reconnaissance will help establish what to look for at the site. In the Eighth Rankine Lecture, Glossop (1968) stated the following truism regarding site exploration: **"If you do not know what you should be looking for in a site investigation, you are not likely to find much of value."** For a highway project, basic sources of geotechnical information should be reviewed to determine landform boundaries and to provide a basis for outlining the project subsurface exploration program. Those sources and functional uses are identified in Table 3-1.

**Table 3-1  
Sources of historical site data (after FHWA, 2002a)**

<b>Source</b>	<b>Functional Use</b>	<b>Location</b>	<b>Examples</b>
<b>Utility Maps</b>	<ul style="list-style-type: none"> <li>Identifies buried utility locations</li> <li>Identifies access restrictions</li> <li>Prevents damage to utilities</li> </ul>	Local agencies/utility companies	Power line identification prior to an intrusive exploration prevents extensive power outage, expensive repairs, and bodily harm
<b>Aerial Photographs</b>	<ul style="list-style-type: none"> <li>Identifies manmade structures</li> <li>Identifies potential borrow source areas</li> <li>Provides geologic and hydrological information which can be used as a basis for site reconnaissance</li> <li>Track site changes over time</li> </ul>	Local Soil Conservation Office, United States Geological Survey (USGS), local library, local & national aerial survey companies	Evaluating a series of aerial photographs may show an area on site which was filled during the time period reviewed
<b>Topographic Maps</b>	<ul style="list-style-type: none"> <li>Provides good index map of site area</li> <li>Allows for estimation of site topography</li> <li>Identifies physical features in the site area</li> <li>Can be used to assess access restrictions</li> </ul>	USGS, State Geological Survey	Engineer identifies access areas/restrictions, identifies areas of potential slope instability; and can estimate cut/fill capacity before visiting the site
<b>Existing Subsurface Exploration Report</b>	<ul style="list-style-type: none"> <li>May provide information on nearby soil/rock type; strength parameters; hydrogeological issues; foundation types previously used; environmental concerns</li> </ul>	USGS, United States Environmental Protection Agency (USEPA), State/local agencies, developers, etc.	A five year old report for a nearby roadway widening project provides geologic, hydrogeologic, and geotechnical information for the area, reducing the scope of the exploration
<b>Geologic Reports and Maps</b>	<ul style="list-style-type: none"> <li>Provides information on nearby soil/rock type and characteristics; hydrogeological issues, environmental concerns</li> </ul>	USGS and State Geological Survey	A twenty year old report on regional geology identifies earth fissure rock types (including fracture and orientation data) and groundwater flow patterns
<b>Water/Brine Well Logs</b>	<ul style="list-style-type: none"> <li>Provide stratigraphy of the site and/or regional area</li> <li>Varied quality from state to state</li> <li>Groundwater levels</li> </ul>	State Geological Survey/Natural Resources, Department of water resources	A boring log of a water supply well two miles from the site area shows site stratigraphy facilitating evaluations of required depth of exploration

**Table 3-1 (Continued)**  
**Sources of historical site data (after FHWA, 2002a)**

<b>Source</b>	<b>Functional Use</b>	<b>Location</b>	<b>Examples</b>
<b>Flood Insurance Maps</b>	<ul style="list-style-type: none"> <li>• Identifies 100 and 500 yr floodplains near water bodies</li> <li>• Caution against construction in a floodplain</li> <li>• Provide information for evaluation of scour potential</li> </ul>	Federal Emergency Management Agency (FEMA), USGS, state/local agencies	Prior to exploration, the flood map shows that the site is in a 100 yr floodplain and the proposed structure is moved to a new location
<b>Soil Survey</b>	<ul style="list-style-type: none"> <li>• Identifies site soil types</li> <li>• Permeability of site soils</li> <li>• Climatic and geologic information</li> </ul>	Local Soil Conservation Service	The local soil survey provides information on near-surface soils to facilitate preliminary borrow source evaluation
<b>Sanborn Fire Insurance Maps</b>	<ul style="list-style-type: none"> <li>• Useful in urban areas</li> <li>• Maps for many cities are continuous for over 100 years.</li> <li>• Identifies building locations and type</li> <li>• Identifies business type at a location (e.g., chemical plant)</li> <li>• May highlight potential environmental problems at an urban site</li> </ul>	State library/Sanborn Company (www.sanborncompany.com)	A 1929 Sanborn map of St. Louis shows that a lead smelter was on site for 10 years. This information prevents an exploration in a contaminated area.

A necessary part involved in review of existing data is to identify the major geologic processes that occurred at the project site because this will permit the geotechnical specialist to develop an understanding of how the local soil and rock formations may have developed. The soil formation process and consideration of landforms in designs of geotechnical features is discussed briefly followed by discussions of subsurface exploration programs.

### **3.1.1 Soil Formations and Landforms**

Soils are a result of the weathering of rocks. In general, rocks are classified as igneous, sedimentary, and metamorphic. Igneous rocks are products of melts (magma) generated an unknown distance below the earth's surface. Sedimentary rocks are cemented and/or compressed materials derived from pre-existing sediments deposited in layers by water or by air. A metamorphic rock is any rock that originates by a process of change from what it was previously. Any former igneous, sedimentary, or metamorphic rock can be metamorphosed (changed) into a new metamorphic rock by an increase in temperature and/or pressure and/or by reaction with surrounding hot fluids and gases. Regardless of the type of rock, most weathering takes place near the ground surface. Rock weathering can occur due to mechanical (physical) and/or chemical processes as follows:

- Mechanical or physical process refers to the process whereby the intact rock breaks into smaller fragments. Physical weathering may be caused by expansion resulting from unloading (e.g., exfoliation or spalling off of the exterior surface of the exposed rock), abrasion, temperature changes (e.g., freeze/thaw), erosion by wind or rain, crystal growth (e.g., ice and other crystals such as salt crystals that form as the result of the capillary action of water containing salts in solution), and organic activity (e.g., forces exerted by growing plants and roots in voids and crevasses of rock).
- Chemical process refers to the process whereby the minerals in the rock are altered into new compounds. Chemical weathering is usually preceded by hydration and hydrolysis and may be caused by, oxidation (e.g., chemical reaction with rainwater), solution (e.g., dissolution of limestone) and/or leaching (e.g., dissolution of the cementing agent in the rock). Chemical weathering commonly occurs by fluids seeping into the fractures caused by mechanical (physical) weathering processes. These fluids are chiefly acids created as rainwater dissolves carbon dioxide from the atmosphere and more carbon dioxide and organic acids from the soil. Most chemical weathering processes result in an increase in volume (that causes an increase in stress within the rock mass), lower density materials (e.g., soils), smaller particle sizes (e.g., clay sizes), and more stable minerals (that may decrease the rate of chemical weathering).

The combined effects of the mechanical and chemical weathering processes vary considerably with climate and the mineralogy of the parent rock. The chemical reactions proceed most rapidly and completely in humid tropics and subtropics and least effectively in cold or arid climates (Goodman, 1993). Thus, in the Arctic regions and deserts, the mechanical processes of physical weathering act virtually alone to gradually breakup the rock into a fractured or rubbled mass whereas, in the tropics, the two weathering processes work together rapidly first to break up the rock and then to alter newly exposed rock surfaces during a project's life.

Once the intact rock is broken into fragments, the rate of weathering depends on the particle size and the climate. In general, small particles weather at a faster rate than large ones due to their larger surface area. The weathering processes can result in particle sizes that are not distinguishable by the naked eye (e.g., colloidal particle size) and can be identified only by equipment such as electron microscopes. Based on particle size, the principal terms used by civil engineers to describe soils are gravel, sand, silt and clay. These terms were discussed in Chapter 2 as a function of the particle sizes they represent and some of their physical characteristics. For example, silt and clay particles are finer than the No. 200 sieve (0.075 mm) and exhibit varying properties in presence of water.

Soils created by a particular geologic process assume characteristic topographic features, called **landforms**, which can be readily identified by the geotechnical specialist. A landform contains soils with generally similar engineering properties and typically extends irregularly over wide areas of a project alignment. Early identification of landforms can be used to optimize the subsurface exploration program. Landforms may be described according to the method of formation as **residual soil landforms** or **transported soil landforms**. Soils commonly associated with these two types of landforms are briefly described as follows:

### 3.1.1.1 Residual Soils

A residual soil landform is one that was formed in its present location through weathering of the parent (or bed) rock. Residual soils tend to be characterized by angular to subangular particles, mineralogy similar to parent rock, and the presence of large angular fragments within the overall soil mass. Because residual soil weathers from parent bedrock, its profile with depth represents a history of the weathering process. Figure 3-2 shows a typical weathering profile for metamorphic and igneous rocks. In Figure 3-2, the weathering profile is divided into three zones: *residual soil*, *weathered rock*, and *unweathered rock*. Deere and Patton (1971) present 12 other weathering-profile classification systems proposed by workers from around the world. Regardless of the weathering-profile classification, the following are some of the properties for such profiles:

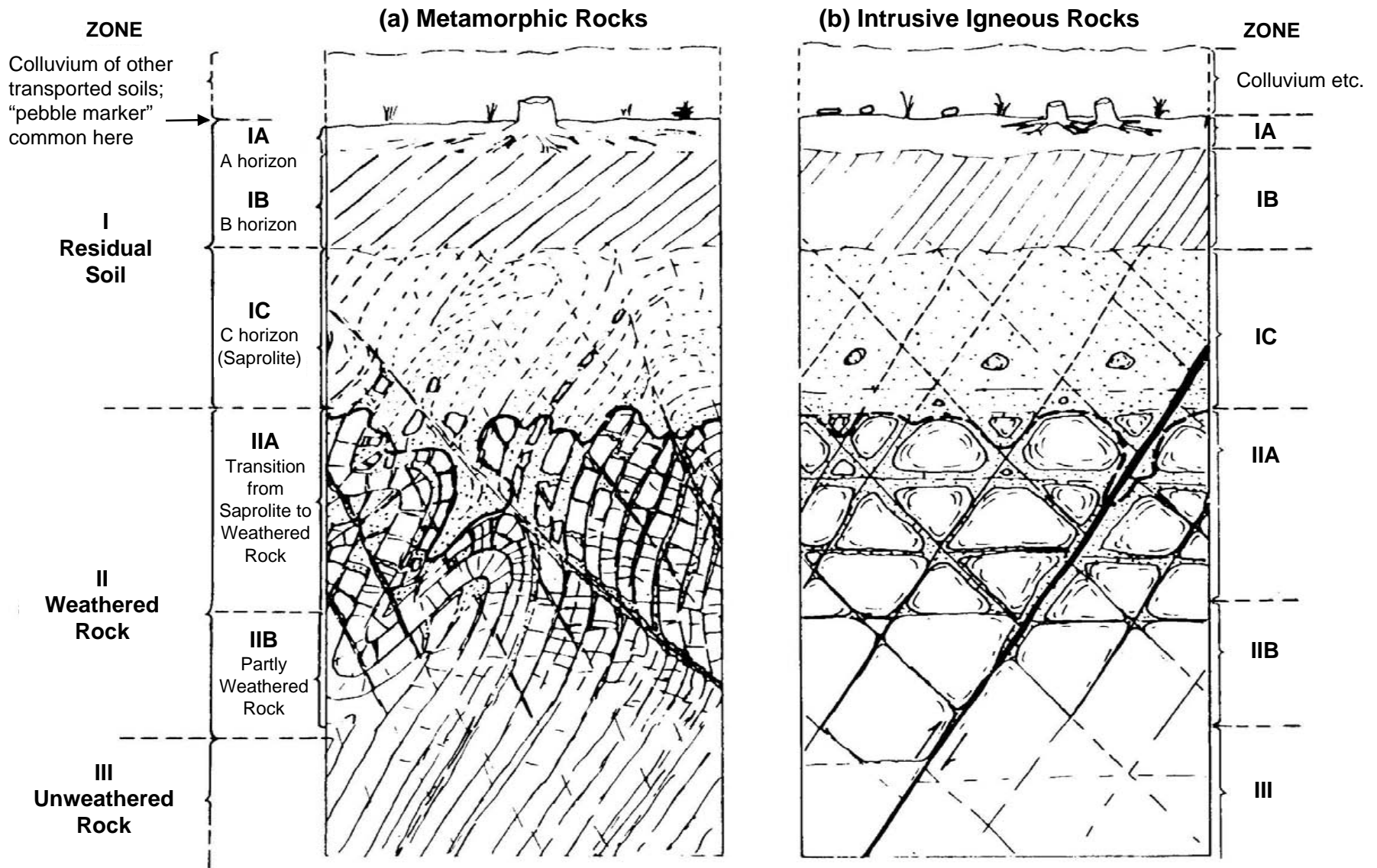


Figure 3-2. Typical weathering profile for metamorphic and igneous rocks (Deere and Patton, 1971).

- The permeability and shear strength gradually change with depth. These two parameters control both the amount of rainfall infiltration and the location of the shear surface when external loads are applied on or in these soils.
- Soil profile thickness and properties depend upon parent bedrock, discontinuities, topography, and climate. Because these factors vary horizontally, the profile can vary significantly over relatively short horizontal distances.
- Deep profiles form in tropical regions where weathering agents are especially strong and advanced stages of chemical weathering form cemented soils called *laterites*. The technical literature often refers to residual soils as tropical soils.
- The material in the transitory zone between residual soil and unweathered rock is called *saprolite*. Saprolites are generally unsaturated, weakly bonded and heterogeneous soils with relict joint systems (Lambe, 1996). Saprolites have widely varying void ratios and widely varying mineralogy and shear strength (Vaughn, *et al.*, 1988).

### 3.1.1.2 Transported Soils

A transported soil is one that was formed from rock weathering at one location and transported by some exterior agent to another location. The transporting agent may be water (principal agent), a glacier, wind, and/or gravity. Often the deposits of transported soils are given names indicative of the mode of transportation causing the deposit, e.g., alluvial deposits, glacial till, etc. Transported soils are characterized by subrounded to rounded particles and a wide variety of particle sizes. Table 3-2 summarizes commonly encountered landforms composed of transported soils, their primary formational process, and their engineering significance.

### 3.1.1.3 Area Concept for Explorations Based on Landforms

Knowledge of the landforms and the engineering properties of the soils and rocks enables the designer to determine the most economical location for a highway alignment and grade, to evaluate design problems for each type of soil or rock, and to determine sources of granular borrow material. Once a landform is identified, the geotechnical specialist can develop an “**area**” **concept** for exploration. In this concept, the lateral extents of landforms in the immediate vicinity of the footprint of the proposed facility are first identified. Then, a limited exploration program (e.g., geologic mapping, geophysical work and some preliminary cone penetration tests and borings) is implemented at strategic locations such that the general characteristics of the landforms are identified. The exploration program can then be refined to obtain specific information on soil types of interest with respect to the footprint of the proposed facility and the anticipated loadings.

**Table 3-2  
Common landforms of transported soils and their engineering significance**

<b>Agent</b>	<b>Landform</b>	<b>Formational Process and General Engineering Significance for Study</b>
Water	Flood Plain	<ul style="list-style-type: none"> <li>• Formed in valleys that are nearly flat and near the high water level of streams. At flood stage the valley is essentially a “flood plain” that is susceptible to widespread shallow flooding.</li> <li>• Generally poor construction site with fine-grained soils and water problems. Potential scour area. Spread footing design below ground will probably require undercut, low foundation pressure and scour protection. Pile foundations probable. Additional shallow explorations required along footing length to determine buried meandering channels. Historic high water levels should be used in design.</li> </ul>
	Coastal Plain	<ul style="list-style-type: none"> <li>• Formed similar to flood plain but in coastal areas.</li> <li>• Consider spread footings for moderate loads except for high water areas. Potential scour area. Soil “set-up” possible for friction piles (see Chapter 9).</li> </ul>
	Terraces	<ul style="list-style-type: none"> <li>• Formed when a stream or water body cuts into a previously deposited sediment or as the stream bed is lowered over geological periods due to normal erosion or to crustal deformations. Terraces are also known as <i>bajadas</i>.</li> <li>• Consider spread footings for lightly loaded foundations.</li> </ul>
	Lakebed (Lacustrine, Varves)	<ul style="list-style-type: none"> <li>• Formed by sedimentation in lake (fresh water) environments. <i>Varves</i> are a particular type of lake deposit formed during glacial periods from seasonal ice melting, which temporarily increased the runoff velocity so that precipitated sand layers alternate with layers of precipitates such as silt or silt-clay made at low velocities.</li> <li>• Suitable only for spread footings to support light loads and even then settlement may be expected. Pile foundation probable and often deep. Obtain undisturbed tube samples for laboratory testing. Consider drilling with “mud” rather than casing. Long-term water observations necessary to determine static water level due to impervious soil. Potential scour area.</li> </ul>
	Deltas	<ul style="list-style-type: none"> <li>• Formed by sediments precipitated at the mouths of rivers or streams into bays, oceans, or lakes.</li> <li>• The use of spread footings must be carefully studied as poor soils often underlie deltaic sands and gravels. The parent material is capable of sustaining high spread footing loads. Piles may be required to penetrate delta material and poor soil. Use casing of adequate size to obtain undisturbed samples of poor soil. Potential scour area.</li> </ul>
	Alluvial Fans. Filled Valleys (Basin Deposits)	<ul style="list-style-type: none"> <li>• Formed similar to delta deposits, but typically found in arid areas where mountain stream runoff flows into wide valleys or on to the plains at the mouths of streams. In arid climates, alluvial fans can become cemented by salts left in the ground by evaporating water or by dropping groundwater. Cemented soils can be loose to dense (e.g., <i>caliche</i>) or open-graded (<i>collapsible</i>).</li> <li>• Consider spread footings for low to moderate loads except at lower elevation of alluvial fans where high water table is possible. In case of collapsible soils, either treat the soils such that collapse potential is mitigated or use deep foundations to bypass such soils. If the caliche is firm to hard, spread foundations can be used.</li> </ul>

**Table 3-2 (continued)**  
**Common landforms of transported soils and their engineering significance**

<b>Agent</b>	<b>Landform</b>	<b>Formation and General Engineering Significance for Study</b>
Ice (Glacier) and meltwater associated with ice	Moraines (Terminal, lateral)	<ul style="list-style-type: none"> <li>• Formed by soil deposits pushed into ridges around the periphery of a glacier. <i>Terminal moraines</i> are ridges of material scraped or bulldozed to the front of a glacier; <i>lateral moraines</i> develop along the sides of a glacier. The moraine may not be a single nicely rolled ridge, but rather a highly serrated, above ground level, earth mass.</li> <li>• Advisable to use spread footings for all foundation loads. Piles should not be used due to very difficult driving and boulders. Core all rock to 10 ft (3.0 m) in case boulders are encountered.</li> </ul>
	Glacial Till (ground moraine)	<ul style="list-style-type: none"> <li>• Glacial Till (also termed ground moraine or simply till) is the deposit of ice-suspended material through the bottom of the glacier. As glaciers melted, materials suspended in the ice precipitated onto the underlying soil or rock to form glacial till. Till deposits are characterized by all sizes of particles with no obvious arrangement. Much of northern US has glacial till.</li> <li>• Where till is unsorted, dense and contains considerable sand and gravel, it is advisable to use spread footings for all foundation loads. Piles should not be used due to difficult driving conditions and boulders. Core all rock encountered to depth of 10 ft (3.0 m) as large boulders may be encountered. Long-term water observations necessary to determine static water level due to soil density.</li> </ul>
	Outwash	<ul style="list-style-type: none"> <li>• Sediments precipitated from glacial melts in the discontinuities between ridges in moraines. Small lakes may temporarily form in depressions behind ridges, producing lacustrine (fresh water) sediments.</li> <li>• Spread footing normally used to support moderate to heavy foundation loads. Piles, if required, will be short. Use large diameter sample spoon to permit representative sample to be obtained as average particle size may jam 1-3/8 in (35.3 mm) sample spoon. Standard penetration test may be erratically high due to large particle sizes. Commercial value as sand and gravel sources since the material often contains very little amount of fines, i.e., particle size less than No. 200 (0.075 mm) sieve.</li> </ul>
	Eskers	<ul style="list-style-type: none"> <li>• Eskers are deposits (usually as ridges) formed by precipitation of water-suspended material flowing in ice tunnels.</li> <li>• Advisable to use spread footings for all loads as soil contains much gravel and is dense. Piles not recommended. Large diameter sample spoon recommended as above for outwash. Commercial value as sand and gravel sources since the material often contains very little amount of fines, i.e., particle size less than No. 200 (0.075 mm) sieve.</li> </ul>
	Drumlins	<ul style="list-style-type: none"> <li>• Drumlins are isolated mounds of glacial debris varying from about 35 (10 m) ft to 230 ft (70 m) high and 650 ft (200 m) to 2600 ft (800 m) long. Most drumlins are of the order of 100 ft (30 m) or less in height and 1000 ft (300 m) or less in length. They often occur in groups called drumlin fields (several).</li> <li>• Suitable for spread footing design with moderate to heavy loads. Piles seldom used due to dense coarse nature of subsoil. Commercial value as sand and gravel sources since the material often contains very little amount of fines, i.e., particle size less than No. 200 (0.075 mm) sieve.</li> </ul>

**Table 3-2 (continued)**  
**Common landforms of transported soils and their engineering significance**

<b>Agent</b>	<b>Landform</b>	<b>Formation and General Engineering Significance for Study</b>
Wind (Aeolian)	Loess	<ul style="list-style-type: none"> <li>• Formed by wind blowing silt and clay with the deposit held together by a montmorillonite binder. Generally derived from glacial outwash in the US. Low density (often less than 90 pcf (14 kN/m<sup>3</sup>)), low wet strength (i.e., collapsible upon water ingress), has the ability to stand on vertical cuts due to cementing agents between particles.</li> <li>• Consider spread footings for low to moderate loads. Heavy loads should be pile supported with the bearing resistance obtained below the loess deposit. Accurate ground water level determination important.</li> </ul>
	Sand Dune	<ul style="list-style-type: none"> <li>• Formed by wind action blowing the sand. Transport occurs mainly along the ground until an obstruction is met, whereupon a dune (or mound) forms. Later winds may demolish the dune and redeposit the material at a new location further downwind. Dune sands tend to be well rounded from abrasion.</li> <li>• Consider spread footings for small foundations not subject to vibratory loading. Heavy structural loads should be supported on friction piles.</li> </ul>
Gravity	Colluvium	<ul style="list-style-type: none"> <li>• Formed by physical and chemical weathering of bedrock. The fragmented particles, given sufficient topographic relief, tend to move down slopes under gravitational forces and accumulate as distinctive deposits along the lower portions of slopes, in topographic depressions, and especially at the base of cliffs.</li> <li>• The characteristics of colluvial materials vary according to the characteristics of the bedrock sources and the climate under which the weathering and transport occur. From an engineering viewpoint, colluvium is weakly stratified and consists of a heterogeneous mixture of soil and rock fragments ranging in size from clay particles to rock more than 3 ft (1 m) in diameter. Because they are found along the lowest portions of valley sides, such deposits frequently need to be partially excavated to allow passage of transportation facilities. The resulting cut slopes are commonly unstable and require constant monitoring and maintenance. Colluvial soils are prone to creep (slow movement with time) and landslides are common in such soils.</li> </ul>
	Talus (Scree)	<ul style="list-style-type: none"> <li>• Talus is colluvium composed of predominantly large fragments. Talus fragments can be huge boulders tens of feet across; however, a lower size limit has not been well defined. With time, the coarse fragments may degrade or finer materials may be added by wind or water transport so that these deposits slowly become infilled with a matrix of fine-grained materials. The degree of infilling of these talus deposits may vary horizontally and vertically.</li> <li>• Rock-supported talus is often inherently unstable and may be hazardous to even walk across. Furthermore, the open structure is porous. Talus deposits are not suitable for engineering structures. Talus deposits could be used to make riprap.</li> </ul>

The area concept is a powerful tool, particularly for linear highway facilities, as it streamlines the subsurface exploration program costs and provides the planning engineer with useful data during the design and construction phases of a project. It also permits early identification of the type and extent of problem soils to be encountered during construction and therefore allows construction costs to be estimated more accurately.

### **3.2 FIELD RECONNAISSANCE**

Application of the area concept requires the use of proper subsurface exploration equipment and techniques. In particular the use of wide area exploration techniques such as remote sensing and geophysical techniques can provide insight of general subsurface conditions in the project area economically. An adequate site exploration can be accomplished only under the direction of a geotechnical specialist who knows the general limitations of the exploration equipment as well as the general demands of the project. A field reconnaissance, preferably with the bridge designer, roadway designer, and project manager, is recommended to assess subsurface conditions prior to establishing a subsurface exploration.

The field reconnaissance should include:

1. Inspection of nearby structures to determine their performance with the particular foundation type utilized. If settlement is suspected, the original structural plans should be reviewed and the structure surveyed by using the original benchmark.
2. For water crossings, inspection of structural footings and the stream banks up and down stream for evidence of scour. Take careful note of the stream bed material. Often large boulders exposed in the stream but not encountered in the borings, are an indication of potential subsurface obstructions to pile installation.
3. Recording the location, type, and depth of any existing structures or abandoned foundations that may infringe on the new highway facility.
4. Relating site conditions to the proposed boring operations. Record potential problems with utilities (overhead and underground), site access, private property, or obstructions.

Figure 3-3 is an example of a field reconnaissance form used to record data pertinent to the site. Upon completion of the site inspection, the geotechnical specialist should prepare a terrain reconnaissance report in which the general suitability of the site is assessed. The report should:

Field Reconnaissance Report  
 \_\_\_\_\_ Department of Transportation

Project No: \_\_\_\_\_ County \_\_\_\_\_ Sta. No. \_\_\_\_\_

Reported By: \_\_\_\_\_ Date \_\_\_\_\_

<p>1. Staking of Line            Well Staked _____            Poorly Staked (We can work) _____            Request Division to Restake _____</p> <p>2. Bench Marks          In Place: Yes _____ No _____          Distance from bridge - m (ft) _____</p> <p>3. Property Owners          Granted Permission: Yes _____ No _____          Remarks on Back _____</p> <p>4. Utilities          Will Drillers Encounter Underground or          Overhead Utilities? Yes _____ No _____          Maybe _____ At Which Holes? _____          What Type? _____          Who to See for Definite Location _____          _____</p> <p>5. Geologic Formation _____</p> <p>6. Surface Soils          Sand _____ Clay _____ Sandy Clay _____          Muck _____ Silt _____ Other _____</p> <p>7. General Site Description          Topography            Level _____ Rolling _____ Hillside _____            Valley _____ Swamp _____ Gullied _____          Groundcover            Cleared _____ Farmed _____ Buildings _____            Heavy Woods _____ Light Woods _____            Other _____          Remarks on Back _____</p> <p>8. Bridge Site          Replacing _____          Widening _____          Relocation _____          Check Appropriate Equipment            Truck Mounted Drill Rig/Cone Rig _____            Track Mounted Drill Rig/Cone Rig _____            Failing 1500 _____            Truck Mounted Skid Rig _____            Skid Rig _____            Rock Coring Rig _____            Wash Boring Equipment _____            Water Wagon _____            Pump _____            Hose _____ m (ft)</p>	<p>8. Bridge Site - Continued          Cut Section - m (ft) _____          Fill Section - m (ft) _____          If Stream Crossing:          Will Pontoons Be Necessary? _____          Can Pontoons Be Placed in Water Easily? _____          _____</p> <p>Can Cable Be Stretched Across Stream?          How Long? _____</p> <p>Is Outboard Motorboat Necessary? _____          Current:          Swift _____ Moderate _____ Slow _____          Describe Streambanks scour.          If Present Bridge Nearby:            Type of Foundation _____          Any Problems Evident in Old Bridge Including          Scour _____            (describe on back)          Is Water Nearby for Wet Drilling - m (ft) _____          Are Abandoned Foundations in Proposed          Alignment? _____</p> <p>9. Ground Water Table          Close to Surface - m (ft) _____          nearby Wells - Depth - m (ft) _____          Intermediate Depth - m (ft) _____          Artesian head - m (ft) _____</p> <p>10. Rock          Boulders Over Area? Yes _____ No _____          Definite Outcrop? Yes _____ No _____          (show sketch on back)          What kind? _____</p> <p>11. Special Equipment Necessary _____</p> <p>12. Remarks on Access          (Describe any Problems on Access)          _____</p> <p>13. Debris and Sanitary Dumps          Stations _____          Remarks _____          _____          _____</p> <p>Reference: Modified from 1978 AASHTO Foundation                    Investigation Manual</p>
---	--

**Figure 3-3. Typical field reconnaissance form.**

1. Flag major potential problems, which may preclude construction.
2. Recommend beneficial shifts in location.
3. Present a general discussion of expected subsurface conditions.
4. Present cost estimate for extraordinary geotechnical treatments.
5. Prepare an estimate of subsurface exploration quantities, costs, and time.

This information should be transmitted to all the groups involved with the project such as the project manager, roadway designer, and bridge designer.

### **3.3 SUBSURFACE EXPLORATION PROGRAM**

The procedures employed in any subsurface exploration program are dependent on a variety of factors that vary from site to site. The project design objectives and the expected subsurface conditions have the major influence on the subsurface explorations. Highway projects necessarily involve both earthwork and structural foundations. Typical boring programs for highways on new alignments are established such that basic information is first gathered along the entire highway alignment and subsequent detailed borings are taken as required at the locations of structures or in problem earthwork areas as disclosed by the initial basic program. Subsurface explorations for widening or improvements of existing highways generally are done in one stage as the location is predetermined.

**Consideration should be given, particularly for large or complex projects, to performing geologic mapping and geophysical explorations after the field reconnaissance and prior to any invasive explorations such as borings.** Geologic mapping and geophysical explorations can be quick and provide a much larger coverage of the project area as compared to invasive explorations. The information from field reconnaissance, geologic mapping and geophysical explorations can then be used to setup the conventional subsurface exploration and testing program. Geophysical explorations are discussed in Section 3.15.

After the field reconnaissance and geophysical explorations are completed, “invasive” explorations using drilled borings and in-situ tests must be performed to obtain in-situ properties and physical samples for identification and testing. The sampling techniques and tools are discussed in Section 3.4 and other sections of this chapter. The objectives for such explorations are as follows:

1. Determine stratigraphy.
  - a. physical description and extent of each stratum.
  - b. thickness and elevation of top and bottom of each stratum.
  
2. For fine-grained soils (each stratum) determine:
  - a. natural moisture contents.
  - b. Atterberg limits.
  - c. stiffness.
  - d. presence of organic materials.
  - e. evidence of desiccation or previous soil disturbance, shearing, or slickensides.
  - f. swelling characteristics.
  - g. unconfined compressive strength - typically estimated from Standard Penetration Tests or Cone Penetration Tests.
  - h. shear strength.
  - i. compressibility.
  
3. For coarse-grained soils (each stratum) determine:
  - a. in-situ density (average and range) typically determined from Standard Penetration Tests or Cone Penetration Tests.
  - b. grain-size distributions (gradation).
  - c. presence of organic materials.
  
4. Determine depth to ground water (for each aquifer if more than one is present).
  - a. piezometric surface over site area: existing, past, and probable range in future (observe at several times).
  - b. perched water table.
  
5. Determine depth to bedrock.
  - a. depth over entire site.
  - b. type of rock.
  - c. extent and character of weathering.
  - d. joints, including distribution, spacing, whether open or closed, and joint infilling.
  - e. faults.
  - f. solution effects in limestone or other soluble rocks.
  - g. core recovery and soundness (RQD).
  - h. hardness and strength.

### 3.4 SAMPLING TECHNIQUES AND TOOLS

The purpose of this section is to provide information on various in-situ testing methods that are currently used to establish site-specific soil and rock properties for design and construction. The execution of a conventional subsurface exploration and testing program usually includes rotary drilling, Standard Penetration Testing (SPT), disturbed and undisturbed sample recovery, and laboratory testing. Although procedures for these commonly performed activities are described in AASHTO and ASTM standards and are well known to most geo-professionals, important testing details are sometimes overlooked that can result in data having marginal quality. This section discusses the importance of carefully selecting and properly conducting the appropriate field and/or laboratory testing method.

In-situ testing methods are increasingly being used on transportation projects, however testing procedures and test limitations are not as well understood as those of the more conventional methods of subsurface exploration and testing such as the use of drilled borings. In this chapter, procedures for various in-situ and laboratory testing methods are presented as they relate to obtaining high quality data for the evaluation of engineering properties of soils and rocks for transportation projects. Information on equipment calibration, measured test parameters, quality control, and the range of ground conditions that apply to each test is also presented.

Several in-situ tests define the geostatigraphy and provide direct measurements of soil properties and geotechnical parameters. The common in-situ tests include: Standard Penetration Test (SPT), Cone Penetration Test (CPT), Piezocone Test (CPTu), Flat Plate Dilatometer Test (DMT), Pressuremeter Test (PMT), and Vane Shear Test (VST). Although the load is applied differently in each test, the purpose of each test is to measure the corresponding response of the soil in an attempt to evaluate the soil's engineering properties, such as strength and/or stiffness. Figure 3-4 depicts these various devices and a graphical representation of how load is applied.

Some state DOTs perform these tests by using agency-owned equipment. In many cases however, the agency may retain an outside contractor for these services either directly or as part of an overall project development package. Several technical reports and manuals are available that describe these test methods. A brief list of these references is provided in Table 3-3. Agencies that perform or contract for these testing services are encouraged to obtain the references identified in Table 3-3. In this manual, only the SPT and the CPT tests will be discussed since they are the most commonly used.

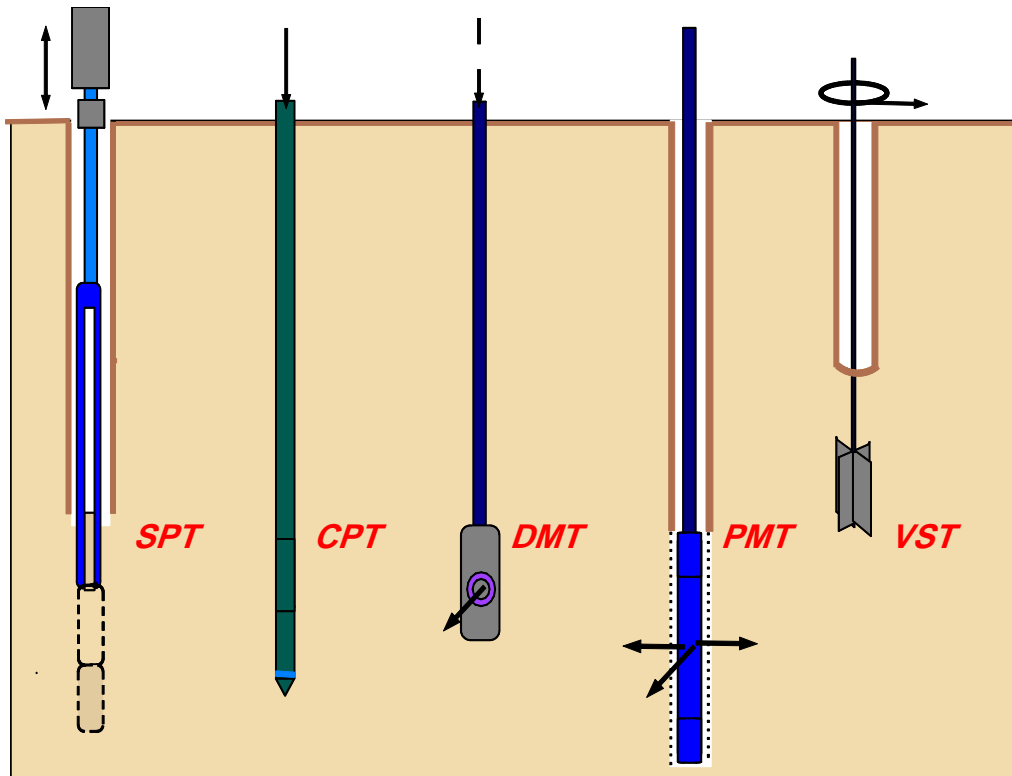


**Figure 3-4. Common in-situ tests for geotechnical site characterization of soils (FHWA, 2002b).**

Boreholes are required for conducting the SPT and normal versions of the PMT and VST. Therefore a drill rig and crew are required for the performance of these tests. Boreholes are not required for the CPT, CPTu, and DMT; therefore these tests are called “direct-push” technologies. Although boreholes are not required for these tests, special mobilized equipment and data acquisition systems are required. Specialized versions of the PMT (i.e., full-displacement type) and VST can be conducted without boreholes. In such cases either standard drill rigs or mobile hydraulic systems (cone trucks) are used to push the probes to the required test depths. Obviously direct push test methods are not suitable in soil profiles that contain boulders, hard cemented layers and bedrock. For such profiles, borehole methods prevail as the testing device may be advanced through the hard layers by coring or non coring techniques. An advantage of direct-push soundings is that cuttings or spoil are not generated, however, this advantage is offset by a significant disadvantage, i.e., no soil sample is retrieved for classification or subsequent laboratory testing. Another advantage of the CPT and CPTu tests is that they provide a continuous record of soil response through the entire depth of the direct push. The other tests are performed at discrete intervals so that the soil’s response is measure at specific depths only. In addition, important layers can be missed with any of the discrete interval test methods.

**Table 3-3**  
**Reference publications on in-situ testing (FHWA, 2002b)**

<b>Test Method</b>	<b>AASHTO/ ASTM Designation</b>	<b>Reference</b>
SPT	AASHTO T206  ASTM D 1586	FHWA (2002b). <i>Subsurface Investigations (Geotechnical Site Characterization)</i> . Report No. FHWA NHI-01-031, Authors: Mayne, P. W., Christopher, B. R., and DeJong, J., Federal Highway Administration, U.S. Department of Transportation.
CPT, CPTu, SCPTu	ASTM D 3341, D5778	FHWA (1992a). <i>The Cone Penetrometer Test</i> . Report No. FHWA NHI-91-043, Authors: Riaund J-L and Miran J., Federal Highway Administration, U.S. Department of Transportation.  Lunne, T., Robertson, P.K., and Powell, J.J.M. (1997) <i>Cone Penetration Testing in Geotechnical Practice</i> , E & F Spon.
DMT	Suggested ASTM Method	FHWA (1992b). <i>The Flat Dilatometer Test</i> . Report No. FHWA NHI-91-044, Authors: Riaund J-L and Miran J., Federal Highway Administration, U.S. Department of Transportation.
PMT	ASTM D 4719	FHWA (1989a). <i>The Pressuremeter Test for Highway Applications</i> . Report No. FHWA IP-89-008, Authors: Briaud J-L, Federal Highway Administration, U.S. Department of Transportation.  Clarke, B.G. (1995) <i>Pressuremeters in Geotechnical Design</i> , Blackie Academic & Professional.
VST	ASTM D 2573	ASTM (1988). <i>Vane Shear Strength Testing in Soils: Field and Laboratory Studies</i> , American Society for Testing and Materials, Committee D-18 on Soil and Rock for Engineering Purposes, Philadelphia, PA.

### 3.5 BORING METHODS

Geotechnical borings are a critical component of any subsurface exploration program. They are performed to satisfy several objectives including those listed below.

- identify the subsurface distribution of materials with distinctive properties, including the presence and thickness of distinct layers;
- retrieve samples of each layer for laboratory tests to determine engineering properties;
- determine depth to groundwater; and
- provide access for the introduction of in-situ testing devices.

There are many types of equipment used in current practice for advancing a soil or rock boring. Typical types of soil borings are listed in Table 3-4(a), rock coring methods in Table 3-4(b), and other exploratory techniques in Table 3-4(c). Detailed information on soil and rock boring procedures can be found in AASHTO (1988), FHWA (2002b), and ASTM D 4700. A brief description of typical soil boring methods is provided below (Day, 1999).

#### 3.5.1 Auger Borings

An auger is an apparatus with a helical shaft that can be manually or mechanically advanced to bore a hole into soil. Large and small diameter augers are shown in Figure 3-5. The practice of advancing a borehole with a mechanical auger consists of rotating the auger while applying a downward pressure on the auger to penetrate soil and possibly weak or weathered rock. The auger may be continuous, where the helix extends along the entire length of the shaft, or discontinuous when the auger helix is at the bottom of the drill stem.

- Discontinuous or single flight auger borings and bucket auger borings. There are basically two types of discontinuous augers: discontinuous flight augers and bucket augers. Commonly available discontinuous flight augers have diameters ranging from 0.25 to 3 ft (0.075 to 1 m) and bucket augers have diameters ranging from 1 to 8 ft (0.3 to 2.5 m). For discontinuous flight auger borings, the auger is periodically removed from the hole and the soil lodged in the grooves of the flight auger is removed. When a bucket auger is used, it too is periodically removed from the hole and the soil in the bucket removed. A casing is generally not used for discontinuous flight and bucket auger borings. Therefore, these methods are not recommended for boreholes deeper than 35 ft (10 m), or where the hole may cave-in during the

excavation of loose or soft soils, or when the boring is below the groundwater table. In firm stiff clays, discontinuous auger borings can be performed to depths in excess of 35 ft (10 m).

- Continuous flight auger borings. As the name implies, continuous flight augers have the auger flights continuous along the entire length of the auger. As shown in Figure 3-6a, there are two types of continuous flight augers: **solid stem** and **hollow stem**. For both of these type augers the drill cuttings are returned to the ground surface via the auger flights. The solid stem auger must be removed from the borehole to allow access to the hole for insertion of sampling or testing devices. Because the auger must be periodically removed from the borehole, a solid stem auger is not appropriate in sands and soft soils or in soil deposits where groundwater is close to the surface. A hollow-stem auger has a circular hollow core that allows for sampling through the center of the auger. As shown in Figure 3-6c, hollow-stem augers come in a variety of diameters. The hollow-stem auger acts like a casing and allows for sampling in loose or soft soils or when the excavation is below the ground water table. A plug (Figure 3-6d) is necessary when hollow stem augers are advanced to prevent cuttings from migrating through the hollow stem. The plug is removed to permit SPT sampling. In loose sands and soft clays extending below the water table, drilling fluids are often used to minimize and mitigate disturbance effects and keep the hole open. The components of the hollow stem auger system are shown in Figure 3-6b.



(a)



(b)

**Figure 3-5. (a) Large diameter auger, (b) Small diameter continuous flight auger.**

**Table 3-4(a)**  
**Soil and soft rock boring methods (FHWA, 2002a)**

<b>Method</b>	<b>Procedure</b>	<b>Applications</b>	<b>Limitations / Remarks</b>
Auger boring (ASTM D 1452)	Dry hole drilled with hand or power auger; samples recovered from auger flights	In soil and soft rock; to identify geologic units and water content above water table	Soil and rock stratification destroyed; sample mixed with water below the water table
Hollow-stem auger boring	Hole advanced by hollow-stem auger; soil sampled below auger as in auger boring above	Typically used in soils that would require casing to maintain an open hole for sampling	Sample limited by larger gravel; maintaining hydrostatic balance in hole below water table is difficult
Wash-type boring	Light chopping and strong jetting of soil; cuttings removed by circulating fluid and discharged into settling tub	Soft to stiff cohesive materials and fine to coarse granular soils	Coarse material tends to settle to bottom of hole; should not be used in boreholes above water table where undisturbed samples are desired.
Becker Hammer Penetration Test (BPT)	Hole advanced using double acting diesel hammer to drive a 6.6-in (168 mm) double-walled casing into the ground. Several sizes are available.	Typically used in soils with gravel and cobbles; casing is driven open-ended if sampling of materials is desired	Skin friction of casing difficult to account for; unsure as to the repeatability of test
Bucket Auger boring	A 2 to 4 ft (0.6 to 1.2 m) diameter drilling bucket with cutting teeth is rotated and advanced. At the completion of each advancement, the bucket is retrieved from the boring and soil is emptied on the ground.	Most soils above water table; can dig harder soils than above types and can penetrate soils with cobbles and boulders if equipped with a rock bucket	Not applicable in running sands; used for obtaining large volumes of disturbed samples and where it is necessary to enter a boring to make observations

**Table 3-4(b)**  
**Rock core drilling methods (FHWA, 2002a)<sup>(1)</sup>**

<b>Method</b>	<b>Procedure</b>	<b>Type of sample</b>	<b>Applications</b>	<b>Limitations / Remarks</b>
Rotary coring of rock (ASTM D 2113; AASHTO T 225)	Outer tube with diamond (or tungsten carbide) bit on lower end rotated to cut annular hole in rock; core protected by stationary inner tube; cuttings flushed upward by drill fluid	Rock cylinder 1 in to 4 in (25 to 100 mm) in diameter and as long as 10 ft (3 m), depending on rock soundness. Standard coring size is 2-1/8 in (54 mm) diameter.	To obtain continuous core in sound rock (percent of core recovered depends on fractures, rock variability, equipment, and driller skill)	Core lost in fracture or variable rock; blockage prevents drilling in badly fractured rock; dip of bedding and joint evident but not strike
Rotary coring of rock, wire line	Same as ASTM D 2113, but core and stationary inner tube retrieved from outer core barrel by lifting device or “overshot” suspended on thin cable (wire line) through special large-diameter drill rods and outer core barrel	Rock cylinder 1-1/8 in to 3-3/8 in (28 to 85 mm) wide and 5 ft to 10 ft (1.5 to 3 m) long	To recover core better in fractured rock which has less tendency for caving during core removal; to obtain much faster cycle of core recovery and resumption of drilling in deep holes	Core lost in fracture or variable rock; blockage prevents drilling in badly fractured rock; dip of bedding and joint evident but not strike
Rotary coring of swelling clay, soft rock	Similar to rotary coring of rock; swelling core retained by third inner plastic liner	Soil cylinder 1-1/8 in to 3-3/8 in (28 to 85 mm) wide and 2 ft to 5 ft (0.6 m to 1.5 m) long encased in plastic tube	In soils and soft rocks that swell or disintegrate rapidly in air (protected by plastic tube)	Sample smaller; equipment more complex than other soil sampling techniques

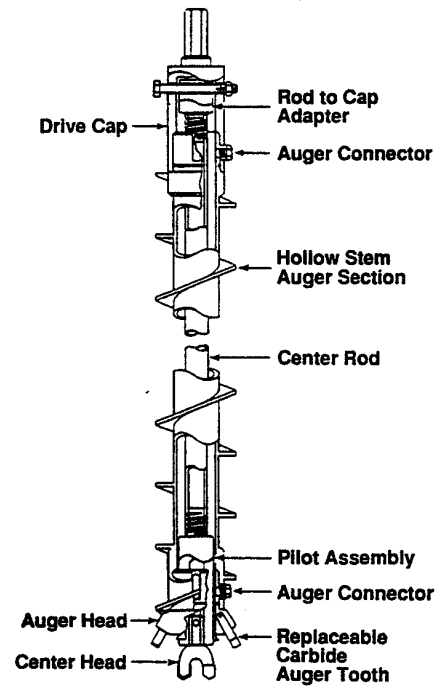
<sup>(1)</sup> See Section 3.6.4 for additional discussion on types of core barrels (i.e., single-, double-, or triple-tube).

**Table 3-4(c)**  
**Other exploratory techniques (FHWA, 2002a)**

<b>Method</b>	<b>Procedure</b>	<b>Type of sample</b>	<b>Applications</b>	<b>Limitations / Remarks</b>
Borehole camera	Inside of core hole viewed by circular photograph or scan	No sample, but a visual representation of the material	To examine stratification, fractures, and cavities in hole walls	Best above water table or when hole can be stabilized by clear water
Pits and Trenches	Pit or trench excavated to expose soils and rocks	Chunks cut from walls of trench; size not limited	To determine structure of complex formations; to obtain samples of thin critical seams such as failure surface	Moving excavation equipment to site, stabilizing excavation walls, and controlling groundwater may be difficult; useful in obtaining depth to shallow rock and for obtaining undisturbed samples on pit/trench sidewalls; pits need to be backfilled
Rotary or cable tool well drill	Toothed cutter rotated or chisel bit pounded and churned	Pulverized	To penetrate boulders, coarse gravel; to identify hardness from drilling rates	Identification of soils or rocks difficult
Percussive Method (jack hammer or air track)	Impact drill used; cuttings removed by compressed air	Rock dust	To locate rock, soft seams, or cavities in sound rock	Drill becomes plugged by wet soil



(a)



(b)



(c)



(d)

**Figure 3-6. (a) Solid stem auger and hollow stem auger, (FHWA, 2002b) (b) Hollow stem auger components (ASTM D 4700), (c) Sizes of hollow stem auger flights (FHWA, 2002b), (d) Outer and inner assembly of hollow stem auger (FHWA, 2002b).**

### 3.5.2 Wash-type Borings

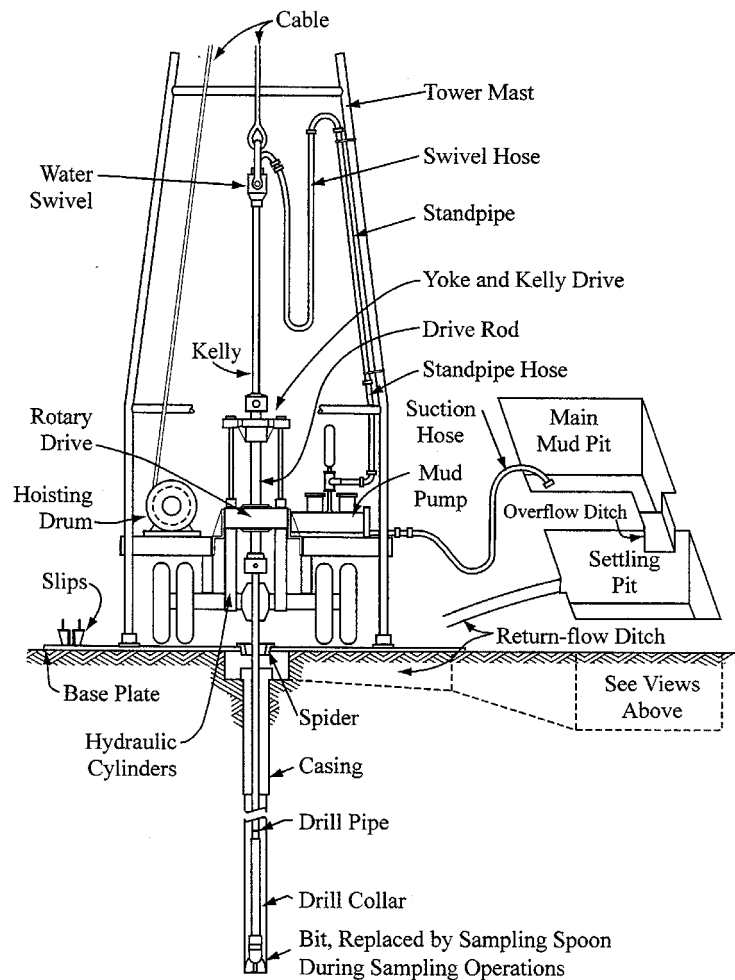
Wash-type borings use circulating drilling fluid (e.g., water or mud) to remove cuttings from the borehole, Figure 3-7. Cuttings are created by the chopping, twisting, and jetting action of the drill bit that breaks the soil or rock into small fragments. Tri-cone bits are often used in dense soil or soft rock. If bentonite or a polymeric drilling mud cannot be used to maintain an open borehole, casings are often used to prevent cave-in of the borehole. The use of casing will require a significant amount of additional time and effort but will result in a protected borehole. When drilling mud is used during subsurface boring, it will be difficult to classify the soil from the auger cuttings because of contamination with the mud. Also, the outside of samples may become coated with drilling mud.

The properties of the drilling fluid and the quantity of water pumped through the drill bit will determine the size of particles that can be removed from the boring with the circulating fluid. In formations containing gravels, cobbles, or larger particles, coarse material may be left at the bottom of the boring. In these instances, cleaning the bottom of the boring with a larger diameter sampler (such as the 3 in (75 mm) OD split barrel sampler) may be needed to obtain a representative sample of the formation.

### 3.5.3 Coring in Rocks

The previously described methods are typically used for soil exploration. The following methods are primarily used for rock exploration.

- *Rotary coring.* This type of coring equipment is most commonly used for rock exploration when an intact core of the rock is desired. Power rotation of the drilling bit is accompanied with introduction of a circulating fluid to remove cuttings from the hole. The drilling bits are specifically designed to core rock, and inner/outer tubes or casings are used to capture the intact core. Table 3-4(b) lists various types of rotary coring techniques for rock, although many of these techniques are also applicable to dense or stiff soil.
- *Percussion drilling.* This type of drilling equipment is often used to penetrate hard rock for subsurface exploration or for the purpose of drilling wells. The drill bit works much like a jackhammer, rising and falling to break up and crush the rock material. Air is commonly used to clean the hole and transport the cuttings to the ground surface. Table 3-4(c) includes a description on the use of the percussion drilling techniques.



(a)



(b)



(c)

**Figure 3-7. (a) Schematic of drilling rig for rotary wash methods (after Hvorslev, 1948), (b) Typical drilling configuration, (c) Settling basin (mud tank).**

## 3.6 SAMPLING METHODS

### 3.6.1 Disturbed Sampling of Soil

Disturbed sampling of soil provides a means to evaluate stratigraphy by visual examination and to obtain soil specimens for laboratory index testing. Disturbed samples are usually collected using split-barrel samplers (Figure 3-8; AASHTO T 206, ASTM D 1586), although several other techniques are available for disturbed sample collection in boreholes (see Table 3-5(a) and 3-5(b)). Shallow disturbed samples can also be obtained by using hand augers and test pits. Direct push methods, such as GeoProbe sampling, can be used to obtain continuous disturbed samples but these methods have limitations in sampling depth similar to those of solid stem and bucket augers (i.e., generally good for depths less than 33 feet (10 meter) unless in firm to stiff clays). Samples obtained via disturbed sampling methods are generally used for index property testing in the laboratory. They should not be used to prepare specimens for consolidation and strength tests.



**Figure 3-8. Split barrel sampler.**

### 3.6.2 Undisturbed Sampling of Soil

Undisturbed soil samples are required for performing laboratory strength and consolidation tests on cohesive soils having consistencies ranging from soft to stiff. High-quality samples for such tests are particularly important for approach embankments and for structural foundations and wall systems that may stress compressible strata. In reality, it is impossible to retrieve truly undisturbed samples since changes in the state of stress in the sample occur upon sampling and removal of the sample from depth. The goal of high-quality undisturbed sampling is to minimize the potential for: (1) alteration of the soil structure; (2) changes in moisture content or void ratio; and (3) changes in chemical composition of the soil. Due to cost and ease of use, the thin-walled Shelby tube (Figure 3-9) is the most commonly used sampler for obtaining relatively undisturbed samples of soft to stiff fine-grained soils.

**Table 3-5(a)**  
**Common samplers to retrieve disturbed soil samples (modified after NAVFAC, 1986a)**

<b>Sampler</b>	<b>Typical Dimensions</b>	<b>Soils that Give Best Results</b>	<b>Method of Penetration</b>	<b>Cause of Low Recovery</b>	<b>Remarks</b>
Split Barrel	Standard is 2 in (50 mm) outside diameter (OD) and 1-3/8 in (35 mm) inside diameter (ID)	All soils finer than gravel size particles that allow sampler to be driven; gravels invalidate drive data; A soil retainer may be required in granular soils.	140 lb (64 kg) hammer driven	Gravel may block sampler	A SPT is performed using a standard penetrometer and hammer (see text); samples are extremely disturbed
Continuous helical-flight auger	Diameters range 3 in to 16 in (75 to 400 mm); penetrations to depths exceeding 50 ft (15 m)	Most soils above water table; will not penetrate hard soils or those containing cobbles or boulders	Rotation	Hard soils, cobbles, boulders	Method of determining soil profile, bag samples can be obtained; log and sample depths must account for lag time between penetration of bit and arrival of sample at surface, to minimize errors in estimated sample depths

**Table 3-5(b)**  
**Common samplers to retrieve disturbed soil samples (modified after NAVFAC, 1986a)**

<b>Sampler</b>	<b>Typical Dimensions</b>	<b>Soils that Give Best Results</b>	<b>Method of Penetration</b>	<b>Cause of Low Recovery</b>	<b>Remarks</b>
Disc auger	Up to 3.5 ft (1 m) diameter; usually has maximum penetration depth of 25 ft (8 m)	Most soils above water table; will not penetrate hard soils or those containing cobbles or boulders	Rotation	Hard soils, cobbles, boulders	Method of determining soil profile, bag samples can be obtained; log and sample depths must account for lag time between penetration of bit and arrival of sample at surface, to minimize errors in estimated sample depths
Bucket auger	Up to 4 ft (1.2 m) diameter common; larger sizes available; with extensions, depth over 80 ft (25 m) are possible	Most soils above water table; can penetrate harder soils than above types and can penetrate soils with cobbles and boulders if equipped with a rock bucket	Rotation	Soil too hard to penetrate	Several bucket types available, including those with ripper teeth and chopping tools; progress is slow when extensions are used
Test boring of large samples, Large Penetration Test (LPT)	2 in to 3 in (50 to 75 mm) ID and 2.5 in to 3.5 in (63 mm to 89 mm) OD samplers (examples, Converse sampler, California Sampler)	In sandy to gravelly soils	Up to 350 lb (160 kg) 350 lb hammer driven	Large gravel, cobbles, and boulders may block sampler	Sample is intact but very disturbed; A resistance can be recorded during penetration, but is <u>not equivalent</u> to the SPT N-value and is more variable due to no standard equipment and methods

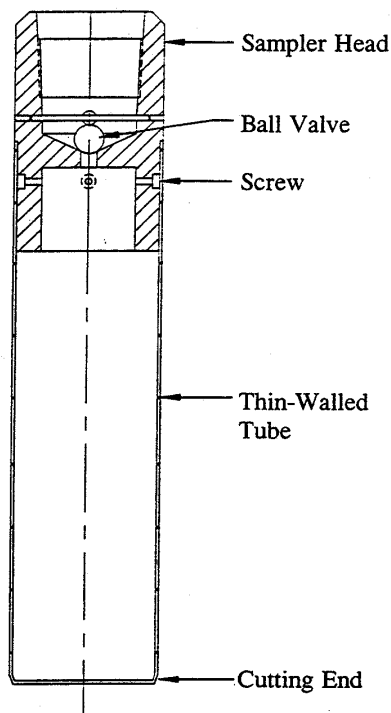


**Figure 3-9. Schematic of thin-walled (Shelby) tube (after ASTM D 4700) and photo of tube with end caps (FHWA, 2002b).**

Thin walled Shelby tube sampling is discussed in Section 3.5.3. Depending upon the in-situ condition of the fine-grained soil (e.g., stiffness and whether significant granular material is in the soil matrix), alternative sampling devices may be used to obtain nominally undisturbed soil samples. These alternative samplers include:

- Stationary piston sampler (Figure 3-10);
- Denison sampler (Figure 3-11);
- Pitcher samplers (Figure 3-12);
- Hydraulic piston sampler (Osterberg Sampler).

Summary information on these samplers is provided in Table 3-6 and detailed procedures for these sampling techniques are provided in FHWA (1997, 2002b). Although not common for typical transportation-related projects, a variety of special samplers are available to obtain samples of soil and soft rocks. These specialty samplers include the retractable plug sampler, the Sherbrooke sampler, and the Laval sampler.

**Table 3-6  
Nominally undisturbed soil samplers (modified after NAVFAC, 1986a)**

<b>Sampler</b>	<b>Typical Dimensions</b>	<b>Soils that Give Best Results</b>	<b>Method of Penetration</b>	<b>Cause of Disturbance or Low Recovery</b>	<b>Remarks</b>
Shelby tube (ASTM D 1587; AASHTO T 207)	3 in (76 mm) OD and 2-7/8 in (73 mm) ID most common; available from 2 in to 5 in (50 to 127 mm) OD; 30 in (760 mm) sampler length standard	Cohesive fine-grained or soft soils; gravelly and very stiff soils will crimp tube	Pressing with relatively rapid, smooth stroke; can be carefully hammer driven but this will induce additional disturbance	Erratic pressure applied during sampling, hammering, gravel particles, crimping of tube edge, improper soil types for sampler, pressing tube greater than 80% of tube length	Simplest device for undisturbed samples; boring should be clean before sampler is lowered; little waste area in sampler; not suitable for hard, dense or gravelly soils
Stationary piston	3 in (76 mm) OD most common; available from 2 in to 5 in (50 to 127 mm) OD; 30 in (760 mm) sampler length standard	Soft to medium clays and fine silts; not for sandy soils	Pressing with continuous, steady stroke	Erratic pressure during sampling, allowing piston rod to move during press, improper soil types for sampler	Piston at end of sampler prevents entry of fluid and contaminating material requires heavy drill rig with hydraulic drill head; samples generally less disturbed compared with Shelby tube; not suitable for hard, dense, or gravelly soil
Hydraulic piston (Osterberg)	3 in (76 mm) OD is most common; available from 2 in to 4 in (50 to 100 mm) OD; 36 in (910 mm) sampler length standard	Silts and clays, some sandy soils	Hydraulic or compressed air pressure	Inadequate clamping of drill rods, erratic pressure	Needs only standard drill rods; requires adequate hydraulic or air capacity to activate sampler; samples generally less disturbed compared with Shelby tube; not suitable for hard, dense, or gravelly soil
Denison	3.5 in to 7 in (89 to 177 mm) OD, producing samples 2-3/8 in to 6.3 in (60 to 160 mm); 24 in (610mm) sampler length	Stiff to hard clay, silt, and sands with some cementation, soft rock	Rotation and hydraulic pressure	Improper operation of sampler; poor drilling procedures	Inner tube face projects beyond outer tube, which rotates; amount of projection can be adjusted; generally takes good samples; not suitable for loose sands and soft clays
Pitcher sampler	4 in (100 mm) OD; uses 3 in (76-mm) diameter Shelby tubes; sample length 24 in (610 mm)	Same as Denison	Same as Denison	Same as Denison	Differs from Denison in that inner tube projection is spring controlled; often ineffective in cohesionless soils
Foil Sampler	Continuous samples 2 in (50 mm) wide and as long as 65 ft (20 m)	Fine grained soils including soft sensitive clays, silts, and varved clays	Pushed into the ground with steady stroke; Pauses occur to add segments to sample barrel	Samplers should not be used in soils containing fragments or shells	Samples surrounded by thin strips of stainless steel, stored above cutter, to prevent contact of soil with tube as it is forced into soil

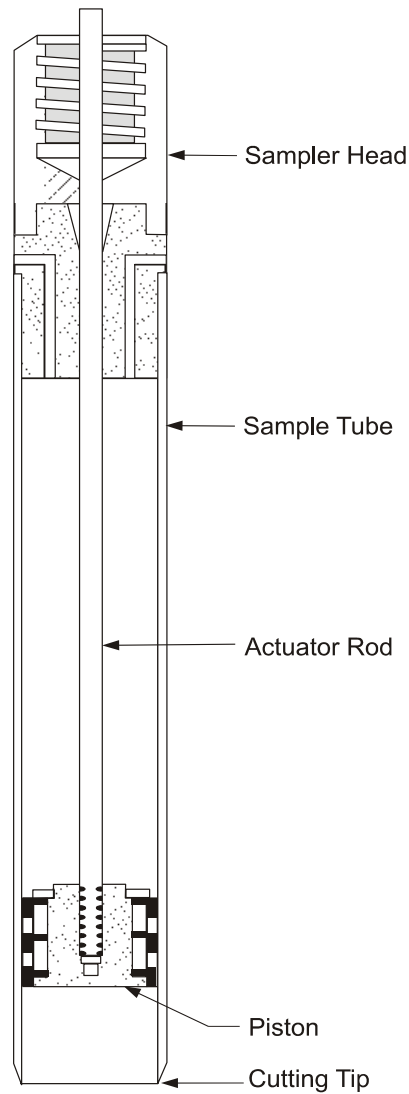


**Figure 3-10. Stationary piston sampler schematic (after ASTM D 4700) and photo (FHWA, 2002b).**

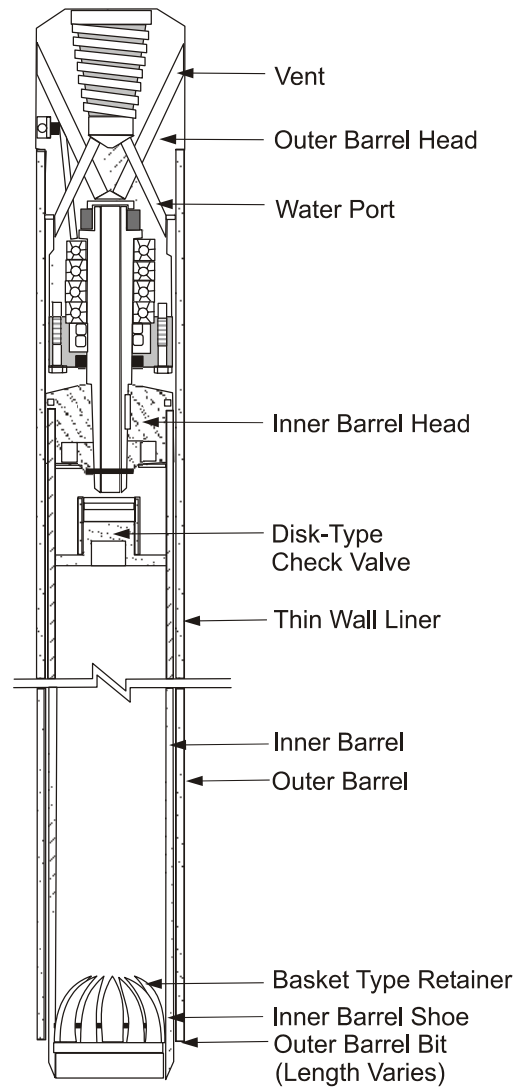


**Figure 3-11. Denison sampler (FHWA, 1997).**

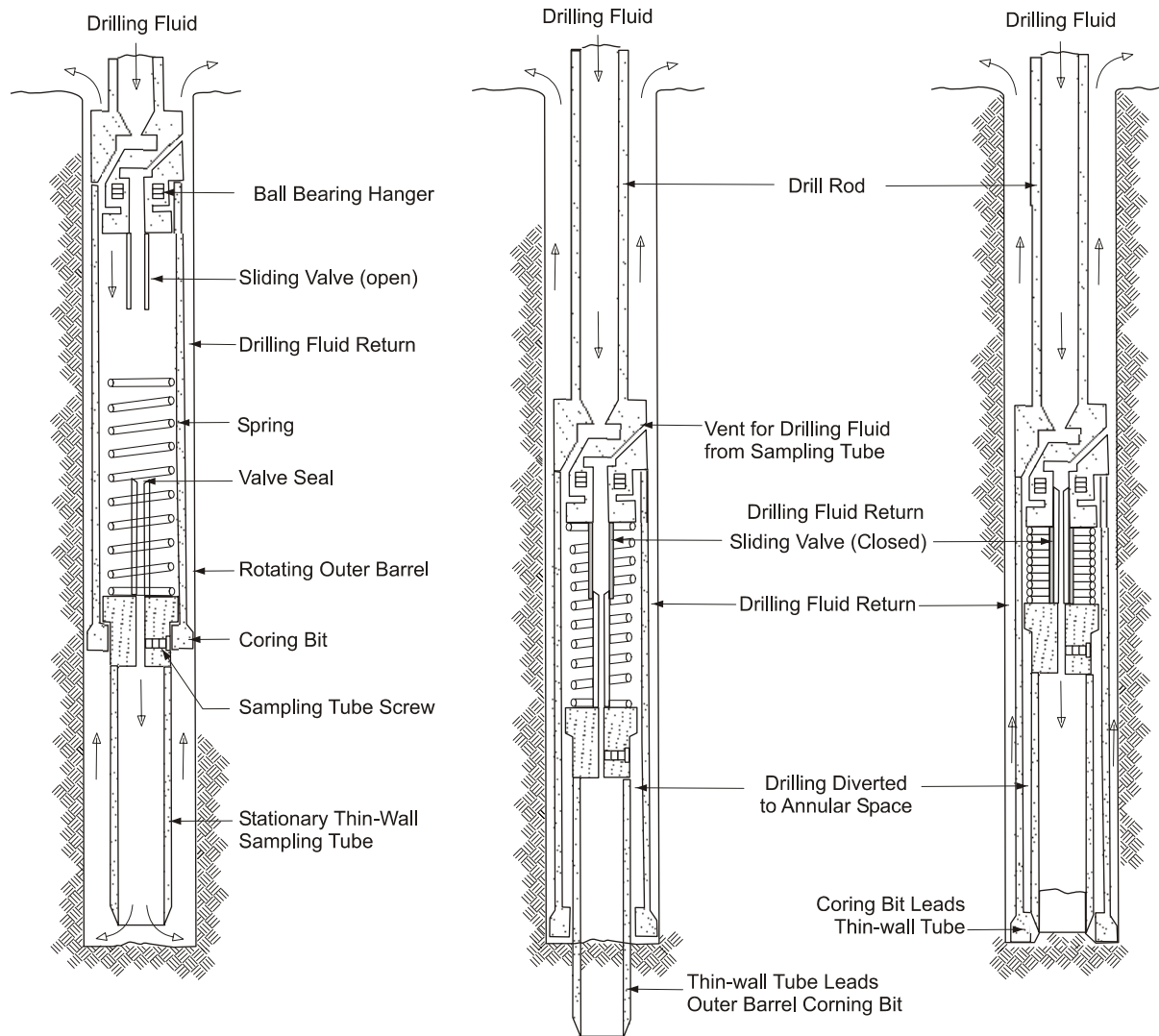


**Figure 3-12. Pitcher sampler (FHWA, 1997, 2002b).**

When dealing with relatively shallow soils that are very stiff, brittle, partially cemented, or that contain coarse gravel or stones, the best method to obtain large relatively undisturbed samples is by block sampling. Block sampling involves isolating a soil column, encasing it in paraffin wax, and covering it with an open-ended box or tube (usually about 12 in (300 mm) square). The bottom is cut, sealed and covered, and the sample is transported to the laboratory. This sampling technique is generally difficult to implement at depths greater than approximately 10 ft (3 m).

### 3.6.3 Thin-Walled (Shelby) Tube Sampling

The importance of appropriate sampling practice using Shelby tubes cannot be over-emphasized. Poor sampling practices, exposure to extreme temperatures, and careless handling of samples can cause sample disturbance that may result in misleading test results that can lead to uneconomical or unsafe designs.

- Geometry of a Thin-Walled Tube: The area ratio (AR) and the inside clearance ratio (ICR) are parameters that are used to evaluate the disturbance potential for different types of soil samplers. These parameters are defined as follows:

$$AR = \frac{D_o^2 - D_i^2}{D_i^2} \times 100 \text{ percent} \quad 3-1a$$

$$ICR = \frac{D_i - D_e}{D_e} \quad 3-1b$$

where  $D_e$  = diameter at the sampler cutting tip,  $D_i$  = inside diameter of the sampling tube, and  $D_o$  = outside diameter of the sampling tube. For a sample to be considered undisturbed, the ICR should be approximately 1 percent and the AR should be 10 percent or less. Using a tube with this ICR value minimizes the friction buildup between the soil sample and the sampler during the advancement of the sampler. Using a tube with an AR value less than 10 percent enables the sampler to cut into the soil with minimal displacement of the soil. Thin-walled tubes (e.g., Shelby tubes) are typically manufactured to meet these specifications, but a thicker walled tube with an ICR of zero is commonly used in the Gulf states (e.g., Texas, Louisiana) to sample very stiff overconsolidated clays. The use of the thicker walled tube minimizes buckling of the sampler in the stiff deposits, and the ICR of zero minimizes sample expansion within the

tube. Additional information on suitable geometry for thin-walled tubes is provided in ASTM D 1587.

- Sample Tube Inspection and Storage: Tubes received from the manufacturer should be inspected to assure that no damage has occurred to the ends of the tubes. Plastic end caps, which will later be used to facilitate securing of the sample, should be placed on the ends of the tube at this time.
- Cleaning Borehole Prior to Sampling: Depending upon the methods used, drilling and sampling procedures will cause some disturbance in the vicinity of the advancing face of a borehole. This is especially the case if a sample is overpushed, if casing is advanced ahead of the borehole, or during continuous sampling operations. It is recommended that a borehole be advanced and cleaned to two to three diameters below the bottom of the previous sample to minimize disturbance. Additionally, after advancement of the borehole, caving may occur at the bottom of the hole. Thus, the bottom of the borehole should be cleaned out thoroughly before the sampling device is advanced. Improper cleaning will lead to severe disturbance of the upper material (accumulated settled material), and possibly disturbance of the entire sample. Cleaning is usually performed by washing materials out of the hole. It should be ensured that the jet holes are not directed downward, for this will erode soft or granular materials to an unknown depth. All settled material should be removed to the edge of the casing. In deep or wide borings, special cleaning augers may be used to decrease time for cleaning and produce a cleaner hole.
- Tube Advancement and Retrieval: Tubes should be advanced without rotation in a smooth and relatively rapid manner. The length of the sampler advancement should be limited to 24 in (600 mm) for a 30 in (760 mm) long tube to minimize friction along the wall of the sampler and allow for loose material in the hole. The amount of recovery should be compared to the advanced length of the sampler to assess whether material has been lost, the sample has swelled, or some caved material has been collected at the top of the tube. The possible presence of caved material should be noted at the top of the tube so that no laboratory moisture content or performance tests are performed on that material. After advancing to the target depth, the drill rod should be rotated one full turn to shear off the bottom of the sample. Prior to shearing, a waiting period of 5 to 15 minutes is recommended for tubes in soft soils to permit the sample to reach equilibrium inside the tube and prevent the sample from falling out the bottom of the tube during retrieval. This waiting period may be reduced for stiffer soils.

- Preparation for Shipment: Upon removal of the sample from the borehole, the ends should be capped with the plastic end caps and the tube should be labeled. The label should be written directly on the tube with a permanent marking pen, and include: (1) tube and boring identification number; (2) sample depth; (3) top and bottom of sample; (4) length of recovery; (5) sampling date; (6) job name and/or number; and (7) sample description. Tube samples that are intended for laboratory performance testing (i.e., strength, consolidation, hydraulic conductivity) should never be extruded from the tube in the field and stored in alternative containers. Samples should be extruded only in the laboratory under controlled conditions. After a thin-walled tube sample has been taken, slough or cuttings from the upper end of the tube should be removed by use of a cleanout tool. The length of sample recovered should be measured and the soil classified for the log. About 1 in (25 mm) of material at the bottom end of the tube should be removed and the cuttings placed in a properly labeled storage jar. Both ends of the tube should then be sealed with at least a 1 in (25 mm) thick layer of microcrystalline (non-shrinking) wax after a plastic disk has been placed to protect the ends of the sample (Figure 3-13a). The use of relatively low temperature wax will minimize shrinkage and potential moisture migration within the sample. The remaining void above the top of the sample should be filled with moist sand. Plastic end caps should then be placed over both ends of the tube and electrician's tape wrapped over the joint between the collar of the cap and the tube and over the screw holes. The capped ends of the tubes are then dipped in molten wax. Alternatively, O-ring packers can be inserted into the sample ends and then sealed (Figure 3-13b). This method of sealing the sample may be preferable as it is cleaner and more rapid than waxing. In both cases, the sample must be sealed to ensure proper preservation of the sample. The tube should be kept vertical, with the top of the sample in the upright position. If the sample needs to be inverted for purposes such as sealing, care should be taken to ensure the sample does not slide within the tube. Samples must be stored upright in a protected environment to prevent freezing, desiccation, and alteration of the moisture content (ASTM D 4220).

Shipment: Sample tubes must to be packed **upright** in accordance with guidelines provided in ASTM D 4220, or in an equivalent sample box. Tubes should be isolated from other sample tubes, and fit snugly in the case to protect against vibration or shock. The cushioning material between the samples should be at least 1 in (25 mm) thick, and the cushioning on the container floor should be at least 2 in (50 mm) thick. The samples should not be exposed to extreme heat or cold. If possible, the geotechnical specialist should deliver the samples to the laboratory or use a special delivery service provider who offers shipping of fragile items (e.g., FedEx) to ship samples. The use of a chain of custody form for sample traceability records is encouraged.

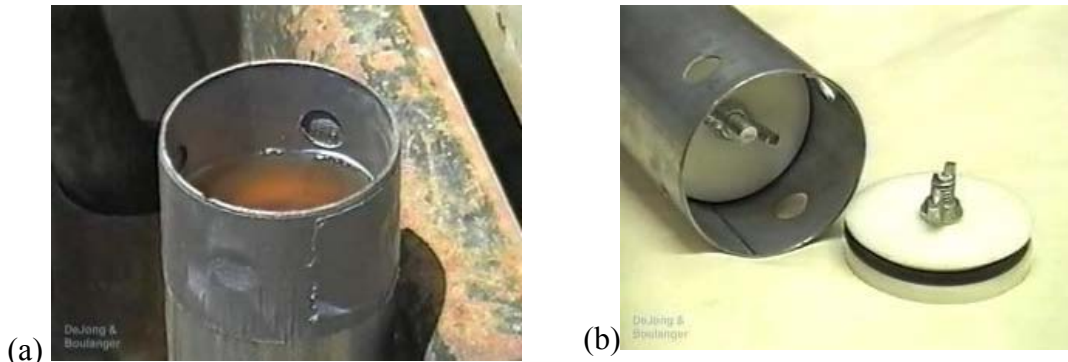


**Figure 3-13. Shelby tube sealing methods, (a) Microcrystalline Wax, (b) O-Ring packer (FHWA, 2002b).**

### 3.6.4 Undisturbed Sampling of Rock (Rock Coring)

When equipment for rock coring is being considered, the dimensions, type of core barrel, type of coring bit, and drilling fluid are important variables. The minimum depth of rock coring should be determined based on the local geology of the site and the type of structure to be constructed. Coring should also be performed to a depth that assures that refusal is not encountered on a boulder. A brief description of issues related to rock coring is provided in this document. Additional information on drilling rigs, methods of circulating drill cuttings (i.e., fluid or air), hole diameters, and casings is provided in ASTM D 2113.

#### 3.6.4.1 Core Barrels

Four different types of core barrels are described in ASTM D 2113 including:

- 1) Single Tube - Figure 3-14(a);
- 2) Rigid Double Tube - Figure 3-14(b);
- 3) Swivel Double Tube - Figure 3-14(c); and
- 4) Triple Tube.

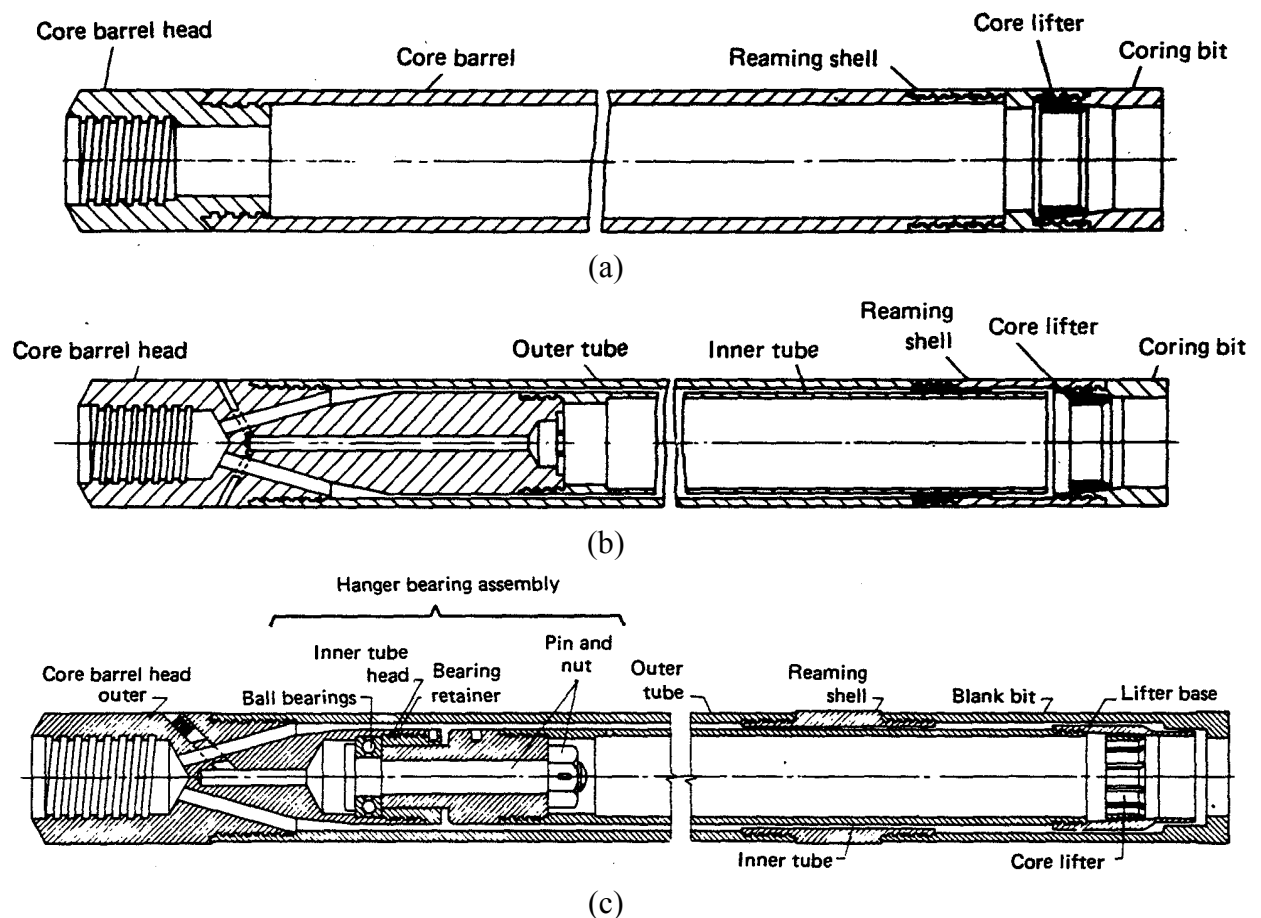


Figure 3-14. (a) Single, (b) and (c) Double tube rock core barrels (FHWA, 1997).

Since the double core barrel isolates the rock from the drilling fluid stream to yield better recovery, it is the minimum standard of core barrel that should be used in practice when an intact core is required for testing. Figure 3-15 shows the outer and inner assembly for a double-tube core barrel. The inner tube of a swivel-type core barrel does not rotate during drilling, which results in less disturbance and better recovery in weak and fractured rock. Rigid type double tube core barrels should not be used where core recovery is a concern. Triple tube swivel-type core barrels will produce better recovery and less core breakage than a double tube barrel.

Most rock coring today is done by use of the wireline method, which was introduced in the 1960s. In this method, an inner tube containing the core is detached from the core barrel assembly when the core barrel is full or a blockage occurs. The tube and core contained in it are pulled to the surface by wire dropped down the string of drill rods. A latch or “overshot assembly,” which snaps on to the top of the inner tube, is used for this purpose. The inner

tube is then rapidly hoisted to surface within the string of drill rods. After the core is removed, the inner tube is dropped down into the outer core barrel and drilling resumes. Thus, the core is retrieved without having to pull all of the rods and production rates, particularly for deep cores, are therefore greater than those for conventional techniques.

Table 3-7 lists the available core sizes. The standard size rock core, NX, has a diameter of 2-1/8 in (54 mm). Generally larger core sizes will lead to less mechanical breakage and yield greater recovery, but the associated cost for drilling will be much higher. Since the size of the core will affect the percent recovery, the core barrel size should be clearly recorded on the log. Additionally, the core barrel length can increase recovery in fractured and weathered rock zones. In these zones a core barrel length of 5 ft (1.5 m) is recommended. Core barrel lengths should not be greater than 10 ft (3 m) under any conditions because of the potential for damage to the long cores.



**Figure 3-15. Double tube core barrel. (a) Outer barrel assembly (b) Inner barrel assembly (FHWA, 2002b).**

#### 3.6.4.2 Coring Bits

The coring bit is the bottommost component of the core barrel assembly. It is the grinding action of this component that cuts the core from the rock mass. The following three basic categories of bits are in use: diamond, carbide and sawtooth (Figure 3-16).

Coring bits are generally selected by the driller and are often approved by the geotechnical specialist. Bit selection should be based on a general knowledge of drill bit performance for the expected formations and the proposed drilling fluid.

**Table 3-7  
Dimensions of core sizes (FHWA, 1997)**

<b>Size</b>	<b>Diameter of Core mm (in)</b>	<b>Diameter of Borehole mm (in)</b>
EX,EXM	21.5 (0.846)	37.7 (1.484)
EWD3	21.2 (0.835)	37.7 (1.484)
AX	30.1 (1.185)	48.0 (1.890)
AWD4, AWD3	28.9 (1.138)	48.0 (1.890)
AWM	30.1 (1.185)	48.0 (1.890)
AQ Wireline, AV	27.1 (1.067)	48.0 (1.890)
BX	42.0 (1.654)	59.9 (2.358)
BWD4, BWD3	41.0 (1.614)	59.9 (2.358)
BXB Wireline, BWC3	36.4 (1.433)	59.9 (2.358)
BQ Wireline, BV	36.4 (1.433)	59.9 (2.358)
NX	54.7 (2.154)	75.7 (2.980)
NWD4,NWD3	52.3 (2.059)	75.7 (2.980)
NXB Wireline, NWC3	47.6 (1.874)	75.7 (2.980)
NQ Wireline, NV	47.6 (1.874)	75.7 (2.980)
HWD4,HXB Wireline, HQ Wireline	61.1 (2.406) 63.5 (2.500)	92.7 (3.650) 96.3 (3.791)
CP, PQ Wireline	85.0 (3.346)	122.6 (4.827)



**Figure 3-16. Coring bits: Diamond (top left), Carbide (top right), and Sawtooth (bottom center) (FHWA, 2002b).**

Diamond coring bits, such as surface set or impregnated-diamond types, are the most versatile since they can produce high-quality cores in soft to extremely hard rock materials (see Figure 3-10, top left). Compared to other types, diamond bits in general permit more rapid coring and, as noted by Hvorslev (1948), exert lower torsional stresses on the core. Lower torsional stresses permit the retrieval of longer cores and cores of smaller diameter. The wide variation in the hardness, abrasiveness, and degree of fracturing encountered in rock has led to the design of bits to meet specific conditions known to exist or expected to be encountered at given sites. Thus, wide variations in the quality, size, and spacing of diamonds, in the composition of the metal matrix, in the face contour, and in the type and number of waterways are found in bits of this type. Similarly, the diamond content and the composition of the metal matrix of impregnated bits are varied to meet differing rock conditions.

Carbide bits use tungsten carbide in lieu of diamonds. There are of several types of carbide bits. The standard type carbide bit is shown in Figure 3-16, top right. Bits of this type are used to core soft to medium hard rock. They are less expensive than diamond bits. However, the rate of drilling is slower than with diamond bits.

Sawtooth bits consist of teeth cut into the bottom of the bit (see Figure 3-10, bottom center). The teeth are faced and tipped with a hard metal alloy such as tungsten carbide to provide water resistance and thereby to increase the life of the bit. Although these bits are less expensive than diamond bits, they do not provide as high a rate of coring and do not have a salvage value. The saw tooth bit is used primarily to core overburden and very soft rock.

An important feature in all bits is the type of waterways provided in the bits for the passage of drilling fluid. Bits are available with so-called “conventional” waterways, which are passages cut on the interior face of the bit, or with bottom discharge waterways, which are internal passages that discharge at the bottom face of the bit behind a metal skirt separating the core from the discharge fluid. Bottom discharge bits should be used when soft rock or rock having soil-filled joints is cored to prevent erosion of the core by the drilling fluid before the core enters the core barrel.

Bit selection is based on the anticipated rock formation as well as the expected drilling fluid. Diamond bits are applicable in all rock types. They permit greater rates of coring than other types of bits. Carbide bits are less expensive than diamond bits and can be used in soft to medium-hard rock. Sawtooth bits are the least expensive of the three, however they have no salvage value. They lead to slower coring and are typically used only in soft rock.

### **3.6.4.3 Drilling Fluid**

In many instances, clear water is used as the drilling fluid in rock coring. If drilling mud is required to stabilize collapsing holes or to seal zones when there is loss of drill water, the geotechnical specialist should be notified to confirm that the type of drilling mud is acceptable. Drilling mud will clog open joints and fractures, which adversely affects permeability measurements and piezometer installations. Drilling fluid should be contained in a settling basin to remove drill cuttings and to allow recirculation of the fluid. Generally, drilling fluids can be discharged onto the ground surface. However, special precautions or handling may be required if the material is contaminated with oil or other substances. Such fluids may require disposal off site. Water flow over the ground surface should be avoided as much as possible. Local environmental agencies should be contacted for permits because some drilling fluids may have adverse effects on local surface and subsurface environments. Certain local agencies may also require implementation of a Storm Water Pollution Prevention Plan (SWPPP).

### **3.6.5 Observations During Rock Core Drilling**

#### **3.6.5.1 Drilling Rate/Time**

The drilling rate should be monitored and recorded on the boring log in the units of minutes per 1 ft (0.3 m). Only time spent advancing the boring should be used to determine the drilling rate.

#### **3.6.5.2 Core Photographs**

Cores in the split core barrel should be photographed immediately upon removal from the borehole. A label should be included in the photograph to identify the borehole, the depth interval and the number of the core run. It may be desirable to get a "close-up" of interesting features in the core. Wetting the surface of the recovered core by using a spray bottle and/or sponge prior to photographing will often enhance the color contrasts of the core.

A tape measure or ruler should be placed across the top or bottom edge of the core box to provide a scale in the photograph. The tape or ruler should be at least 3 ft (1 m) long, and it should have relatively large, high contrast markings to be visible in the photograph.

A color bar chart is often desirable in the photograph to provide indications of the effects of variation in film age, film processing, and the ambient light source. The photographer should strive to maintain uniform light conditions from day to day, and those lighting conditions should be compatible with the type of film selected for the project. The use of a digital camera is a convenient way to circumvent some of the problems associated with the use of film cameras for photographing rock cores.

### **3.6.5.3 Rock Classification**

The rock type and its inherent discontinuities, joints, seams, and other facets should be documented. See Chapter 4 for a discussion of rock description and classification.

### **3.6.5.4 Recovery**

The core recovery is the length of rock core recovered from a core run. The recovery ratio is the ratio of the length of core recovered to the total length of the core drilled on a given run, expressed as either a fraction or a percentage. Core length should be measured along the core centerline. When the recovery is less than the length of the core run, the non-recovered section should be assumed to be at the end of the run unless there is reason to suspect otherwise (e.g., weathered zone, drop of rods, plugging during drilling, loss of fluid, and rolled or re-cut pieces of core). Non-recovery should be marked as NCR (no core recovery) on the boring log, and entries should not be made for bedding, fracturing, or weathering in that interval.

Recoveries greater than 100 percent may occur if core that was not recovered during a run is subsequently recovered in the next run. Recoveries greater than 100 percent should be recorded and adjustments to data should not be made in the field.

### **3.6.5.5 Rock Quality Designation (RQD)**

The RQD is a quantitative measure that represents a modified core recovery percentage. By definition the RQD is the sum of the lengths of all pieces of sound core over 4 in (100 mm) long divided by the length of the core run (Deere, 1963). The correct procedure for measuring RQD is illustrated in Figure 3-17. The RQD is an index of rock quality. Problematic rock that is highly weathered, soft, fractured, sheared, and jointed typically yields lower RQD values than more intact rock. Thus, RQD is simply a measurement of the percentage of "good" rock recovered from an interval of a borehole.

It should be noted that the original definition of RQD reported by Deere (1963) was based on measurements made on NX-size core. Experience in recent years reported by Deere and Deere (1989) indicates that cores with diameters both slightly larger and smaller than NX may be used for computing RQD. The wire line cores using NQ, HQ, and PQ are also considered acceptable. Use of RQD for the smaller BQ and BX sizes is discouraged because of a greater potential for core breakage and loss that would result in a smaller value of RQD.

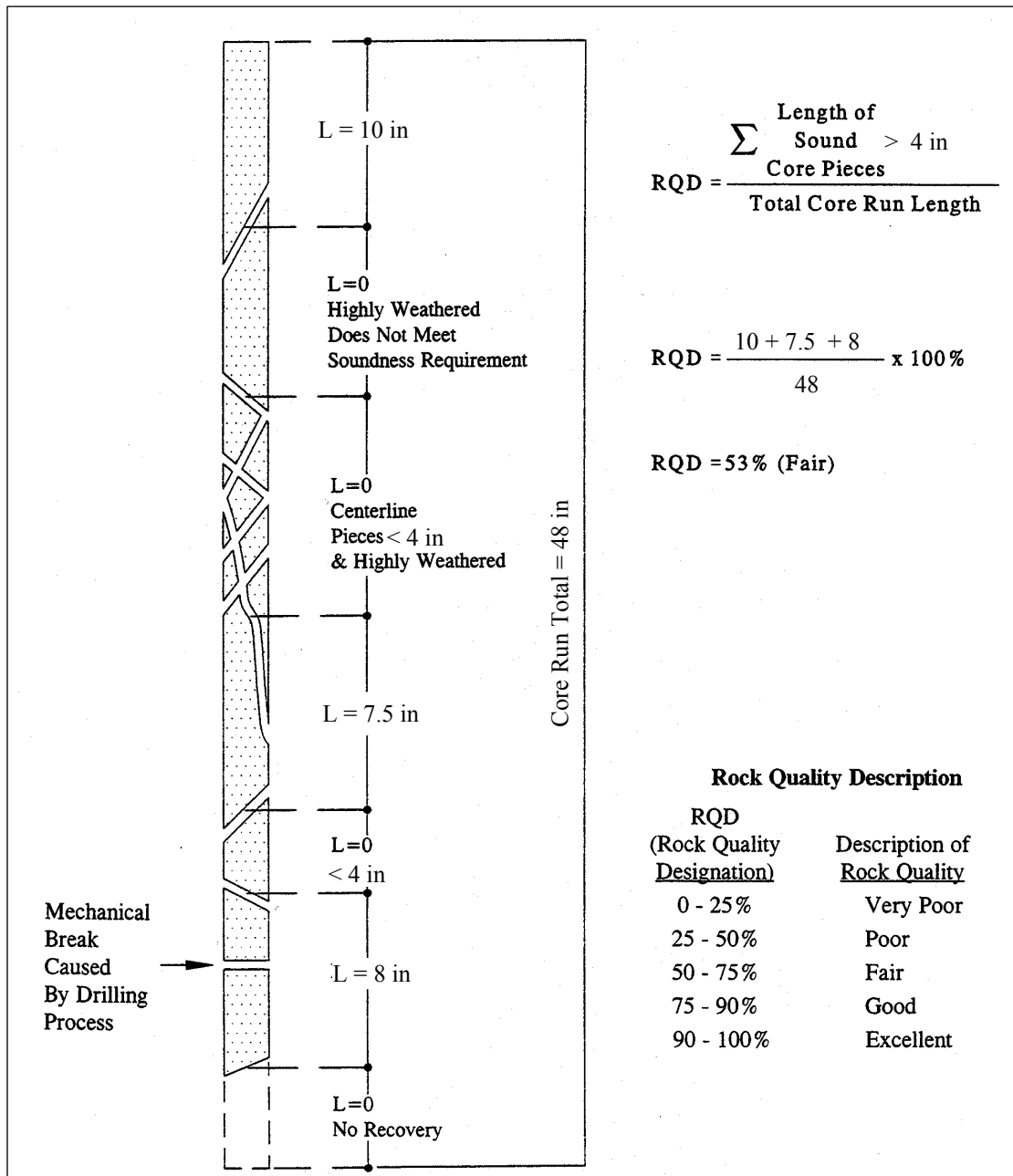
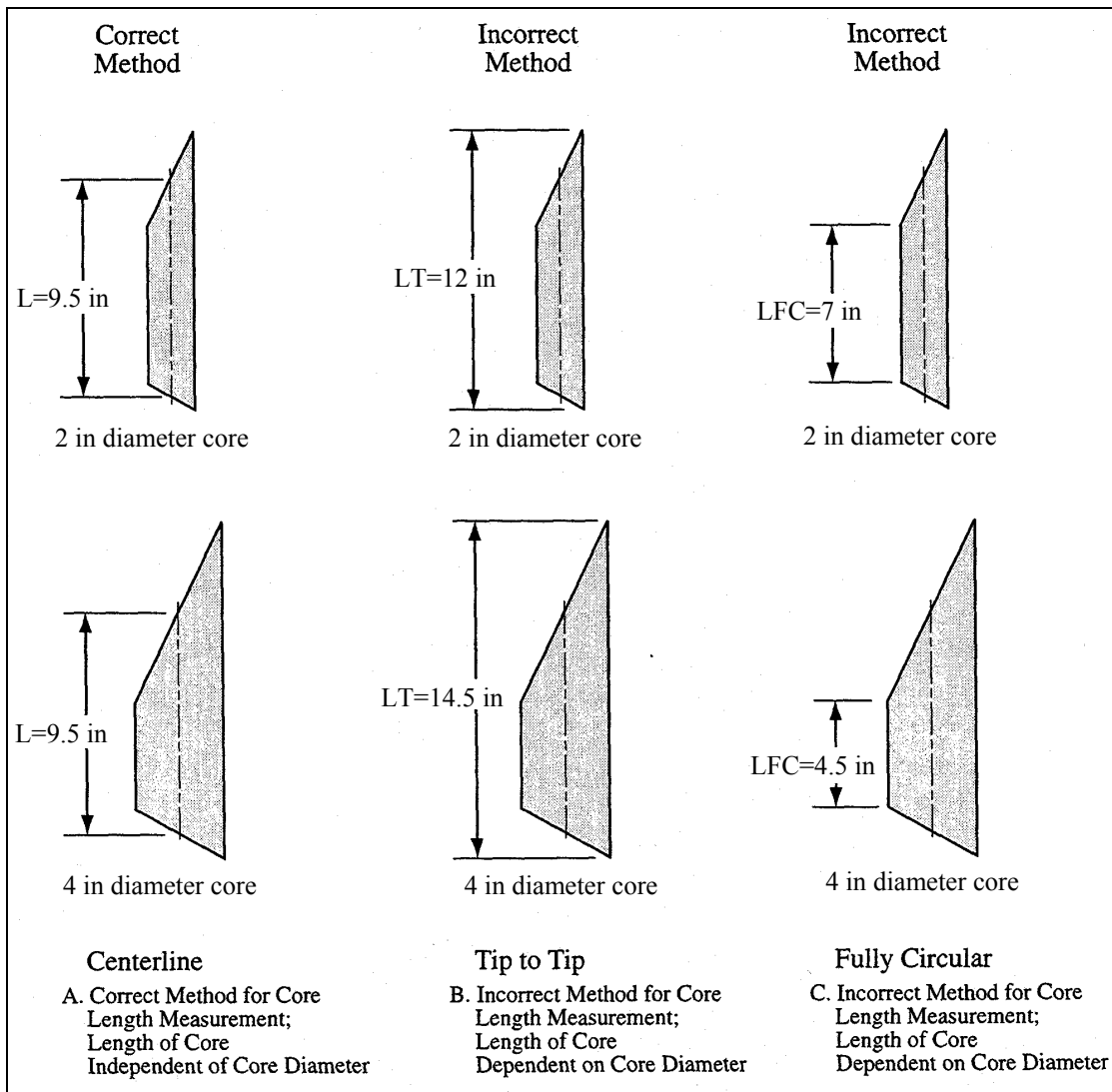


Figure 3-17. Modified core recovery as an index of rock mass quality (FHWA, 1997).

## Length Measurements of Core Pieces

The same piece of core could be measured three ways: along the centerline, from tip to tip, or along the fully circular barrel section (Figure 3-18). The recommended procedure is to measure the core length along the centerline. This method is advocated by the International Society for Rock Mechanics (ISRM), Commission on Standardization of Laboratory and Field Tests (ISRM, 1981). The centerline measurement is preferred because: (1) it results in a standardized RQD not dependent on the core diameter, and (2) it avoids unduly penalizing the rock quality for cases where fractures run parallel to the borehole and are cut by a second set of fractures.



**Figure 3-18. Length measurements for core RQD determination (FHWA, 1997).**

### Assessment of Soundness

Pieces of core which are not "hard and sound" should not be counted for the RQD even though they possess the requisite 4 in (100 mm) length. The purpose of the soundness requirement is to downgrade the rock quality where the rock has been altered and weakened either by agents of surface weathering or by hydrothermal activity. Obviously, in many instances a judgment decision must be made as to whether or not the degree of chemical alteration is sufficient to reject the core piece.

One commonly used procedure is not to count a piece of core if there is any doubt about its meeting the soundness requirement as evidenced by discolored or bleached grains, heavy staining, pitting, or weak grain boundaries. This procedure may unduly penalize the rock quality, but it errs on the side of conservatism. A second procedure that is occasionally used includes the altered rock within the RQD summed percentage, but indicates by means of an asterisk (RQD\*) that the soundness requirements have not been met. The advantage of this method is that the RQD\* will provide some indication of the rock quality with respect to the degree of fracturing, while also noting its lack of soundness.

Core breaks caused by the drilling process should be fitted together and counted as one piece. Drilling breaks are usually evidenced by rough fresh surfaces. For schistose and laminated rocks, it is often difficult to discern the difference between natural breaks and drilling breaks. When in doubt about a break, it should be considered as natural in order to be conservative in the calculation of RQD for most uses. Obviously, this practice would not be conservative when the RQD is used as part of a ripping or dredging estimate.

#### **3.6.5.6 Drilling Fluid Recovery**

The loss of drilling fluid during the advancement of a boring can be indicative of the presence of open joints, fracture zones or voids in the rock mass being drilled. Therefore, the volumes of fluid losses and the intervals over which they occur should be recorded. For example, "no fluid loss" means that no fluid was lost except through spillage and filling the hole. "Partial fluid loss" means that a return was achieved, but the amount of return was significantly less than the amount being pumped in. "Complete water loss" means that no fluid returned to the surface during the pumping operation. A combination of opinions from the field personnel and the driller on this matter will result in the best estimate.

### 3.6.5.7 Core Handling and Labeling

Rock cores from geotechnical explorations should be stored in structurally sound core boxes made of wood or corrugated waxed cardboard (Figure 3-19). Wooden boxes should be provided with hinged lids, with the hinges on the upper side of the box and a latch to secure the lid in a closed position.

Cores should be handled carefully during transfer from barrel to box to preserve mating across fractures and fracture-filling materials. Breaks in core that occur during or after the core is transferred to the core box should be refitted and marked with three short parallel lines across the fracture trace to indicate a mechanical break. Breaks made to fit the core into the core box and breaks made to examine an inner core surface should be marked as such. These deliberate breaks should be avoided unless absolutely necessary. Cores should be placed in the boxes from left to right, top to bottom. When the upper compartment of the box is filled, the next lower (or adjoining) compartment should be filled beginning at the left-hand side, and so on the same way until the box is filled. The depths of the top and bottom of the core and each noticeable gap in the formation should be marked by a clearly labeled wooden spacer block.

If there is less than 100 percent core recovery for a run, a cardboard tube spacer of the same length as the core loss should be placed in the core box either at the depth of core loss, if known, or at the bottom of the run. The depth of core loss, if known, or length of core loss should be marked on the spacer with a black permanent marker. The core box labels should be completed using an indelible black marking pen. An example of recommended core box markings is shown in Figure 3-19. The core box lid should have identical markings both inside and out, and both exterior ends of the box should be marked as shown in Figure 3-19. For angled borings, depths marked on core boxes and boring logs should be those measured along the axis of the boring. The angle and orientation of the boring should be noted on the core box and the boring log.

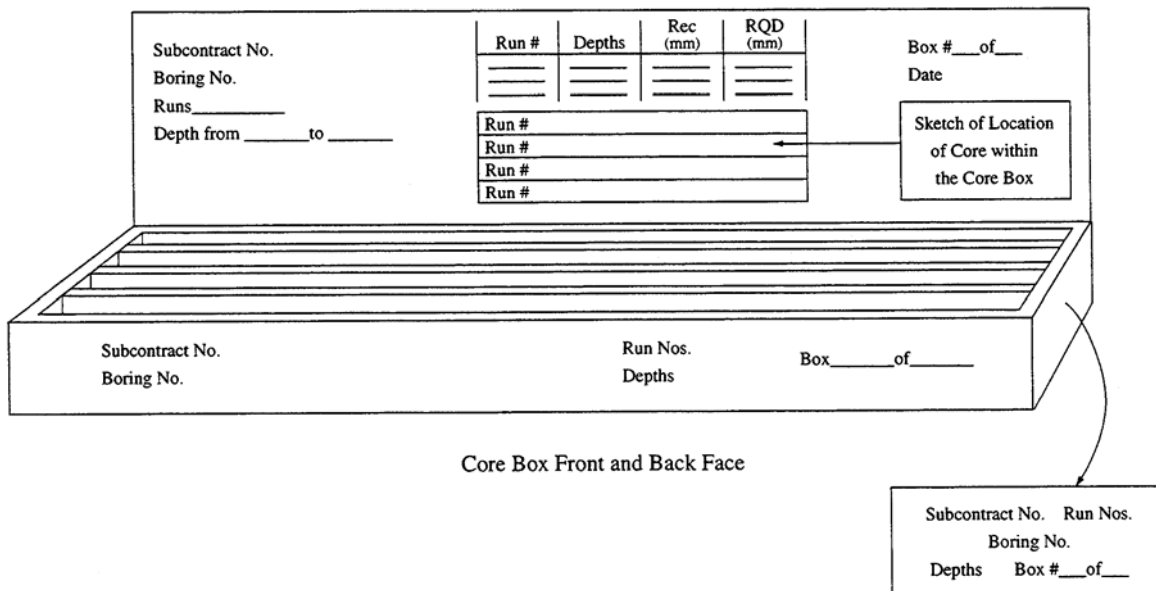


Figure 3-19. Core box for storage of recovered rock and labeling.

### **3.6.5.8 Care and Preservation of Rock Samples**

A detailed discussion of sample preservation and transportation is presented in ASTM D 5079. Four levels of sample protection are identified as follows:

- a) routine care,
- b) special care,
- c) soil-like care, and
- d) critical care.

Routine care in placing rock core in core boxes will be used for most geotechnical explorations. ASTM D 5079 suggests enclosing the core in a loose-fitting polyethylene sleeve prior to placing the core in the core box.

Special care is considered appropriate if the moisture state of the rock core (especially shale, claystone and siltstone) and the corresponding properties of the core may be affected by exposure. Special care can also be applied if it is important to maintain fluids other than water in the sample. Critical care is needed to protect samples against shock and vibration or variations in temperature, or both. For soil-like care, samples should be treated as indicated in ASTM D 4220.

### **3.6.6 Geologic Mapping**

Geologic mapping is the systematic collection of local, detailed geologic data, and, for engineering purposes, is used to characterize and document the condition of a rock mass or outcrop. The data derived from geologic mapping are a portion of the data required for the design of a cut slope or for the stabilization of an existing slope. Geologic mapping can often provide more extensive and less costly information than drilling. Soil and soil-like materials, although occasionally mapped, are not considered in this section. For a detailed discussion of geologic mapping, the reader is referred to the FHWA manual on rock slopes (FHWA, 1998a).

### 3.7 STANDARD PENETRATION TEST (SPT)

The standard penetration test (SPT) is performed during the advancement of a soil boring to obtain a disturbed drive sample (split barrel type) of the soil being penetrated and an approximate measure of its dynamic resistance. The test was introduced by the Raymond Pile Company in 1902 and remains today as the most common in-situ test performed worldwide. The procedures for the SPT are detailed in ASTM D 1586 and AASHTO T 206. A summary of the important features of the test follows.

The SPT involves the driving of a hollow thick-walled tube into the ground and measuring the number of blows to advance the split-barrel sampler having standard dimensions of 2 in (50 mm) outside diameter (OD) and 1-3/8 in (35 mm) inside diameter (ID) a vertical distance of 1 ft (300 mm), see Figure 3-20. A 140 pound (63.5 kilogram) hammer is repeatedly dropped from a height of 30 in (0.76 m) to achieve three successive 6 in (150 mm) increments of penetration. The first recorded increment is considered as a “seating” penetration, while the number of blows to advance the second and third increments are summed to give the N-value (“blow count”) or SPT-resistance (reported in blows per foot (0.3 m)).

The SPT can be halted when a total of 100 blows have been counted or if the number of blows exceeds 50 in any given 6 in (150 mm) increment, or if the sampler fails to advance during 10 consecutive blows. SPT refusal is defined by penetration resistances exceeding 100 blows per 2 in (50 mm), although ASTM D 1586 has re-defined this limit at 50 blows per 1 in (25 mm). If bedrock, or an obstacle such as a boulder, is encountered, the boring may be advanced further by using diamond core drilling or non-core rotary methods (ASTM D 2113; AASHTO T 225) at the discretion of the geotechnical specialist. In certain cases, this SPT criterion may be utilized to define the top of bedrock within a particular geologic setting where boulders are not of concern or not of great impact on the project requirements. The advantages and disadvantages of the SPT are listed in Table 3-8.

**Table 3-8**  
**Advantages and disadvantages of the Standard Penetration Test (SPT)**

<b>Advantages</b>	<b>Disadvantages</b>
<ul style="list-style-type: none"><li>• Obtain both a sample and an N-value</li><li>• Simple and rugged</li><li>• Suitable in many soil types</li><li>• Can be performed in weak rocks</li><li>• Readily available throughout the U.S.</li></ul>	<ul style="list-style-type: none"><li>• Disturbed sample (index tests only)</li><li>• N-value is a crude number for analysis</li><li>• Not applicable in soft clays &amp; loose silts</li><li>• High variability and uncertainty</li><li>• Unreliable in gravelly soils</li></ul>

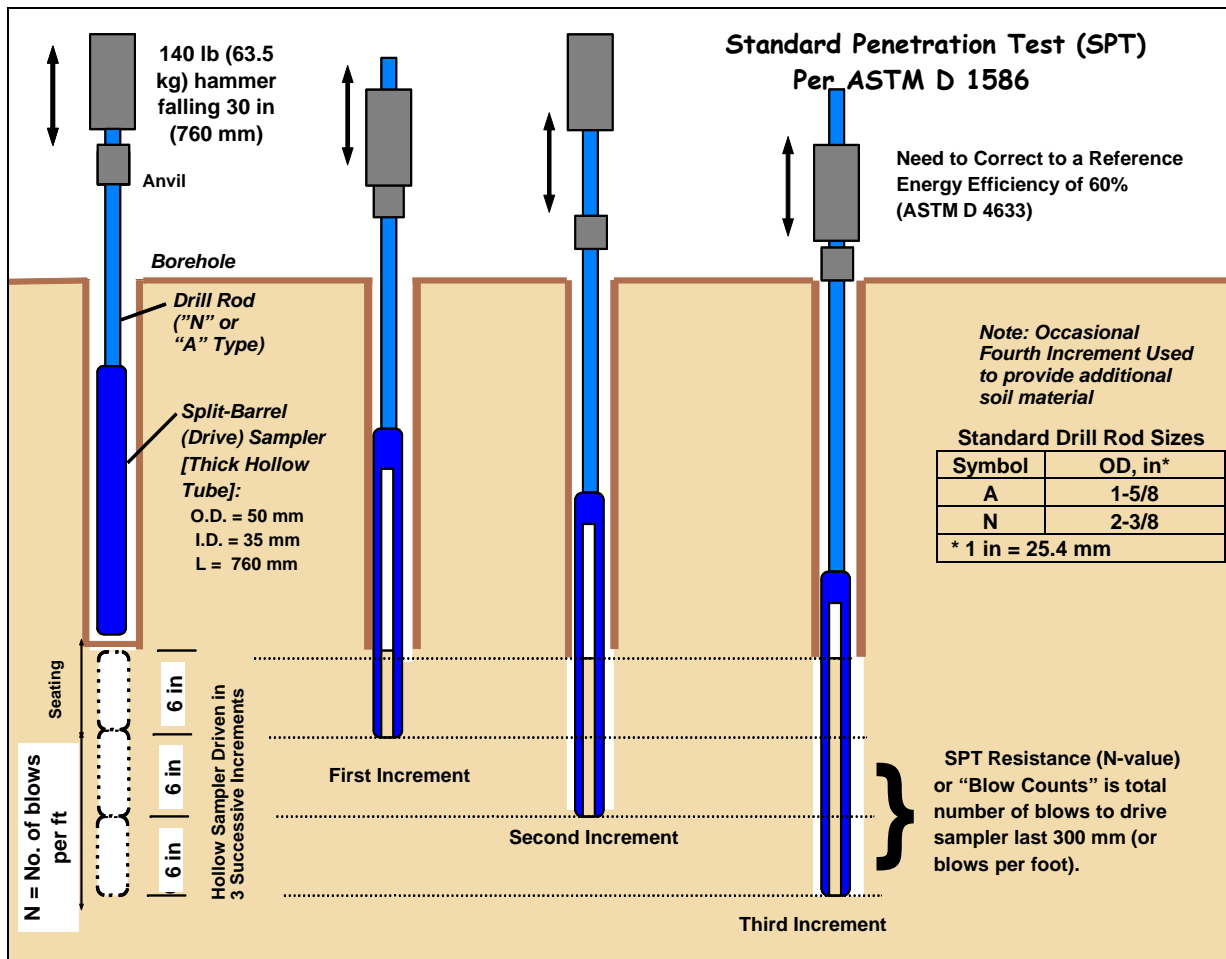


**Figure 3-20. Sequence of driving split-barrel sampler during the Standard Penetration Test (modified after FHWA, 2002b).**

The SPT is conducted at the bottom of a soil boring that has been advanced by use of either flight augers or rotary wash drilling methods. The borehole can be cased or uncased. At regular depth intervals, the drilling process is interrupted to perform the SPT. Generally, at depths shallower than 10 ft (3 m) the SPT is performed continuously or at intervals of 2.5 ft (0.75 m). Below a depth of 10 ft (3 m) the SPT is generally performed at intervals of 5 ft (1.5 m) to the planned end of the boring or refusal. If the borehole extends below the groundwater table, the head of water in the borehole must be maintained at or above the ambient groundwater level to avoid inflow of water and borehole instability.

Liners may be placed inside the split-barrel sampler with the same inside diameter as the cutting shoe, see Figure 3-21a. This allows samples to remain intact during transport to the laboratory. The liners may be arranged in a set of 1-inch (25 mm) high rings in which case “ring” samples of pre-determined height may be obtained. In U.S. practice, it is normal to omit the liner. The resistance of the sampler to driving is altered depending upon whether or not a liner is used (Skempton 1986, Kulhawy and Mayne, 1990). Therefore, **when the liners are used, their use should be clearly mentioned in the boring logs.**

Steel or plastic sampler “catchers” are often required to keep samples of clean granular soils in the split-barrel sampler. Figure 3-21 shows a variety of catchers. They are inserted inside the sampler between the cutting shoe and the sample barrel to help retain loose or flowing materials. These catchers permit the soil to enter the sampler during driving but upon withdrawal they close and thereby retain the sample. **Use of sample catchers should be noted on the boring log.**



(a)



(b)

**Figure 3-21: (a) Stainless steel and brass liners, (b) Sample catchers (FHWA, 2002b).**

### 3.7.1 Energy Efficiency of Hammers

In current U.S. practice, three types of drop hammers and four types of drill rods are used in performing the SPT. Drop hammer types are typically donut, safety, and automatic (see Figure 3-22). Typical drill rod sizes are N or A (see Figure 3-20 for sizes). The test results are highly dependent upon the type of equipment used and the experience of the operator performing the test. One of the more important factors for obtaining useful data from the test is the energy efficiency of the system. The theoretical energy of a free-fall system with the specified mass and drop height is 350 ft-lb (48 kg-m), but the actual energy is less due to a number of factors including frictional losses and eccentric loading that are specific to the hammer drop. The energy efficiency of the rotating cathead and rope system commonly used in the past depends on numerous factors including: type of hammer, number of rope turns, conditions of the sheaves and rotating cathead (e.g., lubricated, rusted, bent, new, old), age of the rope, actual drop height, vertical plumbness, weather and moisture conditions (e.g., wet, dry, freezing), and other variables (see for example Skempton, 1986). In the recent past the trend has been towards the use of automated systems for lifting and dropping the mass in order to minimize these factors. Automated systems provide more reliable and more reproducible results than the rotating cathead and rope system used in the past.

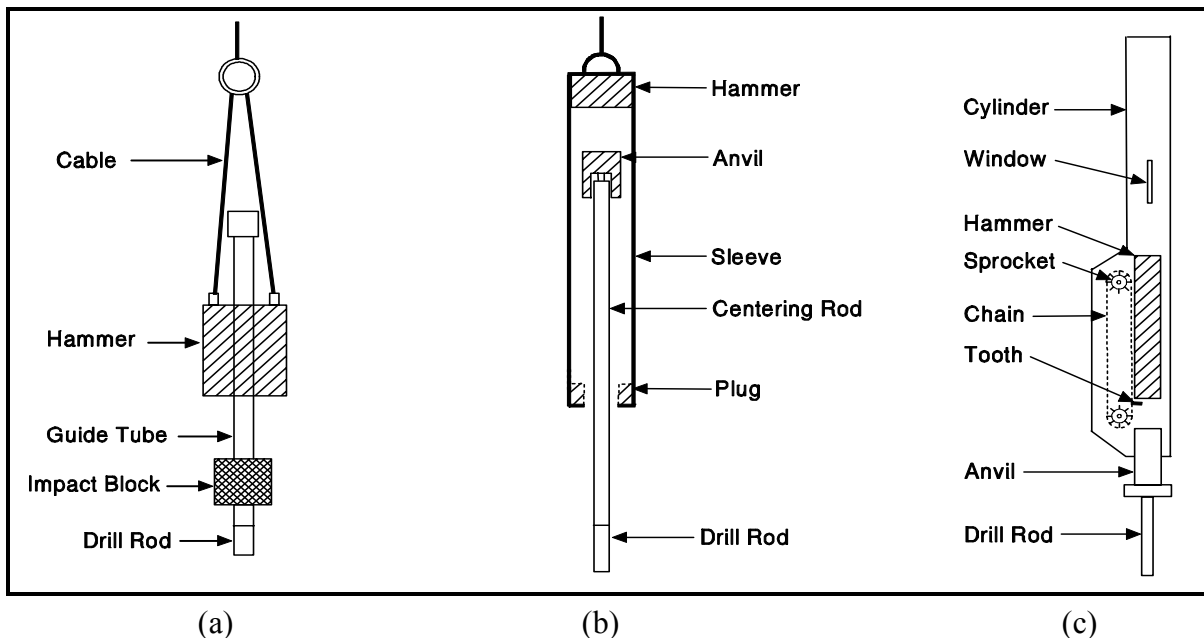


**Figure 3-22. SPT hammer types, (a) Donut, (b) Safety, and (c) Automatic (FHWA, 2006a).**

A calibration of energy efficiency for a specific drill rig and operator is recommended by ASTM D 4633. Instrumented strain gages and accelerometer measurements are used for these calibrations in an attempt to standardize the energy levels. The standard of practice for energy efficiency varies from about 35% to 85% with cathead systems using donut or safety hammers. The average for cathead systems in the United States is approximately 60%. The newer automatic trip-hammers can deliver between 80 to 100% efficiency, depending upon the type of commercial system being used.

If energy efficiency ( $E_f$ ) is measured, then the energy-corrected SPT N-value adjusted to 60% efficiency ( $N_{60}$ ) is given by:

$$N_{60} = (E_f/60) N_{\text{meas}} \quad 3-2$$

where  $N_{\text{meas}}$  is the N-value measured in the field during the test. N-values measured in the field should be corrected to  $N_{60}$  for all soils, if possible. The relative magnitudes of corrections for energy efficiency, sampler lining, rod lengths, and borehole diameter are given by Skempton (1986) and Kulhawy and Mayne (1990), but only as general guidelines. Theoretically it is mandatory to measure  $E_f$  to get the proper correction to  $N_{60}$ . In absence of data, AASHTO (2004 with 2006 Interims) recommends  $E_f = 60$  for rope and cathead systems, i.e., donut and safety hammers and  $E_f = 80$  for automatic hammer systems.

The efficiency may be obtained by comparing either the work done ( $W = F \cdot d = \text{force times displacement}$ ) or the kinetic energy ( $KE = \frac{1}{2}mv^2$ ) with the potential energy of the system ( $PE = mgh$ ), where  $m = \text{mass}$ ,  $v = \text{impact velocity}$ ,  $g = 32.2 \text{ ft/s}^2 = 9.8 \text{ m/s}^2 = \text{gravitational constant}$ , and  $h = \text{drop height}$ . Thus, the energy ratio (ER) is defined as  $W/PE$ , or  $ER = KE/PE$ . **It is important to note that geotechnical foundation practice and engineering usage based on SPT correlations have been developed on the basis of the standard-of-practice, corresponding to an average ER  $\approx$  60 %. Thus, it is recommended to adjust measured N-values ( $N_{\text{meas}}$ ) to  $N_{60}$  values.**

Figure 3-23 exemplifies the need for correcting measured N-values to a reference energy level where the successive SPTs were conducted by alternating the use of donut and safety hammers in the same borehole. The energy ratios were measured for each test and gave  $34 < ER < 56$  for the donut hammer (average = 45%) and  $55 < ER < 69$  for the safety hammer (average = 60%) at this site. The individual trends for the measured N-values from donut and safety hammers are quite apparent in Figure 3-23(a), whereas a consistent profile is obtained in Figure 3-23(b) once the data have been corrected to  $ER = 60\%$ .

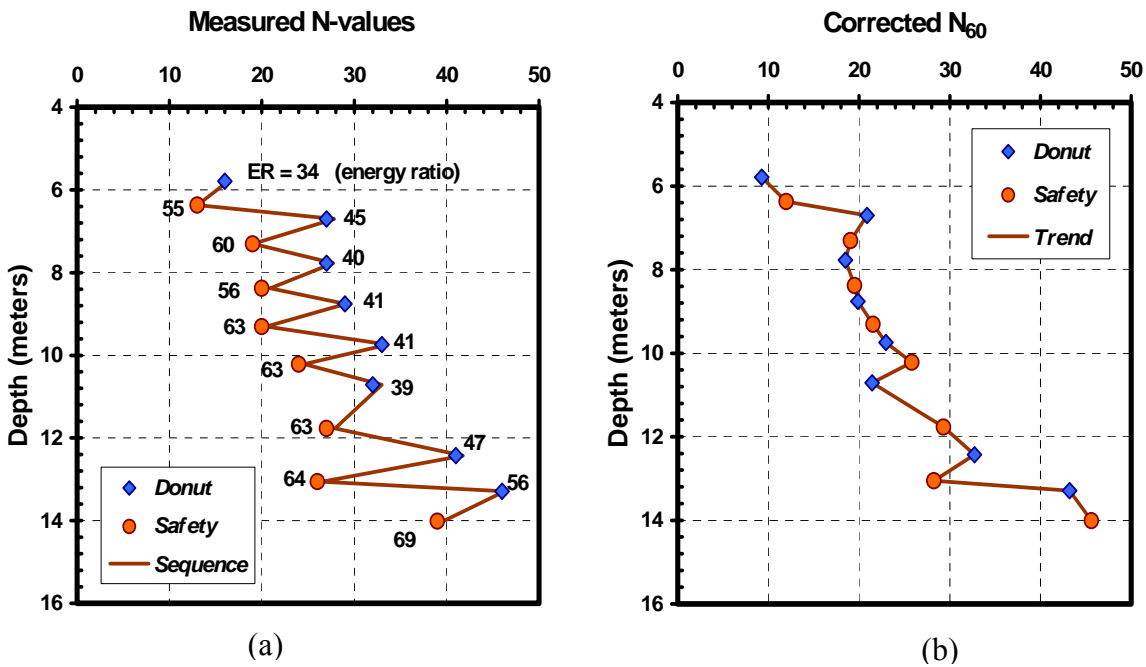


Figure 3-23. SPT N-values from (a) Uncorrected data, and (b) Corrected to 60% efficiency (Data modified after Robertson and Campanella, 1983).

### 3.7.2 Effect of Overburden Stress on N-values

Since N-values of similar materials increase with increasing effective overburden stress, the corrected blow count ( $N_{60}$ ) is often normalized to 1-atmosphere (1 tsf or about 100 kPa) effective overburden stress by using overburden normalization schemes. The energy-corrected blow count normalized for overburden is referred to as  $N_{160}$ , and is equal to:

$$N_{160} = C_N N_{60} \quad 3-3$$

where  $C_N$  is the overburden correction factor (or stress normalization parameter) calculated as (Peck, *et al.*, 1974):

$$C_N = [0.77 \log_{10}(20/p_o)], \text{ and } C_N < 2.0$$

$p_o$  = vertical effective pressure at the depth where the SPT test is performed (tsf)

$N_{60}$  = SPT blow count corrected for hammer efficiency (blows/ft) – refer to Equation 3-2.

Note that the constants in Equation 3-3 are unit dependent therefore the units of  $p_o$  must be tsf. Figure 3-24 presents the overburden correction factor as a function of vertical effective stress.

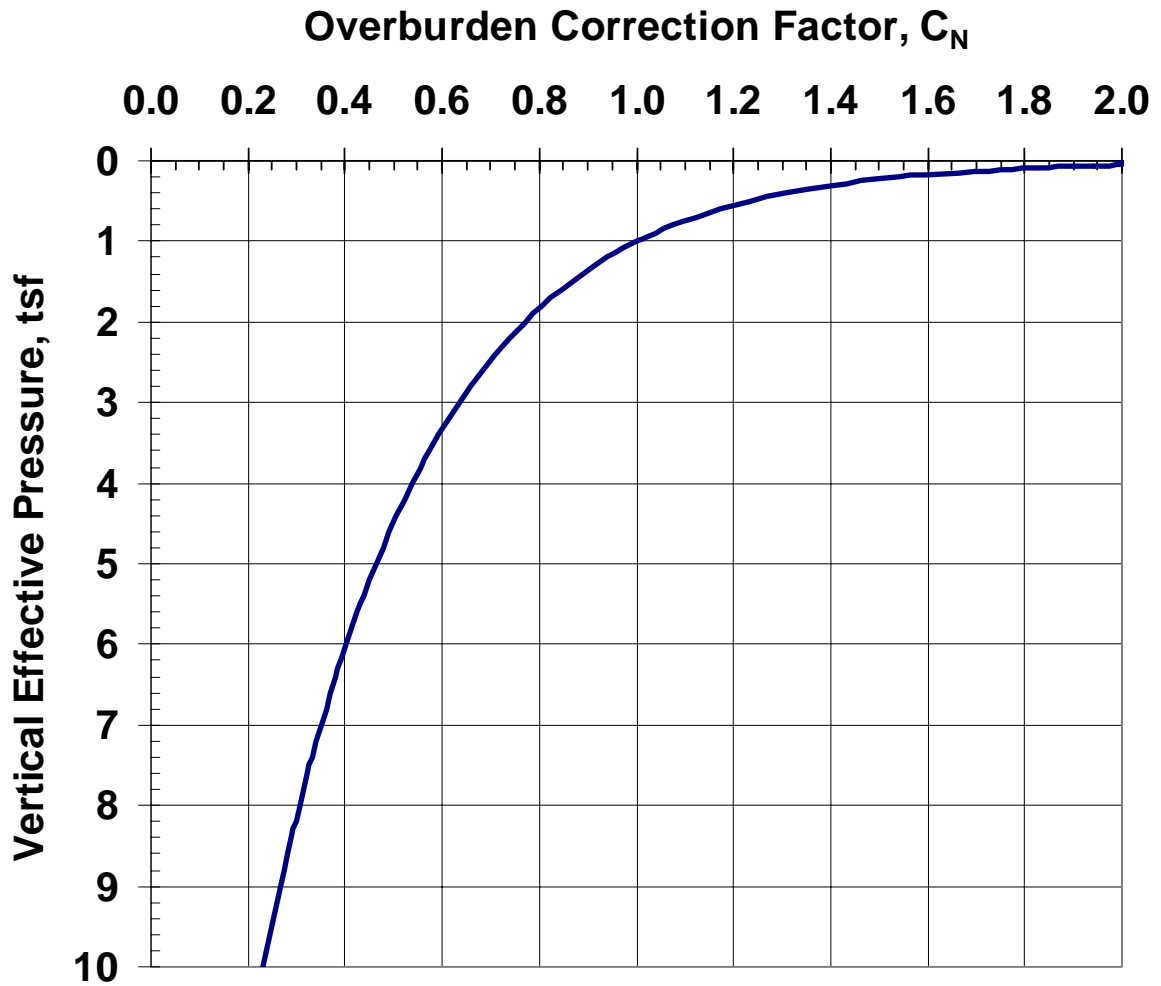


**Figure 3-24. Variation of overburden correction factor,  $C_N$ , as a function of vertical effective stress.**

Caution should be exercised in applying the overburden correction factor to indurated cemented soils, e.g., hard caliche soils encountered in the desert southwest. In such soils, the overburden pressure may not be a direct function of the depth of the soil. Therefore, the overburden correction is not recommended for such soils since it may lead to overly conservative designs.

### 3.7.3 Correlation of SPT N-Values with Basic Soil Characteristics

SPT N-values are an indication of the relative density of cohesionless soils and the consistency of cohesive soil. Table 3-9 shows N-value ranges correlated to the relative density of sands and the consistency of fine-grained soils. It is emphasized that these correlations are unreliable for gravels, silts and clays and should serve only as crude estimates for these materials.

**Table 3-9**  
**Soil properties correlated with Standard Penetration Test values (after Peck, *et al.*, 1974)**

<b>Sands (Reliable)</b>		<b>Silts and Clays (Unreliable)</b>	
<b>N<sub>60</sub></b>	<b>Relative Density</b>	<b>N<sub>60</sub></b>	<b>Consistency</b>
0-4	Very loose	Below 2	Very soft
5-10	Loose	2-4	Soft
11-30	Medium Dense	5-8	Medium
31-50	Dense	9-15	Stiff
Over 50	Very dense	16-30	Very stiff
		Over 30	Hard

#### 3.7.3.1 Applicability of SPTs in Gravelly Soils

The SPT can be performed in a wide variety of soil types as well as weak rocks, however the SPT is not particularly useful in the characterization of gravelly soils. Since the split-spoon inside diameter is 1-3/8 in (35 mm), gravel sizes larger than 1-3/8 in (35 mm) will not enter the spoon. Therefore, soil descriptions may not reflect actual gravel content of the deposit. Also, gravel pieces may plug the end of the spoon and cause the SPT blow count to be erroneously large. Thus, the SPT in such cases produces refusal blow counts (i.e., > 50 blows per 1 in (25 mm)) that are misleading and lead to unconservative designs. In this case, “Large Penetration Tests” (LPTs), such as the Becker Penetration Test (BPT), are more suitable. The LPTs consist of driving a pipe (casing) larger than the standard split spoon sampler into the ground with a pile-driving hammer. While the pipe is being driven, the driving resistance or blow count/ft of penetration is recorded. Unlike the SPT, the LPT blow count is non-standardized and is a function of the drill rod size, pipe (sampler) size, hammer type, and hammer efficiency. Careful energy calibrations are required to correlate the LPT blow counts to SPT N-values. However, this effort may be worthwhile considering that the results of SPT in gravelly soils are unreliable and misleading. Daniel, *et al.* (2003) present methods for evaluating LPT blow counts.

Since the gravel content cannot be measured by the SPT, it is recommended that consideration be given to obtaining bulk samples by drilling large diameter borings with

augers similar to the one shown in Figure 3-5a. The bulk samples obtained from such borings will also help evaluate whether the soil deposit is indeed a gravel deposit or gravels are larger particles floating in a softer soil matrix. The bulk samples will also permit an accurate determination of the Unified Soil Classification System (USCS) designation (see Chapter 4), which will be useful from design as well as constructability considerations.

### 3.7.4 SPT Test Errors

Although the procedures for conducting the SPT test have been standardized, several errors can creep into the test. The most common errors are:

1. Effect of overburden pressure. Soils of the same density will give smaller blow counts near the ground surface. The overburden stress normalization parameter ( $C_N$ ) can be used to correct for this factor.
2. Variations in the 30 in (770 mm) free fall of the drive weight. The drop height is often gauged by eye with the older rotating cathead and rope system. Newer hammer systems automatically release the weight at a height of 30 inches. The energy correction factor accounts for this factor.
3. Interference with the free fall of the drive weight by the guides or the hoist rope required in the rotating cathead and rope system. Newer automatic hammer systems eliminate rope interference. The energy correction factor accounts for this factor.
4. Use of a drive shoe that is damaged or worn from too many "refusal" blow counts ( $N_{\text{meas}} \geq 100$  blows/foot).
5. Failure to seat the sampler properly on undisturbed material in the bottom of the boring.
6. Inadequate cleaning of loosened material (slough) from the bottom of the boring.
7. Failure to maintain sufficient hydrostatic pressure in the borehole during drilling below the groundwater table. Unbalanced hydrostatic pressures between the borehole drill water and the groundwater table can cause the test zone to become "quick." This can happen when a continuous-flight auger is used with the end plugged and with a water level in the hollow stem below that in the hole.
8. Effect of gravel size as discussed in Section 3.7.3.1.

9. Samples retrieved from dilatant soils (fine sands, sandy silts) that exhibit unusually high blow counts should be examined in the field to determine if the sampler drive shoe is plugged. Poor sample recovery is usually an indication of plugging.
10. Careless work on the part of the drill crew.

***The use of qualified and experienced drillers cannot be overemphasized. Agencies that maintain their own drilling personnel and equipment generally achieve much more reliable and consistent results than those that routinely let boring contracts to the lowest bidder.***

Soil type, density, and overburden pressure are the most significant factors affecting SPT N-values (assuming good workmanship and equipment). Table 3-10 lists factors affecting the SPT and SPT results.

Regardless of the impressive list of shortcomings, the SPT is not likely to be abandoned for several reasons:

1. The test is very economical in terms of cost per unit of information.
2. The test results provides soil samples, which can be tested for index properties and visually examined.
3. Long service life of the enormous amount of equipment in use.
4. The accumulation of a large SPT database that is continually expanding.
5. The results of the SPT have been correlated with a number of soil properties to provide estimates of the values of those properties. The estimated values are often used for preliminary designs in lieu of values obtained from tests run specifically to determine those properties.
6. The fact that other methods can be readily used to supplement the SPT when the borings indicate more refinement in sample/data collection.

**Table 3-10****Factors affecting the SPT and SPT results (after Kulhawy and Mayne, 1990)**

<b>Cause</b>	<b>Effects</b>	<b>Influence on SPT N-value</b>
Inadequate cleaning of hole	SPT is performed in loose slough. Therefore soil may become trapped in sampler and may be compressed as sampler is driven, reducing recovery	Increases
Failure to maintain adequate head of water in borehole when test is performed below groundwater level	Bottom of borehole may become "quick"	Decreases
Careless measure of hammer drop	Hammer energy varies (generally variations cluster on low side)	Increases
Hammer weight inaccurate	Hammer energy varies (driller supplies weight; variations of 5 - 7 percent are common)	Increases or decreases
Hammer strikes drill rod collar eccentrically	Hammer energy reduced	Increases
Lack of hammer free fall because of ungreased sheaves, new stiff rope on weight, more than two turns on cathead, incomplete release of rope each drop	Hammer energy reduced	Increases
Sampler driven above bottom of casing	Sampler driven in disturbed, artificially densified soil	Increases greatly
Careless counting of hammer blows	Inaccurate results	Increases or decreases
Use of non-standard sampler	Correlations with SPT sampler invalid	Increases or decreases
Coarse gravel or cobbles in soil	Sampler becomes clogged or impeded	Increases
Use of bent drill rods	Inhibited transfer of energy of sampler	Increases

### **3.8 LOG OF BOREHOLE INFORMATION (“BORING LOGS”)**

The importance of accurate field notes and good logging of boreholes cannot be overemphasized. The logger must realize that a good field description must be recorded. The field-boring log is the major portion of the factual data used in the analysis of foundation conditions.

The boring log is a record that should contain all of the information obtained from a boring whether or not it may seem important at the time of drilling. It is important to record the maximum amount of information accurately. This record is the "field" boring log, as opposed to the "finished" boring log used in the preparation of the geotechnical data report. The finished log is drawn from the data presented in the field log supplemented by the results of visual identifications of samples and classification tests made in the laboratory. A typical boring log form is shown on Figures 3-25. The form presented in Figures 3-25 can be used for recording *field* data as well.

#### **3.8.1 Boring Log Format**

A wide variety of boring log forms are used by various agencies. The specific log to be used for a given type of boring will depend on local practice. The log in Figures 3-25 is just one example of a log used by geotechnical specialists. For detailed information on boring logs, the reader can refer to FHWA (1997, 2002b). The boring log shown in Figures 3-25 is used in this document simply to present the reader with an idea of the basic information that should be included in a boring log. Specific projects will likely require more detailed logs. Often separate logs are used for logging information from borings in soils and rocks unlike the log shown in Figures 3-25, which combines this information.

#### **3.8.2 Duties of the Logger**

The technical background and experience of the person who logs the field information will vary by organization. Some organizations will have a geotechnical engineer, an engineering geologist, a geologist, or a trained technician to accompany the drill crew, while others may train the drill crew foreman to log the borehole. In order to obtain the maximum amount of accurate data, the logger should work closely with the driller and be alert for changes in materials and operations while drilling is being performed. The logger is generally responsible for recording the following basic information on the field boring log:

REGION 3		<u>SUBSURFACE EXPLORATION LOG</u>				HOLE <u>BAF-2</u>						
COUNTY <u>Orange</u>						LINE <u>Baseline</u>						
PROJECT <u>Interstate 0</u>						STA. <u>92+00</u>						
DATE START <u>5/4/92</u>		HAMMER FALL-CASING <u>18"</u>				OFFSET <u>50' Lt</u>						
DATE FINISH <u>5/6/92</u>		HAMMER FALL-SAMPLER <u>30"</u>				SURF. ELEV. <u>996.2</u>						
CASING O.D. <u>2 1/2"</u> I.D. <u>2 1/4"</u>		WEIGHT OF HAMMER-CASING <u>300</u> LBS.				TIME <table border="1" style="display: inline-table; border-collapse: collapse;"> <tr><td style="width: 50px;">4:00 pm</td><td style="width: 50px;">8:00 am</td></tr> <tr><td>5/4/92</td><td>5/6/92</td></tr> </table>			4:00 pm	8:00 am	5/4/92	5/6/92
4:00 pm	8:00 am											
5/4/92	5/6/92											
SAMPLER O.D. <u>2"</u> I.D. <u>1-3/8"</u>		WEIGHT OF HAMMER-SAMPLER <u>140</u> LBS.										
RIG TYPE <u>Acker B-40</u>						DEPTH TO WATER						
CORE BARREL <u>Double Tube</u>						<table border="1" style="display: inline-table; border-collapse: collapse;"> <tr><td style="width: 50px;">10'</td><td style="width: 50px;">10'</td></tr> </table>			10'	10'		
10'	10'											

DEPTH BELOW SURFACE	BLOWS ON CASING	SAMPLE NO.	BLOWS ON SAMPLER					RECOVER (in)	DESCRIPTION OF SOIL AND ROCK	MOIST CONT %
			0	0.5	1.0	1.5	2.0			
0	6	J1	1	2	2		5	GR. FINE TO COARSE SAND MOIST NON PLASTIC		
	19									
	27	J2	1	3	3		10			
	35									
	21	J3	2	5	6		17			
	30	J4	7	9	12		15			
	22									
	25	J5	8	7	15		18			
	24									
10	28	J6	14	20	20		16			
	27	J7	15	18	19					
	36									
	34	J8	13	16	17		17			
	37									
	39	J8	15	10	3		18	15'		
	31									
	40									
	46									
	46									
20	45									
	41	J10	2	4	4		15			
	42									
	56									
	52									
	58									
	50	J11	2	3	3		14	GR. SILTY CLAY MOIST - PLASTIC		
	56									
	52									
	49									
30	58									
	52	J12	1	2	3		18			
	56									
	61									
	63									
	65									

<p>THE SUBSURFACE INFORMATION SHOWN HERE WAS OBTAINED FOR STATE DESIGN AND ESTIMATE PURPOSES. IT IS MADE AVAILABLE TO AUTHORIZED USERS ONLY THAT THEY MAY HAVE ACCESS TO THE SAME INFORMATION AVAILABLE TO THE STATE. IT IS PRESENTED IN GOOD FAITH, BUT IS NOT INTENDED AS A SUBSTITUTE FOR INVESTIGATION, INTERPRETATION OR JUDGMENT OF SUCH AUTHORIZED USERS.</p>	<p>DRILL RIG OPERATOR <u>Klinedinst</u></p> <p>SOIL &amp; ROCK DESCRIP. <u>Chassie</u></p> <p>REGIONAL SOILS ENGR. <u>Cheney</u></p> <p>SHEET <u>1</u> OF <u>2</u></p> <p>STRUCTURE NAME/NO. <u>Apple Freeway #2</u></p>
CONTRACTOR <u>ACME Drilling, Inc. SM</u>	HOLE <u>BAF-2</u>

**Figure 3-25a. Example subsurface exploration log (0 – 35 ft depth).**



1. General description of each soil and rock stratum, and the depth to the top and bottom of each stratum. As noted before, the log demonstrated in Figure 3-25 is intended to be a field log. On the final log, the description of the soil should be much more detailed and follow a specified soil classification system. Soils in the geotechnical engineering community are most often classified according to the Unified Soil Classification System (USCS). For example, the soils between depths 15 ft to 39 ft have been simply described in the field as “GR. SILTY CLAY, MOIST-PLASTIC.” The full classification as per USCS on the final log may read as follows (the detailed description and classification of soils and the USCS are discussed in Chapter 4):

*Soft, wet, gray, high plasticity CLAY, with Silt; Fat CLAY (CH); (Alluvium)*

2. The depth to groundwater at the time it is first encountered and afterwards at the end of each day, at completion of boring, and, if possible, at least 24 hours after completion of the boring.
3. The depth at which each sample is taken, the type of sample taken, its number, and any loss of samples taken during extraction from the hole.
4. The depths at which field tests are made and the results of the test.
5. Information generally required by the log format, such as:
  - Boring number and location.
  - Date of start and finish of the hole.
  - Name of driller (and of logger, if applicable).
  - Elevation at top of hole.
  - Depth of hole and reason for termination.
  - Diameter of any casing used.
  - Size of hammer and free fall used on casing (if driven).
  - Blows per foot to advance casing (if driven).
  - Description and size of sampler.
  - Size of drive hammer and free fall used on sampler in dynamic field tests.
  - Blow count for each 6 in (150 mm) to drive sampler. (Sampler should be driven three 6 in (150 mm) increments or to a total of 100 blows).
  - Type of drilling rig used.

- Type and size of core barrel used.
  - Length of time to drill each core run or foot of core run.
  - Length of each core run and amount of core per run.
  - Recovery of sample in inches and RQD of rock core.
  - Project identification.
6. Notes regarding any other pertinent information and remarks on miscellaneous conditions encountered, such as:
- Depth of observed groundwater, elapsed time from completion of drilling, conditions under which observations were made, and comparison with the elevation noted during reconnaissance (if any).
  - Artesian water pressure.
  - Obstructions encountered.
  - Difficulties in drilling (caving, coring boulders, surging or rise of sands in casing, caverns, etc.).
  - Loss of circulating water and addition of extra drilling water.
  - Drilling mud and casing as needed and why.
  - Odor of recovered sample.
  - Sampler plugged.
  - Poor recovery.
7. Any other information the collection of which may be required by agency policy (e.g., names and associations of visitors to the site, etc.).

### 3.9 CONE PENETRATION TESTING (CPT)

The history of field cone penetrometers began with a design by the Netherlands Department of Public Works in 1930. This "Dutch" cone penetrometer was a mechanical operation using a manometer to read loads. Paired sets of inner and outer rods are pushed into the ground in 8 in (200 mm) intervals. In 1948, electric cones permitted continuous measurements to be taken downhole. In 1965, the addition of sleeve friction measurement devices allowed an indirect means for identifying soil types. Later, in 1974, the electric cone was combined with a piezoprobe to form the first piezocone penetrometer. Most recently, additional sensors have been added to form specialized devices such as the resistivity cone, acoustic cone, seismic cone, vibrocone, cone pressuremeter, and lateral stress cone.

The cone penetration test (CPT) was first introduced in the U.S. in 1965. Since that time, the CPT has developed into one of the most popular in-situ testing methods because it is fast, economical, and provides continuous profiling of the geostratigraphy and allows for continuous in-situ evaluation of soil properties. Depending upon equipment capability as well as soil conditions, 330 to 1150 ft (100 to 350 m) of penetration testing may be completed in one day.

As shown in Figure 3-26, the CPT involves the hydraulic push of an instrumented steel probe into the soil at a constant rate to obtain continuous vertical profiles of stresses and/or other measurements. No borehole, cuttings, or spoil are produced by this test. Testing is conducted in accordance with ASTM D 5778.

The CPT can be used in very soft clays to dense sands. It is not suitable for use in highly indurated or cemented soils or in soils containing significant amounts of gravel and boulders. The advantages and disadvantages of the CPT are listed in Table 3-11.

**Table 3-11**

**Advantages and disadvantages of the Cone Penetration Test (CPT) (FHWA, 2002b)**

<b>Advantages</b>	<b>Disadvantages</b>
<ul style="list-style-type: none"> <li>• Fast and continuous profiling</li> <li>• Economical and productive</li> <li>• Results not operator-dependent</li> <li>• Strong theoretical basis in interpretation</li> <li>• Particularly suitable for soft soils</li> </ul>	<ul style="list-style-type: none"> <li>• High capital investment</li> <li>• Requires skilled operator to run</li> <li>• Electronic drift, noise, and calibration</li> <li>• No soil samples are obtained</li> <li>• Unsuitable for gravel/boulder deposits*</li> </ul>
<p>*Note: Except where special rigs are provided and/or additional drilling support is available.</p>	

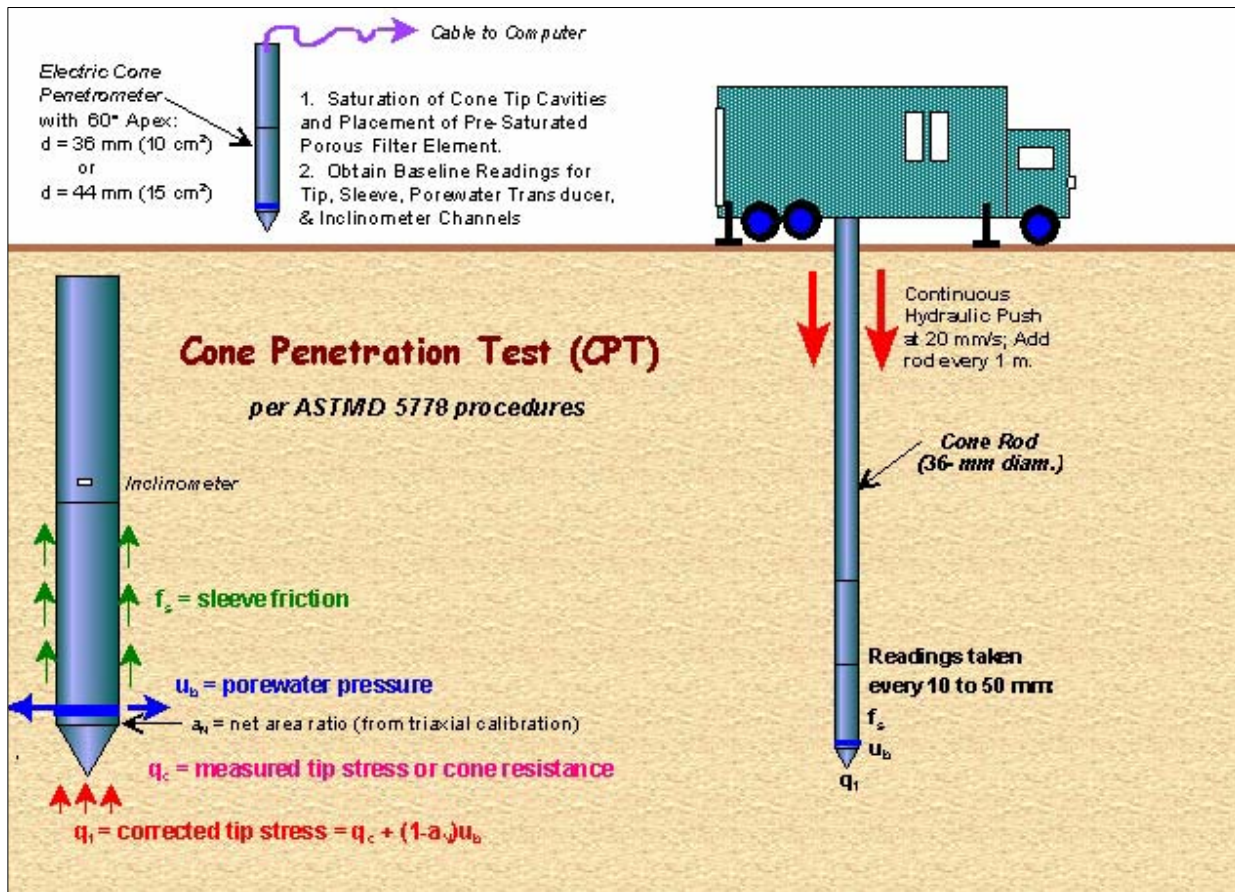


**Figure 3-26. Procedures and components of the Cone Penetration Test (FHWA, 2002b).**

Although the test provides continuous logging of the in-situ response of the soil, which can lead to more accurate and reliable analyses, no soil samples are available for laboratory testing. For that reason the CPT provides an excellent complement to the more conventional soil test boring with SPT measurements and subsequent laboratory testing on retrieved samples.

### 3.9.1 Equipment Description and Operation

Electronic cones are now the dominant cone type used in cone penetration testing. Therefore, mechanical cones are not discussed in this document. Electronic cones may be further divided into three primary types: (a) the standard friction cone (CPT), (b) the piezocone (PCPT or more commonly CPTu), and (c) the seismic cone piezocone (SCPTu). Each of these cones is briefly described here. To assist in following the brief descriptions, the standard terminology regarding the cone penetrometer is shown in Figure 3-27.

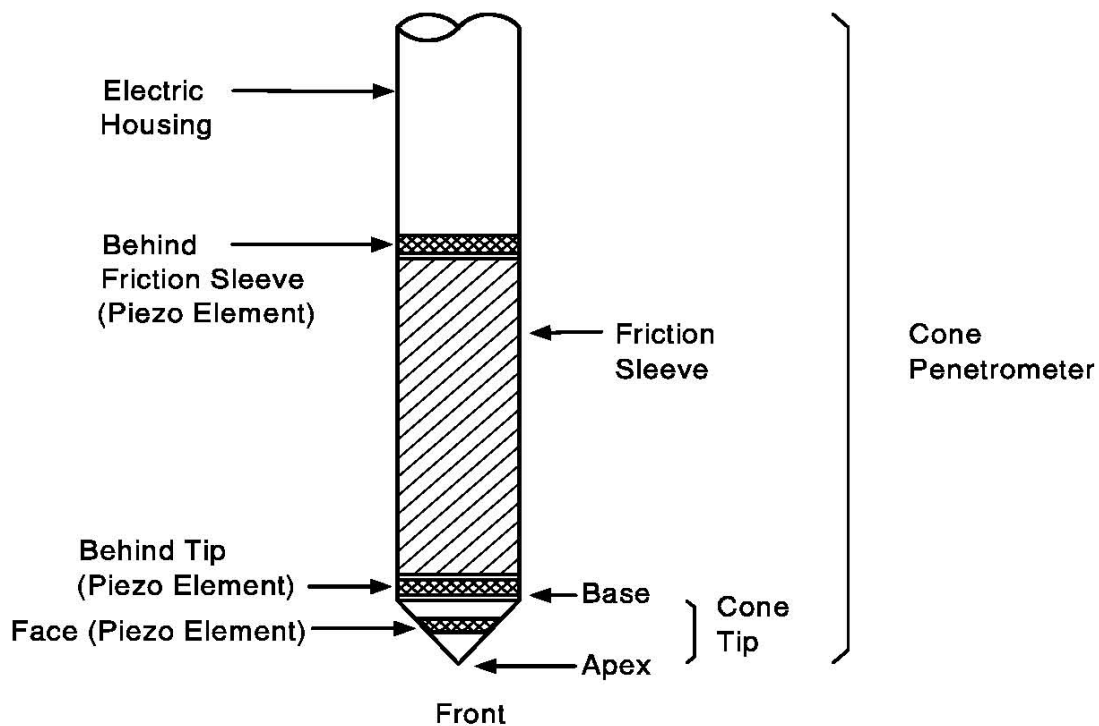


**Figure 3-27. Cone penetrometer terminology (from Robertson and Campanella, 1989).**

### 3.9.2 The Standard Cone Penetration Test (CPT)

The equipment necessary for performing a standard CPT includes a penetrometer, cone rod or drill rod, an electrical cable, a data acquisition system, and a hydraulic actuator attached to equipment that has sufficient reaction mass to advance the penetrometer. The equipment that provides the reaction mass can be a conventional drilling rig, however, a dedicated CPT truck commonly weighing 20 to 25 tons (200 to 250 kN) is more commonly used.

A standard cone penetrometer is a 1.4 in (35.7 mm) diameter cylindrical probe with a 60° conical apex at the tip. The tip has a projected area of 1.6 in<sup>2</sup> (10 cm<sup>2</sup>). The surface area of the sleeve above the cone is 23.3 in<sup>2</sup> (150 cm<sup>2</sup>). More robust penetrometers are available with a 1.7 in (44 mm) diameter body, a 2.3 in<sup>2</sup> (15 cm<sup>2</sup>) projected tip area, and a 31 to 35 in<sup>2</sup> (200 to 225 cm<sup>2</sup>) sleeve surface area. A penetrometer having a projected cone area of 2.3 in<sup>2</sup> (15 cm<sup>2</sup>) will generally provide the same response as one having a projected cone area of 1.6 in<sup>2</sup> (10 cm<sup>2</sup>). The “size” of a cone is defined by its projected tip area, e.g. a 1.6 in<sup>2</sup> (10 cm<sup>2</sup>) cone or a 2.3 in<sup>2</sup> (15 cm<sup>2</sup>) cone. Figure 3-28 shows a number of different cone penetrometers and piezocones.



**Figure 3-28. Cone and piezocone penetrometers (note the quarter for scale) (FHWA, 2002b).**

A section of standard cone rod is typically 3.3 ft (1 m) in length with a 1.4 in (35.7 mm) outer diameter and a 0.9 in (22 mm) inner diameter. Alternatively, the penetrometer can be pushed with standard AW drill rod (1 $\frac{3}{4}$  in (44.4 mm) OD; 1 $\frac{1}{4}$  in (31.8mm) ID) or EW drill rod (1 $\frac{3}{8}$  in (34.9 mm) OD; 15/16 in (23.8 mm) ID).

The cone cable runs through the hollow cone/drill rods and attaches to an electronic data acquisition system at the ground surface. The data acquisition system generally consists of an analog signal conditioner, an analog to digital (A-D) converter, and a computer processor. Current data acquisition systems are attached to one or two computer monitors so the operator and engineer can observe data recorded during the sounding in real time. Real time monitoring allows for decisions to be made in the field with respect to the sounding. This is helpful if auxiliary tests, such as a pore pressure dissipation test, are to be performed in certain soil layers, or if the test is to be terminated once a certain layer is encountered. Printers can be attached to the computer processor to obtain a real-time printout of the data. Printed data are a good backup in case an unforeseen incident causes the computer to crash resulting in the loss of the electronically stored data. Data are typically recorded every  $\frac{3}{4}$  to 2 in (20 to 50 mm) of vertical penetration.

The test procedure for the standard cone penetration test and the nature of the data acquired during the test are described in Sections 3.9.5 and 3.9.6, respectively.

### 3.9.3 The Piezo-cone Penetration Test (CPTu)

The piezo-cone (CPTu) is essentially the same as the standard electronic friction cone except that it includes porous filter piezo-elements that may be located at the cone tip, on the cone face, behind the cone tip, or behind the friction sleeve. These porous filter elements are used to measure pore water pressure during penetration. Saturation of the porous element and cavity is essential to obtain reliable pore water pressure measurements.

### 3.9.4 The Seismic Piezocone Penetration Test (SCPTu)

For the seismic piezocone test (SCPTu), a geophone is located approximately 1.6 feet (500 millimeters) uphole from the cone tip. The geophone detects shear waves generated at the ground surface at intervals of approximately 3 or 5 ft (1 or 1.5 m), corresponding to successive rod additions. If necessary, adjustments should be made if AW or EW rods are used to advance the cone since they typically come in longer lengths.

### 3.9.5 Test Procedures

The test procedure for the CPT consists of hydraulically pushing the cone at a rate of 0.8 in/s (20 mm/s) in accordance with ASTM D 5778 by using either a standard drill rig or a specialized cone truck as the reaction mass (see Figure 3-29). The advance of the probe requires the successive addition of rods at approximately 3 or 5 ft (1 or 1.5 m) intervals. Readings of tip resistance ( $q_t$ ), sleeve friction ( $f_s$ ), inclination ( $i$ ), and pore water pressure ( $u_m$ ) are taken at least every 2 in (50 mm) (i.e., at approximately 2.5-sec intervals). For the seismic cone test, shear wave arrival times ( $t_s$ ) are typically recorded at rod breaks corresponding to 3 or 5 ft (1 or 1.5 m) intervals.



Figure 3-29. Cone penetration testing from cone truck.

### 3.9.6 CPT Profiles

The results of the individual channels of a piezocone penetration test are plotted with depth, as illustrated in a typical plot shown in Figure 3-30. Since soil samples are not obtained with the CPT, an indirect assessment of Soil Behavioral Type (SBT) is inferred by an examination of the readings. The numbers can be processed for use in empirical chart classification systems, or the raw readings can be easily interpreted for soil strata changes. A simplified soil classification chart for a standard electric friction cone is presented in Figure 3-31. The sleeve friction, often expressed in terms of a friction ratio  $R_f = f_s/q_t$ , also is a general indicator of soil type. For example, in sands, usually  $0.5\% < R_f < 1.5\%$ ; and in clays, normally  $3\% < R_f < 10\%$ . In the lower half of the Figure 3-31, the center column shows an approximate relationship between the SPT N-value and the cone tip resistance,  $q_c$ . The SPT N-value obtained from this relationship should be considered to be equivalent to  $N_{160}$ .

### 3.9.7 CPT Profile Interpretation

The CPT sounding shown in Figure 3-30 was taken in the immediate vicinity of the boring recorded in the boring log shown in Figures 3-25. These two logs permit an interesting comparison to be made of the SPT and CPT procedures. In the sounding shown in Figure 3-30, a clayey and sandy stratum (clay, clayey silt, silt, silty sand and sandy silt) occurs from the ground surface to a depth of 10 ft (3 m). These strata are underlain by a thick layer of sand and sandy silt to depth of approximately 20 ft (6 m), which in turn is underlain by a clay layer extending down to a depth of approximately 45 ft (14 m). Finally, a dense gravelly sand layer is encountered, which the cone penetrometer could not penetrate. The SPT tests could however be performed in this dense layer since it was possible to drill into this layer.

Figure 3-30 is a good example that demonstrates the advantage of continuous sounding compared to the samples obtained at discrete intervals using SPT procedures. For example, depending on the sampling interval in the SPT test, the silt layer within the clay layer may not have been undetected. Even if it had been detected, it would not have been possible to estimate its thickness accurately between the locations of the SPT samples because the SPT samples are commonly retrieved at 5 ft (1.5 m) intervals. The implications of this shortcoming can be significant in design. For example, silt consolidates faster than clay. If the designer is not aware of the silt layer, then he/she might design a wick drain surcharge system that, based on a clay layer 25 ft (7.5 m) thick, will take longer to consolidate than what might actually be the case. In fact, the CPT profile in Figure 3-30 shows that only the 15 ft (4.5 m) portion of the clay layer below the silt layer has excess pore pressures, which suggests that it will be the primary source of consolidation settlements.



FHWA

Hole No.:CPT-BAF-2  
Location:APPLE FREEWAY

Cone: 20 Ton St 146  
Date:05:02:92 11:24

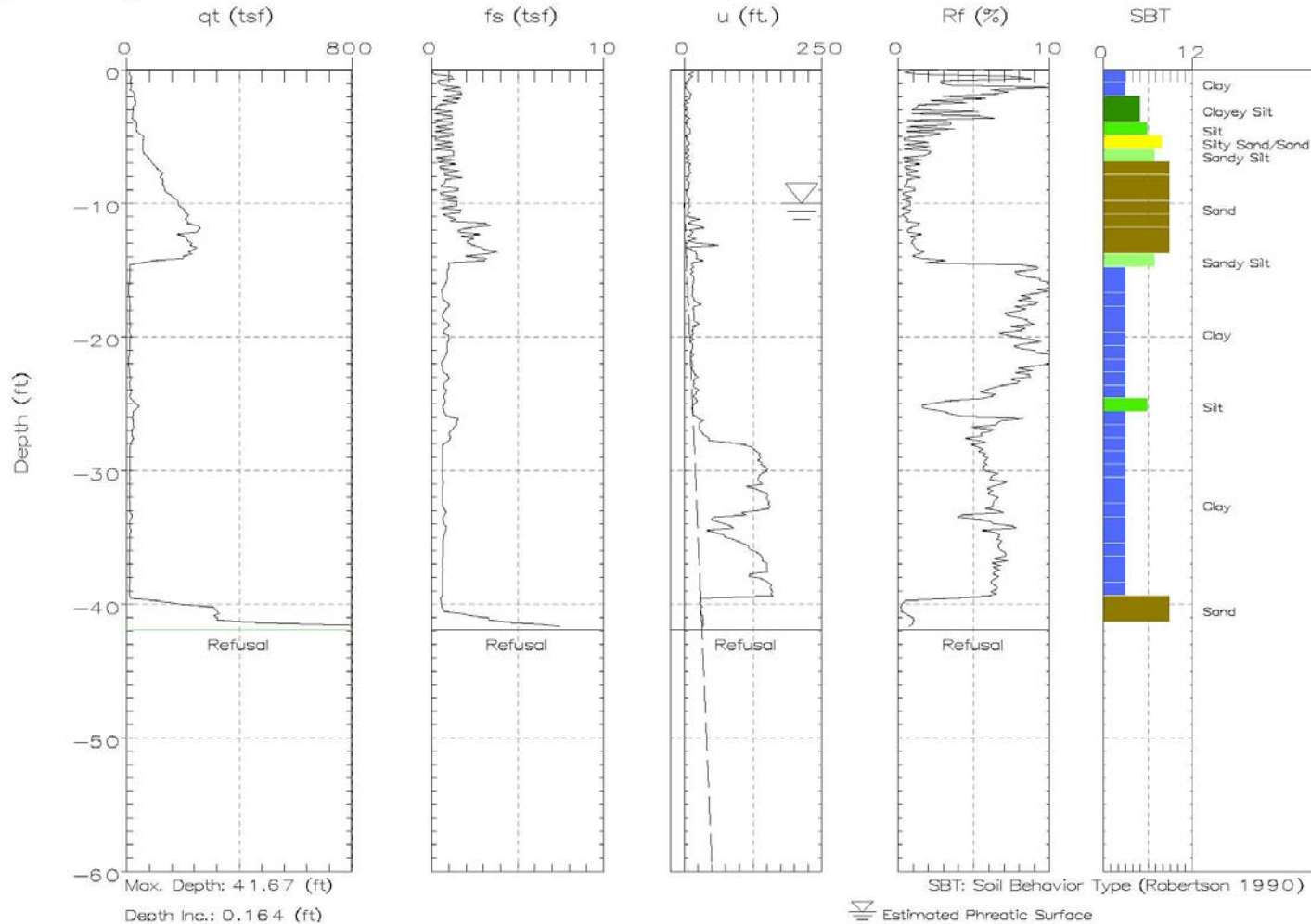
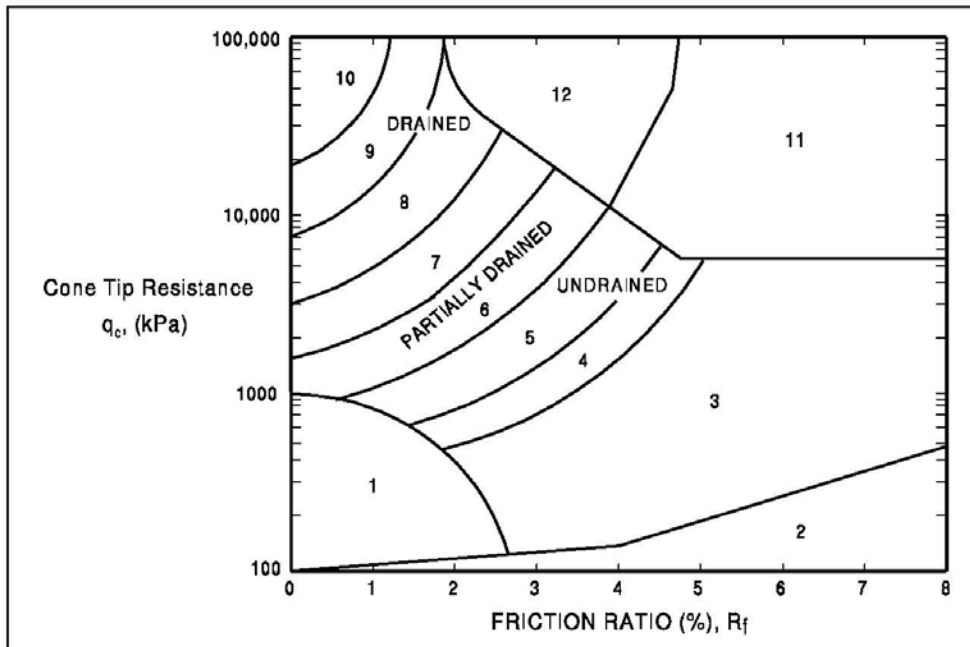


Figure 3-30. Piezo-cone results for Apple Freeway Bridge.

It is important for the reader to understand that CPT procedures do not allow retrieval of physical samples that can be tested in the laboratory to characterize various phenomena such as consolidation and shear strength. Thus, it is most beneficial to use the CPT with another method, such as the boring technique used in the SPT, that allows the retrieval of physical samples for laboratory testing. Performing the CPT before sampling in borings will permit identification of the specific depths where disturbed and undisturbed physical samples should be obtained for laboratory tests.



Zone	$q_c/N$	Soil Behavior Type
1)	2	sensitive fine grained
2)	1	organic material
3)	1	clay
4)	1.5	silty clay to clay
5)	2	clayey silt to silty clay
6)	2.5	sandy silt to clayey silt
7)	3	silty sand to sandy silt
8)	4	sand to silty sand
9)	5	sand
10)	6	gravelly sand to sand
11)	1	very stiff fine grained
12)	2	sand to clayey sand

**Figure 3-31. A commonly used simplified soil classification chart for standard electronic friction cone (after Robertson, *et al.*, 1986).**

### 3.10 DILATOMETER TEST (DMT)

The dilatometer is an in-situ testing device that was developed in Italy in the early 1970s and first introduced in the U.S. in 1979. Like the cone penetrometer, the dilatometer is generally hydraulically pushed into the ground although it may also be driven. When the dilatometer can be pushed into the ground with tests conducted at 8 in (200 mm) increments, 100 to 130 ft (30 to 40 m) of soundings may be completed in a day. The primary utilization of the dilatometer test (DMT) in pile foundation design is the delineation of subsurface stratigraphy and interpreted soil properties. However, it would appear that the CPT/CPTu is generally better suited to this task than the DMT. The DMT may be a potentially useful test for the design of piles subjected to lateral loads. Design methods in this area show promise, but are still in the development stage. For design of axially loaded piles, the DMT has limited direct value. A picture of the DMT equipment is presented in Figure 3-32.

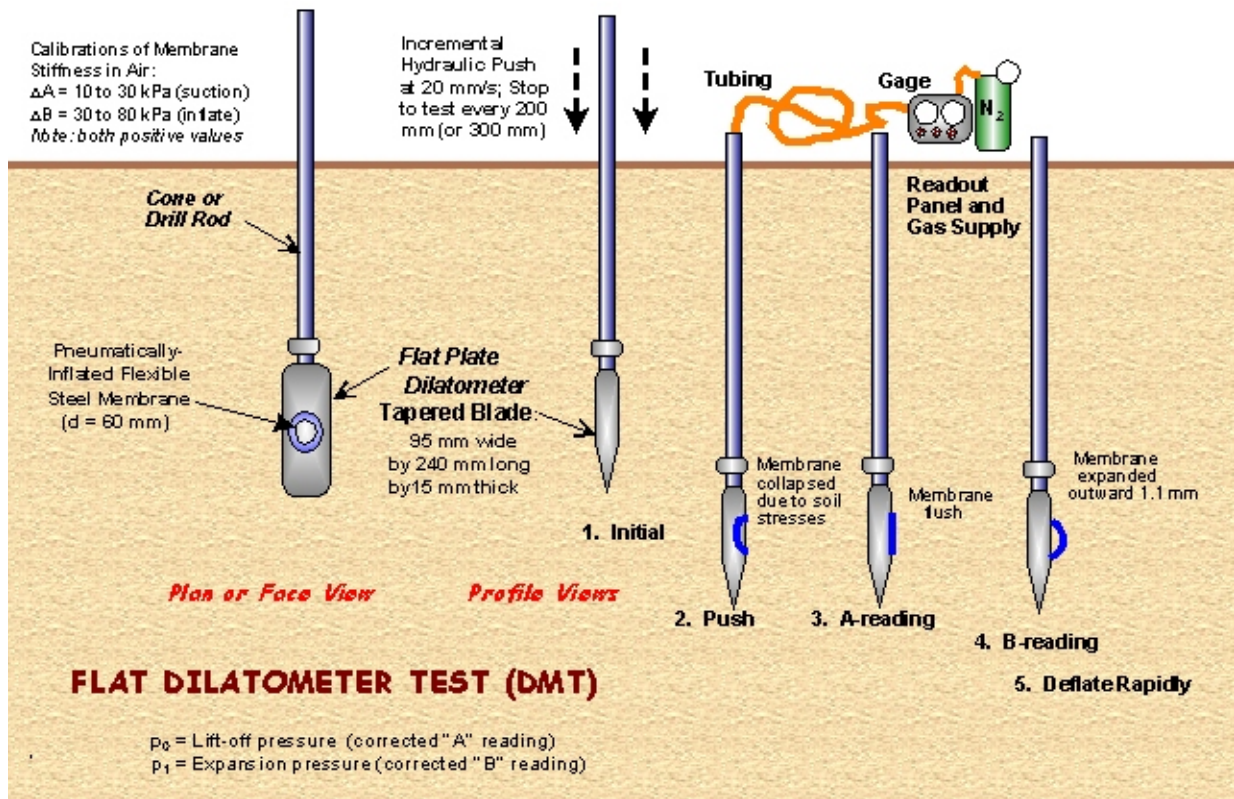


Figure 3-32. Dilatometer test equipment and procedure (FHWA 2002b).

### 3.11 PRESSUREMETER TEST (PMT)

The pressuremeter is an in-situ device used to evaluate soil and rock properties. The pressuremeter has been used in Europe for many years and was introduced into the U.S. in the mid 1970s. The pressuremeter imparts lateral pressures to the soil, and the soil shear strength and compressibility are determined by interpretation of a pressure-volume relationship. The pressuremeter test (PMT) allows a determination of the load-deformation characteristics of soil in axisymmetric conditions. Deposits such as soft clays, fissured clays, sands, gravels and soft rock can be tested with pressuremeters. A pressuremeter test produces information on the elastic modulus of the soil as well as the at rest horizontal earth pressure, the creep pressure, and the soil limit pressure. A schematic of the pressuremeter test is presented in Figure 3-33.

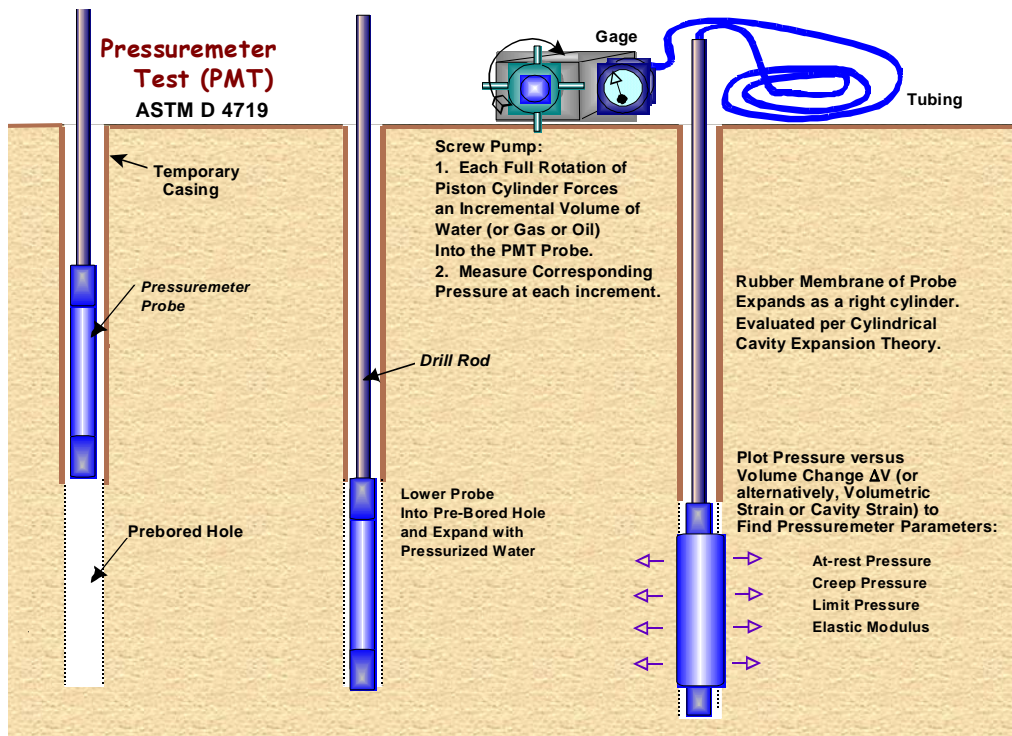


Figure 3-33. Pressuremeter test schematic (FHWA, 2002b).

The utilization of test results is based upon semi-empirical correlations from a large number of tests and observations on actual structures. For piles subjected to lateral loads, the pressuremeter test is a useful design tool and can be used for determination of p-y curves. For design of vertically loaded piles, the pressuremeter test has limited value. Pile design procedures using pressuremeter data have been developed and may be found in FHWA (1989a). Details on test procedures may be found in ASTM D 4719.

### 3.12 VANE SHEAR TEST (VST)

The vane shear test is an in-situ test for determining the undrained shear strength of soft to medium clays. Figure 3-34 is a schematic drawing of the essential components and test procedure. The test consists of forcing a four-bladed vane into undisturbed soil and rotating it until the soil shears. Two shear strengths are usually recorded, the peak shearing strength and the remolded shearing strength. These measurements are used to determine the **sensitivity of clay**, which is defined as the ratio of the peak undrained shearing strength to the remolded undrained shearing strength. Sensitivity,  $S_t$ , allows analysis of the soil resistance to be overcome during pile driving in clays which is useful for pile driveability analyses. It is necessary to measure skin friction along the steel connector rods which must be subtracted to determine the actual shear strength. The VST generally provides the most accurate undrained shear strength values for clays with undrained shear strengths less than 1 ksf (50 kPa). The test procedure has been standardized in AASHTO T 223-74 and ASTM D 2573.

It should be noted that the sensitivity of a clay determined from a vane shear test provides insight into the set-up potential of the clay deposit. However, the sensitivity value is a qualitative and not a quantitative indicator of soil set-up. Classification of clayey soils based on sensitivity values is presented in Table 3-12.

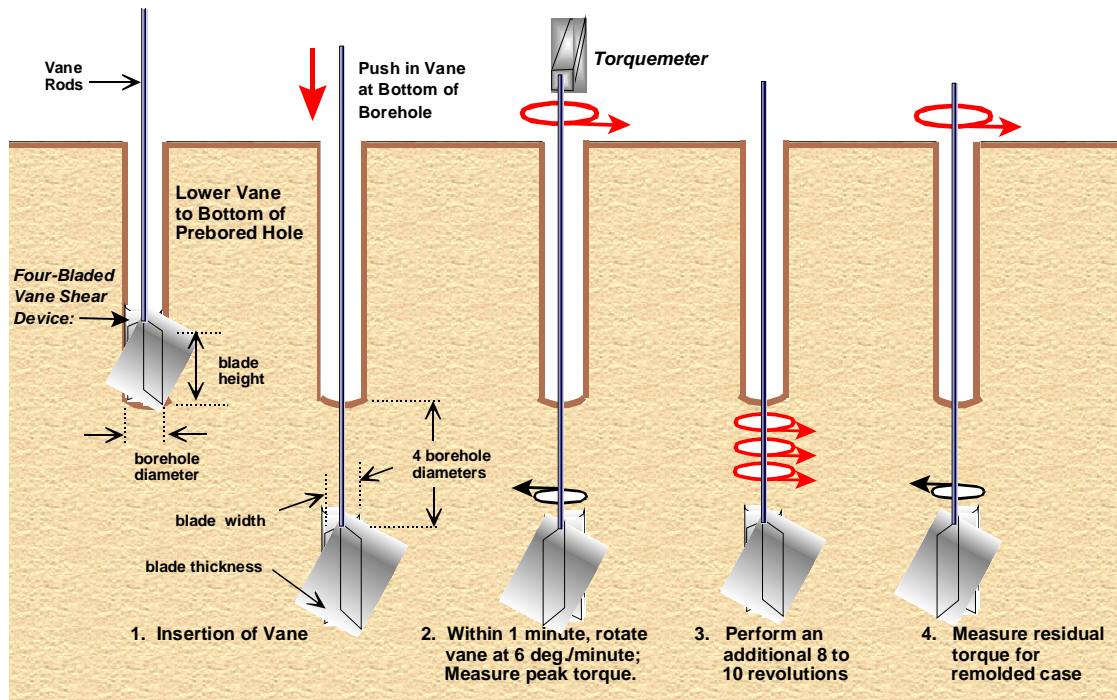


Figure 3-34. Vane shear test equipment and procedure (after FHWA, 2002b).

**Table 3-12**  
**Classification of Sensitivity Values (Mitchell, 1976)**

<b>Classification</b>	<b>Sensitivity, <math>S_t</math></b>
Insensitive	~ 1.0
Slightly sensitive clays	1 – 2
Medium sensitive clays	2 – 4
Very sensitive clays	4 – 8
Slightly quick clays	8 – 16
Medium quick clays	16 – 32
Very quick clays	32 – 64
Extra quick clays	> 64

### **3.13 GROUNDWATER MEASUREMENTS**

Observations of the groundwater level and pore water pressure are an important part of all geotechnical explorations. The identification of groundwater conditions should receive the same level of care given to soil descriptions and samples. Measurements of water entry during drilling and measurements of the groundwater level at least once following drilling should be considered a minimum effort to obtain water level data, unless alternate methods, such as installation of observation wells, are defined by the geotechnical specialist. Detailed information regarding groundwater observations can be obtained from ASTM D 4750 and ASTM D 5092.

#### **3.13.1 Information on Existing Wells**

Many states require the drillers of water wells to file logs of the wells they have drilled. These are good sources of information of the materials encountered and water levels recorded during well installation. The well owners, both public and private, may have records of the water levels after installation, which may provide extensive information on fluctuations of the water level. This information may be available at state agencies regulating the drilling and installation of water wells, such as the Department of Transportation, the Department of Natural Resources, State Geologist, Hydrology Department, Department of Environmental Quality, and Division of Water Resources.

### **3.13.2 Open Borings**

The water level in open borings should be measured after any prolonged interruption in drilling, at the completion of each boring, and at least 12 hours (preferably 24 hours) after completion of drilling. Additional water level measurements should be made at the completion of the field exploration and at other times designated by the engineer. The date and time of each observation should be recorded.

If the borehole has caved, the depth to the collapsed region should be recorded on the boring record as the collapse may have been caused by groundwater conditions. The elevations of the caved depths of certain borings may be consistent with groundwater table elevations at the site. This consistency may become apparent once the subsurface profile is constructed (see Chapters 4 and 11).

Drilling mud obscures observations of the groundwater level owing to filter cake action and the greater specific gravity of the drilling mud compared to that of the water. If drilling fluids are used to advance borings, the drill crew should be instructed to bail the hole prior to making groundwater observations.

### **3.13.3 Observation Wells**

The observation well, also referred to as a piezometer, is the fundamental means for measuring water head in an aquifer and for evaluating the performance of dewatering systems. In theory, a “piezometer” measures the water pressure in a confined aquifer or at a specific horizon of the geologic profile, while an “observation well” measures the level of a water table in an aquifer (Powers, 1992). In practice, however, the two terms are often used interchangeably to describe any device for determining static water head.

The term “observation well” is applied to any well or drilled hole used for the purpose of long-term studies of groundwater levels and pressures. Existing wells and bore holes in which casing is left in place are often used to observe groundwater levels. These, however, are not considered to be as satisfactory as wells constructed specifically for the purpose of measuring groundwater conditions. The latter may consist of a standpipe installed in a previously drilled exploratory hole or a hole drilled solely for use as an observation well.

Details of typical observation well installations are shown in Figure 3-35. The simplest type of observation well is formed by a small-diameter polyvinyl chloride (PVC) pipe set in an open hole. The bottom of the pipe is slotted and capped, and the annular space around the

slotted pipe is backfilled with clean sand. The area above the sand is sealed with bentonite, and the remaining annulus is filled with grout, concrete, or soil cuttings. A surface seal, which is sloped away from the pipe, is commonly formed with concrete in order to prevent the entrance of surface water. The top of the pipe should also be capped to prevent the entrance of foreign material; there should be a small vent hole in the top of the removable cap. In some localities, regulatory agencies may stipulate the manner for installation and closure of observation wells.

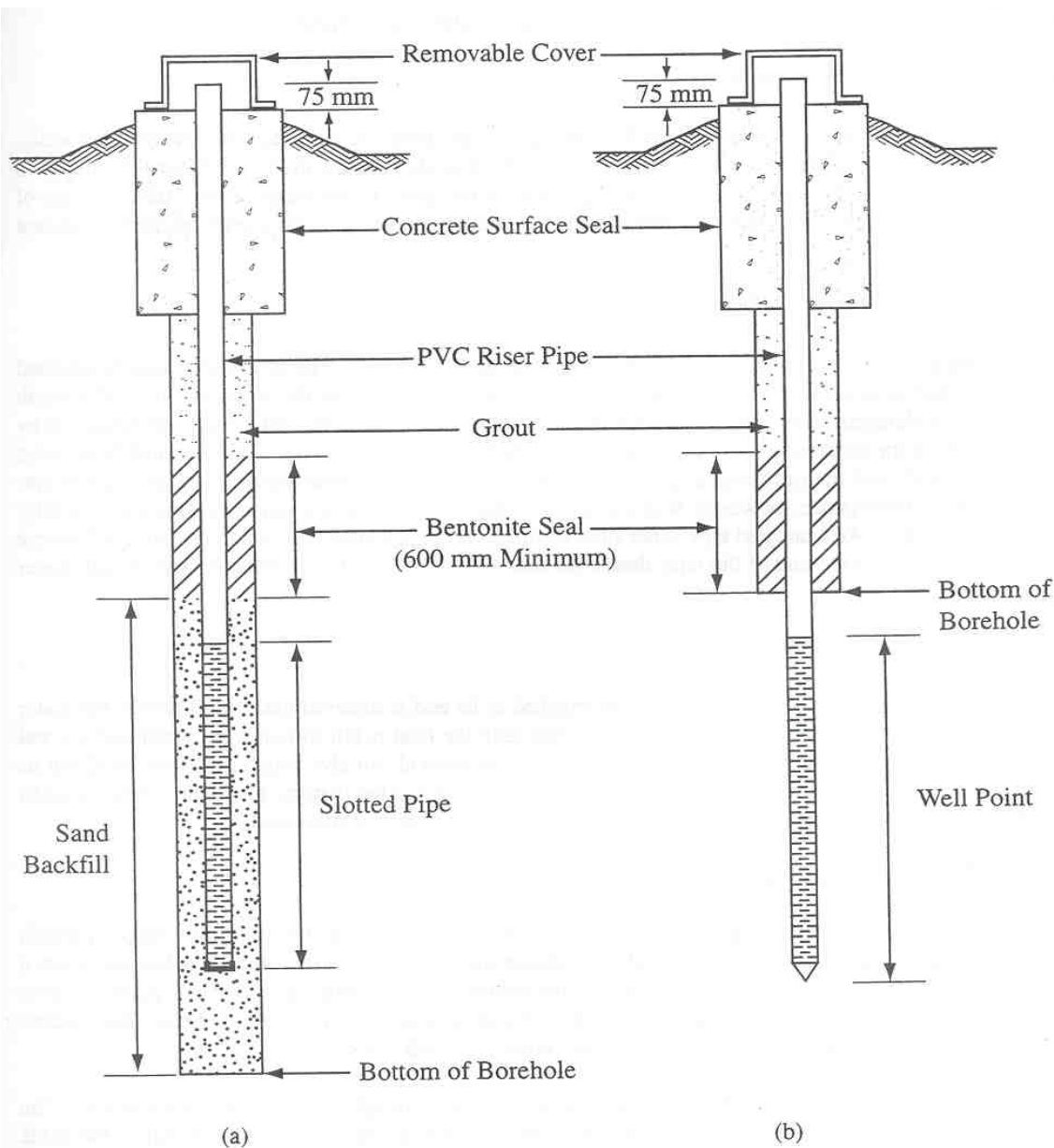


**Figure 3-35. Representative details of observation well installations. (a) Drilled-in-place stand-pipe piezometer, (b) Driven well point (FHWA, 1997).**

Driven or pushed-in well points are another common type of observation well for use in granular soil formations and very soft clay (Figure 3-35b). The well is formed by a stainless steel or brass well point threaded to a galvanized steel pipe. In granular soils, an open boring or rotary wash boring is advanced to a point several inches above the measurement depth and the well point is driven to the desired depth. A seal is commonly required in the boring above the well point with a surface seal at the ground surface. Note that observation wells may require development (see ASTM D 5092) to minimize the effects of installation, drilling fluids, etc. Minimum pipe diameters should allow introduction of a bailer or other pumping apparatus to remove fine-grained materials in the well to improve the response time.

Local jurisdictions may impose specific requirements on “permanent” observation wells, including closure and reporting of the location and construction that must be considered in the planning and installation. Licensed drillers and special fees may be required.

Piezometers are available in a number of designs. Commonly used piezometers are of the pneumatic and the vibrating wire type. Interested readers are directed to Dunnycliff (1988) and FHWA (1997) for a detailed discussion of the various types of piezometers.

### **3.13.4 Water Level Measurements**

A number of devices have been developed for sensing or measuring the water level in observation wells. Following is a brief presentation of three methods that are commonly used to measure the depth to groundwater. In general, common practice is to measure the depth to the water surface by using the top of the casing as a reference, with the reference point at a common orientation (often north) marked or notched on the well casing.

#### **3.13.4.1 Chalked Tape**

In this method a short section at the lower end of a metal tape is chalked. The tape with a weight attached to its end is then lowered until the chalked section has passed slightly below the water surface. The depth to the water is determined by subtracting the depth of penetration of the line into water, as measured by the water line in the chalked section, from the total depth from the top of casing. This is probably the most accurate method, and the accuracy is useful in pump tests where very small drawdowns are significant. The method is cumbersome, however, when a series of rapid readings is taken since the tape must be fully removed each time. An enameled tape is not suitable unless it is roughened with sandpaper so it will accept chalk. The weight on the end of the tape should be small in volume so it does not displace enough water to create an error in the water level.

#### **3.13.4.2 Tape with a Float**

In this method, a tape with a flat-bottomed float attached to its end is lowered until the float hits the water surface and the tape goes slack. The tape is then lifted until the float is felt to touch the water surface and the tape is just taut; the depth to the water surface is then measured. With practice this method can give rough measurements, but its accuracy is poor. A refinement is to mount a heavy whistle, open at the bottom, on a tape. When it sinks in the water, the whistle will give an audible beep as the air within it is displaced.

#### **3.13.4.3 Electric Water-Level Indicator**

This battery operated indicator consists of a weighted electric probe attached to the lower end of a length of electrical cable that is marked at intervals to indicate the depth. When the probe reaches the water a circuit is completed. This condition is registered by a meter mounted on the cable reel. Various manufacturers produce the instrument, utilizing a neon lamp, a horn, or an ammeter as the signaling device. The electric indicator has the advantage that it may be used in extremely small holes.

The instrument should be ruggedly built, since some degree of rough handling can be expected. The distance markings must be securely fastened to the cable. Some models are available in which the cable itself is manufactured as a measuring tape. The sensing probe should be shielded to prevent shorting out against metal risers. When the water is highly conductive, erratic readings can develop in the moist air above the actual water level. Sometimes careful attention to the intensity of the neon lamp or the pitch of the horn will enable the reader to distinguish the true level. A sensitivity adjustment on the instrument can be useful. If oil or iron sludge has accumulated in the observation well, the electric probe will give unreliable readings.

#### **3.13.4.4 Data Loggers**

When timed and frequent water level measurements are required, as for a pump test or slug test, data loggers are useful. Data loggers are in the form of an electric transducer near the bottom of the well that senses changes in water level as changes in pressure. A data acquisition system is used to acquire and store the readings. A data logger can eliminate the need for onsite technicians on night shifts during extended field permeability testing. A further significant saving is in the technician's time back in the office. The preferred models of the data logger not only record the water level readings but permit the data to be downloaded into a personal computer and, with appropriate software, to be quickly reduced

and plotted. These devices are also extremely useful for cases where measurement of artesian pressures is required or where data for tidal corrections during field permeability tests are necessary.

### **3.14 GUIDELINES FOR MINIMUM SUBSURFACE EXPLORATION**

In regard to the scope of the subsurface exploration program for a structure or a geotechnical feature, one must consider the small cost of the borings in relation to the foundation costs. The knowledge gained from a thorough subsurface exploration program will allow the geotechnical specialist to evaluate various candidate foundation schemes and provide recommendations for those that can be built most efficiently and economically on the project site. Without an adequate subsurface exploration program, the result is generally an extremely conservative foundation recommendation.

Planning a subsurface exploration program should include determining the location and depth of borings, test pits, or other procedures to be used and establishing the methods of soil sampling and testing to be employed. Usually, the extent of the work is estimated based on available geological studies, earlier explorations, or records of existing structures. The number of borings and their locations in a site area will depend on the proposed structure, design parameters, access issues, geologic constraints, and expected stratigraphy.

Although no rigid rules apply universally to geotechnical explorations, certain general principles are usually followed in practice. Recommended guidelines for the minimum number of exploration points and their spacing are provided in Table 3-13. This table was developed based on a number of FHWA documents. This table should be used only as a first step in estimating the minimum number of borings for a particular design, as actual boring spacings will be dependent upon the project type and geologic environment. In all cases, it is recommended that the depth of the exploration should be such that the depth of significant influence (DOSI) is explored. For a given configuration of loading, the DOSI may exceed the minimum guidelines in Table 3-13 in which case the depth of exploration should be increased accordingly. Some other general guidance in addition to that in Table 3-13 is as follows:

- In areas underlain by heterogeneous soil deposits and/or rock formations, it will probably be necessary to exceed the minimum guidelines presented in Table 3-13 to capture variations in soil and/or rock type and to assess consistency across the site.

**Table 3-13**  
**Guidelines for minimum number of exploration points and depth of exploration (modified after FHWA, 2002a)**

<b>Application</b>	<b>Minimum Number of Exploration Points and Location of Exploration Points</b>	<b>Minimum Depth of Exploration</b>
Retaining walls	<ul style="list-style-type: none"> <li>(1) A minimum of one exploration point for each retaining wall.</li> <li>(2) For retaining walls more than 100 ft (30 m) in length, exploration points spaced every 100 to 200 ft (30 to 60 m) with locations alternating from in front of the wall to behind the wall.</li> <li>(3) For anchored walls, additional exploration points in the anchorage zone spaced at 100 to 200 ft (30 to 60 m).</li> <li>(4) For soil-nail walls, additional exploration points at a distance of 1.0 to 1.5 times the height of the wall behind the wall spaced at 100 to 200 ft (30 to 60 m).</li> </ul>	<ul style="list-style-type: none"> <li>(1) Investigate to a depth below bottom of wall between 1 and 2 times the wall height or a minimum of 10 ft (3 m) into bedrock.</li> <li>(2) Exploration depth should be great enough to fully penetrate soft highly compressible soils (e.g. peat, organic silt, soft fine grained soils) into competent material of suitable bearing capacity (e.g., stiff to hard cohesive soil, compact dense cohesionless soil, or bedrock).</li> </ul>
Embankment Foundations	<ul style="list-style-type: none"> <li>(1) A minimum of one exploration point every 200 ft (60 m) (erratic conditions) to 400 ft (120 m) (uniform conditions) of embankment length along the centerline of the embankment.</li> <li>(2) At critical locations, (e.g., maximum embankment heights, maximum depths of soft strata) a minimum of three exploration points in the transverse direction to define the existing subsurface conditions for stability analyses.</li> <li>(3) For bridge approach embankments, at least one exploration point at abutment locations.</li> </ul>	<ul style="list-style-type: none"> <li>(1) Exploration depth should be, at a minimum, equal to twice the embankment height unless a hard stratum is encountered above this depth.</li> <li>(2) If soft strata are encountered extending to a depth greater than twice the embankment height, the exploration depth should be great enough to fully penetrate the soft strata into competent material (e.g., stiff to hard cohesive soil, compact to dense cohesionless soil, or bedrock).</li> </ul>
Cut Slopes	<ul style="list-style-type: none"> <li>(1) A minimum of one exploration point every 200 ft (60 m) (erratic conditions) to 400 ft (120 m) (uniform conditions) of slope length.</li> <li>(2) At critical locations (e.g., maximum cut depths, maximum depths of soft strata) a minimum of three exploration points in the transverse direction to define the existing subsurface conditions for stability analyses.</li> <li>(3) For cut slopes in rock, perform geologic mapping along the length of the cut slope.</li> </ul>	<ul style="list-style-type: none"> <li>(1) Exploration depth should be, at a minimum, 15 ft (4.5 m) below the minimum elevation of the cut unless a hard stratum is encountered below the minimum elevation of the cut.</li> <li>(2) Exploration depth should be great enough to fully penetrate through soft strata into competent material (e.g., stiff to hard cohesive soil, compact to dense cohesionless soil, or bedrock).</li> <li>(3) In locations where the base of cut is below ground-water level, increase depth of exploration as needed to determine the depth of underlying pervious strata.</li> </ul>

**Table 3-13 (Continued)**  
**Guidelines for minimum number of exploration points and depth of exploration (after FHWA, 2002a)**

<b>Application</b>	<b>Minimum Number of Exploration Points and Location of Exploration Points</b>	<b>Minimum Depth of Exploration</b>
Shallow Foundations	<ul style="list-style-type: none"> <li>(1) For substructure (e.g., piers or abutments) widths less than or equal to 100 ft (30 m), a minimum of one exploration point per substructure.</li> <li>(2) For substructure widths greater than 100 ft (30 m), a minimum of two exploration points per substructure.</li> <li>(3) Additional exploration points should be provided if erratic subsurface conditions or sloping rock surfaces are encountered.</li> </ul>	<p>Depth of exploration should be:</p> <ul style="list-style-type: none"> <li>(1) great enough to fully penetrate unsuitable foundation soils (e.g., peat, organic silt, soft fine grained soils) into competent material of suitable bearing capacity (e.g. stiff to hard cohesive soil, compact to dense cohesionless soil or bedrock); and</li> <li>(2) <b>at least to a depth where stress increase due to estimated footing load is less than 10% of the applied stress at the base of the footing;</b> and</li> <li>(3) in terms of the width of the footing: at least 2 times for axisymmetric case and 4 times for strip footing (interpolate for intermediate cases); and</li> <li>(4) if bedrock is encountered before the depth required by item (2) above is achieved, exploration depth should be great enough to penetrate a minimum of 10 ft (3 m) into the bedrock, but rock exploration should be sufficient to characterize compressibility of infill material of near-horizontal to horizontal discontinuities.</li> </ul>
Deep Foundations	<ul style="list-style-type: none"> <li>(1) For substructure (e.g., bridge piers or abutments) widths less than or equal to 100 ft (30 m), a minimum of one exploration point per substructure.</li> <li>(2) For substructure widths greater than 100 ft (30 m), a minimum of two exploration points per substructure.</li> <li>(3) Additional exploration points should be provided if erratic subsurface conditions are encountered.</li> <li>(4) Due to large expense associated with construction of rock-socketed shafts, conditions should be confirmed at each shaft location.</li> </ul>	<ul style="list-style-type: none"> <li>(1) In soil, depth of exploration should extend below the anticipated pile or shaft tip elevation a minimum of 20 ft (6 m), or a minimum of two times the maximum pile group dimension, whichever is deeper. All borings should extend through unsuitable strata such as unconsolidated fill, peat, highly organic materials, soft fine-grained soils, and loose coarse-grained soils to reach hard or dense materials.</li> <li>(2) For piles bearing on rock, a minimum of 10 ft (3 m) of rock core shall be obtained at each exploration point location to verify that the boring has not terminated on a boulder.</li> <li>(3) For shafts supported on or extending into rock, a minimum of 10 ft (3 m) of rock core, or a length of rock core equal to at least three times the shaft diameter for isolated shafts or two times the maximum shaft group dimension, whichever is greater, shall be extended below the anticipated shaft tip elevation to determine the physical characteristics of rock within the zone of foundation influence.</li> </ul>

- In the case of embankments, the guidance provided in Table 3-13 for the depth of exploration is the minimum recommended for any transportation facility, i.e., 2 times the height of the embankment. The minimum guidance may not be the same as the DOSI, which is a function of the geometry (crest width, height, configuration of side slopes, and the base width) of the embankment. For the same height of embankment, the DOSI increases as the base width of an embankment increases, and may vary from 4 to 6 times the height of the embankment. An example of this is shown in Figures 2-8 in Chapter 2, which shows that the DOSI can extend to depths much deeper than 2 times the height of the embankment. This may be particularly critical in cases where there are soft soils in the subsurface. Thus, for such situations, the geotechnical specialist should use tools such as the FoSSA program or published elastic solutions (Poulos and Davis, 1974) to determine the depth of exploration.
- For situations where large-diameter rock-socketed shafts will be used or where drilled shafts are being installed in karstic formations, it may be necessary to advance a boring at the location of each shaft.
- In a laterally homogeneous area, drilling or advancing a large number of borings may be redundant, since each sample tested would exhibit similar strength and compressibility properties.
- In all cases, it is necessary to understand how the design and construction of the geotechnical feature will affect the soil and/or rock mass in order to optimize the exploration.

During exploration, each exploration point (e.g., drill hole or CPT sounding) should be designated by a unique identification number to prevent duplication during subsequent explorations. For example, it is not unusual to find projects where borehole numbering was done by only single numbers so that the same designations were used during one or more subsequent explorations. A suggested method to avoid duplication is to designate that all bridge holes begin with the letter "B," followed by the initials of the highway or river being crossed and finally a sequential number. For example, the first boring for a structure on Apple Freeway would be designated DH-BAF-1, where the DH means a "drill hole" where SPTs were performed as opposed to CPT-BAF-1, where the CPT refers to the first CPT sounding performed for a bridge structure on Apple Freeway.

The geotechnical specialist should plot the proposed boring locations on a site topographic map prior to initiation of drilling. Notes taken during the site visit should be reviewed before boring locations are selected so that site access restrictions can be considered. Boring locations should never be selected arbitrarily or randomly. Alternate boring locations should be considered and a contingency plan should be developed in case a boring needs to be relocated due to access restrictions or unexpected geologic conditions (e.g., locate a replacement boring within a maximum of 15 ft (4.5 m) from the location of a boring that could not be drilled at a particular location). Field personnel unfamiliar with the objectives and rationale behind the planning of the site exploration should maintain contact with the person in responsible charge of the field exploration during field activities and discuss issues such as the relocation of a boring with that person. Arbitrary or random boring selection will increase the chances of boring relocation, confusion, and wasted time in the field. Final boring locations should be surveyed and recorded as part of the permanent project record. Elevations and northing and easting should be provided for each boring.

### **3.14.1 Recommendations for Sampling Depth Intervals in Soils**

It is difficult to establish a prescriptive drilling, sampling, and testing protocol that is applicable to all sites. To be most effective the geotechnical specialist should:

- (1) apply conventional guidelines with project-specific requirements and constraints;
- (2) recognize the advantages and limitations of the available sampling devices and in-situ testing methods.

Some general recommendations for minimum sampling depth intervals are as follows:

- For preliminary screening, disturbed samples might be taken continuously in the upper 10 ft (3 m), at 5 ft (1.5 m) intervals up to 100 ft (30 m), and possibly every 10 ft (3 m) at depths greater than 100 ft (30 m).
- Disturbed samples should be taken at every abrupt change in stratum as indicated by a noticeable change in the drilling pressure.
- Where footings are to be placed on natural soil, continuous spoon samples are recommended for a depth equal to 15 ft (4.5 m) or 1.5 times the width of the footing, whichever is greater, as measured below the anticipated footing base elevation.

- For characterization and assessment of design properties in fine-grained soils, a minimum of one undisturbed sample should be taken in each stratum, with additional samples taken at 10- to 20-ft (3 to 6 m) intervals with depth.
- Undisturbed Shelby tube samples should be obtained at 5 ft (1.5 m) intervals in at least one boring in cohesive soils. For cohesive deposits greater than 30 ft (9 m) in depth, the tube sample interval can be increased to 10 ft (3 m). Undisturbed samples may not need to be taken in each boring if the deposit is relatively homogeneous within closely spaced borings.

These minimum guidelines and intervals may need to be increased depending upon the project requirements and site geologic conditions. The sampling interval may need to be increased when soil/rock conditions change frequently with depth; however, these changes need to be considered in the context of the design. Therefore, ongoing communication between field personnel and the office/design engineer is absolutely essential. Once the site stratigraphy has been established, it may not be necessary to sample every time there is a change in stratigraphy if the changes have no impact on design. For example, it may not be necessary to sample alternating layers of coarse-grained deposits where settlement is of concern, and for designs concerned with bearing capacity. Similarly, although samples below the anticipated extent of the area influenced by the load may be reduced, samples should be obtained in case the type of foundation changes between preliminary and final design.

The sampling interval will vary between individual projects and regional geologies. If soils are anticipated to be difficult to sample or trim in the laboratory due to defects (e.g., bent tubes, improper handling, etc.), the frequency of sample collection should be greater than average to offset the number of samples that may be unusable in the laboratory for performance property evaluation (e.g., shear strength). When borings are widely spaced, it may be appropriate to retrieve undisturbed samples in each boring. For closely spaced borings or in deposits of lateral uniformity, undisturbed samples may be needed only in select borings. If a thin clay seam is encountered during drilling and not sampled, the boring may need to be offset and re-drilled to obtain a sample.

It is often quite helpful to combine in-situ soundings with conventional disturbed/undisturbed sampling. For example, by performing CPT or CPTu soundings prior to conventional drilling and sampling, it may be possible to target representative and/or critical areas where samples can be obtained later. This concept was illustrated previously by the discussion in Section 3.9.7 and Figure 3-30. The use of precursor soundings may reduce some of the potential drilling redundancy in heterogeneous environments. Geophysical methods can also

be used to provide useful information on conditions between and even beyond boring locations.

### **3.14.2 Recommendations for Sampling Depth Intervals in Rocks**

For explorations for slopes and foundations within rock, it is important to consider structural geology in addition to the information obtained as part of a rock-coring program. For example, the orientation and characteristics of a clay-filled discontinuity are critical since they can be used to judge whether a rock slope will be stable or unstable or whether a structural foundation will undergo minor or significant settlement. A detailed structural geologic assessment may provide enough information to limit the scope of a rock-coring program significantly or even preclude such a program. For example, drilling and coring may not be required where applied loads are significantly less than the bearing capacity of the rock, where there is no possibility of sliding instability in a rock slope, or where there are extensive rock outcrops from which information can be obtained to establish the subsurface conditions confidently for design and constructability assessments (Wyllie, 1999).

### **3.14.3 Recommendations for Water Level Monitoring in Borings**

The water level in each boring should be observed and the depth below the top of hole recorded on the drill log with the date and time of the reading for each of the following situations:

- a) Water seepage or artesian pressure encountered during drilling. Artesian pressure may be measured by extending drill casing above the ground until flow stops. Report the pressure as the number of ft (m) of head above ground.
- b) Water level at the end of each day and at completion of boring.
- c) Water level 24 hours (minimum) after hole completion. Long term readings may require installation of a perforated plastic tube before abandoning the hole.

A false indication of water level may be obtained when water is used in drilling and adequate time is not permitted after the boring is completed for the water level to stabilize. In low permeability soils, such as clays, more than one week may be required to obtain accurate readings. Proper safety precautions should be taken if a hole is allowed to remain open for such an extended period of time.

### 3.15 GEOPHYSICAL TESTS

As indicated in Section 3.3, geophysical testing can be used as part of the initial site exploration to provide supplementary information to data collected by other means (i.e., borings, test pits, geologic surveys, etc.). Geophysical testing can be used for establishing stratification of subsurface materials, the profile of the top of bedrock, the depth to groundwater, the boundaries of various types of soil deposits, the rippability of hard soil and rock, and the presence and depth of voids, buried pipes, and existing foundations. Data from geophysical testing should always be correlated with information from the direct methods of exploration discussed previously.

#### 3.15.1 Types of Geophysical Tests

There are a number of different types of geophysical in-situ tests that can be used to obtain stratigraphic information from which engineering properties can be estimated. Table 3-14 provides a summary of the various geophysical methods that are currently available in U.S. practice. Further information on the procedures used for these methods is provided in FHWA (2003). Additional general discussion regarding the major test methods listed in Table 3-14 is presented below, with particular emphasis on potential applications to highway engineering.

1. **Seismic Methods:** These methods are becoming increasingly popular for geotechnical engineering practice because they have the potential to provide data regarding the compression and shear wave velocities of the subsurface materials. The shear wave velocity is directly related to small-strain material stiffness, which, in turn, is often correlated to compressive strength and soil/rock type. These techniques are often used for assessing the vertical stiffness profile in a soil deposit and for assessing the location at depth of the interface between soil and rock. Seismic refraction method involves measurement of time of arrival of the initial ground motion generated by the energy source while the seismic reflection method involves measurement of the energy arrival after the initial ground motion.
2. **Electrical Methods:** These methods are usually used to locate voids or locally distinct materials. With regards to highway applications, these procedures may be used to assess the potential for karst activity along a planned transportation corridor, or for locating large underground voids and/or specific underground anomalies such as storage drums and/or tanks. Electrical methods provide qualitative information only and are usually part of a two- or three-phased exploration program.

**Table 3-14  
Geophysical testing techniques (modified after FHWA, 2002a)**

Method	Basic Field Procedures	Applications	Limitations
<b>SEISMIC METHODS</b>			
Seismic Refraction	Impact load is applied to the ground surface. Seismic energy refracts off soil/rock layer interfaces and the <i>time of arrival</i> is recorded on the ground surface using several dozen geophones positioned along a line or performing repeated events using a single geophone.	<ul style="list-style-type: none"> <li>• depth to bedrock</li> <li>• depth to water table</li> <li>• thickness and relative stiffness soil/rock layers</li> </ul>	<ul style="list-style-type: none"> <li>• does not work if stiffness decreases with depth or if soft layer underlies stiff layer</li> <li>• works best when sharp stiffness discontinuity is present</li> </ul>
Spectral-Analysis-of-Surface-Waves (SASW)	Impact load is applied to the ground surface. Surface waves propagate along ground surface and are recorded on the ground surface with two geophones positioned along a line.	<ul style="list-style-type: none"> <li>• depth to bedrock</li> <li>• measurement of shear wave velocity</li> <li>• thickness and stiffness of surface pavement layer</li> <li>• qualitative indicator of cracking in pavement</li> </ul>	<ul style="list-style-type: none"> <li>• resolution decreases significantly with increasing depth</li> <li>• accurate interpretation may require a significant amount of expertise</li> <li>• interpretation is difficult if a stiff layer overlies a soft layer and soft layer properties are desired</li> </ul>
<b>ELECTRICAL METHODS</b>			
DC Resistivity	DC current is applied to the ground by electrodes. Voltages are measured at different points on the ground surface with other electrodes positioned along a line.	<ul style="list-style-type: none"> <li>• depth to water table</li> <li>• inorganic groundwater contamination</li> <li>• groundwater salinity</li> <li>• soil layer thickness</li> <li>• delineation of certain vertical features (e.g., sinkholes, contamination plumes, waste trenches)</li> </ul>	<ul style="list-style-type: none"> <li>• slow; must install electrodes directly in the ground</li> <li>• resolution decreases significantly with increasing depth</li> <li>• resolution is difficult in highly heterogeneous deposits</li> </ul>
Electromagnetics	Electrical coils are held over the ground. Current passing through the coils induces a magnetic field in the ground, which is measured with receiver coils.	<ul style="list-style-type: none"> <li>• groundwater salinity</li> <li>• inorganic groundwater contamination</li> <li>• detection of buried metal objects</li> <li>• delineation of certain vertical features (e.g., sinkholes, contamination plumes, waste trenches)</li> </ul>	<ul style="list-style-type: none"> <li>• extra effort is required to characterize depth of target</li> <li>• resolution decreases significantly with increasing depth</li> </ul>
Ground Penetrating Radar (GPR)	Electromagnetic energy is pulsed into the ground. This energy reflects off boundaries between different soil layers and is measured at the ground surface.	<ul style="list-style-type: none"> <li>• depth to water table</li> <li>• identification of buried objects</li> <li>• thickness of pavement layers</li> <li>• void detection</li> </ul>	<ul style="list-style-type: none"> <li>• not effective below the water table or in clay</li> <li>• depth of penetration is limited to about 30 ft (10 m)</li> </ul>

**Table 3-14  
Geophysical testing techniques (modified after FHWA, 2002a)**

<b>Method</b>	<b>Basic Field Procedures</b>	<b>Applications</b>	<b>Limitations</b>
<b>GRAVITY AND MAGNETIC METHODS</b>			
Gravity	The Earth's gravitational field is measured at the ground surface.	<ul style="list-style-type: none"> <li>• identification of large subsurface voids</li> <li>• identification of large objects possessing unusually high or low densities</li> </ul>	<ul style="list-style-type: none"> <li>• results are non-unique (i.e. more than one subsurface condition can give the same result)</li> <li>• primarily, large-scale reconnaissance tool; applications in highway engineering are limited</li> </ul>
Magnetics	The Earth's magnetic field is measured at the ground surface.	<ul style="list-style-type: none"> <li>• identification of ferrous materials</li> <li>• identification of soil/rock containing large amounts of magnetic minerals</li> </ul>	<ul style="list-style-type: none"> <li>• results are non-unique (i.e. more than one subsurface condition can give the same results)</li> <li>• primarily a large-scale reconnaissance tool; applications in highway engineering are limited</li> </ul>
<b>NEAR-SURFACE NUCLEAR METHODS</b>			
Neutron Moisture Content	Instrument is placed on the ground surface and neutrons are emitted into the ground. Energy of returning neutrons is related to the moisture content in the ground (hydrogen atoms decrease the energy of the neutrons detected at the sensor).	<ul style="list-style-type: none"> <li>• estimate of water content in compacted soil</li> <li>• estimate of asphalt content in asphalt concrete</li> <li>• can be quantitative if properly calibrated to site conditions</li> </ul>	<ul style="list-style-type: none"> <li>• limited exploration depth (a few inches)</li> <li>• possible health and safety hazard if operators not properly trained</li> <li>• will detect hydrogen ion (i.e. gas, clay) in non-water bearing stratum</li> </ul>
Gamma Density	Instrument is placed on the ground surface and gamma radiation is emitted into the ground. Returning gamma energy is a function of material density (denser materials absorb more gamma energy so less is detected at the sensor)	<ul style="list-style-type: none"> <li>• estimate of density of soil or asphalt concrete</li> </ul>	<ul style="list-style-type: none"> <li>• limited exploration depth (less than one foot);</li> <li>• exploration depth further limited to a few inches if ground cannot be penetrated</li> <li>• possible health and safety hazard if operators not properly trained</li> </ul>

**Table 3-14 (continued)**  
**Geophysical testing techniques (modified after FHWA, 2002a)**

<b>Method</b>	<b>Basic Field Procedures</b>	<b>Applications</b>	<b>Limitations</b>
<b>BOREHOLE METHODS</b>			
Crosshole/ Downhole	Energy sources and geophones are placed in boreholes and/or on ground surface; interval travel times are converted into seismic wave velocity as a function of depth in the borehole.	<ul style="list-style-type: none"> <li>• measurement of wave velocities for seismic site response analysis</li> <li>• depth to water table</li> <li>• correlation of lithologic units with surface seismic</li> <li>• identification of thin layers at depth</li> </ul>	<ul style="list-style-type: none"> <li>• requires one or more boreholes and significant support field equipment</li> </ul>
Suspension Logger	Field instrument is placed in a fluid-filled borehole and used to measure P-(compression) and S-(shear) wave velocities in surrounding soil or rock.	<ul style="list-style-type: none"> <li>• measurement of wave velocities for seismic site response analysis</li> <li>• correlation of lithologic units with surface seismic</li> <li>• identification of thin layers at depth</li> </ul>	<ul style="list-style-type: none"> <li>• requires borehole and significant support field equipment, which is expensive</li> <li>• borehole must be fluid-filled</li> </ul>
Electrical Logging	Field instrument is placed in a borehole. Electrical fields are directly applied or electromagnetically induced into surrounding soil or rock and electrical resistivity is measured.	<ul style="list-style-type: none"> <li>• estimate of soil/rock permeability or porosity</li> <li>• identification of inorganic contaminant plumes or saltwater intrusion</li> <li>• identification of thin layers at depth</li> </ul>	<ul style="list-style-type: none"> <li>• requires borehole and significant support field equipment, which is expensive</li> <li>• generally cannot operate in a cased borehole</li> <li>• may require fluid-filled borehole</li> <li>• results may be dependent upon drilling mud salinity</li> </ul>
Nuclear Logging	Field instrument is placed in a borehole. Surrounding soil or rock is irradiated with neutrons particles and/or gamma energy. Energy and neutrons returning to the instrument are measured and related to rock density, porosity and pore fluid type.	<ul style="list-style-type: none"> <li>• estimate of soil/rock type, density, porosity, and pore fluid density</li> <li>• identification of thin layers at depth</li> </ul>	<ul style="list-style-type: none"> <li>• requires borehole and significant support field equipment, which is expensive</li> <li>• possible health and safety hazard if operators are not properly trained</li> </ul>
Lithology Logging	Field instrument is placed in a borehole; naturally occurring electrical fields and radiation levels are related to soil or rock type.	<ul style="list-style-type: none"> <li>• classification of soil or rock type</li> <li>• identification of thin layers at depth</li> </ul>	<ul style="list-style-type: none"> <li>• requires borehole and significant support field equipment, which is expensive</li> <li>• may require fluid-filled borehole</li> <li>• results are dependent upon site-specific conditions and/or borehole fluid salinity</li> </ul>

3. **Gravity and Magnetic Methods:** These methods are similar to electrical methods, except that they rely on correlations between the potential gravitational and/or magnetic influence of voids and subsurface anomalies and measured differences in the earth's micro-gravitational and/or magnetic fields, rather than on changes in electrical fields. These methods provide measurements at specific points unlike seismic and electrical methods that provide measurements over large areas.
4. **Near-surface nuclear methods:** These methods have been used for several years for compaction control of fills in the field. Through careful calibration, it is possible to assess the moisture content and density of compacted soils reliably. These methods have been widely adopted as reliable quantitative methods.
5. **Borehole Methods:** Downhole geophysical methods provide reliable indications of a wide range of soil properties. For example, downhole/crosshole methods provide reliable measures of shear wave velocity. As indicated previously, shear wave velocity is directly related to small-strain stiffness and is correlated to strength and soil/rock type. Although downhole logging methods have seen little use in highway construction, they have been the mainstay for deep geologic characterization in oil exploration. The principal advantage of downhole logging is the ability to obtain several different geophysical tests/indicators by "stringing" these tools together in a deep borehole.

### **3.15.2 Advantages and Disadvantages of Geophysical Tests**

As with the other methods of exploration, geophysical testing offers some advantages and some disadvantages that should be considered before these techniques are recommended for a specific application. These are summarized as follows:

#### **3.15.2.1 Advantages of Geophysical Tests**

1. Many geophysical tests are non-invasive. Therefore such tests offer significant benefits in cases where conventional drilling, testing, and sampling are difficult (e.g., deposits of gravel, talus deposits, etc.) or where potentially contaminated soils may occur in the subsurface.
2. In general, geophysical testing can cover a relatively large geographical area thereby providing the opportunity to characterize large areas with relatively few tests. Geophysical testing is particularly well-suited to projects that have large longitudinal extent such as new highway construction.

3. Geophysical measurements are used to assess the properties of soil and rock at very small strains, typically on the order of 0.001 percent, thereby providing information on truly elastic properties.
4. For the purpose of obtaining information on the subsurface, geophysical methods are relatively inexpensive considering the large area over which they provide information.

### **3.15.2.2 Disadvantages of Geophysical Tests**

1. Most methods work best for situations in which there is a large difference in the property being measured between adjacent subsurface units. In seismic methods, it is difficult to develop good stratigraphic profiling if the general stratigraphy consists of hard material overlying soft material.
2. Each geophysical method has limitations that may be associated with equipment, signal noise, unfavorable site and subsurface conditions, and processing constraints.
3. Results can be non-unique and are generally interpreted qualitatively. Therefore useful results can be obtained only through analyses performed by a geotechnical specialist experienced with the particular testing method.
4. Specialized and more electronically sophisticated equipment is required as compared to the more conventional subsurface exploration tools.

### **3.15.3 Examples of Uses of Geophysical Tests**

The following are a few examples where geophysical testing could be used on highway projects to compliment conventional exploration.

1. Highly Variable Subsurface Conditions: In several geologic settings, the subsurface conditions along a transportation corridor may be expected to be variable. This variability could be from underlying karst development above limestone; alluvial deposits, including buried terrace gravels, across a wide floodplain; buried boulders in a talus slope, etc. For these cases, conventional exploration techniques may be very difficult and if “refusal” is encountered at one depth, there is a strong likelihood that different materials could underlie the region. Development of a preliminary subsurface characterization profile by using geophysical testing could prove advantageous in designing future focused explorations.

2. Regional Studies: Along a transportation corridor it may be necessary to assess the depth to (and through) rippable rock or highly cemented caliche. Alternative alignments may or may not be possible, but the cost implications may be significant. Therefore, it is important to obtain a profile related to rock/soil stiffness. Geophysical testing is a logical consideration for this application as a precursor to invasive explorations.
  
3. Settlement Sensitive Structures: The prior two examples related to cases where the geophysical testing served as the front-end of a multi-phase project. In the case where a settlement-sensitive structure is to be founded on deposits of sands, knowledge of the in-situ modulus of the sand deposit is critical. After the characteristics of the site are assessed, it may be helpful to quantify the deformation modulus by the use of geophysical testing at the specific foundation site.

These examples demonstrate that geophysical testing can play a potentially important role in the subsurface characterization of soils and rocks. As with the other investigative “tools” described in this document, the particular selection of the appropriate technology is very much a function of the site conditions and the goals of the characterization program.

## CHAPTER 4.0

### ENGINEERING DESCRIPTION, CLASSIFICATION AND CHARACTERISTICS OF SOILS AND ROCKS

The geotechnical specialist is usually concerned with the design and construction of some type of geotechnical feature constructed on or out of a geomaterial. For engineering purposes, in the context of this manual, the geomaterial is considered to be primarily rock and soil. A geomaterial intermediate between soil and rock is labeled as an intermediate geomaterial (IGM). These three classes of geomaterials are described as follows:

- **Rock** is a relatively hard, naturally formed solid mass consisting of various minerals and whose formation is due to any number of physical and chemical processes. The rock mass is generally so large and so hard that relatively great effort (e.g., blasting or heavy crushing forces) is required to break it down into smaller particles.
- **Soil** is defined as a conglomeration consisting of a wide range of relatively smaller particles derived from a parent rock through mechanical weathering processes that include air and/or water abrasion, freeze-thaw cycles, temperature changes, plant and animal activity and by chemical weathering processes that include oxidation and carbonation. The soil mass may contain air, water, and/or organic materials derived from decay of vegetation, etc. The density or consistency of the soil mass can range from very dense or hard to loose or very soft.
- **Intermediate geomaterials (IGMs)** are transition materials between soils and rocks. The distinction of IGMs from soils or rocks for geotechnical engineering purposes is made purely on the basis of strength of the geomaterials. Discussions and special design considerations of IGMs are beyond the scope of this document.

The following three terms are often used by geotechnical specialists to describe a geomaterial: **identification**, **description** and **classification**. For soils, these terms have the following meaning:

- **Identification** is the process of determining which components exist in a particular soil sample, i.e., gravel, sand, silt, clay, etc.
- **Description** is the process of estimating the relative percentage of each component to prepare a word picture of the sample (ASTM D 2488). Identification and description are accomplished primarily by both a visual examination and the feel of the sample, particularly when water is added to the sample. Description is usually performed in the

field and may be reevaluated by experienced personnel in the laboratory.

- **Classification** is the laboratory-based process of grouping soils with similar engineering characteristics into categories. For example, the Unified Soil Classification System, USCS, (ASTM D 2487), which is the most commonly used system in geotechnical work, is based on grain size, gradation, and plasticity. The AASHTO system (M 145), which is commonly used for highway projects, groups soils into categories having similar load carrying capacity and service characteristics for pavement subgrade design.

It may be noted from the above definitions that the description of a geomaterial necessarily includes its identification. Therefore, as used in this document, the term “description” is meant to include “identification.”

The important distinction between classification and description is that standard AASHTO or ASTM laboratory tests must be performed to determine the classification. It is often unnecessary to perform the laboratory tests to classify every sample. Instead soil technicians are trained to identify and describe soil samples to an accuracy that is acceptable for design and construction purposes. ASTM D 2488 is used for guidance in such visual and tactile identification and description procedures. These visual/tactile methods provide the basis for a preliminary classification of the soil according to the USCS and AASHTO system.

During progression of a boring, the field personnel should describe only the soils encountered. Group symbols associated with classification should not be used in the field. It is important to send the soil samples to a laboratory for accurate visual description and classification by a laboratory technician experienced in soils work, as this assessment will provide the basis for later testing and soil profile development. Classification tests can be performed in the laboratory on representative samples to verify the description and assign appropriate group symbols based on a soil classification system (e.g., USCS). If possible, the moisture content of every sample should be determined since it is potentially a good indicator of performance. The test to determine the moisture content is simple and inexpensive to perform.

## 4.01 Primary References

The primary references for this Chapter are as follows:

ASTM (2006). *Annual Book of ASTM Standards – Sections 4.02, 4.08, 4.09 and 4.13*. ASTM International, West Conshohocken, PA.

AASHTO (2006). *Standard Specifications for Transportation Materials and Methods of Sampling and Testing*, Parts I and II, American Association of State Highway and Transportation Officials, Washington, D.C.

FHWA (2002a). *Geotechnical Engineering Circular 5 (GEC5) - Evaluation of Soil and Rock Properties*. Report No FHWA-IF-02-034. Authors: Sabatini, P.J, Bachus, R.C, Mayne, P.W., Schneider, J.A., Zettler, T.E., Federal Highway Administration, U.S. Department of Transportation.

## 4.1 SOIL DESCRIPTION

Soil description/identification is the systematic naming of individual soils in both written and spoken forms (ASTM D 2488, AASHTO M 145). Soil classification is the grouping of soils with similar engineering properties into a category by using the results of laboratory-based index tests, e.g., group name and symbol (ASTM D 2487, AASHTO M 145). It is important to distinguish between a visual description of a soil and its classification in order to minimize potential conflicts between general visual evaluations of soil samples in the field and more precise laboratory evaluations supported by index tests.

The soil's description should include as a **minimum**:

- Apparent consistency (e.g., soft, firm, etc. for fine-grained soils) or density adjective (e.g., loose, dense, etc. for coarse-grained soils);
- Water content condition adjective (e.g., dry, moist, wet);
- Color description (e.g., brown, gray, etc.);
- Main soil type name, often presented in all capital letters (e.g. SAND, CLAY);
- Descriptive adjective for main soil type (e.g., fine, medium, coarse, well-rounded, angular, etc. for coarse-grained soils; organic, inorganic, compressible, laminated, etc., for fine-grained soils);
- Particle-size distribution adjective for gravel and sand (e.g., uniform, well-graded,

gap-graded);

- Plasticity adjective (e.g., high, low) and soil texture (e.g., rough, smooth, slick, waxy, etc.) for inorganic and organic silts or clays;
- Descriptive term for minor type(s) of soil (with, some, trace, etc.);
- Minor soil type name with "y" added if the fine-grained minor component is less than 30 percent but greater than 12 percent or the coarse-grained minor component is 30 percent or more (e.g., silty for fine grained minor soil type, sandy for coarse-grained minor soil type);
- Descriptive adjective “with” if the fine-grained minor soil type is 5 to 12 percent (e.g., with clay) or if the coarse-grained minor soil type is less than 30 percent but 15 percent or more (e.g., with gravel). Note: some practices use the descriptive adjectives “some” and “trace” for minor components;
- Inclusions (e.g., concretions, cementation);
- Geological name (e.g., Holocene, Eocene, Pleistocene, Cretaceous), if known, in parenthesis or in notes column.

The various elements of the soil description are generally stated in the order given above. For example, a soil description might be presented as follows:

*Fine-grained soils:* Soft, wet, gray, high plasticity CLAY, with f. Sand; (Alluvium)

*Coarse-grained soils:* Dense, moist, brown, silty m-f SAND, with f. Gravel to c. Sand; (Alluvium)

When minor changes occur within the same soil layer (e.g., a change in apparent density), the boring log should indicate a description of the change, such as “same, except very dense.”

#### **4.1.1 Consistency and Apparent Density**

The consistency of fine-grained soils and apparent density of coarse-grained soils can be estimated from the energy-corrected SPT N-value,  $N_{60}$ . The consistency of clays and silts varies from very soft to firm to stiff to hard. The apparent density of coarse-grained soil ranges from very loose to dense to very dense. Suggested guidelines for estimating the in-place apparent density or consistency of soils are given in Tables 4-1 and 4-2, respectively.

**Table 4-1**  
**Evaluation of the apparent density of coarse-grained soils (after Peck, *et al.*, 1974)**

$N_{60}$	Apparent Density	Relative Density, %
0 – 4	Very loose	0 – 20
>4 - 10	Loose	20 – 40
>10 - 30	Medium dense	40 – 70
>30 - 50	Dense	70 – 85
>50	Very Dense	85 – 100
The above guidance may be misleading in gravelly soils.		

**Table 4-2**  
**Evaluation of the consistency of fine-grained soils (after Peck, *et al.*, 1974)**

$N_{60}$	Consistency	Unconfined Compressive Strength, $q_u$ , ksf (kPa)	Results of Manual Manipulation
<2	Very soft	< 0.5 (<25)	Specimen (height = twice the diameter) sags under its own weight; extrudes between fingers when squeezed.
2 - 4	Soft	0.5 – 1 (25 – 50)	Specimen can be pinched in two between the thumb and forefinger; remolded by light finger pressure.
4 - 8	Medium stiff	1 – 2 (50 – 100)	Can be imprinted easily with fingers; remolded by strong finger pressure.
8 - 15	Stiff	2 – 4 (100 – 200)	Can be imprinted with considerable pressure from fingers or indented by thumbnail.
15 - 30	Very stiff	4 – 8 (200 – 400)	Can barely be imprinted by pressure from fingers or indented by thumbnail.
>30	Hard	> 8 >400	Cannot be imprinted by fingers or difficult to indent by thumbnail.
Note that $N_{60}$ -values should <u>not</u> be used to determine the design strength of fine grained soils.			

The apparent density or consistency of the soil formation can vary from these empirical correlations for a variety of reasons. Judgment remains an important part of the visual identification process. Field index tests (e.g., smear test, dried strength test, thread test) which will be described in the next section are suggested as aids in estimating the consistency of fine grained soils.

In some cases the sampler may pass from one layer into another of markedly different properties; for example, from a dense sand into a soft clay. In attempting to identify apparent

density, an assessment should be made as to what part of the blow count corresponds to each layer since the sampler begins to reflect the presence of the lower layer before it actually reaches it.

#### 4.1.2 Water Content (Moisture)

The relative amount of water present in the soil sample should be described by an adjective such as dry, moist, or wet as indicated in Table 4-3.

**Table 4-3**  
**Adjectives to describe water content of soils (ASTM D 2488)**

Description	Conditions
Dry	No sign of water and soil dry to touch
Moist	Signs of water and soil is relatively dry to touch
Wet	Signs of water and soil definitely wet to touch; granular soil exhibits some free water when densified

#### 4.1.3 Color

The color must be described when the sample is first retrieved in the field at the as-sampled water content since the color may change with changes in the water content. Primary colors should be used (brown, gray, black, green, white, yellow, red). Soils with different shades or tints of basic colors are described by using two basic colors; e.g., gray-green. Some agencies may require use of the Munsell color system (USDA, 1993). When the soil is marked with spots of color, the term “mottled” can be applied. Soils with a homogeneous texture but having color patterns that change and are not considered mottled can be described as “streaked.”

#### 4.1.4 Type of Soil

The constituent parts of a given soil type are defined on the basis of texture in accordance with particle-size designators separating the soil into coarse-grained, fine-grained, and highly organic designations. Soil with more than 50 percent by weight of the particles larger than the U.S. Standard No. 200 sieve (0.075 mm) is designated coarse-grained. Soil (inorganic and organic) with 50 percent or more by weight of the particles finer than the No. 200 sieve (0.075 mm) is designated fine-grained. Soil primarily consisting of less than 50 percent by volume of organic matter, dark in color, and with an organic odor is designated as organic soil. Soil with organic content more than 50 percent is designated as peat. The soil type designations used by FHWA follow ASTM D 2487; i.e., gravel, sand, silt, clay, organic silt, organic clay, and peat.

#### 4.1.4.1 Coarse-Grained Soils (Gravel and Sand)

Coarse-grained soils consist of a matrix of either gravel or sand in which more than 50 percent by weight of the soil is retained on the No. 200 sieve (0.075 mm). Coarse-grained soils may contain fine-grained soil, i.e., soils passing the No. 200 sieve (0.075 mm), but the percent by weight of the fine-grained portion is less than 50 percent. The gravel and sand components are defined on the basis of particle size as indicated in Table 4-4. The particle-size distribution is identified as well graded or poorly graded. Well graded coarse-grained soil contains a good representation of all particle sizes from largest to smallest, with  $\leq 12$  percent fines. Poorly graded coarse-grained soil is uniformly graded, i.e., most of the coarse-grained particles are about the same size, with  $\leq 12$  percent fines. Gap graded coarse grained soil can be either a well graded or poorly graded soil lacking one or more intermediate sizes within the range of the gradation.

Gravels and sands may be described by adding particle-size distribution adjectives in front of the soil type in accordance with the criteria given in Table 4-5. Based on correlation with laboratory tests, the following simple field identification tests can be used as an aid in identifying granular soils.

**Table 4-4**  
**Particle size definition for gravels and sands (after ASTM D 2488)**

Component	Grain Size	Determination
Boulders*	12" + (300 mm +)	Measurable
Cobbles*	3" to 12" (300 mm to 75 mm)	Measurable
Gravel		
Coarse	$\frac{3}{4}$ " – 3" (19 mm to 75 mm)	Measurable
Fine	$\frac{3}{4}$ " to #4 sieve ( $\frac{3}{4}$ " to 0.187") (19 mm to 4.75 mm)	Measurable
Sand		
Coarse	#4 to #10 sieve (0.19" to 0.079") (4.75 mm – 2.00 mm)	Measurable and visible to the eye
Medium	#10 to #40 sieve (0.079" to 0.017") (2.00 mm – 0.425 mm)	Measurable and visible to the eye
Fine	#40 to #200 sieve (0.017" to 0.003") (0.425 mm- 0.075 mm)	Measurable but barely discernible to the eye
*Boulders and cobbles are not considered soil or part of the soil's classification or description, except under miscellaneous description; i.e., with cobbles at about 5 percent (volume).		

**Table 4-5**

**Adjectives for describing size distribution for sands and gravels (after ASTM D 2488)**

<b>Particle-Size Adjective</b>	<b>Abbreviation</b>	<b>Size Requirement</b>
Coarse	c.	< 30% m-f sand or < 12% f. gravel
Coarse to medium	c-m	< 12% f. sand
Medium to fine	m-f	< 12% c. sand and > 30% m. sand
Fine	f.	< 30% m. sand or < 12% c. gravel
Coarse to fine	c-f	> 12% of each size <sup>1</sup>

<sup>1</sup> 12% and 30% criteria can be modified depending on fines content. The key is the shape of the particle-size distribution curve. If the curve is relatively straight or dished down, and coarse sand is present, use c-f, also use m-f sand if a moderate amount of m. sand is present. If one has any doubts, determine the above percentages based on the amount of sand or gravel present.

**Feel and Smear Tests:** A pinch of soil is handled lightly between the thumb and fingers to obtain an impression of the grittiness (i.e., roughness) or softness (smoothness) of the constituent particles. Thereafter, a pinch of soil is smeared with considerable pressure between the thumb and forefinger to determine the degrees of grittiness (roughness), or the softness (smoothness) of the soil. The following guidelines may be used:

- Coarse- to medium-grained sand typically exhibits a very gritty feel and smear.
- Coarse- to fine-grained sand has less gritty feel, but exhibits a very gritty smear.
- Medium- to fine-grained sand exhibits a less gritty feel and smear that becomes softer (smoother) and less gritty with an increase in the fine sand fraction.
- Fine-grained sand exhibits a relatively soft feel and a much less gritty smear than the coarser sand components.
- Silt components less than about 10 percent of the total weight can be identified by a slight discoloration of the fingers after smear of a moist sample. Increasing silt increases discoloration and softens the smear.

**Sedimentation Test:** A small sample of soil is shaken in a test tube filled with water and allowed to settle. The time required for the particles to fall a distance of 4-inches (100 mm) is about 1/2 minute for particle sizes coarser than silt. About 50 minutes would be required for particles of 0.0002 in (0.005 mm) or smaller (often defined as "clay size") to settle out.

For sands and gravels containing more than 5 percent fines, the type of inorganic fines (silt or clay) can be identified by performing a shaking/dilatancy test. See fine-grained soils section.

**Visual Characteristics:** Sand and gravel particles can be readily identified visually, but silt particles are generally indistinguishable to the eye. With an increasing silt component, individual sand grains become obscured, and when silt exceeds about 12 percent, the silt almost entirely masks the sand component from visual separation. Note that gray fine-grained sand visually appears to contain more silt than the actual silt content.

#### **4.1.4.2 Fine-Grained Soils**

Fine-grained soils are those having 50 percent or more by weight pass the No. 200 sieve. The so-called fines are either inorganic or organic silts and/or clays. To describe fine-grained soils, plasticity adjectives and soil-type adjectives should be used to further define the soil's plasticity and texture. The following simple field identification tests can be used to estimate the degree of plasticity of fine-grained soils.

**Shaking (Dilatancy) Test** (Holtz and Kovacs, 1981). Water is dropped or sprayed on a portion of a fine-grained soil sample mixed and held in the palm of the hand until it shows a wet surface appearance when shaken or bounced lightly in the hand or a sticky nature when touched. The test involves lightly squeezing the wetted soil sample between the thumb and forefinger and releasing it alternatively to observe its reaction and the speed of the response. Soils that are predominantly silty (nonplastic to low plasticity) will show a dull dry surface upon squeezing and a glassy wet surface immediately upon release of the pressure. This phenomenon becomes less and less pronounced in soils with increasing plasticity and decreasing dilatancy,

**Dry Strength Test** (Holtz and Kovacs, 1981). A relatively undisturbed portion of the sample is allowed to dry out and a fragment of the dried soil is pressed between the fingers. Fragments which cannot be crumbled or broken are characteristic of clays with high plasticity. Fragments which can be disintegrated with gentle finger pressure are characteristic of silty materials of low plasticity. Thus, in generally, fine-grained materials with relatively high dry strength are clays of high plasticity and those with relatively little dry strength are predominantly silts.

**Thread Test** (After Burmister, 1970). Moisture is added to or worked out of a small ball (about 1.5 in (40 mm) diameter) of fine grained soil and the ball kneaded until its consistency approaches medium stiff to stiff (compressive strength of about 2,100 psf (100 kPa)). This condition is observed when the material just starts to break or crumble. A thread is then rolled out between the palm of one hand and the fingers of the other to the smallest diameter possible before disintegration of the sample occurs. The smaller the thread achieved, the higher the plasticity of the soil. Fine-grained soils of high plasticity will have threads smaller

than 0.03 in (3/4 mm) in diameter. Soils with low plasticity will have threads larger than 0.12 in (3 mm) in diameter.

**Smear Test** (FHWA, 2002b). A fragment of soil smeared between the thumb and forefinger or drawn across the thumbnail will, by the smoothness and sheen of the smear surface, indicate the plasticity of the soil. A soil of low plasticity will exhibit a rough textured, dull smear while a soil of high plasticity will exhibit a slick, waxy smear surface.

Table 4-6 identifies field methods to approximate the plasticity range for the dry strength, thread, and smear tests.

**Table 4-6**  
**Field methods to describe plasticity (FHWA, 2002b)**

<b>Plasticity Range</b>	<b>Adjective</b>	<b>Dry Strength</b>	<b>Smear Test</b>	<b>Thread Smallest Diameter, in (mm)</b>
0	Nonplastic	none - crumbles into powder with mere pressure	gritty or rough	ball cracks
1 - 10	low plasticity	low - crumbles into powder with some finger pressure	rough to smooth	1/4 – 1/8 (6 to 3)
>10 - 20	medium plasticity	medium - breaks into pieces or crumbles with considerable finger pressure	smooth and dull	1/16 (1.5)
>20 - 40	high plasticity	high - cannot be broken with finger pressure; spec. will break into pieces between thumb and a hard surface	Shiny	0.03 (0.75)
>40	very plastic	very high - can't be broken between thumb and a hard surface	very shiny and waxy	0.02 (0.5)

#### 4.1.4.3 Highly Organic Soils

Colloidal and amorphous organic materials finer than the No. 200 sieve (0.075 mm) are identified and classified in accordance with their drop in plasticity upon oven drying (ASTM D 2487). Further identification markers are:

1. dark gray and black and sometimes dark brown colors, although not all dark colored soils are organic;
2. most organic soils will oxidize when exposed to air and change from a dark gray/black color to a lighter brown; i.e., the exposed surface is brownish, but when the sample is pulled apart the freshly exposed surface is dark gray/black;
3. fresh organic soils usually have a characteristic odor that can be recognized,

- particularly when the soil is heated;
4. compared to inorganic soils, less effort is typically required to pull the material apart and a friable break is usually formed with a fine granular or silty texture and appearance;
  5. workability of organic soils at the plastic limit is weaker and spongier than an equivalent inorganic soil;
  6. the smear, although generally smooth, is usually duller and appears more silty than an equivalent inorganic soil's; and
  7. the organic content of organic soils can also be determined by the combustion test method (AASHTO T 267, ASTM D 2974).

Fine-grained soils, where the organic content appears to be less than 50 percent of the volume (about 22 percent by weight), should be described as soils with organic material or as organic soils such as clay with organic material or organic clays etc. If the soil appears to have an organic content greater than 50 percent by volume it should be described as peat. The engineering behavior of soils below and above the 50 percent dividing line is entirely different. It is therefore critical that the organic content of soils be determined both in the field and in the laboratory (AASHTO T 267, ASTM D 2974). Simple field or visual laboratory identification of soils as organic or peat is neither advisable nor acceptable.

It is very important not to confuse topsoil with organic soils or peat. Topsoil is the relatively thin layer of soil found on the surface composed of partially decomposed organic materials, such as leaves, grass, small roots etc. Topsoil contains many nutrients that sustain plant and insect life and should not be used to construct geotechnical features or to support engineered structures.

#### **4.1.4.4 Minor Soil Type(s)**

Two or more soil types may be present in many soil formations,. When the percentage of the fine-grained minor soil type is less than 30 percent but greater than 12 percent, or the total sample or the coarse-grained minor component is 30 percent or more of the total sample, the minor soil type is indicated by adding a "y" to its name (e.g., f. gravelly, c-f. sandy, silty, clayey). Note the gradation adjectives are given for granular soils, while the plasticity adjective is omitted for the fine-grained soils.

When the percentage of the fine-grained minor soil type is 5 to 12 percent or for the coarse-grained minor soil type is less than 30 percent but 15 percent or more of the total sample, the minor soil type is indicated by adding the descriptive adjective "with" to the group name (i.e., with clay, with silt, with sand, with gravel, and/or with cobbles).

Some local practices also use the descriptive adjectives “some” and “trace” for minor components as follows:

- "trace" when the percentage is between 1 and 12 percent of the total sample; or
- "some" when the percentage is greater than 12 percent and less than 30 percent of the total sample.

#### **4.1.4.5 Inclusions**

Additional inclusions or characteristics of the sample can be described by using "with" and the descriptions described above. For example:

- with petroleum odor
- with organic matter
- with foreign matter (roots, brick, etc.)
- with shell fragments
- with mica
- with parting(s), seam(s), etc. of (give soil's complete description)

#### **4.1.4.6 Other Descriptors**

Depending on local conditions, the soils may be described based on reaction to HCl acid, and type and degree of cementation. ASTM D 2488 provides guidance for such descriptors.

#### **4.1.4.7 Layered Soils**

Soils of different types can be found in repeating layers of various thickness. It is important that all such formations and their thicknesses are noted. Each layer is described as if it is a non-layered soil by using the sequence for soil descriptions discussed above. The thickness and shape of layers and the geological type of layering are noted according to the descriptive terms presented in Table 4-7. The thickness designation is given in parentheses before the type of layer or at the end of each description, whichever is more appropriate.

Examples of descriptions for layered soils are:

- Medium stiff, moist to wet 0.2 to 0.75 in (5 to 20 mm) interbedded seams and layers of gray, medium plastic, silty CLAY and lt. gray, low plasticity SILT; (Alluvium).

- Soft moist to wet varved layers of gray-brown, high plasticity CLAY (0.2 to 0.75-in (5 to 20 mm)) and nonplastic SILT, trace f. sand (0.4 to 0.6 in (10 to 15 mm)); (Alluvium).

**Table 4-7**  
**Descriptive terms for layered soils (NAVFAC, 1986a)**

Type of Layer	Thickness	Occurrence
Parting	< 1/16" (< 1.5 mm)	
Seam	1/16 to 1/2" (1.5 mm to 12 mm)	
Layer	1/2" to 12" (12 mm to 300 mm)	
Stratum	> 12" (>300 mm)	
Pocket		Small erratic deposit
Lens		Lenticular deposit
Varved (also layered)		Alternating seams or layers of silt and/or clay and sometimes fine sand
Occasional		One or less per 12" (300 mm) of thickness or laboratory sample inspected
Frequent		More than one per 12" (300 mm) of thickness or laboratory

#### 4.1.4.8 Geological Name

The soil description should include the geotechnical specialist's assessment of the origin of the soil unit and the geologic name, if known. This information is generally placed in parentheses or brackets at the end of the soil description or in the field notes column of the boring log. Some examples include:

- a. *Washington, D.C.*-Cretaceous Age Material with SPT N-values between 30 and 100: Very hard gray-blue silty CLAY (CH), moist [**Potomac Group Formation**]
- b. *Newport News, VA*-Miocene Age Marine Deposit with SPT N-values around 10 to 15: Stiff green sandy CLAY (CL) with shell fragments, calcareous [**Yorktown Formation**].
- c. *Tucson, AZ* – Holocene Age Alluvial Deposit with SPT N-values around 35: Cemented clayey SAND (SC), dry [**Pantano Formation**].

## 4.2 SOIL CLASSIFICATION

As previously indicated, final identification with classification is best performed in the laboratory. This process will lead to more consistent final boring logs and avoid conflicts with field descriptions. The Unified Soil Classification System (USCS) group name and symbol (in parenthesis) appropriate for the soil type in accordance with AASHTO M 145 (or ASTM D 3282) or ASTM D 2487 is the most commonly used system in geotechnical work and is covered in this section. For classification of highway subgrade material, the AASHTO classification system (see Section 4.2.2) is used. The AASHTO classification system is also based on grain size and plasticity.

### 4.2.1 Unified Soil Classification System (USCS)

The Unified Soil Classification System (ASTM D 2487) groups soils with similar engineering properties into categories based on grain size, gradation and plasticity. Table 4-8 provides a simplification of the group breakdown based on percent passing No. 200 sieve (0.075 mm) and Table 4-9 provides an outline of the complete laboratory classification method. The procedures, along with charts and tables, for classifying coarse-grained and fine-grained soils follow.

**Table 4-8**

**Basic USCS soil designations based on percent passing No. 200 sieve (0.075 mm) (after ASTM D 2487; Holtz and Kovacs, 1981)**

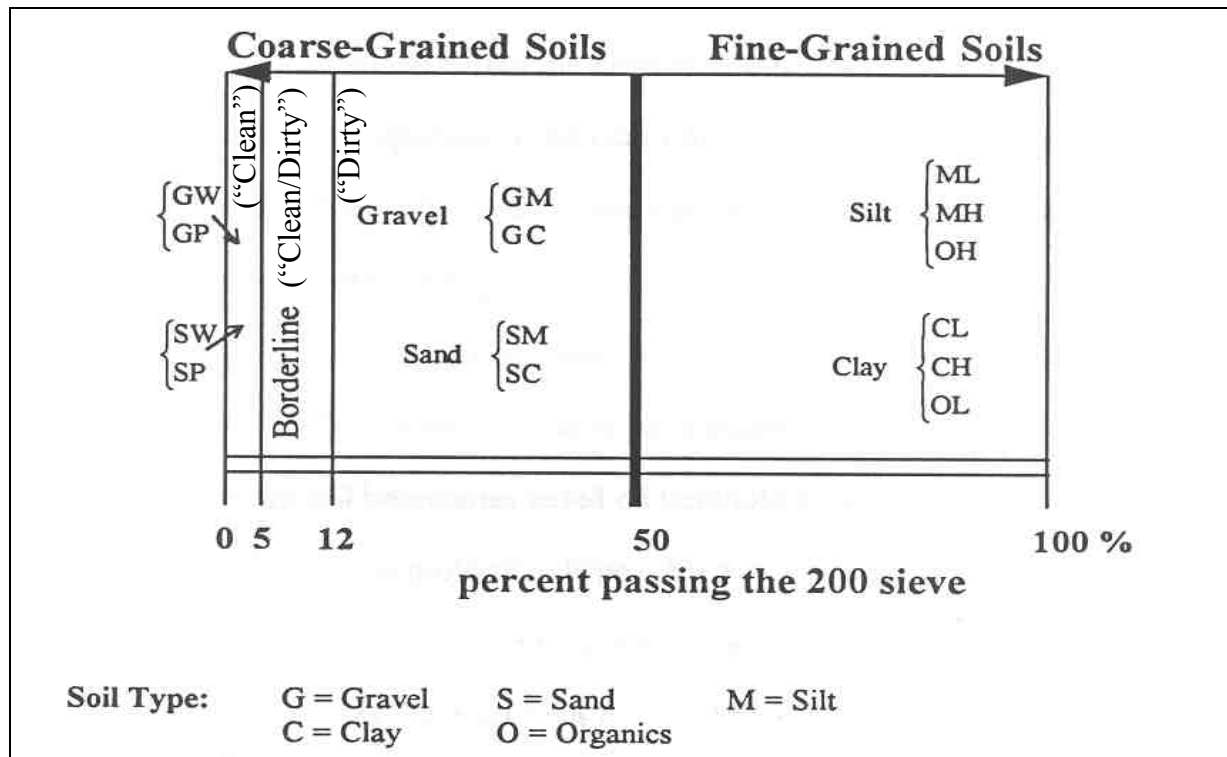


**Table 4-9**  
**Soil classification chart (laboratory method) (after ASTM D 2487)**

Criteria for Assigning Group Symbols and Group Names Using Laboratory Tests <sup>a</sup>			Soil Classification	
<b>COARSE-GRAINED SOILS (Sands and Gravels) - more than 50% retained on No. 200 (0.075 mm) sieve</b> <b>FINE-GRAINED (Silts and Clays) - 50% or more passes the No. 200 (0.075 mm) sieve</b>			<b>Group Symbol</b>	<b>Group Name<sup>b</sup></b>
<b>GRAVELS</b>  More than 50% of coarse Fraction retained on No. 4 Sieve	CLEAN GRAVELS	$C_u \geq 4$ and $1 \leq C_c \leq 3^e$	GW	Well-graded gravel <sup>f</sup>
	< 5% fines	$C_u < 4$ and/or $1 > C_c > 3^e$	GP	Poorly-graded gravel <sup>f</sup>
	GRAVELS WITH FINES	Fines classify as ML or MH	GM	Silty gravel <sup>f,g,h</sup>
		Fines classify as CL or CH	GC	Clayey gravel <sup>f,g,h</sup>
<b>SANDS</b>  50% or more of coarse fraction passes No. 4 Sieve	CLEAN SANDS	$C_u \geq 6$ and $1 \leq C_c \leq 3^e$	SW	Well-graded Sand <sup>i</sup>
	< 5% fines <sup>d</sup>	$C_u < 6$ and/or $1 > C_c > 3^e$	SP	Poorly-graded sand <sup>i</sup>
	SANDS WITH FINES	Fines classify as ML or MH	SM	Silty sand <sup>g,h,i</sup>
		Fines classify as CL or CH	SC	Clayey sand <sup>g,h,i</sup>
<b>SILTS AND CLAYS</b>  Liquid limit less than 50	Inorganic	PI > 7 and plots on or above "A" line <sup>j</sup>	CL	Lean clay <sup>k,l,m</sup>
		PI < 4 or plots below "A" line <sup>j</sup>	ML	Silt <sup>k,l,m</sup>
	Organic	$\frac{\text{Liquid limit - overdried}}{\text{Liquid limit - not dried}} < 0.75$	OL	Organic clay <sup>k,l,m,n</sup>
				Organic silt <sup>k,l,m,o</sup>
<b>SILTS AND CLAYS</b>  Liquid limit 50 or more	Inorganic	PI plots on or above "A" line	CH	Fat clay <sup>k,l,m</sup>
		PI plots below "A" line	MH	Elastic silt <sup>k,l,m</sup>
	Organic	$\frac{\text{Liquid limit - oven dried}}{\text{Liquid limit - not dried}} < 0.75$	OH	Organic clay <sup>k,l,m,p</sup>
				Organic silt <sup>k,l,m,q</sup>
<b>Highly fibrous organic soils</b>	Primary organic matter, dark in color, and organic odor		Pt	Peat

**Table 4-9 (Continued)**  
**Soil classification chart (laboratory method) (after ASTM D 2487)**

NOTES:

- a Based on the material passing the 3 in (75 mm) sieve.
- b If field sample contained cobbles and/or boulders, add “with cobbles and/or boulders” to group name.
- c Gravels with 5 to 12% fines require dual symbols:  
     GW-GM, well-graded gravel with silt  
     GW-GC, well-graded gravel with clay  
     GP-GM, poorly graded gravel with silt  
     GP-GC, poorly graded gravel with clay
- d Sands with 5 to 12% fines require dual symbols:  
     SW-SM, well-graded sand with silt  
     SW-SC, well-graded sand with clay  
     SP-SM, poorly graded sand with silt  
     SP-SC, poorly graded sand with clay
- e  $C_u = \frac{D_{60}}{D_{10}}$      $C_c = \frac{(D_{30})^2}{(D_{10})(D_{60})}$   
     [C<sub>u</sub>: Uniformity Coefficient; C<sub>c</sub>: Coefficient of Curvature]
- f If soil contains ≥ 15% sand, add “with sand” to group name.
- g If fines classify as CL-ML, use dual symbol GC-GM, SC-SM.
- h If fines are organic, add “with organic fines” to group name.
- i If soil contains ≥ 15% gravel, add “with gravel” to group name.
- j If the liquid limit and plasticity index plot in hatched area on plasticity chart, soil is a CL-ML, silty clay.
- k If soil contains 15 to 29% plus No. 200 (0.075 mm), add “with sand” or “with gravel,” whichever is predominant.
- l If soil contains ≥ 30% plus No. 200 (0.075mm), predominantly sand, add “sandy” to group name.
- m If soil contains ≥ 30% plus No. 200 (0.075 mm), predominantly gravel, add “gravelly” to group name.
- n PI ≥ 4 and plots on or above “A” line.
- o PI < 4 or plots below “A” line.
- p PI plots on or above “A” line.
- q PI plots below “A” line.

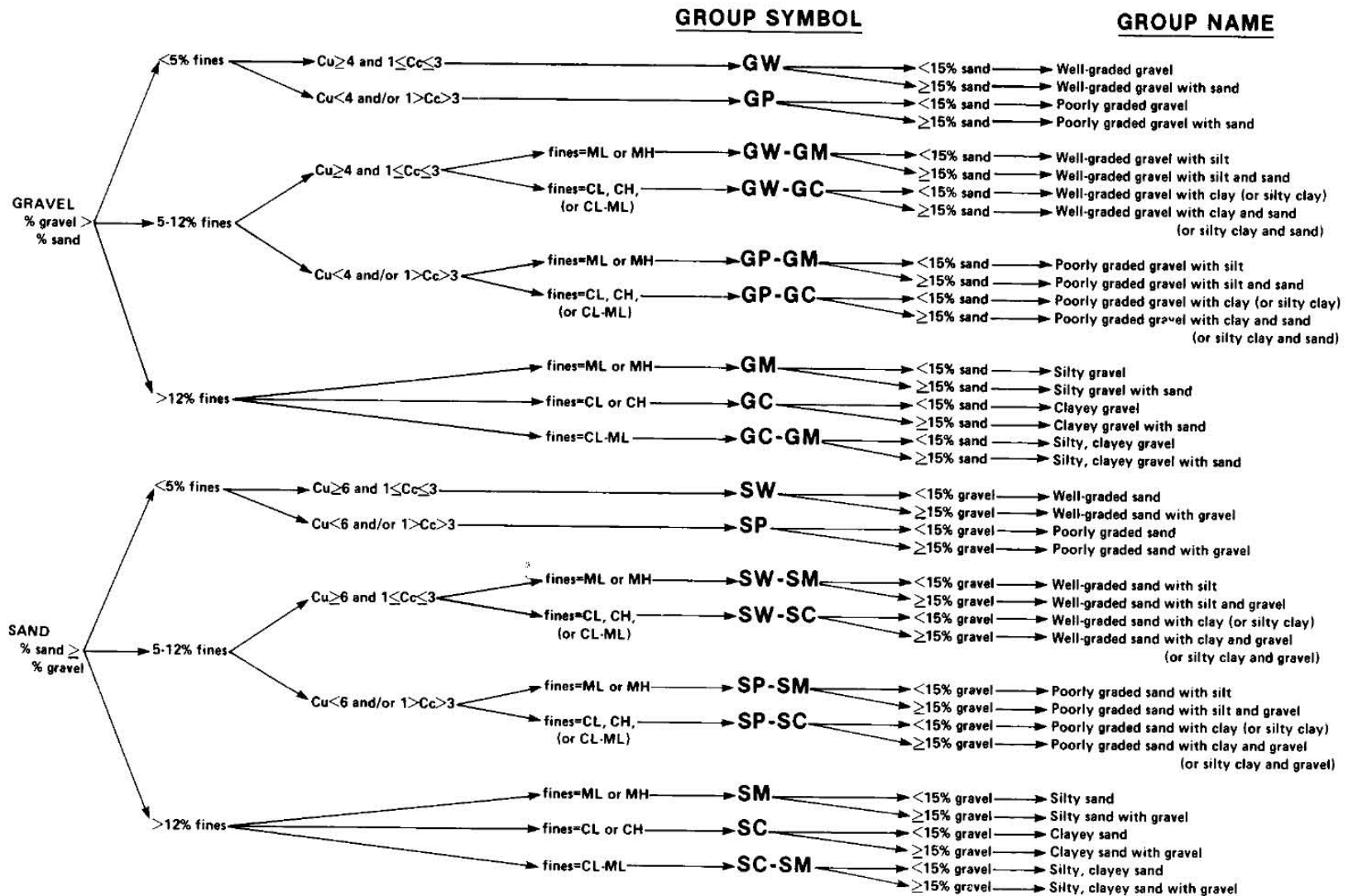


Figure 4-1: Flow chart to determine the group symbol and group name for coarse-grained soils (ASTM D 2487).

#### 4.2.1.1 Classification of Coarse-Grained Soils

Coarse-grained soils are defined as those in which 50 percent or more by weight are retained on the No. 200 sieve (0.075 mm). The flow chart to determine the group symbol and group name for coarse-grained soils is given in Figure 4-1. This figure is identical to Figure 3 in ASTM D 2487 except for the recommendation to capitalize the primary soil type; e.g., GRAVEL.

- **The shape of the grain-size distribution (GSD) curve or “gradation curve” as it is frequently called, is one of the more important aspects in a soil classification system for coarse-grained soils.** The shape of the gradation curve can be characterized by a pair of “shape” parameters called the coefficient of uniformity,  $C_u$ , and the coefficient of curvature,  $C_c$ , to which numerical values may be assigned. By assigning numerical values to such shape parameters it becomes possible to compare grain-size distribution curves for different soils without having to plot them on the same diagram. In order to define shape parameters certain characteristic particle sizes must be identified that are common to all soils. Since the openings of a sieve are square, particles of many different shapes are able to pass through a sieve of given size even though the abscissa on the gradation curve is expressed in terms of particle “diameter,” which implies a spherical-shaped particle. Therefore, the “diameter” shown on the gradation curve is an effective diameter so that the characteristic particle sizes that must be identified to define the shape parameters are in reality effective grain sizes (EGS).

A useful EGS for the characterizing the shape of the gradation curve is the grain size for which 10 percent of the soil by weight is finer. This EGS is labeled  $D_{10}$ . This size is convenient because Hazen (1911) found that the ease with which water flows through a soil is a function of the  $D_{10}$ . In other words, Hazen found that the sizes smaller than the  $D_{10}$  affected the permeability more than the remaining 90 percent of the sizes. Therefore, the  $D_{10}$  is a logical choice as a characteristic particle size. Other convenient sizes were found to be the  $D_{30}$  and the  $D_{60}$ , which pertain to the grain size for which thirty and sixty percent, respectively, of the soil by weight is finer. These EGSs are used as follows in the Unified Soil Classification System (USCS) for the classification of coarse grained soils.

- **Slope of the gradation curve:** The shape of the curve could be defined relative to an arbitrary slope of a portion of the gradation curve. Since one EGS has already been identified as the  $D_{10}$ , the slope of the gradation curve could be described by identifying another convenient point (EGS) that is “higher” on the curve. Hazen

selected this other convenient size as the  $D_{60}$  that indicates the particle size for which 60 percent of the soil by weight is finer. The slope between the  $D_{60}$  and the  $D_{10}$  can then be related to the degree of uniformity of the sample through a parameter called the “Coefficient of Uniformity” or the “Uniformity Coefficient,”  $C_u$ , which is expressed as follows:

$$C_u = \frac{D_{60}}{D_{10}} \quad 4-1$$

- **Curvature of the gradation curve:** The second “shape” parameter is used to evaluate the curvature of the gradation curve between the two arbitrary points,  $D_{60}$  and  $D_{10}$ . A third EGS,  $D_{30}$ , that indicates the particle size for which 30 percent of the soil by weight is finer, is chosen for this purpose. The curvature of the slope between the  $D_{60}$  and the  $D_{10}$  can then be related to the three EGS’ through a parameter called the “Coefficient of Curvature” or the “Coefficient of Concavity” or the “Coefficient of Gradation,”  $C_c$ , which is expressed as follows:

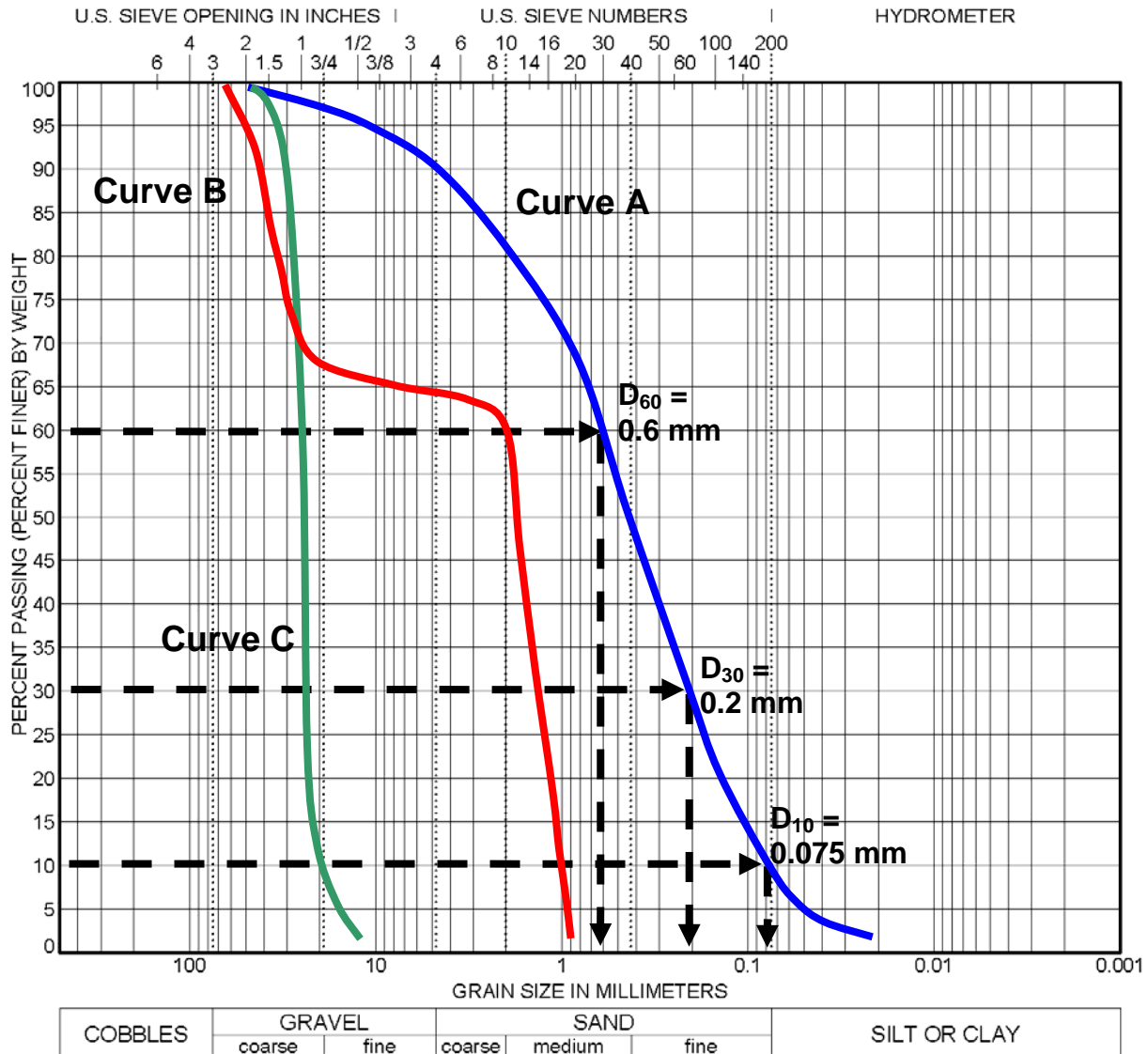
$$C_c = \frac{D_{30}^2}{D_{60} \times D_{10}} \quad 4-2$$

By use of the two “shape” parameters,  $C_u$  and  $C_c$ , the uniformity of the coarse-grained soil (gravel and sand) can now be classified as well-graded (non-uniform), poorly graded (uniform), or gap graded (uniform or non-uniform). Table 4-10 presents criteria for such classifications.

**Table 4-10**  
**Gradation based on  $C_u$  and  $C_c$  parameters**

Gradation	Gravels	Sands
Well-graded	$C_u \geq 4$ and $1 < C_c < 3$	$C_u \geq 6$ and $1 < C_c < 3$
Poorly graded	$C_u < 4$ and $1 < C_c < 3$	$C_u < 6$ and $1 < C_c < 3$
Gap graded*	$C_c$ not between 1 and 3	$C_c$ not between 1 and 3
*Gap-graded soils may be well-graded or poorly graded. In addition to the $C_c$ value it is recommended that the shape of the GSD be the basis for definition of gap-graded.		

$C_u$  and  $C_c$  are statistical parameters and provide good initial guidance. However, **the plot of the GSD curve must always be reviewed in conjunction with the values of  $C_u$  and  $C_c$  to avoid incorrect classification.** Examples of the importance of reviewing the GSD curves are presented in Figure 4-2 and discussed subsequently.



Curve	D <sub>10</sub> (mm)	D <sub>30</sub> (mm)	D <sub>60</sub> (mm)	C <sub>u</sub>	C <sub>c</sub>	Gradation
A	0.075	0.2	0.6	8.0	0.9	Well graded (1)
B	1	1.5	2	2.0	1.12	Poorly graded - Gap graded (2)
C	19	25	27	1.4	1.2	Poorly graded

(1) Soil does not meet C<sub>u</sub> and C<sub>c</sub> criteria for well-graded soil but GSD curve clearly indicates a well-graded soil

(2) The C<sub>u</sub> and C<sub>c</sub> parameters indicate a uniform (or poorly) graded material, but the GSD curve clearly indicates a gap-graded soil.

Note: For clarity only the D<sub>10</sub>, D<sub>30</sub>, and D<sub>60</sub> sizes for Curve A are shown on the figure.

**Figure 4-2. Evaluation of type of gradation for coarse-grained soils.**

**Discussion of Figure 4-2:** Curve A in Figure 4-2 has  $C_u = 8$  and  $C_c = 0.9$ . The soil represented by Curve A would not meet the criteria listed in Table 4-10 for well-graded soil, but yet an examination of the GSD curve shows that the soil is well-graded. Examination of the GSD curve is even more critical for the case of gap graded soils because the largest particle size evaluated by parameters  $C_u$  and  $C_c$  is  $D_{60}$  while the gap grading may occur at a size larger than  $D_{60}$  size as shown for a 2/3:1/3 proportion of gravel: sand mix represented by Curve B in Figure 4-2. Based on the criteria in Table 4-10, the soil represented by Curve B would be classified as a uniform or poorly graded soil which would be an incorrect classification. Such incorrect classifications can and do occur on construction sites where the contractor may (a) simply mix two stockpiles of uniformly graded soils leftover from a previous project. (b) use multiple sand and gravel pits to obtain borrow soils, and/or (c) mix soils from two different seams or layers of poorly graded material in the same gravel pit. Figure 4-2 is an illustration on the importance of evaluating the shape of the GSD curve in addition to the statistical parameters  $C_u$  and  $C_c$ . Practical aspects of the engineering characteristics of granular soils are discussed in Section 4.4.

#### 4.2.1.2 Classification of Fine-Grained Soils

Fine-grained soils, or “fines,” are those in which 50 percent or more by weight pass the No. 200 (0.075 mm) sieve. The classification of fine-grained soils is accomplished by use of the plasticity chart (Figure 4-3). For fine-grained organic soils, Table 4-11 may be used. Inorganic silts and clays are those that do not meet the organic criteria as given in Table 4-11. The flow charts to determine the group symbol and group name for fine-grained soils are given in Figure 4-4a and 4-4b. These figures are identical to Figures 1a and 1b in ASTM D 2487 except that they are modified to show the soil type capitalized; e.g., CLAY. Dual symbols are used to classify organic silts and clays whose liquid limit and PI plot above the "A"-line, for example, CL-OL instead of OL and CH-OH instead of OH. To describe the fine-grained soil types more fully, plasticity adjectives and soil types used as adjectives should be used to further define the soil type's texture, plasticity, and location on the plasticity chart (see Table 4-12). Examples using Table 4-11 are given in Table 4-12. An example description of fine-grained soils is as follows:

*Soft, wet, gray, high plasticity CLAY, with f. Sand; Fat CLAY (CH); (Alluvium)*

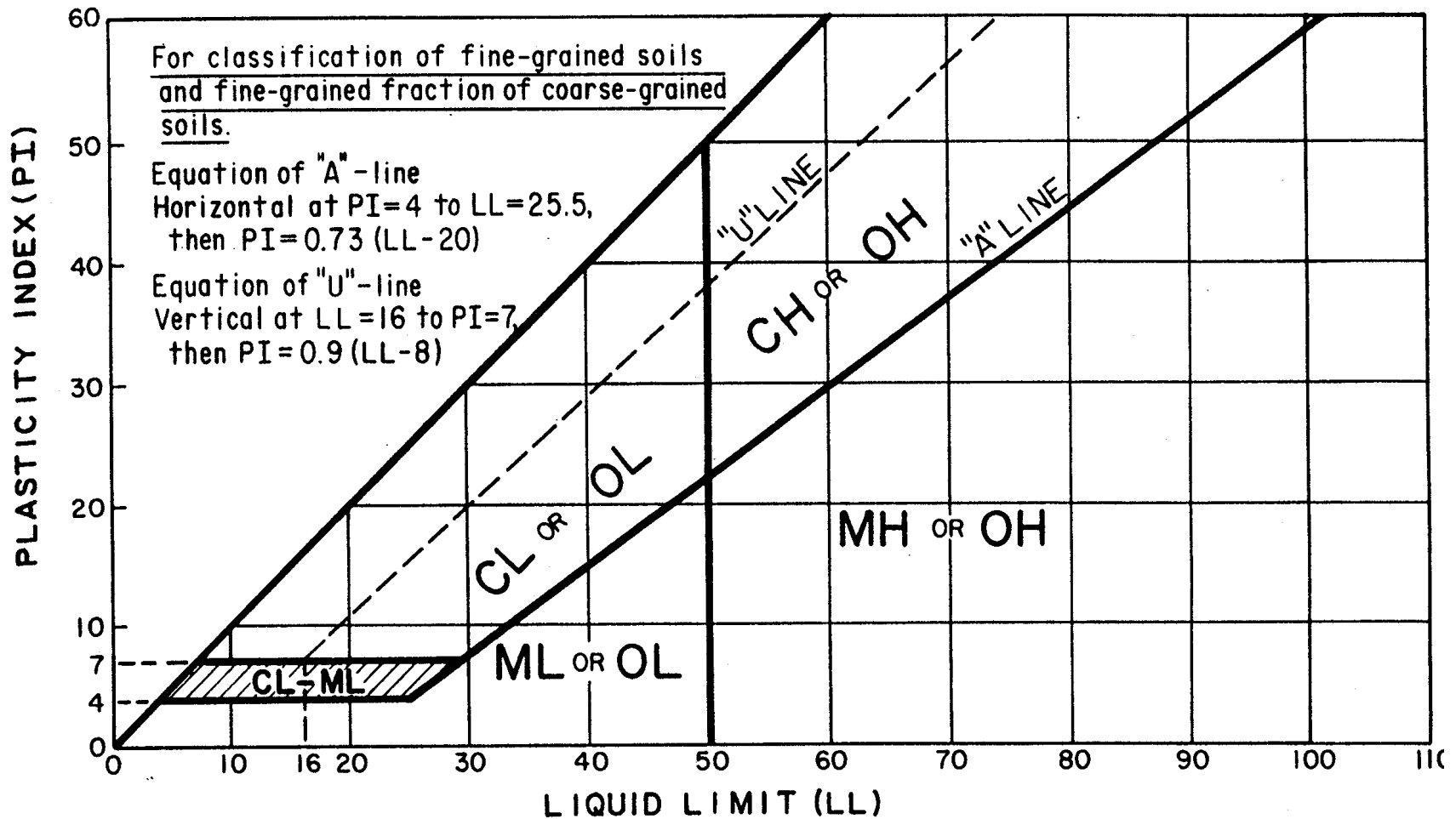


Figure 4-3. Plasticity chart for Unified Soil Classification System (ASTM D 2487).

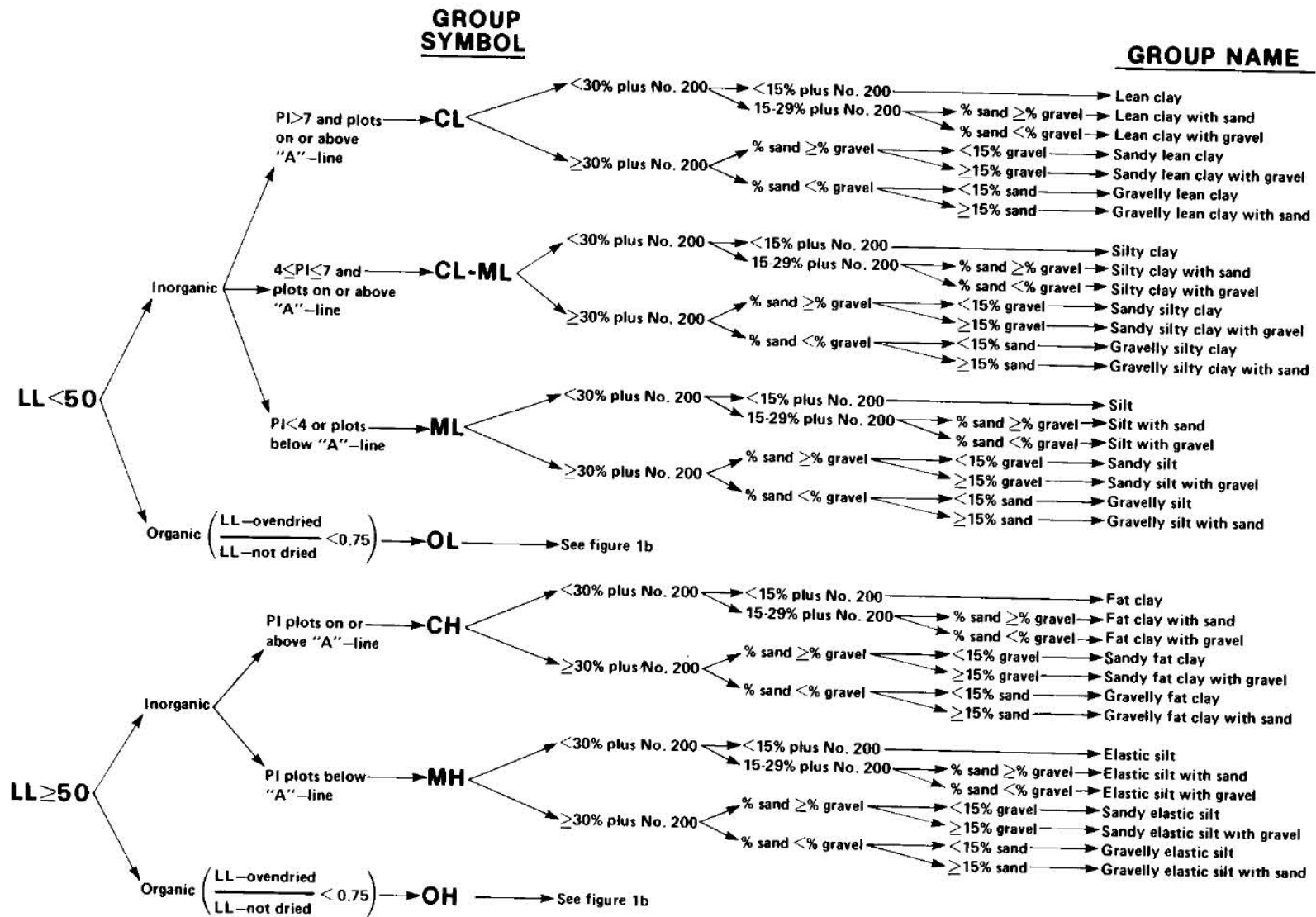


Figure 4-4a. Flow chart to determine the group symbol and group name for fine-grained soils (ASTM D 2487).

**GROUP SYMBOL**

**GROUP NAME**

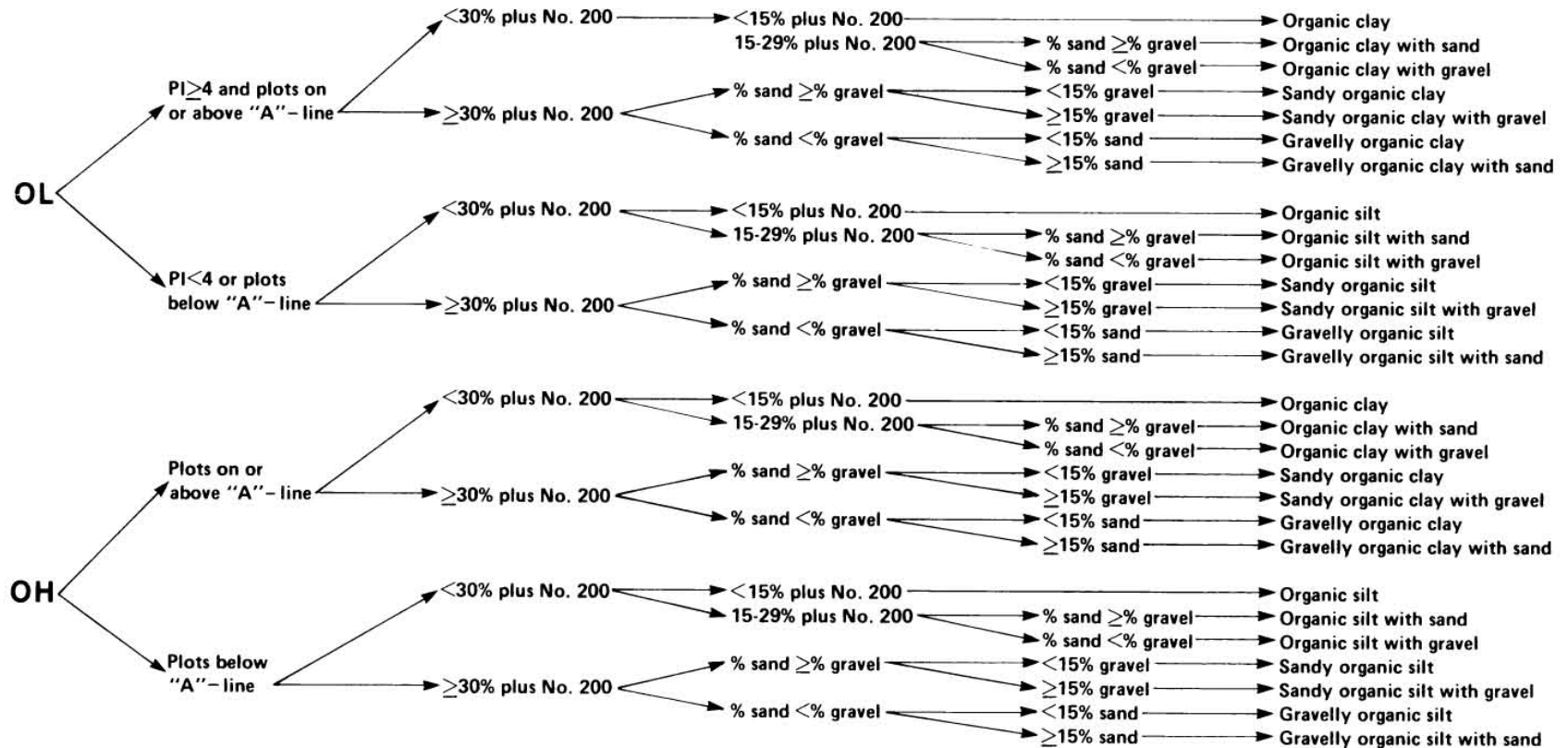


Figure 4-4b. Flow chart to determine the group symbol and group name for organic soils (ASTM D 2487).

**Table 4-11**  
**Soil plasticity descriptors (based on Figures 4-3, 4-4a and 4-4b)**

Plasticity Index Range	Plasticity Adjective	Adjective for Soil Type, Texture, and Plasticity Chart Location		
		ML & MH (Silt)	CL & CH (Clay)	OL & OH (Organic Silt or Clay) <sup>1</sup>
0	nonplastic	-	-	ORGANIC SILT
1 - 10	low plasticity	-	silty	ORGANIC SILT
>10 - 20	medium plasticity	Clayey	silty to no adj.	ORGANIC clayey SILT
>20 - 40	high plasticity	Clayey	-	ORGANIC silty CLAY
>40	very plastic	Clayey	-	ORGANIC CLAY

Soil type is the same for above or below the “A”-line; the dual group symbol (CL-OL or CH-OH) identifies the soil types above the “A”-line.

**Table 4-12**  
**Examples of description of fine-grained soils (based on Figures 4-3, 4-4a and 4-4b)**

Group Symbol	PI	Group Name	Complete Description For Main Soil Type (Fine-Grained Soil)
CL	9	lean CLAY	low plasticity silty CLAY
ML	7	SILT	low plasticity SILT
ML	15	SILT	medium plastic clayey SILT
MH	21	elastic SILT	high plasticity clayey SILT
CH	25	fat CLAY	high plasticity silty CLAY or high plasticity CLAY, depending on smear test (for silty relatively dull and not shiny or just CLAY for shiny, waxy)
OL	8	ORGANIC SILT	low plasticity ORGANIC SILT
OL	19	ORGANIC SILT	medium plastic ORGANIC clayey SILT
CH	>40	fat CLAY	very plastic CLAY

#### 4.2.2 AASHTO Soil Classification System

The AASHTO soil classification system is shown in Table 4-13. The AASHTO classification system is useful in determining the relative quality of the soil material for use in earthwork structures, particularly embankments, subgrades, subbases and bases.

According to this system, soil is classified into seven major groups, A-1 through A-7. Soils classified under groups A-1, A-2 and A-3 are granular materials where 35% or less of the particles pass through the No. 200 sieve (0.075 mm). Soils where more than 35% pass the No. 200 sieve (0.075 mm) are classified under groups A-4, A-5, A-6 and A-7. Soils where more than 35% pass the No. 200 sieve (0.075 mm) are mostly silt and clay-size materials. The classification procedure is shown in Table 4-13. The classification system is based on the following criteria:

- i Grain Size: The grain size terminology for this classification system is as follows:
  - Gravel**: fraction passing the 3 in (75 mm) sieve and retained on the No. 10 (2 mm) sieve.
  - Sand**: fraction passing the No. 10 (2 mm) sieve and retained on the No. 200 (0.075 mm) sieve
  - Silt and clay**: fraction passing the No. 200 (0.075 mm) sieve
  
- ii Plasticity: The term *silty* and *clayey* are used as follows:
  - Silty**: use when the fine fractions of the soil have a plasticity index of 10 or less.
  - Clayey**: use when the fine fractions have a plasticity index of 11 or more.
  
- iii. If cobbles and boulders (size larger than 3 in (75 mm)) are encountered they are excluded from the portion of the soil sample on which the classification is made. However, the percentage of material is recorded.

To evaluate the quality of a soil as a highway subgrade material, a number called the *group index* (GI) is also incorporated along with the groups and subgroups of the soil. The group index is written in parenthesis after the group or subgroup designation. The group index is given by Equation 4-3 where F is the percent passing the No. 200 (0.075 mm) sieve, LL is the liquid limit, and PI is the plasticity index.

$$GI = (F-35)[0.2+0.005(LL-40)] + 0.01(F-15) (PI-10) \quad 4-3$$

**Table 4-13**

**AASHTO soil classification system based on AASHTO M 145 (or ASTM D 3282)**

<b>GENERAL CLASSIFICATION</b>	<b>GRANULAR MATERIALS</b> (35 percent or less of total sample passing No. 200 sieve (0.075 mm))							<b>SILT-CLAY MATERIALS</b> (More than 35 percent of total sample passing No. 200 sieve (0.075 mm))			
<b>GROUP CLASSIFICATION</b>	A-1		A-3	A-2				A-4	A-5	A-6	A-7
	A-1-a	A-1-b		A-2-4	A-2-5	A-2-6	A-2-7				A-7-5, A-7-6
<b>Sieve analysis, percent passing:</b>											
No. 10 (2 mm)	50 max.										
No. 40 (0.425 mm)	30 max.	50 max.	51 min.								
No. 200 (0.075 mm)	15 max.	25 max.	10 max.	35 max.	35 max.	35 max.	35 max.	36 min.	36 min.	36 min.	36 min.
<b>Characteristics of fraction passing No 40 (0.425 mm)</b>											
Liquid limit				40 max.	41 min.	40 max.	41 min.	40 max.	41 min.	40 max.	41 min.
Plasticity index	6 max.		NP	10 max.	10 max.	11 min.	11 min.	10 max.	10 max.	11 min.	11 min.*
<b>Usual significant constituent materials</b>	Stone fragments, gravel and sand		Fine sand	Silty or clayey gravel and sand				Silty soils		Clayey soils	
<b>Group Index**</b>	0		0	0		4 max.		8 max.	12 max.	16 max.	20 max.
<b>Classification procedure:</b>											
With required test data available, proceed from left to right on chart; correct group will be found by process of elimination. The first group from left into which the test data will fit is the correct classification.											
*Plasticity Index of A-7-5 subgroup is equal to or less than LL minus 30. Plasticity Index of A-7-6 subgroup is greater than LL minus 30 (see Fig 4-5).											
**See group index formula (Eq. 4-3). Group index should be shown in parentheses after group symbol as: A-2-6(3), A-4(5), A-7-5(17), etc.											

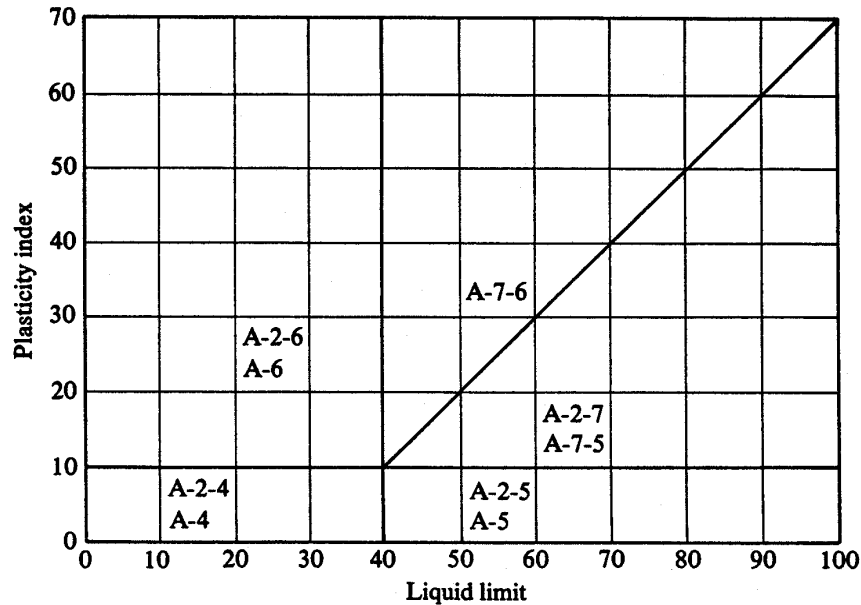


**Figure 4-5. Range of liquid limit and plasticity index for soils in groups A-2, A-4, A-5, A-6 and A-7 per AASHTO M 145 (or ASTM D 3282).**

The first term of Equation 4-3 is the partial group index determined from the liquid limit. The second term is the partial group index determined from the plasticity index. Following are some rules for determining group index:

- If Equation 4-3 yields a negative value for GI, it is taken as zero.
- The group index calculated from Equation 4-3 is rounded off to the nearest whole number, e.g.,  $GI=3.4$  is rounded off to 3;  $GI=3.5$  is rounded off to 4.
- There is no upper limit for the group index.
- The group index of soils belonging to groups A-1-a, A-1-b, A-2-4, A-2-5, and A-3 will always be zero.
- When the group index for soils belonging to groups A-2-6 and A-2-7 is calculated, the partial group index for PI should be used, or

$$GI=0.01(F-15) (PI-10) \quad 4-4$$

**In general, the quality of performance of a soil as a subgrade material is inversely proportional to the group index.**

A comparison of the USCS and AASHTO system is shown in Figures 4-6 and 4-7.

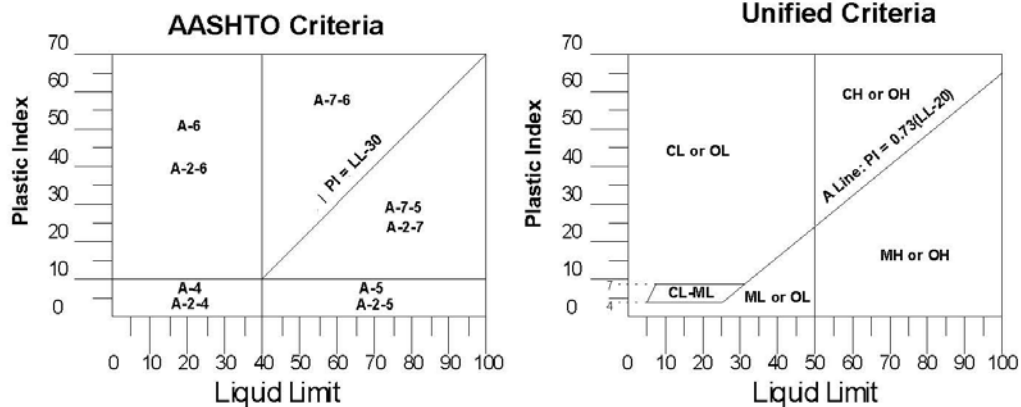
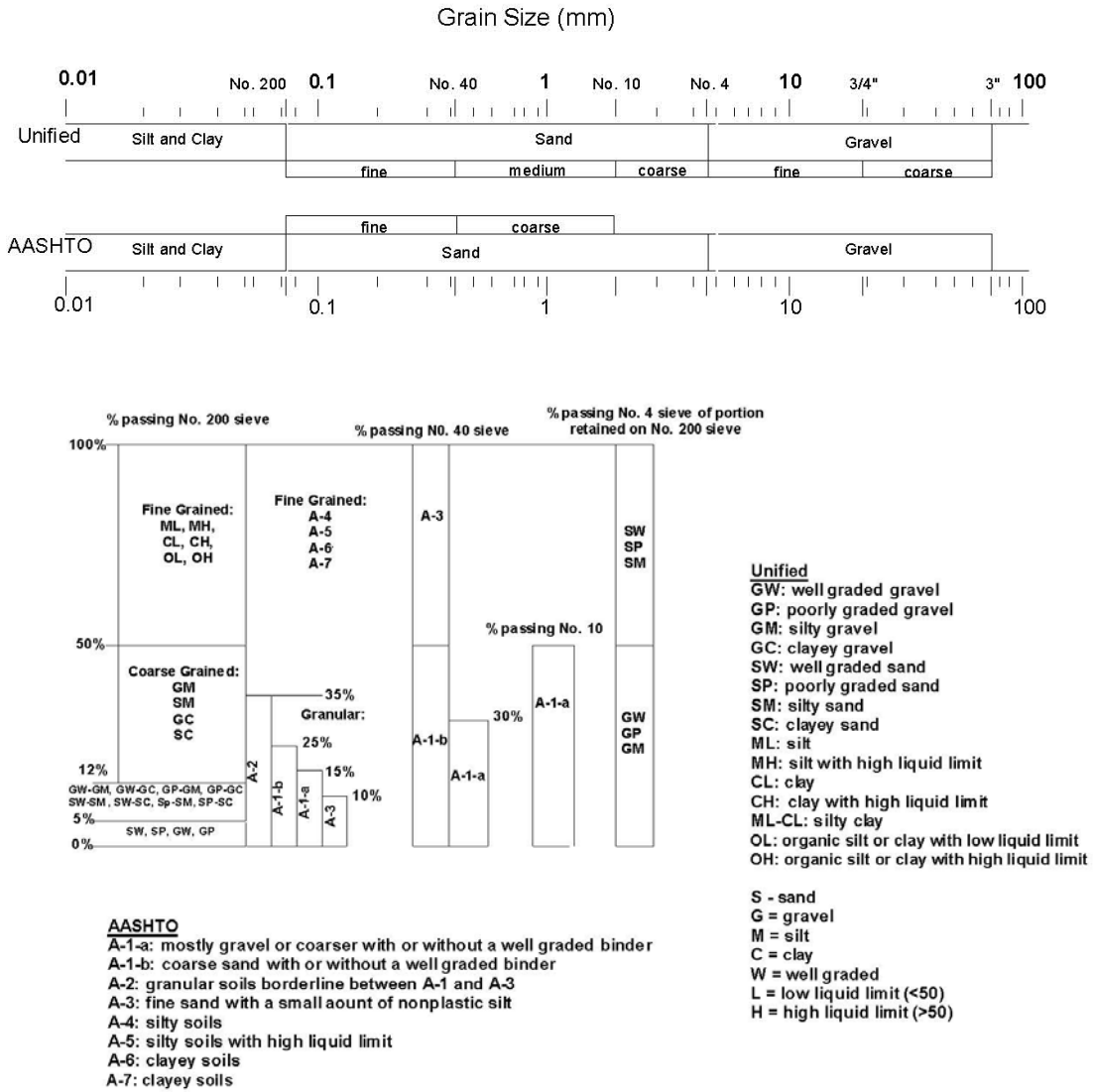


**Figure 4-6. Comparison of the USCS with the AASHTO soil classification system (after Utah DOT – Pavement Design and Management Manual, 2005).**

Soil Group in Unified System	Comparable Soil Groups in AASHTO System			Soil Group in AASHTO System	Comparable Soil Groups in Unified System		
	Most Probable	Possible	Possible but Improbable		Most Probable	Possible	Possible but Improbable
GW	A-1-a	—	A-2-4, A-2-5, A-2-6, A-2-7	A-1-a	GW, GP	SW, SP	GM, SM
GP	A-1-a	A-1-b	A-3, A-2-4, A-2-5, A-2-6, A-2-7	A-1-b	SW, SP, GM, SM	GP	—
GM	A-1-b, A-2-4, A-2-5, A-2-7	A-2-6	A-4, A-5, A-6, A-7-5, A-7-6, A-1-a	A-3	SP	—	SW, GP
GC	A-2-6, A-2-7	A-2-4, A-6	A-4, A-7-6, A-7-5	A-2-4	GM, SM	GC, SC	GW, GP SW, SP
SW	A-1-b	A-1-a	A-3, A-2-4, A-2-5, A-2-6, A-2-7	A-2-5	GM, SM	—	GW, GP, SW, SP
SP	A-3, A-1-b	A-1-a	A-2-4, A-2-5, A-2-6, A-2-7	A-2-6	GC, SC	GM, SM	GW, GP SW, SP
SM	A-1-b, A-2-4, A-2-5, A-2-7	A-2-6, A-4, A-5	A-6, A-7-5, A-7-6, A-1-a	A-2-7	GM, GC, SM, SC	—	GW, GP, SW, SP
SC	A-2-6, A-2-7	A-2-4, A-6, A-4, A-7-6	A-7-5	A-4	ML, OL	CL, SM, SC	GM, GC
ML	A-4, A-5	A-6, A-7-5	—	A-5	OH, MH, ML, OL	—	SM, GM
CL	A-6, A-7-6	A-4	—	A-6	CL	ML, OL, SC	GC, GM, SM
OL	A-4, A-5	A-6, A-7-5, A-7-6	—	A-7-5	OH, MH	ML, OL, CH	GM, SM, GC, SC
MH	A-7-5, A-5	—	A-7-6	A-7-6	CH, CL	ML, OL, SC	OH, MH, GC, GM, SM
CH	A-7-6	A-7-5	—				
OH	A-7-5, A-5	—	A-7-6				
Pt	—	—	—				

Figure 4-7. Comparison of soil groups in the USCS with the AASHTO Soil Classification Systems (Holtz and Kovacs, 1981).

### **4.3 ENGINEERING CHARACTERISTICS OF SOILS**

The major engineering characteristics of the main soil groups discussed in the previous section as related to foundation design are summarized as follows. A discussion on the practical aspects of the engineering characteristics is presented for granular and fine-grained soils following these summaries.

#### **4.3.1 Engineering Characteristics of Coarse-Grained Soils (Sands and Gravels)**

- Generally very good foundation material for supporting structures and roads.
- Generally very good embankment material.
- Generally the best backfill material for retaining walls.
- Might settle under vibratory loads or blasts.
- Dewatering may be difficult in open-graded gravels due to high permeability.
- Generally not frost susceptible.

#### **4.3.2 Engineering Characteristics of Fine-Grained Soils (Inorganic Clays)**

- Generally possess low shear strength.
- Plastic and compressible.
- Can lose part of shear strength upon wetting.
- Can lose part of shear strength upon disturbance.
- Can shrink upon drying and expand upon wetting.
- Generally very poor material for backfill.
- Generally poor material for embankments.
- Can be practically impervious.
- Clay slopes are prone to landslides.

#### **4.3.3 Engineering Characteristics of Fine-Grained Soils (Inorganic Silts)**

- Relatively low shear strength.
- High capillarity and frost susceptibility.
- Relatively low permeability.
- Frost heaving susceptibility
- Difficult to compact.

#### **4.3.4 Engineering Characteristics of Organic Soils**

The term organic designates those soils, other than topsoil, that contain an appreciable amount of vegetative matter and occasionally animal organisms in various states of decomposition. Any soil containing a sufficient amount of organic matter to influence its engineering properties is called an organic soil. The organic matter is objectionable for three main reasons:

1. Reduces load carrying capacity of soil.
2. Increases compressibility considerably.
3. Frequently contains toxic gasses that are released during the excavation process.

Generally organic soils, whether peat, organic clays, organic silts, or even organic sands, are not used as construction materials.

#### **4.4 PRACTICAL ASPECTS OF ENGINEERING CHARACTERISTICS OF COARSE-GRAINED SOILS**

Grain size distribution is the single most important element in the design of structures on, in, or composed of granular soils. As discussed in Chapter 2, grain size distribution is determined by sieving a dried soil sample of known weight through a nest of U.S. Standard sieves with decreasing mesh opening sizes. Figures 2-3 and 4-2 presented sample grain size distribution curves, also known as gradation curves, and introduced the terminology “well graded,” “poorly graded,” and “gap graded.”

Much can be learned about a soil’s behavior from the shape and location of the curve. For instance, the “well graded” curve shown in Figure 4-2 represents a non-uniform soil with a wide range of particle sizes that are evenly distributed. Densification of a well-graded soil causes the smaller particles to move into the voids between the larger particles. As the voids in the soil are reduced, the density and strength of the soil increase. Specifications for select structural fill should contain required ranges of different particle sizes so that a dense, non-compressible backfill can be achieved with reasonable compactive effort. For example, the well-graded soil represented by Curve A shown in Figure 4-2 could be specified by providing the gradation limits listed in Table 4-14.

As shown by Curve C in Figure 4-2, a poorly graded or uniform soil is composed of a narrow range of particle sizes. When compaction is attempted, inadequate distribution of particle sizes prevents reduction of the volume of voids by infilling with smaller particles. Such uniform soils should be avoided as select fill material. However, uniform soils do have an

important use as drainage materials. The relatively large and permanent void spaces act as conduits to carry water. Obviously, the larger the average particle size the larger the void space. The "French drain" is an example of the engineering use of a coarse uniform soil. Table 4-15 presents a typical specification for drainage materials having a narrow band of particle sizes. For material specifications related to drain material, it is important to specify that gap-graded materials shall not be acceptable. This is because gap-graded materials have variable permeabilities that may cause malfunction of the drain with associated damage to the geotechnical feature associated with the drain.

**Table 4-14**  
**Example gradation limits of well-graded granular material**  
 (see Curve A in Figure 4-2)

Sieve Size	Percent Passing by Weight
2" (50.8 mm)	100
#10 (2 mm)	75-90
#40 (0.425 mm)	40-60
#200 (0.075 mm)	0 – 15

**Table 4-15**  
**Example gradation limits of drainage materials**  
 (see Curve C in Figure 4-2)

Sieve Size	Percent Passing by Weight
2" (50.8 mm)	100
1 ½" (37.5 mm)	90-100
¾" (19 mm)	0-15

#### **4.5 PRACTICAL ASPECTS OF ENGINEERING CHARACTERISTICS OF FINE-GRAINED SOILS**

As indicated in Chapter 2, the plasticity index (PI) is the difference between the liquid limit (LL) and the plastic limit (PL). The PI represents the range of water content over which the soil remains plastic. In general, the greater the PI, the greater the amount of clay particles present and the more plastic the soil. The more plastic a soil, the more likely it will be to have the following characteristics:

1. Be more compressible.
2. Have greater potential to shrink upon drying and/or swell upon wetting.
3. Be less permeable.

In addition to the PI, the Liquidity Index (LI) is a useful indicator of the engineering characteristics of fine-grained soils. Table 2-4 in Chapter 2 identifies the strength and deformation characteristics of fine-grained soils in terms of the LI.

## 4.6 DESCRIPTION OF ROCK

When providing rock descriptions, geotechnical specialists should use technically correct geological terms. Local terms in common use may be acceptable if they help describe distinctive characteristics. Rock cores should be logged when wet for consistency of color description and greater visibility of rock features such as hairline fractures. The guidelines presented in the ISRM (1981), should be reviewed for additional information regarding logging procedures for core drilling.

The rock's lithologic description should include as a minimum the following items:

- Rock type
- Color
- Grain size and shape
- Texture (stratification/foliation)
- Mineral composition
- Weathering and alteration
- Strength
- Other relevant notes

The various elements of the rock's description should be stated in the order listed above, for example:

"Limestone, light gray, very fine-grained, thin-bedded, unweathered, strong"

The rock description should include identification of discontinuities and fractures. The description should also include a drawing of the naturally occurring fractures and mechanical breaks.

### 4.6.1 Rock Type

Rocks are classified according to their origin into three major divisions: igneous, sedimentary, and metamorphic (see Table 4-16). These three groups are subdivided into types according to mineral and chemical composition, texture, and internal structure. For some projects a library of hand samples and photographs representing lithologic rock types present in the project area should be maintained.

**Table 4-16**  
**Rock groups and types (FHWA, 1997)**

<b>Igneous</b>		
Intrusive (Coarse Grained)	Extrusive (Fine Grained)	Pyroclastic
Granite Syenite Diorite Diabase Gabbro Peridotite Pegmatite	Rhyolite Trachyte Andesite Basalt	Obsidian Pumice Tuff
<b>Sedimentary</b>		
Clastic (Sediment)	Chemically Formed	Organic Remains
Shale Mudstone Claystone Siltstone Sandstone Conglomerate Limestone, oolitic	Limestone Dolomite Gypsum Halite	Chalk Coquina Lignite Coal
<b>Metamorphic</b>		
Foliated		Non-foliated
Slate Phyllite Schist Gneiss		Quartzite Amphibolite Marble Hornfel

## 4.6.2 Color

Colors should be consistent with a Munsell Color Chart (USDA, 1993) and recorded for both wet and dry conditions as appropriate.

## 4.6.3 Grain Size and Shape

The grain size description should be classified according to the terms presented in Table 4-17. Table 4-18 is used to classify the shape of the grains. The grain size descriptions are consistent with those used in the USCS for soil particles.

**Table 4-17**  
**Terms to describe grain size (typically for sedimentary rocks)**

Description	Grain Size (mm)	Characteristic of Individual Grains
Very coarse grained	#4 (> 4.75)	Can be easily distinguished by eye
Coarse grained	#10 to #4 (2.00 -4.75)	Can be easily distinguished by eye
Medium grained	#40 to #10 (0.425 -2.00)	Can be distinguished by eye
Fine grained	#200 to #40 (0.075-0.425)	Can be distinguished by eye with difficulty
Very fine grained	< #200 (< 0.075)	Cannot be distinguished by unaided eye

**Table 4-18**  
**Terms to describe grain shape (for sedimentary rocks)**

Description	Characteristic
Angular	Showing very little evidence of wear. Grain edges and corners are sharp. Secondary corners are numerous and sharp.
Subangular	Showing some evidence of wear. Grain edges and corners are slightly rounded off. Secondary corners are slightly less numerous and slightly less sharp than in angular grains.
Subrounded	Showing considerable wear. Grain edges and corners are rounded to smooth curves. Secondary corners are reduced greatly in number and highly rounded.
Rounded	Showing extreme wear. Grain edges and corners are smoothed off to broad curves. Secondary corners are few in number and rounded.
Well-rounded	Completely worn. Grain edges or corners are not present. No secondary edges or corners are present.

#### 4.6.4 Stratification/Foliation

Significant non-fracture structural features should be described. The thickness should be described by using the terms in Table 4-19. The orientation of the bedding/foliation should be measured from the horizontal or with respect to the core axis.

**Table 4-19. Terms to describe stratum thickness**

<b>Descriptive Term</b>	<b>Stratum Thickness in (mm)*</b>
Very Thickly bedded	(> 1 m)
Thickly bedded	(0.5 to 1.0 m)
Thinly bedded	(50 mm to 500 mm)
Very Thinly bedded	(10 mm to 50 mm)
Laminated	(2.5 mm to 10 mm)
Thinly Laminated	(< 2.5 mm)
* Conventionally measured in m or mm. (1 m = 3.28 ft; 25.4 mm = 1 in)	

#### 4.6.5 Mineral Composition

The mineral composition should be identified by a geologist based on experience and the use of appropriate references. The most abundant mineral should be listed first, followed by minerals in decreasing order of abundance. For some common rock types, the mineral composition need not be specified (e.g. dolomite, limestone).

#### 4.6.6 Weathering and Alteration

Weathering and alteration is due to the weathering processes discussed in Chapter 3, e.g., physical, chemical and thermal mechanisms. Terms and abbreviations used to describe weathering and alteration are presented in Table 4-20.

#### 4.6.7 Strength

The point load test described in Chapter 5 is recommended for the measurement of sample strength. The point-load index,  $I_s$ , obtained from the point load test should be converted to uniaxial compressive strength. Categories and terminology for describing rock strength based on the uniaxial compressive strength are presented in Table 4-21. Table 4-21 also presents guidelines for common qualitative assessments of strength that can be performed with the aid of a geologist's hammer and a pocket knife while the geotechnical specialist is mapping or doing primary logging of core at the drill rig site. The field estimates should be confirmed where appropriate by comparison with selected laboratory tests.

**Table 4-20**  
**Terms to describe rock weathering and alteration (ISRM, 1981)**

<b>Grade (Term)</b>	<b>Description</b>
I (Fresh)	Rock shows no discoloration, loss of strength, or other effects of weathering/alteration
II (Slightly Weathered/Altered)	Rock is slightly discolored, but not noticeably lower in strength than fresh rock
III (Moderately Weathered/Altered)	Rock is discolored and noticeably weakened, but less than half is decomposed; a minimum 2 in (50 mm) diameter sample cannot be broken readily by hand across the rock fabric
IV (Highly Weathered/Altered)	More than half of the rock is decomposed; rock is weathered so that a minimum 2 in (50 mm) diameter sample can be broken readily by hand across the rock fabric
V (Completely Weathered/Altered)	Original minerals of rock have been almost entirely decomposed to secondary minerals even though the original fabric may be intact; material can be granulated by hand
VI (Residual Soil)	Original minerals of rock have been entirely decomposed to secondary minerals, and original rock fabric is not apparent; material can be easily broke by hand

**Table 4-21**  
**Terms to describe rock strength (ISRM, 1981)**

<b>Grade (Description)</b>	<b>Field Identification</b>	<b>Approximate Range of Uniaxial Compressive Strength, psi (kPa)</b>
R0 (Extremely Weak Rock)	Can be indented by thumbnail	35 - 150 (250) - (1,000)
R1 (Very Weak Rock)	Can be peeled by pocket knife	150 - 725 (1,000) - (5,000)
R2 (Weak Rock)	Can be peeled with difficulty by pocket knife	725 - 3,500 (5,000) - (25,000)
R3 (Medium Strong Rock)	Can be indented 3/16 in (5 mm) with sharp end of pick	3,500 - 7,000 (25,000) - (50,000)
R4 (Strong Rock)	Requires one blow of geologist's hammer to fracture	7,000 - 15,000 (50,000) - (100,000)
R5 (Very Strong Rock)	Requires many blows of geologist's hammer to fracture	15,000 - 36,000 (100,000) - (250,000)
R6 (Extremely Strong Rock)	Can only be chipped with blows of geologist's hammer	> 36,000 (>250,000)

#### 4.6.8 Hardness

Hardness is commonly assessed by the scratch test. Descriptions and abbreviations used to describe rock hardness are presented in Table 4-22.

**Table 4-22**  
**Terms to describe rock hardness (FHWA, 2002b)**

<b>Description (Abbr)</b>	<b>Characteristic</b>
Soft (S)	Reserved for plastic material alone.
Friable (F)	Easily crumbled by hand, pulverized or reduced to powder.
Low Hardness (LH)	Can be gouged deeply or carved with a pocket knife.
Moderately Hard (MH)	Can be readily scratched by a knife blade; scratch leaves a heavy trace of dust and scratch is readily visible after the powder has been blown away.
Hard (H)	Can be scratched with difficulty; scratch produces little powder and is often faintly visible; traces of the knife steel may be visible.
Very Hard (VH)	Cannot be scratched with pocket knife. Leave knife steel marks on surface.

#### 4.6.9 Rock Discontinuity

Discontinuity is the general term for any mechanical break in a rock mass that has zero or low tensile strength. Discontinuity is the collective term used for most types of joints, weak bedding planes, weak schistosity planes, weakness zones, and faults. The spacing between discontinuities is defined as the perpendicular distance between adjacent discontinuities. The spacing should be measured perpendicular to the planes in the set. Table 4-23 presents guidelines to describe discontinuity spacing.

Discontinuities should be described as closed, open, or filled. **Aperture** is the term used to describe the perpendicular distance separating the adjacent rock walls of an open discontinuity in which the intervening space is air- or water-filled. **Width** is the term used to describe the distance separating the adjacent rock walls of filled discontinuities. The terms presented in Table 4-24 should be used to describe apertures. Terms such as "wide," "narrow" and "tight" are used to describe the width of discontinuities such as thickness of veins, fault gouge filling, or joints openings. Guidelines for use of such terms are presented in Tables 4-23 and 4-24.

**Table 4-23. Terms to describe discontinuities (after ISRM, 1981)**

<b><u>Discontinuity Type</u></b> F - Fault J - Joint Sh - Shear Fo - Foliation V - Vein B - Bedding	<b><u>Amount of Infilling</u></b> Su - Surface Stain Sp - Spotty Pa - Partially Filled Fi - Filled No - None	<b><u>Discontinuity Spacing (m)*</u></b> EW - Extremely Wide (>6) VW - Very Wide (2-6) W - Wide (0.6-2) M - Moderate (0.2-0.6) C - Close (0.06-0.2) VC - Very Close (0.02-0.06) EC - Extremely close (<0.02)
<b><u>Discontinuity Width (mm)*</u></b> W - Wide (12.5-5.0) MW - Moderately Wide (2.5-12.5) N - Narrow (1.25-2.5) VN - Very Narrow (<1.25) T - Tight (~ 0)		<b><u>Surface Shape of Joint</u></b> Wa - Wavy Pl - Planar St - Stepped Ir - Irregular
<b><u>Type of Infilling</u></b> Cl - Clay Ca - Calcite Ch - Chlorite Fe - Iron Oxide Gy - Gypsum/Talc H - Healed No - None Py - Pyrite Qz - Quartz Sd - Sand	<b><u>Roughness of Surface</u></b> Slk - Slickensided (surface has smooth, glassy finish with visual evidence of striations) S - Smooth (surface appears smooth and feels so to the touch) SR - Slightly Rough (asperities on the discontinuity surface are distinguishable and can felt) R - Rough (some ridges and side-angle steps are evident; asperities are clearly visible, and discontinuity surface feels very abrasive) V - Very Rough (near-vertical steps and ridges occur on the discontinuity surface)	
* Conventionally measured in m or mm. (1 m = 3.28 ft; 1 in = 25.4 mm)		

**Table 4-24. Terms to classify discontinuities based on aperture size (ISRM, 1981)**

<b>Aperture (mm)*</b>	<b>Description</b>	
<0.1 0.1 - 0.25 0.25 - 0.5	Very tight Tight Partly open	"Closed Features"
0.5 - 2.5 2.5 - 10 > 10	Open Moderately open Wide	"Gapped Features"
1-100 100-1000 >1 m	Very wide Extremely wide Cavernous	"Open Features"
* Conventionally measured in mm, cm or m. (1 m = 3.28 ft; 1 in = 25.4 mm)		

For faults or shears that are not thick enough to be represented on the boring log, the measured thickness is recorded numerically in millimeters.

Discontinuities are further characterized by the surface shape of the joint and the roughness of its surface in addition to the fill material separating the adjacent rock walls of the discontinuities. Filling is characterized by its type, amount, width (i.e., perpendicular distance between adjacent rock walls) and strength. If non-cohesive fillings are identified, then the filling should be identified qualitatively, e.g., fine sand. Refer to Table 4-23 for guidelines to characterize these features.

#### **4.6.10 Fracture Description**

Naturally occurring fractures are numbered and described by using the same terminology that is used for discontinuities. The number of naturally occurring fractures observed in each 1 ft (0.5 m) of core should be recorded as the fracture frequency. Mechanical breaks, thought to have occurred during drilling, are not counted. The following criteria can be used to identify natural breaks:

1. A rough brittle surface with fresh cleavage planes in individual rock minerals suggests an artificial fracture.
2. A generally smooth or somewhat weathered surface with soft coating or infilling materials, such as talc, gypsum, chlorite, mica, or calcite indicates a natural discontinuity.
3. In rocks showing foliation, cleavage or bedding it may be difficult to distinguish between natural discontinuities and artificial fractures when the discontinuities are parallel with the incipient weakness planes. If drilling has been carried out carefully then the questionable breaks should be counted as natural features to be on the conservative side.
4. Depending upon the drilling equipment, part of the length of core being drilled may occasionally rotate with the inner barrels in such a way that grinding of the surfaces of discontinuities and fractures occurs. In weak rock types it may be very difficult to decide if the resulting rounded surfaces represent natural or artificial features. When in doubt, conservatively assume that they are natural.

The fracture description can be strongly time dependent and moisture content dependent in the case of certain varieties of shales and mudstones that have relatively weakly developed

diagenetic bonds. A diagenetic bond is the bond that is formed in a deposited sediment by chemical and physical processes during its conversion to rock. A frequent problem is "discing," in which an initially intact core separates into discs on incipient planes. The process generally becomes noticeable perhaps within a few minutes of core recovery. This phenomenon is experienced in several different forms:

1. Stress relief cracking and swelling by the initially rapid release of strain energy in cores recovered from areas of high stress, especially in the case of shaley rocks.
2. Dehydration cracking experienced in the weaker mudstones and shales that may reduce RQD values from 100 percent to 0 percent in a matter of minutes. The initial integrity might possibly have been due to negative pore water pressure.
3. Slaking and cracking experienced by some of the weaker mudstones and shales when they are subjected to wetting and drying.

Any of these forms of "discing" may make logging of fracture frequency unreliable. Whenever such conditions are anticipated, core should be logged by a geotechnical specialist as it is being recovered and at subsequent intervals until the phenomenon is predictable.

#### **4.6.11 Rock Mass Classification**

In determining the rock strength for transportation facilities constructed in, on, or of rock, it is most important to account for the presence of discontinuities, such as joints, faults or bedding planes. Therefore, for most conditions, the **rock mass** strength properties, rather than the intact rock properties must be determined for use in design. The rock mass is the in-situ, fractured rock that will almost always have significantly lower strength than the intact rock because of discontinuities that divide the rock mass into blocks. Therefore, the strength of the rock mass will depend on such factors as the shear strength of the surfaces of the blocks, the spacing and continuous length of the discontinuities and their alignment relative to the direction of loading. These factors were identified in the previous sections. Using these factors, Bieniawski (1989) proposed a method for estimating rock mass properties from an index that characterizes the overall properties of the rock mass quality. This index is known as the **rock mass rating (RMR)**. Originally developed for tunnel support design, the RMR has been adopted by AASHTO (2004 with 2006 Interims) because the RMR is determined from readily measurable parameters. Table 4-25 identifies the following five measurable parameters and assigns relative ratings to each parameter:

**Table 4-25**  
**Geomechanics classification of rock masses (AASHTO 2004 with 2006 Interims)**

PARAMETER		RANGES OF VALUES							
1	Strength of intact rock material	Point load strength index	>1,200 psi	600 to 1,200 psi	300 to 600 psi	150 to 300 psi	For this low range – uniaxial compressive test is preferred		
		Uniaxial compressive strength	>30,000 psi	15,000 to 30,000 psi	7,500 to 15,000 psi	3,600 to 7,500 psi	1,500 to 3,600 psi	500 to 1,500 psi	150 to 500 psi
	Relative Rating	15	12	7	4	2	1	0	
2	Drill core quality RQD	90% to 100%	75% to 90%	50% to 75%	25% to 50%	<25%			
	Relative Rating	20	17	13	8	3			
3	Spacing of joints	>10 ft	3 to 10 ft	1 to 3 ft	2 in. to 1 foot	<2 in.			
	Relative Rating	30	25	20	10	5			
4	Condition of joints	<ul style="list-style-type: none"> <li>• Very rough surfaces</li> <li>• Not continuous</li> <li>• No separation</li> <li>• Hard joint wall rock</li> </ul>	<ul style="list-style-type: none"> <li>• Slightly rough surfaces</li> <li>• Separation &lt;0.05”</li> <li>• Hard joint wall rock</li> </ul>	<ul style="list-style-type: none"> <li>• Slightly rough surfaces</li> <li>• Separation &lt;0.05”</li> <li>• Soft joint wall rock</li> </ul>	<ul style="list-style-type: none"> <li>• Slickensided surfaces - or -</li> <li>• Gouge &lt;0.2 in thick – or-</li> <li>• Joints open 0.05-0.2”</li> <li>• Continuous joints</li> </ul>	<ul style="list-style-type: none"> <li>• Soft gouge &gt;0.2” thick - or -</li> <li>• Joints open &gt;0.2”</li> <li>• Continuous joints</li> </ul>			
	Relative Rating	25	20	12	6	0			
5	Ground water conditions (use one of the three evaluation criteria as appropriate to the method of exploration)	Inflow per 30 ft tunnel length	None	<400 gallons/hr	400 to 2,000 gallons/hr	>2,000 gallons/hr			
		Ratio= joint water pressure/ major principal stress	0	0.0 to 0.2	0.2 to 0.5	>0.5			
		General Conditions	Completely Dry	Moist only (interstitial water)	Water under moderate pressure	Severe water problems			
	Relative Rating	10	7	4	0				

Note: 1 psi = 6.895 kPa; 1 in = 25.4 mm

1. Strength of intact rock material.
2. Drill core quality as expressed by RQD.
3. Spacing of joints.
4. Condition of joints.
5. Ground water conditions.

The RMR is determined as the sum of the five relative ratings. The RMR should be adjusted in accordance with the criteria in Table 4-26. **The rock classification should be determined in accordance with Table 4-27 where RMR refers to the adjusted value.**

**Table 4-26**  
**Geomechanics rating adjustment for joint orientations**  
**(after AASHTO 2004 with 2006 Interims)**

Orientations of joints		Very favorable	Favorable	Fair	Unfavorable	Very Unfavorable
Ratings	Tunnels	0	-2	-5	-10	-12
	Foundations	0	-2	-7	-15	-25
	Slopes	0	-5	-25	-50	-60

**Table 4-27**  
**Geomechanics rock mass classes determined from total ratings**  
**(AASHTO 2004 with 2006 Interims)**

RMR (Note 1)	100 to 81	80 to 61	60 to 41	40 to 21	<20
Class No.	I	II	III	IV	V
Description	Very good rock	Good rock	Fair rock	Poor rock	Very poor rock
Note 1: RMR is adjusted for structural application and rock joint orientation as per Table 4-26 prior to evaluating the Class No.					

## 4.7 SUBSURFACE PROFILE DEVELOPMENT

The mark of successfully accomplishing a subsurface exploration is the ability to draw a subsurface profile of the project site complete with soil types, rock interfaces, and the relevant design properties. The subsurface profile is a visual display of subsurface conditions as interpreted from all of the methods of explorations and testing described previously. Uncertainties in the development of a subsurface exploration usually indicate the need for additional explorations or testing. Because of the diverse nature of the geologic processes that contribute to soil formation, actual subsurface profiles can be extremely varied both vertically and horizontally, and can differ significantly from interpreted profiles developed from boring logs. Therefore, subsurface profiles developed from boring logs should contain some indication that the delineation between strata do not necessarily suggest that distinct boundaries exist between the strata or that the interpolations of strata thickness between borings are necessarily correct. The main purpose of subsurface profiles is to provide a starting point for design and not necessarily to present an accurate description of subsurface conditions.

In the optimum situation, the subsurface profile is developed in stages. First, a rough profile is established from the driller's logs by the geotechnical specialist. The object is to discover any obvious gaps or question marks while the drill crew is still at the site so that additional work can be performed immediately. Once a crew has left the site, a delay of months may occur before their schedule permits them to reoccupy the site, not to mention the additional cost to remobilize/demobilize. The drilling inspector or crew chief should be required to call the project geotechnical specialist when the last scheduled boring has begun to request instructions for any supplemental borings.

When all borings are completed and laboratory visuals and moisture content data received, the initial subsurface profile should be revised. Estimated soil layer boundaries and accurate soil descriptions should be established for soil deposits. Estimated bedrock interfaces should be identified. Most importantly, the depth to perched or regional groundwater should be indicated. The over-complication of the profile by noting minute variations between adjacent soil samples can be avoided by:

1. Reviewing the geologic history of the site, e.g., if the soil map denotes a lakebed deposit overlying a glacial till deposit, do not subdivide the lakebed deposit because adjacent samples have differing amounts of silt and clay. Realize before breaking down the soil profile that probably only two layers exist and variations are to be expected within each. Important variations such as the average thickness of silt and clay varves can be noted adjacent to the visual description of the layer.

2. Remembering that the soil samples examined are only a minute portion of the soil underlying the site and must be considered in relation to adjacent samples as well as adjacent borings.

A few simple rules should be followed at this stage to interpret the available data properly:

1. Review the USDA Soil Survey map for the county and determine major surface and near-surface deposits that can be expected at the site.
2. Examine the subsurface log containing SPT results and the laboratory visual descriptions with accompanying moisture contents.
3. Review representative soil samples to check laboratory identifications and to calibrate your interpretations with those of the laboratory technicians who performed the visual description.
4. Establish rational mechanics for drawing the soil profile. For example:
  - a. Use a vertical scale of 1 in equals 10 ft or 20 ft; generally, any smaller scale tends to compress data visually and prevent proper interpretation.
  - b. Use a horizontal scale equal to the vertical scale, if possible, to simulate actual relationships. However, the total length should be kept within 36 inches (920 millimeter) to permit review in a single glance.

When the subsurface layer boundaries and descriptions have been established, determine the extent and details of laboratory testing. Do not casually read the driller's log and randomly select certain samples for testing. Plan the test program intelligently from the subsurface profile and for the proposed feature. Identify major soil deposits and assign appropriate tests for the design project under investigation.

The final subsurface profile is the geotechnical specialist's best interpretation of all available subsurface data. The final subsurface profile should include the following:

- interpreted boundaries of soil and rock
- the average physical properties of the soil layers, e.g., unit weight, shear strength, etc.
- a visual description of each layer including USCS symbols for soil classification
- location of the ground water level, and

- notations for special items such as boulders, artesian pressure, etc.

If the inclusion of all of the information listed above clutters the subsurface profile, then complementary tables containing some of that information should be developed to accompany the profile. Figures 4-8 and 4-9 show a typical boring location plan and an interpreted subsurface profile. Note that **the interpreted boundaries of rock and groundwater profiles are for internal agency use. Such interpretations should not be presented in bid documents.** Another example of boring location plan and subsurface profile is presented in Chapter 11 (Geotechnical Reports).

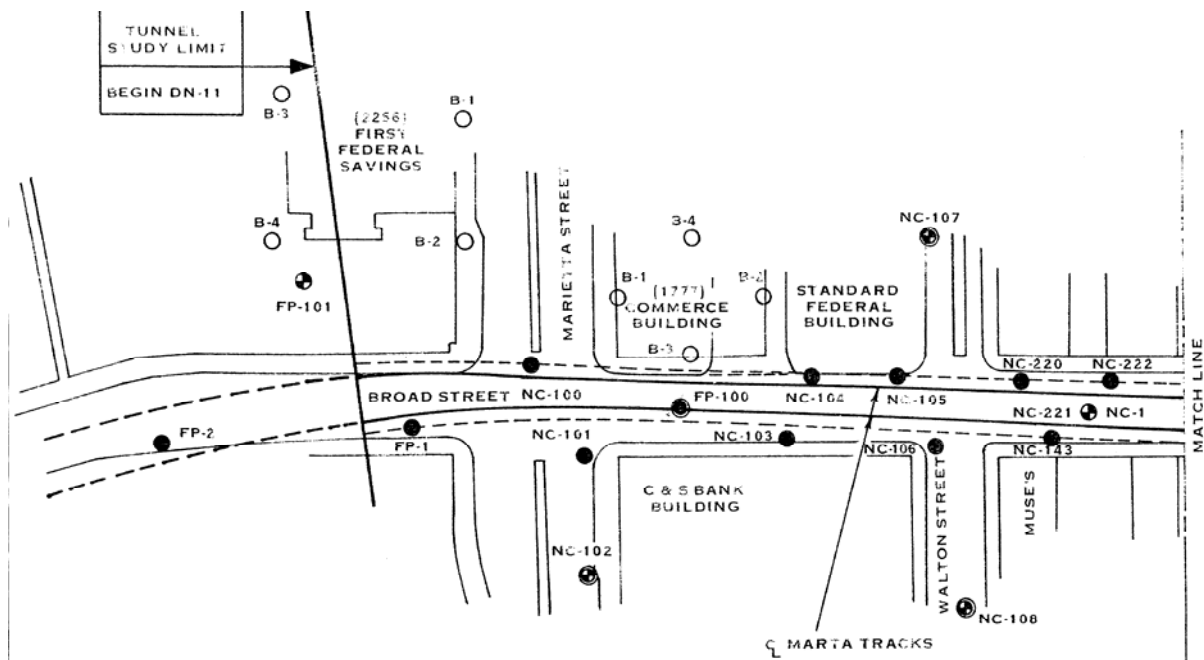
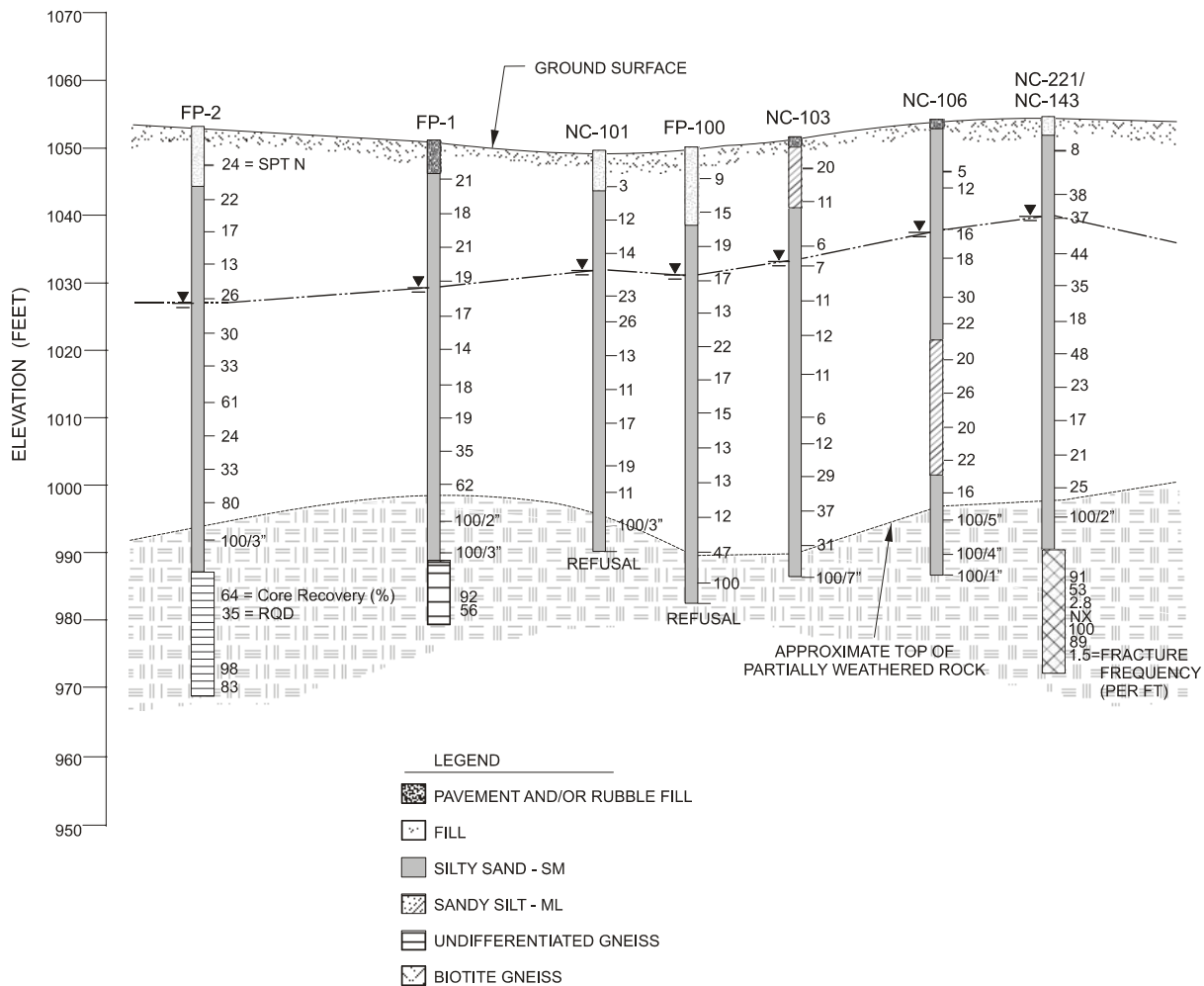


Figure 4-8. Example boring location plan (FHWA, 2002a).



**Figure 4-9. Example interpreted subsurface profile (FHWA, 2002a).**

#### 4.7.1 Use of Historical Data in Development of Subsurface Profile

Data from historical boring logs from the area can be used to supplement data provided by the current boring logs in developing a subsurface profile, however, such historical logs need to be reviewed carefully well in advance of drilling activities to ensure that the data are accurate. In some cases, boring log locations are referenced to the center alignment of a roadway without the location of the borehole having been actually surveyed. It is imperative to ensure that a consistent coordinate system is used to establish the correct relative location of all borings. Since borings would have likely been performed over an extended period of time or for different contracts along a roadway alignment (i.e., project centerlines are commonly changed during project development), it is possible that coordinate systems will not be consistent. Simply stated, if a historical boring cannot be located confidently on a site

plan, then the boring has limited usefulness for establishing stratigraphy. Also, it is likely that different drill rigs with different operators and different energy efficiencies were used in the collection of SPT data on historical boring logs. This factor must also be recognized when an attempt is made to correlate engineering properties to SPT blow count values. However, the geotechnical specialist should realize that while there may be potential limitations in the use of historical borings, it is necessary to review these borings relative to the design under consideration. As an example, a historical boring may indicate a thick layer of very soft clay as evidenced by the description “weight of rod/weight of hammer” in the SPT recording box of the log at a large number of test depths. While shear strength and consolidation properties cannot be reliably estimated based on SPT blow count values, the historical boring may provide useful information concerning the depth to a firm stratum.

Most DOTs have collected large amounts of subsurface data from previous investigations within their states. Unfortunately, much of these data are archived with related project data once the project has been completed, and thus may not be readily available or accessible for use during future projects. Additionally, the subsurface data may not be fully utilized if the locations of the borings are not identified properly or if the plan drawing of the project site is not maintained with the boring logs. To overcome this problem, many DOTs currently use longitude and latitude to identify the boring locations, in lieu of or in conjunction with the conventional positioning format that uses station and offset. Unfortunately, the vast majority of the historical subsurface boring information is available only on paper. Therefore, a considerable amount of work is required to convert that data into electronic form before it can be fully appreciated and used to establish an electronic database of the subsurface information.

Several DOTs have recently commenced using electronic boring records for their projects. Not only does the use of electronic boring records provide a redundancy to compliment the paper copy, but it also preserves data in a way that has the potential for automated electronic data management. One method of electronic data management increasingly used by DOTs involves the use of a centralized electronic database in conjunction with Geographic Information System (GIS) techniques to locate and identify borings on a plan. In its most simplistic form, the electronically stored data are managed and assessed visually by using GIS software, where each boring location is identified on a plan map. An appropriately developed database and GIS can be used to great advantage by the DOT. Specifically, in addition to the previously mentioned advantages of having electronic data records compliment paper logs, it is possible to:

1. catalog borings that were conducted previously;
2. inventory data regarding specific problematic formations across the state; and

3. develop cross sections that depict subsurface conditions across a site or within a region.

This type of application of electronic boring records and data base accessibility can facilitate the development of subsequent subsurface investigations that are appropriately focused and that optimize the utility of existing data.

## **CHAPTER 5.0 LABORATORY TESTING FOR GEOTECHNICAL DESIGN AND CONSTRUCTION**

Laboratory testing of soils and rocks is a fundamental element of geotechnical engineering. The complexity of testing required for a particular project may range from a simple moisture content determination to sophisticated triaxial strength testing. A laboratory test program should be well-planned to optimize the test data for design and construction. The geotechnical specialist, therefore, should recognize the project's issues ahead of time so as to optimize the testing program, particularly strength and consolidation testing.

Laboratory testing of samples recovered during subsurface investigations is the most common technique to obtain values of the engineering properties necessary for design. A laboratory-testing program consists of “index tests” to obtain general information on categorizing materials, and “performance tests” to measure specific properties that characterize soil behavior for design and constructability assessments (e.g., shear strength, compressibility, hydraulic conductivity, etc.). This chapter provides information on common laboratory test methods for soils and rocks including testing equipment, general procedures related to each test, and parameters measured by the tests.

### **5.01 Primary References**

The primary references for this Chapter are as follows:

ASTM (2006). *Annual Book of ASTM Standards – Sections 4.02, 4.08, 4.09 and 4.13*. ASTM International, West Conshohocken, PA.

AASHTO (2006). *Standard Specifications for Transportation Materials and Methods of Sampling and Testing*, Parts I and II, American Association of State Highway and Transportation Officials, Washington, D.C.

FHWA (2002a). *Geotechnical Engineering Circular 5 (GEC5) - Evaluation of Soil and Rock Properties*. Report No FHWA-IF-02-034. Authors: Sabatini, P.J, Bachus, R.C, Mayne, P.W., Schneider, J.A., Zettler, T.E., Federal Highway Administration, U.S. Department of Transportation.

## **5.1 QUALITY ASSURANCE FOR LABORATORY TESTING**

Laboratory testing will be required for most projects. Therefore, it is necessary to select the appropriate types and quantities of laboratory tests to be performed. A careful review of all data obtained during the field investigation and a thorough understanding of the preliminary design of geotechnical, structural and hydraulic features of the project are essential to develop an appropriately scoped laboratory testing program. In some cases owners may hire external testing laboratories to perform select tests. It is necessary that testing requests be clear and sufficiently detailed. Unless specialized testing is required, the owner should require that all testing be performed in accordance with the appropriate specifications for laboratory testing such as those codified in AASHTO and/or ASTM. Several tables are presented in this chapter that summarize various common tests for soils and rocks per AASHTO and ASTM standards. In order to assure that the results of laboratory testing are representative, several precautions must be taken before the tests themselves are performed. These precautions include: sample tracking, sample storage, sample handling to prevent sample disturbance, and sample selection. Discussion of each of these precautions follows.

### **5.1.1 Sample Tracking**

Whether the laboratory testing is performed in-house or is subcontracted, samples will likely be assigned a laboratory identification number that differs from the identification number assigned in the field. A list should be prepared to match the laboratory identification number with the field identification number. This list can also be used to provide tracking information to ensure that each sample arrived at the lab. When laboratory testing is requested, both the field identification number and the laboratory identification number should be used on the request form. An example request form is shown in Figure 5-1. A spreadsheet or database program is useful to manage sample identification data.

### **5.1.2 Sample Storage**

Undisturbed soil samples should be transported and stored so that the moisture content is maintained as close as possible to the natural conditions (AASHTO T 207, ASTM D 4220 and D 5079). Samples should not be placed, even temporarily, in direct sunlight. Shelby tubes should be stored in an upright position with the top side of the sample up in a humid room with relative humidity above 90%.

Long-term storage of soil samples in Shelby tubes is not recommended. As storage time increases, moisture will migrate within the tube. Potential for disturbance and moisture migration within the sample will increase with time, and samples tested 30 days after their retrieval should be noted on the laboratory data sheet. Excessive storage time can lead to



Long-term storage of soil samples in Shelby tubes is not recommended for another reason. During long term storage the sample tubes may corrode. Corrosion accompanied by adhesion of the soil to the tube may result in the development of such a large sidewall resistance that some soils may experience internal failures during extrusion. Often these failures cannot be seen by the naked eye; x-ray radiography (ASTM D 4452) will likely be necessary to confirm the presence of such conditions. If these samples are tested as “undisturbed” specimens, the results may be misleading.

### **5.1.3 Sample Handling**

Careless handling of nominally undisturbed soil samples after they have been retrieved may cause major disturbances that could influence test results and lead to serious design and construction consequences. Samples should always be handled by experienced personnel in a manner that ensures that the sample maintains structural integrity and its natural moisture condition. Saws and knives used to prepare soil specimens should be clean and sharp. Preparation time should be kept to a minimum, especially where the maintenance of the moisture content is critical. Specimens should not be exposed to direct sun, freezing, or precipitation.

### **5.1.4 Effects of Sample Disturbance**

As a soil sample is removed from the ground during a conventional soil investigation, its in-situ effective stress condition is being changed. In addition, nominally undisturbed specimens taken from samples obtained from drilled boreholes will become disturbed as a result of the drilling itself, sampling, sample extrusion, and sample trimming to form a specimen for testing. These processes will also change the effective stress condition in the soil sample, i.e., the effective stress in the soil at the time after a sample is trimmed and prepared for testing is different from that of the same soil in the ground. Therefore the utmost care should be taken to minimize the effect of these processes in order for the results of laboratory tests to represent the in-situ soil behavior accurately.

### **5.1.5 Specimen Selection**

The selection of representative specimens for testing is one of the most important aspects of sampling and testing procedures. Selected specimens must be representative of the formation or deposit being investigated. The geotechnical specialist should study the boring logs, understand the geology of the site, and visually examine the samples before selecting the test specimens. Samples should be selected on the basis of their color, physical appearance, structural features and an understanding of the disturbance of the samples. Specimens should be selected to represent all types of materials present at the site, not just the worst or the best.

Samples with discontinuities and intrusions may fail prematurely in the laboratory. The first inclination would be to test these samples. However, if these features are small and randomly located, they may not necessarily cause such failures in the field. Therefore samples having such local features should be noted, but not necessarily selected for testing since such samples may not be representative of the stratum in terms of its response to applied loads.

Certain considerations regarding laboratory testing, such as when, how much, and what type, can be decided only by an experienced geotechnical specialist. The following minimal criteria should be considered when the scope of the laboratory testing program is being determined:

- Project type (bridge, embankment, building, reconstruction or new construction, etc.)
- Size of the project (geographic extent).
- Loads to be imposed on the foundation soils (geometry, type, direction and magnitude).
- Performance requirements for the project (e.g., settlement and lateral deformation limitations).
- Vertical and horizontal variations in the subsurface profile as determined from boring logs and visual identification of subsurface material types in the laboratory.
- Known or suspected peculiarities of subsurface strata at the project location (e.g., swelling soils, collapsible soils, organics, etc.)
- Presence of visually observed intrusions, slickensides, fissures, concretions, etc.

The selection of tests should be considered preliminary until the geotechnical specialist is satisfied that the test results are sufficient to develop reliable subsurface profiles and provide the parameters needed for design.

## **5.2 LABORATORY TESTING FOR SOILS**

Table 5-1 provides a listing of commonly-performed soil laboratory tests. Tables 5-2 and 5-3 provide a summary of typical soil index and performance tests, respectively. Additional information on these tests is provided in subsequent sections.

**Table 5-1  
Commonly performed laboratory tests on soils (after FHWA, 2002a)**

Test Category	Name of Test	Test Designation	
		AASHTO	ASTM
Visual Identification	Practice for Description and Identification of Soils (Visual-Manual Procedure)	-	D 2488
	Practice for Description of Frozen Soils (Visual-Manual Procedure)	-	D 4083
Index Properties	Test Method for Determination of Water (Moisture) Content of Soil by Direct Heating Method	T 265	D 2216
	Test Method for Specific Gravity of Soils	T 100	D 854; D 5550
	Method for Particle-Size Analysis of Soils	T 88	D 422
	Test Method for Classification of Soils for Engineering Purposes	M 145	D 2487; D 3282
	Test Method for Amount of Material in Soils Finer than the No. 200 (0.075 mm) Sieve		D 1140
	Test Method for Liquid Limit, Plastic Limit, and Plasticity Index of Soils	T 89; T 90	D 4318
Compaction	Test Method for Laboratory Compaction Characteristics of Soil Using Standard Effort (12,375 ft. lbs/ft <sup>3</sup> )	T 99	D 698
	Test Method for Laboratory Compaction Characteristics of Soil Using Modified Effort (56,250 ft.lbs/ft <sup>3</sup> )	T 180	D 1557
Strength Properties	Test Method for Unconfined Compressive Strength of Cohesive Soil	T 208	D 2166
	Test Method for Unconsolidated, Undrained Compressive Strength of Cohesive Soils in Triaxial Compression	T 296	D 2850
	Test Method for Consolidated, Undrained Compressive Strength of Cohesive Soils in Triaxial Compression	T 297	D 4767
	Method for Direct Shear Test of Soils under Consolidated Drained Conditions	T 236	D 3080
	Test Methods for Modulus and Damping of Soils by the Resonant-Column Method	-	D 4015
	Test Method for Laboratory Miniature Vane Shear Test for Saturated Fine-Grained Clayey Soil	-	D 4648
	Test Method for CBR (California Bearing Ratio) of Laboratory-Compacted Soils	-	D 1883
	Test Method for Resilient Modulus of Soils	T 294	-
Consolidation, Swelling, Collapse Properties	Test Method for Resistance R-Value and Expansion Pressure of Compacted Soils	T 190	D 2844
	Test Method for One-Dimensional Consolidation Properties of Soils	T 216	D 2435
	Test Method for One-Dimensional Consolidation Properties of Soils Using Controlled-Strain Loading	-	D 4186
	Test Methods for One-Dimensional Swell or Settlement Potential of Cohesive Soils	T 258	D 4546
Permeability	Test Method for Measurement of Collapse Potential of Soils	-	D 5333
	Test Method for Permeability of Granular Soils (Constant Head)	T 215	D 2434
Corrosivity (Electro-chemical)	Test Method for Measurement of Hydraulic Conductivity of Saturated Porous Materials Using a Flexible Wall Permeameter	-	D 5084
	Test Method for pH for Peat Materials	-	D 2976
	Test Method for pH of Soils	-	D 4972
	Test Method for pH of Soil for Use in Corrosion Testing	T 289	G 51
	Test Method for Sulfate Content	T 290	D 4230
	Test Method for Resistivity	T 288	D 1125; G57
Organic Content	Test Method for Chloride Content	T 291	D 512
	Test Methods for Moisture, Ash, and Organic Matter of Peat and Other Organic Soils	T 194	D 2974

**Table 5-2  
Methods for index testing of soils (after FHWA, 2002a)**

Test	Procedure	ASTM and/or AASHTO	Applicable Soil Types	Applicable Soil Properties	Limitations / Remarks
Moisture content, $w_n$	Dry soil in oven at $100 \pm 5$ °C	D 2216 T 265	Gravel, sand, silt, clay, peat	$e_o, \gamma$	Simple index test for all materials.
Unit weight and density	Extract a tube sample; measure dimensions and weight;	D 2216 T 265	Soils where undisturbed samples can be taken, i.e., silt, clay, peat	$\gamma_t, \gamma_{dry}, \rho_{tot}, \rho_{dry}, p_t$	Not appropriate for clean granular materials where undisturbed sampling is not possible. Very useful index test.
Atterberg limits, LL, PL, PI, SL, LI	LL – Moisture content associated with closure of the groove at 25 blows of specimen in Casagrande cup PL – Moisture content associated with crumbling of rolled soil at 1/8-in (3mm)	D 4318 T 89 T 90	Clays, silts, peat; silty and clayey sands to determine whether SM or SC	Soil classification and used in consolidation parameters	Not appropriate in non-plastic granular soil. Recommended for all plastic materials.
Mechanical sieve	Place air dry material on a series of successively smaller screens of known opening size and vibrate to separate particles of a specific equivalent diameter	D 422 T 88	Gravel, sand, silt	Soil classification	Not appropriate for clay soils. Useful, particularly in clean and dirty granular materials.
Wash sieve	Flush fine particles through a U.S. No. 200 (0.075 mm) sieve with water.	C 117 D 1140 T 88	Sand, silt, clay	Soil classification	Needed to assess fines content in dirty granular materials.
Hydrometer	Allow particles to settle, and measure specific gravity of the solution with time.	D 422 D 1140 T 88	Fine sand, silt, clay	Soil classification	Helpful to assess relative quantity of silt and clay.
Sand Equivalent	Sample passing No. 4 (4.75 mm) sieve is separated into sand and clay size particles	D 2419 T 176	Gravel, Sand, silt, clay	Aggregate classification Compaction	Useful for aggregates
Specific gravity of solids	The volume of a known mass of soil is compared to the known volume of water in a calibrated pycnometer	D 854 D 5550 T 100	Sand, silt, clay, peat	Used in calculation of $e_o$	Particularly helpful in cases where unusual solid minerals are encountered.
Organic content	After performing a moisture content test at 110 °C (230° F), the sample is ignited in a muffle furnace at 440 °C (824° F) to measure the ash content.	D 2974 T 194	All soil types where organic matter is suspected to be a concern	Not related to any specific performance parameters, but samples high in organic content will likely have high compressibility.	Recommended on all soils suspected to contain organic materials.

Symbols used in Table 5-2

$e_o$ : in-situ void ratio       $\gamma_{dry}$ :dry unit weight       $\gamma$ : unit weight       $p_t$ : total vertical stress  
 $\rho_{dry}$ :dry density       $\rho_{tot}$ :total density       $\gamma_t$ :total unit weight

**Table 5-3  
Methods for performance testing of soils (after FHWA, 2002a)**

Test	Procedure	Applicable Soil Types	Soil Properties	Limitations / Remarks
1-D oedometer	Incremental loads are applied to a soil specimen confined by a rigid ring; deformation values are recorded with time; loads are typically doubled for each increment and applied for 24 hours each.	Primarily clays and silts; granular soils can be tested, but typically are not.	$p_c$ , OCR, $C_c$ , $C_{ce}$ , $C_r$ , $C_{re}$ , $C_a$ , $C_{ae}$ , $c_v$ , $k$	Recommended for fine grained soils. Results can be useful index to other critical parameters.
Constant rate of strain oedometer	Loads are applied such that $\Delta u$ is between 3 and 30 percent of the applied vertical stress during testing	Clays and silts; not applicable to free draining granular soils.	$p_c$ , $C_c$ , $C_{ce}$ , $C_r$ , $C_{re}$ , $c_v$ , $k$	Requires special testing equipment, but can reduce testing time significantly.
Unconfined compression (UC)	A specimen is placed in a loading apparatus and sheared under axial compression with no confinement.	Clays and silts; cannot be performed on granular soils or fissured and varved materials	$S_{u,UC}$	Provides rapid means to approximate undrained shear strength, but disturbance effects, test rate, and moisture migration will affect results.
Unconsolidated undrained (UU) triaxial shear	The specimen is not allowed to consolidate under the confining stress, and the specimen is loaded at a quick enough rate to prevent drainage.	Clays and silts	$S_{u,UU}$	Sample must be nearly saturated. Sample disturbance and rate effects will affect measured strength.
Isotropic consolidated drained compression (CIDC)	The specimen is allowed to consolidate under the confining stress, and then is sheared at a rate slow enough to prevent build-up of pore water pressures.	Sands, silts, clays	$\phi'$ , $c'$ , $E$	Can be run on clay specimen, but time consuming. Best triaxial test to obtain deformation properties.
Isotropic consolidated undrained compression (CIUC)	The specimen is allowed to consolidate under the confining stress with drainage allowed, and then is sheared with no drainage allowed, but pore water pressures measured.	Sands, silts, clays, peats	$\phi'$ , $c'$ , $S_{u,CIUC}$ , $E$	Recommended to measure pore pressures during test. Useful test to assess effective stress strength parameters. Not recommended for measuring deformation properties.
Direct shear	The specimen is sheared on a forced failure plane at a constant rate, which is a function of the hydraulic conductivity of the specimen.	Compacted fill materials; sands, silts, and clays	$\phi'$ , $\phi'_r$	Requires assumption of drainage conditions. Relatively easy to perform.

Test	Procedure	Applicable Soil Types	Soil Properties	Limitations / Remarks
Flexible Wall Permeameter	The specimen is encased in a membrane, consolidated, backpressure saturated, and measurements of flow with time are recorded for a specific gradient.	Relatively low permeability materials ( $k \leq 1 \times 10^{-5}$ cm/s); clays & silts	k	Recommended for fine grained materials. Backpressure saturation required. Confining stress needs to be provided. System permeability must be at least an order of magnitude greater than that of the specimen. Time needed to allow inflow and outflow to stabilize.
Rigid Wall Permeameter	The specimen is placed in a rigid wall cell, vertical confinement is applied, and flow measurements are recorded with time under constant head or falling head conditions.	Relatively high permeability materials; sands, gravels, and silts	k	Need to control gradient. Not for use in fine grained soils. Monitor for sidewall leakage.

Symbols used in Table 5-3

$\phi'$ : peak effective stress friction angle	OCR: overconsolidation ratio	$C_{ce}$ : modified compression index
$\phi'_r$ : residual effective stress friction angle	$c_v$ : vertical coefficient of consolidation	$C_r$ : recompression index
$c'$ : effective stress cohesion intercept	E: Young's modulus	$C_{re}$ : modified recompression index
$s_u$ : undrained shear strength	k: hydraulic conductivity	$C_\alpha$ : secondary compression index
$p_c$ : preconsolidation stress	$C_c$ : compression index	$C_{\alpha e}$ : modified secondary compression index

## 5.3 LABORATORY INDEX TESTS FOR SOILS

### 5.3.1 General

Data generated from laboratory index tests provide an inexpensive way to assess soil consistency and variability among samples collected from a site. Information obtained from index tests is used to select samples for engineering property testing as well as to provide an indicator of general engineering behavior. For example, a soil with a high plasticity index (PI) can be expected to have high compressibility, low hydraulic conductivity, and high swell potential. Common index tests discussed in this section include moisture content, unit weight (wet density), Atterberg limits, particle size distribution, visual classification, specific gravity, and organic content. Index testing should be conducted on each type of soil material on every project. Information from index tests should be assessed prior to a final decision regarding the specimens selected for subsequent performance testing.

### 5.3.2 Moisture Content

The moisture (or water) content test is one of the simplest and least expensive laboratory tests to perform. Moisture content is defined as the ratio of the weight of the water in a soil specimen to the dry weight of the specimen. Natural moisture contents ( $w_n$ ) of sands are typically  $0 \leq w_n \leq 20$  %, whereas for inorganic and insensitive silts and clays, the typical range is  $10 \leq w_n \leq 40$  %. However, for clays it is possible to have more water than solids (i.e.,  $w_n > 100\%$ ), depending upon the mineralogy, formation environment, and structure of the clay. Therefore, soft and highly compressible clays, as well as sensitive, quick, or organically rich clays, can exhibit water contents in the range of  $40 \leq w_n \leq 300$  % or more.

Moisture content can be tested a number of different ways including: (1) a drying oven (ASTM D 2216); (2) a microwave oven (ASTM D 4643); or (3) a field stove or blowtorch (ASTM D 4959). While the microwave or field stove (or blowtorch) methods provide a rapid evaluation of moisture content, potential errors inherent with these methods require confirmation of results obtained by using ASTM D 2216. The radiation heating induced by the microwave oven and the excessive temperature induced by the field stove may release water entrapped in the soil structure (adsorbed water) that would normally not be released at 230° F (110° C), the maximum temperature specified by ASTM D 2216. Therefore, the microwave oven and field stove methods may yield greater values of moisture content than would occur from ASTM D 2216.

Field measurements of moisture content often rely on a field stove or microwave due to the speed of testing. For control of compacted material, it is common to use a nuclear gauge

(ASTM D 3017) in the field to assess moisture contents rapidly. Nuclear gage readings may indicate widely varying moisture contents for micaceous soils, i.e., soils containing a significant amount of mica particles. Results from nuclear techniques should be “calibrated” or confirmed by using the drying oven method (ASTM D 2216).

Moisture contents of soils as determined from in-situ moisture content tests may be altered during sampling, sample handling, and sample storage. Because the top end of the sample tube may contain water or collapse material from the borehole, moisture content tests should not be performed on material near the top of the tube. Also, as storage time increases, moisture will migrate within a specimen and lead to altered values of moisture content. If the sample is not properly sealed, moisture loss through drying of the sample will likely occur.

### 5.3.3 Unit Weight

The terms density ( $\rho$ ) and unit weight ( $\gamma$ ) are often incorrectly used interchangeably. The correct usage is that density implies mass while unit weight implies weight measurements. Density and unit weight are related through the gravitational constant ( $g$ ) as follows:  $\gamma = \rho g$ . In this document they will be referenced as “density (unit weight)” if the usage is independent of the specific definition.

In the laboratory, soil unit weight and mass density are easily measured on tube (undisturbed) samples of natural soils. The moist (total) mass density is  $\rho_t = M_t/V_t$ , where  $M_t$  is the total mass of the soil sample including the mass of the moisture in the pores and  $V_t$  is the total volume of the soil sample. Similarly the dry mass density is given by  $\rho_d = M_s/V_t$ , where  $M_s$  is the mass of the solid component of the soil sample and  $V_t$  is the total volume of the soil sample. Likewise, the moist unit weight is  $\gamma_t = W_t/V_t$ , where  $W_t$  is the total weight including the weight of the water in the pores and  $V_t$  is the total volume of the soil sample. Similarly, the dry unit weight is defined as  $\gamma_d = W_s/V_t$  where  $W_s$  is the weight of the solid component of the soil sample and  $V_t$  is the total volume of the soil sample. The relationship between the total and dry mass density and unit weight in terms of natural moisture content,  $w$ , is given by:

$$\rho_d = \frac{\rho_t}{1 + w} \quad 5-1$$

Since  $\gamma = \rho g$  the relationship between total and dry unit weight is given by:

$$\gamma_d = \frac{\gamma_t}{1 + w} \quad 5-2$$

Field measurements of soil mass density (unit weight) are generally restricted to shallow surface samples such as those obtained during placement of compacted fills. In those cases, field measurements of soil mass density (unit weight) can be accomplished by using drive tubes (ASTM D 2937), the sand cone method (ASTM D 1556), or a nuclear gauge (ASTM D 2922). To obtain unit weights or mass densities with depth, either high-quality thin-walled tube samples must be obtained (ASTM D 1587), or relatively expensive geophysical logging by gamma ray techniques (ASTM D 5195) can be employed.

Table 5-4 presents typical unit weights along with a range of void ratios for a variety of soils.

### 5.3.4 Particle Size Distribution

Particle size distributions by mechanical sieve and hydrometer analyses are useful for soil classification purposes. Procedures for grain size analyses are contained in ASTM D 422 and AASHTO T88. Testing is accomplished by shaking air-dried material through a stack of sieves having decreasing opening sizes. Table 2-3 in Chapter 2 listed U.S. standard sieve sizes and their associated opening sizes. Each successive screen in the stack has a smaller opening to capture progressively smaller particles. The amount retained on each sieve is collected, dried and weighed to determine the percentage of material passing that sieve size. An example of how to determine the grain size distribution from sieve data is shown in Figure 5-2. The grain size distribution curve corresponding to the data in Figure 5-2 is presented in Figure 5-3.

Testing of the finer grained particles is accomplished by suspending the chemically dispersed particles in a water column and measuring the change in the specific gravity of the liquid as the particles fall from suspension. This part of the test is commonly referred to as a hydrometer analysis.

Obviously, obtaining a representative specimen is an important aspect of this test. When soil samples are dried or washed for testing, it may be necessary to break up the soil clods. Care should be taken to avoid crushing of soft carbonate or sand particles. If the soil contains a substantial amount of fibrous organic materials, these may tend to plug the sieve openings during washing. The material settling over the sieve during washing should be constantly stirred to avoid plugging.

**Table 5-4**

**Typical particle sizes, uniformity coefficients, void ratios and unit weights (from Kulhawy and Mayne, 1990)**

Soil Type	Approximate Particle Size, mm			Uniformity Coefficient	Void Ratio		Normalized Unit Weight				
	D <sub>max</sub>	D <sub>min</sub>	D <sub>60</sub>		D <sub>60</sub> /D <sub>10</sub>	e <sub>max</sub>	e <sub>min</sub>	Dry $\gamma_{dry}/\gamma_w$		Saturated $\gamma_{sat}/\gamma_w$	
				Min				Max	Min	Max	
Uniform granular soil											
Equal spheres (theoretical)	-	-	-	1.0	0.92	0.35	-	-	-	-	-
Standard Ottawa sand	0.84	0.59	0.67	1.1	0.80	0.50	1.47	1.76	1.49	2.10	
Clean, uniform sand	-	-	-	1.2 to 2.0	1.00	0.40	1.33	1.89	1.35	2.18	
Uniform, inorganic silt	0.05	0.005	0.012	1.2 to 2.0	1.10	0.40	1.28	1.89	1.30	2.18	
Well-graded granular soil											
Silty sand	2.0	0.005	0.02	5 to 10	0.90	0.30	1.39	2.04	1.41	2.28	
Clean, fine to coarse sand	2.0	0.05	0.09	4 to 6	0.95	0.20	1.36	2.21	1.38	2.37	
Micaceous sand	-	-	-	-	1.20	0.40	1.22	1.92	1.23	2.21	
Silty sand and gravel	100	0.005	0.02	15 to 300	0.85	0.14	1.43	2.34	1.44	2.48	
Silty or sandy clay	2.0	0.001	0.003	10 to 30	1.80	0.25	0.96	2.16	1.60	2.36	
Gap-graded silty clay with gravel or larger	250	0.001	-	-	1.00	0.20	1.35	2.24	1.84	2.42	
Well-graded gravel, sand, silt, and clay	250	0.001	0.002	25 to 1,000	0.70	0.13	1.60	2.37	2.00	2.50	
Clay (30 to 50% < 2 $\mu$ size)	0.05	0.5 $\mu$	0.001	-	2.40	0.50	0.80	1.79	1.51	2.13	
Colloidal clay (over 50% < 2 $\mu$ size)	0.01	10Å	-	-	12.00	0.60	0.21	1.70	1.14	2.05	
Organic silt	-	-	-	-	3.00	0.55	0.64	1.76	1.39	2.10	
Organic clay (30 to 50% < 2 $\mu$ size)	-	-	-	-	5.40	0.70	0.48	1.60	1.30	2.00	

Note:  $\gamma_w = 62.4$  pcf (9.80 kN/m<sup>3</sup>);  $\mu = 10^{-3}$  mm; Å : Angstrom =  $10^{-7}$  mm

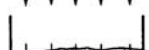
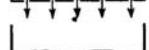
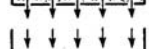
U.S. Standard sieve Nos	Total dry weight of soil sample sieved 200.0 g	Retained on sieve		Cumulative retained		Cumulative passing	
		g	%	g	%	g	%
1	2	3	4	5	6	7	8
	G						
4		0.00	0.00	0.00	0.00	200.00	100.00
10		2.84	1.42	2.84	1.42	197.16	98.58
20		5.66	2.83	8.50	4.25	191.50	95.75
40		46.04	23.02	54.54	27.27	145.46	72.72
60		44.00	22.00	98.54	49.27	101.46	50.73
100		23.64	11.82	122.18	61.09	77.82	38.91
140		11.26	5.63	133.44	66.72	66.56	33.28
200		63.16	31.58	196.60	98.30	3.40	1.70
-200 (Pan)		3.40	1.70	200.00	100.00		
		200.00g	100.00%				

Figure 5-2. Example grain size distribution based on sieve analysis (Jumikis, 1962).

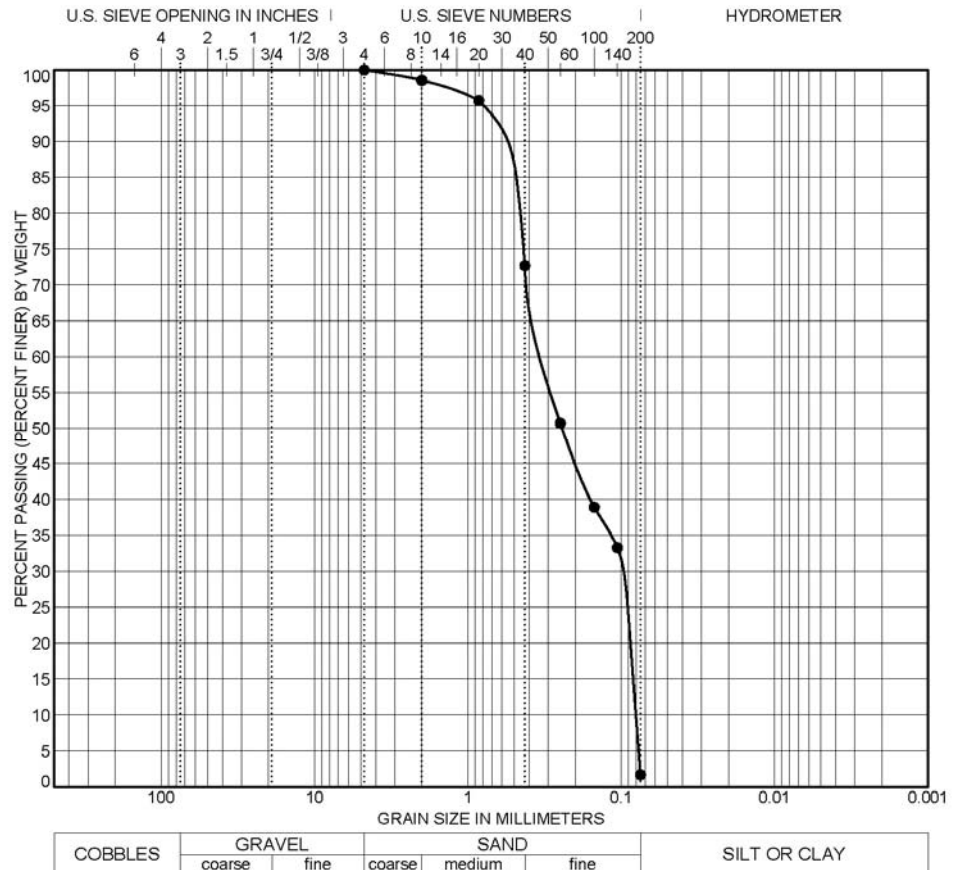


Figure 5-3. Grain size distribution curve based on data in Figure 5-2.

Particle size testing is relatively straightforward, but the results can be misleading if procedures are not performed correctly and/or if equipment is not maintained in good working condition. If the sieve screen is distorted, large particles may be able to pass through sieve openings that typically would retain the particles. Material lodged within the sieve from previous tests could become dislodged during shaking, thereby increasing the weight of material retained on the following sieve. Therefore, sieves should be cleaned thoroughly after each test. A wire brush may distort finer sieve meshes during cleaning, so a plastic brush should be used to clean the U.S. No. 40 (0.425 mm) sieve and finer. Openings of fine mesh No. 200 sieve (0.075 mm)) are easily distorted as a result of normal handling and use. Therefore, fine-mesh sieves should be replaced often. A simple way to determine whether sieves should be replaced is to examine the stretch of the sieve fabric on its frame periodically. The fabric should remain taut; if it sags, it has been distorted and should be replaced. A common cause of serious errors is the use of “dirty” sieves. Some soil particles, because of their shape, size or adhesion characteristics, have a tendency to lodge in the sieve openings. This is especially true of the fine mesh sieves.

Representative samples of fine-grained soils (i.e., samples containing more than 50% of particles with diameter less than the U.S. No. 200 sieve size (0.075 mm) ) should not be oven dried prior to testing because some particles may cement together leading to a calculated lower fines content from mechanical sieve analyses than is actually present. When fine-grained particles are a concern, the wash sieve method (ASTM D 1140) should be performed to assess the fines content.

If the clay-size content is an important parameter, hydrometer analyses should be performed even though the hydrometer test provides only approximate results due to oversimplified assumptions. However, the results can still be used as a general index of silt and clay-size content. Depending upon the chemical makeup of the fine grained particles, the traditional sodium hexametaphosphate solution used to disperse the clay-size particles may not provide adequate dispersion. If the clay-size particles are not dispersed, the hydrometer data leads to the interpretation of a lower than actual clay-size content. In some cases the concentration of the dispersing agent may need to be increased or a different dispersing agent may need to be used. If the sieve and hydrometer analyses are performed correctly, the gradation curve should be continuous over a range that includes all particle sizes.

### 5.3.4.1 Sand Equivalent

The sand equivalent test is a rapid test to show the relative proportions of fine dust or claylike materials in aggregate (or soils). A sample of aggregate passing the No. 4 sieve (4.75-mm) sieve and a small amount of flocculating solution are poured into a graduated cylinder and are agitated to loosen the claylike coatings from the sand particles. The sample is then irrigated with additional flocculation solution forcing the claylike material into suspension above the sand. After a prescribed sedimentation period, the height of flocculated clay and height of sand are determined. The sand equivalent is determined from the ratio of the height of the sand to height of the clay and expressed as a percentage. Cleaner aggregates will have higher sand equivalent values. For asphalt pavements, agencies often specify a minimum sand equivalent around 25 to 35 (Roberts, *et al.*, 1996). Higher values are used in case of compacted structural fill which may support structures (see Section 8.6).

### 5.3.5 Atterberg Limits

The Atterberg limits of a fine grained soil represent the moisture content at which the physical state of the soil changes. The tests for the Atterberg limits are referred to as index tests because they serve as an indication of several physical properties of the soil, including strength, permeability, compressibility, and shrink/swell potential. These limits also provide a relative indication of the plasticity of the soil, where plasticity refers to the ability of a silt or clay to retain water without changing state from a semi-solid to a viscous liquid. In geotechnical engineering practice, the Atterberg limits generally refer to the liquid limit (LL), plastic limit (PL), and shrinkage limit (SL). The limits were defined and discussed in Chapter 2. In this chapter the definition is extended further in terms of quantifiable parameters that permit their measurements in the laboratory. These quantifiable definitions are as follows:

- Liquid Limit (LL) - This limit represents the moisture content at which any increase in moisture content will cause a plastic soil to behave as a viscous liquid. The LL is defined as the moisture content at which a standard groove cut in a remolded sample will close over a distance of ½-inch (13 mm) at 25 blows of the liquid limit device (Figure 5-4). The test is performed on material passing a US Standard No. 40 sieve (0.425 mm). During the test the material is brought to various moisture contents, usually by adding water. The plot of moisture contents vs. blows required to close the groove is called a “flow curve” and the value of the liquid limit moisture content is obtained from the flow curve at 25 blows.



**Figure 5-4. Some of the equipment used for Atterberg limits testing of soil.**

- Plastic Limit (PL) - This limit represents the moisture content at which the transition between the plastic and semisolid state of a soil occurs. The PL is defined as the moisture content at which a thread of soil just crumbles when it is carefully rolled out by hand to a diameter of 1/8-inch (3 mm).
- Shrinkage Limit (SL) – This limit represents the moisture content corresponding to the change between the semisolid to solid state of the soil. The SL is also defined as the moisture content at which any further reduction in moisture content will not result in a decrease in the volume of the soil.

Based on the above index values, there are two useful related indices, namely, the Plasticity Index (PI) and the Liquidity Index (LI), which were defined in Chapter 2 as follows:

$$PI = LL - PL \quad 2-11$$

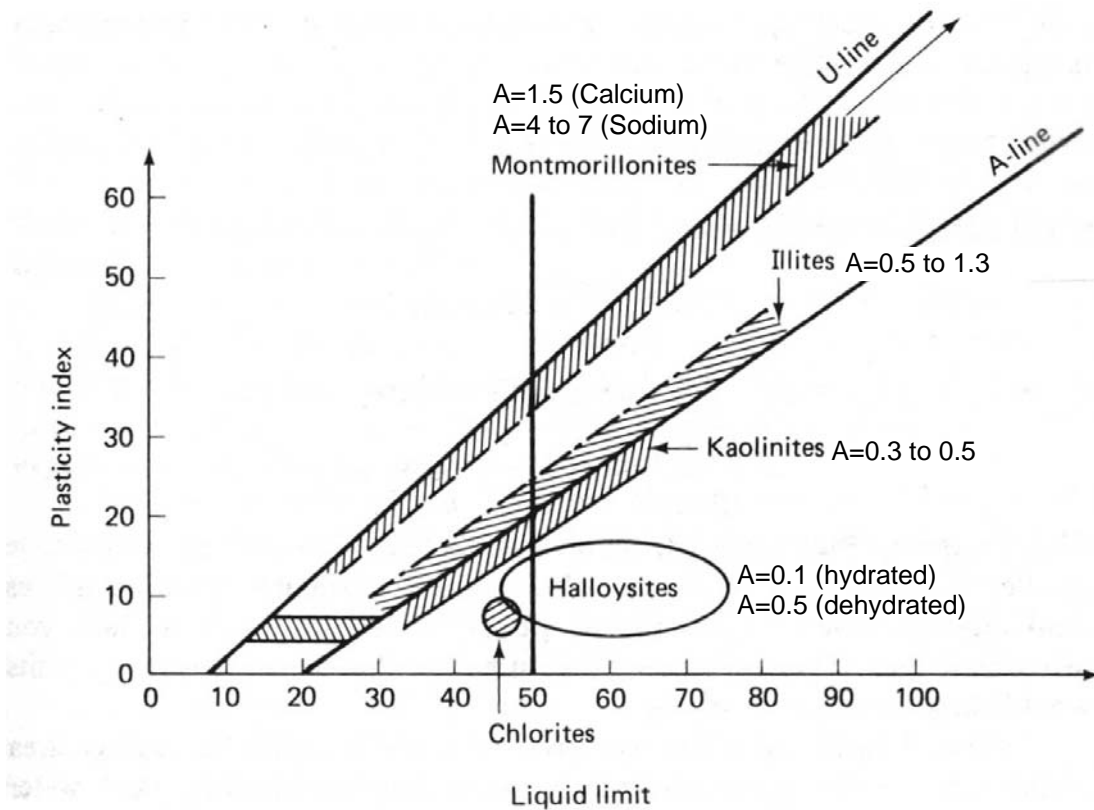
$$LI = \frac{w - PL}{PI} \quad 2-12$$

where  $w$  is the natural (in-situ) water content of the soil. Numerous engineering correlations have been developed that relate PI and LI to clay soil properties, including undrained and drained strength to PI and compression index to LI.

Another useful index proposed by Skempton (1953) based on the proportion of clay and PI is known as the “Activity Index.” The activity index of a clay soil is denoted by  $A$  and is generally defined as follows:

$$A = \frac{PI}{CF}$$

where CF is the clay fraction is usually taken as the percentage by weight of the soil with a particle size less than 0.002 mm. Clays with  $0.75 < A < 1.25$  are classified as “normal” clays while those with  $A < 0.75$  are “inactive” and  $A > 1.25$  are “active.” Values of activity index, A, can be correlated to the type of clay mineral that, in turn, provides important information relative to the expected behavior of a clay soil. A clay soil that consists predominantly of the clay mineral montmorillonite behaves very differently from a clay soil composed predominantly of kaolinite. Figure 5-5 also shows the activities of various clay minerals and their location on the Casagrande’s plasticity chart. The symbol for the activity index (A) in Figure 5-5 should not be confused with the “A-line” also shown in the figure.



Activity Index, A, of other minerals			
Attapulgite	0.5-1.2	Mica (muscovite)	0.2
Allophane	0.5-1.2	Quartz	0
Calcite	0.2		

**Figure 5-5. Location of clay minerals on the Casagrande Plasticity Chart and Activity Index values (after Skempton, 1953, Mitchell, 1976, Holtz and Kovacs, 1981).**

**Modified Activity Index,  $A_m$ :** Based on their studies regarding the swell potential of compacted natural and artificial clay soils, Seed *et al.* (1962) proposed that for natural clay soils compacted as per the requirements of ASTM D 698 and Atterberg limits determined by ASTM D 4318 (AASHTO T 89, T 90), a Modified Activity Index,  $A_m$ , defined as follows is more appropriate:

$$A_m = \frac{PI}{CF - 5} \quad 5-4$$

The above definition is used to define the swell potential of soils (see Section 5.7).

### 5.3.5.1 Significance of the “A-line” and “U-line” on Plasticity Chart

As shown in Figure 4-3 in Chapter 4, the equation for the A-line and U-line are:

$$A - \text{line} : PI = 0.73 (LL - 20) \quad 5-5$$

$$U - \text{line} : PI = 0.9(LL - 8) \quad 5-6$$

The A-line generally separates soils whose behavior is more claylike (points plotting above the A-Line) from those that exhibit a behavior more characteristic of silt (points plotting below the A-line). The A-line also separates organic (below) from inorganic (above) soils. The  $LL = 50$  line generally represents the dividing line between silt, clay and organic fractions of the soil that exhibit low plasticity ( $LL < 50$ ) and high plasticity ( $LL > 50$ ). The U-line shown in Figure 5-5 represents the upper range of PI and LL coordinates that have been found for soils. When the limits of any soil plot above the U-line, the results should be considered spurious and the tests should be rerun. Note that in Figure 5-5 the clay mineral montmorillonite plots well above the A-line and just below the U-line. If a soil plots in this range, it probably contains a significant amount of the clay mineral montmorillonite that expands in presence of water.

### 5.3.6 Specific Gravity

The specific gravity of solids ( $G_s$ ) is a measure of solid particle density and is referenced to an equivalent volume of water. Specific gravity of solids is defined as  $G_s = (M_s/V_s) / \rho_d$  where  $M_s$  is the mass of the soil solids and  $V_s$  is the volume of the soil solids and  $\rho_d$  is the mass density of water = 1,000 kg/m<sup>3</sup> or 1 Mg/m<sup>3</sup>. This formulation represents the theoretically correct definition of specific gravity and can be rewritten as  $G_s = \rho_s / \rho_d$ .

However, since  $\gamma = \rho g$  the gravitational constant appears in both the numerator and denominator of the expression and the equation for  $G_s$  can also be given as  $G_s = \gamma_s/\gamma_w$  where  $\gamma_s$  = unit weight of solid particles in the soil mass and  $\gamma_w$  = unit weight of water = 62.4 pcf (1,000 kg/m<sup>3</sup> or 1 Mg/m<sup>3</sup>).

The typical values of specific gravity of most soils lie within the narrow range of  $G_s = 2.7 \pm 0.1$ . Exceptions include soils with appreciable organics (e.g., peat), ores (e.g., mine tailings), or calcareous (high calcium carbonate content) constituents (e.g., caliche). It is common to assume a reasonable  $G_s$  value within the range listed above for preliminary calculations. Laboratory testing by AASHTO T100 or ASTM D 854 or D 5550 can be used to confirm the magnitude of  $G_s$ , particularly on projects where little previous experience exists and unusually low or high unit weights are measured.

### 5.3.7 Organic Content

A visual assessment of organic materials may be very misleading in terms of engineering analysis. Laboratory test method AASHTO T194 or ASTM D 2974 should be used to evaluate the percentage of organic material in a specimen where the presence of organic material is suspected based on field information or from previous experience at a site. The test involves weighing and heating a previously dried sample to a temperature of 824°F (440°C) and holding this temperature until no further change in weight occurs. At this temperature, the organics in the sample turn to ash and the sample is re-weighed. Therefore, with the assumption that the weight of the ash is negligible, the percentage of organic matter is the ratio of the difference in weight before and after heating the sample to 824°F (440°C) to the weight of the original dried sample. The sample used for the test can be a previously dried sample from a moisture content evaluation. Usually organic soils can be distinguished from inorganic soils by their characteristic odor and their dark gray to black color. In doubtful cases, the liquid limit should be determined for an oven-dried sample (i.e., dry preparation method) and for a sample that is not pre-dried before testing (i.e., wet preparation method). If drying decreases the value of the liquid limit by about 30 percent or more, the soil may usually be classified as organic (Terzaghi, *et al.*, 1996).

Soils with relatively high organic contents have the ability to retain water. Water retention may result in higher moisture content, higher primary and secondary compressibility, and potentially higher corrosion potential. Organic soils may or may not be relatively weak depending on the nature of the organic material. Highly organic fibrous peats can exhibit high strengths despite having a very high compressibility. In some instances such soils may even exhibit tensile strength.

### **5.3.8 Electro Chemical Classification Tests**

Electro chemical classification tests provide the geotechnical specialist with quantitative information related to the aggressiveness of the soil conditions with respect to corrosion and the potential for deterioration of typical foundation materials. Electro chemical tests include determination of pH, resistivity, sulfate ion content, sulfides, and chloride ion content. Depending on the application, limits of these electro chemical properties are established based on various factors such as corrosion rates for metals and disintegration rates for concrete. Tests to characterize the aggressiveness of a soil environment are important for design applications that include metallic elements, especially for ground anchors comprised of high strength steel and for metallic reinforcements in mechanically stabilized earth walls. ASTM and AASHTO test procedures are listed under “Corrosivity (Electrochemical)” in Table 5-1.

### **5.3.9 Laboratory Classification**

In addition to field identification (ASTM D 2488), soils should be classified in the laboratory by using the Unified Soil Classification System (USCS) in accordance with ASTM D 2487 or by the AASHTO soil classification system in accordance with AASHTO T 145. These two systems were discussed in Chapter 4. The USCS will be used throughout the remainder of this document. Classification in the laboratory occurs in a controlled environment and more time can be spent on this classification than the identification exercise performed in the field. Laboratory and/or field identification is also important so that defects and features of the soil can be recorded that would not typically be noticed from index testing or standard classification. Some of the features include degree of calcium carbonate cementation, mica content, joints, and fractures.

## 5.4 CONSOLIDATION TESTING

### 5.4.1 Process of Consolidation

As discussed in Chapter 2, consolidation is a time-dependent decrease in the volume of a soil mass under applied loading. In highway design, static loading is represented by the permanent load placed on the soil by embankments and structures. Depending on the configuration of the load and the subsurface conditions, the stress increase due to the externally applied loads may extend below the water table where all the voids are filled with water. An applied load will cause the soil grains to readjust to a more compact position to carry the load. This readjustment cannot take place until the water, which is incompressible, escapes from the voids.

As discussed in Chapter 2, the rate of the readjustment of the soil particles is a function of the void size, which controls the rate at which the water can escape from the voids. The settlement associated with the readjustment of the soil particles due to migration of water out of the voids is known as **primary consolidation**.

The amount of primary consolidation will depend on the initial void ratio of the soil. The greater the initial void ratio, the more water that can be squeezed out, and the greater the primary consolidation. The rate at which primary consolidation occurs is dependent on the rate at which the water is squeezed out of the soil voids. **Secondary compression** occurs after primary consolidation is complete. Secondary compression occurs under constant load. It is caused by the soil particles reorienting or deforming under constant load at a very slow rate. This process is known as “**creep**” and it occurs in most soils when they are subjected to long-term applied loads. Therefore, secondary compression is also a time-dependent process. However, secondary compression is not dependent on water being squeezed out of the soil as is consolidation. That is why it is called “secondary compression” and not “secondary consolidation.” Primary consolidation accounts for the major portion of settlement in saturated fine-grained soils. Primary consolidation and secondary compression both contribute significantly to settlements in organic soil.

Some natural deposits of fine-grained soils experienced compression in geologic history due to the weight of glaciers, due to the weight of overlying soil that has been eroded, or due to desiccation. Since their void ratios were substantially reduced in the past by these processes, these soils are less compressible today. Such soils are called “**preconsolidated**” or “**overconsolidated**” since they have been subjected to greater stresses in the past than exist at present. This concept is important because overconsolidated soils can be reloaded such as by the load from an embankment or bridge substructure without settling appreciably until the

currently applied load exceeds the preconsolidation load. Saturated fine-grained soil deposits, which have never consolidated under loads other than the current loads, are called “**normally consolidated.**” On the other end of the spectrum, soils whose present loading induces stresses in the soil that are greater than the maximum effective stress they have experienced in the past are called “**under consolidated.**” This means that the consolidation process under the existing loading is on-going and the soil will continue to consolidate until that process is complete, even if no additional loads are applied.

#### **5.4.2 Consolidation Testing**

To predict the amount of consolidation in saturated fine-grained and organic soils, adequate testing must be performed. An undisturbed soil sample should be obtained in the field with a Shelby tube sampler. The oedometer or one-dimensional consolidometer is the primary laboratory equipment used to evaluate consolidation and settlement potential of fine-grained soils. A consolidation test is typically performed on a specimen obtained from an undisturbed sample retrieved from the deposit of fine-grained soils to evaluate the consolidation characteristics of the soil and define the settlement-time relationship of the in-situ soils under proposed foundation loads. The equipment for a consolidation test includes:

1. A loading device that applies a vertical load to the soil specimen,
2. A metal ring (fixed or free) that laterally confines the soil specimen and restricts deformation to the vertical direction only (i.e., only one-dimensional compression is modeled),
3. Porous discs placed on the top and bottom of the sample to allow the sample to drain,
4. A dial indicator or linear variable differential transducer (LVDT) to measure vertical displacement. Properly calibrated, each device should provide the same accuracy, but the electronic output of an LVDT can be incorporated into an automated recording system for quicker, more efficient, and higher resolution readings.
5. A timer to assess the duration of loading increments. Monitoring of time for manual systems can be accommodated by use of a wall clock with a second hand. The internal clock of a computer is used for automated systems
6. A surrounding container to permit the specimen to remain submerged during the test.

Figure 5-6 shows a schematic of a consolidation test. The consolidation-loading device may be a weighted lever arm as shown in Figure 5-7b, a pneumatic device, or an automated

loading frame as shown in Figure 5-7c. Automated loading frames are recommended for use in production testing because they provide the most flexibility in testing options. The pneumatic device provides flexibility in loads and load increment ratios (LIR) that can be applied during testing. A weighted lever arm provides a robust, relatively simple system for consolidation testing, however, because data are generally recorded manually, it is difficult to expedite testing or vary the loading schedule since data reduction cannot typically be performed in real time.

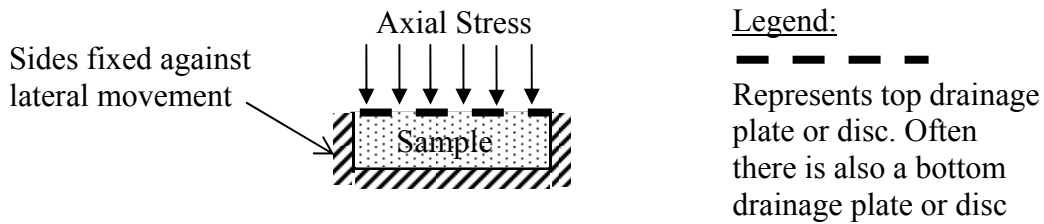


**Figure 5-6. Schematic of a consolidation test.**

Consolidation cells may be either fixed ring or floating ring. Friction and drag are created in the ring as the specimen compresses in relation to the ring. In a fixed ring test the sample compresses from the top only, potentially resulting in high incremental side shear forces. In a floating ring test the sample compresses from the top and bottom thus providing the advantage of minimizing drag forces. However, the floating ring method has the following disadvantages: it is more difficult to set up; it has the potential for sidewall leakage that would result in an inaccurate assessment of the rate of consolidation, and soil may squeeze out near the junction of the sidewall and the bottom porous disc. Because of these disadvantages, the fixed ring method is most commonly used.

### 5.4.3 Procedures

The consolidation properties of fine-grained soils are evaluated in the laboratory by using the one-dimensional consolidation test. The most common laboratory method is the incremental load (IL) method (ASTM D 2435). The weighted lever arm oedometer shown in Figure 5-7b is commonly used for performing the procedure. The automated load-frame apparatus shown in Figure 5-7c provides higher quality test results compared to the weighted lever apparatus. High-quality undisturbed samples obtained by using Shelby tubes (ASTM D 1587), piston samplers, or other special samplers are preferred for laboratory consolidation tests.



(a)



(b)



(c)

**Figure 5-7. (a) Components of consolidation test equipment, (b) Weighted lever arm - incremental load consolidation apparatus, (c) Automated load-frame and computerized consolidation apparatus (Photographs courtesy of GeoComp Corporation).**

#### 5.4.4 Presentation and Understanding the Consolidation Test Results

The consolidation test should be run in such a way that sufficient time is allowed for the applied pressure (total stress) increment to be transmitted from the pore water, where it acts initially as a excess pore water pressure, to the soil structure where it ultimately becomes an applied effective stress increment. The time it takes for this transfer to occur is the basis for the process being called “consolidation” and not “compression.” Therefore, the effective stress corresponding to the applied pressure is generally plotted versus void ratio. The resulting “**consolidation curve**” permits an evaluation of the preconsolidation pressure and values for other parameters pertaining to the consolidation characteristics of the soil sample.

Plots of void ratio versus effective pressure on arithmetic and logarithmic scales are shown in Figure 5-8. The semi log plot is more widely used in practice and will be used in subsequent sections of this manual. The consolidation curve on the void ratio versus semi log pressure plot is commonly referred to as the “**e-log p**” relationship. As discussed in detail in Chapter 7 and as shown on Figure 5-8, the slope of the loading portion of the e-log p curve is called the compression index, which is denoted by the symbol  $C_c$ . The slope of the re-load portion of the e-log p curve is called the re-compression index; it is denoted by the symbol  $C_r$ .

Some geotechnical specialists prefer to use a plot of percent strain versus log of pressure instead of the e-log p plot. In this case the slope of the virgin compression portion of the consolidation curve is called the modified compression index denoted by the symbol  $C_{ce}$  and the slope of the rebound portion of the curve is called the modified recompression index denoted by the symbol  $C_{re}$ . The modified indices reflect the relationship between strain and void ratio, i.e., strain ( $\epsilon$ ) =  $\Delta e / (1 + e_o)$ . Therefore, to convert the strain-based indices ( $C_{ce}$  and  $C_{re}$ ) to the void-ratio-based indices ( $C_c$  and  $C_r$ ) multiply the strain based values by  $(1 + e_o)$ . Void-ratio-based values (e-log p) will be used in the remainder of this manual.

Analysis of consolidation test data allows the engineer to determine:

##### 1. Initial Void Ratio ( $e_o$ )

The value of the initial void ratio is very important because it defines the amount of void space at the start of the loading. It is this initial void space that will be reduced as the water is squeezed out of the voids with time. The initial void ratio  $e_o$  is a key parameter used in settlement computations to determine the magnitude of settlement.

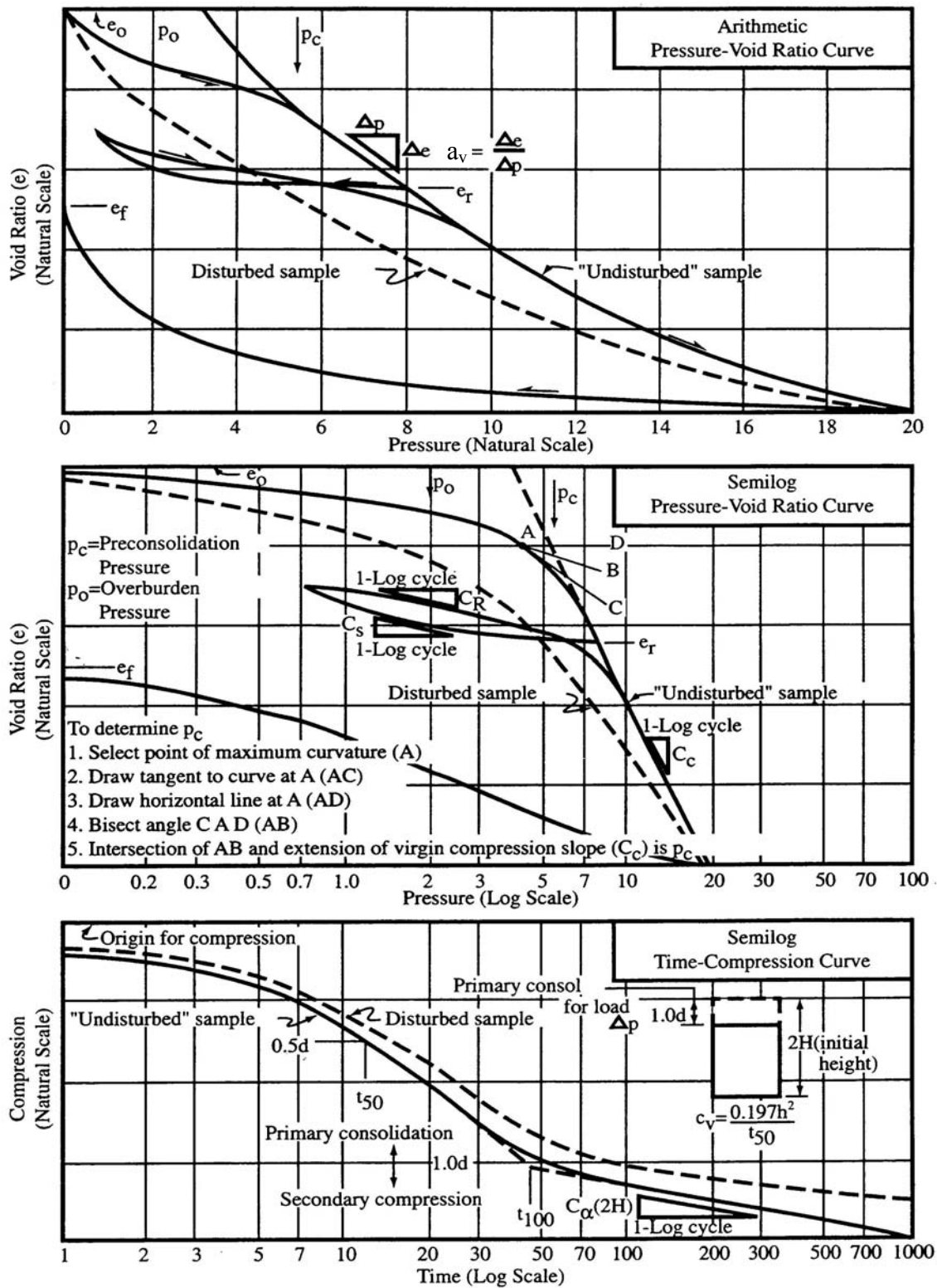


Figure 5-8. Consolidation test relationships (after NAVFAC, 1986a).

## 2. **Preconsolidation Pressure ( $p_c$ )**

The  $e$ -log  $p$  relationship generally displays a distinct break at approximately the maximum past effective stress ( $p_c$ ). The graphical technique developed by Casagrande (1936) is generally used to determine the value of  $p_c$ , which is known as preconsolidation pressure. The Casagrande procedure is included in the middle portion of Figure 5-8 and is discussed in detail in Chapter 7.

The maximum effective stress to which a soil has been loaded in the past will have a major influence on the amount of settlement to be expected under a proposed loading. In fact, 10 times more settlement may occur in a normally consolidated soil than a preconsolidated soil for equal load increments up to the preconsolidation pressure. Values of preconsolidation pressure should be carefully established for the entire depth of the fine-grained soil deposit under consideration. Normally, a minimum, maximum and most probable value of  $p_c$  will be determined from laboratory test results and plotted as a range with depth.

## 3. **Compression Index ( $C_c$ )**

The slope of the consolidation curve beyond  $p_c$  is called the compression index ( $C_c$ ). It is a measure of the load-deformation characteristic of the soil during “virgin” compression.

## 4. **Recompression Index ( $C_r$ )**

An unload/reload segment of the consolidation curve is also shown in Figure 5-8. The slope of the reload curve is called the recompression index ( $C_r$ ). It is a measure of the load-deformation characteristic of the soil upon reloading after some amount of load release. As is obvious in Figure 5-8, the slope of the reload portion of the consolidation curve is not as steep as the slope of the virgin portion of the curve since the void ratio change accompanying the virgin loading is unrecoverable. Figure 5-8 also shows that if, upon reloading, the applied pressure exceeds the pressure from which the soil was unloaded, the slope of the reload curve reverts back to the virgin compression slope,  $C_c$ . In general,  $C_c \approx 10 C_r$ .

## 5. Coefficient of Consolidation ( $c_v$ )

The coefficient of consolidation is an indicator of the rate of drainage during consolidation. The value may be determined by the  $t_{50}$  (log time) method or the  $t_{90}$  (square root of time) method. Both of these methods are described in Chapter 7 (Approach Roadway Deformations). As shown in the bottom portion of Figure 5-8, the compression-log time curve for a given load increment is used to determine the coefficient of consolidation ( $c_v$ ), which is a measure of the time rate of primary consolidation. The value of  $c_v$  is determined for each load increment. These values are sometimes plotted on a separate axis below the consolidation curve .

## 6. Secondary Compression Index ( $C_\alpha$ )

Of great importance in organic materials, secondary compression may account for the majority of settlement that takes place over a long period of time in such soils. The compression-log time curve for a given load increment is used to determine the secondary compression index ( $C_\alpha$ ), which is basically the slope of the curve over one log cycle beyond the time required for primary consolidation ( $t_{100}$ ) as shown in the bottom portion of Figure 5-8.

## 7. Effects of Sample Disturbance on Consolidation Test Results

The influence of sample disturbance on consolidation test results is shown on Figure 5-8 by the dashed lines. The dash lines indicate that disturbance:

- a. Eliminates the distinct break in the  $e$ -log  $p$  curve at the preconsolidation pressure ( $p_c$ ).
- b. Lowers the estimated value of the preconsolidation pressure ( $p_c$ ) and the measured value of the compression index ( $C_c$ ).
- c. Decreases the measured values of  $c_v$ .
- d. Increases the recompression index ( $C_r$ ).
- e. Decreases the secondary compression index ( $C_\alpha$ ).

**The general effects of disturbance are (a) under- or over-prediction of the magnitude of expected settlement and (b) over-prediction of the time for its occurrence.**

The importance of the consolidation test results as applied to design is summarized below. The test results may be applied to project design after a series of tests have been completed to represent the total depth of the fine-grained soil deposit. The two most important predictions are:

1. **The amount of settlement.** The value is determined by analyzing the consolidation curve between the existing overburden pressure and the final pressure induced by the highway load at various depths. The amount of settlement may vary dramatically depending upon the maximum past pressure to which the soil has been loaded. The total amount of long-term settlement should include an estimate of settlement due to secondary compression, especially for times past the time for 100% primary consolidation if that is less than the design life of the constructed facility.
2. **The time for settlement.** The time for primary consolidation to occur may be estimated from the results of the compression versus time plots at loads between the overburden pressure and final pressure induced by the applied load. The important factors in the settlement-time relationship are:
  - (a) Time required is proportional to the square of the longest distance required for water to drain from the deposit. This distance is the thickness of the layer if water drains in one direction only (generally vertically upward to the surface), and one-half the layer thickness if more permeable soils exist above and below the consolidating layer.
  - (b) Time required for consolidation varies inversely with the coefficient of consolidation.
  - (c) Rate of settlement decreases as time increases.

Settlement computations based on consolidation test results are demonstrated in Chapter 7 (Approach Roadway Deformations).

#### 5.4.5 Comments on the Consolidation Tests

The consolidation test results are necessary to assess the consolidation properties of the soil. As will be shown in subsequent sections of this document, the consolidation test is one of the most important tests for fine-grained soil as it provides data regarding stress history and compressibility. It is important to consider all laboratory testing variables and their potential effects on the values of soil properties computed from the test results. Information that will need to be provided to a laboratory for a consolidation test includes the loading schedule (i.e., magnitude and duration of loads). It is important to evaluate the loading schedule to be used, especially the duration of loading since time is required for the applied total stress increment to be transferred from the pore water to the soil structure so that it becomes an effective stress acting on the soil mass. Important issues related to consolidation tests are discussed below.

- **Loading Sequence:** The loading sequence selected for a consolidation test will depend on the type of soil being tested and the particular application being considered for the project (e.g., embankment, shallow foundation). The selection of a loading sequence should never be left to the discretion of the laboratory. As an example, if the clay soil is heavily overconsolidated, it is possible that a laboratory-determined maximum load for the consolidation test will not be sufficient to exceed  $p_c$ .
- **Range of Applied Loads:** The range of applied loads for the test should well exceed the effective stresses that are required for settlement analyses. This range should cover the smallest and largest effective stresses anticipated in the field and will depend on depth, foundation loads, and excavations. The anticipated preconsolidation stress should be exceeded by at least a factor of four during the laboratory test. If the preconsolidation stress is not significantly exceeded during the loading schedule,  $p_c$ , and  $C_c$  (or  $C_{ce}$ ) may be underestimated due to specimen disturbance effects.
- **Load Increment Ratio (LIR):** By definition the  $LIR = \Delta\sigma / \sigma_{initial}$  where  $\Delta\sigma$  is the incremental stress and  $\sigma_{initial}$  is the previous stress. A  $LIR=1$  corresponds to a doubling of the vertical stress applied to the specimen at each successive load increment during a consolidation test. A LIR of 1 is commonly used for most tests. Experience with soft sensitive soils suggests that as the stress approaches the value of  $p_c$ , a smaller LIR will facilitate a better estimate of  $p_c$ . Typically, laboratories provide a unit cost for a consolidation test that may be based on 6 to 8 load increments with a separate cost for each additional increment.

- **Unload-Reload Cycle:** It is recommended that an unload-reload cycle be performed, especially for cases where accurate settlement predictions are required, specifically to obtain a value for  $C_r$ . Since most samples will inevitably be somewhat disturbed, a  $C_r$  value based on the initial loading of a consolidation test sample will be greater than that for an undisturbed sample, resulting in an overestimation of settlements in the overconsolidated region. A value of  $C_r$  based on an unload-reload cycle is more likely to be representative of the actual behavior of the soil in the overconsolidated region.
- **Duration of Load Increment:** The duration of each load increment should be selected to ensure that the sample is approximately 100 percent consolidated prior to application of the next load increment. For relatively low to moderate plasticity silts and clays, durations of 3 to 12 hours will be appropriate for loads in the normally consolidated range. For fibrous organic materials, primary consolidation may be completed in 15 minutes for each load increment. For high plasticity materials, the duration for each load increment may need to be 24 hours or more to ensure complete primary consolidation and to evaluate secondary compression behavior. Conversely, primary consolidation may occur in less than 3 hours for loads less than  $p_c$ .

If the time period is too short for a given load increment (i.e., the sample is not allowed to achieve approximately 100 percent consolidation before the next load increment is applied), then values of  $C_c$  may be underestimated and values of  $c_v$  may be overestimated. The duration of time required, however, can be optimized by using pneumatic, hydraulic, or electro-mechanical loading systems that include automated loading and data acquisition systems. Continuous deformation versus time measurements and the square root of time method described in Chapter 7 (Approach Embankment Deformations) can be used to estimate the beginning and end of primary consolidation during the test. Once the end of primary consolidation is detected, the system can automatically apply the next load increment. Alternatively, some laboratories can provide real-time deformation versus log time plots to enable the engineer to evaluate whether 100 percent primary consolidation has been achieved.

- **Secondary Compression:** In cases where secondary compression is important (e.g., organic soils), secondary compression should be assessed on the basis of the deformation versus log-time response. The consolidation test for each load increment should be run long enough to establish a linear trend between vertical displacement and log time.

## 5.4.6 Useful Correlations between Consolidation Parameters and Index Values

This section presents some useful correlations between consolidation parameters and other index values. These correlations can be used by the designer to check the validity of the laboratory tests results or to develop a prediction of the range of values of consolidation parameters that can be expected from yet-to-be performed consolidation tests. **It must be emphasized that predictions based on correlations should never be substituted for proper testing and that any assumptions regarding consolidation parameters should always be verified through testing.**

### 5.4.6.1 Compression Index, $C_c$

Over 70 different equations have been published for correlating  $C_c$  with the index properties of clays. Table 5-5 lists some of the more useful correlations. Figure 5-9 shows correlations between natural water content and  $C_c$  for fine-grained soils, peats and shales **Note that the coordinates in Figure 5-9 are both logarithmic so that values of  $C_c$  can vary by as much as a factor of 5 with respect to the average trend line in these empirical correlations. Values of  $C_c$  obtained from Table 5-5 or Figure 5-9 should not be used for final design.**

**Table 5-5  
Correlations for  $C_c$  (modified after Holtz and Kovacs, 1981)**

Correlation	Soil
$C_c = 0.156 e_o + 0.0107^{(1)}$ $C_c \approx 0.5 G_s (PI/100)^{(2)}$	All Clays
$C_c = 0.30 (e_o - 0.27)$	Inorganic, silt, silty clay
$C_c = 0.009 (LL - 10)^{(3)}$	Clay of medium to slight sensitivity ( $S_t < 4, LL < 100$ ) <sup>(4)</sup>
$C_c = 0.0115 w_n^{(5)}$	Organic Soils, Peat
$C_c = 0.75 (e_o - 0.50)$	Low plasticity clays
<sup>(1)</sup> $e_o$ = initial void ratio, <sup>(2)</sup> PI = Plasticity Index, <sup>(3)</sup> LL=Liquid Limit, <sup>(4)</sup> $S_t$ = sensitivity = Undisturbed undrained shear strength/Remolded undrained shear strength (see Table 3-12 in Chapter 3, <sup>(5)</sup> $w_n$ = natural water content	

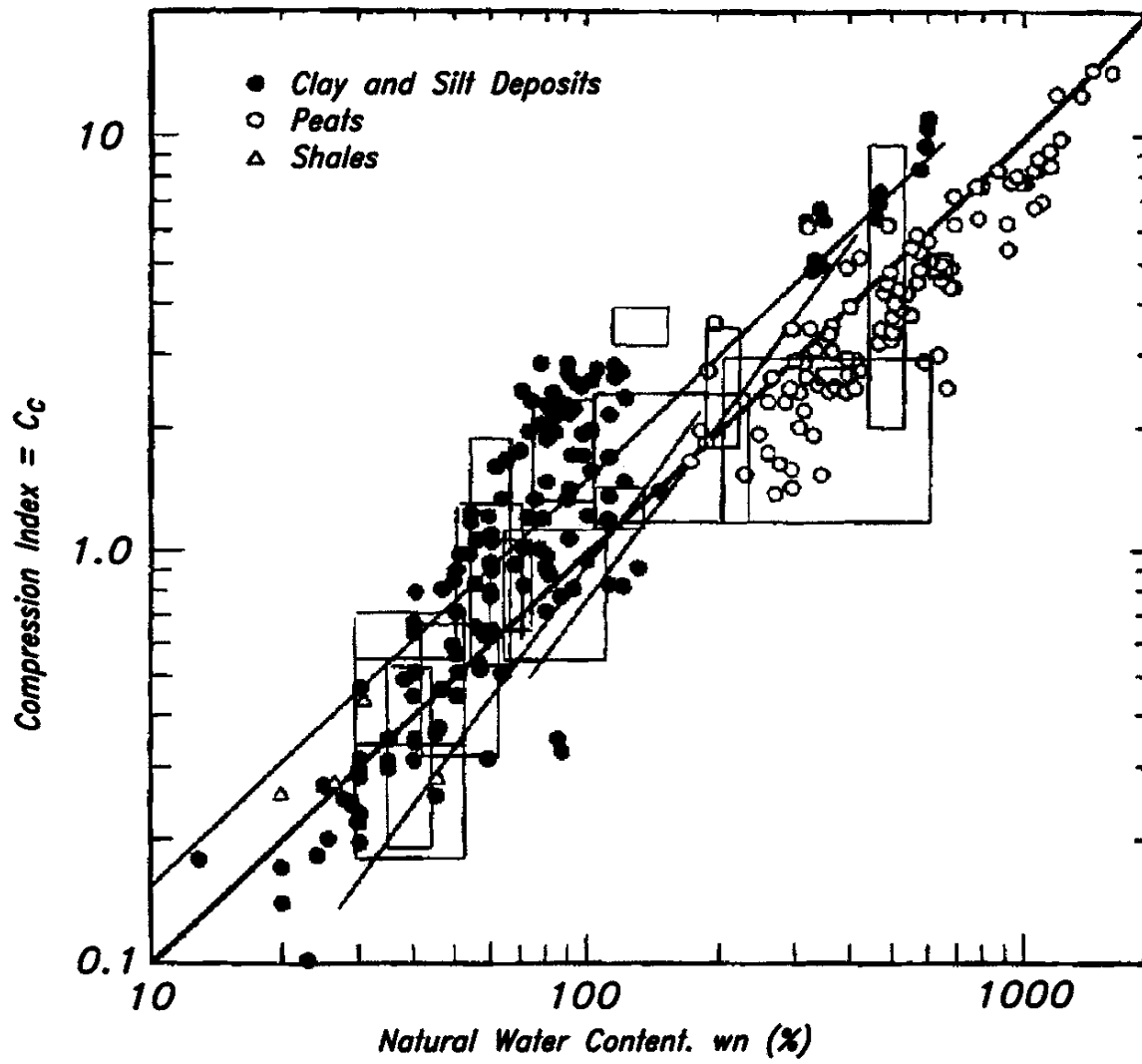


Figure 5-9. Empirical correlation between compression index and natural (in-situ) water content (from Terzaghi, *et al.*, 1996).

#### 5.4.6.2 Recompression Index, $C_r$

The ratio of  $C_r / C_c$  typically ranges from 0.02 to 0.20 (Terzaghi, and Peck, 1967). The low value is typical of highly structured and bonded soft clay or silt, while the largest ratio corresponds to micaceous silts and fissured stiff clays and shales. In reality, the value of  $C_r$  depends on whether loading or unloading is occurring, since some hysteresis effects develop when the soil is subjected to cycles of loading and unloading.

Generally, it is sufficiently accurate to assume  $C_r$  is constant for most clay deposits. It may not be adequate to rely on a single value of  $C_r$  for loading and unloading in the case of highly structured soft clays or stiff clay shales. In the case of highly structured soft clays the initial value of  $C_r$  is steep as a result of flocculation (edge to face structure of clays) and bonding that allows the soil to be stable at high void ratios until the stress exceeds the preconsolidation pressure (Terzaghi and Peck, 1967). The subsequent rebound slope can be significantly different from the initial  $C_r$ .

#### 5.4.6.3 Coefficient of Vertical Consolidation, $c_v$

Because of the wide range of permeabilities that exist in soils (see Table 5-10), the coefficient of consolidation can itself vary widely, from less than 10 ft<sup>2</sup>/yr ( $\approx 1$  m<sup>2</sup>/yr) for clays of low permeability to 10,000 ft<sup>2</sup>/yr ( $\approx 1,000$  m<sup>2</sup>/yr) or more for very sandy clays, fissured clays and weathered rocks. Some typical values for clays are given in Table 5-6 and an approximate correlation with liquid limit is shown in Figure 5-10.

Just as permeabilities in the horizontal and vertical directions can be significantly different due to variations in soil particle orientation, non-homogeneity, etc., so too can the in situ coefficient of horizontal consolidation,  $c_h$ , be much different from the coefficient of vertical consolidation  $c_v$  measured in the laboratory for the same reasons. For example, the in situ coefficient of horizontal consolidation,  $c_h$ , for clays containing fissures or fine bands of sand, may often be much greater than  $c_v$  measured in the laboratory for the clay alone. In such cases, the in-situ  $c_h$  may govern the actual rate of consolidation under field loading conditions.

**Table 5-6**  
**Typical values of coefficient of vertical consolidation,  $c_v$**   
**(after Carter and Bentley, 1991)**

Soil	$c_v$		
	( $\text{cm}^2/\text{s} \times 10^{-4}$ )	( $\text{m}^2/\text{yr}$ )	( $\text{ft}^2/\text{yr}$ )
Boston Blue Clay (CL)	40±20	12±6	135±70
Organic silt (OH)	2-10	0.6-3	7-34
Glacial lake clays (CL)	6.5-8.7	2.0-2.7	22-30
Chicago silty clay (CL)	8.5	2.7	29
Swedish medium sensitive clays (CL-CH)			
1. laboratory	0.5-0.7	0.1-0.2	1.7-2.4
2. field	0.7-3.0	0.2-1.0	2.4-10.2
San Francisco Bay Mud (CL)	2-4	0.6-1.2	6.8-13.6
Mexico City clay (MH)	0.9-1.5	0.3-0.5	3.1-5.1

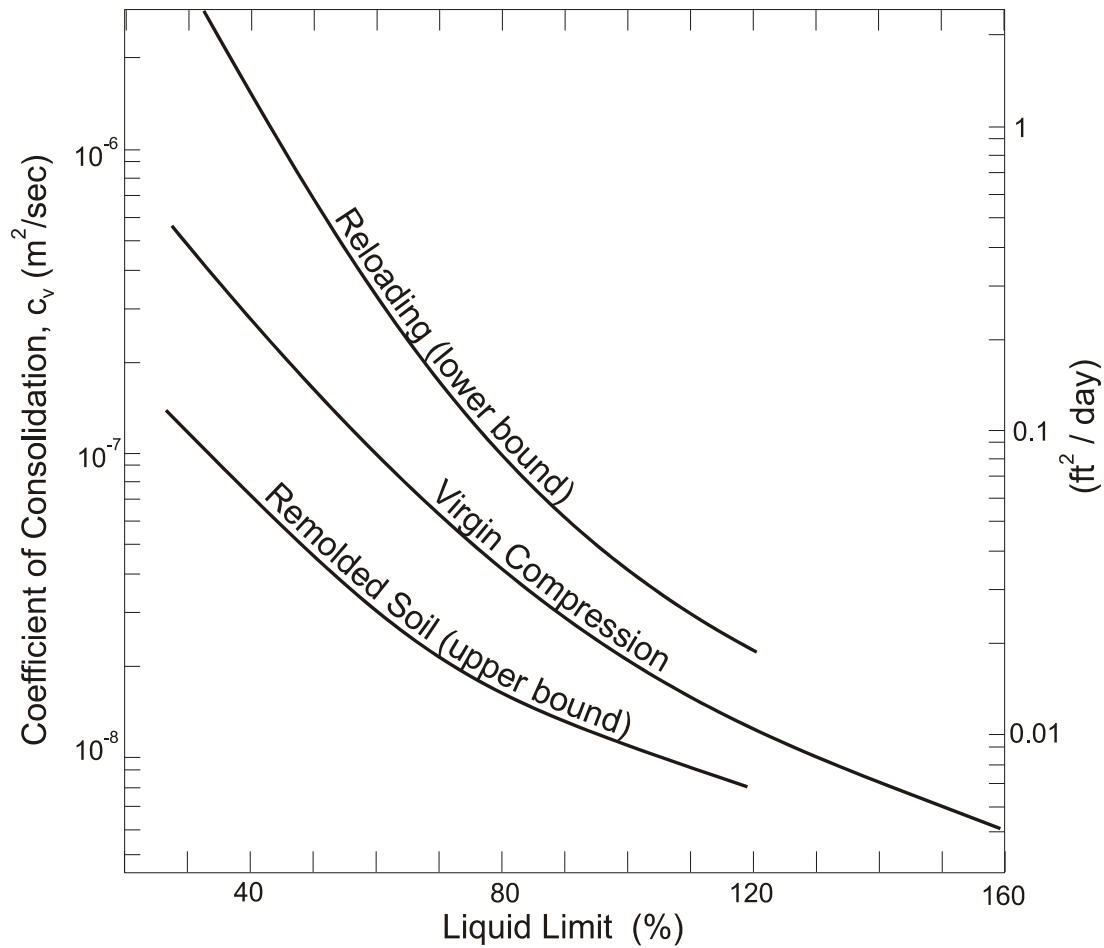


**Figure 5-10. Approximate correlations between  $c_v$  and LL (NAVFAC, 1986a).**

#### 5.4.6.4 Coefficient of Secondary Compression, $C_\alpha$

Table 5-7 presents typical values of  $C_\alpha$  in terms of  $C_c$  for various geomaterials. As shown below by Equations 5-7, the coefficient,  $C_\alpha$ , may be expressed either in units of strain ( $C_{\alpha\varepsilon}$ ) or void ratio ( $C_{\alpha e}$ ) per log cycle of time. As indicated previously, to convert void-ratio-based consolidation curve indices to strain-based indices divide the void-ratio-based values by  $(1 + e_0)$ .

$$C_{\alpha\varepsilon} = \frac{d\varepsilon}{d(\log t)}; \quad C_{\alpha e} = \frac{de}{d(\log t)}; \quad C_{\alpha\varepsilon} = \frac{C_{\alpha e}}{(1 + e_0)} \quad 5-7$$

$C_{\alpha e}$  is usually assumed to be related to  $C_c$  with values of  $C_{\alpha e}/C_c$  typically in the range 0.025-0.006 for inorganic soils and 0.035-0.085 for organic soils. Figure 5-11 presents a correlation between  $C_{\alpha e}$  and natural water content.

**Table 5-7**  
**Typical Values of  $C_{\alpha e}/C_c$  (Terzaghi, et al., 1996)**

Soil	$C_\alpha/C_c$
Granular soils including rockfill	$0.02 \pm 0.01$
Shale and mudstone	$0.03 \pm 0.01$
Inorganic clays and silts	$0.04 \pm 0.01$
Organic clays and silts	$0.05 \pm 0.01$
Peat and muskeg	$0.06 \pm 0.01$

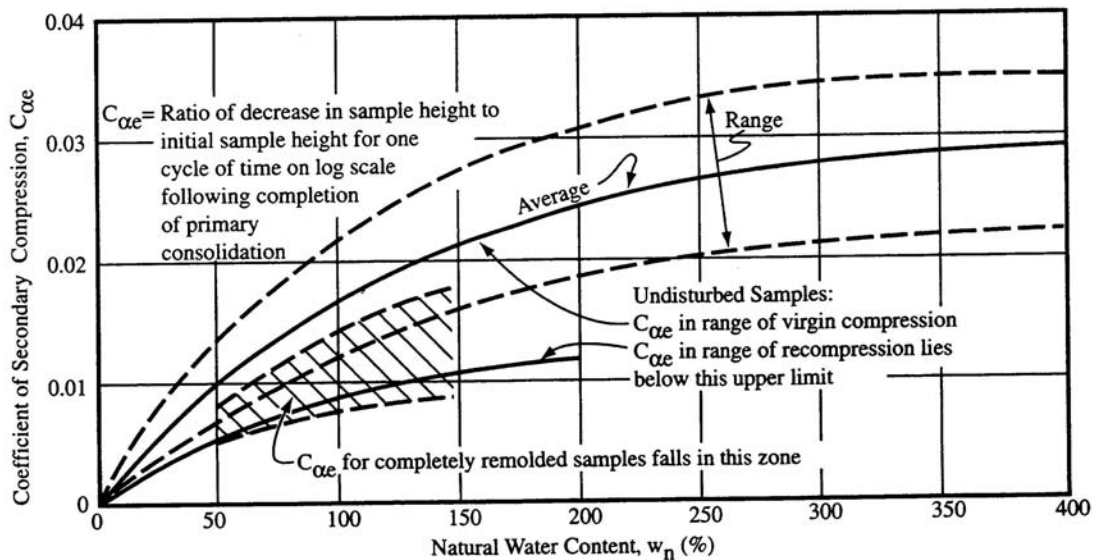


**Figure 5-11. Correlation between  $C_{\alpha e}$  and natural water content (NAVFAC, 1986a).**

## 5.5 SHEAR STRENGTH OF SOILS

The shear strength of soils is extremely important to foundation design. In addition, slopes of all kinds, including hills, river banks, and man-made cuts and fills, stay in place only because of the shear strength of the material of which they are composed. Knowledge of the shear strength of soil is important for the design of structural foundations, embankments, retaining walls, pavements, and cuts. Table 5-8 provides a summary of specific issues related to the design and construction of typical highway design elements that should be considered in developing and implementing a laboratory and in-situ testing program for evaluating soil shear strength.

### 5.5.1 Concept of Frictional and Cohesive Strengths

The concept of shear strength was introduced in Chapter 2 where it was shown to be comprised of two components, **friction** ( $\phi$ ) and **cohesion** ( $c$ ). In terms of the classification of soils introduced in Chapter 3, these two components of the shear strength can be generalized as follows:

1. Coarse-grained soils, such as gravel and sand, and fine-grained silt, derive strength primarily from friction between particles. Therefore they are considered to be “**cohesionless**” or “**frictional**” soils and are often denoted as “ $\phi$ -soils.”
2. Fine-grained soils, composed mainly of clay, derive strength primarily from the electro-chemical attraction, or bond, between particles. Therefore they are considered to be “**cohesive**” soils and are often denoted as “c-soils.”
3. Mixtures of cohesionless and cohesive soils derive strength from both interparticle friction and bonding. Such soils are commonly denoted as “**c- $\phi$  soils**.”

#### 5.5.1.1 Strength Due to Friction

The strength due to friction between soil particles is dependent on the stress state of the soil (e.g., overburden pressure) and the angle of internal friction ( $\phi$ ) between the particles. As discussed in Chapter 2, the frictional resistance of soil is equal to the normal stress,  $\sigma_n$ , times the tangent of friction angle,  $\phi$ . The tangent of  $\phi$  is equal to the coefficient of friction ( $\mu$ ) between the soil particles.

**Table 5-8**  
**Summary of issues relevant to shear strength evaluation in support of the design of**  
**typical geotechnical features (after FHWA, 2002a)**

Design Element	Issues Relevant to Shear Strength Evaluation
Shallow Foundation	<ul style="list-style-type: none"> <li>• Soil shear strength information required for depths up to 2 times the width of the footing, unless weak zones are found below this depth. The depth of bottom of footing will be based, in part, on requirements with respect to frost penetration depths and scour depths.</li> </ul>
Drilled Shaft	<ul style="list-style-type: none"> <li>• The excavation of a hole to construct a drilled shaft results in stress relief and disturbance in the soil that ultimately results in a reduction in shear strength from that corresponding to in-situ (i.e., before construction) conditions. The magnitude of the stress relief and disturbance will depend upon the method of construction, soil type, saturation condition, and type of strength (e.g., side shear or end bearing).</li> </ul>
Driven Pile	<ul style="list-style-type: none"> <li>• The shear strength of the soil may vary significantly between the time when the pile (or pile group) is first driven and tested to the time when the superstructure loads are applied to the pile (or pile group). The time-dependent phenomena of strength increase is referred to as “<b>pile set-up</b>” and is often observed for driven piles in saturated normally consolidated (NC) to moderately over consolidated (OC) clay and fine-grained material. A decrease in strength with time is referred to as “<b>relaxation</b>” and is often observed for heavily OC clays, dense silts, dense fine sands, and weak laminated rock. Shear strengths should therefore be evaluated for both long and short term conditions.</li> <li>• Changes in site conditions that affect the in-situ the effective stress state may increase or decrease shear strength and pile capacity. These may include site dewatering or additional surface loading from an embankment.</li> <li>• An increase in granular soil strength may occur due to densification during driving. This increased strength will need to be considered such that an appropriate pile driving system can be selected for construction.</li> </ul>
Retaining Walls	<ul style="list-style-type: none"> <li>• The analysis of non-gravity cantilevered and anchored walls requires an evaluation of earth pressures on the active side and passive side of the excavation. For undrained loadings in some clayey soils, particularly low to medium plasticity materials, there can be a large difference in undrained strength between the strength used for the active side and the passive side of the excavation.</li> <li>• For soils that may exhibit peak, fully softened, and residual conditions, an estimate of the tolerable deflection of the wall system needs to be made and this deflection used to select the appropriate strength condition for analysis.</li> </ul>
Slopes	<ul style="list-style-type: none"> <li>• The shear strength of discontinuities (e.g., fissures) in soil (and rock) needs to be evaluated since it may represent the critical (i.e., lowest) shear strength for design.</li> <li>• Weathering and other physiochemical reactions may occur at a quick enough rate to weaken soil bonds and reduce shear strength.</li> <li>• Strength loss may occur in cut slopes due to soil softening (in presence of water) and continuing deformations. Large deformation residual strengths should be used for long-term analyses.</li> </ul>

The equation for frictional resistance,  $\tau$ , is written in terms of normal stress,  $\sigma_n$ , as follows:

$$\tau = \sigma_n \tan \phi \quad 5-8$$

The coefficient of friction,  $\tan \phi$ , between individual particles depends on both their mineral hardness and surface roughness. However, the measured friction angle of a soil sample or deposit also depends on the density of the mass caused by interlocking of particles. For a detailed discussion of factors affecting frictional resistance, the reader is referred to textbooks such as by Holtz and Kovacs (1981).

### 5.5.1.2 Strength Due to Cohesion

The concept of cohesive strength is more difficult to explain and often misunderstood. The designer must develop a good understanding of this concept otherwise there will be a disconnect between reality and the design of some structures, e.g., the first bench cut in shoring.

There are two types of cohesion in soils: **true cohesion** and **apparent cohesion**. These are briefly discussed as follows (after Mitchell, 1976):

1. **True cohesion** may result from chemical cementation (just like in rocks) and/or forces of attraction (e.g., electrostatic and electromagnetic attractions) between colloidal ( $10^{-3}$  mm to  $10^{-6}$  mm) clay particles. True cohesion is stress-independent unlike frictional resistance that is a function of normal stress.
2. **Apparent cohesion** may develop because of capillary stresses and mechanical interlocking as follows:
  - **Capillary stresses** develop between particles in a partially saturated soil due to surface tension in the water. The surface tension (negative pressure) in the water produces an equal and opposite effective stress between the soil particles, which results in an apparent cohesion since it too is stress-independent. The magnitude of this type of apparent cohesion can be extremely large, especially in fine-grained soils. Such capillary stresses can be overcome by an increase in the degree of saturation.

- **Apparent mechanical forces** are often exhibited by the interlocking of rough (angular) soil particles. The interlock between the soil particles can offer some resistance to shear stresses even in the absence of a normal stress. This type of apparent cohesion is often the cause of cohesion measured in compacted soils. However, such apparent mechanical forces are susceptible to significant reduction by vibrations and other types of mechanical disturbance.

Figure 5-12 presents a graphical representation of the potential contribution of various mechanisms of cohesion. It can be seen that true cohesion in soils exists only when the particle size is colloidal. Unless the complete soil sample is composed of colloidal particles, true cohesion due to interparticle attraction cannot be relied on. Cementation by deposition is often observed in arid environments (e.g., desert southwest), but it is difficult to quantify. As indicated above, capillary stresses can provide a large apparent cohesion, but such cohesion can be overcome by saturation. Since cohesion cannot be defined with confidence, its contribution to long-term shear strength in  $c-\phi$  soils is often disregarded or greatly minimized by using only a small value such as 100 to 500 psf (5 to 25 kPa). For purely cohesive soils, the designer should be careful in evaluating the cohesion for long-term design purposes. Further discussion on apparent cohesion in the context of compacted soils is included in Section 5.8.4.1.

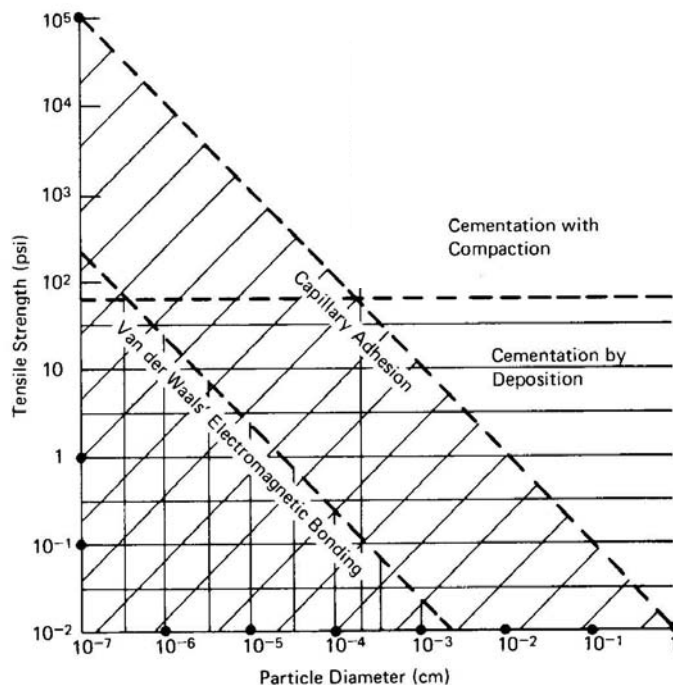


**Figure 5-12. Potential contributions of various bonding mechanisms to cohesive strength (after Ingles, 1962).**

### 5.5.1.3 Simplified Expression for Shear Strength of Soils

As indicated in Chapter 2, the shear strength,  $\tau$ , of soils is expressed simplistically by two additive components as follows:

$$\tau = c + \sigma_n \tan \phi \quad 5-9$$

In terms of effective stresses, the effective shear strength,  $\tau'$ , can be re-written as follows:

$$\tau' = c' + (\sigma_n - u) \tan \phi' = c' + \sigma' \tan \phi' \quad 5-10$$

where  $u$  is the pore water pressure,  $c'$  is the effective cohesion,  $\sigma'$  is the effective normal stress, and  $\phi'$  is the effective friction angle.

The shear strength soil is influenced by many factors including the effective stress state, mineralogy, packing arrangement of the soil particles, soil hydraulic conductivity, rate of loading, stress history, sensitivity, and other variables. As a result, **the shear strength of soil is not a unique property**. The following sections present and discuss various laboratory tests to determine the shear strength for various types of construction and loading conditions. Typical laboratory strength tests are introduced including the unconfined compression test (AASHTO T208; ASTM D 2166), the triaxial test (AASHTO T234; ASTM D 4767), and the direct shear test (AASHTO T236; ASTM D 3080). A detailed discussion on testing equipment and procedures is beyond the scope of this document. The interested reader should review the AASHTO and ASTM standards for detailed information on testing equipment and procedures. The following sections also describe information that must be conveyed to a laboratory testing firm to ensure that the strength testing is performed consistent with the requirements imposed by the design (e.g., selection of confining pressures consistent with the imposed loads).

## 5.5.2 Strength Testing of Soils in the Laboratory

The shear strength of a soil is the maximum shear stress that the soil structure can resist before failure. Failure is generally defined as continuing displacement without an increase in applied stress. Since the water filling the pores has no shear strength, shear stresses are carried by the structure of soil grains. However, the shear strength of the soil structure is indirectly dependent on the pressure in the pore water, which influences the friction term as shown by the excess pore water pressure term,  $u$ , in Equation 5-10. Foundation designers must consider the effects of expected construction operations on the subsoils when planning

a test program. For example, when a highway embankment or structural footing is suddenly placed on a soft clay deposit, the pore water initially carries all the load and the available shear strength does not increase until drainage begins and the excess pore water pressure decreases. In planning a test program for such a situation the designer should request unconsolidated undrained (UU) triaxial tests to determine the undrained shear strength of the soil which, in this case, would be the critical strength value, i.e., the initial shear strength before consolidation begins. Additional consolidated undrained (CU) or consolidated drained (CD) tests would also be used to determine the increase in shear strength as consolidation occurs and excess pore water pressures dissipate. These results can be used to determine alternate methods of applying the loads safely, especially if the undrained strength is insufficient to sustain the proposed loading. Stage construction involves placement of an increment of load and a waiting period to allow strength gain through excess pore water pressure dissipation so the soil deposit can safely support the next load increment.

The majority of strength tests are conducted on cohesive soils since obtaining undisturbed samples of non-cohesive soils is difficult. Strength tests on cohesive soils are usually conducted on high quality undisturbed samples obtained from thin wall sampling tubes. The preferred test for most projects where cohesive soils are involved is the triaxial compression test. The number and types of tests must be selected by the designer to suit the project conditions. For each test the designer should clearly indicate the consolidation or confining pressure to be used. These pressures are determined from the  $p_o$  diagram for each specific project (refer to Chapter 2 for discussion of the  $p_o$  diagram). The range usually extends from the effective overburden pressure to the pressure induced by the highway loading. The program objective should be to establish a profile of soil strength with depth. Soil strength parameters are frequently expressed as a ratio of shear strength over the effective overburden pressure ( $\tau/p_o$ ).

The most common laboratory soil strength tests are:

- Unconfined compression test
- Triaxial compression test, and
- Direct shear test

Each of these tests is briefly discussed below. For the triaxial compression and the direct shear tests, it is important that each test be performed on a new sample. **The practice of performing multi-stage shear strength tests on a single sample is not recommended.**

### 5.5.2.1 Unconfined Compression (UC) Tests

The unconfined compression test is a quick, relatively inexpensive means to obtain an estimation of the undrained shear strength of cohesive specimens. In this test a cylindrical specimen of the soil is loaded axially as shown in Figure 5-13 without any lateral confinement to the specimen, at a sufficiently high rate to prevent drainage. Since there is no confinement, residual negative pore pressures that may exist in the sample following sample preparation generally control the state of effective stress in the sample. The shear stresses induced in the specimen by the axial load result in a shear failure. The magnitude of the shear stress at the moment of failure represents the shear strength of the soil under these conditions of loading and drainage. Therefore, the shear strength obtained from this test is called the “undrained shear strength ( $s_u$ ).” In most cases, the value of undrained shear strength obtained from an unconfined compression test is conservative. The maximum axial compressive stress measured at failure represents the compressive strength of the soil under these conditions of loading, drainage, and confinement. Therefore, the compressive strength obtained from this test is called the “unconfined compressive strength ( $q_u$ ).” These two strengths terms should not be confused; one is a shear strength the other a compressive strength. It can be shown graphically by a Mohr’s circle construction (Appendix B) that the undrained shear strength ( $s_u$ ) is equal to one-half the unconfined compressive strength ( $q_u$ ).

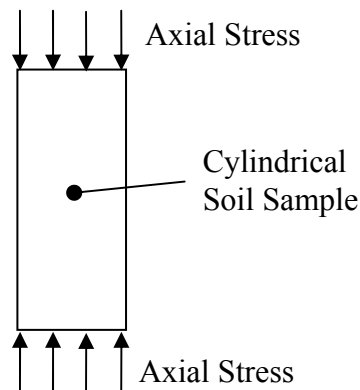


**Figure 5-13. Schematic of an unconfined compression test.**

The unconfined compression test cannot be performed on granular soils, dry or crumbly soils, silts, peat, or fissured or varved materials. Because there is no control over the effective stress state of the specimen, this test is not recommended for evaluating strength properties for compressible clay soils subjected to embankment or structural foundation loads. The reliability of this test decreases with increasing sampling depth because the sample tends to swell after removal from the ground due to confining stress release. The

swelling results in greater particle separation and reduced shear strength. Testing the full diameter extruded specimen as soon as possible after removal from the tube can:

- minimize swelling
- reduce disturbance
- preserve the natural moisture content.

Unfortunately, despite these shortcomings, this test is commonly used in practice because of its simplicity and low cost.

### 5.5.2.2 Triaxial Tests

The triaxial test is very versatile in the sense that the shear strength can be evaluated under compression as well as extension loading conditions. A schematic of triaxial compression test is shown in Figure 5-14 where the axial stress is greater than the confining stress. Lateral pressures at various depths below the ground surface can be simulated by confining pressures. Note that the confining pressures acts on the entire sample and is equal to the axial stress before the application of an axial stress increment. Typically, failure of the sample is caused by increasing the axial stress (compression) until a shear failure takes place. In an extension test, the confining pressures are increased while keeping the axial stress constant. Pore water pressures during the test can be measured.

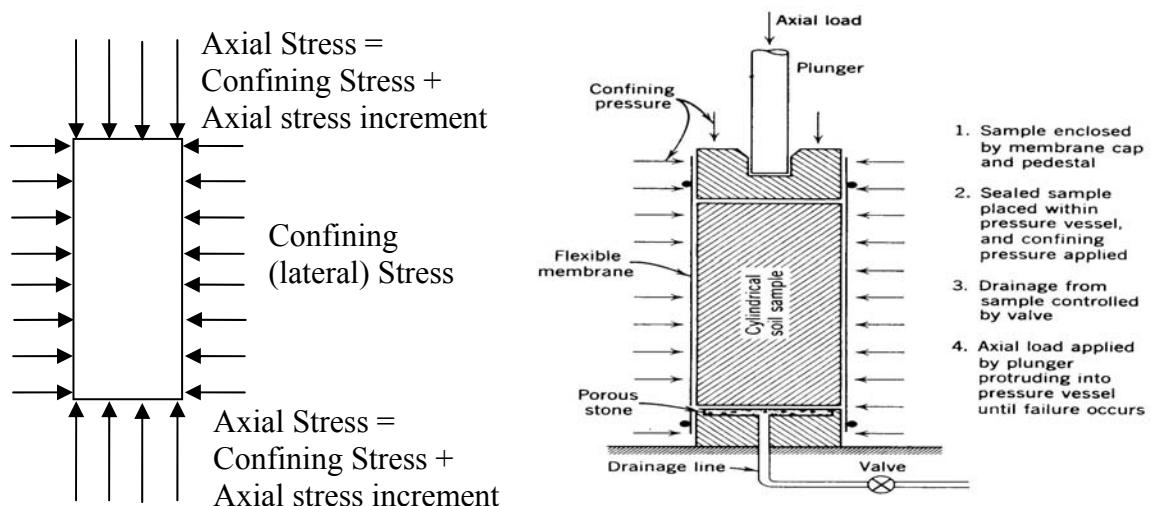


**Figure 5-14. Schematic of a triaxial compression test (Lambe and Whitman, 1979).**



(a)



(b)

**Figure 5-15. (a) Failure of a loose sand specimen in a triaxial cell; and (b) Load frame, pressure panel, and computerized data acquisition system (Photographs courtesy of GeoComp Corporation).**

Equipment – Triaxial systems today use electronic instrumentation to provide continuous monitoring and periodic acquisition of test data (see Figure 5-15b). Force is measured by using a force transducer or load cell that is typically mounted outside the triaxial cell. More advanced systems have the transducer incorporated within the testing cell to reduce the effects of rod-friction. Linear variable differential transducers (LVDTs) are used to monitor deformations. Additionally, volume measurements can be taken with a device that makes use of an LVDT to measure the rise or fall of a bellofram cylinder. This change in movement is calibrated to the volume of water taken in or pushed out of the sample. Pressure transducers are mounted on the base of the test cell to monitor the confining pressure within the cell and the pore water pressure within the sample.

### ***Unconsolidated-Undrained (UU) Test***

In the UU test, no drainage or consolidation is allowed during either the application of the confining pressure or the application of the axial load that induces shear stress. The shear stresses induced in the specimen by the axial load result in failure. As indicated in Section 5.5.2, the UU test models the response of a soil that has been subjected to a rapid application of an axial load such as that due to construction of an embankment. It is difficult to obtain repeatable results for UU testing due to the effects of sample disturbance. The accuracy of the UU test is dependent on the soil sample retaining its original structure until testing occurs. The undrained shear strength of the soil,  $s_u$ , is measured in this test.

### ***Consolidated-Drained (CD) Test***

In the CD test, the specimen is allowed to consolidate completely under the confining pressure prior to the application of axial load, i.e., the confining pressure acts as an effective stress throughout the soil specimen. The axial load is applied at a rate slow enough to allow drainage of pore water so that there is no buildup of excess pore water pressures, i.e., the stresses imposed by the axial load are effective stresses. The shear stresses induced in the specimen by the axial load result in failure. The time required to conduct this test in low permeability soil may be as long as several months. Therefore it is not common to conduct a CD test on low permeability soils. The CD test models the long-term (drained) condition in soil. Effective stress strength parameters (i.e.,  $\phi'$  and  $c'$ ) are evaluated from the results of the CD test.

### ***Consolidated-Undrained (CU) Test***

The initial part of the CU test is similar to the CD test in that the specimen is allowed to consolidate under the confining pressure. However, unlike the CD test, the axial load is applied with the drainage lines closed in the CU test. Thus, during shearing there is continual development (+ or -) of excess pore water pressure. The rate of axial load application for this test is more rapid than that for a CD test. Pore pressures are typically measured during the CU test so that both total stress and effective stress strength parameters can be obtained. Recall that total stress equals effective stress + pore water pressure as expressed by Equation 2-13. The pore water pressure may be + or - depending upon whether the specimen dilates or compresses during application of the axial load. The shear stresses induced in the specimen by the axial load result in failure. The effective stress parameters evaluated for most soils based on CU testing with excess pore water pressure measurements will be similar to those obtained from CD testing, thus making CD tests unnecessary for typical applications.

During triaxial testing, the confining pressure, which acts uniformly over the entire specimen, is considered to be the minor principal stress. By definition, a principal stress is one that acts on a plane where shear stress is zero. The interface between the soil and the membrane isolating it from the fluid in the chamber is assumed to be frictionless during the entire test, i.e. no shear stresses develop along the circumference of the specimen. Likewise, the applied axial load causes a normal stress to act on the top and bottom of the specimen. As shown in Figure 5-14, this vertical normal stress acts in addition to the confining pressure. Therefore, the combined vertical stress acting on the top and bottom of the specimen during the triaxial test is considered to be the major principal stress not only because the plane (horizontal) on which it acts is orthogonal to the minor principal stress plane (vertical), but



### 5.5.2.3 Direct Shear Tests

The oldest form of shear test upon soil is the direct shear test, first used by Coulomb (1776). A schematic of the essential elements of the direct shear apparatus are shown in Figure 5-17. The soil is held in a box that is split across its middle; the bottom portion of the box is usually fixed against lateral movement. A confining normal force,  $N$ , is applied, and then a tangential shear force,  $T$ , is applied so as to cause relative displacement between the two parts of the box. The magnitude of the shear force is recorded as a function of the shear displacement, and usually, the change in thickness of the soil sample is also recorded. Although it is widely used in practice, the direct shear device lacks a number of features that limit its applicability. For example, there is no way to control the confining pressure. Also, since there is no way to measure excess pore water pressures generated during shearing of saturated clay specimens, use of the direct shear test is generally limited to cohesionless soils.

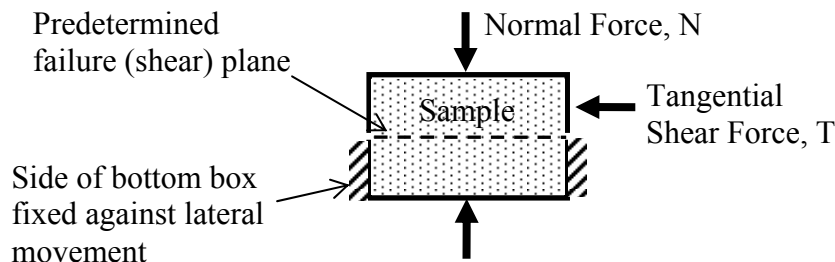


**Figure 5-17. Schematic of the Direct Shear Test.**

Equipment – The apparatus and procedures for direct shear testing are discussed in ASTM D 3080. A specimen is prepared in a split square or circular box. Figure 5-18 shows a circular specimen. The specimen is sheared as one part of the box is displaced horizontally with respect to the other. Generally, the lower part of the box is fixed against lateral movement and the shear force is applied to the upper part of the box through a loading frame as shown in Figure 5-18. The central two of the six screws visible in the top portion of the box extend into the bottom portion and are used to hold the assembly together while the specimen is being prepared. This shear box assembly is then placed in a reservoir which could be filled with water to allow saturation of the specimen prior to shearing. Before the test is begun, the two central screws are removed and the four corner screws, which rest on the top surface of the bottom portion of the box, are turned to slightly raise the top part of the box so that there is no contact between it and the bottom part of the box. This is done to prevent the error that would result from the frictional resistance between the two boxes at their contact. Load cells are used to monitor the shear force and LVDTs are used to monitor both horizontal and

vertical deformation. By use of this instrumentation, as well as a loading frame that provides a constant rate of horizontal deformation, it is possible to automate the direct shear test.



**Figure 5-18. Direct shear testing box (Photograph courtesy of GeoComp Corporation).**

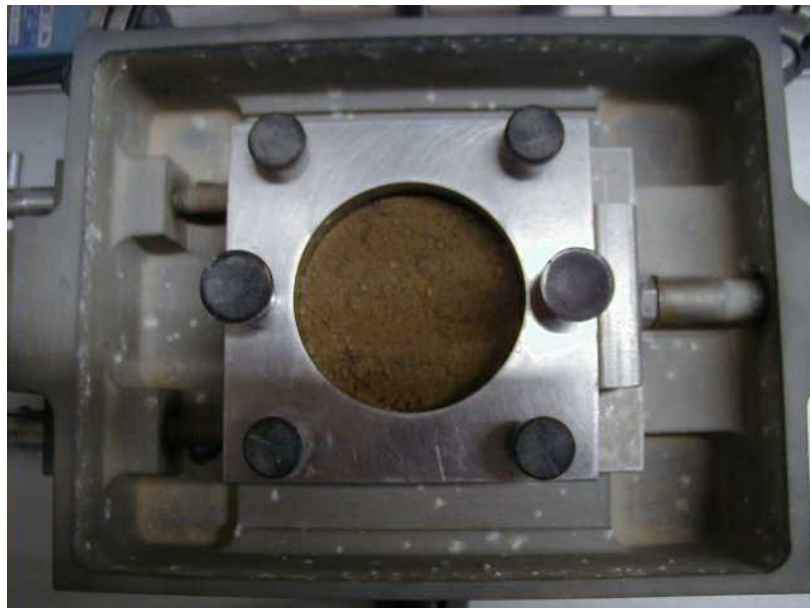


**Figure 5-19. Soil sample mounted in direct shear testing apparatus (Photograph courtesy of GeoComp Corporation).**

Test Procedures – In the direct shear test, the soil is first consolidated under an applied normal stress. After consolidation is completed, which will be virtually instantaneous in cohesionless soils, the specimen is sheared directly at a constant rate. The rate of shear is typically selected as a function of the hydraulic conductivity of the specimen. Direct shear testing is commonly performed on compacted materials used for embankment fills and retaining structures. Direct shear testing can also be performed on natural materials. However, the lack of control on soil specimen drainage makes the evaluation of undrained strength unreliable. The direct shear test can also be used to evaluate the drained strength of natural materials by shearing the sample at a rate slow enough to ensure that no significant pore water pressures develop, however there is no way to verify this condition by measurement.

In addition to providing data that allows the determination of the peak effective stress friction angle ( $\phi'$ ), the direct shear test data can also be used for the evaluation of effective stress residual strengths ( $c'_r \approx 0$ ;  $\phi'_r$ ). The effective stress residual strength parameters are necessary for stability and landslide analyses. Residual strengths are associated with very large shear strains along a predefined or preferential slip surfaces that result in very large deformations. Data from a reversing direct shear test can also be used to evaluate residual shear strengths. In a reversing direct shear test, the direction of shearing in the test is reversed several times thereby causing the accumulation of displacements at the slip surface.

A characteristic of the direct shear test that distinguishes it from the triaxial test is that the shear failure in the direct shear device is forced to occur on a horizontal plane so that the orientations of the major and minor principal stress planes are not apparent. Ordinarily this characteristic is considered to be a disadvantage of the direct shear test. However this characteristic is advantageous for designs involving geosynthetics where the shearing resistance of the interface between the soil and the geosynthetic or between two pieces of geosynthetic is often required. Direct shear machines have been modified to test the interface shear strength between various types of engineering materials, as described in ASTM D 5321.

### **5.5.3 Factors Affecting Strength Testing Results**

It is important for the designer to realize that all laboratory tests on soils must be carefully performed. This is particularly important for strength testing since the use of strength parameters are a key to successful foundation design. The following seven factors in particular affect the results of strength testing:

1. Sample disturbance
2. Mode of shearing
3. Confining pressures
4. Specimen size
5. Saturation
6. Displacement at failure
7. Rate of shearing and strain required to reach peak strength

A detailed discussion of each of these factors is presented in FHWA (2002a). In addition to recognizing the effect of the factors that can affect the strength testing results, it is extremely important for the designer to perform the proper tests depending on project requirements. The selection of an appropriate test to be used to provide relevant information for a particular geotechnical structure should consider, at a minimum, the following questions:

- (1) How fast will construction occur relative to the hydraulic conductivity of the soil (i.e., should drained or undrained strength tests be performed)?
- (2) How does the direction of applied load affect measured shear strengths and the appropriate strength to be used for an analysis?
- (3) How do the expected levels of deformation for the geotechnical structure affect the selection of shear strength? and
- (4) How does the manner in which the feature is constructed affect the shear strength to be used in analysis?

#### **5.5.4 Comparison of Laboratory and Field Strengths**

Soil samples are obtained from the ground for laboratory testing by sampling from boreholes and sealing and transporting these samples to the laboratory. The degree of disturbance affecting the samples will vary according to the type of soil, sampling method and the skill of the driller. At best some disturbance will occur from the removal of in-situ stresses during sampling and from the preparation of specimens in the laboratory for testing. In general, disturbance tends to reduce the shear strength obtained from unconfined or unconsolidated tests and increase the shear strength obtained from consolidated tests. There is, therefore, considerable merit in measuring the in-situ shear strength. The field vane shear test discussed in Chapter 3 is the most commonly used field test for direct measurement of the undrained shear strength of soft to medium clays. In reviewing the different types of field and laboratory tests available to determine the undrained shear strength in clays, the designer should expect the field vane shear test to provide the most accurate value of  $s_u$ , with UC and UU tests yielding lower results and CU tests yielding slightly higher results.

It is important that the results of in-situ tests be interpreted carefully and calibrated with laboratory tests. Without careful calibrations, the in-situ tests can yield inaccurate results.

### 5.5.5 Selection of Design Shear Strength

Frequently, on a large project the designer will receive a large quantity of undrained shear strength test results from both the field and laboratory. This data must be synthesized to permit rational interpretation of the results. The tests should be analyzed on a hole-by-hole basis. All tests from one hole should be reviewed and the results for each type of test should be plotted separately versus depth to determine the pattern of strength variation for each test type and to assess the reliability of the data, e.g., a CU test result that is lower than a UC test result at the same depth should be considered suspect. The general pattern of shear strength results should show an increase in strength with depth in a normally consolidated clay deposit. Overconsolidated clays may exhibit this pattern only at greater depths since the amount of preconsolidation increases shear strength in the upper portions of the soil deposit. Section 5.14 presents values of the coefficient of variation of measured soil properties that should be taken into account while selecting the final design shear strength.

### 5.5.6 Correlations of Shear Strength Parameters with Index Parameters

This section presents some useful correlations between shear strength parameters and other index values or field conditions. These correlations may be used by the designer to check the general validity of the laboratory test results or to develop a preliminary assessment about the shear strength characteristics of the soils on the project site. In the latter case, it must be emphasized that predictions based on correlations alone should never be used for design and that any assumptions regarding shear strength parameters must always be verified through testing.

#### 5.5.6.1 Undrained Shear Strength of Cohesive Soils

For most saturated clays tested under quick undrained conditions, the angle of shearing resistance,  $\phi_u$ , is zero. This means that the shear strength of the clay is a fixed value and is equal to the apparent cohesion,  $c_u$ , at a specific moisture content and preconsolidation pressure. A value for the undrained shear strength may be crudely estimated for a sample for which uncorrected SPT N-values are known by molding a specimen of the clay between the fingers and by applying the observations indicated in Table 4-2 in Chapter 4. However, as noted in the footnote of Table 4-2, **the values of SPT blow count listed there should not be used to determine the design strength of fine grained soils.**

## Undrained Shear Strength

For most normally consolidated clays the undrained shear strength ( $s_u$ ) is proportional to the effective overburden pressure ( $p_o$ ). For such soils, Skempton (1957) proposed the relationship shown in Figure 5-20 between the  $s_u/p_o$  and plasticity index (PI). Figure 5-20 also includes results obtained by a number of other researchers. As can be seen in the figure, the composite of all findings varies so much that **such relations should be used with caution**. However, such correlations, particularly the correlation by Skempton (1957), are useful for obtaining preliminary estimates and for checking laboratory results of project-specific tests performed on normally consolidated clays.

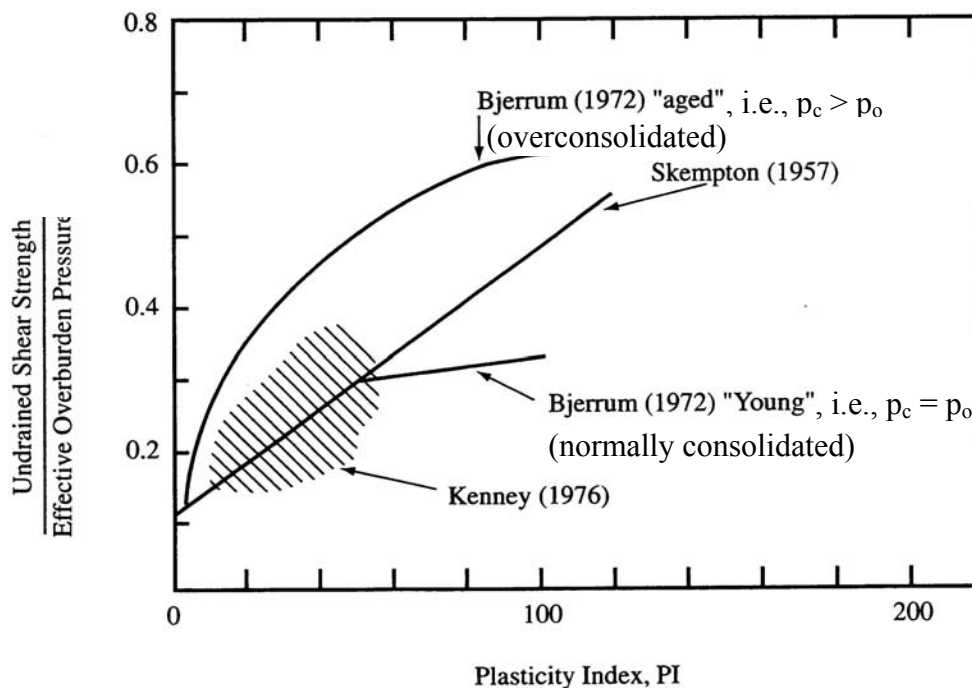


**Figure 5-20. Relationship between the ratio of undrained shear strength to effective overburden pressure and plasticity index for normally consolidated and overconsolidated clays (after Holtz and Kovacs, 1981).**

The shear strength of undisturbed clays depends on the consolidation history of the clay as well as its fabric characteristics. In general, the undrained strength ratio,  $s_u/p_o$ , increases with increasing overconsolidation as measured by the overconsolidation ratio, OCR. **It is recommended that laboratory tests be performed to determine the undrained strength ratio for overconsolidated clays rather than relying on any published correlations.** In practical terms, it is more straightforward to measure the undrained shear strength of overconsolidated clays than to predict it from other indices.

### 5.5.6.2 Drained and Effective Shear Strength of Cohesive Soils

It is often important to carry out stability calculations in terms of effective stresses. The soil strength parameters,  $c'$  and  $\phi'$ , used in these calculations should be obtained from either drained direct shear box or drained triaxial tests or from CU triaxial tests with pore water pressure measurements (giving  $\phi'_{cu}$  and  $c'_{cu}$ ). Generally, there is a minor difference in the results obtained from these two tests for saturated clays because the soil is being tested under different boundary conditions and stress paths. In-situ tests such as CPTs can also be used to estimate the drained and effective shear strength parameters of cohesive soils.

For clays, empirical correlations have been developed to relate  $\phi'$  to the plasticity characteristics of the soil. Figure 5-21 shows a slight trend of  $\phi'$  decreasing with increasing PI. The existence of these relationships arises because both PI and shear strength reflect the clay mineral composition of the soil; as the clay mineral content increases, the PI increases and the strength decreases. From Figure 5-21, it can be seen that the drained friction angle values can be  $\pm 8^\circ$  in variance with respect to the dashed trend line.

Considering the overall importance of  $\phi'$  in stability calculations, foundations design, and landslide analyses, it is essential to assess  $\phi'$  directly by means of consolidated drained direct shear tests, consolidated drained triaxial tests, or consolidated undrained triaxial tests with pore water pressure measurements. The consequences of merely estimating  $\phi'$  can be economically unwise. As an example, in stability analyses for relatively long, shallow slip surfaces that may be associated with a landslide, the required forces that would need to be resisted by some form of stabilization system (e.g., retaining wall, micropiles) would vary significantly depending on the drained friction angle of the soil. It is highly recommended that geotechnical designers develop historical data summaries of  $\phi'$  versus PI to check the validity of future test results.

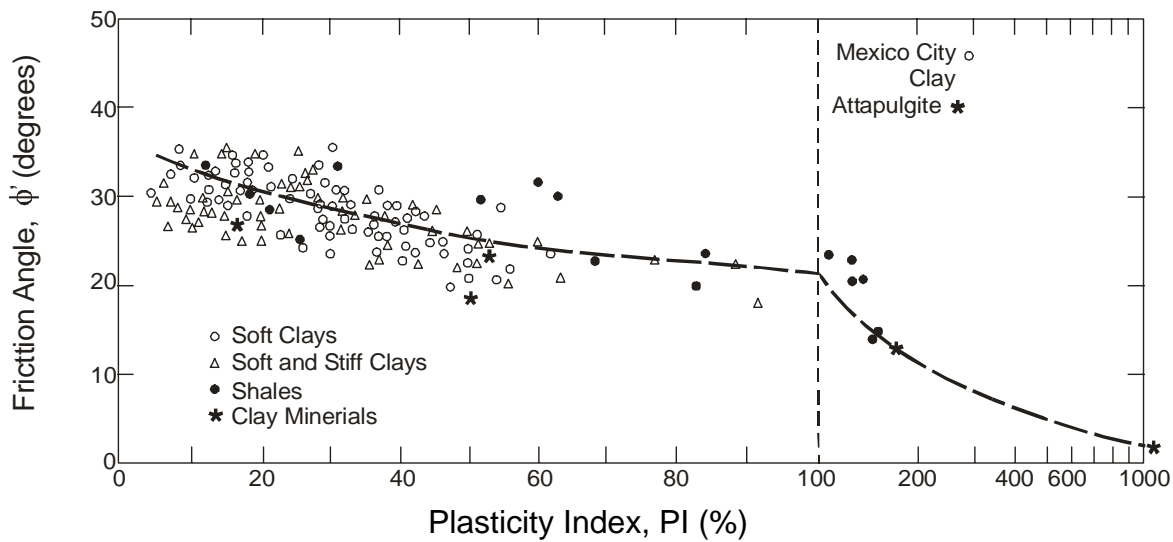
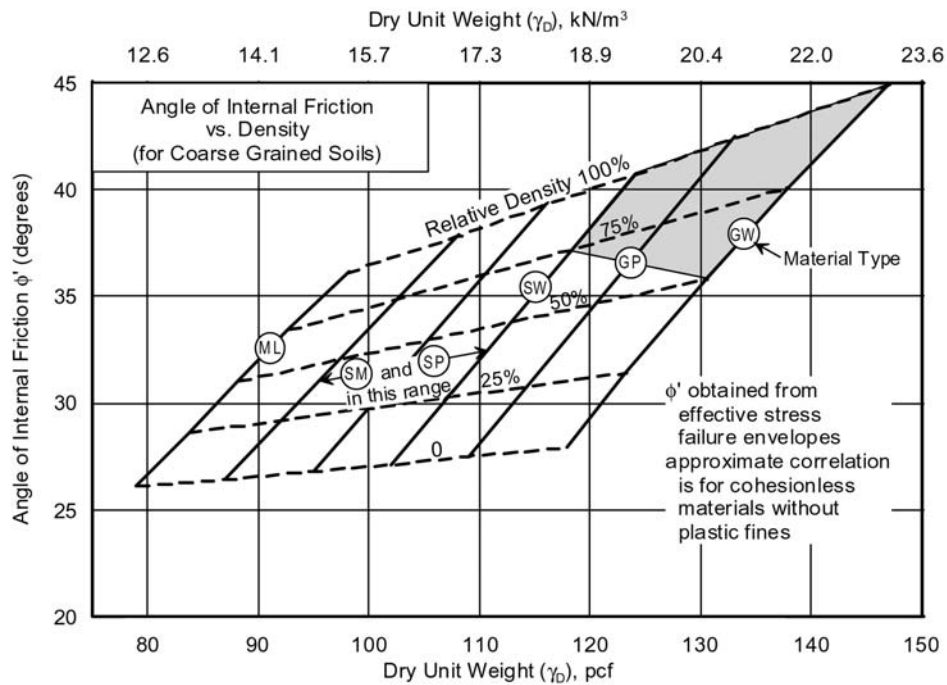


**Figure 5-21. Relationships between  $\phi$  and PI. (after Terzaghi, *et al.*, 1996).**

### 5.5.6.3 Shear Strength of Cohesionless Soils

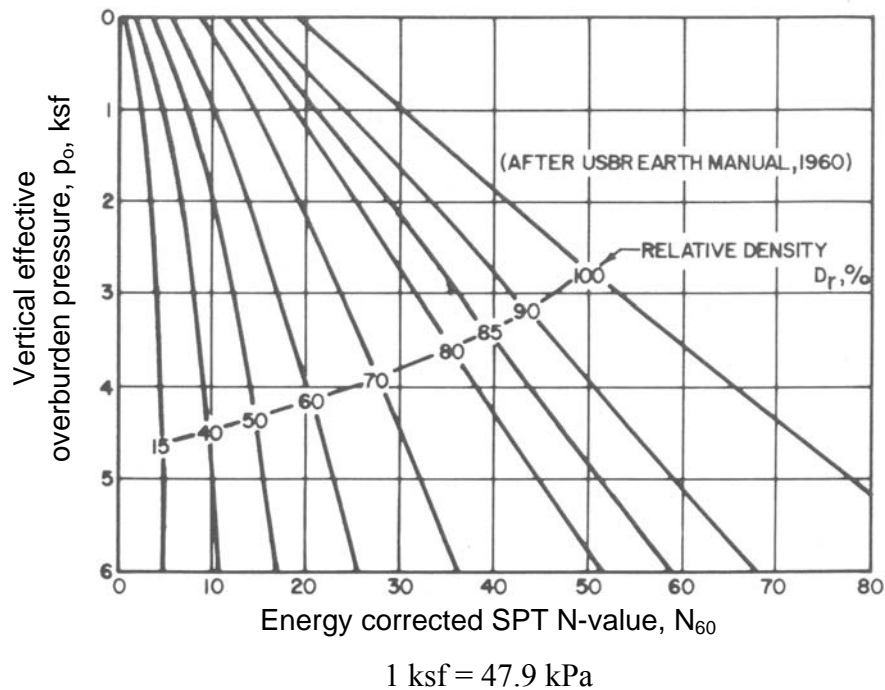
Because of their high permeability, pore water pressures do not build up significantly when cohesionless soils are subjected to shearing forces. The complication of total and effective stresses is therefore avoided and the phenomenon of apparent cohesion, or undrained shear strength does not occur. Consequently, the shear strength of cohesionless soils is defined exclusively in terms of frictional resistance between the grains, as measured by the angle of shearing resistance,  $\phi$ . Typical values of  $\phi$  for sands and gravels are given in Figure 5-22 as a function of dry unit weight and relative density. The material types indicated in the figure relate to the Unified Classification System (USCS).

Figure 5-22 requires determination of relative density. A reasonable estimate of relative density can be obtained from Figure 5-23. Figure 5-23 was originally developed based on data obtained using rope and cathead operated hammers. Thus, it is recommended that an energy corrected SPT N-value, i.e.,  $N_{60}$ , be used as shown in Figure 5-23. However, note that Figure 5-23 is a function of both N-value and the vertical effective overburden pressure,  $p_o$ . Therefore,  $N_{60}$ -value should not be corrected for overburden pressure, i.e.,  $C_N=1.0$  (see Section 3.7.2) while using Figure 5-23.



Note: Use caution in the shaded portion of the chart due to the potential for unreliable SPT N-values in gravels

**Figure 5-22. Correlation between relative density, material classification and angle of internal friction for coarse-grained soils (NAVFAC, 1986a).**



**Figure 5-23. Correlation between relative density and SPT resistance (NAVFAC, 1986a).**

## **5.6 PERMEABILITY**

### **5.6.1 General**

Permeability, also known as hydraulic conductivity, is one of the major parameters used in selecting soils for various types of construction. In some cases, it may be desirable to place a high-permeability fill immediately under a pavement surface or behind a wall to facilitate the removal of water. In other cases, such as retention pond dikes, it may be detrimental to use high-permeability materials. Permeability also significantly influences the choice of backfill materials for various elements such as trenches and retaining walls.

Unlike the fill soils discussed in the previous paragraph, the permeability of a natural soil is strongly influenced by its macroscopic structure, e.g., clays containing fissures or fine bands of sand will have permeabilities that are many times greater than that of the clay material itself. Also, stratified soils often have horizontal permeabilities that are many times the vertical permeability. Because of the small size of laboratory specimens and the way they are obtained and prepared, large scale in-situ features are absent and test results do not give a true indication of field values in soils with a pronounced macro-structure. Moreover, laboratory tests usually constrain water to flow vertically through the specimen whereas the horizontal permeability may be much greater, and hence of overriding importance, so far as site conditions are concerned. Field permeability tests overcome these shortcomings, but, since the pattern of water flow from a well used to determine in situ permeabilities can only be estimated, interpretation of the field test results is difficult and uncertain. Thus, one set of problems is exchanged for another.

### **5.6.2 Equipment**

Laboratory permeability testing is performed to determine the permeability or hydraulic conductivity ( $k$ ) of a soil specimen. For natural soils, tests are conducted on specimens from tube samples. For fill and borrow soils, tests are performed on compacted materials. Two types of tests are commonly performed, the rigid wall test (AASHTO T215; ASTM D 2434) and the flexible wall test (ASTM D 5084).

The equipment for the rigid wall test includes a rigid wall permeameter, a water tank, a vacuum pump, and manometer tubes (see Figure 5-24). The permeameter must be large enough to minimize sidewall leakage. Therefore, the diameter of the rigid wall device should be at least 8 to 12 times that of the largest soil particle in the sample being tested. Frequently, the side wall of the cylinder is coated with petroleum jelly to prevent sidewall leakage. Porous stones and filter paper placed on the top and bottom of the test specimen to

prevent soil particle erosion by retaining fine particles must not restrict flow through the soil otherwise the permeability of the porous stones or filter paper will be measured. A vacuum pump is used to remove air from the sample and to help saturate the specimen prior to testing. In a rigid wall test saturation is performed from the bottom of the specimen upward (see ASTM D 2434). Manometer outlets should be available on the sides of the cell to measure head loss over the specimen.

Rigid wall permeameters are not recommended for low permeability (i.e.,  $k \leq 2 \times 10^{-5}$  ft/min ( $1 \times 10^{-6}$  cm/s)) soils due to the potential for sidewall leakage. Rigid wall permeameters are typically used for sandy and gravelly soils (ASTM D 2434) with a permeability greater than  $2 \times 10^{-2}$  ft/min ( $1 \times 10^{-3}$  cm/s). Rigid wall systems are used for granular materials because the permeability of the flexible wall system (valves, pore stones, tubing, etc.) may be less than that of the specimen. Therefore the flexible wall system itself may affect the permeability value of granular soils and a measured value of permeability lower than that of the specimen may result.



**Figure 5-24. Rigid wall permeameter (Photograph courtesy of GeoComp Corporation).**



**Figure 5-25. Flexible wall permeameter (Photograph courtesy of GeoComp Corporation).**

The equipment for a flexible wall test includes a flexible wall permeameter cell, a cell reservoir, a headwater reservoir, a tailwater reservoir, top and base caps, a flexible membrane, porous stones, and filter paper (see Figure 5-25). The specimen can be tested over a range of confining stresses under backpressure saturation. The separate headwater and tailwater reservoirs can be monitored, and falling head or constant head tests can be performed. Since the flexible membrane encases the specimen, side leakage is prevented. Flexible wall permeameter cells consist of influent and effluent lines as well as porous stones and filter paper. The hydraulic conductivity of the system should be tested before a soil specimen is tested to ensure that the system's conductivity is at least one order of magnitude greater than that anticipated for the soil. The triaxial cell can be used as a flexible wall permeameter. In fact, permeability measurements are often made as part of a drained triaxial (CD) test.

The determination of permeability by testing is predicated on the validity of Darcy's Law for laminar flow through porous media. If any of the assumptions of Darcy's Law are violated, the results of permeability testing will be invalid.

### 5.6.3 Procedures

Flexible wall permeameters (ASTM D 5084) are used for materials with a hydraulic conductivity ( $k$ ) less than or equal to  $2 \times 10^{-2}$  ft/min ( $1 \times 10^{-3}$  cm/sec). The flexible membrane used to encase the specimen prevents sidewall leakage for fine-grained soils that are likely to occur in a rigid wall system. The confining stress of the hydraulic conductivity test should be specified to the laboratory. As confining stress increases, the hydraulic conductivity of fine grained soils will typically decrease due to consolidation of the specimen and reduction of void ratio. The confining stress should be equal to the anticipated effective stress-state in the soil.

The hydraulic gradient, defined as the difference in hydraulic head across the specimen divided by the length of the specimen, should also be specified to the laboratory. Typical hydraulic gradients in field situations are less than 5, however the use of such a small gradient in the laboratory will result in extremely long testing times for materials having hydraulic conductivities less than  $2 \times 10^{-5}$  ft/min ( $1 \times 10^{-6}$  cm/sec). If the hydraulic gradient across the specimen is too high, turbulent flow will occur and Darcy's Law will be violated with the result that the measured hydraulic conductivity will be less than that which will occur in the field. Suggested values of hydraulic gradient, as presented in Table 5-9, are a function of the anticipated hydraulic conductivity.

Saturation of the specimen is necessary to achieve accurate results. A hydraulic conductivity test should be ended when steady flow is occurring. The flow through the permeameter is considered to be steady when four or more consecutive hydraulic conductivity measurements fall within  $\pm 25$  percent of the average  $k$  value if  $k$  is greater than  $1 \times 10^{-8}$  cm/sec, or if four or more measurements fall within  $\pm 50$  percent of the average if  $k$  is less than  $1 \times 10^{-8}$  cm/sec.

**Table 5-9**  
**Recommended maximum hydraulic gradient for permeability testing**

<b>Hydraulic Conductivity, cm/sec*</b>	<b>Recommended Maximum Hydraulic Gradient</b>
$1 \times 10^{-3}$ to $1 \times 10^{-4}$	2
$1 \times 10^{-4}$ to $1 \times 10^{-5}$	5
$1 \times 10^{-5}$ to $1 \times 10^{-6}$	10
$1 \times 10^{-6}$ to $1 \times 10^{-7}$	20
less than $1 \times 10^{-7}$	30
* Conventionally expressed in cm/sec. [ $1 \text{ cm/sec} \approx 2 \text{ ft/min} = 0.6 \text{ m/min}$ ]	

#### 5.6.4 Useful Correlations of Permeability with Index Values

The typical range of permeability values for various soil types and USCS groups is presented in Table 5-10, which is based on information originally presented by Casagrande and Fadum (1940). Superimposed on Table 5-10 are “typical soil groups” identified by their USCS symbols (Carter and Bentley, 1991). The range of permeability values corresponding to those groups is typical for compacted soils of that type where compaction is according to ASTM D 1557. Typical permeability values for highway construction materials are given in Table 5-11.

Numerous correlations of permeability with grain size can be found in the literature. Figure 5-26 presents logarithmic plots of  $k$  versus  $D_{10}$ , based on experimental results. Figure 5-26 includes the well known Hazen’s formula. All the correlations shown in Figure 5-26 were developed for sands and gravels. The great range of particle size present in most clays and the effects of clay mineralogy make such correlations of limited use for clays.

Hazen’s equation is the most common correlation equation used to estimate permeability for sands ( $k \geq 10^{-3}$  cm/sec). This equation is written as:

$$k = C(D_{10})^2 \quad 5-14$$

where:  $k$  is the permeability in cm/s;

$C$  = a coefficient ranging from 0.4 to 1.2 depending on sand size/sorting; and

$D_{10}$  = effective grain size in mm at 10% passing by weight as determined from sieve analysis.

Hazen’s equation should be used with caution since it provides very approximate estimates of  $k$  applicable only to clean sands having less than 5% passing the No. 200 sieve (0.075 mm) and with  $D_{10}$  sizes between 0.1 and 3.0 mm (Holtz and Kovacs, 1981). Hazen’s equation is valid only for  $k \geq 10^{-3}$  cm/sec.

**Table 5-10**  
**Typical permeability values in soils (after Carter and Bentley, 1991)**

	$10^{-11}$	$10^{-10}$	$10^{-9}$	$10^{-8}$	$10^{-7}$	$10^{-6}$	$10^{-5}$	$10^{-4}$	$10^{-3}$	$10^{-2}$	$10^{-1}$	1
	m/s											
Coefficient of permeability (log scale)	$10^{-9}$	$10^{-8}$	$10^{-7}$	$10^{-6}$	$10^{-5}$	$10^{-4}$	$10^{-3}$	$10^{-2}$	$10^{-1}$	1	10	100
	cm/s											
Permeability:	Practically impermeable			Very low		Low		Medium		High		
Drainage conditions:	Practically impermeable				Poor			Good				
Typical soil groups:	GC → GM →			SM		SW →		GW →				
	CH		SC	MH		SM-SC		SP →		GP →		
			MC-CL									
Soil types:	Homogeneous clays below the zone of weathering			Silts, fine sands, silty sands, glacial till, stratified clays				Clean sands, sand and gravel mixtures			Clean gravels	
				Fissured and weathered clays and clays modified by the effects of vegetation								

Note: The arrow adjacent to group classes indicates that permeability values can be greater than the typical value shown.

**Table 5-11**  
**Typical permeability values for highway materials (after Krebs and Walker, 1971)**

Materials	Permeability (cm/sec)
Uniformly graded coarse aggregate	40 - $4 \times 10^{-1}$
Well-graded aggregate without fines	$4 \times 10^{-1}$ - $4 \times 10^{-3}$
Concrete sand, low dust content	$7 \times 10^{-2}$ - $7 \times 10^{-4}$
Concrete sand, high dust content	$7 \times 10^{-4}$ - $7 \times 10^{-6}$
Silty and clayey sands	$10^{-5}$ - $10^{-7}$
Compacted silt	$7 \times 10^{-6}$ - $7 \times 10^{-8}$
Compacted clay	Less than $10^{-7}$
Bituminous concrete (new pavements)*	$4 \times 10^{-3}$ - $4 \times 10^{-6}$
Portland cement concrete	less than $10^{-8}$

\* Values as low as  $10^{-8}$  have been reported for sealed, traffic compacted highway pavement.

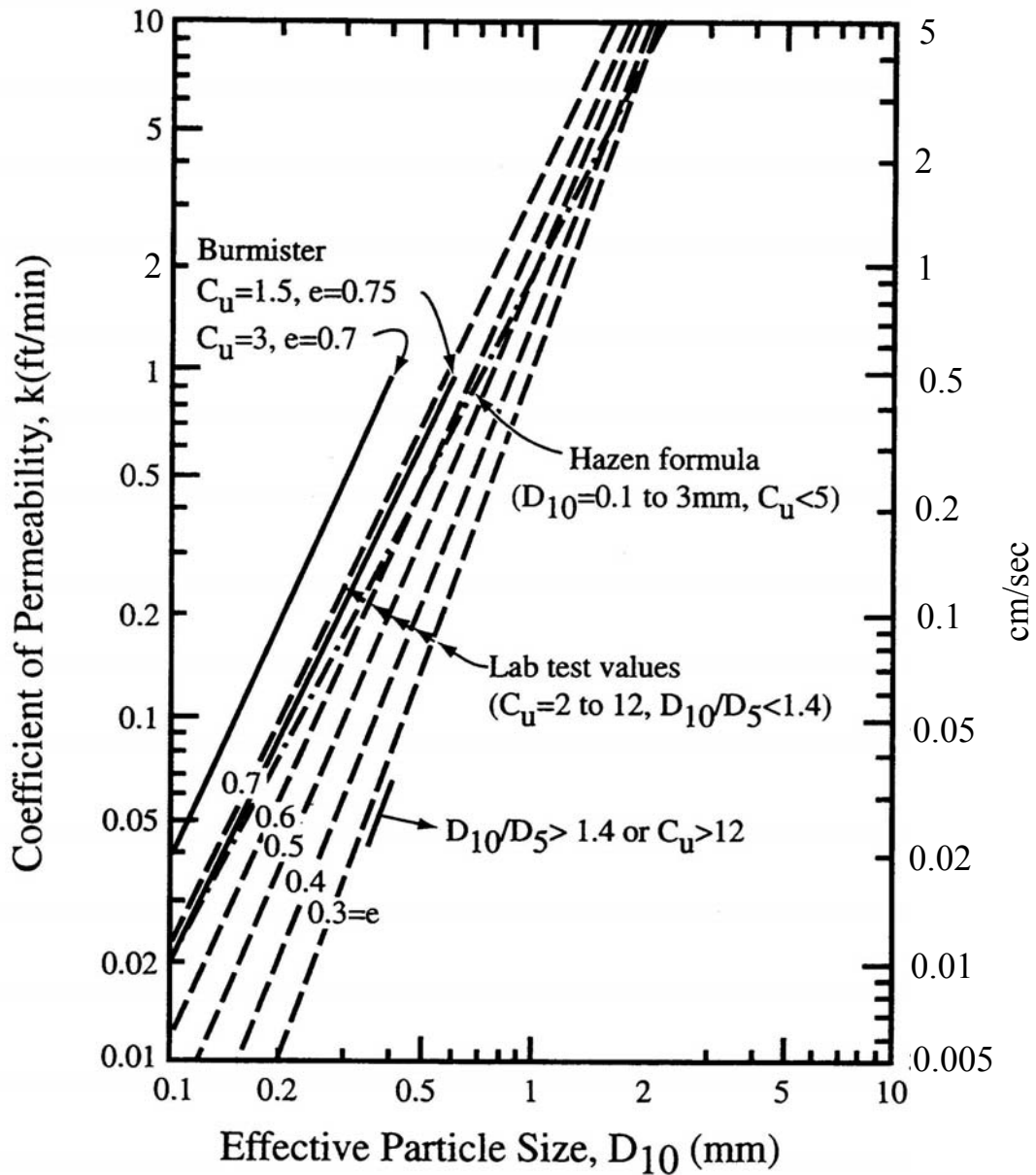


Figure 5-26. The permeability of sands and gravels (after NAVFAC, 1986a).

Note: In Figure 5-26, correlations shown are for remolded compacted sands and sand-gravel mixtures with  $C_u$  values as indicated.

## **5.7 VOLUME CHANGE PHENOMENA DUE TO LOADING AND MOISTURE**

Depending on mineralogy and depositional patterns, natural soils can exhibit either swell (expansion) or collapse under various degrees of loading and moisture ingress. Moisture may be in liquid or frozen form. For foundation design, it is very important to recognize and evaluate the potential for soils to swell or collapse. It is important to realize that these phenomena happen in both natural and compacted soils. Every year millions of dollars are spent dealing with the consequences of swelling (expanding) and collapsing soils. This section briefly discusses these two mechanisms and the tests that can be performed to evaluate the swell (expansion) and collapse potentials.

### **5.7.1 Swell Potential of Clays**

Swelling is a characteristic reaction of some clays to water ingress. The potential for swell depends on the mineralogical composition of the soil fines. While montmorillonite (smectite) exhibits a high degree of swell potential, illite has no to moderate swell potential, and kaolinite exhibits almost none. The percentage of volumetric swell of a soil depends on the amount and type of clay, its relative density, the compaction moisture content and dry density, permeability, location of the groundwater table, the presence of vegetation and trees, overburden pressure, etc. Expansive soils are found throughout the U.S., however, damage caused by expansive clays is most prevalent in certain parts of California, Wyoming, Colorado, and Texas, where the climate is considered to be semi-arid and periods of intense rainfall are followed by long periods of drought. This pattern of wet and dry cycles results in periods of extensive near-surface drying and desiccation crack formation. During intense precipitation, water enters the deep cracks causing the soil to swell; upon drying, the soil will shrink. This weather pattern results in cycles of swelling and shrinking that can be detrimental to the performance of pavements, slabs on-grade, and retaining walls built on or in such soils.

Deep-seated volume changes in expansive soils are rare. More common are volume changes within the upper 3-10 feet (1- 3 m) of a soil deposit. These upper few feet are more likely to be affected by seasonal moisture content changes due to climatic changes. The zone over which volume changes are most likely to occur is defined as the active zone. The active zone can be evaluated by plotting the moisture content with depth for samples taken during the wet season and for samples taken during the dry season at the same location. The depth at which the moisture content becomes nearly constant is the limit of the active zone depth, which is also referred to as the depth of seasonal moisture change. The active zone is an important consideration in foundation design. In the design of piles or drilled shafts, it is important to recognize that full side friction resistance may not be realized in this zone. As

the soil undergoes cycles of shrinking and swelling, it may lose contact with the pile or shaft. Alternatively, as the soil swells, it may impose significant uplift pressures on the foundation element.

In the field, the presence of surface desiccation cracks and/or fissures in a clay deposit is an indication of expansion potential. Experience has indicated that the most problematic expansive near-surface soils are typically highly plastic, stiff, fissured, overconsolidated clays. Several classification methods are used to identify expansive soils in the laboratory. Currently, there is not a standard classification procedure; different methods are used in various locations across the U.S. Typically, methods include the use of Atterberg limits and/or clay size percentage to describe a soil qualitatively as having low, medium, high, or very high expansion potential. Generally, soils with a plasticity index less than 15 percent will not exhibit expansive behavior. For soils with a plasticity index greater than 15 percent, the clay content of the soil should be evaluated in addition to the Atterberg limits. Figure 5-27 shows the swelling potential of natural soils and soils compacted to standard Proctor procedures (ASTM D 698) as a function of modified activity index,  $A_m$ , (Equation 5-4) and clay fraction.

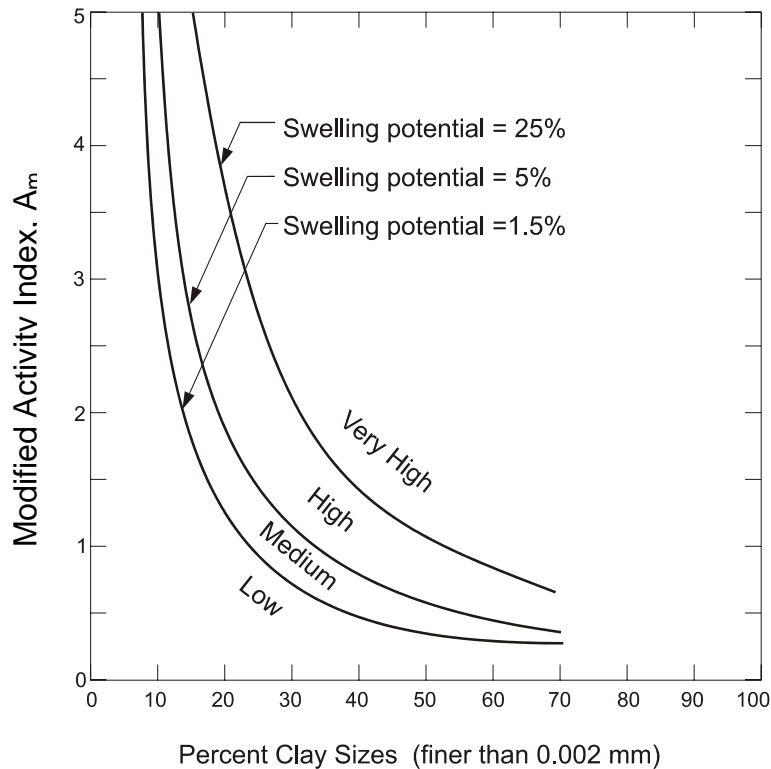


**Figure 5-27. Classification of swell potential for soils (after Seed *et al.*, 1962).**

### 5.7.1.1 Evaluation of Expansion (Swell) Potential

For situations where it is necessary to construct a facility in and around expansive soils, it will be necessary to estimate the magnitude of swell, i.e., surface heave, and the corresponding swelling pressures that may occur if the soil becomes wetted. The swelling pressure represents the magnitude of pressure that would be necessary to resist the tendency of the soil to swell. A one-dimensional swell potential test can be performed in an oedometer on undisturbed or recompacted samples according to AASHTO T256 or ASTM D 4546. In this test, the swell potential is evaluated by observing and measuring the swell of a laterally confined specimen when it is lightly surcharged and flooded with water. Alternatively, if the swelling pressure is to be measured, the height of the specimen is kept constant by adding load after the specimen is inundated. The swelling pressure is then defined as the vertical pressure necessary to maintain zero volume change. Swelling pressures in some expansive soils may be so large that the loads imposed by lightweight structures or pavements do little to counteract the swelling.

The use of the one-dimensional swell potential test to evaluate in-situ swell potential of natural and compacted clay soils has limitations including:

- Lateral swell and lateral confining pressure are not simulated in the laboratory. The calculated magnitude of swell in the vertical direction may not be a reliable estimate of soil expansion for structures that are not confined laterally (e.g., bridge abutments);
- The rate of swell calculated in the laboratory will not likely be indicative of the rate of swell experienced in the field. Laboratory tests cannot simulate the actual availability of water in the field.

It should be noted that there is a lack of a standard definition of swell potential in the technical literature based in part on variations in the test procedures, e.g., the condition of the test specimen (remolded or undisturbed), the magnitude of the surcharge, etc. Therefore the geotechnical specialist must be sure that the conditions used in the laboratory swell test simulate those expected in the field. In general, soils classified as CL or CH according to the USCS and A-6 or A-7 according to the AASHTO classification system should be considered potentially expansive.

### 5.7.2 Collapse Potential of Soils

There are several types of soils that can experience collapse under moisture ingress. Examples of such soils are wind-blown deposits such as loess, or alluvial soils deposited in arid or semi-arid environments where evaporation of soil moisture takes place at such a rapid rate that the deposits do not have time to consolidate under their self weight or where the deposits are cemented by precipitated salts. Such soils are predominantly composed of silts and some clay. Typically, the structure of such soils is flocculated and the soil particles are held together by “clay bridges” or some other cementing agent such as calcium carbonate. In both cases disturbed samples obtained from these deposits are generally classified as silt. When dry or at low moisture content the in-situ material gives the appearance of a stable deposit. At elevated moisture contents these soils generally undergo sudden changes in volume and collapse. **Full saturation is not required to realize collapse of such soils; often collapse of the soil structure occurs at moisture contents corresponding to pre-collapse degrees of saturation between 50 to 70%.** Such soils, unlike other non-cohesive soils, will stand on almost a vertical slope until inundated. Collapse-susceptible soils typically have a low relative density, a low unit weight and a high void ratio. Figure 5-28 is a useful tool for assessing whether a soil is collapsible or not based on LL and dry unit weight.

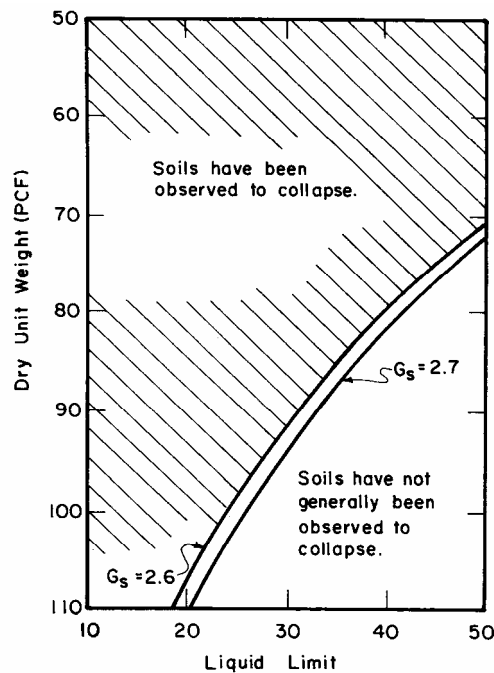


Figure 5-28. Chart for evaluation of collapsible soils (after Holtz and Hilf, 1961).

Structures founded on such soils may be seriously damaged if the soils are inundated and collapse. Therefore, if a soil is suspected to be collapse susceptible, then it is of primary importance to estimate the magnitude of potential collapse that may occur if the soil becomes wetted. To do this, a one-dimensional collapse potential test can be performed in an oedometer on undisturbed or recompacted samples according to ASTM D 5333. For this test, a sample is placed in an oedometer at its natural or compacted moisture content and the vertical pressure on the sample is increased in increments to the anticipated final loading in the field. Readings of vertical deformation are taken during the loading sequence. At the anticipated final load level, water is introduced to the sample and the resulting deformation due to collapse is recorded. The percent collapse (%C) is defined as:

$$\%C = \frac{100 \Delta H_c}{H_o} \quad 5-15$$

where  $\Delta H_c$  is the change in height upon wetting and  $H_o$  is the initial height of the specimen. Conceptually, C is a strain. Therefore, for a soil layer with a given thickness, H, the settlement due to collapse,  $s_{collapse}$ , if the entire thickness is inundated may be calculated as:

$$s_{collapse} = H \left( \frac{\%C}{100} \right) \quad 5-16$$

The collapse potential (CP) is calculated as the percent collapse (%C) of a soil specimen subjected to a total load of 4 ksf (200 kPa) as measured by using procedures specified in ASTM D 5333. The CP is an index value used to compare the susceptibility of various soils to collapse. Table 5-12 provides a relative indication of the degree of severity for various values of CP.

**Table 5-12**  
**Qualitative assessment of collapse potential (after ASTM D 5333)**

<b>Collapse Potential (CP)</b>	<b>Severity of Problem</b>
0	None
0.1 to 2%	Slight
2.1 to 6%	Moderate
6.1 to 10%	Moderately Severe
>10%	Severe

### 5.7.3 Expansion of Soils due to Frost Action

The expansion of soils due to frost action is commonly known as **frost heave**. Three conditions are required for frost heave to occur. These are (a) freezing surface, (b) source of water, and (c) fine grained soils in which capillary rise can occur. Frost action in soils can have important engineering consequences as follows (after Holtz and Kovacs, 1981):

- The volume of the soil can immediately increase about 10% just due to the volumetric expansion of water upon freezing.
- The formation of ice crystals and lenses in the soil can cause heaving and damage to light surface structures such as small buildings, and highway pavements. Frost action can also displace retaining walls due to increased lateral pressures.

When water in saturated fine-grained soils freezes, it forms lenses of ice oriented roughly parallel to the surface exposed to low temperature (Terzaghi, *et al.*, 1996). Due to the inherent variability in the distribution of pore space, soils affected by frost action do not freeze and expand uniformly. Therefore, just as with swelling and collapsing soils, differential movement occur, and causes structural damage. Upon thawing, the moisture content of the soil increases which leads to reduction in shear strength and a consequent reduction in bearing capacity. Thus, the freeze-thaw cycle results in significant distress to structures and in particular highway pavements.

Only fine-grained soils are susceptible to frost action. However, the critical grain size marking the boundary between soils that are subject to ice-lens formation and those that are not depends on the uniformity of the soil, i.e., the distribution of pore space. The following conditions noted by Terzaghi, *et al.* (1996) may be used as a general guide for evaluating the frost susceptibility of soils:

- In perfectly uniform soils, i.e., a single particle size soils, ice lenses do not develop unless the grains are smaller than 0.01 mm.
- Uniform soils must contain at least 10% of grains smaller than 0.02 mm.
- In mixed-grain soils, ice lenses form when grains with a size less than 0.02 mm constitute at least 3% of the total aggregate.

- In soils with less than 1% of grains smaller than 0.02 mm, ice lenses are not formed under any conditions which may be encountered in the field.

Common frost susceptible soils include silts (ML, MH), silty sands (SM), and low plasticity clays (CL, CL-ML). One of the most common methods to mitigate the detrimental effects of frost is to place the foundations below the anticipated frost depth. The depth of frost action depends primarily on air temperature below freezing and duration, soil permeability and soil water content. Figure 5-29 can be used for a preliminary estimate of the frost depth. More positive measures to mitigate damage due to frost action include lowering of the ground water table and, depending on the depth of the frost penetration, removal of the frost susceptible soils in the subgrade or foundation. Use of impervious membranes, chemical additives, and even foamed insulation (Styrofoam) under highways, buildings, and railroads have been successfully employed (Holtz and Kovacs, 1981).

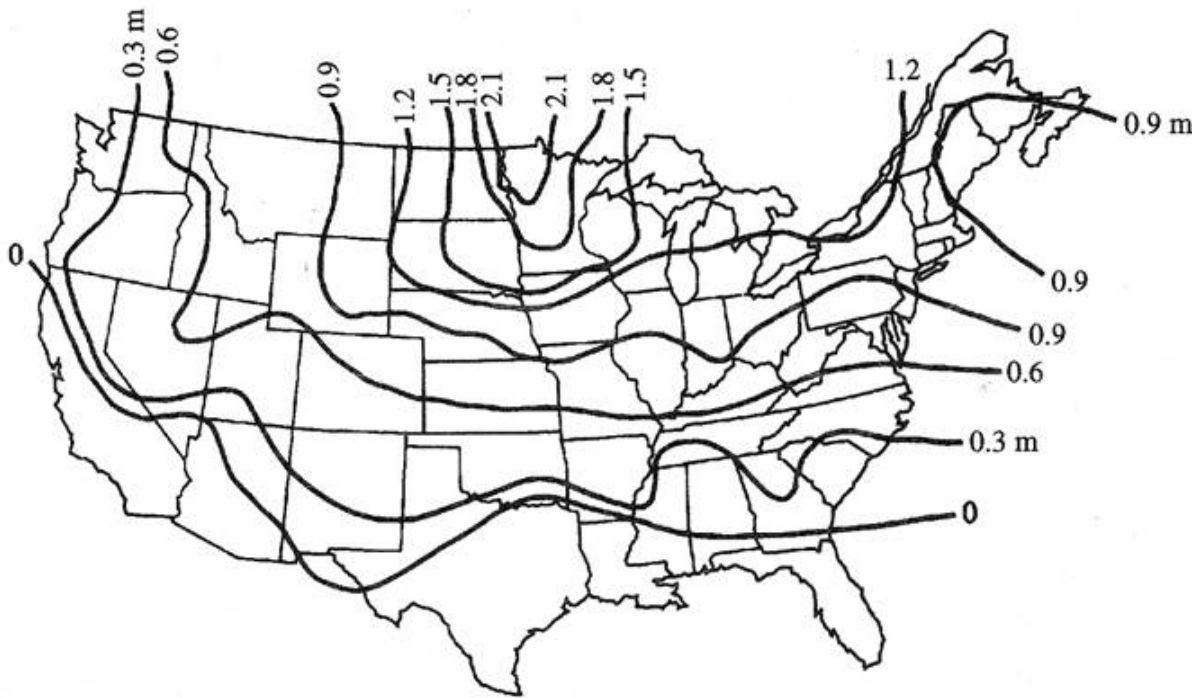


**Figure 5-29. Approximate frost depth map for United States (Bowles, 1996).  
(1 m = 3.28 ft)**

## 5.8 COMPACTION CHARACTERISTICS OF SOIL

### 5.8.1 Concept of Compaction

In the construction of highway embankments, earth dams, retaining walls, structural foundations and many other facilities, loose soils must be compacted to increase their densities. Compaction is the process of densifying soil under controlled moisture conditions by application of a given amount and type of energy. Compaction increases the density of the soil, which generally leads to:

- an increase in the strength and stiffness characteristics of the soil,
- a decrease in the amount of undesirable settlement of structures under both static and dynamic loads,
- a reduction in soil permeability, and
- an increase in the stability of slopes and embankments.

Unless compaction is properly controlled, there is a potential that the volume change phenomena described in Section 5.7 (swell, collapse and frost heave) can occur.

The density of compacted soils is measured in terms of the dry unit weight,  $\gamma_d$ , of the soil. The dry unit weight is a measure of the amount of solid materials present in a unit volume of soil. The greater the amount of solid materials, the stronger and more stable the soil will be. Pertinent parameters for evaluating the results of laboratory and field compaction tests are:

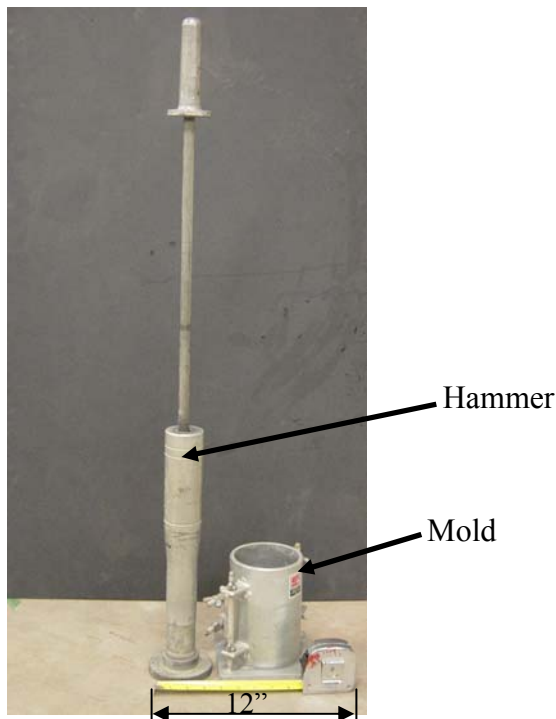
- dry “density” or dry “unit weight.”
- compaction water content.
- type of energy input, e.g., impact, static, vibratory, kneading.
- amount of energy input expressed in ft-lbs/ft<sup>3</sup>.

Table 5-13 presents a summary of the characteristics of the most commonly used laboratory compaction tests. Figure 5-30 shows a typical hammer and a mold which is used for performing compaction tests in the laboratory. A comparison of the various values in Table 5-13 reveals that the energy level in the Modified Proctor compaction (MPC) test is 4.5 times that for the Standard Proctor compaction (SPC) test.

**Table 5-13**  
**Characteristics of laboratory compaction tests**

Common Name	ASTM (AASHTO) Designation	Mold Dimensions			Hammer		No. of Layers	Blows/ Layer	Energy (ft-lbs/ft <sup>3</sup> )
		Diam. (in)	Height (in)	Vol. (ft <sup>3</sup> )	Wt. (lbs)	Drop Ht. (in)			
Standard Proctor	D 698 (T 99)	4	4½	1/30	5.5	12	3	25	12,375
Modified Proctor	D 1557 (T 180)	4	4½	1/30	10	18	5	25	56,250

Note: Both tests are performed on minus No. 4 (4.75 mm) fraction of the soil.



**Figure 5-30. Hammer and mold for laboratory compaction test (tape measure is for scale purpose only).**

### 5.8.2 Test Procedures

At least 3 (preferably 5) samples of the same type of soil are prepared at various water contents and compacted according to the requirements listed in Table 5-13. Following compaction, the moist unit weight of the compacted soil ( $\gamma_t$ ) in the mold is easily calculated as the weight of the soil (measured) divided by the volume of the mold (constant = 1/30 ft<sup>3</sup>). The water content (w) is determined as per ASTM D 2216-05 and the dry unit weight is then calculated as (see Table 2-2 in Chapter 2):

$$\gamma_d = \frac{\gamma_t}{(1 + w)}$$

The dry unit weight (pcf (kN/m<sup>3</sup>)) for each compacted sample is plotted versus its compaction moisture content (%). The resulting curve is called a **compaction curve**. Figure 5-31 shows compaction curves for the same soil using Standard Proctor compaction (SPC) test parameters and Modified Proctor compaction (MPC) test parameters as listed in Table 5-13. The typical compaction curves as presented in Figure 5-31 have the following characteristics:

- **Maximum dry density** ( $\gamma_{d-max}$ ) is the dry density corresponding to the peak of the compaction curve for a given type and amount of input energy. Note from Figure 5-31, that the SPC  $\gamma_{d-max}$  is less than the MPC  $\gamma_{d-max}$ . Note from Table 5-13 that although the type of energy (impact) is the same for both SPC and MPC, the amount of energy in the MPC test is 4.5 times that of the SPC test.
- **Optimum moisture content** ( $w_{opt}$ ) is the compaction water content at which the soil attains its maximum dry density for a given input energy. Note from Figure 5-31, that the SPC  $w_{opt}$  is greater than the MPC  $w_{opt}$ .

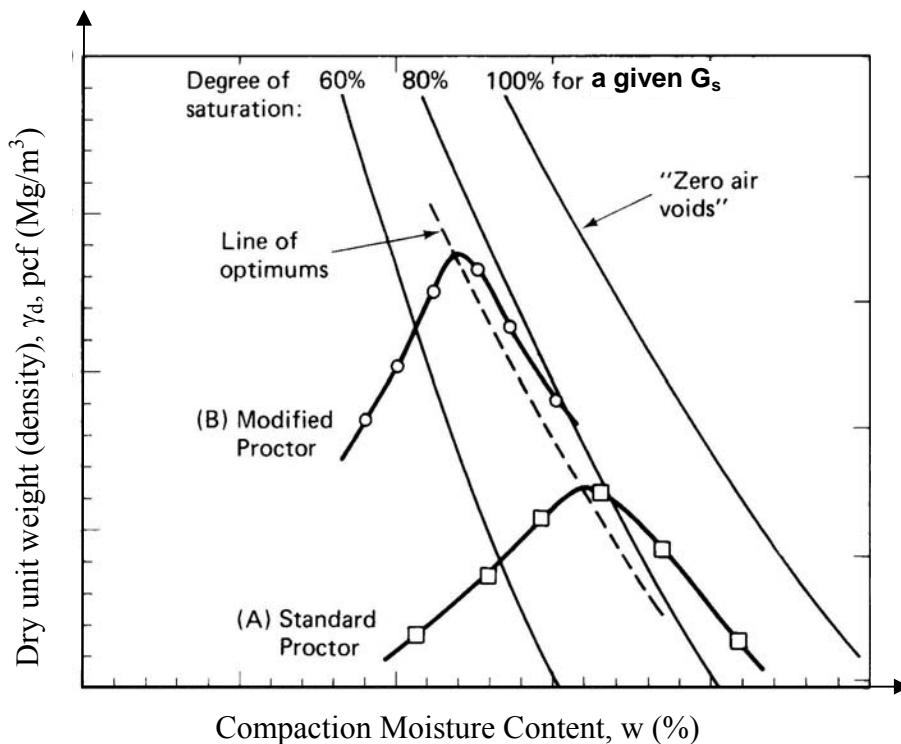


**Figure 5-31. Compaction curves (after Holtz and Kovacs, 1981).**

- **Zero air voids curve** is the curve that corresponds to  $S=100\%$  regardless of the amount or type of energy input. The importance of the zero-air-voids curve is that it denotes the limits of compaction, i.e., if the moisture content of a fill is too high for a given amount of input energy, the compacted fill may begin to “pump” as its voids become fully saturated with moisture. This can happen even at low moisture contents if the input energy is very large as may be the case with too many passes of a too heavy a piece of compaction equipment. Points on the zero air voids curve are calculated from the basic equation for dry unit weight given by Equation 5-18 by setting  $S=1$  and choosing arbitrary values of compaction moisture content within the range of the compaction curve.

$$\gamma_d = \frac{G_s \gamma_w}{(1 + e)} = \frac{G_s \gamma_w}{\left(1 + \frac{wG_s}{S}\right)} \quad 5-18$$

where:  $G_s$  = specific gravity of solid particles

$\gamma_w$  = unit weight of water

$e$  = void ratio

$w$  = water content expressed as a decimal

$S$  = degree of saturation expressed as a decimal.

Note that the  $S=100\%$  (zero air voids) curve is calculated for a specific value of  $G_s$ , in this case 2.7. Curves corresponding to other degrees of saturation can be calculated in the same way by setting  $S=80$  for the 80% saturation curve,  $S=60$  for the 60% saturation curve and so forth. The saturation curve for a degree of saturation less than 100% is often useful for developing compaction specifications for silty soils since such soils frequently have sharply peaked compaction curves. Therefore, they can begin to “pump” even though the degree of saturation is less than 100%.

- **Line of optimums** - As its name suggests the “line of optimums” is obtained by passing a curve through the peaks of the compaction curves that were developed for a certain type of soil compacted at various energy input levels. Testing laboratories frequently develop such curves for various types of soil based on information in their job files. The line of optimums can be used as a guide for developing compaction specifications where no laboratory test data are available.

The above observations are true for all types of soils and apply to all methods of compaction. The most important concept about compaction curves as discussed above is that an increase in the amount of compaction (more energy) results in an increase in the maximum dry density and a corresponding decrease in the optimum moisture content. Therefore, this concept should be recognized when the geotechnical specialist is required to develop specifications for field compaction of soils.

### **5.8.3 Implication of Laboratory Tests on Field Compaction Specifications**

With reference to Figure 5-31 it is obvious that for a given compaction curve the same dry unit weight can be obtained at two different compaction moisture contents, one below optimum and the other above optimum. For fine-grained soils this difference in moisture contents relates to a difference in soil structure that may affect engineering properties such as shear strength and permeability.

It is very important that compaction specifications be given in terms of three parameters: the compaction energy (Standard or Modified Proctor), the desired dry density expressed as a percentage of the maximum dry density, and the compaction moisture content expressed as a range (+ or -) with respect to the optimum moisture content. For example, since the input energy of Modified Proctor is greater than the input energy of Standard Proctor (see Table 5-13) the Modified Proctor curve plots above the Standard Proctor curve so that 95% of MPC  $\gamma_{d-max}$  may be greater than 100% of SPC  $\gamma_{d-max}$ . Likewise, a compaction moisture content of 1 or 2% above optimum for modified Proctor compaction may be below the standard Proctor optimum moisture content.

Unfortunately, laboratory compaction curves mainly serve as guidelines for field compaction. This approach is inconsistent because the impact type of energy input in the laboratory is not the same as the type of energy delivered by the equipment commonly used in construction. Figure 5-32 illustrates this point by presenting the types of compactive effort (static, vibratory, kneading) corresponding to the equipment typically used in practice. Note that none of the compaction processes in Figure 5-32 involves impact type of energy that is used to determine the compaction characteristics of the soils in a laboratory SPC or MPC test.

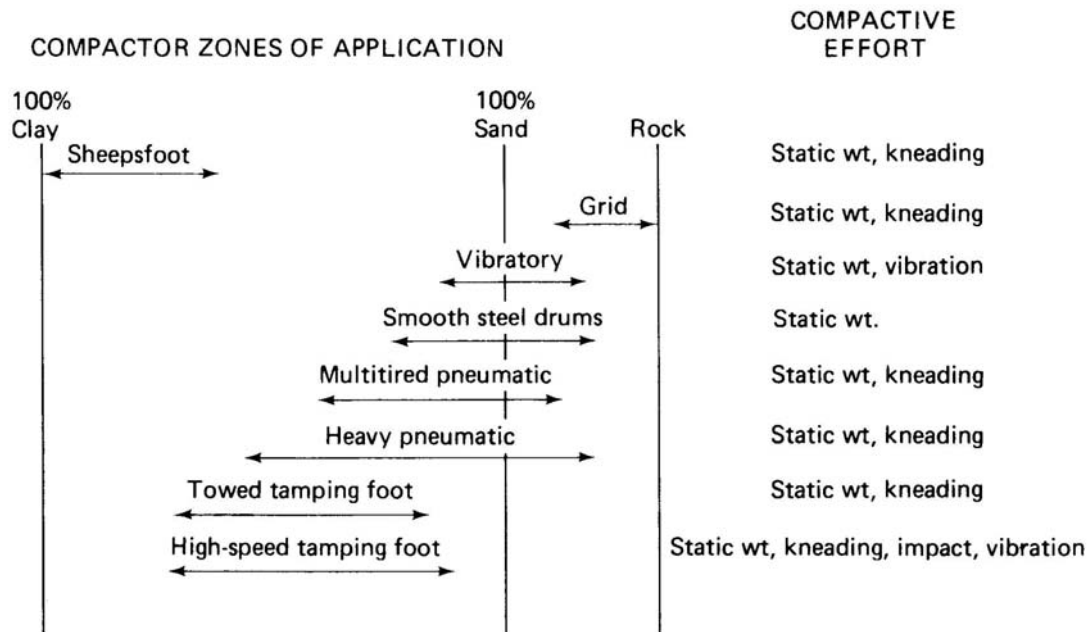


**Figure 5-32. Compactors recommended for various types of soil and rock (Schroeder, 1980).**

Due to the obvious disconnect between the types of energy in the laboratory and the field, some method is needed to express the laboratory-measured compaction parameters, i.e., maximum dry unit weight ( $\gamma_{d-max}$ ) and optimum moisture content ( $w_{opt}$ ), in terms of field compaction. Most commonly, this relationship is achieved by so-called **performance based or end-product specifications** wherein a certain **relative compaction, RC**, also known as **percent compaction**, is specified. The RC is simply the ratio of the desired field dry unit weight,  $\gamma_{d field}$ , to the maximum dry density measured in the laboratory,  $\gamma_{d max}$ , expressed in percent as follows:

$$RC = \frac{\gamma_{d field}}{\gamma_{d max}} \times 100\% \quad 5-19$$

The relative compaction, RC, is not the same as relative density,  $D_r$ , that was defined in Chapter 2. Relative density applies only to granular soils with fines less than 12% (ASTM D 2049), while relative compaction is used across a wide variety of soils. Lee and Singh (1971) published the following relationship between RC and  $D_r$  based on a statistical evaluation of 47 different granular soils compacted by using Modified Proctor energy (Wright, *et al.*, 2003).

$$D_r = 0\% \text{ for } RC = 80\%$$

$$D_r = 100\% \text{ for } RC = 100\%$$

Assuming a linear interpolation, the above relationship can be expressed as follows:

$$D_r(\%) = 5[RC(\%) - 80] \quad 5-20$$

or

$$RC(\%) = 80 + \frac{D_r(\%)}{5} \quad 5-21$$

In terms of Standard Proctor, Equations 5-20 and 5-21 are approximately as follows:

$$D_r(\%) = 5[RC(\%) - 85] \quad 5-22$$

or

$$RC(\%) = 85 + \frac{D_r(\%)}{5} \quad 5-23$$

Figure 5-33 presents the above equations in a graphical format. Table 5-14 presents the values of  $D_r$  for values of RC values ranging from 85% to 100% for MPC and from 90% to 105% for SPC.

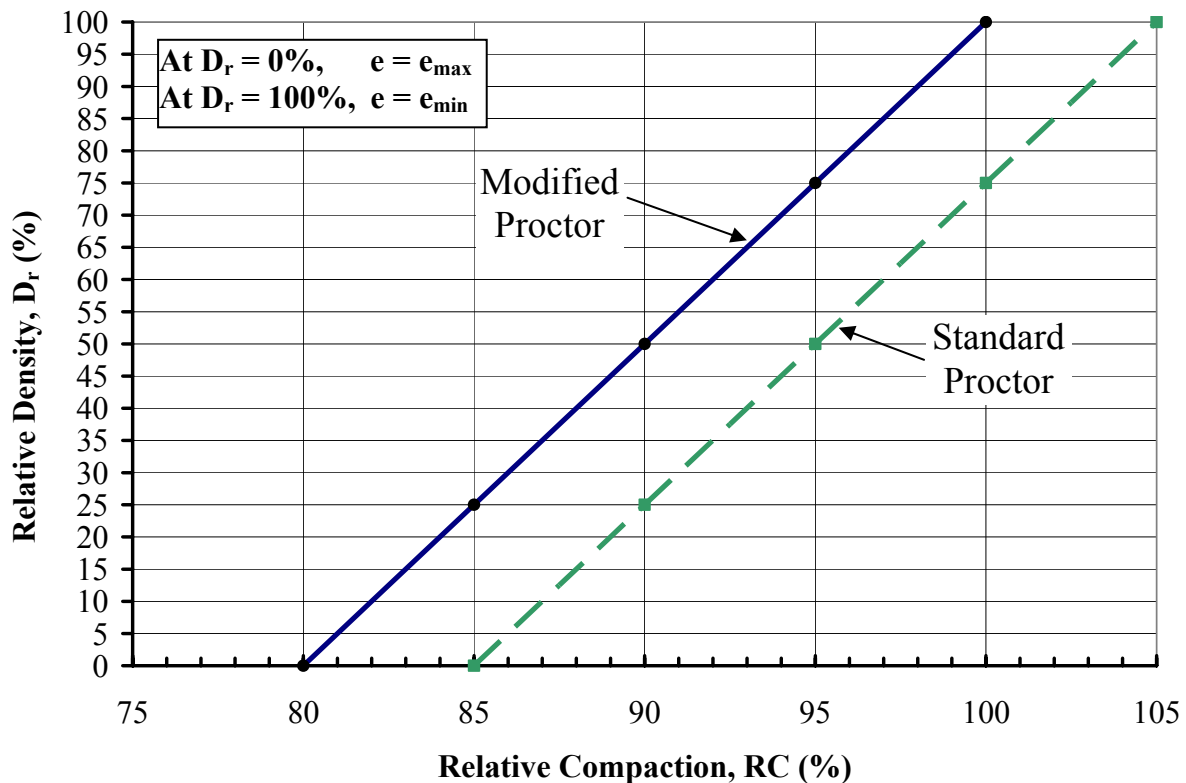


**Figure 5-33. Relative density, relative compaction and void ratio concepts.**

**Table 5-14**  
**Some values of  $D_r$  as a function of RC**  
**based on Modified and Standard Proctor Compaction Test**

RC (%) MPC (SPC)*	$D_r$ (%)	RC (%) MPC (SPC)*	$D_r$ (%)	RC (%) MPC (SPC)*	$D_r$ (%)
85 (90)	25	90 (95)	50	95 (100)	75
86 (91)	30	91 (96)	55	96 (101)	80
87 (92)	35	92 (97)	60	97 (102)	85
88 (93)	40	93 (98)	65	98 (103)	90
89 (94)	45	94 (99)	70	99 (104)	95
				100 (105)	100
* MP: Modified Proctor; SP: Standard Proctor					

Figure 5-33 and Table 5-14 indicates that for every 1% increase in RC, the increase in  $D_r$  is 5% regardless of compaction energy. This is rather significant when it is realized that the shear strength parameter,  $\phi$ , of granular soils is a direct function of relative density as shown in Figure 5-22 and as illustrated by the following simple computations:

- Based on Figure 5-22, the angle of internal friction for well-graded sands (SW soils) for values of  $D_r$  between 50% and 100% varies from 33° to 41°. From Table 5-14, values of  $D_r$  between 50% and 100% correspond to RC values of 90 and 100%, respectively for Modified Proctor and 95 and 105%, respectively for Standard Proctor. In other words, for SW soils, for every 1% increase in RC, the angle of internal friction increases by 0.8°.
- Alternatively, the increase in the coefficient of friction,  $\tan \phi$ , would be  $\tan(41^\circ) / \tan(33^\circ) = 1.33$  or a 33% increase over a 10% change in RC. In other words, there is a 3.3% increase in shear strength for every 1% increase in RC.

Select materials are often specified in the construction of transportation facilities such as embankments, foundations, and pavement sub-bases and bases. The select materials are granular soils as discussed in Chapters 6 (Slope Stability), 7 (Approach Roadway Deformations), 8 (Shallow Foundations) and 10 (Earth Retaining Structures). The above simple example illustrates the importance of carefully specifying RC for such materials. RC values of 90 to 100% of standard Proctor values are commonly used. Based on Table 5-14, this range of RC corresponds to a  $D_r$  between 25% and 75%.

For most transportation applications, the RC value is prescribed in **performance based specifications**. In this case, it does not matter which equipment or type of compaction energy the contractor chooses to use as long as the end-product meets the specified RC. The prudent contractor would choose the equipment according to the type of soil. Often the contractor chooses to use the equipment he/she owns or is cheapest to lease or rent. Unfortunately, this equipment may not always be the most efficient equipment for the work. Figure 5-32 can be used as a preliminary guide in selecting the type of equipment and mode of compaction energy as a function of soil type. In Figure 5-32 the “100%” above the word clay on the left and the word sand on the right indicates boundaries for the range of soils types in between, e.g. 100% clay means that the soil to be compacted is all fine grained, therefore use of a sheepsfoot roller is recommended. The figure also suggests that a sheepsfoot roller can be used for various soil mixtures consisting of up to approximately 35% fine grained soils and 70 % coarse grained soils.

An example of the influence of the choice of compaction equipment and energy is shown in Figure 5-34. Assume that Curve 1 is obtained from laboratory tests to develop the compaction curve for a borrow material that the contractor has identified for a given project. Further assume that the specification for the project requires that  $RC = 90\%$ . If M represents the point of maximum dry density,  $\gamma_{dmax}$ , then  $RC=90\%$  would mean that Points P and Y represent the limits of Curve 1 within which the contractor has to operate. In other words, the contractor cannot use compaction moisture contents less than a or c on the compaction moisture content axis.

To properly evaluate the choice of the compaction equipment, the contractor should perform compaction tests at various RC values in the laboratory to develop a line of optimums and a family of curves similar to Curve 2 and 3 shown in Figure 5-34. Once this data is developed, then it can be observed from Figure 5-34, that the most economical water content would be that corresponding to point R along the line of optimums, i.e., the moisture content given by Point b on the X-axis. Point R represents the minimum compactive effort to attain  $RC=90\%$ . To avoid inadequate compaction and risk failed field quality control tests, a prudent contractor usually aims to achieve somewhat higher dry density. Thus, the contractor often chooses to select a target curve similar to Curve 2 and aim to maintain moisture content in Zone B.

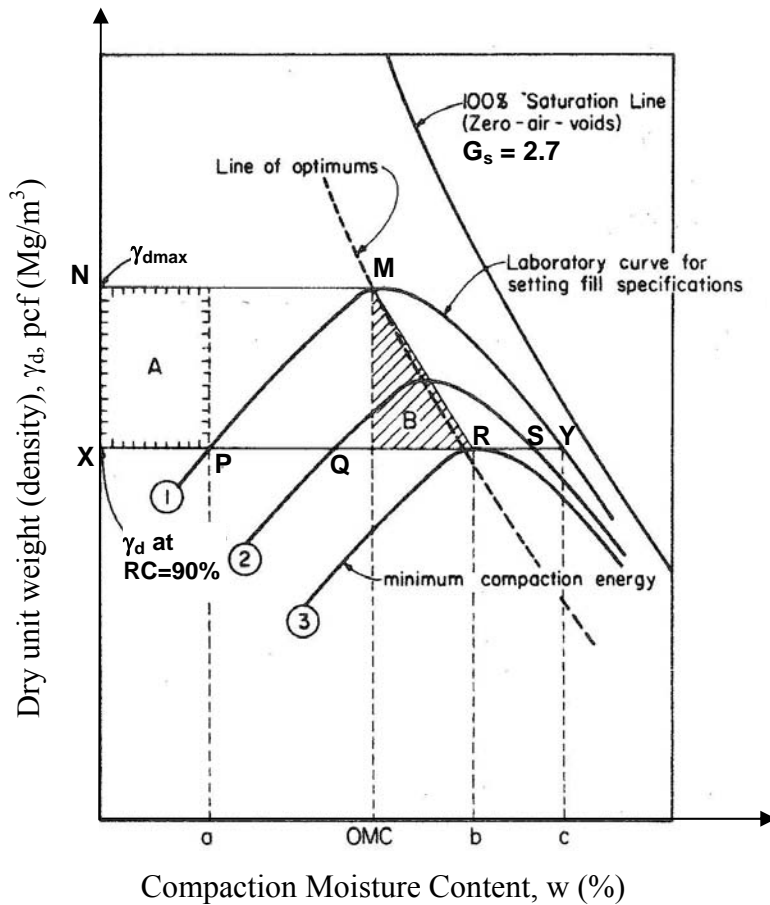


**Figure 5-34. Example evaluation of economical field compaction conditions (after Bowles, 1979)**

#### 5.8.4 Engineering Characteristics of Compacted Soils

Typical values for the engineering characteristics of compacted soils are given in Table 5-15. The values of the engineering properties refer to soils compacted to maximum dry density by using the standard Proctor test. The data in Table 5-15 are based on more than 1500 soil tests performed by the Bureau of Reclamation in Denver, CO. The large majority of soils were from 17 western states in the U.S. with some foreign soils (USBR, 1960). The background information for the values in Table 5-15 is given in the notes section of the table.

**Table 5-15**  
**Average engineering properties of compacted inorganic soils (after USBR, 1960)**

USCS	Standard Proctor Compaction (ASTM D 698/AASHTO T 99)		As Compacted Cohesion, c' psi (kPa)	Saturated Cohesion, c' <sub>sat</sub> psi (kPa)	Friction Angle, φ' (deg)	Void Ratio, e [Permeability, k (ft/yr)]
	Maximum Dry Density, pcf (kN/m <sup>3</sup> )	Optimum Moisture Content (%)				
GW	>119 (>18.7)	<13.3	*	*	>38	* [27,000±13,000]
GP	>110 (>17.3)	<12.4	*	*	>37	* [64,000±34,000]
GM	>114 (>17.9)	<14.5	*	*	>34	* [>0.3]
GC	>115 (>18.1)	<14.7	*	*	>31	* [>0.3]
SW	119±5 (18.7±0.8)	13.3±2.5	5.7±0.6 (39±4)	*	38±1	0.37±* [*]
SP	110±2 (17.3±0.3)	12.4±1.0	3.3±0.9 (23±6)	*	37±1	0.50±0.03 [>15.0]
SM	114±1 (17.9±0.2)	14.5±0.4	7.4±0.9 (51±6)	2.9±1.0 (20±7)	34±1	0.48±0.02 [7.5±4.8]
SM-SC	119±1 (18.7±0.2)	12.8±0.5	7.3±3.1 (50±21)	2.1±0.8 (14±6)	33±4	0.41±0.02 [0.8±0.6]
SC	115±1 (18.1±0.2)	14.7±0.4	10.9±2.2 (75±15)	1.6±0.9 (11±6)	31±4	0.48±0.01 [0.3±0.2]
ML	103±1 (16.2±0.2)	19.2±0.7	9.7±1.5 (67±10)	1.3±* (9±*)	32±2	0.63±0.02 [0.59±0.23]
ML-CL	109±2 (17.1±0.3)	16.8±0.7	9.2±2.4 (63±17)	3.2±* (22±*)	32±3	0.54±0.03 [0.13±0.07]
CL	108±1 (17.0±0.2)	17.3±0.3	12.6±1.5 (87±10)	1.9±0.3 (13±2)	28±2	0.56±0.01 [0.08±0.03]
MH	82±4 (12.9±0.6)	36.3±3.2	10.5±4.3 (72±30)	2.9±1.3 (20±9)	25±3	1.15±0.12 [0.16±0.10]
CH	94±2 (14.8±0.3)	25.5±1.2	14.9±4.9 (103±34)	1.6±0.86 (11±6)	19±5	0.80±0.04 [0.05±0.05]

Notes:

1. The entry ± indicates 90 percent confidence limits of the average value; \* denotes insufficient data.
2. For permeability, 1 ft/yr ≈ 10<sup>-6</sup> cm/sec.
3. All shear strengths, void ratios and permeabilities were determined on samples prepared at Standard Proctor maximum dry density and optimum moisture content.
4. The values of cohesion, c', and friction angle, φ', are based on a straight-line Mohr strength envelope on an effective stress basis. The value c'<sub>sat</sub> was obtained by saturating the sample and shearing it to failure. Consolidated-undrained (CU) triaxial tests were used to determine all the shear strengths.
5. Since all laboratory tests, except large-sized permeability tests, were performed on the minus No. 4 (4.75 mm) fraction of soil, data on average values for gravels are not available for most properties. However, an indication as to whether these average values will be greater than or less than the average values for the corresponding sand group are given in the table (note entries with > or < symbol).
6. Void ratio was derived from the maximum dry density and specific gravity of the soil.
7. In USCS, there are no upper boundaries of liquid limit of MH and CH soils. The maximum limits for MH and CH soils tested by USBR (1960) were 81% and 88%, respectively. Soils with higher liquid limits than these will have inferior engineering properties.

#### 5.8.4.1 Effect of Increase in Moisture Content on Shear Strength of Compacted Soils

The cohesion values,  $c'$  (as-compacted) and  $c'_{\text{sat}}$  (after saturation of compacted soil) listed in Table 5-15 are instructive in the context of the apparent cohesion concept discussed in Section 5.5.1.2. In the soil's compacted state at optimum moisture content (OMC), the capillary stresses and the apparent mechanical forces assume their peak values at that particular compaction energy. Capillary stress, as discussed in Section 5.5.1.2, is due to surface tension in the water between individual soil grains. The magnitude of capillary stress is larger in fine-grained soils than coarse-grained soils as demonstrated by the increasing values of  $c'$  in Table 5-15 as the soil type changes from granular to fine-grained.

The same trend is observed with the  $c'_{\text{sat}}$  values. However, the values of  $c'_{\text{sat}}$  are approximately 10% (for CH soils) to 40% (for SM soils) of the corresponding  $c'$  values. This drastic reduction in cohesive strength is attributable to the effect of capillary stresses being significantly reduced by the increase in moisture content required to reach saturation resulting in much lower apparent cohesive strengths. The reduction may also represent loss of apparent mechanical forces due to reduction in the interlocking of the particles because of the lubricating effect of water.

**Based on the above discussions, it is important to ensure that compacted soils are protected against increases in moisture content because the strength of such soils will decrease with associated detrimental effects on the facilities they support.**

### 5.9 ELASTIC PROPERTIES OF SOILS

The stress-strain behavior of soils and rocks is highly nonlinear or inelastic. However, as indicated in Chapter 2, elastic theory provides a convenient first order approximation to stresses and strains induced in soils by external loads. A pair of elastic constants is required when elastic theory is used to solve such problems, e.g., elastic modulus ( $E$ ) and Poisson's ratio ( $\nu$ ), or shear modulus ( $G$ ) and bulk modulus ( $B$ ), or some other pair of elastic constants. The pair of  $E$  and  $\nu$  is most widely used since both parameters are readily measurable. Consequently, many of the elastic equations in geotechnical engineering are formulated with this pair. Therefore, typical values of  $E$  and  $\nu$  for soils are presented in this section.

The elastic properties of soils may be measured from laboratory stress-strain curves such as those shown in Figure 5-16. The elastic properties,  $E_s$  and  $\nu$ , of a soil may be estimated from empirical relationships presented in Table 5-16 for **preliminary** design or for final design

where the prediction of deformation is not critical to the performance of the structure, i.e., when the structural design can tolerate the potential inaccuracies inherent in the correlations. The definition of  $E_s$  is not always consistent for the various correlations and methods of in-situ measurement. FHWA (2002a) provides additional details regarding the definition and determination of  $E_s$ . Where evaluation of elastic settlement is critical to the design of the foundation or selection of the foundation type, in-situ methods such as pressuremeter or dilatometer tests should be used for evaluating the modulus of the impacted strata.

The modulus of elasticity for normally consolidated cohesionless soils tends to increase with depth. An alternative method of defining the soil modulus for granular soils is to assume that the modulus,  $E_s$ , increases linearly with depth, starting at zero at the ground surface, in accordance with the following equation:

$$E_s \text{ (tsf)} = n_h \times z \quad 5-24$$

where:  $n_h$  = rate of increase of soil modulus with depth as defined in Table 5-17 (tsf/ft)  
 $z$  = depth in feet below the ground surface (ft)

The formulation provided in Equation 5-24 is used primarily for analysis of lateral response or buckling of deep foundations.

## **5.10 COMMON SENSE GUIDELINES FOR LABORATORY TESTING OF SOILS**

Sampling and testing of soils is one of the first and most important steps in the design and construction of all types of structures. Omissions or errors introduced here, if undetected, will be carried through the process of design and construction and will often result in costly and possibly unsafe facilities. Table 5-18 lists topics that should be considered for proper handling of samples, preparation of test specimens, and laboratory test procedures. Table 5-18 should in no way be construed as being a complete list of guidelines to avoid possible errors and omissions in handling or testing of soil specimens; there are more. These are just some of the more common ones.

**Table 5-16**  
**Elastic constants of various soils (after AASHTO 2004 with 2006 Interims)**

Soil Type	Typical Range of Young's Modulus Values, $E_s$ (tsf)	Poisson's Ratio, $\nu$
Clay: Soft sensitive Medium stiff to stiff Very stiff	25-150 150-500 500-1,000	0.4-0.5 (undrained)
Loess	150-600	0.1-0.3
Silt	20-200	0.3-0.35
Fine Sand: Loose Medium dense Dense	80-120 120-200 200-300	0.25
Sand: Loose Medium dense Dense	100-300 300-500 500-800	0.20-0.36 0.30-0.40
Gravel: Loose Medium dense Dense	300-800 800-1,000 1,000-2,000	0.20-0.35 0.30-0.40
<b>Estimating <math>E_s</math> from SPT N-value</b>		
Soil Type	$E_s$ (tsf)	
Silts, sandy silts, slightly cohesive mixtures	4 $N_{160}$	
Clean fine to medium sands and slightly silty sands	7 $N_{160}$	
Coarse sands and sands with little gravel	10 $N_{160}$	
Sandy gravel and gravels	12 $N_{160}$	
<b>Estimating <math>E_s</math> (tsf) from <math>q_c</math> static cone resistance</b>		
Sandy soils	$2q_c$ where ( $q_c$ is in tsf)	
Note: 1 tsf = 95.76 kPa		

**Table 5-17**  
**Rate of increase of soil modulus with depth  $n_h$  (tsf/ft) for sand**  
**(AASHTO 2004 with 2006 Interims)**

Consistency	Dry or Moist	Submerged
Loose	30	15
Medium	80	40
Dense	200	100
Note: 1 tsf/ft = 314.7 kPa/m		

**Table 5-18**  
**Common sense guidelines for laboratory testing of soils**

1. Protect samples to prevent moisture loss and structural disturbance.
2. Carefully handle samples during extrusion; samples being extruded should be properly supported upon their exit from the tube.
3. Avoid long term storage of soil samples in Shelby tubes.
5. Properly number and identify samples.
5. Store samples in properly controlled environments.
6. Visually examine and identify soil samples after removal of smear from the sample surface.
7. Use pocket penetrometer or miniature vane only for an indication of consistency not strength.
8. Carefully select "representative" specimens for testing.
9. Have a sufficient number of samples to select from.
10. Always consult the field logs for proper selection of samples.
11. Recognize disturbances caused by sampling, the presence of cuttings, drilling mud or other foreign matter.
12. Do not depend solely on the visual identification of soils for classification.
13. Always perform organic content tests when classifying soils as peat or organic. Visual classifications of organic soils may be very misleading.
15. Do not dry soils in overheated or underheated ovens.
15. Discard old worn-out equipment; old sieves for example, particularly fine (<No. 40) mesh ones need to be inspected and replaced often; worn compaction molds or compaction hammers should be checked and replaced if needed. An error in the volume of a compaction mold is amplified 30x when translated to unit volume.
16. Performance of Atterberg limits tests requires carefully adjusted drop height of the liquid limit machine and proper rolling of plastic limit specimens.
17. Do not use tap water for tests where distilled water is specified.
18. Properly cure stabilization test specimens.
19. Never assume that all samples are saturated as received.
20. Perform saturation by applying properly staged back pressures of adequate magnitude.
21. Use properly fitting o-rings, membranes, etc. in triaxial or permeability tests.
22. Evenly trim ends and sides of undisturbed samples.
23. Be careful to identify and report slickensides and natural fissures.
25. Do not mistakenly identify failures due slickensides as shear failures.
25. Do not use stress-strain curves from unconfined compression test results to determine elastic moduli.
26. Incremental loading of consolidation tests should be performed only after the completion of the primary stage.
27. Use proper loading rate for strength tests.
28. Do not guesstimate e-log p curves from accelerated, incomplete consolidation tests.
29. Avoid "reconstructing" soil specimens, disturbed by sampling or handling, for undisturbed testing.
30. Correctly label all laboratory test specimens.
31. Do not take shortcuts by using non-standard equipment or non-standard test procedures.
32. Periodically calibrate testing equipment and maintain calibration records.
33. Always test a sufficient number of samples to obtain representative results in variable material.
34. Take proper precautions to assure the safety of personnel when performing any test procedure.

## 5.11 LABORATORY TESTS FOR ROCK

### 5.11.1 Introduction

This section provides information on common laboratory test methods for rock including testing equipment, general procedures related to each test, and parameters measured by the tests. Table 5-19 provides a list of commonly performed laboratory tests for rock associated with typical projects for highway applications. Although other laboratory test methods for rock are available including triaxial strength testing, rock tensile strength testing, and durability testing related to rock soundness, most design procedures for structural foundations and slopes on or in rock are developed based on empirical rules related to RQD, degree of fracturing, and the unconfined compressive strength of the rock. The use of more sophisticated laboratory testing for rock properties is usually limited to the most critical projects. Details on other laboratory testing procedures for rock are provided in FHWA, (1997). Table 5-20 provides summary information on the typical rock index and performance tests.

**Table 5-19**  
**Common rock tests performed in the laboratory**

<b>Test Category</b>	<b>Name of Test</b>	<b>ASTM Test Designation</b>
Point Load Strength	Suggested method for evaluating point-load strength	D 5731
Compressive Strength	Compressive strength of intact rock core specimen (in unconfined compression)	D 2938
Direct Shear Strength	Laboratory direct shear strength tests for rock specimens under constant normal stress	D 5607
Durability	Slake durability of shales and similar weak rocks	D 4644
Strength-Deformation	Elastic moduli of intact rock core specimens in uniaxial compression	D 3148

**Table 5-20**

**Summary information on laboratory test methods for rock (FHWA, 2002a)**

<b>Test</b>	<b>Procedure</b>	<b>Applicable Rock Types</b>	<b>Applicable Rock Properties</b>	<b>Limitations / Remarks</b>
Point-Load Strength Test	Rock specimens in the form of core, cut blocks, or irregular lumps are broken by application of concentrated load through a pair of spherically truncated, conical platens.	Generally not appropriate for rock with uniaxial compressive strength less than 520 ksf (25 MPa)	Provides an index of uniaxial compressive strength	Can be performed in the field with portable equipment or in the laboratory; in soft or weak rock, test results need to be adjusted to account for platen indentation
Unconfined Compressive Strength of Intact Rock Core	A cylindrical rock specimen is placed in a loading apparatus and sheared under axial compression with no confinement until peak load and failure are obtained.	Intact rock core	Uniaxial compressive strength	Simplest and fastest test to evaluate rock strength; fissures or other anomalies will often cause premature failure
Laboratory Direct Shear Test	A rock specimen is placed in the lower half of the shear box and encapsulated in either synthetic resin or mortar. The specimen must be positioned so that the line of shear force lies in the plane of the discontinuity to be investigated. The specimen is then mounted in the upper shear box and the normal load and shear force are applied.	Used to assess peak and residual shear strength of discontinuity	Peak and residual shear strength	May need to perform in-situ direct shear test if design is controlled by potential slip along a discontinuity filled with very weak material
Elastic Moduli of Intact Rock Core	Procedure is similar to that for unconfined compressive strength of intact rock. Lateral strains are also measured	Intact rock core	Modulus and Poisson's ratio	Modulus values (and Poisson's ratio) vary due to nonlinearity of stress-strain curve.
Slake Durability	Dried fragments of rock are placed in a drum made of wire mesh that is partially submerged in distilled water. The drum is rotated, the sample dried, and the sample is weighed. After two cycles of rotating and drying, the weight loss and the shape of size of the remaining rock fragments are recorded.	Shale or other soft or weak rocks	Index of degradation potential of rock	

### 5.11.2 Point-Load Strength Test

The point load strength test is used to estimate the unconfined compressive strength of rock. Both core samples and fractured rock samples can be tested. The test is conducted by compressing a piece of the rock between two points on cone-shaped platens (see Figure 5-35) until the rock specimen breaks in tension between these two points. Each of the cone points has a 1/5 in (5 mm) radius of curvature and the cone bodies themselves include a 60° apex angle. The equipment is portable, and tests can be carried out quickly and inexpensively in the field. Because the point load test provides an index value for the compressive strength, usual practice is to calibrate the results with a limited number of uniaxial compression tests on prepared core samples. The point load test is also used with other index values to assess the degradation potential of shales.

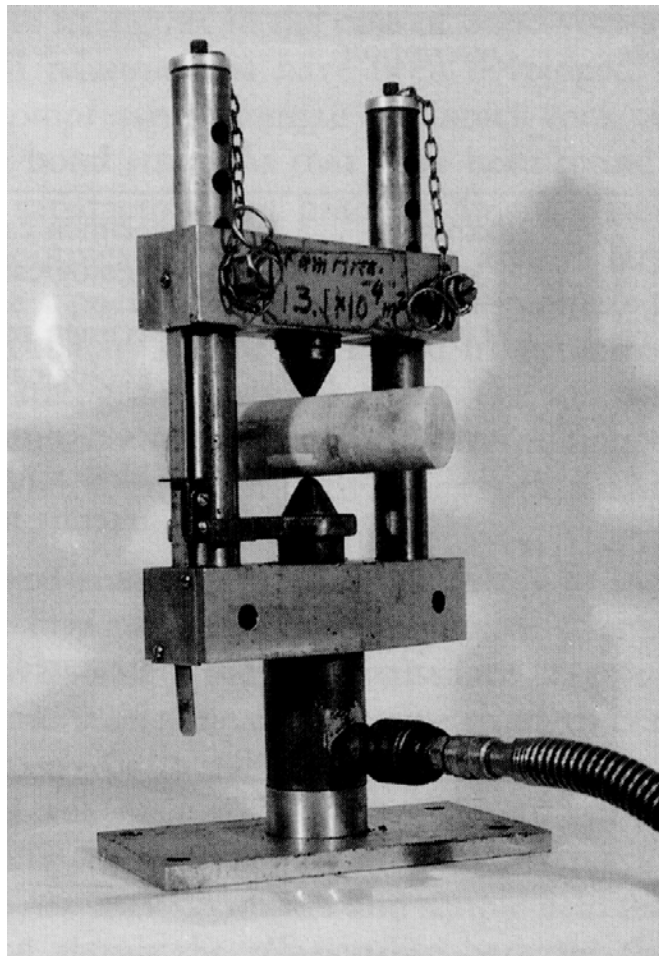


**Figure 5-35. Point load strength test equipment (Wyllie, 1999).**

If the distance between the contact points of the platens is  $D$  and the breaking load is  $P$ , then the point load strength,  $I_s$ , is calculated as:

$$I_s = \frac{P}{D_e^2} \quad 5-25$$

where  $D_e$  is the equivalent core diameter given by:

- (1)  $D_e = D^2$  for diametral tests; or
- (2)  $D_e = 4 \times A$  for axial, block, or lump tests where  $A = W \times D$ . The area  $A$  is the minimum cross-sectional area of a lump sample for a plane through the platen contact points where  $W$  is the specimen width.

The size-corrected point load strength index,  $I_{s(50)}$  of a rock specimen is defined as the value of  $I_s$  that would have been measured by a diametral test with  $D = 2$  in (50 mm). For tests performed on specimens other than 2 in (50 mm) in diameter, the results can be standardized to the size-corrected point load strength index according to:

$$I_{s(50)} = k_{PLT} I_s \quad 5-26$$

The value of the size correction factor,  $k_{PLT}$ , is given by:

$$k_{PLT} = \left( \frac{D}{50} \right)^{0.45} \quad (D \text{ in mm}) \quad 5-27$$

It has been found that, on average, the uniaxial compressive strength,  $\sigma_c$ , is about 20 to 25 times the point load strength index, with a value of 24 commonly used, i.e.,

$$\sigma_c = 24 I_{s(50)} \quad 5-28$$

However, tests on many different types of rock show that the  $\sigma_c / I_{s(50)}$  ratio can vary between 15 and 50, especially for anisotropic rocks. Consequently, the most reliable results are obtained if a series of uniaxial calibration tests are carried out. Point load test results are not acceptable if the failure plane lies partially along a pre-existing fracture in the rock, or is not coincident with the line between the platens. For tests in weak rock where the platens indent

the rock, the test results should be adjusted by measuring the amount of indentation and correcting the distance D (Wyllie, 1999).

### **5.11.3 Unconfined Compressive Strength of Intact Rock Core**

The unconfined compressive strength of intact rock core can be evaluated by using ASTM D 2938. In this test, rock specimens of regular geometry, generally rock cores, are used. The rock core specimen is cut to length so that the length to diameter ratio is 2.5 to 3.0 and the ends of the specimen are machined flat. ASTM D 2938 provides tolerance requirements related to the flatness of the ends of the specimen, the perpendicularity of the ends of the specimens, and the smoothness of the length of the specimen. The specimen is placed in a loading frame, see Figure 5-36a. Axial load is then continuously applied to the specimen at a uniform rate until peak load and failure are obtained. The unconfined or uniaxial compressive strength of the specimen is calculated by dividing the maximum load carried by the specimen during the test by the initial cross-sectional area of the specimen.

This test is more expensive than the point load strength test, but it is also more accurate with respect to in situ strength. Careful consideration of the design requirements should be made before deciding which test to perform, the unconfined compression test, a performance test, or the simpler point load strength test, an index test.

### **5.11.4 Elastic Modulus of Intact Rock Core**

The test to determine the elastic modulus of intact rock is performed similarly to the unconfined compressive test discussed previously, except that deformation is monitored during application of load. This test is performed when it is necessary to estimate both the elastic modulus and the Poisson's ratio of the intact rock core. Because of this dual purpose, it is common to measure both axial (or vertical) and lateral (or diametral) strain during compression. It is preferable to use strain gauges glued directly to the rock surface (see Figure 5-36b) as compared to LVDTs mounted on the platens since slight imperfections at the contact between the platens and the rock may lead to movements that are not related to strain in the rock (Wyllie, 1999).



(a)



(b)

**Figure 5-36. (a) Unconfined compression strength test on intact rock core, (b) Use of strain gage on intact rock core sample for measurement of stress-strain characteristics. (Photographs courtesy of Geomechanics Laboratory, University of Arizona).**

### 5.11.5 Laboratory Direct Shear Test

The apparatus and procedures for direct shear testing are discussed in ASTM D 5607. The direct shear test is typically used to evaluate the shear strength of a rock discontinuity. Overall, the equipment for the direct shear test on rock is similar to that for soil including a direct shear testing machine, a device for applying normal pressure, and vertical and horizontal displacement monitoring devices. A schematic of the test set up is shown in Figure 5-37. For testing rock specimens, an encapsulating material such as a high strength gypsum cement is poured around the specimen in the upper and lower holding ring. The specimen is sheared as one holding ring is displaced horizontally with respect to the other such that the discontinuity surface is exactly parallel to the direction of the shear load. Load cells are used to monitor the shear force and LVDTs or dial gauges are used to monitor both horizontal and vertical deformation. Multiple LVDTs should be used to monitor vertical deformation and potential rotation of the specimen in the vertical plane.

Typically, the results of a direct shear test on rock are presented on two separate plots: one a plot of shear stress versus shear displacement and the other a plot of normal displacement versus shear displacement. Normal stresses should be adjusted to account for potential decreases in the shear contact area. After the sample is sheared, the sample is reset to its original position, the normal load is increased, and another test is performed. Each test will produce a pair of shear stress and normal stress values for both peak and residual conditions. The friction angle of the discontinuity surface can be evaluated from this data.

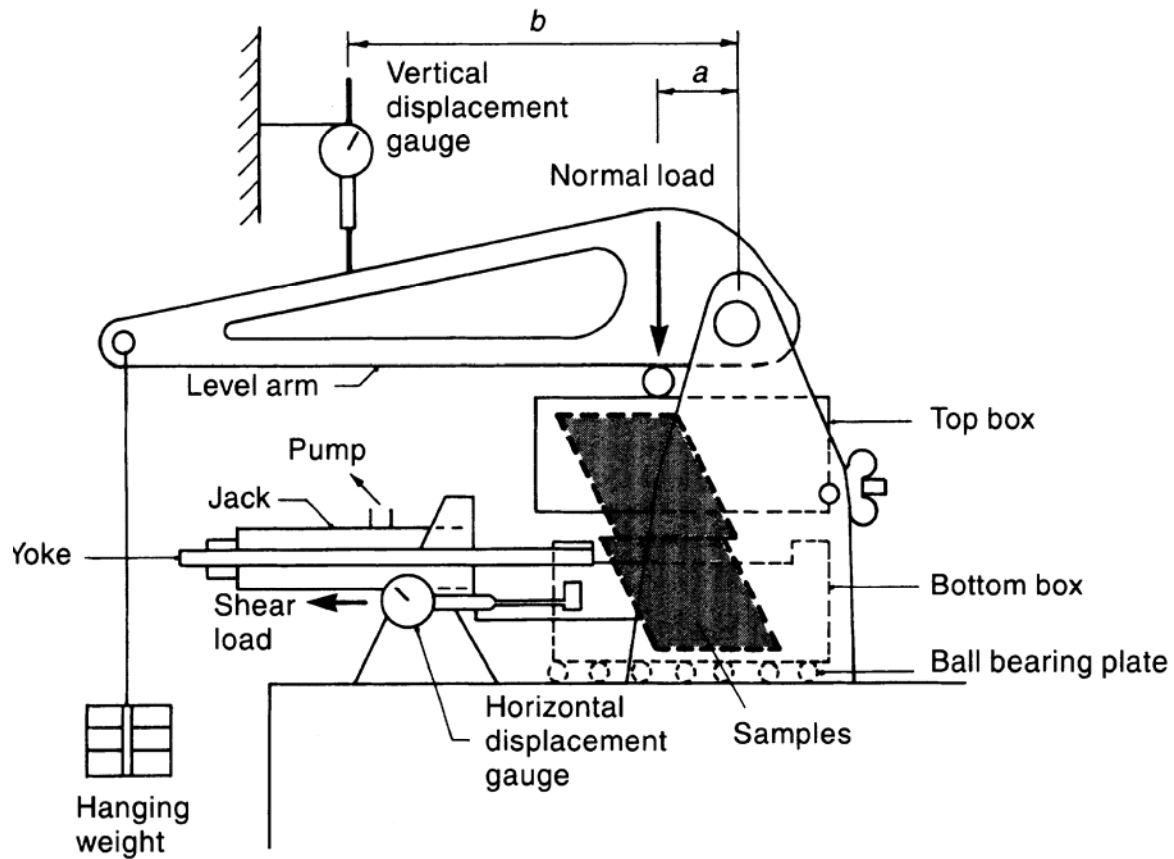


Figure 5-37. Laboratory direct shear testing equipment for rock (Wyllie, 1999).

## 5.12 ELASTIC PROPERTIES OF ROCKS

Preliminary estimates of the elastic modulus of intact rock can be made from Table 5-21. Note that some of the rock types identified in the table are not present in the U.S. As discussed in Chapter 4, **it is extremely important to use the elastic modulus of the rock mass for computation of in-situ displacements of rock under applied loads. Use of the intact modulus will result in unrealistic and unconservative estimates of displacement.** Section 5.12.1 presents some guidance for estimating the elastic modulus of a rock mass.

Poisson's ratio for rock should be determined from tests on intact rock core. Where tests on rock core are not practical, Poisson's ratio may be estimated from Table 5-22.

**Table 5-21**  
**Summary of elastic moduli for intact rock (AASHTO 2004 with 2006 Interims).**

Rock Type	No. of Values	No. of Rock Types	Elastic Modulus, $E_i$ (psi $\times 10^6$ )			Standard Deviation (psi $\times 10^6$ )
			Maximum	Minimum	Mean	
Granite	26	26	15.5	0.93	7.64	3.55
Diorite	3	3	16.2	2.48	7.45	6.19
Gabbro	3	3	12.2	9.8	11.0	0.97
Diabase	7	7	15.1	10.0	12.8	1.78
Basalt	12	12	12.2	5.20	8.14	2.60
Quartzite	7	7	12.8	5.29	9.59	2.32
Marble	14	13	10.7	0.58	6.18	2.49
Gneiss	13	13	11.9	5.13	8.86	2.31
Slate	11	2	3.79	0.35	1.39	0.96
Schist	13	12	10.0	0.86	5.97	3.18
Phyllite	3	3	2.51	1.25	1.71	0.57
Sandstone	27	19	5.68	0.09	2.13	1.19
Siltstone	5	5	5.76	0.38	2.39	1.65
Shale	30	14	5.60	0.001	1.42	1.45
Limestone	30	30	13.0	0.65	5.7	3.73
Dolostone	17	16	11.4	0.83	5.22	3.44

Note: 1 psi = 6.895 kPa

**Table 5-22**  
**Summary of Poisson's ratio for intact rock (AASHTO 2004 with 2006 Interims)**

Rock Type	No. of Values	No. of Rock Types	Poisson's Ratio, $\nu$			Standard Deviation
			Maximum	Minimum	Mean	
Granite	22	22	0.39	0.09	0.20	0.08
Gabbro	3	3	0.20	0.16	0.18	0.02
Diabase	6	6	0.38	0.20	0.29	0.06
Basalt	11	11	0.32	0.16	0.23	0.05
Quartzite	6	6	0.22	0.08	0.14	0.05
Marble	5	5	0.40	0.17	0.28	0.08
Gneiss	11	11	0.40	0.09	0.22	0.09
Schist	12	11	0.31	0.02	0.12	0.08
Sandstone	12	9	0.46	0.08	0.20	0.11
Siltstone	3	3	0.23	0.09	0.18	0.06
Shale	3	3	0.18	0.03	0.09	0.06
Limestone	19	19	0.33	0.12	0.23	0.06
Dolostone	5	5	0.35	0.14	0.29	0.08

### 5.12.1 Elastic Modulus of Rock Mass

The elastic modulus of a rock mass ( $E_m$ ) shall be taken as the lesser of the intact modulus of a sample of rock core ( $E_i$ ) or the modulus computed from one of the following equations:

$$E_m = 145000 \times [10^{(RMR-10)/40}] \quad 5-29$$

where:  $E_m$  = Elastic modulus of the rock mass (psi)

RMR = Rock Mass Rating (see Chapter 4)

Note that in almost all cases, the elastic modulus of the rock mass,  $E_m$ , is less than the elastic modulus of the intact rock,  $E_i$ .

The elastic modulus of the rock mass can also be determined from the following equation:

$$E_m = E_m/E_i \times E_i \quad 5-30$$

where  $E_i$  is the elastic modulus of the intact rock.  $E_m/E_i$  is basically a reduction factor to account for discontinuities in the rock mass and can be determined by using the guidance in

Table 5-23. In using Table 5-23, it is important that the elastic modulus for the intact rock,  $E_i$ , be determined from tests rather than by using the data in Table 5-21. For critical or large structures, determination of rock mass modulus ( $E_m$ ) by in-situ tests may be warranted. A discussion of suitable in-situ tests can be found in FHWA (2002a).

**Table 5-23**  
**Estimation of  $E_m$  based on RQD (AASHTO 2004 with 2006**  
**Interims).**

RQD (Percent)	$E_m/E_i$	
	Closed Joints	Open Joints
100	1.00	0.60
70	0.70	0.10
50	0.15	0.10
20	0.05	0.05
Note: Refer to Chapter 3 for guidance on determination of RQD and a description of rock joints.		

### 5.13 COMMON SENSE GUIDELINES FOR LABORATORY TESTING OF ROCKS

As with soils, omissions or errors introduced during laboratory testing of rock, if undetected, will be carried through the process of design and construction and will often result in costly and possibly unsafe facilities. Table 5-24 lists topics that should be considered and given proper attention so that a reasonable assessment of the rock properties will be assured and an optimization of the geotechnical investigation can be realized in terms of economy, performance, and safety. Guidance in proper handling and storage of rock cores may be found in ASTM D 5079.

**Table 5-24**  
**Common sense guidelines for laboratory testing of rocks**

1. Provide protection of samples to avoid moisture loss and structural disturbance.
2. Clearly indicate proper numbering and identification of samples.
3. Store samples in controlled environments to prevent drying, overheating & freezing.
5. Take care in the handling and selection of “representative” specimens for testing.
5. Consult the field logs while selecting test specimens.
6. Recognize disturbances and fractures caused by coring procedures.
7. Maintain trimming and testing equipment in good operating condition.
8. Use properly fitting, platens, o-rings and membranes in triaxial, uniaxial, and shear tests.
9. Maintain tolerances in trimming of ends and sides of intact cores.
10. Document frequency, spacing, conditions and infilling of joints and discontinuities.
11. Periodically calibrate instruments used to measure load, deflection, temperatures and time.
12. Use a properly-determined loading rate for strength tests.
13. Photo document samples cores, fracture patterns and test specimens for possible use in a report.
15. Carefully align and level all specimens in directional loading apparatuses and test frames.
15. Record initial baselines, offsets, and eccentricities prior to testing.
16. Save remnant rock pieces after destructive testing by uniaxial, triaxial and direct shear tests.
17. Conduct nondestructive tests (i.e., porosity, unit weight, ultrasonics) prior to destructive strength tests (compression, tensile, shear).
18. Take proper precautions to assure the safety of personnel when any test procedure is performed.

## 5.14 PRACTICAL ASPECTS FOR LABORATORY TESTING

A poor understanding sometimes exists among geologists, structural engineers, and some foundation engineers about the type and amount of laboratory testing required for design of geotechnical features whether they happen to be structural foundations or earthwork. This weakness may render subsequent analyses useless. Organizations that have neither the proper testing facilities nor trained soils laboratory personnel should contract testing to competent AASHTO/ASTM certified private testing firms. This solution can be effective only if the project foundation designer can confidently request the necessary testing and review the results to select design values. A fair estimate of the costs associated with a private testing laboratory may be obtained by assuming the following number of person-days (pd) per test and multiplying by current labor costs:

- visual description of an SPT sample including moisture content (0.05 pd),
- visual description of a tube sample including moisture content and unit weight (0.1 pd),
- classification tests (0.7 pd),
- undrained triaxial test (0.9 pd),
- drained triaxial test (2.0 pd),
- consolidation test (2.0 pd).

These values include all work required to present a completed test result to the foundation designer. Alternatively, most private testing laboratories provide a schedule of services and associated costs that can be used to obtain a more accurate estimate of the cost of a proposed laboratory test program.

Blanket consultant contracts "to perform testing necessary for design" usually result in unnecessarily large quantities of testing being performed, much of which does not apply to the project geotechnical issues. For example, if a multi span structure is crossing an area having a soft clay surface deposit underlain by sands, inordinate amounts of time and money should not be spent to determine the strength and consolidation parameters of the soft clay layer at pier and abutment locations in great detail. Generally a pile foundation will be designed by using SPT N-values and the only laboratory testing that may be needed in the soft clay layer may be to estimate drag forces on the piles. Also, non-standard strength testing such as torvanes, penetrometers, etc., which are not covered by ASTM or AASHTO standards, should not be permitted. Such devices should be used only for field index tests to determine consistency.

## 5.15 VARIABILITY OF MEASURED PROPERTIES

Chapters 3, 4 and 5 presented methodologies to perform subsurface explorations, to describe identify, and classify subsurface materials, and to implement and interpret a laboratory test program. The topics covered in these chapters are presented in the temporal sequence in which they are performed on an actual project. Therefore, the geotechnical specialist should continuously evaluate the results of laboratory tests with respect to the initial subsurface model prepared as part of Step 1 of the flow chart presented in Figure 3-1 of Chapter 3. Table 5-25 presents the values of the coefficient of variation of measured properties that should be taken into consideration as the subsurface model is finalized for engineering design. The data in Table 5-25 can be used by the geotechnical specialist as follows:

- Perform sensitivity (parametric) studies to evaluate the effect of variability in properties with respect to the subsurface profile and the type, magnitude and direction of the anticipated loading and establish the best-case and worst-case scenarios,
- Evaluate the need to perform additional explorations,
- Exercise judgment with respect to the results of engineering analyses and designs and convey the uncertainty to the project team, in particular to the structural engineer, and
- Establish the need for instrumentation to monitor the performance of the facility during and after construction .

The finalization of the subsurface model should be performed by a geotechnical specialist who is experienced in the design and construction aspects of the proposed facility. Active input should be sought from the field inspectors and the laboratory personnel who were actually involved in the collection of the data. At this stage, it is recommended that the geotechnical specialist seek a peer review from one or more **qualified and experienced** geotechnical specialist(s) with the specific purpose of having them evaluate whether or not the collected data and subsurface model is adequate to permit a cost-effective design of the facility. The experienced geotechnical specialist(s) can also provide information on potential value analysis alternatives (value engineering) for the design of the facility based on the collected data. The importance of such peer reviews cannot be overemphasized. Finally, the owner of the facility should be informed of the findings so that the owner can make decisions such as authorizing more field explorations and/or laboratory tests or modifying the facilities as appropriate based on the results of the geotechnical investigation thus far.

**Table 5-25**  
**Values of coefficient of variation, V, for geotechnical properties and in situ tests**  
**(after Duncan, 2000)**

Measured or interpreted parameter value	Coefficient of Variation, V (Note 1)
Unit weight, $\gamma$	3 to 7 %
Buoyant unit weight, $\gamma_b$	0 to 10 %
Effective stress friction angle, $\phi'$	2 to 13 %
Undrained shear strength, $s_u$	13 to 40 %
Undrained strength ratio ( $s_u/p_o$ )	5 to 15 %
Compression index, $C_c$	10 to 37 %
Preconsolidation pressure, $p_c$	10 to 35 %
Hydraulic conductivity of saturated clay, k	68 to 90 %
Hydraulic conductivity of partially-saturated clay, k	130 to 240 %
Coefficient of consolidation, $c_v$	33 to 68 %
Standard penetration blow count, N	15 to 45 %
Electric cone penetration test, $q_c$	5 to 15 %
Mechanical cone penetration test, $q_c$	15 to 37 %
Vane shear test undrained strength, $s_{uVST}$	10 to 20 %
Note 1: Coefficient of Variation, V, is defined as standard deviation divided by the average (mean) value expressed as a percentage.	

## **CHAPTER 6.0**

### **SLOPE STABILITY**

Ground stability must be assured prior to consideration of other foundation related items. Embankment foundation problems involve the support of the embankment by natural soil. Problems with embankments and structures occasionally occur that could be prevented by initial recognition of the problem and appropriate design. Stability problems most often occur when the embankment is to be built over soft soils such as low strength clays, silts, or peats. Once the soil profile, soil strengths, and depth of ground water table have been determined by field explorations and/or field and laboratory testing, the stability of the embankment can be analyzed and a factor of safety estimated. If the embankment is found to be unstable, measures can then be taken to stabilize the foundation soils.

As illustrated in Figure 6-1, there are four major types of instability that should be considered in the design of embankments over weak foundation soils. Recommendations on how to recognize, analyze, and solve each of the first three problems are presented in this chapter. Lateral squeeze is more closely related to the evaluation of foundation deformation and is discussed in Chapter 7 (Approach Roadway Deformations).

The stability problems illustrated in Figure 6-1 can be classified as “internal” or “external.” “Internal” embankment stability problems generally result from the selection of poor quality embankment materials and/or improper placement of the embankment fills and/or improper placement requirements. The infinite slope failure mode is an example of an “internal” stability problem; often such a failure is manifested as sloughing of the surface of the slope. Internal stability can be assured through project specifications by requiring granular materials with minimum gradation and compaction requirements. An example of a typical specification for approach roadway construction is presented in Chapter 7. The failure modes shown in Figure 6-1b, c and d, can be classified as “external” stability problems.

#### **6.01 Primary Reference**

The primary reference for this chapter is as follows:

FHWA (2001a). *Soil Slope and Embankment Design Reference Manual*. Report No. FHWA NHI-01-026, Authors: Collin, J. G., Hung, J. C., Lee, W. S., Munfakh, G., Federal Highway Administration, U.S. Department of Transportation.

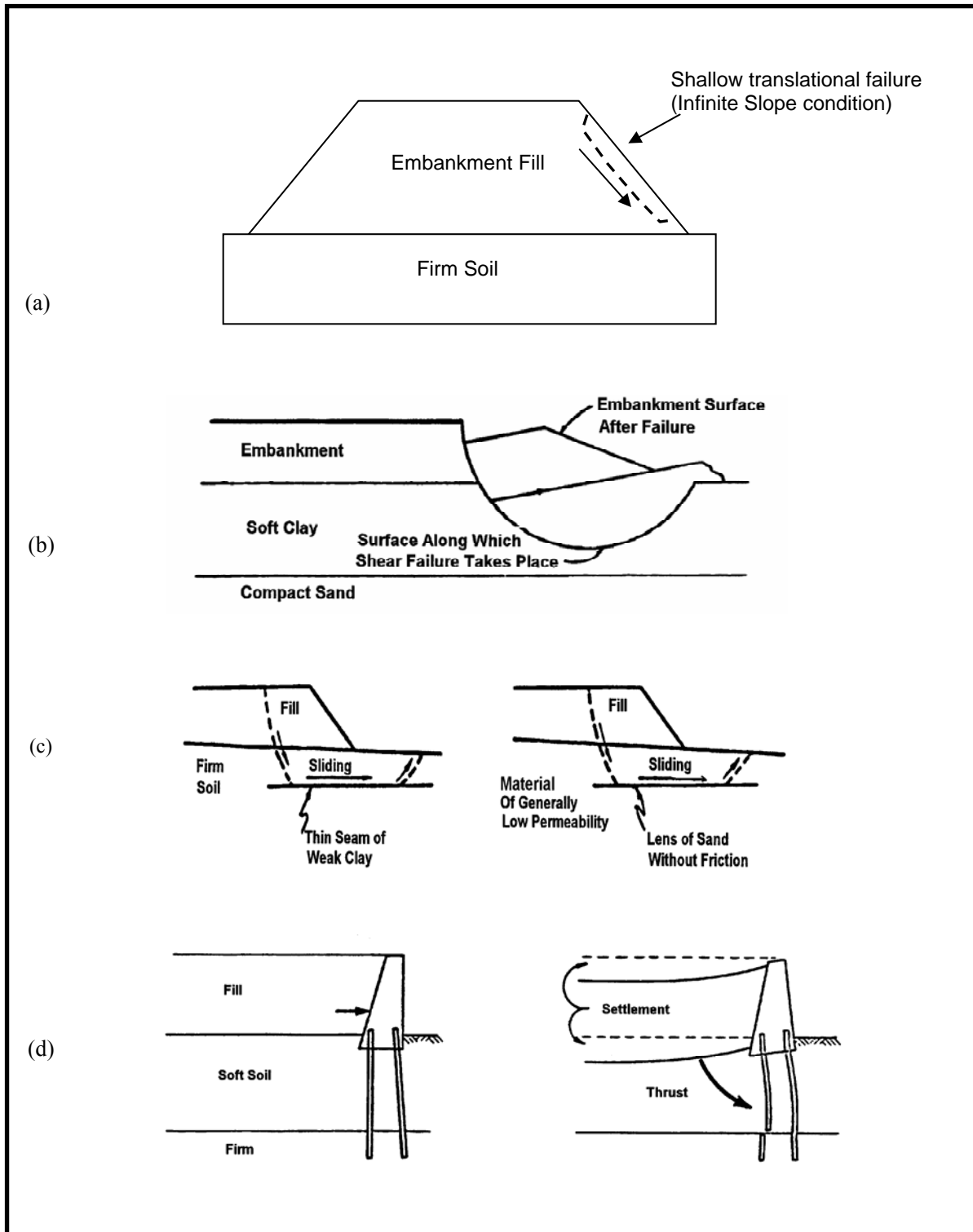


**Figure 6-1. Embankment failures: (a) Infinite slope failure in embankment fill, (b) Circular arc failure in embankment fill and foundation soil, (c) Sliding block failure in embankment fill and foundation soil, and (d) Lateral squeeze of foundation soil.**

## 6.1 EFFECTS OF WATER ON SLOPE STABILITY

Very soft, saturated foundation soils or ground water generally play a prominent role in geotechnical failures in general. They are certainly major factors in cut slope stability and in the stability of fill slopes involving both “internal” and “external” slope failures. The effect of water on cut and fill slope stability is briefly discussed below.

- **Importance of Water**

Next to gravity, water is the most important factor in slope stability. The effect of gravity is known, therefore, water is the key factor in assessing slope stability.

- **Effect of Water on Cohesionless Soils**

In cohesionless soils, water does not affect the angle of internal friction ( $\phi$ ). The effect of water on cohesionless soils below the water table is to decrease the intergranular (effective) stress between soil grains ( $\sigma'_n$ ), which decreases the frictional shearing resistance ( $\tau'$ ).

- **Effect of Water on Cohesive Soils**

Routine seasonal fluctuations in the ground water table do not usually influence either the amount of water in the pore spaces between soil grains or the cohesion. The attractive forces between soil particles prevent water absorption unless external forces such as pile driving, disrupt the grain structure. However, certain clay minerals do react to the presence of water and cause volume changes of the clay mass.

An increase in absorbed moisture is a major factor in the decrease in strength of cohesive soils as shown schematically in Figure 6-2. Water absorbed by clay minerals causes increased water contents that decrease the cohesion of clayey soils. These effects are amplified if the clay mineral happens to be expansive, e.g., montmorillonite.

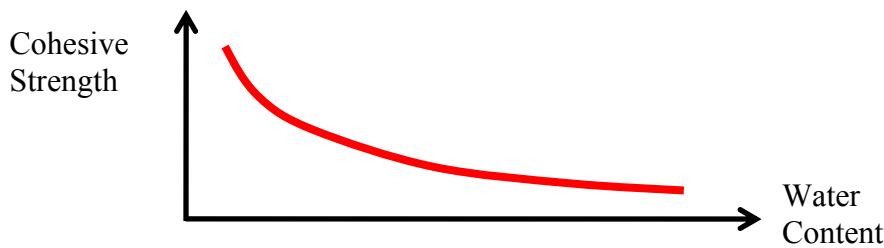


**Figure 6-2. Effect of water content on cohesive strength of clay.**

- **Fills on Clays**

Excess pore water pressures are created when fills are placed on clay or silt. Provided the applied loads do not cause the undrained shear strength of the clay or silt to be exceeded, as the excess pore water pressure dissipates consolidation occurs, and the shear strength of the clay or silt increases with time. For this reason, the factor of safety increases with time under the load of the fill.

- **Cuts in Clay**

As a cut is made in clay the effective stress is reduced. This reduction will allow the clay to expand and absorb water, which will lead to a decrease in the clay strength with time. For this reason, the factor of safety of a cut slope in clay may decrease with time. Cut slopes in clay should be designed by using effective strength parameters and the effective stresses that will exist in the soil after the cut is made.

- **Slaking - Shales, Claystones, Siltstones, etc.**

Sudden moisture increase in weak rocks can produce a pore pressure increase in trapped pore air accompanied by local expansion and strength decrease. The "slaking" or sudden disintegration of hard shales, claystones, and siltstones results from this mechanism. If placed as rock fill, these materials will tend to disintegrate into a clay soil if water is allowed to percolate through the fill. This transformation from rock to clay often leads to settlement and/or shear failure of the fill. Index tests such as the jar-slake test and the slake-durability test used to assess slaking potential are discussed in FHWA (1978).

## 6.2 DESIGN FACTOR OF SAFETY

A minimum factor of safety as low as 1.25 is used for highway embankment side slopes. This value of the safety factor should be increased to a minimum of 1.30 to 1.50 for slopes whose failure would cause significant damage such as end slopes beneath bridge abutments, major retaining structures and major roadways such as regional routes, interstates, etc. The selection of the design safety factor for a particular project depends on:

- The method of stability analysis used (see Section 6.4.5).
- The method used to determine the shear strength.
- The degree of confidence in the reliability of subsurface data.
- The consequences of a failure.
- How critical the application is.

## 6.3 INFINITE SLOPE ANALYSIS

A slope that extends for a relatively long distance and has a consistent subsurface profile may be analyzed as an infinite slope. The failure plane for this case is parallel to the surface of the slope and the limit equilibrium method can be applied readily.

### 6.3.1 Infinite Slopes in Dry Cohesionless Soils

A typical section or “slice” through the potential failure zone of a slope in a dry cohesionless soil, e.g., dry sand, is shown in Figure 6-3, along with its free body diagram. The weight of the slice of width  $b$  and height  $h$  having a unit dimension into the page is given by:

$$W = \gamma b h \quad 6-1$$

where  $\gamma$  is the effective unit weight of the dry soil. For a slope with angle  $\beta$  as shown in Figure 6-3, the normal ( $N$ ) and tangential ( $T$ ) force components of  $W$  are determined as follows:

$$N = W \cos \beta \quad \text{and} \quad 6-2$$

$$T = W \sin \beta \quad 6-3$$

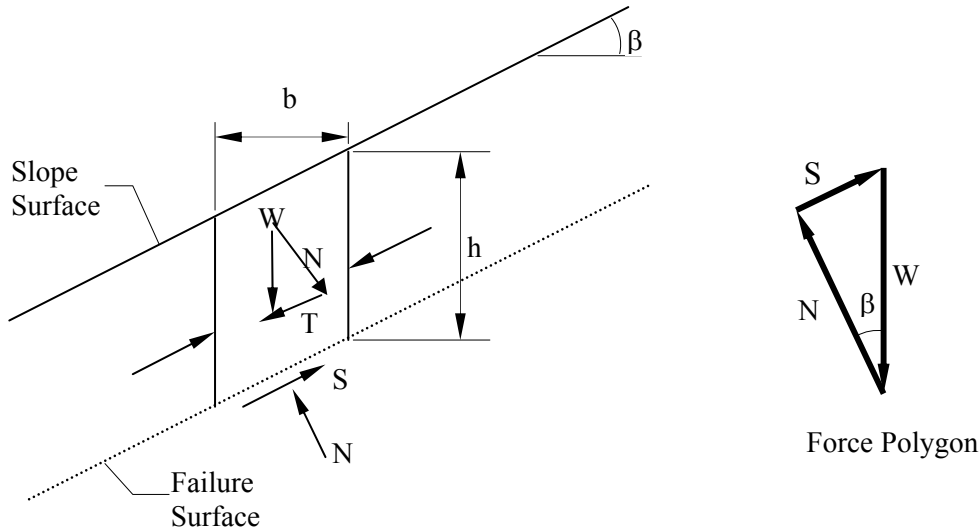


**Figure 6-3. Infinite slope failure in dry sand.**

The available shear strength along the failure plane is given by:

$$S = N \tan \phi \quad 6-4$$

The factor of safety (FS) is defined as the ratio of available shear strength to strength required to maintain stability. Thus, the FS will be given by:

$$FS = \frac{S}{T} = \frac{N \tan \phi}{W \sin \beta} = \frac{(W \cos \beta) \tan \phi}{W \sin \beta} = \frac{\tan \phi}{\tan \beta} \quad 6-5$$

For an infinite slope analysis, the FS is independent of the slope depth,  $h$ , and depends only on the angle of internal friction,  $\phi$ , and the angle of the slope,  $\beta$ . The slope is said to have reached **limit equilibrium** when  $FS=1.0$ . Also, at a  $FS = 1.0$ , the maximum slope angle will be limited to the angle of internal friction,  $\phi$ .

### 6.3.2 Infinite Slopes in $c-\phi$ Soils with Parallel Seepage

If a saturated slope in a  $c-\phi$  soil has seepage parallel to the surface of the slope as shown in Figure 6-4, the same limit equilibrium concepts may be applied to determine the FS, which will now depend on the effective normal force ( $N'$ ). In the following analysis, effective shear strength parameters,  $c'$  and  $\phi'$  are used.

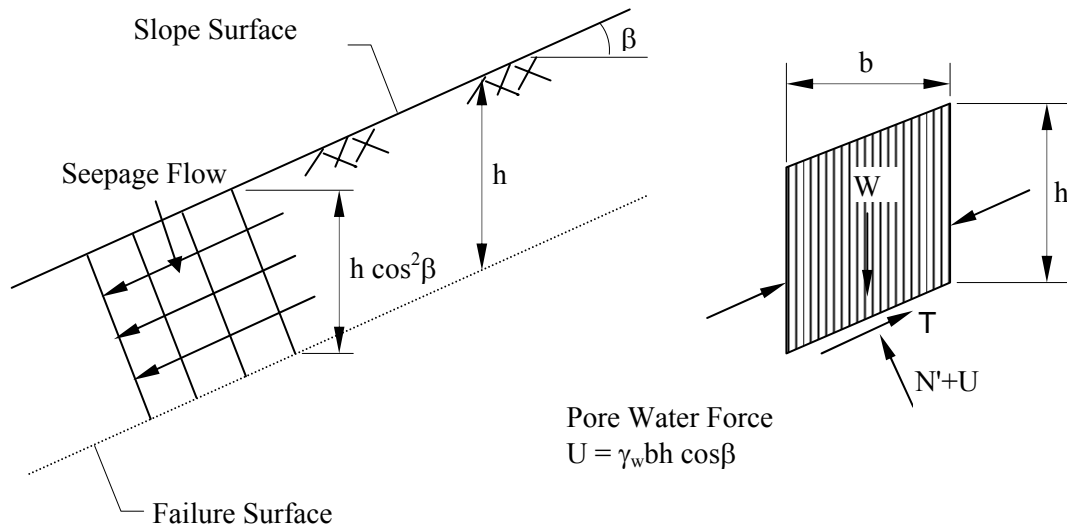


**Figure 6-4. Infinite slope failure in a c- $\phi$  soil with parallel seepage.**

From Figure 6-4, the pore water force acting on the base of a typical slice having a unit dimension into the page is:

$$U = \left( \gamma_w h \cos^2 \beta \right) \frac{b}{\cos \beta} = \gamma_w b h \cos \beta \quad 6-6$$

where h is any depth less than or equal to the depth of saturation and b is a unit width.

The available frictional strength, S, along the failure plane will depend on  $\phi'$  and the effective normal force,  $N' = N - U$ , where N is the total normal force. The equation for S is:

$$S = c' \frac{b}{\cos \beta} + (N - U) \tan \phi' \quad 6-7$$

The factor of safety for this case will be:

$$FS = \frac{S}{T} = \frac{(c' b / \cos \beta) + (N - U) \tan \phi'}{W \sin \beta} \quad 6-8$$

By substituting  $W = \gamma_{sat} b h$  into the above expression and rearranging terms, the FS is given by:

$$FS = \frac{c' + h (\gamma_{sat} - \gamma_w) (\cos^2 \beta) \tan \phi'}{\gamma_{sat} h \sin \beta \cos \beta} \quad 6-9$$

where  $\gamma' = (\gamma_{sat} - \gamma_w)$ .

For  $c' = 0$ , the above expression may be simplified to:

$$FS = \frac{\gamma'}{\gamma_{sat}} \frac{\tan \phi'}{\tan \beta} \quad 6-10$$

From Equation 6-10 it is apparent that for a *cohesionless* material with parallel seepage, the FS is also independent of the slope depth,  $h$ , just as it is for a dry cohesionless material as given by Equation 6-5. The difference is that the FS for the dry material is reduced by the factor  $\gamma'/\gamma_{sat}$  for saturated cohesionless materials to account for the effect of seepage. For typical soils, this reduction will be about 50 percent in comparison to dry slopes.

The above analysis can be generalized if the seepage line is assumed to be located at a normalized height,  $m$ , above the failure surface where  $m = z/h$ . In this case, the FS is:

$$FS = \frac{c' + h \cos^2 \beta [(1 - m) \gamma_m + m \gamma'] \tan \phi'}{h \sin \beta \cos \beta [(1 - m) \gamma_m + m \gamma_{sat}]} \quad 6-11$$

and  $\gamma_{sat}$  and  $\gamma_m$  are the saturated and moist unit weights of the soil below and above the seepage line. The above equation may be readily reformulated to determine the critical depth of the failure surface in a  $c'$ - $\phi'$  soil for any seepage condition.



### 6.4.1 Simple Rule of Thumb for Factor of Safety

A rule of thumb based on simplified bearing capacity theory can be used to make a preliminary "guestimate" of the factor of safety (FS) against circular arc failure for an embankment built on a clay foundation without presence of free water. The rule of thumb is as follows:

$$FS \cong \frac{6 c}{\gamma_{Fill} \times H_{Fill}} \quad 6-13$$

Where:  $c$  = unit cohesion of clay foundation soil (psf)  
 $\gamma_{Fill}$  = unit weight fill (pcf)  
 $H_{Fill}$  = height of fill (feet)

Since the rule of thumb assumes that there is no influence from groundwater,  $c$  and  $\gamma_{Fill}$  are effective stress parameters.

For example, the factor of safety for the proposed embankment illustrated in Figure 6-6 can be computed as follows:

$$FS = \frac{(6)(1,100 \text{ psf})}{(130 \text{ pcf})(30 \text{ ft})} = 1.69 \quad \text{Use Rule of Thumb 6-13}$$

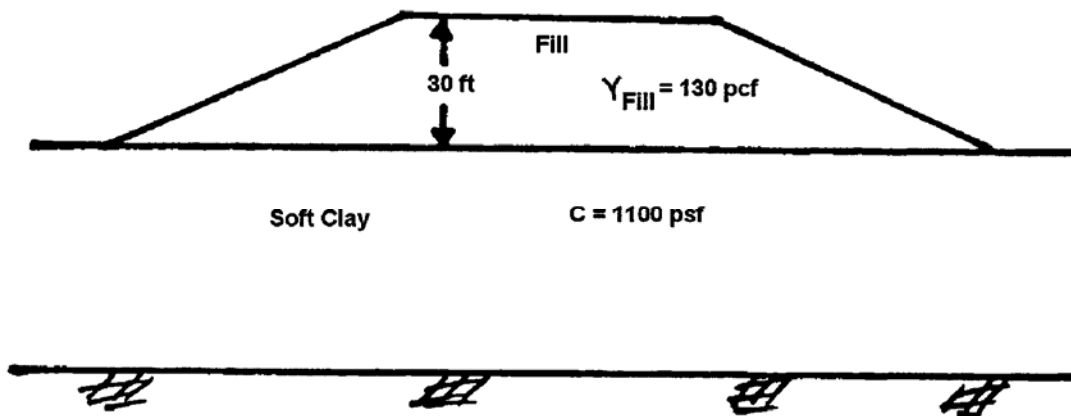


Figure 6-6. Example proposed embankment.

**The factor of safety computed by using this rule of thumb should never be used for final design.** This simple equation obviously does not take into account such factors as fill strength or fill slope angle and does not identify the location of a critical failure surface. **If**

**the factor of safety computed by using the rule of thumb is less than 2.5, a more sophisticated stability analysis is required.**

However, this rule of thumb can be helpful very early in the design stage to make a quick preliminary check on whether stability may be a problem and if more detailed analyses should be conducted. It can also be of use in the field while borings and sampling are being performed. For example, if in-situ vane shear tests are being carried out as part of the field investigation for a proposed embankment, the geotechnical specialist can use the vane strength with Equation 6-13 to estimate the FS in the field. This estimate can aid in directing the drilling, sampling, and testing program while the drill crew is at the site and help insure that critical strata are adequately explored and sampled. Finally, the FS calculated by the rule of thumb can be used to check for *gross* errors in computer output or input.

#### **6.4.2 Stability Analysis Methods (General)**

There are several available methods that can be used to perform a circular arc stability analysis for an approach embankment over soft ground. The simplest basic method is known as the **Normal or Ordinary Method of Slices**, also known as Fellenius' method (Fellenius, 1936) or the Swedish circle method of analysis. The Ordinary Method of Slices can easily be performed by hand calculations and is also a method by which the computation of driving and resisting forces is straightforward and easily demonstrated. For this method, the failure surface is assumed to be the arc of a circle as shown in Figure 6-7 and the factor of safety against sliding along the failure surface is defined as the ratio of the moment of the total available resisting forces on the trial failure surface to the net moment of the driving forces due to the embankment weight, that is:

$$FS = \frac{\text{Sum of Resisting Forces} \times \text{Moment Arm (R)}}{\text{Sum of Driving Forces} \times \text{Moment Arm (R)}} \quad 6-14$$

Note that since the method consists of computing the driving and resisting forces along the failure arc, the moment arm R is the same for both the driving and resisting forces. Thus, Equation 6-14 reduces to:

$$FS = \frac{\text{Sum of Resisting Forces}}{\text{Sum of Driving Forces}} \quad 6-14a$$

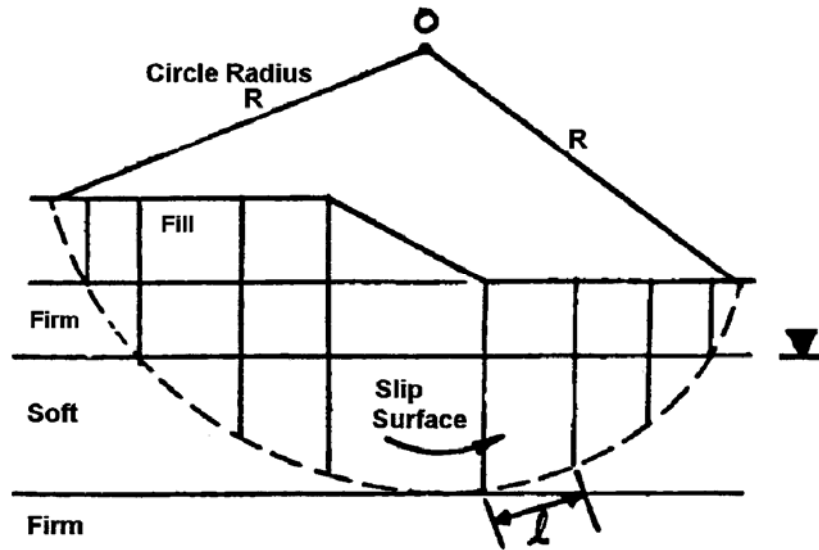


Figure 6-7. Geometry of Ordinary Method of Slices.

For slope stability analysis, the mass within the failure surface is divided into vertical slices as shown in Figures 6-7 and 6-8. A typical vertical slice and its free body diagram is shown in Figure 6-9 for the case where water is not a factor. The case with the presence of water is shown in Figure 6-10. The following assumptions are then made in the analysis using Ordinary Method of Slices:

1. The available shear strength of the soil can be adequately described by the Mohr-Coulomb equation:

$$\tau = c + (\sigma - u) \tan \phi \quad 6-15$$

where:

- $\tau$  = effective shear strength
- $c$  = cohesion component of shear strength
- $(\sigma - u) \tan \phi$  = frictional component of shear strength
- $\sigma$  = total normal stress on the failure surface at the base of a slice due to the weight of soil and water above the failure surface
- $u$  = water uplift pressure against the failure surface
- $\phi$  = angle of internal friction of soil
- $\tan \phi$  = coefficient of friction along failure surface

2. The factor of safety is the same for all slices.
3. The factors of safety with respect to cohesion ( $c$ ) and friction ( $\tan \phi$ ) are equal.
4. Shear and normal forces on the sides of each slice are ignored.
5. The water pressure ( $u$ ) is taken into account by reducing the total weight of the slice by the water uplift force acting at the base of the slice.

Equation 6-15 is expressed in terms of total strength parameters. The equation could easily have been expressed in terms of effective strength parameters. Therefore, the convention to be used in the stability analysis, be it total stress or effective stress, should be chosen and specified. In soil problems involving water, the engineer may compute the normal and tangential forces by using either total soil weights and boundary water forces (both buoyancy and unbalanced hydrostatic forces) or submerged (buoyant) soil weights and unbalanced hydrostatic forces. The results are the same. When total weight and boundary water forces are used, the equilibrium of the entire block is considered. When submerged weights and hydrostatic forces are used, the equilibrium of the mineral skeleton is considered. The total weight notation is used herein as this method is the simplest to compute.

### 6.4.3 Ordinary Method of Slices - Step-By-Step Computation Procedure

To compute the factor of safety for an embankment by using the Ordinary Method of Slices, the step-by-step computational procedure is as follows:

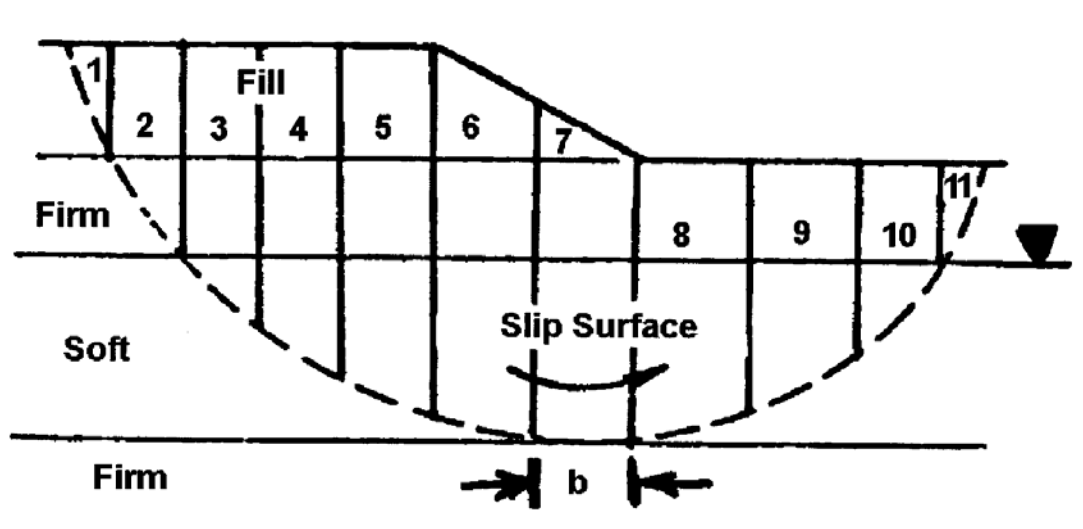


Figure 6-8. Example of dividing the failure mass in slices.

**Step 1. Draw a cross-section of the embankment and foundation soil profile on a scale of either 1-inch = 10 feet or 1-inch = 20 feet scale both horizontal and vertical.**

**Step 2. Select a circular failure surface such as shown in Figure 6-7.**

**Step 3. Divide the circular mass above the failure surface into 10 - 15 vertical slices as illustrated in Figure 6-8.**

To simplify computation, locate the vertical sides of the slices so that the bottom of any one slice is located entirely in a single soil layer or at the intersection of the ground water level and the circle.

Locate the top boundaries of vertical slices at breaks in the slope. The slice widths do not have to be equal. For convenience assume a one-foot (0.3 m) thick section of embankment. This unit width simplifies computation of driving and resisting forces.

Also, as shown in Figure 6-9 and 6-10 the driving and resisting forces of each slice act at the intersection of a vertical line drawn from the center of gravity of the slice to the failure circle to establish a centroid point on the circle. Lines (called rays) are then drawn from the center of the circle to the centroid point on the circular arc. The  $\alpha$  angles are then measured from the vertical to each ray.

When the water table is sloping, use Equation 6-16 to calculate the water pressure on the base of the slice:

$$u = h_w \gamma_w \cos^2 \alpha_w \quad 6-16$$

where:  $\alpha_w$  = slope of water table from horizontal in degrees.

$h_w$  = depth from ground water surface to the centroid point on the circle.

**Step 4: Compute the total weight ( $W_T$ ) of each slice.**

For illustration, the resisting and driving forces acting on individual slices with and without water pressure are shown on Figures 6-9 and 6-10.

To compute  $W_T$ , use total soil unit weight,  $\gamma_t$ , both above and below the water table.

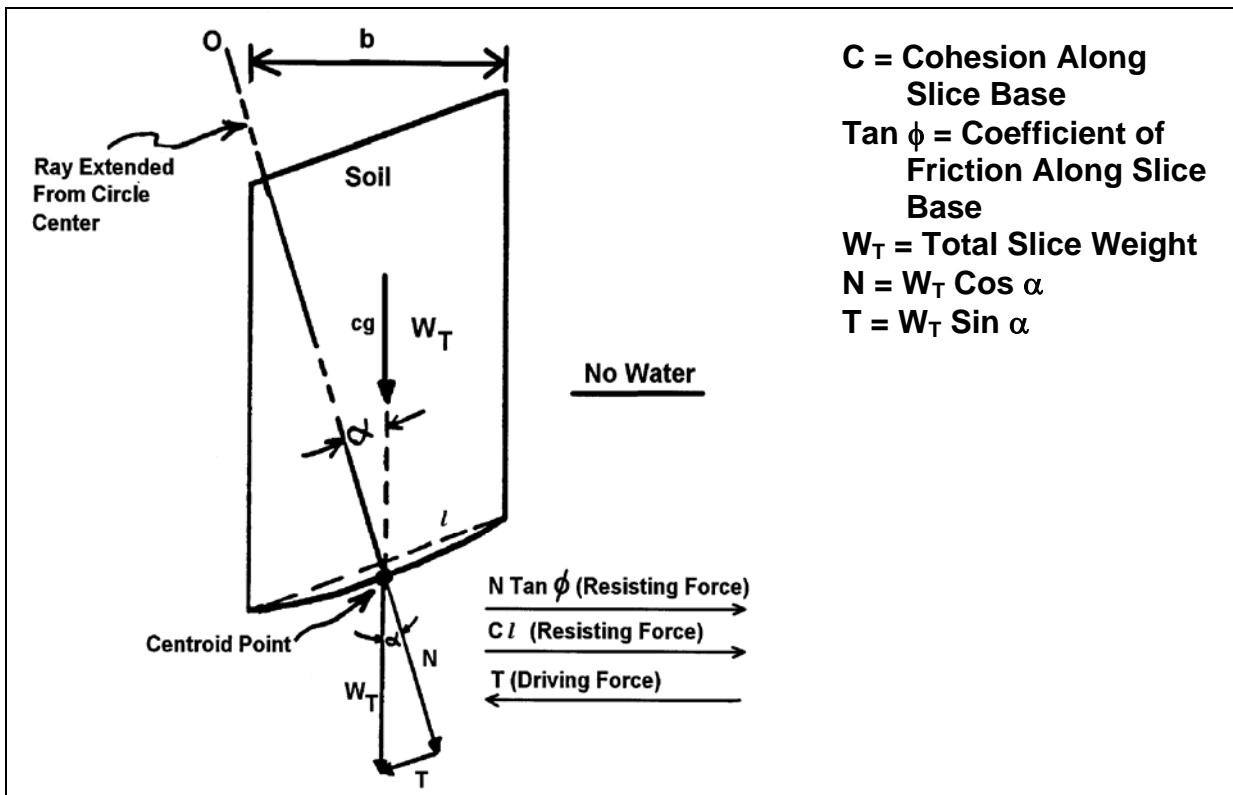


Figure 6-9. Forces on a slice without water effect.

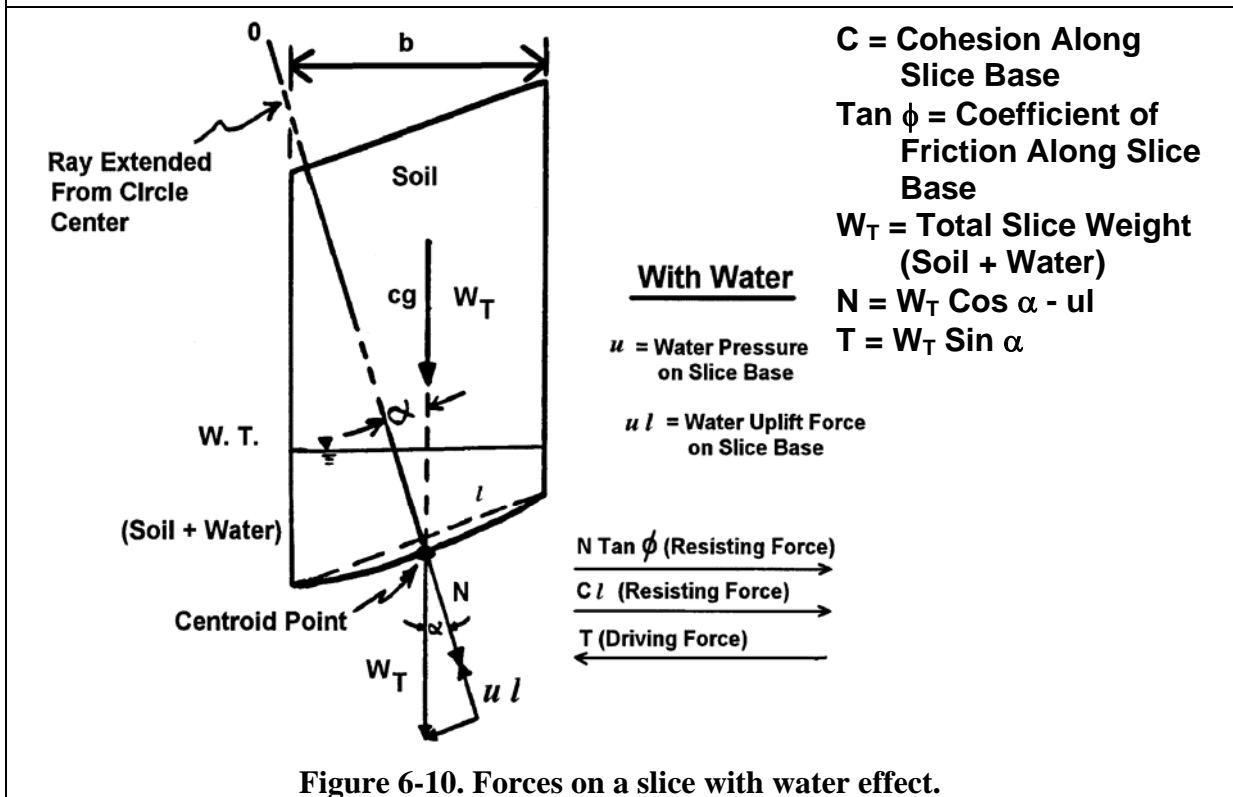


Figure 6-10. Forces on a slice with water effect.

$$W_T = \gamma_t \times \text{Average Slice Height} \times \text{Slice Width} \quad 6-17$$

For example: Assume

$$\gamma_t = 120 \text{ pcf (18.9 kN/m}^3\text{)}$$

$$\text{Average height of slice} = 10 \text{ ft (3 m)}$$

$$\text{Slice width} = 10 \text{ ft (3 m)}$$

Then for a unit thickness into the plane of the paper,  $W_T = (120 \text{ pcf}) (10 \text{ ft}) (10 \text{ ft}) (1 \text{ ft}) = 12,000 \text{ lbs (53.3 kN)}$

**Step 5: Compute frictional resisting force for each slice depending on location of ground water table.**

$$N = W_T \cos \alpha \quad 6-18a$$

$$N' = W_T \cos \alpha - ul \quad 6-18b$$

$N$  = total normal force acting against the slice base

$N'$  = effective normal force acting against the slice base

$W_T$  = total weight of slice (from Step 4 above)

$\alpha$  = angle between vertical and line drawn from circle center to midpoint (centroid) of slice base (Note:  $\alpha$  is also equal to the angle between the horizontal and a line tangent to the base of the slice)

$u$  = water pressure on the base of the slice = average height of water,  $h_w \times \gamma_w$ .  
Use  $\gamma_w = 62.4 \text{ pcf (9.8 kN/m}^3\text{)}$

$l$  = arc length of slice base. To simplify computations, take  $l$  as the secant to the arc.

$ul$  = water uplift force against base of the slice per unit thickness into the plane of the paper.

$\phi$  = internal friction angle of the soil.

$\tan \phi$  = coefficient of friction along base of the slice.

Note that **the effect of water is to reduce the normal force against the base of the slice and thus reduce the frictional resisting force.** To illustrate this reduction, take the same slice used in Step 4 and compute the friction resistance force for the slice with no water and then for the ground water table located 5 feet above the base of the slice.

Assume:  $\phi = 25^\circ$   $\alpha = 20^\circ$   $l = 11 \text{ ft (3.3 m)}$

If there is no water in the slice,  $u l = 0$  and Equation 6-18b reverts to Equation 6-18a and the total frictional resistance can be computed as follows:

$$N = W_T \cos \alpha = (12,000 \text{ lbs}) (\cos 20^\circ) = 11,276 \text{ lbs (50.18 kN)}$$
$$N \tan \phi = (11,276 \text{ lbs}) (\tan 25^\circ) = 5,258 \text{ lbs (23.4 kN)}$$

If there is 5-ft of water above the midpoint of the slice, Equation 6-18b is used directly and the effective frictional resistance is computed as follows:

$$u l = (h_w)(\gamma_w)(l) = (5 \text{ ft})(62.4 \text{ pcf})(11 \text{ ft})(1 \text{ ft}) = 3,432 \text{ lbs (15.3 kN)}$$
$$N' = W_T \cos \alpha - u l = 11,276 \text{ lbs} - 3,432 \text{ lbs} = 7,844 \text{ lbs (34.9 kN)}$$
$$N' \tan \phi = (7,844 \text{ lbs}) (\tan 25^\circ) = 3,658 \text{ lbs (16.3 kN)}$$

**Step 6: Compute cohesive resisting force for each slice.**

$c$  = cohesive soil strength  
 $l$  = length of slice base

Example:  $c = 200 \text{ psf (9.6 kPa)}$   
 $l = 11 \text{ ft (3.6 m)}$   
 $cl = (200 \text{ psf})(11 \text{ ft})(1 \text{ ft}) = 2,200 \text{ lbs (9.8 kN)}$

**Step 7: Compute tangential driving force, T, for each slice.**

$$T = W_T \sin \alpha \quad 6-19$$

T is the component of total weight of the slice,  $W_T$ , acting tangent to the slice base.  
T is the driving force due to the weight of both soil and water in the slice.

Example: Given  $W_T = 12,000 \text{ lbs (53.3 kN)}$   
 $\alpha = 20^\circ$   
 $T = W_T \sin \alpha = (12,000 \text{ lbs})(\sin 20^\circ) = 4,104 \text{ lbs (18.2 kN)}$





#### 6.4.4 Recommended Stability Methods

The basic static forces on a typical slice are shown in Figure 6-12. The limit equilibrium method of slices is based on the principles of statics, i.e., summation of moments, vertical forces, and horizontal forces. The Ordinary Method of Slices ignores both interslice shear ( $I_S$ ) and interslice normal ( $I_N$ ) forces and satisfies only moment equilibrium. There are many other methods available for performing a slope stability analysis besides the Ordinary Method of Slices. These include the Bishop Method (Bishop, 1955), the Simplified Janbu Method (Janbu, 1954) and the Spencer Method (Spencer, 1967). These methods are primarily variations and refinements of the Ordinary Method of Slices. The differences among these more refined methods lie in the assumptions made regarding the interslice shear and normal forces acting on the sides of slices. The Bishop Method, also known as the Simplified Bishop Method, includes interslice normal forces ( $I_N$ ) but ignores interslice shear ( $I_S$ ) forces. Again, Bishop's method satisfies only moment equilibrium. The Simplified Janbu Method is similar to the Bishop Method in that it includes the interslice normal ( $I_N$ ) forces and ignores the interslice shear ( $I_S$ ) forces. The difference between the Bishop Method and the Simplified Janbu Method is that the Simplified Janbu Method satisfies only horizontal force equilibrium, as opposed to moment equilibrium. The Spencer Method considers both normal and shear interslice side forces as well as moments. Therefore the Spencer Method is theoretically more rigorous than the other methods.

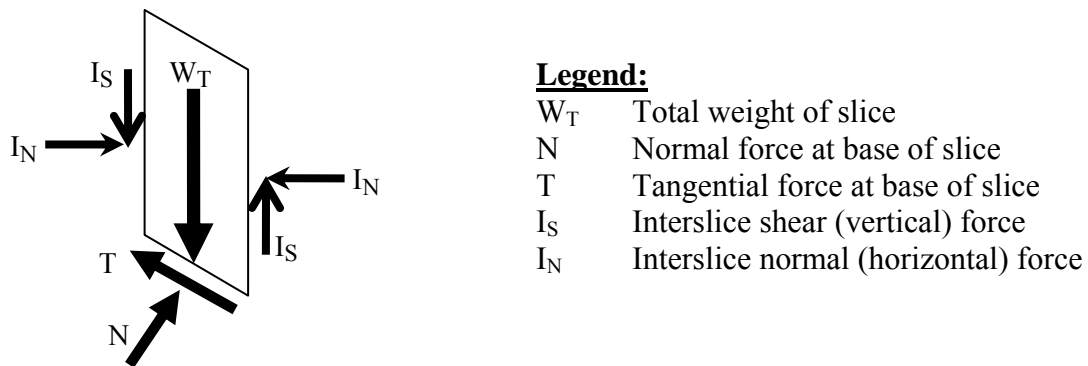


**Figure 6-12. Typical static forces on a slice of sliding mass without seepage.**

The Ordinary Method of Slices is more conservative and gives unrealistically lower factors of safety than the Bishop Method or the other more refined methods. The only reason for inclusion of the Ordinary Method of Slices here is to demonstrate the principles of slope stability. For purely cohesive soils the Ordinary Method of Slices and Bishop's method give identical results. For soils that have frictional strength, the Bishop Method should be used as a minimum. While none of the methods is 100 percent correct theoretically, currently available procedures such as Bishop's method, Janbu's Simplified method or Spencer's method are sufficiently accurate for practical analysis and design. For more information on these and other slope stability methods, the reader is referred to FHWA (2001a).

The method of analysis that should be used to determine a factor of safety depends on the soil type, the source of the soil strength parameters, the level of confidence in the values, and the type of slope that is being designed. Slope stability analyses should be performed only by qualified and experienced geotechnical specialists. Guidelines recommended for the analysis of slope stability are given in Table 6-1.

**Table 6 -1. Slope stability guidelines for design**

<b>Foundation Soil Type</b>	<b>Type of Analysis</b>	<b>Source of Strength Parameters (see Chapter 5)</b>	<b>Remarks (see Note 1)</b>
Cohesive	<b>Short-term</b> (embankments on soft clays – immediate end of construction – $\phi = 0$ analysis).	<ul style="list-style-type: none"> <li>• UU or field vane shear test or CU triaxial test.</li> <li>• Use undrained strength parameters at <math>p_o</math></li> </ul>	Use <b>Bishop Method</b> . An angle of internal friction should not be used to represent an increase of shear strength with depth. The clay profile should be divided into convenient layers and the appropriate cohesive shear strength assigned to each layer.
	<b>Stage construction</b> (embankments on soft clays – build embankment in stages with waiting periods to take advantage of clay strength gain due to consolidation).	<ul style="list-style-type: none"> <li>• CU triaxial test. Some samples should be consolidated to higher than existing in-situ stress to determine clay strength gain due to consolidation under staged fill heights.</li> <li>• Use undrained strength parameters at appropriate <math>p_o</math> for staged height.</li> </ul>	Use <b>Bishop Method</b> at each stage of embankment height. Consider that clay shear strength will increase with consolidation under each stage. Consolidation test data needed to estimate length of waiting periods between embankment stages. Piezometers and settlement devices should be used to monitor pore water pressure dissipation and consolidation during construction.
	<b>Long-term</b> (embankment on soft clays and clay cut slopes).	<ul style="list-style-type: none"> <li>• CU triaxial test with pore water pressure measurements or CD triaxial test.</li> <li>• Use effective strength parameters.</li> </ul>	Use <b>Bishop Method</b> with combination of cohesion and angle of internal friction (effective strength parameters from laboratory test).
	<b>Existing failure planes</b>	<ul style="list-style-type: none"> <li>• Direct shear or direct simple shear test. Slow strain rate and large deflection needed.</li> <li>• Use residual strength parameters.</li> </ul>	Use <b>Bishop, Janbu or Spencer Method</b> to duplicate previous shear surface.
Granular	<b>All types</b>	<ul style="list-style-type: none"> <li>• Obtain effective friction angle from charts of standard penetration resistance (SPT) versus friction angle or from direct shear tests.</li> </ul>	Use <b>Bishop Method</b> with an effective stress analysis.
Note 1: Methods recommended represent minimum requirement. More rigorous methods such as Spencer’s method should be used when a computer program has such capabilities.			

#### 6.4.5 Remarks on Safety Factor

For side slopes of routine highway embankments, a minimum design safety factor of 1.25 **as determined by the Ordinary Method of Slices** is used. For slopes that would cause greater damage upon failure, such as end slopes beneath bridge abutments, major retaining structures, and major roadways such as regional routes, interstates, etc., the design safety factor should be increased to at least 1.30 to 1.50. For cut slopes in fine-grained soils, which can lose shear strength with time, a design safety factor of 1.50 is desirable.

### 6.5 CRITICAL FAILURE SURFACE

The step-by-step procedure presented in the preceding section illustrates how to compute the factor of safety for one selected circular arc failure surface. The complete analysis requires that a large number of assumed failure surfaces be checked in order to find the critical one, i.e., the surface with the lowest factor of safety. This task would obviously be a tedious and time consuming operation if done by hand. Therefore a computer program becomes a valuable tool for performing such computations. Any method for stability analysis is easily adapted to computer solution. For critical circle methods a grid of possible circle centers is defined, and a range of radius values established for each. The computer can be directed to perform stability analyses for each circle center over the range of radii and then to print out all the safety factors or just the minimum one and its radius. A plot of minimum safety factor for each circle center in the form of contours can be used to define the location of the most critical circle and the minimum safety factor as shown in Figure 6-13. The radius of the most critical surface can be used to locate the intersection points of the circle with the ground surface above and below the slope. This is useful in identifying structures above and below the slope that may be potentially impacted by slope instability.

Figure 6-13 shows just one of several ways that computer programs can be used to search for the most critical failure surface. It is beyond the scope of this manual to discuss these in detail. However, the following points should be noted as one uses a computer program for locating the most critical failure surface:

1. Check multiple circle center locations and compare the lowest safety factors. There may be more than one “local” minimum and a single circle center location may not necessarily locate the lowest safety factor for the slope.

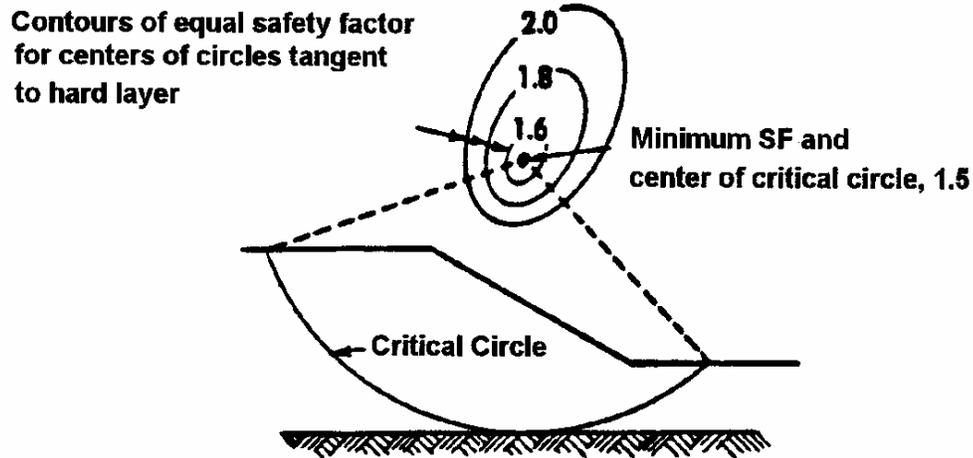


**Figure 6-13. Location of critical circle by plotting contours of minimum safety factors for various trial circles.**

2. Search all areas of the slope to find the lowest safety factor. The designer may find multiple areas of the slope where the safety factors are low and comparable. In this case, the designer should try to identify insignificant failure modes that lead to low safety factors for which the consequences of failure are small. This is often the case in cohesionless soils, where the lowest safety factor is found for a shallow failure plane located close the slope face.
3. Review the soil stratigraphy for “secondary” geological features such as thin relatively weak zones where a slip surface can develop. Often, circular failure surfaces are locally modified by the presence of such weak zones. Therefore computer software capable of simulating such failures should be used. Some of the weak zones may be man-made, e.g., when new fills are not adequately keyed into existing fills for widening projects.
4. Conduct stability analyses to take into account all possible loading and unloading schemes to which the slope might be subjected during its design life. For example, if the slope has a detention basin next to it, then it might be prudent to evaluate the effect of water on the slope, e.g., perform an analysis for a rapid drawdown condition.
5. Use the drained or undrained soil strength parameters as appropriate for the conditions being analyzed
6. Use stability charts to develop a “feel” for the safety factor that may be anticipated. Stability charts are discussed in the next section. Such charts may also be used to verify the results of computer solutions.

## 6.6 DESIGN (STABILITY) CHARTS

Slope stability charts are useful for preliminary analysis to compare alternates that may be examined in more detail later. Chart solutions also provide a quick means of checking the results of detailed analyses. Engineers are encouraged to use these charts before performing a computer analysis in order to determine the approximate value of the factor of safety. The chart solution allows some quality control and a check for the subsequent computer-generated solutions.

Slope stability charts are also used to back-calculate strength values for failed slopes, such as landslides, to aid in planning remedial measures. In back-calculating strength values a factor of safety of unity is assumed for the conditions at failure. Since soil strength often involves both cohesion and friction, there are no unique values that will give a factor of safety equal to one. Therefore, selection of the most appropriate values of cohesion and friction depends on local experience and judgment. Since the friction angle is usually within a narrow range for many types of soils and can be obtained by laboratory tests with a certain degree of confidence, it is generally fixed for the back-calculations in practice and the value of cohesion is varied until a factor of safety of one is obtained.

The major shortcoming in using design charts is that most charts are for ideal, homogeneous soil conditions that are not typically encountered in practice. Design charts have been devised with the following general assumptions:

1. Two-dimensional limit equilibrium analysis.
2. Simple homogeneous slopes.
3. Slip surfaces of circular shapes only.

**It is imperative that the user understands the underlying assumptions for the charts before using them for the design of slopes.**

Regardless of the above shortcomings, many practicing engineers use these charts for non-homogeneous and non-uniform slopes with different geometrical configurations. To do this correctly, one must use an average slope inclination and weighted averages of  $c$ ,  $\phi$ , or  $c'$ ,  $\phi'$  or  $c_u$  calculated on the basis of the proportional length of slip surface passing through different relatively homogeneous layers. Such a procedure is extremely useful for preliminary analyses and saves time and expense. In most cases, the results are checked by performing detailed analyses using more suitable and accurate methods, for example, one of the methods of slices discussed previously.

### 6.6.1 Historical Background

Some of the first slope stability charts were published by Taylor (1948). Since then various charts were developed by many investigators. Two of the most common stability charts are presented in this manual. These were developed by Taylor (1948) and Janbu (1968).

### 6.6.2 Taylor's Stability Charts

Taylor's Stability Charts (Taylor, 1948) were derived from solutions based on circular failure surfaces for the stability of simple, homogeneous, finite slopes without seepage (i.e., condition of effective stress). The general equations that Taylor developed as the basis for his stability charts are relationships between the height (H) and inclination ( $\beta$ ) of the slope, the unit weight of the soil ( $\gamma$ ), and the values of the soil's *developed (mobilized)* shear strength parameters,  $c_d$  and  $\phi_d$ . These developed (mobilized) quantities are as follows:

$$c_d = \frac{c'}{F_c}; \quad \tan \phi_d = \frac{\tan \phi'}{F_\phi} \quad 6-21$$

Where  $F_c$  is the average factor of safety with respect to cohesion and  $F_\phi$  is the average factor of safety with respect to friction angle, i.e.,  $\phi_d = \arctan(\tan \phi' / F_\phi)$ . As an approximation, the following equation may be used for the developed friction angle:

$$\phi_d \approx \frac{\phi'}{F_\phi} \quad 6-22$$

However, for soils possessing both frictional and cohesive components of strength, the factor of safety in slope stability analyses generally refers to the overall factor of safety with respect to shearing strength, FS, which equals  $\tau/\tau_d$  where  $\tau$  = shear strength and  $\tau_d$  = the developed (mobilized) shear strength. Therefore, the general Mohr-Coulomb expression for developed shear strength in terms of combined factors of safety is:

$$\tau_d = \frac{\tau}{FS} = \frac{c'}{F_c} + \sigma' \frac{\tan \phi}{F_\phi} \quad 6-23$$

Equation 6-23 can be re-written in terms of developed shear strength parameters as follows:

$$\tau_d = c_d + \sigma' \tan \phi_d \quad 6-24$$

There are an unlimited number of combinations of  $F_c$  and  $F_\phi$  that can result in a given value of FS. However, Equations 6-21 and 6-23 suggest that for the case where the value of  $F_c = F_\phi$ , the factor of safety with respect to shearing strength, FS, also equals that value. The importance of this condition will be illustrated in Section 6.6.2.1 by an example problem.

To simplify the determination of the factor of safety, Taylor calculated the stability of a large number of slopes over a wide range of slope angles and developed friction angles,  $\phi_d$ . He represented the results by a dimensionless number that he called the “Stability Number,”  $N_s$ , which he defined as follows:

$$N_s = \frac{c_d}{\gamma H} = \frac{c'}{F_c \gamma H} \quad 6-25$$

Equation 6-25 can be rearranged to provide an expression for  $F_c$  as a function of the Stability Number and three variables,  $c'$ ,  $H$  and  $\gamma$ , as follows:

$$F_c = \frac{c'}{N_s \gamma H} \quad 6-26$$

Taylor published his results in the form of curves that give the relationship between  $N_s$  and slope angle,  $\beta$ , for various values of developed friction angles,  $\phi_d$ , as shown in Figure 6-14. Note that factors of safety do not appear in the chart. The chart is divided into two zones, A and B. As shown in the inset for Zone A, the critical circle for steep slopes passes through the toe of the slope with the lowest point on the failure arc at the toe of the slope. As shown in the inset for Zone B, for shallower slopes the lowest point of the critical circle is not at the toe, and three cases must be considered as follows:

- **Case 2:** For shallow slope angles or small developed friction angles the critical circle may pass below the toe of the slope. This condition corresponds to Case 2 in the inset for Zone B. The values of  $N_s$  for this case are given in the chart by the long dashed curves.

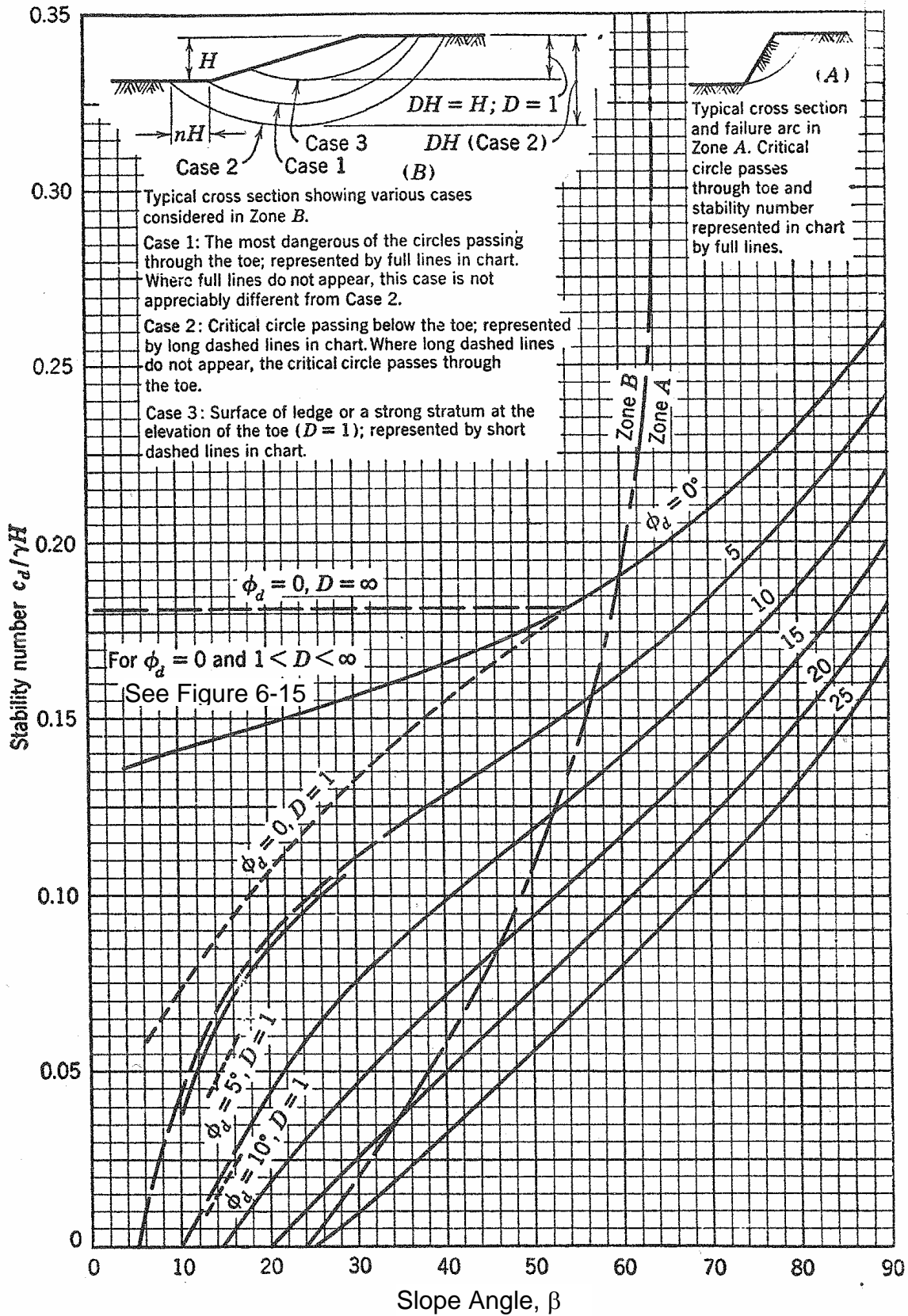


Figure 6-14. Taylor's chart for soils with friction angle (after Taylor, 1948).

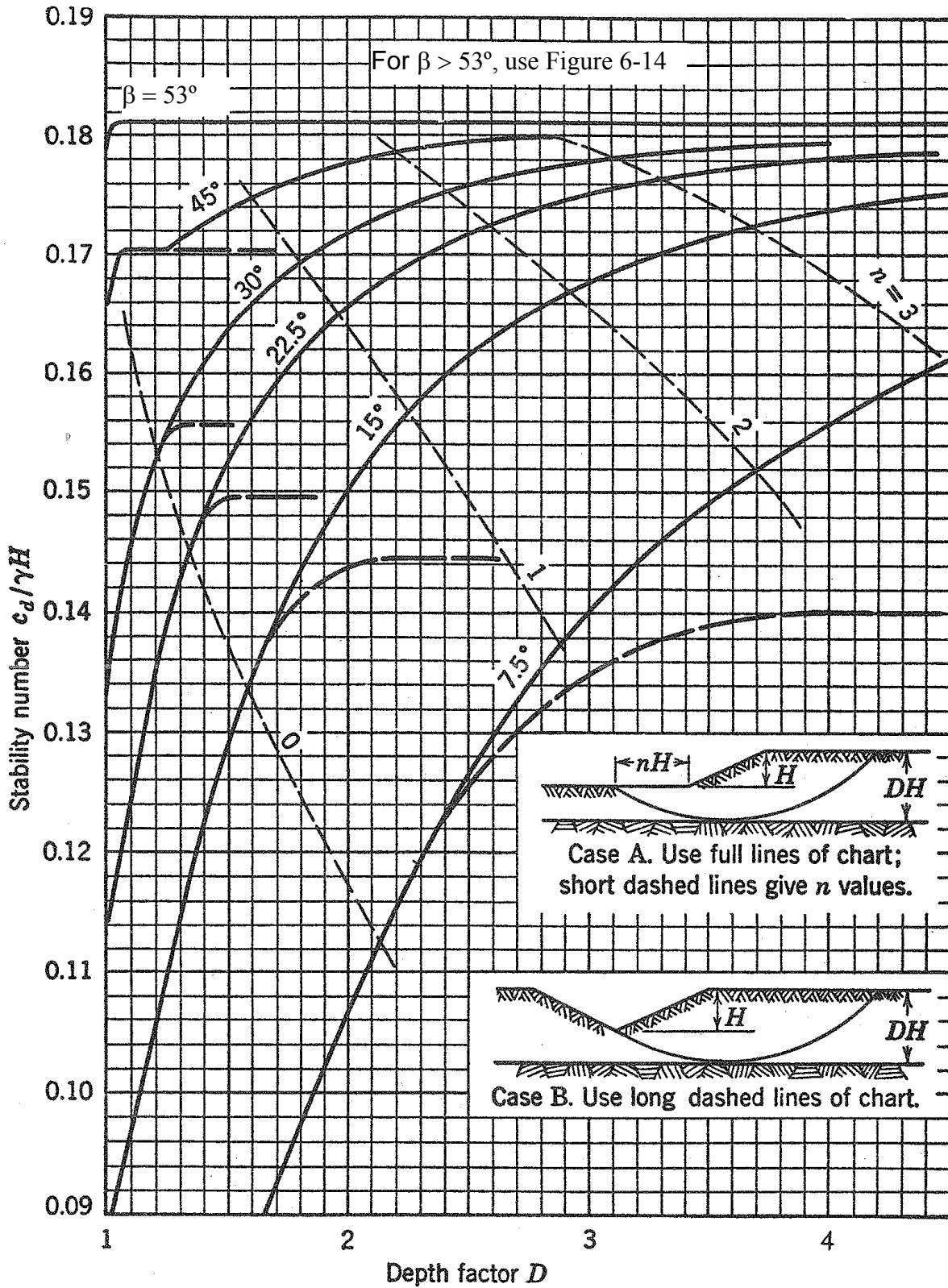


Figure 6-15. Taylor's chart for  $\phi' = 0$  conditions for slope angles ( $\beta$ ) less than  $54^\circ$  (after Taylor, 1948).

- **Case 1:** Where long dashed curves do not appear in the chart, the critical circle passes through the toe. This condition corresponds to Case 1. Stability numbers for Case 1 are given by the solid lines in the chart both when there is and when there is not a more dangerous circle that passes below the toe, i.e., the curves for Case 1 are an extension of the curves that correspond to a toe circle failure in Zone A. In both Case 1 and Case 2 the failure circle passes through the soil below the toe of the slope. The depth ratio,  $D$ , which is a multiple of the slope height  $H$ , is used to define the depth ( $DH$ ) from the top of the slope to an underlying strong material through which the failure circle does not pass.
- **Case 3:** This case corresponds to the condition where there is an underlying strong layer at the elevation of the toe ( $D=1$ ). This case is represented by short dashed lines in the chart.

**Comment on  $\phi_d = 0$  condition:** The condition of  $\phi_d = 0$  in Taylor's Stability Chart is somewhat misleading since, as noted previously, Taylor's charts were derived for simple slopes without seepage, i.e., for an effective stress analysis. The condition of " $\phi_d = 0$ " was used by Taylor to simplify the analysis and permit generation of the stability charts by assuming that shear strength is constant with depth. Basically, in the Mohr-Coulomb equation, Taylor assumed an average intergranular pressure,  $\sigma'_{avg}$  instead of an actual value of  $\sigma'$  which varies with depth. Since stability analyses are much simpler to perform when the shear strength is constant, he introduced this concept into his stability charts by considering the effective cohesion to be the average shear strength and by considering the friction angle to be zero. Thus the condition where  $\phi_d = 0$  is merely an example of substitution of an average value for a variable quantity. However, in the context of Taylor's definition of  $\phi_d = 0$ , the stability charts are often used in practice for estimating the factor of safety and location of the critical circle in a homogeneous saturated clay in undrained shear.

As shown in Figure 6-14, the critical circle for the " $\phi_d = 0$ " case passes below the toe for slopes with inclinations less than  $53^\circ$ . In practice the depth to which the failure circle extends is limited by an underlying strong material. Thus, the value of  $N_s$  for this case is greatly dependent on this limiting value of depth. The chart shown in Figure 6-15 is used exclusively for the " $\phi_d = 0$ " case and supplements the curves shown in Figure 6-14 for that condition. The coordinates in Figure 6-15 allow the chart to be used easily and enable the user to evaluate a number of parameters that may be of interest in practice. For example, the chart can be used to determine  $nH$ , which is the distance from the toe of the slope to where the critical failure surface passing below the toe may be expected to emerge.

### 6.6.2.1 Determination of the Factor of Safety for a Slope

As indicated in Section 6.6.2, in order to use Taylor's charts to determine the minimum overall factor of safety with respect to shear strength for a slope of given height  $H$  and inclination  $\beta$  having soil properties  $\gamma$ ,  $c'$  and  $\phi'$ , the condition  $FS = F_c = F_\phi$  must be satisfied. The general computational approach is as follows:

1. Assume a reasonable value for the common factors of safety  $FS = F_c = F_\phi$ .
2. Use Equations 6-21 to calculate the corresponding values of  $c_d$  and  $\phi_d$ .
3. For the given value of  $\beta$  and the calculated value of  $\phi_d$ , read the corresponding value of the stability number  $N_s$  from Figure 6-14.
4. Use an inverted form of Equation 6-26 to calculate the slope height  $H$  corresponding to the assumed factor of safety.
5. If the calculated value of  $H$  is within an acceptable distance of the actual height, e.g.,  $\pm 0.5$  feet, the assumed value of the common factor of safety represents the minimum overall factor of safety of the slope with respect to shear strength,  $F_s$ .
6. If the calculated value of  $H$  is not within the desired acceptable range, the process is repeated with a new assumed value of the common factor of safety until the recomputed value of  $H$  falls within that range.
7. The new assumed value of the common factor of safety for subsequent iterations is generally less than the previously chosen value if the calculated value of  $H$  is less than the actual value of  $H$ . Conversely, a larger value of the new common factor of safety is assumed if the calculated value of  $H$  is greater than the actual value of  $H$ .

The use of Taylor's chart is illustrated by the following example.

**Example 6-1:** Determine the factor of safety for a 30 ft high fill slope. The slope angle is  $30^\circ$ . The fill is constructed with soil having the following properties:

Total unit weight,  $\gamma = 120$  pcf;      Effective cohesion,  $c' = 500$  psf

Effective friction angle,  $\phi' = 20^\circ$

#### **Solution:**

First assume a common factor of safety of 1.6 for both cohesion and friction angle so that  $F_c = F_\phi = 1.6$ . Since  $F_\phi = 1.6$ , the developed friction angle,  $\phi_d$ , can be computed as follows:

$$\phi_d = \arctan \left( \frac{\tan \phi'}{F_\phi} \right) = \arctan \left( \frac{\tan 20^\circ}{1.6} \right) = 12.8^\circ$$

For  $\phi_d = 12.8^\circ$ , and  $\beta = 30^\circ$ , the value of the stability number  $N_s$  from Figure 6-14 is approximately 0.065. Thus, from Equation 6-26

$$0.065 = \frac{500 \text{ psf}}{(1.6) (120 \text{ pcf}) (H)}$$

or

$$H = \frac{500 \text{ psf}}{(1.6) (120 \text{ pcf}) (0.065)} = 40.1 \text{ ft}$$

Since computed height  $H = 40.1$  ft is greater than the actual height of 30-ft, the value of the common safety factor must be greater than 1.6. Assume  $F_c = F_\phi = 1.9$  and recompute as follows:

If  $F_\phi = 1.9$ , then  $\phi_d = 10.8^\circ$  and  $N_s$  from Figure 6-14 is approximately 0.073 based on which the recomputed value of  $H$  is as follows:

$$H = \frac{500 \text{ psf}}{(1.9) (120 \text{ pcf}) (0.073)} = 30.04 \text{ ft}$$

The height of 30.04 ft is virtually identical to the correct height of 30 ft. Therefore, the minimum factor of safety with respect to shearing strength is approximately 1.9.

### **Alternate Graphical Approach**

An alternate graphical approach for determining the minimum factor of safety with respect to shearing strength is also available. The procedure is as follows:

1. Assume a reasonable value for  $F_\phi$  and calculate  $\phi_d$ .
2. For the given value of  $\beta$  and the calculated value of  $\phi_d$  read the corresponding value of the stability number  $N_s$  from Figure 6-14.
3. Use Equation 6-26 to calculate  $F_c$ .
4. Repeat the process for at least two other assumed values of  $F_\phi$  over a range of expected factors of safety so that at least three pairs of  $F_\phi$  and  $F_c$  are obtained.
5. Plot the calculated points on  $F_c$  versus  $F_\phi$  coordinates and draw a curve through the points.
6. Draw a line through the origin that represents  $F_c = F_\phi$ .
7. The minimum overall factor of safety of the slope with respect to shear strength is the value of factor of safety at the intersection of the calculated with the  $F_c = F_\phi$  line.

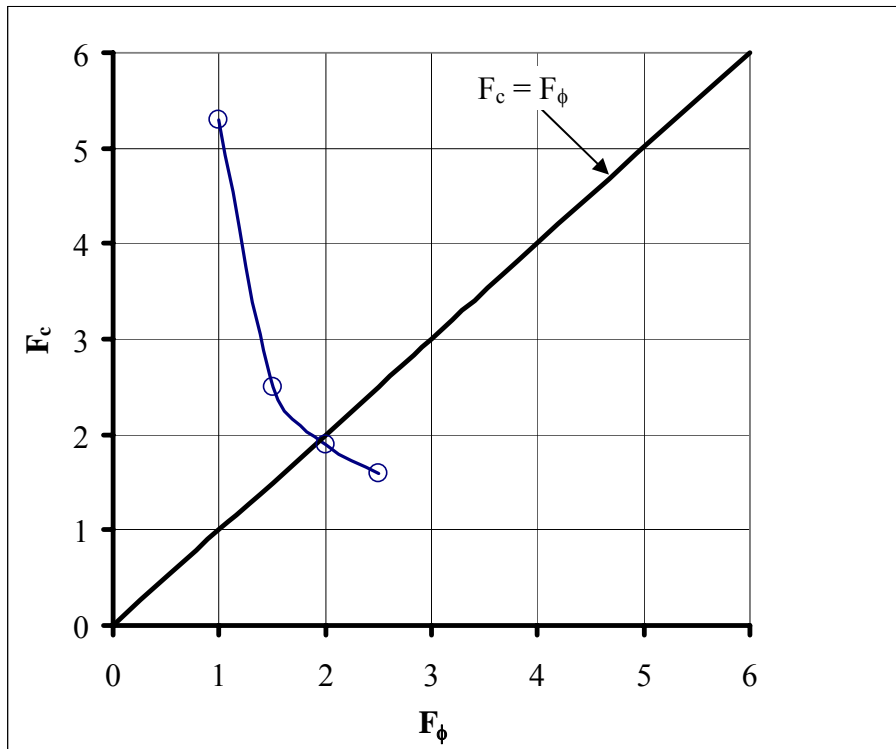
**Example 6-1a:** Solve Example 6-1 by using the alternate graphical approach.

**Solution:**

Set up a table for ease of computation (steps 1 through 4) as follows:

Assumed $F_\phi$	Calculated $\phi_d$	$N_s$ from Figure 6-14	Calculated $F_c$
1.0	20	0.026	5.3
1.5	14	0.055	2.5
2.0	10	0.075	1.9
2.5	8	0.087	1.6

As shown in the figure below, plot the data as per steps 5 and 6 of the procedure. Read the value of  $F_c = F_\phi = 1.95$  at the intersection of plotted curves. This value is the minimum factor of safety with respect to shearing strength, FS. This value is close to the value of 1.9 calculated in Example 6-1. This example problem is also solved by the use of a computer program, ReSSA, in Appendix D and the computer analysis yielded a FS =1.96 which is close to the values computed by the use of stability chart.



### 6.6.3 Janbu's Stability Charts

Janbu (1968) published stability charts for slopes in soils with uniform strength for  $\phi = 0$  and  $\phi > 0$  conditions. These charts are presented in Figures 6-16 through 6-19. This series of charts accounts for several different conditions and provides factors for surcharge loading at the top of the slope, submergence, and tension cracks that can be expected to influence the design of typical highway slopes.

The stability chart for slopes in soils with uniform shear strength throughout the depth of the layer and with  $\phi = 0$  is shown in Figure 6-16. Charts for correction factors for the conditions when surcharge loads, submergence and tension cracks are present are shown in Figures 6-17 through 6-19. Step-by-step guidance for the use Janbu's charts follows.

#### **Steps for using Janbu's Charts on Figures 6-16 through 6-19, for $\phi = 0$ material.**

- Step 1.** Use the chart at the bottom of Figure 6-16 to determine the position of the center of the critical circle, which is located at a coordinate point defined by  $X_o$ ,  $Y_o$  with respect to a cartesian coordinate system whose origin is at the toe of the slope. Following are some guidelines that can be used to identify the critical center:
- For slopes steeper than  $53^\circ$ , the critical circle passes through the toe. For slopes flatter than  $53^\circ$ , the critical circle passes below the toe.
  - In addition to the toe circle, at least four circles with different depths below the toe,  $D$ , should be analyzed to ensure that the actual minimum factor of safety and the actual critical circle have been found. The following suggestions may be used to select the circles (Duncan and Wright, 2005):
    - If there is water outside the slope, a circle passing above the water may be critical.
    - If a soil layer is weaker than the one above it, the critical circle may extend into the lower (weaker) layer. This applies to layers both above and below the toe.
    - If a soil layer is stronger than the one above it, the critical circle may be tangent to the top of the stronger layer.

For each of the assumed circles, perform Steps 2 to 6.

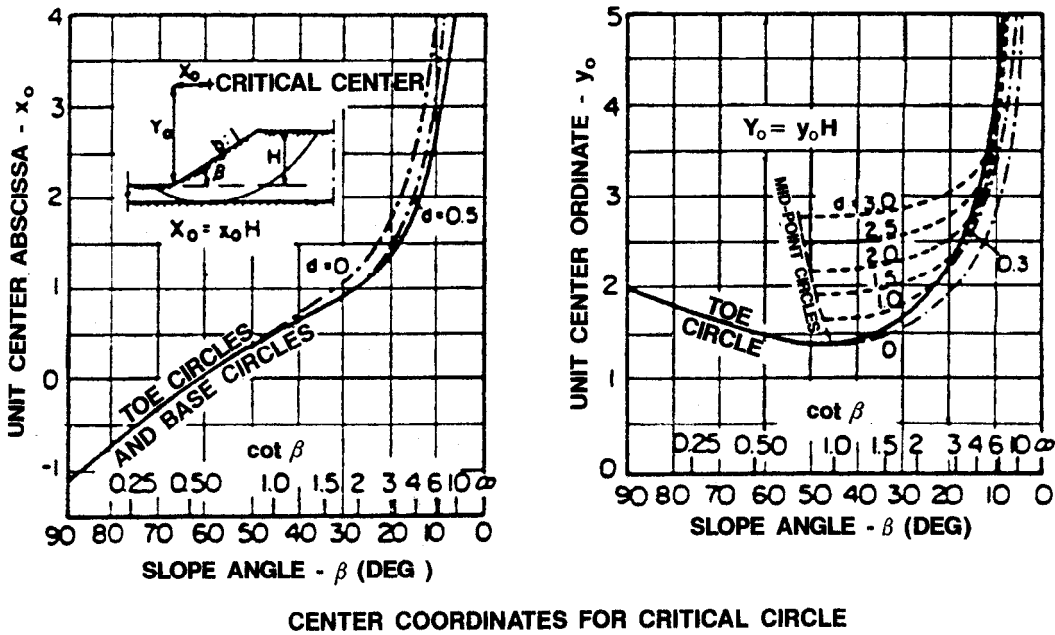
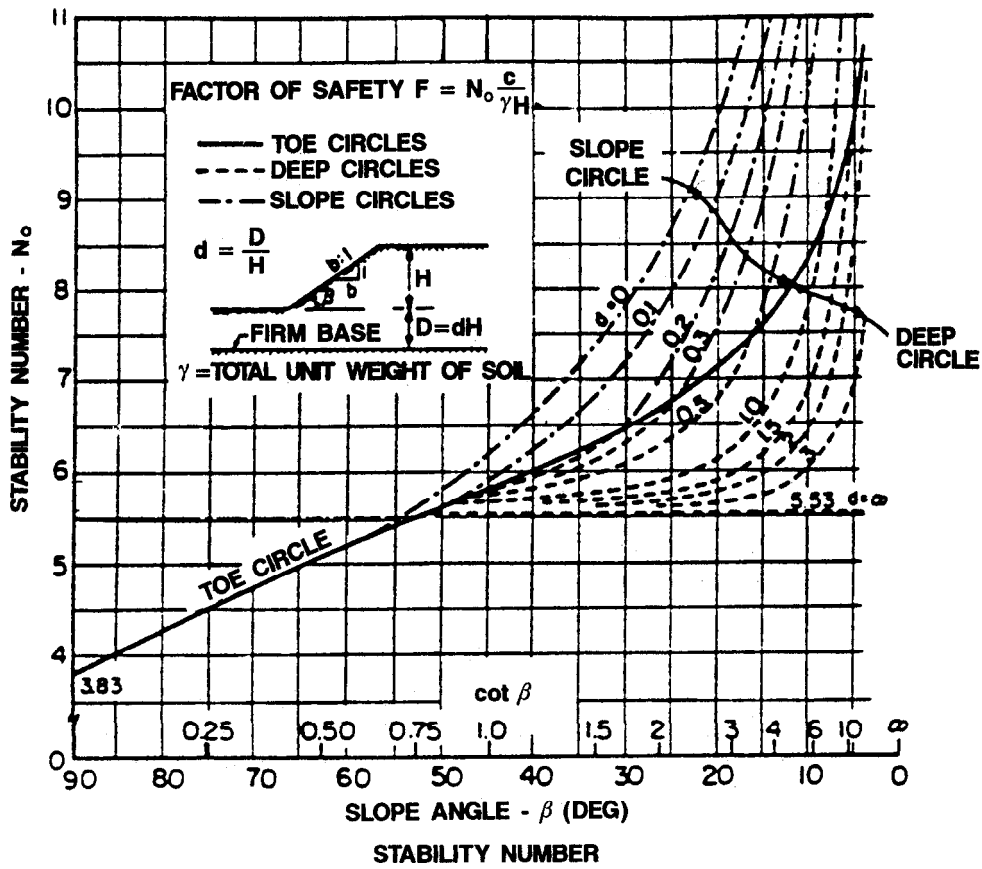


Figure 6-16. Stability charts for  $\phi = 0$  soils (Janbu, 1968).

**Step 2.** Using the assumed critical circle as a guide, estimate the average value of strength,  $c$ , by calculating the weighted average of the strengths along the failure surface. The number of degrees intersected along the arc by each soil layer as a percentage of the entire angle subtended by the arc is used as the weighting factor.

**Step 3.** Calculate the depth factor,  $d$  where  $d = D/H$ . (Note that the depth factor,  $d$ , for Janbu's charts is different from the depth ratio  $D$  for Taylor's chart.)

**Step 4.** Calculate  $P_d$  by using the following equation:

$$P_d = (\gamma H + q - \gamma_w H_w) / (\mu_t \mu_q \mu_w) \quad 6-27$$

where:  $q$  = surcharge load

$\gamma_w$  = unit weight of water

$H_w$  = depth of water outside the slope

$\mu_t$  = tension crack correction factor (Figure 6-17)

$\mu_q$  = surcharge correction factor (Figure 6-18, top)

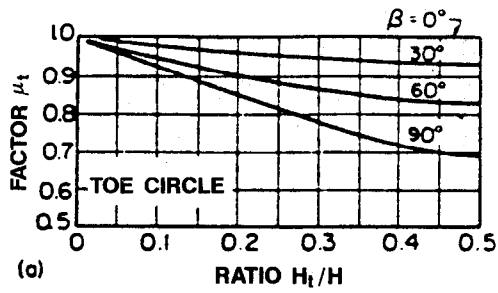
$\mu_w$  = submergence correction factor (Figure 6-18, bottom)

**Step 5.** Use the chart at the top of Figure 6-16 to determine the value of the stability number,  $N_o$ , which depends on the slope angle  $\beta$ , and the value of  $d$ .

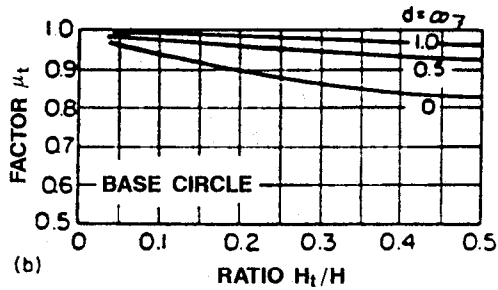
**Step 6.** Calculate the factor of safety (FS) by using the following equation:

$$FS = N_o c / P_d \quad 6-28$$

**Step 7.** Repeat Steps 2 to 6 for all the circles assumed in Step 1. Compare the FS to obtain the most critical circle as the circle with the lowest FS. If it appears that the minimum FS is for a circle close to the toe, i.e.,  $d=0$ , then it is prudent to check if the critical failure surface is within the height of the slope,  $H$ . In this case, the toe of the slope is adjusted to the point of intersection of assumed circle with the slope and all dimensions, (i.e.,  $D$ ,  $H$ , and  $H_w$ ) are adjusted accordingly in the calculations and steps 1 to 6 are repeated (Duncan and Wright, 2005).



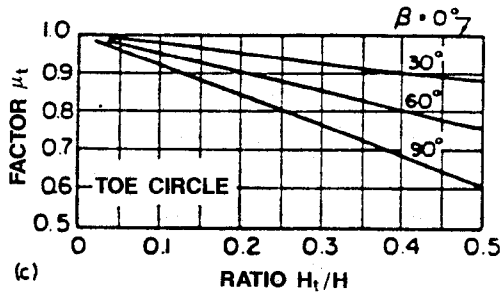
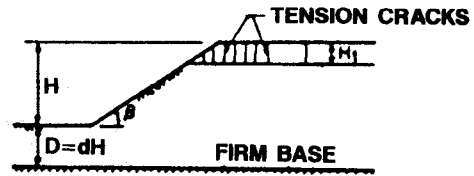
(a)



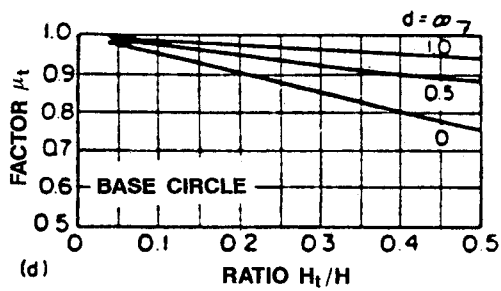
(b)

No water in crack i.e., no hydrostatic pressure in crack

KEY SKETCH



(c)



(d)

Crack filled with water, i.e., full hydrostatic pressure in crack

KEY SKETCH

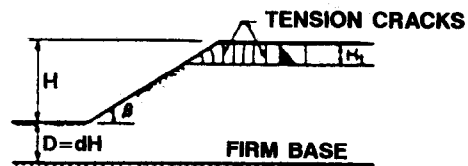
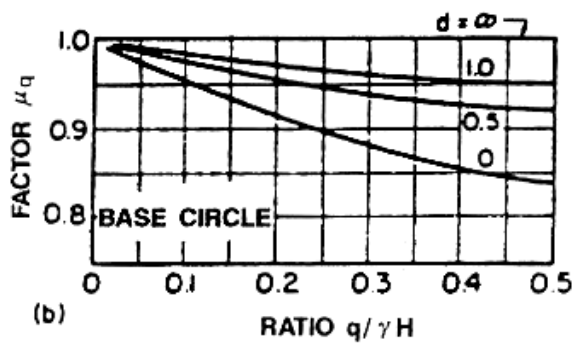
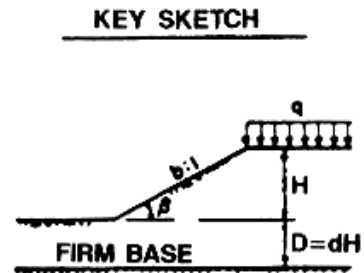
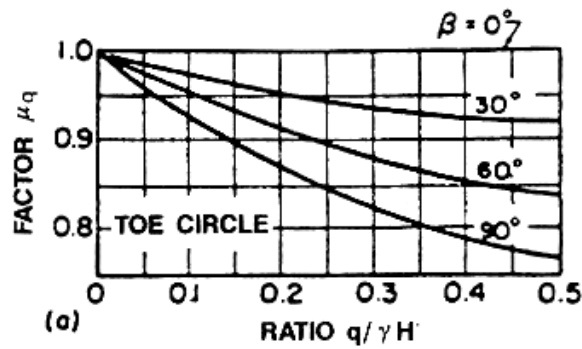
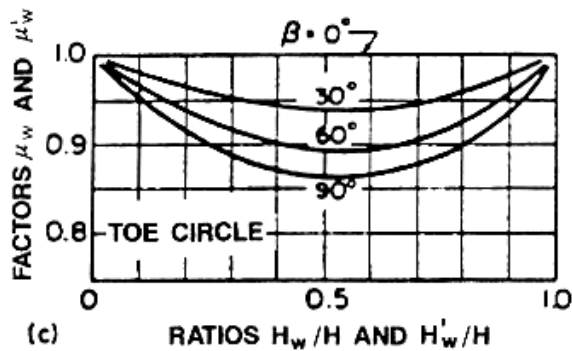


Figure 6-17. Reduction factors to account for tension cracks to be used with stability charts for  $\phi=0$  and  $\phi > 0$  soils (Janbu, 1968).



REDUCTION FACTORS FOR SUBMERGENCE ( $\mu_w$ ) AND SEEPAGE ( $\mu'_w$ )



KEY SKETCHES

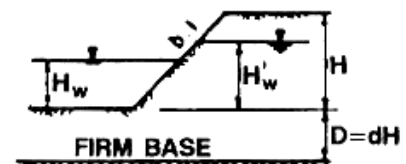
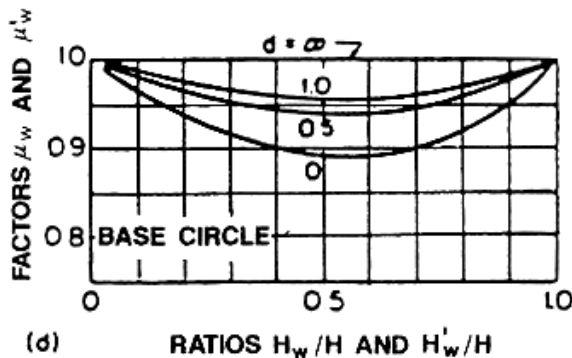
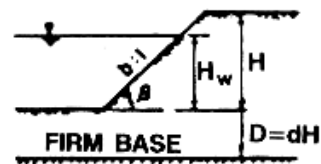


Figure 6-18. Reduction factors to account for surcharge (upper) and submergence and/or seepage (lower) to be used with stability charts for  $\phi=0$  and  $\phi > 0$  soils (Janbu, 1968).

**Steps for using Janbu's Charts on Figures 6-17 through 6-19, for  $\phi > 0$  materials.**

**Step 1.** Use judgment to estimate the location of the critical circle. For most conditions of simple slopes in uniform soils with  $\phi > 0$ , the critical circle passes through the toe of the slope. The critical stability numbers given in Figure 6-19 were developed from analyses of toe circles.

Where conditions are not uniform and there is a weak layer beneath the toe of the slope, a circle passing beneath the toe may be more critical than a toe failure. Figure 6-19 may be used to calculate the factor of safety for such cases provided the values of  $c$  and  $\phi$  used in the analysis represent the correct average values for the circle considered.

If there is a weak layer above the toe of the slope, a circle passing above the toe of the slope may be more critical. Similarly, if there is water outside the toe of the slope, a circle passing above the water may be more critical. When these types of circles are analyzed, the value of  $H$  should be equal to the height from the base of the weak layer, or the water level, to the top of the slope.

**Step 2.** Use the estimated circle in Step 1 as a guide to estimate the average values of  $c$  and  $\phi$ . This can be done by calculating the weighted average values of  $c$  and  $\phi$ . The number of degrees intersected along the arc by each soil layer as a percentage of the entire angle subtended by the arc is used as the weighting factor for each parameter.

**Step 3.** Calculate  $P_d$  by using Equation 6-27.

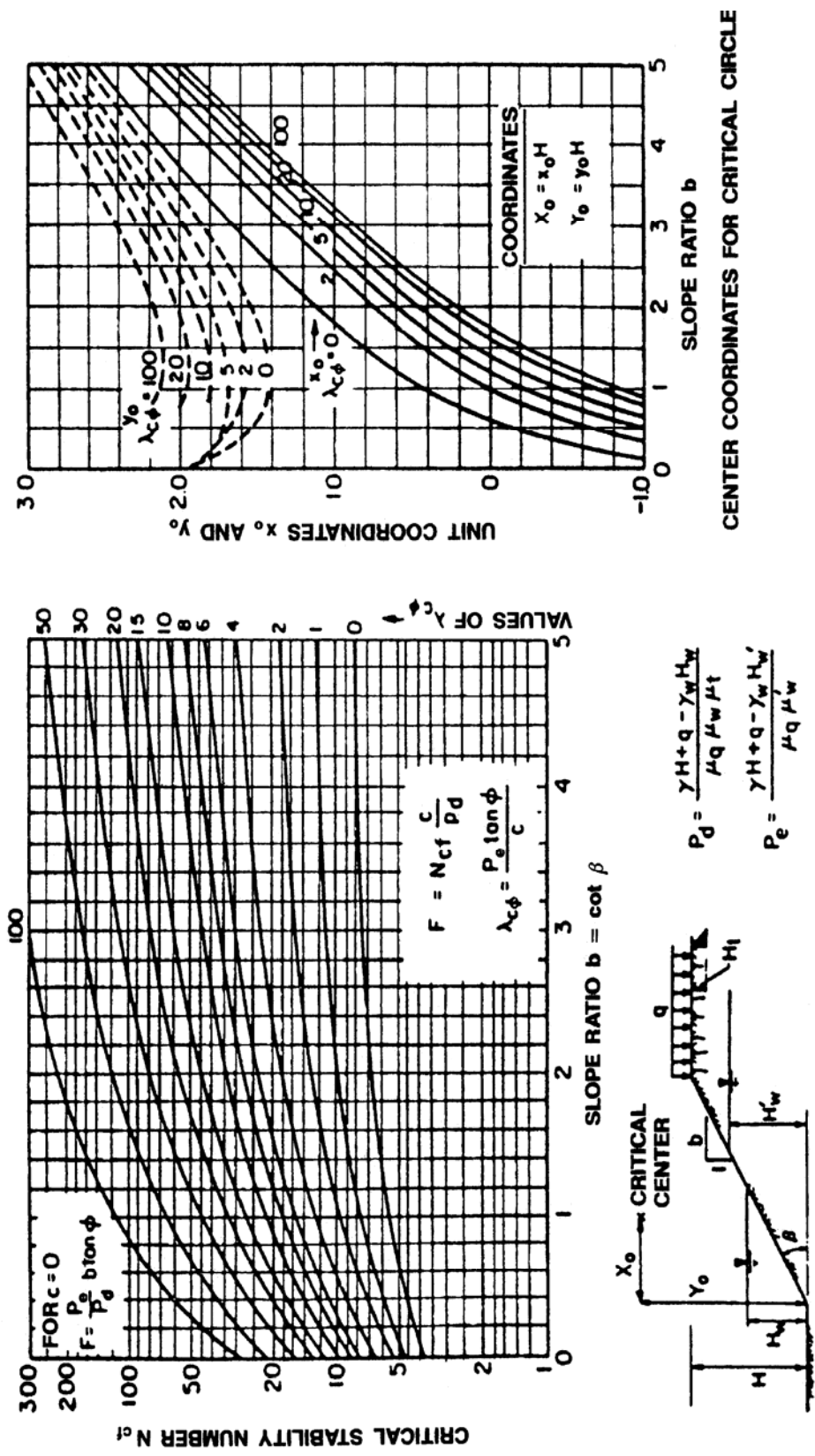
**Step 4.** Calculate  $P_e$  by using the following equation:

$$P_e = (\gamma H + q - \gamma_w H'_w) / (\mu_q \mu'_w) \quad 6-29$$

where:  $H'_w$  = height of water within the slope (Figure 6-18, bottom)

$\mu_q$  = surcharge correction factor (Figure 6-18, top)

$\mu'_w$  = seepage correction factor (Figure 6-18, bottom)



$$P_d = \frac{\gamma H + q - \gamma_w H_w}{\mu_q \mu_w \mu_t}$$

$$P_e = \frac{\gamma H + q - \gamma_w H_w'}{\mu_q \mu_w'}$$

( IN FORMULA FOR  $P_e$  TAKE  $q = 0, \mu_q = 1$  FOR UNCONSOLIDATED CONDITION )

Figure 6-19. Stability charts for  $\phi > 0$  (Janbu, 1968).

**Step 5.** Calculate the dimensionless parameter  $\lambda_{C\phi}$  by using the following equation:

$$\lambda_{C\phi} = P_e \tan\phi/c \quad 6-30$$

For  $c=0$ ,  $\lambda_{C\phi}$  is infinite therefore skip to Step 6.

**Step 6.** Use the chart in Figure 6-19 to determine the value of the critical stability number,  $N_{cf}$ , which is dependent on the slope angle,  $\beta$ , and the value of  $\lambda_{C\phi}$ .

**Step 7.** Calculate the factor of safety for the slope as follows:

$$\text{For } c > 0 \quad \text{FS} = N_{cf} c / P_d \quad 6-31$$

$$\text{For } c = 0 \quad \text{FS} = P_e b \tan \phi / P_d \quad 6-32$$

**Step 8.** Determine the actual location of the critical circle by using the chart on the right side of Figure 6-19. The center of the circle is located at a coordinate point defined by  $X_o$ ,  $Y_o$  with respect to a cartesian coordinate system whose origin is at the toe of the slope. The circle passes through the toe of the slope (the origin), except for slopes flatter than  $53^\circ$ , where the critical circle passes tangent to the top of firm soil or rock. If the critical circle is much different from the one assumed in Step 1 for the purpose of determining the average strength, Steps 2 through 8 should be repeated.

If a slope contains more than one soil layer, it may be necessary to calculate the factor of safety for circles at more than one depth. If the underlying soil layer is weaker than the layer above it, the critical circle will extend into the lower layer, and either a toe circle or a deep circle within this layer will be critical. If the underlying soil layer is stronger than the layer above it, the critical circle may or may not extend into the lower layer, depending on the relative strengths of the two layers. Both possibilities should be examined (Duncan and Wright, 2005).

The use of Janbu's charts is illustrated by the following example.

**Example 6-2:** Figure 6-20 shows a 35 ft high slope with a grade of 1.5H:1V. The soil properties within the slope and under it are shown on the figure. Groundwater is immediately under the slope. Calculate the factor of safety for a toe circle by using total stress analysis based on the soil properties shown. (Note: The circle in Figure 6-20 is plotted in Step 5 of the solution.)

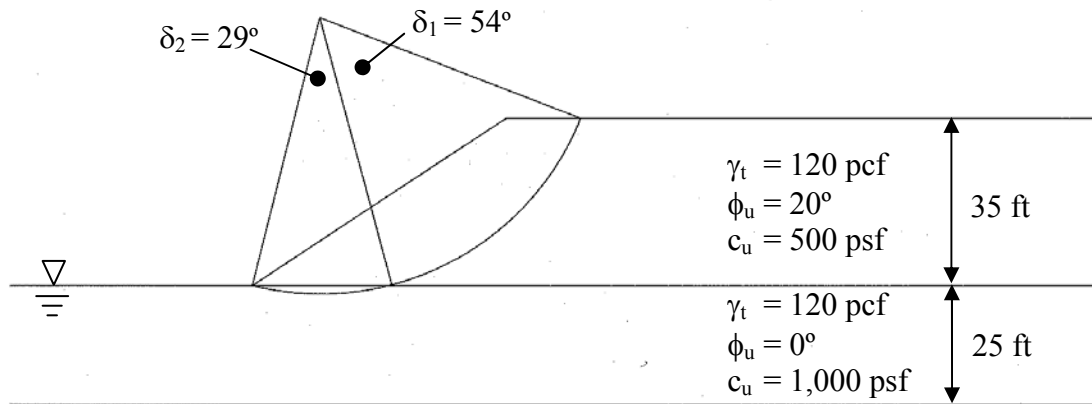


**Figure 6-20. Data for Example 6-2.**

**Solution:**

The correction factors  $\mu_t$ ,  $\mu_q$ ,  $\mu_w$  and  $\mu'_w$  are all equal to 1.0 since there is no tension crack ( $H_t = 0$ ), no surcharge on the slope ( $q = 0$ ), no water above the toe of the slope ( $\gamma_w H_w = 0$ ), and no seepage out of the slope ( $\gamma_w H'_w = 0$ ).

1. Calculate  $P_d$  by using Equation 6-27 as follows:

$$P_d = (\gamma H + q - \gamma_w H_w) / (\mu_t \mu_q \mu_w)$$

$$P_d = (120 \text{ pcf})(35 \text{ ft}) / [(1)(1)(1)] = 4,200 \text{ psf}$$

2. Calculate  $P_e$  by using Equation 6-29 as follows:

$$P_e = (\gamma H + q - \gamma_w H'_w) / (\mu_q \mu'_w)$$

$$P_e = (120 \text{ pcf})(35 \text{ ft}) / [(1)(1)] = 4,200 \text{ psf}$$

3. For a toe circle, it is likely that a segment of the circle will pass through the soil below the toe and the average shear strength parameters along the circle will be different than those for the two layers. However, since at this stage the length of the segment passing through the soil below the toe is unknown, assume that the shear strength values of the soil within the slope height are representative and calculate the parameter  $\lambda_{C\phi}$  by using Equation 6-30 as follows:

$$\lambda_{C\phi} = P_e \tan\phi / c = (4,200 \text{ psf}) (\tan 20^\circ) / (500 \text{ psf}) = 3.06$$

4. From Figure 6-19 obtain the approximate center coordinates of the critical circle by using  $b=1.5$  and  $\lambda_{C\phi} = 3.06$  as follows

$$x_o \approx 0.4 \quad y_o \approx 1.6$$

$$\text{Thus, } X_o = (H)(x_o) = (35 \text{ ft})(0.4) = 14 \text{ ft}$$

$$Y_o = (H)(y_o) = (35 \text{ ft})(1.6) = 56 \text{ ft}$$

5. Plot the critical circle on the given slope, as shown in Figure 6-20. Note that the subtended angles for the failure circle within the slope and the foundation are  $\delta_1 = 54^\circ$  and  $\delta_2 = 29$  degrees, respectively.
6. Calculate  $c_{av}$ ,  $\tan \phi_{av}$  and  $\lambda_{C\phi}$  based on the angular distribution of the failure surface within the slope and foundation soil using  $\delta_1$  and  $\delta_2$  as follows:

$$c_{av} = [(54^\circ)(500 \text{ psf}) + (29^\circ)(1,000 \text{ psf})] / (54^\circ + 29^\circ) = 674.7 \text{ psf}$$

$$\tan \phi_{av} = [(54^\circ)(\tan 20^\circ) + (29^\circ)(\tan 0^\circ)] / (54^\circ + 29^\circ) = 0.236 \quad (\text{or } \phi_{av} = 13.3^\circ)$$

Thus, according to Equation 6-30;

$$\lambda_{C\phi} = P_e \tan \phi / c = (4,200 \text{ psf})(0.236) / (674.7 \text{ psf}) = 1.47 \approx 1.5$$

7. From Figure 6-19 obtain the center coordinates of the critical circle by using  $b=1.5$  and  $\lambda_{C\phi} = 1.5$  as follows

$$x_o \approx 0.5 \quad y_o \approx 1.55$$

$$\text{Thus, } X_o = (H)(x_o) = (35 \text{ ft})(0.5) = 17.5 \text{ ft}$$

$$Y_o = (H)(y_o) = (35 \text{ ft})(1.55) = 54.3 \text{ ft}$$

This circle is close to the circle obtained in the previous iteration, so retain  $\lambda_{C\phi} = 1.5$  and  $c_{av} = 674.7 \text{ psf}$ .

8. From Figure 6-19, obtain  $N_{cf} = 10.0$  for  $b = 1.5$  and  $\lambda_{C\phi} = 1.5$ .
9. Calculate the factor of safety, FS, by using Equation 6-28 as follows :

$$FS = N_o c / P_d = (10)(674.7 \text{ psf}) / (4,200 \text{ psf})$$

$$FS = 1.61$$

This calculation sequence is only for a given circle. This sequence is repeated for several circles and the resulting FS compared to find the minimum FS. With the advent of computer programs, this method is now more often used to verify the results of the computer generated most critical circle rather than computing the minimum FS by repeating the above sequence of calculations for several circles.

## 6.7 SLIDING BLOCK FAILURE

A "sliding block" type failure can occur where:

1. the foundation soil contains thin seams of weak clay or organic soils,
2. a shallow layer of weak soil exists at the ground surface and is underlain by firm soil, and
3. the foundation soil contains thin sand or silt lenses sandwiched between less permeable soil. The weak layers or lenses provide a plane of weakness along which sliding can occur. In the case of sand or silt lenses trapped between less permeable soils, the mechanism that can cause sliding is as follows. As the fill load is placed, the water pressure is increased in the sand or silt lense. Since the water cannot escape due to the impermeable soil above and below, the sand or silt loses frictional strength as a result of the intergranular effective stress between soil grains being decreased due to the excess pore water pressure.

Typical "sliding block" type failures are illustrated in Figure 6-21. When sliding occurs, an active wedge type failure occurs through the fill and a passive wedge type failure occurs below the fill toe as soil in the toe area is pushed out of the way. The sliding mass moves essentially as a block, thus the term "sliding block." These concepts are illustrated in Figure 6-22.

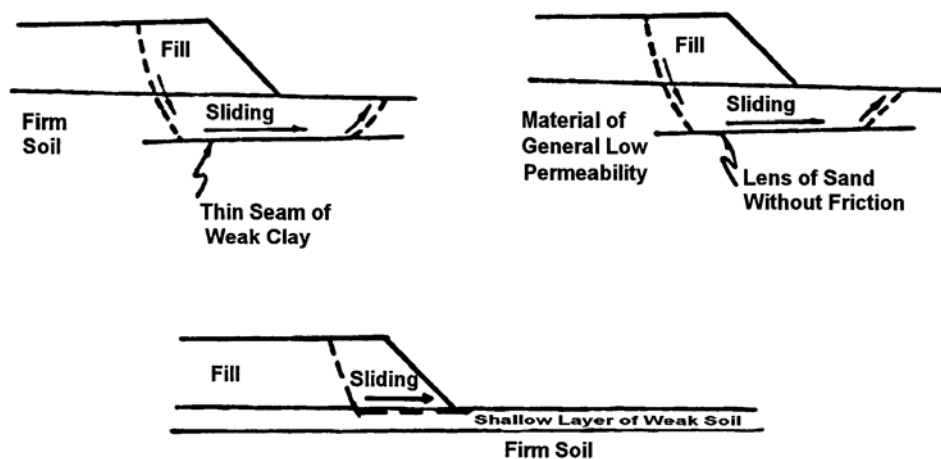


**Figure 6-21. Sliding block failure mechanism.**

### 6.7.1 Sliding Block – Hand Method of Analysis

A simple sliding block analysis to estimate the factor of safety against sliding is straightforward and can be performed easily and quickly by hand. For the analysis, the potential sliding block is divided into three parts; (1) an active wedge at the head of the slide, (2) a central block, and (3) a passive wedge at the toe as shown in Figure 6-22.

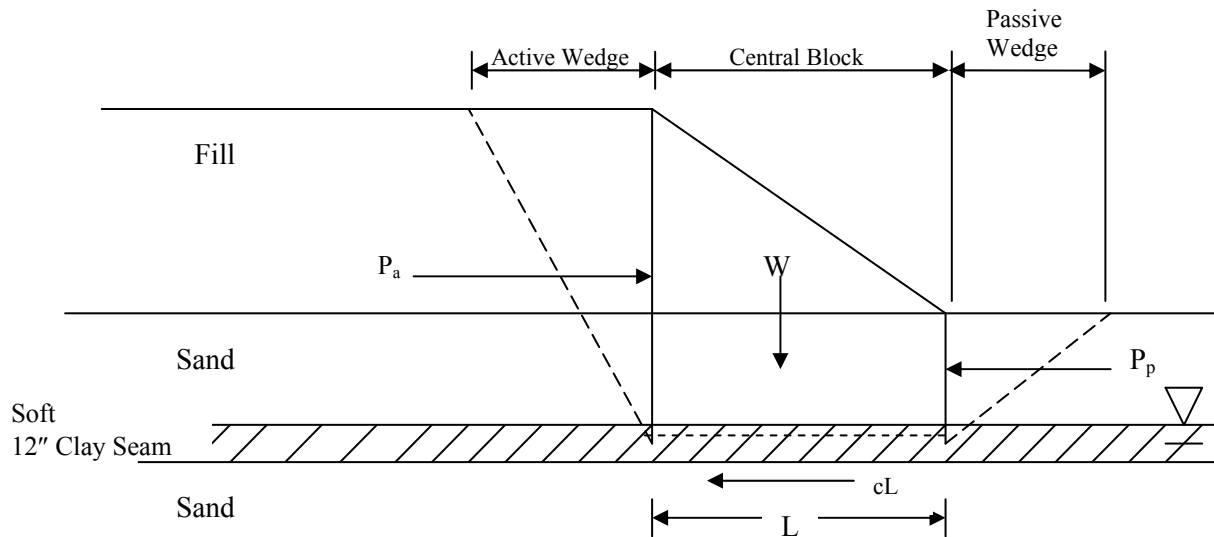


**Figure 6-22. Geometry and force components for sliding block analysis.**

For the problem illustrated in Figure 6-22, the factor of safety would be computed by summing forces horizontally, to give:

$$FS = \frac{\text{Horizontal Resisting Forces}}{\text{Horizontal Driving Forces}} = \frac{P_p + cL}{P_a} \quad 6-33$$

where:  $P_a$  = Active force (driving)  
 $P_p$  = Passive force (resisting)  
 $cL$  = Resisting force due to cohesion of clay

The assumption is made that the loading is rapid so that there is no frictional component of resistance. For convenience of computation of a 1 ft thick slice of embankment is assumed.

Several trial locations of the active and passive wedges must be checked to determine the minimum factor of safety. Note that since wedge type failures occur at the head and toe of the slope, similar to what occurs behind retaining walls, the active and passive forces are

assumed to act against vertical planes that are treated as "imaginary" retaining walls, and the active and passive forces are computed the same as for retaining wall problems.

### 6.7.1.1 Computation of Forces - Simple Sliding Block Analysis

For the simple sliding block problem illustrated Figure 6-22 the forces used to compute the factor of safety can be calculated by using the Rankine approach as follows:

#### Driving Force – Rankine Active Force

$$P_a = 1/2 \gamma H^2 K_a \quad 6-34$$

Where:  $P_a$  = active force (kips) (kN)  
 $\gamma$  = unit weight of soil in the active wedge (kcf) (kN/m<sup>3</sup>)  
 $H$  = height of soil layer in active wedge (ft) (m)  
 $K_a$  = active earth pressure coefficient for level ground surface  
 $K_a = (1 - \sin\phi)/(1 + \sin\phi) = \tan^2(45^\circ - \phi/2)$  (see Chapter 2)  
 $\phi$  = angle of internal friction of soil in the active wedge.

#### Resisting Force – Rankine Passive Force

$$P_p = 1/2 \gamma H^2 K_p \quad 6-35$$

Where:  $P_p$  = passive force (kips) (kN)  
 $\gamma$  = unit weight of soil in the passive wedge (kcf) (kN/m<sup>3</sup>)  
 $H$  = height of soil layer in passive wedge (ft) (m)  
 $K_p$  = passive earth pressure coefficient for level ground surface  
 $K_p = (1 + \sin\phi)/(1 - \sin\phi) = \tan^2(45^\circ + \phi/2)$  (see Chapter 2)  
 $\phi$  = angle of internal friction of soil in the passive wedge.

**Resisting Force (kips or kN) = Clay cohesion (c in ksf or kPa) x  
 Length of central wedge (L in ft or m)**

#### Computation Tips:

The following design tips should be kept in mind when a sliding block analysis is performed.

1. Be aware that the active or passive wedge can pass through more than one soil type with different strengths or unit weights. If that is the case then the active or passive

pressure distribution changes at the boundary between the different soils. This abrupt change in pressure is due to a change in either the angle of internal friction that affects the value of the earth pressure coefficient  $K_a$  or  $K_p$  and/or a change in the unit weight of the soil. The easiest way to handle this condition is to compute the active or passive earth pressure distribution diagram for each soil. There may be a discontinuity in the pressure diagram at the boundary between the two different soil layers. Then compute the active or passive force for each segment of the pressure distribution diagram from the area of each segment.

2. When the active or passive pressure is being computed for soils below the ground water table, the buoyant (effective) unit weight of the soil must be used.

The step-by step procedure for the Sliding Block Method of Analysis is illustrated by the following numerical example.

**Example 6-3:** Find the safety factor for the 20 ft high embankment illustrated in Figure 6-23 by using the simple sliding block method and Rankine earth pressure coefficients. Consider a 1 ft wide strip of the embankment into the plane of the paper.

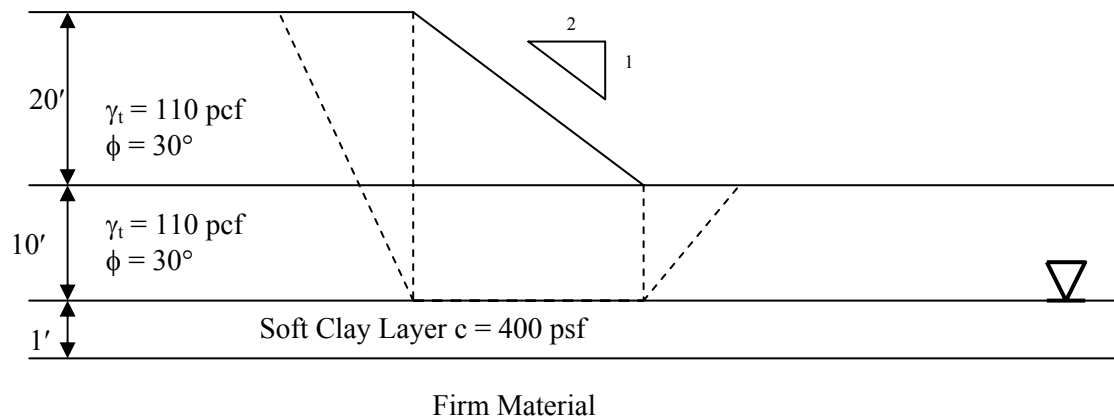


**Figure 6-23. Example simple sliding block method using Rankine pressure coefficients.**

### Solution

**Step 1:** Compute driving force,  $P_a$ , by using Equation 6-34

- Active Driving Force ( $P_a$ ) by using Equation 6-34

$$P_a = \frac{1}{2} \gamma_t H^2 K_a \quad (\text{use } \gamma_t \text{ as the water table is below the failure plane})$$

$$K_a = \tan^2 \left( 45 - \frac{\phi}{2} \right) = \tan^2 \left( 45 - \frac{30^\circ}{2} \right) = 0.33$$

$$P_a = \frac{1}{2} (0.110 \text{ kcf})(30 \text{ ft})^2 (0.33)(1 \text{ ft}) = 16.5 \text{ kips}$$

**Step 2:** Compute resisting forces

- Central Block Resistance

$$c_l = (0.400 \text{ ksf})(40 \text{ ft})(1 \text{ ft}) = 16.0 \text{ kips} \quad (71.1 \text{ kN})$$

- Passive Resisting Force by using Equation 6-35

$$P_p = \frac{1}{2} \gamma_t H^2 K_p$$

$$K_p = \tan^2 \left( 45 + \frac{\phi}{2} \right) = \tan^2 \left( 45 + \frac{30^\circ}{2} \right) = 3.0$$

$$P_p = \left( \frac{1}{2} \right) (0.110 \text{ kcf})(10 \text{ ft})^2 (3)(1 \text{ ft}) = 16.5 \text{ kips}$$

**Step 3:** Compute factor of safety by using Equation 6-33

$$\text{Safety Factor} = \frac{c_l + P_p}{P_a} = \frac{16.0 \text{ kips} + 16.5 \text{ kips}}{16.5 \text{ kips}} = 1.97$$

### 6.7.2 Computation of Forces - Complicated Sliding Block Analysis

The Rankine approach is a useful tool to portray the mechanism of a planar failure condition. However a general force diagram applicable to a more difficult sliding block type problem can account for the effects of water pressure, cohesion, friction, and a sloping failure plane in

the analysis. This analysis procedure, which is described in FHWA (2001a), can be used both to estimate the factor of safety for assumed failure surfaces in design or to "back-analyze" sliding block landslide problems.

Computer solutions are also available for failure modes defined by planar and non-circular surfaces. However most of those solutions do not use the simplified Rankine block approach but rather a more complex failure plane such as that used in Janbu's method. In general a computer solution is preferred for these planar failure problems because of the flexibility they offer in handling a variety of conditions that result in a more complex failure plane.

## **6.8 SLOPE STABILITY ANALYSIS USING COMPUTER PROGRAMS**

Slope stability procedures are well suited to computer analysis due to the interactive nature of the solution. Also, the simplified hand solution procedures do not properly account for interslice forces, irregular failure surfaces, seismic forces, and external loads such as line load surcharges or tieback forces. Several user-friendly computer programs exist to analyze two-dimensional slope stability problems. One of the advantages of a computer program is that it allows parametric studies to be performed by varying parameters of interest, e.g., shear strength parameters. More complex computer programs are available for three dimensional slope stability analysis. As a minimum, a basic two-dimensional slope stability program is recommended for routine use.

Desirable geotechnical features of such a program should include:

- Multiple analysis capability
  - a. Circular arc (Bishop)
  - b. Non-circular (Janbu)
  - c. Sliding block
  
- Variable input parameters to account for specific conditions
  - a. Heterogeneous soil systems
  - b. Pseudo-static seismic loads
  - c. Ground anchor forces
  - d. Piezometric levels
  
- Random generation of multiple failure surfaces with an option to analyze a specific failure surface.

Desirable software features include:

- User-friendly input screens including a summary screen that shows the cross section and soil boundaries in profile.
- Help screens and error tracking messages.
- Expanded output options for both resisting forces in friction, cohesion or tieback computations and driving forces in static or dynamic computations.
- Ordered output and plotting capability for the failure surface of 10 minimum safety factors.
- Documentation of program.

A major problem for software users is technical support, maintenance and update of programs. Slope stability programs are in a continual process of improvement that can be expected to continue indefinitely. Highway agencies should implement only software that is documented and verified and for which the seller agrees to provide full technical support, maintenance and update. The following web page for the FHWA National Geotechnical Team contains links to distributors of FHWA software:

<http://www.fhwa.dot.gov/engineering/geotech/index.cfm>

Similar services are provided for commercially available slope stability programs such as the ReSSA (2001), SLOPE/W, SLIDE, STABL series (e.g., PCSTABL, XSTABL, GSTABL), and UTEXAS. Appendix D provides an overview of use of the ReSSA program.

Finally, it is extremely important for the designer to understand that the design is only as good as the input parameters. Therefore, the designer should put major emphasis where it belongs, which is on:

- Investigation
- Sampling
- Testing
- Development of soil profile
- Design soil strengths
- Ground water table location

Computer programs are only tools that aid in the design. The answers are only as good as the input data. Don't get carried away with plugging in the numbers and examining the results. You may learn the "garbage in - garbage out" principle the hard way.

## **6.9 IMPROVING THE STABILITY OF EMBANKMENTS**

There are usually several technically feasible solutions to a stability problem. The chosen solution should be the most economical considering the following factors:

1. Available materials.
2. Quantity and cost of materials.
3. Construction time schedules.
4. Line and grade requirements.
5. Right-of-way issues.

### **6.9.1 Embankment Stability Design Solutions**

Table 6-2 presents a summary of practical solutions to mitigate embankment stability problems. Figures 6-24 to 6-26 illustrate some of the mitigation methods listed in Table 6-2. One of the solutions listed in Table 6-2 is the use of ground improvement. This solution can be used for cases where the internal stability of the embankment is not an issue due to the use of competent embankment materials, but the foundation materials are weak enough to affect the stability of the embankment slope. By improving the ground under the embankment, the resistance along the failure surface within the foundation is improved, thereby increasing the safety factor against slope failure. Relatively poor soils can be reinforced with geosynthetics to offset their low shear strength so that acceptable embankments can be constructed.

Another solution is related to reinforcement of the embankment soils themselves. This solution can be used where the foundation is adequate but the locally available soils may not be suitable for construction of embankments at the desired slope angles. In this case, the embankment soils may be strengthened by the inclusion of reinforcements. Such slopes are called reinforced soil slopes (RSS). The RSS technology can be used to construct slopes at angles up to 69-degrees from horizontal. The RSS design method is discussed here as an example of a remediation method. Only the basics of the RSS design method are presented herein. Detailed design procedures for RSS technology can be found in FHWA (2001b).

### **6.9.2 Design Approach for Reinforced Soil Slopes**

The design of internal reinforcement for safe, steep slopes requires a rigorous analysis. The design of the reinforcement for this application is critical, as failure of the reinforcement would result in failure of the slope. The overall design requirements for reinforced slopes are similar to those for unreinforced slopes. The factor of safety must be adequate for both the short-term and long-term conditions and for all possible modes of failure.

**Table 6-2**  
**Practical design solutions to mitigate embankment stability problems**

*1. Relocate highway alignment.	A line shift of the highway to an area having better soils may be the most economical solution.
*2. Reduce grade line. (flatten slope)	A reduction in grade line will decrease the weight of the embankment and will improve stability (Figure 6-24).
3. Counterweight berms.	A counterweight berm outside of the center of rotation, as illustrated in (Figure 6-25), provides an additional resisting moment that increases the factor of safety. Berms should be built concurrently with the embankment. The embankment should never be completed prior to berm construction since the critical time for shear failure is at the end of embankment construction. The top surface of a berm should be sloped to drain water away from the embankment. Also, care should be exercised in selection of materials and compaction specifications to assure the design unit weight will be achieved for berm construction.
4. Excavation of soft soil and replacement with shear key.	The strength of soft soils is often insufficient to support embankments. In such cases, the soft soils are excavated and replaced with granular material that acts like a shear key (Figure 6-26).
5. Displacement of soft soil.	For deep soft deposits, excavation is difficult. The soft soil can be displaced by generating continuous shear failures along the advancing fill front until the embankment is on firm bottom. The mudwave forced up in front of the fill must be excavated to insure continuous displacement and prevent large pockets of soft soil from being trapped under the fill
6. Slow rate or stage	Many weak subsoils will tend to gain strength during the loading process as consolidation occurs and pore water pressures dissipate. For soils that consolidate relatively fast, such as some silts and silty clays, this method is practical. Proper instrumentation is desirable to monitor the state of stress in the soil during the loading period to insure that loading does not proceed so rapidly that a shear failure occurs. Typical instrumentation consists of slope inclinometers to monitor stability, piezometers to measure excess pore water pressure, and settlement devices to measure the amount and rate of settlement. Planning of the instrumentation program and data interpretation should be done by a qualified and experienced geotechnical engineer. This option could also be used if weak subsoils are pretreated with wick drains
7. Lightweight embankment.	In some areas of the country lightweight materials such as blast furnace slag, shredded rubber tires, or expanded shale are available. The slag material weighs about 80 pcf (12.6 kN/m <sup>3</sup> ). Sawdust fill weighs about 50 pcf (7.9 kN/m <sup>3</sup> ) and has a friction angle of 35° or more. Expanded Polystyrene Foam (EPS) is available throughout the country and weighs 1 to 3 pcf (0.15 to 0.5 kN/m <sup>3</sup> ). Use of such materials decreases the driving force. Typical advantages and disadvantages of the use of such materials, and specifications for lightweight fills are included in FHWA (2006b).
8. Ground improvement	Recently developed techniques such as stone columns, soil mixing, geosynthetics, soil nailing, ground anchors, and grouting can be used to increase resisting forces. Specialty contractors should be considered for these design solutions.
9. Reinforcement of embankment soils.	The embankment soils can be strengthened by incorporating reinforcements with the compacted soil. The reinforcement generally permits steeper slopes compared to unreinforced embankments.

\*Always consider these solutions first since they are relatively simple and inexpensive.

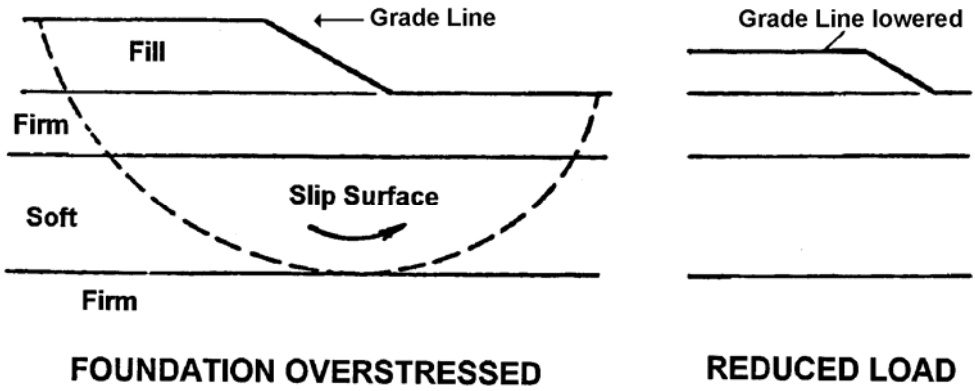


Figure 6-24. Reduction of grade line to improve slope stability.

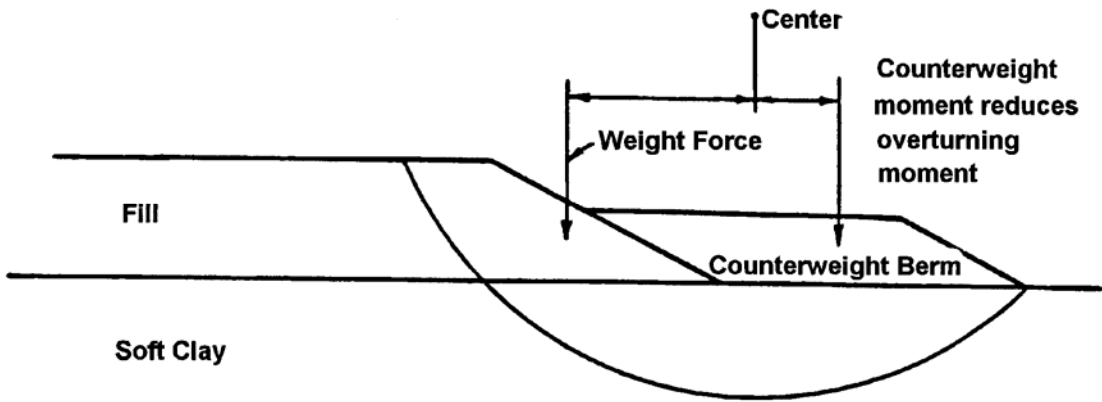


Figure 6-25. Use of counterweight berm to improve slope stability.

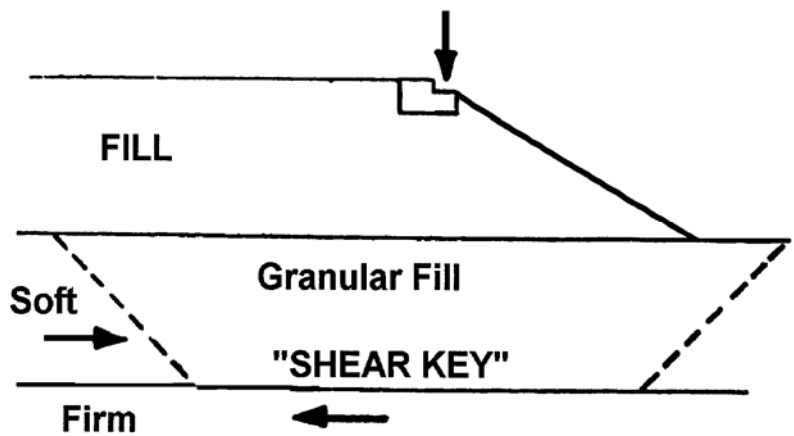
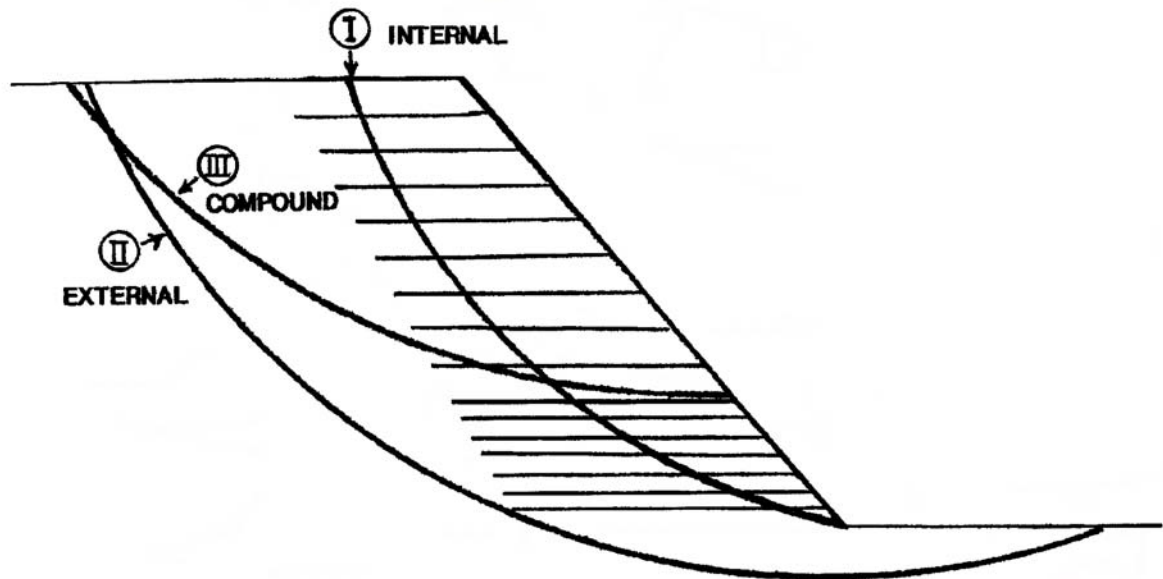


Figure 6-26. Use of shear key to improve slope stability.

As illustrated in Figure 6-27, there are three possible failure modes for reinforced slopes:

1. Internal - the failure plane passes through the reinforcing elements.
2. External - the failure surface passes behind and underneath the reinforced mass. The reinforced mass is the mass of soil that contains the reinforcements.
3. Compound - the failure surface passes behind and through the reinforced soil mass.



**Figure 6-27. Failure modes for Reinforced Soil Slopes.**

In some cases, the calculated minimum safety factor can be approximately equal in two or even all three modes if the reinforcement strengths, lengths, and vertical spacing are optimized (FHWA, 2001b). FHWA (2001b) contains a detailed discussion of the analysis and design of RSS'. A convenient chart solution is presented in this manual for preliminary feasibility-level design of the RSS.

### **6.9.2.1 Preliminary Feasibility Design of RSS**

A preliminary design for a feasibility evaluation can be easily made by the use of design charts. These charts can also be used for the final design of low slopes, i.e., slope height less than 20 ft (6 m), where the consequences of failure are not critical. Figure 6-28 is a widely used chart that presents a simplified method based on a two-part, wedge-type failure surface. Use of the chart is limited by the assumptions noted on the figure. Figure 6-28 is not

intended to be a single design tool. Other design charts available from the literature could also be used, e.g., FHWA (2001b), Leshchinsky and Perry (1987).

The procedure for using the charts shown in Figure 6-28 is as follows:

1. For an assumed (desired) safety factor,  $F$ , determine the factored friction angle,  $\phi'_f$ , in degrees as follows (Note: this is similar to the factored friction angle in Taylor's stability chart):

$$\phi'_f = \arctan \left( \frac{\tan \phi'}{F} \right)$$

2. Using  $\phi'_f$  read the force coefficient  $K$  from Part A and determine  $T_{S-MAX}$  as follows:

$$T_{S-MAX} = 0.5 K \gamma_f (H')^2$$

where  $H' = H + q/\gamma$  is the effective height,  $q$  = surcharge, and  $\gamma_f$  = fill unit weight.

3. Determine the length of the reinforcement at the top,  $L_T$ , and bottom,  $L_B$ , of the slope from Part B.
4. Determine the distribution of reinforcement:
  - For low slope heights ( $H \leq 20$  ft) assume a uniform reinforcement distribution, and use  $T_{S-MAX}$  to determine the spacing or the required tension,  $T_{MAX}$ , for each reinforcement layer.
  - For high slope heights ( $H > 20$  ft), divide the slope into two or three reinforcement zones of equal height, and use a factored  $T_{S-MAX}$  in each zone for spacing or design tension requirements.

For 2 zones:

$$T_{Bottom} = 3/4 T_{S-MAX}$$

$$T_{Top} = 1/4 T_{S-MAX}$$

For 3 zones:

$$T_{Bottom} = 1/2 T_{S-MAX}$$

$$T_{Middle} = 1/3 T_{S-MAX}$$

$$T_{Top} = 1/6 T_{S-MAX}$$

The force is assumed to be uniformly distributed over the entire zone.

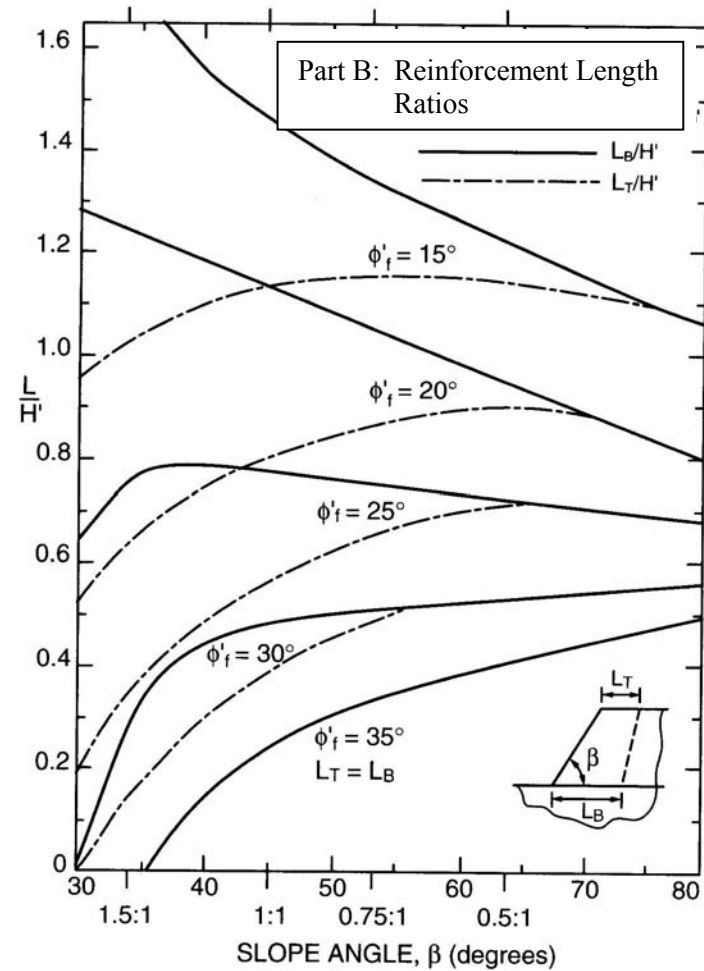
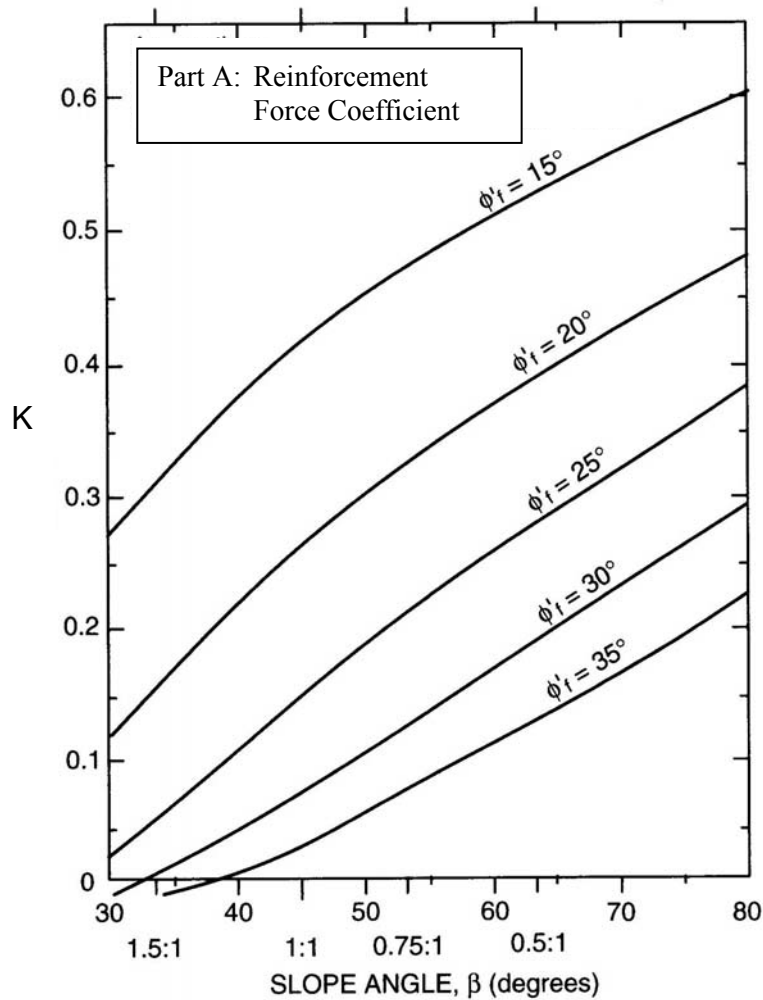


Chart assumptions:

(1) extensible reinforcement, (2) slopes constructed with uniform cohesionless soils ( $c=0$ ), (3) no pore water pressures within slope, (4) competent, level foundation soils, (5) no seismic forces, (6) uniform surcharge,  $q$ , not greater than  $0.2\gamma_f H$ , (7) relatively high soil/reinforcement interface friction angle =  $0.9\phi'$  (may not be appropriate for some geotextiles).

**Figure 6-28. Chart solution for determining the reinforcement strength requirements (after Schmertmann, *et al.*, 1987).**

- Determine the requirements for vertical spacing of the reinforcement,  $S_v$ , or the maximum design tension,  $T_{MAX}$ , for each reinforcement layer.
- For each zone, calculate  $T_{MAX}$  for each reinforcing layer in that zone based on an assumed  $S_v$  or, if the allowable reinforcement strength is known, calculate the minimum vertical spacing and number of reinforcing layers,  $N$ , required for each zone based on Equation 6-36 and the use of consistent units.

$$T_a R_c = T_d = \frac{T_{zone} S_v}{H_{zone}} = \frac{T_{zone}}{N} \quad 6-36$$

where:

$T_a$  = sum of available tensile force per width of reinforcement for all reinforcement layers.

$R_c$  = coverage ratio of the reinforcement that equals the width of the reinforcement,  $b$ , divided by the horizontal spacing  $S_h$ .

$S_v$  = vertical spacing of reinforcement; multiples of compacted layer thickness for ease of construction.

$T_{zone}$  = maximum reinforcement tension required for each zone.  
=  $T_{S-MAX}$  for low slopes ( $H < 20$  ft)

$H_{zone}$  = height of zone.  
=  $T_{top}$ ,  $T_{middle}$ , and  $T_{Bottom}$  for high slopes ( $H > 20$  ft)

$N$  = number of reinforcement layers.

- In general, use short (4 - 6.5 ft (1.2 - 2 m)) lengths of reinforcement layers to maintain a maximum vertical spacing of 16 in (400 mm) or less for face stability and compaction quality. This short reinforcement should be placed in continuous layers and need not be as strong as the primary load bearing reinforcement, but it must be strong enough to survive construction (e.g., minimum survivability requirements for geotextiles in road stabilization applications in AASHTO M-288) and provide localized tensile reinforcement to the surficial soils.

For detailed analyses required for final design, refer to FHWA (2001b). The computer program ReSSA (2001) noted earlier, can perform analysis and design of reinforced soil slopes using the methods described in FHWA (2001b).

## 6.10 IMPROVING THE STABILITY OF CUT SLOPES

The two most common types of cut slope failures are deep-seated and shallow surface failures. Both of these types of failure and their mitigation are discussed in this section.

### 6.10.1 Deep Seated Failure

A deep seated failure usually occurs in slopes cut into clay. The clay has insufficient shear strength to support the slope, and shear failure generally occurs along a circular arc. If the clay contains water-bearing silt or sand layers, seepage forces will also contribute to the instability. Figure 6-29 shows an example of a deep seated failure and a possible design solution. Table 6-3 lists typical design solutions to potential cut slope stability problems in clay.

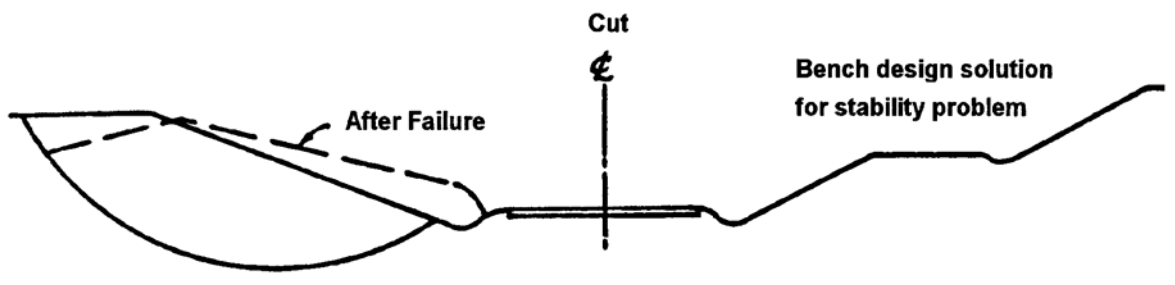


**Figure 6-29. Deep seated slope failure (left) and bench slope design (right) to prevent slope failure.**

**Table 6-3**

**Typical design solutions to mitigate cut slope stability problems**

Design Solution	Effect on Stability
a. Flatten slope.	Reduces driving force.
b. Bench slope.	Reduces driving force.
c. Buttress toe.	Increases resisting force.
d. Lower water table.	Reduces seepage force.
e. Reinforcement (e.g., nails)	Increases resisting force

**The design of cut slopes in clay should NOT be based on the undrained strength of the clay determined by tests on samples obtained before the cut is made.** Designs based on undrained strength will be unconservative since the effective stress is reduced when the cut is made because load is removed. This decrease in effective stress allows the clay to swell and

lose strength if water is made available to the clay as shown in Figure 6-30. Therefore, the design of cut slopes in clays should be based on effective strength parameters so that the reduction in effective stress resulting from the excavation can be taken into account. It is important to remember that an undrained clay in a cut gradually weakens and may fail long after construction.

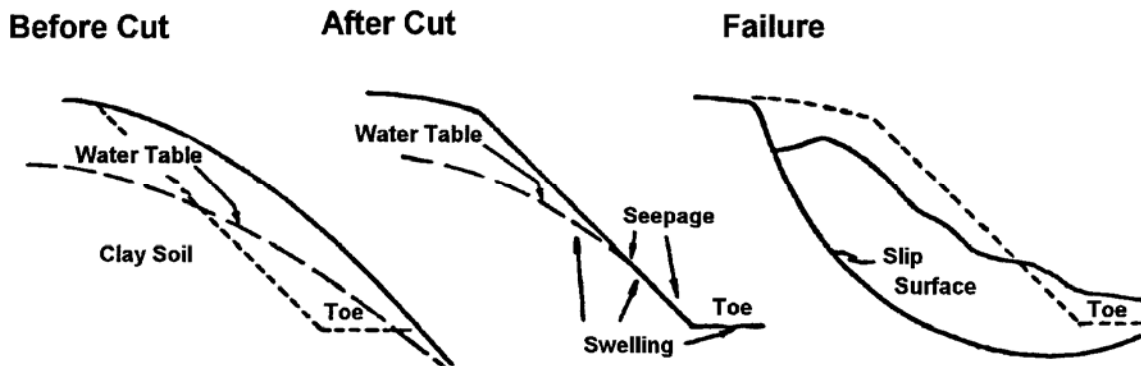


**Figure 6-30: Typical cut slope failure mechanism in clay soils.**

### 6.10.2 Shallow Surface Failures

Shallow surface failures (sloughs) are most common in cut slopes in layered clay or silt. This type of failure may involve either an entire slope or local areas in the slope. The prime cause of shallow surface failures is water seepage. Water seepage reduces the strength of the surface soils, causing them to slide or flow.

Sloughing of slopes due to ground water seepage can often be remedied by placing a 2-3 ft (0.6-1 m) thick rock or gravel blanket over the critical area. The blanket reduces the seepage forces, drains the water, and acts as a counter-weight on the unstable soil. The blanket should be "keyed" into the ditch at the toe of the slope. The key should extend about 4 feet (1.2 m) below the ditch line and be about 4 ft (1.2 m) wide. A geotextile should be placed both under the key and against the slope before placement of the gravel blanket. Construction of the gravel blanket should proceed from the toe upwards. The most effective placement is by a dozer that will track over and compact the lower areas of the gravel blanket while the upper areas are being constructed.

### **6.10.3 Factor of Safety - Cut Slopes**

As indicated previously, a minimum design safety factor of 1.25 is used for routine highway embankment side slopes. A minimum factor of safety against sliding of 1.50 is recommended for the stability of cut slopes in fine-grained soils. The greater factor of safety for cut slopes is based upon the knowledge that cut slopes may deteriorate with time as a result of natural drainage conditions that embankments generally do not experience. In addition, there is a greater degree of uncertainty about the homogeneity of the soils in cut slopes than in embankment slopes that are engineered and constructed under controlled conditions.

[THIS PAGE INTENTIONALLY BLANK]

## CHAPTER 7.0

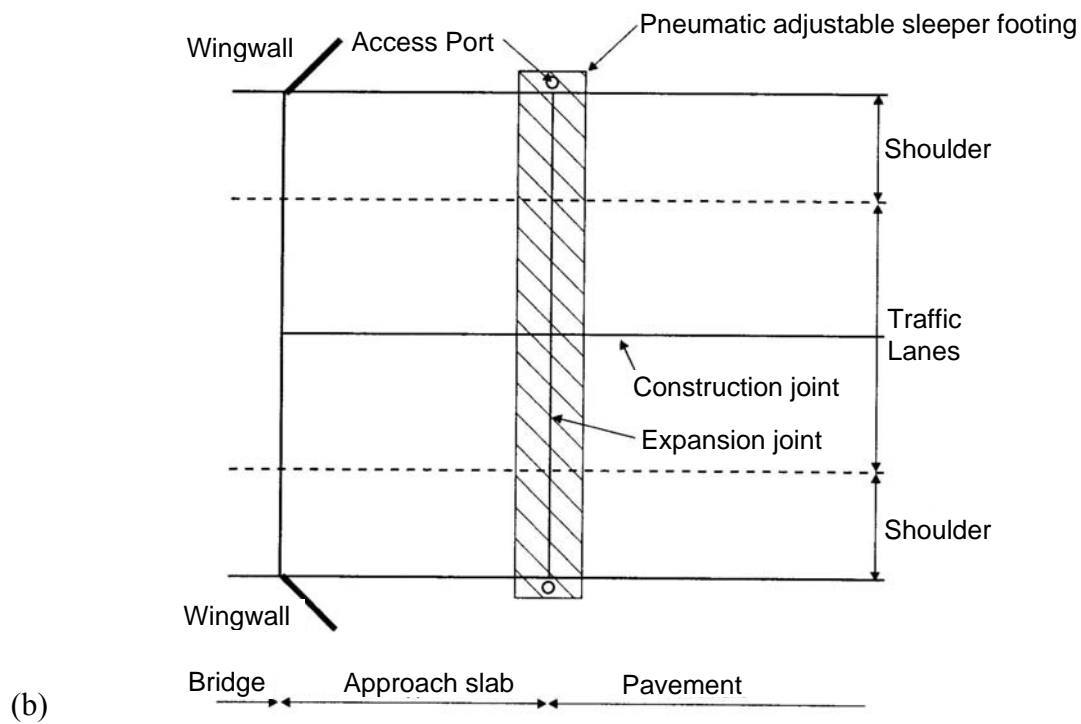
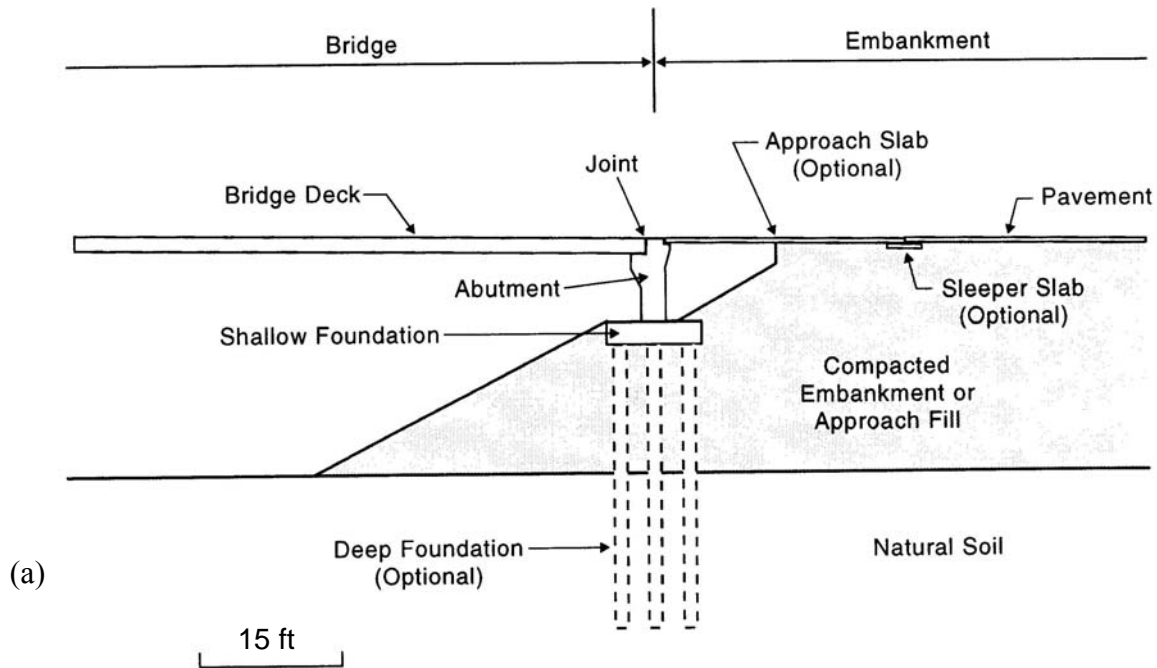
### APPROACH ROADWAY DEFORMATIONS

Often roadways are constructed on embankment fills to meet the requirements of the vertical grade of a roadway alignment. Fills placed to accommodate the vertical profile as the roadway approaches a bridge are often referred to as “approach embankment fills” or “approach roadway fills.” Typical elements of a bridge approach system are shown in Figure 7-1. The abutment configuration may vary as shown in Figure 7-2. An abutment fill slope is also referred to as an “end-slope.” The common element to all types of abutments is an approach fill. Deformation, both vertical and lateral, of approach fills is the most prevalent foundation problem in highway construction. The embankment deformation near a bridge structure, leads to the ubiquitous “bump at the end of the bridge.” Figure 7-3 shows some of the problems leading to the existence of the bump.

Approach slabs are often used by most state agencies to provide a smooth transition between the bridge deck and the roadway pavement. The slab usually is designed to withstand some embankment settlement and a reduction in subgrade support near the abutment. Joints must be provided to accommodate cyclic thermal movements of the bridge deck, abutment and roadway pavement. Figure 7-1b shows one common joint set. However, if the approach embankments are not properly engineered, the approach slab merely moves the bump at the end of the bridge to the approach slab-roadway interface. Unlike stability problems, the results of approach embankment deformations are seldom catastrophic but the cost of perpetual maintenance of continuing deformation can be immense. The difficulty in preventing these problems is not so much a lack of technical knowledge as a lack of communication between personnel involved in the roadway design and those involved in the structural design and construction.

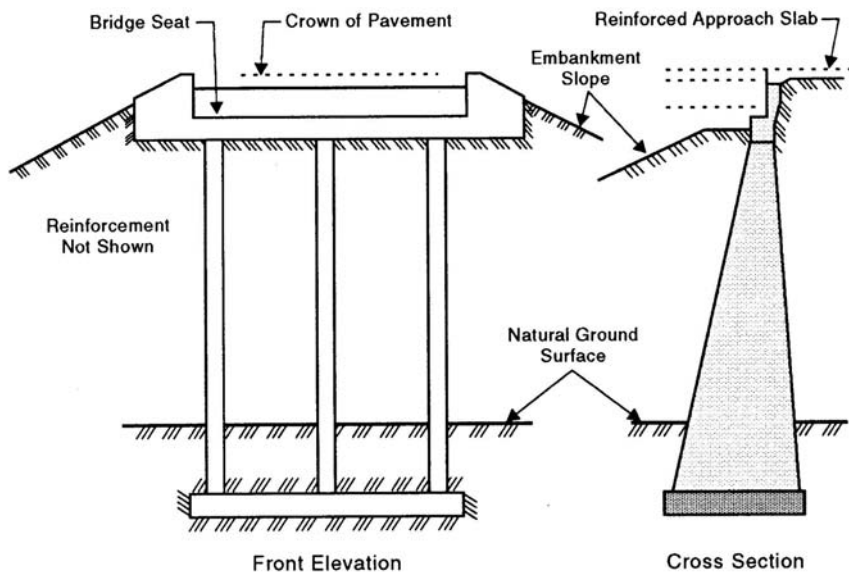
#### 7.1 TYPICAL APPROACH ROADWAY DEFORMATION PROBLEMS

Roadway designers allow use of inexpensive available soils for approach fills to reduce project costs. The bridge structures are necessarily designed for little or no deformation to maintain specified highway clearances and to insure integrity of structural members. In most agencies the responsibility for approach embankment design is not defined as a structural issue, which results in roadway embankment requirements being used up to the structure. In reality, **the approach embankment requires special materials and placement criteria to prevent internal deformations and to mitigate external deformations.** A discussion of the types of deformation associated with approach fills follows.

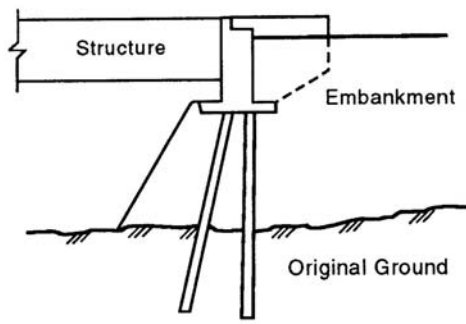


Note: This plan detail is only one way of handling the bridge/fill interface. An approach slab with expansion between the superstructure and the approach slab without a sleeper slab is another.

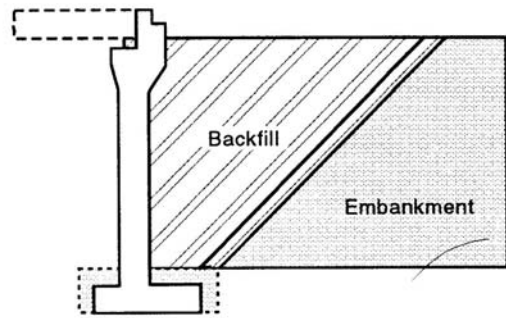
**Figure 7-1. (a) Elements of a bridge approach system, (b) Plan view of an approach system (modified after NCHRP, 1997).**



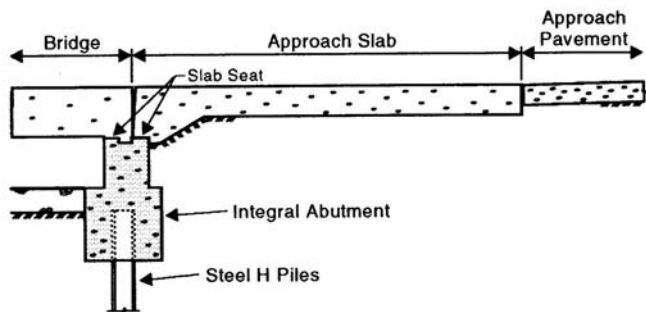
Typical Spill-Through Abutment



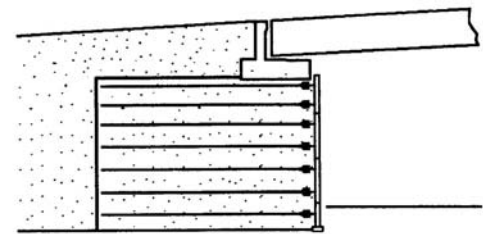
Typical Perched Abutment



Typical Full-Height Closed or High Abutment



Typical Integral Abutment



Mechanically Stabilized Abutment ("True" bridge abutment)

Figure 7-2. Types of abutments (modified after NCHRP, 1990).

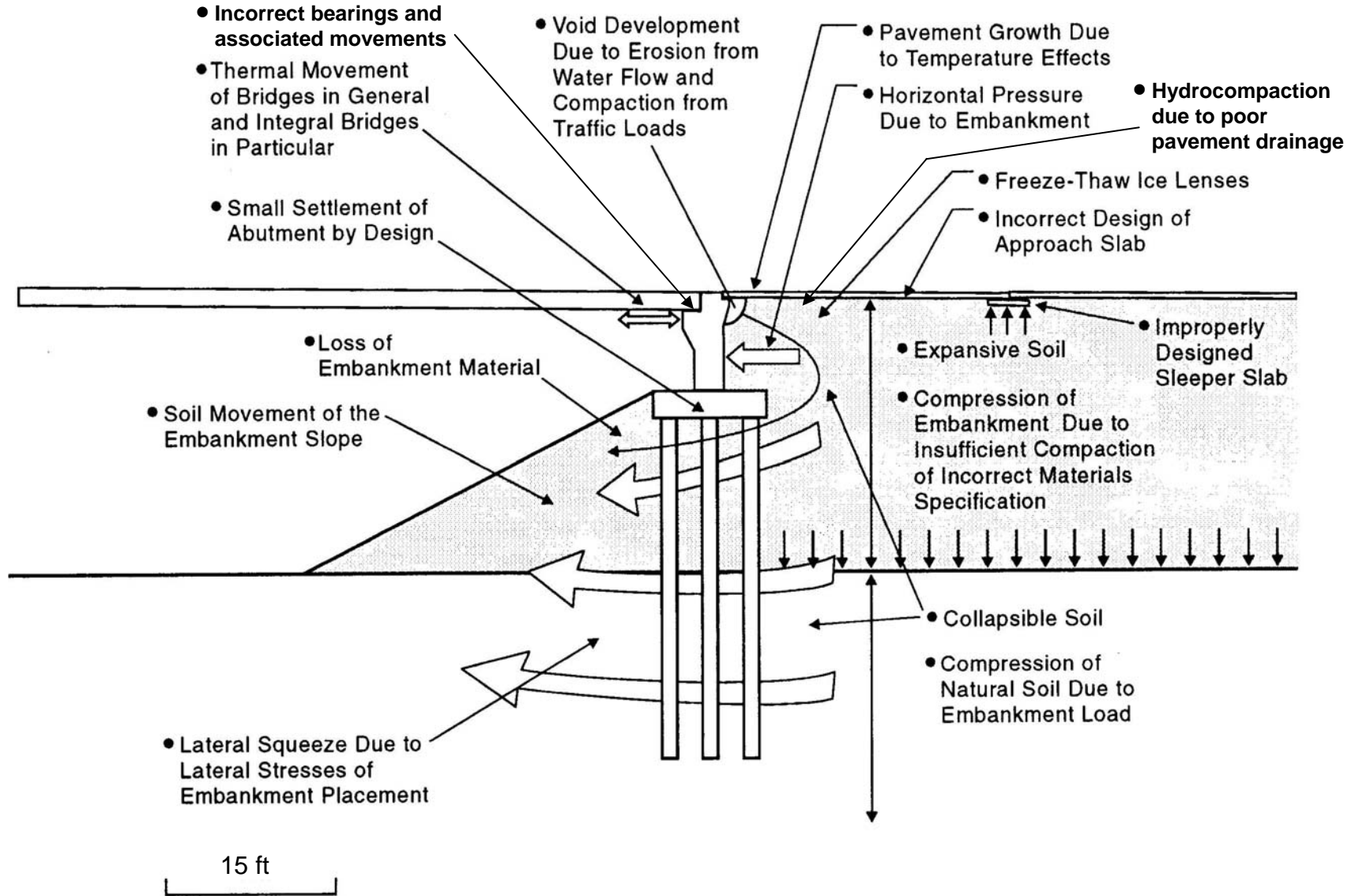


Figure 7-3. Problems leading to the existence of a bump (modified after NCHRP, 1997).

Most state agencies, as noted earlier, use bridge approach slabs to provide a transitional roadway between the pavement on the approach embankment and the actual structure of the bridge. Due to the deformation of the approach embankment fills for various reasons shown in Figure 7-3, these slabs can settle and/or rotate creating problems for the abutment as well as the joints. Depending on the configuration of the approach slab, e.g., how the slab is connected to the abutment and/or the wing walls, voids may develop under the slab as the approach fill settles. Such voids can then fill with water, which can further compound the problem, e.g., water pressures acting against structural elements, softening of the soils with associated reduction in strength, freeze-thaw issues, etc. Due to the above considerations, design problems with approach roadway embankments are classified as follows:

- Internal deformation **within** the embankment
- External deformation in native soils **below** the embankment

As mentioned previously, it is important to realize that the deformation considerations for the embankment include both vertical as well as lateral deformations. Vertical deformations are commonly referred to as “settlements.” Lateral deformations can result in rotation of the structure that is commonly referred to as “tilting.”

**Internal deformation** is a direct result of compression of the materials used in the construction of the embankment fill. The importance of adequate drainage with respect to the internal behavior of the embankment cannot be overemphasized. Poor drainage can (a) cause softening of the embankment soils leading to vertical and lateral deformations, (b) reduce the stability of soils near the slope leading to lateral deformations and associated vertical deformations near the crest of the slope, and (c) potentially lead to migration of fill material and creation of voids or substantial vertical and lateral deformations.

**External deformation** is due to the vertical and lateral deformation of the foundation soils on which the embankment is placed. Furthermore, deformation of foundation soils may include both immediate and consolidation deformations depending on the type of foundation soils. Lateral squeeze of the foundation soils can occur if the soils are soft and if their thickness is less than the width of the end slope of the embankment. Consolidation settlement and lateral squeeze are not an issue within embankment fills since coarse-grained soils placed under controlled compaction conditions are generally used.

This chapter discusses internal as well as external deformations of approach fills. Design solutions to mitigate the detrimental effect of these deformations are presented. Guidelines for construction monitoring are also provided.

## **7.2 INTERNAL DEFORMATION WITHIN EMBANKMENTS**

Internal deformation within embankments can be easily controlled by using fill materials that have the ability to resist the anticipated loads imposed on them. A well constructed soil embankment will not excessively deform internally if quality control is exercised with regard to material and compaction. Standard specifications and construction drawings should be prepared for the approach embankment area, normally designated to extend 50 ft (15 m) behind the wingwall. The structural designer should have the responsibility for selecting the appropriate cross section for the approach embankment depending on selection of the foundation type. A typical approach embankment cross section is shown in Figure 7-4.

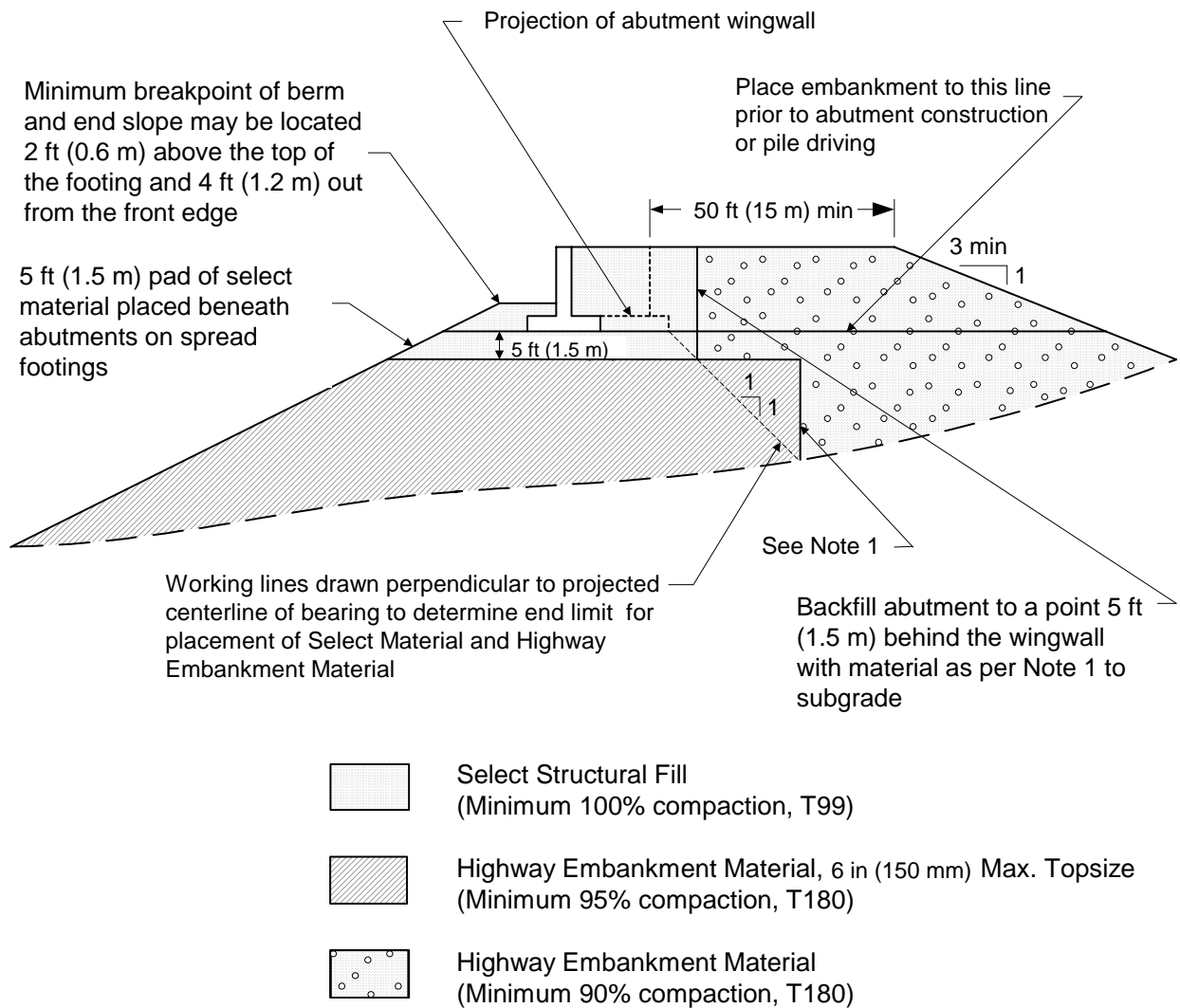
Special attention should be given to the interface area between the structure and the approach embankment, as this is where the "bump at the end of the bridge" occurs. The reasons for the bump are (a) poor compaction of embankment material near the structure, (b) migration of fine soil into drainage material, and (c) loss of embankment material due to poor drainage details as discussed earlier. Poor compaction is usually caused by restricted access of standard compaction equipment. Proper compaction can be achieved by optimizing the soil gradation in the interface area to permit compaction to maximum density with minimum effort. Figure 7-5 shows a detail for placement of drainage material. Considerations for the specification of select structural backfill and underdrain filter material to minimize the "bump" problem are included in the next two sections. Similar drainage results can be obtained by the use of prefabricated geocomposite drains that are attached to the backwall and connected to an underdrain.

### **7.2.1 General Considerations for Select Structural Backfill**

Select structural backfill is usually placed in relatively small quantities and in relatively confined areas. Structural backfill specifications must be designed to ensure construction of a durable, dense backfill. Table 7-1 lists considerations for the specification of select structural backfill.

### **7.2.2 General Considerations for Drainage Aggregate**

The drainage aggregate, such as that used for underdrain filters, should consist of crushed stone, sand, gravel or screened gravel. Suggested gradation for drainage aggregate is provided in Table 7-2. The AASHTO standard gradation No. 57 or 67 should be equally suitable.



Note 1: Highway embankment material and select material shall be placed simultaneously of the vertical payment line

**Figure 7-4. Suggested approach embankment details.**

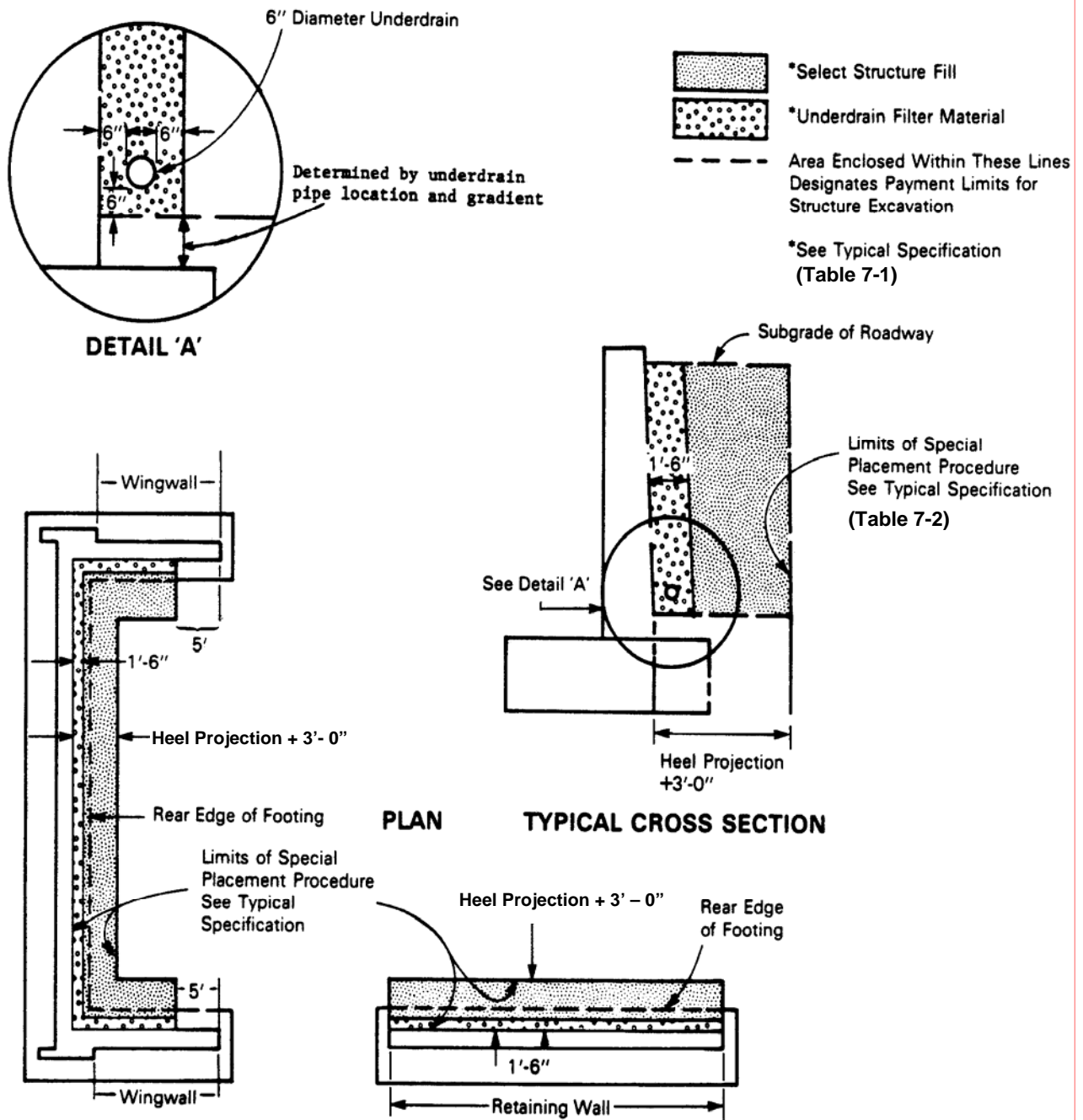


**Figure 7-5. Structural backfill placement limits for porous drainage aggregate.**  
 (1 ft = 0.3 m; 1 in = 25.4 mm)

**Table 7-1  
General considerations for specification of select structural backfill**

<b>Consideration</b>	<b>Comment</b>								
Lift Thickness	Limit to 6" to 8" (150 mm to 200 mm), so compaction is possible with small equipment.								
Topsize (largest particle size)	Limit to less than $\frac{3}{4}$ of lift thickness.								
Gradation/Percent Fines	Use well graded soil for ease of compaction. Typical gradation is as follows: <table border="1" data-bbox="548 569 1414 722"> <thead> <tr> <th><b>Sieve Size</b></th> <th><b>Percent Passing (by weight)</b></th> </tr> </thead> <tbody> <tr> <td>4-in (100 mm)</td> <td>100</td> </tr> <tr> <td>No. 40 (0.425 mm)</td> <td>0 to 70</td> </tr> <tr> <td>No. 200 (0.075 mm)</td> <td>0 to 15</td> </tr> </tbody> </table> <p>The limitation on percent fines (particles smaller than No. 200 sieve) is to prevent piping and allow gravity drainage. For rapid drainage, consideration may be given to limiting the percent fines to 5%.</p>	<b>Sieve Size</b>	<b>Percent Passing (by weight)</b>	4-in (100 mm)	100	No. 40 (0.425 mm)	0 to 70	No. 200 (0.075 mm)	0 to 15
<b>Sieve Size</b>	<b>Percent Passing (by weight)</b>								
4-in (100 mm)	100								
No. 40 (0.425 mm)	0 to 70								
No. 200 (0.075 mm)	0 to 15								
Plasticity Index	The plasticity index (PI) should not exceed 10 to control long-term deformation.								
Durability	This consideration attempts to address breakdown of particles and resultant settlement. The material should be substantially free of shale or other soft, poor-durability particles. Where the agency elects to test for this requirement, a material with a magnesium sulfate soundness loss exceeding 30 should be rejected.								
T99 Density Control	Small equipment cannot achieve AASHTO T180 densities. Minimum of 100 percent of standard Proctor maximum density is required.								
Compatibility	Particles should not move into voids of adjacent fill or drain material								

**Table 7-2  
Suggested gradation for drainage aggregate**

<b>Sieve Size</b>	<b>Percent Passing (by weight)</b>
1-in (25.4 mm)	100
$\frac{1}{2}$ -in (12.7 mm)	30 to 100
No. 3 (6.3 mm)	0 to 30
No. 10 (2.00 mm)	0 to 10
No. 20 (0.85 mm)	0 to 5

As with the select backfill, the soundness of the drainage aggregate should be tested. The drainage aggregate should have a loss not exceeding 20 percent by weight after four (4) cycles of the magnesium sulfate soundness test.

The maximum loose lift thickness for the drainage aggregate should not exceed 6 in (150 mm). Placement and compaction operations should be conducted in a manner so as to insure that the top surface of each lift of the drainage aggregate should not be contaminated by the adjacent backfill materials. Compaction of the drainage aggregate is commonly achieved by two passes of a vibratory compactor approved by the engineer. No compaction control tests are normally required for the drainage aggregate.

### **7.2.3 Use of Geosynthetics to Control Internal Deformations**

In geographic areas where select materials are not available, the use of geosynthetic materials to reinforce the abutment backfill and approach area can reduce the bump at the end of the bridge. Such reinforced fills can be designed by using the principles of Reinforced Soil Slopes (RSS) discussed in Chapter 6 (Slope Stability)

It is suspected that high dynamic loads are routinely induced in the abutment backfill due to vehicle impact loads. Poorly designed or constructed drainage layers or non-durable drainage aggregate can cause either piping of fines or accelerated pavement subsidence due to breakdown of aggregates. As indicated previously, the use of geotextiles or geocomposite drains can be an effective method of minimizing internal embankment deformation and the resulting “bump at the end of the bridge.”

## **7.3 EXTERNAL DEFORMATION IN FOUNDATION SOILS BELOW EMBANKMENTS**

Once the issue of internal deformation within fills has been addressed, the designer must concentrate on the evaluation of the deformation of foundation soils and any engineered soils on which the fills will be placed. As explained in Chapter 2, deformations in foundation soils under embankments occur due to the pressure imposed by the embankments. Depending on the type of foundation soils, one or both of the following deformations may occur:

- Immediate (elastic) deformation
- Consolidation (or long-term) deformation

Immediate or elastic deformations occur in all soils regardless of whether they are cohesive or cohesionless. Consolidation deformations typically occur in fine-grained soils that are saturated at the time additional loads are applied. Many and varied procedures exist for computation of these types of deformations. Two methods are presented in this chapter; one each for cohesionless and cohesive soils. However, there is a critical first step that is common to both modes of deformation. This first step involves the estimation of the stress distribution within the foundation soils due to the pressures imposed by the embankment fills. This step is discussed next.

### 7.3.1 Procedure for Estimating Stress Distribution in Foundation Soils under Fills

The basic steps involved in estimating stresses in native soils under fills are as follows:

1. Develop a soil profile including soil unit weights, SPT results ( $N_{160}$ ), moisture contents and interpreted consolidation test values.
2. Draw effective overburden pressure ( $p_o$ ) diagram with depth.
3. Plot total embankment pressure ( $p_f$ ) on the  $p_o$  diagram at ground surface level.
4. Distribute the total embankment pressure with depth by using the appropriate pressure coefficient charts presented in Figure 7-6.

(Note: The charts in Figure 7-6 are limited to only two locations, Section B-B and Section C-C, and assume that the end and side slopes have the same grades. Programs such as FoSSA (2003) may be used for case of unequal end and side slopes, or if pressure coefficients at locations other than along Section B-B or C-C are desired.)

***The principles to remember are: (1) stresses induced in the soil from an embankment load are distributed with depth in proportion to the embankment width, and (2) the additional stresses in the soil decrease with depth.***

Following is a step-by-step procedure to use the chart in Figure 7-6. A worked example is presented afterwards to illustrate the use of the chart numerically:

- Step 1. Determine the distance  $b_f$  from the centerline of the approach embankment to the midpoint of side slope. Multiply the numerical value of " $b_f$ " by the appropriate values shown to the right of the chart to develop the depths at which the distributed pressures will be computed, e.g.,  $0.2b_f$ ,  $0.4b_f$ , etc.

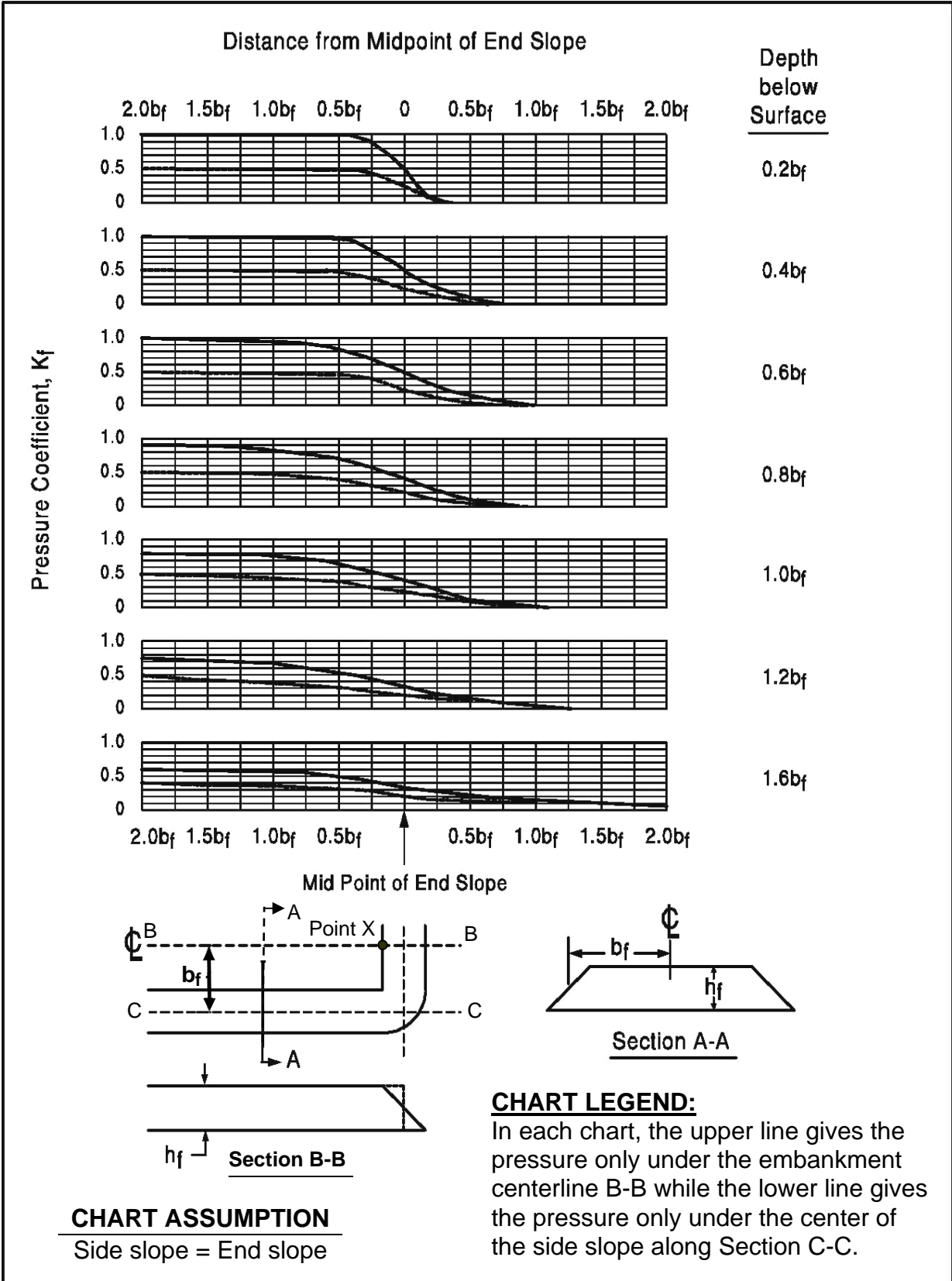


Figure 7-6. Pressure coefficients beneath the end of a fill (after NYSDOT).

Step 2. Select the point X on the approach embankment where the vertical stress prediction is desired, normally at the intersection of the centerline of the embankment and the abutment. In this case the side slope is called the end slope. Measure the distance from X to the midpoint of the end slope. Return to the chart and scale that distance as a multiple of  $b_f$  on the horizontal axis from the appropriate side of the midpoint centerline line of the end slope.

Step 3. Read vertically up or down from the plotted distance on the horizontal axes to the various curves corresponding to depth below surface. The " $K_f$ " value on the left vertical axis should be read and recorded on a computation sheet with the corresponding depth. Note that the upper line gives the pressure under the embankment centerline (Section B-B) while the lower line gives the pressure under the mid of the side slope (Section C-C).

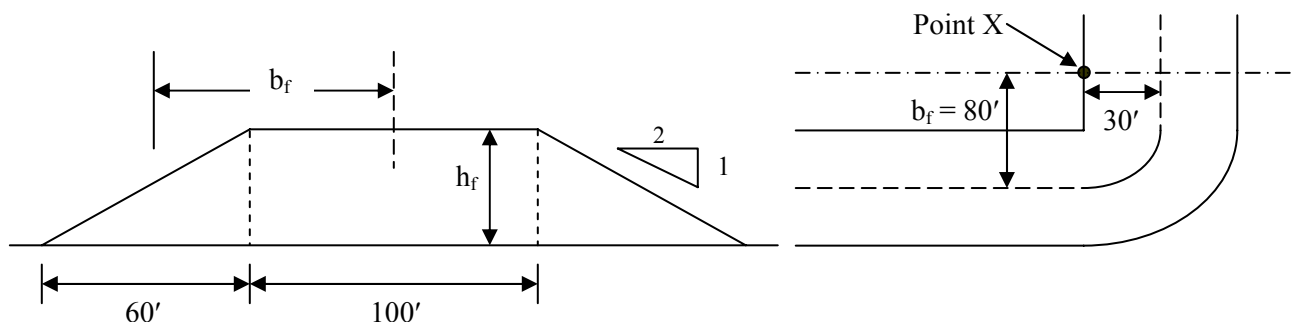
Step 4. Multiply each " $K_f$ " value by the value of total embankment pressure ( $\gamma_f h_f$ ) to determine the amount of the pressure increment ( $\Delta p$ ) transmitted to each depth, where  $\gamma_f$  is the unit weight of the embankment fill soil and  $h_f$  is height of the embankment fill.

The application of this step-by-step procedure and the charts shown on Figure 7-6 to a typical embankment problem is illustrated by the following worked example problem.

**Example 7-1:** The geometry of a fill slope is as follows:

Fill height  $h_f = 30$  ft; Fill unit weight  $\gamma_f = 100$  pcf

End and side slopes (2H:1V); Embankment top width = 100 ft



**Find:** The stress increase ( $\Delta p$ ) under the proposed abutment centroid (Point X) at a depth of  $0.8 b_f$  below the base of the fill.

**Solution:**

Figure 7-6 will be used to determine the stress increase. To use the chart first compute the following quantities:

- Distance from midpoint of end slope to Point X = 30 ft.
- Distance from centerline to mid point of side slope  $b_f = (100 \text{ ft}/2) + (60 \text{ ft}/2) = 80 \text{ ft}$ .

Enter stress distribution chart for a depth of  $0.8b_f = (0.8)(80 \text{ ft}) = 64 \text{ ft}$  and a distance measured from the ***midpoint of the end slope to Point X expressed as a multiple of  $b_f$***  =  $(30 \text{ ft}/80 \text{ ft}) b_f = 0.38 b_f$ . Enter the plot with this value to the left of the value of zero on the abscissa, i.e., upslope from the midpoint on the end slope.

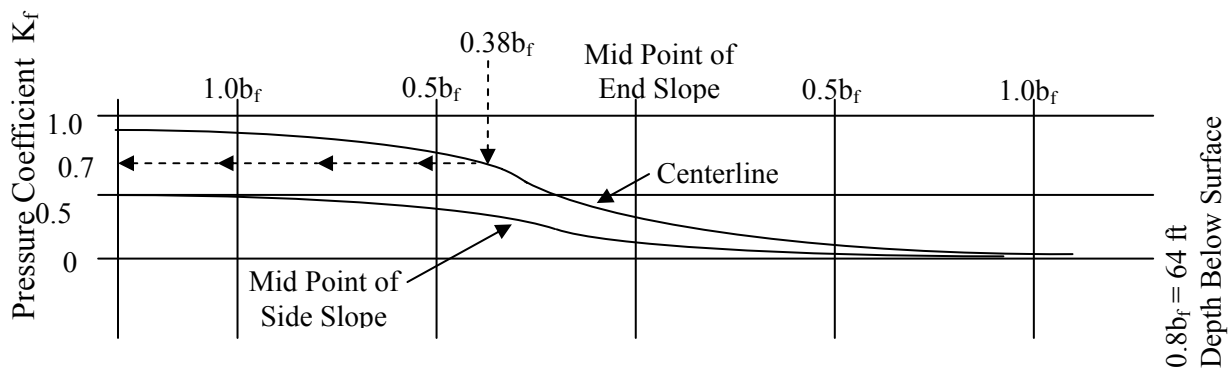
In Figure 7-6 read  $K_f = 0.7$  from the chart for  $0.8b_f$ . Therefore, at a depth of 64 ft below the embankment at Point X

$$\Delta p = K_f \gamma_f h_f$$

$$\Delta p = (0.7) (100 \text{ pcf}) (30 \text{ ft}) = 2,100 \text{ psf}$$

Repeat the above steps for distances to other points along the centerline of the embankment expressed as a multiple of  $b_f$  and measured (+ and -) from the midpoint of end slope to develop the horizontal distribution of vertical stress increases due to the embankment at a depth of 64 ft below and beyond the base of the end slope along the embankment centerline.

**Horizontal Distribution of Vertical Stress Increases Below and Beyond the End Slope at a Depth of 64-ft Below the Embankment**



## 7.4 COMPUTATION OF IMMEDIATE SETTLEMENT

All geomaterials, whether cohesionless or cohesive, will experience settlements immediately after application of loads. Whether or not the settlements will continue with time after the application of the loads will be a function of how quickly the water can drain from the voids as explained in Chapter 2. Long-term consolidation-type settlements are generally not experienced in cohesionless soils where pore water can drain quickly or in dry or slightly moist cohesive soils where significant amounts of pore water are not present. Therefore, embankment settlements caused by consolidation of cohesionless or dry cohesive soil deposits are frequently ignored as they are much smaller compared to immediate settlements in such soils. Consolidation type settlement for saturated cohesive soils is discussed in Section 7.5.

Many methods have been published in the geotechnical literature for the computation of immediate settlements in soils or rocks. These methods vary from the use of rules of thumb based on experience to the use of complex nonlinear elasto-plastic constitutive models. All methods are based on some form of estimate of soil compressibility. In the geotechnical literature, soil compressibility is expressed using several different terms such as “bearing capacity index,” “compression index,” “elastic modulus,” “constrained modulus,” etc.

For computing external embankment settlements, the method by Hough (1959) as modified by AASHTO (2004 with 2006 Interims) can be used since it is simple and provides a first-order conservative estimate of immediate settlements. The original Hough method (Hough, 1959) was based on uncorrected SPT N-values and included recommendations for cohesionless as well as cohesive soils such as sandy clay and remolded clay. AASHTO modified the Hough (1959) method for use with  $N_{160}$  values and eliminated the recommendations for sandy clay and remolded clay. Since the method presented here is AASHTO’s version of the Hough method, it will be referred to as the “Modified Hough” method.

Even after the modifications, the settlements estimated by Modified Hough method are usually overestimated by a factor of 2 or more based on the data in FHWA (1987). While such conservative estimates may be acceptable from the viewpoint of the earthwork quantities (see discussion regarding compaction factor in Section 7.4.1.1), they may be excessive with respect to the behavior of the structures founded within, under or near the embankment. In cases where structures are affected by embankment settlement, more refined estimates of the immediate settlements are warranted. **For more refined estimates of immediate settlements it is recommended that the designer use either the modified method of Schmertmann, *et al.* (1978), which takes into account the strain distribution**

with depth, or the D'Appolonia (1968, 1970) method, which takes into account the effect of preconsolidation. Both methods provide equally suitable results. Schmertmann's modified method is presented in Chapter 8 (Shallow Foundations).

#### 7.4.1 Modified Hough Method for Estimating Immediate Settlements of Embankments

The following steps are used in Modified Hough method to estimate immediate settlement:

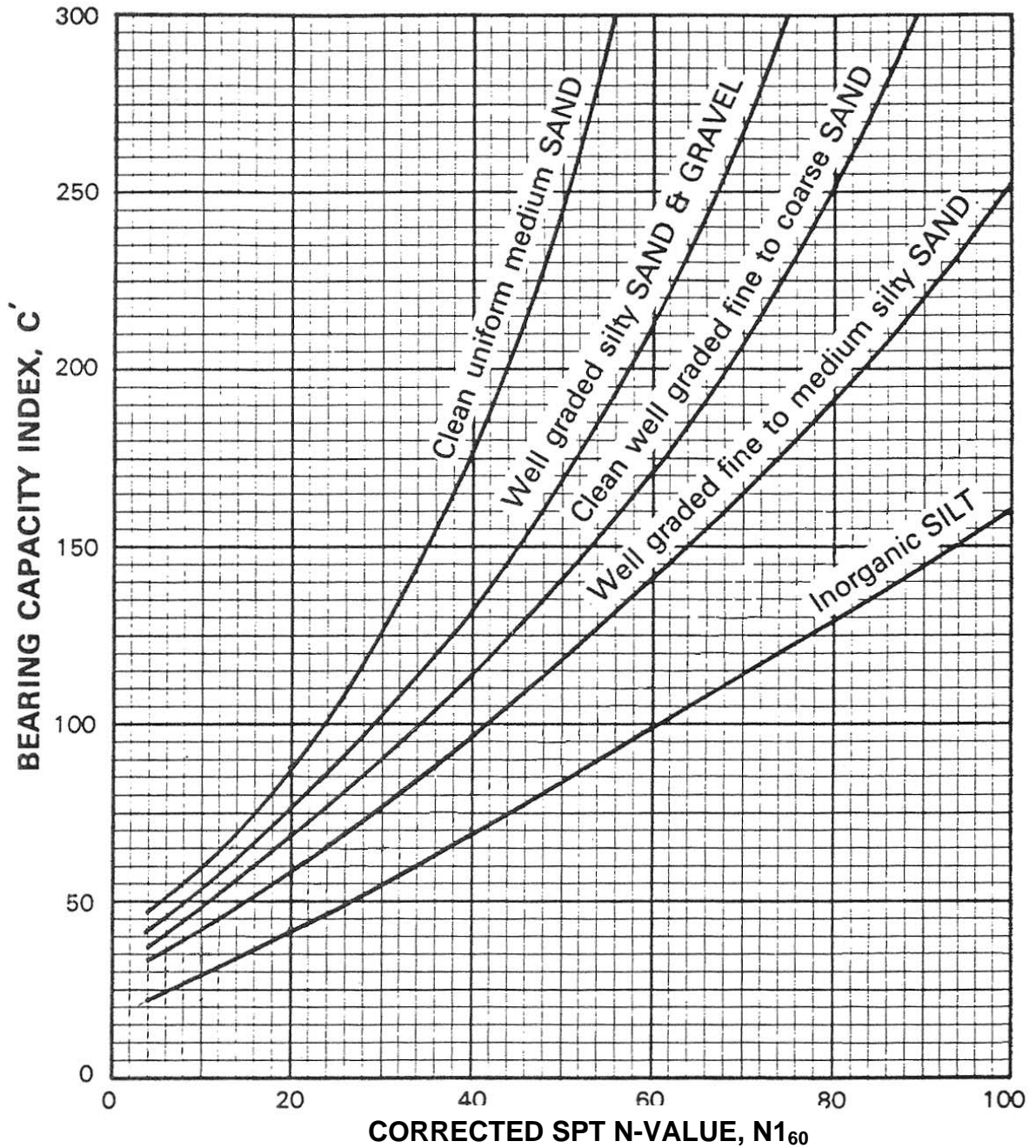
- Step 1. Determine the bearing capacity index ( $C'$ ) by entering Figure 7-7 with  $N_{160}$  value and the visual description of the soil.
- Step 2. Compute settlement by using the following equation. Subdivide the total thickness of the layer impacted by the applied loads into 10 ft  $\pm$  (3 m  $\pm$ ) increments and sum the incremental solutions:

$$\Delta H = H \left( \frac{1}{C'} \right) \log_{10} \frac{p_o + \Delta p}{p_o} \quad 7-1$$

- where:
- $\Delta H$  = settlement of subdivided layer (ft)
  - $H$  = thickness of subdivided soil layer considered (ft)
  - $C'$  = bearing capacity index (Figure 7-7)
  - $p_o$  = existing effective overburden pressure (psf) at center of the subdivided layer being considered. For shallow surface deposits, a minimum value of 200 psf should be used to prevent unrealistic settlement predictions.
  - $\Delta p$  = distributed embankment pressure (psf) at center of the subdivided layer being considered

Note that the term  $p_o + \Delta p$  represents the final pressure applied to the foundation subsoil,  $p_f$ .

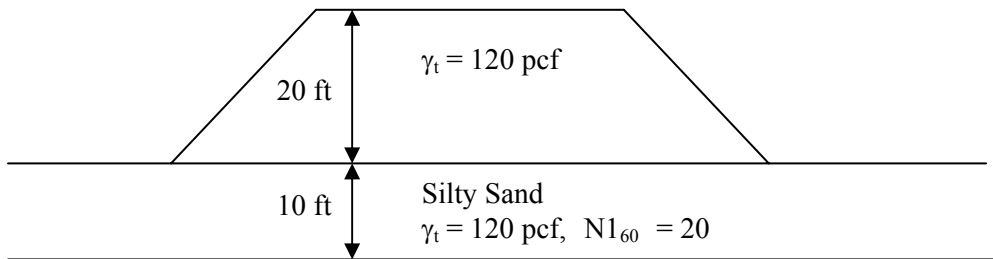
A key point is that the logarithm term in Equation 7-1 incorporates the fundamental feature of dissipation of applied stress with depth. The use of Modified Hough method is illustrated numerically in Example 7-2.



(Note: The “Inorganic SILT” curve should generally not be applied to soils that exhibit plasticity because N-values in such soils are unreliable)

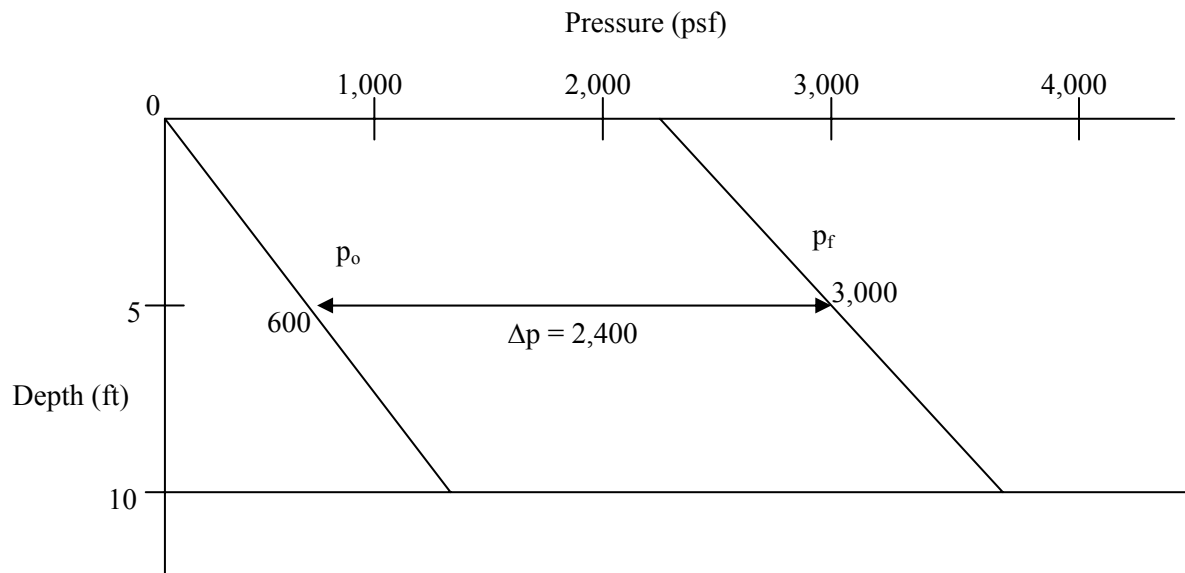
**Figure 7-7. Bearing capacity index (C') values used in Modified Hough method for computing immediate settlements of embankments (AASHTO, 2004 with 2006 Interims; modified after Hough, 1959).**

**Example 7-2:** For the geometry shown in the following figure, determine the settlement at the center of a wide embankment placed on a silty sand layer by using Modified Hough method and the  $p_o$  diagram.



**Solution:**

The original overburden pressure at the center of the 10 ft thick silty sand deposit can be computed as  $p_o = (10 \text{ ft}/2) (120 \text{ pcf}) = 600$  psf. Since, the embankment is “wide” the stress does not practically dissipate with depth. Therefore, increase in the stress at this depth due to the 20 ft high wide embankment can be computed as  $\Delta p = (20 \text{ ft}) (120 \text{ pcf}) = 2,400$  psf. The  $p_o$  diagram based on these values of  $p_o$  and  $\Delta p$  is shown below.



From Figure 7-7, find  $C'$  for “silty sand.” Using  $N_{160} = 20$  and the “silty sand” curve,  $C' \approx 58$ . Find immediate settlement using Equation 7-1 as follows:

$$\Delta H = H \left( \frac{1}{C'} \right) \log_{10} \frac{p_o + \Delta p}{p_o}$$

$$\Delta H = 10 \text{ ft} \left( \frac{1}{58} \right) \log_{10} \frac{600 \text{ psf} + 2,400 \text{ psf}}{600 \text{ psf}} = 0.12 \text{ ft} = 1.44 \text{ in}$$

#### 7.4.1.1 Comments on the Computed Settlement of Embankments

The implication of the amount of embankment settlement is that when the embankment is completed, additional fill will be required to bring the top of the embankment to the design grade. For example, a 1 in (25 mm) settlement on a 60-ft (18 m) wide, 1-mile (5,280 ft or 1,610 m) long embankment will result in a need for approximately 1,000 yd<sup>3</sup> (~750 m<sup>3</sup>) of additional fill. Some state agencies refer to such settlement estimates as the “compaction factor” and note it in the contract plans so that the contractor can make appropriate allowances in the bid price to accommodate the additional embankment fill material needed to achieve the required design grades. It is in this regard the conservative estimate of the settlement resulting from the Modified Hough method may be acceptable and may even be preferable to prevent construction change orders.

### 7.5 COMPUTATION OF CONSOLIDATION (LONG-TERM) SETTLEMENTS

Unless the geomaterial is friable, consolidation settlements in fine-grained saturated soils occur over a period of time as a function of the permeability of the soils. This concept was introduced in discussed in Chapter 2 by using the spring-piston analogy. The features of the laboratory consolidation test were discussed in Chapter 5. In this chapter the data obtained from the consolidation test are used to demonstrate the computation of long-term settlements due to the consolidation phenomena, i.e., primary consolidation and secondary compression.

Theoretically, a necessary condition for consolidation settlement is that the soil must be saturated, i.e., degree of saturation,  $S = 100\%$ . While the laboratory test for moisture content of a soil is inexpensive and relatively straightforward to perform and generally yields reliable, reproducible results, there are a number of parameters in consolidation analysis that cannot be determined with confidence as indicated by the data in Table 5-25. Therefore, depending on the magnitude and configuration of the load with respect to the size and moisture content of the compressible soil layer, it is possible that consolidation settlements may occur in soils that are judged to be “nearly saturated” but not “fully saturated.” This is because such nearly saturated soils may approach full saturation after application of a load of sufficient magnitude to cause the pore spaces filled with air to compress (immediate settlement) to the extent that the degree of saturation is virtually 100%. Therefore, the geotechnical specialist should carefully evaluate the in-situ degree of saturation with respect to the degree of saturation of the soil sample at the beginning and end of the consolidation test. The geotechnical specialist should also carefully evaluate the reliability of other parameters determined during the performance of the consolidation test to make an informed judgment regarding the potential for consolidation settlements to occur. Unnecessarily

conservative assumptions regarding the magnitude and time rate of consolidation settlements may lead to recommendations for deep foundations or for unnecessary implementation of costly ground improvement measures.

Settlement resulting from primary consolidation may take months or even years to be completed. Furthermore, because soil properties may vary beneath the location of loading, the duration of the primary consolidation and the amount of settlement may also vary with the location of the applied load, resulting in differential settlement. If such settlements are not within tolerable limits the geotechnical feature as well as a structure founded on or in it may be damaged. In the case of embankments, differential settlements that occur along the longitudinal axis of the embankment because of changes in thickness and/or consolidation properties of underlying clays can cause transverse cracking on the surface of the embankment where pavement structures are usually constructed.

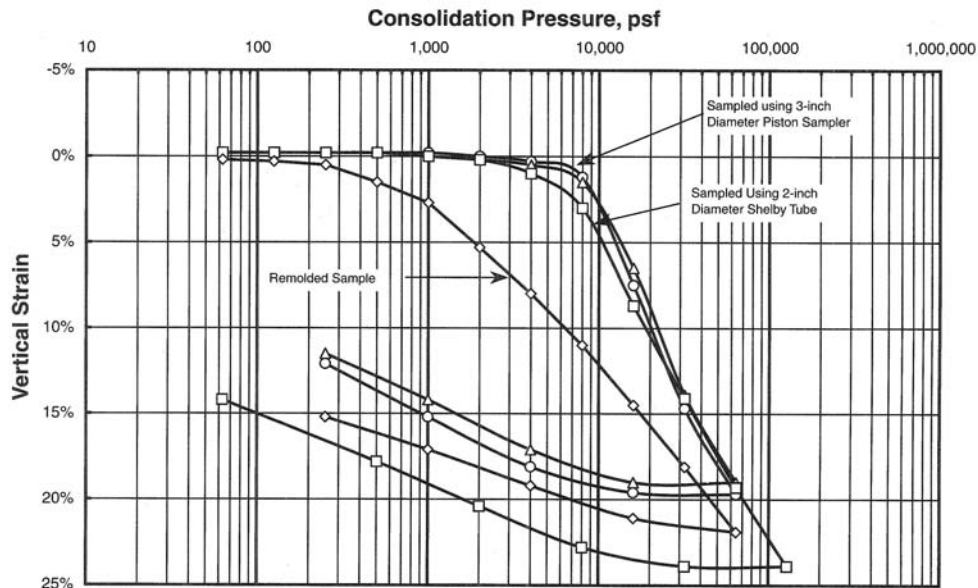
When the areal extent of the applied load is wide compared to the thickness of the compressible layer beneath it, a large portion of the soil will consolidate vertically (one-dimensionally) with very little lateral displacement because of the constraining forces exerted by the neighboring soil elements. However, when the areal extent of the applied load is smaller than the thickness of the compressible layer or when there is a finite soft layer at a certain depth below the loaded area, significant lateral stresses and associated deformations can occur as shown earlier in Figure 2-16 in Chapter 2. Back-to-back retaining walls and a narrow embankment for an approach ramp on soft soils are examples of this condition. Due to the potential for significant lateral stresses and associated lateral deformations, the geotechnical specialist should carefully evaluate the loading geometry with respect to subsurface conditions and ascertain whether the problem is 1-D or 3-D. This type of evaluation is important because 3-D deformations can affect a number of facilities such as buried utilities, bridge foundations, and the stability of embankment slopes.

The determination of the vertical component of 3-D consolidation deformation is commonly based on the one-dimensional consolidation test (ASTM D 2435). Typically, the results of the one-dimensional consolidation test are expressed in an  $e$ -log  $p$  plot which is the so-called “consolidation curve.” As indicated in Chapter 5, settlement due to consolidation can be estimated from the slope of the consolidation curve. This procedure is generally used in practice despite the fact that not all of the points beneath the embankment undergo one-dimensional consolidation. However, before the laboratory test results are used, it is very important to correct the consolidation curves for the effects of sampling. Thus, before proceeding with the discussion of computing consolidation settlements, the correction of the laboratory consolidation curves is discussed.

### 7.5.1 Correction of Laboratory One-Dimensional Consolidation Curves

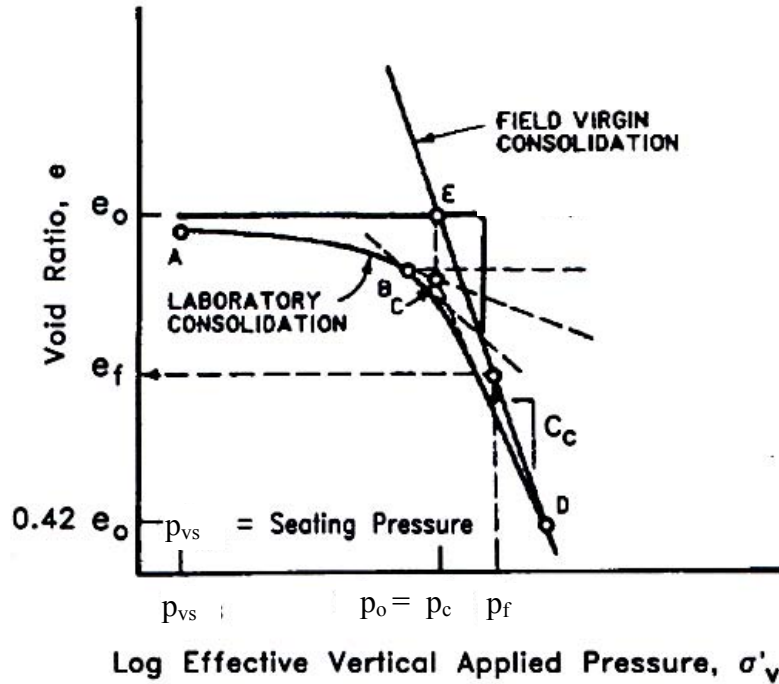
As indicated in Chapter 3, the process of sampling soils will cause some disturbance no matter how carefully the samples are taken. This sampling disturbance will affect virtually all measured physical properties of the soil. The sampling disturbance will usually cause the “break” in the laboratory consolidation curve to occur at a lower maximum past vertical pressure ( $p_c$ ) than would be measured for a truly undisturbed specimen. The effect of disturbance from the sampling procedure is illustrated in Figure 7-8 where, for the sake of comparison, the vertical strain rather than void ratio ( $e$ ) is plotted versus the logarithm of the vertical effective stress.

Figure 7-8 shows three consolidation curves for a red-colored plastic clay from Fond du Lac, Wisconsin. Samples were taken alternately with 3 in (75 mm) and 2 in (50 mm) thin walled samplers. The 3 in (50 mm) sampler apparently caused less disturbance than the 2 in (50 mm) sampler. The curve for the remolded sample is the flattest curve without a well defined break between reloading and virgin compression.

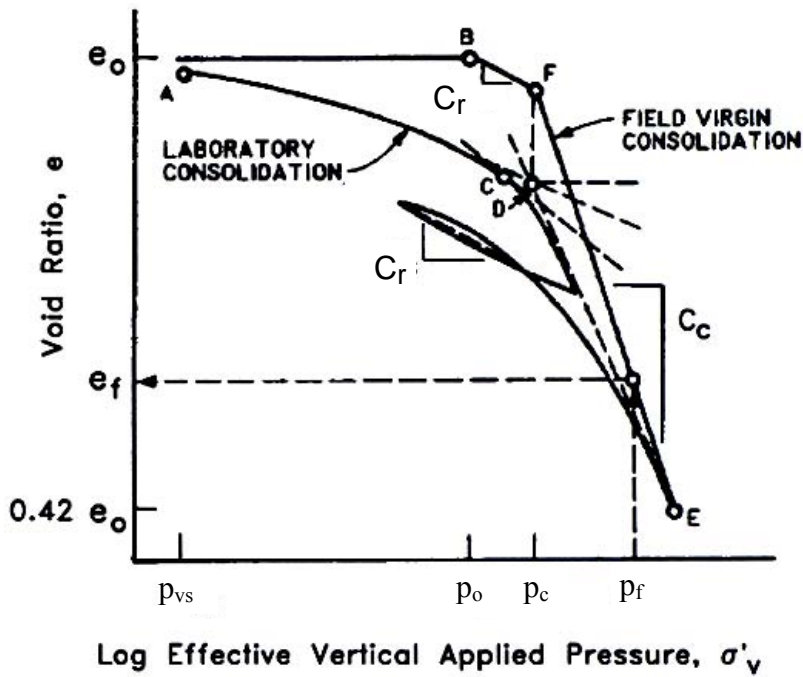


**Figure 7-8. Effect of sample disturbance on the shape of the one-dimensional consolidation curve (Reese, *et al.*, 2006).**

Even for good quality samples, it is still necessary to “correct” the  $e$ -log  $p$  curve since no sampling technique is perfect. There are several methods available to correct the consolidation curve. The laboratory curve can be corrected according to Figures 7-9a and 7-9b for normally consolidated and overconsolidated soils, respectively. Table 7-3 presents the reconstruction procedures.



(a.) NORMALLY CONSOLIDATED SOIL



(b.) OVERCONSOLIDATED SOIL

Figure 7-9. Construction of field virgin consolidation relationships (adapted from USACE, 1994).

**Table 7-3**  
**Reconstruction of virgin field consolidation curve (modified from USACE, 1994).**

Step	Description
<b>a. Normally Consolidated Soil (Figure 7-9a)</b>	
1	By eye choose the point B at the point of minimum radius of curvature (maximum curvature) of the laboratory consolidation curve.
2	Plot point C by the Casagrande construction procedure: (1) Draw a horizontal line through point B; (2) Draw a line tangent to the consolidation curve at point B; (3) Draw the bisector between the horizontal and tangent lines; and (4) Draw a line tangent to the “virgin” portion of the laboratory consolidation curve. Point C is the intersection of the tangent to the virgin portion of the laboratory curve with the bisector. Point C indicates the maximum preconsolidation (past) pressure $p_c$ .
3	Plot point E at the intersection of a horizontal line through $e_o$ and the vertical extension of point C, that corresponds to $p_c$ as found from Step 2. The value of $e_o$ is given as the initial void ratio prior to testing in the consolidometer.
4	Plot point D on the laboratory virgin consolidation curve at a void ratio $e = 0.42e_o$ . Extend the laboratory virgin consolidation curve to that void ratio if necessary. On the basis of many laboratory tests, Schmertmann (1955) found that the laboratory curve for various degrees of disturbance intersects the field virgin curve at a value of $e = 0.42e_o$ .
5	The field virgin consolidation curve is the straight line determined by points E and D.
6	The field compression index, $C_c$ , is the slope of the line ED.
<b>b. Overconsolidated Soil (Figure 7-9b)</b>	
1	Plot point B at the intersection of a horizontal line through the given $e_o$ and the vertical line representing the initial estimated in situ effective overburden pressure $p_o$ .
2	Draw a line through point B parallel to the mean slope, $C_r$ , of the rebound laboratory curve.
3	Plot point D by using Step 2 in Table 7-3a for normally consolidated soil.
4	Plot point F by extending a vertical line through point D up through the intersection of the line of slope $C_r$ extending through B.
5	Plot point E on the laboratory virgin consolidation curve at a void ratio $e = 0.42e_o$ .
6	The field virgin consolidation curve is the straight line through points F and E. The field reload curve is the straight line between points B and F.
7	The field compression index, $C_c$ , is the slope of the line FE.

## 7.5.2 Computation of Primary Consolidation Settlements

Depending upon the magnitude of the existing effective stress relative to the maximum past effective stress at a given depth, in-situ soils can be considered normally consolidated, overconsolidated (preconsolidated), or underconsolidated. The behavior of in-situ soils to additional loads is highly dependent upon the stress history. The overconsolidation ratio, OCR, which is a measure of the degree of overconsolidation in a soil is defined as  $p_c/p_o$ . The value of OCR provides a basis for determining the effective stress history of the clay at the time of the proposed loading as follows:

- OCR = 1 - the clay is considered to be “normally consolidated” under the existing load, i.e., the clay has fully consolidated under the existing load ( $p_c = p_o$ ).
- OCR > 1 - the clay is considered to be “overconsolidated” under the existing load, i.e., the clay has consolidated under a load greater than the load that currently exists ( $p_c > p_o$ ).
- OCR < 1 – the clay is considered to be “underconsolidated” under the existing load, i.e., consolidation under the existing load is still occurring and will continue to occur under that load until primary consolidation is complete, even if no additional load is applied ( $p_c < p_o$ ).

The manner in which primary settlements are computed for each of these three conditions varies as will be discussed in the following sections.

### 7.5.2.1 Normally Consolidated Soils

The settlement of a geotechnical feature or a structure resting on  $n$  layers of normally consolidated soils ( $p_c = p_o$ ) can be computed from Figure 7-10a where  $n$  is the number of layers into which the consolidating layer is divided:

$$S_c = \sum_i^n \frac{C_c}{1 + e_o} H_o \log_{10} \left( \frac{p_f}{p_o} \right) \quad 7-2$$

where:

- $C_c$  = compression index
- $e_o$  = initial void ratio
- $H_o$  = layer thickness
- $p_o$  = initial effective vertical stress at the center of layer  $n$
- $p_f$  =  $p_o + \Delta p$  = final effective vertical stress at the center of layer  $n$ .

The final effective vertical stress is computed by adding the stress change due to the applied load to the initial vertical effective stress. The total settlement will be the sum of the compressions of the n layers of soil.

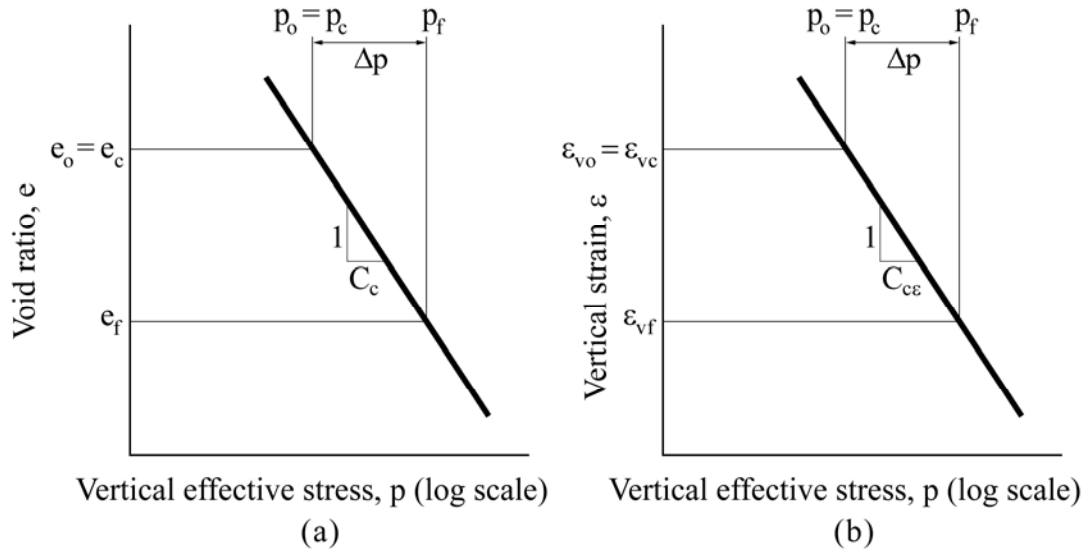


**Figure 7-10. Typical consolidation curve for normally consolidated soil, (a) Void ratio versus vertical effective stress and (b) Vertical strain versus vertical effective stress.**

Normally the slope of the virgin portion of the  $e$ -log  $p$  curve is determined from the corrected one-dimensional consolidation curve measured on specimens taken from each relevant soil in the stratigraphic profile. The procedure for determining the corrected curve is presented in Table 7-6a. Common correlations for estimating  $C_c$  were presented in Section 5.4.6.1 of Chapter 5 and can be used to check laboratory results.

Sometimes the consolidation data is presented in terms of vertical strain ( $\epsilon_v$ ) instead of void ratio. In this case the slope of the virgin portion of the modified consolidation curve is called the modified compression index and is denoted as  $C_{ce}$  as shown in Figure 7-10b. Settlement is computed by using Equation 7-3 for normally consolidated soils where all of the other terms are defined as for Equation 7-2.

$$S_c = \sum_1^n H_o C_{ce} \log_{10} \left( \frac{p_f}{p_o} \right) \quad 7-3$$

By comparing Equations 7-2 and 7-3, it can be seen that  $C_{ce} = C_c / (1 + e_o)$

### 7.5.2.2 Overconsolidated (Preconsolidated) Soils

If the water content of a clay layer below the water table is closer to the plastic limit than the liquid limit, the soil is likely overconsolidated, i.e.,  $OCR > 1$ . This means that in the past the clay was subjected to a greater stress than now exists. Preconsolidation could have occurred because of any number of factors including but not limited to the weight of glaciers which is especially prevalent in the northern tier of states and in the northeast, the weight of a natural soil deposit that has since eroded away, the weight of a previously placed fill that has since been removed, loads due to structures that have since been demolished, desiccation, etc.

As a result of preconsolidation, the field state of stress will reside on the initially flat portion of the  $e$ - $\log p$  curve. Figures 7-11a and 7-11b illustrate the case where a load increment,  $\Delta p$ , is added so that the final stress,  $p_f$ , is greater than the maximum past effective stress,  $p_c$ . For this condition, the settlements for the case of  $n$  layers of overconsolidated soils will be computed from Equation 7-4 or Equation 7-5 that correspond to Figure 7-11a and 7-11b, respectively.

$$S = \sum_1^n \frac{H_o}{1 + e_o} \left( C_r \log_{10} \frac{p_c}{p_o} + C_c \log_{10} \frac{p_f}{p_c} \right) \quad 7-4$$

$$S = \sum_1^n H_o \left( C_{re} \log_{10} \frac{p_c}{p_o} + C_{ce} \log_{10} \frac{p_f}{p_c} \right) \quad 7-5$$

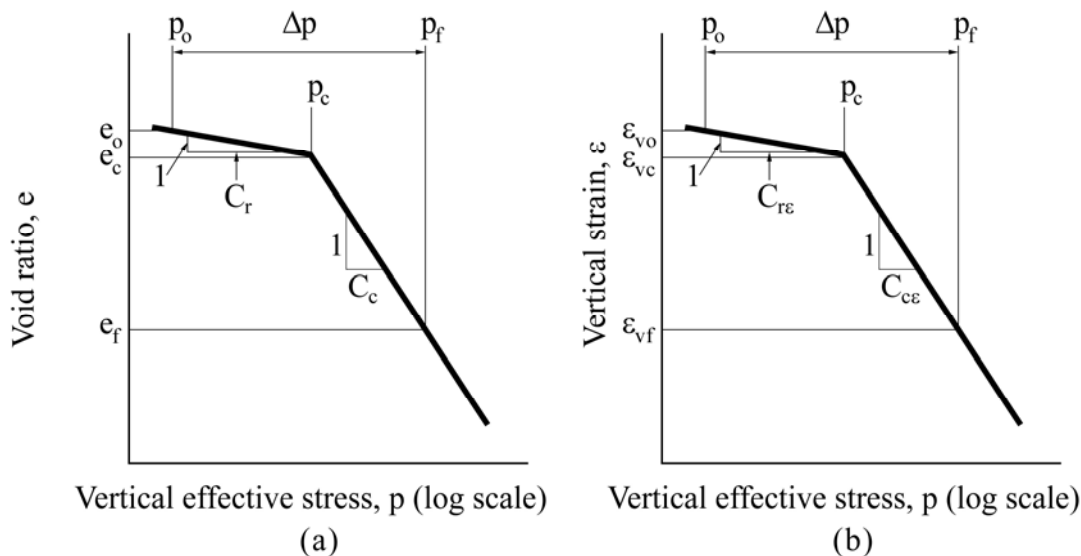


**Figure 7-11. Typical consolidation curve for overconsolidated soil, (a) Void ratio versus vertical effective stress and (b) Vertical strain versus vertical effective stress.**

The total settlement is computed by summing the settlements computed from each subdivided compressible layer within the zone of influence ( $Z_I$ ). The assumption is made that the initial and final stress calculated at the center of each sublayer is representative of the average stress for the sublayer, and the material properties are reasonably constant within the sublayer. The sublayers are typically 5 ft (1.5 m) to 10 ft (3 m) thick in highway applications. In cases where the various stratigraphic layers represent combinations of both normally and overconsolidated soils, the settlement is computed by using the appropriate combinations of Equations 7-2 through 7-5.

### 7.5.2.3 Underconsolidated Soils

Underconsolidation is the term used to describe the effective stress state of a soil that has not fully consolidated under an existing load, i.e.,  $OCR < 1$ . Consolidation settlement due to the existing load will continue to occur under that load until primary consolidation is complete, even if no additional load is applied. This condition is shown in Figure 7-12 by  $\Delta p_o$ . Therefore, any additional load increment,  $\Delta p$ , would have to be added to  $p_o$ . Consequently, if the soil is not recognized as being underconsolidated, the actual total primary settlement due to  $\Delta p_o + \Delta p$  will be greater than the primary settlement computed for an additional load  $\Delta p$  only, i.e., the settlement may be under-predicted. As a result of under-consolidation, the field state of stress will reside entirely on the virgin portion of the consolidation curve as shown in Figure 7-12. The settlements for the case of  $n$  layers of under-consolidated soils are computed by Equation 7-6 or Equation 7-7 that correspond to Figure 7-12a and 7-12b, respectively.

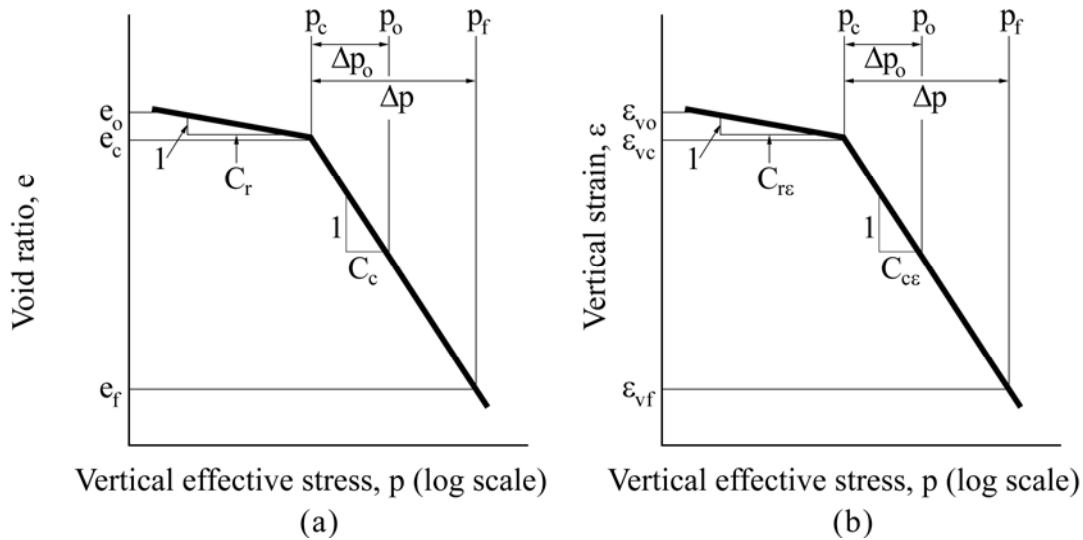


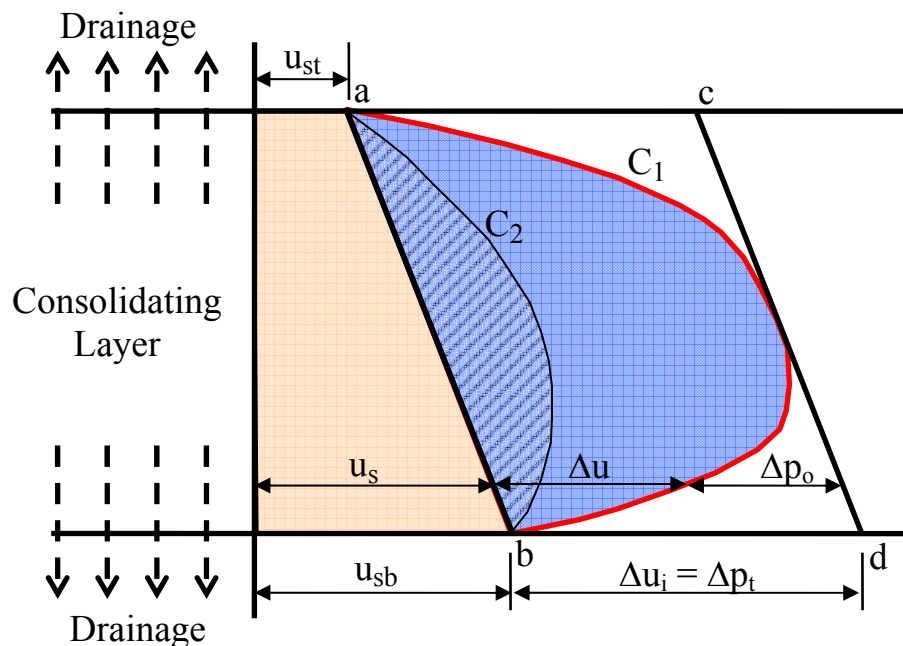
**Figure 7-12. Typical consolidation curve for under-consolidated soil – (a) Void ratio versus vertical effective stress and (b) Vertical strain versus vertical effective stress.**

$$S = \sum_1^n \frac{H_o}{1 + e_o} \left( C_c \log_{10} \frac{p_o}{p_c} + C_c \log_{10} \frac{p_f}{p_o} \right) \quad 7-6$$

$$S = \sum_1^n H_o \left( C_{c\varepsilon} \log_{10} \frac{p_o}{p_c} + C_{c\varepsilon} \log_{10} \frac{p_f}{p_o} \right) \quad 7-7$$

### 7.5.3 Consolidation Rates (Time Rate of Consolidation Settlement)

The rate of consolidation should be considered for the design of geotechnical features and structures on compressible clay. For example, a geotechnical feature such as an embankment will settle relative to a bridge foundation supported on piles, creating an undesirable “bump at the end of the bridge.” Hence, time rate of consolidation, as well as differential settlements between the bridge and embankment, is important. The concept of time rate of consolidation is explained with respect to Figure 7-13.



- Definitions:
- $u_{st}$  = hydrostatic pore water pressure at top of layer
  - $u_{sb}$  = hydrostatic pore water pressure at bottom of layer
  - $u_s$  = hydrostatic pore water pressure at any depth
  - $\Delta u_i$  = initial excess pore water pressure
  - $\Delta u$  = excess pore water pressure at any depth after time  $t$
  - $u_t = u_s + \Delta u$  = total pore water pressure at any depth after time  $t$

**Figure 7-13. Diagram illustrating consolidation of a layer of clay between two pervious layers (modified after Terzaghi, *et al.* 1996).**

- The initial hydrostatic pore water pressure distribution,  $u_s$ , is assumed to be linear in a layer of saturated clay. Line a-b in Figure 7-13 shows the initial hydrostatic pore water pressure distribution through a clay layer at a certain depth below the ground water elevation where  $u_{st}$  is the pore water pressure at the top of the clay layer and  $u_{sb}$  is the pore water pressure at the bottom of the clay layer. Experimental measurement of pore pressures in saturated clays subjected to one-dimensional loading indicate that when a load is applied the pore water pressure will instantaneously increase an amount equal to the total vertical stress increment,  $\Delta p_t$ , uniformly throughout the entire thickness of the consolidating layer as shown by a-c-d-b in Figure 7-13. The initial increase in the pore water pressure,  $\Delta u_i$ , above the static value is called the initial excess pore water pressure and it is equal to  $\Delta p_t$ . The total initial pore water pressure which is the sum of the hydrostatic pressure and the initial excess pore water pressures is shown as line c-d in Figure 7-13.
- With time, water will drain out of the consolidating layer to relieve the excess pore water pressure and the applied total vertical stress increment,  $\Delta p_t$ , will be slowly transferred to the soil particles, i.e., at any given time after application of the load, the initial excess pore water pressure will decrease at all depths to an excess pore water pressure having a value less than of  $\Delta u_i$ . The pattern of the excess pore water pressure at any given time is not parallel to line c-d, but is curvilinear similar to curve  $C_1$  in Figure 7-13. Curves such as  $C_1$  and  $C_2$  are known as *isochrones* because they are lines of equal time. The difference between the line a-b and curve  $C_1$ , for example, represents the excess pore water pressure,  $\Delta u$ , at any point within the consolidating layer at any time after application of the vertical load stress increment,  $\Delta p_t$ .
- If the clay layer is confined between two sand layers that are more permeable, the initial excess pore water pressure will drop immediately to zero at the drainage boundaries as shown in Figure 7-13 and the total vertical stress increment  $\Delta p_t$  and will be equal to the effective vertical stress increment,  $\Delta p_o$ . The rate of this transfer with depth depends upon the boundary drainage conditions. With time, the vertical distribution of excess pore water pressure within the consolidating layer will evolve from the initial distribution (a-c-d-b), to the  $C_1$  distribution, to the  $C_2$  distribution, and finally to the initial distribution of the hydrostatic pressure represented by line a-b.
- At any depth, the difference between a pore water pressure isochrone, such as  $C_1$ , and the initial excess pore water pressure c-d is equal to the effective vertical stress increment,  $\Delta p_o$ , i.e., the amount of  $\Delta p_t$  that has been transferred to the soil structure. Since the isochrone  $C_1$  develops after a certain period of time, the difference between  $C_1$  and c-d

also represents the distribution of the effective stress increments with depth at a given time after application of load.

- Note that the distribution shown in Figure 7-13 pertains only to the specific boundary drainage condition where a more permeable material exists above and below the consolidating clay layer. In this case the clay layer is considered to be “doubly drained” with the longest distance to a drainage boundary being half the layer thickness. If the clay layer is underlain by a less permeable material (e.g., rock), drainage will occur in only one direction and the isochrones at a given time will be different from those shown for double drainage in Figure 7-13. In this case the clay layer is considered to be “singly drained” with the longest distance to a drainage boundary being the entire layer thickness. During the consolidation process the principle of effective stress will be in operation at every depth, i.e.,  $\Delta p_t = \Delta u + \Delta p_o$  and settlement will be occurring due to the effective stress increment  $\Delta p_o$ . The drainage boundary condition will affect the time it takes for settlement to occur, but it has no effect on the magnitude of settlement, which is determined by use of the equations presented previously in which settlement is a function of  $\Delta p_o$  only.

### 7.5.3.1 Percent Consolidation

As indicated previously, immediately after application of load,  $\Delta u$ , will drop to zero at the drainage boundaries because the water will drain immediately into the more pervious layers. Since the excess pore water pressure is zero at the drainage boundaries, the soil there has undergone 100% consolidation. However, at interior points, the pore water pressure dissipates more slowly with time depending on the permeability of the compressible soil. At any time after application of a load, the actual degree or percentage of consolidation at a given depth is defined as  $(\Delta u_i - \Delta u) / \Delta u_i$ , where  $\Delta u$  is the excess pore water pressure at that depth at that time and  $\Delta u_i$  = the initial excess pore water pressure which, as indicated previously, equals the total stress increment  $\Delta p_t$ . Thus, where  $\Delta u_i = \Delta u$  (i.e., at the instant of loading), the percent consolidation is zero. When  $\Delta u = 0$  (i.e., at the end of consolidation), the percent consolidation is 100. This relationship is valid at any depth within the consolidating layer at any time from the instant of loading to the completion of primary consolidation.

While plots of the type shown in Figure 7-13 give an indication of the pore pressure variation within the consolidating layer at any time and are useful to explain the theory of consolidation, from a practical viewpoint it is usually more beneficial to obtain the *average* degree or percent of consolidation,  $U$ , within the entire layer to indicate when the entire clay

layer has undergone a certain average amount of consolidation of say 10, 50, or 80 percent. With reference to Figure 7-13, the average degree of consolidation at any time is defined as the difference between the area under the initial excess pore water pressure curve (a-c-d-b) and the area under the isochrone at that time, e.g., the cross hatched area under isochrone  $C_2$  divided by the area under the initial excess pore water pressure curve (a-c-d-b). The result is expressed as a percentage. Therefore, at the instant  $\Delta p_t$  is applied the area under the isochrone is exactly equal to the area (a-c-d-b) as indicated above and the average percent consolidation ( $U$ ) equals zero. At the end of primary consolidation all excess pore water pressures have dissipated and the area under the isochrone is zero. Thus, the average percent consolidation ( $U$ ) equals 100. Since, according to the principle of effective stress,  $\Delta p_t = \Delta u + \Delta p_o$ , the amount of settlement at any time after the application of load is directly related to the amount of consolidation that has taken place up to that time. As a practicality the average degree of consolidation at any time,  $t$ , can be defined as the ratio of the settlement at that time,  $S_t$ , to the settlement at the end of primary consolidation,  $S_{ultimate}$ , when excess pore water pressures are zero throughout the consolidating layer, i.e.,  $U = S_t/S_{ultimate}$ . This relationship is used to develop a so-called “settlement-time curve” as will be discussed later.

Table 7-4 shows the average degree of consolidation ( $U$ ) corresponding to a normalized time expressed in terms of a time factor,  $T_v$ , where:

$$T_v = \frac{c_v t}{H_d^2} \quad , \quad \text{which can be written as} \quad t = \frac{T_v H_d^2}{c_v} \quad 7-8$$

where:

- $c_v$  = coefficient of consolidation (ft<sup>2</sup>/day) (m<sup>2</sup>/day)
- $H_d$  = the longest distance to a drainage boundary (ft) (m)
- $t$  = time (day).

Any consistent set of units can be used in Equation 7-8 since  $T_v$  is dimensionless. As indicated previously, the longest drainage distance of a soil layer confined by more permeable layers on both ends is equal to one-half of the layer thickness. When confined by a more permeable layer on one side and an impermeable boundary on the other side, the longest drainage distance is equal to the layer thickness. The value of the dimensionless time factor  $T_v$  may be determined from Table 7-4 for any average degree of consolidation,  $U$ . The actual time,  $t$ , it takes for this percent of consolidation to occur is a function of the boundary drainage conditions, i.e., the longest distance to a drainage boundary, as indicated by Equation 7-8. By using the normalized time factor,  $T_v$ , settlement time can be computed for various percentages of settlement due to primary consolidation, to develop a predicted settlement-time curve. A typical settlement-time curve for a clay deposit under an embankment loading is shown in Figure 7-14.

**Table 7-4**  
**Average degree of consolidation, U, versus Time Factor,  $T_v$ ,**  
**for uniform initial increase in pore water pressure**

U %	$T_v$
0	0.000
10	0.008
20	0.031
30	0.071
40	0.126
50	0.197
60	0.287
70	0.403
80	0.567
90	0.848
93.1	1.000
95.0	1.163
98.0	1.500
99.4	2.000
100.0	Infinity



**Figure 7-14. Typical settlement-time curve for clay under an embankment loading.**

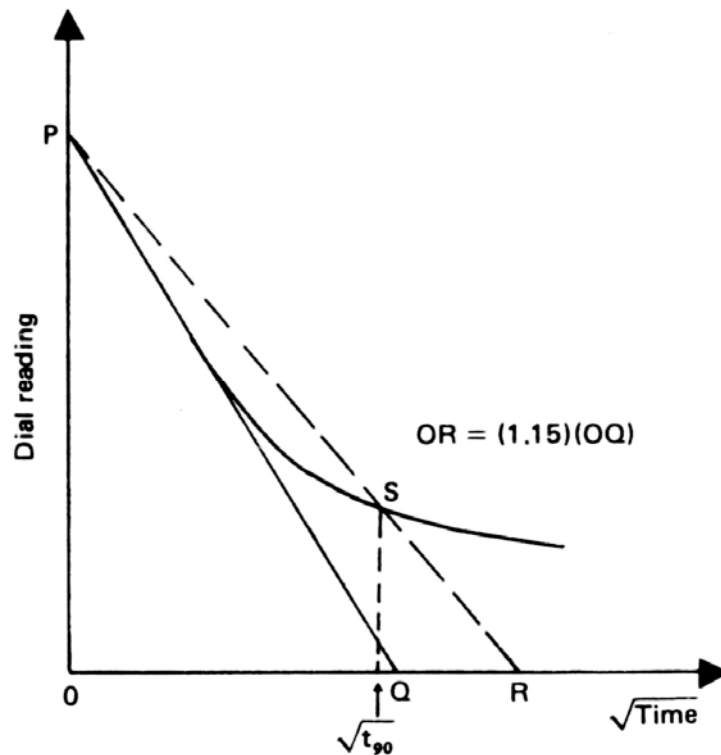
### 7.5.3.2 Step-by-Step Procedure to Determine Amount and Time for Consolidation

The step-by-step process for determining the amount of and time for consolidation to occur for a single-stage construction of an embankment on soft ground is outlined below:

1. From laboratory consolidation test data determine the  $e$ -log  $p$  curve and estimate the change in void ratio that results from the added weight of the embankment. Create the virgin field consolidation curve by using the guidelines presented in Table 7-3.
2. Determine if the foundation soil is normally consolidated, overconsolidated or under-consolidated.
3. Use Equations 7-2 to 7-7 to compute the primary consolidation settlement for normally consolidated, overconsolidated and under-consolidated foundation soils.
4. Determine  $c_v$  from laboratory consolidation test data. Two graphical procedures are commonly used for this determination are the **logarithm-of-time method** ( $\log t$ ) proposed by Casagrande and Fadum (1940) and the **square-root-of-time method** ( $\sqrt{t}$ ) proposed by Taylor (1948). These methods are shown in Figures 7-15 and 7-16, respectively. Because both methods are different approximations of theory, they do not give the same answers. Often the  $\sqrt{t}$  method gives slightly greater values of  $c_v$  than the  $\log t$  method.
5. Use Equation 7-8 to calculate the time to achieve 90% - 95% primary consolidation.

For a more detailed discussion on the consolidation theory, the reader is referred to Holtz and Kovacs (1981). An alternative approach to hand calculations is the use of a computerized method. For example, program FoSSA (2003) by ADAMA Engineering, Version 1.0 licensed to FHWA, which was introduced in Chapter 2, calculates the time rate of settlement for various boundary conditions including the effects of staged construction and strip drains in addition to calculating the stresses and settlements. FoSSA (2003) also allows for simulation of multiple layers undergoing simultaneous consolidation. In any event, the step-by-step hand calculations can serve to verify the correctness of benchmark cases and thereby be used to ascertain the correctness of any computerized procedure.





**Step-by-step procedure:**

1. Plot the dial reading and the corresponding square-root-of-time,  $\sqrt{t}$ .
2. Draw the tangent PQ to the early portion of the plot.
3. Draw a line PR such that  $OR = (1.15)(OQ)$ .
4. The abscissa of the point S (i.e., the intersection of PR and the consolidation curve) will give  $\sqrt{t_{90}}$ , i.e., the square-root-of-time for 90% consolidation.
5. Determine  $c_v$  from Equation 7-8 for  $U=90\%$ . From Table 7-4, the value of  $T_v$  for  $U=90\%$  is 0.848. Thus,  $c_v$  can be determined as follows:

$$c_v = \frac{0.848 H_d^2}{t_{90}}$$

**Figure 7-16. Square-root-of-time method for determination of  $c_v$ .**

**Comments on  $c_v$  value:** The value of  $c_v$  is determined for a given load increment. It varies from increment to increment and is different for loading and unloading. Moreover,  $c_v$ , usually varies considerably among samples of the same soil. Therefore, **if the actual rate of consolidation is critical to the design, as in certain stability problems where excess pore water pressures must be known accurately, pore pressures must actually be measured in the field as construction proceeds.**

Regardless of whether hand-calculations or computerized methods are used, the important factors to remember are:

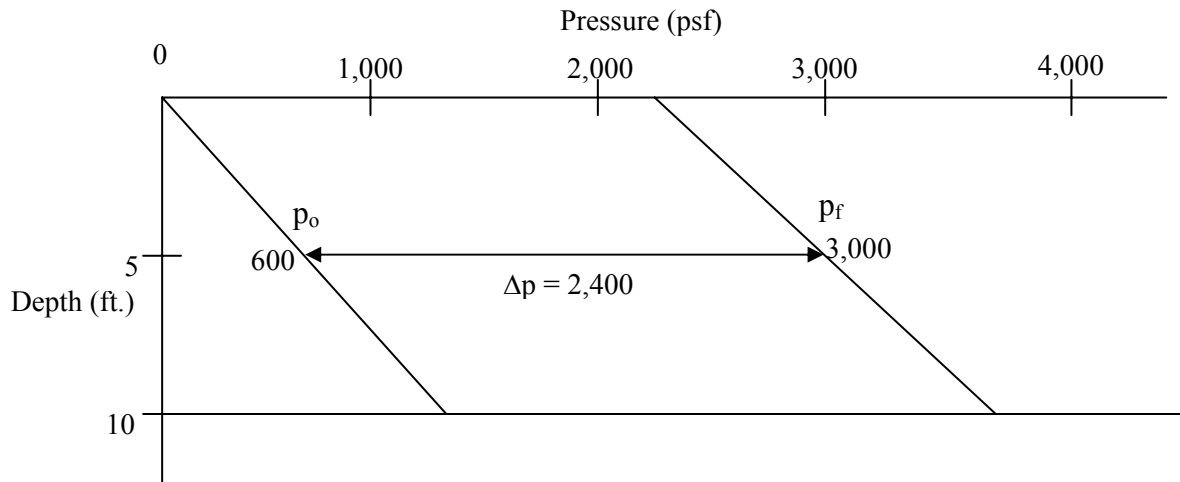
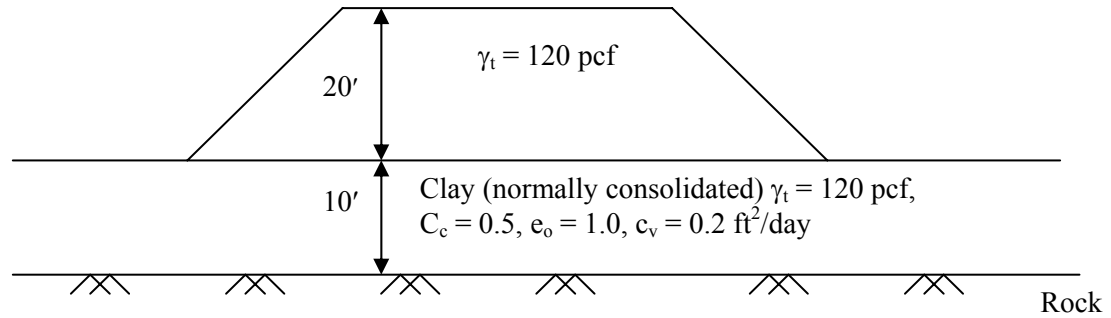
- the time required for consolidation is proportional to the square of the longest distance required for water to drain from the deposit and,
- the rate of settlement decreases as time increases.

The maximum length of vertical drainage path,  $H_d$ , bears further explanation. This term should not be confused with the  $H$  term in the equation for the computation of the settlement magnitude.  $H$  is an arbitrarily selected value usually representing a portion of the total compressible layer thickness. For calculating the magnitude of settlement the sum of the sublayer  $H$  values must equal the total thickness of the clay layer. For calculating the time rate of settlement, the  $H_d$  term in Equation 7-8 is the maximum vertical distance that a water molecule must travel to escape from the compressible layer to a more permeable layer. In the case of a 20 ft (6 m) thick clay layer bounded by a sand layer on top and a virtually impermeable rock stratum on the bottom, the  $H_v$  term would equal to 20 ft (6 m). The water molecule must travel from the bottom of the layer to the top of the layer to escape, i.e., single drainage. However, if the clay layer was bounded top and bottom by more permeable sand deposits, the  $H_v$  distance would be 10 ft (3 m). The water molecule in this case, needs only to travel from the center of the layer to either boundary to escape, i.e., double drainage. However, regardless of the boundary drainage conditions, the sum of the sublayer  $H$  values must equal 20 ft (6 m) in the settlement computations.

The mechanism for determining the maximum horizontal path for escape of a water molecule is similar. The influence of horizontal drainage may be significant if the width of the loaded area is small. For instance, during consolidation under a long, narrow embankment, a water molecule can escape by traveling a distance equal to one half the embankment width. However, for very wide embankments the beneficial effect of lateral drainage may be small as the time for lateral escape of a water molecule increases as the square of one-half the embankment width.

The concepts of consolidation settlement and time rates of consolidation with reference to an embankment loading are illustrated by the following example.

**Example 7-3:** Determine the magnitude of and the time for 90% consolidation for the primary settlement of a “wide” embankment by using the  $p_o$  diagram.



**Solution:**

Since the embankment is “wide,” the vertical stress at the base of the embankment is assumed to be the same within the 10-ft thick clay layer. Since soil is normally consolidated, use Equation 7-2 to determine the primary consolidation settlement as follows:

$$\Delta H = H \frac{C_c}{1 + e_o} \log_{10} \frac{p_o + \Delta p}{p_o}$$

$$\Delta H = 10 \text{ ft} \left( \frac{0.5}{1 + 1.0} \right) \log_{10} \frac{600 \text{ psf} + 2,400 \text{ psf}}{600 \text{ psf}} = 1.75 \text{ ft} = 21 \text{ inches (0.53 m)}$$

Find time for 90% consolidation use  $T_v = 0.848$  from Table 7-4. Assume single vertical drainage due to impervious rock underlying clay layer and use Equation 7-8 to calculate the time required for 90% consolidation to occur.

$$t_{90} = \frac{TH_d^2}{c_v}$$

$$t_{90} = \frac{(0.848)(10 \text{ ft})^2}{0.2 \text{ ft}^2 / \text{day}} = 424 \text{ days}$$

#### 7.5.4 Secondary Compression of Cohesive Soils

Secondary compression is the process whereby the soil continues to displace vertically after the excess pore water pressures are dissipated to a negligible level i.e., primary compression is essentially completed. Secondary compression is normally evident in the settlement-log time plot when the specimen continues to consolidate beyond 100 percent of primary consolidation, i.e., beyond  $t_{100}$ , as shown in Figure 7-15. An example is shown in Figure 7-17, where secondary compression occurs beyond  $t_{100} = 392$  mins. There are numerous hypotheses as to the reason for the secondary compression. The most obvious reason is associated with the simplifications involved in the theory of one-dimensional consolidation derived by Terzaghi. More rigorous numerical solutions accounting for the simplifications can often predict apparent secondary compression effects.

The magnitude of secondary compression is estimated from the coefficient of secondary compression,  $C_\alpha$ , as determined from laboratory tests by using Equation 7-9 that is derived from Figure 7-17.

$$C_\alpha = \frac{\Delta e}{\log_{10} \left( \frac{t_{2 \text{ lab}}}{t_{1 \text{ lab}}} \right)} \quad 7-9$$

where:  $t_{1 \text{ lab}}$  = time when secondary compression begins and is typically taken as the time when 90 percent of primary compression has occurred

$t_{2 \text{ lab}}$  = an arbitrary time on the curve at least one log-cycle beyond  $t_{90}$  or the time corresponding to the service life of the structure

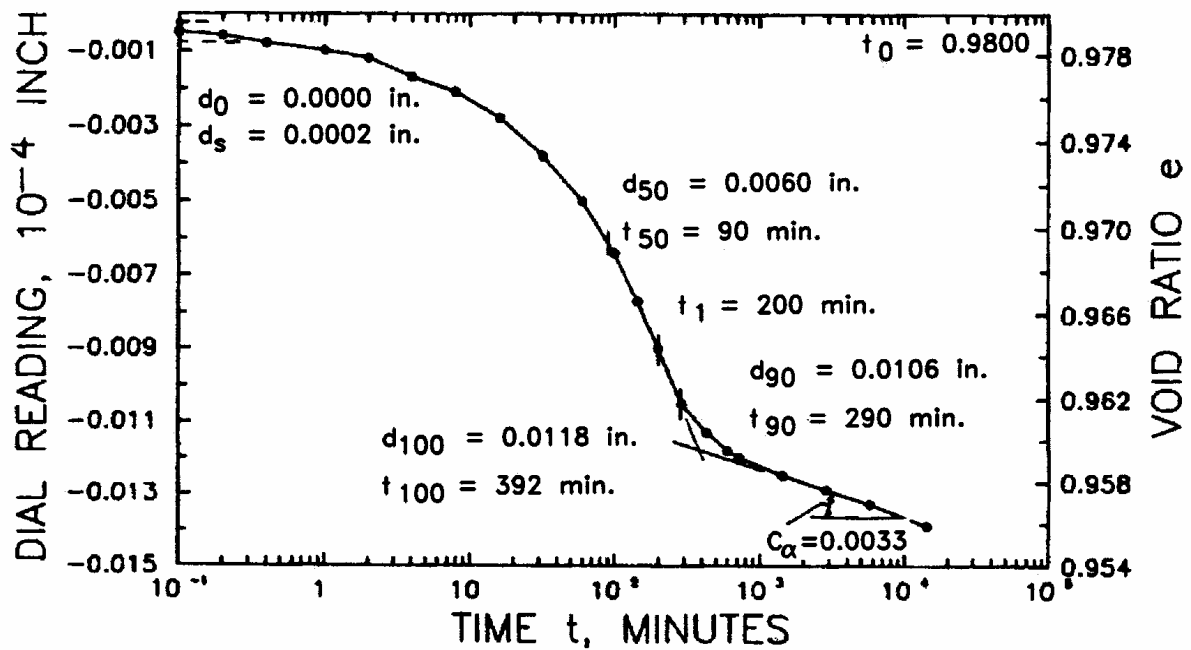


**Figure 7-17: Example time plot from one-dimensional consolidometer test for determination of secondary compression (USACE, 1994). (1 in = 25.4 mm)**

The settlement due to secondary compression ( $S_s$ ) is then determined from Equation 7-10.

$$S_s = \frac{C_\alpha}{1 + e_o} H_c \log_{10} \left( \frac{t_2}{t_1} \right) \quad 7-10$$

where:  $t_1$  = time when approximately 90 percent of primary compression has occurred for the actual clay layer being considered as determined from Equation 7-8.

$t_2$  = the service life of the structure or any other time of interest.

The values of  $C_\alpha$  can be determined from the dial reading vs. log time plots associated with the one-dimensional consolidation test as shown in Figure 7-17. Typical ranges of the ratio of  $C_\alpha/C_c$  presented in Section 5.4.6.4 of Chapter 5 can be used to check laboratory test results.

## 7.6 LATERAL SQUEEZE OF FOUNDATION SOILS

When the geometry of the applied load is larger than the thickness of the compressible layer or when there is a finite soft layer within the depth of significant influence (DOSI) below the loaded area, significant lateral stresses and associated lateral deformations can occur as shown earlier in Figure 2-16 in Chapter 2. For example, as shown in Figure 7-18, if the thickness of a soft soil layer beneath an embankment fill is such that it is less than the width,  $b_e$ , of an end or side slope, then the soft soil may squeeze out.

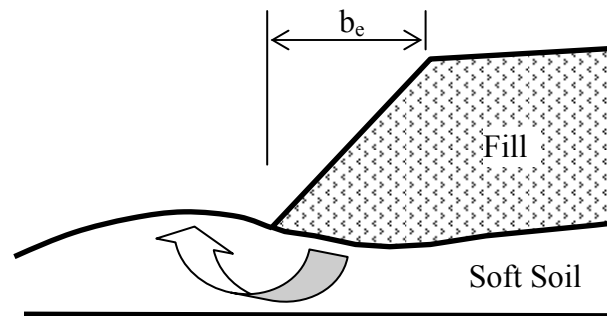


**Figure 7-18. Schematic of lateral squeeze phenomenon.**

The lateral squeeze phenomenon is due to an unbalanced load at the surface of the soft soil. The lateral squeeze behavior may be of two types, (a) short-term undrained deformation that results from a local bearing capacity type of deformation, or (b) long-term drained, **creep**-type deformation. **Creep refers to the slow deformation of soils under sustained loads over extended periods of time and can occur at stresses well below the shear strength of the soil.** As discussed in Section 5.4.1, secondary compression is a form of creep deformation while primary consolidation is not.

The lateral squeeze phenomenon can be observed in the field. For example, field observations and measurements have shown that some bridge abutments supported on piles driven through compressible soils tilted toward the embankment fill. Many of the abutments experienced large horizontal movements resulting in damage to the structure. The cause of this problem is attributed to the unbalanced fill load, which "squeezes" the soil laterally as discussed previously. This "lateral squeeze" of the soft foundation soil can apply enough lateral thrust against the piles to bend or even shear the piles. This problem is illustrated in Figure 7-19. The bridge abutment may tilt forward or backward depending on a number of factors including the relative configuration of the fill and the abutment, the relative stiffness of the piles or shafts and the soft deposit, the strength and thickness of the soft layer, rate of construction of the fill, and depth to bearing layer.

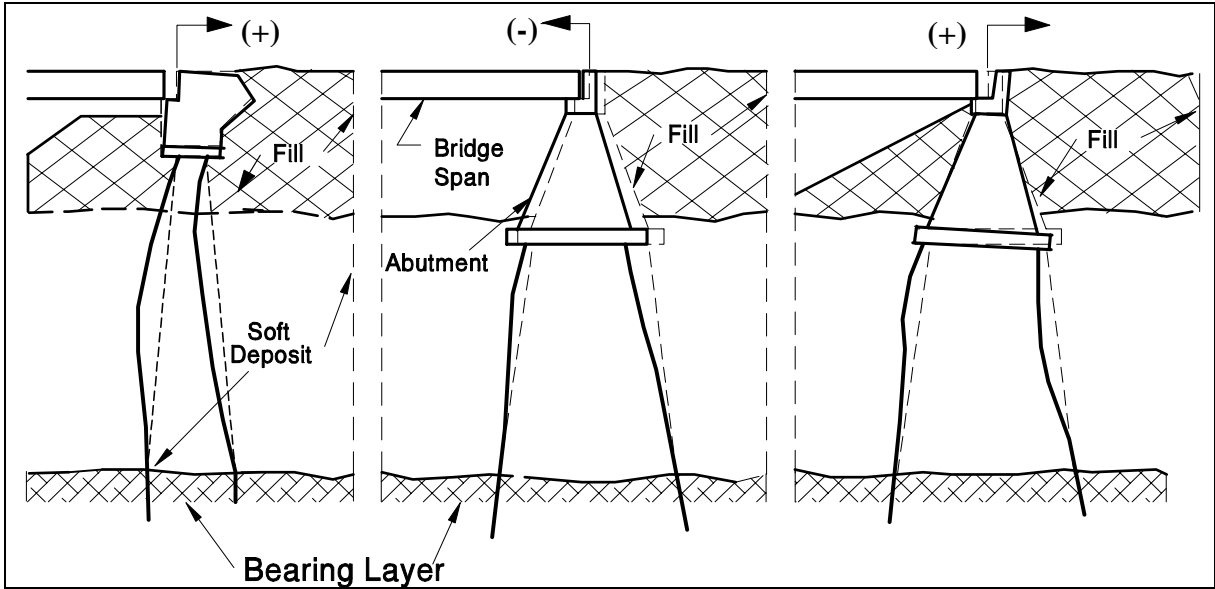


Figure 7-19. Examples of abutment tilting due to lateral squeeze (FHWA, 2006a).

### 7.6.1 Threshold Condition for Lateral Squeeze

Experience has shown that lateral squeeze of the foundation soil can occur and abutment tilting may result if the surface load applied by the weight of the fill exceeds 3 times the undrained shear strength,  $s_u$ , of the soft foundation soil, i.e.,

$$(\gamma)(H) > 3s_u \quad 7-11$$

where,  $\gamma$  is the unit weight of the fill and  $H$  is the height of the fill. The possibility of abutment tilting can be evaluated in design by using the above relationship. Whether the lateral squeeze will be short-term or long-term can be determined by evaluating the consolidation rate of settlement with respect to the rate of application of the load. For practical purposes, the unit weight of an embankment fill can be assumed to be approximately 125 pcf (19.7 kN/m<sup>3</sup>). The undrained shear strength,  $s_u$ , of the foundation soil can be determined either from in-situ field vane shear tests or from laboratory triaxial tests on high quality undisturbed Shelby tube samples.

### 7.6.2 Calculation of the Safety Factor against Lateral Squeeze

The safety factor against failure by squeezing,  $FS_{SQ}$ , may be calculated by Equation 7-12 (Silvestri, 1983). The geometry of the problem and the forces involved are shown in Figure 7-20.

$$FS_{SQ} = \left[ \frac{2s_u}{\gamma D_s \tan \theta} \right] + \left[ \frac{4.14s_u}{\gamma H} \right] \quad 7-12$$

- where:
- $\theta$  = angle of slope
  - $\gamma$  = unit weight of the fill
  - $D_s$  = depth of soft soil beneath the toe of the end slope or side slope of the fill
  - $H$  = height of the fill
  - $s_u$  = undrained shear strength of soft soil beneath the fill

Caution is advised when Equation 7-12 is used. It was found that when  $FS_{SQ} < 2$ , a rigorous slope stability analysis and possibly advanced numerical analysis, e.g., finite element analysis should be performed. When the depth of the soft layer,  $D_s$ , is greater than the base width of the end slope,  $b=H/\tan\theta$ , general slope stability behavior governs the design. In that case, the methods described in Chapter 6 (Slope Stability) may be used to evaluate the stability of the foundation soils.

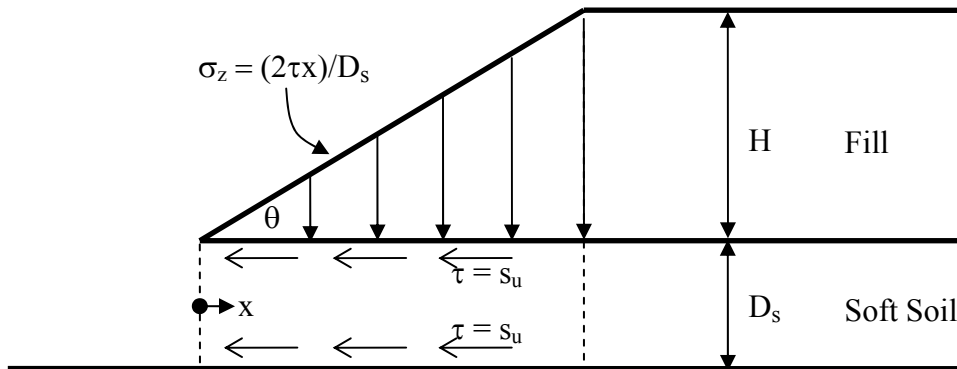


**Figure 7-20. Definitions for calculating safety factor against lateral squeeze (after Silvestri, 1983).**

### 7.6.3 Estimation of Horizontal Movement of Abutments

The amount of horizontal movement the abutment may experience can also be estimated in design. Information from case histories for nine structures where measurements of abutment movements occurred is documented in Table 7-5.

The data presented in Table 7-5 provides a basis for estimating horizontal movement for abutments under similar conditions, provided a reasonable estimate of the post-construction fill settlement is made by using data from consolidation tests on high quality undisturbed Shelby tube samples. Note that the data for the abutments listed in Table 7-5 shows the horizontal movement (tilt) to range from 6 to 33% of the vertical fill settlement, with the average being 21%. Therefore, as a first approximation, it can be said that if the fill load exceeds the  $3s_u$  limit prescribed by Equation 7-11, then the horizontal movement (tilt) of an abutment can be reasonably estimated as approximately 25% of the vertical fill settlement for the conditions listed in Table 7-5.

**Table 7-5**  
**Summary of abutment movements (Nicu, *et al.*, 1971)**

Foundation	Fill Settlement (inches)	Abutment Settlement (inches)	Abutment Tilting (inches)	Ratio of Abutment Tilting to Fill Settlement
Steel H-piles	16	Unknown	3	0.19
Steel H-piles	30	0	3	0.10
Soil bridge	24	24	4	0.17
Cast-in-place pile	12	3.5	2.5	0.19
Soil bridge	12	12	3	0.25
Steel H-piles	48	0	2	0.06
Steel H-piles	30	0	10	0.33
Steel H-piles	5	0.4	0.5 to 1.5	0.1 to 0.3
Timber Piles	36	36	12	0.33

## 7.7 DESIGN SOLUTIONS - DEFORMATION PROBLEMS

Both the magnitude and time rate of settlement can affect fill structures, which in turn may affect the performance of other structures such as bridge abutments that are built within or in the vicinity of the fills. There are various methods to reduce the magnitude and time rate of settlement. All of these methods can be considered as ground improvement and are discussed in detail in FHWA (2006b). Two of these methods are briefly discussed in this manual. The reader is referred to FHWA (2006b) for further details. Solutions to prevent abutment tilting due to lateral squeeze are discussed in Section 7.7.3.

### **7.7.1 Reducing the Amount of Settlement**

Settlement can be reduced by either increasing the resistance or reducing the load. Several ground improvement methods that are particularly suitable for reducing the amount of settlement are noted below.

#### **7.7.1.1 Category 1 - Increasing the Resistance**

Common ground improvement techniques that increase resistance include the following:

- Excavation and recompaction.
- Excavation and replacement.
- Vertical inclusions such as stone columns, shafts and piles. Embankments supported in this way are known as column supported embankments.
- Horizontal inclusions such as geosynthetics.
- Grouting, e.g., soil mixing, jet grouting.
- Dynamic compaction.

#### **7.7.1.2 Category 2 - Reducing the Load**

Common load reduction techniques include the following:

- Reduce grade line (reduction in height and/or flattening the slope)
- Use lightweight fill material, e.g., expanded shale, foamed concrete, geofoam.
- Bypass the soft layer with a deep foundation. Deep foundations may be used in conjunction with a load transfer platform (see FHWA 2006b).

### **7.7.2 Reducing Settlement Time**

Often the major design consideration related to a settlement problem is the time for the settlement to occur. Low permeability clays and silty clays can take a long time to consolidate under an applied load. The settlement time is critical on most projects because it has a direct impact on construction schedules and delays increase project costs. Settlement time is also important to the maintenance personnel of a highway agency. The life cycle cost of annual regrading and resurfacing of settling roadways is usually far greater than the cost of design treatments to eliminate settlement before or during initial construction.

The two most common methods used to accelerate settlement and reduce settlement time are:

1. Application of surcharge.
2. Installation of vertical drains in the foundation soils.

Note that both of the above techniques lead to an increase in the resistance. These techniques are briefly discussed below and their use is illustrated in the Apple Freeway example in Appendix A.

### 7.7.2.1 Surcharge Treatment

An embankment surcharge is constructed to a predetermined height, usually 1 to 10 ft (0.3 to 3 m) above final grade elevation based on settlement calculations. The surcharge is maintained for a predetermined waiting period (typically 3 to 12 months) based on settlement-time calculations. Depending upon the strength of the consolidating layer(s) the surcharge may have to be constructed in stages. The actual dimensions of the surcharge and the waiting period for each stage depend on the strength and drainage properties of the foundation soil as well as the initial height of the proposed embankment. The length of the waiting period can be estimated by using laboratory consolidation test data. The actual settlement occurring during embankment construction is then monitored with geotechnical instrumentation. When the settlement with surcharge equals the settlement originally estimated for the embankment, the surcharge is removed, as illustrated in Figure 7-21.

If the surcharge is not removed after the desired amount of settlement has occurred, then additional settlement will continue to occur. Note that the stability of a surcharged embankment must be checked as part of the embankment design to ensure that an adequate short term safety factor exists. The stability is often field verified by monitoring with instrumentation such as inclinometers, piezometers and settlement points as discussed later.

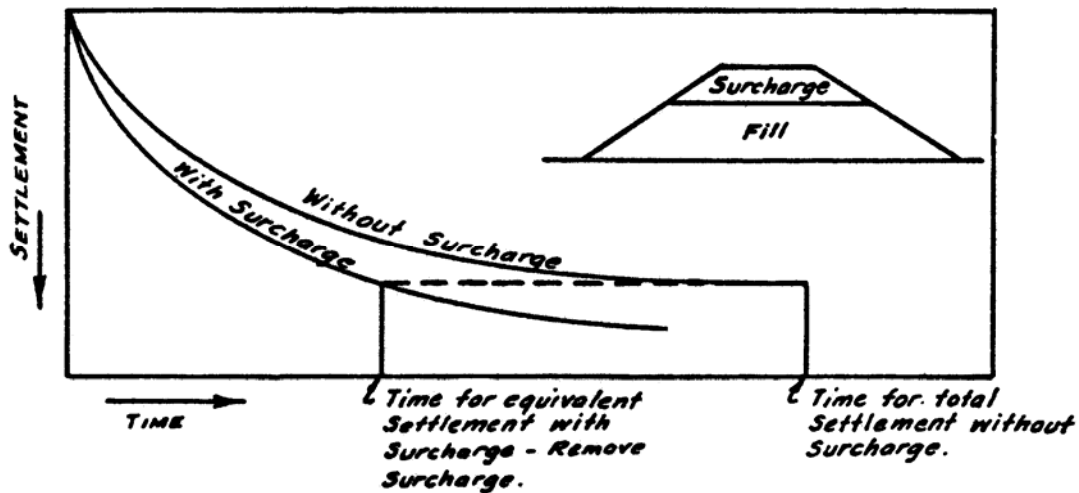
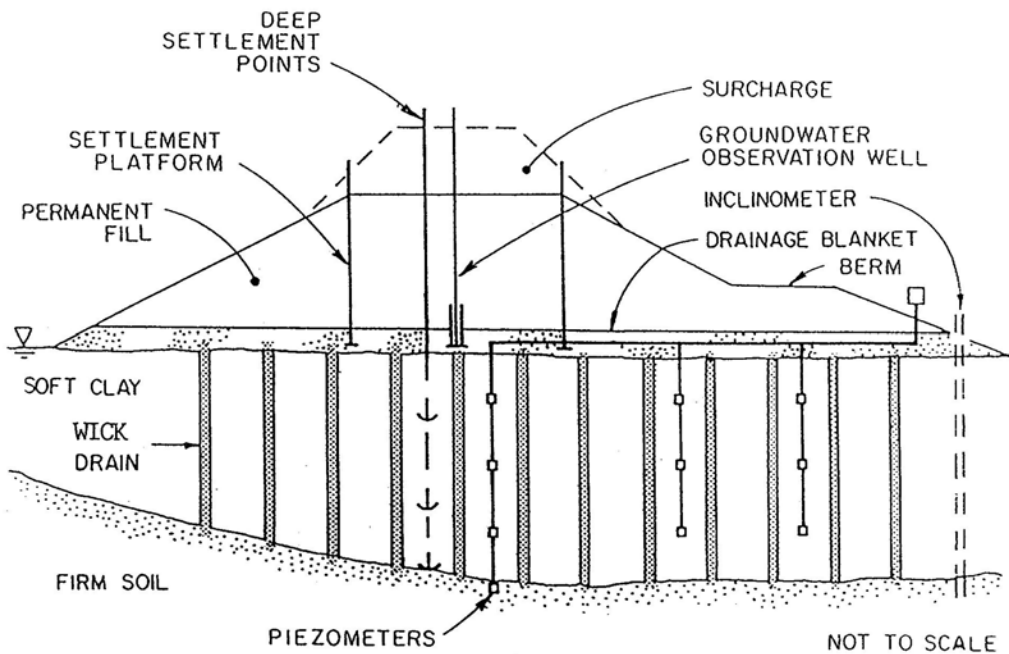


Figure 7-21. Determination of surcharge time required to achieve desired settlement.

### 7.7.2.2 Vertical Drains

Primary consolidation of some highly plastic clays can take many years to be completed. Surcharging alone may not be effective in reducing settlement time sufficiently since the longest distance to a drainage boundary may be significant. In such cases, vertical drains can be used to accelerate the settlement, either with or without surcharge treatment. The vertical drains accelerate the settlement rate by reducing the drainage path the water must travel to escape from the compressible soil layer to half the horizontal distance between drains, as illustrated in Figure 7-22. In most applications, a permeable sand blanket, 2 to 3 ft (0.6 to 1 m) thick, should be placed on the ground surface to permit free movement of water away from the embankment area and to create a working platform for installation of the drains. The drains are installed prior to placement of the embankment. The applied pressure from the embankment generates excess pore water pressure.

Recall that the consolidation time is proportional to the square of the length of the longest drainage path. Thus if the length of the drainage path is shortened by 50%, the consolidation time is reduced by a factor of four. Vertical drains and sand blankets should have high permeability to allow the water squeezed out of the subsoil to travel relatively quickly through the drains and the blanket.



**Figure 7-22. Use of vertical drains to accelerate settlement (NCHRP, 1989).**

Wick drains are small prefabricated drains consisting of a plastic core that is wrapped with geotextile. Wick drains are typically 4 inches (100 mm) wide and about 1/4 inch (7 mm) thick. The drains are produced in rolls that can be fed into a mandrel. Wick drains are installed by pushing or vibrating a mandrel into the ground with the wick drain inside. When the bottom of the compressible soil is reached, the mandrel is withdrawn and the trimmed portion of the wick drain left in the ground. To minimize smear of the compressible soil, the cross-sectional area of the mandrel is recommended to be limited to a maximum of about 10 in<sup>2</sup> (6,450 mm<sup>2</sup>). Predrilling of dense soil deposits may be required in some cases to reach the design depth. Use of wick drains in the United States began in the early 1970s. Design and construction guidance on the use of wick drains is provided in FHWA (1986, 2006b).

The feasibility of a surcharge solution should always be considered first since vertical drains are generally more expensive.

### **7.7.3 Design Solutions to Prevent Abutment Tilting**

A recommended solution to minimize abutment-tilting is to induce settlement of the fill before the abutment piles or shafts are installed. If the construction time schedule or other factors do not permit pre-consolidation of the foundation soils before the piles or shafts are installed, then abutment tilting issues can be mitigated by the following design provisions:

1. Use sliding plate expansion shoes large enough to accommodate the anticipated horizontal movement.
2. Make provisions to fill in the bridge deck expansion joint over the abutment by inserting either metal plate fillers or larger neoprene joint fillers.
3. Design the deep foundations for downdrag forces due to settlement. This solution does not improve the horizontal displacement effects.
4. Use backward battered piles at the abutment and particularly at the wingwalls.
5. Use lightweight fill materials to reduce driving forces

Displacements should also be monitored during and after construction so that the predicted movements can be compared to actual displacements. Displacements should be monitored by survey monuments or protected prisms installed on the face of the abutment and wingwalls and should be tied into permanent benchmarks.

## 7.8 PRACTICAL ASPECTS OF EMBANKMENT SETTLEMENT

Few engineers realize the influence of embankment construction on the response of subsoils. The total weight of an embankment has an impact on the type of foundation treatment that may be appropriate. For instance, a relatively low height embankment of 10 ft (3 m) may be effectively surcharged because the additional surcharge weight could be 30 to 40 percent of the proposed embankment weight. However, when the embankment height exceeds 50 ft (15 m) the influence of a 5 or 10 ft (1.5 or 3 m) trapezoid of soil on top of this heavy 50 ft (15 m) mass is small and probably not cost-effective. Conversely, as the embankment height increases, the use of a shallow foundation for support of the abutment becomes more attractive. A 30 ft (9 m) high, 50 ft (15 m) long approach embankment weighs about 15,000 tons (130 MN) compared to the insignificant weight of a total (stub type) abutment loading that may equal 1,000 tons (9 MN). The width of an embankment also has an effect on total settlement. Wider embankments cause a pressure increase deeper into the subsoil. As might be expected, wider embankments may also cause more immediate and consolidation settlement and increase the time for consolidation to occur.

Recent developments in computer software readily permit computer analysis of approach embankment settlement. Programs such as FoSSA (2003), discussed in Chapter 2, allow the user to compute settlements along abutments and to evaluate the effects of settlements on pipes buried in end slopes or pipes placed diagonally under approach fills.

## 7.9 CONSTRUCTION MONITORING AND QUALITY ASSURANCE

Approach embankment construction should be clearly defined in standard drawings as to materials and limits of placement. Such standards assure uniformity in construction due to the familiarity of the construction personnel with the operations being performed and results expected. Designers should attempt to use standard details wherever possible. Attempts at small changes in materials or limits are generally counterproductive to good construction where repetition of good practice is an important factor.

The philosophy of approach embankment details is to insure adequate bearing capacity for abutments or piers placed in the embankment and to minimize settlement of the pavement or footing. Typical highway embankments require compaction to 90 percent of maximum dry density (AASHTO T180) to control pavement settlement. **Designers should specify materials and compaction control as shown in Figure 7-4, to limit differential settlement between the structure and approach fill.** If piles are used to support footings in

fill, the largest particle size of embankment material should be limited to 6 in (150 mm) to ease pile installation either by driving or pre-drilling. If spread footings are used, a minimum of 5 ft (1.5 m) of select material compacted to 100 percent of maximum dry density (AASHTO T99) should be placed beneath the footing and extended beyond the wingwalls. This layer provides uniform support for the footing and a rigid transition between the structure and the fill to minimize differential settlement. Construction control is usually referenced to percent compaction on the standard design drawings.

### **7.9.1 Embankment Construction Monitoring by Instrumentation**

The observational approach to design involves monitoring subsoil behavior during early construction stages to verify design and to predict responses to subsequent construction. Basic soil mechanics concepts can be used to predict future subsoil behavior accurately if data from instrumentation are analyzed after initial construction loads have been placed. Occasionally a design problem arises that is unique or extremely critical and that can be safely solved only by utilizing the observational approach.

Embankment placement must be carefully observed and monitored on projects where stability and/or settlement are critical. The monitoring should include visual observation by the construction inspection staff and the use of instrumentation. Without the aid of various forms of instrumentation, it is impossible to determine accurately what is happening to the foundation. Instrumentation can be used to warn of imminent failure or to indicate whether settlement is occurring as predicted. The type of instruments to be used and where they will be placed should be planned by a qualified and experienced geotechnical specialist. Actual interpretation and analysis of the data should also be performed by someone with a background in soil mechanics; however, the project engineer and inspector should understand the purpose of each type of instrumentation and how the data are to be used.

#### **7.9.1.1 Inspector's Visual Observation**

In areas of marginal embankment stability, the inspector should walk the surface of the embankment daily looking for any sign of cracking or movement. Hairline cracks often develop at the embankment surface just prior to failure. If the inspector discovers any such features, all fill operations should cease immediately. All instrumentation should be read immediately. The geotechnical specialist should be notified. Subsequent readings will indicate when it is safe to resume operations. Unloading by removal of fill material or other mitigation methods are sometimes necessary to prevent an embankment failure.

### 7.9.1.2 Types of Instrumentation

The typical instrumentation specified to monitor foundation performance on projects where stability and settlement are critical consists of:

1. **Slope Inclinometers** are used to monitor subsurface lateral deformation. A slope inclinometer typically consists of a 3 in (75 mm) internal diameter (ID) plastic tube with four grooves cut at 90-degree intervals around the inside. The slope inclinometer tube is installed in a borehole. The bottom of the slope inclinometer tube must be founded in firm soil or rock. A readout probe that fits into the grooves is lowered down the tube and angular deflection of the tube is measured. The amount and location of horizontal movement in the foundation soil can then be measured. For embankments built over very soft subsoils, telescoping inclinometer casing should be used to account for vertical consolidation. In soft ground conditions, several inches of lateral movement due to squeeze may occur without shear failure as the embankment is built. Therefore, from a practical construction control standpoint, the rate of movement rather than the amount is the better indicator of imminent failure. Slope inclinometer readings should be made often during the critical embankment placement period, daily if fill placement is proceeding rapidly, and readings should be plotted immediately on a movement versus time plot. Fill operations should cease if a sudden increase in the rate of movement occurs.
2. **Piezometers** indicate the amount of excess pressure build-up within the water-saturated pores of the soil. There are critical levels to which the water pressure in the subsoil will increase just prior to failure. The geotechnical specialist can estimate the critical water pressure level during design. Normally, the primary function of piezometers during fill placement is to warn of failures. Once the embankment placement is complete, the piezometers are used to measure the rate of consolidation. There are several different types of piezometers. The simplest is the open standpipe type, which is essentially a well point with a metal or plastic pipe attached to it. The pipe is extended up through the fill in sections as the fill height increases. This type of open well piezometer has the disadvantage that the pipes are susceptible to damage if hit by construction equipment. Also, the response time of open well piezometers is often too slow in soft clays to warn of potential embankment failure. There are several types of remote piezometers that eliminate the requirement for extending a pipe up through the fill. The remote units consist of a piezometer transducer that is sealed in a borehole with leads carried out laterally under the base of the embankment to a readout device that records the pore water pressure measured by the transducer. Pneumatic or vibrating wire piezometers

have a more rapid response to changes in pore water pressure than open-stand pipe piezometers.

3. **Settlement devices** are used to measure the amount and rate of settlement of the foundation soil due to the load from the embankment. Typically they are installed on or just below the existing ground surface before any fill is placed. The simplest settlement device is a settlement plate usually a 3 or 4 ft (0.9 to 1.2 m square plywood mat or steel plate with a vertical reference rod (usually  $\frac{3}{4}$  in (19 mm) pipe) attached to the plate. The reference rods are normally added 4 ft (1.2 m) at a time as the height of the embankment increases. The elevation of the top of the reference rod is surveyed periodically to measure the foundation settlement. Remote pneumatic settlement devices are also available. As with the remote piezometer devices, the remote settlement devices have the advantage of not having a reference rod extending up through the fill.

### 7.9.1.3 Typical Locations for Instruments

Instrument installations should be spaced approximately 250 to 500 ft (75 to 150 m) along the roadway alignment in critical areas. Typical locations of instruments for an embankment over soft ground are shown in Figure 7-23:

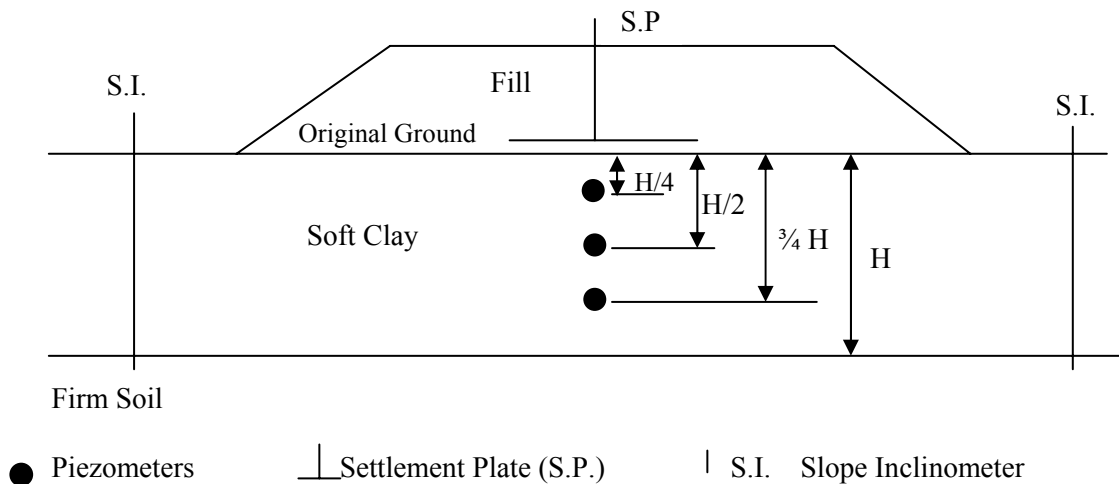


**Figure 7-23. Typical locations for various types of monitoring instruments for an embankment constructed over soft ground.**

[THIS PAGE INTENTIONALLY BLANK]



U.S. Department of Transportation  
Federal Highway Administration

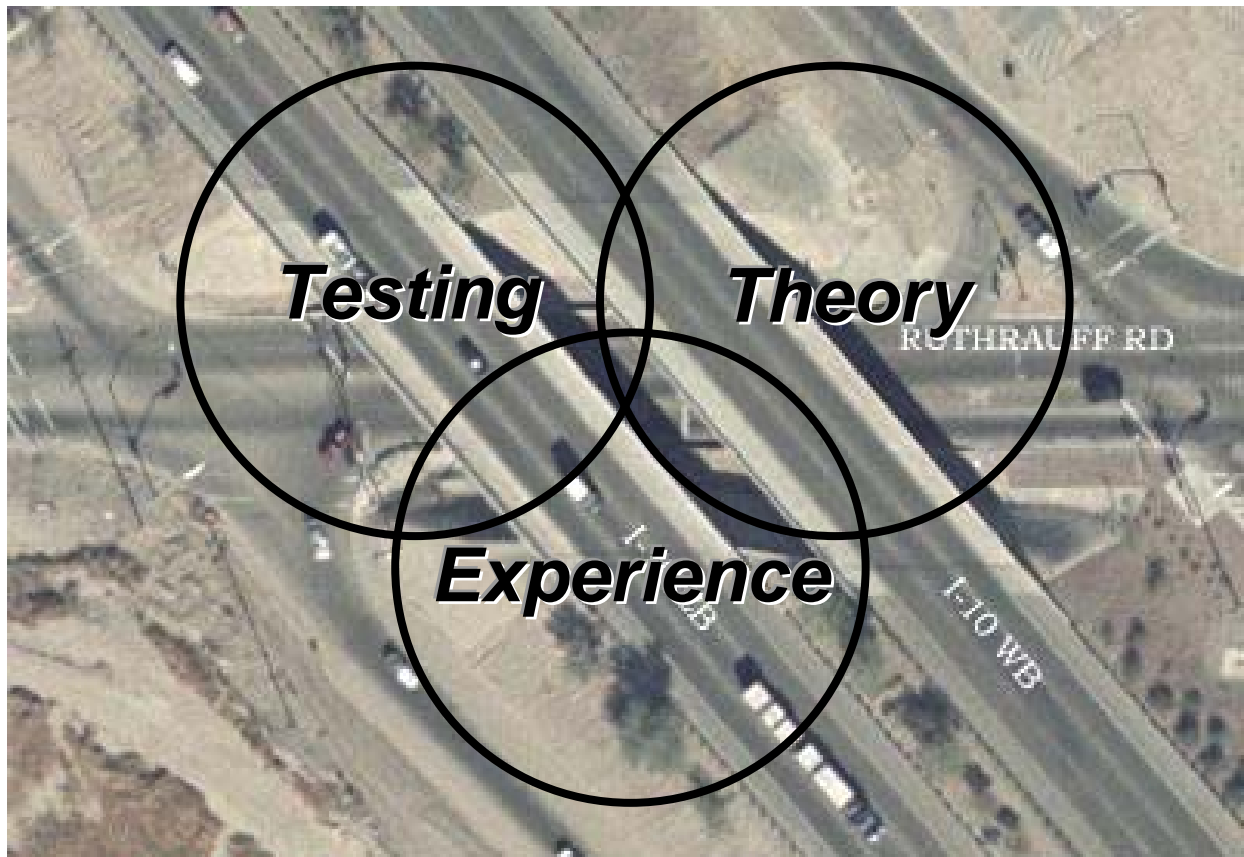
Publication No. FHWA NHI-06-089  
December 2006

**NHI Course No. 132012**

---

# **SOILS AND FOUNDATIONS**

**Reference Manual – Volume II**



*National Highway Institute*

## **NOTICE**

The contents of this report reflect the views of the authors, who are responsible for the facts and the accuracy of the data presented herein. The contents do not necessarily reflect policy of the Department of Transportation. This report does not constitute a standard, specification, or regulation. The United States Government does not endorse products or manufacturers. Trade or manufacturer's names appear herein only because they are considered essential to the objective of this document.

**Technical Report Documentation Page**

1. Report No. FHWA-NHI-06-089	2. Government Accession No.	3. Recipient's Catalog No.	
4. Title and Subtitle  SOILS AND FOUNDATIONS REFERENCE MANUAL – Volume II		5. Report Date December 2006	
		6. Performing Organization Code	
7. Author(s) Naresh C. Samtani*, PE, PhD and Edward A. Nowatzki*, PE, PhD		8. Performing Organization Report No.	
9. Performing Organization Name and Address Ryan R. Berg and Associates, Inc. 2190 Leyland Alcove, Woodbury, MN 55125 * NCS GeoResources, LLC 640 W Paseo Rio Grande, Tucson, AZ 85737		10. Work Unit No. (TRAIS)	
		11. Contract or Grant No. DTFH-61-02-T-63016	
12. Sponsoring Agency Name and Address National Highway Institute U.S. Department of Transportation Federal Highway Administration, Washington, D.C. 20590		13. Type of Report and Period Covered	
		14. Sponsoring Agency Code	
15. Supplementary Notes FHWA COTR – Larry Jones FHWA Technical Review – Jerry A. DiMaggio, PE; Silas Nichols, PE; Richard Cheney, PE; Benjamin Rivers, PE; Justin Henwood, PE. Contractor Technical Review – Ryan R. Berg, PE; Robert C. Bachus, PhD, PE; Barry R. Christopher, PhD, PE <i>This manual is an update of the 3<sup>rd</sup> Edition prepared by Parsons Brinckerhoff Quade &amp; Douglas, Inc, in 2000. Author: Richard Cheney, PE. The authors of the 1<sup>st</sup> and 2<sup>nd</sup> editions prepared by the FHWA in 1982 and 1993, respectively, were Richard Cheney, PE and Ronald Chassie, PE.</i>			
16. Abstract  The Reference Manual for Soils and Foundations course is intended for design and construction professionals involved with the selection, design and construction of geotechnical features for surface transportation facilities. The manual is geared towards practitioners who routinely deal with soils and foundations issues but who may have little theoretical background in soil mechanics or foundation engineering. The manual's content follows a project-oriented approach where the geotechnical aspects of a project are traced from preparation of the boring request through design computation of settlement, allowable footing pressure, etc., to the construction of approach embankments and foundations. Appendix A includes an example bridge project where such an approach is demonstrated. Recommendations are presented on how to layout borings efficiently, how to minimize approach embankment settlement, how to design the most cost-effective pier and abutment foundations, and how to transmit design information properly through plans, specifications, and/or contact with the project engineer so that the project can be constructed efficiently.  The objective of this manual is to present recommended methods for the safe, cost-effective design and construction of geotechnical features. Coordination between geotechnical specialists and project team members at all phases of a project is stressed. Readers are encouraged to develop an appreciation of geotechnical activities in all project phases that influence or are influenced by their work.			
17. Key Words		18. Distribution Statement	
Subsurface exploration, testing, slope stability, embankments, cut slopes, shallow foundations, driven piles, drilled shafts, earth retaining structures, construction.		No restrictions.	
19. Security Classif. (of this report)	20. Security Classif. (of this page)	21. No. of Pages	22. Price
UNCLASSIFIED	UNCLASSIFIED	594	

[THIS PAGE INTENTIONALLY BLANK]

## **PREFACE**

This update to the Reference Manual for the Soils and Foundations course was developed to incorporate the guidance available from the FHWA in various recent manuals and Geotechnical Engineering Circulars (GECs). The update has evolved from its first two versions prepared by Richard Cheney and Ronald Chassie in 1982 and 1993, and the third version prepared by Richard Cheney in 2000.

The updated edition of the FHWA Soils and Foundations manual contains an enormous amount of information ranging from methods for theoretically based analyses to “rules of thumb” solutions for a wide range of geotechnical and foundation design and construction issues. It is likely that this manual will be used nationwide for years to come by civil engineering generalists, geotechnical and foundation specialists, and others involved in transportation facilities. That being the case, the authors wish to caution against indiscriminate use of the manual’s guidance and recommendations. The manual should be considered to represent the minimum standard of practice. The user must realize that there is no possible way to cover all the intricate aspects of any given project. Even though the material presented is theoretically correct and represents the current state-of-the-practice, engineering judgment based on local conditions and knowledge must be applied. This is true of most engineering disciplines, but it is especially true in the area of soils and foundation engineering and construction. For example, the theoretical and empirical concepts in the manual relating to the analysis and design of deep foundations apply to piles installed in the glacial tills of the northeast as well as to drilled shafts installed in the cemented soils of the southwest. The most important thing in both applications is that the values for the parameters to be used in the analysis and design be selected by a geotechnical specialist who is intimately familiar with the type of soil in that region and intimately knowledgeable about the regional construction procedures that are required for the proper installation of such foundations in local soils.

### **General conventions used in the manual**

This manual addresses topics ranging from fundamental concepts in soil mechanics to the practical design of various geotechnical features ranging from earthworks (e.g., slopes) to foundations (e.g., spread footings, driven piles, drilled shafts and earth retaining structures). In the literature each of these topics has developed its own identity in terms of the terminology and symbols. Since most of the information presented in this manual appears in other FHWA publications, textbooks and publications, the authors faced a dilemma on the regarding terminology and symbols as well as other issues. Following is a brief discussion on such issues.

- **Pressure versus Stress**

The terms “pressure” and “stress” both have units of force per unit area (e.g., pounds per square foot). In soil mechanics “pressure” generally refers to an applied load distributed over an area or to the pressure due to the self-weight of the soil mass. “Stress,” on the other hand, generally refers to the condition induced at a point within the soil mass by the application of an external load or pressure. For example, “overburden pressure,” which is due to the self weight of the soil, induces “geostatic stresses” within the soil mass. Induced stresses cause strains which ultimately result in measurable deformations that may affect the behavior of the structural element that is applying the load or pressure. For example, in the case of a shallow foundation, depending upon the magnitude and direction of the applied loading and the geometry of the footing, the pressure distribution at the base of the footing can be uniform, linearly varying, or non-linearly varying. In order to avoid confusion, the terms “pressure” and “stress” will be used interchangeably in this manual. In cases where the distinction is important, clarification will be provided by use of the terms “applied” or “induced.”

- **Symbols**

Some symbols represent more than one geotechnical parameter. For example, the symbol  $C_c$  is commonly used to identify the coefficient of curvature of a grain size distribution curve as well as the compression index derived from consolidation test results. Alternative symbols may be chosen, but then there is a risk of confusion and possible mistakes. To avoid the potential for confusion or mistakes, the Table of Contents contains a list of symbols for each chapter.

- **Units**

English units are the primary units in this manual. SI units are included in parenthesis in the text, except for equations whose constants have values based on a specific set of units, English or SI. In a few cases, where measurements are conventionally reported in SI units (e.g., aperture sizes in rock mapping), only SI units are reported. English units are used in example problems. Except where the units are related to equipment sizes (e.g., drill rods), all unit conversions are “soft,” i.e., approximate. Thus, 10 ft is converted to 3 m rather than 3.05 m. The soft conversion for length in feet is rounded to the nearest 0.5 m. Thus, 15 ft is converted to 4.5 m not 4.57 m.

- **Theoretical Details**

Since the primary purpose of this manual is to provide a concise treatment of the fundamental concepts in soil mechanics and an introduction to the practical design of various geotechnical features related to highway construction, the details of the theory underlying the methods of analysis have been largely omitted in favor of discussions on the application of those theories to geotechnical problems. Some exceptions to this general approach were made. For example, the concepts of lateral earth pressure and bearing capacity rely too heavily on a basic understanding of the Mohr's circle for stress for a detailed presentation of the Mohr's circle theory to be omitted. However, so as not to encumber the text, the basic theory of the Mohr's circle is presented in Appendix B for the reader's convenience and as an aid for the deeper understanding of the concepts of earth pressure and bearing capacity.

- **Standard Penetration Test (SPT) N-values**

The SPT is described in Chapter 3 of this manual. The geotechnical engineering literature is replete with correlations based on SPT N-values. Many of the published correlations were developed based on SPT N-values obtained with cathead and drop hammer methods. The SPT N-values used in these correlations do not take in account the effect of equipment features that might influence the actual amount of energy imparted during the SPT. The cathead and drop hammer systems typically deliver energy at an estimated average efficiency of 60%. Today's automatic hammers generally deliver energy at a significantly higher efficiency (up to 90%). When published correlations based on SPT N-values are presented in this manual, they are noted as  $N_{60}$ -values and the measured SPT N-values should be corrected for energy before using the correlations.

Some researchers developed correction factors for use with their SPT N-value correlations to address the effects of overburden pressure. When published correlations presented in this manual are based upon values corrected for overburden they are noted as  $N_{160}$ . Guidelines are provided as to when the  $N_{60}$ -values should be corrected for overburden.

- **Allowable Stress Design (ASD) and Load and Resistance Factor Design (LRFD) Methods**

The design methods to be used in the transportation industry are currently (2006) in a state of transition from ASD to LRFD. The FHWA recognizes this transition and has developed separate comprehensive training courses for this purpose. Regardless of whether the ASD or LRFD is used, it is important to realize that the fundamentals of soil mechanics, such as the

determination of the strength and deformation of geomaterials do not change. The only difference between the two methods is the way in which the uncertainties in loads and resistances are accounted for in design. Since this manual is geared towards the fundamental understanding of the behavior of soils and the design of foundations, ASD has been used because at this time most practitioners are familiar with that method of design. However, for those readers who are interested in the nuances of both design methods Appendix C provides a brief discussion on the background and application of the ASD and LRFD methods.

## ACKNOWLEDGEMENTS

The authors would like to acknowledge the following events and people that were instrumental in the development of this manual.

- Permission by the FHWA to adapt the August 2000 version of the Soils and Foundations Workshop Manual.
- Provision by the FHWA of the electronic files of the August 2000 manual as well as other FHWA publications.
- The support of Ryan R. Berg of Ryan R. Berg and Associates, Inc. (RRBA) in facilitating the preparation of this manual and coordinating reviews with the key players.
- The support provided by the staff of NCS Consultants, LLC, (NCS) - Wolfgang Fritz, Juan Lopez and Randy Post (listed in alphabetical order of last names). They prepared some graphics, some example problems, reviewed selected data for accuracy with respect to original sources of information, compiled the Table of Contents, performed library searches for reference materials, and checked internal consistency in the numbering of chapter headings, figures, equations and tables.
- Discussions with Jim Scott (URS-Denver) on various topics and his willingness to share reference material are truly appreciated. Dov Leshchinsky of ADAMA Engineering provided copies of the ReSSA and FoSSA programs which were used to generate several figures in the manual as well as presentation slides associated with the course presentation. Robert Bachus of Geosyntec Consultants prepared Appendices D and E. Allen Marr of GeoComp Corporation provided photographs of some laboratory testing equipment. Pat Hannigan of GRL Engineers, Inc. reviewed the driven pile portion of Chapter 9. Shawn Steiner of ConeTec, Inc. and Salvatore Caronna of gINT Software prepared the Cone Penetration Test (CPT) and boring logs, respectively, shown in Chapter 3 and Appendix A. Robert (Bob) Meyers (NMDOT), Ted Buell (HDR-Tucson) and Randy Simpson (URS-Phoenix) provided comments on some sections (particularly Section 8.9).
- Finally, the technical reviews and recommendations provided by Jerry DiMaggio, Silas Nichols, Benjamin Rivers, Richard Cheney (retired) and Justin Henwood of the FHWA, Ryan Berg of RRBA, Robert Bachus of GeoSyntec Consultants, Jim Scott of URS, and Barry Christopher of Christopher Consultants, Inc., are gratefully acknowledged.

## **SPECIAL ACKNOWLEDGEMENTS**

A special acknowledgement is due of the efforts of Richard Cheney and Ronald Chassie for their work in the preparation of the previous versions of this manual. It is their work that made this course one of the most popular FHWA courses. Their work in developing this course over the past 25 years is acknowledged.

With respect to this manual, the authors wish to especially acknowledge the in-depth review performed by Jerry DiMaggio and time he spent in direct discussions with the authors and other reviewers. Such discussions led to clarification of some existing guidance in other FHWA manuals as well as the introduction of new guidance in some chapters of this manual.

<b>SI CONVERSION FACTORS</b>				
<b>APPROXIMATE CONVERSIONS FROM SI UNITS</b>				
<b>Symbol</b>	<b>When You Know</b>	<b>Multiply By</b>	<b>To Find</b>	<b>Symbol</b>
<b>LENGTH</b>				
mm	millimeters	0.039	inches	in
m	meters	3.28	feet	ft
m	meters	1.09	yards	yd
Km	kilometers	0.621	miles	mi
<b>AREA</b>				
mm <sup>2</sup>	square millimeters	0,0015	square inches	in <sup>2</sup>
m <sup>2</sup>	square meters	10.758	square feet	ft <sup>2</sup>
m <sup>2</sup>	square meters	1.188	square yards	yd <sup>2</sup>
ha	hectares	2.47	acres	ac
km <sup>2</sup>	square kilometers	0.386	square miles	mi <sup>2</sup>
<b>VOLUME</b>				
ml	milliliters	0.034	fluid ounces	fl oz
l	liters	0.264	gallons	gal
m <sup>3</sup>	cubic meters	35.29	cubic feet	ft <sup>3</sup>
m <sup>3</sup>	cubic meters	1.295	cubic yards	yd <sup>3</sup>
<b>MASS</b>				
g	grams	0.035	ounces	oz
kg	kilograms	2.205	pounds	lb
Tones	tonnes	1.103	US short tons	tons
<b>TEMPERATURE</b>				
°C	Celsius	1.8°C + 32	Fahrenheit	°F
<b>WEIGHT DENSITY</b>				
kN/m <sup>3</sup>	kilonewtons / cubic meter	6.36	Pound force / cubic foot	pcf
<b>FORCE and PRESSURE or STRESS</b>				
N	newtons	0.225	pound force	lbf
kN	kilonewtons	225	pound force	lbf
kPa	kilopascals	0.145	pound force / square inch	psi
kPa	kilopascals	20.88	pound force / square foot	psf
<b>PERMEABILITY (VELOCITY)</b>				
cm/sec	centimeter/second	1.9685	feet/minute	ft/min

[THIS PAGE INTENTIONALLY BLANK]

**SOILS AND FOUNDATIONS  
VOLUME II**

**TABLE OF CONTENTS**

	Page
<b>LIST OF FIGURES</b> .....	vii
<b>LIST OF TABLES</b> .....	xii
<b>LIST OF SYMBOLS</b> .....	xiv
<b>8.0 SHALLOW FOUNDATIONS</b> .....	8-1
8.01 Primary References .....	8-1
8.1 GENERAL APPROACH TO FOUNDATION DESIGN .....	8-1
8.1.1 Foundation Alternatives and Cost Evaluation .....	8-2
8.1.2 Loads and Limit States for Foundation Design .....	8-3
8.2 TYPES OF SHALLOW FOUNDATIONS .....	8-4
8.2.1 Isolated Spread Footings .....	8-4
8.2.2 Continuous or Strip Footings .....	8-6
8.2.3 Spread Footings with Cantilevered Stemwalls .....	8-7
8.2.4 Bridge Abutments .....	8-7
8.2.5 Retaining Structures .....	8-9
8.2.6 Building Foundations .....	8-9
8.2.7 Combined Footings .....	8-9
8.2.8 Mat Foundations .....	8-11
8.3 SPREAD FOOTING DESIGN CONCEPT AND PROCEDURE .....	8-12
8.4 BEARING CAPACITY .....	8-15
8.4.1 Failure Mechanisms .....	8-16
8.4.1.1 General Shear .....	8-16
8.4.1.2 Local Shear .....	8-18
8.4.1.3 Punching Shear .....	8-18
8.4.2 Bearing Capacity Equation Formulation .....	8-18
8.4.2.1 Comparative Effect of Various Terms in Bearing Capacity Formulation .....	8-22
8.4.3 Bearing Capacity Correction Factors .....	8-23
8.4.3.1 Footing Shape (Eccentricity and Effective Dimensions) .....	8-24
8.4.3.2 Location of the Ground Water Table .....	8-27
8.4.3.3 Embedment Depth .....	8-28
8.4.3.4 Inclined Base .....	8-29
8.4.3.5 Inclined Loading .....	8-29
8.4.3.6 Sloping Ground Surface .....	8-30
8.4.3.7 Layered Soils .....	8-30
8.4.4 Additional Considerations Regarding Bearing Capacity Correction Factors .....	8-32

8.4.5	Local or Punching Shear.....	8-33
8.4.6	Bearing Capacity Factors of Safety .....	8-35
	8.4.6.1 Overstress Allowances.....	8-35
8.4.7	Practical Aspects of Bearing Capacity Formulations .....	8-36
	8.4.7.1 Bearing Capacity Computations .....	8-36
	8.4.7.2 Failure Zones .....	8-38
8.4.8	Presumptive Bearing Capacities .....	8-40
	8.4.8.1 Presumptive Bearing Capacity in Soil .....	8-40
	8.4.8.2 Presumptive Bearing Capacity in Rock .....	8-40
8.5	SETTLEMENT OF SPREAD FOOTINGS.....	8-44
8.5.1	Immediate Settlement .....	8-44
	8.5.1.1 Schmertmann’s Modified Method for Calculation of Immediate Settlements.....	8-45
	8.5.1.2 Comments on Schmertmann’s Method.....	8-47
	8.5.1.3 Tabulation of Parameters in Schmertmann’s Method .....	8-52
8.5.2	Obtaining Limiting Applied Stress for a Given Settlement.....	8-54
8.5.3	Consolidation Settlement.....	8-54
8.6	SPREAD FOOTINGS ON COMPACTED EMBANKMENT FILLS.....	8-55
8.6.1	Settlement of Footings on Structural Fills .....	8-57
8.7	FOOTINGS ON INTERMEDIATE GEOMATERIALS (IGMs) AND ROCK.....	8-58
8.8	ALLOWABLE BEARING CAPACITY CHARTS .....	8-60
8.8.1	Comments on the Allowable Bearing Capacity Charts .....	8-62
8.9	EFFECT OF DEFORMATIONS ON BRIDGE STRUCTURES.....	8-64
8.9.1	Criteria for Tolerable Movements of Bridges.....	8-68
	8.9.1.1 Vertical Movements.....	8-68
	8.9.1.2 Horizontal Movements .....	8-69
8.9.2	Loads for Evaluation of Tolerable Movements Using Construction Point Concept.....	8-70
8.10	SPREAD FOOTING LOAD TESTS.....	8-72
8.11	CONSTRUCTION INSPECTION .....	8-73
	8.11.1 Structural Fill Materials.....	8-73
	8.11.2 Monitoring .....	8-75
<b>9.0</b>	<b>DEEP FOUNDATIONS .....</b>	<b>9-1</b>
9.1	TYPES OF DEEP FOUNDATIONS AND PRIMARY REFERENCES.....	9-3
	9.1.1 Selection of Driven Pile or Cast-in-Place (CIP) Pile Based on Subsurface Conditions .....	9-5
	9.1.2 Design and Construction Terminology.....	9-5
9.2	DRIVEN PILE DESIGN-CONSTRUCTION PROCESS.....	9-7
9.3	ALTERNATE DRIVEN PILE TYPE EVALUATION.....	9-18
	9.3.1 Cost Evaluation of Alternate Pile Types.....	9-19
9.4	COMPUTATION OF PILE CAPACITY .....	9-20
	9.4.1 Factors of Safety .....	9-23
9.5	DESIGN OF SINGLE PILES.....	9-29
	9.5.1 Ultimate Geotechnical Capacity of Single Piles in	

	Cohesionless Soils .....	9-29
	9.5.1.1 Nordlund Method.....	9-29
9.5.2	Ultimate Geotechnical Capacity of Single Piles in Cohesive Soils.....	9-47
	9.5.2.1 Total Stress – $\alpha$ -method.....	9-47
	9.5.2.2 Effective Stress – $\beta$ -method.....	9-52
9.5.3	Ultimate Geotechnical Capacity of Single Piles in Layered Soils.....	9-59
9.5.4	Plugging of Open Pile Sections .....	9-60
9.5.5	Time Effects on Pile Capacity .....	9-64
	9.5.5.1 Soil Setup.....	9-64
	9.5.5.2 Relaxation .....	9-65
9.5.6	Additional Design and Construction Considerations.....	9-66
9.5.7	The DRIVEN Computer Program .....	9-67
9.5.8	Ultimate Capacity of Piles on Rock and in Intermediate Geomaterials (IGMs) .....	9-75
9.6	DESIGN OF PILE GROUPS.....	9-76
9.6.1	Axial Compression Capacity of Pile Groups .....	9-78
	9.6.1.1 Cohesionless Soils .....	9-78
	9.6.1.2 Cohesive Soils.....	9-79
	9.6.1.3 Block Failure of Pile Groups .....	9-81
9.6.2	Settlement of Pile Groups .....	9-82
	9.6.2.1 Elastic Compression of Piles .....	9-82
	9.6.2.2 Settlement of Pile Groups in Cohesionless Soils.....	9-83
	9.6.2.3 Settlement of Pile Groups in Cohesive Soils .....	9-84
9.7	DESIGN OF PILES FOR LATERAL LOAD .....	9-84
9.8	DOWNDRAG OR NEGATIVE SHAFT RESISTANCE .....	9-87
9.9	CONSTRUCTION OF PILE FOUNDATIONS.....	9-90
9.9.1	Selection of Design Safety Factor Based on Construction Control.....	9-90
9.9.2	Pile Driveability.....	9-90
	9.9.2.1 Factors Affecting Drivability .....	9-91
	9.9.2.2 Driveability Versus Pile Type.....	9-93
9.9.3	Pile Driving Equipment and Operation .....	9-94
9.9.4	Dynamic Pile Driving Formulae.....	9-97
9.9.5	Dynamic Analysis of Pile Driving.....	9-100
9.9.6	Wave Equation Methodology .....	9-103
	9.9.6.1 Input to Wave Equation Analysis .....	9-105
	9.9.6.2 Output Values from Wave Equation Analysis.....	9-106
	9.9.6.3 Pile Wave Equation Analysis Interpretation.....	9-106
9.9.7	Driving Stresses .....	9-108
9.9.8	Guidelines for Assessing Pile Drivability.....	9-109
9.9.9	Pile Construction Monitoring Considerations .....	9-112
9.9.10	Dynamic Pile Monitoring .....	9-114
	9.9.10.1 Applications .....	9-115
	9.9.10.2 Interpretation of Results and Correlation with Static Pile Load Tests .....	9-117
9.10	CAST-IN-PLACE (CIP) PILES .....	9-119
9.11	DRILLED SHAFTS.....	9-123

9.11.1	Characteristics of Drilled Shafts .....	9-124
9.11.2	Advantages of Drilled Shafts .....	9-125
9.11.1.1	Special Considerations for Drilled Shafts .....	9-126
9.11.3	Subsurface Conditions and Their Effect on Drilled Shafts.....	9-126
9.12	ESTIMATING AXIAL CAPACITY OF DRILLED SHAFTS.....	9-127
9.12.1	Side Resistance in Cohesive Soil.....	9-129
9.12.1.1	Mobilization of Side Resistance in Cohesive Soil .....	9-130
9.12.2	Tip Resistance in Cohesive Soil .....	9-131
9.12.2.1	Mobilization of Tip Resistance in Cohesive Soil.....	9-131
9.12.3	Side Resistance in Cohesionless Soil.....	9-132
9.12.3.1	Mobilization of Side Resistance in Cohesionless Soil .....	9-133
9.12.4	Tip Resistance in Cohesionless Soil .....	9-133
9.12.4.1	Mobilization of Tip Resistance in Cohesionless Soil.....	9-134
9.12.5	Determination of Axial Shaft Capacity in Layered Soils or Soils with Varying Strength with Depth.....	9-136
9.12.6	Group Action, Group Settlement, Downdrag and Lateral Loads ..	9-136
9.12.7	Estimating Axial Capacity of Shafts in Rocks.....	9-140
9.12.7.1	Side Resistance in Rocks.....	9-140
9.12.7.2	Tip Resistance in Rocks .....	9-141
9.12.8	Estimating Axial Capacity of Shafts in Intermediate GeoMaterials (IGM's) .....	9-142
9.13	CONSTRUCTION METHODS FOR DRILLED SHAFTS.....	9-142
9.14	QUALITY ASSURANCE AND INTEGRITY TESTING OF DRILLED SHAFTS.....	9-146
9.14.1	The Standard Crosshole Sonic Logging (CSL) Test .....	9-146
9.14.2	The Gamma Density Logging (GDL) Test.....	9-149
9.14.3	Selecting the Type of Integrity Test for Quality Assurance .....	9-152
9.15	STATIC LOAD TESTING FOR DEEP FOUNDATIONS.....	9-153
9.15.1	Reasons for Load Testing .....	9-153
9.15.2	Advantages of Static Load Testing.....	9-153
9.15.3	When to Load Test.....	9-154
9.15.4	Effective Use of Load Tests.....	9-156
9.15.4.1	Design Stage .....	9-156
9.15.4.2	Construction Stage.....	9-156
9.15.5	Prerequisites for Load Testing.....	9-157
9.15.6	Developing a Static Load Test Program.....	9-158
9.15.7	Compression Load Tests.....	9-158
9.15.7.1	Compression Test Equipment.....	9-160
9.15.7.2	Recommended Compression Test Loading Method.....	9-165
9.15.7.3	Presentation and Interpretation of Compression Test Results.....	9-165
9.15.7.4	Plotting the Failure Criteria .....	9-166
9.15.7.5	Determination of the Ultimate (Failure) Load.....	9-167
9.15.7.6	Determination of the Allowable Geotechnical Load .....	9-168
9.15.7.7	Load Transfer Evaluations.....	9-168
9.15.8	Other Compression Load Tests.....	9-171

	9.15.8.1 The Osterberg Cell Method .....	9-171
	9.15.8.2 Statnamic Test Method .....	9-176
	9.15.9 Limitations of Compression Load Tests .....	9-179
	9.15.10 Axial Tension and Lateral Load Tests .....	9-179
<b>10.0</b>	<b>EARTH RETAINING STRUCTURES .....</b>	<b>10-1</b>
10.01	Primary References .....	10-4
10.1	CLASSIFICATION OF EARTH RETAINING STRUCTURES .....	10-4
10.1.1	Classification by Load Support Mechanism .....	10-4
10.1.2	Classification by Construction Method .....	10-6
10.1.3	Classification by System Rigidity .....	10-7
10.1.4	Temporary and Permanent Wall Applications .....	10-7
10.1.5	Wall Selection Considerations .....	10-8
10.2	LATERAL EARTH PRESSURES .....	10-8
10.2.1	At-Rest Lateral Earth Pressure .....	10-10
10.2.2	Active and Passive Lateral Earth Pressures .....	10-12
10.2.3	Effect of Cohesion on Lateral Earth Pressures .....	10-16
10.2.4	Effect of Wall Friction and Wall Adhesion on Lateral Earth Pressures .....	10-16
10.2.5	Theoretical Lateral Earth Pressures in Stratified Soils .....	10-23
10.2.6	Semi Empirical Lateral Earth Pressure Diagrams .....	10-24
10.2.7	Lateral Earth Pressures in Cohesive Backfills .....	10-24
10.3	LATERAL PRESSURES DUE TO WATER .....	10-27
10.4	LATERAL PRESSURE FROM SURCHARGE LOADS .....	10-29
10.4.1	General .....	10-29
10.4.2	Uniform Surcharge Loads .....	10-31
10.4.3	Point, Line, and Strip Loads .....	10-31
10.5	WALL DESIGN .....	10-35
10.5.1	Steps 1, 2, and 3 – Established Project Requirements, Subsurface Conditions, Design Parameters .....	10-36
10.5.2	Step 4 – Select Base Dimension Based on Wall Height .....	10-37
10.5.3	Step 5 – Select Lateral Earth Pressure Distribution .....	10-37
10.5.4	Step 6 – Evaluate Bearing Capacity .....	10-41
10.5.4.1	Shallow Foundations .....	10-41
10.5.4.2	Deep Foundations .....	10-42
10.5.5	Step 7 – Evaluate Overturning and Sliding .....	10-43
10.5.6	Step 8 – Evaluate Global Stability .....	10-44
10.5.7	Step 9 – Evaluate Settlement and Tilt .....	10-45
10.5.8	Step 10 – Design Wall Drainage Systems .....	10-45
10.5.8.1	Subsurface Drainage .....	10-46
10.5.8.2	Drainage System Components .....	10-48
10.5.8.3	Surface Water Runoff .....	10-50
10.6	EXTERNAL STABILITY ANALYSIS OF A CIP CANTILEVER WALL .....	10-52
10.7	CONSTRUCTION INSPECTION .....	10-56

<b>11.0</b>	<b>GEOTECHNICAL REPORTS .....</b>	<b>11-1</b>
11.01	Primary References.....	11-1
11.1	TYPES OF REPORTS.....	11-1
11.1.1	Geotechnical Investigation Reports.....	11-2
11.1.2	Geotechnical Design Reports.....	11-3
11.1.3	GeoEnvironmental Reports.....	11-6
11.2	DATA PRESENTATION.....	11-7
11.2.1	Boring Logs .....	11-7
11.2.2	Boring Location Plans .....	11-8
11.2.3	Subsurface Profiles .....	11-9
11.3	TYPICAL SPECIAL CONTRACT NOTES .....	11-11
11.4	SUBSURFACE INFORMATION MADE AVAILABLE TO BIDDERS	11-14
11.5	LIMITATIONS (DISCLAIMERS) .....	11-15
<b>12.0</b>	<b>REFERENCES.....</b>	<b>12-1</b>

**APPENDICES**

**APPENDIX A: APPLE FREEWAY PROJECT**

**APPENDIX B: MOHR’S CIRCLE AND ITS APPLICATIONS IN GEOTECHNICAL ENGINEERING**

**APPENDIX C: LOAD AND RESISTANCE FACTOR DESIGN (LRFD)**

**APPENDIX D: USE OF THE COMPUTER PROGRAM ReSSA**

**APPENDIX E: USE OF THE COMPUTER PROGRAM FoSSA**

## LIST OF FIGURES

<u>Figure</u>	<u>Caption</u>	<u>Page</u>
8-1	Geometry of a typical shallow foundation (FHWA, 2002c; AASHTO, 2002) ...	8-5
8-2	Isolated spread footing (FHWA, 2002c).....	8-5
8-3	Continuous strip footing (FHWA, 2002c) .....	8-6
8-4	Spread footing with cantilever stemwall at bridge abutment .....	8-8
8-5	Abutment/wingwall footing, I-10, Arizona .....	8-8
8-6	Footing for a semi-gravity cantilever retaining wall (FHWA, 2002c) .....	8-9
8-7	Combined footing (FHWA, 2002c) .....	8-10
8-8	Spill-through abutment on combination strip footing (FHWA, 2002c) .....	8-10
8-9	Typical mat foundation (FHWA, 2002c).....	8-11
8-10	Shear failure versus settlement considerations in evaluation of allowable bearing capacity .....	8-13
8-11	Design process flow chart – bridge shallow foundation (modified after FHWA, 2002c).....	8-14
8-12	Bearing capacity failure of silo foundation (Tschebotarioff, 1951) .....	8-15
8-13	Boundaries of zone of plastic equilibrium after failure of soil beneath continuous footing (FHWA, 2002c) .....	8-16
8-14	Modes of bearing capacity failure (after Vesic, 1975) (a) General shear (b) Local shear (c) Punching shear .....	8-17
8-15	Bearing capacity factors versus friction angle.....	8-20
8-16	Notations for footings subjected to eccentric, inclined loads (after Kulhawy, 1983) .....	8-25
8-17	Eccentrically loaded footing with (a) Linearly varying pressure distribution (structural design), (b) Equivalent uniform pressure distribution (sizing the footing).....	8-26
8-18	Modified bearing capacity factors for continuous footing on sloping ground, (after Meyerhof, 1957, from AASHTO 2004 with 2006 Interims) .....	8-31
8-19	Modes of failure of model footings in sand (after Vesic, 1975, AASHTO 2004 with 2006 Interims).....	8-33
8-20	Approximate variation of depth ( $d_o$ ) and lateral extent ( $f$ ) of influence of footing as a function of internal friction angle of foundation soil .....	8-39
8-21	(a) Simplified vertical strain influence factor distributions, (b) Explanation of pressure terms in equation for $I_{zp}$ (after Schmertmann, <i>et al.</i> , 1978) .....	8-46
8-22	Example allowable bearing capacity chart .....	8-60
8-23	Components of settlement and angular distortion in bridges (after Duncan and Tan, 1991).....	8-65
9-1	Situations in which deep foundations may be needed (Vesic, 1977; FHWA, 2006a).....	9-2
9-2	Deep foundations classification system (after FHWA, 2006a) .....	9-4
9-3	Driven pile design and construction process (after FHWA, 2006a).....	9-8
9-4	Typical load transfer profiles (FHWA, 2006a).....	9-24
9-5	Soil profile for factor of safety discussion (FHWA, 2006a).....	9-26

9-6	Nordlund's general equation for ultimate pile capacity (after Nordlund, 1979).....	9-31
9-7	Relationship of $\delta/\phi$ and pile soil displacement, $V$ , for various types of piles (after Nordlund, 1963) .....	9-36
9-8	Design curves for evaluating $K_\delta$ for piles when $\phi = 25^\circ$ (after Nordlund, 1963) .....	9-37
9-9	Design curves for evaluating $K_\delta$ for piles when $\phi = 30^\circ$ (after Nordlund, 1963) .....	9-38
9-10	Design curves for evaluating $K_\delta$ for piles when $\phi = 35^\circ$ (after Nordlund, 1963) .....	9-39
9-11	Design curves for evaluating $K_\delta$ for piles when $\phi = 40^\circ$ (after Nordlund, 1963) .....	9-40
9-12	Correction factor, $C_F$ for $K_\delta$ when $\delta \neq \phi$ (after Nordlund, 1963).....	9-41
9-13	Chart for estimating $\alpha_t$ coefficient and bearing capacity factor $N'_q$ (FHWA, 2006a) .....	9-44
9-14	Relationship between maximum unit pile toe resistance and friction angle for cohesionless soils (after Meyerhof, 1976).....	9-45
9-15	Adhesion values for driven piles in mixed soil profiles, (a) Case 1: piles driven through overlying sands or sandy gravels, and (b) Case 2: piles driven through overlying weak clay (Tomlinson, 1980).....	9-49
9-16	Adhesion factors for driven piles in stiff clays without different overlying Strata (Case 3) (Tomlinson, 1980).....	9-50
9-17	Chart for estimating $\beta$ coefficient as a function of soil type $\phi'$ (after Fellenius, 1991).....	9-57
9-18	Chart for estimating $N_t$ coefficients as a function of soil type $\phi'$ angle (after Fellenius, 1991).....	9-58
9-19	Plugging of open end pipe piles (after Paikowsky and Whitmann, 1990) .....	9-61
9-20	Plugging of H-piles (FHWA, 2006a).....	9-61
9-21	DRIVEN project definition screen .....	9-69
9-22	DRIVEN soil profile screen – cohesive soil.....	9-69
9-23	DRIVEN cohesive soil layer properties screen .....	9-70
9-24	DRIVEN soil profile screen – cohesionless soil.....	9-70
9-25	DRIVEN cohesionless soil layer properties screen .....	9-71
9-26	DRIVEN soil profile screen – Pile type selection drop down menu and pile detail screen .....	9-71
9-27	DRIVEN toolbar output and analysis options .....	9-72
9-28	DRIVEN output tabular screen.....	9-73
9-29	DRIVEN output graphical screen for end of driving.....	9-74
9-30	DRIVEN output graphical screen for restrrike .....	9-74
9-31	Stress zone from single pile and pile group (after Tomlinson, 1994).....	9-77
9-32	Overlap of stress zones for friction pile group (after Bowles, 1996) .....	9-77
9-33	Measured dissipation of excess pore water pressure in soil surrounding full scale pile groups (after O'Neill, 1983) .....	9-80
9-34	Three dimensional pile group configuration (after Tomlinson, 1994) .....	9-81
9-35	Equivalent footing concept (after Duncan and Buchignani, 1976) .....	9-85

9-36	Stress distribution below equivalent footing for pile group (FHWA, 2006a) ...	9-86
9-37a	Common downdrag situation due to fill weight (FHWA, 2006a) .....	9-88
9-37b	Common downdrag situation due to ground water lowering (FHWA, 2006a) .	9-88
9-38	Typical components of a pile driving system .....	9-95
9-39	Typical components of a helmet .....	9-96
9-40	Hammer-pile-soil system .....	9-100
9-41	Typical Wave Equation models (FHWA, 2006a).....	9-104
9-42	Summary of stroke, compressive stress, tensile stress, and driving capacity vs. blow count (blows/ft) for air-steam hammer.....	9-107
9-43	Graph of diesel hammer stroke versus blow count for a constant pile capacity .....	9-108
9-44	Suggested trial hammer energy for Wave Equation analysis .....	9-109
9-45	Pile and driving equipment data form.....	9-113
9-46	Typical force and velocity traces generated during dynamic measurements ..	9-116
9-47	Cast-in-Place (CIP) pile design and construction process (modified after FHWA, 2006a).....	9-120
9-48	Typical drilled shaft and terminology (after FHWA, 1999).....	9-124
9-49	Portions of drilled shafts not considered in computing ultimate side resistance (FHWA, 1999) .....	9-129
9-50	Load-transfer in side resistance versus settlement for drilled shafts in cohesive soils (FHWA, 1999).....	9-130
9-51	Load-transfer in tip resistance versus settlement for drilled shafts in cohesive soils (FHWA, 1999).....	9-132
9-52	Load-transfer in side resistance versus settlement for drilled shafts in cohesionless soils (FHWA, 1999) .....	9-134
9-53	Load-transfer in tip resistance versus settlement for drilled shafts in cohesionless soils (FHWA, 1999) .....	9-136
9-54	Steps in construction of drilled shafts by the dry method (a) drill, (b) clean, (c) position concrete cage, (d) place concrete .....	9-143
9-55	Steps in construction of drilled shafts by the wet method (a) start drilling and introduce slurry (bentonite or polymer) in the excavation PRIOR to the encountering the known piezometric level, (b) continue drilling with slurry in the excavation, (c) clean the excavation and slurry, (d) position reinforcement cage, and (e) place concrete by tremie .....	9-144
9-56	Steps in construction of drilled shafts by the casing method (a) start drilling and introduce casing in the excavation PRIOR to encountering the known piezometric level and/or caving soil, (b) advance the casing through the soils prone to caving, (c) clean the excavation, (d) position reinforcement cage, and (e) place concrete and remove the casing if it is temporary .....	9-144
9-57	Photographs of exhumed shafts (a) shaft where excavation was not adequately clean, (b) shaft where excavation was properly cleaned (FHWA, 2002d) .....	9-145
9-58	Schematic of CSL test (Samtani, <i>et al.</i> , 2005).....	9-147
9-59	Single plot display format for the CSL data for shaft with five tubes (Samtani, <i>et al.</i> , 2005).....	9-148

9-60	Schematic of GDL Test (Samtani, <i>et al.</i> , 2005).....	9-150
9-61	Single plot display format for the GDL data for shaft with four tubes (Samtani, <i>et al.</i> , 2005).....	9-151
9-62	Basic mechanism of a compression pile load test.....	9-159
9-63	Typical arrangement for applying load in an axial compressive test (FHWA, 1992c) .....	9-161
9-64	Load application and monitoring components (FHWA, 2006a) .....	9-162
9-65	Load test movement monitoring components (FHWA, 2006a).....	9-163
9-66	Typical compression load test arrangement with reaction piles (FHWA, 2006a) .....	9-163
9-67	Typical compression load test arrangement using a weighted platform (FHWA, 2006a) .....	9-164
9-68	Presentation of typical static pile load-movement results (a) Davisson’s method, (b) Double-tangent method.....	9-166
9-69	Example of residual load effects on load transfer evaluation (FHWA, 2006a) .....	9-170
9-70	Sister bar vibrating wire gages for concrete embedment (FHWA, 2006a) .....	9-170
9-71	Are-weldable vibrating wire strain gage attached to H-pile (Note: protective channel cover shown on left) (FHWA, 2006a).....	9-171
9-72	Comparison of reaction mechanism between Osterberg Cell and Static test ..	9-172
9-73	Some details of the O-cell test (after <a href="http://www.bridgebuildermagazine.com">www.bridgebuildermagazine.com</a> ) .....	9-173
9-74	Photograph of an O-cell .....	9-173
9-75	O-cell assembly attached to a reinforcing cage with other instrumentation....	9-174
9-76	Schematic of Statnamic test.....	9-177
9-77	Photograph of Statnamic test arrangement, showing masses being accelerated inside gravel-filled sheath.....	9-177
10-1	Schematic of a retaining wall and common terminology .....	10-1
10-2	Variety of retaining walls (after O’Rourke and Jones, 1990) .....	10-3
10-3	Classification of earth retaining systems (after O’Rourke and Jones, 1990)....	10-5
10-4	Effect of wall movement on wall pressures (after Canadian Foundation Engineering Manual, 1992) .....	10-9
10-5	Coulomb coefficients $K_a$ and $K_p$ for sloping wall with wall friction and sloping cohesionless backfill (after NAVFAC, 1986b).....	10-13
10-6	(a) Wall Pressures for a cohesionless soil, and (b) Wall pressures for soil with a cohesion intercept – with groundwater in both cases (after Padfield and Mair, 1984) .....	10-15
10-7	Wall friction on soil wedges (after Padfield and Mair, 1984) .....	10-16
10-8	Comparison of plane and log-spiral failure surfaces (a) Active case and (b) Passive case (after Sokolovski, 1954).....	10-20
10-9	Passive coefficients for sloping wall with wall friction and horizontal backfill (Caquot and Kerisel, 1948, NAVFAC, 1986b) .....	10-21
10-10	Passive coefficients for vertical wall with wall friction and sloping backfill (Caquot and Kerisel, 1948, NAVFAC, 1986b).....	10-22
10-11	Pressure distribution for stratified soils .....	10-23
10-12	Computation of lateral pressures for static groundwater case .....	10-27

10-13	(a) Retaining wall with uniform surcharge load and (b) Retaining wall with line loads (railway tracks) and point loads (catenary support structure).....	10-30
10-14	Lateral pressure due to surcharge loadings (after USS Steel, 1975) .....	10-32
10-15	Potential failure mechanisms for rigid gravity and semi-gravity walls .....	10-35
10-16	Typical dimensions (a) Cantilever wall, (b) Counterfort wall (Teng, 1962)...	10-38
10-17	Design criteria for cast-in-place (CIP) concrete retaining walls (after NAVFAC, 1986b).....	10-39
10-18	CIP abutment with integral wingwalls.....	10-40
10-19	Typical movement of pile-supported cast-in-place (CIP) wall with soft foundation .....	10-42
10-20	Resistance against sliding from keyed foundation .....	10-43
10-21	Typical modes of global stability (after Bowles, 1996).....	10-44
10-22	Potential sources of subsurface water .....	10-46
10-23	Typical retaining wall drainage alternatives.....	10-47
10-24	Drains behind backfill in cantilever wall in a cut situation .....	10-48
11-1	Example table of contents for a geotechnical investigation report.....	11-4
11-2	Example table of contents for a geotechnical design report .....	11-5
11-3	Example boring location plan for retaining walls RW-11 and RW-12 retaining an on-ramp to a freeway .....	11-9
11-4	Subsurface profile along the baseline between retaining walls RW-11 and RW-12 shown in Figure 11-3 .....	11-10

## LIST OF TABLES

<u>No.</u>	<u>Caption</u>	<u>Page</u>
8-1	Estimation of friction angle of cohesionless soils from Standard Penetration Tests (after AASHTO, 2004 with 2006 Interims, FHWA, 2002c).....	8-19
8-2	Bearing Capacity Factors (AASHTO, 2004 with 2006 Interims) .....	8-20
8-3	Variation in bearing capacity with changes in physical properties or dimensions .....	8-23
8-4	Shape correction factors (AASHTO, 2004 with 2006 Interims) .....	8-27
8-5	Correction factor for location of ground water table (AASHTO 2004 with 2006 Interims) .....	8-27
8-6	Depth correction factors (Hansen and Inan, 1970; AASHTO, 2004 with 2006 Interims).....	8-28
8-7	Inclined base correction factors (Hansen and Inan, 1970; AASHTO, 2004 with 2006 Interims).....	8-29
8-8	Allowable bearing pressures for fresh rock of various types (Goodman, 1989) .....	8-42
8-9	Presumptive values of allowable bearing pressures for spread foundations on rock (modified after NAVFAC, 1986a, AASHTO 2004 with 2006 Interims).....	8-43
8-10	Suggested values of allowable bearing capacity (Peck, <i>et al.</i> , 1974) .....	8-43
8-11	Values of parameters used in settlement analysis by Schmertmann's method..	8-53
8-12	Typical specification of compacted structural fill used by WSDOT (FHWA, 2002c) .....	8-57
8-13	Shape and rigidity factors, $C_d$ , for calculating settlements of points on loaded areas at the surface of a semi-infinite elastic half space (after Winterkorn and Fang, 1975).....	8-59
8-14	Tolerable movement criteria for bridges (FHWA, 1985; AASHTO, 2002, 2004).....	8-68
8-15	Example of settlements evaluated at various critical construction points .....	8-71
8-16	Inspector responsibilities for construction of shallow foundations .....	8-74
9-1	Pile type selection based on subsurface and hydraulic conditions .....	9-6
9-2	Typical piles and their range of loads and lengths.....	9-18
9-3	Pile type selection pile shape effects .....	9-19
9-4	Cost savings recommendations for pile foundations (FHWA, 2006a).....	9-21
9-5	Recommended factor of safety based on construction control method .....	9-25
9-6a	Design table for evaluating $K_s$ for piles when $\omega = 0^\circ$ and $V = 0.10$ to $1.00 \text{ ft}^3/\text{ft}$ (FHWA, 2006a) .....	9-42
9-6b	Design table for evaluating $K_s$ for piles when $\omega = 0^\circ$ and $V = 1.0$ to $10.0 \text{ ft}^3/\text{ft}$ (FHWA, 2006a) .....	9-43
9-7	Approximate range of $\beta$ and $N_t$ coefficients (Fellenius, 1991).....	9-53
9-8	Soil setup factors (after FHWA, 1996).....	9-65
9-9	Responsibilities of design and construction engineers .....	9-92
9-10	Summary of example results from wave equation analysis.....	9-106

9-11	Maximum allowable stresses in pile for top driven piles (after AASHTO, 2002, FHWA, 2006a).....	9-110
9-12	Osterberg cells for drilled shafts.....	9-174
9-13	Osterberg cells for driven piles.....	9-174
10-1	Wall friction and adhesion for dissimilar materials (after NAVFAC, 1986b)	10-18
10-2	Design steps for gravity and semi-gravity walls.....	10-36
10-3	Suggested gradation for backfill for cantilever semi-gravity and gravity retaining walls.....	10-37
10-4	Inspector responsibilities for a typical CIP gravity and semi-gravity wall project .....	10-56

## LIST OF SYMBOLS

### Chapter 8

A	Angular distortion
A'	Effective footing area
AASHTO	American Association of State Highway and Transportation Officials
ASD	Allowable stress design
B	Width
$B'_f$	Effective footing width
$b_c, b_\gamma, b_q$	Base inclination correction factors
$B_f$	Footing width
$B_f^*$	Modified footing width for bearing capacity analysis of footings on sands
c	Cohesion of soil
$c^*$	Reduced effective cohesion for punching shear
$C_1$	Correction factor for embedment depth
$C_2$	Correction factor for time-dependent settlement increase
$C_c$	Compression indices
$C_d$	Shape and rigidity factors
$C_{w\gamma}, C_{wq}$	Groundwater correction factors
$D_f$	Depth of embedment
$D_I$	Maximum depth of strain influence
$D_{IP}$	Depth to maximum strain influence factor
DL	Dead load
$d_o$	Depth of influence of footing
DOSI	Depth of Significant Influence
$d_q$	Embedment depth correction factor
$D_r$	Relative density of sand
$D_w$	Depth of water table
E	Elastic modulus of soil
$e_B$	Eccentricity in direction of footing width
$e_L$	Eccentricity in direction of footing length
$E_m$	Young's modulus of rock mass
$e_o$	Initial void ratio
f	Lateral extent of influence of footing
FD	Foundation design specialist
FHWA	Federal Highway Administration
FS	Factor of safety
ft	Foot
GT	Geotechnical specialist
$H_c$	Thickness of soil layer considered
IGM	Intermediate geomaterial
$I_z$	Strain influence factor
$I_{zB}$	Strain influence factor at footing elevation
$I_{zP}$	Maximum strain influence factor
kPa	Kilopascal
L	Length

$L'_f$	Effective footing length
$L_f$	Footing length
LL	Live load
LRFD	Load resistance factor design
MPa	Megapascal
MSE	Mechanically stabilized earth
n	Number of soil layers
N	SPT blow count value
$N_{160}$	SPT blow count corrected for depth and hammer efficiency
$N_c, N_q, N_\gamma$	Bearing capacity factors
$N_{cq}, N_{\gamma q}$	Bearing capacity factors modified for sloping ground surface
$N_s$	Slope stability factor
OCR	Overconsolidation ratio
P	Applied footing load
$p_o$	Effective overburden pressure
$p_{op}$	effective stress at depth of peak strain influence factor
psf	Pounds per square foot
q	Uniform surcharge pressure at the base of the footing
$q_{all}$	Allowable bearing capacity
$q_{eq}$	Equivalent uniform bearing pressure
$q_{max}$	Maximum bearing pressure under the footing
$q_{min}$	Minimum bearing pressure under the footing
$q_{ult\ gross}$	Gross ultimate bearing capacity
$q_{ult\ net}$	Net ultimate bearing capacity
$q_{ult}$	Ultimate bearing capacity
RQD	Rock quality designation
S	Settlement
S, 2S, 3S	Settlement contours
$S_c, S_q, S_\gamma$	Shape correction factors
$S_i$	Settlement of i-th soil layer
SL	Distance between adjacent foundations (span length)
SLS	Serviceability limit state
$S_t$	Sensitivity of clay
ST	Structural specialist
t	time
tsf	Tons per square foot
ULS	Ultimate limit state
X	Modification factor for determination of elastic modulus
$z_i$	Depth to soil layer i
$\alpha$	Footing inclination from horizontal
$\gamma$	Unit weight of soil
$\gamma'$	Effective unit weight of soil
$\gamma_a$	Unit weight of soil above the footing
$\gamma_b$	Submerged unit weight of soil
$\delta$	Differential settlement
$\delta_v$	Vertical settlement at surface

$\Delta H$	Consolidation settlement
$\Delta H_i$	Settlement factor for soil layer i
$\Delta p$	Net load intensity at foundation depth
$\nu$	Poisson's ratio
$\phi$	Angle of internal friction
$\phi^*$	Reduced effective soil friction angle for punching shear
$\phi'$	Effective angle of internal friction

## Chapter 9

A	Cross-sectional area of the pile
AASHTO	American Association of State Highway and Transportation Officials
$A_p$	Cross-sectional area of an unplugged pile
API	American Petroleum Institute
$a_s$	Acceleration of the drilled corresponding to $F_{so}$
$A_s$	Shaft surface area
ASD	Allowable stress design
$A_{si}$	Pile interior surface area
ASTM	American Society for Testing and Materials
$A_t$	Pile toe area
$A_t$	Tip area of rock socket
b	Pile diameter or width
B	Width of the pile group
BPF	Blows per foot
C	Wave propagation velocity of pile material
$c_a$	Pile adhesion
$C_d$	Pile perimeter at depth d
$C_F$	Correction factor for $K_s$ when $\delta \neq \phi$
CIDH	Cast-in-drilled hole
CIP	Cast-in-place
COR	Coefficient of restitution
cps	counts per second
CPT	Cone penetration test
CSL	Cross-hole sonic logging
CSLT	Cross-hole sonic logging tomography
$c_u$	Average undrained shear strength
$c_{u1}$	Weighted average of the undrained shear strength over the depth of pile embedment for the cohesive soils along the pile group perimeter
$c_{u2}$	Average undrained shear strength of the cohesive soils at the base of the pile group to a depth of 2B below pile toe level
D	Pile embedment length
d	Center to center distance
d	Depth
D	Diameter of the shaft
D	Distance from ground surface to bottom of clay layer or pile toe
$D_R$	Diameter of rock socket
E	Modulus of elasticity of pile material

$E_i$	Intact rock modulus
$E_m$	Rock mass modulus
$E_n$	Driving energy
EN	Engineering News
$E_r$	Manufacturer's rated hammer energy
$f_c$	28-day compressive strength of concrete
FHWA	Federal Highway Administration
$f_{pe}$	Pile prestress
FS	Factor of safety
$f_s$	Unit shaft resistance
$f_{si}$	Interior unit shaft resistance
$f_{si}$	Ultimate unit load transfer in side resistance
$f_{so}$	Exterior unit shaft resistance
$F_{so}$	Force measured by the load cell at the point at which the slope of the rebound curve is zero
$f_{so}$	Ultimate unit shaft resistance
$f_y$	Yield stress of steel
$g$	Acceleration of gravity
GDL	Gamma-gamma density logging
H	Distance of ram fall
$I_f$	Influence factor for group embedment
IGM	Intermediate geomaterial
IR	Impulse response
$k$	Constant which varies from 0.1 to 1 based on hammer type
$K_s$	Earth pressure coefficient
$K_\delta$	Coefficient of lateral earth pressure at depth $d$
$L$	Effective length of the pile
$L_R$	Length of rock socket
LRFD	Load and resistance factor design
LVDT	Linear variable displacement transducer
$M$	Mean
$n$	Number of piles in group
$N$	Number of layers used in the analysis
$N$	SPT blows per foot
$N'$	SPT value corrected for overburden pressure
$N'_q$	Bearing capacity factor
$\bar{N}'$	Average corrected SPT $N_{160}$ value within depth $B$ below pile toe
$\bar{N}1$	Average corrected SPT $N_{160}$ for each soil layer
$N1$	Overburden corrected blowcount
$N_{160}$	Overburden-normalized energy-corrected blowcount
$N_{60}$	Energy-corrected SPT-N value adjusted to 60% efficiency
$N_b$	Number of hammer blows per 1 inch final penetration
$N_c$	Bearing capacity factor
NCHRP	National Cooperative of Highway Research Program
NDT	Non-destructive test
NML	Neutron moisture logging

$N_t$	Toe bearing capacity coefficient
P	Safe pile load
$p_a$	Atmospheric pressure (2.12ksf or 101kPa)
$p_d$	Average effective overburden pressure at the midpoint of each soil layer
$p_d$	Effective overburden pressure at the center of depth increment $\Delta d$
PDA	Pile driving analyzer
$p_f$	Design foundation pressure
$p_o$	Effective overburden pressure
$p_o$	Effective overburden stress at depth $z_i$
PSL	Perimeter sonic logging
$p_t$	Effective overburden pressure at the pile toe
PVC	Polyvinyl chloride
Q	Test load
$Q_a$	Allowable geotechnical soil resistance
$Q_a$	Design load
QA	Quality assurance
$Q_{avg}$	Average load in the pile
$Q_h$	Applied Pile Head Load
$Q_s$	Ultimate skin capacity
$Q_{sr}$	Ultimate side resistance in rock
$q_{SR}$	Unit skin resistance of rock
$Q_t$	Ultimate tip (base or end) capacity
$q_L$	Limiting unit toe resistance
$q_t$	Unit toe resistance or unit end bearing
$Q_{tr}$	Ultimate tip resistance in rock
$q_{tr}$	Unit tip resistance of rock
$Q_u$	Ultimate geotechnical pile capacity or ultimate axial load or ultimate pile capacity
$q_u$	Uniaxial compressive strength of rock
$Q_u$	Ultimate capacity of each individual pile in the pile group
$Q_{ug}$	Ultimate capacity of the pile group
$Q_{ult}$	Ultimate axial capacity
R	Total soil resistance against the pile
$R_1, R_2$	Deflection readings at measuring points
RQD	Rock quality designation
$R_s$	Total skin resistance
$R_s$	Ultimate shaft resistance
$R_{s1}, R_{s2}, R_{s3}$	Resistance in different soil layers
$R_t$	Total toe resistance
$R_t$	Ultimate toe resistance
$R_t(\max)$	Maximum ultimate toe resistance
$R_t$	Estimated toe resistance
$R_t$	Pile toe resistance
$R_T$	Total static resistance of the drilled shaft
$R_u$	Ultimate pile capacity
$R_{ult}$	Delivered hammer energy for an assigned driving soil resistance

s	Estimated total settlement
S	Pile penetration per blow
SD	Standard deviation
SE	Sonic echo
$s_f$	Settlement at failure
SPT	Standard penetration test
SRD	Soil resistance to driving
$s_{ui}$	Undrained shear strength in a layer $\Delta z_i$
$s_{ut}$	Undrained shear strength of the soil at the tip of the shaft
$s_u$	Undrained shear strength
TL	Temperature logging
TTI	Texas Transportation Institute
$u_k$	Hydrostatic pore water pressure
US	Ultra-seismic
$u_s$	Excess pore water pressure
V	Computed velocity
V	Volume per foot for pile segment
$V_C$	Theoretical compression wave velocity in concrete
VR	Velocity reductions
W	Weight of pile
W	Weight of ram
W	Weight of shaft
WEA	Wave equation analysis
$w_p$	Weight of the plug
$W_s$	Total weight of the drilled shaft
WSDOT	Washington State Department of Transportation
z	Depth of the penetration
Z	Length of the pile group
$z_i$	Depth to the center of the $i^{\text{th}}$ layer
$\alpha_i$	Adhesion factor in a layer $\Delta z_i$
$\alpha_t$	Dimensionless factor dependent on pile depth-width relationship
$\delta$	Interface friction angle between pile and soil
$\eta_g$	Pile group efficiency
$\Psi$	Ratio of undrained shear strength of soil to effective overburden pressure
$\Delta$	Elastic deformation
$\Delta d$	Length of pile segment
$\Delta L$	Elastic shortening of the pile
$\Delta L$	Length of pile between two measured points under no load condition
$\Delta z$	Thickness of layer i
$\alpha$	Adhesion factor
$\alpha_E$	Reduction factor to account for jointing in rock
$\beta$	Bjerrum-Burland beta coefficient
$\phi'$	Effective soil friction angle
$\phi$	Soil friction angle
$\gamma'_i$	Effective unit weight of the $i^{\text{th}}$ layer

$\sigma_a$	AASHTO allowable working stress
$\omega$	Angle of pile taper measured from the vertical

## Chapter 10

AASHTO	American Association of State Highway and Transportation Officials
ASTM	American Society for Testing and Materials
B	Base width
$c'$	Effective cohesion
$c_a$	adhesion between concrete and soil
CIP	Cast-in-place
$c_w$	Wall adhesion
e	Eccentricity
ERS	Earth retaining structures
FHWA	Federal Highway Administration
$FS_{bc}$	Factor of safety against bearing capacity failure
$FS_s$	Factor of safety against sliding
H	Height of retaining wall
$h_w$	Distance from ground surface to water table
K	Ratio of horizontal to vertical stress
$K_a$	Coefficient of active earth pressure
$K_{ac}$	Coefficient of active earth pressure adjusted for wall adhesion
$K_o$	Coefficient of lateral earth pressure “at rest”
$K_p$	Coefficient of passive earth pressure
$K_{pc}$	Coefficient of passive earth pressure adjusted for wall adhesion
$\bar{m}$	Coefficient to relate wall height to distance of load from retaining wall
$\bar{n}$	Coefficient to relate wall height to depth from ground surface
MSE	Mechanically stabilized earth
OCR	Over consolidation ratio
$p_0$	Vertical pressure at a given depth
$p_a'$	Active effective pressure
$p_h$	Lateral earth pressure at a given depth
$p_p'$	Passive effective pressure
$q, q_s$	Vertical surcharge load
$Q_1, Q_2, Q_p$	Surcharge loads
$q_{eq}$	Equivalent uniform bearing pressure
$q_{max}$	Maximum bearing pressure
$q_{min}$	Minimum bearing pressure
SOE	Support of excavation
u	Pore water pressure
W	Weight at base of wall
Y	Horizontal deformation of retaining wall
z	Depth from surface
$z_w$	Depth from water table
$\beta$	Angle of slope
$\theta$	Slope of wall backface
$\Omega$	Dimensionless coefficient

$\Delta p_h$	Increase in lateral earth pressure due to vertical surcharge
$\delta$	Wall friction
$\delta_b$	friction angle between soil and base
$\gamma'$	Effective soil unit weight
$\gamma$	Soil unit weight
$\gamma_{sat}$	Saturated soil unit weight
$\gamma_w$	Unit weight of water
$\phi$	Angle of internal friction of soil
$\phi'$	Effective (drained) friction angle

[THIS PAGE INTENTIONALLY BLANK]

## **CHAPTER 8.0**

### **SHALLOW FOUNDATIONS**

Foundation design is required for all structures to ensure that the loads imposed on the underlying soil will not cause shear failures or damaging settlements. The two major types of foundations used for transportation structures can be categorized as “shallow” and “deep” foundations. This chapter first discusses the general approach to foundation design including consideration of alternative foundations to select the most cost-effective foundation. Following the general discussion, the chapter then concentrates on the topic of shallow foundations.

#### **8.01 Primary References:**

The two primary references for shallow foundations are:

FHWA (2002c). *Geotechnical Engineering Circular 6 (GEC 6), Shallow Foundations*. Report No. FHWA-SA-02-054, Author: Kimmerling, R. E., Federal Highway Administration, U.S. Department of Transportation.

AASHTO (2004 with 2006 Interims). *AASHTO LRFD Bridge Design Specifications*, 3rd Edition, American Association of State Highway and Transportation Officials, Washington, D.C.

#### **8.1 GENERAL APPROACH TO FOUNDATION DESIGN**

The duty of the foundation design specialist is to establish the most economical design that safely conforms to prescribed structural criteria and properly accounts for the intended function of the structure. Essential to the foundation engineer’s study is a rational method of design, whereby various foundation types are systematically evaluated and the optimum alternative selected. The following foundation design approach is recommended:

1. Determine the direction, type and magnitude of foundation loads to be supported, tolerable deformations and special constraints such as:
  - a. Underclearance requirements that limit allowable total settlement.
  - b. Structure type and span length that limits allowable deformations and angular distortions.
  - c. Time constraints on construction.
  - d. Extreme event loading and construction load requirements.

In general, a discussion with the structural engineer about a preliminary design will provide this information and an indication of the flexibility of the constraints.

2. Evaluate the subsurface investigation and laboratory testing data with regard to reliability and completeness. The design method chosen should be commensurate with the quality and quantity of available geotechnical data, i.e., **don't use state-of-the-art computerized analyses if you have not performed a comprehensive subsurface investigation to obtain reliable values of the required input parameters.**
3. Consider alternate foundation types where applicable as discussed below.

### **8.1.1 Foundation Alternatives and Cost Evaluation**

As noted earlier, the two major alternate foundation types are the “shallow” and “deep” foundations. Shallow foundations are discussed in this chapter. Deep foundation alternatives including piles and drilled shafts are discussed in the next chapter. Proprietary foundation systems should not be excluded as they may be the most economical alternative in a given set of conditions. Cost analyses of all feasible alternatives may lead to the elimination of some foundations that were otherwise qualified under the engineering study. Other factors that must be considered in the final foundation selection are the availability of materials and equipment, the qualifications and experience of local contractors and construction companies, as well as environmental limitations/considerations on construction access or activities.

Whether it is for shallow or deep foundations, it is recommended that foundation support cost be defined as the total cost of the foundation system divided by the load the foundation supports in tons. Thus, the cost of the foundation system should be expressed in terms of **dollars per ton load** that will be supported. For an equitable comparison, the total foundation cost should include all costs associated with a given foundation system including the need for excavation or retention systems, environmental restrictions on construction activities, e.g., vibrations, noise, disposal of contaminated excavated spoils, pile caps and cap size, etc. For major projects, if the estimated costs of alternative foundation systems during the design stage are within 15 percent of each other, then alternate foundation designs should be considered for inclusion in contract documents. If alternate designs are included in the contract documents, both designs should be adequately detailed. For example, if two pile foundation alternatives are detailed, the bid quantity pile lengths should reflect the estimated pile lengths for each alternative. Otherwise, material costs and not the installed foundation

cost will likely determine the low bid. Use of alternate foundation designs will generally provide the most cost effective foundation system.

A conventional design alternate should generally be included with a proprietary design alternate in the final project documents to stimulate competition and to anticipate value engineered proposals from contractors.

### **8.1.2 Loads and Limit States for Foundation Design**

Foundations should be proportioned to withstand all anticipated loads safely including the permanent loads of the structure and transient loads. Most design codes specify the types of loads and load combinations to be considered in foundation design, e.g., AASHTO (2002). These load combinations can be used to identify the “limit” states for the foundation types being considered. A limit state is reached when the structure no longer fulfills its performance requirements. There are several types of limit states that are related to maximum load-carrying capacity, serviceability, extreme event and fatigue. Two of the more common limit states are as follows:

- An **ultimate limit state** (ULS) corresponds to the maximum load-carrying capacity of the foundation. This limit state may be reached through either structural or geotechnical failure. An ultimate limit state corresponds to collapse. The ultimate state is also called the **strength limit state** and includes the following failure modes for shallow foundations:
  - bearing capacity of soil exceeded,
  - excessive loss of contact, i.e., eccentricity,
  - sliding at the base of footing,
  - loss of overall stability, i.e., global stability,
  - structural capacity exceeded.
  
- A **serviceability limit state** (SLS) corresponds to loss of serviceability, and occurs before collapse. A serviceability limit state involves unacceptable deformations or undesirable damage levels. A serviceability limit state may be reached through the following mechanisms:
  - Excessive differential or total foundation settlements,
  - Excessive lateral displacements, or
  - Structural deterioration of the foundation.

The serviceability limit state for transportation structures is based upon economy and the quality of ride. The cost of limiting foundation movements should be compared to the cost of designing the superstructure so that it can tolerate larger movements, or of correcting the consequences of movements through maintenance, to determine minimum life cycle cost. More stringent criteria may be established by the owner.

All relevant limit states must be considered in foundation design to ensure an adequate degree of safety and serviceability. Therefore, all foundation design is geared towards addressing the ULS and the SLS. In this manual, the allowable stress design (ASD) approach is used. Further discussion on ASD and other design methods such as the Load and Resistance Factor Design (LRFD) can be found in Appendix C.

## **8.2 TYPES OF SHALLOW FOUNDATIONS**

The geometry of a typical shallow foundation is shown in Figure 8-1. Shallow foundations are those wherein the depth,  $D_f$ , of the foundation is small compared to the cross-sectional size (width,  $B_f$ , or length,  $L_f$ ). This is in contradistinction to deep foundations, such as driven piles and drilled shafts, whose depth of embedment is considerably larger than the cross-section dimension (diameter). The exact definition of shallow or deep foundations is less important than an understanding of the theoretical assumptions behind the various design procedures for each type. Stated another way, it is important to recognize the theoretical limitations of a design procedure that may vary as a function of depth, such as a bearing capacity equation. Common types of shallow foundations are shown in Figures 8-2 through 8-9.

### **8.2.1 Isolated Spread Footings**

Footings with  $L_f/B_f$  ratio less than 10 are considered to be isolated footings. Isolated spread footings (Figure 8-2) are designed to distribute the concentrated loads delivered by a single column to prevent shear failure of the soil beneath the footing. The size of the footing is a function of the loads distributed by the supported column and the strength and compressibility characteristics of the bearing materials beneath the footing. For bridge columns, isolated spread footings are typically greater than 10 ft by 10 ft (3 m by 3 m). These dimensions increase when eccentric loads are applied to the footing. Structural design of the isolated footing includes consideration for moment resistance at the face of the column in the short direction of the footing, as well as shear and punching around the column.

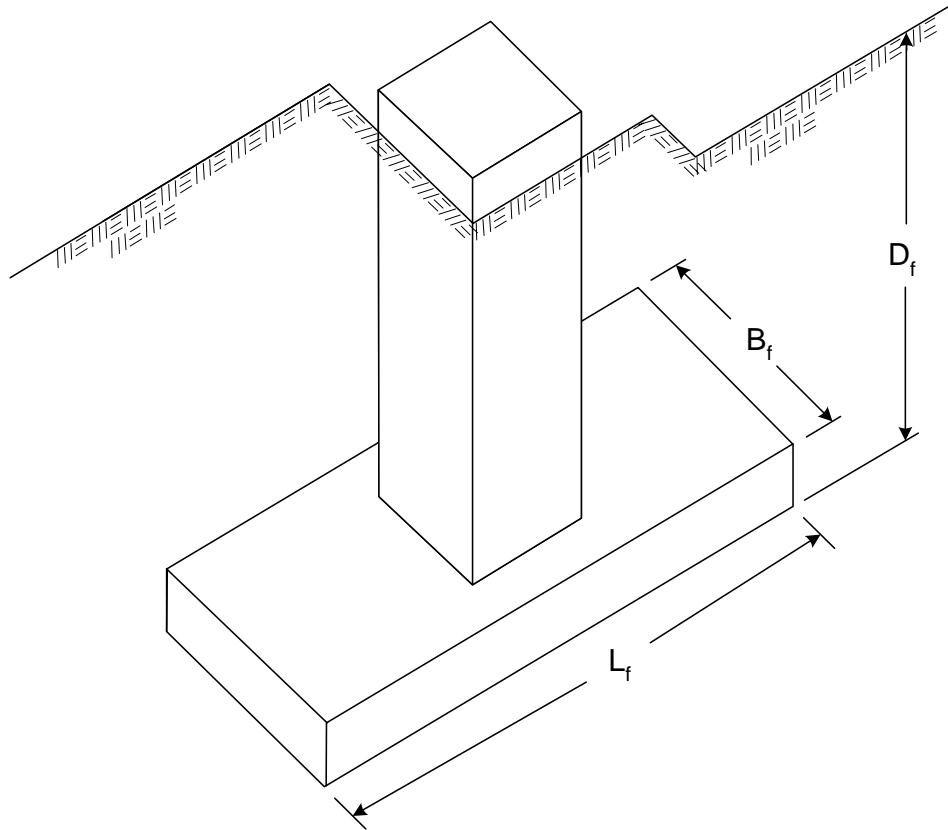


**Figure 8-1. Geometry of a typical shallow foundation (FHWA, 2002c, AASHTO 2002).**

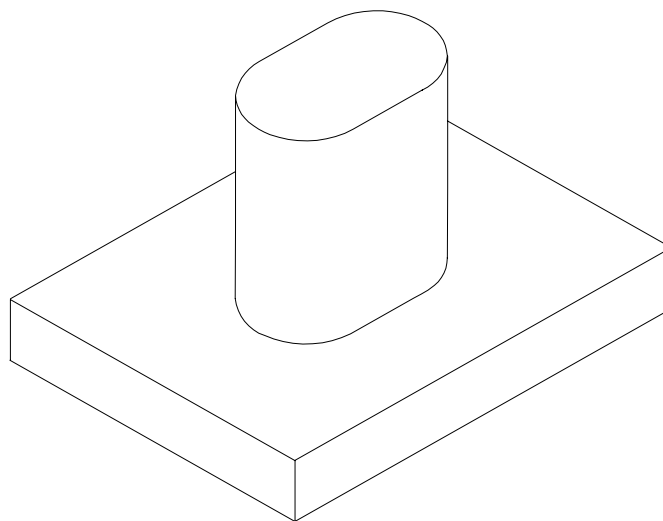


**Figure 8-2. Isolated spread footing (FHWA, 2002c).**

## 8.2.2 Continuous or Strip Footings

The most commonly used type of foundation for buildings is the continuous strip footing (Figure 8-3). For computation purposes, footings with an  $L_f/B_f$  ratio  $\geq 10$  are considered to be continuous or strip footings. Strip footings typically support a single row of columns or a bearing wall to reduce the pressure on the bearing materials. Strip footings may tie columns together in one direction. Sizing and structural design considerations are similar to those for isolated spread footings with the exception that plane strain conditions are assumed to exist in the direction parallel to the long axis of the footing. This assumption affects the depth of significant influence (DOSI), i.e., the depth to which applied stresses are significantly felt in the soil. For example, in contrast with isolated footing where the DOSI is between 2 to 4 times the footing width, the DOSI in the case of the strip footings will always be at least 4 times the width of the footing as discussed in Section 2.4.1 of Chapter 2. The structural design of strip footings is generally governed by beam shear and bending moments.

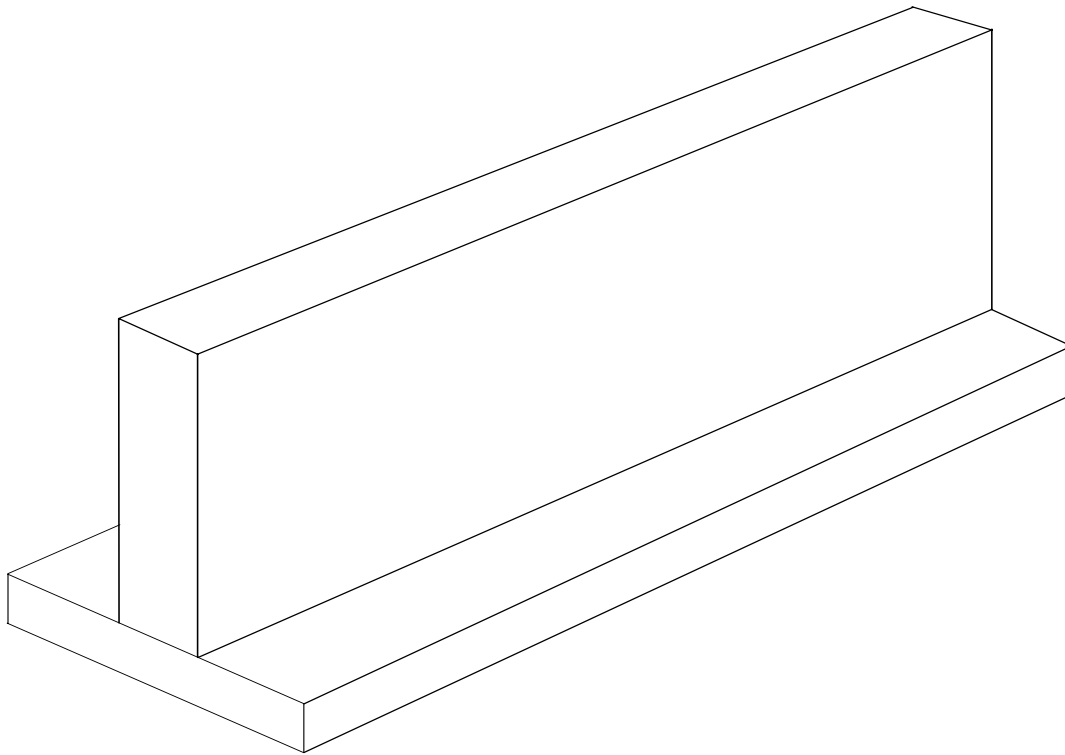


**Figure 8-3. Continuous strip footing (FHWA, 2002c).**

### **8.2.3 Spread Footings with Cantilevered Stemwalls**

An earth retaining system consisting of a spread footing supporting a cantilevered retaining wall is frequently used to resist lateral loads applied by a backfill and other external loads that may be acting on top of the backfill (refer to Figures 8-4 and 8-5). The system must offer resistance to both vertical and horizontal loads as well as to overturning moments. The spread footing is designed to resist overturning moments and vertical eccentric loads caused by the lateral earth pressures and the horizontal components of the externally applied loads acting on the cantilever stemwall. The wall itself is designed as a simple cantilevered structure to resist the lateral earth pressures imposed by the backfill and other external loads that may be applied on top of the backfill.

### **8.2.4 Bridge Abutments**

Bridge abutments are required to perform numerous functions, including the following:

- Retain the earthen backfill behind the abutment.
- Support the superstructure and distribute the loads to the bearing materials below the spread footing, assuming that a spread footing is the foundation system chosen for the abutment.
- Provide a transition from the approach embankment to the bridge deck.
- Depending on the structure type, accommodate shrinkage and temperature movements within the superstructure.

Spread footings with cantilevered stemwalls are well suited to perform these multiple functions. The general arrangement of a bridge abutment with a spread footing and a cantilevered stemwall is shown in Figures 8-4 and 8-5. In the case of weak soils at shallow depths, deep foundations, such as drilled shafts or driven piles, are often used to support the abutment. There are several other abutment types such as those that use mechanically stabilized earth (MSE) walls with spread foundations on top or with deep foundation penetrating through the MSE walls. Several different types of bridge abutments are shown in Figure 7-2 in Chapter 7.

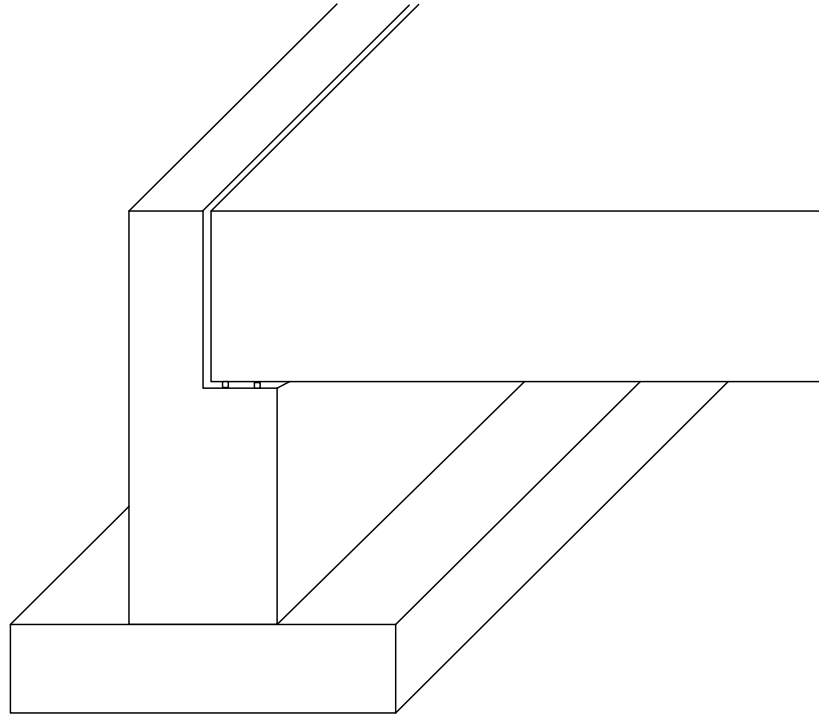


**Figure 8-4. Spread footing with cantilever stemwall at bridge abutment.**



**Figure 8-5. Abutment/wingwall footing, I-10, Arizona.**

### 8.2.5 Retaining Structures

The foundations for semi-gravity concrete cantilever retaining walls (inverted “T” walls) are essentially shallow spread footings. The wall derives its ability to resist loads from a combination of the dead weight of the backfill on the heel of the wall footing and the structural cantilever of the stem (Figure 8-6).

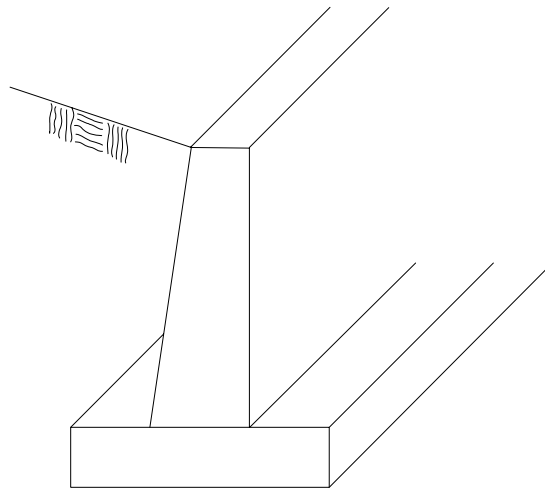


**Figure 8-6. Footing for a semi-gravity cantilever retaining wall (FHWA, 2002c).**

### 8.2.6 Building Foundations

When a building stemwall is buried, partially buried or acts as a basement wall, the stemwall resists the lateral earth pressures of the backfill. Unlike bridge abutments where the bridge structure is usually free to move horizontally on the abutment or the semi-gravity cantilever wall, the tops or the ends of the stemwalls in buildings are frequently restrained by other structural members such as beams, floors, transverse interior walls, etc. These structural members provide lateral restraint that affects the magnitude of the design lateral earth pressures

### 8.2.7 Combined Footings

Combined footings are similar to isolated spread footings except that they support two or more columns and are rectangular or trapezoidal in shape (Figure 8-7). They are used primarily when the column spacing is non-uniform (Bowles, 1996) or when isolated spread footings become so closely spaced that a combination footing is simpler to form and construct. In the case of bridge abutments, an example of a combined footing is the so-called

“spill-through” type abutment (Figure 8-8). This configuration was used during some of the initial construction of the Interstate Highway System on new alignments where spread footings could be founded on competent native soils. Spill-through abutments are also used at stream crossings to make sure that foundations are below the scour depth of the stream.

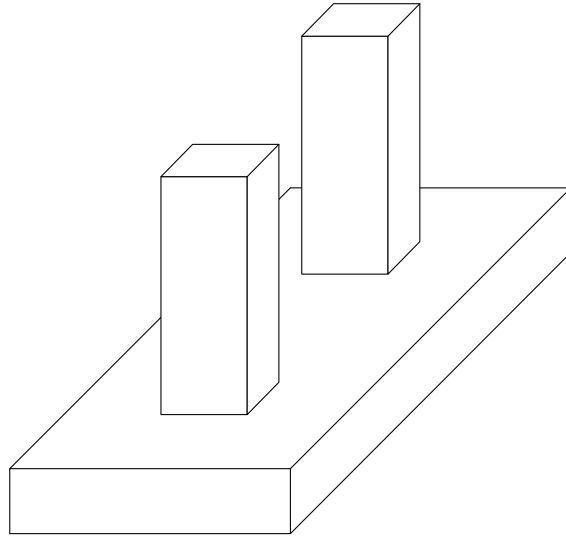


**Figure 8-7. Combined footing (FHWA, 2002c).**

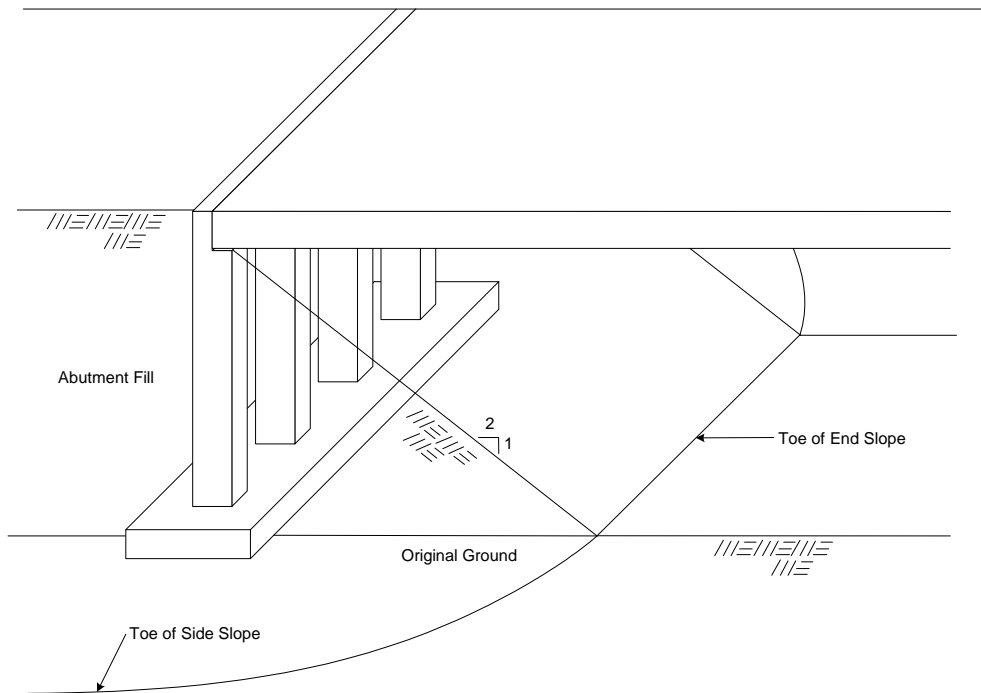


**Figure 8-8. Spill-through abutment on combination strip footing (FHWA, 2002c).**

Due to the frame action that develops with combined footings, they can be used to resist large overturning or rotational moments in the longitudinal direction of the column row.

There are a number of approaches for designing and constructing combined footings. The choice depends on the available space, load distribution among the columns supported by the footing, variations of soil properties supporting the footing, and economics.

### 8.2.8 Mat Foundations

A mat foundation consists of a single heavily reinforced concrete slab that underlies the entire structure or a major portion of the structure. Mat foundations are often economical when spread footings would cover more than about 50 percent of the plan area of the structure's footprint (Peck, *et al.*, 1974). A mat foundation (Figure 8-9) typically supports a number of columns and/or walls in either direction or a uniformly distributed load such as that imposed by a storage tank. The principal advantage of a mat foundation is its ability to bridge over local soft spots, and to reduce differential movement.

Structures founded on relatively weak soils may be supported economically on mat foundations. Column and wall loads are transferred to the foundation soils through the mat foundation. Mat foundations distribute the loads over a large area, thus reducing the intensity of contact pressures. Mat foundations are designed with sufficient reinforcement and thickness to be rigid enough to distribute column and wall loads uniformly. Although differential settlements may be minimized by the use of mat foundations, greater uniform settlements may occur because the zone of influence of the applied stress may extend to considerable depth due to the larger dimensions of the mat. Often a mat also serves as the base floor level of building structures.

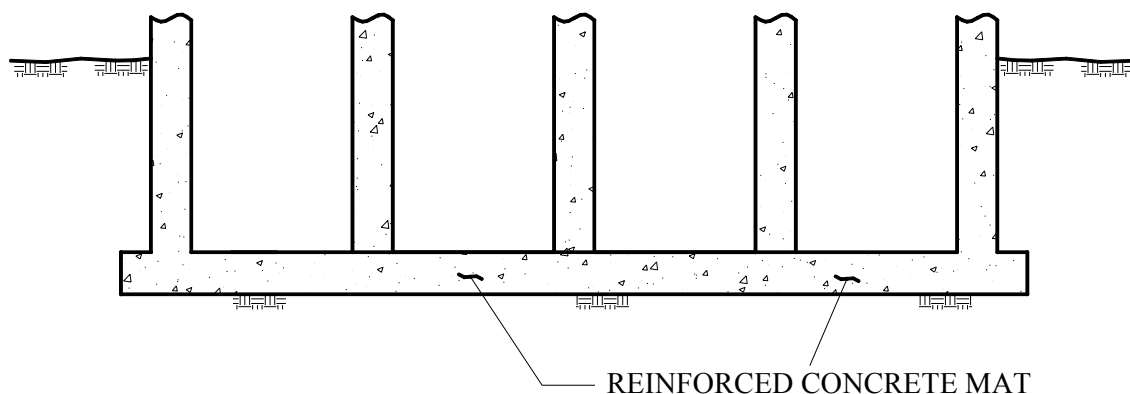


**Figure 8-9. Typical mat foundation (FHWA, 2002c).**

Mat foundations have limited applicability for bridge support, except where large bridge piers, such as bascules or other movable bridge supports, bear at relatively shallow depth without deep foundation support. This type of application may arguably be a deep foundation, but the design of such a pier may include consideration of the base of the bascule pier as a mat. Discussion of mat foundation design is included in FHWA (2002c).

A more common application of mat foundations for transportation structures includes lightly loaded rest area or maintenance facilities such as small masonry block structures, sand storage bins or sheds, or box culverts constructed as a continuous structure.

### 8.3 SPREAD FOOTING DESIGN CONCEPT AND PROCEDURE

The geotechnical design of a spread footing is a two-part process. First the allowable soil bearing capacity must be established to ensure stability of the foundation and determine if the proposed structural loads can be supported on a reasonably sized foundation. Second, the amount of settlement due to the actual structural loads must be predicted and the time of occurrence estimated. Experience has shown that settlement is usually the controlling factor in the decision to use a spread footing. This is not surprising since structural considerations usually limit tolerable settlements to values that can be achieved only on competent soils not prone to a bearing capacity failure. Thus, the **allowable bearing capacity** of a spread footing is defined as the lesser of:

- The applied stress that results in a shear failure divided by a suitable factor of safety (FS); this is a criterion based on an **ultimate limit state** (ULS) as discussed previously.
- or
- The applied stress that results in a specified amount of settlement; this is a criterion based on a **serviceability limit state** (SLS) as discussed previously.

Both of the above considerations are a function of the least lateral dimension of the footing, typically called the footing width and designated as  $B_f$  as shown in Figure 8-1. The effect of footing width on allowable bearing capacity and settlement is shown conceptually in Figure 8-10. The allowable bearing capacity of a footing is usually controlled by shear-failure considerations for narrow footing widths as shown in Zone A in Figure 8-10. As the footing width increases, the allowable bearing capacity is limited by the settlement potential of the soils supporting the footing within the DOSI which is a function of the footing width as discussed in Section 2.4 of Chapter 2. Stated another way, as the footing width increases, the stress increase “felt” by the soil may decrease but the effect of the applied stress will extend

more deeply below the footing base. Therefore, settlements may increase depending on the type of soils within the DOSI. This is schematically shown in Zone B in Figure 8-10.

The concept of decreasing allowable bearing capacity with increasing footing width for the settlement controlled cases is an important concept to understand. In such cases, the allowable bearing capacity is the value of the applied stress at the footing base that will result in a given settlement. Since the DOSI increases with increasing footing width, the only way to limit the settlements to a certain desired value is by reducing the applied stress. The more stringent the settlement criterion the less the stress that can be applied to the footing which in turn means that the allowable bearing capacity is correspondingly less. This is conceptually illustrated in Figure 8-10 wherein it is shown that decreasing the settlement, i.e., going from 3S to 2S to S decreases the allowable bearing capacity at a given footing width. An example of the use of the chart is presented in Section 8.8.

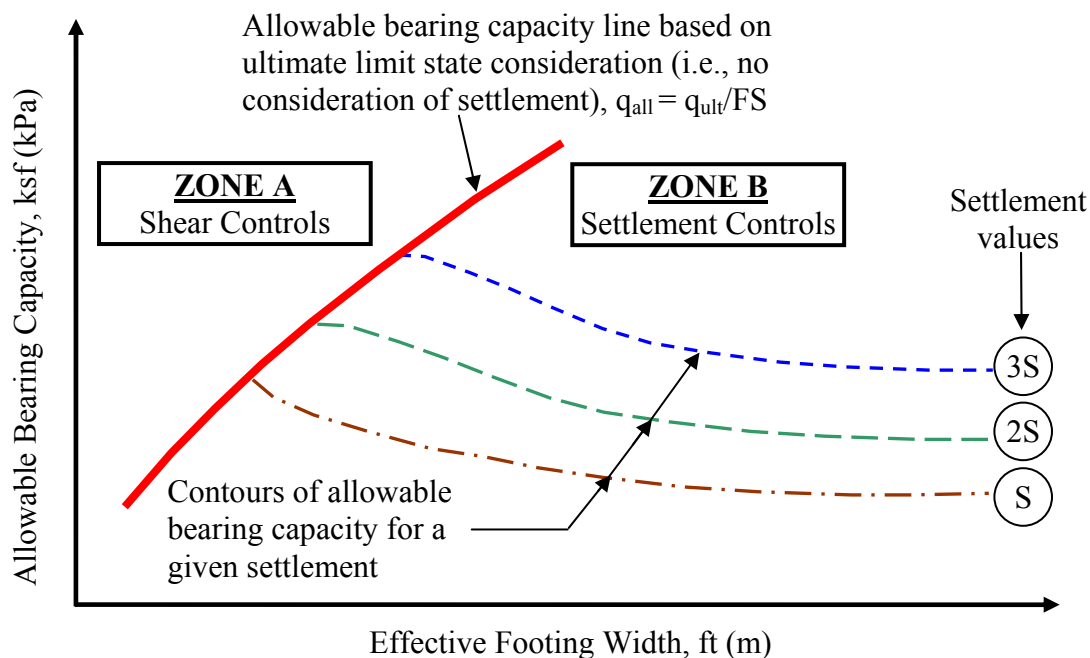


**Figure 8-10. Shear failure versus settlement considerations in evaluation of allowable bearing capacity.**

The design process flow chart for a bridge supported on spread footings is shown in Figure 8-11. In the flow chart, the foundation design specialist is a person with the skills necessary to address both geotechnical and structural design. Section 8.4 discusses the bearing capacity aspects while Section 8.5 discusses the settlement aspects of shallow foundation design.

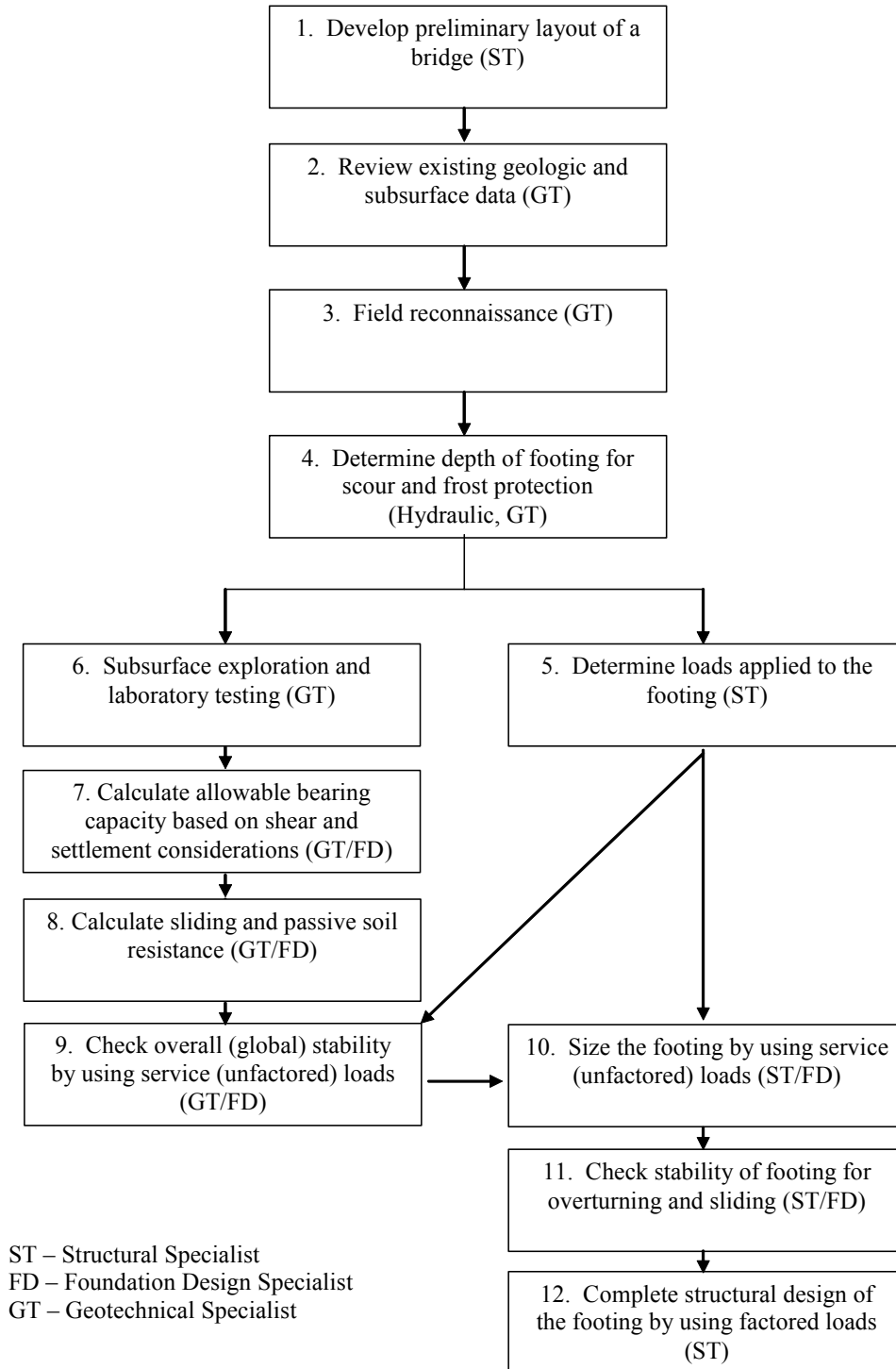


**Figure 8-11. Design process flow chart – bridge shallow foundation (modified after FHWA, 2002c).**

## 8.4 BEARING CAPACITY

This section discusses bearing capacity theory and its application toward computing allowable bearing capacities for shallow foundations.

A foundation failure will occur when the footing penetrates excessively into the ground or experiences excessive rotation (Figure 8-12). Either of these excessive deformations may occur when,

- (a) the shear strength of the soil is exceeded, and/or
- (b) large uneven settlement and associated rotations occur.

The failure mode that occurs when the shear strength is exceeded is known as a bearing capacity failure or, more accurately, an **ultimate bearing capacity failure**. Often, large settlements may occur prior to an ultimate bearing capacity failure and such settlements may impair the serviceability of the structure, i.e., the ultimate limit state (ULS) has not been exceeded, but the serviceability limit state (SLS) has. In this case, to control the settlements within tolerable limits, the footprint and/or depth of the structure below the ground may be dimensioned such that the imposed bearing pressure is well below the ultimate bearing capacity.



**Figure 8-12. Bearing capacity failure of silo foundation (Tschebotarioff, 1951).**

## 8.4.1 Failure Mechanisms

The type of bearing capacity failure is a function of several factors such as the type of the soil, the density (or consistency) of the soil, shape of the loaded surface, etc. This section discusses three failure mechanisms.

### 8.4.1.1 General Shear

When a footing is loaded to the ultimate bearing capacity, a condition of plastic flow develops in the foundation soils. As shown in Figure 8-13, a triangular wedge beneath the footing, designated as Zone I, remains in an elastic state and moves down into the soil with the footing. Although only a single failure surface (CD) is shown in Zone II, radial shear develops throughout Zone II such that radial lines of failure extending from the Zone I boundary (CB) change length based on a logarithmic spiral until they reach Zone III. Although only a single failure surface (DE) is shown in Zone III, a passive state of stress develops throughout Zone III at an angle of  $45^\circ - (\phi'/2)$  from the horizontal. This configuration of the ultimate bearing capacity failure, with a well-defined failure zone extending to the surface and with bulging of the soil occurring on both sides of the footing, is called a “general shear” type of failure. General shear-type failures (Figure 8-14a) are believed to be the prevailing mode of failure for soils that are relatively incompressible and reasonably strong.

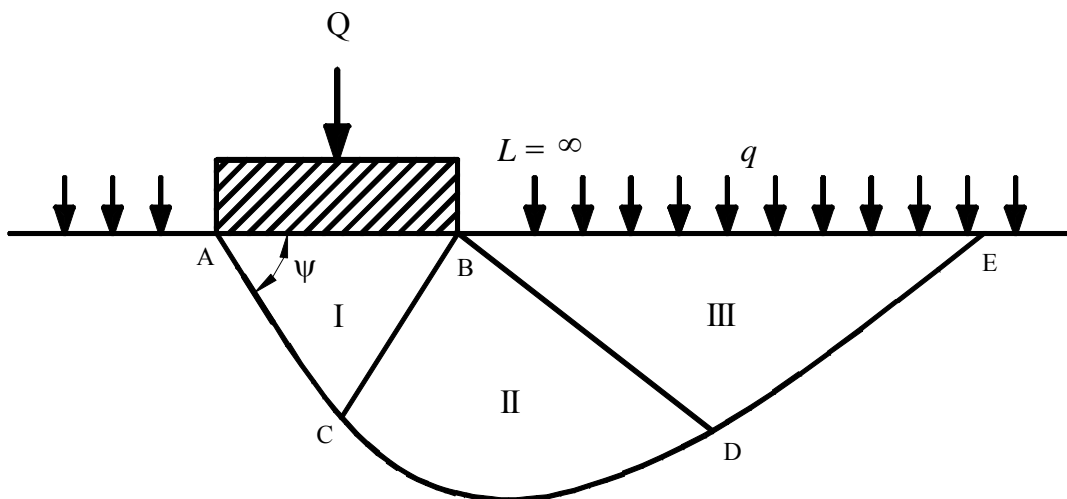


**Figure 8-13. Boundaries of zone of plastic equilibrium after failure of soil beneath continuous footing (FHWA, 2002c).**

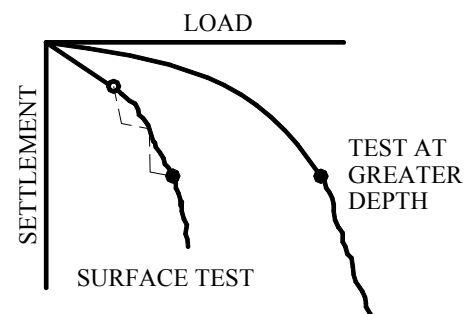
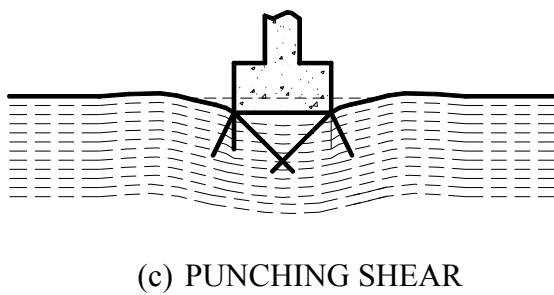
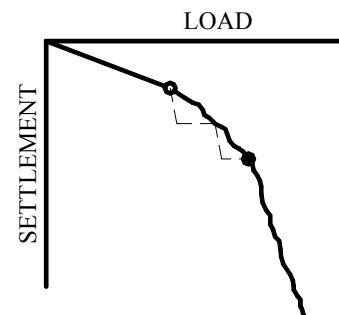
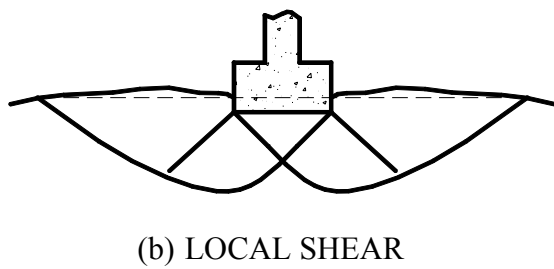
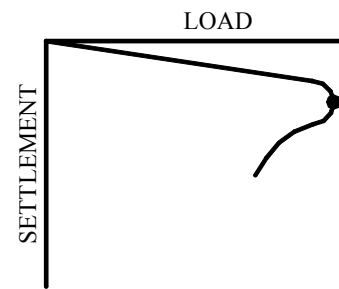
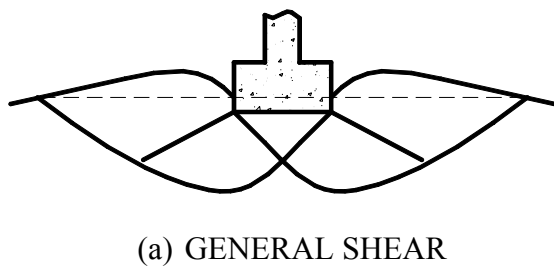


**Figure 8-14. Modes of bearing capacity failure (after Vesic, 1975) (a) General shear (b) Local shear (c) Punching shear**

### 8.4.1.2 Local Shear

Local shear failure is characterized by a failure surface that is similar to that of a general shear failure but that does not extend to the ground surface. In the case of a local shear failure the failure zone ends somewhere in the soil below the footing (Figure 8-14b). Local shear failure is accompanied by vertical compression of soil below the footing and visible bulging of soil adjacent to the footing, but not by sudden rotation or tilting of the footing. Local shear failure is a transitional condition between general and punching shear failure. Local shear failures may occur in soils that are relatively loose compared to soils susceptible to general shear failure.

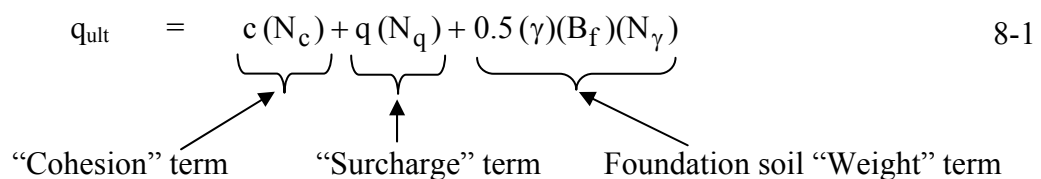
### 8.4.1.3 Punching Shear

Punching shear failure is characterized by vertical shear around the perimeter of the footing and is accompanied by a vertical movement of the footing and compression of the soil immediately below the footing. The soil outside the loaded area is not affected significantly (Figure 8-14c). The ground surface adjacent to the footing moves downward instead of bulging as in general and local shear failure. Punching shear failure generally occurs in loose or compressible soils, in weak soils under slow (drained) loading, and in dense sands for deep footings subjected to high loads.

Note that from a perspective of bridge foundation design, soils so obviously weak as to experience local or punching shear failure modes should be avoided for supporting shallow foundations. Additional guidance on dealing with soils that fall in the intermediate or local shear range of behavior is provided in Section 8.4.5.

## 8.4.2 Bearing Capacity Equation Formulation

In essence, the bearing capacity failure mechanism is similar to the embankment slope failure mechanism discussed in Chapter 6. In the case of footings, the ultimate bearing capacity is equivalent to the stress applied to the soil by the footing that causes shear failure to occur in the soil below the footing base. For a concentrically loaded rigid strip footing with a rough base on a level homogeneous foundation material without the presence of water, the gross ultimate bearing capacity,  $q_{ult}$ , is expressed as follows (after Terzaghi, 1943):

$$q_{ult} = c(N_c) + q(N_q) + 0.5(\gamma)(B_f)(N_\gamma) \quad 8-1$$


“Cohesion” term
“Surcharge” term
Foundation soil “Weight” term

- where:  $c$  = cohesion of the soil (ksf) (kPa)
- $q$  = total surcharge at the base of the footing =  $q_{\text{appl}} + \gamma_a D_f$  (ksf) (kPa)
- $q_{\text{appl}}$  = applied surcharge (ksf)(kPa)
- $\gamma_a$  = unit weight of the overburden material above the base of the footing causing the surcharge pressure (kcf) (kN/m<sup>3</sup>)
- $D_f$  = depth of embedment (ft) (m) (Figure 8-1)
- $\gamma$  = unit weight of the soil under the footing (kcf) (kN/m<sup>3</sup>)
- $B_f$  = footing width, i.e., least lateral dimension of the footing (ft) (m) (Figure 8-1)
- $N_q$  = bearing capacity factor for the “surcharge” term (dimensionless)
- $= e^{\pi \tan \phi} \tan^2 \left( 45^\circ + \frac{\phi}{2} \right)$  8-2
- $N_c$  = bearing capacity factor for the “cohesion” term (dimensionless)
- $= (N_q - 1) \cot \phi$  for  $\phi > 0^\circ$  8-3
- $= 2 + \pi = 5.14$  for  $\phi = 0^\circ$  8-4
- $N_\gamma$  = bearing capacity factor for the “weight” term (dimensionless)
- $= 2 (N_q + 1) \tan(\phi)$  8-5

Many researchers proposed different expressions for the bearing capacity factors,  $N_c$ ,  $N_q$ , and  $N_\gamma$ . The expressions presented above are those used by AASHTO (2004 with 2006 Interims). These expressions are a function of the friction angle,  $\phi$ . Table 8-1 can be used to estimate friction angle,  $\phi$ , from corrected SPT N-value,  $N_{160}$ , for cohesionless soils. Otherwise, the friction angle can be measured directly by laboratory tests or in situ testing. The values of  $N_c$ ,  $N_q$ , and  $N_\gamma$  as computed for various friction angles by Equations 8-3/8-4, 8-2, and 8-5, respectively are included in Table 8-1 and in Figure 8-15. Computation of ultimate bearing capacity is illustrated in Example 8-1.

**Table 8-1**  
**Estimation of friction angle of cohesionless soils from Standard Penetration Tests**  
**(after AASHTO, 2004 with 2006 Interims; FHWA, 2002c)**

Description	Very Loose	Loose	Medium	Dense	Very Dense
Corrected SPT $N_{160}$	0	4	10	30	50
Approximate $\phi$ , degrees*	25 – 30	27 – 32	30 – 35	35 – 40	38 – 43
Approximate moist unit weight, ( $\gamma$ ) pcf*	70 – 100	90 – 115	110 – 130	120 – 140	130 – 150
* Use larger values for granular material with 5% or less fine sand and silt. Note: Correlations may be unreliable in gravelly soils due to sampling difficulties with split-spoon sampler as discussed in Chapter 3.					

**Table 8-2**  
**Bearing Capacity Factors (AASHTO, 2004 with 2006 Interims)**

$\phi$	$N_c$	$N_q$	$N_\gamma$	$\phi$	$N_c$	$N_q$	$N_\gamma$
0	5.14	1.0	0.0	23	18.1	8.7	8.2
1	5.4	1.1	0.1	24	19.3	9.6	9.4
2	5.6	1.2	0.2	25	20.7	10.7	10.9
3	5.9	1.3	0.2	26	22.3	11.9	12.5
4	6.2	1.4	0.3	27	23.9	13.2	14.5
5	6.5	1.6	0.5	28	25.8	14.7	16.7
6	6.8	1.7	0.6	29	27.9	16.4	19.3
7	7.2	1.9	0.7	30	30.1	18.4	22.4
8	7.5	2.1	0.9	31	32.7	20.6	26.0
9	7.9	2.3	1.0	32	35.5	23.2	30.2
10	8.4	2.5	1.2	33	38.6	26.1	35.2
11	8.8	2.7	1.4	34	42.2	29.4	41.1
12	9.3	3.0	1.7	35	46.1	33.3	48.0
13	9.8	3.3	2.0	36	50.6	37.8	56.3
14	10.4	3.6	2.3	37	55.6	42.9	66.2
15	11.0	3.9	2.7	38	61.4	48.9	78.0
16	11.6	4.3	3.1	39	67.9	56.0	92.3
17	12.3	4.8	3.5	40	75.3	64.2	109.4
18	13.1	5.3	4.1	41	83.9	73.9	130.2
19	13.9	5.8	4.7	42	93.7	85.4	155.6
20	14.8	6.4	5.4	43	105.1	99.0	186.5
21	15.8	7.1	6.2	44	118.4	115.3	224.6
22	16.9	7.8	7.1	45	133.9	134.9	271.8

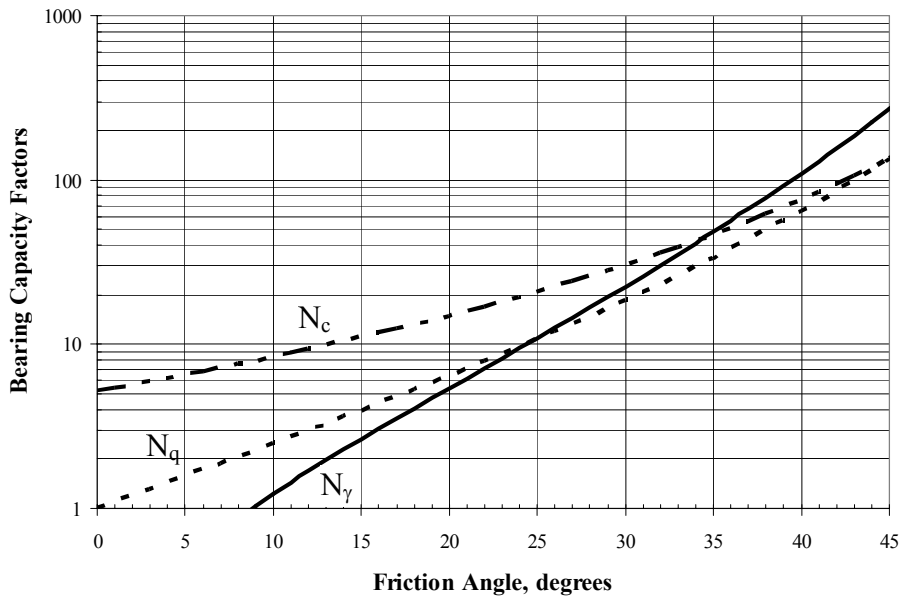
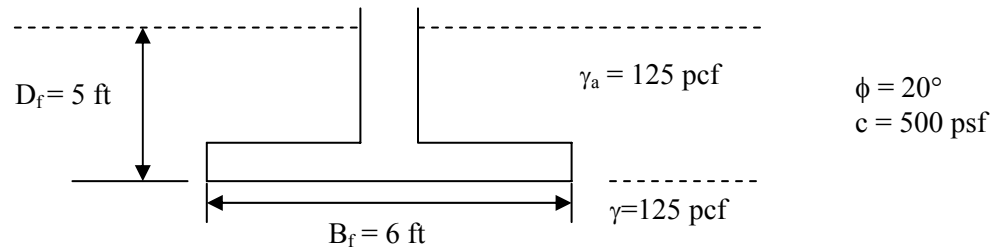


**Figure 8-15. Bearing capacity factors versus friction angle.**

**Example 8-1:** Determine the ultimate bearing capacity for a rigid strip footing with a rough base having the dimensions shown in the sketch below. Assume that the footing is concentrically loaded and that the total unit weight below the base of the footing is equal to the total unit weight above the base of the footing, i.e., in terms of the symbols used previously,  $\gamma = \gamma_a$ . First assume that the ground water table is well below the base of the footing and therefore it has no effect on the bearing capacity. Then, assume that the groundwater table is at the base of the footing and recompute the ultimate bearing capacity.



**Solution:**

Assume a general shear condition and enter Table 8-2 for  $\phi = 20^\circ$  and read the bearing capacity factors as follows:

$N_c = 14.8$ ,  $N_q = 6.4$ ,  $N_\gamma = 5.4$ . These values can also be read from Figure 8-15.

$$q_{ult} = c(N_c) + \gamma_a(D_f)(N_q) + 0.5(\gamma)(B_f)(N_\gamma)$$

$$\begin{aligned} q_{ult} &= (500 \text{ psf})(14.8) + (125 \text{ pcf})(5 \text{ ft})(6.4) + 0.5(125 \text{ pcf})(6 \text{ ft})(5.4) \\ &= 7,400 \text{ psf} + 4,000 \text{ psf} + 2,025 \text{ psf} \\ q_{ult} &= 13,425 \text{ psf} \end{aligned}$$

Effect of water: If the ground water table is at the base of the footing, i.e., a depth of 5 ft from the ground surface, then effective unit weight should be used in the “weight” term as follows:

$$\begin{aligned} q_{ult} &= (500 \text{ psf})(14.8) + (125 \text{ pcf})(5 \text{ ft})(6.4) + 0.5(125 \text{ pcf} - 62.4 \text{ pcf})(6 \text{ ft})(5.4) \\ &= 7,400 \text{ psf} + 4,000 \text{ psf} + 1,014 \text{ psf} \\ q_{ult} &= 12,414 \text{ psf} \end{aligned}$$

Sections 8.4.2.1 and 8.4.3.2 further discuss the effect of water on ultimate bearing capacity.

### 8.4.2.1 Comparative Effect of Various Terms in Bearing Capacity Formulation

In Equation 8-1, the first term is called the “cohesion” term, the second term is called the “surcharge” term since it represents the loads above the base of the footing, and the third term is called the “weight” term since it represents the weight of the foundation soil in the failure zone below the base of the footing. Consider now the effect that each of these terms has on the computed value of the ultimate bearing capacity ( $q_{ult}$ ).

- **Purely cohesive soils,  $\phi = 0$  (corresponds to undrained loading):** In this case, the last term is zero ( $N_\gamma = 0$  for  $\phi = 0$ ) and the first term in Equation 8-1 is a constant. Therefore the ultimate bearing capacity is a function of only the cohesion as it appears in the cohesion term in Equation 8-1 and the depth of embedment of the footing as it appears in the surcharge term in Equation 8-1. For this case, the footing width has no influence on the ultimate bearing capacity.
- **Purely frictional or cohesionless soils,  $c = 0$  and  $\phi > 0$ :** In this case, there will be large changes in ultimate bearing capacity when properties and/or dimensions are changed. The embedment effect is particularly important. Removal of the soil over an embedded footing, either by excavation or scour, can substantially reduce its ultimate bearing capacity and result in a lower factor of safety than required by the design. Removal of the soil over an embedded footing can also cause greater settlement than initially estimated. Similarly, a rise in the ground water level to the ground surface will reduce the effective unit weight of the soil by making the soil buoyant, thus reducing the surcharge and unit weight terms by essentially one-half.

Table 8-3 shows how bearing capacity can vary with changes in physical properties or dimensions. Notice that for a given value of cohesion, the effect of the variables on the bearing capacity in cohesive soils is minimal. Only the embedment depth has an effect on bearing capacity in cohesive soils. Also note that a rise in the ground water table does not influence cohesion. Interparticle bonding remains virtually unchanged unless the clay is reworked or the clay contains minerals that react with free water, e.g., expansive minerals.

Table 8-3 also shows that for a given value of internal friction angle, the effect on cohesionless soils is significant when dimensions are changed and/or a rise in the water table takes place. The embedment effect is particularly important. Removal of soil from over an embedded footing, either by excavation or scour, can substantially reduce the ultimate bearing capacity and possibly cause catastrophic shear failure. Rehabilitation or repair of an existing spread footing often requires excavation of the soil above the footing. If the effect of this removal on bearing capacity is not considered, the footing may move downward resulting in structural distress.

**Table 8-3**

**Variation in bearing capacity with changes in physical properties or dimensions**

Properties and Dimensions	Cohesive Soil	Cohesionless Soil
	$\phi = 0$ $c = 1,000$ psf $q_{ult}$ (psf)	$\phi = 30^\circ$ $c = 0$ $q_{ult}$ (psf)
A. <u>Initial situation</u> : $\gamma = 120$ pcf, $D_f = 0'$ , $B_f = 5'$ deep water table	5,140	6,720
B. <u>Effect of embedment</u> : $\gamma = 120$ pcf,, $D_f = 5'$ , $B_f = 5'$ , deep water table	5,740	17,760
C. <u>Effect of width</u> : $\gamma = 120$ pcf, $D_f = 0'$ , $B_f = 10'$ deep water table	5,140	13,440
D. <u>Effect of water table at surface</u> : $\gamma' = 57.6$ pcf, $D_f = 0'$ , $B_f = 5'$	5,140	3,226

**8.4.3 Bearing Capacity Correction Factors**

A number of factors that were not included in the derivations discussed earlier influence the ultimate bearing capacity of shallow foundations. Note that Equation 8-1 assumes a rigid strip footing with a rough base, loaded through its centroid, that is bearing on a level surface of homogeneous soil. Various correction factors have been proposed by numerous investigators to account for footing shape adjusted for eccentricity, location of the ground water table, embedment depth, sloping ground surface, an inclined base, the mode of shear, local or punching shear, and inclined loading. The general philosophy of correcting the theoretical ultimate bearing capacity equation involves multiplying each of the three terms in the bearing capacity equation by empirical factors to account for the particular effect. Each correction factor includes a subscript denoting the term to which the factor should be applied: “c” for the cohesion term, “q” for the surcharge term, and “ $\gamma$ ” for the weight term. Each of these factors and suggestions for their application are discussed separately below. In most cases these factors may be used in combination.

The general form of the ultimate bearing capacity equation, including correction terms, is:

$$q_{ult} = cN_c s_c b_c + qN_q C_{wq} s_q b_q d_q + 0.5\gamma B_f N_\gamma C_{w\gamma} s_\gamma b_\gamma \tag{8-6}$$

where:  $s_c$ ,  $s_\gamma$  and  $s_q$  are **shape correction factors**

$b_c$ ,  $b_\gamma$  and  $b_q$  are **base inclination correction factors**

$C_{w\gamma}$  and  $C_{wq}$  are **groundwater correction factors**

$d_q$  is an **embedment depth correction factor** to account for the shearing resistance along the failure surface passing through cohesionless material above the bearing elevation. Recall that the embedment is modeled as a surcharge pressure applied at the bearing elevation. To be theoretically correct, the “q” in the surcharge term consists of two components, one the embedment depth surcharge to which the correction factor applies, the other an applied surcharge such as the traffic surcharge to which the correction factor, by definition, does not apply. Therefore, theoretically the “q” in the surcharge term should be replaced with  $(q_a + \gamma D_f d_q)$  where  $q_a$  is defined as an applied surcharge for cases where applied surcharge is considered in the analysis;

$N_c$ ,  $N_q$  and  $N_\gamma$  are **bearing capacity factors** that are a function of the friction angle of the soil.  $N_c$ ,  $N_q$  and  $N_\gamma$  can be obtained from Table 8-2 or Figure 8-15 or they can be computed by Equation 8-3/8-4, 8-2 and 8-5, respectively. As discussed in Section 8.4.3.6,  $N_c$  and  $N_\gamma$  are replaced with  $N_{cq}$  and  $N_{\gamma q}$  for the case of sloping ground or when the footing is located near a slope. In these cases the  $N_q$  term is omitted.

The following sections provide guidance on the use of the bearing capacity correction factors, and whether or not certain factors should be used in combination.

#### **8.4.3.1 Footing Shape (Eccentricity and Effective Dimensions)**

The following two issues are related to footing shape:

- Distinguishing a strip footing from a rectangular footing. The general bearing capacity equation is applicable to strip footings, i.e., footings with  $L_f/B_f \geq 10$ . Therefore, footing shape factors should be included in the equation for the ultimate bearing capacity for rectangular footings with  $L_f/B_f$  ratios less than 10.
- Use of the effective dimensions of footings subjected to eccentric loads. Eccentric loading occurs when a footing is subjected to eccentric vertical loads, a combination

of vertical loads and moments, or moments induced by shear loads transferred to the footing. Abutments and retaining wall footings are examples of footings subjected to this type of loading condition. Moments can also be applied to interior column footings due to skewed superstructures, impact loads from vessels or ice, seismic loads, or loading in any sort of continuous frame. Eccentricity is accounted for by distributing the non-uniform pressure distribution due to the eccentric load as an equivalent uniform pressure over an “effective area” that is smaller than the actual area of the original footing such that the point of application of the eccentric load passes through the centroid of the “effective area.” The eccentricity correction is usually applied by reducing the width ( $B_f$ ) and length ( $L_f$ ) such that:

$$B'_f = B_f - 2e_B \quad 8-7$$

$$L'_f = L_f - 2e_L \quad 8-8$$

where, as shown in Figure 8-16,  $e_B$  and  $e_L$  are the eccentricities in the  $B_f$  and  $L_f$  directions, respectively. These eccentricities are computed by dividing the applied moment in each direction by the applied vertical load. It is important to maintain consistent sign conventions and coordinate directions when this conversion is done. The reduced footing dimensions  $B'_f$  and  $L'_f$  are termed the effective footing dimensions. When eccentric load occurs in both directions, the equivalent uniform bearing pressure is assumed to act over an effective fictitious area,  $A'$ , where (AASHTO, 2004 with 2006 Interims):

$$A' = B'_f L'_f \quad 8-9$$

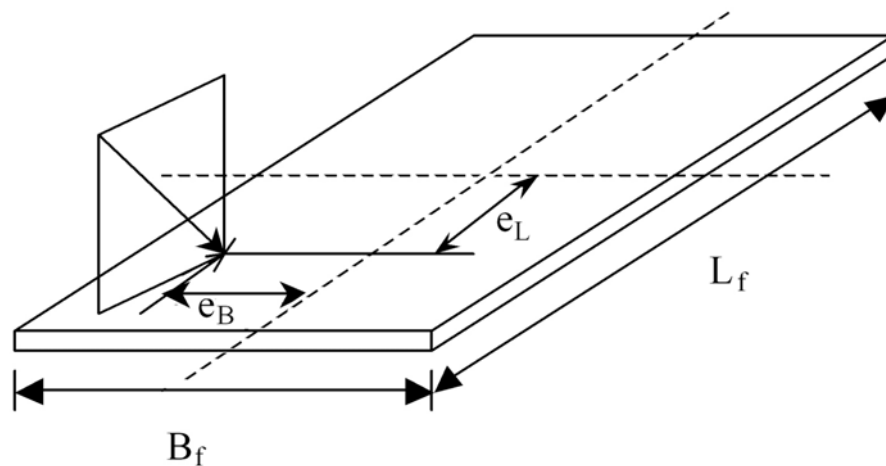


**Figure 8-16. Notations for footings subjected to eccentric, inclined loads (after Kulhawy, 1983).**

The concept of an effective area loaded by an equivalent uniform pressure is an approximation made to account for eccentric loading and was first proposed by Meyerhof (1953). Therefore, the equivalent uniform pressure is often referred to as the “**Meyerhof pressure.**” The concept of equivalent footing and Meyerhof pressure is used for geotechnical analysis during sizing of the footing, i.e., bearing capacity and settlement analyses. However, the structural design of a footing should be performed using the actual trapezoidal or triangular pressure distributions that model the pressure distribution under an eccentrically loaded footing more conservatively. A comparison of the two loading distributions is shown in Figure 8-17.

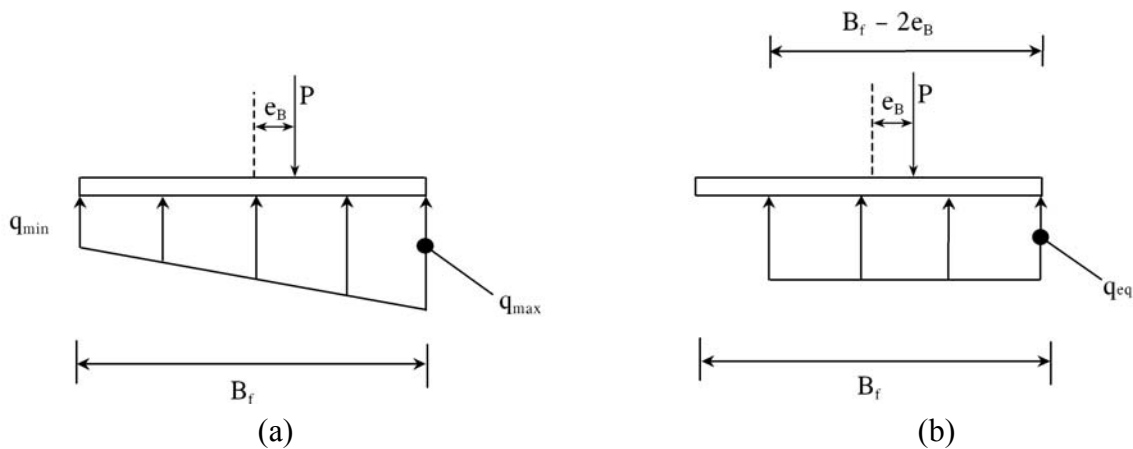


**Figure 8-17. Eccentrically loaded footing with (a) Linearly varying pressure distribution (structural design), (b) Equivalent uniform pressure distribution (sizing the footing).**

Limiting eccentricities are defined to ensure that zero contact pressure does not occur at any point beneath the footing. These limiting eccentricities vary for soil and rock. Footings founded on soil should be designed such that the eccentricity in any direction ( $e_B$  or  $e_L$ ) is less than one-sixth ( $1/6$ ) of the actual footing dimension in the same direction. For footings founded on rock, the eccentricity should be less than one-fourth ( $1/4$ ) of the actual footing dimension. If the eccentricity does not exceed these limits, a separate calculation for stability with respect to overturning need not be performed. If eccentricity does exceed these limits, the footing should be resized.

The shape correction factors are summarized in Table 8-4. For eccentrically loaded footings, AASHTO (2004 with 2006 Interims) recommends use of the effective footing dimensions,  $B'_f$  and  $L'_f$ , to compute the shape correction factors. However, in routine foundation design, use of the effective footing dimensions is not practical since the effective dimensions will

change for various load cases. Besides, the difference in the computed shape correction factors for actual and effective footing dimensions will generally be small. Therefore the geotechnical engineer should make reasonable assumptions about the footing shape and dimensions and compute the correction factors by using the equations in Table 8-4.

**Table 8-4**  
**Shape correction factors (AASHTO, 2004 with 2006 Interims)**

Factor	Friction Angle	Cohesion Term ( $s_c$ )	Unit Weight Term ( $s_\gamma$ )	Surcharge Term ( $s_q$ )
Shape Factors, $s_c, s_\gamma, s_q$	$\phi = 0$	$1 + \left( \frac{B_f}{5L_f} \right)$	1.0	1.0
	$\phi > 0$	$1 + \left( \frac{B_f}{L_f} \right) \left( \frac{N_q}{N_c} \right)$	$1 - 0.4 \left( \frac{B_f}{L_f} \right)$	$1 + \left( \frac{B_f}{L_f} \tan \phi \right)$
<i>Note:</i> Shape factors, $s$ , should not be applied simultaneously with inclined loading factors, $i$ . See Section 8.4.3.5.				

#### 8.4.3.2 Location of the Ground Water Table

If the ground water table is located within the potential failure zone above or below the base of a footing, buoyant (effective) unit weight should be used to compute the overburden pressure. A simplified method for accounting for the reduction in shearing resistance is to apply factors to the two terms in the bearing capacity equation that include a unit weight term. Recall that the cohesion term is neither a function of soil unit weight nor effective stress. The ground water factors may be computed by interpolating values between those provided in Table 8-5 ( $D_w$  = depth to water from ground surface).

**Table 8-5**  
**Correction factor for location of ground water table**  
**(AASHTO, 2004 with 2006 Interims)**

$D_w$	$C_{w\gamma}$	$C_{wq}$
0	0.5	0.5
$D_f$	0.5	1.0
$> 1.5B_f + D_f$	1.0	1.0
<i>Note:</i> For intermediate positions of the ground water table, interpolate between the values shown above.		

### 8.4.3.3 Embedment Depth

Because the effect on bearing capacity of the depth of embedment was accounted for by considering it as an equivalent surcharge applied at the footing bearing elevation, the effect of the shearing resistance due to the failure surface actually passing through the footing embedment cover was neglected in the theory. If the backfill or cover over the footing is known to be a high-quality, compacted granular material that can be assumed to remain in place over the life of the footing, additional shearing resistance due to the backfill can be accounted for by including in the surcharge term the embedment depth correction factor,  $d_q$ , shown in Table 8-6. Otherwise, the depth correction factor can be conservatively omitted.

**Table 8-6**  
**Depth correction factors**  
**(Hansen and Inan, 1970; AASHTO, 2004 with 2006 Interims)**

Friction Angle, $\phi$ (degrees)	$D_f/B_f$	$d_q$
32	1	1.20
	2	1.30
	4	1.35
	8	1.40
37	1	1.20
	2	1.25
	4	1.30
	8	1.35
42	1	1.15
	2	1.20
	4	1.25
	8	1.30
<i>Note:</i> The depth correction factor should be used only when the soils above the footing bearing elevation are as competent as the soils beneath the footing level; otherwise, the depth correction factor should be taken as 1.0.		

Spread footings should be located below the depth of frost potential due to possible frost heave considerations discussed in Section 5.7.3. Figure 5-29 may be used for preliminary guidance on depth of frost penetration. Similarly, footings should be located below the depth of scour to prevent undermining of the footing.

#### 8.4.3.4 Inclined Base

In general, inclined footings for bridges should be avoided or limited to inclination angles,  $\alpha$ , less than about 8 to 10 degrees from the horizontal. Steeper inclinations may require keys, dowels or anchors to provide sufficient resistance to sliding. For footings inclined to the horizontal, Table 8-7 provides equations for the correction factors to be used in Equation 8-6.

**Table 8-7**  
**Inclined base correction factors (Hansen and Inan, 1970; AASHTO, 2004 with 2006 Interims)**

Factor	Friction Angle	Cohesion Term (c)	Unit Weight Term ( $\gamma$ )	Surcharge Term (q)
		$b_c$	$b_\gamma$	$b_q$
Base Inclination	$\phi = 0$	$1 - \left( \frac{\alpha}{147.3} \right)$	1.0	1.0
Factors, $b_c, b_\gamma, b_q$	$\phi > 0$	$b_q - \left( \frac{1 - b_q}{N_c \tan \phi} \right)$	$(1 - 0.017\alpha \tan \phi)^2$	$(1 - 0.017\alpha \tan \phi)^2$
$\phi$ = friction angle, degrees; $\alpha$ = footing inclination from horizontal, upward +, degrees				

#### 8.4.3.5 Inclined Loading

A convenient way to account for the effects of an inclined load applied to the footing by the column or wall stem is to consider the effects of the axial and shear components of the inclined load individually. If the vertical component is checked against the available bearing capacity and the shear component is checked against the available sliding resistance, the inclusion of load inclination factors in the bearing capacity equation can generally be omitted. The bearing capacity should, however, be evaluated by using effective footing dimensions, as discussed in Section 8.4.3.1 and in the footnote to Table 8-4, since large moments can frequently be transmitted to bridge foundations by the columns or pier walls. **The simultaneous application of shape and load inclination factors can result in an overly conservative design.**

Unusual column geometry or loading configurations should be evaluated on a case-by-case basis relative to the foregoing recommendation before the load inclination factors are omitted. An example might be a column that is not aligned normal to the footing bearing surface. In this case, an inclined footing may be considered to offset the effects of the inclined load by providing improved bearing efficiency (see Section 8.4.3.4). Keep in mind that bearing surfaces that are not level may be difficult to construct and inspect.

### 8.4.3.6 Sloping Ground Surface

Placement of footings on or adjacent to slopes requires that the designer perform calculations to ensure that both the bearing capacity and the overall slope stability are acceptable. The bearing capacity equation should include corrections recommended by AASHTO as adapted from NAVFAC (1986b) to design the footings. Calculation of overall (global) stability is discussed in Chapter 6.

For sloping ground surface, Equation 8-6 is modified to include terms  $N_{cq}$  and  $N_{\gamma q}$  that replace the  $N_c$  and  $N_\gamma$  terms. The modified version is given by Equation 8-10. There is no surcharge term in Equation 8-10 because the surcharge effect on the slope side of the footing is ignored.

$$q_{ult} = c(N_{cq})s_c b_c + 0.5\gamma B_f(N_{\gamma q})C_{w\gamma}s_\gamma b_\gamma \quad 8-10$$

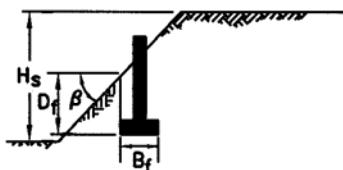
Charts are provided in Figure 8-18 to determine  $N_{cq}$  and  $N_{\gamma q}$  for footings on (Figure 8-18a) or close to (Figure 8-18d) slopes for cohesive ( $\phi = 0^\circ$ ) and cohesionless ( $c = 0$ ) soils. As indicated in Figure 8-18d, the bearing capacity is independent of the slope angle if the footing is located beyond a distance, 'b,' of two to six times the foundation width, i.e., the situation is identical to the case of horizontal ground surface.

Other forms of Equation 8-10 are available for cohesive soils ( $\phi = 0^\circ$ ). However, because footings located on or near slopes consisting of cohesive soils, they are likely to have design limitations due to either settlement or slope stability, or both, the presentation of these equations is omitted here. The reader is referred to NAVFAC (1986a, 1986b) for discussions of these equations and their applications and limitations.

Equation 8-10, which includes the width term for cohesionless soils, is useful in designing footings constructed within bridge approach fills. In this case, obtain  $N_{\gamma q}$  from Figure 8-18(c) or 8-18(f) and then compute the ultimate bearing capacity by using Equation 8-10.

### 8.4.3.7 Layered Soils

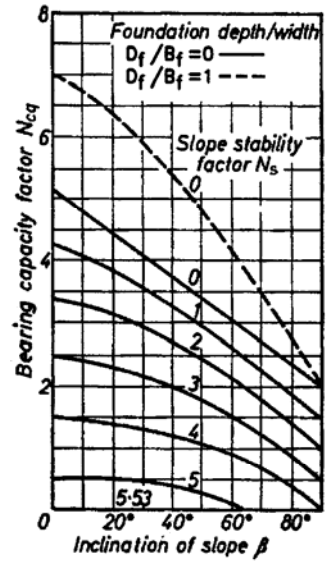
For layered soils, the reader is referred to the guidance provided in AASHTO (2004 with 2006 Interims).



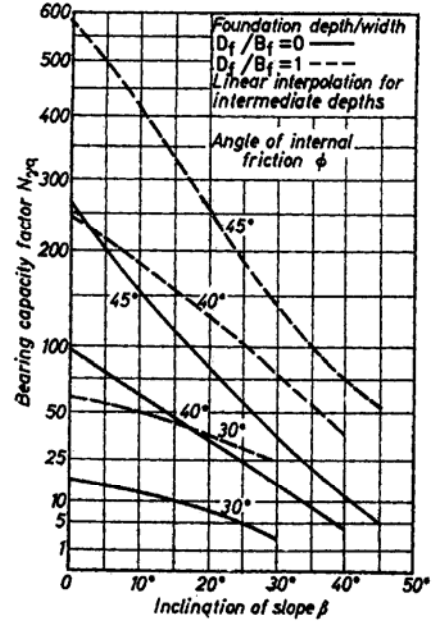
$$N_s = 0 \text{ (FOR } B_f < H_s)$$

$$N_s = \frac{\gamma H_s}{c} \text{ (FOR } B_f \geq H_s)$$

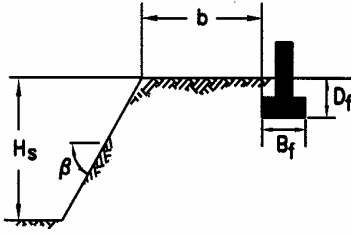
(a) Geometry



(b) Cohesive Soil ( $\phi=0$ )



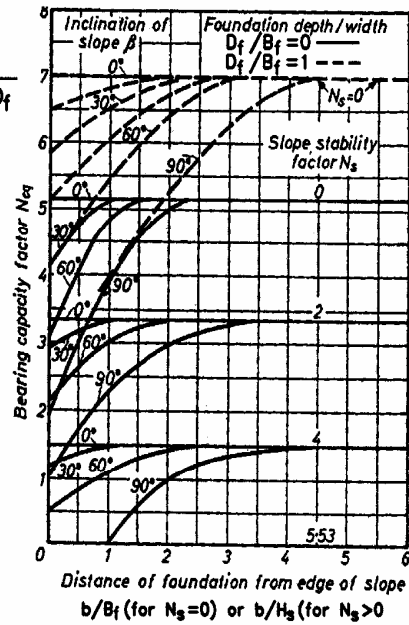
(c) Cohesionless Soil ( $c=0$ )



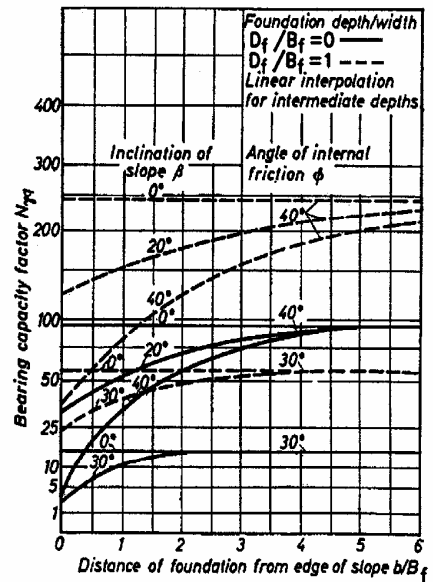
$$N_s = 0 \text{ (FOR } B_f < H_s)$$

$$N_s = \frac{\gamma H_s}{c} \text{ (FOR } B_f \geq H_s)$$

(d) Geometry



(e) Cohesive Soil ( $\phi=0$ )



(f) Cohesionless Soil ( $c=0$ )

**Figure 8-18. Modified bearing capacity factors for continuous footing on sloping ground (after Meyerhof, 1957, from AASHTO, 2004 with 2006 Interims)**

#### 8.4.4 Additional Considerations Regarding Bearing Capacity Correction Factors

The inherent or implied factor of safety of a settlement-limited allowable bearing capacity relative to the computed ultimate bearing capacity is usually large enough to render the magnitude of the application of the individual correction factors small. Some comments in this regards are as follows:

- AASHTO (2002) guidelines recommend calculating the shape factors,  $s$ , by using the effective footing dimensions,  $B'_f$  and  $L'_f$ . However, the original references (e.g., Vesic, 1975) do not specifically recommend using the effective dimensions to calculate the shape factors. Since the geotechnical engineer typically does not have knowledge of the loads causing eccentricity, it is recommended that the full footing dimensions be used to calculate the shape factors according to the equations given in Table 8-4 for use in computation of ultimate bearing capacity.
- Bowles (1996) also recommends that the shape and load inclination factors ( $s$  and  $i$ ) should not be combined.
- In certain loading configurations, the designer should be careful in using inclination factors together with shape factors that have been adjusted for eccentricity (Perloff and Baron, 1976). The effect of the inclined loads may already be reflected in the computation of the eccentricity. Thus an overly conservative design may result.

Further, the bearing capacity correction factors were developed with the assumption that the correction for each of the terms involving  $N_c$ ,  $N_\gamma$  and  $N_q$  can be found independently. The bearing capacity theory is an idealization of the response of a foundation that attempts to account for the soil properties and boundary conditions. Bearing capacity analysis of foundations is frequently limited by the geotechnical engineer's ability to determine material properties accurately as opposed to inadequacies in the theory used to develop the bearing capacity equations. Consider Table 8-2 and note that a one degree change in friction angle can result in a 10 to 15 percent change in the factors  $N_c$ ,  $N_\gamma$  and  $N_q$ . Determination of the in situ friction angle to an accuracy of  $1^\circ$  is virtually impossible. Also note that the value of  $N_\gamma$  more than doubles when the friction angle increases from  $35^\circ$  to  $40^\circ$ . Clearly, the uncertainties in the material properties will control the uncertainty of a bearing capacity computation to a large extent. **The importance of the application of the correction factors is therefore secondary to adequate assessment of the inherent strength characteristics of the foundation soil through correctly performed field investigations and laboratory testing.**

Unfortunately, very few spread footings of the size used for bridge support have been load-tested to failure. Therefore, the evaluation of ultimate bearing capacity is based primarily on theory and laboratory testing of small-scale footings, with modification of the theoretical equations based on observation.

#### 8.4.5 Local or Punching Shear

Several references, including AASHTO (2004 with 2006 Interims), recommend reducing the soil strength parameters if local or punching shear failure modes can develop. Figure 8-19 shows conditions when these modes can develop for granular soils. The recommended reductions are shown in Equations 8-11 and 8-12.

$$c^* = 0.67c \quad 8-11$$

$$\phi^* = \tan^{-1} (0.67 \tan \phi) \quad 8-12$$

where:  $c^*$  = reduced effective stress soil cohesion for punching shear (tsf (MPa))  
 $\phi^*$  = reduced effective stress soil friction angle for punching shear (degrees)

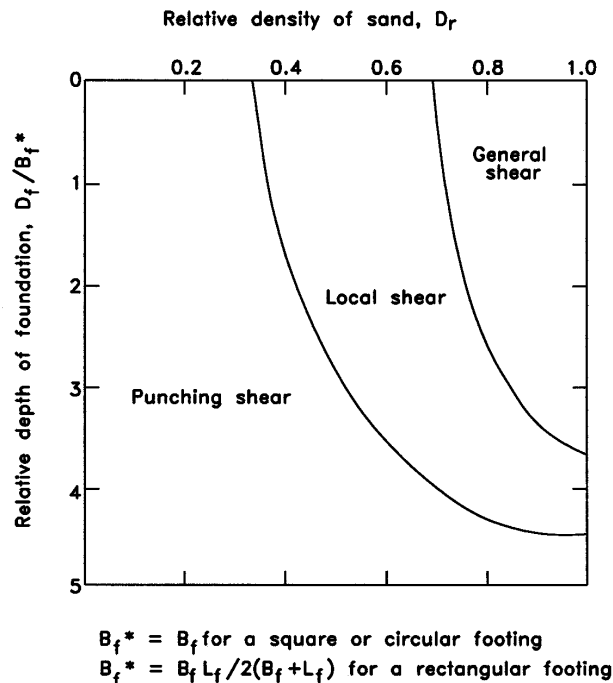


**Figure 8-19. Modes of failure of model footings in sand (after Vesic, 1975; AASHTO, 2004 with 2006 Interims)**

Soil types that can develop local or punching shear failure modes include loose sands, quick clays (i.e., clays with sensitivity,  $S_t > 8$ ; see Table 3-12 in Chapter 3), collapsible sands and silts, and brittle clays ( $OCR > 4$  to 8). As indicated in Section 3.12, **sensitivity of clay** is defined as the ratio of the peak undrained shearing strength to the remolded undrained shearing strength. These soils present potential “problem” conditions that should be identified through a comprehensive geotechnical investigation. In general, these problem soils will have other characteristics that make them unsuitable for the support of shallow foundations for bridges, including large settlement potential for loose sands, sensitive clays and collapsible soils. Brittle clays exhibit relatively high strength at small strains, but they generally undergo significant reduction in strength at larger strains (strain-softening). This behavior should be identified and quantified through the field and laboratory testing program and compared to the anticipated stress changes resulting from the shallow foundation and ground slope configuration under consideration.

Although local or punching shear failure modes can develop in loose sands or when very narrow footings are used, this local condition seldom applies to bridge foundations because spread footings are not used on obviously weak soils. In general, relatively large footing sizes are needed for structural stability of bridge foundations.

The geotechnical engineer may encounter the following two situations where the application of the one-third reduction according to Equation 8-12 can result in an unnecessarily over-conservative design.

- The first is when a footing bears on a cohesionless soil that falls in the local shear portion of Figure 8-19. Note that a one-third reduction in the tangent of a friction angle of 38 degrees, a common value for good-quality, compacted, granular fill, results in a 73 percent reduction in the bearing capacity factor  $N_q$ , and an 81 percent reduction in  $N_\gamma$ . Also note that Figure 8-19 does not consider the effect of large footing widths, such as those used for the support of bridges. **Therefore, provided that settlement potential is checked independently and found to be acceptable, spread footings on normally consolidated cohesionless soils falling within the local shear portion of Figure 8-19 should not be designed by using the one-third reduction according to Equation 8-12.**
- The second situation is when a spread footing bears on a compacted structural fill. The relative density of compacted structural fills as compared to compactive effort, i.e., percent relative compaction, indicates that for fills compacted to a minimum of 95 percent of maximum dry density as determined by AASHTO T 180, the relative

density should be at or above 75 percent (see Figure 5-33 in Chapter 5). This relationship is consistent with the excellent performance history of spread footings in compacted structural fills (FHWA, 1982). Therefore, the one-third reduction should not be used in the design of footings on compacted structural fills constructed with good quality, granular material.

#### 8.4.6 Bearing Capacity Factors of Safety

The minimum factor of safety applied to the calculated ultimate bearing capacity will be a function of:

- The confidence in the design soil strength parameters  $c$  and  $\phi$ ,
- The importance of the structure, and
- The consequence of failure.

Typical minimum factors of safety for shallow foundations are in the range of 2.5 to 3.5. A minimum factor of safety against bearing capacity failure of 3.0 is recommended for most bridge foundations. This recommended factor of safety was selected through a combination of applied theory and experience. **Uncertainty in the magnitudes of the loads and the available soil bearing strength are combined into this single factor of safety.** The general equation to compute the allowable bearing capacity as a function of safety factor is:

$$q_{\text{all}} = \frac{q_{\text{ult}}}{\text{FS}} \quad 8-13$$

where:  $q_{\text{all}}$  = allowable bearing capacity (ksf) (kPa)  
 $q_{\text{ult}}$  = ultimate bearing capacity (ksf) (kPa)  
FS = the applied factor of safety

##### 8.4.6.1 Overstress Allowances

Allowable Strength Design (ASD) criteria permit the allowable bearing capacity to be exceeded for certain load groups (e.g., seismic) by a specified percentage that ranges from 25 to 50 percent (AASHTO, 2002). These overstress allowances are permitted for short-duration, infrequently occurring loads and may also be applied to calculated allowable bearing capacities. Construction loading is often a short-duration loading and may be considered for overstress allowances. **Overstress allowances should not be permitted for cases where soft soils are encountered within the depth of significant influence (DOSI) or durations are such that temporary loads may cause unacceptable settlements.**

## 8.4.7 Practical Aspects of Bearing Capacity Formulations

This section presents some useful practical aspects of bearing capacity formulations. Several interesting observations are made here that provide practical guidance in terms of implementation and interpretation of the bearing capacity formulation and computed results.

### 8.4.7.1 Bearing Capacity Computations

The procedure to be used to compute bearing capacity is as follows:

1. Review the structural plans to determine the proposed footing widths. In the absence of data assume a pier footing width equal to  $1/3$  the pier column height and an abutment footing width equal to  $1/2$  the abutment height.
2. Review the soil profile to determine the position of the groundwater table and the interfaces between soil layer(s) that exist within the appropriate depth below the proposed footing level.
3. Review soil test data to determine the unit weight, friction angle and cohesion of all of the impacted soils. In the absence of test data, estimate these values for coarse-grained granular soils from SPT N-values (refer to Table 8-3). NOTE SPT N-values in cohesive soils should not be used to determine shear strengths for final design since the reliability of SPT N-values in such soils is poor.
4. Use Equation 8-6 with appropriate correction factors to compute the ultimate bearing capacity. The general case (continuous footing) may be used when the footing length is 10 or more times the footing width. Also the bearing capacity factor  $N_\gamma$  will usually be determined for a rough base condition since most footings are poured concrete. However the smoothness of the contact material must be considered for temporary footings such as wood grillages (rough), or steel supports (smooth) or plastic sheets (smooth). The safety factor for the bearing capacity of a spread footing is selected both to limit the amount of soil strain and to account for variations in soil properties at footing locations.
5. The mechanism of the general bearing capacity failure is similar to the embankment slope failure mechanism. However, the footing analysis is a 3-dimensional analysis as opposed to the 2-dimensional slope stability analysis. The bearing capacity factors  $N_c$ ,  $N_q$  and  $N_\gamma$  relate to the actual volume of soil involved in the failure zones. A

cursory study of the failure cross sections in Figure 8-13, discloses that the depth and lateral extent of the failure zones and the values of  $N_c$ ,  $N_q$  and  $N_\gamma$  are determined by the dimensions of the wedge-shaped zone directly below the footing. As the friction angle increases, the depth and width of the failure zones increase, i.e., more soil is impacted and more shear resistance is mobilized, thereby increasing the bearing capacity.

6. Substantial downward movement of the footing is required to mobilize the shearing resistance within the entire failure zone completely. Besides providing a margin of safety on shear strength properties, the relatively large safety factor of 3 commonly used in the design of footings controls the amount of strain necessary to mobilize the allowable bearing capacity fully. Settlement analysis (Section 8.5) is recommended to compute the allowable bearing capacity corresponding to a specified limiting settlement. That allowable bearing capacity may result in a factor of safety with respect to ultimate bearing capacity much larger than 3.
7. In reporting the results of bearing capacity analyses, the footing width that was used to compute the bearing capacity should always be included. Most often the geotechnical engineer must assume a footing width since bearing capacity analyses are completed before structural design begins. It is recommended that bearing capacity be computed for a range of possible footing widths and those values be included in the foundation report with a note stating that if other footing widths are used, the geotechnical engineer should be contacted. The state of the practice today is for the geotechnical engineer to develop location-specific bearing capacity charts on which allowable bearing capacity is plotted versus footing width for a family of curves representing specific values of settlement. Refer to Figure 8-10 for a schematic example of such a chart.
8. The **net** ultimate bearing pressure is the difference between the gross ultimate bearing pressure and the pressure that existed due to the ground surcharge at the bearing depth before the footing was constructed,  $q$  ( $= \gamma_a D_f$ ). The net ultimate bearing pressure can thus be computed by subtracting the ground surcharge ( $q$ ) from Equation 8-6:

$$q_{ult \text{ net}} = q_{ult} - q \quad 8-14$$

$$q_{ult \text{ net}} = cN_c s_c b_c + q(N_q - 1) C_{wq} s_q b_q d_q + 0.5\gamma B_f N_\gamma C_{w\gamma} s_\gamma b_\gamma \quad 8-15$$

The structural designer will typically include the self-weight of the concrete footing and the backfill over the footing (approximately equal to  $\gamma_a D_f$ ) in the loads that contribute to the applied bearing stress. Therefore, if the geotechnical engineer computes and reports a net ultimate bearing pressure, the effect of the surcharge directly over the footing area is counted twice. Reporting an allowable bearing capacity computed from a net ultimate bearing pressure is conservative and generally not recommended provided that a suitable factor of safety is maintained against bearing capacity failure. If the geotechnical engineer chooses to report an allowable bearing capacity computed from a net ultimate bearing pressure, this fact should be clearly stated in the foundation report.

#### 8.4.7.2 Failure Zones

Certain practical information based on the geometry of the failure zone is as follows:

1. The bearing capacity of a footing is dependent on the strength of the soil within a depth of approximately 1.5 times footing width below the base of the footing unless much weaker soils exist just below this level, in which case a potential for punching shear failure may exist. Continuous soil samples and SPT N-values should be routinely specified within this depth. If the borings for a structure are done long before design, a good practice is to obtain continuous split spoon samples for the top 15 ft (4.5 m) of each boring where footings may be placed on natural soil. The cost of this sampling is minimal but the knowledge gained is great. At a minimum, continuous sampling to a depth of 15 ft (4.5 m) will generally provide the following information:
  - a. thickness of existing topsoil.
  - b. location of any thin zones of unsuitable material.
  - c. accurate determination of depth of existing fill.
  - d. improved ground water determination in the critical zone.
  - e. representative samples in this critical zone to permit reliable determination of strength parameters in the laboratory and confident assessment of bearing capacity.
2. Often questions arise during excavation near existing footings as to the effect of soil removal adjacent to the footing on the bearing capacity of that footing. In general, for weaker soils the zone of lateral influence extends outside the footing edge less than twice the footing width. Reductions in bearing capacity can be estimated by

considering the effects of surcharge removal within these zones. The theoretical lateral extent of this zone is shown in Figure 8-20. This figure is also useful in determining the effects of ground irregularities on bearing capacity or the effects of footing loads on adjacent facilities.

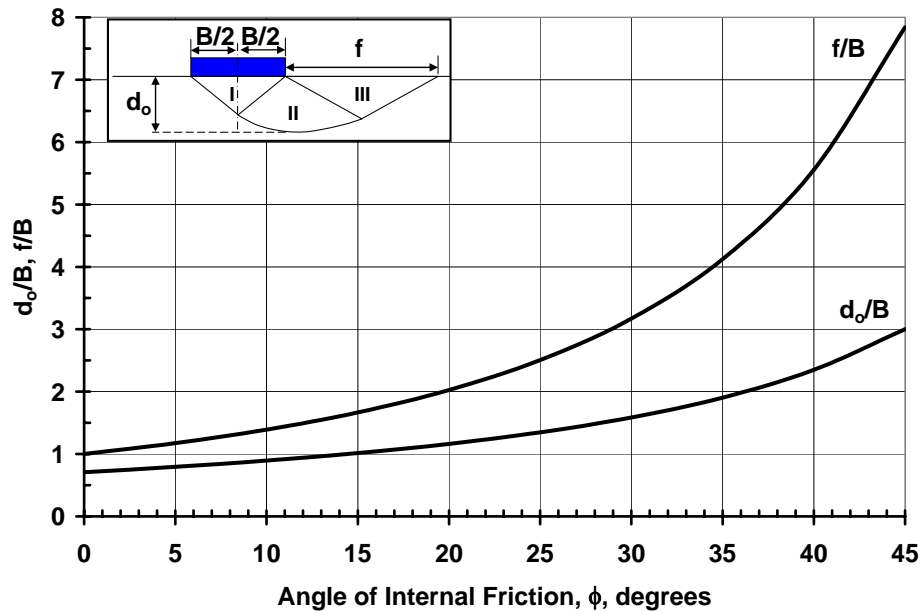


**Figure 8-20. Approximate variation of depth ( $d_o$ ) and lateral extent ( $f$ ) of influence of footing as a function of internal friction angle of foundation soil.**

As noted earlier, the general mechanism by which soils resist a footing load is similar to the foundation of an embankment resists shear failure. The load to cause failure must exceed the available soil strength within the failure zone. When failure occurs the footing plunges into the ground and causes an uplift of the soil adjacent to the sides of the footing. The resistance to failure is based on the soil strength and the amount of soil above the footing. Therefore, the bearing capacity of a footing can be increased by:

1. replacing or densifying the soil below the footing prior to construction.
2. increasing the embedment of the footing below ground, provided no weak soils exist within 1.5 times the footing width.

Common examples of improving bearing capacity are the support of temporary footings on pads of gravel or the embedment of mudsills a few feet below ground to support falsework. The design of these support systems is primarily done by bearing capacity analysis in which the results of subsurface explorations and testing are used. Structural engineers who review falsework designs should carefully check the soil bearing capacity at foundation locations.

## 8.4.8 Presumptive Bearing Capacities

Many building codes include provisions that arbitrarily limit the amount of loading that may be applied on various classes of soils by structures subject to code regulations. These limiting loads are generally based on bearing pressures that have been observed to result in acceptable settlements. The implication is that on the basis of experience alone it may be presumed that each designated class of soil will safely support the loads indicated without the structure undergoing excessive settlements. Such values listed in codes or in the technical literature are termed presumptive bearing capacities.

### 8.4.8.1 Presumptive Bearing Capacity in Soil

**The use of presumptive bearing capacities for shallow foundations bearing in soils is not recommended for final design of shallow foundations for transportation structures, especially bridges.** Guesses about the geology and nature of a site and the application of a presumptive value from generalizations in codes or in the technical literature are not a substitute for an adequate site-specific subsurface investigation and laboratory testing program. As an exception, presumptive bearing values are sometimes used for the preliminary evaluation of shallow foundation feasibility and estimation of footing dimensions for preliminary constructability or cost evaluations.

### 8.4.8.2 Presumptive Bearing Capacity in Rock

Footings on intact sound rock that is stronger and less compressible than concrete are generally stable and do not require extensive study of the strength and compressibility characteristics of the rock. However, site investigations are still required to confirm the consistency and extent of rock formations beneath a shallow foundation.

Allowable bearing capacities for footings on relatively uniform and sound rock surfaces are documented in applicable building codes and engineering manuals. Many different definitions for sound rock are available. **In simple terms, however, “sound rock” can generally be defined as a rock mass that does not disintegrate after exposure to air or water and whose discontinuities are unweathered, closed or tight, i.e., less than about 1/8 in (3 mm) wide and spaced no closer than 3 ft (1 m) apart.** Table 8-8 presents allowable bearing pressures for intact rock recommended in selected local building codes (Goodman, 1989). These values were developed based on experience in sound rock formations, with the intention of satisfying both bearing capacity and settlement criteria in order to provide a satisfactory factor of safety. However, the use of presumptive values may lead to overly conservative and costly foundations. In such cases, most codes allow for a

variance if the request is supported by an engineering report. Site-specific investigation and analysis is strongly encouraged.

In areas where building codes are not available or applicable, other recommended presumptive bearing values, such as those listed in Table 8-9, may be used to determine the allowable bearing pressure for sound rock. For footings designed by using these published values, the elastic settlements are generally less than 0.5 in (13 mm). Where the rock is reasonably sound, but fractured, the presumptive values listed in Tables 8-8 and 8-9 should be reduced by limiting the bearing pressures to tolerable settlements based on settlement analyses. Most building codes also provide reduced recommended bearing pressures to account for the degree of fracturing.

Peck, *et al.* (1974) presented an empirical correlation of presumptive allowable bearing pressure with Rock Quality Designation (RQD), as shown in Table 8-10. If the recommended value of allowable bearing pressure exceeds the unconfined compressive strength of the rock or allowable stress of concrete, the allowable bearing pressure should be taken as the lower of the two values. Although the suggested bearing values of Peck, *et al.* (1974) are substantially greater than most of the other published values and ignore the effects of rock type and conditions of discontinuities, they provide a useful guide for an upper-bound estimation as well as an empirical relationship between allowable bearing values and the intensity of fracturing and jointing (Table 8-10). Note that with a slight increase of the degree of fracturing of the rock mass, for example when the RQD value drops from 100 percent to 90 percent, the recommended bearing capacity value is reduced drastically from 600 ksf (29 MPa) to 400 ksf (19 MPa).

In no instance should the allowable bearing capacity exceed the allowable stress of the concrete used in the structural foundation. Furthermore, Peck, *et al.* (1974) also suggest that the average RQD for the bearing rock within a depth of the footing width ( $B_f$ ) below the base of the footing should be used if the RQD values within the depth are relatively uniform. If rock within a depth of  $0.5B_f$  is of poorer quality, the RQD of the poorer quality rock should be used to determine the allowable bearing capacity.

**Table 8-8****Allowable bearing pressures for fresh rock of various types (Goodman, 1989)**

Rock Type	Age	Location	Allowable Bearing Pressure tsf (MPa)
Massively bedded limestone <sup>5</sup>		U.K. <sup>6</sup>	80 (3.8)
Dolomite	L. Paleoz.	Chicago	100 (4.8)
Dolomite	L. Paleoz.	Detroit	20-200 (1.0 – 9.6)
Limestone	U. Paleoz.	Kansas City	20-120 (0.5 – 5.8)
Limestone	U. Paleoz.	St. Louis	50-100 (2.4 – 4.8)
Mica schist	Pre-Camb.	Washington	20-40 (0.5 – 1.9)
Mica schist	Pre-Camb.	Philadelphia	60-80 (2.9 – 3.8)
Manhattan schist	Pre-Camb.	New York	120 (5.8)
Fordham gneiss	Pre-Camb.	New York	120 (5.8)
Schist and slate	-	U.K. <sup>6</sup>	10-25 (0.5 – 1.2)
Argillite	Pre-Camb.	Cambridge, MA	10-25 (0.5 – 1.2)
Newark shale	Triassic	Philadelphia	10-25 (0.5 – 1.2)
Hard, cemented shale	-	U.K. <sup>6</sup>	40 (1.9)
Eagleford shale	Cretaceous	Dallas	13-40 (0.6 – 1.9)
Clay shale	-	U.K. <sup>6</sup>	20 (1.0)
Pierre shale	Cretaceous	Denver	20-60 (1.0 – 2.9)
Fox Hills sandstone	Tertiary	Denver	20-60 (1.0 – 2.9)
Solid chalk	Cretaceous	U.K. <sup>6</sup>	13 (0.6)
Austin chalk	Cretaceous	Dallas	30-100 (1.4 – 4.8)
Friable sandstone and claystone	Tertiary	Oakland	8-20 (0.4 – 1.0)
Friable sandstone (Pico formation)	Quaternary	Los Angeles	10-20 (0.5 – 1.0)

*Notes:*

<sup>1</sup> According to typical building codes; reduce values accordingly to account for weathering or unrepresentative fracturing

<sup>2</sup> Values from Thorburn (1966) and Woodward, Gardner and Greer (1972).

<sup>3</sup> When a range is given, it relates to usual range in rock conditions.

<sup>4</sup> Sound rock that rings when struck and does not disintegrate. Cracks are unweathered and open less than 10 mm.

<sup>5</sup> Thickness of beds greater than 3 ft (1 m), joint spacing greater than 2 mm; unconfined compressive strength greater than 160 tsf (7.7 MPa) (for a 4 in (100 mm) cube).

<sup>6</sup> Institution of Civil Engineers Code of Practice 4.

**Table 8-9**

**Presumptive values of allowable bearing pressures for spread foundations on rock  
(modified after NAVFAC, 1986a, AASHTO 2004 with 2006 Interims)**

Type of Bearing Material	Consistency In Place	Allowable Bearing Pressure tsf (MPa)	
		Range	Recommended Value for Use
Massive crystalline igneous and metamorphic rock: granite, diorite, basalt, gneiss, thoroughly cemented conglomerate (sound condition allows minor cracks)	Hard, sound rock	120-200 (5.8 - 9.6)	160 (7.7)
Foliated metamorphic rock: Slate, schist (sound condition allows minor cracks)	Medium-hard, sound rock	60-80 (2.9-3.8)	70 (3.4)
Sedimentary rock; hard cemented shales, siltstone, sandstone, limestone without cavities	Medium-hard, sound rock	30-50 (1.4-2.4)	40 (1.9)
Weathered or broken bedrock of any kind except highly argillaceous rock (shale). RQD less than 25	Soft rock	16-24 (0.8-1.2)	20 (1)
Compacted shale or other highly argillaceous rock in sound condition	Soft rock	16-24 (0.8-1.2)	20 (1)

*Notes:*

1. For preliminary analysis or in the absence of strength tests, design and proportion shallow foundations to distribute their loads by using presumptive values of allowable bearing pressure given in this table. Modify the nominal value of allowable bearing pressure for special conditions described in notes 2 through 8.
2. The maximum bearing pressure beneath the footing produced by eccentric loads that include dead plus normal live load plus permanent lateral loads shall not exceed the above nominal bearing pressure.
3. Bearing pressures up to one-third in excess of the nominal bearing values are permitted for transient live load from wind or earthquake. If overload from wind or earthquake exceeds one-third of nominal bearing pressures, increase allowable bearing pressures by one-third of nominal value.
4. Extend footings on soft rock to a minimum depth of 1.5 in (40 mm) below adjacent ground surface or surface of adjacent floor, whichever elevation is the lowest.
5. For footings on soft rock, increase allowable bearing pressures by 5 percent of the nominal values for each 1 ft (300 mm) of depth below the minimum depth specified in Note 4.
6. Apply the nominal bearing pressures of the three categories of hard or medium hard rock shown above where the base of the foundation lies on rock surface. Where the foundation extends below the rock surface, increase the allowable bearing pressure by 10 percent of the nominal values for each additional 1ft (300 mm) of depth extending below the surface.
7. For footings smaller than 3 ft (1 m) in the least lateral dimension, the allowable bearing pressure shall be the nominal bearing pressure multiplied by the least lateral dimension.
8. If the above-recommended nominal bearing pressure exceeds the unconfined compressive strength of intact specimen, the allowable pressure equals the unconfined compressive strength.

**Table 8-10**

**Suggested values of allowable bearing capacity (Peck, *et al.*, 1974)**

RQD (%)	Rock Mass Quality	Allowable Pressure ksf (MPa)
100	Excellent	600 (29)
90	Good	400 (19)
75	Fair	240 (12)
50	Poor	130 (6)
25	Very Poor	60 (3)
0	Soil-like	20 (1)

## **8.5 SETTLEMENT OF SPREAD FOOTINGS**

The controlling factor in the design of a spread footing is usually tolerable settlement. Estimation of settlement may be routinely accomplished with adequate geotechnical data and knowledge of the structural loads. The accuracy of the estimation is only as good as the quality of the geotechnical data and the estimation of the actual loads. Settlements of spread footings are frequently overestimated by engineers for the following reasons:

1. The structural load causing the settlement is overestimated. In the absence of actual structural loads, geotechnical engineers conservatively assume that the footing pressure equals the maximum allowable soil bearing pressure.
2. Settlement occurring during construction is not subtracted from total predicted amounts (See discussion in Section 8.9 for more details).
3. Preconsolidation of the subsoil is not accounted for in the analysis. Preconsolidation may be due to a geologic load applied in past time or to removal of significant amounts of soil in construction prior to placement of the foundation. This error can cause a grossly overestimated settlement.

As explained in Chapter 7, there are two primary types of settlement, immediate (short-term) and consolidation (long-term). The procedures for computing these settlements under spread footings are similar to those under embankments as discussed in Chapter 7. The following sections illustrate the computation of immediate and consolidation settlements.

### **8.5.1 Immediate Settlement**

As noted in Chapter 7, there are several methods available to evaluate immediate settlements. Modified Hough's method was introduced in Chapter 7 and was illustrated by an example. Modified Hough's method can also be applied to shallow foundations by using the same approach demonstrated in Chapter 7. Studies conducted by FHWA (1987) indicate that Modified Hough's procedure is conservative and over-predicts settlement by a factor of 2 or more. Such conservatism may be acceptable for the evaluation of the settlement of embankments due to reasons discussed in Chapter 7. However, in the case of shallow foundations such conservatism may lead to unnecessary use of costlier deep foundations in cases where shallow foundations may be viable. Therefore, use of a more rigorous procedure such Schmertmann's modified method (1978) is recommended for shallow foundations, and is presented here.

### 8.5.1.1 Schmertmann's Modified Method for Calculation of Immediate Settlements

An estimate of the immediate settlement,  $S_i$ , of spread footings can be made by using Equation 8-16 as proposed by Schmertmann, *et al.* (1978).

$$S_i = C_1 C_2 \Delta p \sum_{i=1}^n \Delta H_i \quad \text{where} \quad \Delta H_i = H_c \left( \frac{I_z}{XE} \right) \quad 8-16$$

where:  $I_z$  = strain influence factor from Figure 8-21a. The dimension  $B_f$  represents the least lateral dimension of the footing after correction for eccentricities, i.e. use least lateral effective footing dimension. The strain influence factor is a function of depth and is obtained from the strain influence diagram. The strain influence diagram is easily constructed for the axisymmetric case ( $L_f/B_f = 1$ ) and the plane strain case ( $L_f/B_f \geq 10$ ) as shown in Figure 8-21a. The strain influence diagram for intermediate conditions can be determined by simple linear interpolation.

$n$  = number of soil layers within the zone of strain influence (strain influence diagram).

$\Delta p$  = **net** uniform applied stress (load intensity) at the foundation depth (see Figure 8-21b).

$E$  = elastic modulus of layer  $i$  based on guidance provided in Table 5-16 in Chapter 5.

$X$  = a factor used to determine the value of elastic modulus. If the value of elastic modulus is based on correlations with  $N_{160}$ -values or  $q_c$  from Table 5-16 in Chapter 5, then use  $X$  as follows.

$X = 1.25$  for axisymmetric case ( $L_f/B_f = 1$ )

$X = 1.75$  for plane strain case ( $L_f/B_f \geq 10$ )

Use interpolation for footings with  $1 < L_f/B_f \leq 10$

If the value of elastic modulus is estimated based on the range of elastic moduli in Table 5-16 or other sources use  $X = 1.0$ .

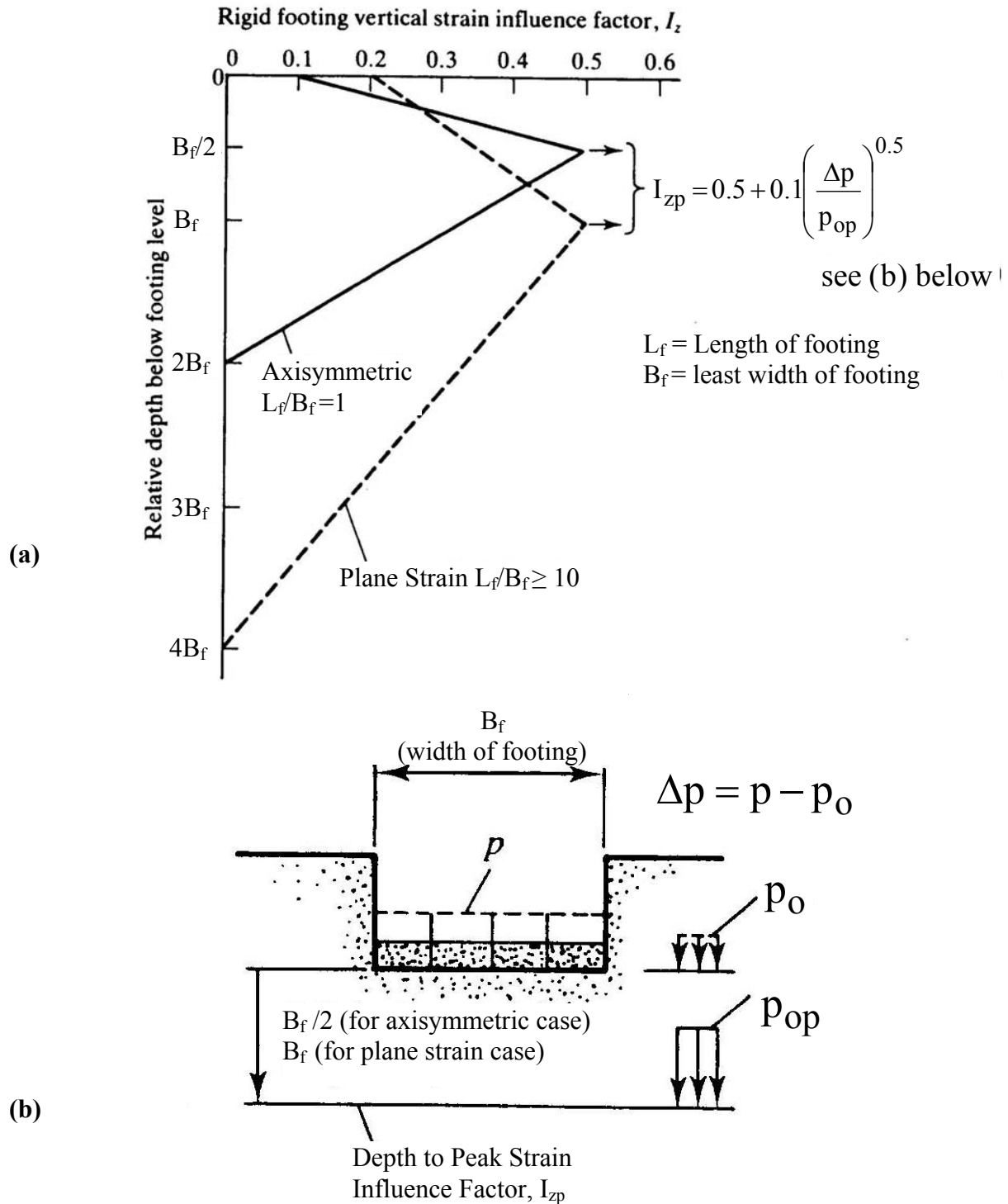


**Figure 8-21. (a) Simplified vertical strain influence factor distributions, (b) Explanation of pressure terms in equation for  $I_{zp}$  (after Schmertmann, *et al.*, 1978).**

$C_1$  = a correction factor to incorporate the effect of strain relief due to embedment where:

$$C_1 = 1 - 0.5 \left( \frac{p_o}{\Delta p} \right) \geq 0.5 \quad 8-17$$

where  $p_o$  is effective in-situ overburden stress at the foundation depth and  $\Delta p$  is the net foundation pressure as shown in Figure 8-21b

$C_2$  = a correction factor to incorporate time-dependent (creep) increase in settlement for  $t$  (years) after construction where:

$$C_2 = 1 + 0.2 \log_{10} \left( \frac{t(\text{years})}{0.1} \right) \quad 8-18$$

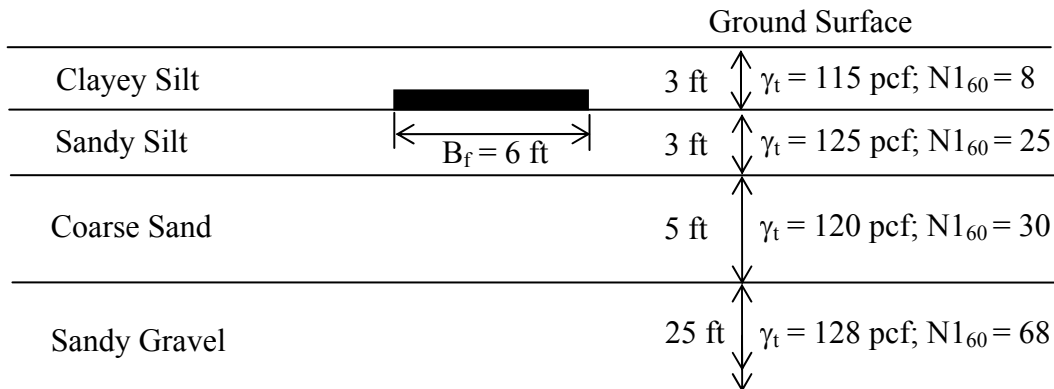
### 8.5.1.2 Comments on Schmertmann's Method

- **Effect of lateral strain:** Schmertmann and his co-workers based their method on the results of displacement measurements within sand masses loaded by model footings, as well as finite element analyses of deformations of materials with nonlinear stress-strain behavior that expressly incorporated Poisson's ratio. Therefore, the effect of the lateral strain on the vertical strain is included in the strain influence factor diagrams.
- **Effect of preloading:** The equations used in Schmertmann's method are applicable to normally loaded sands. If the sand was pre-strained by previous loading, then the actual settlements will be overpredicted. Schmertmann, *et al.* (1978) recommend a reduction in settlement after preloading or other means of compaction of half the predicted settlement. Alternatively, in case of preloaded soil deposits, the settlement can be computed by using the method proposed by D'Appolonia (1968, 1970), which includes explicit consideration of preloading.
- **$C_2$  correction factor:** The time duration,  $t$ , in Equation 8-18 is set to 0.1 years to evaluate the settlement immediately after construction, i.e.,  $C_2 = 1$ . If long-term creep deformation of the soil is suspected then an appropriate time duration,  $t$ , can be used in the computation of  $C_2$ . **As explained in Sections 5.4.1 and 7.6, creep deformation is not the same as consolidation settlement.** This factor can have an important influence on the reported settlement since it is included in Equation 8-16 as a multiplier. For example, the  $C_2$  factor for time durations of 0.1 yrs, 1 yr, 10 yrs and 50 yrs are 1.0, 1.2, 1.4 and 1.54, respectively. In cohesionless soils and unsaturated fine-grained cohesive

soils with low plasticity, time durations of 0.1 yr and 1 yr, respectively, are generally appropriate and sufficient for cases of static loads. Where consolidation settlement is estimated in addition to immediate settlement,  $C_2 = 1$  should be used.

The use of Schmertmann's modified method to calculate immediate settlement is illustrated numerically in Example 8-2.

**Example 8-2:** A 6 ft x 24 ft footing is founded at a depth of 3 ft below ground elevation with the soil profile and average  $N_{160}$  values shown. Determine the settlement in inches (a) at the end of construction and (b) 1 year after construction. There is no groundwater. The footing is subjected to an applied stress of 2,000 psf.



**Solution:**

**Step 1:** Begin by drawing the strain influence diagram. The  $L_f/B_f$  ratio for the footing is  $24'/6' = 4$ . From Figure 8-21(a), determine the value of the strain influence factor at the base of the footing,  $I_{ZB}$ , as follows:

$$I_{ZB} = 0.1 \text{ for axisymmetric case } (L_f/B_f = 1)$$

$$I_{ZB} = 0.2 \text{ for plane strain case } (L_f/B_f \geq 10)$$

Difference between axisymmetric  $L_f/B_f$  and plane strain  $L_f/B_f = 9$

Difference between axisymmetric  $I_{ZB}$  and plane strain  $I_{ZB} = 0.1$

Use linear interpolation for  $L_f/B_f = 4$ :

$\Delta(L_f/B_f)$  with respect to axisymmetric  $L_f/B_f = 4 - 1 = 3$ . Therefore

$$I_{ZB} = 0.1 + \frac{(0.2 - 0.1)}{9}(3) = 0.1 + \frac{0.1}{3} = 0.133$$

**Step 2:** Determine the maximum depth of influence,  $D_I$ , as follows:

$$D_I = 2B_f \quad \text{for } L_f/B_f = 1$$

$$D_I = 4B_f \quad \text{for } L_f/B_f > 10$$

By using linear interpolation  $L_f/B_f = 4$  as before:

$\Delta (L_f/B_f)$  with respect to axisymmetric  $L_f/B_f = 4-1 = 3$ . Therefore

$$D_I = 2B_f + \frac{(4B_f - 2B_f)}{9}(3) = 2B_f + \frac{2B_f}{3} = \frac{6B_f + 2B_f}{3} = \frac{8B_f}{3}$$

$$D_I = \frac{8}{3}(6 \text{ ft}) = 16 \text{ ft}$$

**Step 3:** Determine the depth to the peak strain influence factor,  $D_{IP}$ , as follows:

$$\text{From Figure 8-21(a)} \quad D_{IP} = B_f/2 \quad \text{for } L_f/B_f = 1$$

$$D_{IP} = B_f \quad \text{for } L_f/B_f > 10$$

Use linear interpolation for  $L_f/B_f = 4$ :

$\Delta (L_f/B_f)$  with respect to axisymmetric  $L_f/B_f = 4-1 = 3$ . Therefore

$$D_{IP} = \frac{B_f}{2} + \frac{\left(B_f - \frac{B_f}{2}\right)}{9}(3) = \frac{B_f}{2} + \frac{B_f}{6} = \frac{3B_f + B_f}{6} = \frac{4B_f}{6}$$

$$D_{IP} = \frac{4}{6}(6 \text{ ft}) = 4 \text{ ft}$$

**Step 4:** Determine the value of the maximum strain influence factor,  $I_{ZP}$ , as follows:

$$I_{ZP} = 0.5 + 0.1 \left( \frac{\Delta p}{p_{op}} \right)^{0.5}$$

$$\Delta p = 2,000 \text{ psf} - 3 \text{ ft}(115 \text{ pcf}) = 1,655 \text{ psf}$$

$$p_{op} = 3 \text{ ft}(115 \text{ pcf}) + 3 \text{ ft}(125 \text{ pcf}) + 1 \text{ ft}(120 \text{ pcf})$$

$$p_{op} = 345 \text{ psf} + 375 \text{ psf} + 120 \text{ psf} = 840 \text{ psf}$$

$$I_{ZP} = 0.5 + 0.1 \sqrt{\frac{1,655 \text{psf}}{840 \text{psf}}} = 0.64$$

**Step 5:** Draw the  $I_Z$  vs. depth diagram as follows and divide it into convenient layers by using the following guidelines:

- The depth of the peak value of the strain influence is fixed. To aid in the computation, develop the layering such that one of the layer boundaries occurs at this depth even though it requires that an actual soil layer be sub-divided.
- Limit the top layer as well as the layer immediately below the peak value of influence factor,  $I_{zp}$ , to  $2/3B_f$  or less to adequately represent the variation of the influence factor within  $D_{IP}$ .
- Limit maximum layer thickness to 10 ft (3 m) or less.
- Match the layer boundary with the subsurface profile layering.

In accordance with the above guidelines, the influence depth of 16 ft is divided into 4 layers as shown below. Since the strain influence diagram starts at the base of the footing, the thickness of Layer 1 corresponds to the thickness of the sandy silt layer shown in the soil profile. Likewise, Layer 4 corresponds to the thickness of the sandy gravel layer that has been impacted by the strain influence diagram. The sum of the thicknesses of Layers 2 and 3 correspond to the thickness of the coarse sand layer shown in the soil profile. The subdivision is made to account for the strain influence diagram going through its peak value within the coarse sand layer. The minimum and maximum layer thicknesses are 1 ft (Layer 2) and 8 ft (Layer 4), respectively. The layer boundaries are shown by solid lines while the layer centers are shown by dashed lines.

**Step 6:** Determine value of elastic modulus  $E_s$  from Table 5-16 from Chapter 5.

Layer 1: Sandy Silt:  $E = 4N_{160}$  tsf

Layer 2: Coarse Sand:  $E = 10N_{160}$  tsf

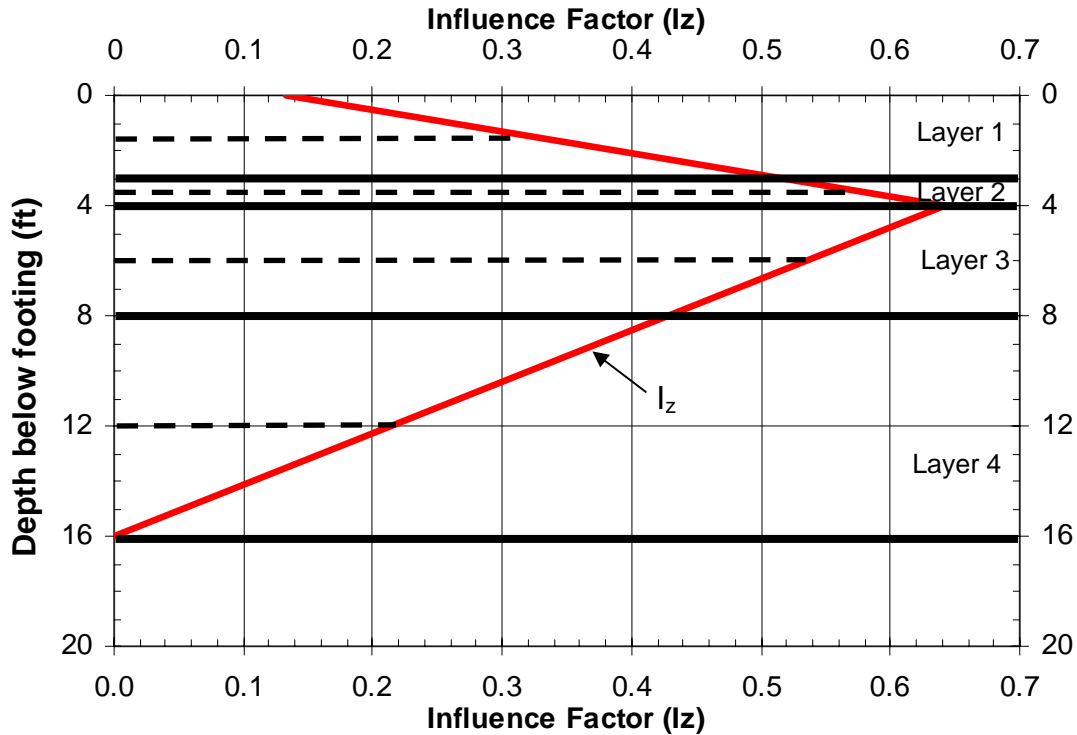
Layer 3: Coarse Sand:  $E = 10N_{160}$  tsf

Layer 4: Sandy Gravel:  $E = 12N_{160}$  tsf

Since the elastic modulus  $E_s$  is based on correlations with  $N_{160}$ -values obtained from Table 5-16, calculate the X multiplication factor as follows:

$X = 1.25$  for  $L_f/B_f = 1$

$X = 1.75$  for  $L_f/B_f \geq 10$



Use linear interpolation for  $L_f/B_f = 4$

$\Delta (L_f/B_f)$  with respect to axisymmetric  $L_f/B_f = 4-1 = 3$

$$X = 1.25 + \frac{(1.75 - 1.25)}{9}(3) = 1.42$$

**Step 7:** Using the thickness of each layer,  $H_c$ , and the relevant values for that particular layer, determine the settlement by setting up a table as follows:

Layer	$H_c$ (inches)	$N_{160}$	$E$ (tsf)	$XE$ (tsf)	$Z_1$ (ft)	$I_z$ at $Z_i$	$\Delta H_i = \frac{I_z}{XE} H_c$ (in/tsf)
1	36	25	100	142	1.5	0.323	0.0819
2	12	30	300	426	3.5	0.577	0.0163
3	48	30	300	426	6	0.533	0.0601
4	96	68	816	1,159	12	0.213	0.0177
$\Sigma H_i =$							<b>0.1760</b>

**Step 8:** Determine embedment factor ( $C_1$ ) and creep factor ( $C_2$ ) as follows:

a) Embedment factor

$$C_1 = 1 - 0.5 \left( \frac{p_o}{\Delta p} \right) = 1 - 0.5 \left( \frac{3 \text{ ft} \times 115 \text{ pcf}}{1655 \text{ psf}} \right) = 0.896$$

b) Creep Factor

$$C_2 = 1 + 0.2 \log_{10} \left( \frac{t(\text{years})}{0.1} \right)$$

- For end of construction  $t(\text{yrs}) = 0.1 \text{ yr}$  (1.2 months)

$$C_2 = 1 + 0.2 \log_{10} \left( \frac{0.1}{0.1} \right) = 1.0$$

- For end of 1 year:

$$C_2 = 1 + 0.2 \log_{10} \left( \frac{1}{0.1} \right) = 1.2$$

**Step 9:** Determine the settlement at end of construction as follows:

$$S_i = C_1 C_2 \Delta p \sum H_i$$

$$S_i = (0.896)(1.0) \left( \frac{1,655 \text{ psf}}{2,000 \text{ psf/tsf}} \right) \left( 0.1760 \frac{\text{in}}{\text{tsf}} \right)$$

$$S_i = 0.130 \text{ inches}$$

**Step 10:** Determine the settlement after 1 year as follows:

$$S_i = 0.130 \text{ inches} \left( \frac{1.2}{1.0} \right) = 0.156 \text{ inches}$$

### 8.5.1.3 Tabulation of Parameters in Schmertmann's Method

To facilitate computations, Table 8-11 presents a tabulation of the various parameters involved in computation of settlement by Schmertmann's method. This table was generated by using the linear interpolation scheme demonstrated in Example 8-2. Linear interpolation may be used for  $L_f/B_f$  values between those presented in Table 8-11.

Table 8-11

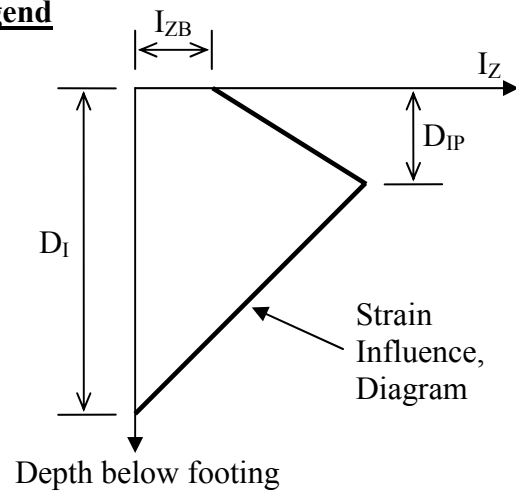
Values of parameters used in settlement analysis by Schmertmann's method

$L_f/B_f$	$I_z$ at footing base, $I_{zB}$	Depth to $I_{zp}$ , $D_{IP}$	Depth of $I_z$ diagram, $D_1$	X factor	$L_f/B_f$	$I_z$ at footing base, $I_{zB}$	Depth to $I_{zp}$ , $D_{IP}$	Depth of $I_z$ diagram, $D_1$	X factor
		Note 1	Note 1	Note 2			Note 1	Note 1	Note 2
<b>1.00</b>	<b>0.100</b>	<b>0.500</b>	<b>2.000</b>	<b>1.250</b>	<b>6.00</b>	<b>0.156</b>	<b>0.778</b>	<b>3.111</b>	<b>1.528</b>
1.25	0.103	0.514	2.056	1.264	6.25	0.158	0.792	3.167	1.542
1.50	0.106	0.528	2.111	1.278	6.50	0.161	0.806	3.222	1.556
1.75	0.108	0.542	2.167	1.292	6.75	0.164	0.819	3.278	1.569
<b>2.00</b>	<b>0.111</b>	<b>0.556</b>	<b>2.222</b>	<b>1.306</b>	<b>7.00</b>	<b>0.167</b>	<b>0.833</b>	<b>3.333</b>	<b>1.583</b>
2.25	0.114	0.569	2.278	1.319	7.25	0.169	0.847	3.389	1.597
2.50	0.117	0.583	2.333	1.333	7.50	0.172	0.861	3.444	1.611
2.75	0.119	0.597	2.389	1.347	7.75	0.175	0.875	3.500	1.625
<b>3.00</b>	<b>0.122</b>	<b>0.611</b>	<b>2.444</b>	<b>1.361</b>	<b>8.00</b>	<b>0.178</b>	<b>0.889</b>	<b>3.556</b>	<b>1.639</b>
3.25	0.125	0.625	2.500	1.375	8.25	0.181	0.903	3.611	1.653
3.50	0.128	0.639	2.556	1.389	8.50	0.183	0.917	3.667	1.667
3.75	0.131	0.653	2.611	1.403	8.75	0.186	0.931	3.722	1.681
<b>4.00</b>	<b>0.133</b>	<b>0.667</b>	<b>2.667</b>	<b>1.417</b>	<b>9.00</b>	<b>0.189</b>	<b>0.944</b>	<b>3.778</b>	<b>1.694</b>
4.25	0.136	0.681	2.722	1.431	9.25	0.192	0.958	3.833	1.708
4.50	0.139	0.694	2.778	1.444	9.50	0.194	0.972	3.889	1.722
4.75	0.142	0.708	2.833	1.458	9.75	0.197	0.986	3.944	1.736
<b>5.00</b>	<b>0.144</b>	<b>0.722</b>	<b>2.889</b>	<b>1.472</b>	<b>10.00</b>	<b>0.200</b>	<b>1.000</b>	<b>4.000</b>	<b>1.750</b>
5.25	0.147	0.736	2.944	1.486	<b>&gt; 10</b>	<b>0.200</b>	<b>1.000</b>	<b>4.000</b>	<b>1.750</b>
5.50	0.150	0.750	3.000	1.500					
5.75	0.153	0.764	3.056	1.514					

**Notes:**

1. The depths are obtained by multiplying the value in this column by the footing width,  $B_f$ .
2. If elastic modulus is not based on SPT or CPT, then  $X=1.0$ . See Section 8.5.1.1 for a discussion on values of X factor.

**Legend**



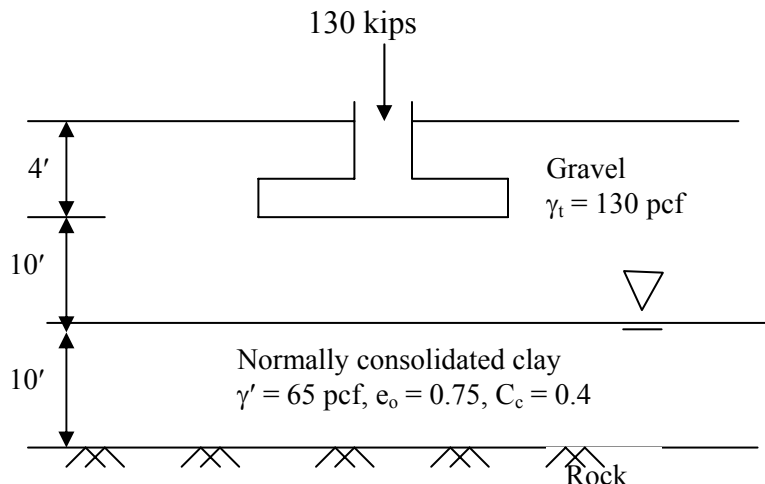
### 8.5.2 Obtaining Limiting Applied Stress for a Given Settlement

As indicated in Section 8.3, the allowable bearing capacity based on settlement considerations is defined as “the applied stress that results in a specified amount of settlement.” Thus, the quantity of interest is often the limiting applied stress for a specified amount of settlement. In this case, Equation 8-16 can be inverted and solved to obtain the limiting applied stress,  $\Delta p$ , for a given settlement,  $S_i$ . By repeating the computation for a range of settlement values, the curves shown in Zone B of Figure 8-10 can be generated. It is important to realize that the applied stress computed by the inverted form of Equation 8-16 is a uniform stress. Consequently, that value of stress should be compared to the Meyerhof equivalent uniform pressure ( $q_{eq}$ ) acting on an effective footing width as shown in Figure 8-17b and not the maximum stress ( $q_{max}$ ) of the trapezoidal pressure distribution on the total footing width as shown in Figure 8-17a. It is for this reason that the X-axis of an allowable bearing capacity chart refers to an effective footing width and not total footing width.

### 8.5.3 Consolidation Settlement

The procedures to compute consolidation settlements discussed in Chapter 7 can be applied to spread footings also. The following example illustrates the method for determining consolidation settlement due to a load applied to a spread footing.

**Example 8-3:** Determine the settlement of the 10 ft  $\times$  10 ft square footing due to a 130 kip axial load. Assume the gravel layer is incompressible.



**Solution:**

Find overburden pressure,  $p_o$ , at center of clay layer

$$p_o = (14 \text{ ft} \times 130 \text{ pcf}) + (5 \text{ ft} \times 65 \text{ pcf}) = 2,145 \text{ psf}$$

Find change in pressure ( $\Delta p$ ) at center of clay layer due to applied load. Use the approximate 2:1 stress distribution method discussed in Section 2.5 of Chapter 2.

$$\Delta p = \frac{130 \text{ kips}}{(10 \text{ ft} + 15 \text{ ft})^2} = \frac{130 \text{ kips}}{625 \text{ ft}} = 0.208 \text{ ksf} = 208 \text{ psf}$$

Use Equation 7-2 to calculate the magnitude of consolidation settlement.

$$\Delta H = H \frac{C_c}{1 + e_o} \log_{10} \left( \frac{p_o + \Delta p}{p_o} \right)$$
$$\Delta H = 10 \text{ ft} \left( \frac{0.4}{1 + 0.75} \right) \log_{10} \left( \frac{2,145 \text{ psf} + 208 \text{ psf}}{2,145 \text{ psf}} \right) = 0.09 \text{ ft} = 1.1 \text{ in}$$

In reality, the magnitude of the total settlement of the foundation would be the sum of the consolidation settlement of the clay and the immediate settlement of the gravel. The gravel was assumed to be incompressible in this example. However, in practice, the component of the total settlement due to the immediate settlement of the gravel would be determined by using Schmertmann's method with only that portion of the strain influence diagram in the gravel being considered.

## 8.6 SPREAD FOOTINGS ON COMPACTED EMBANKMENT FILLS

Geotechnical engineers have long recognized the desirability of placing footings on engineered fills. In general, the load imposed by the weight of the fill is many times that of the imposed footing load. If adequate time is allowed for the foundation soils to settle under the fill load, subsequent application of a smaller structural load will result in negligible settlement of the structure. In bridge construction, common practice is to build the approach embankment excluding the area to be occupied by the abutment and allow settlement to occur prior to abutment construction. Details of the settlement of approach embankment fills are presented in Chapter 7.

Field evaluation of spread footings placed in or on engineered fills constructed of select granular material, show that spread footings provide satisfactory performance, i.e., minimal vertical and lateral displacements, if all relevant factors are considered in the design of the embankment and the footing. A performance evaluation of spread footings on compacted embankment fills was conducted through a joint study between FHWA and the Washington State Department of Transportation (FHWA, 1982). A visual inspection was made of the structural condition of 148 highway bridges supported by spread footings on engineered fills throughout the State of Washington. The approach pavements and other bridge appurtenances were also inspected for damage or distress that could be attributed to the use of spread footings on engineered fill. This review, in conjunction with detailed survey investigations of the foundation movement of 28 selected bridges, was used to evaluate the performance of spread footings on engineered fills. None of the bridges investigated displayed any safety problems or serious functional distress. The study concluded that spread footings can provide a satisfactory alternative to deep foundations, especially when high embankments of good quality borrow materials are constructed over satisfactory foundation soils. Further studies were made to substantiate the feasibility of using spread footings in lieu of more expensive deep foundation systems. Cost analyses showed that spread footings were 50 to 65 percent less expensive than the alternate choice of deep foundations. Studies of foundation movement showed that bridges easily tolerated differential settlements of 1 to 3 inches (25 to 75 mm) without serious distress.

In addition to the FHWA (1982) study which was limited to the bridges in the State of Washington, a nationwide study of 314 bridges was conducted (FHWA, 1985). The nationwide study arrived at similar conclusions. Unfortunately many agencies continue to disregard spread footings as alternative foundations for highway structures. Yet another study (NCHRP, 1983), states the following:

"In summary, it is very clear that the tolerable settlement criteria currently used by most transportation agencies are extremely conservative and are needlessly restricting the use of spread footings for bridge foundations on many soils. Angular distortions of 1/250 of the span length and differential vertical movements of 2 to 4 inches (50 to 100 mm), depending on span length, appear to be acceptable, assuming that approach slabs or other provisions are made to minimize the effects of any differential movements between abutments and approach embankments. Finally, horizontal movements in excess of 2 inches (50 mm) appear likely to cause structural distress. The potential for horizontal movements of abutments and piers should be considered more carefully than is done in current practice."

It is recommended that **compacted structural fills used for supporting spread footings should be a select and specified material that includes sand- and gravel-sized particles. Furthermore, the fill should be compacted to a minimum relative compaction of 95% based on Modified Proctor compaction energy. This structural fill should extend for the entire embankment below the footing.** FHWA (2002c) notes that the Washington Department of Transportation (WSDOT) successfully used the gradation listed in Table 8-12 to design spread footings for the I-5 Kalama Interchange. WSDOT limited the maximum bearing pressures to 3 tsf (290 kPa) and the measured settlements were found to be less than 1.5 in (40 mm) within the fill. In addition to WSDOT, the Nevada Department of Transportation (NDOT) commonly uses spread foundations founded within compacted structural embankment fills.

Direct shear testing of materials such as those described in Table 8-12 is not practical on a project-by-project basis since such materials require large specialized test equipment. Therefore the design of spread footings on compacted sand and gravel is based on a combination of experience and the results of infrequent large-scale laboratory testing on specified gradations of select fill materials. Materials specifications are then developed based on the specified gradations to ensure good quality control during construction. This procedure helps ensure that the conclusions from the laboratory tests are valid for the construction practices used to place the fills.

**Table 8-12**  
**Typical specification of compacted structural fill used by WSDOT (FHWA, 2002c)**

Sieve Size	Percent Passing
4" (100 mm)	100
2" (50 mm)	75 – 100
No. 4 (4.75 mm)	50 – 80
No. 40 (0.425 mm)	30 max
No. 200 (0.075 mm)	7 max
Sand Equivalent (See Note 1)	42 min
<b>Notes:</b>	
1. See Section 5.3.4.1 in Chapter 5 for a discussion of sand equivalent test.	

### **8.6.1 Settlement of Footings on Structural Fills**

Calculation of the settlement of a spread footing supported in or on an engineered fill requires an assumption about the compressibility of the fill material. Because structural fills should be constructed of good-quality granular materials and by following good construction techniques, the estimation of settlement lends itself to the application of the methods

discussed in this Chapter. To estimate settlements of footings in structural fills by Schmertmann's method, an assumption must be made about the SPT N-value that is representative of the engineered fill.

FHWA (1987) used a SPT N-value of 32 blows per foot corrected for overburden pressure as a representative value for estimating settlement in structural fills. This value of SPT N-value corresponds to a relative density,  $D_r$ , of approximately 85 percent at an overburden stress of about 1 tsf (100 kPa) (FHWA, 1987); this is confirmed by the data in Figure 5-23. Based on Figure 5-33 or Equation 5-21, this value of  $D_r$  is at approximately 97% relative compaction based on Modified Proctor compaction energy (ASTM D 1557). Under such compacted conditions, and in the absence of other SPT data in structural fills, the settlement of a footing supported on structural fill can be estimated by using an assumed corrected SPT N-value ( $N_{160}$ ) of 32. However, a relative compaction of 95% based on Modified Proctor compaction energy is often used. For this case, a corrected SPT N-value ( $N_{160}$ ) of 23 is more appropriate.

## 8.7 FOOTINGS ON INTERMEDIATE GEOMATERIALS (IGMs) AND ROCK

The assumption made in this chapter is that intermediate geomaterials (IGMs) are stiff and strong enough that bearing capacity and settlement considerations will generally not govern the design of a spread footing supported on such a material. If a settlement estimate is necessary for shallow foundations supported on an IGM or rock, a method based on elasticity theory is probably the best approach. As with any of the methods for estimating settlement that use elasticity theory, the accuracy of the values estimated for the elastic parameter(s) required by the method is a major factor in determining the reliability of the predicted settlements.

Equation 8-19 may be used to compute the settlement of a shallow spread footing founded on rock based on Young's modulus of the intact rock. In this equation, the stress applied at the top of the rock surface can be calculated by using the stress distribution methods presented in Chapter 2.

$$\delta_v = \frac{C_d \Delta p B_f (1 - \nu^2)}{E_m} \quad 8-19$$

where:  $\delta_v$  = vertical settlement at surface  
 $C_d$  = shape and rigidity factors (Table 8-13)

- $\Delta p$  = change in stress at top of rock surface due to applied footing load
- $B_f$  = footing width or diameter
- $\nu$  = Poisson's ratio (refer to Table 5-22 in Chapter 5)
- $E_m$  = Young's modulus of rock mass (see Section 5.12.1 in Chapter 5)

The elastic modulus of IGMs and some rocks may be measurable by in situ testing with equipment such as the pressuremeter (FHWA 1989a), the dilatometer (FHWA 1992b), and plate load tests or flat jacks. ASTM standards are available for each of these in situ tests and they provide details regarding performance and the interpretation of the test data. The method for determining elastic modulus based on RMR discussed in Chapter 5.

To preserve the stability of footings on IGMs or rock, the geotechnical engineer must evaluate the potential for a global stability failure and the potential of limitations of the allowable bearing capacity because of the presence of rock mass discontinuities. The bearing capacity of IGMs derived from sedimentary rock can dramatically decrease when the IGM is exposed to weathering and moisture.

**Table 8-13**

**Shape and rigidity factors,  $C_a$ , for calculating settlements of points on loaded areas at the surface of a semi-infinite elastic half space (after Winterkorn and Fang, 1975)**

Shape	Center	Corner	Middle of Short Side	Middle of Long Side	Average
Circle	1.00	0.64	0.64	0.64	0.85
Circle (rigid)	0.79	0.79	0.79	0.79	0.79
Square	1.12	0.56	0.76	0.76	0.95
Square (rigid)	0.99	0.99	0.99	0.99	0.99
Rectangle (length/width):					
1.5	1.36	0.67	0.89	0.97	1.15
2	1.52	0.76	0.98	1.12	1.30
3	1.78	0.88	1.11	1.35	1.52
5	2.10	1.05	1.27	1.68	1.83
10	2.53	1.26	1.49	2.12	2.25
100	4.00	2.00	2.20	3.60	3.70
1000	5.47	2.75	2.94	5.03	5.15
10000	6.90	3.50	3.70	6.50	6.60

## 8.8 ALLOWABLE BEARING CAPACITY CHARTS

The concept of an allowable bearing capacity chart was discussed in Section 8.3. The curves shown in Figure 8-10 can be obtained by performing computations for allowable bearing capacity and settlement for a range of values of footing widths by using the procedures described in Sections 8.4 to 8.7. This section presents an example bearing capacity chart and a step-by-step procedure to use such a chart for the sizing of footings.

**Example 8-3:** The abutments of a bridge will be founded on spread foundations similar to the configuration shown in Figure 8-4. The length,  $L_f$ , of the abutment footing is 130 ft. The minimum depth of embedment,  $D_f$ , of the footing base is 5 ft. The geotechnical engineer developed a bearing capacity chart based on site-specific subsurface data. This chart is shown in Figure 8-22. Determine the footing width,  $B_f$ , such that the settlement of the footing is less than or equal to 1 in.

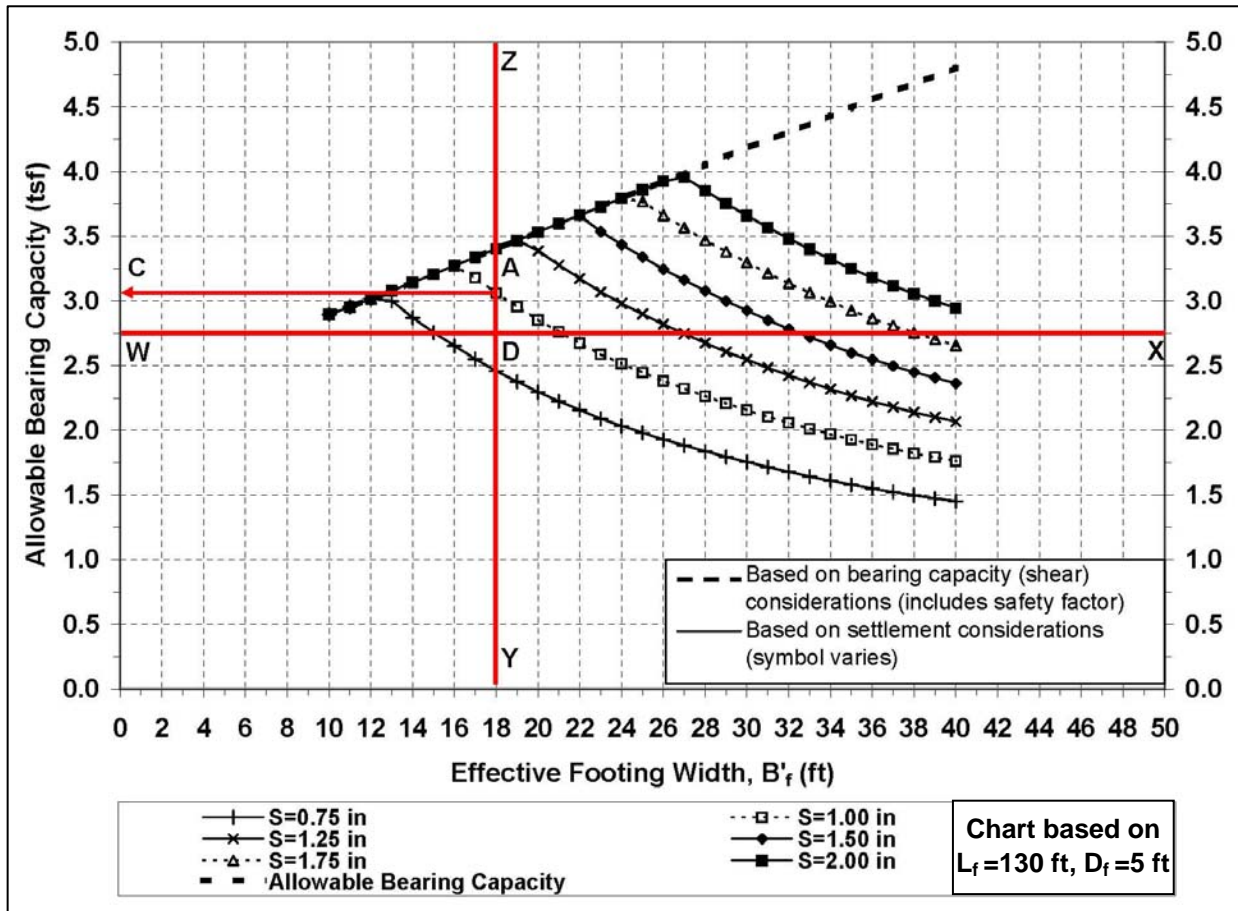


Figure 8-22. Example allowable bearing capacity chart.

**Solution:**

**Step 1:**

Assume a footing width,  $B_f$ , and compute the equivalent **net** uniform (Meyerhof) bearing pressure,  $q_{eu}$ , at the base of the footing. The equivalent net uniform bearing pressure,  $q_{eu}$ , is obtained by dividing the resultant vertical load,  $R$ , by the effective area,  $A'$ , of the footing as follows:

$$q_{eu} = R/A'$$

The resultant vertical load, i.e., the vertical component of the resultant load, should be determined by using the **unfactored** dead load, plus the **unfactored** component of live and impact loads assumed to extend to the footing level (Section 4.4.7.2 of AASHTO, 2002). The effective area,  $A'$ , is determined as follows based on Equation 8-7, 8-8 and 8-9:

$$A' = B'_f L'_f = (B_f - 2e_B) (L_f - 2e_L)$$

where  $e_B$  and  $e_L$  are the eccentricities of the resultant load,  $R$ , in the  $B_f$  and  $L_f$  directions, respectively, as indicated in Figure 8-16. The eccentricities,  $e_B$  and  $e_L$  should be such that they are less than  $B_f/6$  and  $L_f/6$ , respectively to ensure that no uplift occurs anywhere within the base of the footing. In cases where there is no load eccentricity, the effective length,  $L'_f$ , and the effective width,  $B'_f$ , are equal to the actual length,  $L_f$ , and actual width,  $B_f$ , respectively.

For the example problem stated above, assume for the sake of illustration that the computed equivalent net uniform bearing pressure,  $q_{eu}$ , at the base of the footing is 2.75 tsf for a retaining wall footing that is 130 ft long ( $L_f = L'_f$ ), has an effective width,  $B'_f$ , of 18 ft, and is embedded 5 ft.

**Step 2:**

Since the minimum required allowable bearing capacity has to be at least equal to the net equivalent uniform bearing pressure,  $q_{eu}$ , draw a horizontal line on the chart corresponding to the value of  $q_{eu}$ . Thus, for the example problem, draw a horizontal line WX on the chart corresponding to a value of 2.75 tsf as shown in Figure 8-22. This horizontal line will intersect the curves of equal settlement, e.g.,  $S=0.75$  in,  $S = 1.0$  in and so on as shown in Figure 8-22.

### **Step 3:**

Draw a vertical line YZ for the effective footing width,  $B'_f$ , of 18 ft. Like the horizontal line, WX, the vertical line, YZ, will intersect the curves of equal settlement, e.g.,  $S=0.75$  in,  $S = 1.0$  in as shown in Figure 8-22.

### **Step 4:**

From the point of intersection of the vertical line, YZ, with the appropriate acceptable settlement curve (1.00-in for this example) draw a horizontal line to the Y-axis to determine the allowable bearing capacity. By drawing the horizontal line, AC, it can be determined that the allowable bearing capacity corresponding to an effective footing width of 18 ft is approximately 3.2 tsf (see Point C in Figure 8-22). This value is greater than the  $q_{eu}$  value of 2.75 tsf and therefore the footing whose effective width,  $B'_f$ , is 18 ft is acceptable.

An alternative way to evaluate the acceptability of a footing size is to determine the estimated settlement corresponding to the computed equivalent net uniform bearing pressure,  $q_{eu}$ , and compare it with the acceptable settlement. From the bearing capacity chart for the example problem, it can be seen that at an effective footing width,  $B'_f$ , of 18 ft and a  $q_{eu}$  value of 2.75 tsf, the estimated settlement will be approximately 0.88 in (see Point D that falls between the  $S=0.75$  in and  $S=1.00$  in curves in Figure 8-22). This value of estimated settlement is less than the limiting settlement of 1 in and is therefore acceptable.

### **Step 5:**

Repeat Steps 1 to 4 as necessary to optimize the footing design or to resize the footing based on the “available” allowable bearing capacity. In this example, the “available” allowable bearing capacity for an 18 ft wide footing is 3.2 tsf which is greater than the required value of 2.75 tsf. Thus, it is possible that the footing width can be reduced. During the optimization process, linear interpolation within the limits of the data presented in the chart is acceptable. However, extrapolation of data is not advisable.

## **8.8.1 Comments on the Allowable Bearing Capacity Charts**

- A factor of safety, FS, against ultimate bearing capacity (shear) failure is included in the computations that yield the steeply rising line on the left side of the chart, i.e., the line that is based on bearing capacity considerations. Since the settlement based allowable bearing capacity curves plot on the right side of the bearing capacity line, the actual factor of safety against shear failure will be higher than the assumed minimum FS.

- The effective footing width,  $B'_f$ , on the X-axis of the charts represents the least lateral effective dimension of the footing. The footing size determined from the chart is a function of the depth of embedment of the footing,  $D_f$ , and the length of the footing,  $L_f$ . The depth of embedment,  $D_f$ , is the vertical distance between the lowest finished permanent ground surface above the footing to the base of the footing. Each bearing capacity chart is developed for a given footing length,  $L_f$ , and a minimum depth of embedment,  $D_f$ . Therefore, these quantities must be clearly labeled on the chart as shown in Figure 8-22. If the actual dimensions of  $D_f$  and/or  $L_f$  vary by more than  $\pm 10\%$  from those noted on the charts then a new chart should be developed for the actual values of  $D_f$  and  $L_f$ .
- Finally, each bearing capacity chart should be specific to a given foundation element and should be developed based on location-specific geotechnical data. Consequently the charts should not be used for foundations at locations other than at which they are applicable.

## 8.9 EFFECT OF DEFORMATIONS ON BRIDGE STRUCTURES

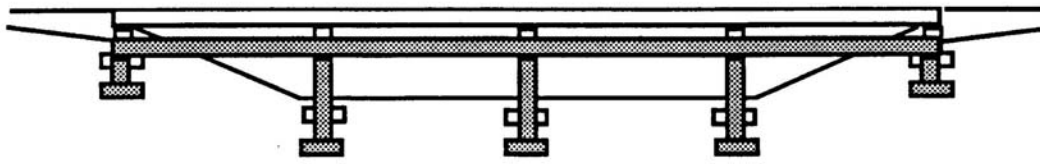
Bridge foundations and other geotechnical features such as approach embankments should be designed so that their deformations (settlements and/or lateral movements) will not cause damage to the bridge structure. Uneven displacements of bridge abutments and pier foundations can affect the quality of ride and the safety of the traveling public as well as the structural integrity of the bridge. Such movements often lead to costly maintenance and repair measures. Therefore, it is important that the geotechnical specialist as well as the structural engineer fully understand the effect of deformations of geotechnical features on bridge structures.

FHWA (1985) and Duncan and Tan (1991) studied tolerable movements for bridges and found that “foundation movements would become intolerable for some other reason before reaching a magnitude that would create intolerable rider discomfort.” The “other” reasons might include reduction of clearance at overpasses and drainage considerations, as discussed later. Therefore, if movements are within a tolerable range with regard to structural distress for the bridge superstructure, they will also be acceptable with respect to user comfort and safe vehicle operation. The severity of the consequences of uneven movements of bridge structures, superstructure as well as substructure, increases with the magnitude of the settlements and lateral movements. Both of these components of bridge movements are discussed below.

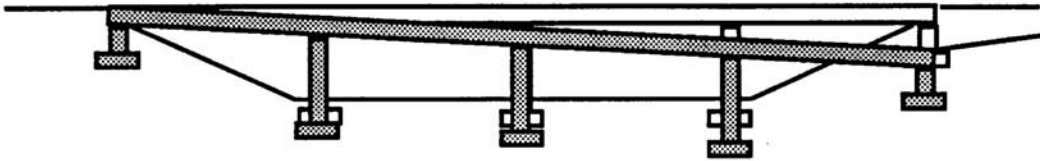
### A. Settlement

Settlement can be subdivided into the following three components, which are illustrated in Figure 8-23 (Duncan and Tan, 1991):

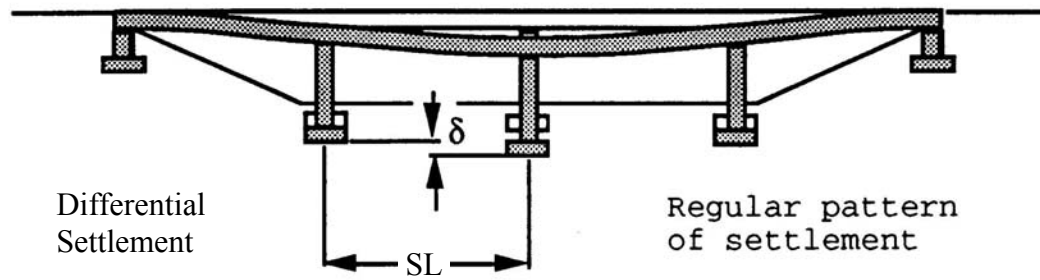
1. **Uniform settlement:** In this case, all bridge support elements settle equally. Even though the bridge support elements settle equally, they can cause differential settlement with respect to the approach embankment and associated features such as approach slabs and utilities that are commonly located in or across the end-spans of bridges. Such differential settlement can create several problems. For example, it can reduce the clearance of the overpass, create a bump at the end of the bridge, change grades at the end of the bridge causing drainage problems, and distort underground utilities at the interfaces of the bridge and approaches.



Uniform Settlement

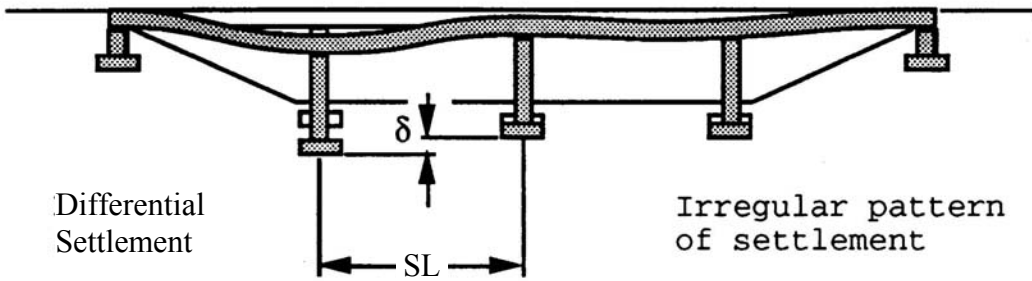


Tilt (Rotation)



Differential Settlement

Regular pattern of settlement



Differential Settlement

Irregular pattern of settlement

A = Angular Distortion

$$A = \frac{\text{Difference in Settlement Between Foundations}}{\text{Distance Between Foundations}} = \frac{\delta}{SL}$$

**Figure 8-23. Components of settlement and angular distortion in bridges (after Duncan and Tan, 1991).**

Although uniform settlements may be computed theoretically, from a practical viewpoint it is not possible for the bridge structure to experience truly uniform settlement due to a combination of many factors including, but not limited to, the variability of loads and soil properties

2. **Tilt or rotation:** Tilt or rotation occurs mostly in single span bridges with stiff superstructures. Tilt or rotation may not cause distortion of the superstructure and associated damage, but due to its differential movement with respect to the facilities associated with approach embankments, tilt or rotation can create problems similar to those of uniform settlement that were discussed above, e.g., a bump at the end of the bridge, drainage problems, and damage to underground utilities.
3. **Differential settlement:** Differential settlement directly results in deformation of the bridge superstructure. As shown in Figure 8-23, two different patterns of differential settlement can occur. These are:
  - a. **Regular pattern:** In this case, the settlement increases progressively from the abutments towards the center of the bridge
  - b. **Irregular pattern:** In this case, the settlement at each support location varies along the length of the bridge.

Both of the above patterns of settlement lead to angular distortion, which is defined as the ratio of the difference in settlement between two points divided by the distance between the two points. For bridge structures, the two points to evaluate the differential settlement are commonly selected as the distance between adjacent support elements, SL, as shown in Figure 8-23. Depending on the type of connections between the superstructure and support columns (pinned or fixed) and the locations of expansion and construction joints along the bridge deck (mid-span or elsewhere), the irregular pattern of differential settlement has the potential to create greater structural distress than the regular pattern of differential settlement. The distress may occur due to increased internal stresses associated with flexure and/or shear of the bridge superstructure and is generally manifested by cracks in the bridge deck and/or girders at support locations.

In addition to the problems they create in the bridge superstructure, differential settlements can create the same problems as uniform settlements discussed earlier, i.e., problems with bumps at the junctures with approach slabs, problems with drainage, problems with clearance at underpasses, etc.

## **B. Horizontal Movements**

Horizontal movements cause more severe and widespread problems than do equal magnitudes of vertical settlement. The types of problems that arise as a result of differential horizontal movements between bridge decks and abutments, or between adjacent spans of bridges, include the following (Duncan and Tan, 1991):

- Shearing of anchor bolts,
- Excessive opening of expansion joints,
- Reduced effectiveness of expansion joints when clearance is reduced,
- Complete closing of expansion joints and jamming of bridge decks into abutments or adjacent spans,
- Shifting of abutments when expansion joints jam,
- Severe damage to abutment walls, approach slabs or bridge decks due to excessive loads when expansion joints jam,
- Distortion and damage to bearing devices,
- Excessive tilting of rockers,
- Damage to rail curbs, sidewalks and parapets.

## **C. Reliability of Estimation of Movements**

All analytical methods used for estimating movements are based on certain assumptions. Therefore, there is an inherent uncertainty associated with the estimated values of movements. The uncertainty of estimated differential settlement is larger than the uncertainty of the estimated settlement at the two support elements used to calculate the differential settlement, e.g., between abutment and pier, or between piers. For example, if one support element settles less than the amount estimated while the other support element settles the amount estimated, the actual differential settlement will be larger than the difference between the two values of estimated settlement at the support elements. Duncan and Tan (1991) suggest the following assumptions to estimate the likely value of differential settlement:

- The settlement of any support element could be as large as the value calculated by using conservative procedures, and
- At the same time, the settlement of the adjacent support element could be zero.

Use of these conservative assumptions would result in an estimated maximum possible differential settlement equal to the largest settlement calculated at either end of any span.

## 8.9.1 Criteria for Tolerable Movements of Bridges

### 8.9.1.1 Vertical Movements

The FHWA (1985) study used the following definition of intolerable movement:

“Movement is not tolerable if damage requires costly maintenance and/or repairs and a more expensive construction to avoid this would have been preferable.”

This definition is somewhat subjective based on the cost and practical problems involved in the repair and maintenance or use of an alternative more expensive construction technique. FHWA (1985) studied data for 56 simple span bridges and 119 continuous span bridges and chose to express the definition for tolerable movement quantitatively in terms of limiting angular distortion as shown in Table 8-14.

**Table 8-14**

**Tolerable movement criteria for bridges (FHWA, 1985; AASHTO 2002, 2004)**

<b>Limiting Angular Distortion, <math>\delta/SL</math></b>	<b>Type of Bridge</b>
0.004	Multiple-span (continuous span) bridges
0.005	Single-span bridges

Note:  $\delta$  is differential settlement,  $SL$  is the span length. The quantity,  $\delta/SL$ , is dimensionless and is applicable when the same units are used for  $\delta$  and  $SL$ , i.e., if  $\delta$  is expressed in inches then  $SL$  should also be expressed in inches.

For example, the criteria in Table 8-14 suggest that for a 100 ft (30 m) span, a differential settlement of 4.8 inches (120 mm) is acceptable for a continuous span and 6 inches (150 mm) is acceptable for a simple span.

Such relatively large values of differential settlements create concern for structural designers, who often arbitrarily limit the criteria to one-half to one-quarter of the values listed in Table 8-14. While there are no technical reasons for structural designers to set such arbitrary additional limits for the criteria listed in Table 8-14, there are often practical reasons based on the tolerable limits of deformation of other structures associated with a bridge, e.g., approach slabs, wingwalls, pavement structures, drainage grades, utilities on the bridge, deformations that adversely affect quality of ride, etc. Thus, the relatively large differential settlements based on Table 8-14, should be considered in conjunction with functional or performance criteria not only for the bridge structure itself but for all of the associated facilities. The following steps are suggested in this regard:

- Step 1: Identify all possible facilities associated with the bridge structure, and the tolerance of those facilities to movements.
- Step 2: Due to the inherent uncertainty associated with estimated values of settlement, determine the differential settlement by using the conservative assumptions described earlier. It is important that the estimation of differential settlement is based on a realistic evaluation of the sequence and magnitude of the loads as described in Section 8.9.2.
- Step 3: Compare the differential settlement from Step 2 with the various tolerances identified in Step 1 and in Table 8-14. Based on this comparison identify the critical component of the facility. Review this critical component to check if it can be relocated or if it can be designed to more relaxed tolerances. Repeat this process as necessary for other facilities. In some cases, a simple re-sequencing of the construction of the facility based on the construction sequence of the bridge may help mitigate the issues associated with intolerable movements.

The above approach will help to develop project-specific limiting angular distortion criteria that may differ from the general guidelines listed in Table 8-14.

### **8.9.1.2 Horizontal Movements**

Based on a survey of bridges, FHWA (1985) found that horizontal movements less than 1 in (25 mm) were almost always reported as being tolerable, while horizontal movements greater than 2 in (50 mm) were quite likely to be considered to be intolerable. Based on this observation, FHWA (1985) recommended that horizontal movements be limited to 1.5 in (38 mm). The data presented by FHWA (1985) showed that horizontal movements tended to be more damaging when they were accompanied by settlement than when they were not. The estimation of magnitude of horizontal movements should take into account the movements associated with considerations of slope instability and lateral squeeze as discussed in Chapter 6 and 7, respectively.

Abutments are often designed for active lateral earth pressure conditions, which require a certain amount of movement (see Chapter 9). Depending on the configuration of the bridge end spans and expansion joints, horizontal movements of an abutment can be restrained, however, such restraint can lead to an increase in the lateral earth pressures above the active earth pressures normally used in design. Design of expansion joints should allow for sufficient movement to keep earth pressures at or close to their design values and still allow the joints to perform properly under all temperature conditions.

## 8.9.2 Loads for Evaluation of Tolerable Movements Using Construction Point Concept

Most designers use the criteria described in Section 8.9.1 as if a bridge structure is instantaneously wished into place, i.e., all the loads are applied at the same time. In reality, loads are applied gradually as construction proceeds. Consequently, settlements will also occur gradually as construction proceeds. There are several critical construction points that should be evaluated separately by the designer. Table 8-15 illustrates this critical construction concept for a bridge abutment footing that was constructed as part of a 2-span bridge in the southwest United States. The prestressed concrete beam bridge is 64.4 ft (19.6 m) wide and 170 ft (52 m) long. The bridge is continuous with mechanically stabilized earth (MSE) walls wrapped around both of the abutments. The abutments are fixed for shear transfer through semi-integral diaphragms connected to spread footings on top of the MSE walls.

Even though the total settlement cited in Table 8-15 is 7.5 inches, in reality only 2.0 in is significant because it occurs progressively during the first 10 years the bridge is in service. (Note that immediately after construction the net settlement was estimated to be only 0.5 in even though the total settlement computed at this stage is 5.0 in)

The pier for this bridge is supported by a group of pipe piles and was estimated to experience a settlement of approximately 0.5 in. To compute the worst angular distortion, it was assumed that the pier would not experience settlement while the abutment would experience the full estimated settlement. Thus, the angular distortion criterion where 0 in settlement is assumed at the pier yields the following results for an 85 ft span (1/2 of the 170 ft long bridge):

- *With Construction Point Concept*

$$\text{Angular Distortion, } A = (2.0 \text{ in} - 0.0 \text{ in}) / (85 \text{ ft} \times 12 \text{ in/ft}) = 2.0 \text{ in} / 1,020 \text{ in} = 0.002$$

In this case, A is one-half of the limiting angular distortion of 0.004 as per Table 8-14. Therefore, the settlements are acceptable.

- *Without Construction Point Concept*

$$\text{Angular Distortion, } A = (7.5 \text{ in} - 0.0 \text{ in}) / (85 \text{ ft} \times 12 \text{ in/ft}) = 7.5 \text{ in} / 1,020 \text{ in} = 0.0073$$

Since  $A > 0.004$ , the angular distortion is deemed intolerable.

**Table 8-15****Example of settlements evaluated at various critical construction points**

<b>Construction Point</b>	<b>Estimated Net Applied Stress<sup>1</sup> (psf)</b>	<b>Settlement (inches)<sup>2</sup></b>	<b>Net Settlement (inches)</b>
I. Embankment only	2,770	3.4	-
II. MSE Wall + Spread footing (no deck)	6,020	5.0	1.6 (during construction)
III. MSE Wall + Spread footing + Deck (DL + LL)	6,520	5.5	0.5 (= 5.5 – 5.0)
IV. MSE Wall + Spread Footing + Deck (DL+LL) + Creep <sup>3</sup>	6,520	7.5	2.0 (= 7.5 – 5.5)

Notes:

1. The 2 ft depth of embedment for the MSE wall was taken into account while estimating the net applied stress from new construction.
2. Settlement analyses were performed by using Schmertmann's method (1978) that allows for estimation of long-term (creep) settlement. In this project, relatively dry, low plastic fine grained soils were encountered that could possibly deform for some time after construction.
3. A time period of 1.5 months was assumed for each Point II and III analyses. For this duration, the creep component of the deformation was less than 5% of the settlements reported above for Point II and III. Conservatively, a time period of 10 years was assumed for the creep deformations for Point IV, after which it was assumed that no significant creep deformations would occur. Note, that the net settlement of 2.0 inches between construction Point III and IV is attributed entirely to creep settlement.

In this example, if the designer did not take into account the various construction points when evaluating settlement, then not only would the angular distortion criteria listed in Table 8-15 not be met but it would also likely lead to implementation of costly and unnecessary ground improvement measures. This approach was used successfully for 55 bridges constructed as part of the I25/I40 (“BIG I”) traffic interchange in Albuquerque, NM. This critical construction point approach permitted the use of true bridge abutments, i.e., spread footings on top of MSE walls, on 28 of the 55 bridges on the BIG I project, which resulted in significant cost savings for the New Mexico Department of Transportation (NMDOT). The project was completed in 2001 and all of the bridges have performed well to date (2006).

A key point in evaluating settlements at critical construction points is that the approach requires close coordination between the structural and geotechnical specialists. In the case of the BIG I project, the structural specialist performed a realistic evaluation of the loads and construction sequence and communicated them to the geotechnical specialist, who then evaluated the settlements for those loads. As demonstrated by the above example, this approach resulted in a realistic evaluation of the deformation of the bridge structure. This critical construction point approach can also often help in making other decisions such as the need for costly ground improvement measures.

## **8.10 SPREAD FOOTING LOAD TESTS**

Spread footing load tests can be used to verify both bearing capacity and settlement predictions. Briaud and Gibbens (1994) present the results of predicted and measured behavior of five spread footings on sand. Full scale tests have been done on predominantly granular soils. An example is the I-359 project in Tuscaloosa, Alabama where dead load was placed on 12 ft x 12 ft (3.7 m x 3.7 m) footings to create a foundation contact pressure of over 4 tsf (383 kPa). A settlement of 0.1 in (2.5 mm) was recorded when the footing concrete was placed. The greatest settlement recorded after application of the load was also approximately 0.1 in (2.5 mm). Spread footing load tests can help develop confidence in the use of such foundations for transportation structures.

## **8.11 CONSTRUCTION INSPECTION**

Construction inspection requirements for shallow foundations are similar to those for other concrete structures. In some cases, agencies may have inspector checklists for construction of shallow foundations. Table 8-16 provides a summary of construction inspection check points for shallow foundations. Throughout construction, the inspector should check submittals for completeness before transmitting them to the engineer.

### **8.11.1 Structural Fill Materials**

Fill requirements should be strictly adhered to because the fill must perform within expected limits with respect to strength and, more importantly, within tolerance for differential settlement. Sometimes the area for construction of the fill is small, such as behind abutment and wingwalls. In such situations, the use of hand compactors or smaller compaction equipment may be necessary.

When the construction of structural fills that will support shallow foundations is being monitored, particular attention should be paid to the following items:

- The material should be tested for gradation and durability at sufficient frequency to ensure that the material being placed meets the specification.
- The specified level of compaction must be obtained in the fill. Testing, if applicable, should be performed in accordance with standard procedures and at the recommended intervals or number of tests per lift.

If a surcharge fill is required for pre-loading, it should be verified that the unit weight of the surcharge fill meets the value assumed in the design.

**Table 8-16**

**Inspector responsibilities for construction of shallow foundations**

<b>CONTRACTOR SET UP</b>
<ul style="list-style-type: none"> <li>• Review plans and specifications.</li> <li>• Review contractor’s schedule.</li> <li>• Review test results and certifications for pre-approved materials, e.g., cement, coarse and fine aggregate.</li> <li>• Confirm that the contractor’s stockpile and staging area are consistent with locations shown on plans.</li> <li>• Discuss anticipated ground conditions and potential problems with the contractor.</li> <li>• Review the contractor’s survey results against the plans.</li> </ul>
<b>EXCAVATION</b>
<ul style="list-style-type: none"> <li>• Verify that excavation slopes and/or structural excavation support is consistent with the plans.</li> <li>• Confirm that limits of any required excavations are within right-of-way limits shown on the plans.</li> <li>• Confirm that all unsuitable materials, e.g., sod, snow, frost, topsoil, soft/muddy soils, are removed to the limits and depths shown on the plans and the excavation is backfilled with properly compacted granular material. <b>The in-place bearing stratum of soil or rock should be checked to verify the in-situ condition and the degree of improvement achieved by the contractor’s preparation approach. Some soil types can become remolded and weakened from disturbance. If the conditions deviate from those anticipated in the geotechnical report and/or the plans and specifications, the geotechnical engineer should be consulted to determine if additional measures are necessary.</b></li> <li>• Confirm that leveling and proof-rolling of the foundation area is consistent with the requirements of the specifications. Probing is recommended for verification of subgrade.</li> <li>• Confirm that contractor’s excavation operations do not result in significant water ponding.</li> <li>• Confirm that existing drainage features, utilities, and other features are protected.</li> <li>• Identify areas not shown on the plans where unsuitable material exists and notify engineer.</li> </ul>
<b>SHALLOW FOUNDATION</b>
<ul style="list-style-type: none"> <li>• Approve footing foundation condition before concrete is poured.</li> <li>• Confirm reinforcement strength, size, and type consistent with the specifications.</li> <li>• Confirm consistency of the contractor’s outline of the footing (footing size and bottom of footing depth) with the plans.</li> <li>• Confirm location and spacing of reinforcing steel consistent with the plans.</li> <li>• Confirm water/cement ratio and concrete mix design consistent with the specifications.</li> <li>• Record concrete volumes poured for the footing.</li> <li>• Confirm appropriate concrete curing times and methods as provided in the specifications.</li> <li>• Confirm that concrete is not placed on ice, snow, or otherwise unsuitable ground.</li> <li>• Confirm that concrete is being placed in continuous horizontal layers and that the time between successive layers is consistent with the specifications.</li> </ul>
<b>POST INSTALLATION</b>
<ul style="list-style-type: none"> <li>• Verify pay quantities.</li> </ul>

### **8.11.2 Monitoring**

The elevations of constructed foundations should be checked before and after the structural load is applied. The measurements made at those times will serve as a baseline for the long-term monitoring of the bridge. Subsequently, additional survey measurements should be made to confirm satisfactory performance or to identify whether potentially harmful settlements are occurring. It may be important to check the completion of fill settlements before foundation construction if the fill was constructed over soft compressible soils. As indicated in Chapter 7, settlement plates, horizontal inclinometers, or other types of instrumentation are typically installed in such cases. The lateral displacement potential can be greater than the vertical movements; therefore, if conditions warrant, monitoring may also include complete survey coordinates and possibly more accurate instrumentation.

Monitoring may also be necessary to evaluate the impact of the new construction on neighboring facilities or the ground surface. Such concerns could be monitored with simple survey tag lines with benchmarks and monitoring hubs and telltales to measure lateral deviations and vertical subsidence/heave. Greater reliability may require more sophisticated instrumentation, such as inclinometers, strain gages, extensometers and tiltmeters. Surveys of the pre-construction condition of neighboring structures should be conducted, particularly in congested urban areas. The instrumentation program should be developed with a consideration of the anticipated performance, risks and potential consequences. Parameters should be identified that are critical to project success and appropriate instrumentation selected. A key to successful use of instrumentation is to measure, plot and interpret the data in a timely manner to be able to take corrective measures, if needed.

[THIS PAGE INTENTIONALLY BLANK]

## CHAPTER 9.0 DEEP FOUNDATIONS

Foundation design and construction involves assessment of factors related to engineering and economics. As discussed in Chapter 8, the selection of the most feasible foundation system requires consideration of both shallow and deep foundation types in relation to the characteristics and constraints of the project and site conditions. Situations commonly exist where shallow foundations are inappropriate for support of structural elements. These situations may be related either to the presence of unsuitable soil layers in the subsurface profile, adverse hydraulic conditions, or intolerable movements of the structure. Deep foundations are designed to transfer load through unsuitable subsurface layers to suitable bearing strata. Typical situations that require the use of deep foundations are shown in Figure 9-1 and briefly discussed below.

- Figure 9-1(a) shows the most common case in which the upper soil strata are too compressible or too weak to support heavy vertical loads. In this case, deep foundations transfer loads to a deeper dense stratum and act as toe bearing foundations. In the absence of a dense stratum within a reasonable depth, the loads must be gradually transferred, mainly through soil resistance along shaft, Figure 9-1(b). An important point to remember is that deep foundations transfer load through unsuitable layers to suitable layers. **The foundation designer must define at what depth suitable soil layers begin in the soil profile.**
- Deep foundations are frequently needed because of the relative inability of shallow footings to resist inclined, lateral, or uplift loads and overturning moments. Deep foundations resist uplift loads by shaft resistance, Figure 9-1(c). Lateral loads are resisted either by vertical deep foundations in bending, Figure 9-1(d), or by groups of vertical and battered foundations, which combine the axial and lateral resistances of all deep foundations in the group, Figure 9-1(e). Lateral loads from overhead highway signs and noise walls may also be resisted by groups of deep foundations, Figure 9-1(f).
- Deep foundations are often required when scour around footings could cause loss of bearing capacity at shallow depths, Figure 9-1(g). In this case the deep foundations must extend below the depth of scour and develop the full capacity in the support zone below the level of expected scour. FHWA (2001c) scour guidelines require the geotechnical analysis of bridge foundations to be performed on the basis that all stream bed materials in the scour prism have been removed and are not available for bearing or lateral support. Costly damage and the need for future underpinning can be avoided by properly designing for scour conditions.

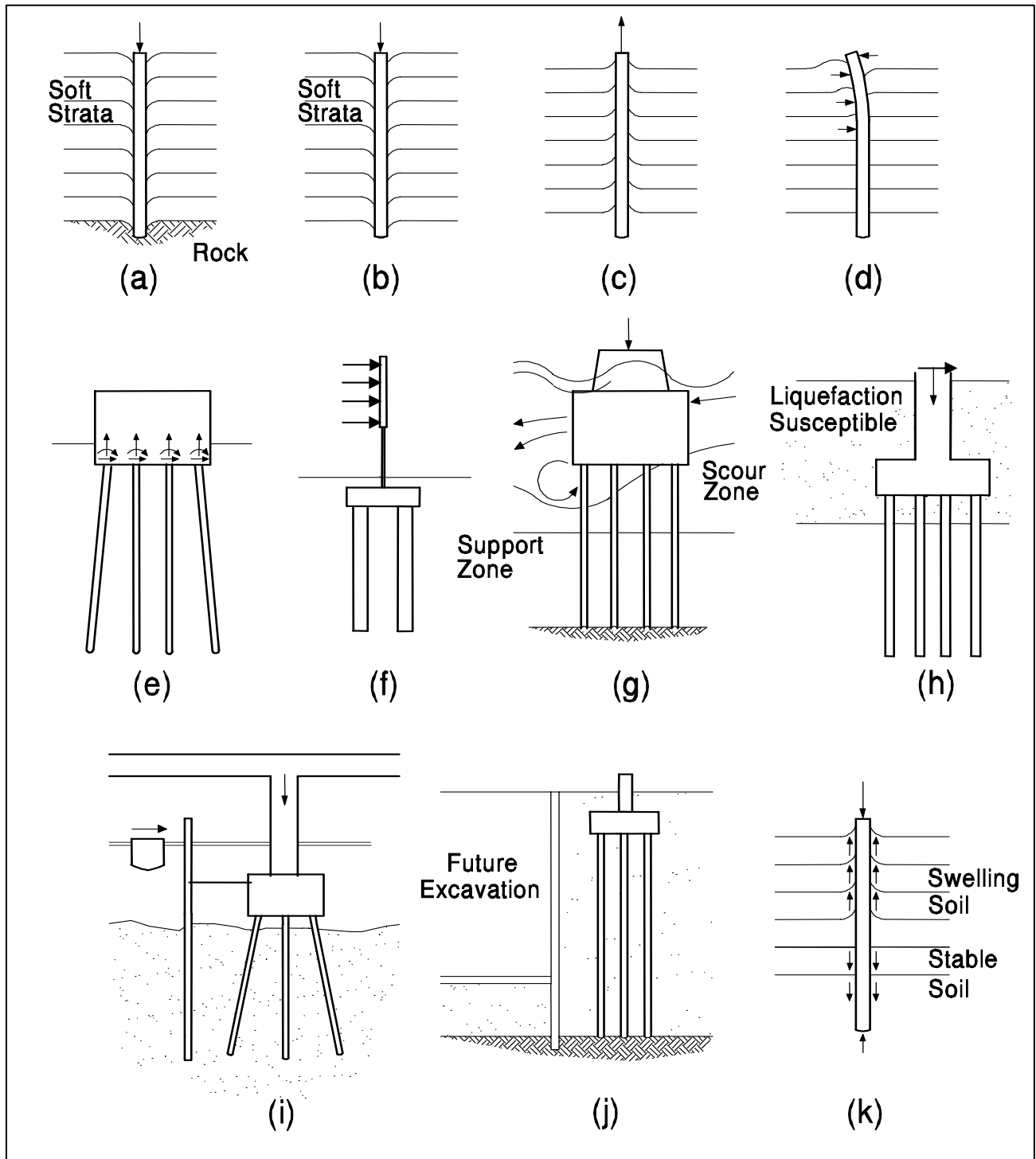


**Figure 9-1. Situations in which deep foundations may be needed (Vesic, 1977; FHWA, 2006a).**

- Soils subject to liquefaction in a seismic event may also dictate that a deep foundation be used, Figure 9-1(h). Seismic events can induce significant lateral loads to deep foundations. During a seismic event, liquefaction-susceptible soils offer less lateral resistance as well as reduced shaft resistance to a deep foundation. Liquefaction effects on deep foundation performance must be considered for deep foundations in seismic areas.
- Deep foundations are often used as fender systems to protect bridge piers from vessel impact, Figure 9-1(i). Fender system sizes and group configurations vary depending upon the magnitude of vessel impact forces to be resisted. In some cases, vessel impact loads must be resisted by the bridge pier foundation elements. Single deep foundations may also be used to support navigation aids.
- In urban areas, deep foundations may occasionally be needed to support structures adjacent to locations where future excavations are planned or could occur, Figure 9-1(j). Use of shallow foundations in these situations could require future underpinning in conjunction with adjacent construction.
- Deep foundations are used in areas of expansive or collapsible soils to resist undesirable seasonal movements of the foundations. Deep foundations under such conditions are designed to transfer foundation loads, including uplift or downdrag, to a level unaffected by seasonal moisture movements, Figure 9-1(k).

## 9.1 TYPES OF DEEP FOUNDATIONS AND PRIMARY REFERENCES

There are numerous types of deep foundations. Figure 9-2 shows a deep foundation classification system based on type of material, configuration, installation technique and equipment used for installation. This chapter discusses the driven pile and drilled shaft foundation types based on the information in the following primary references:

FHWA (2006a) *Design and Construction of Driven Pile Foundations - Vol. I and II*, Report No. FHWA-NHI-05-042 and FHWA-NHI-05-043, Authors: Hannigan, P.J., G.G. Goble, G. Thendean, G.E. Likins and F. Rausche., Federal Highway Administration, U.S. Department of Transportation.

FHWA (1999). *Drilled Shafts: Construction Procedures and Design Methods*. Report No. FHWA-IF-99-025, Authors: O’Neill, M. W. and Reese, L. C. Federal Highway Administration, U.S. Department of Transportation.

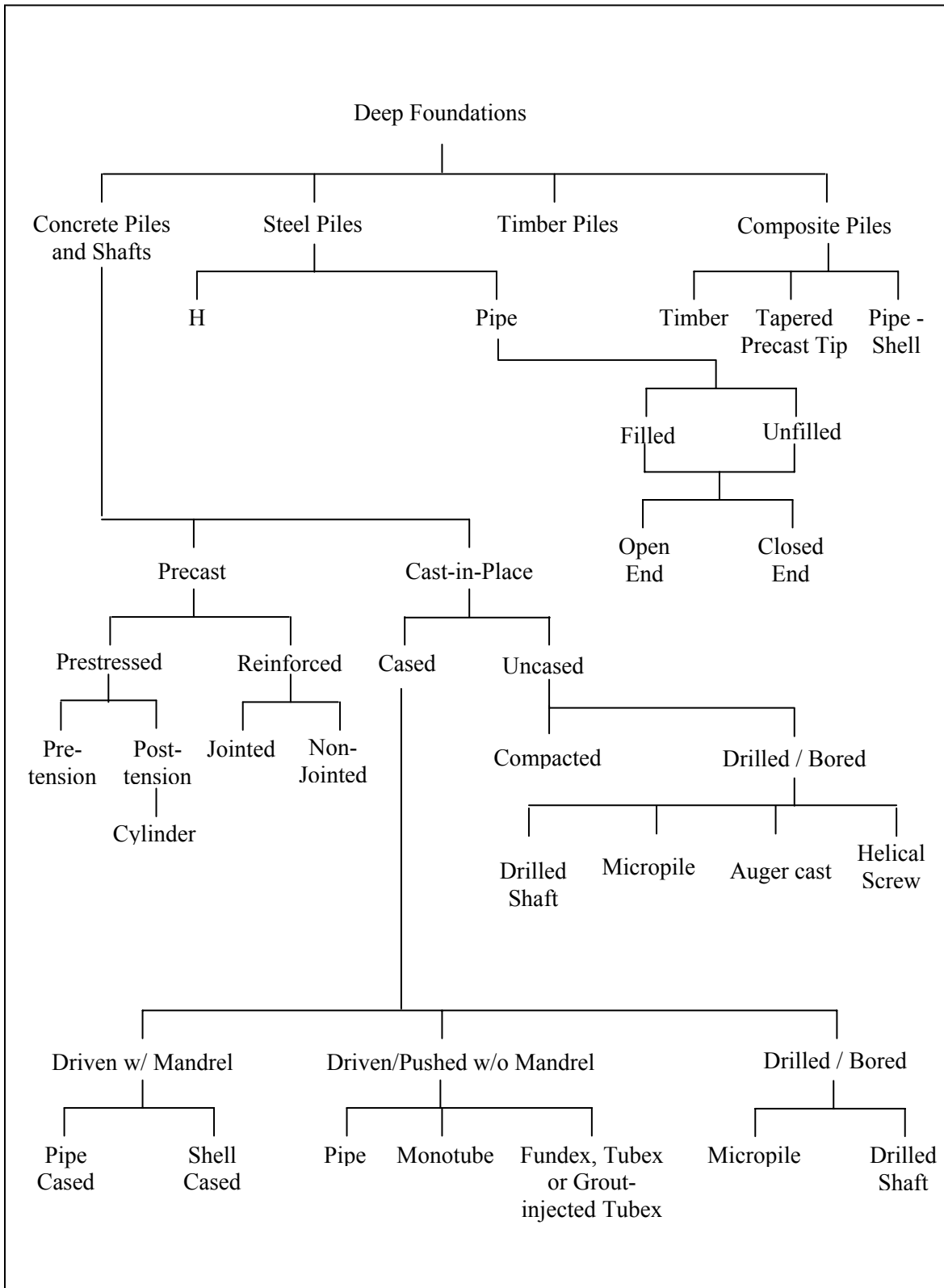


**Figure 9-2. Deep foundation classification system (after FHWA, 2006a).**

Micropiles and auger-cast piles are rapidly gaining in popularity as viable types of deep foundations for transportation structures. These types of piles are not addressed in this chapter. Guidance for these types of piles can be found in the following FHWA manuals.

FHWA (2005a). “Micropile Design and Construction,” Report No. FHWA NHI-05-039, Authors: Sabatini, P.J., Tanyu, B., Armour., P., Groneck, P., and Keeley, J., National Highway Institute, Federal Highway Administration, U.S. Department of Transportation.

FHWA (2006c) “Geotechnical Engineering Circular No. 8, Continuous Flight Auger Piles,” Authors: Brown, D. and Dapp, S., Federal Highway Administration, U.S. Department of Transportation.

### **9.1.1 Selection of Driven Pile or Cast-in-Place (CIP) Pile Based on Subsurface Conditions**

For many years the use of a deep foundation has meant security to many designers. For example, the temptation to use driven piles under every facility is great because detailing of plans is routine, quantity estimate is neat, and safe structural support is apparently assured. Often, designers do not consider other pile alternatives such as cast-in-place (CIP) piles. Figure 9-2 shows a variety of CIP pile types. The most common CIP pile type is the drilled shaft which, as indicated earlier, is the only CIP pile type discussed in this chapter. The selection of appropriate pile types for any project should include a consideration of subsurface conditions as the first step. Table 9-1 provides a discussion of driven pile versus drilled shafts for various subsurface conditions. Sections 9.2 to 9.9 discuss the details of the driven pile foundation systems while Sections 9.10 to 9.14 discuss the CIP pile types with emphasis on drilled shafts.

### **9.1.2 Design and Construction Terminology**

Just as with the design of other geotechnical features, there is a specific terminology associated with design of various deep foundations. Examples of terminology are “static pile capacity,” “ultimate pile capacity,” “allowable pile capacity,” “driving capacity,” “restrike capacity,” “shaft resistance in piles,” “side resistance in drilled shafts,” “toe resistance for piles,” “base or tip resistance for drilled shafts,” etc. This terminology has been ingrained in the technical literature, FHWA manuals, various text books and AASHTO. Herein, the terminology in various primary references listed above will be used for driven piles and drilled shafts. The first time a specific phrase or term appears in the text, it will be highlighted in **bold text**.

For all deep foundations, the capacity of the foundation is a function of the geotechnical and the structural aspects. The geotechnical aspect is a function of the resistance from the ground while

the structural aspect is a function of the structural section and the structural properties of the pile. In this chapter, the primary emphasis is on the geotechnical aspects of the deep foundations. Structural aspects are discussed only to the extent that they may be relevant, e.g., the structural capacity of a pile relative to the driving stresses induced during the driven pile installation process.

**Table 9-1**  
**Pile type selection based on subsurface and hydraulic conditions**

<b>Typical Problem</b>	<b>Recommendations</b>
Boulders overlying bearing stratum	Use heavy nondisplacement driven pile with a reinforced tip or manufactured point and include contingent predrilling item in contract. Depending on the size of the boulders, large diameter drilled shaft may be feasible.
Loose cohesionless soil	Use tapered pile to develop maximum skin friction. For drilled shafts, side-support in form of casing or slurry will be required making it costlier than the driven pile option
Negative shaft resistance	Use smooth steel pile to minimize drag adhesion, and avoid battered piles. Minimize the magnitude of drag force when possible. In case of drilled shafts use casing to minimize drag load.
Deep soft clay	Use rough concrete pile to increase adhesion and rate of pore water dissipation. Drilled shaft is possible but side-support in form of casing or slurry will be required making it costlier than driven pile option.
Artesian Pressure	Do not use mandrel driven thin-wall shells as generated hydrostatic pressure may cause shell collapse; pile heave common to closed-end pipe. In case of drilled shaft, a slurry drilling will be required.
Scour	Do not use tapered piles unless large part of taper extends well below scour depth. Design permanent pile capacity to mobilize soil resistance below scour depth. Large drilled shaft is likely a better option compared to a group of piles.
Coarse Gravel Deposits	Use precast concrete piles where hard driving expected in coarse soils. DO NOT use H-piles or open end pipes as nondisplacement piles will penetrate at low blow count and cause unnecessary overruns. Drilled shaft is likely a better option for coarse gravel deposit.

## 9.2 DRIVEN PILE DESIGN-CONSTRUCTION PROCESS

The driven pile design and construction process has aspects that are unique in all of structural design. Because the driving characteristics are related to pile capacity for most soils, they can be used to improve the accuracy of the pile capacity estimate. In general, the various methods of determining pile capacity from dynamic data such as driving resistance with wave equation analysis and dynamic measurements are considerably more accurate than the static analysis methods based on subsurface exploration information. **It must be clearly understood that the static analysis based on the subsurface exploration information usually has the function of providing an *estimate* of the pile length prior to field installation. The final driving criterion is usually a blow count that is established after going to the field and the individual pile penetrations may vary depending on the soil variability. Furthermore, pile driveability is a very important aspect of the process and must be considered during the design phase.**

*The key point to understand in a driven pile design is that the pile should be designed such that it (a) can be driven to the design depth without damage, and (b) sustain the loads with the design factor of safety during the service life of the structure.* If the design is completed and the piles cannot be driven, large costs can be generated. It is absolutely necessary that the design and construction phases be linked in a way that does not exist elsewhere in construction.

The driven pile design-construction process is outlined in the flow chart of Figure 9-3. This flow chart will be discussed block by block using the numbers in the blocks as a reference and it will serve to guide the designer through all of the tasks that must be completed.

### **Block 1: Establish Global Project Performance Requirements**

The first step in the entire process is to determine the general structure requirements.

1. Is the project a new bridge, a replacement bridge, a bridge renovation, a retaining wall, a noise wall, or sign or light standard?
2. Will the project be constructed in phases or all at one time?
3. What are the general structure layout and approach grades?
4. What are the surficial site characteristics?

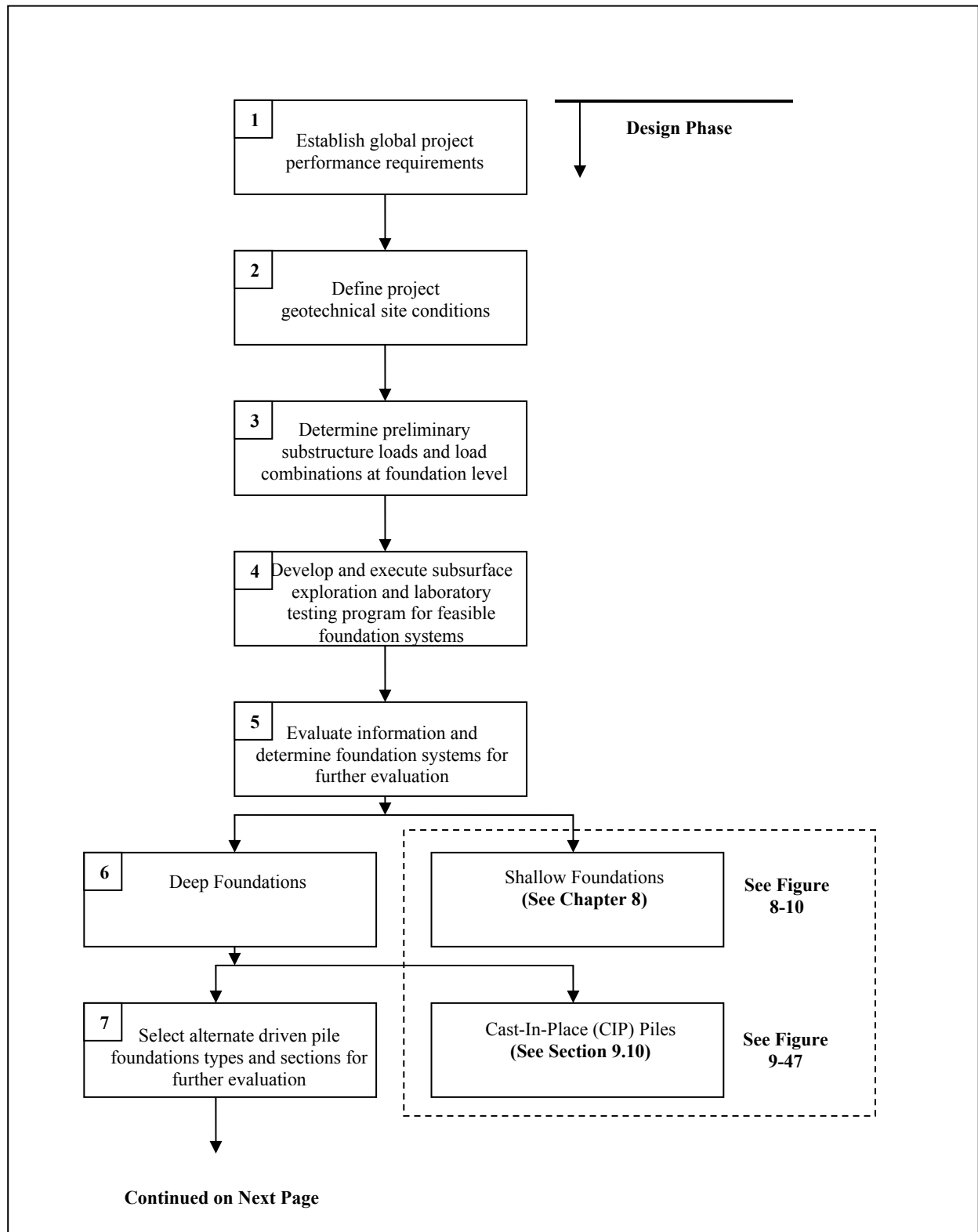


**Figure 9-3. Driven pile design and construction process (after FHWA 2006a).**

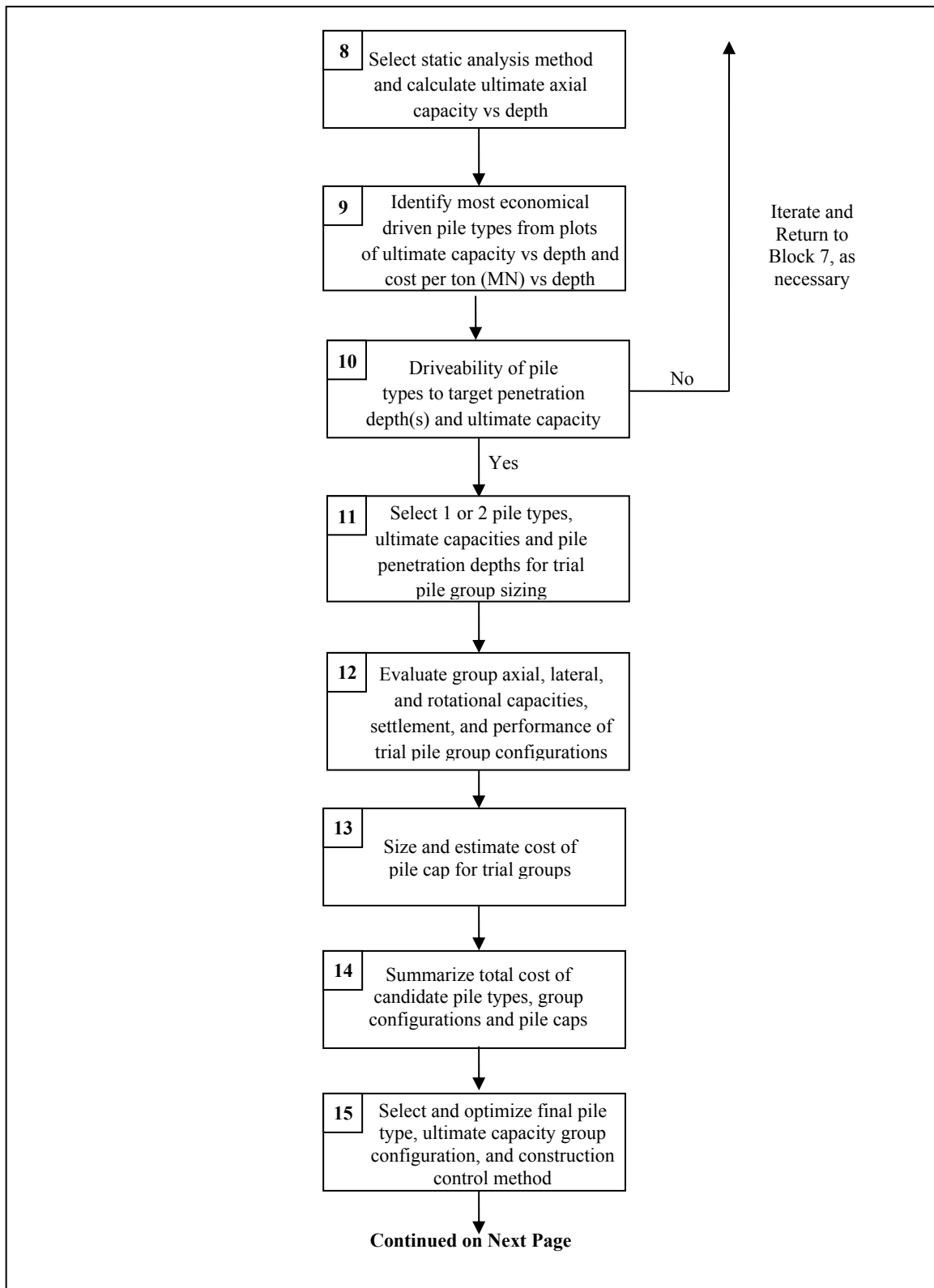


**Figure 9-3 (Continued). Driven pile design and construction process (after FHWA 2006a).**

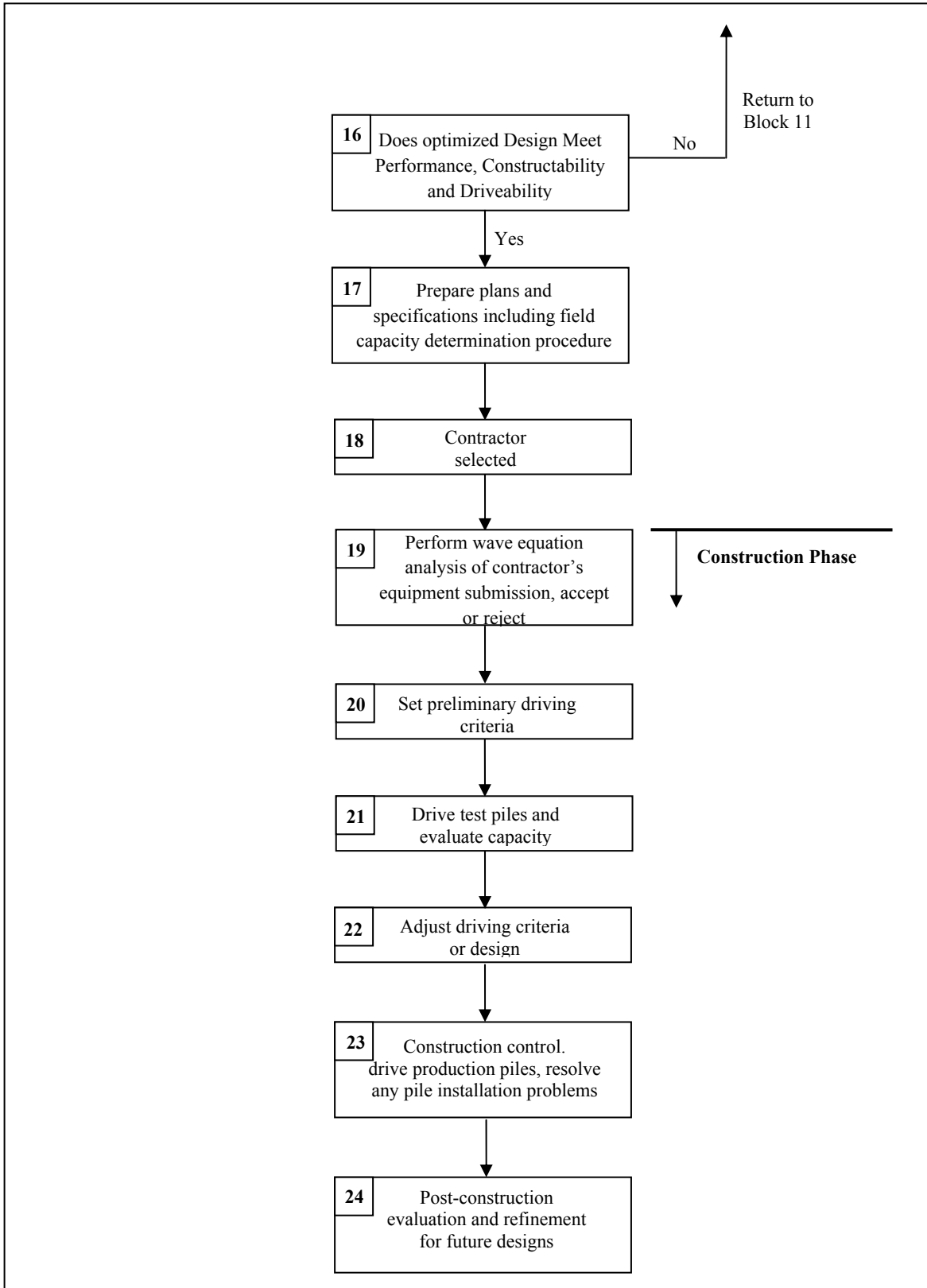


**Figure 9-3 (Continued). Driven pile design and construction process (after FHWA 2006a).**

5. Is the structure subjected to any special design events such as seismic, scour, downdrag, debris loading, vessel impact, etc.? If there are special design events, the design requirements should be reviewed at this stage so that these can be factored into the site investigation.
6. What are the approximate foundation loads? What are the deformation or deflection requirements (total settlement, differential settlement, lateral deformations, tolerances)?
7. Are there site environmental issues that must be considered in the design (specific limitation on noise, vibrations, etc.)?

### **Block 2: Define Project Geotechnical Site Conditions**

A great deal can be learned about the foundation requirements with even a very general understanding of the site geology. For small structures, this may involve only a very superficial investigation such as a visit to the site. The foundation design for very large structures may require extensive geologic studies and review of geologic maps. Based on the geologic studies, the project team should consider possible modifications in the structure that may be desirable for the site under consideration

Frequently there is information available on foundations that have been constructed in the area. This information can be of assistance in avoiding problems. Both subsurface exploration information and foundation construction experience should be collected *prior* to beginning the foundation design. Unfortunately, this step is not often done in practice.

### **Block 3: Determine Preliminary Substructure Loads and Load Combinations at the Foundation Level**

Substructure loads and reasonable vertical and lateral deformation requirements should be established at this time. This issue was considered in Block 1. The result of that effort has probably matured in the intervening time which might be quite long for some projects and is now better defined. It is imperative that the foundation specialist obtain a completely defined and unambiguous set of foundation loads and performance requirements in order to proceed through the foundation design process. Accurate load information and performance criteria are essential in the development and implementation of an adequate subsurface exploration program for the planned structure.

#### **Block 4: Develop and Execute Subsurface Exploration Program for Feasible Foundation Systems**

Based on the information obtained in Blocks 1-3, it is possible to make decisions regarding the necessary information that must be obtained for the feasible foundation systems at the site. The subsurface exploration program and the associated laboratory testing must meet the needs of the design problem that is to be solved at a cost consistent with the size and importance of the structure. The results of the subsurface exploration program and the laboratory testing are used to prepare a subsurface profile and identify critical cross sections. These tasks are covered in greater detail in Chapters 3, 4, and 5.

#### **Block 5: Evaluate Information and Select Candidate Foundation Systems**

The information collected in Blocks 1-4 must be evaluated and candidate foundation systems selected for further consideration. The first question to be decided is whether a shallow or a deep foundation is required. This question will be answered based primarily on the strength and compressibility of the site soils, the proposed loading conditions, scour depth, the project performance criteria and the foundation cost. If settlement and scour are not a problem for the structure, then a shallow foundation will probably be the most economical solution. Ground improvement techniques in conjunction with shallow foundations should also be evaluated. Shallow and deep foundation interaction with approach embankments must also be considered. If the performance of a shallow foundation exceeds the limitations imposed by the structure performance criteria, a deep foundation must be used. The design of ground improvement techniques is not covered in this manual and can be found in FHWA (2006b). Information on design considerations for shallow foundations can be found in Chapter 8.

#### **Block 6: Deep Foundations**

The decision on deep foundation type is now between driven piles and other deep foundation systems. These other deep foundation systems are primarily drilled shafts, but would also include micropiles, auger cast piles, and other drilled-in deep foundation systems as shown in Figure 9-2. The questions that must be answered in deciding between driven piles and other deep foundation systems will center on the relative costs of available, possible systems. Foundation support cost can be conveniently calculated based on a cost per unit of load carried. In addition, constructability must be considered. Design guidance on drilled shafts can be found in Section 9.10 of this chapter. Guidance for other deep foundation systems such as micro-piles and auger cast piles can be found in the references listed in Section 9.1.

## **Block 7: Select Candidate Driven Pile Types for Further Evaluation**

At this point on the flow chart, the primary concern is for the design of a driven pile foundation. The pile type must be selected consistent with the applied load per pile. Consider this problem. The general magnitude of the column or pier loads is known from the information obtained in Blocks 1 and 3. However, a large number of combinations of pile capacities and pile types can satisfy the design requirements. Should twenty, 225 kip (1000 kN) capacity piles be used to carry a 4,500 kip (20,000 kN) load, or would it be better to use ten, 450 kip (2,000 kN) capacity piles? This decision should consider both the structural capacity of the pile and the realistic geotechnical capacities of the pile type for the soil conditions at the site, the cost of the available alternative piles, and the capability of available construction contractors to drive the selected pile. Of course, there are many geotechnical factors that must also be considered. At this point in the design process, 2 to 5 candidate pile types and/or sections that meet the general project requirements should be selected for further evaluation. Pile type and selection considerations are covered in Section 9.3.

At this stage the loads must also be firmly established. In Block 1, approximate loads were determined, which were refined in Block 3. At the early stages of the design process the other aspects of the total structural design were probably not sufficiently advanced to establish the final design loads. By the time that Block 6 has been reached, the structural engineer should have finalized the various loads. One common inadequacy that is sometimes discovered when foundation problems arise is that the foundation loads were never really accurately defined at the final stage of the foundation design.

If there are special design events to be considered, they must be included in the determination of the loads. Vessel impact will be evaluated primarily by the structural engineer and the results of that analysis will give pile loads for that case. There may be stiffness considerations in dealing with vessel impact since the design requirement is basically a requirement that some vessel impact energy be absorbed by the foundation system.

Scour presents a different requirement. The loads due to the forces from the stream must be determined as specified in the AASHTO (2002), Section 3.18. The requirements of this AASHTO section should be included in the structural engineer's load determination process. The depth of scour must also be determined as directed in AASHTO (2002), Section 4.3.5. In the design process, it must be assured that the pile will still have adequate capacity after scour.

In many locations in the country, seismic loads will be an important contributor to some of the critical pile load conditions. Since the 1971 San Fernando Earthquake, significant emphasis has

been placed on seismic design considerations in the design of highway bridges. The AASHTO Standard Specifications for Highway Bridges has been substantially expanded to improve the determination of the seismic loads. Usually the structural engineer will determine the seismic requirements. Frequently the behavior of the selected pile design will affect the structural response and hence the pile design loads. In this case, there will be another loop in the design process that includes the structural engineer. The geotechnical engineer should review the seismic design requirements in Division I-A of AASHTO (2002) for a general understanding of the design approach.

**Block 8:      Select Static Analysis Method and Calculate Ultimate Capacity vs Depth**

A static analysis method(s) applicable to the pile type(s) under consideration and the soil conditions at the site should now be selected. Static analysis methods are covered in detail in Section 9.4. The ultimate axial capacity versus depth should then be calculated for all candidate pile types and sections.

**Block 9:      Identify Most Economical Candidate Pile Types and/or Sections**

The next step is to develop and evaluate plots of the ultimate axial static capacity versus pile penetration depth and the pile support cost versus pile penetration depth for each candidate pile type and/or section. The support cost, which is the cost per ton (kN) supported, is the ultimate capacity at a given penetration depth divided by the pile cost to reach that penetration depth. The pile cost can be calculated from the unit cost per ft (m) multiplied by the pile length to the penetration depth. These plots should be evaluated to identify possible pile termination depths to obtain the lowest pile support cost. This process is briefly discussed in Section 9.3.

**Block 10:     Calculate Driveability of Candidate Pile Types**

Candidate pile types should now be evaluated for driveability. Can the candidate pile type and/or section be driven to the required capacity and penetration depth at a reasonable pile penetration resistance (blow count) without exceeding allowable driving stresses for the pile material? This analysis is performed by using the wave equation theory. All of the necessary information is available except the hammer selection. Since the hammer to be used on the job will be known only after the contractor is selected, possible hammers must be identified to make sure that the pile is driveable to the capacity and depth required.

Pile driveability, wave equation analysis and allowable pile driving stresses are discussed in Section 9.9.

If candidate pile types or sections do not meet driveability requirements they are dropped from further evaluation or modified sections must be chosen and evaluated. For H-piles and pipe piles it may be possible to increase the pile section without increasing the soil resistance to driving. For concrete piles an increase in section usually means a larger pile size. Therefore, an increase in soil resistance must also be overcome. Hence, some section changes may cause the design process to revisit Block 8. If all candidate pile types fail to meet driveability requirements, the design process must return to Block 7 and new candidate pile types must be selected.

**Block 11: Select 1 or 2 Final Candidate Pile Types for Trial Group Sizing**

The most viable candidate pile types and/or sections from the cost and driveability evaluations in Blocks 9 and 10 should now be evaluated for trial group sizing by using the final loads and performance requirements. Multiple pile penetration depths and the resulting ultimate capacity at those depths should be used to establish multiple trial pile group configurations for each candidate pile type. These trial configurations should then be carried forward to Block 13.

**Block 12: Evaluate Capacity, Settlement, and Performance of Trial Groups**

The trial group configurations should now be evaluated for axial group capacity, group uplift, group lateral load performance, and settlement. These computations and analysis procedures are described in Section 9.6.

**Block 13: Size and Estimate Pile Cap Cost for Trial Groups**

The size and thickness of the pile cap for each trial group should be evaluated, and the resulting pile cap cost estimated. It is not necessary to design the cap reinforcement at this time only to determine cap size. Pile cap cost is a key component in selecting the most cost effective pile type and should not be overlooked.

**Block 14: Summarize Total Cost of Final Candidate Piles**

The total cost of each candidate pile should now be determined. A given pile type may have several total cost options depending upon the pile penetration depths, ultimate capacities, group configurations, and pile cap sizes carried through the design process. The cost of any special construction considerations and environmental restrictions should also be included in the total cost for each candidate pile.

### **Block 15: Select and Optimize Final Pile Type, Capacity, and Group Configuration**

Select the final pile foundation system including pile type, section, length, ultimate capacity and group configuration for final design. A complete evaluation of lateral and rotational resistance of the group should be performed. The design should be optimized for final structure loads, performance requirements, and construction efficiency.

### **Block 16: Does Optimized Design Meet All Requirements?**

The final pile type, section, capacity and group configuration optimized in Block 15 should be evaluated so that all performance requirements have been achieved. If the optimization process indicates that a reduced pile section can be used, the driveability of the optimized pile section must be checked by a wave equation driveability analysis. This analysis should also consider what influence the group configuration and construction procedures (e.g., cofferdams, etc.) may have on pile installation conditions.

### **Block 17: Prepare Plans and Specifications, Set Field Capacity Determination Procedure**

When the design has been finalized, plans and specifications can be prepared and the procedures that will be used to verify pile capacity can be defined. It is important that all of the quality control procedures are clearly defined for the bidders to avoid claims after construction is underway. In the past a pile load specified on the basis of dynamic formulae was a design or working load since a factor of safety is contained in the formula. Modern methods for determining pile capacity always use ultimate loads with a factor of safety (or in LRFD a resistance factor) selected and applied. This modern approach should also be made clear in the project specifications so that the contractor has no question regarding the driving requirements. Procedures should be in place that address commonly occurring pile installation issues such as obstructions and driveability.

### **Block 18: Contractor Selection**

After the bidding process is complete, a contractor is selected. The contractor should be qualified and experienced in the installation of driven piles for the type of structure being built.

### **Block 19: Perform Wave Equation Analysis of Contractor's Equipment Submission**

At this point the engineering effort shifts to the field. The contractor will submit a description of the pile driving equipment that he intends to use on the project for the engineer's evaluation. Wave equation analyses are performed to determine the driving resistance that must be achieved in the field to meet the required capacity and pile penetration depth. Driving stresses are determined and evaluated. If all conditions are satisfactory, the equipment is approved for driving. Some design specifications make this information advisory to the contractor rather than mandatory. Section 9.8 provides additional information in this area.

On smaller projects, a dynamic formula may be used to evaluate driveability. In this case, the modified Gates Formula should be used. If a dynamic formula is used, then driveability and hammer selection will be based on the driving resistance given by the formula only, since stresses are not determined. Dynamic formula usage is covered in Section 9.9.

### **Block 20: Set Preliminary Driving Criteria**

Based on the results of the wave equation analysis of Block 19 (or on smaller projects the modified Gates Formula) and any other requirements in the design, the preliminary driving criteria can be set.

### **Block 21: Drive Test Pile and Evaluate Capacity**

The test pile(s), if required, are driven to the preliminary criteria developed in Block 19. Driving requirements may be defined by penetration depth, driving resistance, dynamic monitoring results or a combination of these conditions. The capacity can be evaluated by driving resistance from wave equation analysis, the results of dynamic monitoring, static load test, the modified Gates Formula, or a combination of these. Dynamic monitoring is described in Section 9.9. Static load test procedures are discussed in greater detail at the end of this chapter.

### **Block 22: Adjust Driving Criteria or Design**

At this stage the final conditions can be set or, if test results from Block 21 indicate the capacity is inadequate, the driving criteria may have to be changed. In a few cases, it may be necessary to make changes in the design that will return the process as far back as Block 8.

In some cases, it is desirable to perform preliminary field testing before final design. When the job is very large and the soil conditions are difficult, it may be possible to achieve substantial

cost savings by having results from a design stage test pile program, including actual driving records at the site, as part of the bid package.

**Block 23: Construction Control**

After the driving criteria are set, the production pile driving begins. Quality control and assurance procedures have been established and are applied. Problems may arise and must be handled as they occur in a timely fashion.

**Block 24: Post-Construction Evaluation and Refinement of Design**

After completion of the foundation construction, the design should be reviewed and evaluated for its effectiveness in satisfying the design requirements and also its cost effectiveness.

**9.3 ALTERNATE DRIVEN PILE TYPE EVALUATION**

The selection of appropriate driven pile types for any project involves the consideration of several design and installation factors including pile characteristics, subsurface conditions and performance criteria. This selection process should consider the factors listed in Table 9-1, Table 9-2 and Table 9-3. Table 9-2 summarizes typical pile characteristics and uses. Table 9-3 presents the placement effects of pile shape characteristics.

**Table 9-2  
Typical piles and their range of loads and lengths**

<b>Type of Pile</b>	<b>Typical Axial Design Loads</b>	<b>Typical Lengths</b>
Timber	20-110 kips (100 – 500 kN)	15-120 ft (5-37 m)*
Precast / Prestressed Reinforced Concrete	90-225 kips (400-1,000 kN) for reinforced 90-1000 kips (400-4,500 kN) for prestressed	30-50 ft (10-15m) for reinforced 50-130 ft (15-40m) for prestressed
Steel H	130-560 kips (600-2,500 kN)	15-130 ft (5-40 m)
Steel Pipe (without concrete core)	180-560 kips (800-2,500 kN)	15-130 ft (5-40 m)
Steel Pipe (with concrete core)	560-3400 kips (2,500-15,000 kN)	15-130 ft (5-40 m)
* 15-75 ft (5-23 m) for Southern Pine; 15-120 ft (5-37 m) for Douglas Fir		

**Table 9-3  
Pile type selection pile shape effects**

<b>Shape Characteristics</b>	<b>Pile Types</b>	<b>Placement Effects</b>
Displacement	Steel Pipe (Closed end), Precast Concrete	<ul style="list-style-type: none"> <li>• Increase lateral ground stress</li> <li>• Densify cohesionless soils, remolds and weakens cohesive soils temporarily</li> <li>• Set-up time may be 6 months in clays for pile groups</li> </ul>
Nondisplacement	Steel H, Steel Pipe (Open end)	<ul style="list-style-type: none"> <li>• Minimal disturbance to soil</li> <li>• Not suited for friction piles in coarse granular soils. Piles often have low driving resistances in these deposits making field capacity verification difficult thereby often resulting in excessive pile lengths.</li> </ul>
Tapered	Timber, Monotube, Tapertube, Thin-wall shell	<ul style="list-style-type: none"> <li>• Increased densification of soils with less disturbance, high capacity for short length in granular soils</li> </ul>

In addition to the considerations provided in the Tables 9-1, 9-2 and 9-3, the problems posed by the specific project location and topography must be considered in any pile selection process. Following are some of the problems usually encountered:

1. Noise and vibration from driven pile installation may affect pile type selection, and require special techniques such as predrilling and/or vibration monitoring of adjacent structures.
2. Remote areas may restrict driving equipment size and, therefore, pile size.
3. Local availability of certain materials and the capability of local contractors may have decisive effects on pile selection.
4. Waterborne operations may dictate use of shorter pile sections due to pile handling limitations.
5. Steep terrain may make the use of certain pile equipment costly or impossible.

### **9.3.1 Cost Evaluation of Alternate Pile Types**

Often several different pile types meet all the requirements for a particular structure. In such cases, the final choice should be made on the basis of a cost analysis that assesses the over-all cost of the foundation alternatives. This requires that candidate pile types be

carried forward in the design process for determination of the pile section requirements for design loads and constructability. The cost analysis for the candidate pile types should include uncertainties in execution, time delays, cost of load testing programs, as well as the differences in the cost of pile caps and other elements of the structure that may differ among alternatives. For major projects, alternate foundation designs should be considered for inclusion in the contract documents if there is a potential for cost savings.

For driven pile foundation projects, the total foundation cost can be separated into three major components as follows:

- The pile cost
- The pile cap cost, and
- The construction control method cost

For most pile types, the pile cost can usually be assumed as linear with depth based on unit price. However, this may not be true for very long concrete piles or long, large section steel piles. These exceptions may require the cost analysis to reflect special transportation, handling, or splicing costs for concrete piles or extra splice time and cost for steel piles. Table 9-4 presents cost savings recommendations to be considered during the evaluation of pile foundations. Expressing the cost of candidate pile types in terms of dollars per ton capacity would allow comparison of alternative pile types in a rational manner. Details of this approach, i.e., expressing costs in \$/ton, are presented in FHWA (2006a).

#### **9.4 COMPUTATION OF PILE CAPACITY**

Once the allowable structural load has been determined for prospective pile alternates, the pile length required to support that load must be determined. For many years this length determination was considered part of the "art of foundation engineering." In recent years more rational analytic procedures have been developed. Static analyses provide a useful design tool to select the most economical pile alternates. The methods that follow are established procedures that account for the variables in pile length determination. The "art" remains in selecting appropriate soil strength values for the conditions and ascertaining the effects of pile installation on these values. For the typical project two static analyses will be required; the first to determine the length required for permanent support of the structures, and the second to determine the soil resistance to be overcome during driving to achieve the estimated length. It must be stressed that each new site represents a new problem with unique conditions. Experience with similar sites should not replace but should refine the rational analysis methods presented herein. This section discusses the concept of static capacity of the pile based on a rational approach.

**Table 9-4. Cost savings recommendations for pile foundations (FHWA, 2006a)**

Factor	Inadequacy of Older Methods	Cost Saving Recommendations	Remarks
A. Design structural load capacity of piles.	1. Allowable pile material stresses may not address site-specific considerations.	1. Use realistic allowable stresses for pile materials in conjunction with adequate construction control procedures, (i.e., load testing, dynamic pile monitoring and wave equation). 2. Determine potential pile types and carry candidate pile types forward in the design process. 3. Optimize pile size for loads.	1. Rational consideration of Factors A and B may decrease cost of a foundation by 25 percent or more. 2. Significant cost savings can be achieved by optimization of pile type and section for the structural loads with consideration of pile driveability requirements.
B. Design geotechnical capacity of soil and rock to carry load transferred by piles.	1. Inadequate subsurface explorations and laboratory testing. 2. Rules of thumb and prescribed values used in lieu of static design may result in overly conservative designs. 3. High potential for change orders and claims.	1. Perform thorough subsurface exploration including in-situ and laboratory testing to determine design parameters. 2. Use rational and practical methods of design. 3. Perform wave equation driveability analysis. 4. Use design stage pile load testing on large pile driving projects to determine load capacities (load tests during design stage).	1. Reduction of safety factor can be justified because some of the uncertainties about load carrying capacities of piles are reduced. 2. Rational pile design will generally lead to shorter pile lengths and/or smaller number of piles.
C. Alternate foundation design.	1. Alternate foundation designs are rarely used even when possibilities of cost savings exist by allowing alternates in contract documents.	1. For major projects, consider inclusion of alternate foundation designs in the contract documents if estimated costs of feasible foundation alternatives are within 15 percent of each other.	1. Alternative designs often generate more competition which can lead to lower costs.
D. Plans and specifications.	1. Unrealistic specifications. 2. Uncertainties due to inadequate subsurface explorations force the contractors to inflate bid prices.	1. Prepare detailed contract documents based on thorough subsurface explorations, understanding of contractors' difficulties and knowledge of pile techniques and equipment. 2. Provide subsurface information to the contractor.	1. Lower bid prices will result if the contractor is provided with all the available subsurface information. 2. Potential for contract claims is reduced with realistic specifications.
E. Construction determination of pile load capacity during installation.	1. Often used dynamic formulas such as Engineering News formula are unreliable. Correlations between load capacities determined from Engineering News formula and static load tests indicate safety factors ranging from less than 1 (i.e. failure) to about 20 (i.e. excessive foundation cost).	1. Eliminate use of dynamic formulas for construction control as experience is gained with the wave equation analysis. 2. Use wave equation analysis coupled with dynamic monitoring for construction control and load capacity evaluation. 3. Use pile load tests on projects to substantiate capacity predictions by wave equation and dynamic monitoring.	1. Reduced factor of safety may allow shorter pile lengths and/or smaller number of piles. 2. Pile damage due to excessive driving can be eliminated by using dynamic monitoring equipment. 3. Increased confidence and lower risk results from improved construction control.

The **static capacity** of a pile can be defined as the sum of soil/rock resistances along the pile shaft and at the pile toe available to support the imposed loads on the pile. Static analyses are performed to determine the ultimate capacity of an individual pile and of a pile group as well as the deformation response of a pile group to the applied loads. The **ultimate capacity** of an individual pile and of a pile group is defined as the smaller of:

- (1) the capacity of the surrounding soil/rock medium to support the loads transferred from the pile(s) or,
- (2) the structural capacity of the pile(s).

Soil-structure interaction analysis methods are used to determine the deformation response of piles and pile groups to lateral loads; such methods can also be used for deformation evaluation under vertical loads. The results from these analyses as well as the results of static analysis of pile group settlement are compared to the performance criteria established for the structure.

The ultimate geotechnical pile capacity,  $Q_u$ , of a pile in homogeneous soil may be expressed as follows in terms of the **shaft (commonly known as “skin”) resistance**,  $R_s$ , **toe resistance**,  $R_t$ , and the weight,  $W$ , of the pile:

$$Q_u = R_s + R_t - W \quad 9-1$$

In most cases, such as H-Piles and open ended pipe piles, the weight  $W$  is small compared to the shaft and toe resistance and is neglected. However, the weight of pipe piles, particularly large diameter pipes, filled with concrete may be significant and may be included in the analysis. In this chapter, the  $W$  term is neglected. Equation 9-1, without the  $W$  term, may also be expressed in the form

$$Q_u = f_s A_s + q_t A_t \quad 9-2$$

where  $f_s$  is the **unit shaft resistance** over the shaft surface area,  $A_s$ , and  $q_t$  is the **unit toe resistance** over the pile toe area,  $A_t$ . The above equations for pile bearing capacity assume that both the pile toe and the pile shaft have moved sufficiently with respect to the adjacent soil to simultaneously develop the ultimate shaft and toe resistances. Generally, the displacement needed to mobilize the shaft resistance is smaller than that required to mobilize the toe resistance. This simple rational approach has been commonly used for all piles except very large diameter piles where such an approach may not be valid.

Figure 9-4 illustrates typical load transfer profiles for a single pile. The load transfer distribution can be obtained from a static load test where strain gages or telltale rods are attached to a pile at different depths along the pile shaft. Figure 9-4 shows the measured ultimate axial load,  $Q_u$ , in the pile plotted against depth. **The shaft resistance transferred to the soil is represented by  $R_s$ , and  $R_t$  represents the resistance at the pile toe.** In Figure 9-4(a), the load transfer distribution for a pile with no shaft resistance is illustrated. In this case the full axial load at the pile head is transferred to the pile toe. In Figure 9-4(b), the axial load versus depth for a uniform shaft resistance distribution typical of a cohesive soil is illustrated. Figure 9-4(c) presents the axial load in the pile versus depth for a triangular shaft resistance distribution typical of cohesionless soils.

#### 9.4.1 Factors of Safety

The results of static analyses yield a **geotechnical ultimate pile capacity**,  $Q_u$ . The **allowable geotechnical soil resistance (geotechnical pile design load)**,  $Q_a$ , is selected by dividing the **geotechnical ultimate pile capacity**,  $Q_u$ , by a **factor of safety** as follows.

$$Q_a = \frac{Q_u}{\text{Factor of Safety}} \quad 9-3$$

The range of the factor of safety, FS, has depended primarily upon the reliability of the particular method of static analysis with consideration of the following items:

1. The level of confidence in the input parameters. The level of confidence is a function of the type and extent of the subsurface exploration and laboratory testing of soil and rock materials.
2. Variability of the soil and rock.
3. Method of static analysis.
4. Effects of and consistency of the proposed pile installation method.
5. Level of construction control (static load test, dynamic analysis, wave equation analysis, Gates dynamic formula).

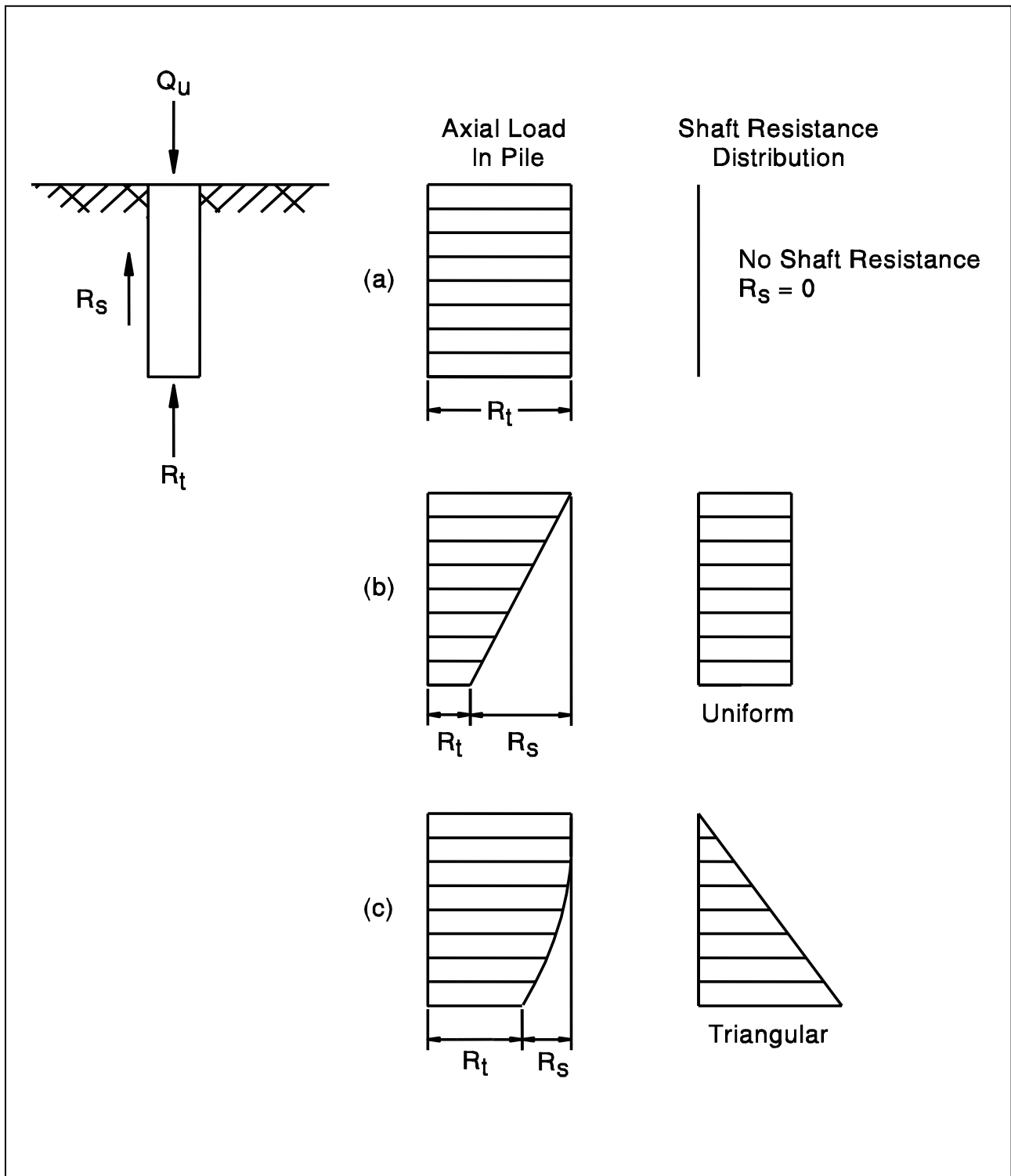


Figure 9-4. Typical load transfer profiles (FHWA, 2006a).

A large number of static analysis methods are documented in the literature with specific recommendations on the factor of safety to be used with each method. These recommended factors of safety have routinely disregarded the influence of the construction control method used to complement the static analysis computation. As part of the overall design process, it is important that the foundation designer qualitatively assess the validity of the chosen design analysis method and the reliability of the geotechnical design parameters.

While the range of static analysis factors of safety in the past was from 2 to 4, most of the static analysis methods recommended a factor of safety of 3. As foundation design loads increased over time, the use of higher factors of safety often resulted in pile installation problems. In addition, experience has shown that construction control methods have a significant influence on pile capacity. Therefore, **the factor of safety used in a static analysis calculation should be based upon the construction control method specified.** Provided that the procedures recommended in this manual are used for the subsurface exploration and analysis, the factors of safety in Table 9-5 are recommended based on the specified construction control method. The factor of safety for other test methods not included in Table 9-5 should be determined by the individual designer.

**Table 9-5. Recommended factor of safety based on construction control method**

<b>Construction Control Method</b>	<b>Factor of Safety</b>
Static load test with wave equation analysis	2.00
Dynamic testing with wave equation analysis	2.25
Indicator piles with wave equation analysis	2.50
Wave equation analysis	2.75
Gates dynamic formula	3.50

The pile design load should be supported by soil resistance developed only in soil layers that contribute to long term load support. The soil resistance from soils subject to scour, or from soil layers above soft compressible soils should not be considered. The following example problem will be used to clarify the use of the factor of safety in static pile capacity calculations for determination of the pile design load as well as for determination of the soil resistance to pile driving.

Consider a pile to be driven through the soil profile described in Figure 9-5. The proposed pile type penetrates through a sand layer subject to scour in the 100-year flood into an underlying very soft clay layer unsuitable for long term support and then into competent support materials. The soil resistances from the scour-susceptible sand layer and soft clay layer do not contribute to long term load support and should not be included in the soil resistance for support of the design load. In this example, static load testing with wave equation analysis will be used for construction control. Therefore, a factor of safety of 2.0 should be applied to the ultimate soil resistance calculated in suitable support layers in the static analysis. It should be noted that this approach is for scour conditions under the 100-year or overtopping flood events and that a different approach would apply for the superflood or 500-year event. For a superflood, a minimum factor of safety of 1.0 is used. This minimum factor of safety is determined by dividing the maximum pile load by the sum of the shaft and toe resistances available below scour depth.

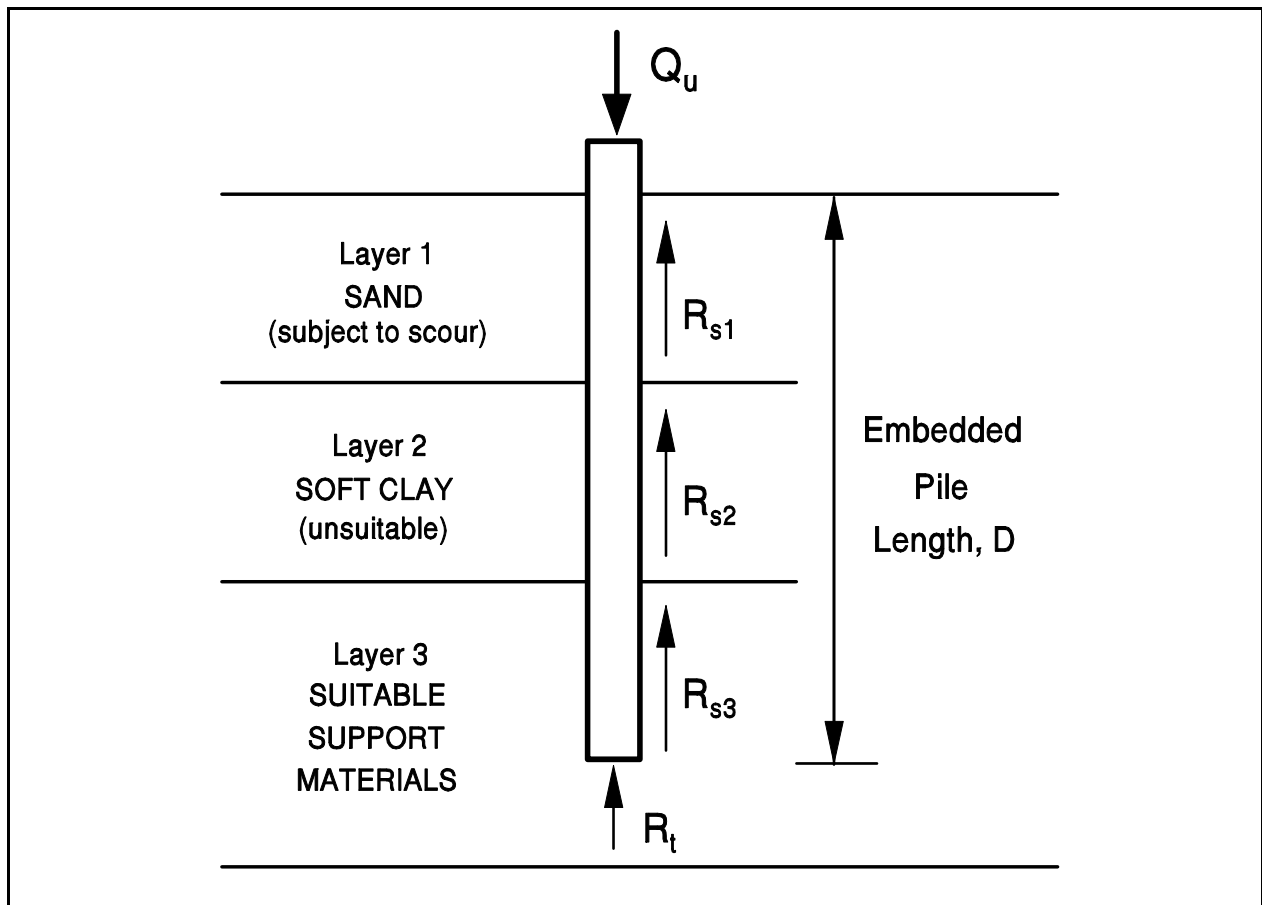


**Figure 9-5. Soil profile for factor of safety discussion (FHWA, 2006a).**

In the static analysis, a trial pile penetration depth is chosen and an ultimate pile capacity,  $Q_u$ , is calculated. This ultimate capacity includes the soil resistance calculated from all soil layers including the shaft resistance in the scour susceptible layer,  $R_{s1}$ , the shaft resistance in the unsuitable soft clay layer,  $R_{s2}$  as well as the resistance in suitable support materials along the pile shaft,  $R_{s3}$ , and at the pile toe resistance,  $R_t$ .

$$Q_u = R_{s1} + R_{s2} + R_{s3} + R_t$$

The design load,  $Q_a$ , is the sum of the soil resistances from the suitable support materials divided by a factor of safety, FS. As noted earlier, a factor of safety of 2.0 is used in the equation below because of the planned construction control with static load testing. Therefore,

$$Q_a = (R_{s3} + R_t) / (FS=2)$$

The design load may also be expressed as the sum of the ultimate capacity minus the calculated soil resistances from the scour susceptible and unsuitable layers divided by the factor of safety. In this alternative approach, the design load is expressed as follows:

$$Q_a = (Q_u - R_{s1} - R_{s2}) / (FS=2)$$

The result of the static analysis is then the estimated pile penetration depth,  $D$ , the design load for that penetration depth,  $Q_a$ , and the calculated ultimate capacity,  $Q_u$ .

For preparation of construction plans and specifications, the **calculated geotechnical ultimate capacity**,  $Q_u$ , is specified. Note that if the construction control method changes after the design stage, the required ultimate capacity and the required pile penetration depth for the ultimate capacity will also change. This is apparent when the previous equation for the design load is expressed in terms of the ultimate capacity as follows:

$$Q_u = R_{s1} + R_{s2} + (Q_a)(FS=2)$$

A static analysis should also be used to calculate the **soil resistance to driving**, SRD, that must be overcome to reach the estimated pile penetration depth necessary to develop the ultimate capacity. This information is necessary for the designer to select a pile section with the driveability to overcome the anticipated soil resistance and for the contractor to properly size equipment. Driveability aspects of design are discussed in Section 9.9.

In the SRD calculation, a factor of safety is not used. The soil resistance to driving is the sum of the soil resistances from the scour susceptible and unsuitable layers plus the soil resistance in the suitable support materials to the estimated penetration depth.

$$SRD = R_{s1} + R_{s2} + R_{s3} + R_t$$

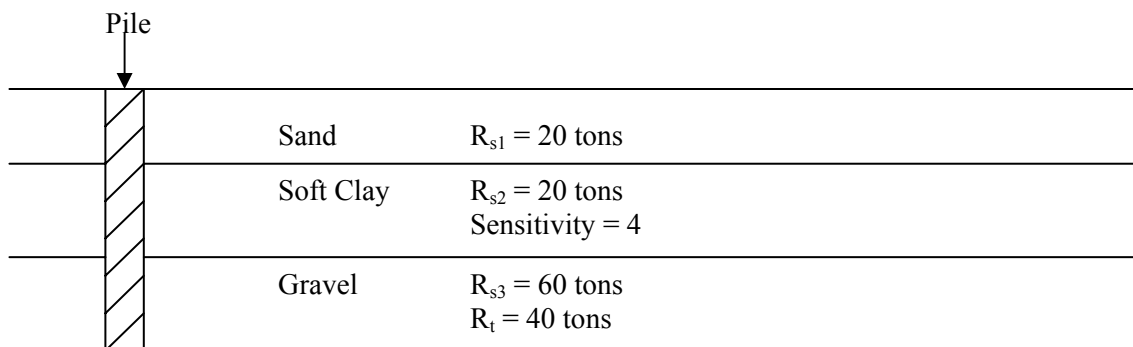
Soil resistances in this calculation should be the resistance at the time of driving. Hence time dependent changes in soil strengths due to **soil setup or relaxation** should be considered (see Table 5-8 in Chapter 5 for brief explanation of these terms and Section 9.5.5 for more discussion). For the example presented in Figure 9-5, the driving resistance from the unsuitable clay layer would be reduced by the sensitivity of the clay. Therefore,  $R_{s2}$  would be  $R_{s2} / 2$  for a clay with a sensitivity of 2. The soil resistance to driving to depth D would then be as follows

$$SRD = R_{s1} + R_{s2}/2 + R_{s3} + R_t$$

This example problem considers only the driving resistance at the final pile penetration depth. In cases where piles are driven through hard or dense layers above the estimated pile penetration depth, the soil resistance to penetrate these layers should also be calculated. Additional information on the calculation of time dependent soil strength changes is provided in Section 9.9 of this chapter.

The concepts discussed above are illustrated numerically in Example 9-1:

**Example 9-1:** Find the ultimate capacity and driving capacity for the pile from the data listed in the profile. The hydraulic specialist determined that the sand layer is susceptible to scour. The geotechnical specialist determined that the soft clay layer is unsuitable for providing resistance.



**Solution:**

$$\begin{aligned}\text{Ultimate capacity} &= R_{s3} + R_t \\ &= 60 \text{ tons} + 40 \text{ tons} = 100 \text{ tons}\end{aligned}$$

$$\begin{aligned}\text{Driving capacity} &= R_{s1} + (R_{s2}/\text{Sensitivity}) + R_{s3} + R_t \\ &= 20 \text{ tons} + \frac{20 \text{ tons}}{4} + 60 \text{ tons} + 40 \text{ tons} = 125 \text{ tons}\end{aligned}$$

## 9.5 DESIGN OF SINGLE PILES

Numerous static analysis methods are available for calculating the ultimate capacity of a single pile. The following sections of this chapter will present recommended analysis methods for piles in cohesionless, cohesive, and layered soil profiles. For additional methods based on N-values, and cone penetration test results the reader is referred to FHWA (2006a). Regardless of the method used to evaluate the static capacity of a pile, it must be understood that the factor of safety is not based on the method of analysis but on the construction control as discussed in Section 9.4. Furthermore, the pile length determined from a static analysis is just an *estimate* prior to going into the field.

### 9.5.1 Ultimate Geotechnical Capacity of Single Piles in Cohesionless Soils

The geotechnical ultimate capacity of a single pile in a cohesionless soil is the sum of shaft and toe resistances ( $Q_u = R_s + R_t$ ). The calculation assumes that the shaft resistance and toe bearing resistance can be determined separately and that these two factors do not affect each other. The Nordlund method is recommended herein for computation of ultimate capacity of single piles in cohesionless soils.

#### 9.5.1.1 Nordlund Method

The Nordlund method (1963) is based on field observations and considers pile taper and soil displacement in calculating the shaft resistance. The method also accounts for the differences in soil-pile coefficient of friction for different pile materials. The method is based on the results of several load test programs in cohesionless soils. Several pile types were used in these test programs including timber, H, closed end pipe, Monotubes and Raymond step-taper piles. These piles, which were used to develop the method's design curves, had pile widths generally in the range of 10 to 20 inches (250 to 500 mm). The Nordlund Method tends to overpredict pile

capacity for piles with widths larger than 24 inches (600 mm) and all sizes of open-ended pipe piles.

According to the Nordlund method, the geotechnical ultimate capacity,  $Q_u$ , of a pile in cohesionless soil is the sum of the shaft resistance,  $R_s$  and the toe resistance,  $R_t$ . Nordlund suggests the shaft resistance is a function of the following variables:

1. The friction angle of the soil.
2. The friction angle on the sliding surface between pile material and soil, i.e., the interface friction angle
3. The taper of the pile.
4. The effective unit weight of the soil.
5. The pile length.
6. The minimum pile perimeter.
7. The volume of soil displaced.

The Nordlund equation for computing the geotechnical ultimate capacity of a pile is as follows (see Figure 9-6 for illustration of variables):

$$Q_u = \sum_{d=0}^{d=D} K_{\delta} C_F p_d \frac{\sin(\delta + \omega)}{\cos \omega} C_d \Delta d + \alpha_t N'_q A_t p_t \quad 9-4$$

- where:
- $d$  = depth.
  - $D$  = embedded length of the pile.
  - $K_{\delta}$  = coefficient of lateral earth pressure at depth  $d$ .
  - $C_F$  = correction factor for  $K_{\delta}$  when  $\delta \neq \phi$ .
  - $p_d$  = effective overburden pressure at the center of depth increment  $\Delta d$ .
  - $\delta$  = interface friction angle between pile and soil.
  - $\omega$  = angle of pile taper from vertical.
  - $\phi$  = soil friction angle.
  - $C_d$  = pile perimeter at depth  $d$ .
  - $\Delta d$  = length of pile segment.
  - $\alpha_t$  = dimensionless factor dependent on pile depth-width relationship.
  - $N'_q$  = bearing capacity factor.
  - $A_t$  = pile toe area.
  - $p_t$  = effective overburden pressure at the pile toe.

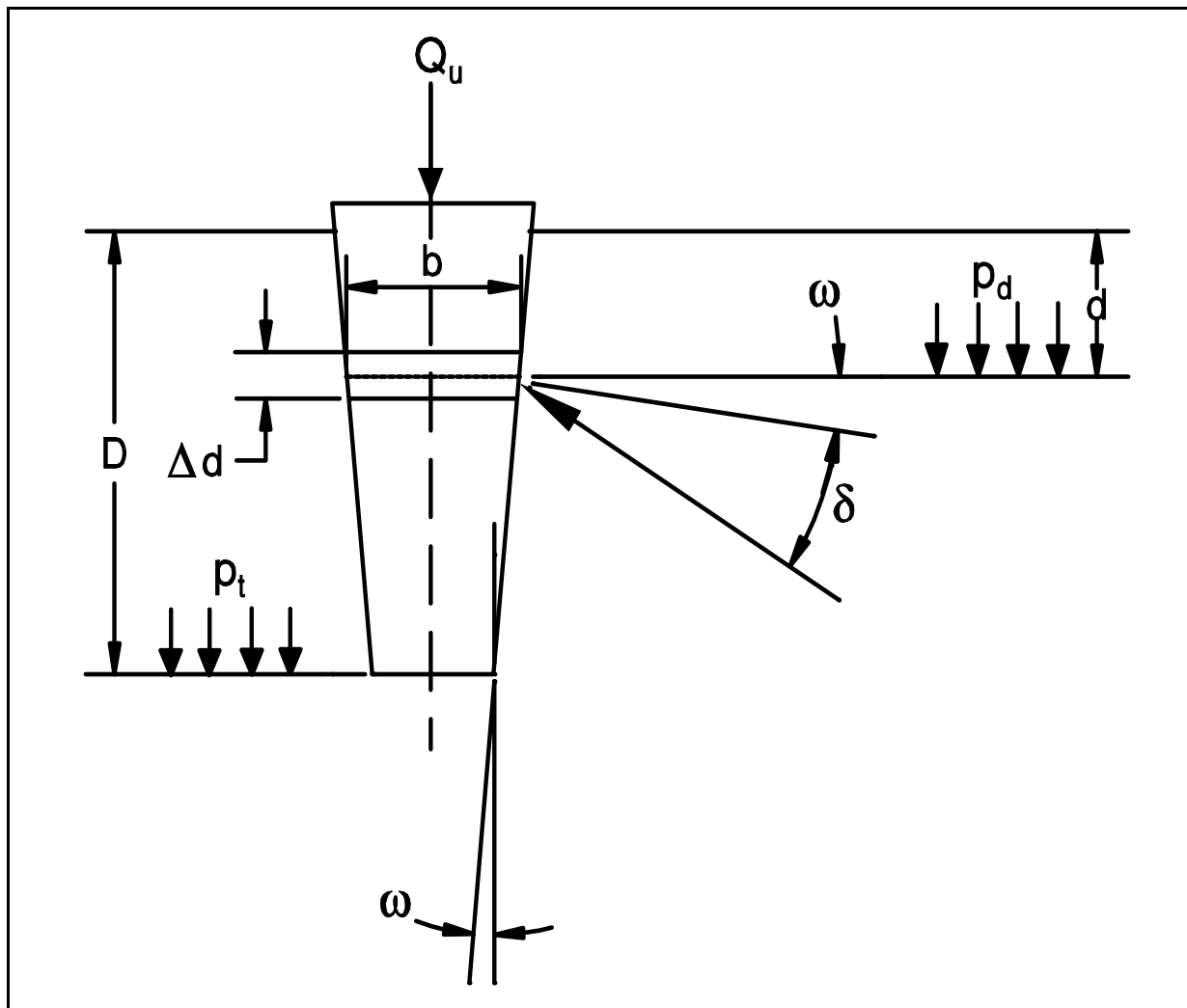


Figure 9-6. Nordlund's general equation for ultimate pile capacity (after Nordlund, 1979).

For a pile of uniform cross section ( $\omega=0$ ) and embedded length  $D$ , driven in soil layers of the same effective unit weight and friction angle, the Nordlund equation becomes:

$$Q_u = K_\delta C_F p_d \sin \delta C_d D + \alpha_t N'_q A_t p_t \quad 9-5$$

The soil friction angle  $\phi$  influences most of the calculations in the Nordlund method. In the absence of laboratory test data,  $\phi$  can be estimated from corrected SPT  $N_{160}$  values. Therefore, Equation 3-3 in Chapter 3 should be used for correcting field  $N$  values. The corrected SPT  $N_{160}$  values may then be used in Table 8-1 of Chapter 8 to estimate the soil friction angle,  $\phi$ .

Nordlund (1979) updated the method but did not place a limiting value on the shaft resistance. However, Nordlund recommended that the effective overburden pressure at the pile toe,  $p_t$ , used for computing the pile toe resistance be limited to 3 ksf (150 kPa).

### **STEP BY STEP PROCEDURE FOR USING NORDLUND METHOD**

Steps 1 through 6 are for computing the shaft resistance and steps 7 through 9 are for computing the pile toe resistance.

**STEP 1** Delineate the soil profile into layers and determine the  $\phi$  angle for each layer.

- a. Construct  $p_o$  diagram using procedure described in Chapter 2.
- b. Using Figure 3-24, correct SPT field  $N$  values for overburden pressure and obtain corrected SPT  $N_{160}$  values. Delineate soil profile into layers based on corrected SPT  $N_{160}$  values.
- c. Determine  $\phi$  angle for each layer from laboratory or in-situ test data.
- d. In the absence of laboratory or in-situ test data, determine the average corrected SPT  $N_{160}$  value,  $\bar{N}_1$ , for each soil layer and estimate  $\phi$  angle from Table 8-1 in Chapter 8.

**STEP 2** Determine  $\delta$ , the interface friction angle between the pile and soil based on displaced soil volume,  $V$ , and the soil friction angle,  $\phi$ .

- a. Compute volume of soil displaced per unit length of pile,  $V$ .
- b. Enter Figure 9-7 with  $V$  and determine  $\delta/\phi$  ratio for pile type under consideration. Note that  $\delta/\phi$  may be greater than 1.0 for taper piles to account for the development of passive resistance along the length of the pile due to pile taper.
- c. Calculate  $\delta$  from  $\delta/\phi$  ratio.

**STEP 3** Determine the coefficient of lateral earth pressure,  $K_\delta$ , for each  $\phi$  angle.

- a. Determine  $K_\delta$  for  $\phi$  angle based on displaced volume,  $V$ , and pile taper angle,  $\omega$ , by using either Figure 9-8, 9-9, 9-10, or 9-11 and the appropriate procedure described in Step 3b, 3c, 3d, or 3e.
- b. If the displaced volume is 0.1, 1.0 or 10.0 ft<sup>3</sup>/ft, which corresponds to one of the curves provided in Figures 9-8 through 9-11, and the  $\phi$  angle is one of those provided,  $K_\delta$  can be determined directly from the appropriate figure.
- c. If the displaced volume is 0.1, 1.0 or 10.0 ft<sup>3</sup>/ft, which corresponds to one of the curves provided in Figures 9-8 through 9-11, but the  $\phi$  angle is other than those provided, use linear interpolation to determine  $K_\delta$  for the required  $\phi$  angle. Tables 9-6a and 9-6b also provide interpolated  $K_\delta$  values at selected displaced volumes versus  $\phi$  angle for uniform piles ( $\omega = 0$ ).
- d. If the displaced volume is other than 0.1, 1.0 or 10.0 ft<sup>3</sup>/ft, which corresponds to one of the curves provided in Figures 9-8 through 9-11, and the  $\phi$  angle corresponds to one of those provided, use log linear interpolation to determine  $K_\delta$  for the required displaced volume. Tables 9-6a and 9-6b also provide interpolated  $K_\delta$  values at selected displaced volumes versus  $\phi$  angle for uniform piles ( $\omega = 0$ ).
- e. If the displaced volume is other than 0.1, 1.0 or 10.0 ft<sup>3</sup>/ft, which correspond to one of the curves provided in Figures 9-8 through 9-11, and the  $\phi$  angle is other than one of those provided, first use linear interpolation to determine  $K_\delta$  for the required  $\phi$  angle at the displaced volume curves provided for 0.1, 1.0 or 10.0 ft<sup>3</sup>/ft. Then use log linear interpolation to determine  $K_\delta$  for the required displaced volume. Tables 9-6a and 9-6b also provide interpolated  $K_\delta$  values at selected displaced volumes versus  $\phi$  angle for uniform piles ( $\omega = 0$ ).

**STEP 4** Determine the correction factor,  $C_F$ , to be applied to  $K_\delta$  if  $\delta \neq \phi$ .

Use Figure 9-12 to determine the correction factor for each  $K_\delta$ . Enter figure with  $\phi$  angle and  $\delta/\phi$  value to determine  $C_F$ .

**STEP 5** Compute the average effective overburden pressure at the midpoint of each soil layer,  $p_d$  (ksf).

**Note:** A limiting value is not applied to  $p_d$ .

**STEP 6** Compute the shaft resistance in each soil layer. Sum the shaft resistance from each soil layer to obtain the ultimate shaft resistance,  $R_s$  (kips). For a pile of uniform cross-section embedded in a uniform soil profile

$$R_s = K_\delta C_F p_d \sin \delta C_d D \quad 9-6$$

For H-piles in cohesionless soils, the "box" area should generally be used for shaft resistance calculations, i.e., the pile perimeter  $C_d$  should be considered as two times flange width plus two times the section height. Additional discussion on the behavior of open pile sections is presented in Section 9.5.4.

**STEP 7** Determine the  $\alpha_t$  coefficient and the bearing capacity factor,  $N'_q$ , from the  $\phi$  angle near the pile toe.

- a. Enter Figure 9-13(a) with  $\phi$  angle near pile toe to determine  $\alpha_t$  coefficient based on pile length to diameter ratio.
- b. Enter Figure 9-13(b) with  $\phi$  angle near pile toe to determine,  $N'_q$ .
- c. If  $\phi$  angle is estimated from SPT data, compute the average corrected SPT  $N_{160}$  value over the zone from the pile toe to 3 diameters below the pile toe.

**STEP 8** Compute the effective overburden pressure at the pile toe,  $p_t$  (ksf).

**Note:** The limiting value of  $p_t$  is 3 ksf (150 kPa).

**STEP 9** a. Compute the ultimate toe resistance,  $R_t$  (kips).

$$R_t = \alpha_t N'_q A_t p_t \quad 9-7a$$

- b. Compute the maximum ultimate toe resistance,  $R_t$  (max)

$$R_t (\text{max}) = q_L A_t \quad 9-7b$$

$q_L$  value is obtained as follows:

1. Enter Figure 9-14 with  $\phi$  angle near pile toe determined from laboratory or in-situ test data.
  2. Enter Figure 9-14 with  $\phi$  angle near the pile toe estimated from Table 8-1 in Chapter 8 and the average corrected SPT N1 near toe as described in Step 7.
- c. Use lesser of the two  $R_t$  values obtained from Equations 9-7a and 9-7b.

For steel H and unfilled open end pipe piles, use only steel cross section area at pile toe unless there is reasonable assurance and previous experience that a soil plug will form at the pile toe. The assumption of a soil plug would allow the use of a box area at H pile toe and total pipe cross section area for open end pipe pile. Additional discussion on the behavior of open pile sections is presented in Section 9.5.4.

- STEP 10** Compute the ultimate geotechnical pile capacity,  $Q_u$  (kips).

$$Q_u = R_s + R_t$$

- STEP 11** Compute the allowable geotechnical soil resistance,  $Q_a$  (kips).

$$Q_a = \frac{Q_u}{\text{Factor of Safety}}$$

The factor of safety used in the calculation should be based upon the construction control method to be specified. Recommended factors of safety based on construction control method are listed in Table 9-5.

The concepts discussed above are illustrated numerically in Example 9-2.

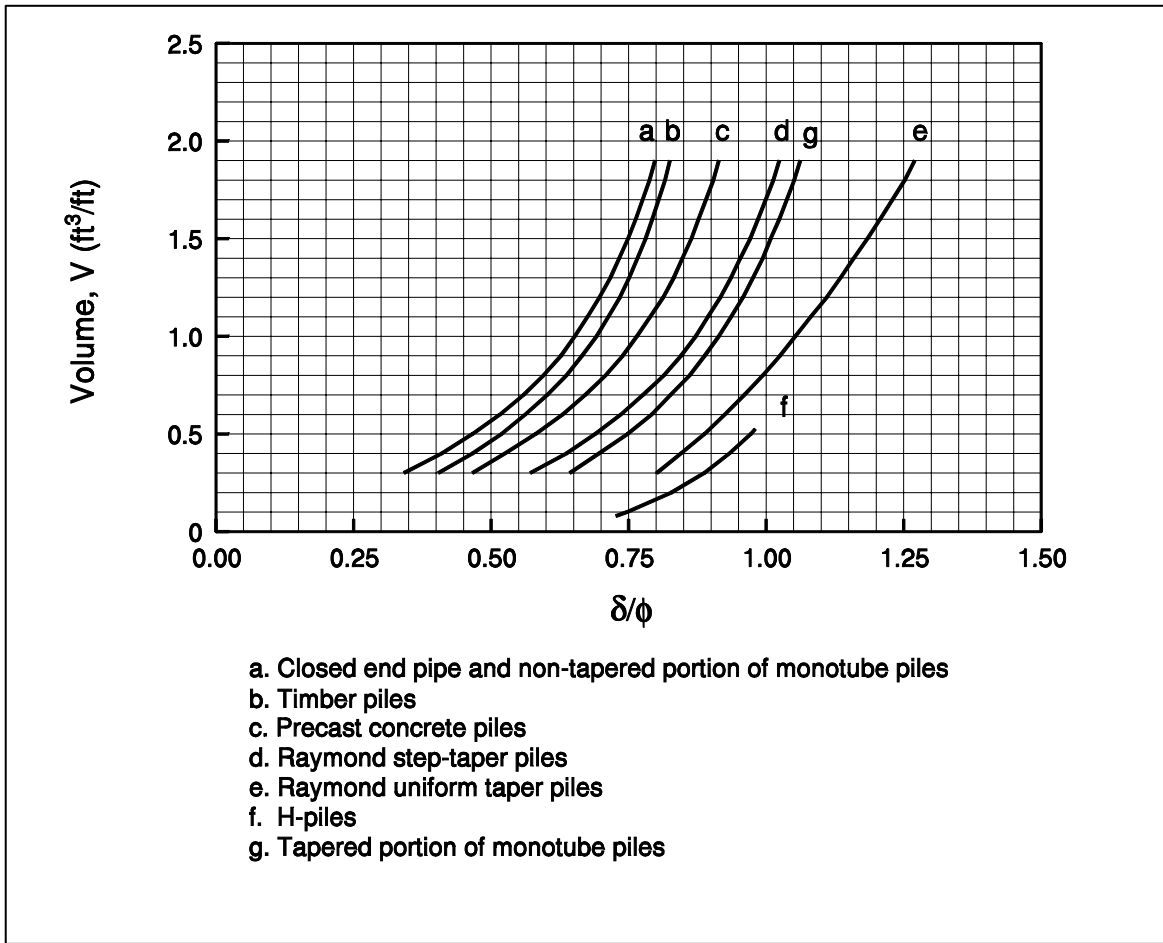


**Figure 9-7. Relationship of  $\delta/\phi$  and pile soil displacement,  $V$ , for various types of piles (after Nordlund, 1963).**

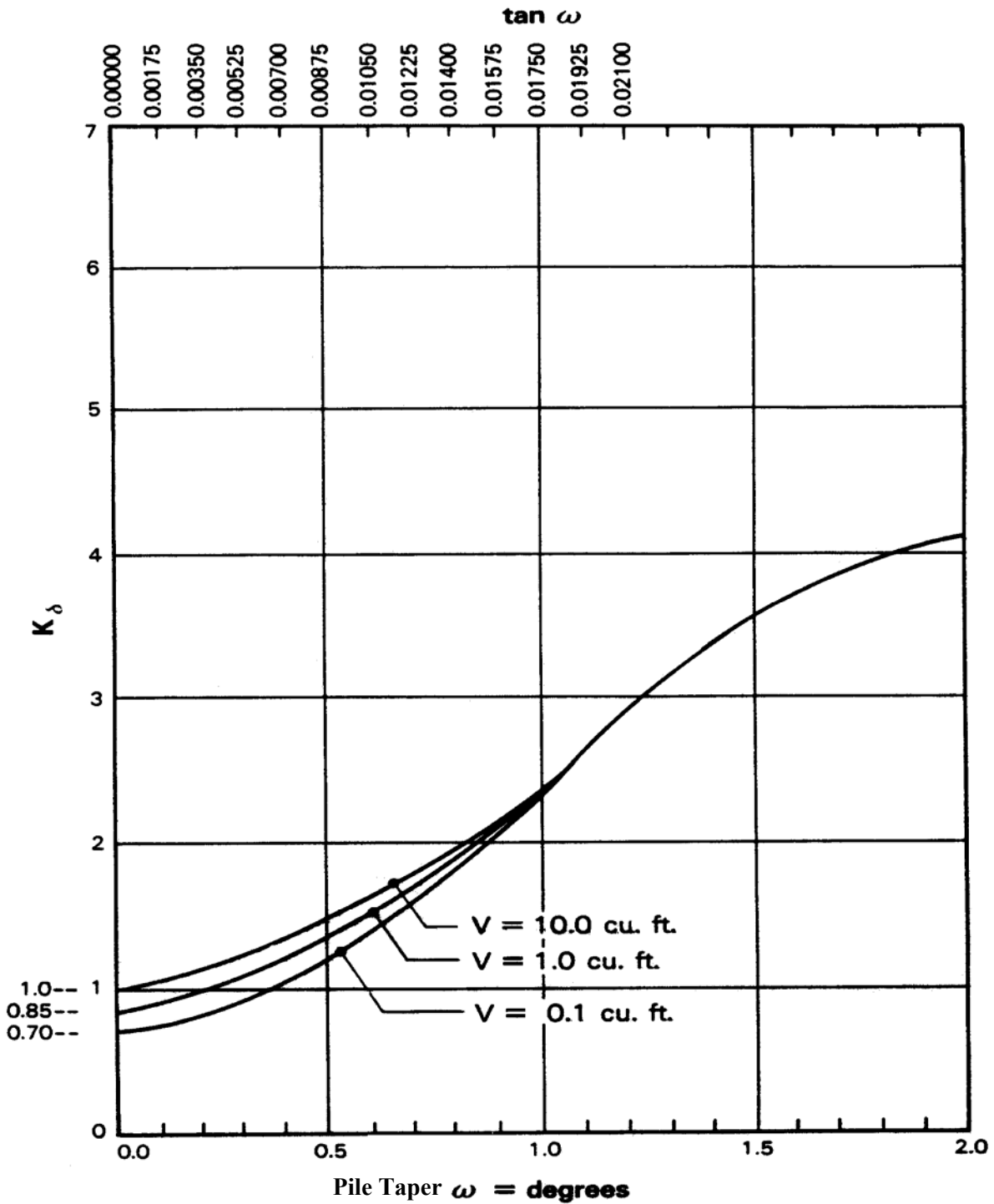


Figure 9-8. Design curves for evaluating  $K_{\delta}$  for piles when  $\phi = 25^{\circ}$  (after Nordlund, 1963).

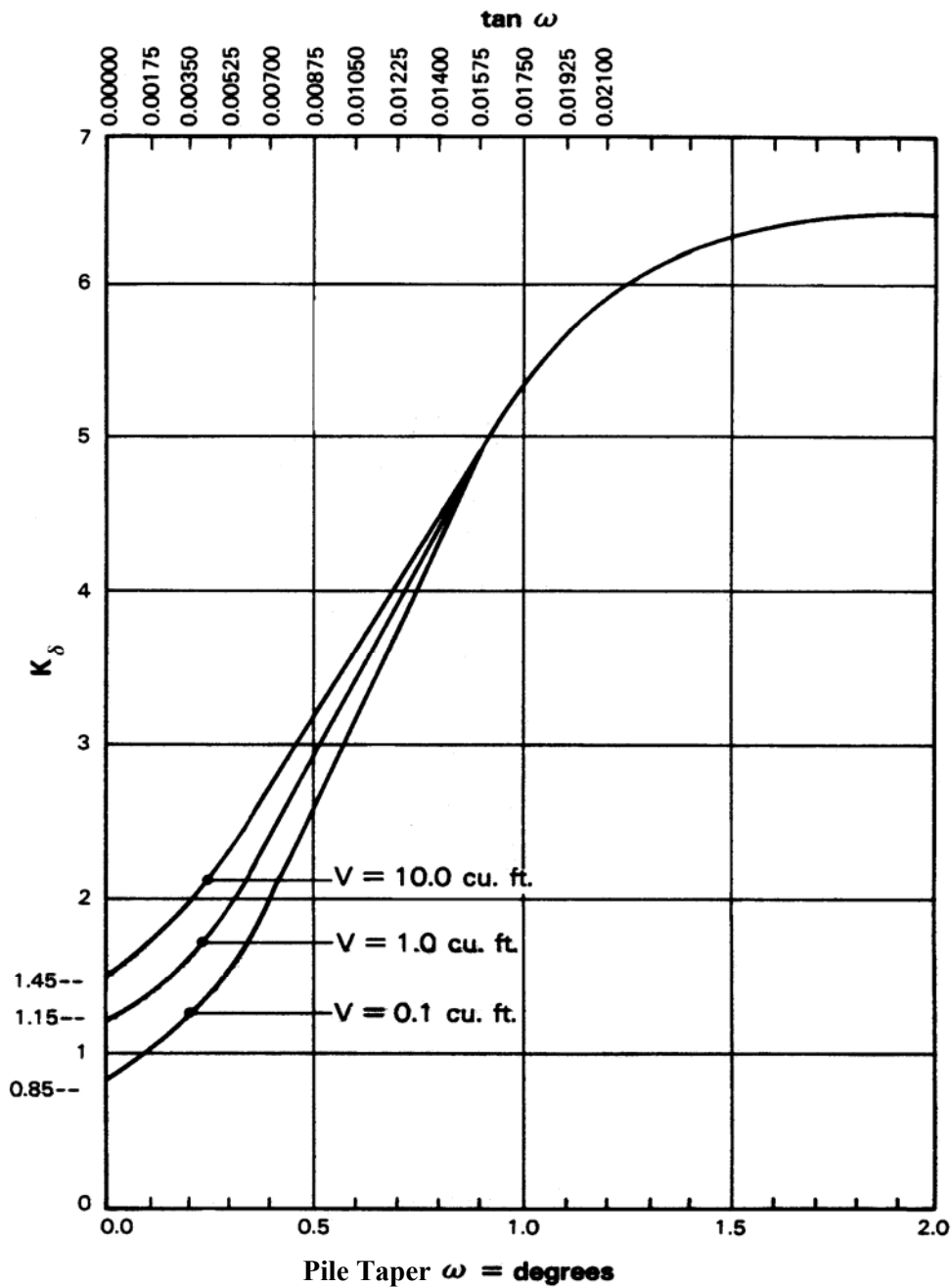


Figure 9-9. Design curves for evaluating  $K_{\delta}$  for piles when  $\phi = 30^{\circ}$  (after Nordlund, 1963).

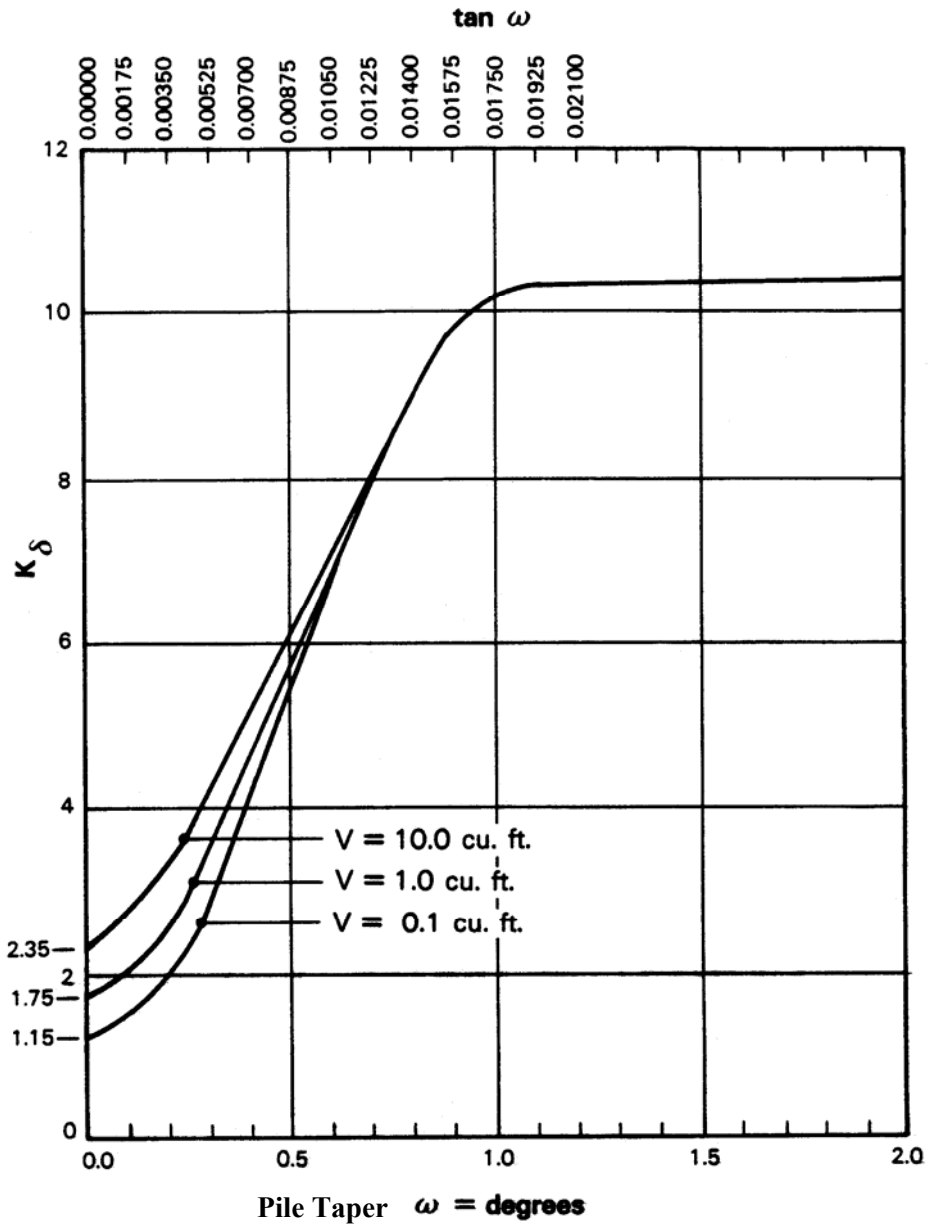


Figure 9-10. Design curves for evaluating  $K_{\delta}$  for piles when  $\phi = 35^{\circ}$  (after Nordlund, 1963).

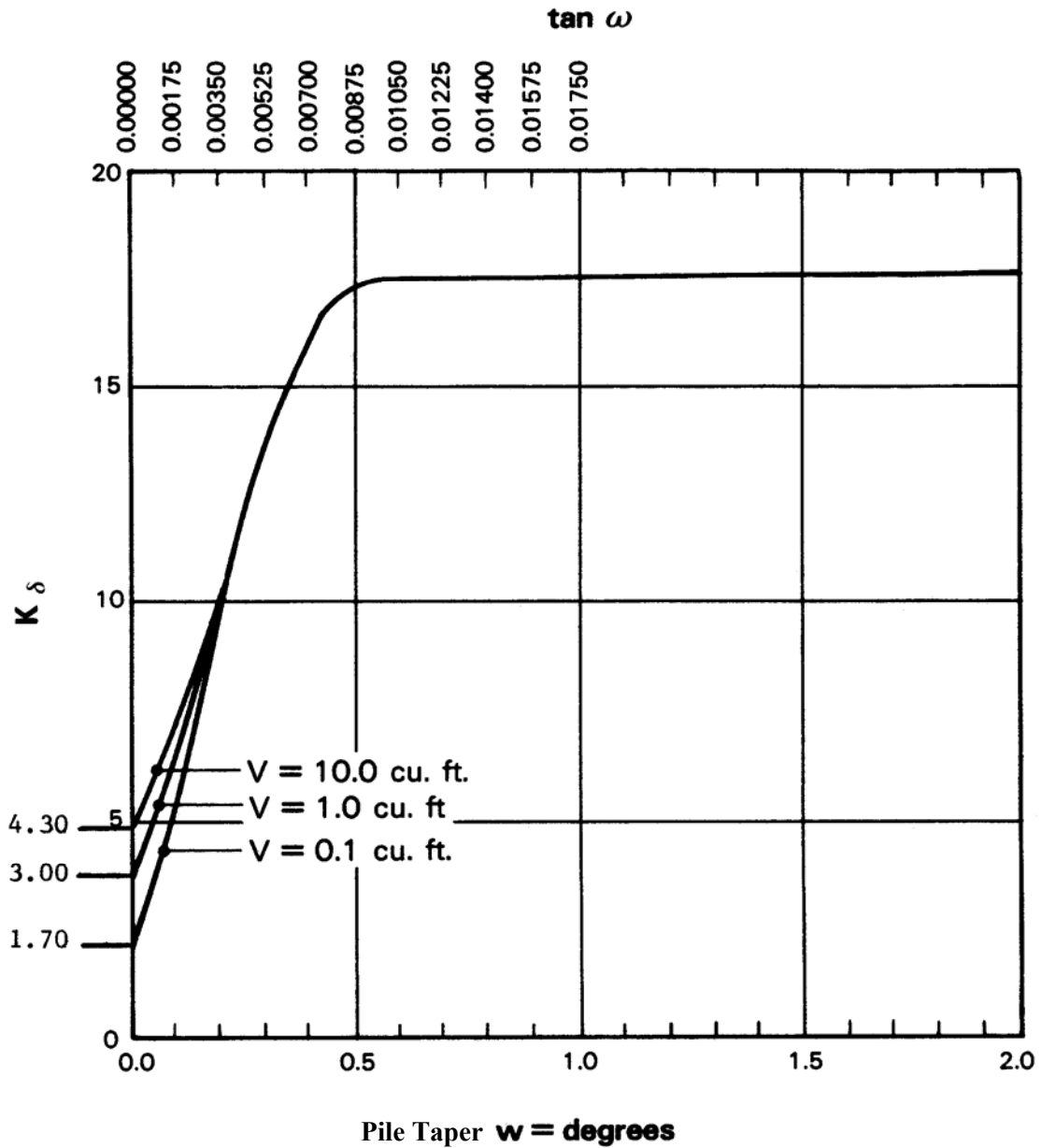


Figure 9-11. Design curves for evaluating  $K_{\delta}$  for piles when  $\phi = 40^{\circ}$  (after Nordlund, 1963).

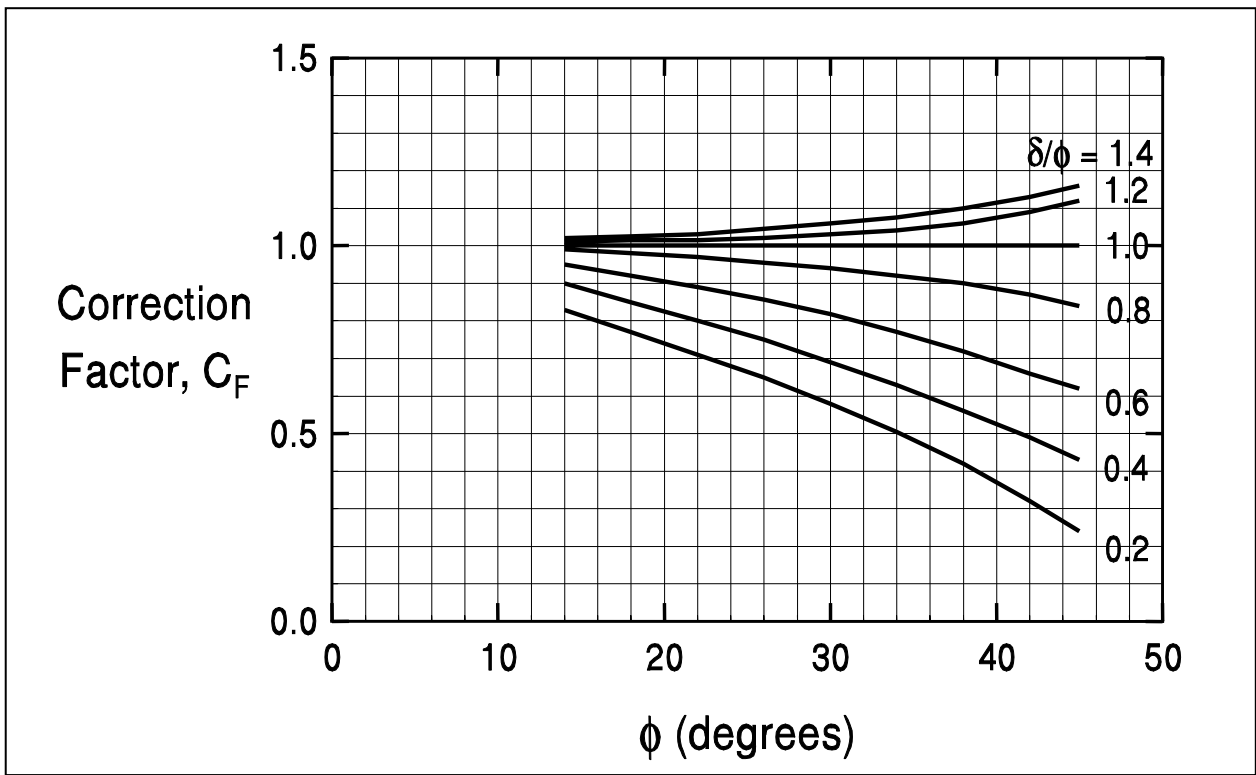


Figure 9-12. Correction factor,  $C_F$  for  $K_\delta$  when  $\delta \neq \phi$  (after Nordlund, 1963).

**Table 9-6(a)****Design table for evaluating  $K_{\delta}$  for piles when  $\omega = 0^{\circ}$  and  $V = 0.10$  to  $1.00$  ft<sup>3</sup>/ft (FHWA, 2006a)**

$\phi$	Displaced Volume -V (ft <sup>3</sup> /ft)									
	0.10	0.20	0.30	0.40	0.50	0.60	0.70	0.80	0.90	1.00
25	0.70	0.75	0.77	0.79	0.80	0.82	0.83	0.84	0.84	0.85
26	0.73	0.78	0.82	0.84	0.86	0.87	0.88	0.89	0.90	0.91
27	0.76	0.82	0.86	0.89	0.91	0.92	0.94	0.95	0.96	0.97
28	0.79	0.86	0.90	0.93	0.96	0.98	0.99	1.01	1.02	1.03
29	0.82	0.90	0.95	0.98	1.01	1.03	1.05	1.06	1.08	1.09
30	0.85	0.94	0.99	1.03	1.06	1.08	1.10	1.12	1.14	1.15
31	0.91	1.02	1.08	1.13	1.16	1.19	1.21	1.24	1.25	1.27
32	0.97	1.10	1.17	1.22	1.26	1.30	1.32	1.35	1.37	1.39
33	1.03	1.17	1.26	1.32	1.37	1.40	1.44	1.46	1.49	1.51
34	1.09	1.25	1.35	1.42	1.47	1.51	1.55	1.58	1.61	1.63
35	1.15	1.33	1.44	1.51	1.57	1.62	1.66	1.69	1.72	1.75
36	1.26	1.48	1.61	1.71	1.78	1.84	1.89	1.93	1.97	2.00
37	1.37	1.63	1.79	1.90	1.99	2.05	2.11	2.16	2.21	2.25
38	1.48	1.79	1.97	2.09	2.19	2.27	2.34	2.40	2.45	2.50
39	1.59	1.94	2.14	2.29	2.40	2.49	2.57	2.64	2.70	2.75
40	1.70	2.09	2.32	2.48	2.61	2.71	2.80	2.87	2.94	3.0

**Table 9-6(b)**

**Design table for evaluating  $K_{\delta}$  for piles when  $\omega = 0^\circ$  and  $V = 1.0$  to  $10.0 \text{ ft}^3/\text{ft}$  (FHWA, 2006a)**

$\phi$	Displaced Volume –V (ft <sup>3</sup> /ft)									
	1.0	2.0	.3.0	4.0	5.0	6.0	7.0	8.0	9.0	10.0
25	0.85	0.90	0.92	0.94	0.95	0.97	0.98	0.99	0.99	1.00
26	0.91	0.96	1.00	1.02	1.04	1.05	1.06	1.07	1.08	1.09
27	0.97	1.03	1.07	1.10	1.12	1.13	1.15	1.16	1.17	1.18
28	1.03	1.10	1.14	1.17	1.20	1.22	1.23	1.25	1.26	1.27
29	1.09	1.17	1.22	1.25	1.28	1.30	1.32	1.33	1.35	1.36
30	1.15	1.24	1.29	1.33	1.36	1.38	1.40	1.42	1.44	1.45
31	1.27	1.38	1.44	1.49	1.52	1.55	1.57	1.60	1.61	1.63
32	1.39	1.52	1.59	1.64	1.68	1.72	1.74	1.77	1.79	1.81
33	1.51	1.65	1.74	1.80	1.85	1.88	1.92	1.94	1.97	1.99
34	1.63	1.79	1.89	1.96	2.01	2.05	2.09	2.12	2.15	2.17
35	1.75	1.93	2.04	2.11	2.17	2.22	2.26	2.29	2.32	2.35
36	2.00	2.22	2.35	2.45	2.52	2.58	2.63	2.67	2.71	2.74
37	2.25	2.51	2.67	2.78	2.87	2.93	2.99	3.04	3.09	3.13
38	2.50	2.81	2.99	3.11	3.21	3.29	3.36	3.42	3.47	3.52
39	2.75	3.10	3.30	3.45	3.56	3.65	3.73	3.80	3.86	3.91
40	3.00	3.39	3.62	3.78	3.91	4.01	4.10	4.17	4.24	4.30

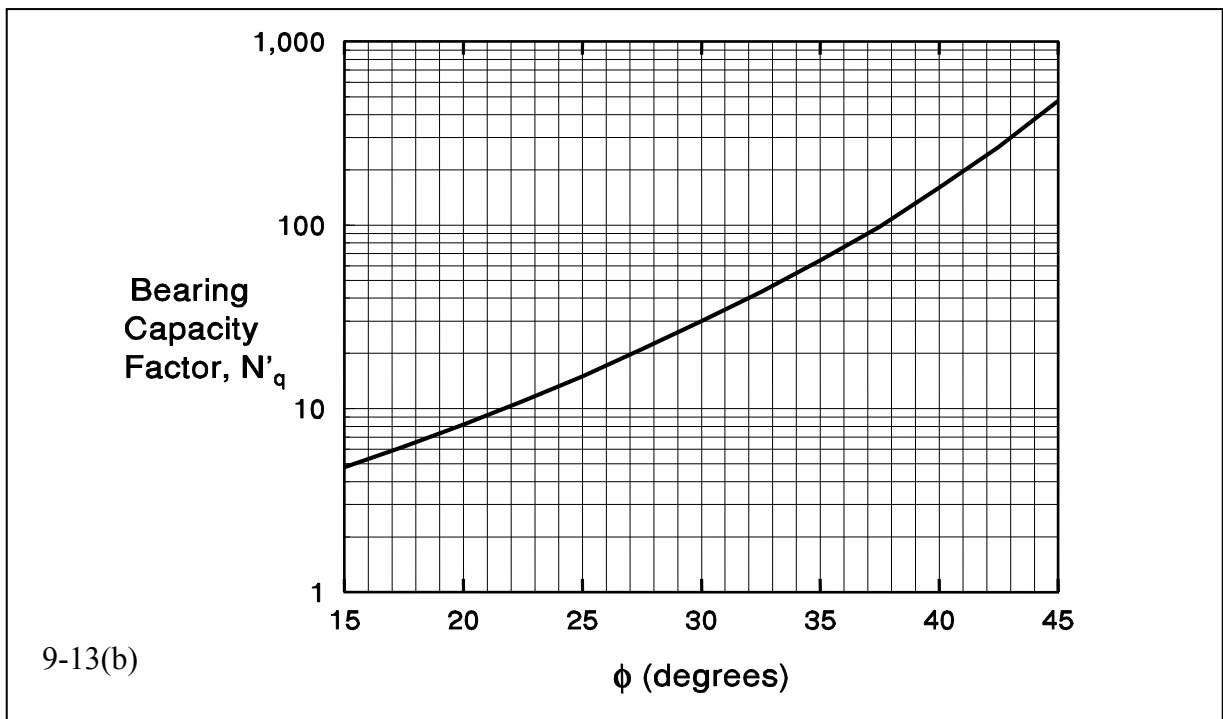
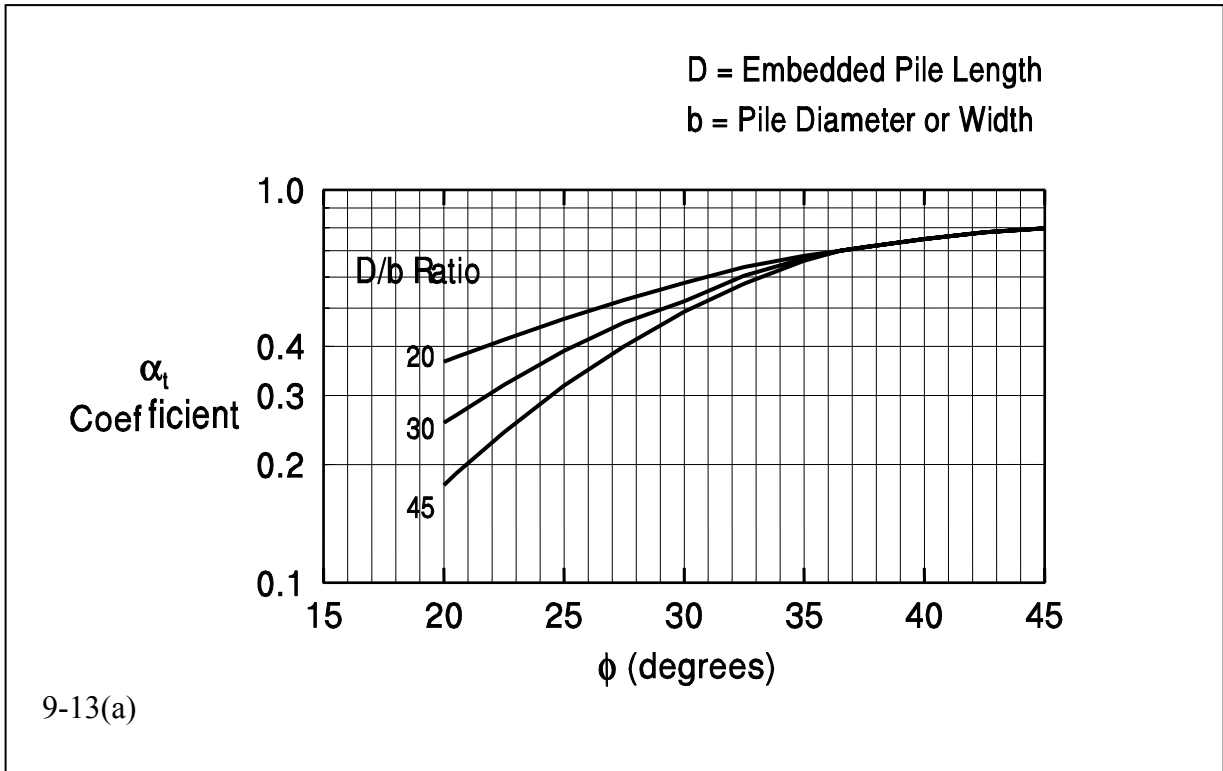


**Figure 9-13. Chart for estimating  $\alpha_t$  coefficient and bearing capacity factor  $N'_q$  (FHWA, 2006a).**

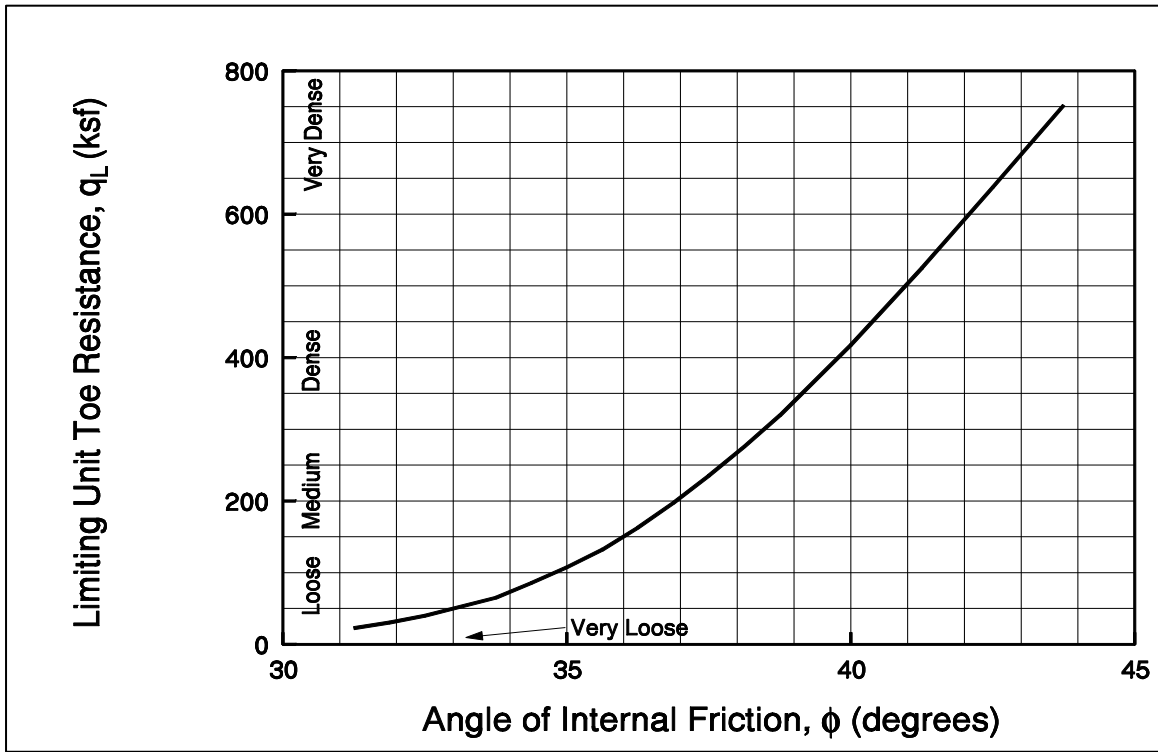
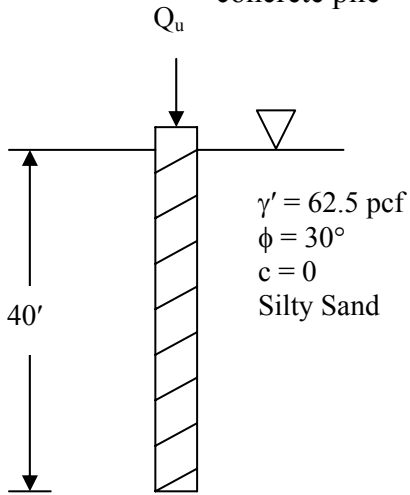


**Figure 9-14. Relationship between maximum unit pile toe resistance and friction angle for cohesionless soils (after Meyerhof, 1976).**

**Example 9-2:** Determine the ultimate geotechnical pile capacity,  $Q_u$ , for the 1 sq ft precast concrete pile



Since  $\omega = 0$ , use Equation 9-5

$$Q_u = K_\delta C_F p_d \sin \delta C_d D + A_t \alpha_t p_t N'_q$$

where the following terms are known from the problem

$$A_t = 1 \text{ sq.ft}$$

$$p_t = 40 \gamma' = 2,500 \text{ psf}$$

$$p_d = 20 \gamma' = 1,250 \text{ psf}$$

$$\omega = 0^\circ, D = 40 \text{ ft}, C_d = 4 \text{ ft}$$

**Solution:**

**Find Shaft Resistance,  $R_s$ :**

Use Figures 9-7, 9-9, and 9-12 with  $\phi = 30^\circ$

From Figure 9-7 – For  $V = 1 \text{ ft}^3/\text{ft}$ , and curve “c” for precast concrete piles;

$$\frac{\delta}{\phi} = 0.76, \quad \text{Since } \phi = 30^\circ, \quad \delta = 22.8^\circ$$

From Figure 9-9 – For  $\omega = 0$ ,  $V = 1 \text{ ft}^3/\text{ft}$ ;  $K_\delta = 1.15$

From Figure 9-12 – For  $\frac{\delta}{\phi} = 0.76$ ;  $C_F = 0.9$

$$R_s = K_\delta C_F p_d \sin \delta C_d D$$

Equation 9-6

$$R_s = (1.15)(0.9)(1,250 \text{ psf})(\sin 22.8^\circ)(4 \text{ ft})(40 \text{ ft}) = 80,216 \text{ lbs}$$

$$R_s = 40.1 \text{ tons}$$

**Find Toe Resistance,  $R_t$ :**

Use Figure 9-13(b) to find  $N'_q$  and  $\alpha_t$  for  $\phi = 30^\circ$

$$N'_q = 30; \alpha_t = 0.5 \text{ (for } \frac{D}{B} = 40)$$

$$R_t = A_t \alpha_t p_t N'_q = (1 \text{ ft}^2)(0.5)(2,500 \text{ psf}) 30 = 37,500 \text{ lbs} = 18.75 \text{ tons}$$

Equation 9-7a

Check limiting point resistance from Figure 9-14,  $q_L \approx 10 \text{ ksf} \approx 5 \text{ tsf}$

$$R_t = q_L A_t = (5 \text{ tsf})(1 \text{ ft}^2) = 5 \text{ tons} \quad \therefore R_t = 5 \text{ tons}$$

Equation 9-7b

**Compute Ultimate Capacity,  $Q_u$ :**

$$Q_u = R_s + R_t = 40.1 + 5 = 45.1 \text{ tons}$$

## 9.5.2 Ultimate Geotechnical Capacity of Single Piles in Cohesive Soils

The ultimate geotechnical capacity of a pile in cohesive soil may also be expressed as the sum of the shaft and toe resistances or  $Q_u = R_s + R_t$ . The shaft and toe resistances can be calculated from static analysis methods using soil boring and laboratory test data in either total stress or effective stress methods. The  $\alpha$ -method is a total stress method that uses undrained soil shear strength parameters for calculating static pile capacity in cohesive soil. The  $\alpha$ -method will be presented in Section 9.5.2.1. The effective stress method, or  $\beta$ -method, uses drained soil strength parameters for capacity calculations. Since the effective stress method may be used for calculating static pile capacity in cohesive as well as cohesionless soils, this method will be presented in Section 9.5.2.2. Alternatively, in-situ CPT test results can also be used to calculate pile capacity in cohesive soils from cone sleeve friction and cone tip resistance values. CPT-based methods as well as other methods are discussed in FHWA (2006a).

The shaft resistance of piles driven into cohesive soils is frequently as much as 80 to 90% of the total capacity. Therefore, it is important that the shaft resistance of piles in cohesive soils be estimated as accurately as possible.

### 9.5.2.1 Total Stress – $\alpha$ -method

For piles in clay, a total stress analysis is often used where ultimate capacity is calculated from the undrained shear strength of the soil. This approach assumes that the shaft resistance is independent of the effective overburden pressure and that the unit shaft resistance can be expressed in terms of an empirical adhesion factor times the undrained shear strength.

#### Shaft Resistance

The unit shaft resistance,  $f_s$ , is equal to the adhesion,  $c_a$ , which is the shear stress between the pile and soil at failure. This may be expressed in equation form as:

$$f_s = c_a = \alpha c_u \quad 9-8$$

in which  $\alpha$  is an empirical factor applied to the average undrained shear strength,  $c_u$ , of undisturbed clay along the embedded length of the pile. The coefficient  $\alpha$  depends on the nature and strength of the clay, magnitude of load, pile dimension, method of pile installation, and time effects. The values of  $\alpha$  vary within wide limits and decrease rapidly with increasing shear strength.

The adhesion factor,  $\alpha$ , is a function of the soil stratigraphy and pile embedment. Three common cases are as follows:

- Case 1: Piles driven into stiff clays through overlying sands or sandy gravels
- Case 2: Piles driven into stiff clays through overlying soft clays
- Case 3: Piles driven into stiff clays without overlying different strata

Figure 9-15 presents the adhesion factor,  $\alpha$ , versus the undrained shear strength of the soil as a function of unique soil stratigraphy and pile embedment for Case 1 and Case 2. The adhesion factor from these soil stratigraphy cases should be used only for determining the adhesion in a stiff clay layer in that specific condition as follows:

- **Case 1:** The top graph in Figure 9-15 may be used to select the adhesion factor when piles are driven through a sand or sandy gravel layer and into an underlying stiff clay stratum. This case results in the highest adhesion factors as granular material is dragged into the underlying clays. The greater the pile penetration into the clay stratum, the less influence the overlying granular stratum has on the adhesion factor. Therefore, for the same undrained shear strength, the adhesion factor decreases with increased pile penetration into the clay stratum.
- **Case 2:** The bottom graph in Figure 9-15 should be used to select the adhesion factor when piles are driven through a soft clay layer overlying a stiff clay layer. In this case, the soft clay is dragged into the underlying stiff clay stratum thereby reducing the adhesion factor of the underlying stiff clay soils. The greater the pile penetration into the underlying stiff clay soils, the less the influence the overlying soft clays have on the stiff clay adhesion factor. Therefore, the stiff clay adhesion factor increases with increasing pile penetration into the stiff clay soils.

Figure 9-16 presents the adhesion factor,  $\alpha$ , versus the undrained shear strength of the soil for piles driven in stiff clays without any different overlying strata, i.e., Case 3. In stiff clays, a gap often forms between the pile and the soil along the upper portion of the pile shaft. In this case, the shallower the pile penetration into a stiff clay stratum the greater the effect the gap has on the shaft resistance that develops. Hence, the adhesion factor for a given shear strength is reduced at shallow pile penetration depths and increased at deeper pile penetration depths.

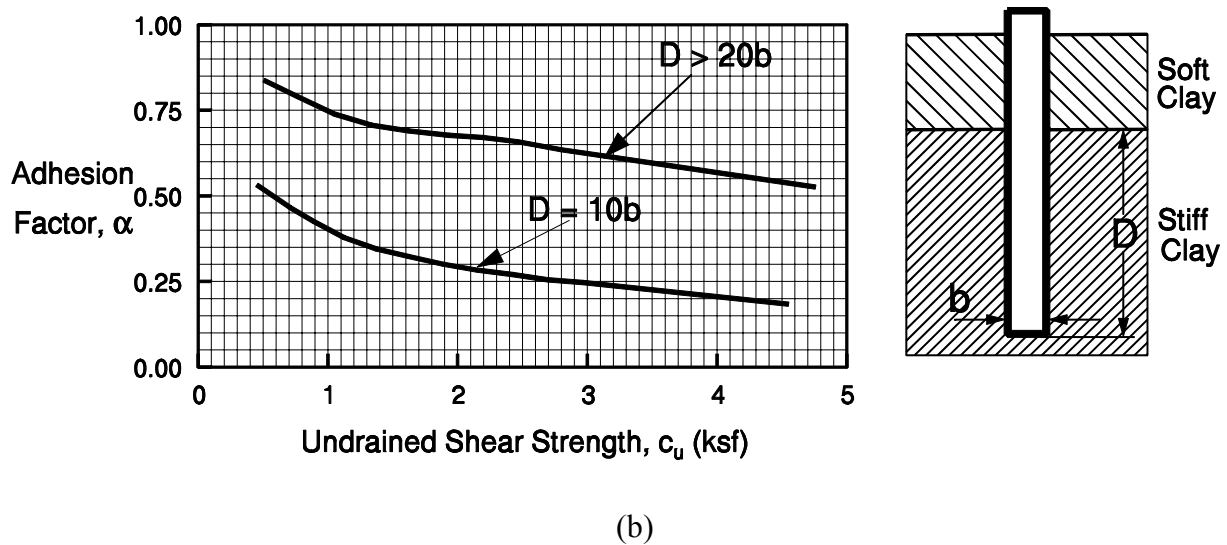
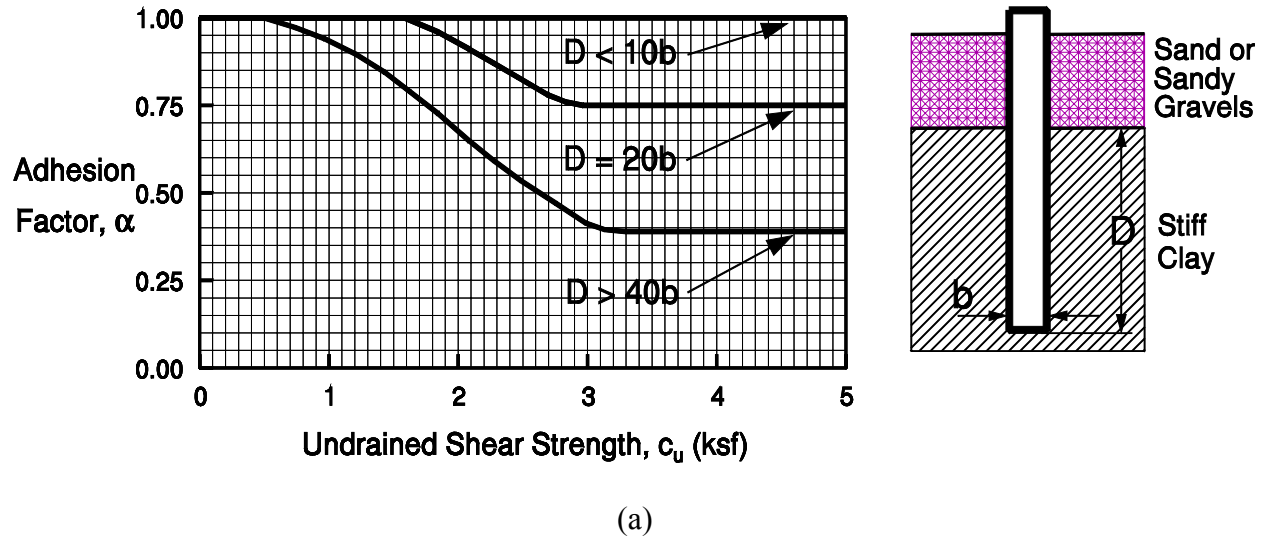


**Figure 9-15. Adhesion values for driven piles in mixed soil profiles, (a) Case 1: piles driven through overlying sands or sandy gravels, and (b) Case 2: piles driven through overlying weak clay (Tomlinson, 1980).**

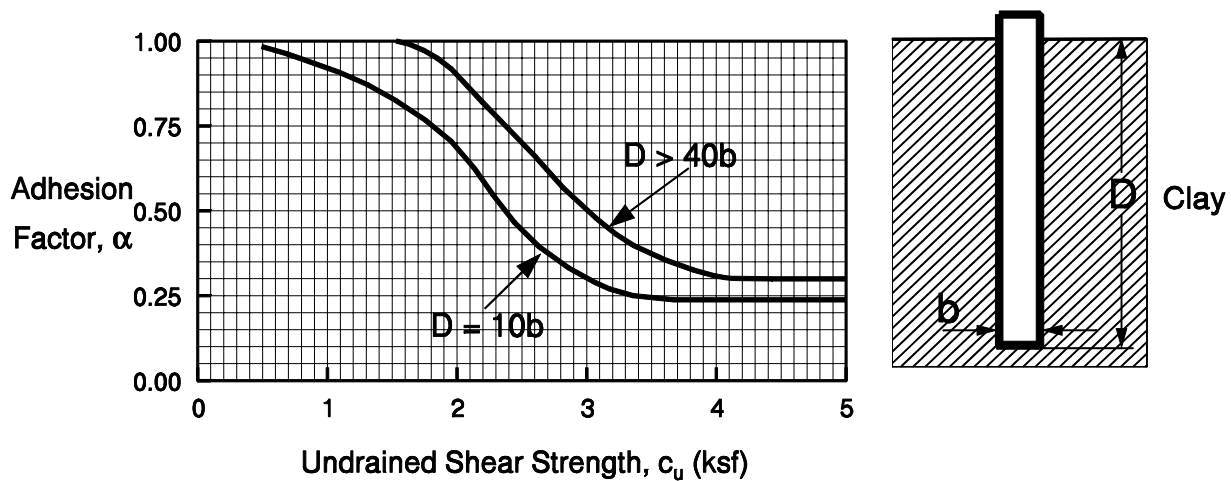


**Figure 9-16. Adhesion values for driven piles in stiff clays without different overlying strata (Case 3) (Tomlinson, 1980).**

The following should be considered by the designer while using Figures 9-15 and 9-16:

- For a soil profile consisting of clay layers of significantly different consistencies such as soft clays over stiff clays, adhesion factors should be determined for each individual clay layer.
- In clays with large shrink-swell potential, static capacity calculations should ignore the shaft resistance from the adhesion in the shrink-swell zone. During dry times, shrinkage will create a gap between the clay and the pile in this zone, therefore the shaft resistance should not be relied upon for long term support.
- In cases where either Figures 9-15b or 9-16 could be used, the inexperienced user should select and use the smaller value obtained from either figure. All users should confirm the applicability of a selected design chart in a given soil condition with local correlations between static capacity calculations and static load tests results.
- In the case of H piles in cohesive soils, the shaft resistance should not be calculated from the surface area of the pile, but rather from the sub-divided perimeter area of the four sides. The shaft resistance for H-piles in cohesive soils consists of the sum of the adhesion,  $c_a$ , times the flange surface area along the exterior of the two flanges, plus the undrained shear strength of the soil,  $c_u$ , times the section height surface area of the two remaining sides. This computation can be approximated by determining the adhesion and multiplying the

adhesion by the H-pile "box perimeter" area. Further discussion on this topic is included in Section 9.5.4.

### **Toe Resistance**

The unit toe resistance in a total stress analysis for homogeneous cohesive soil is as follows:

$$q_t = c_u N_c \quad 9-9$$

The term  $N_c$  is a dimensionless bearing capacity factor that depends on the pile diameter and the depth of embedment and  $c_u$  is the undrained shear strength of the material at and below the toe of the pile. The bearing capacity factor,  $N_c$ , is usually taken as 9 for deep foundations.

It should be remembered that the movement required to mobilize the toe resistance is several times greater than that required to mobilize the shaft resistance. At the movement required to fully mobilize the toe resistance, the shaft resistance may have decreased to a residual value. Therefore, the contribution of the toe resistance to the ultimate pile capacity in cohesive soils is sometimes ignored except in hard cohesive deposits such as glacial tills.

### **STEP BY STEP PROCEDURE FOR - " $\alpha$ -METHOD"**

**STEP 1** Delineate the soil profile into layers and determine the adhesion,  $c_a$ , from Figure 9-15 and 9-16 as appropriate. for each layer.

Enter the appropriate figure with the undrained shear strength of the soil,  $c_u$ , and determine adhesion or adhesion factor based on the ratio of the embedded pile length in clay,  $D$ , and the pile diameter,  $b$ . Use the  $D/b$  curve for the appropriate soil and embedment condition.

**STEP 2** For each soil layer, compute the unit shaft resistance,  $f_s$  in ksf (kPa).

$$f_s = c_a = \alpha c_u$$

where:  $c_a$  = adhesion and  $\alpha$  = adhesion factor.

**STEP 3** Compute the shaft resistance in each soil layer and the ultimate shaft resistance,  $R_s$ , in kips (kN), from the sum of the shaft resistance from each layer.

$$R_s = f_s A_s \quad 9-10$$

where:  $A_s$  = pile-soil surface area in  $\text{ft}^2$  ( $\text{m}^2$ ) = (pile perimeter) x (length).

**STEP 4** Compute the unit toe resistance,  $q_t$  in ksf (kPa).

$$q_t = 9 c_u$$

where:  $c_u$  = undrained shear strength of soil at the pile toe in ksf (kPa)

**STEP 5** Compute the ultimate toe resistance,  $R_t$  in kips (kN).

$$R_t = q_t A_t \quad 9-11$$

where:  $A_t$  = Area of pile toe in  $\text{ft}^2$  ( $\text{m}^2$ ).

**STEP 6** Compute the ultimate geotechnical pile capacity,  $Q_u$  in kips (kN).

$$Q_u = R_s + R_t$$

**STEP 7** Compute the allowable geotechnical soil resistance,  $Q_a$  in kips (kN).

$$Q_a = \frac{Q_u}{\text{Factor of Safety}}$$

The factor of safety in this static calculation should be based on the specified construction control method as described in Section 9.4 of this chapter. Factors of safety for various construction control methods are listed in Table 9-5.

### 9.5.2.2 Effective Stress – $\beta$ -method

Static capacity calculations in cohesionless, cohesive, and layered soils can also be performed by using an effective stress based method. Effective stress based methods were developed to model the long term drained shear strength conditions. Therefore, the effective soil friction angle,  $\phi'$ , should be used in parameter selection.

In an effective stress analysis, the unit shaft resistance is calculated from the following expression:

$$f_s = \beta p_o \quad 9-12$$

where:  $\beta$  = Bjerrum-Burland beta coefficient =  $K_s \tan \delta$ .  
 $p_o$  = average effective overburden pressure along the pile shaft, in ksf (kPa).  
 $K_s$  = earth pressure coefficient.  
 $\delta$  = interface friction angle between pile and soil.

The unit toe resistance is calculated from:

$$q_t = N_t p_t \quad 9-13$$

where:  $N_t$  = toe bearing capacity coefficient.  
 $p_t$  = effective overburden pressure at the pile toe in ksf (kPa).

Recommended ranges of  $\beta$  and  $N_t$  coefficients as a function of soil type and  $\phi'$  angle from Fellenius (1991) are presented in Table 9-7. Fellenius (1991) notes that factors affecting the  $\beta$  and  $N_t$  coefficients consist of the soil composition including the grain size distribution, angularity and mineralogical origin of the soil grains, the original soil density and density due to the pile installation technique, the soil strength, as well as other factors. Even so,  $\beta$  coefficients are generally within the ranges provided and seldom exceed 1.0.

**Table 9-7**  
**Approximate range of  $\beta$  and  $N_t$  coefficients (Fellenius, 1991)**

Soil Type	$\phi'$	$\beta$	$N_t$
Clay	25 – 30	0.23 - 0.40	3 - 30
Silt	28 – 34	0.27 - 0.50	20 - 40
Sand	32 – 40	0.30 - 0.60	30 - 150
Gravel	35 – 45	0.35 - 0.80	60 - 300

For sedimentary cohesionless deposits, Fellenius (1991) states that  $N_t$  ranges from about 30 to a high of 120. In very dense non-sedimentary deposits such as glacial tills,  $N_t$  can be much higher, but it can also approach the lower bound value of 30. In clays, Fellenius (1991) notes that the toe resistance calculated by using an  $N_t$  of 3 is similar to the toe resistance calculated from an analysis where undrained shear strength is used. Therefore, the use of a relatively low value of the  $N_t$  coefficient in clays is recommended unless local correlations suggest higher values are appropriate.

Graphs of the ranges in  $\beta$  and  $N_t$  coefficients versus the range in  $\phi'$  angle as suggested by Fellenius are presented in Figure 9-17 and 9-18, respectively. These graphs may be helpful in selection of  $\beta$  or  $N_t$ . The inexperienced user should select conservative  $\beta$  and  $N_t$  coefficients. As with any design method, the user should also confirm the appropriateness of a selected  $\beta$  or  $N_t$  coefficient in a given soil condition with local correlations between static capacity calculations and static load test results.

It should be noted that the effective stress method places no limiting values on either the shaft or toe resistance.

### **STEP BY STEP PROCEDURE FOR THE EFFECTIVE STRESS METHOD**

- STEP 1** Delineate the soil profile into layers and determine  $\phi'$  angle for each layer.
- a. Construct  $p_o$  diagram by using previously described procedures in Chapter 2.
  - b. Divide soil profile throughout the pile penetration depth into layers and determine the effective overburden pressure,  $p_o$ , in ksf (kPa) at the midpoint of each layer.
  - c. Determine the  $\phi'$  angle for each soil layer from laboratory or in-situ test data.

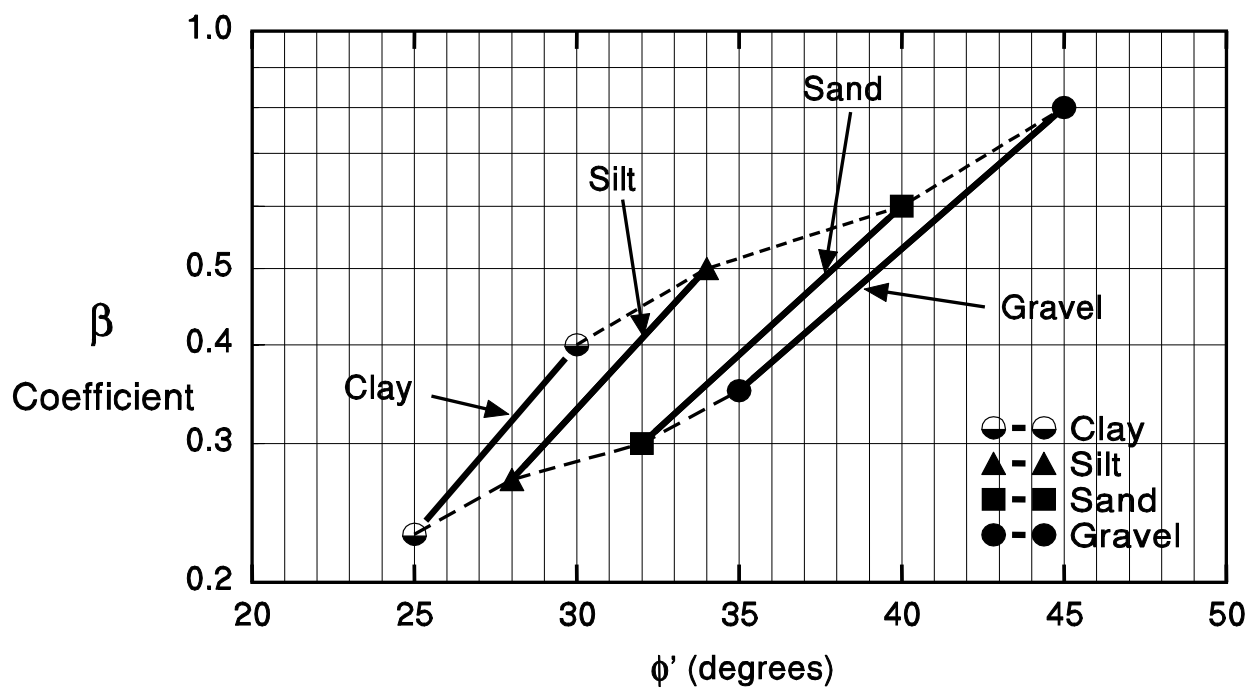


Figure 9-17. Chart for estimating  $\beta$  coefficient as a function of soil type  $\phi'$  (after Fellenius, 1991).

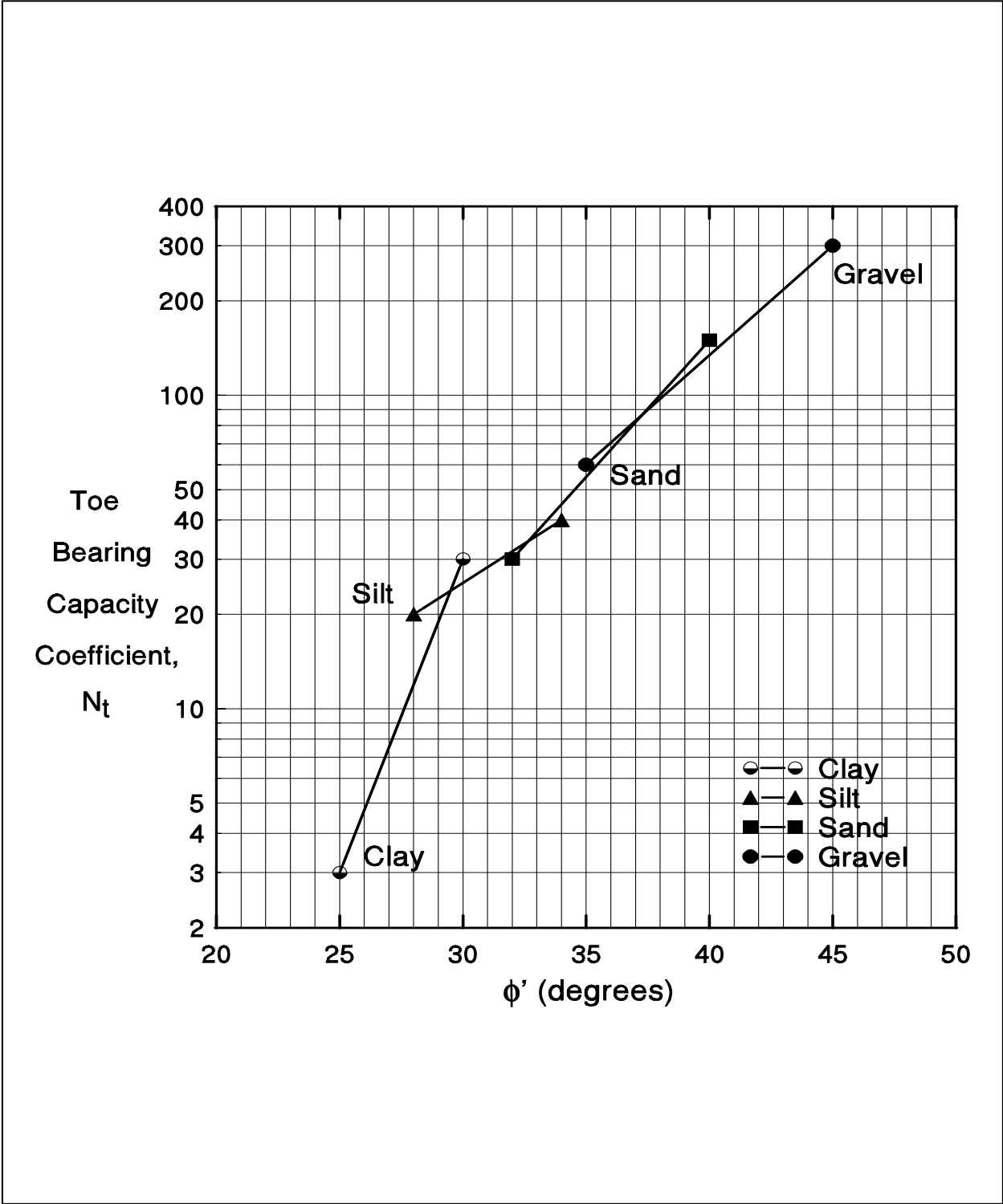


Figure 9-18. Chart for estimating  $N_t$  coefficients as a function of soil type  $\phi'$  angle (after Fellenius, 1991).

- d. In the absence of laboratory or in-situ test data for cohesionless layers, determine the average corrected SPT N1 value for each layer and estimate  $\phi'$  angle from Table 8-1 in Chapter 8.

**STEP 2** Select the  $\beta$  coefficient for each soil layer.

- a. Use local experience to select  $\beta$  coefficient for each layer.
- b. In the absence of local experience, use Table 9-7 or Figure 9-17 to estimate the  $\beta$  coefficient from the  $\phi'$  angle for each layer.

**STEP 3** For each soil layer compute the unit shaft resistance,  $f_s$  in ksf (kPa).

$$f_s = \beta p_o$$

**STEP 4** Compute the shaft resistance in each soil layer and the ultimate shaft resistance,  $R_s$  in kips (kN) from the sum of the shaft resistance from each soil layer.

$$R_s = \sum f_s A_s$$

where:  $A_s$  = pile-soil surface area in  $\text{ft}^2$  ( $\text{m}^2$ ) = (pile perimeter) x (length).

**STEP 5** Compute the unit toe resistance,  $q_t$  in ksf (kPa).

$$q_t = N_t p_t$$

- a. Use local experience to select  $N_t$  coefficient.
- b. In the absence of local experience, estimate  $N_t$  from Table 9-7 or Figure 9-18 based on  $\phi'$  angle.
- c. Calculate the effective overburden pressure at the pile toe,  $p_t$  in ksf (kPa).

**STEP 6** Compute the ultimate toe resistance,  $R_t$  in kips (kN).

$$R_t = q_t A_t$$

where:  $A_t$  = area of the pile toe in  $\text{m}^2$  ( $\text{ft}^2$ ).

**STEP 7** Compute the ultimate geotechnical pile capacity,  $Q_u$  in kips (kN).

$$Q_u = R_s + R_t$$

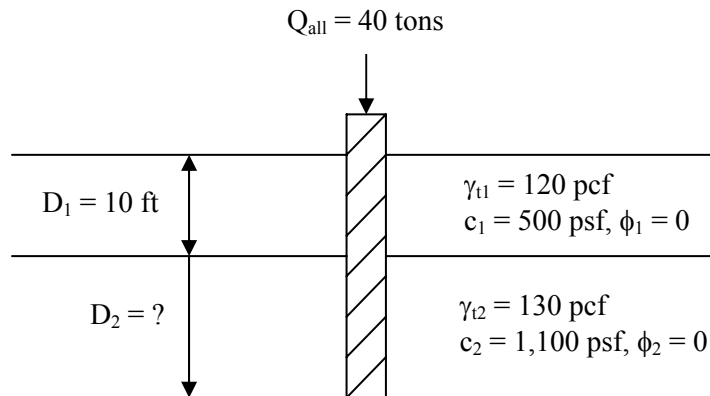
**STEP 8** Compute the allowable geotechnical soil resistance,  $Q_a$  in kips (kN).

$$Q_a = \frac{Q_u}{\text{Factor of Safety}}$$

The factor of safety in this static calculation should be based on the specified construction control method as described in Section 9.4 of this chapter. Recommended factors of safety based on construction control methods are listed in Table 9-5

The concepts discussed above are illustrated numerically in Example 9-3.

**Example 9-3:** Determine the required pile length to resist a 40 tons load with a safety factor of 2. Assume no toe resistance for the 1 ft<sup>2</sup> precast concrete pile. Site specific tests have indicated that the adhesion may be assumed equal to cohesion.



**Solution:**

$$Q_u = R_{s1} + R_{s2} \quad (\text{Note: No toe resistance, i.e. } 9 c_u A_t = 0)$$

$$Q_u = c_{a1} A_{s1} + c_{a2} A_{s2}$$

$$Q_u = c_{a1} C_{d1} D_1 + c_{a2} C_{d2} D_2$$

where  $C_{d1}$  and  $C_{d2}$  are pile perimeters within depths  $D_1$  and  $D_2$

$$C_{d1} = C_{d2} = 4 \times 1 \text{ ft} = 4 \text{ ft}$$

From the problem statement, for site-specific conditions, adhesion = cohesion. Therefore,

$$c_{a1} = c_1 = 500 \text{ psf}$$

$$c_{a2} = c_2 = 1,100 \text{ psf}$$

$$Q_u = 40 \text{ tons} \times \text{FS} = 40 \text{ tons} \times 2 = 80 \text{ tons}$$

$$80 \text{ tons} = (500 \text{ psf})(4 \text{ ft})(10 \text{ ft}) + (1,100 \text{ psf})(4 \text{ ft})D_2$$

$$80 \text{ tons} = 20,000 \text{ lbs} + 4,400 D_2 \text{ lbs/ft}$$

$$80 \text{ tons} = 10 \text{ tons} + 2.2 D_2 \text{ tons/ft}$$

Solve for  $D_2$ ,

$$D_2 = \frac{80 \text{ tons} - 10 \text{ tons}}{2.2 \text{ tons/ft}} \approx 32 \text{ ft}$$

$$\therefore \text{Total pile length required} = 32 \text{ ft} + 10 \text{ ft} \approx 42 \text{ ft}$$

### 9.5.3 Ultimate Geotechnical Capacity of Single Piles in Layered Soils

The ultimate capacity of piles in layered soils can be calculated by combining the methods previously described for cohesionless and cohesive soils. For example, a hand calculation combining the Nordlund method from Section 9.5.1.1 for cohesionless soil layers with the  $\alpha$ -method from Section 9.5.2.1 for cohesive soil layers could be used. The effective stress method as described in Section 9.5.2.2 could also be used for layered soil profiles.

#### 9.5.4 Plugging of Open Pile Sections

Open pile sections include open end pipe piles and H-piles. The use of open pile sections has increased, particularly where special design events dictate large pile penetration depths. When open pile sections are driven, they may behave as low displacement piles and "cookie cut" through the soil, or act as displacement piles if a soil plug forms near the pile toe. It is generally desired that open sections remain unplugged during driving and plugged under static loading conditions.

Stevens (1988) reported that plugging of pipe piles in clays does not occur during driving if pile accelerations along the plug zone are greater than 22g. Holloway and Beddard (1995) reported that hammer blow size influenced the dynamic response of the soil plug. With a large hammer blow, the plug "slipped" under the dynamic event whereas under a lesser hammer blow the pile encountered toe resistance typical of a plugged condition. From a design perspective, these cases indicate that pile penetration of open sections can be facilitated if the pile section is designed to accommodate a large pile hammer. Wave equation analyses can provide calculated accelerations at selected pile segments.

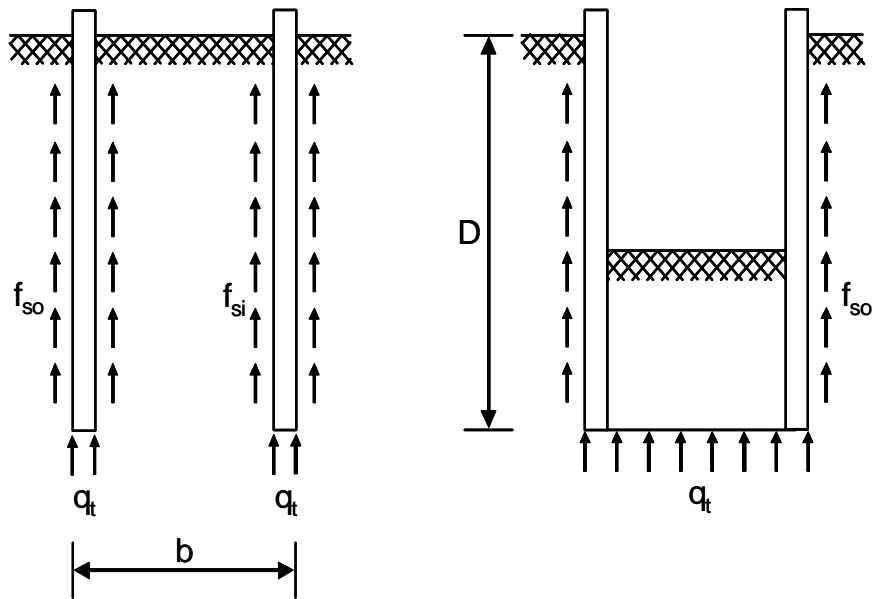
Static pile capacity calculations must determine whether an open pile section will exhibit plugged or unplugged behavior. Studies by O'Neill and Raines (1991), Raines, *et al.* (1992), as well as Paikowsky and Whitman (1990) suggest that plugging of open pipe piles in medium dense to dense sands generally begins at a pile penetration-to-pile-diameter ratio of 20, but can occur in cases where the ratio is as high as 35. For pipe piles in soft to stiff clays, Paikowsky and Whitman (1990) reported plugging occurs at penetration-to-pile-diameter ratios of 10 to 20.

The above studies suggest that plugging in any soil material is probable under static loading conditions once the penetration-to-pile-diameter ratio exceeds 20 in dense sands and clays, or 20 to 30 in medium sands. An illustration of the difference in the soil resistance mechanism that develops on a pipe pile with an open and plugged toe condition is presented in Figure 9-19. Paikowsky and Whitman (1990) recommend that the static capacity of an open end pipe pile be calculated from the lesser of the following equations:

$$\text{Plugged Condition:} \quad Q_u = f_{so} A_s + q_t A_t \quad 9-15a$$

$$\text{Unplugged Condition:} \quad Q_u = f_{so} A_s + f_{si} A_{si} + q_t A_p - w_p \quad 9-15b$$

where:  $Q_u$  = ultimate pile capacity in kips (kN).  
 $f_{so}$  = exterior unit shaft resistance in ksf (kPa).



(a) Open Toe Condition

(b) Plugged Toe Condition

Figure 9-19. Plugging of open end pipe piles (after Paikowsky and Whitman, 1990).

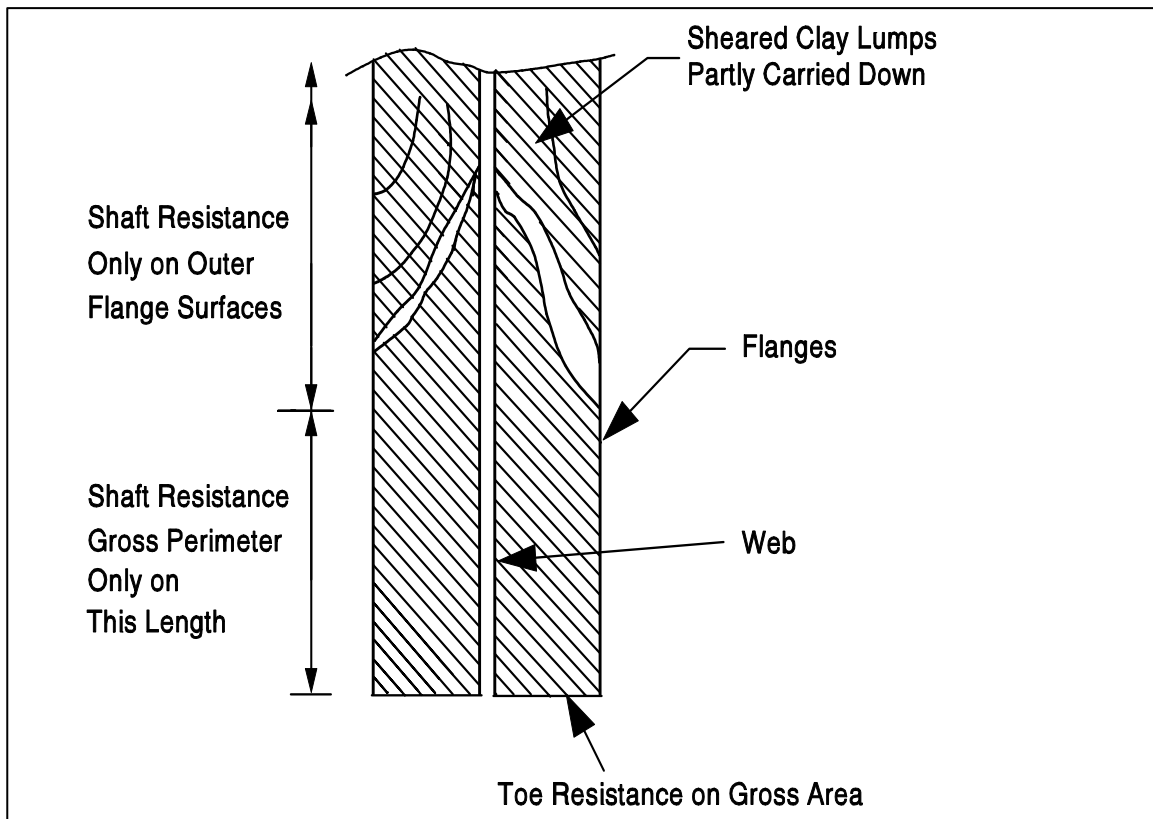


Figure 9-20. Plugging of H-piles (FHWA, 2006a).

$A_s$	= pile exterior surface area in ft <sup>2</sup> (m <sup>2</sup> )
$f_{si}$	= interior unit shaft resistance in ksf (kPa)
$A_{si}$	= pile interior surface area in ft <sup>2</sup> (m <sup>2</sup> )
$q_t$	= unit toe resistance in ksf (kPa)
$A_t$	= toe area of a plugged pile in ft <sup>2</sup> (m <sup>2</sup> )
$A_p$	= cross sectional area of an unplugged pile in ft <sup>2</sup> (m <sup>2</sup> )
$w_p$	= weight of the plug in kips (kN)

Static pile capacity calculations for open end pipe piles in cohesionless soils should be performed by using the Paikowsky and Whitman (1990) equations. Toe resistance should be calculated by using the Tomlinson limiting unit toe resistance of 105 ksf (5000 kPa), once Meyerhof's limiting unit toe resistance, determined from Figure 9-14, exceeds 105 ksf (5000 kPa). For open end pipe piles in predominantly cohesive soils, the Tomlinson equation should be used.

The soil stresses and displacements induced by driving an open pile section and a displacement pile section are not the same. Hence, a lower unit toe resistance,  $q_t$ , should be used for calculating the toe capacity of open end pipe piles compared to a typical closed end condition. The value of the interior unit shaft resistance in an open end pipe pile is typically on the order of 1/3 to 1/2 the exterior unit shaft resistance, and is influenced by soil type, pile diameter, and pile shoe configuration. These factors will also influence the length of the soil plug that may develop.

For open end pipe piles in cohesionless soils, Tomlinson (1994) recommends that the static pile capacity be calculated using a limiting value of 105 ksf (5000 kPa) for the unit toe resistance, regardless of the pile size or soil density. Tomlinson states that higher unit toe resistances do not develop, because yielding of the soil plug rather than bearing capacity failure of the soil below the plug governs the capacity.

For open end pipe piles driven in stiff clays, Tomlinson (1994) recommends that the static pile capacity for cohesive soils be calculated as follows when field measurements confirm a plug is formed and carried down with the pile:

$$Q_u = 0.8 c_a A_s + 4.5 c_u A_t \quad 9-16$$

where:	$Q_u$	= ultimate pile capacity in kips (kN)
	$c_a$	= pile adhesion from Figure 9-15 in ksf (kPa)
	$A_s$	= pile-soil surface area in ft <sup>2</sup> (m <sup>2</sup> )
	$c_u$	= average undrained shear strength at the pile toe in ksf (kPa)

$A_t$  = toe area of a plugged pile in  $\text{ft}^2$  ( $\text{m}^2$ )

The plugging phenomenon in H-piles can be equally difficult to analyze. However, the distance between flanges of an H-pile is smaller than the inside diameter of most open end pipe piles. Therefore, it can usually be assumed that an H-pile will be plugged under static loading conditions and the “box” area of the pile toe can be used for static calculation of the toe capacity in cohesionless and cohesive soils, i.e., area = flange width x section height. The toe capacity for H-piles driven to rock is usually governed by the pile structural strength. In that case, the toe capacity is calculated based on the steel cross sectional area, and should not include the area of a soil plug, if any.

For H-piles in cohesionless soils, arching between the flanges can usually be assumed, and the "box" perimeter can be used for shaft resistance calculations, i.e., perimeter = 2 x flange width + 2 x section height. In most cohesive soils, the shaft resistance is calculated from the sum of the adhesion,  $c_a$ , along the exterior of the two flanges plus the undrained shear strength of the soil,  $c_u$ , times the section height surface area of the two remaining sides of the "box" due to soil-to-soil shear along these two faces. Figure 9-20 illustrates that calculation of shear resistance for H-piles in stiff clays can still be problematic. Sheared clay lumps can develop above the plug zone, in which case the shaft resistance may develop only along the exterior surfaces of the flanges in the sheared lump zone.

The above discussions highlight the point that a higher degree of uncertainty often exists for static pile capacity calculations of open pile sections than for displacement piles. Soil plug formation and plug response is often different under static and dynamic loading. Such differences can complicate pile capacity evaluations of open pile sections with all dynamic methods (wave equation, dynamic testing, and dynamic formulas). Therefore, a static load test is recommended to verify calculated capacity for large diameter open end pipe piles, greater than 18 in (450 mm), or for H-piles designed to carry their load primarily in shaft resistance.

### 9.5.5 Time Effects on Pile Capacity

The soil is greatly disturbed when a pile is driven into the soil. As the soil surrounding the pile recovers from the installation disturbance, a time dependent change in pile capacity often occurs. Frequently piles driven in saturated clays, and loose to medium dense silts or fine sands gain capacity after driving has been completed. This phenomenon is called **soil setup**. Occasionally piles driven into dense saturated fine sands, dense silts, or weak laminated rocks such as shale, will exhibit a decrease in capacity after the driving has been completed. This phenomenon is called **relaxation**. Case history discussions on soil setup and relaxation may be found in Fellenius, *et al.* (1989), and Thompson and Thompson (1985), respectively.

#### 9.5.5.1 Soil Setup

When saturated cohesive soils are compressed and disturbed due to pile driving, large excess pore water pressures develop. These excess pore water pressures are generated partly from the shearing and remolding of the soil and partly from radial compression as the pile displaces the soil. The excess pore water pressures cause a reduction in the effective stresses acting on the pile, and thus a reduction in the soil shear strength. The reduction in soil shear strength results in a reduced pile capacity during driving, and for a period of time afterwards.

After driving, the excess pore water pressures will dissipate primarily through radial flow of the pore water away from the pile. With the dissipation of pore water pressures, the soil reconsolidates and shear strength increases. This increase in soil shear strength results in an increase in the static pile capacity and is called **soil setup**. A similar decrease in resistance to pile penetration with subsequent soil setup may occur in loose to medium dense, saturated, fine grained sands or silts. The magnitude of the gain in capacity depends on soil characteristics, pile material and pile dimensions.

Because the pile capacity may increase after the end of driving, pile capacity assessments should be made from static load testing or **restriking** performed **after** equilibrium conditions in the soil have been re-established. The time for the return of equilibrium conditions is highly variable and depends on soil type and degree of soil disturbance. Piezometers installed within three diameters of the pile can be used to monitor pore pressure dissipation with time. Effective stress static pile capacity calculation methods can be used to evaluate the increase in capacity with time once pore pressures are quantified.

Static load testing or **restrike** testing of piles in fine grained soils should not be conducted until after pore pressures dissipate and return to equilibrium. In the absence of site-specific pore water

pressure data from piezometers, it is suggested that static load testing or restriking of piles in clays and other predominantly fine grained soils be delayed for at least two weeks after driving and preferably for a longer period. In sandy silts and fine sands, pore pressures generally dissipate more rapidly. In these more granular deposits, five days to a week is often a sufficient time delay.

FHWA (1996) calculated general soil setup factors based on the predominant soil type along the pile shaft. The **soil setup factor** was defined as the failure load from a static load test divided by the end-of-drive wave equation capacity. These results are presented in Table 9-20. The data base for this study was comprised of 99 test piles from 46 sites. The number of sites and the percentage of the data base in a given soil condition is included in the table. While these soil set-up factors may be useful for preliminary estimates, soil setup is better estimated based on site-specific data gathered from pile restriking, dynamic measurements, static load testing, and local experience.

Komurka, *et al.*, (2003) summarized the current practice in estimating and measuring soil setup in a report to the Wisconsin Highway Research Program. This report summarizes the mechanisms associated with soil setup development and reviews several empirical relationships for estimating set-up.

**Table 9-8**  
**Soil setup factors (after FHWA, 1996)**

Predominant Soil Type Along Pile Shaft	Range in Soil Set-up Factor	Recommended Soil Set-up Factors*	Number of Sites and (Percentage of Data Base)
Clay	1.2 - 5.5	2.0	7 (15%)
Silt - Clay	1.0 - 2.0	1.0	10 (22%)
Silt	1.5 - 5.0	1.5	2 (4%)
Sand - Clay	1.0 - 6.0	1.5	13 (28%)
Sand - Silt	1.2 - 2.0	1.2	8 (18%)
Fine Sand	1.2 - 2.0	1.2	2 (4%)
Sand	0.8 - 2.0	1.0	3 (7%)
Sand - Gravel	1.2 - 2.0	1.0	1 (2%)
* Confirmation with local experience recommended			

### 9.5.5.2 Relaxation

The ultimate capacity of driven piles can also decrease with time following driving. This is known as **relaxation** and it has been observed in dense, saturated, fine grained soils such as non-cohesive silts and fine sands, as well as in some shales. In these cases, the driving process is believed to cause the dense soil near the pile toe to dilate, thereby generating negative excess

pore water pressures, i.e., suction. In accordance with the principle of effective stress, the negative pore water pressures temporarily increase the effective stresses acting on the pile, resulting in a temporarily higher soil strength and driving resistance. When these negative excess pore water pressures dissipate, the effective stresses acting on the pile decrease, as does the pile capacity. Relaxation in weak laminated rocks has been attributed to a release of locked-in horizontal stresses (Thompson and Thompson, 1985).

Because the pile capacity may decrease due to relaxation after the end of driving, pile capacity assessments from static load testing or restriking should be made after equilibrium conditions in the soil have been re-established. In the absence of site-specific pore water pressure data from piezometers, it is suggested that static load testing or restriking of piles in dense silts and fine sands be delayed for five days to a week after driving, or longer if possible. In relaxation-prone shales, it is suggested that static load testing or restrike testing be delayed a minimum of two weeks after driving.

Published cases of the relaxation magnitude of various soil types are quite limited. However, data from Thompson and Thompson (1985) as well as Hussein, *et al.* (1993) suggest relaxation factors for piles founded in some shales can range from 0.5 to 0.9. The **relaxation factor** is defined as the failure load from a static load test divided by the pile capacity at the end of initial driving. Relaxation factors of 0.5 and 0.8 have also been observed in two cases where piles were founded in dense sands and extremely dense silts, respectively. The importance of evaluating time dependent decreases in pile capacity for piles founded in these materials cannot be over emphasized.

### **9.5.6 Additional Design and Construction Considerations**

The previous sections of this chapter addressed routine static analysis procedures for pile foundation design. However, the designer should be aware of additional design and construction considerations that can influence the reliability of static analysis procedures in estimating pile capacity. These issues include effects of predrilling or jetting, construction dewatering and soil densification on pile capacity. Pile-driving-induced vibrations can also influence the final design and results of static calculations if potential vibration levels dictate changes in pile type or installation procedures. These topics are outside the scope of this manual and the reader is referred to FHWA (2006a) for guidance.

### 9.5.7 The DRIVEN Computer Program

The FHWA developed the computer program DRIVEN in 1998 for calculation of static pile capacity. The DRIVEN program can be used to calculate the capacity of open and closed end pipe piles, H-piles, circular or square solid concrete piles, timber piles, and Monotube piles. The program results can be displayed in both tabular and graphical form. Analyses may be performed in either English or SI units and can be switched between units during analyses (FHWA, 1998b). The DRIVEN manual and software Version 1.2, released in March 2001, can be downloaded from [www.fhwa.dot.gov/bridge/geosoft.htm](http://www.fhwa.dot.gov/bridge/geosoft.htm).

In the DRIVEN program, the user inputs the soil profile consisting of the soil unit weights and strength parameters including the percentage strength loss during driving. For the selected pile type, the program calculates the pile capacity versus depth for the entire soil profile using the Nordlund and  $\alpha$ -methods in cohesionless and cohesive layers, respectively. User-input percentage soil strength losses during driving are used to calculate the ultimate pile capacity at the time of driving as well as during restrike.

The DRIVEN program includes several analysis options that facilitate pile design. These options include:

- **Soft compressible soils:** The shaft resistance from unsuitable soil layers defined by the user is subtracted from the calculation of ultimate pile capacity.
- **Scourable soils:** Based on a user-input depth, the calculated shaft resistance from scourable soils due to local scour is subtracted from the calculation of ultimate pile capacity. In the case of channel degradation scour, the reduction in pile capacity from the loss of shaft resistance in the scour zone as well as the influence of the reduced effective overburden pressure from soil removal on the capacity calculated in the underlying layers is considered.
- **Pile Plugging:** DRIVEN handles pile plugging based on the recommendations presented in Section 9.5.4 of this manual.

The initial DRIVEN program screen is the Project Definition Screen illustrated in Figure 9-21. In this screen the user inputs the project information as well as the number of soil layers. Inputs for three water table elevations are provided. The water table at the time of drilling is used for correction of SPT N values for overburden pressure if that option is selected by the user. The

water table at the time of restrike / driving affects the effective overburden pressure in the static capacity calculations at those times. The static calculation at the time of driving includes soil strength losses. The restrike static calculations include the long term soil strength. The water table at the ultimate condition is used in the calculation of effective overburden pressure for the static capacity calculation under an extreme event.

The Soil Profile screen for a two layer soil profile is shown in Figure 9-22. A mouse click on the Select Graph Option will bring up the Cohesive Soil Layer Properties screen shown in Figure 9-23. The user can then select how the adhesion is calculated. The general adhesion option attributed to “Tomlinson 1979” in Figure 9-23 is based upon the data presented in Figure 9-16, i.e., piles without different overlying strata. The bottom option in the Cohesive Soil Layer Properties screen shown in Figure 9-23 allows the user to enter an adhesion value of their choice. This bottom option may be useful with the data presented in Figures 9-15 and 9-16 or site data from specific load test..

The Soil Profile screen for a two layer profile with cohesionless soil properties is presented in Figure 9-24. The user can input the same or different soil friction angles to be used in the shaft resistance and end bearing calculations in the layer. The user can also input SPT N values and let the program compute the soil friction angle from a correlation developed by Peck, *et al.* (1974) as shown in Figure 9-25. However, it is recommended that the user manually select the soil friction angle rather than use this program option as factors influencing the N value -  $\phi$  angle correlation such as SPT hammer type and sample recovery are not considered by the program.

Both cohesive and cohesionless soil profile screens request the user to provide the percentage strength loss of the soil type during driving. This is sometimes difficult for the user to quantify. Insight into appropriate values of driving strength loss can be gathered from the soil setup factors presented in Section 9.5.5. The percent driving strength loss needed for input into DRIVEN can be then be calculated from:

$$\% \text{ Driving Strength Loss} = 1 - [1 / \text{setup factor}]$$

After the soil input has been entered, the user must select a pile type from a drop down menu located on the Soil Profile screen. A pile detail screen will appear for the pile type selected requesting additional information on the depth to the top of the pile and the pile properties. These DRIVEN screens are presented in Figure 9-26.

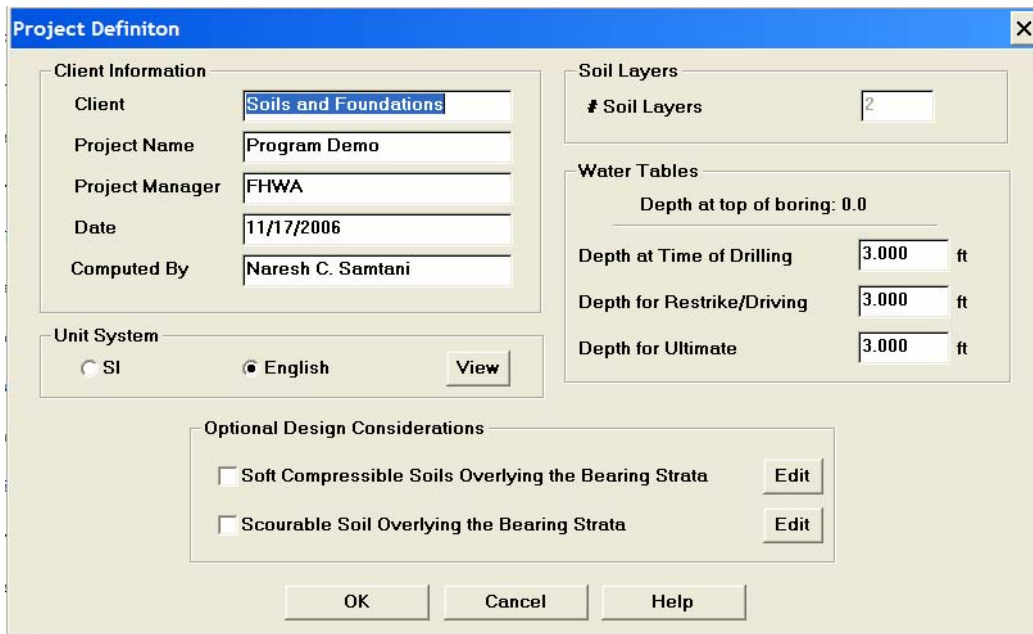


Figure 9-21. DRIVEN Project Definition screen.

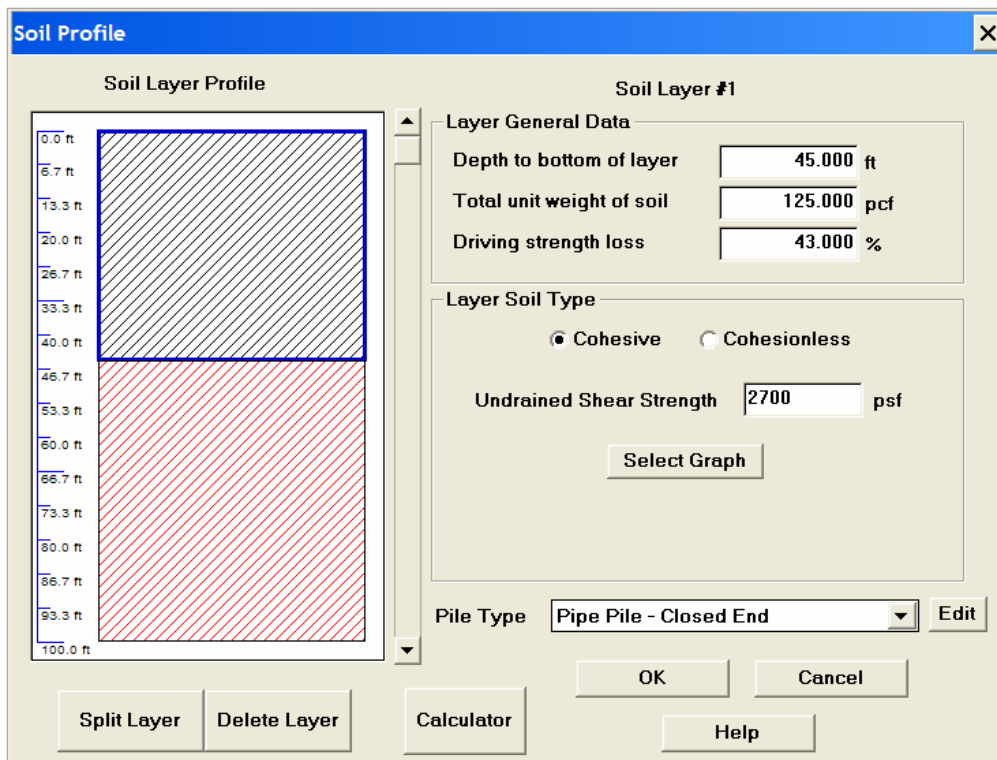


Figure 9-22. DRIVEN Soil Profile screen – cohesive soil.



Figure 9-23. DRIVEN Cohesive Soil Layer Properties screen.

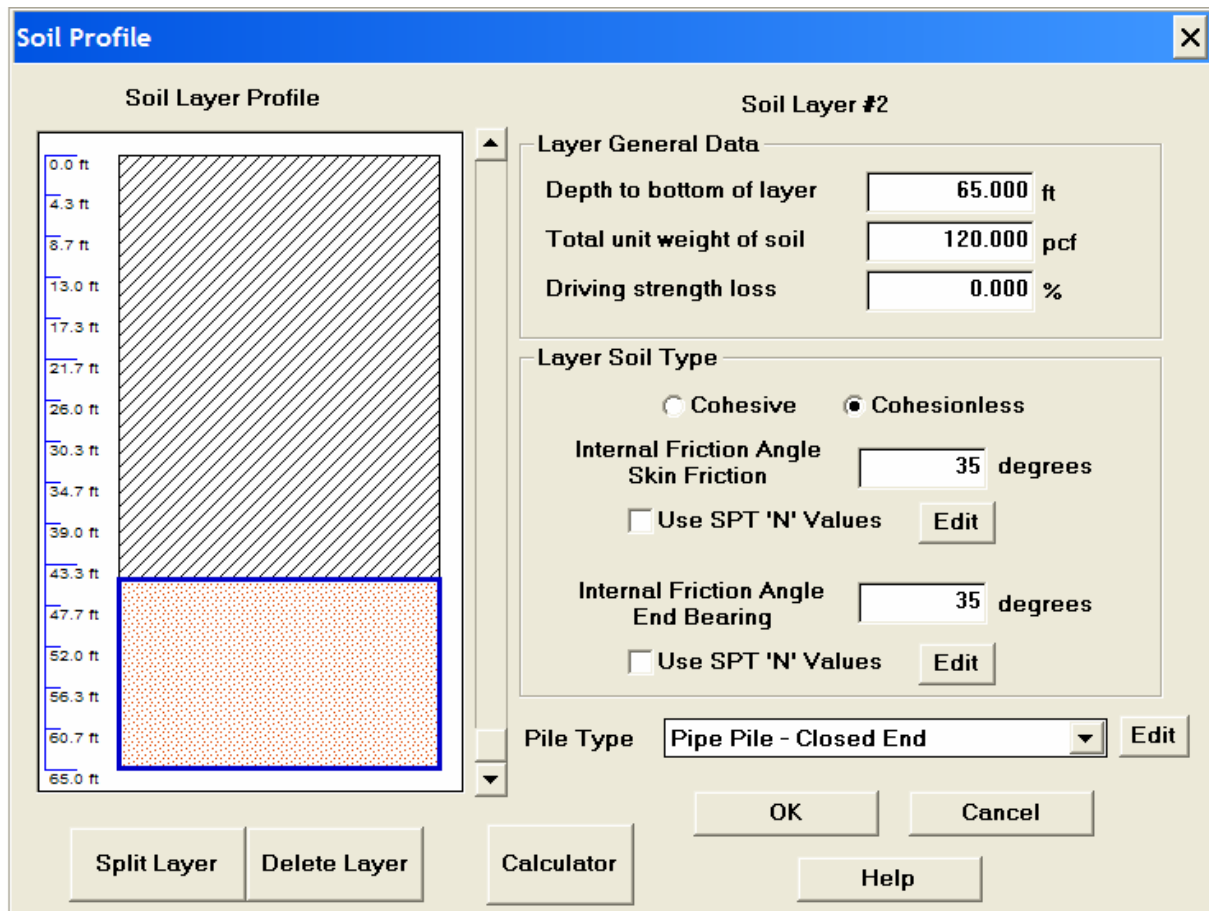


Figure 9-24. DRIVEN Soil Profile screen – cohesionless soil.

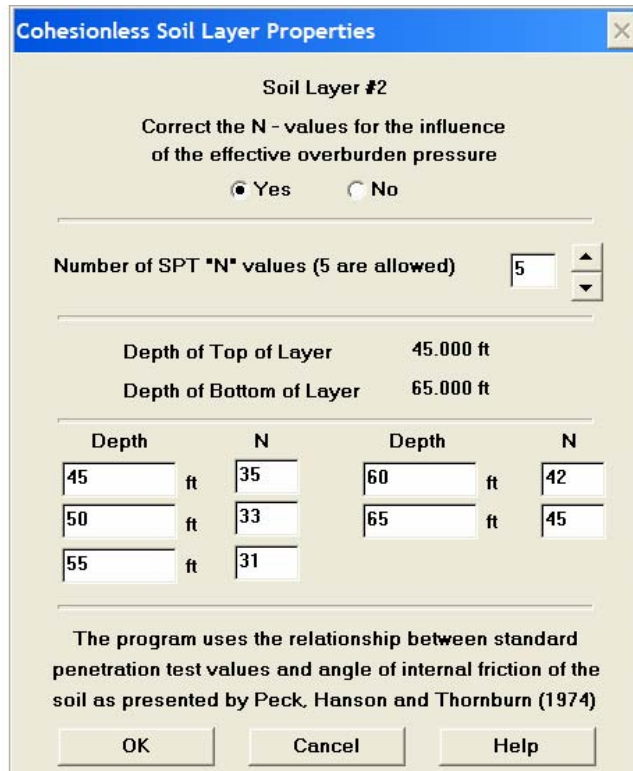


Figure 9-25. DRIVEN Cohesionless Soil Layer Properties screen.

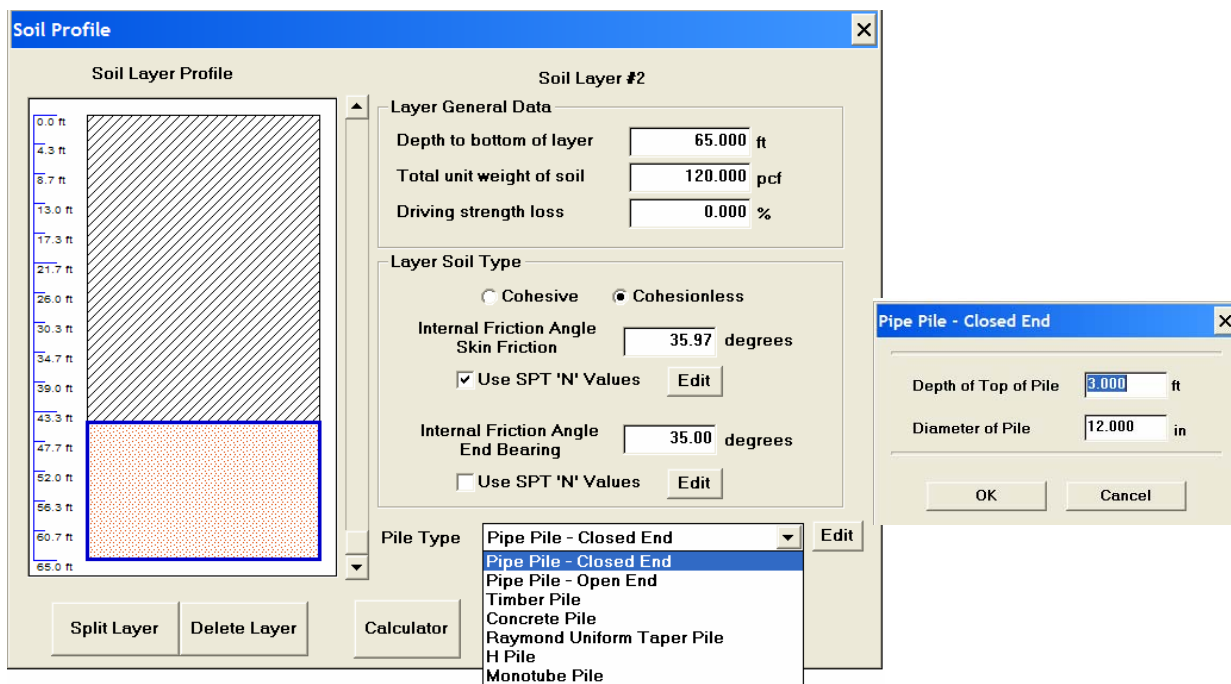
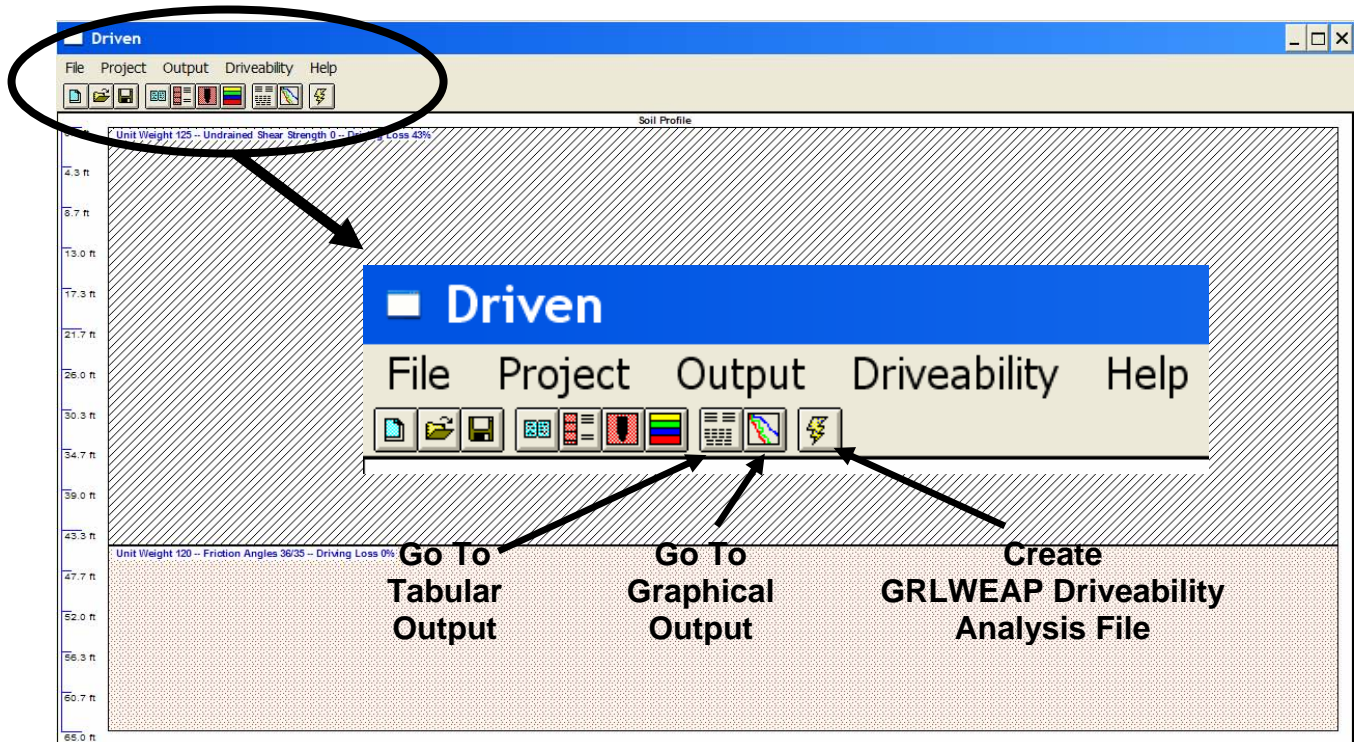


Figure 9-26. DRIVEN Soil Profile screen - Pile type selection drop down menu and pile detail screen.

Once all soil and pile information is entered, the user can review the static capacity calculations in tabular or graphical form by a mouse click on the appropriate icon in the program toolbar. The toolbar icons for tabular and graphical output are identified in Figure 9-27. The Output-Tabular screen is shown in Figure 9-28. A summary of the input data and the results of the analysis will be printed if the user clicks on the report button. Analysis output can also be presented graphically as shown in Figures 9-28 and 9-29 for driving and restrrike static analyses, respectively. The ultimate capacity versus depth from shaft resistance, toe resistance, and the combined shaft and toe resistance can be displayed by clicking on “skin friction,” “end bearing,” and “total capacity” on the Plots menu of the Output-Graphical screen, capacity changes with time or from extreme events can be reviewed by clicking on “restrrike,” “driving,” and “ultimate” on the Plot Set menu of the Output-Graphical screen.

The program also generates the soil input file required for a driveability study in the commonly used GRLWEAP wave equation program. The GRLWEAP file created by DRIVEN is compatible with the Windows versions of GRLWEAP. However, the DRIVEN file must be identified as a pre 2002 input file in the current version of GRLWEAP.

Additional DRIVEN program capabilities are described in the DRIVEN Program User’s Manual by FHWA (1998b).



**Figure 9-27. DRIVEN toolbar output and analysis options.**

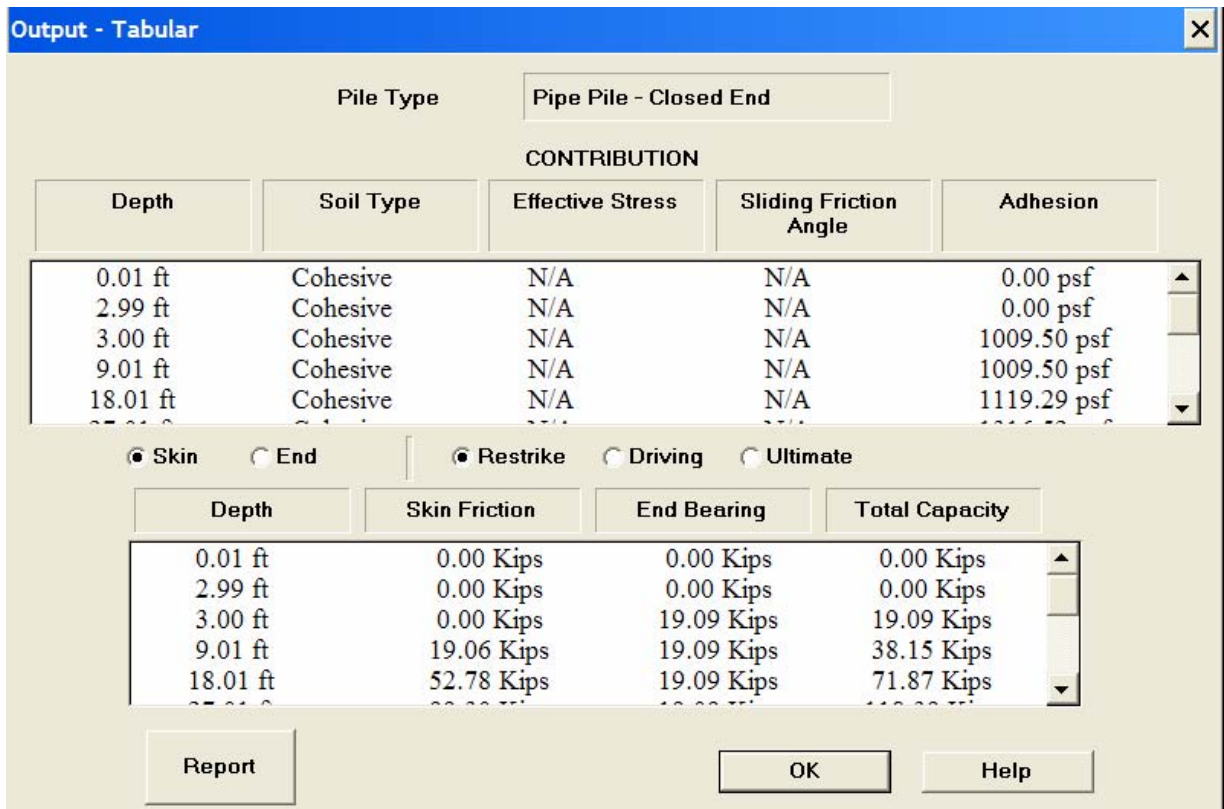


**Figure 9-28. DRIVEN Output Tabular screen.**

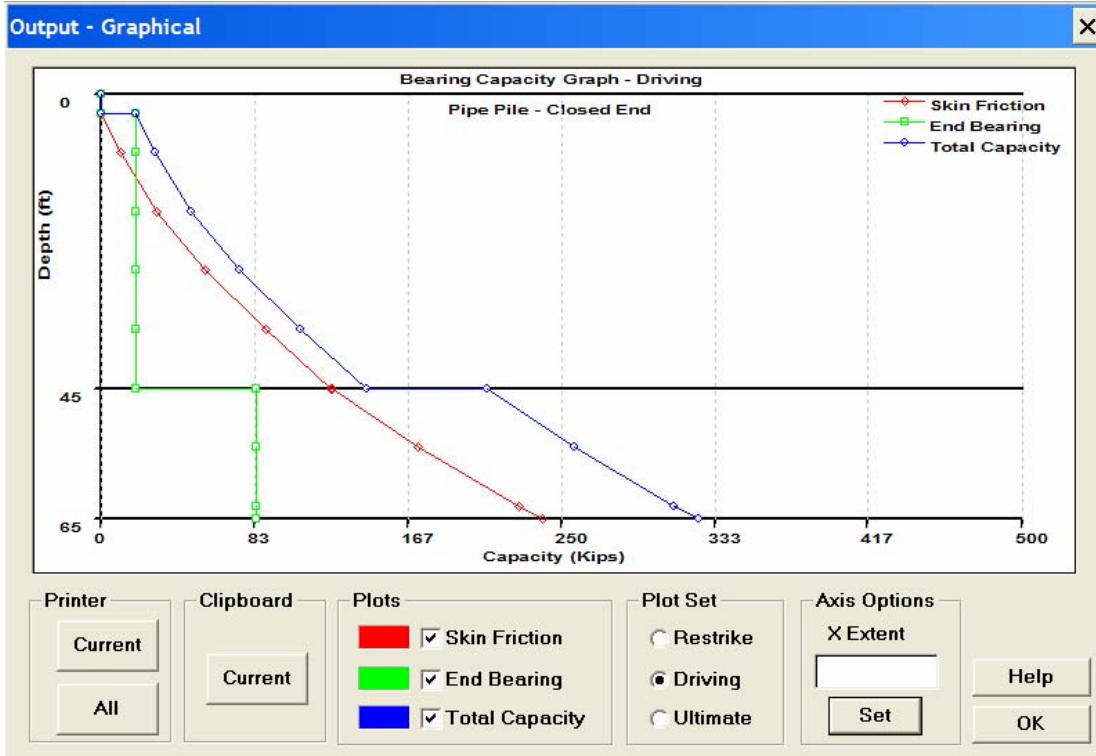


Figure 9-29. DRIVEN Output-Graphical screen for end of driving.

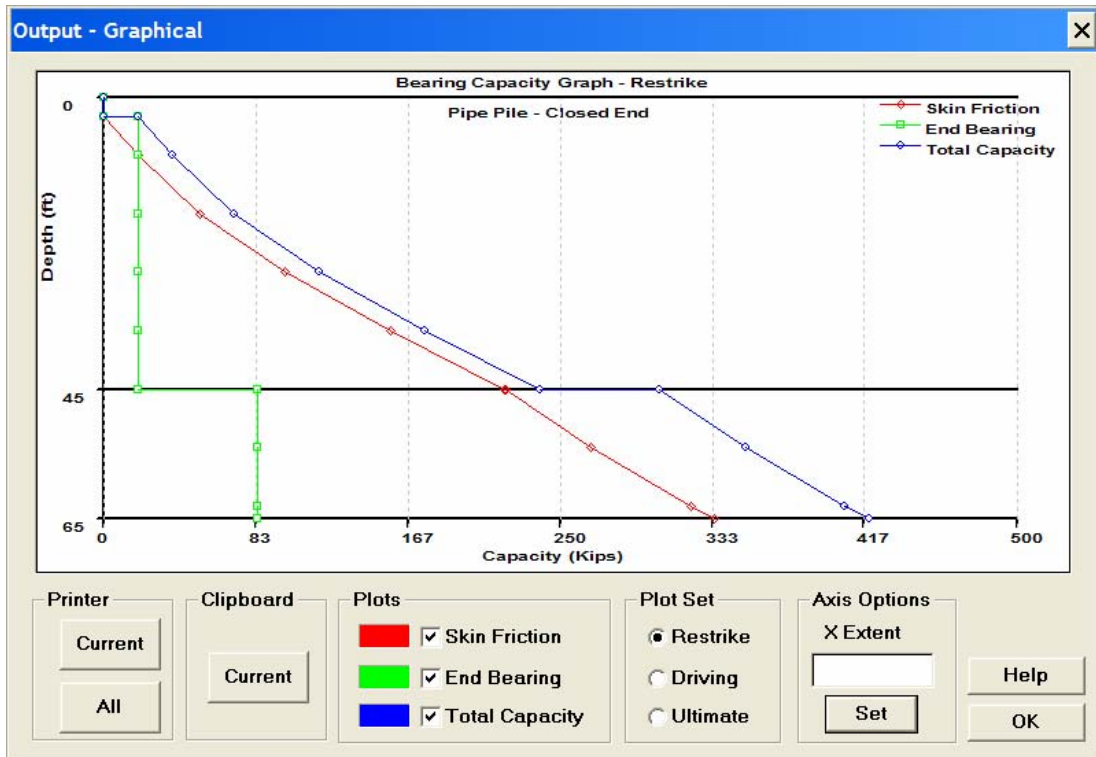


Figure 9-30. DRIVEN Output -Graphical screen for restrike.

### **9.5.8 Ultimate Capacity of Piles on Rock and in Intermediate Geomaterials (IGMs)**

Pile foundations on rock are normally designed to carry large loads. For pile foundations driven to rock, which include steel H-piles, pipe piles or precast concrete piles, the exact area in contact with the rock, the depth of penetration into rock, as well as the quality of rock are largely unknown. Therefore, the determination of load capacity of driven piles on rock should be made on the basis of driving observations, local experience and load tests.

Rock Quality Designation (RQD) values can provide a qualitative assessment of rock mass as discussed in Chapter 3. Except for soft weathered rock, the structural capacity of toe bearing pile will generally be less than the capacity of rock of fair to excellent quality as described in Figure 3-17 in Chapter 3. The structural capacity, which is based on the allowable design stress for the pile material, will therefore govern the pile capacity in many cases.

Small diameter piles supported on fair to excellent quality rock may be loaded to their allowable structural capacity. Piles supported on soft weathered rock, such as shale or other types of very poor or poor quality rock, should be designed based on the results of pile load tests. Similarly, for driven piles that penetrate into soft rocks or IGMs, the ultimate capacity may include the contribution of shaft resistance if a static load test is performed to verify the magnitude of the shaft resistance.

## 9.6 DESIGN OF PILE GROUPS

The previous sections of this chapter dealt with design procedures for single piles. However piles for almost all highway structures are installed in groups due to the heavy foundation loads. This section of the chapter will address the foundation design procedures for evaluating the axial compression capacity of pile groups as well as the settlement of pile groups under axial compression loads. The axial compression capacity and settlement of pile groups are interrelated and are therefore presented in sequence.

The efficiency of a pile group in supporting the foundation load is defined as the ratio of the ultimate capacity of the group to the sum of the ultimate capacities of the individual piles comprising the group. This may be expressed in equation form as:

$$\eta_g = \frac{Q_{ug}}{nQ_u} \quad 9-17$$

where:  $\eta_g$  = pile group efficiency  
 $Q_{ug}$  = ultimate capacity of the pile group  
 $n$  = number of piles in the pile group  
 $Q_u$  = ultimate capacity of each individual pile in the pile group

If piles are driven into compressible cohesive soil or into dense cohesionless material underlain by compressible soil, then the ultimate axial compression capacity of a pile group may be less than that of the sum of the ultimate axial compression capacities of the individual piles. In this case, the pile group has a group efficiency of less than 1. In cohesionless soils, the ultimate axial compression capacity of a pile group is generally greater than the sum of the ultimate axial compression capacities of the individual piles comprising the group. In this case, the pile group has a group efficiency greater than 1.

The settlement of a pile group is likely to be many times greater than the settlement of an individual pile carrying the same per pile load as each pile in the group. Figure 9-31(a) illustrates that for a single pile, only a relatively small zone of soil around and below the pile toe is subjected to vertical stress. Figure 9-31(b) illustrates that for a pile group, a much larger zone of soil around and below the pile group is stressed. The settlement of the pile group may be large depending on the compressibility of the soils within the stressed zone.

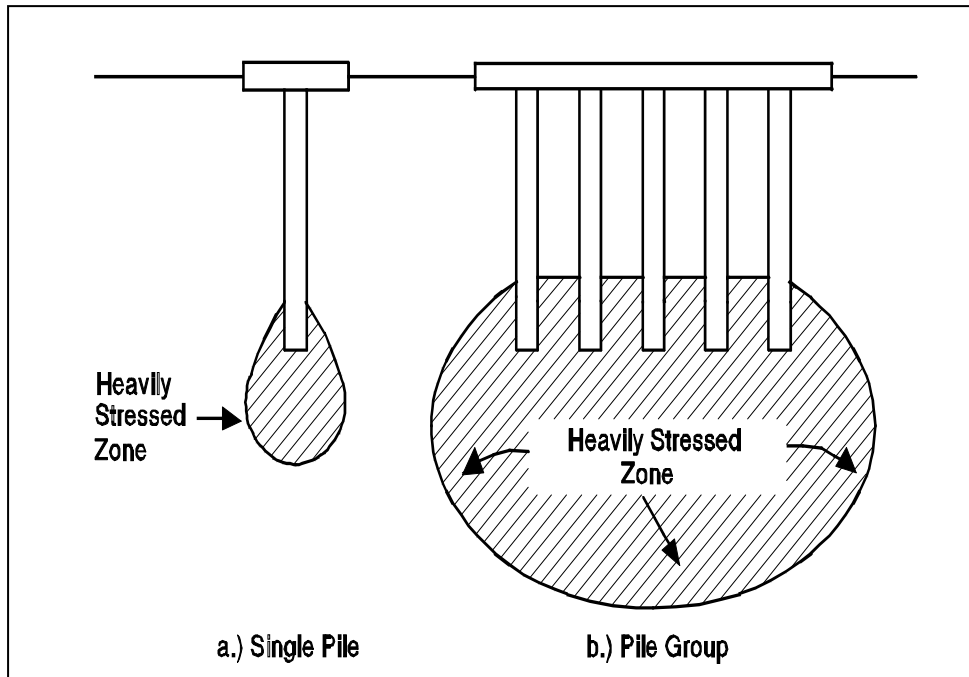


Figure 9-31. Stress zone from single pile and pile group (after Tomlinson, 1994).

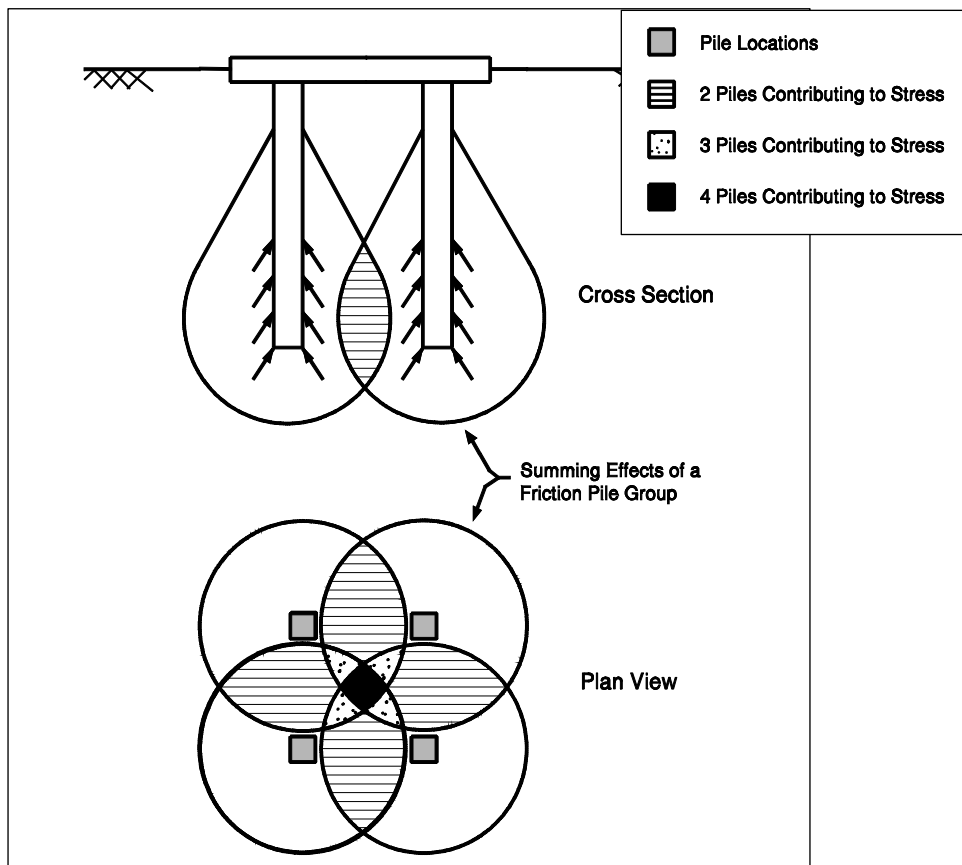


Figure 9-32. Overlap of stress zones for friction pile group (after Bowles, 1996).

The soil supporting a pile group is also subject to overlapping stress zones from individual piles in the group. The overlapping effect of stress zones for a pile group supported by shaft resistance is illustrated in Figure 9-32.

## **9.6.1 Axial Compression Capacity of Pile Groups**

### **9.6.1.1 Cohesionless Soils**

In cohesionless soils, the ultimate group capacity of driven piles with a center to center spacing of less than 3 pile diameters is greater than the sum of the ultimate capacity of the individual piles. The greater group capacity is due to the overlap of individual soil compaction zones around each pile, which increases the shaft resistance due to soil densification. Piles in groups at center to center spacings greater than three times the average pile diameter generally act as individual piles.

Design recommendations for estimating group capacity for driven piles in cohesionless soil are as follows:

1. The ultimate group capacity for driven piles in cohesionless soils not underlain by a weak deposit may be taken as the sum of the individual ultimate pile capacities, provided jetting or predrilling was not used in the pile installation process. Jetting or predrilling can result in group efficiencies less than 1. Therefore, jetting or predrilling should be avoided whenever possible or controlled by detailed specifications when necessary.
1. If a pile group founded in a firm bearing stratum of limited thickness is underlain by a weak deposit, then the ultimate group capacity is the smaller value of either the sum of the ultimate capacities of the individual piles, or the group capacity against block failure of an equivalent pier, consisting of the pile group and enclosed soil mass punching through the firm stratum into the underlying weak soil. From a practical standpoint, block failure in cohesionless soils can only occur when the center to center spacing of the piles is less than 2 pile diameters, which is less than the minimum center to center spacing of 2.5 diameters allowed by the AASHTO code (2002). The method shown for cohesive soils presented in the Section 9.6.1.3 may be used to evaluate the possibility of a block failure.
3. Piles in groups should not be installed at center to center spacings less than 3 times the average pile diameter. A minimum center to center spacing of 3 diameters is recommended to optimize group capacity and minimize installation problems.

### 9.6.1.2 Cohesive Soils

In the absence of negative shaft resistance, the group capacity in cohesive soil is usually governed by the sum of the ultimate capacities of the individual piles, with some reduction due to overlapping zones of shear deformation in the surrounding soil. Negative shaft resistance is described in Section 9.8 and often occurs when soil settlement transfers load to the pile. The AASHTO (2002) code states that the group capacity is influenced by whether or not the pile cap is in firm contact with the ground. If the pile cap is in firm contact with the ground, the soil between the piles and the pile group act as a unit.

The following design recommendations are for estimating ultimate pile group capacity in cohesive soils. The lesser of the ultimate pile group capacity, calculated from Steps 1 to 4, should be used.

1. For pile groups driven in clays with undrained shear strengths of less than 2 ksf (95 kPa) and for the pile cap not in firm contact with the ground, a group efficiency of 0.7 should be used for center to center pile spacings of 3 times the average pile diameter. If the center to center pile spacing is greater than 6 times the average pile diameter, then a group efficiency of 1.0 may be used. Linear interpolation should be used for intermediate center to center pile spacings.
2. For pile groups driven in clays with undrained shear strengths less than 2 ksf (95 kPa) and for the pile cap in firm contact with the ground, a group efficiency of 1.0 may be used.
3. For pile groups driven in clays with undrained shear strength in excess of 2 ksf (95 kPa), a group efficiency of 1.0 may be used regardless of the pile cap - ground contact.
4. Calculate the ultimate pile group capacity against block failure by using the procedure described in Section 9.6.1.3.
5. Piles in groups should not be installed at center to center spacings less than 3 times the average pile diameter and not less than 3 ft (1 m).

It is important to note that the driving of pile groups in cohesive soils can generate large excess pore water pressures. The excess pore water pressures can result in short term group efficiencies on the order of 0.4 to 0.8 for 1 to 2 months after installation. As these excess pore water pressures dissipate, the pile group efficiency will increase. Figure 9-33 presents observations on the dissipation of excess pore water pressure versus time for pile groups driven in cohesive soils.

Depending upon the group size, the excess pore water pressures typically dissipate within 1 to 2 months after driving. However, in very large groups, full excess pore water pressure dissipation may take up to a year.

If a pile group will experience the full group load shortly after construction, the foundation designer must evaluate the reduced group capacity that may be available for load support. In these cases, piezometers should be installed to monitor pore pressure dissipation with time. Effective stress capacity calculations can then be used to determine if the increase in pile group capacity versus time during construction meets the load support requirements.

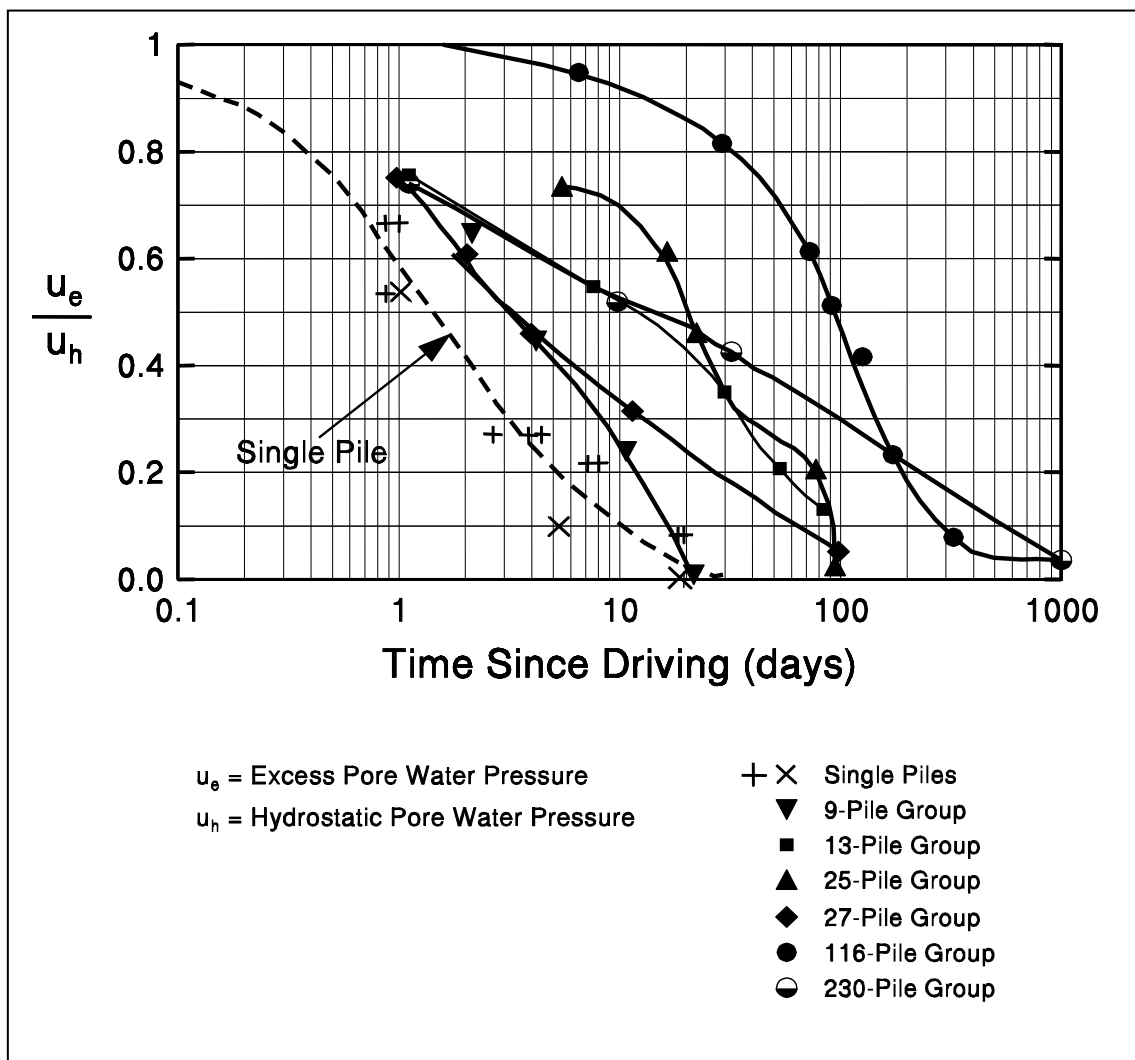


Figure 9-33. Measured dissipation of excess pore water pressure in soil surrounding full scale pile groups (after O'Neill, 1983).

### 9.6.1.3 Block Failure of Pile Groups

Block failure of pile groups is generally a design consideration only for pile groups in soft cohesive soils or in cohesionless soils underlain by a weak cohesive layer. For a pile group in cohesive soil as shown in Figure 9-34, the ultimate capacity of the pile group against a block failure is provided by the following expression:

$$Q_{ug} = 2D (B + Z) c_{u1} + B Z c_{u2} N_c \quad 9-18$$

- where:
- $Q_{ug}$  = ultimate group capacity against block failure
  - $D$  = embedded length of piles
  - $B$  = width of pile group
  - $Z$  = length of pile group
  - $c_{u1}$  = weighted average of the undrained shear strength over the depth of pile embedment for the cohesive soils along the pile group perimeter
  - $c_{u2}$  = average undrained shear strength of the cohesive soils at the base of the pile group to a depth of  $2B$  below pile toe level
  - $N_c$  = bearing capacity factor

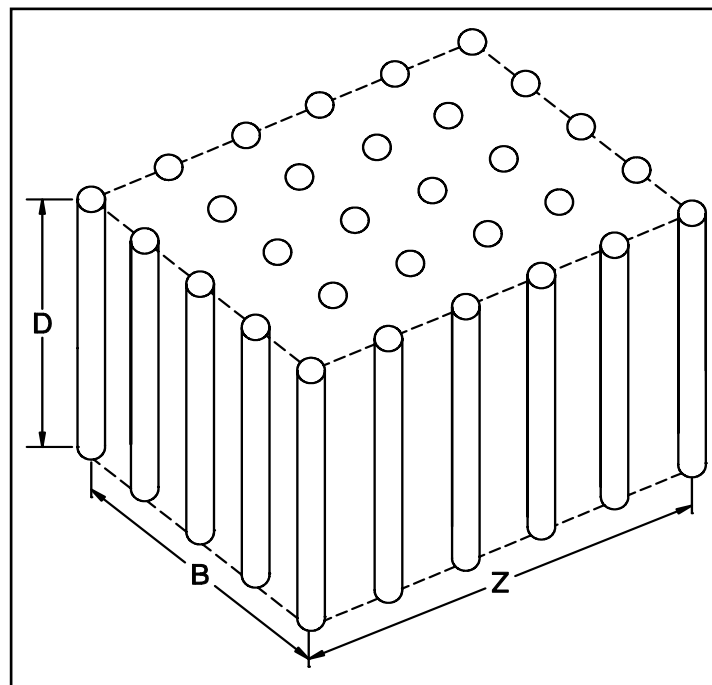


**Figure 9-34. Three dimensional pile group configuration (after Tomlinson, 1994).**

If a pile group will experience the full group load shortly after construction, the ultimate group capacity against block failure should be calculated by using the remolded or a reduced shear strength rather than the average undrained shear strength for  $c_{ul}$ .

The bearing capacity factor,  $N_c$ , for a rectangular pile group is generally 9. However, for pile groups with relatively small pile embedment depths and/or relatively large widths,  $N_c$  should be calculated from the following equation where the terms  $D$ ,  $B$  and  $Z$  are as shown in Figure 9-34.

$$N_c = 5 \left( 1 + \frac{D}{5B} \right) \left( 1 + \frac{B}{5Z} \right) \leq 9 \quad 9-19$$

In the evaluation of possible block failure of pile groups in cohesionless soils underlain by a weak cohesive deposit, the weighted average unit shaft resistance for the cohesionless soils should be substituted for  $c_{ul}$  in calculating the ultimate group capacity. The pile group base strength determined from the second part of the ultimate group capacity equation should be calculated by using the strength of the underlying weaker layer.

## 9.6.2 Settlement of Pile Groups

Pile groups supported in and underlain by cohesionless soils will produce only elastic or immediate settlements. This means that the settlements will occur almost immediately as the pile group is loaded. Pile groups supported in and underlain by cohesive soils may produce both elastic settlements that will occur almost immediately and consolidation settlements that will occur over a period of time. In highly over-consolidated clays, the majority of the foundation settlement will occur almost immediately. Consolidation settlements will generally be the major source of foundation settlement in normally consolidated clays.

Methods for estimating settlement of pile groups are provided in the following sections. Methods for estimating single pile settlements are not provided in this document because piles are usually installed in groups.

### 9.6.2.1 Elastic Compression of Piles

The methods for computing pile group settlement discussed in the following sections consider soil settlements only and do not include the settlement caused by elastic compression of pile material due to the imposed axial load. Therefore, the elastic compression should also be computed and added to the group settlement estimates of soil settlement to obtain the total settlement. The elastic compression can be computed by the following expression:

$$\Delta = \frac{Q_a L}{A E} \quad 9-20$$

where:  $\Delta$  = elastic compression of pile material in inches (mm)  
 $Q_a$  = design axial load in pile in kips (kN)  
 $L$  = length of pile in inches (mm)  
 $A$  = pile cross sectional area in in<sup>2</sup> (mm<sup>2</sup>)  
 $E$  = modulus of elasticity of pile material in ksi (kPa)

The modulus of elasticity for steel piles is 30,000 ksi (207,000 MPa). For concrete piles, the modulus of elasticity varies with concrete compressive strength and is generally on the order of 4,000 psi (27,800 MPa). The elastic compression of short piles is relatively small and can often be neglected in design.

### 9.6.2.2 Settlement of Pile Groups in Cohesionless Soils

Meyerhof (1976) recommended the settlement of a pile group in a homogeneous sand deposit not underlain by a compressible soil be conservatively estimated by the following expressions in U.S. units:

$$s = \frac{4 p_f \sqrt{B} I_f}{\bar{N}'} \quad \text{For silty sand, use: } s = \frac{8 p_f \sqrt{B} I_f}{\bar{N}'} \quad 9-21$$

where:  $s$  = estimated total settlement in inches  
 $p_f$  = design foundation pressure in ksf = group design load divided by group area  
 $B$  = width of pile group in ft  
 $\bar{N}'$  = average corrected SPT  $N_{160}$  value within a depth  $B$  below pile toe  
 $I_f$  = influence factor for group embedment =  $1 - [D / 8B] \geq 0.5$   
 $D$  = pile embedment depth in ft

### 9.6.2.3 Settlement of Pile Groups in Cohesive Soils

Terzaghi and Peck (1967) proposed that pile group settlements could be evaluated using an equivalent footing situated at a depth of  $D/3$  above the pile toe. This concept is illustrated in Figure 9-35. For a pile group consisting of only vertical piles, the equivalent footing has a plan area  $(B)(Z)$  that corresponds to the perimeter dimensions of the pile group as shown in Figure 9-34. The pile group load over this plan area is then the bearing pressure transferred to the soil through the equivalent footing. The load is assumed to spread within the frustum of a pyramid of side slopes at  $30^\circ$  and to cause uniform additional vertical pressure at lower levels. The pressure at any level is equal to the load carried by the group divided by the plan area of the base of the frustum at that level. Once the equivalent footing dimensions have been established then the settlement of the pile group can be estimated by using the procedures described in Chapter 8 (Shallow Foundations).

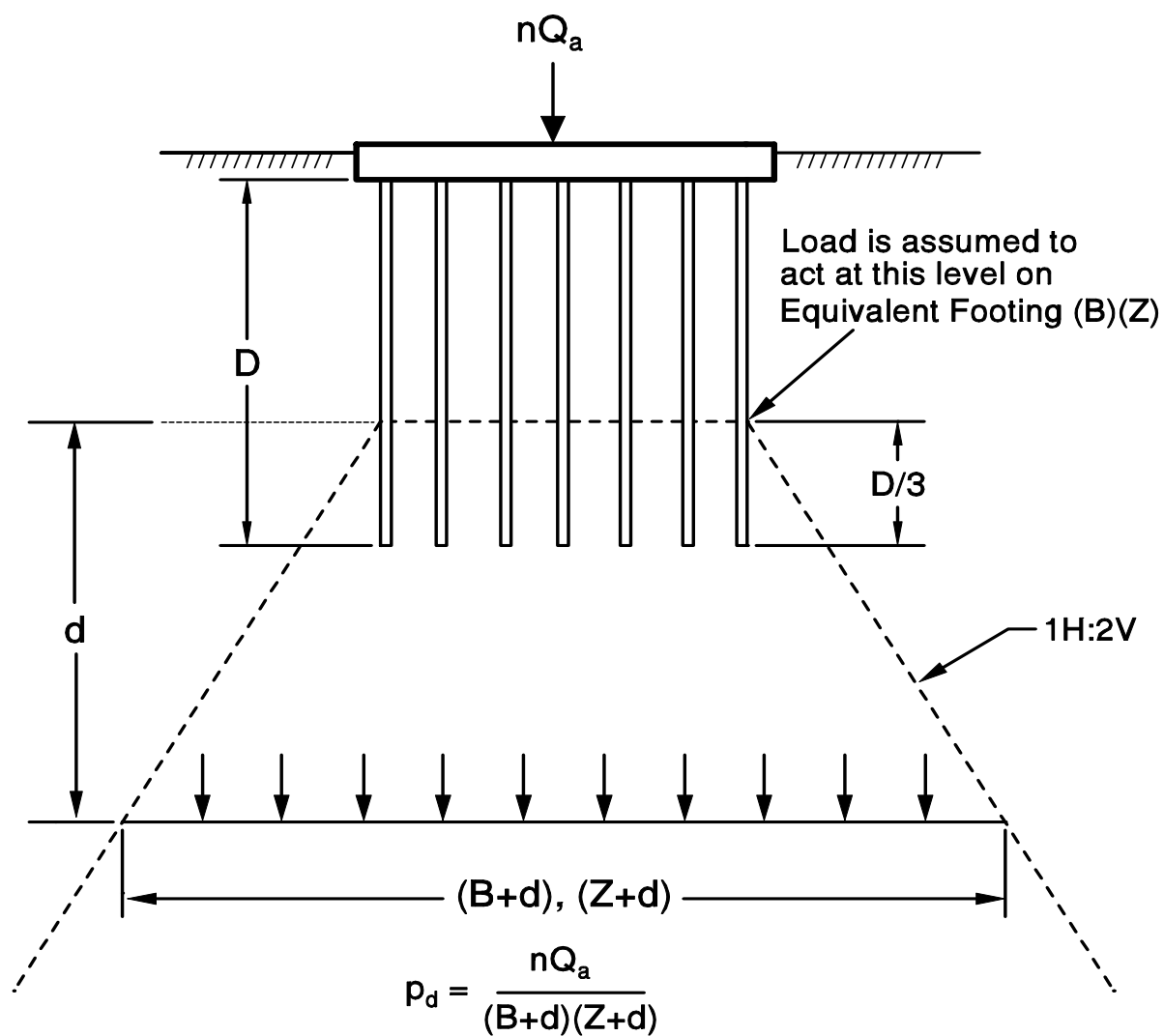
Rather than fixing the equivalent footing at a depth of  $D/3$  above the pile toe for all soil conditions, the depth of the equivalent footing should be adjusted based upon soil stratigraphy and load transfer mechanism to the soil. Figure 9-36 presents the recommended location of the equivalent footing for the following load transfer and soil resistance conditions:

- a) toe bearing piles in hard clay or sand underlain by soft clay
- b) piles supported by shaft resistance in clay
- c) piles supported in shaft resistance in sand underlain by clay
- d) piles supported by shaft and toe resistance in layered soil profile

Note that Figures 9-35 and 9-36 assume that the pile group consists only of vertical piles. If a group of piles contains battered piles, then they should be included in the determination of the equivalent footing width only if the stress zones from the battered piles overlap with those from the vertical piles.

## 9.7 DESIGN OF PILES FOR LATERAL LOAD

The interaction of a pile-soil system subjected to lateral load has long been recognized as a complex function of nonlinear response characteristics of both pile and soil. The theory and design method for analyzing laterally loaded piles is beyond the scope of this document. Guidance on lateral load analysis is provided in FHWA (1994). The program LPILE is commonly used to evaluate the behavior of single piles under lateral loads. FHWA (2006a) discusses the use of LPILE program for piles subjected to lateral loads.



Note: Pile Group has Plan Dimension of B and Z

**Figure 9-35. Equivalent footing concept (after Duncan and Buchignani, 1976).**

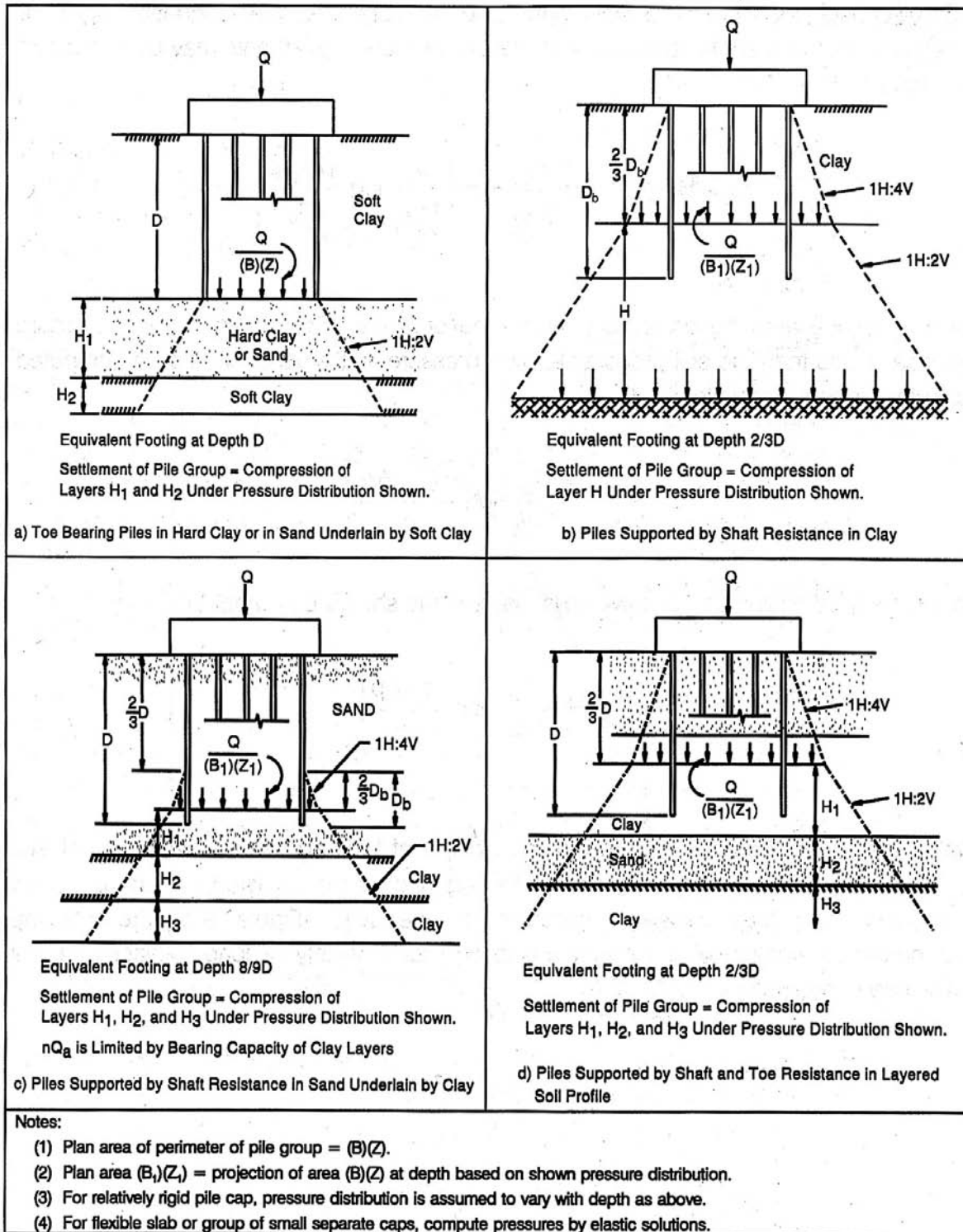


Figure 9-36. Stress distribution below equivalent footing for pile group (FHWA, 2006a).

## 9.8 DOWNDRAG OR NEGATIVE SHAFT RESISTANCE

When piles are installed through a soil deposit undergoing consolidation, the resulting relative downward movement of the soil around piles induces "**downdrag**" forces on the piles. These "downdrag" force is also called negative shaft resistance. Negative shaft resistance is the reverse of the usual positive shaft resistance developed along the pile surface that allows the soil to support the applied axial load. The downdrag force increases the axial load on the pile and can be especially significant on long piles driven through compressible soils. Therefore, the potential for negative shaft resistance must be considered in pile design. Batter piles should be avoided in soil conditions where relatively large soil settlements are expected because of the additional bending forces imposed on the piles, which can result in pile deformation and damage.

Settlement computations should be performed to determine the amount of settlement the soil surrounding the piles is expected to undergo after the piles are installed. The amount of relative settlement between soil and pile that is necessary to mobilize negative shaft resistance is about 0.4 to 0.5 inches (10 to 12 mm). At that amount of movement, the maximum value of negative shaft resistance is equal to the soil-pile adhesion. The negative shaft resistance can not exceed this value because slip of the soil along the pile shaft occurs at this value. It is particularly important in the design of friction piles to determine the depth at which the pile will be unaffected by negative shaft resistance. Only below that depth can positive shaft resistance provide support to resist vertical loads.

The most common situation where large negative shaft resistance develops occurs when fill is placed over a compressible layer immediately prior to, or shortly after piles are driven. This condition is shown in Figure 9-37(a). Negative shaft resistance can also develop whenever the effective overburden pressure is increased on a compressible layer through which a pile is driven as for example in the case of lowering of the ground water table as illustrated in Figure 9-37(b).

NCHRP (1993) presents the following criteria for identifying when negative shaft resistance may occur. If any one of these criteria is met, negative shaft resistance should be considered in the design. The criteria are:

1. The total settlement of the ground surface will be larger than 4 in (100 mm).
2. The settlement of the ground surface after the piles are driven will be larger than 0.4 in (10 mm).

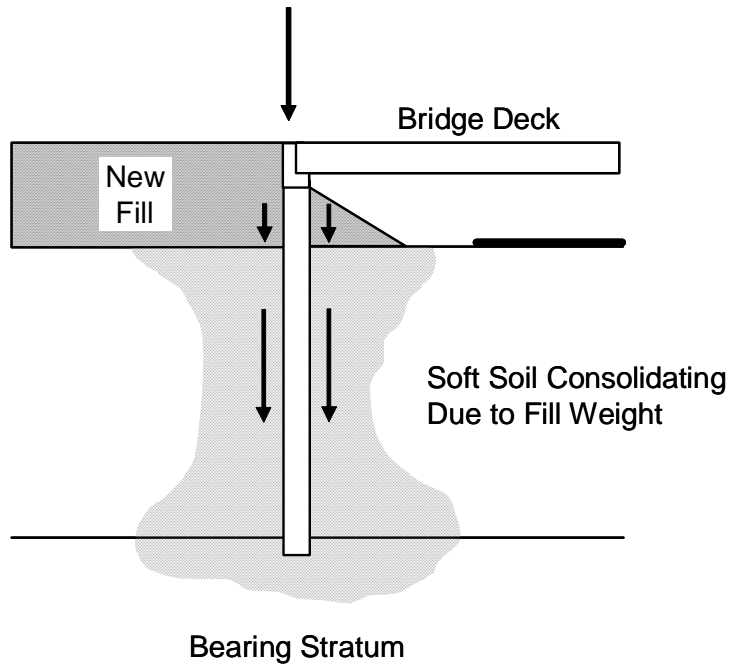


**Figure 9-37(a). Common downdrag situation due to fill weight (FHWA, 2006a).**

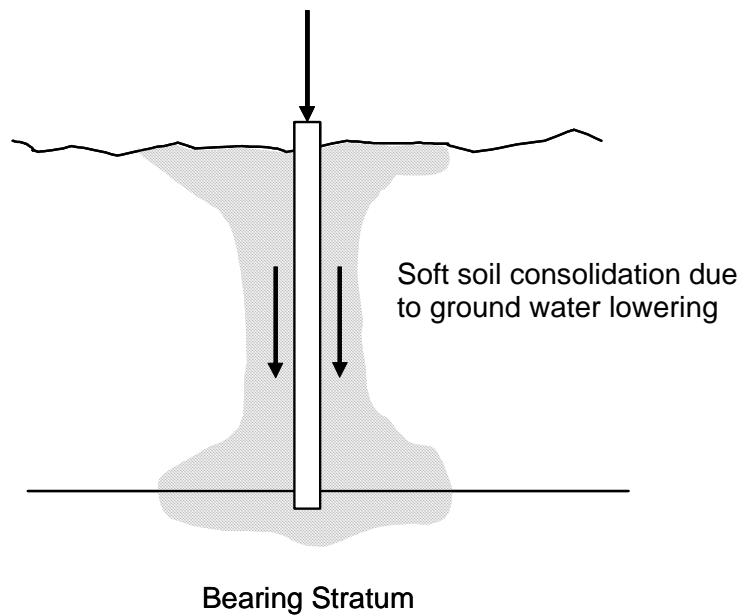


**Figure 9-37(b). Common downdrag situation due to ground water lowering (FHWA, 2006a).**

3. The height of the embankment to be placed on the ground surface exceeds 6.5 ft (2 m).
4. The thickness of the soft compressible layer is larger than 30 ft (10 m).
5. The water table will be lowered by more than 13 ft (4 m).
6. The piles will be longer than 80 ft (25 m).

For pile groups, the total downdrag load should not be calculated by summation of the downdrag load on each pile in the group. Rather, the downdrag load should be computed based on the perimeter surface area of the group block.

FHWA (2006a) presents several different methods for determining negative shaft resistance. In situations where the negative shaft resistance on piles is relatively large such that a reduction in the pile design load is impractical, negative shaft resistance forces can be handled or reduced by using one or more of the following techniques:

- Reduce soil settlement, e.g. by preloading the soil
- Use lightweight fill material
- Use a friction reducer such as bitumen and plastic wrap. These reducers are prone to being scrapped off during driving and are not considered to be reliable.
- Increase allowable pile-stress
- Prevent direct contact between soil and pile, e.g., pile sleeves

The above options for reducing negative shaft resistance are discussed in FHWA (2006a).

## 9.9 CONSTRUCTION OF PILE FOUNDATIONS

Construction control of pile operations is a much more difficult proposition than for spread footings. During footing placement an inspector can easily examine a prepared footing area and observe the concrete footing being poured to assure a quality foundation. Piles derive their support below ground. Direct quality control of the finished product is not possible. Therefore, substantial control must be maintained over the peripheral operations leading to the incorporation of the pile into the foundation. In general terms, control is exercised in two areas; the pile material, and the installation equipment. These items are interrelated since changes in one may affect the others. It is mandatory that pile foundation installation be considered during design to insure that the piles shown on the plans can be installed. This section discusses the installation and construction monitoring aspects of driven pile foundations.

### 9.9.1 Selection of Design Safety Factor Based on Construction Control

The topic of selection of a suitable design safety factor based on construction control was discussed in Section 9.4. It is reiterated that the factor of safety used should be based on the construction control method used for capacity verification. **The factor of safety applied to the design load should increase with the increasing unreliability of the method used for determining ultimate pile capacity during construction.** The recommended factors of safety on the design load for various construction control methods were presented in Table 9-5. The factor of safety for other test methods not included in Table 9-5 should be determined by the individual designer.

### 9.9.2 Pile Driveability

Greater pile penetration depths are increasingly being required to satisfy performance criteria in special design events such as scour, vessel impact, ice and debris loading, and seismic events. Therefore, the ability of a pile to be driven to the required depth has become increasingly more important and must be evaluated in the design stage. **Pile driveability refers to the ability of a pile to be driven to a desired depth and/or capacity.** All of the previously described static analysis methods are meaningless if the pile cannot be driven to the required design depth without sustaining damage. **The limit of pile driveability is the maximum soil resistance a pile can be driven either without sustaining damage or a refusal driving resistance with a properly sized driving system.**

Primary factors controlling the ultimate geotechnical capacity of a pile are the **pile details** (type and length), **subsurface data**, and the method of **installation**. Table 9-9 highlights these factors

and the items to be included in the plans and specifications that are the design engineer's responsibility. Also included in Table 9-9 are the items to be checked for quality assurance that are the construction engineer's responsibility. Since the pile type, length and method of installation can be specified, it is often erroneously assumed that the pile can be installed as designed to the estimated depth. However, the pile must have sufficient driveability to overcome the soil resistance encountered during driving in order to reach the estimated or specified depth. If a pile section does not have a driveability limit in excess of the soil resistance to be overcome during driving, it will not be driveable to the desired depth. **The failure to evaluate pile driveability is one of the most common deficiencies in driven pile design practice.**

In evaluating the driveability of a pile, the soil disturbance during installation and the time dependent soil strength changes should be considered. Both soil setup and relaxation have been described earlier in this chapter. For economical pile design, the foundation designer must match the soil resistance to be overcome at the time of driving with the pile impedance, the pile material strength, and the pile driving equipment. These factors are discussed in the following section.

### **9.9.2.1 Factors Affecting Driveability**

A pile must satisfy two aspects of driveability. First, the pile must have sufficient stiffness to transmit driving forces large enough to overcome soil resistance. Second, the pile must have sufficient structural strength to withstand the driving forces without damage.

The primary controlling factor on pile driveability is the pile impedance, which is defined as  $EA/C$ , where  $E$  is the elastic modulus of pile material,  $A$  is the cross-sectional area of the pile and  $C$  is the wave propagation velocity of pile material. Since  $E$  and  $C$  are constant for a given type of pile, only increasing the pile cross sectional area,  $A$ , will improve the pile driveability. For steel H-piles, the designer can improve pile driveability by increasing the H-pile section without increasing the H-pile size. The driveability of steel pipe piles can be improved by increasing the pipe wall thickness. For open ended pipe piles, an inside-fitting cutting shoe can improve driveability by delaying the formation of a soil plug and thereby reducing the soil resistance to be overcome. Most concrete piles are solid cross sections. Therefore, increasing the pile area to improve driveability is usually accompanied by an increase in the soil resistance to driving.

**Table 9-9. Responsibilities of design and construction engineers**

<b>Item</b>	<b>Design Engineer's Responsibilities</b>	<b>Construction Engineer's Responsibilities</b>
Pile Details	Include in plans and specifications: <ol style="list-style-type: none"> <li>a. Material and strength: concrete, steel, or timber.</li> <li>b. Cross section: diameter, tapered or straight, and wall thickness.</li> <li>c. Special coatings for corrosion or downdrag.</li> <li>d. Splices, toe protection, etc.</li> <li>e. Estimated pile tip elevation.</li> <li>f. Estimated pile length.</li> <li>g. Pile design load and ultimate capacity.</li> <li>h. Allowable driving stresses.</li> </ol>	Quality control testing or certification of materials.
Subsurface Data	Include in plans and specifications: <ol style="list-style-type: none"> <li>a. Subsurface profile.</li> <li>b. Soil resistance to be overcome to reach estimated length.</li> <li>c. Minimum pile penetration requirements.</li> <li>d. Special notes: boulders, artesian pressure, buried obstructions, time delays for embankment fills, etc.</li> </ol>	Report major discrepancies in soil profile to the designer.
Installation	Include in plans and specifications: <ol style="list-style-type: none"> <li>a. Method of hammer approval.</li> <li>b. Method of determining ultimate pile capacity.</li> <li>c. Compression, tension, and lateral load test requirements (as needed) including specification for tests and the method of interpretation of test results.</li> <li>d. Dynamic testing requirements (as needed).</li> <li>f. Limitations on vibrations, noise, and head room.</li> <li>g. Special notes: spudding, predrilling, jetting, set-up period, etc.</li> </ol>	<ol style="list-style-type: none"> <li>a. Confirm that the hammer and driving system components agree with the contractor's approved submittal.</li> <li>b. Confirm that the hammer is maintained in good working order and the hammer and pile cushions are replaced regularly.</li> <li>c. Determination of the final pile length from driving resistance, estimated lengths and subsurface conditions.</li> <li>d. Pile driving stress control.</li> <li>e. Conduct pile load tests.</li> <li>f. Documentation of field operations.</li> <li>g. Ensure quality control of pile splices, coatings, alignment and driving equipment.</li> </ol>

A lesser factor influencing pile driveability is the pile material strength. The influence of pile material strength on driveability is limited, since strength does not alter the pile impedance. However, a pile with a higher pile material strength can tolerate higher driving stresses that may allow a larger pile hammer to be used. Use of larger hammer may allow a slightly higher capacity to be obtained before driving refusal or pile damage occurs.

Other factors that may affect pile driveability include the characteristics of the driving system such as ram weight, stroke, and speed, as well as the actual system performance in the field. The dynamic soil response can also affect pile driveability. Soils may have higher damping characteristics or elasticity than assumed, both of which can reduce pile driveability. These factors are discussed in Section 9.9.3 and 9.9.6.

Even if the pile structural capacity and geotechnical capacity both indicate a high pile capacity could be used, a high pile capacity may still not be obtainable because driving stresses may exceed allowable driving stress limits. A pile cannot be driven to an ultimate static capacity that is as high as the structural capacity of the pile because of the additional dynamic resistance or damping forces generated during pile driving. The allowable static design stresses in pile materials specified by various codes generally represent the static stress levels that can be consistently developed with normal pile driving equipment and methods. Maximum allowable design and driving stresses are presented in Section 9.9.7.

### **9.9.2.2 Driveability Versus Pile Type**

Driveability should be checked during the design stage of all driven piles. It is particularly important for closed end steel pipe piles where the impedance of the steel casing may limit pile driveability. Although the designer may attempt to specify a thin-wall pipe without mandrel in order to save material cost, a thin wall pile may lack the driveability to develop the required ultimate capacity or to achieve the necessary pile penetration depth. Wave equation analyses should be performed in the design stage to select the pile section and wall thickness.

Steel H-piles and open-end pipe piles, prestressed concrete piles, and timber piles are also subject to driveability limitations. This is particularly true as allowable design stresses increase and as special design events such as scour require increased pile penetration depths. The driveability of long prestressed concrete piles can be limited by the pile's tensile strength.

The following sections discuss the various aspects related to pile driveability. First, the pile driving equipment and operation (Section 9.9.3) is introduced followed by the fundamental pile driving formula (Section 9.9.4), basics of the dynamic analysis of pile driving (Section 9.9.5),

use of wave equation methodology to perform dynamic analysis of pile driving (Section 9.9.6), discussion of driving stresses (Section 9.9.7), and some useful guidelines to assess the results of wave equation analysis in terms of pile driveability (Section 9.9.8). General pile construction monitoring considerations are discussed in Section 9.9.10 followed by a brief description of the elements of dynamic pile monitoring in Section 9.9.11.

### 9.9.3 Pile Driving Equipment and Operation

Proper inspection of pile driving operations requires that the inspector have a basic understanding of pile driving equipment. Estimation of "as driven pile capacity" is usually based on the number of hammer blows needed to advance the pile a given distance. Each hammer blow transmits a given amount of energy to the pile. The total number of blows is the total energy required to move the pile a given distance. This energy can then be related to soil resistance and supporting capacity. However, pile inspection entails more than counting blows of the hammer.

The energy transmitted to the pile by a given hammer can vary greatly depending on the equipment used by the contractor. Energy losses can occur by poor alignment of the driving system, improper or excessive cushion material, improper appurtenances, or a host of other reasons. As the energy losses increase, additional blows are required to move the pile. The manufacturer's rated hammer energy is based on minimal energy losses. Assumptions that the hammer is delivering its rated energy to the pile can prove dangerous if substantial energy is lost in the driving system. Artificially high blow counts can result in acceptance of driven pile lengths, which are shorter than that necessary for the required pile capacity.

Important elements of the driving system include the **leads**, the **hammer cushion**, the **helmet**, and for concrete piles, the **pile cushion**. Typical components of a pile driving system are shown in Figure 9-38. The leads are used to align the hammer and the pile such that every hammer blow is delivered concentrically to the pile system. The helmet holds the top of the pile in proper alignment and prevents rotation of the pile during driving. Typical components of a helmet are shown in Figure 9-39. The hammer and the helmet "ride" in the leads so that hammer - pile alignment is assured.

All impact pile driving equipment, except some gravity hammers should be equipped with a suitable thickness of hammer cushion material. The function of the hammer cushion is to prevent damage to the hammer or pile and insure uniform energy delivery per blow to the pile. Hammer cushions must be made of durable manufactured materials provided in accordance with the hammer manufacturer's guidelines. All wood, wire rope and asbestos hammer cushions are

specifically disallowed and should not be used. The thicker the hammer cushion, the less the amount of energy transferred to the pile. Mandatory use of a durable hammer cushion material, which will retain uniform properties during driving, is necessary to relate blow count to pile capacity accurately. Non-durable materials, which deteriorate during driving, cause erratic energy delivery to the pile and prevent the use of blow counts to determine pile capacity.

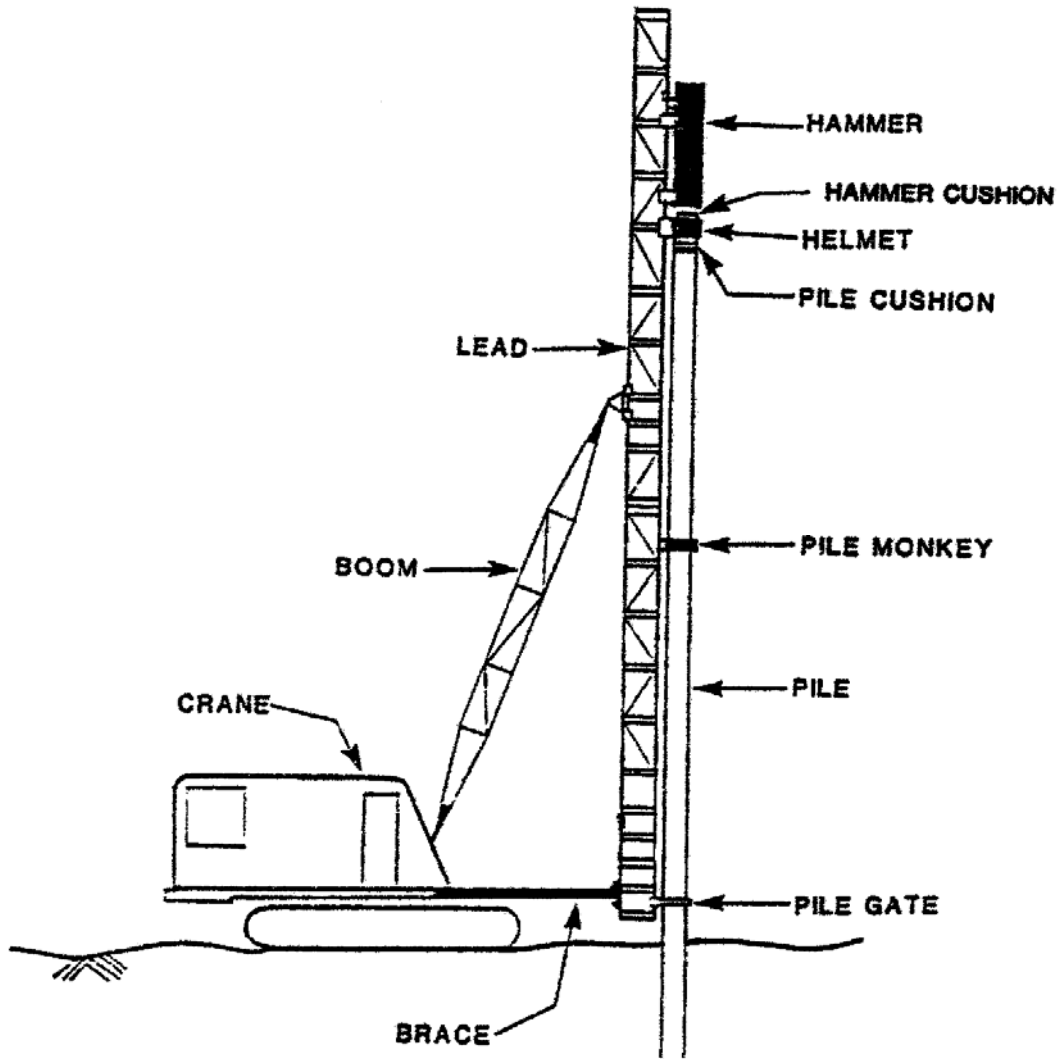
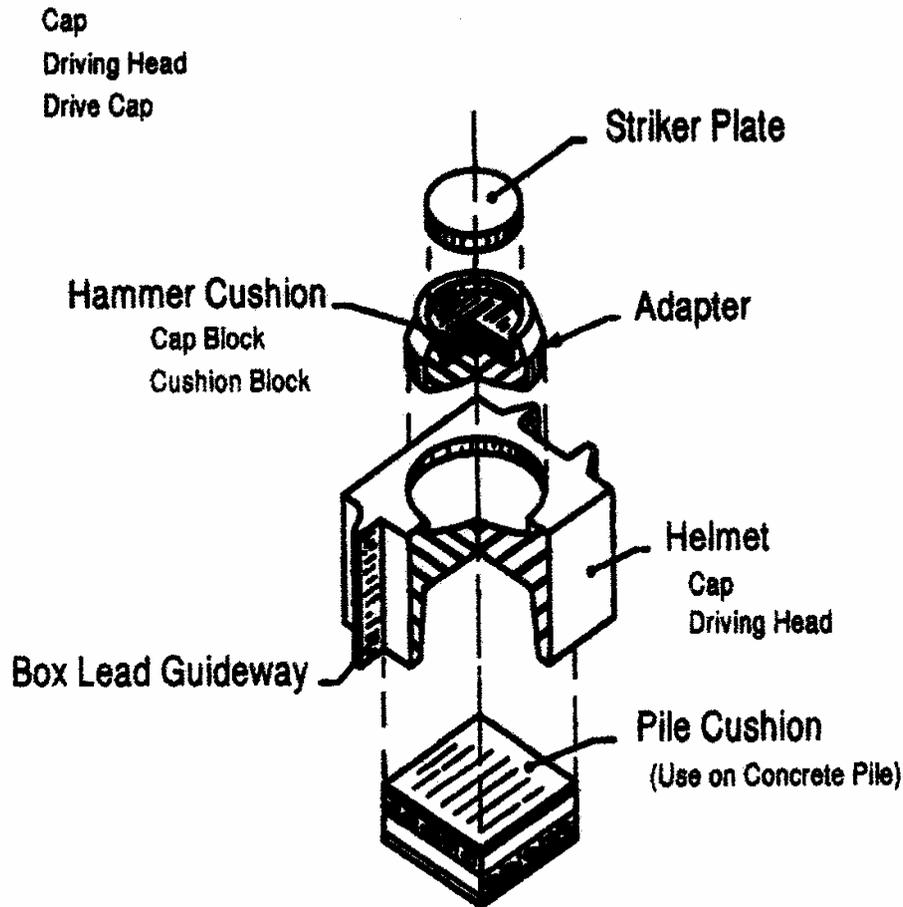


Figure 9-38. Typical components of a pile driving system.

## Helmet (Complete Unit)



Note: The helmet shown is for nomenclature only. Various sizes and types are available to drive H, pipe, concrete (shown) and timber piles. A system of inserts or adapters is utilized up inside of the helmet to change from size to size and shape to shape.

**Figure 9-39. Typical components of a helmet.**

The heads of concrete piles must be protected by a pile cushion made of hardwood or plywood. The minimum thickness of pile cushion placed on the pile head should not be less than four inches. A new pile cushion should be provided for each pile.

A non-routine element called a **follower** may be used in the driving system, particularly for piles driven below water. Followers cause substantial and erratic reduction in the hammer energy transmitted to the pile due to the follower is flexibility, poor connection to the pile head, frequent misalignment, etc. Reliable correlation of blow count with pile capacity is impossible when followers are used. Special monitoring with devices such as the Pile Driving Analyzer (PDA) (FHWA, 2006a) should be specified when followers are used.

#### 9.9.4 Dynamic Pile Driving Formulae

In the 1800s, the fundamental pile driving formula was established to relate dynamic driving forces to available pile bearing capacity. The formula was based on a simple energy balance between the kinetic energy of the ram at impact and the resulting work done on the soil, i.e., a distance of pile penetration against a soil resistance. The concept assumed a pure Newtonian impact with no energy loss. The fundamental formula was expressed as follows:

WORK DONE ON SOIL = KINETIC ENERGY INPUT

$$RS = WH = 12 E_n \quad 9-22$$

where: W = weight of the ram in pounds  
H = distance of ram fall in feet  
R = total soil resistance against the pile (driving capacity) in pounds  
S = pile penetration per blow (set) in inches  
E<sub>n</sub> = driving energy (ft-lbs), which is converted to in-lbs for unit consistency by multiplying by 12.

An inherent difficulty in the pile driving operation is that only a portion of the ram's kinetic energy actually causes penetration of the pile. Studies indicate that typically only 30 to 65 percent of the rated energy is passed through to the pile. Much of the energy is lost in either heat (soil friction, hammer mechanism, pile material, etc.) or strain (elastic compression of the cushion, the pile and the surrounding soil). For example, if the elastic shortening of the pile ( $\Delta L$ ) is  $RL/AE$ , where  $L$  = the effective length of the pile in inches,  $A$  = the cross sectional area of the pile in  $\text{in}^2$ , and  $E$  = modulus of elasticity of the pile material in  $\text{lbs}/\text{in}^2$ , then the average shortening along the length of the pile would be  $\Delta L/2$  and the energy lost due to elastic compression of the pile would be  $R(\Delta L/2)$  or  $R^2L/2AE$ . Therefore, if all losses are ignored except those due to elastic compression of the pile, then Equation 9-22 can be re-written as:

$$RS = 12 E_n - \frac{R^2 L}{2AE} \quad 9-23a$$

If the pile is driven through reasonably uniform soil the effective length,  $L$ , is the full length of pile penetration. If the pile is driven through relatively firm soil into a weaker substratum, the effective length is generally taken as the length from the head of the pile to the depth of the weak substratum.

If  $k$  is defined as  $RL/2AE$  then Equation 9-23a can be re-written as:

$$RS = 12 E_n - Rk \quad 9-23b$$

When Equation 9-23b is solved for total soil resistance ( $R$ ) the result is the Engineering News pile driving formula:

$$R = \frac{12 E_n}{S + k} \quad 9-24$$

The Engineering News (EN) pile driving formula was first published in the *Engineering News* in the year 1888. The EN formula is commonly, but incorrectly termed the ENR formula since the publishers of the *Engineering News* merged with the McGraw-Hill Publishing Company in 1917 to produce the *Engineering News-Record*. The EN formula was developed for wood piles driven by a drop hammer. As expressed by Equation 9-24, the EN formula is for driving resistance. Subsequently, in an attempt to develop a relationship between driving resistance and bearing capacity, the equation was modified to provide the safe load that a pile could withstand to the input energy and set per blow. The basic assumption in the modification of the original EN formula is that the safe working load ( $P$ ) is one-sixth of the driving resistance. Therefore, the basic EN formula as we know it today is:

$$P = \frac{R}{6} = \frac{2E_n}{S + k} \quad 9-25$$

where:

- $E_n$  = driving energy (ft-lbs).
- $S$  = pile penetration per blow (set) in inches.
- $k$  = constant based on hammer type = 0.1 for single acting steam hammer and 1 for drop hammer.

According to Hough (1957), the basic assumption that the safe working load ( $P$ ) is one-sixth of the driving resistance is not the same as applying a factor of safety of 6 to the ultimate bearing capacity under static load. The real factor of safety for the EN formula may be considerably more or even less than 6 under certain conditions

Most engineers are not aware (1) that the EN formula was originally developed for timber piles, or (2) that the EN formula has a built-in factor of safety of 6. Sowers (1979) states the following about the EN formula:

"The EN formula was derived from observations of the driving of wood piles in sand with free-falling drop hammers. Numerous pile load tests show that the real factor of safety of the formula can be as low as 2/3 and as high as 20. For wood piles driven with free-falling drop hammers and for lightly loaded short piles driven with a steam hammer, the EN formulas give a crude indication of pile capacity. For other conditions they can be very misleading."

In 1988 the Washington State DOT published a study (WSDOT, 1988) based on high quality pile load test data that showed the EN formula to be the least reliable of the 10 dynamic formulae that were analyzed. Subsequent studies by FHWA as part of the Demonstration Project 66 (precursor of the FHWA (2006a) manual) confirmed the unreliability of the EN formula, particularly for higher pile loads where actual safety factors are too frequently less than 1.0.

The WSDOT and FHWA studies resulted in both organizations replacing EN in their specifications with the Gates dynamic formula. However, the Gates dynamic formula, which was originally developed based on correlations with static load test data, is usually restricted to piles that have driving capacities less than 600 kips. The Gates formula, was modified by FHWA for driving capacity as shown below:

$$R_u = 1.75 \sqrt{E_r} \log_{10}(10N_b) - 100 \quad 9-26a$$

- where:
- $R_u$  = the ultimate pile capacity (kips)
  - $E_r$  = the manufacturer's rated hammer energy (ft-lbs) at the **field observed ram stroke**
  - $N_b$  = the number of hammer blows per 1 inch at final penetration

The number of hammer blows per foot of pile penetration required to obtain the ultimate pile capacity is calculated as follows:

$$N/ft = 12 (10^x) \quad 9-26b$$

- where:  $x = [(R_u + 100)/(1.75 \sqrt{E_r})] - 1$

### 9.9.5 Dynamic Analysis of Pile Driving

An examination of the pile driving process discloses that the concept of a Newtonian impact does not apply. When viewed in slow motion, the ram does not immediately rebound from the pile after impact. The ram transfers force to the pile head over a finite period of time that depends on the properties of the hammer-pile-soil system. A force pulse is created that travels down the pile in a **wave** shape. The amplitude of the wave will decay due to system damping properties before reaching the pile tip. The force in the wave, which reaches the tip, will "pull" the pile tip into the soil before the wave is reflected back up the pile. After reflection, an amount of permanent "set" of the pile tip will remain. This process is crudely shown in Figure 9-40 for the hammer-pile-soil system.

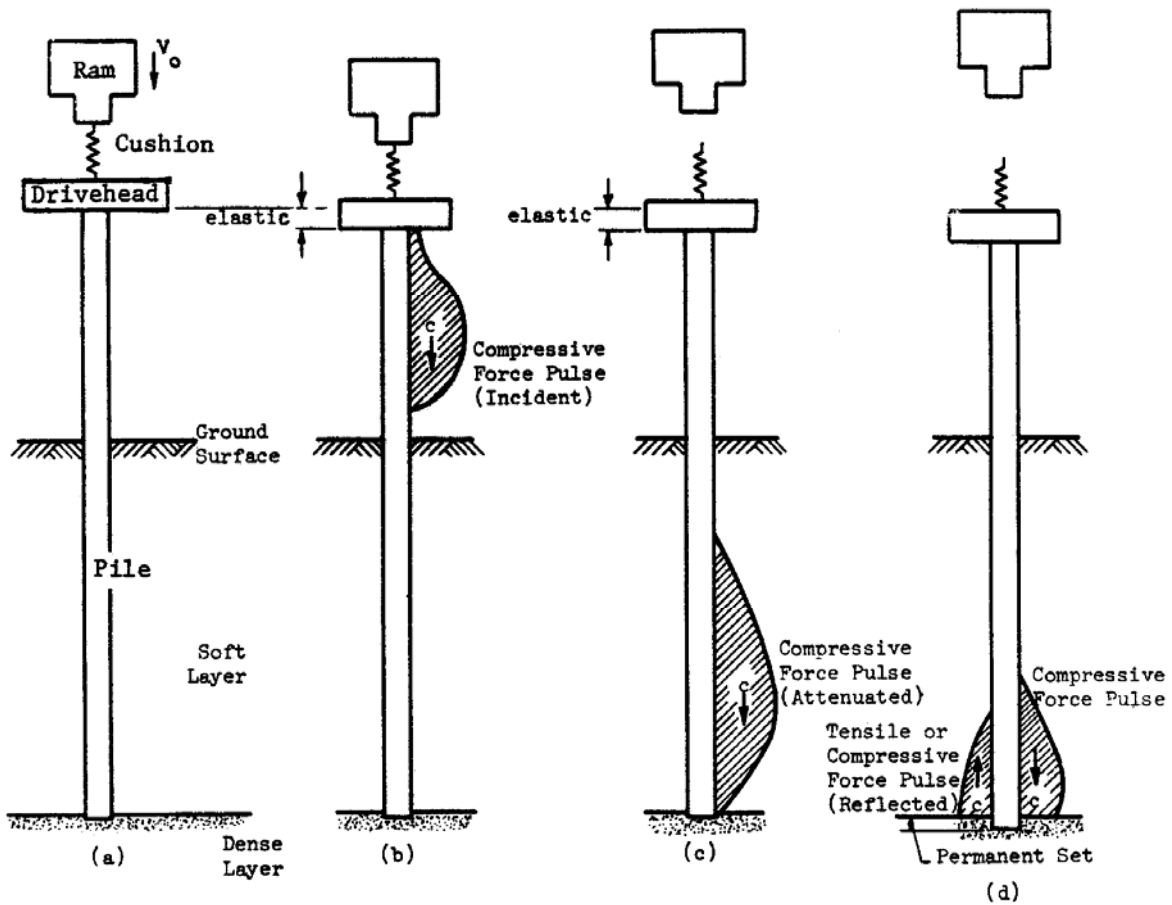


Figure 9-40. Hammer-pile-soil system.

The analysis of the force pulse wave is commonly known as the **wave equation analysis** (WEA). In a WEA a number of variables such as pile length and flexibility are accounted for in addition to the variations in the contractor's driving system and the project soils. Therefore, WEA represents a significant improvement over dynamic formulas. The approach was developed by E.A.L. Smith (1960), and after the rationality of the approach had been recognized, several researchers developed a number of computer programs. For example, the Texas Department of Highways supported research at the Texas Transportation Institute (TTI) in an attempt to determine driving stresses and reduce concrete pile damage by using a realistic analysis method. FHWA sponsored the development of both the TTI program (Hirsch, *et al.*, 1976) and WEAP (Goble and Rausche, 1976). FHWA supported the development of WEAP to obtain analysis results backed by measurements taken on construction piles during installation for a variety of hammer models. WEAP was updated several times under FHWA sponsorship until 1986 (Goble and Rausche, 1986). Later, additional options, improved data files, refined mathematical representations and modern user conveniences were added to this program on a proprietary basis, and the program is now known as GRLWEAP (Pile Dynamics, Inc. 2005). TNOWAVE is a similar program developed in the Netherlands since 1970s and is popular in Europe and elsewhere. Similar computer programs based on the method of characteristics have been developed such as PDPWAVE (Bielefeld and Middendorp, 1992).

The wave equation approach has been subjected to a number of checks and correlation studies. Studies on the performance of WEAP have produced publications demonstrating that program's performance and utility (e.g., Blendy 1979, Soares, *et al.* 1984, Rausche, *et al.*, 2004). In the WEA approach, it is recognized that each element in the hammer-pile-soil system affects the pile penetration and stresses caused in the pile. A few characteristics of each element are discussed below before the WEA methodology is discussed in detail.

## **1. Hammer**

- Pile hammers can be categorized into two main types: impact hammers and vibratory hammers. There are numerous types of impact hammers having variations in the types of power source, configurations, and rated energies.
- Mechanical efficiency determines what percentage of rated energy is transmitted by the ram. Typical values of mechanical efficiency for hammers in good condition are 50% for double or differential acting air hammers, 67% for single acting air/steam hammers, 80% for diesel hammers, and 80 to 95% for hydraulic hammers.

- Force wave shape characteristics are different for different hammer types. The shape affects pile stress and pile penetration.

## **2. Pile and Appurtenances (Cushions, Helmets, etc.)**

- The stiffness of appurtenances such as the hammer cushion is defined by the cross sectional area times the modulus of elasticity divided by the thickness. The stiffness has a major effect on both blow count and stress transfer to the pile. These elements must not degrade during driving as observed blow count will decrease and pile stresses increase.
- As noted in Section 9.9.2.1, pile impedance affects pile driveability. The cross sectional area of the pile does not control pile driveability. As an example, an HP 14x117 has a cross-sectional area of 34.4 in<sup>2</sup> (0.22 m<sup>2</sup>) and an impedance of 61.4 k-s/ft (900 kN-s/m). A 12 in square concrete pile has a cross-sectional area of 144 in<sup>2</sup> (0.93 m<sup>2</sup>) and an impedance of 57.9 k-s/ft (845 kN-s/m). Hence, the H pile has better driveability even though it has approximately 25% of the cross-sectional area of the concrete pile.

## **3. Soil**

- Soil strength may be permanently or temporarily changed during driving. Piles being driven into soil that contains large percentages of fines may require restrikes to estimate long term capacity due to effects of set-up or relaxation.
- The damping properties of the soil surrounding the pile can have a dramatic effect on the observed blow count. An increase in damping decreases driveability. Damping parameters can be estimated by soil type or from basic index test data. Consideration of the dynamic aspects of the field pile driving operation is necessary so that the driving characteristics can be related to the static pile capacity. Foundation designers should routinely consider the potential for dynamic effects such as set-up and include provisions for field observations such as restrikes. In addition, construction control of pile driving should account for basic dynamic parameters that influence blow count and pile stress. Some of these parameters can be controlled by specification; others require use of a pile wave equation analysis.

### 9.9.6 Wave Equation Methodology

The wave equation analysis (WEA) is a tool to understand the variable involved in pile driving. In a WEA, the hammer, helmet, and pile are modeled by a series of segments each consisting of a concentrated mass and a weightless spring. A schematic of the wave equation hammer-pile-soil model is presented in Figure 9-41. The hammer and pile segments are approximately 3 ft in length. Spring stiffness and mass values are calculated from the cross sectional area, modulus of elasticity, and specific weight of the corresponding pile section. Hammer and pile cushions are represented by additional springs whose stiffnesses are calculated from area, modulus of elasticity, and thickness of the cushion materials. In addition, coefficients of restitution (COR) are usually specified to model energy losses in cushion materials and in all segments that can separate from their neighboring segments by a certain slack distance. The COR is equal to unity for a perfectly elastic collision that preserves all energy and is equal to zero for a perfectly plastic condition that loses all deformation energy. The usual condition of partially elastic collisions is modeled with an intermediate COR value.

The soil resistance along the embedded portion of the pile and at the pile toe is represented by both static and dynamic components. Therefore, both a static and a dynamic soil resistance force acts on every embedded pile segment. The static soil resistance forces are modeled by elasto-plastic springs and the dynamic soil resistance by dashpots. The displacement at which the soil changes from elastic to plastic behavior is referred to as the soil "quake,"  $q$ . The dynamic soil resistance is proportional to a damping factor,  $J$ , times the pile velocity times the assigned static soil resistance. The parameters  $q$  and  $J$  are shown in lower left hand corner of Figure 9-41. In simple terms,  $q$ , is a parameter used in determination of static resistance while  $J$  is a parameter used in determination of dynamic resistance.

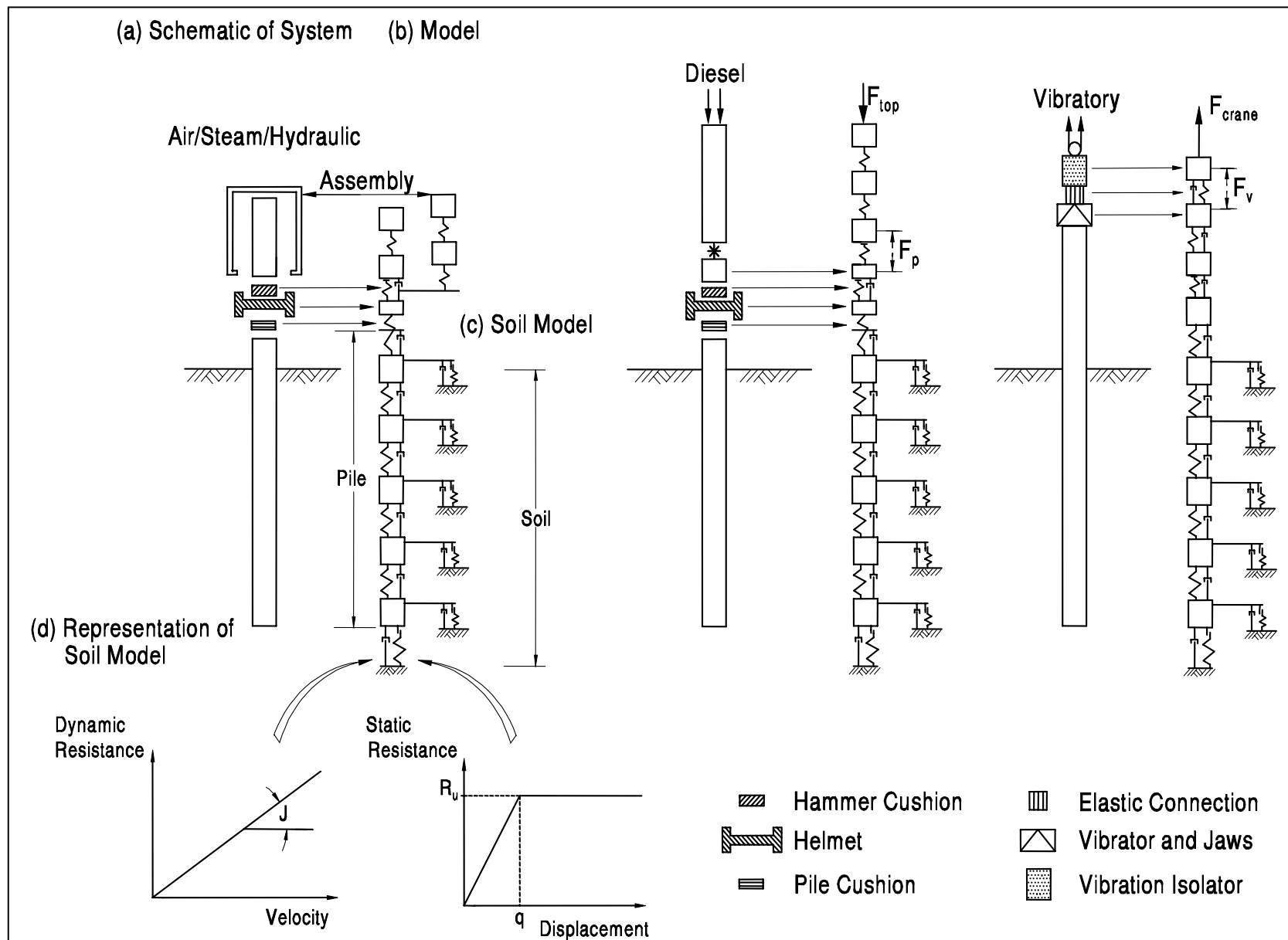


Figure 9-41. Typical Wave Equation models (FHWA 2006a).

### 9.9.6.1 Input to Wave Equation Analysis

In a typical wave equation analysis, parameters defining the hammer, pile (plus appurtenances), and soil systems are needed. The confidence level that can be assigned to the output is directly related to how well the project-specific input parameters are known. The basic input parameters are discussed below.

- **Hammer Data:** Hammer input properties are usually well known from a manufacturers' database. In a driveability analysis, hammer types are selected based on the soil resistance to be overcome. In construction monitoring analysis the contractor submits the intended driving system for review and approval. If a satisfactory driving system is submitted and approved, then the only major concern in construction is that the hammer is in good working condition as was assumed for the input.
- **Driving System or Appurtenance Data:** The driving system or appurtenance data consists of information on hammer cushion, helmet including striker plate, inserts, adapters, etc. and pile cushion in case of concrete piles. The properties of cushions, for both hammer and pile, are especially critical. Only manufactured materials whose properties remain reasonably constant during driving can be used with confidence. The actual cushion thickness used in the field must be checked and discrepancies reported so that the wave equation analysis can be modified.
- **Pile Data:** Required pile data consists of total length, cross-sectional area, elastic modulus and weight, all as a function of depth. This is the pile profile. *The wave analysis cannot predict pile length.* This fact is commonly misunderstood by engineers. Pile length is determined by static analysis procedures and then used as input to pile wave analyses. One exception is a "driveability analysis" where pile behavior is assessed at various depths. The cross sectional area of the pile is frequently varied in design analyses to determine which section is both driveable and cost effective. Increasing the pile section has the effect of improving driveability as well as reducing pile stresses.
- **Soil Data:** Soil data input requires both an understanding of site-specific soil properties and the effects of pile driving on those properties. Dynamic properties such as damping and quake are roughly correlated with soil type. These properties are best determined by experienced geotechnical specialist. The driving soil resistance and its distribution are determined from the static analysis. The driving soil resistance may be substantially greater than the design load times the safety factor; particularly for piles in scour situations. Also the dynamic effects of pile driving on soil resistance must be

considered by an experienced geotechnical specialist to determine set-up or relaxation values for ultimate soil resistance. These dynamic effects are frequently overlooked, which can result in large variations between estimated and actual pile lengths.

### 9.9.6.2 Output Values from Wave Equation Analysis

The results of a wave equation analysis include the predicted blow count, pile stresses, and delivered hammer energy for an assigned driving soil resistance,  $R_{ult}$ , and for given hammer, driving system (appurtenance), pile and soil conditions. **Each wave equation analysis is for the specific pile length that was considered in the analysis.** A summary table of the results obtained from a wave equation analysis is shown in Table 9-10. The data shown in Table 9-10 was generated for a specific site where a pile length of 50 ft (15 m) was being analyzed.

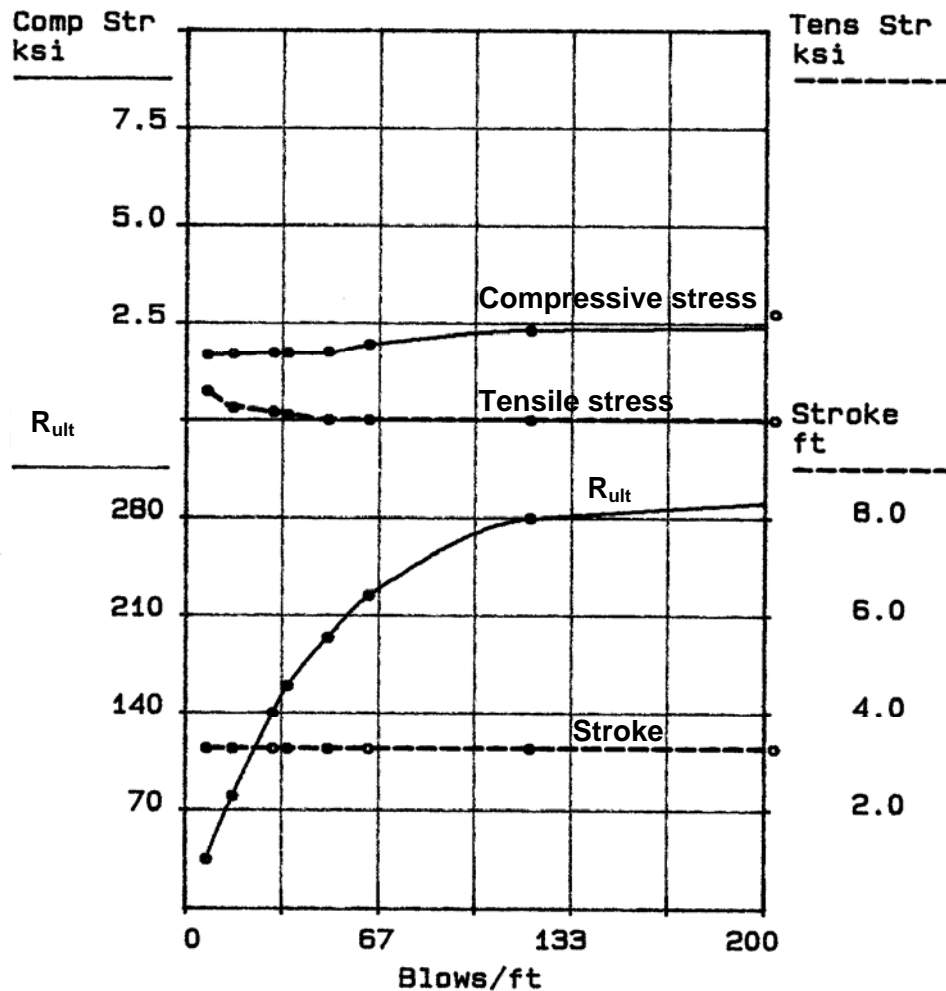
**Table 9-10**  
**Summary of example results from wave equation analysis**

$R_{ult}$ kips	Blow Count BPF	Stroke (EQ) ft	Tensile Stress ksi	Compressive Stress ksi	Transfer Energy ft-kip
35.0	7	3.27	-0.73	1.68	13.6
80.0	16	3.27	-0.32	1.71	13.6
140.0	30	3.27	-0.20	1.73	13.0
160.0	35	3.27	-0.14	1.73	13.0
195.0	49	3.27	-0.00	1.75	12.8
225.0	63	3.27	0.0	1.96	12.7
280.0	119	3.27	0.0	2.34	12.6
350.0	841	3.27	0.0	2.75	12.5

Note that for each driving resistance ( $R_{ult}$ ), a value of blow count, hammer stroke, tensile stress, compressive stress, and transferred energy has been computed. The data is also commonly shown in graphical form as noted in Figure 9-42.

### 9.9.6.3 Pile Wave Equation Analysis Interpretation

The data in Table 9-10, when plotted as shown in Figure 9-42, presents the predicted relationship between pile hammer blow count and other variables for the situation when the pile is embedded 50 ft (15 m) in the ground. The plot, which relates the ultimate capacity to penetration resistance, is known as a **bearing graph**. The data in Table 9-10 is interpreted in the field by comparing them with the measured blow count at a pile penetration of 50 ft (15 m) as follows. When the pile reaches 50 ft (15 m), if the blow count is 49, the driving resistance is 195 kips (867 kN), the stroke is 3.27 ft (0.99 m), the tensile stress is zero ksi, the compressive stress is 1.75 ksi (12,069 kPa), and transferred energy is 12.8 ft-kips (17.3 m-kN). If the blow count had been 63 the driving resistance would have been predicted to be 225 kips (1,000 kN), etc.



**WAVE EQUATION BEARING GRAPH**

**Figure 9-42. Summary of stroke, compressive stress, tensile stress, and driving capacity vs. blow count (blows/ft) for air-steam hammer.**

Note that Table 9-10 is an example for an air-steam hammer and the stroke is constant for all blow counts. Diesel hammers operate at different strokes depending on the pile-soil properties. A pile wave summary table for a diesel hammer will display a predicted combination of blow count and stroke that is necessary to achieve the driving capacity. In fact, there are numerous combinations of blow count and stroke that correspond to a particular driving resistance. These combinations may be computed and plotted for a selected driving resistance. A typical plot of diesel hammer stroke versus blow count is shown in Figure 9-43 for a constant resistance of 240 kips (1,067 kN).

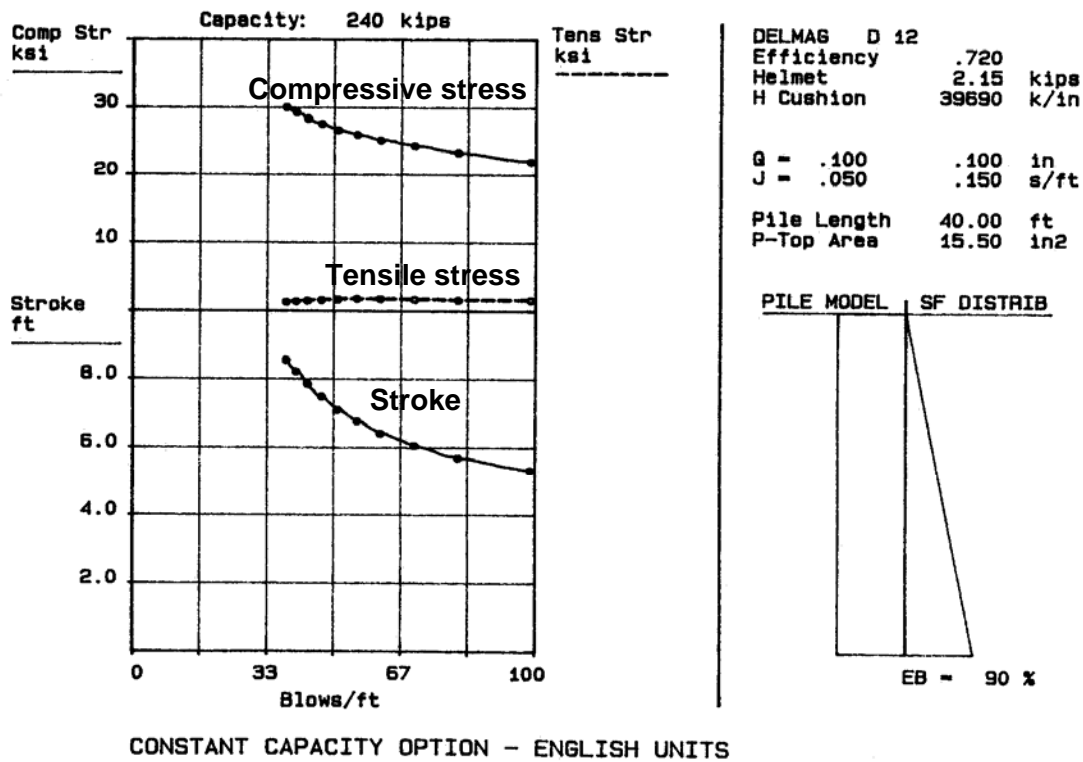


Figure 9-43. Graph of diesel hammer stroke versus blow count for a constant pile capacity.

A wave equation bearing graph is substantially different from a similar graph generated from a dynamic formula. The wave equation bearing graph is associated with a single driving system, hammer stroke, pile type, soil profile, and a particular pile length. If any one of the above items is changed, the bearing graph will also change.

### 9.9.7 Driving Stresses

In almost all cases, the highest stress levels occur in a pile during driving. High driving stresses are necessary to cause pile penetration. The pile must be stressed to overcome the ultimate soil resistance, plus any dynamic resistance forces, in order to be driven to the design depth and load. The high strain rate and temporary nature of the loading during pile driving allow a substantially higher driving stress limitation than for the static design case. Wave equation analyses can be used for predicting driving stresses prior to installation. During installation, dynamic testing can be used to monitor driving stresses.

The stresses predicted by the wave equation analysis should be compared to safe stress levels. This comparison is usually performed for the tensile and compressive stress shown at the computed driving resistance for the estimated pile length. Table 9-11 presents a summary of design and driving stresses for various types of driven piles.

### 9.9.8 Guidelines for Assessing Pile Driveability

The last operation in pile design is to insure that the pile can be driven to the estimated length without damage. For this purpose a trial wave equation analysis is done with an appropriately sized hammer. Figure 9-44 can be used to choose a reasonable hammer for wave analysis. In general, the suggested hammer energies in Figure 9-44 are less than the optimum energy necessary to drive the appropriate pile cross section. Judgment should be used in selecting the hammer size. If initial wave equation analysis yield high blow counts and low stresses the hammer size should be increased.

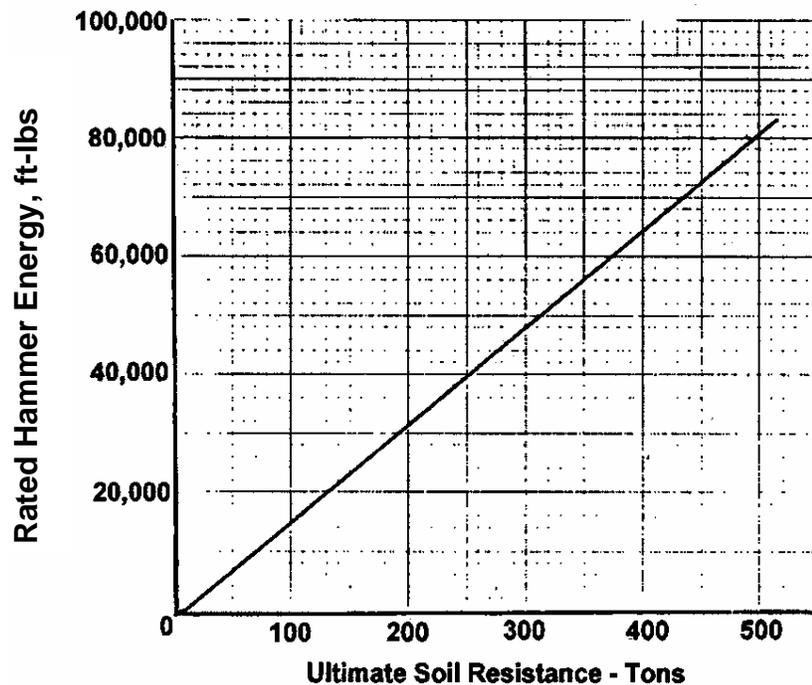


Figure 9-44. Suggested trial hammer energy for wave equation analysis.

During design, a wave equation analysis should be performed to determine if a reasonable range of hammer energies can drive the proposed pile section without exceeding the allowable driving stresses listed in Table 9-11 and a reasonable range of hammer blows, i.e., 30 to 144 bpf for friction piles and higher blows of short duration for end bearing piles. This concept is illustrated numerically by Example 9-4.



**Example 9-4:** Determine if the 14 inch square concrete pile can be driven to a driving capacity of 225 kips by using the wave equation output summary provided. Assume the concrete compressive strength,  $f_c$ , is 4000 psi and the pile prestress,  $f_{pe}$ , is 700 psi.

**Wave equation output summary**

<b>R<sub>ult</sub> kips</b>	<b>Blow Count BPF</b>	<b>Stroke (EQ) ft</b>	<b>Tensile Stress ksi</b>	<b>Compressive Stress ksi</b>	<b>Transfer Energy ft-kip</b>
35.0	7	3.27	-0.73	1.68	13.6
80.0	16	3.27	-0.32	1.71	13.6
140.0	30	3.27	-0.20	1.73	13.0
160.0	35	3.27	-0.14	1.73	13.0
195.0	49	3.27	-0.00	1.75	12.8
225.0	63	3.27	0.0	1.96	12.7
280.0	119	3.27	0.0	2.34	12.6
350.0	841	3.27	0.0	2.75	12.5

**Solution:**

Acceptable driveability depends on achieving the desired driving capacity at hammer blows between 30 and 144 bpf without exceeding the allowable compressive and tensile driving stress.

1. At  $R_{ult} = 225$  kips, blow count = 63 bpf                      O.K.(between 30 and 144)
2. The allowable driving stresses based on Table 9-11, for prestressed precast concrete piles are calculated as follows:
  - Compressive stress allowed =  $0.85 f_c - f_{pe} = 0.85 (4,000 \text{ psi}) - 700 \text{ psi} = 2,700 \text{ psi}$ ,
  - Actual maximum compressive stress up to 225 kips from wave equation output summary is 1.96 ksi or 1,960 psi  $\leq 2,700$  psi allowed value.      O.K.
  - Tensile stress allowed =  $3 (f_c)^{1/2} + f_{pe} = 3 (4,000 \text{ psi})^{1/2} + 700 \text{ psi} = 890 \text{ psi}$
  - Actual maximum tensile stress up to 225 kips from wave equation output summary is 0.730 ksi or 730 psi  $\leq 890$  psi allowed value.      O.K.

Therefore, the analyzed pile-hammer system can be approved.

### 9.9.9 Pile Construction Monitoring Considerations

The approval of a contractor's driving equipment is an example of design and construction coordination. It is recommended to use the wave equation analysis to determine if the contractor's equipment is adequate to drive the pile to the estimated length without pile damage. The steps in this procedure are as follows:

1. The pile specifications should include a statement similar to:

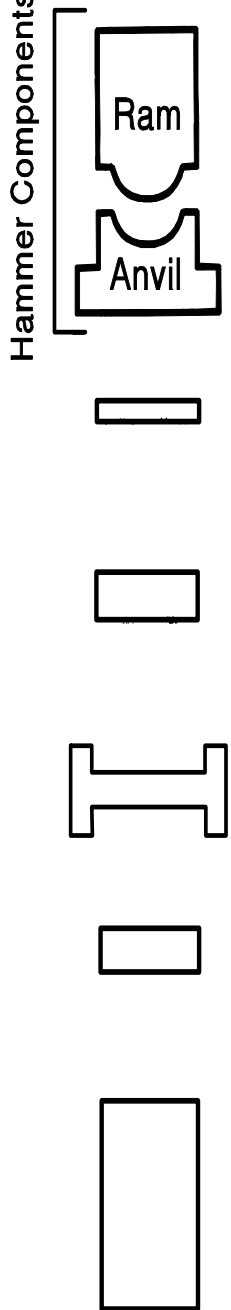
"All pile driving equipment to be furnished by the contractor shall be subject to the approval of the engineer. Prerequisite to such approval, the contractor shall submit the following:

- a. A completed pile and driving equipment data form (Figure 9-45) for each hammer proposed for the project.
- b. A wave equation analysis performed by a professional engineer for each proposed hammer at least to the soil resistance value listed on the plans.

Contractor notification of acceptance or rejection of the hammer will be made within 14 days of receipt of the data form and wave equation analysis."

In this case the contractor is charged with performing the wave equation analysis. In some cases, the owner may perform the analysis.

2. The designer should also receive a copy of the data form and the results of wave equation analysis. An independent wave equation analysis should be performed to verify the submitted results and in some cases to establish driving criteria for the piles. The designer should check the results for reasonableness. For example, 30 to 144 blows per foot are considered reasonable for friction piles. Greater blow counts can be permitted for end bearing piles since the duration of high blow counts is short. Then the stresses at that blow count are checked to determine if the values are below the allowable driving stress of the pile material. If these items are satisfied, the equipment can be approved and the information sent to the construction engineer. The results of the wave equation analysis may be transmitted to the field with a recommendation to reject or approve the hammer.
3. The procedure for the changing of approved hammers during the contract is the same.

Contract No.: _____ Project: _____ County: _____	Structure Name and/or No.: _____ Pile Driving Contractor or Subcontractor: _____ _____ (Piles driven by)
<div style="writing-mode: vertical-rl; transform: rotate(180deg); font-weight: bold;">Hammer Components</div> 	Manufacturer: _____ Model No.: _____ Hammer Type: _____ Serial No.: _____ Manufacturers Maximum Rated Energy: _____ (Joules) (ft-k) Stroke at Maximum Rated Energy: _____ (meters) (ft) Range in Operating Energy: _____ to _____ (Joules) (ft-k) Range in Operating Stroke: _____ to _____ (meters) (ft) Ram Weight: _____ (kips) (kN) Modifications: _____ _____ _____
	<b>Hammer</b>
	<b>Striker Plate</b> Weight: _____ (kips) (kN) Diameter: _____ (in) (mm) Thickness: _____ (in) (mm)
	<b>Hammer Cushion</b> Material #1 _____ Material #2 _____ (for Composite Cushion) Name: _____ Name: _____ Area: _____ (in <sup>2</sup> ) (cm <sup>2</sup> ) Area: _____ (in <sup>2</sup> ) (mm <sup>2</sup> ) Thickness/Plate: _____ (in) (mm) Thickness/Plate: _____ (in) (mm) No. of Plates: _____ No. of Plates: _____ Total Thickness of Hammer Cushion: _____ (in) (mm)
	<b>Helmet (Drive Head)</b> Weight: _____ including inserts (kips) (kN)
<b>Pile Cushion</b> Material: _____ Area: _____ (in <sup>2</sup> ) (cm <sup>2</sup> ) Thickness/Sheet: _____ (in) (mm) No. of Sheets: _____ Total Thickness of Pile Cushion: _____ (in) (mm)	
<b>Pile</b> Pile Type: _____ Wall Thickness: _____ (in) (mm) Taper: _____ Cross Sectional Area: _____ (in <sup>2</sup> ) (mm <sup>2</sup> ) Weight/ft (m): _____ Ordered Length: _____ (ft) (m) Design Load: _____ (kips) (kN) Ultimate Pile Capacity: _____ (kips) (kN) Description of Splice: _____ _____ Driving Shoe/Closure Plate Description: _____ _____ Submitted By: _____ Date: _____ Telephone No.: _____ Fax No.: _____	

**Figure 9-45. Pile and driving equipment data form (after FHWA, 2006a).**

During production operations, the engineer will check if the necessary blow count is attained at the estimated length shown on the pile driving information form. The resistance is generally acceptable if the blow count is within 10 percent of that expected, or if the expected blow count is achieved within 5 ft (1.5 m) of the estimated length. The construction engineer should be aware that blow counts greater than expected will cause an increase in pile stress. If necessary an upper blow count limit may need to be established to prevent damage.

If either radically different blow counts (greater or less) than those predicted from wave equation analysis or damage are observed during the driving process, the foundation designer should be contacted immediately. The phone number of the foundation designer should be on the information form.

It should be realized that pile driving is not by any means an exact science and actual blow counts and pile lengths may be expected to vary somewhat even in the same footing. The objective of construction monitoring of pile driving is to ensure that the pile is capable of supporting the design load safely. This means that the pile is not damaged and adequate soil resistance is mobilized for support. Both these items can be checked from the wave equation analysis output.

The use of wave equation analysis for construction monitoring provides the engineer with a method to predict the behavior of the driven piles during installation. While this prediction is superior to previous methods of estimating driveability, the optimal method of determining pile driveability is to obtain dynamic measurements during pile installation. Dynamic test methods commonly employ accelerometers and strain gages attached to the pile during driving to measure real time strains and accelerations produced during the driving process. Field computers use these measurements to develop driving variables, which the inspector can use to:

- Monitor hammer and driving system performance,
- Evaluate driving stresses and pile integrity, and,
- Verify pile capacity

Additional details of the dynamic test procedure are discussed in the following section.

#### **9.9.10 Dynamic Pile Monitoring**

Dynamic test methods use measurements of strain and acceleration taken near the pile head as a pile is driven or restruck with a pile driving hammer. These dynamic measurements can be used to evaluate the performance of the pile driving system, calculate pile installation stresses, assess pile integrity, and estimate static pile capacity. Dynamic test results can be further evaluated by

using signal matching techniques to determine the relative distribution of soil resistance along the pile, as well as representative dynamic soil properties for use in wave equation analyses. This section provides a brief discussion of the equipment and methods of analysis associated with dynamic measurements.

A typical dynamic monitoring system consists of a minimum of two strain transducers and two accelerometers bolted to diametrically opposite sides of the pile to monitor strain and acceleration and account for nonuniform hammer impacts and pile bending. Because of nonuniform impacts and bending, the use of two diametrically opposite mounted strain transducers is essential for a valid test. The reusable strain transducers and accelerometers are generally attached two to three diameters below the pile head. Almost any driven pile type (concrete, steel pipe, H, Monotube, timber, etc.) can be tested with the pile preparation for each pile type varying slightly.

As the pile is struck by a pile hammer, the strains and accelerations detected by the corresponding gages on the pile are converted into forces and velocities. Typical force and velocity traces generated during dynamic measurements are shown in Figure 9-46. These traces are processed to obtain an estimate of the static pile capacity at the time of testing and for pile design. The additional information obtained and displayed includes compressive and tensile stresses in the pile, transferred energy to the pile, and the force and velocity at the top of the pile throughout the duration of the hammer impact. An experienced operator can use this data to evaluate the performance of the pile driving system and the condition of the pile. The results of the dynamic monitoring are enhanced by the post-testing evaluation in which signal matching is used with computer analysis to verify the correctness of assumed dynamic inputs including damping, quake and load transfer distribution.

ASTM D 4945 contains a detailed description of the equipment requirements and test procedure for dynamic pile load testing.

#### **9.9.10.1 Applications**

Dynamic pile monitoring costs much less and requires less time than static pile load testing. Important information can be obtained regarding the behavior of both the pile-soil system and the pile driving system that is not available from a static pile load test. Determination of driving stresses and pile integrity with dynamic test methods has facilitated the use of fewer, higher capacity piles in foundations through better pile installation control. Some of the applications of dynamic pile testing are discussed below (FHWA, 2006a).

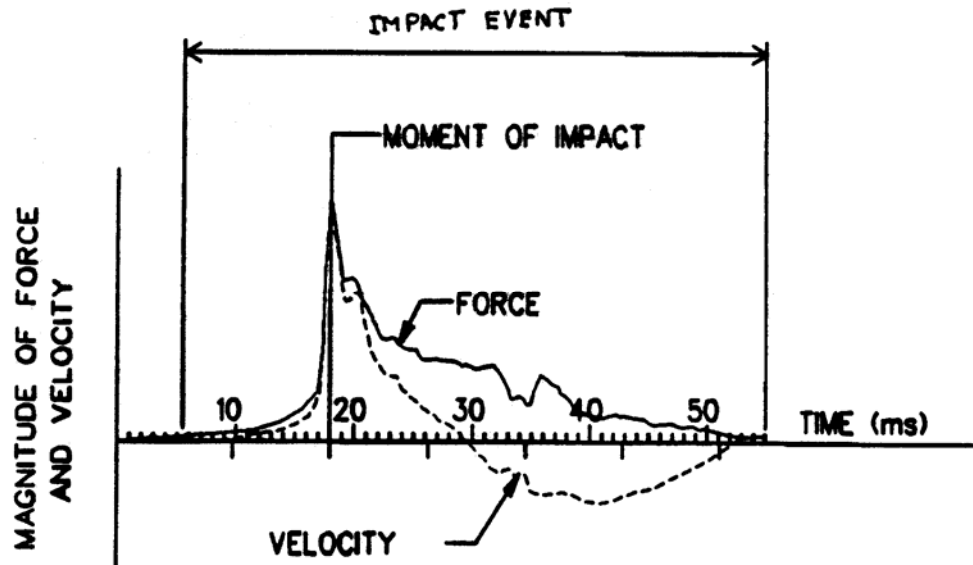


Figure 9-46. Typical force and velocity traces generated during dynamic measurements.

- **Static Pile Capacity**

- a. Evaluation of static pile capacity at the time of testing. Soil setup or relaxation potential can be also assessed by restriking several piles and comparing restrike capacities with end-of-initial driving capacities.
- b. Assessments of static pile capacity versus pile penetration depth can be obtained by testing from the start to the end of driving. This can be helpful in profiling the depth to the bearing stratum and thus the required pile lengths.
- c. Signal matching computer analysis can provide refined estimates of static capacity, assessment of soil resistance distribution, and soil quake and damping parameters for input into a wave equation analysis.

- **Hammer and Driving System Performance**

- a. Calculation of energy transferred to the pile for comparison with the manufacturer's rated energy and wave equation predictions which indicate hammer and drive system performance. Energy transfer can also be used to determine effects of changes in hammer cushion or pile cushion materials on pile driving resistance.

- b. Determination of drive system performance under different operating pressures, strokes, or changes in hammer maintenance by comparative testing of hammers, or of a single hammer over an extended period of use.
- c. Identification of hammer performance problems, such as preignition problems with diesel hammers or preadmission problems in air/steam hammers.
- d. Determination of whether soil behavior or hammer performance is responsible for changes in observed driving resistances.

- **Driving Stresses and Pile Integrity**

- a. Calculation of compression and tension driving stresses. In cases with driving stress problems, this information can be helpful when evaluating adjustments to pile installation procedures are being evaluated. Calculated stresses can also be compared to specified driving stress limits.
- b. Determination of the extent and location of pile structural damage. With dynamic pile monitoring costly extraction may not be necessary to confirm or quantify damage suspected from driving records.
- c. Stress distribution throughout pile by using signal matching computer analysis.

#### **9.9.10.2 Interpretation of Results and Correlation with Static Pile Load Tests**

The results of dynamic pile monitoring should be interpreted by an experienced geotechnical specialist who has had the opportunity to observe and evaluate the results from many dynamically test piles and can detect the signs, not always readily apparent, of unusual soil-pile response, pile damage, erratic hammer operation or testing equipment malfunction. It is important that the geotechnical specialist performing the evaluation should have attained an appropriate level of expertise through qualifying examinations by providers of dynamic testing services.

Interpretation of the results of dynamic pile measurements also requires an awareness of the differences in behavior of dynamically and statically loaded piles. Improper correlations of dynamic and static pile loads test may be caused by the following:

- **Incorrectly assumed soil damping, quake and load transfer parameters.** This source of discrepancy can be minimized by performing a post-test computerized analysis to match

measured and computed relationships between force and velocity to determine the most appropriate parameters.

- **Time-related changes in pile capacity.** Depending on soil type and pile characteristics, the capacity of a pile may increase or, less commonly, decrease with time. The principal causes are time-related changes of pore water pressure in cohesive soils and stress relaxation in cohesionless soils. The effects can be assessed by “restriking” the pile at various time intervals after driving and comparing the observed “restrike” capacity to the driving capacity obtained during the initial drive. The pile capacity should be determined during the first few “good” hammer blows during re-strike. When comparing the results of dynamic testing against those of a static pile load test, at least one dynamic test should be performed after completion of static testing.
- **Inadequate pile tip displacement.** Pile tip displacement during dynamic testing may be inadequate to mobilize full end bearing. Frictional resistance between a pile and the surrounding soil is mobilized at a fraction of the pile movement necessary to mobilize full end bearing resistance. A penetration resistance of 10 blows/inch (10 blows/25.4 mm) or higher, may produce insufficient strain in the soil to mobilize full end resistance. This results in an underestimate of the end bearing capacity. For many types of piles, the estimate can be improved by performing a force-velocity match both for the initial drive and for the restrike data. The tip capacity derived from the initial drive is combined with skin resistance from the restrike to obtain the total pile capacity. However, this method may not be applicable for open-ended pipe, H-piles, and precast cylinder piles. In the case of these types of piles, only the structural area of the pile can mobilize the toe bearing during installation. This value of toe bearing may be significantly less than the value that may be experienced in the static load test, since the soil in the static load test will adhere to the pile with time and create a plug.

## **9.10 CAST-IN-PLACE (CIP) PILES**

There are a variety of cast-in-place (CIP) piles as shown in Figure 9-2. In contrast to the driven piles wherein piles manufactured in a factory are driven in the ground, in the case of CIP piles, the load resisting element is constructed in a pre-drilled hole. The load resisting element is often a combination of steel and CIP concrete. As shown previously in Figure 9-2, there are a variety of CIP piles, e.g., drilled shafts, micropiles, auger cast piles, etc.

The design and construction process for CIP piles is shown in Figure 9-47. This process is similar to that for driven piles shown in Figure 9-3 for Blocks 1 to 18. It is in the construction phase where there are major differences between the driven piles and CIP piles. Blocks 19 to 24 are briefly discussed below:

### **Block 19: Review Contractor's Installation Procedures**

The potential that the CIP piles will perform as designed is heavily dependent on the techniques employed by the contractor during construction. For example, soil excavation technique will not be suitable for excavation in IGMs or rocks. The contractor should be required to submit a detailed CIP pile construction procedure that will be reviewed by the geotechnical engineer.

### **Block 20: Set Preliminary Installation Criteria**

Based on the evaluation of the contractor's proposed installation procedures with respect to project installation criteria and any other requirements in the design and specifications, the preliminary approval of the contractor's equipment and procedures can be given. If the contractor's installation procedures are not acceptable, then the process returns to Block 19.

### **Block 21: Install Test Piles and Evaluate Constructability**

Usually, the first CIP pile on a project is considered to be a "test" pile wherein the contractor's proposed equipment and installation procedures are evaluated in the field. Often, where prior experience is not available, the first pile is required to be installed as a sacrificial pile at a location away from the footprint of the production piles. The constructability evaluation of the test pile is critical. Non-destructive (integrity) tests are recommended at this stage to evaluate the quality of the constructed product.

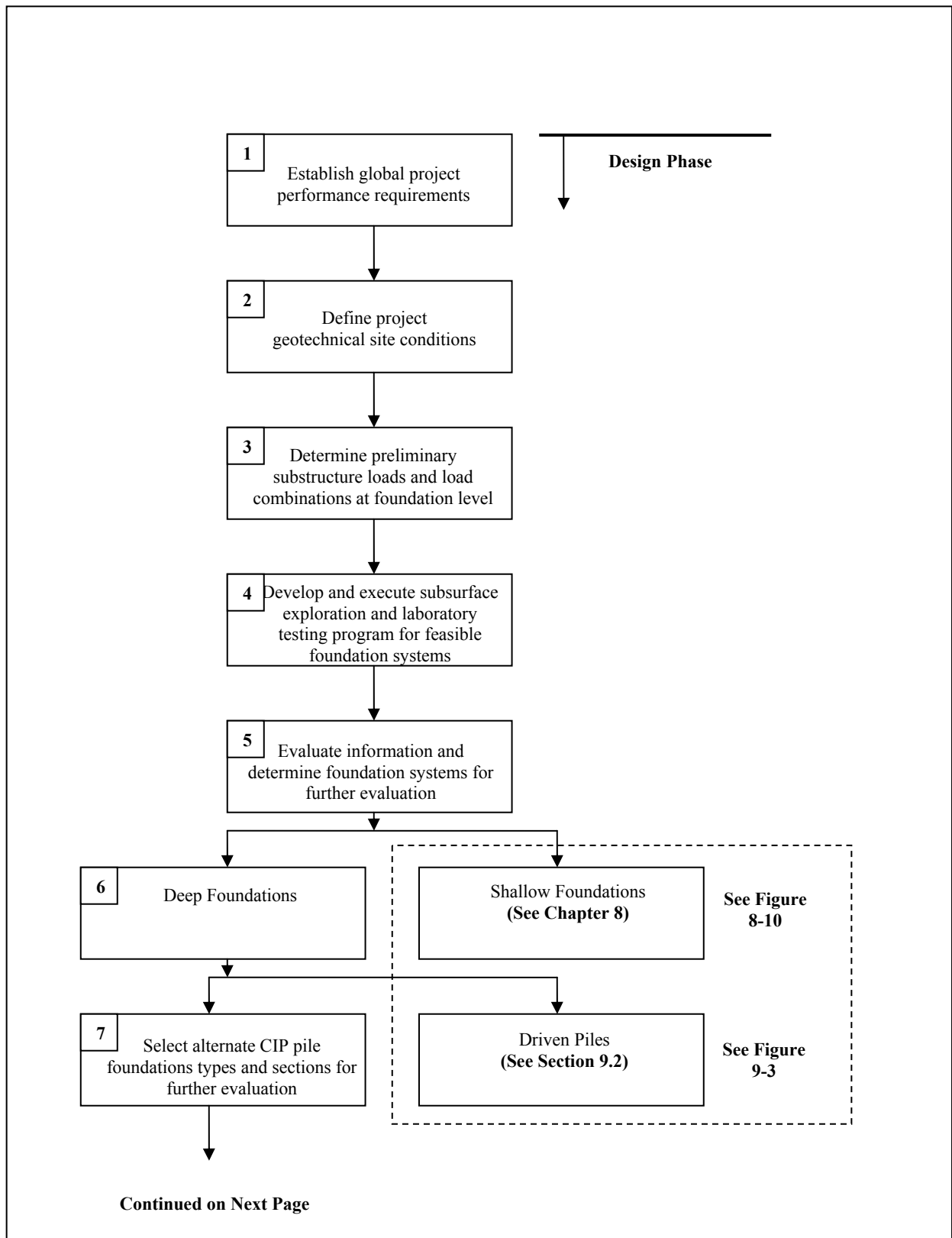


**Figure 9-47. Cast-in-Place (CIP) pile design and construction process (modified after FHWA 2006a).**

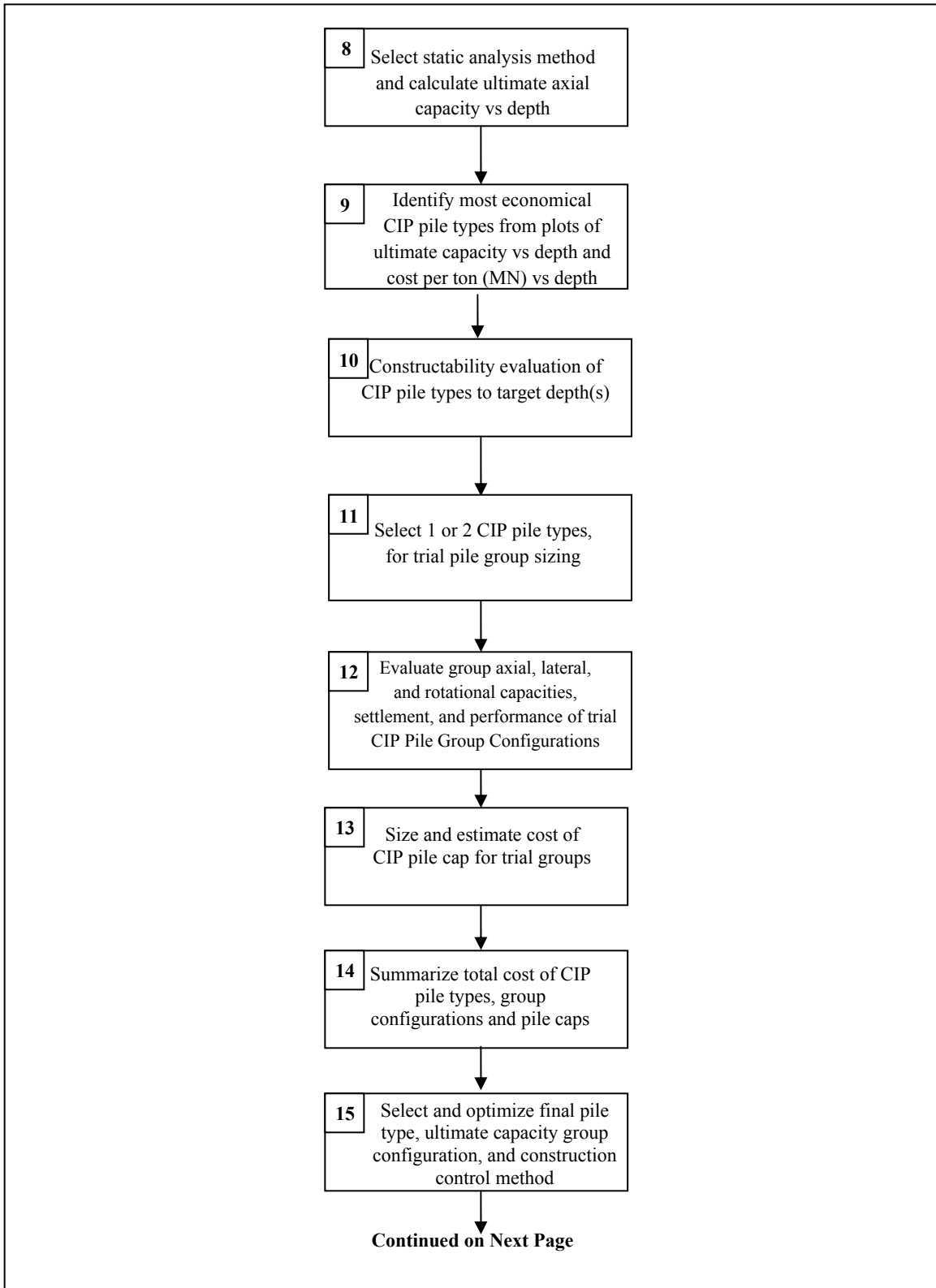


**Figure 9-47 (Continued). Cast-in-Place (CIP) pile design and construction process (modified after FHWA 2006a).**

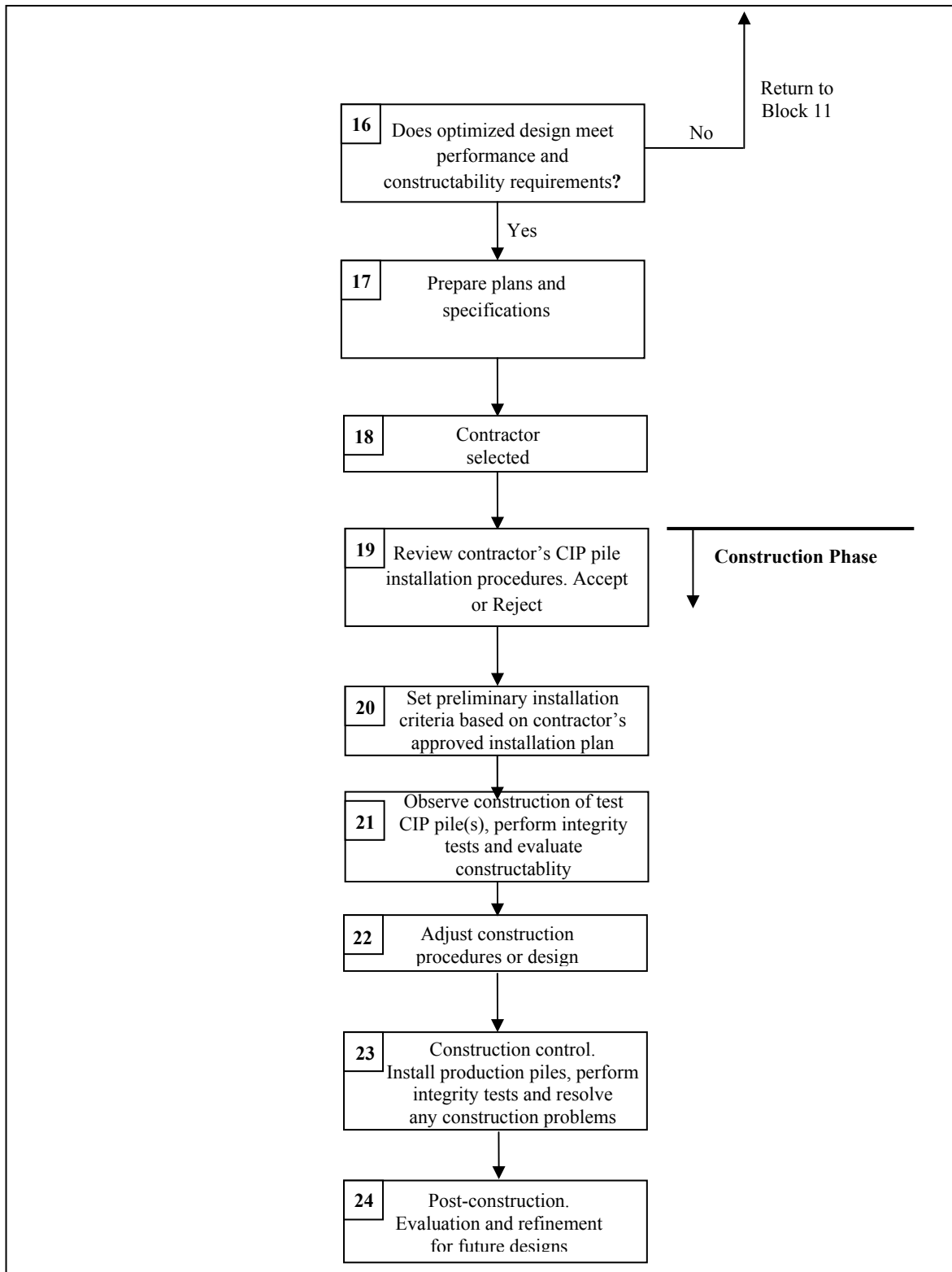


**Figure 9-47 (Continued). Cast-in-Place (CIP) pile design and construction process (modified after FHWA 2006a).**

## **Block 22: Adjust Construction Procedures**

In this step, an adjustment in the contractor's construction procedures may be required prior to construction of the production piles. If significant adjustments are necessary, then another test pile may be warranted.

## **Block 23: Construction Control**

After the test CIP pile has been successfully constructed, the same construction procedures are applied for the production piles unless different subsurface conditions are encountered that may warrant alternative construction techniques. In this case another test pile may be required. Quality control and assurance procedures including integrity tests are implemented as discussed in Section 9.14. Problems may arise and must be handled in a timely fashion as they occur.

## **Block 24: Post-Construction Evaluation and Refinement of Design**

After completion of the foundation construction, the project should be reviewed and evaluated for its effectiveness in satisfying the project requirements and also its cost effectiveness. The evaluation should be performed from the viewpoint of refining the construction and design procedures as appropriate for future projects.

## **9.11 DRILLED SHAFTS**

A drilled shaft is a form of cast-in-place (CIP) pile. A drilled shaft is a machine- and/or hand-excavated shaft in soil or rock that is filled with concrete and reinforcing steel, with the primary purpose of providing structural support. A drilled shaft is usually circular in cross section and may be belled at the base to provide greater bearing area. A typical drilled shaft is shown in Figure 9-48. Other terminology commonly used to describe a drilled shaft includes: drilled pier, drilled caisson, bored pile and cast-in-drilled hole (CIDH). Rectangular drilled shafts are called barrettes.

Vertical load is resisted by the drilled shaft in base bearing and side friction. Horizontal load is resisted by the shaft in horizontal bearing against the surrounding soil or rock.

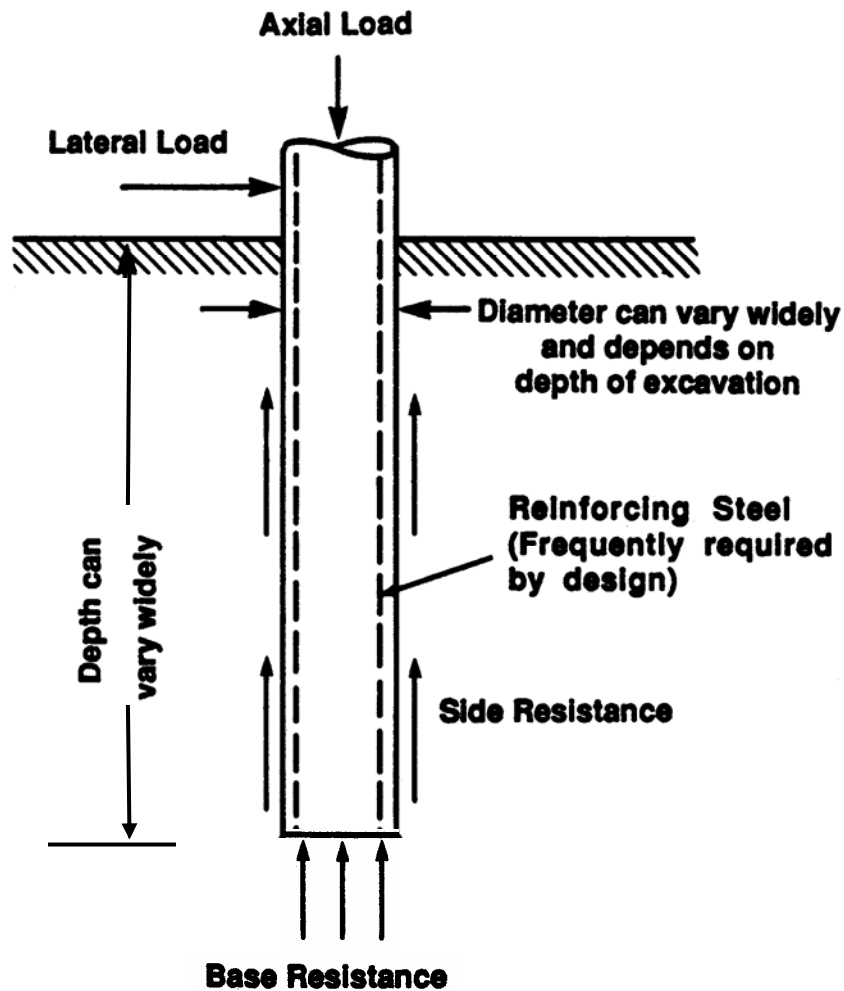


Figure 9-48. A typical drilled shaft and terminology (after FHWA, 1999).

### 9.11.1 Characteristics of Drilled Shafts

The following special features distinguish drilled shafts from driven pile foundations:

1. The drilled shaft is constructed in a drilled hole, unlike the driven pile.
2. Wet concrete is cast and cures directly against the soil in the borehole. Temporary steel casing may be necessary for stabilization of the open hole and may or may not be extracted.
3. The construction method for drilled shafts is adapted to suit the subsurface conditions.

### 9.11.2 Advantages of Drilled Shafts

Following are the advantages of drilled shafts.

- a. Construction equipment is normally mobile and construction can proceed rapidly.
- b. The excavated material and the drilled hole can often be examined to ascertain whether or not the soil conditions at the site agree with the estimated soil profile. For end-bearing situations, the soil beneath the tip of the drilled shaft can be probed for cavities or for weak soil.
- c. Changes in geometry of the drilled shaft may be made during the course of the project if the subsurface conditions so dictate.
- d. The heave and settlement at the ground surface due to installation will normally be very small.
- e. The personnel, equipment, and materials for construction is usually readily available.
- f. The noise level from the equipment is less than for some other methods of construction.
- g. The drilled shaft is applicable to a wide variety of subsurface conditions. For example, it is possible to drill through a layer of cobbles and into hard rock for many feet. It is also possible to drill through frozen ground.
- h. A single drilled shaft can sustain very large loads so that a pile cap may not be needed.
- i. Databases that contain documented load-transfer information are available. These databases allow confident designs of drilled shafts to be made in which load-transfer both in end bearing and in side resistance can be considered.
- j. The shaft occupies less area than the footing and thus can be built closer to railroads, existing structures and constricted areas.
- k. Drilled shafts may be more economical than spread footing construction, especially when the foundation support layer is deeper than 10' below the ground or at water crossings.

### **9.11.2.1 Special Considerations for Drilled Shafts**

- a. Construction procedures are critical to the quality of the drilled shaft. Knowledgeable inspection is required.
- b. Drilled shafts are not normally used in deep deposits of soft clay or in situations where artesian pressures exist.
- c. Static load tests to verify the ultimate capacity of large diameter shafts are very costly.

### **9.11.3 Subsurface Conditions and Their Effect on Drilled Shafts**

Subsurface investigation for drilled shaft designs must include an assessment of the potential methods of shaft construction as well as a determination of soil properties. The standard method for obtaining soil characteristics is similar to pile foundations and involves laboratory testing of undisturbed samples and the use of in situ techniques including the standard penetration test. Constructability is difficult to assess from routine geotechnical investigations. Critical items such as hole caving, dewatering, rock drilling and obstructions can best be examined by drilling a full diameter test shaft hole during the exploration or design phase of the project. These test holes are usually done by local drilled shaft contractors under a short form contract. Prospective bidders should be invited to observe the construction of the test hole. A detailed log should be made of the test hole including items such as type of drilling rig, rate of drilling, type of drill tools and augers used, etc. Such information should be made available for bidders.

#### **Subsurface Conditions Affecting Construction**

- a. The stability of the subsurface soils against caving or collapse when the excavation is made will determine whether or not a casing is necessary. The dry method of construction can be used only where the soils will not cave or collapse. The casing method must be used if there is danger of caving or collapse.
- b. The existence of groundwater at the site must be determined and what rate of flow can be expected into a shaft excavation. This knowledge will permit selection of appropriate slurry type and dosage to support the sides and the bottom of the shaft during drilling and subsequent placement of reinforcing cage and concrete. The groundwater can be regional groundwater or perched water.
- c. Any artesian water conditions must be clearly identified in the contract documents. Artesian water flowing could spoil the concrete placement, or cause collapse or

heaving at the excavation. Flowing water can create similar problems during concrete placement as it can leach the cement grout out of the concrete mix. Conventional slurry-assisted drilling alone may not be adequate in cases where artesian pressure is encountered and casing may be required.

- d. The presence of cobbles or boulders can cause difficulties in drilling. It is sometimes not easy to extract large pieces of rock, especially with smaller diameter shafts.
- e. The presence of existing foundations or structures.
- f. The presence of landfill that could contain material that cannot be easily excavated, such as an old car body.
- g. The presence of rock may require more sophisticated drilling methods.
- h. The presence of a weak stratum just below the base of the drilled shaft. For this situation drilling may have to be extended below the weak stratum.

## **9.12 ESTIMATING AXIAL CAPACITY OF DRILLED SHAFTS**

The procedures for estimation of drilled shaft capacity have improved significantly over the past decade. The major reason for this improvement is a database that has been developed on load transfer in skin friction and in end bearing based on load tests in a broad range of geomaterials. It is now well established that drilled shafts can carry a substantial portion of applied loads in skin friction. As with pile foundations, the ultimate skin friction is mobilized at a relatively small downward movement of the shaft relative to the soil. End bearing resistance is developed in relation to the amount of deflection at the tip.

Separate analyses are required to determine skin friction and end bearing contributions in different soil types and rock. Details of these analyses can be found in FHWA (1999). The basic formulation for drilled shaft capacity in soils and rocks, excerpted from FHWA (1999), is presented herein. The discussions in this manual regarding drilled shaft axial capacity are limited to drilled shafts of uniform cross-section, with vertical alignment, concentric axial loading, and a relatively horizontal ground surface. The reader is referred to FHWA (1999) for procedures to incorporate the effects of enlarged base, group action, and sloping ground.

The ultimate axial capacity ( $Q_{ult}$ ) of the drilled shaft is determined as follows for compression and uplift loading, respectively:

$$Q_u = Q_s + Q_t - W \quad 9-34a$$

$$Q_u \leq 0.7Q_s + W \quad 9-34b$$

where:  $Q_u$  = total ultimate axial capacity of the foundation  
 $Q_s$  = ultimate skin (side) capacity  
 $Q_t$  = ultimate tip (base or end) capacity  
 $W$  = weight of the shaft.

Note that in contra-distinction to the ultimate capacity equation for driven piles (see Equation 9-1), the weight term is included for the drilled shaft since the weight of a shaft is usually much larger than that of a pile. The shaft weight can therefore act as a load in the downward direction or act as a resistance in uplift.

Similar to the driven piles, the **allowable geotechnical soil resistance**,  $Q_a$ , is determined as follows:

$$Q_a = \frac{Q_u}{FS} \quad 9-35$$

where FS = factor of safety which typically varies between 2 to 3. If load tests are not performed then the shaft should be designed for a minimum factor of safety of 2.5 (AASHTO, 2002). This minimum recommended factor of safety is based on an assumed normal level of field quality control during shaft construction as per the requirements of FHWA (2002d). If a normal level of field quality control as required by FHWA (2002d) cannot be assured, larger minimum factors of safety such as 3.0 are recommended. If a site-specific load test is performed, consideration may be given to reducing the factor of safety from 2.5 to 2.0.

Shafts in cohesive soils may be designed by total and effective stress methods of analysis, for undrained and drained conditions, respectively. Shafts in cohesionless soils should be designed by effective stress methods of analysis for drained loading conditions. Formulations for both cohesive and cohesionless soils using allowable stress design (ASD) are presented herein based FHWA (1999) and AASHTO (2002). For LRFD based formulations the reader is referred to AASHTO (2004 with 2006 Interims).

### 9.12.1 Side Resistance in Cohesive Soil

For cylindrical shafts in cohesive soils loaded under undrained loading conditions, the **ultimate side resistance** may be estimated by using the following expression:

$$Q_s = \pi D \sum_{i=1}^N \alpha_i s_{ui} \Delta z_i \quad 9-36$$

Where,  $D$  is the diameter of the shaft and  $\alpha_i$  and  $s_{ui}$  are the adhesion factor and undrained shear strength, respectively, in a layer  $\Delta z_i$ . The adhesion factor,  $\alpha$ , is given as follows.

$$\alpha = 0.55 \quad \text{for } s_u/p_a \leq 1.5 \quad 9-37a$$

$$\alpha = 0.55 - 0.1(s_u/p_a - 1.5) \quad \text{for } 1.5 < s_u/p_a \leq 2.5 \quad 9-37b$$

where  $p_a$  = atmospheric pressure (=1.06 tsf = 2.12 ksf = 14.7 psi = 101kPa). The units of  $s_{ui}$  and  $p_a$  should be dimensionally consistent.

The **ultimate unit load transfer in side resistance** at any depth  $f_{si}$  is given as follows:

$$f_{si} = \alpha_i s_{ui} \quad 9-38$$

As illustrated in Figure 9-49, the top and bottom 5-ft of the shaft should not be included in the development of the ultimate skin resistance. Environmental, long-term loading or construction factors may dictate that a depth greater than the top 5-ft should be ignored in estimating  $Q_s$ .

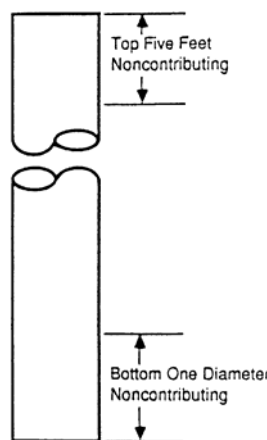


**Figure 9-49. Portions of drilled shafts not considered in computing ultimate side resistance (FHWA, 1999).**

Effective stress methods for computing  $Q_s$  described in Section 9.10.2.3 may be used for the following cases:

- For shafts in cohesive soils under drained loading conditions, and
- In the zones where time-dependent changes in soil shear strength may occur, e.g., swelling of expansive clay or downdrag from a consolidating clay.

### 9.12.1.1 Mobilization of Side Resistance in Cohesive Soil

Figure 9-50 presents the load-transfer characteristics for side resistance in cohesive soils. The curves presented indicate the proportion of the ultimate side resistance ( $Q_s$ ) mobilized at various magnitudes of settlement. It can be seen that the full ultimate side resistance is mobilized at displacements of 0.2% to 0.8% of the shaft diameter. Thus, for a 4-ft diameter shaft in cohesive soil, full side resistance will be mobilized at vertical displacements in the range of 1/8" to 3/8" (3 mm to 10 mm).

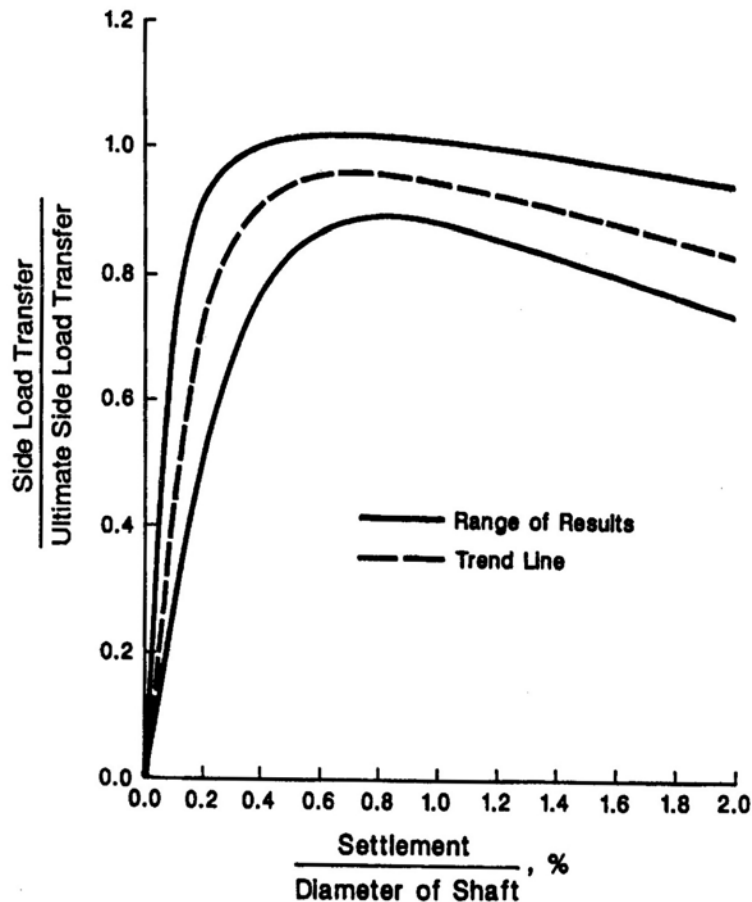


**Figure 9-50. Load-transfer in side resistance versus settlement for drilled shafts in cohesive soils (FHWA, 1999).**

### 9.12.2 Tip Resistance in Cohesive Soil

For axially loaded shafts in cohesive soil subjected to undrained loading conditions, the ultimate tip resistance of drilled shafts may be estimated by using the following relationship:

$$Q_t = q_t A_t = N_c s_{ut} A_t \quad 9-39$$

Where  $q_t$  is the unit tip resistance,  $N_c$  is a bearing capacity factor,  $s_{ut}$  is the undrained shear strength of the soil at the tip of the shaft and  $A_t$  is the tip area of the shaft. Values of the bearing capacity factor,  $N_c$ , may be determined by using the following relationship.

$$N_c = 6.0[1+0.2(z/D)]; \quad N_c \leq 9 \quad 9-40$$

where  $z$  is the depth of the penetration of the shaft and  $D$  is the diameter of the shaft. The units of  $z$  and  $D$  should be consistent.

The limiting value of unit end bearing ( $q_t = N_c s_{ut}$ ) is 80 ksf. The value of 80 ksf is not a theoretical limit but a limit based on the largest measured values. A higher limiting value may be used if it is based on the results of a load test, or previous successful experience in similar soils under similar loading conditions.

The value of  $s_{ut}$  should be determined from the results of in-situ and/or laboratory testing of undisturbed samples obtained within a depth of 2.0 diameters below the tip of the shaft. If the soil within 2.0 diameters of the tip has  $s_{ut} < 0.5$  ksf, the value of  $N_c$  should be multiplied by 0.67.

#### 9.12.2.1 Mobilization of Tip Resistance in Cohesive Soil

Figure 9-51 presents the load-transfer characteristics for tip resistance in cohesive soils. The curves presented indicate the proportion of the ultimate tip resistance ( $Q_t$ ) mobilized at various magnitudes of settlement. It can be seen that the ultimate tip resistance,  $Q_t$ , is fully mobilized at displacements of 2% to 5%. Thus, for a 4-ft diameter shaft in cohesive soil, full tip resistance will be mobilized at vertical displacements in the range of 1" to 2.5" (25 mm to 65 mm). Conversely, if the shaft settles less than these values, then full tip resistance may not be mobilized. For example, if the shaft settles only 1% of the shaft diameter then approximately 60% of the tip resistance will be mobilized as indicated by the trendline shown in Figure 9-51. For smaller tolerable settlements, the mobilized tip resistance will be similarly smaller. If one limits the deformation to between 0.2% and 0.8% to be consistent with full mobilization of side resistance in cohesive soil, then from Figure 9-51, it can be seen that only approximately 10 to 50% of the tip resistance will be available based on the trendline.

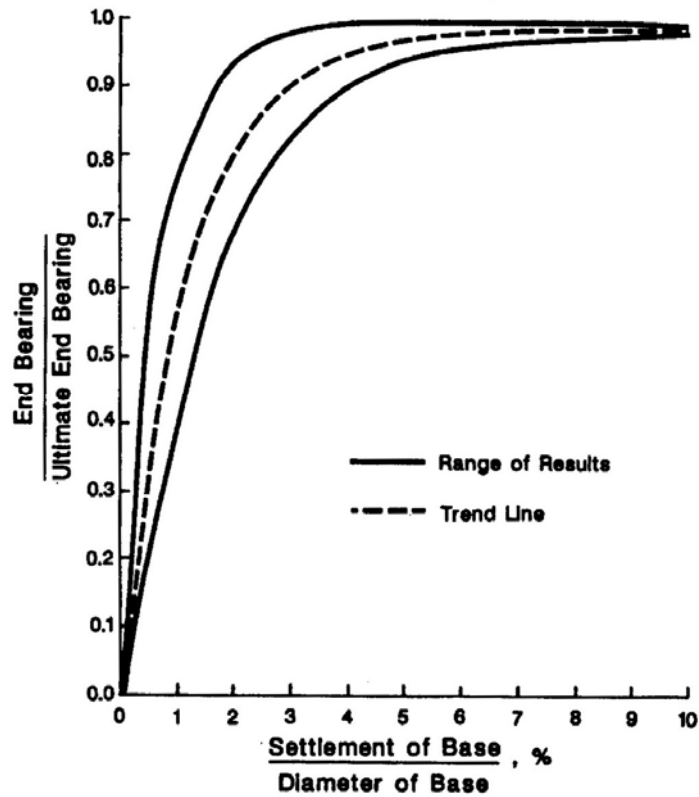


**Figure 9-51. Load-transfer in tip resistance versus settlement for drilled shafts in cohesive soils (FHWA, 1999).**

The above examples of shaft settlements clearly demonstrate the need to perform detailed settlement analyses by using Figure 9-50 and 9-51 to estimate the shaft resistance based on consistent deformations. For shafts in cohesive soil under drained loading conditions,  $Q_t$ , may be estimated by using the procedure described in Section 9.12.3.1 for cohesionless (drained) soils.

### 9.12.3 Side Resistance in Cohesionless Soil

For cylindrical shafts in cohesionless soil or for effective stress analysis of cylindrical shafts in cohesive soils under drained loading conditions, the ultimate side resistance of axially loaded drilled shafts may be estimated by using the following equation:

$$Q_s = \pi D \sum_{i=1}^N \beta_i p_o \Delta z_i \tag{9-41}$$

where:  $\beta_i = 1.5 - 0.135\sqrt{z_i}$  with  $1.2 > \beta_i > 0.25$  9-42

In above equations  $D$  is the shaft diameter,  $N$  is the number of layers used in the analysis,  $z_i$  is the depth in feet to the center of the  $i^{\text{th}}$  layer and  $p_o$  is the effective overburden pressure at the center of the  $i^{\text{th}}$  layer. The ultimate unit load transfer in side resistance at any depth  $f_{si}$  is given as follows:

$$f_{si} = \beta_i p_o \quad 9-43$$

The limiting value of  $f_{si}$  for shafts in cohesionless soils is 4 ksf (191 kPa).

### 9.12.3.1 Mobilization of Side Resistance in Cohesionless Soil

Figure 9-52 presents the load-transfer characteristics for side resistance in cohesionless soils. The curves presented indicate the proportion of the ultimate side resistance ( $Q_s$ ) mobilized at various magnitudes of settlement. It can be seen that the full ultimate side resistance,  $Q_s$ , is fully mobilized at displacements of 0.1% to 1.0% of the shaft diameter. Thus, for a 4-ft diameter shaft in cohesionless soil, full side resistance will be mobilized at vertical displacements in the range of 0.05" to 0.5" (1.3 to 13 mm).

### 9.12.4 Tip Resistance in Cohesionless Soil

For axially load drilled shafts in cohesionless soils or for effective stress analysis of axially loaded drilled shafts in cohesive soils, the ultimate tip resistance may be estimated by using the following equation:

$$Q_t = q_t A_t \quad 9-44$$

The value of  $q_t$  may be determined from the results of standard penetration testing using  $N_{60}$  blow count readings within a depth of  $2B$  below the tip of the shaft as follows:

$$\text{For } N_{60} \leq 75: \quad q_t = 1.2N_{60} \quad \text{in ksf} \quad 9-45a$$

$$\text{For } N_{60} > 75: \quad q_t = 90 \text{ ksf} \quad 9-45b$$

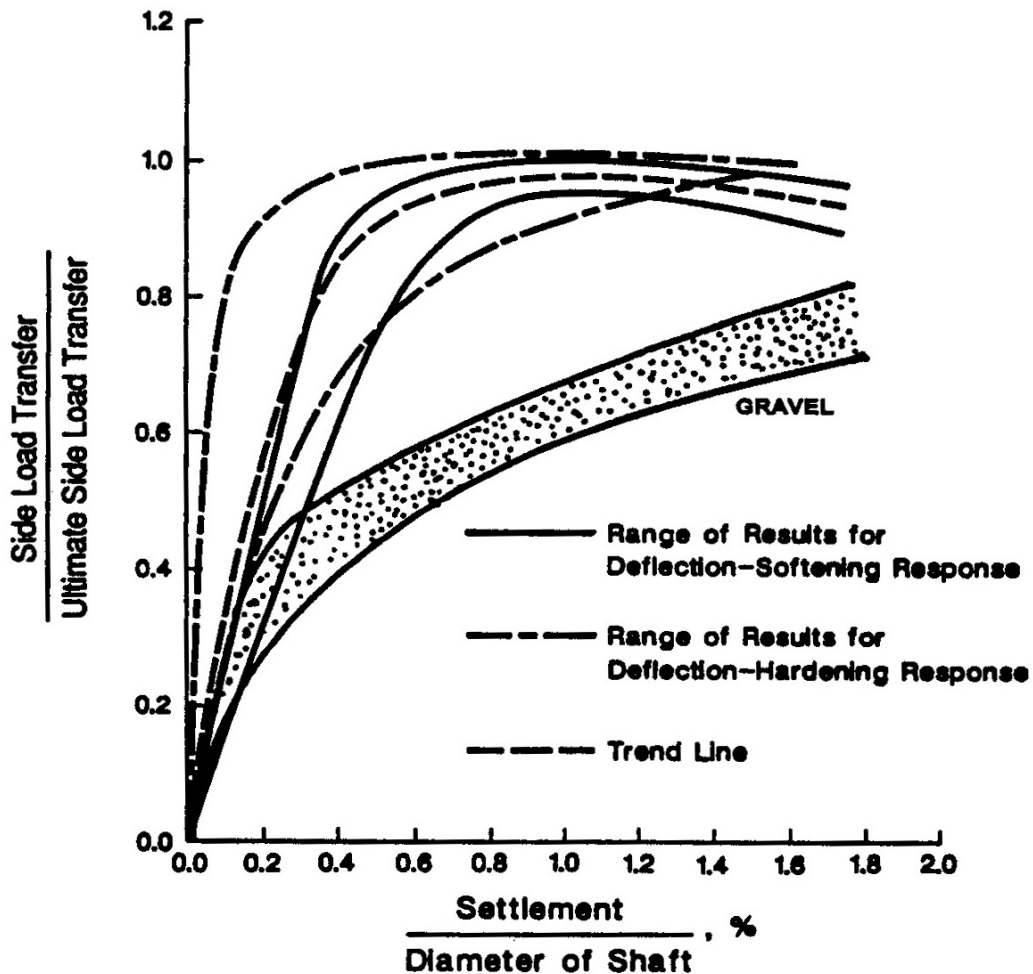


Figure 9-52. Load-transfer in side resistance versus settlement for drilled shafts in cohesionless soils (FHWA, 1999).

#### 9.12.4.1 Mobilization of Tip Resistance in Cohesionless Soil

Figure 9-53 presents the load-transfer characteristics for tip resistance in cohesionless soils. The curves presented indicate the proportion of the ultimate tip resistance ( $Q_t$ ) mobilized at various magnitudes of settlement. It can be seen that the ultimate tip resistance,  $Q_t$ , is fully mobilized at displacements of approximately 5%. Thus, for a 4-ft diameter shaft in cohesive soil, full tip resistance will be mobilized at vertical displacements of approximately 2.4-inches. Conversely, if the shaft settles less than this value, then full tip resistance may not be mobilized. For example if the shaft settles only 1% of the shaft diameter then approximately 30% of the tip resistance will be mobilized as indicated by the trendline shown in Figure 9-53. For smaller settlements, the mobilized tip resistance will be similarly smaller. If one limits the deformation to between

0.1% and 1% to be consistent with full mobilization of side resistance in cohesionless soils, then from Figure 9-53, it can be seen that only approximately 5 to 30% of the tip resistance will be available based on the trendline.

Compared to similar examples for cohesive soils, it can be seen that deformation compatibility is more critical in cohesionless soils due to the relatively large deformation of 5% of shaft diameter that is required to mobilize full tip resistance. This reinforces the need to perform detailed settlement analyses by using Figure 9-52 and 9-53 to estimate the shaft resistance based on consistent deformations.

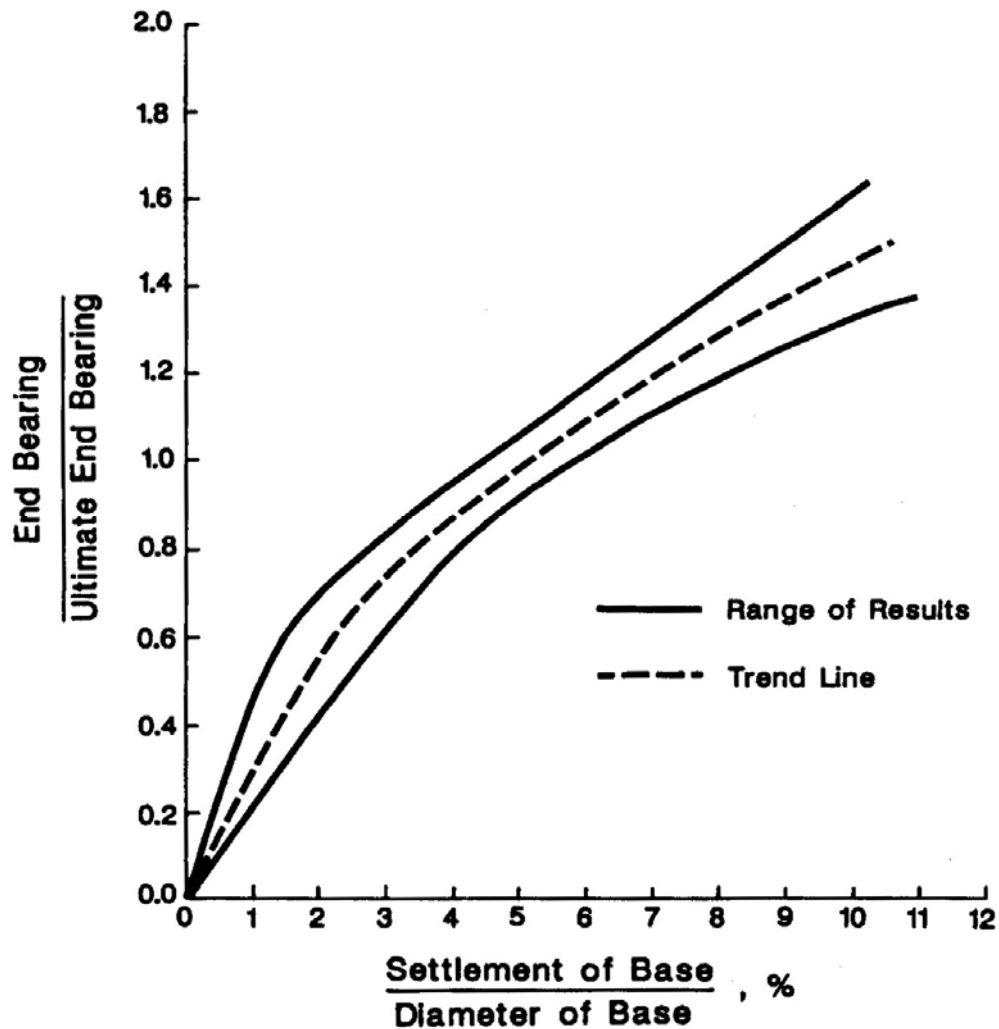


Figure 9-53. Load-transfer in tip resistance versus settlement for drilled shafts in cohesionless soils (FHWA, 1999).

### **9.12.5 Determination of Axial Shaft Capacity in Layered Soils or Soils with Varying Strength with Depth**

The design of shafts in layered soil deposits or soil deposits having variable strength with depth requires evaluation of soil parameters characteristic of the respective layers or depth. The side resistance,  $Q_s$ , in such soil deposits may be estimated by dividing the shaft into layers according to soil type and properties, determining  $Q_s$  for each layer, and summing the values for each layer to obtain the total load  $Q_s$ . If the soil below the shaft tip is of variable consistency,  $Q_t$ , may be estimated using the strength properties of the predominant soil strata within a depth of 2 shaft diameters below the shaft tip. While summing the resistances, particular attention must be paid to deformation compatibility.

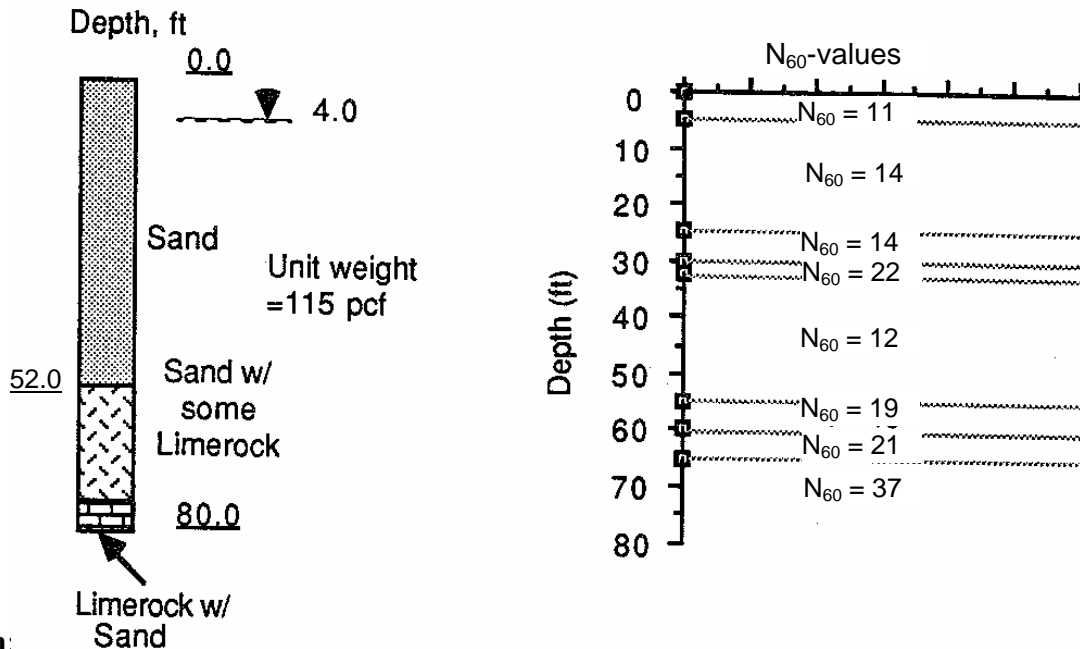
For shafts extending through soft compressible layers to firm soil or rock, consideration should be given to the effects of negative skin friction due to the potential consolidation settlement of soils surrounding the shaft. Where the shaft tip would bear on a thin firm soil layer underlain by a softer soil unit, the shaft should be extended through the softer soil unit to eliminate the potential for a punching shear failure into the softer deposit.

### **9.12.6 Group Action, Group Settlement, Downdrag and Lateral Loads**

These topics are similar to those for pile foundations. Their detailed discussion is beyond the scope of this manual. The reader is referred to FHWA (1999) for discussion of these topics.

The concepts regarding axial capacity of drilled shafts in cohesionless or drained cohesive soils are illustrated numerically by Example 9-5. The concepts regarding axial capacity of drilled shafts in layered soils are illustrated numerically by Example 9-6.

**Example 9-5:** Size a shaft to resist 170 tons of vertical design load in the soil profile shown below. Assume a factor of safety (FS) of 2.5.



**Solution:**

The ultimate geotechnical axial load = (FS) (Design Load) = (2.5) (170 tons) = 425 tons. Assume a straight-sided drilled shaft with a diameter of 3-ft and a length of 60-ft. Thus,  $\pi(D) = 9.42\text{-ft}$

Use Equation 9-41 to determine ultimate skin resistance,  $Q_s = \pi D \sum_{i=1}^N \gamma_i z_i \beta_i \Delta z_i$

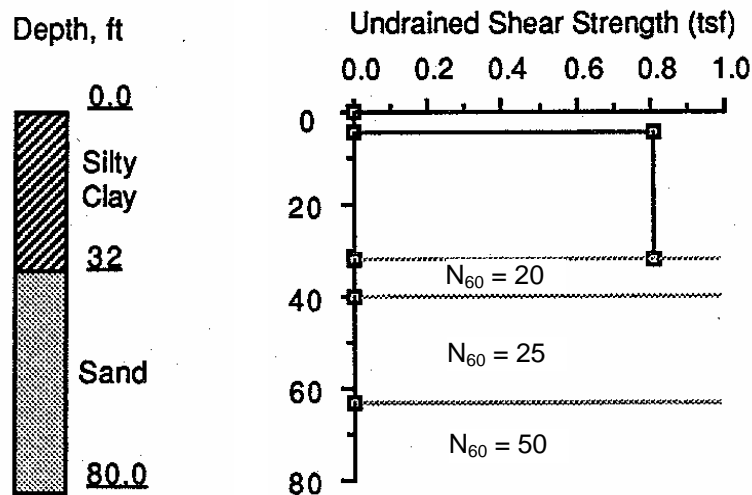
Depth Interval, $\Delta z$ , ft	Surface Area per depth interval, $\Delta z(\pi)(D)$ , ft <sup>2</sup>	Average effective vertical (overburden) stress, $p_o = \gamma z_i$ tsf	$\beta$ $\beta_i = 1.5 - 0.135\sqrt{z_i}$ with $1.2 > \beta_i > 0.25$	$\Delta Q_s$ Tons
0 - 4	37.7	0.115	1.20	5.20
4 - 30	245.0	0.572	0.94	131.70
30 - 60	282.7	1.308	0.59	218.20
<b>Q<sub>s</sub></b>				<b>355.10</b>

Base resistance ( $N_{60}=21$  at 60-ft). Using Equation 9-45a  $q_t = 1.2N_{60} = 25.2 \text{ ksf} = 12.6 \text{ tsf}$   
 $A_t = 7.07 \text{ ft}^2$  Therefore,  $Q_t = (7.07 \text{ ft}^2) (12.6 \text{ tsf}) = 89.1 \text{ tons}$

Thus, ultimate geotechnical axial resistance,  $Q_{ult}$  is given by:

$$Q_u = 355.1 + 89.1 = 444.2 \text{ tons} \approx 440 \text{ tons} > 425 \text{ tons} \quad \text{Okay.}$$

**Example 9-6:** Determine the shaft length to resist 150 tons of vertical design load in the mixed (clay on sand) soil profile shown below. Assume a safety factor of 2.5. Assume a total unit weight of 125 pcf for clay and 115 pcf for sand. Water table is at a depth of 17-ft. Assume depth of zone of seasonal moisture change to be 5-ft. Once the shaft is sized for ultimate load, check the deformation under design load of 150 tons.



**Solution:**

For a factor of safety of 2.5, the ultimate axial load is computed to be  $(2.5)(150 \text{ tons}) = 375 \text{ tons}$ .

For a straight-sided shaft with a diameter of 3.0-ft and a depth of penetration of 50-ft,  $\pi(D) = 9.42\text{-ft}$

Use Equation 9-36 and 9-41,

$$Q_s = \pi D \sum_{i=1}^N \alpha_i s_{ui} \Delta z_i$$

$$Q_s = \pi D \sum_{i=1}^N \gamma'_i z_i \beta_i \Delta z_i$$

Soil	Depth Interval, $\Delta z$ , ft	Surface Area per depth interval, $\Delta z(\pi)(D)$ , ft <sup>2</sup>	Shear Strength or Average effective vertical (overburden) stress, tsf	$\alpha$ or $\beta$	$\Delta Q_s$ Tons
Clay	0 – 5	--	--	0.00	0
Clay	5-32	254.5	0.80 (shear strength)	$\alpha = 0.55^*$	112.0
Sand	32-50	169.6	$\{(17 \text{ ft} \times 125 \text{ pcf}) + (32 \text{ ft} - 17 \text{ ft})(125 \text{ pcf} - 62.4 \text{ pcf}) + 9 \text{ ft}(115 \text{ pcf} - 62.4 \text{ pcf})\} / 2,000 = 3537.4 \text{ psf} / 2,000 = 1.769 \text{ tsf}$	$\beta = 0.64^{**}$	192.0
* From Equation 9-37a				$Q_s$	304.0
** From Equation 9-42, $\beta_i = 1.5 - 0.135\sqrt{z_i}$ At mid-depth of sand layer, $z_i = 32 \text{ ft} + (50 \text{ ft} - 32 \text{ ft})/2 = 41 \text{ ft}$ At $z_i = 41 \text{ ft}$ , $\beta_i = 1.5 - 0.135\sqrt{41 \text{ ft}} \approx 0.64$					

Base resistance ( $N_{60}=25$  at 50 ft)

Use Equation 9-45a

$$q_t = 1.2N_{60} = 1.2(25) = 30 \text{ ksf} = 15 \text{ tsf}$$

$$A_t = 7.07 \text{ ft}^2$$

$$Q_t = (7.07 \text{ ft}^2)(15.0 \text{ tsf}) = 106 \text{ tons}$$

Total ultimate axial resistance,  $Q_{ult}$  is given by:

$$Q_u = 304.0 + 106.0 = 416.0 \text{ tons} > 375 \text{ tons} \quad \text{Okay.}$$

#### Check of settlement under design load (150 tons)

Because most of the load in side resistance and all of the end bearing are derived from sand, Figures 9-52 and 9-53 will be used to estimate settlement. A settlement near the upper bound in both figures will be selected as a conservative estimate.

A settlement of 0.15 percent of the diameter is selected for the average settlement of the sides, or 0.06-inch. That would indicate that about 138 tons is carried in side resistance, and about 12 tons is carried in bearing, assuming that the shaft is essentially incompressible.

Comment: The settlement solution appears to be reasonable.

### 9.12.7 Estimating Axial Capacity of Shafts in Rocks

Drilled shafts are commonly socketed into rock to limit axial displacements, increase load capacity and/or provide fixity for resistance to lateral loading.

Typically, axial compression load is carried solely by the side resistance on a shaft socketed into rock until a total shaft vertical displacement on the order of 0.4 inches occurs, i.e., elastic compression of the concrete plus downward movement of the shaft under load. At this displacement, the ultimate side resistance in rock,  $Q_{sr}$ , is mobilized and slip occurs between the concrete and rock. As a result of this slip, any additional load is transferred to the tip.

The design procedures assume the socket is constructed in reasonably sound rock that is not significantly affected by construction, i.e., the rock does not rapidly degrade upon excavation and/or exposure to air or water, and is cleaned prior to concrete placement, i.e., the rock surface is free of soil and other debris. If the rock is degradable, consideration of special construction procedures, larger socket dimensions, or reduced socket capacities should be considered.

#### 9.12.7.1 Side Resistance in Rocks

For drilled shafts socketed into rock, shaft resistance may be evaluated as follows (Horvath and Kenney, 1979):

$$Q_{sr} = \pi D_r L_r q_{sr} \quad 9-46$$

$$q_{sr} = 0.65(\alpha_E)(p_a) \left( \frac{q_u}{p_a} \right)^{0.5} < 0.65(p_a) \left( \frac{f'_c}{p_a} \right)^{0.5} \quad 9-47$$

where:  $D_r$  = diameter of rock socket (ft)  
 $L_r$  = length of rock socket (ft)  
 $q_{sr}$  = unit skin resistance of rock (tsf)  
 $q_u$  = uniaxial compressive strength of rock (tsf)  
 $p_a$  = atmospheric pressure = 1.06 tsf

$\alpha_E$  =  $E_M/E_i$  = reduction factor to account for jointing in rock as provided in Table 5-23 in Chapter 5, where  $E_M$  is the elastic modulus of the rock mass and  $E_i$  is the elastic modulus of intact rock

$f'_c$  = 28-day compressive strength of concrete (tsf)

Equation 9-46 applies to the case where the side of the rock socket is considered to be smooth or where the rock is drilled using a drilling slurry. Significant additional shaft resistance may be achieved if the borehole is specified to be artificially roughened by grooving. Methods to account for increased shaft resistance due to borehole roughness are provided in FHWA (1999).

Equation 9-46 should be used only for intact rock. When the rock is highly jointed, the calculated  $q_{sr}$  should be reduced to arrive at a final value for design. The procedure is as follows:

- Step 1. Evaluate the ratio of rock mass modulus to intact rock modulus (i.e.,  $E_m/E_i$ ) by using Table 5-23 in Chapter 5.
- Step 2. Evaluate the reduction factor,  $\alpha_E = E_M/E_i$ , by using Table 5-23.
- Step 3. Calculate  $q_{sr}$  according to Equation 9-47.

### 9.12.7.2 Tip Resistance in Rocks

If the rock below the base of the drilled shaft to a depth of 1.0 diameter is either intact or tightly jointed, i.e., there are no compressible materials or gouge-filled seams, and the depth of the socket is greater than 1.5 diameters, then the tip resistance of the rock may be evaluated as follows (FHWA, 1999):

$$Q_{tr} = A_t q_{tr} \quad 9-48$$

$$q_{tr} = 2.5 q_u \quad 9-49$$

where:  $A_t$  = tip area of rock socket

$q_{tr}$  = unit tip resistance, which is evaluated in terms of  $q_u$ , where  $q_u$  = unconfined compressive strength of intact rock (tsf)

If the rock below the base of the shaft is jointed and the joints have random orientation, then the reader should refer to the procedures in FHWA (1999).

### 9.12.8 Estimating Axial Capacity of Shafts in Intermediate GeoMaterials (IGMs)

Intermediate geomaterials (IGMs) are the transitory materials between soils and rocks. IGMs are defined by FHWA (1999) as follows:

- Cohesive IGM – clay shales or mudstones with an undrained shear strength,  $s_u$ , of 2.5 to 25 tsf, and
- Cohesionless – granular tills or granular residual soils with  $N_{60}$  greater than 50 blows/ft.

For detailed information regarding the estimation of shaft resistances in IGM's, the reader should consult FHWA (1999).

### 9.13 CONSTRUCTION METHODS FOR DRILLED SHAFTS

There are three basic methods for construction of drilled shafts. These are (a) dry method, (b) wet method and (c) casing method. Each of these methods is briefly presented below.

#### 1. Dry Method

The dry method is applicable to soils above the water table that will not cave or slump when the hole is drilled to its full depth. A soil that meets this specification is a homogeneous stiff clay. The dry method can be employed in some instances with sands above the water table if the sands have some cohesion, or if they will stand for a period of time because of apparent cohesion.

The dry method can be used for soils below the water table if the soils are low in permeability so that only a small amount of water will seep into the hole during the time the excavation is open.

The dry method consists of drilling a hole using an auger or bucket drill without casing, cleaning the bottom of the excavation, placing a rebar cage and then filling the hole with concrete. The 4 steps involved in construction of a drilled shaft by the dry method are shown in Figure 9-54.

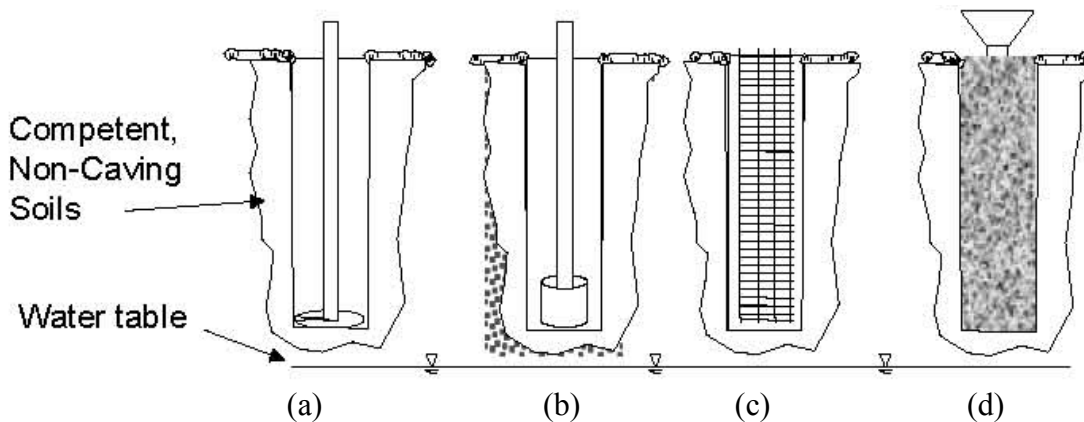


**Figure 9-54. Steps in construction of drilled shafts by the dry method (a) drill, (b) clean, (c) position reinforcement cage, and (d) place concrete.**

## 2. Wet Method

Bentonite or polymer slurry is introduced into the excavation to prevent caving or deformation of loose or permeable soils. The wet method is commonly used while drilling under the groundwater level. Drilling by use of an auger or clamshell mounted on a Kelly bar continues through the slurry. When the desired depth is reached, the excavation is cleaned and the rebar cage is lowered into the slurried hole. Concrete is then tremie-poured into the hole. Slurry is displaced by the heavier concrete and collected at the surface in a sump. The slurry may again be used in another hole. Figure 9-55 shows the 5-step process of shaft construction using wet method.

## 3. Casing Method

The casing method is applicable to sites where soil conditions are such that caving or excessive deformation will occur when a hole is excavated. An example of such a site is a clean sand below the water table. This method employs a cylindrical steel casing inside the excavation to support the caving soil. The excavation is made by driving, vibrating, or pushing a heavy casing to the proposed founding level and by removing the soil from within the casing either continuously as excavation proceeds or in one sequence after the casing has reached the desired depth. Slurry may be required if the excavation is advanced below the ground water table. The excavation is cleaned and the rebar cage is lowered into the excavation. Concrete is then placed, by tremie if the excavation is slurried, and the casing removed. The casing is sometimes permanently left in place. Figure 9-56 shows the 5-step process of shaft construction using the casing method.

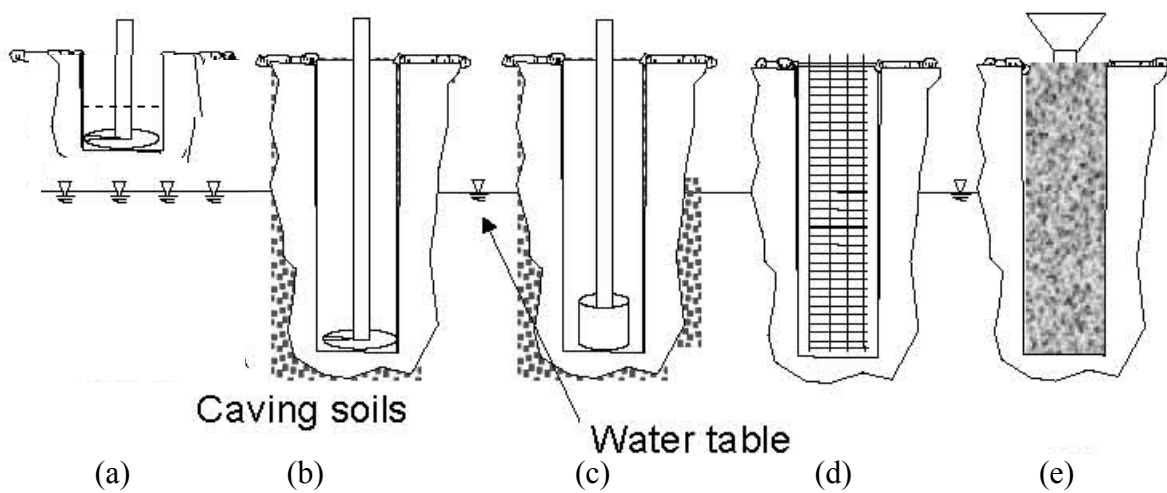


**Figure 9-55. Steps in construction of drilled shafts by the wet method (a) start drilling and introduce slurry (bentonite or polymer) in the excavation PRIOR to encountering the known piezometric level, (b) continue drilling with slurry in the excavation, (c) clean the excavation and slurry, (d) position reinforcement cage, and (e) place concrete by tremie.**

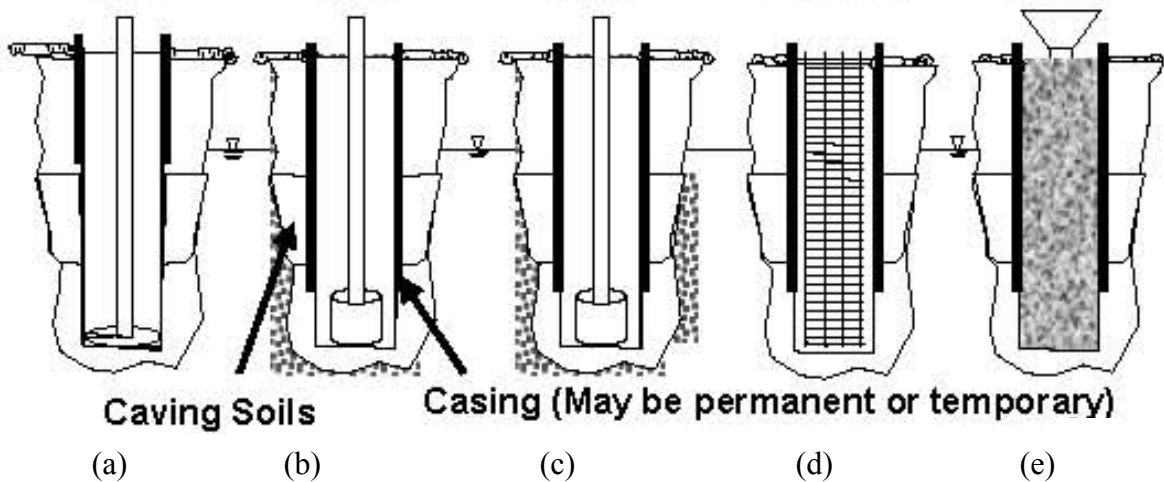


**Figure 9-56. Steps in construction of drilled shafts by the casing method (a) start drilling and introduce casing in the excavation PRIOR to encountering the known piezometric level and/or caving soil, (b) advance the casing through the soils prone to caving, (c) clean the excavation, (d) position reinforcement cage, and (e) place concrete and remove the casing if it is temporary.**

It is critical that the correct construction method be chosen for a given project. Unlike driven piles, which are assembled under controlled conditions and then driven into the ground, drilled shafts are “manufactured” on-site. Thus, the quality of the constructed drilled shaft will be only as good as the quality of the construction processes. In particular, the side and tip resistances are directly affected by the construction processes. While each of the steps in Figures 9-54 to 9-56 are important, **the most important step is related to cleaning of the shaft excavation. There are many considerations involved in the proper cleaning of shafts that are beyond the scope of this manual.** Figure 9-57a shows a photograph of a shaft in which the excavation was not cleaned properly, while Figure 9-57b shows a photograph of a shaft where the cleaning was adequate. These photographs clearly illustrate the need for proper cleaning of the shaft excavation. A detailed discussion of the drilled shaft construction and inspection processes including procedures to assure adequate cleaning can be found in FHWA (1999) and FHWA (2002d).

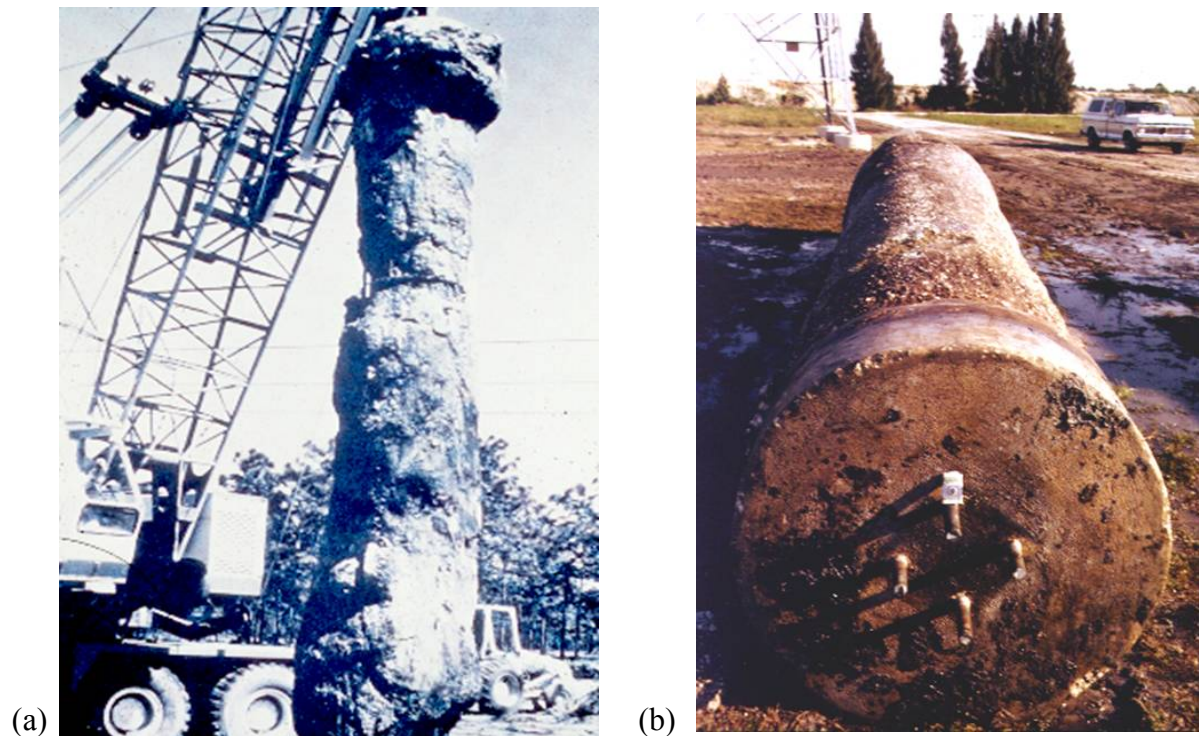


**Figure 9-57. Photographs of exhumed shafts (a) shaft where excavation was not adequately cleaned, (b) shaft where excavation was properly cleaned (FHWA, 2002d).**

## 9.14 QUALITY ASSURANCE AND INTEGRITY TESTING OF DRILLED SHAFTS

Unlike piles, which are manufactured in a factory (e.g., steel pipe piles) or a casting yard (e.g., precast concrete piles), drilled shafts are “manufactured” at the site. Anomalies often develop during the construction of drilled shafts as shown in Figure 9-57a. An anomaly is a deviation from an assumed uniform geometry of the shaft and/or from the required physical properties of the shaft. Typical anomalies may include necking or bulbing, “soft bottom” conditions, voids or soil intrusions, poor quality concrete, debonding, lack of concrete cover over the reinforcement steel and honey-combing. Non-destructive test (NDT) methods are used for Quality Assurance (QA) integrity testing of drilled shaft foundations to identify anomalies.

NDT testing techniques can be categorized as external and internal. External NDT techniques are used at the surface of the concrete structure when access to the interior of the concrete is not available. Examples of external NDT techniques include Sonic Echo (SE), Impulse Response (IR) or Ultra-seismic (US). Internal NDT techniques are used when testing equipment can access the interior of a concrete structure through either cast-in-place access tubes or cored access paths, or through cast-in-place equipment within the concrete (e.g., strain gages). **Commonly used internal NDT techniques include standard Cross-hole Sonic Logging (CSL) with zero-offset measurements and Gamma-Gamma Density Logging (GDL).** Both of these techniques are described below. Other more specialized internal NDT techniques include the Neutron Moisture Logging (NML) and Temperature Logging (TL). All of the NDT methods are discussed in FHWA (2003). Summaries of the methods are given in FHWA (1999), FHWA (2002d) and by Samtani, *et al.* (2005).

### 9.14.1 The Standard Crosshole Sonic Logging (CSL) Test

In the standard CSL test method, an ultrasonic transmitter or source and receiver probes are first lowered to the bottom of a pair of water-filled pre-installed access tubes as shown in Figure 9-58. It is common industry practice to locate the access tubes inside the reinforcing cage. The two probes are then pulled up simultaneously such that the probes are level with each other, i.e., zero-offset. The travel time of the ultrasonic wave between the tubes is recorded along with the amplitude of the signal as a function of every inch of depth. This test procedure is repeated for all possible paired combination of access tubes along the outer perimeter as well as across the inner diagonal of the shaft as shown in the inset Plan View in Figure 9-58. Typically, one tube per foot diameter of the shaft is installed for CSL tests. Thus, for 6-ft diameter shaft, 6 tubes are used. The minimum number of tubes should be 3.

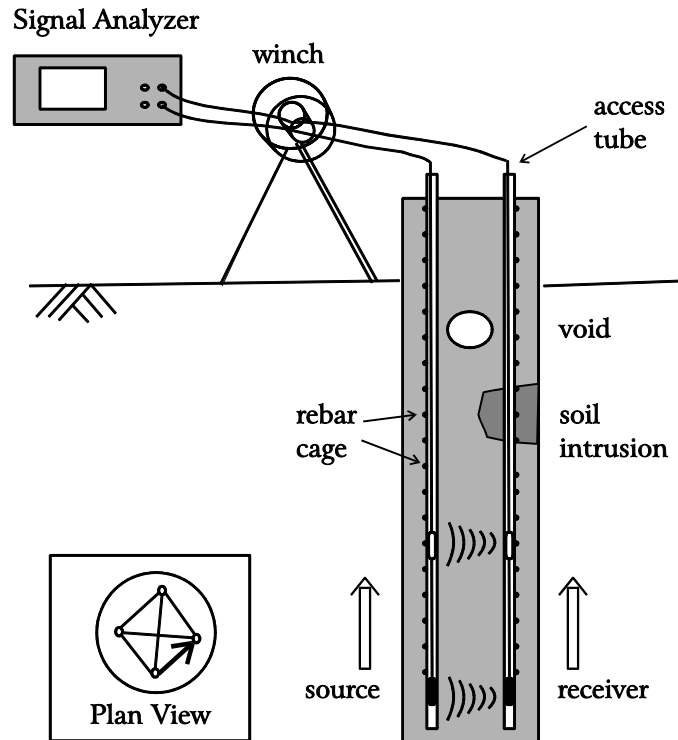


Figure 9-58. Schematic of CSL Test (Samtani, *et al.*, 2005).

The measured travel time,  $t$ , between two tubes with a known center to center distance,  $d$ , is expressed in terms of velocity as:  $V = d/t$ . This computed velocity,  $V$ , is compared with the theoretical compressional wave velocity,  $V_c$ , in concrete. The theoretical ultrasonic wave velocity in competent concrete with unconfined compressive strength,  $f'_c$ , in the range from 3,000 to 5,000 psi is approximately 10,000 to 11,500 ft/sec, respectively (Samtani *et al.*, 2005). As a comparison, the sonic velocity in water and air is approximately 5,000 ft/sec and 1,000 ft/sec, respectively. The computed velocity is compared with the theoretical velocity and expressed in terms of velocity reductions,  $VR = (1 - V/V_c)(100)\%$ . A qualitative rating is assigned to the concrete based on VR, as follows:

<u>VR</u>	<u>Rating</u>
0-10%	Good
10-20%	Questionable
>20%	Poor

The ratings are partially based on the estimated reduction in strength of concrete in anomalous zones. For example, if  $VR=10\%$  at a given location in a shaft, then the  $f'_c$  at that location is approximately 65% of the nominal 28-day  $f'_c$  value of the concrete in that shaft. Similarly, a concrete with  $VR=20\%$  implies that  $f'_c$  at that location is 40% of the 28-day strength.

With the exception of voids and possibly honeycombs, the locations of poor concrete can be confirmed by checking the signal amplitudes. Weaker concrete absorbs the energy of the sonic wave more than sounder concrete and this phenomenon is reflected in lower signal amplitudes. Thus, if the measurements in the shaft indicate lower velocity and lower signal amplitudes then they typically point to anomalous zones due to soil intrusions or poor quality concrete. An example single plot display format that includes velocity and signal amplitude profiles is shown in Figure 9-59. In this particular case, it can be seen that a soft bottom condition in the shaft is reflected at the very bottom of the profile by a drastic change in both in the velocity and amplitude profiles.

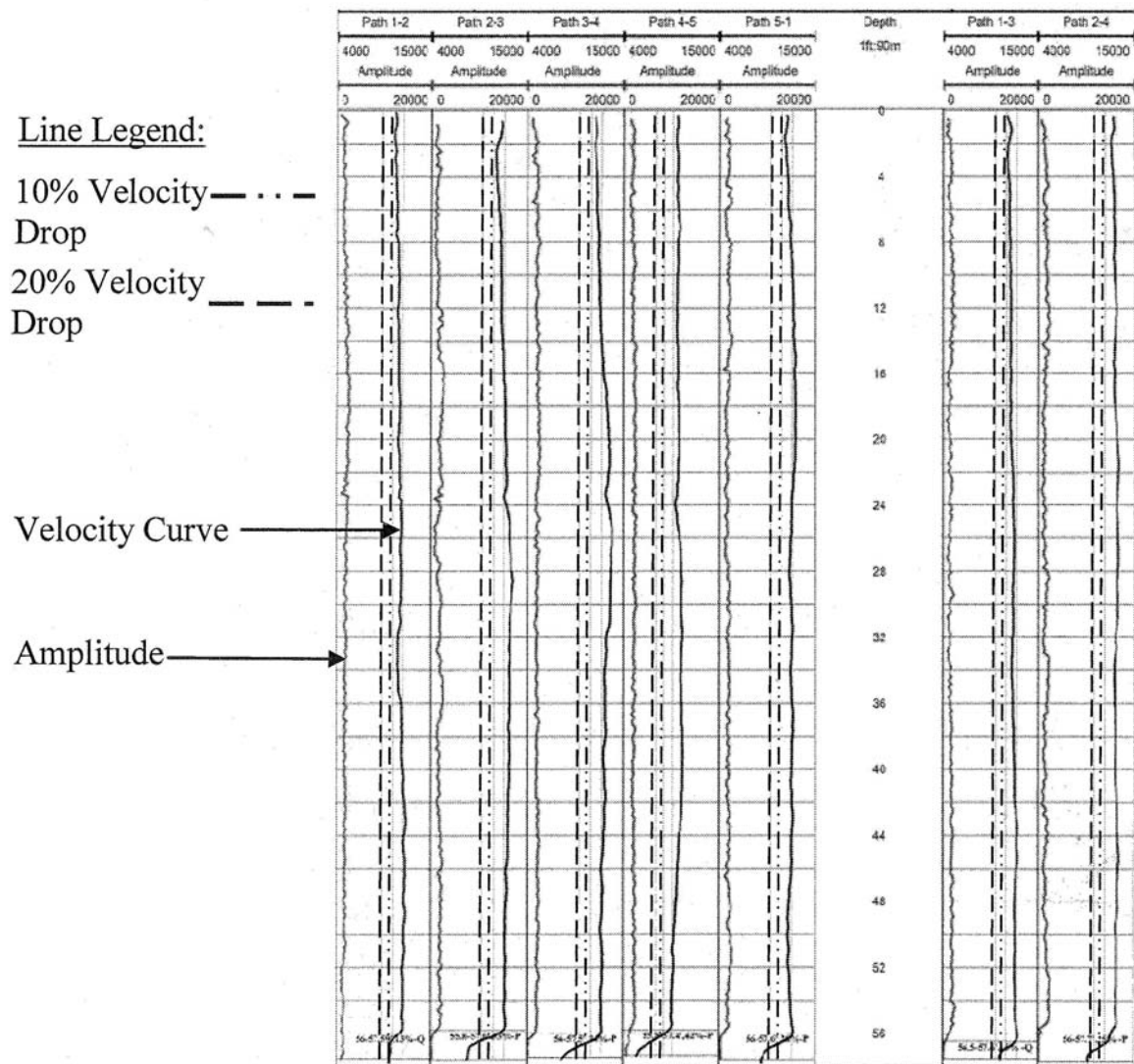


**Figure 9-59. Single plot display format for the CSL data for shaft with five tubes (Samtani, *et al.*, 2005).**

If the tubes debond from the concrete, i.e., there is a small air gap between the outer surface of the tube and the concrete of the shaft, then the CSL test will record a partial or complete loss of signal depending on the extent of the debonding around the perimeter of the tube at that location. Debonding can occur with Schedule 40 PVC access tubes particularly near the ground surface or above the groundwater table where temperature gradients are generally greater. For Schedule 40 PVC tubes, the debonding may occur within a week after placement of concrete as the concrete sets and tends to shrink away from the tubes. Thus, if Schedule 40 PVC tubes are used, then it is generally recommended to perform the CSL tests within 2 to 3 days after concrete placement. A thicker wall PVC tube, such as a Schedule 80 tube, may help extend this timeframe because it is able to withstand the higher temperature gradients better than a thinner PVC tube. Longer time frames can be achieved by the use of steel tubes that experience minimal to no debonding. Therefore, many owners tend to specify steel tubes to alleviate the debonding problems. However, in doing so, the owners are giving up an advantage of the PVC tubes in that they can serve as access paths to repair the shafts should an anomaly be identified by the CSL test since the PVC tubes can be cut open at any depth by use of a high velocity water jet, commonly known as the “water knife.” Use of a water knife is much more difficult, if not impossible, in steel due to the practical limitation of generating a very high water velocity at depth within the access tubes.

Cross-hole Sonic Logging Tomography (CSLT) using multi-offset CSL method is a logical newer extension of the CSL technique and is starting to gain acceptance. The Perimeter Sonic Logging (PSL) is yet another new variation in which zero-offset or multi-offset CSL may be performed in PVC tubes attached to the outside of the reinforcing cage. Samtani, *et al.* (2005) and FHWA (2003) provide summaries of these methods

#### **9.14.2 The Gamma Density Logging (GDL) Test**

A typical field setup for the GDL test is shown in Figure 9-60. In this test a weak Cesium-137 (radioactive) source emits gamma rays into the surrounding medium. A small fraction of the gamma ray photons are reflected back to the probe due to Compton scattering. The intensity of the reflected photons is recorded by a NaI scintillation crystal as counts per second (cps). The measured count rate (*cps*) depends on the electron density of the surrounding medium, which is proportional to the mass per unit volume. The instrument is calibrated by placing the probe in an environment of known density in order to convert the measured count rate (*cps*) into the units of density or unit weight, e.g. lb/ft<sup>3</sup> (pcf).

In the GDL test, the radius of the investigation is largely governed by ½ of the source-detector spacing. Good concrete conditions will result in a near continuous alignment of the data.

Anomalous zones due to soil intrusions, poor concrete or voids are characterized by low density which leads to a high count rate.

A typical GDL log is shown in Figure 9-61. In a GDL log, the measured gamma ray intensity count rate (cps) is presented in terms of unit weight (pcf). In Figure 9-61, the results are plotted in 4 separate sub-plots from the tested access tubes. Each individual sub-plot depicts the GDL results from a 14-inch source-detector separation (corresponding to about 5- to 6-inch radius of investigation) presented in a magnified density scale of 130-180 pcf. Also, in each sub-plot, the mean as well as the minus 2 (-2) and minus three (-3) standard deviation (SD) from mean curves are displayed as vertical guidelines. Depths, in feet, are measured from the top of the shaft and are shown on the vertical axis.

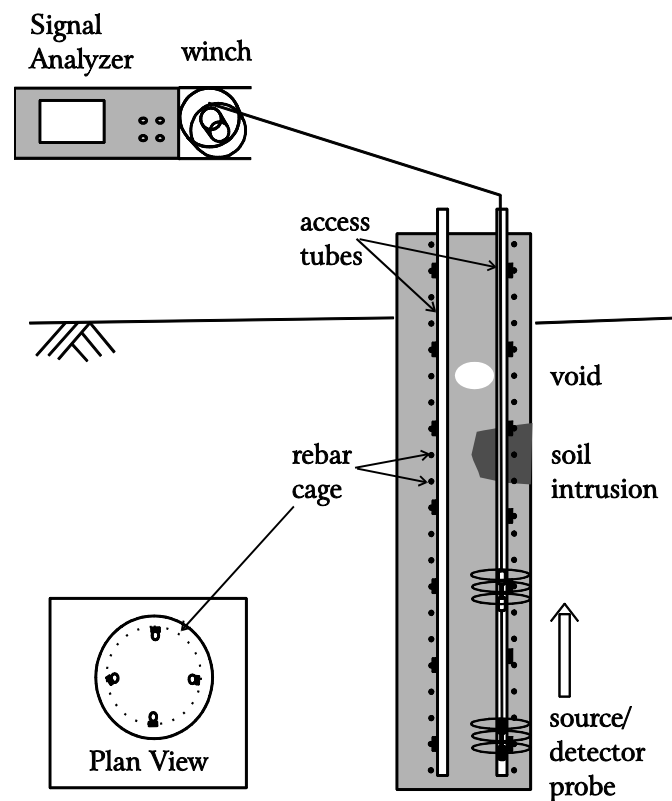


**Figure 9-60. Schematic of GDL Test (Samtani, *et al.*, 2005).**

The results of GDL tests are used to define “questionable” concrete conditions as a zone with reduction in unit weight between -2SD and -3SD and “poor” concrete conditions as a zone with reduction in unit weight of greater than -3SD from the mean (M). These criteria are based on the observation that a cps data set approximates a standard normal distribution probability function in which 99.73% of the data is within  $M \pm 3SD$ . Therefore, when data points are identified

beyond 3SDs, they are considered to represent an anomaly. While these definitions are generally accepted, it is not widely recognized that the computation of M and SD varies during presentation of the results by various testers/agencies. Some testers or agencies define the M and SD with respect to a given tube while others may define these quantities based on all tubes within a shaft, i.e. ignore the variation of steel density and hole geometry, or all tubes from a group of shafts that may form a single overall foundation element for a superstructure. Obviously, the definition of the concrete quality will be different based on the definition of the M and SD. Therefore, the user should be careful with the interpretation of the GDL test data.

Unlike the CSL test, the GDL is not affected much by debonding of the tubes from the concrete. Therefore, a PVC tube is generally used, although steel can also be used with GDL testing. It must be recognized, however, that the thicker or denser the tube material, the lower the measured counts per second (cps) since the tube itself will absorb some of the electrons. Therefore, the user of the data should review the calibration data and check whether the tube type used during calibration is consistent with that used in the actual shaft and the density of the shaft reinforcement.

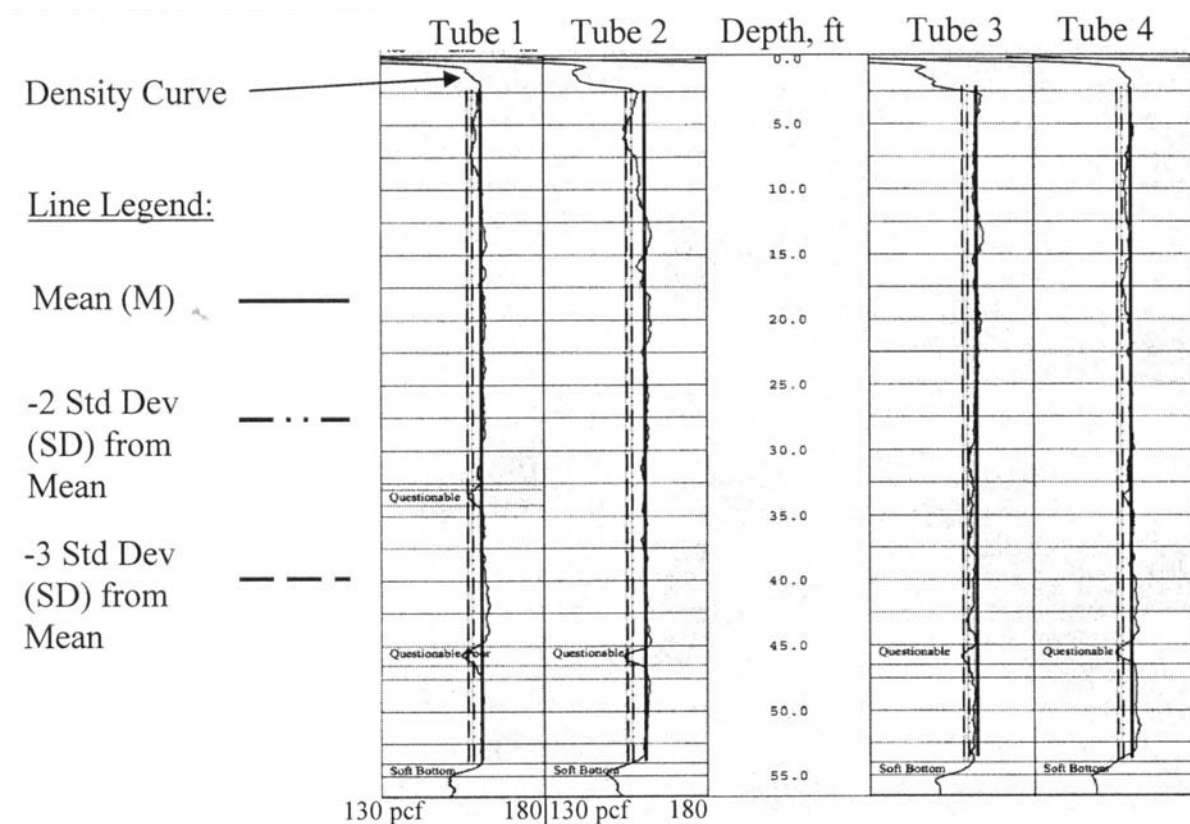


**Figure 9-61. Single plot display format for the GDL data for shaft with four tubes (Samtani, *et al.*, 2005).**

### **9.14.3 Selecting the Type of Integrity Test for Quality Assurance**

Most agencies use either the CSL or GDL test method to evaluate the structural integrity of a constructed shaft. As shown in Figure 9-58, the CSL test evaluates the area of the shaft between the tubes. Since the tubes are commonly located on the inside of the cage, this means that only the portion of the shaft within the reinforcing cage is evaluated. On the other hand, the GDL test evaluates a portion of the shaft immediately surrounding a tube. In other words, GDL evaluates a zone inside and outside the reinforcing cage as shown in Figure 9-60. Due to the different portions of the shaft evaluated by the CSL and GDL tests, it is recommended that both tests be performed to assure an evaluation of the concrete inside and outside the reinforcing cage.

## **9.15 STATIC LOAD TESTING OF DEEP FOUNDATIONS**

Static load testing of deep foundations is the most accurate method of determining load capacity. Depending upon the size of the project, static load tests may be performed either during the design stage or the construction stage. Conventional load test types include the **axial compression, axial tension or lateral load tests**.

The purpose of this section is to provide an overview of static testing and its importance as well as to describe the basic test methods and interpretation techniques. For additional details on load testing for deep foundations, the reader is referred to FHWA (1992c) and ASTM D 1143. It may be noted that ASTM D 1143 was not re-approved in 2006. Therefore, as of the publication date of this manual, there is no accepted ASTM standard for static load tests. However, for the purposes of this manual, the latest ASTM D 1143 prior to 2006 is adequate from the viewpoint of the basic aspects of load testing.

### **9.15.1 Reasons for Load Testing**

1. To minimize risks to the structure by confirming the suitability of the deep foundation to support the design load with an appropriate factor of safety.
2. It is the most positive way for determining the capacity of deep foundations.
3. To develop information for use in the design and/or construction of a deep foundation.
4. Implementation of new static or dynamic analysis methods or procedures.
5. Calibrations of new design procedures such as the Load and Resistance Factor Design (LRFD).

### **9.15.2 Advantages of Static Load Testing**

The advantages of performing static load tests are summarized as follows:

1. A static load test allows a more rational design. Confirmation of pile-soil capacity through static load testing is considerably more reliable than capacity estimates from static capacity analyses and dynamic formulas.

2. An improved knowledge of deep foundation-soil behavior is obtained that may allow a reduction in deep foundations lengths or an increase in the design load, either of which may result in potential savings in foundation costs.
3. With the improved knowledge of deep foundation-soil behavior, a lower factor of safety may be used on the design load. A factor of safety of 2.0 is generally applied to design loads confirmed by load tests as compared to a factor of safety of 3.5 used on design loads in the Modified Gates dynamic formula. Hence, a cost savings potential again exists (Refer to Table 9-5).
4. The ultimate geotechnical capacity determined from load testing allows confirmation that the design load may be adequately supported at the planned foundation penetration depth.

Engineers are sometimes hesitant to recommend a static load test because of cost concerns or potential time delays in design or construction. While the cost of performing a static load test should be weighed against the anticipated benefits, cost alone should not be the determining factor.

Delays to a project in the design or construction stage usually occur when the decision to perform static load tests is added late in the project. Such delays can be minimized by determining early in the project whether a static load test program should be performed. In the construction stage, delays can be minimized by clearly specifying the number and locations of static load tests to be performed as well as the time necessary for the engineer to review the results. In addition, the specifications should state that the static test must be performed prior to ordering pile lengths or commencing production driving. In this way, the test results are available to the design and construction engineer early in the project so that the maximum benefits can be obtained. At the same time the contractor is also aware of the test requirements and analysis duration and can schedule the project accordingly.

### **9.15.3 When to Load Test**

The following criteria, adapted and modified from FHWA (1992c), summarize conditions when pile load testing can be effectively utilized:

1. When substantial cost savings can be realized. This is often the case on large projects involving either friction piles to prove that lengths can be reduced or end bearing piles to prove that the design load can be increased. Testing can also be justified if the savings obtained by using a lower factor of safety equals or exceeds the testing cost.

2. When a safe design load is uncertain due to limitations of an engineer's experience base or due to unusual site or project conditions.
3. When subsurface conditions vary considerably across the project, but can be delineated into zones of similar conditions. Static tests can then be performed in representative areas to delineate foundation variation.
4. When a significantly greater load is contemplated relative to typical design loads and practice.
5. When time dependent changes in deep foundation capacity are anticipated as a result of soil setup or relaxation.
6. Verification of new design or testing methods.
7. When new, unproven deep foundation types and/or pile installation procedures are utilized.
8. When existing deep foundations will be reused to support a new structure with heavier design loads.
9. When a reliable assessment of uplift capacity or lateral behavior is important.
10. When, during construction, the estimated ultimate capacity determined by using dynamic formulas or dynamic analysis methods differs from the estimated capacity at that depth determined by static analysis. For example, H-piles that "run" when driven into loose to medium dense sands and gravels.
11. Calibrations of new design procedures such as the Load and Resistance Factor Design (LRFD).

Experience has also shown that load tests will typically confirm that pile lengths can be reduced at least 15 percent versus the lengths that would be required by the Engineering News (EN) formula on projects where piles are supported predominantly by shaft resistance. This 15 percent pile length reduction was used to establish the following “rule of thumb” formula to compute the total estimated pile length that the project must have to make the load test cost effective based purely on material savings alone.

$$\text{Total estimated pile length in feet on project} \geq \frac{\text{cost of load test}}{(0.15) (\text{cost / ft of pile})} \quad 9-50$$

The above formula may not be valid for drilled shafts since the EN formula is not applicable.

#### **9.15.4 Effective Use of Load Tests**

##### **9.15.4.1 Design Stage**

The best information for design of a deep foundation is provided by the results of a load testing program conducted during the design phase. The number of static tests, types of piles/shafts to be tested, method of driving and test load requirements, method of shaft excavation should be selected by the geotechnical and structural engineers responsible for design. A cooperative effort between the two is necessary. The following are the advantages of load testing during the design stage.

- a. Allows load testing of several different pile/shaft types and lengths resulting in the design selection of the most economical pile/shaft foundation.
- b. Confirm driveability to minimum penetration requirements and suitability of foundation capacity at estimated pile penetration depths.
- c. Establishes preliminary driving criteria for production piles.
- d. Pile driving information released to bidders should reduce their bid "contingency."
- e. Confirm the excavation and excavation support methods for drilled shafts.
- e. Reduces potential for claims related to pile driving problems or shaft excavation methods.
- f. Allows the results of the load test program to be reflected in the final design and specifications.

##### **9.15.4.2 Construction Stage**

Load testing at the start of construction may be the only practical time for testing on smaller projects that can not justify the cost of a design stage program. Construction stage static tests are invaluable to confirm that the design loads are appropriate and that the pile installation procedure

is satisfactory. Driving of test piles and load testing is frequently done to determine the pile order length at the beginning of construction. These results refine the estimated pile lengths shown on the plans and establish minimum pile penetration requirements.

### **9.15.5 Prerequisites for Load Testing**

In order to plan and implement a static load testing program adequately, the following information should be obtained or developed.

1. A detailed subsurface exploration program at the test location. A load test is not a substitute for a subsurface exploration program.
2. Well defined subsurface stratigraphy including engineering properties of soil materials and identification of groundwater conditions.
3. Static pile capacity analyses to select pile type(s) and length(s) as well as to select appropriate location(s) for load test(s).
4. For drilled shafts, caliper-logging to determine the exact dimensions of the shaft excavation. Caliper-logging is required because the actual dimensions of excavations in geomaterials can vary significantly from the diameter of the drilling tool due to a variety of geologic factors or drilling considerations. Calipers are available in either mechanical or electronic configurations. Determination of the exact dimensions of the excavation is the key to proper interpretation of the load test results.
5. For drilled shafts, integrity testing should be performed prior to the load test to determine whether the shaft needs to be structurally repaired so that it has enough structural capacity to sustain the test loads.

### **9.15.6 Developing a Static Load Test Program**

The goal of a static load test program should be clearly established. The type and frequency of tests should be selected to provide the required knowledge for final design purposes or construction verification. A significantly different level of effort and instrumentation is required if the goal of the load test program is simply to confirm the ultimate pile capacity or if detailed load-transfer information is desired for final design. The following items should be considered during the planning stage of the load test program so that the program provides the desired information.

1. The capacity of the loading apparatus (reaction system and jack) should be specified so that the test pile(s) may be loaded to plunging failure. A loading apparatus designed to load a pile to only twice the design load is usually insufficient to obtain plunging failure. Hence, the true factor of safety on the design load cannot be determined, and the full benefit from performing the static test is not realized.
2. Specifications should require use of a load cell and spherical bearing plate as well as dial gages with sufficient travel to allow accurate measurements of load and movement at the pile head. Where possible, deformation measurements should also be made at the pile toe and at intermediate points to allow for an evaluation of shaft and toe bearing resistance.
3. The load test program should be supervised by a person experienced in this field of work.
4. A test pile installation record should be maintained with installation details appropriately noted. Too often, only the hammer model and driving resistance are recorded on a test pile log. Additional items such as hammer stroke (particularly at final driving), fuel setting, accurately determined final set, installation aids used and depths at which they are used, predrilling, driving times, stops for splicing, etc., should be recorded.
5. Use of dynamic monitoring equipment on the load test pile is recommended for estimates of pile capacity at the time of driving, evaluation of drive system performance, calculation of driving stresses, and subsequent refinement of soil parameters for wave equation analysis.

### **9.15.7 Compression Load Tests**

Deep foundations are most often tested in compression, but they can also be tested in tension or for lateral load capacity. Figure 9-62 illustrates the basic mechanism of performing a compression pile load test. This mechanism normally includes the following steps:

1. The pile is loaded incrementally from the pile head according to some predetermined loading sequence, or it can be loaded at a continuous, constant rate.
2. Measurements of load, time, and movement at the pile head and at various points along the pile shaft are recorded during the test.
3. A load movement curve is plotted.

4. The failure load and the movement at the failure load are determined by one of several methods of interpretation.
5. The movement is usually measured only at the pile head. However, the pile can be instrumented to determine movement anywhere along the pile. Telltales (solid rods protected by tubes) shown in Figure 9-62 or strain gages may be used to obtain this information.

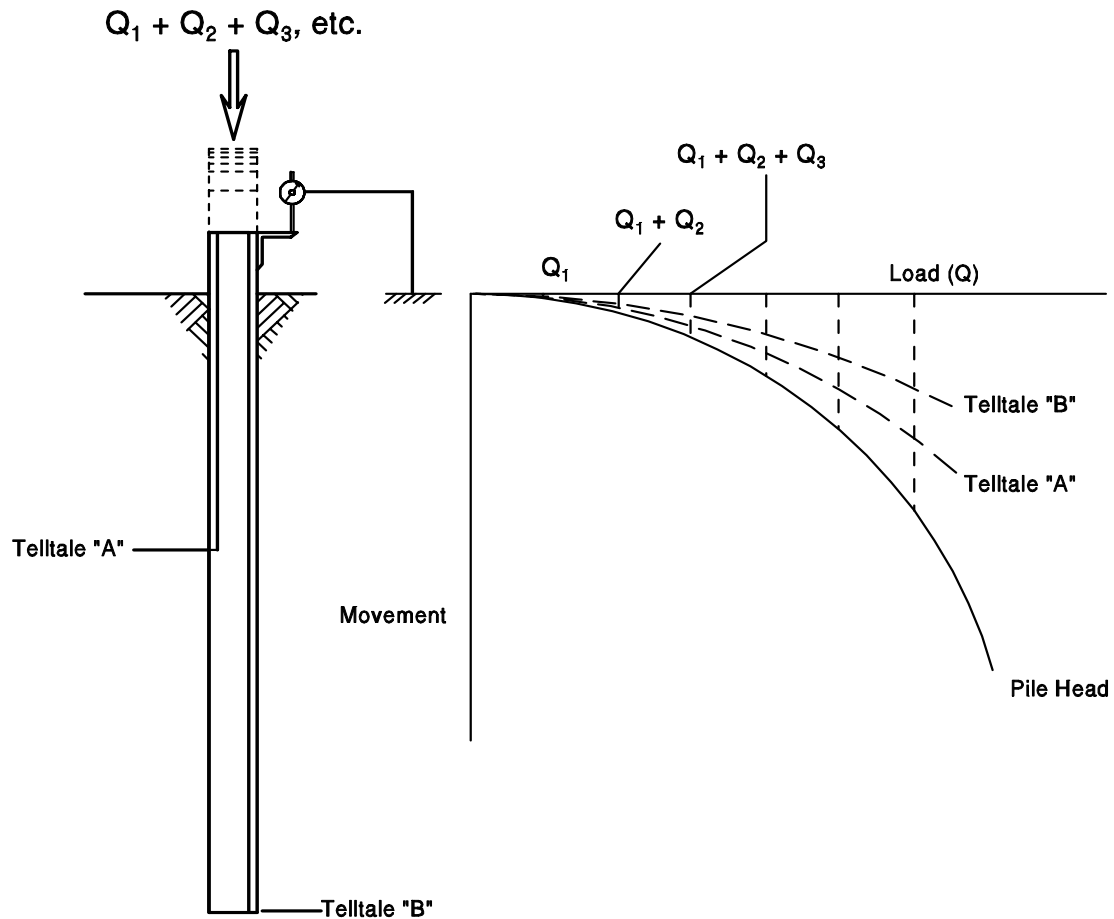


**Figure 9-62. Basic mechanism of a compression pile load test (FHWA, 2006a).**

### 9.15.7.1 Compression Test Equipment

ASTM D1143 recommends several alternative systems for (1) applying compressive load to the pile, and (2) measuring movements. Most often, compressive loads are applied by hydraulically jacking against a beam that is anchored by piles or ground anchors, or by jacking against a weighted platform. A schematic of a typical compression load test setup is presented in Figure 9-63. The primary means of measuring the load applied to the pile should be with a calibrated load cell. The jack load should also be recorded from a calibrated pressure gage, such as the Bourdon gage shown in Figure 9-63. To minimize eccentricities in the applied load, a spherical bearing plate should be included in the load application arrangement.

Axial pile or shaft head movements are usually measured by dial gages or LVDT's that measure movement between the pile head and an independently supported reference beam. ASTM requires the dial gages or LVDT's have a minimum of 2 inches (50 mm) of travel and a precision of at least 0.01 inches (0.25 mm). It is preferable to have gages with a minimum travel of 3 inches (75 mm) and with a precision of 0.001 inches (0.025 mm) particularly when testing long piles that may undergo large elastic deformations under load. A minimum of two dial gages or LVDT's mounted equidistant from the center of the pile and diametrically opposite to each other should be used. Two backup systems consisting of a scale, mirror, and wire system should be provided with a scale precision of 0.01 inches (0.25 mm). The backup systems should also be mounted on diametrically opposite pile faces. Both the reference beams and backup wire systems are to be independently supported with a clear distance of not less than 8 ft (2.5 m) between supports and the test pile. A remote backup system consisting of a survey level should also be used in case reference beams or wire systems are disturbed during the test.

ASTM D 1143 specifies that the clear distance between a test pile and reaction piles be at least 5 times the maximum diameter of the reaction pile or test pile, whichever has the greater diameter if not the same pile type, but not less than 7 ft (2 m). If a weighted platform is used, ASTM D 1143 requires the clear distance between the cribbing supporting the weighted platform and the test pile exceed 5 ft (1.5 m).

Photographs of the load application and movement monitoring components are presented in Figures 9-64 and 9-65. A typical compression load test arrangement using reaction piles is presented in Figure 9-66 and a weighted platform arrangement is shown in Figure 9-67. Additional details on load application as well as head load and movement measurements may be found in ASTM D1143 as well as in FHWA (1992c).

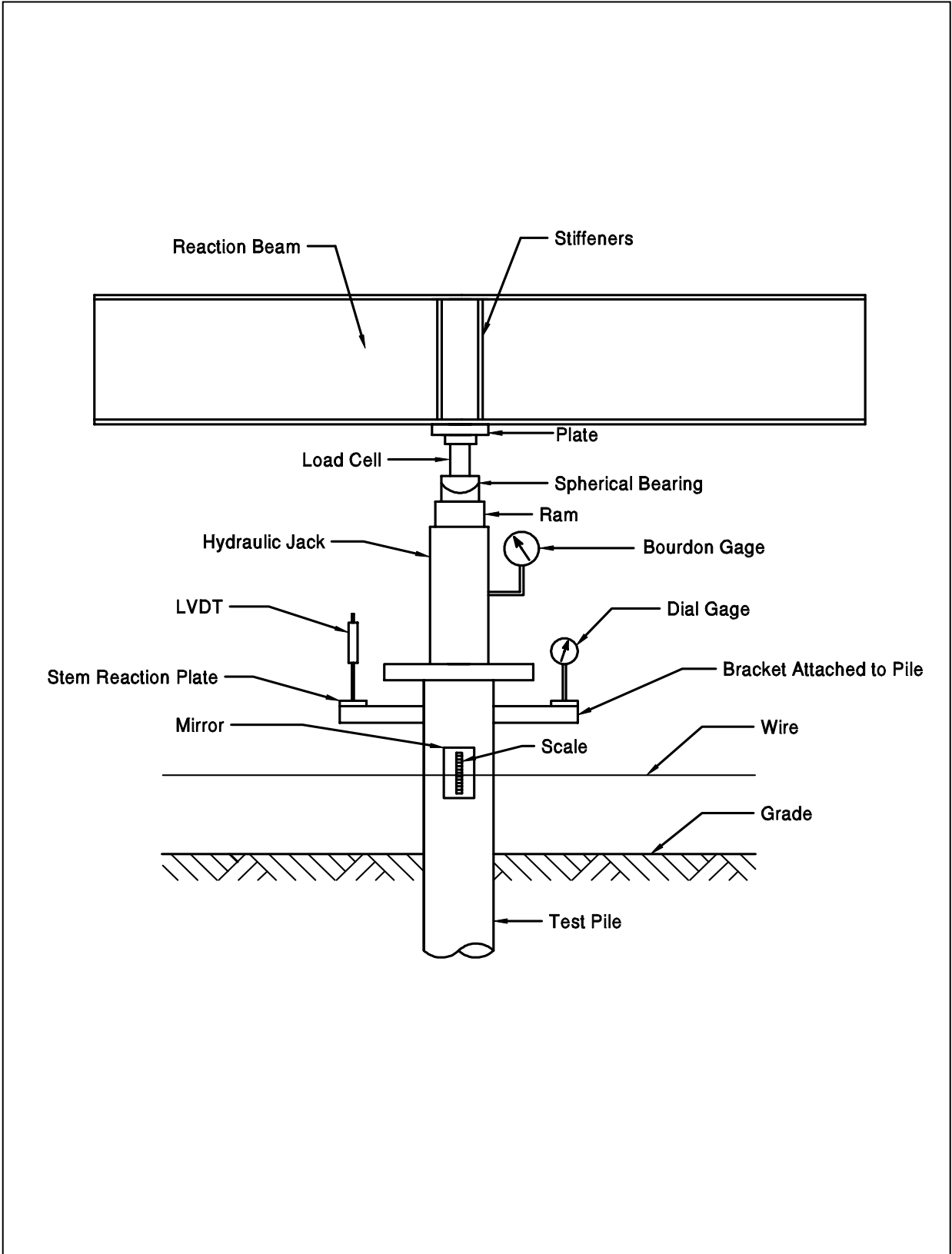


**Figure 9-63. Typical arrangement for applying load in an axial compressive test (FHWA, 1992c).**

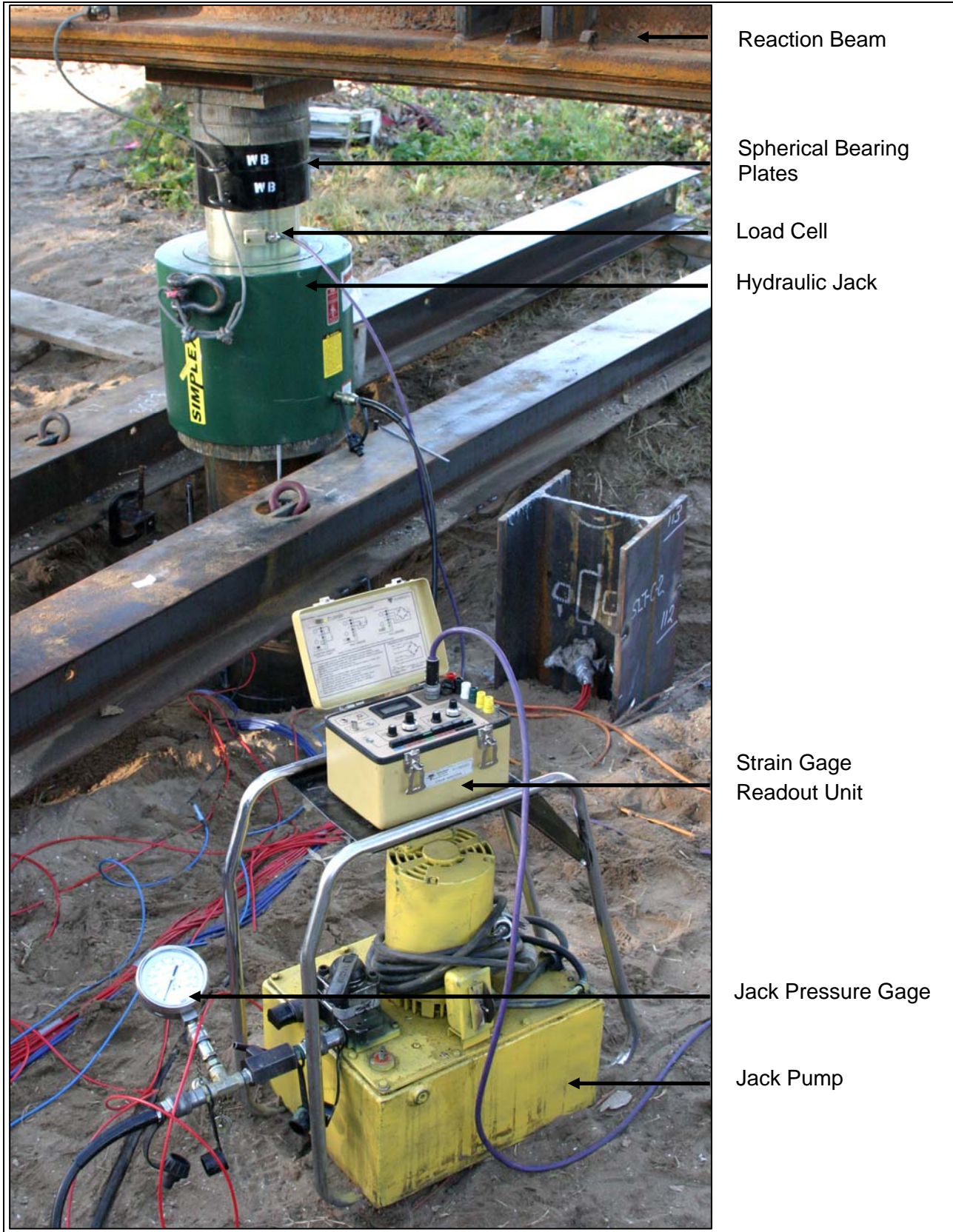


**Figure 9-64. Load test load application and monitoring components (FHWA, 2006a).**



**Figure 9-65. Load test movement monitoring components (FHWA, 2006a).**

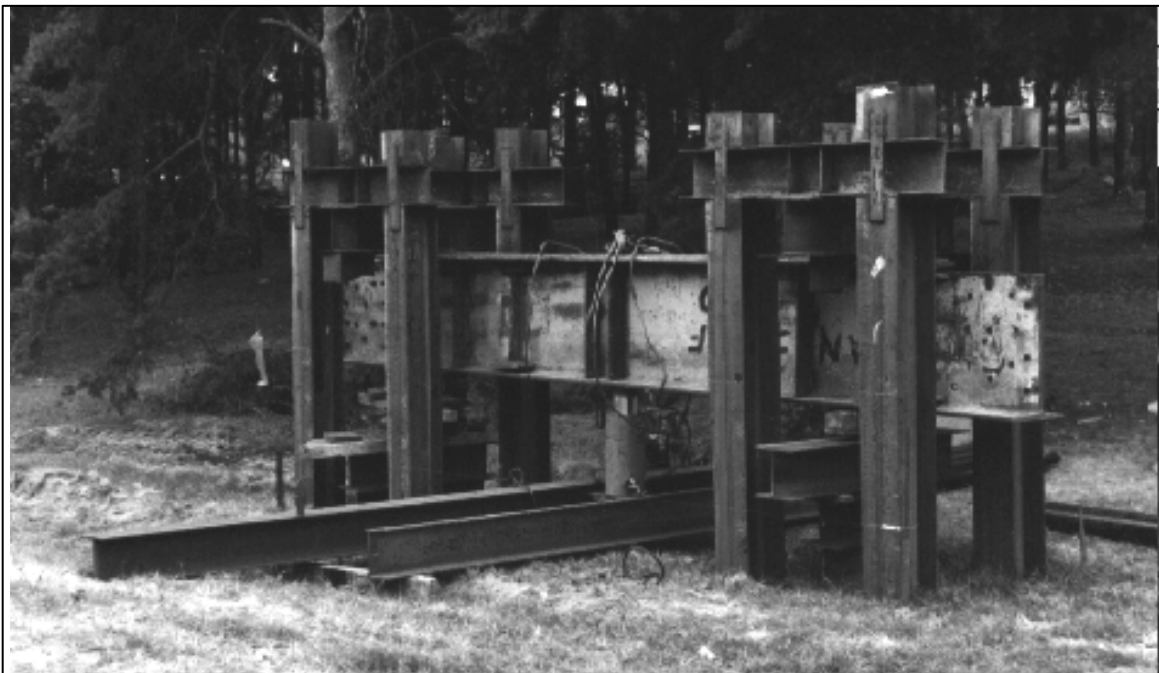


**Figure 9-66. Typical compression load test arrangement with reaction piles (FHWA, 2006a).**



**Figure 9-67. Typical compression load test arrangement using a weighted platform (FHWA, 2006a).**

### **9.15.7.2 Recommended Compression Test Loading Method**

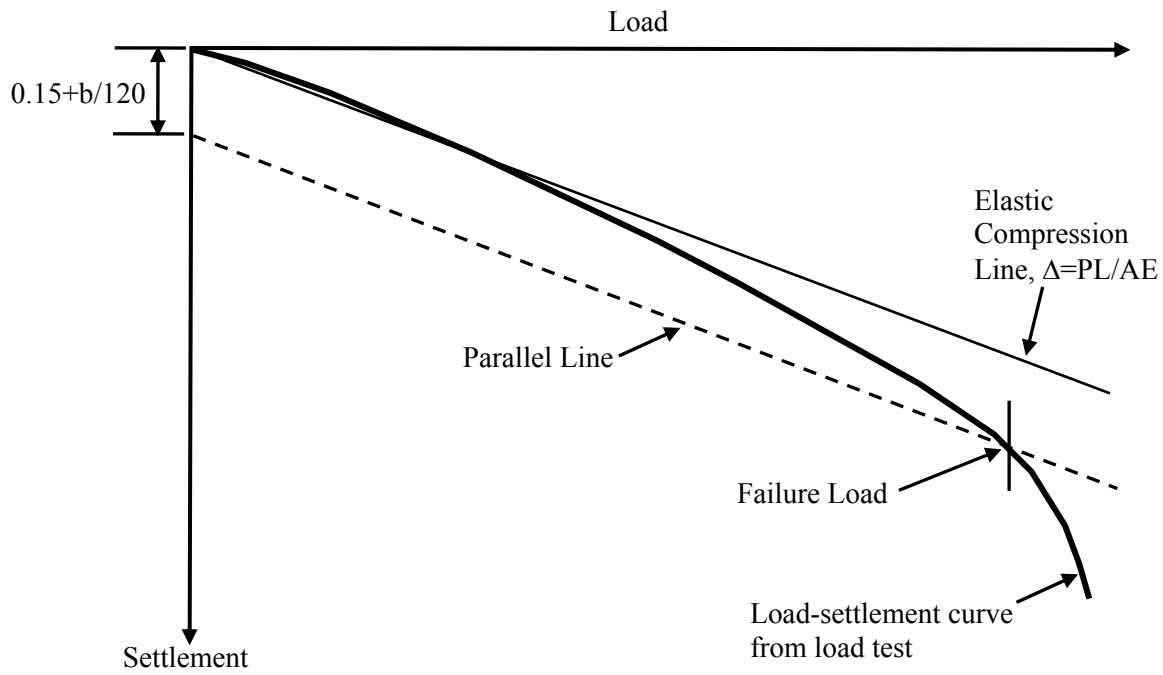
It is extremely important that standardized load testing procedures are followed. Several loading procedures are detailed in ASTM D 1143. The quick load test method is recommended. This method replaces traditional methods where each load increment was held for extended periods of time. The quick test method requires that load be applied in increments of 10 to 15% of the pile design load with a constant time interval of 2½ minutes or as otherwise specified between load increments. Readings of time, load, and gross movement are to be recorded immediately before and after the addition of each load increment. This procedure is to continue until continuous jacking is required to maintain the test load or the capacity of the loading apparatus is reached, whichever occurs first. Upon reaching and holding the maximum load for 5 minutes, the pile is unloaded in four equal load decrements, each of which is held for 5 minutes. Readings of time, load, and gross movement are once again recorded immediately after, 2½ minutes after, and 5 minutes after each load reduction, including the zero load.

### **9.15.7.3 Presentation and Interpretation of Compression Test Results**

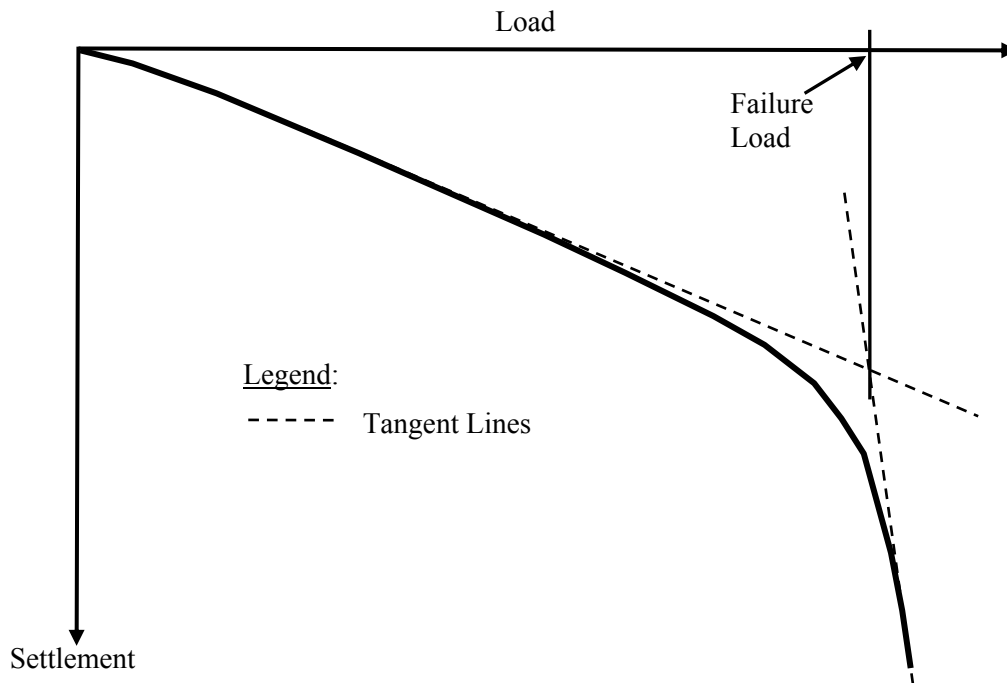
The results of load tests should be presented in a report conforming to the requirements of ASTM D 1143. A load-movement curve similar to the one shown in Figure 9-68 should be plotted for interpretation of test results.

The literature abounds with different methods of defining the failure load from static load tests. Methods of interpretation based on maximum allowable gross movements, which do not take into account the elastic deformation of the pile shaft, are not recommended. These methods overestimate the allowable capacities of short piles and underestimate the allowable capacities of long piles. Methods that account for elastic deformation and are based on a specified failure criterion provide a better understanding of pile performance and provide more accurate results.

AASHTO (2002) and FHWA (1992c) recommend pile compression test results be evaluated by using an offset limit method as proposed by Davisson (1972). The “double-tangent” is more commonly used for drilled shafts. These methods are shown in Figure 9-68 and are discussed in the following sections.



(a)



(b)

**Figure 9-68. Presentation of typical static pile load-movement results, (a) Davisson's method, (b) Double-tangent method.**

#### 9.15.7.4 Plotting the Failure Criteria

Figure 9-68a shows the load-movement curve from a typical pile load test. To facilitate the interpretation of the test results, the scales for the loads and movements are selected so that the line representing the elastic deformation  $\Delta$  of the pile is inclined at an angle of about  $20^\circ$  from the load axis. The elastic deformation  $\Delta$  is computed from:

$$\Delta = \frac{QL}{AE} \quad 9-51$$

Where:  $\Delta$  = elastic deformation in inches (mm)  
Q = test load in kips (kN)  
L = pile length in inches (mm)  
A = cross sectional area of the pile in  $\text{in}^2$  ( $\text{m}^2$ )  
E = modulus of elasticity of the pile material in ksi (kPa)

#### 9.15.7.5 Determination of the Ultimate (Failure) Load

For pile diameters less than 24 in (610 mm), the ultimate or failure load  $Q_f$  of a pile is that load which produces a movement of the pile head equal to:

$$\text{In US Units} \quad s_f = \Delta + \left( 0.15 + \frac{b}{120} \right) \quad 9-52$$

where:  $s_f$  = settlement at failure in inches  
b = pile diameter or width in inches  
 $\Delta$  = elastic deformation of total pile length in inches

A failure criterion line parallel to the elastic deformation line is plotted as shown in Figure 9-68a. The point at which the observed load-movement curve intersects the failure criterion is by definition the failure load. If the load-movement curve does not intersect the failure criterion line, the pile has an ultimate capacity in excess of the maximum applied test load.

For pile diameters greater than 24 in (610 mm), additional pile toe movement is necessary to develop the toe resistance. For pile diameters greater than 24 in (610 mm), the failure load can be defined as the load that produces at movement at the pile head equal to:

*In US Units*

$$s_f = \Delta + \left( \frac{b}{30} \right)$$

9-53

For drilled shafts, the failure load is commonly determined based on the “double-tangent” method shown in Figure 9-68b. Alternatively, the failure load is often defined as the test load corresponding to 5% of the shaft diameter because such a movement represents a large movement given that the drilled shafts are often much larger in diameter than driven piles.

### 9.15.7.6 Determination of the Allowable Geotechnical Load

The allowable geotechnical load is usually determined by dividing the ultimate load,  $Q_u$ , by a suitable factor of safety. A factor of safety of 2.0 is recommended by AASHTO (2002) and is often used. However, larger factors of safety may be appropriate under the following conditions:

- a. Where soil conditions are highly variable.
- b. Where a limited number of load tests are specified.
- c. For friction piles in clay, where group settlement may control the allowable load.
- d. Where the total movement that can be tolerated by the structure is exceeded.
- e. For piles installed by means other than impact driving, such as vibratory driving or jetting.

### 9.15.7.7 Load Transfer Evaluations

FHWA (1992c) provides a method for evaluation of the soil resistance distribution from telltales embedded in a load test pile. The average load in the pile,  $Q_{avg}$ , between two measuring points can be determined as follows:

$$Q_{avg} = A E \frac{R_1 - R_2}{\Delta L} \quad 9-54$$

Where:

- $\Delta L$  = length of pile between two measuring points under no load condition
- A = cross sectional area of the pile
- E = modulus of elasticity of the pile
- $R_1$  = deflection readings at upper of two measuring points
- $R_2$  = deflection readings at lower of two measuring points

If the  $R_1$  and  $R_2$  readings correspond to the pile head and the pile toe respectively, then an estimate of the shaft and toe resistances may be computed. For a pile with an assumed constant uniform soil resistance distribution, Fellenius (1990) states that an estimate of the toe resistance,  $R_t$ , can be computed from the applied pile head load,  $Q_h$  by the following equation.

$$R_t = 2 Q_{avg} - Q_h \quad 9-55$$

The applied pile head load,  $Q_h$ , is chosen as close to the failure load as possible. For a pile with an assumed linearly increasing triangular soil resistance distribution, the estimated toe resistance may be calculated by using the following equation:

$$R_t = 3 Q_{avg} - 2 Q_h \quad 9-56$$

The estimated shaft resistance can then be calculated from the applied pile head load minus the toe resistance.

During driving, residual loads can be locked into a pile that does not completely rebound after a hammer blow, i.e., return to a condition of zero stress along its entire length. This mechanism is particularly true for flexible piles, piles with large frictional resistances, and piles with large toe quakes. Load transfer evaluations performed by using telltale measurements described above assume that no residual loads are locked in the pile during driving. Therefore, the load distribution calculated from the above equations would not include residual loads. If measuring points  $R_1$  and  $R_2$  correspond to the pile head and pile toe of a pile that has locked-in residual loads, the calculated average pile load would also include the residual loads. This inclusion of residual loads would result in a lower toe resistance being calculated than actually exists as depicted in Figure 9-69. Additional details on telltale load transfer evaluation, including residual load considerations, may be found in Fellenius (1990).

When detailed load transfer data is desired, telltale measurements alone are insufficient since residual loads cannot be directly accounted for. Dunncliff (1988) suggests that weldable vibrating wire strain gages be used on steel piles and sister bars with vibrating wire strain gages be embedded in concrete piles for detailed load transfer evaluations. A geotechnical instrumentation specialist should be used to select the appropriate instrumentation to withstand pile handling and installation, to determine the redundancy required in the instrumentation system, to determine the appropriate data acquisition system, and to reduce and report the data acquired from the instrumentation program.

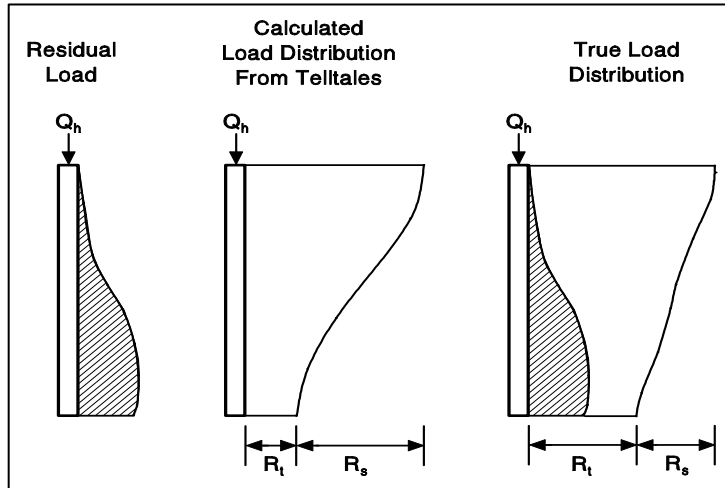


**Figure 9-69. Example of residual load effects on load transfer evaluation (FHWA, 2006a).**

A sister bar vibrating wire strain gage for embedment in concrete or concrete filled pipe piles is shown in Figure 9-70 and an arc-weldable vibrating wire strain gage attached to a steel H-pile is presented in Figure 9-71. When detailed load-transfer data is desired, a data acquisition system should be used.



**Figure 9-70. Sister bar vibrating wire gages for concrete embedment (FHWA, 2006a).**

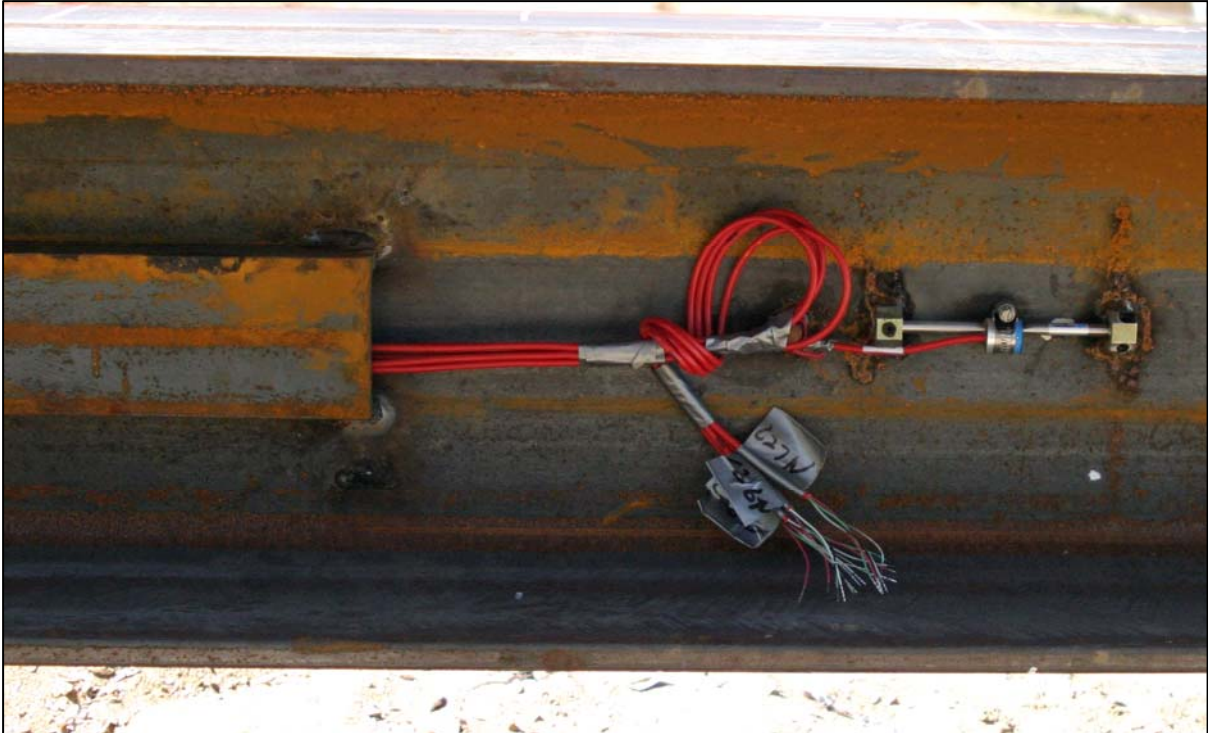


**Figure 9-71. Arc-weldable vibrating wire strain gage attached to H-pile. (Note: protective channel cover shown on left) (FHWA, 2006a).**

### **9.15.8 Other Compression Load Tests**

Two methods of load testing were introduced in recent years that have been used to varying degrees by highway agencies for testing drilled shafts. These methods are the Osterberg Cell<sup>®</sup> and the Statnamic<sup>®</sup> methods, both of which are proprietary methods. Both of these techniques can routinely be used for test loads in range of 10,000 to 15,000 kips. The Osterberg Cell<sup>®</sup> test can apply loads up to 50,000 kips. Both, driven piles and cast-in-place piles, e.g., drilled shafts, can be tested by these methods. Although the details of each method are beyond the scope of this manual, a brief description follows on each method. Additional details are presented in primary references for this chapter (FHWA, 2006a; FHWA, 1999).

#### **9.15.8.1 The Osterberg Cell<sup>®</sup> Method**

Instead of using a conventional jack, reaction frame and reaction anchor system, the axial loading test can be performed by applying the load with an expendable jack and load cell cast within the test shaft. This jack - load cell is called an Osterberg Cell<sup>®</sup> after its inventor, Jorj Osterberg and the test in which the Osterberg Cell<sup>®</sup> is used is commonly known as the O-Cell<sup>®</sup> test. A schematic of the O-Cell<sup>®</sup> test in comparison with a static load test with a

reaction frame is shown in Figure 9-72. Figure 9-73 shows some details for the O-Cell<sup>®</sup> test. Figure 9-74 shows a photograph of an O-cell. Figure 9-75 shows a photograph of an O-Cell<sup>®</sup> assembly attached to a reinforcing cage just prior to the cage being placed into a drilled shaft excavation.

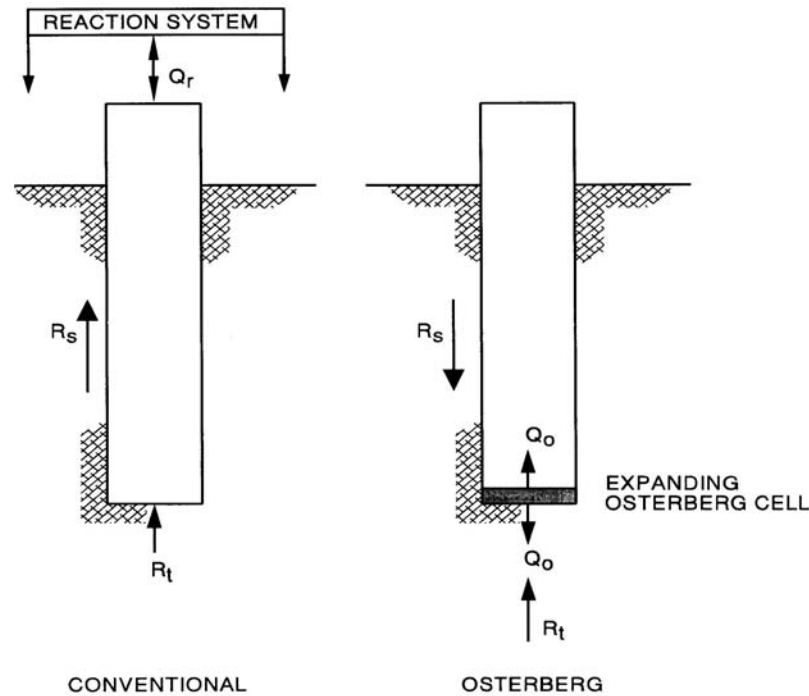


**Figure 9-72. Comparison of reaction mechanism between Osterberg Cell<sup>®</sup> and Static test.**

The principle of operation is very simple. The Osterberg Cell<sup>®</sup> consists essentially of two plates (pistons) of a prescribed diameter between which there is an expandable chamber that can hold pressurized fluid, usually oil or water. The upper and lower plates on the cell can be field welded to steel plates, usually at least 2 in (50 mm) thick, whose diameters are approximately equal to that of the test shaft. The chamber is pressurized by pumping from a reservoir on the ground surface. The unique feature of this device is that the pistons being pressurized have standard diameters that are approximately the full diameter of the cell, which may be up to 32 in (800 mm). Therefore, the pressurized fluid is acting on a very large area, unlike a conventional ram in which the area of the piston is usually small. This characteristic allows the Osterberg Cell<sup>®</sup> to apply very large loads with relatively low hydraulic pressures. Standard models with a diameter of 32 in (800 mm) are capable of applying loads of up to 3,000 tons (26.7 MN). Smaller sizes are also available from the supplier with consequently smaller capacities. The Osterberg Cell<sup>®</sup> is manufactured in a variety of sizes for both drilled shaft installations and driven pile installations as shown in Tables 9-12 and 9-13, respectively.

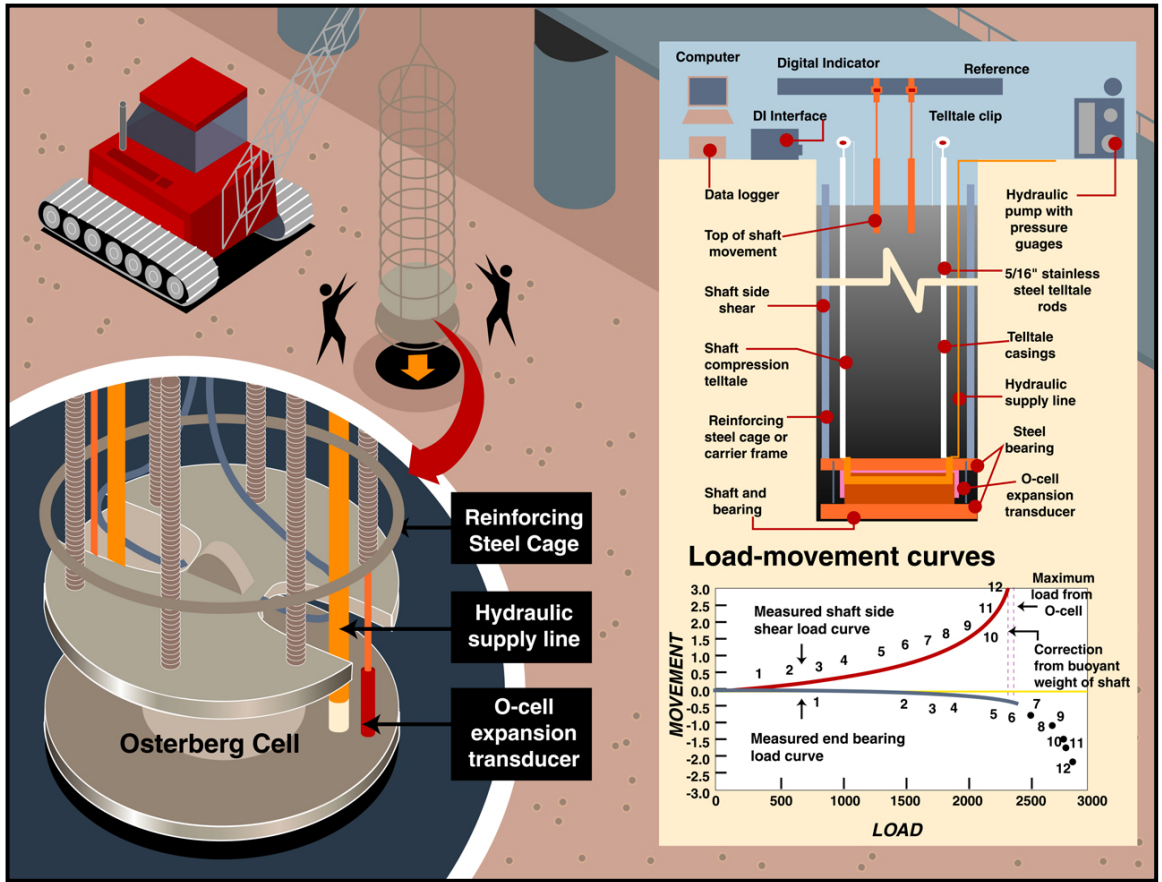
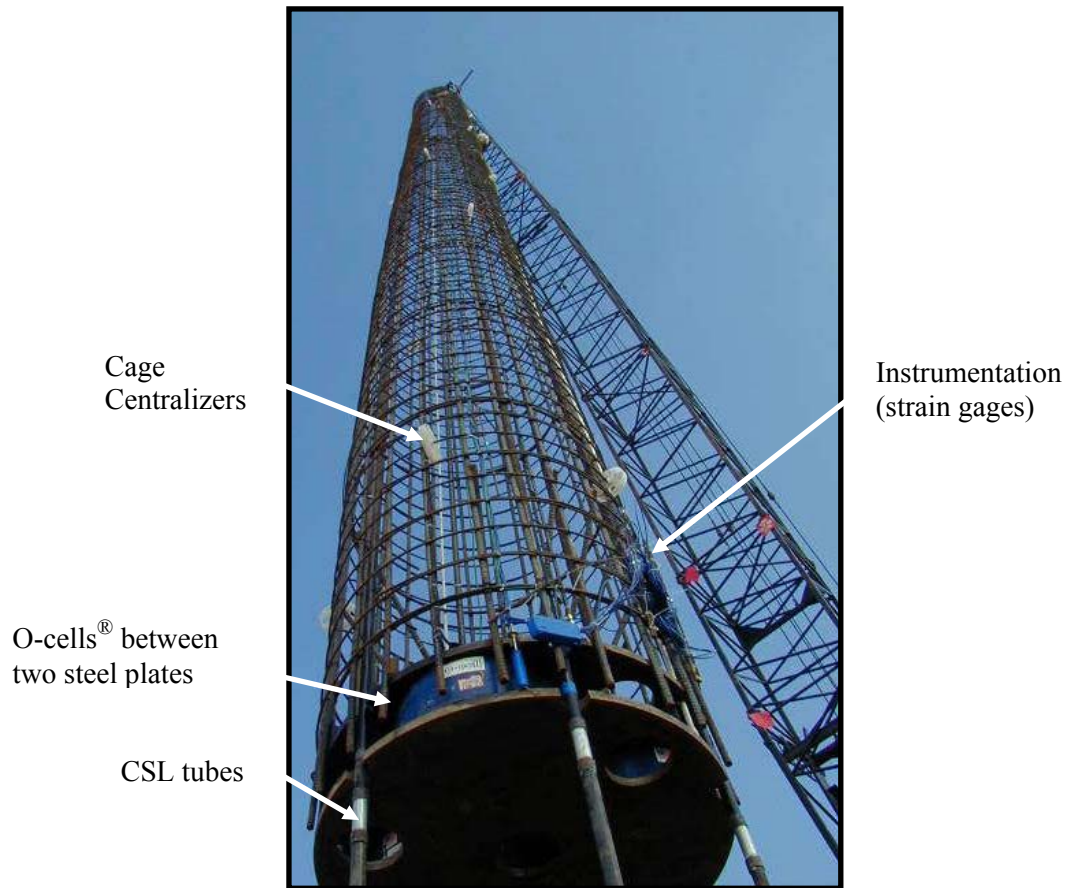


Figure 9-73. Some details of the O-Cell<sup>®</sup> test (after [www.bridgebuildermagazine.com](http://www.bridgebuildermagazine.com)).



Figure 9-74. Photograph of an O-Cell<sup>®</sup>.



**Figure 9-75. O-Cell<sup>®</sup> assembly attached to a reinforcing cage with other instrumentation.**

**Table 9-12. Osterberg Cells<sup>®</sup> for drilled shafts**

Size	Diameter Inches	Height Inches	Capacity Tons	Weight Pounds
5	5.25	5.18	75	32
9	9.00	10.75	200	190
13	13.00	11.65	400	300
21	21.25	11.65	1,200	800
26	26.25	11.65	1,800	1,230
34	34.25	12.37	3,000	2,015

Note: 1 in = 25.4 mm; 1 ton = 8.9 kN

**Table 9-13. Osterberg Cells<sup>®</sup> for driven piles**

Size – Inches	Capacity – Tons	Stroke - Inches	Description of Pile
14	200	6	Round-steel pipe
14	300	6	Square-precast Concrete
18	900	8	Round-steel pipe
30	950	9	Square-precast Concrete

Note: 1 in = 25.4 mm; 1 ton = 8.9 kN

The load being applied to the drilled shaft is usually monitored by measuring the pressure in the fluid being applied by the pump. The Osterberg Cell<sup>®</sup> will therefore need to be calibrated in a testing machine prior to installation to obtain a relationship between the measured pressure and the load applied by the cell. Ordinarily, a calibration is provided by the supplier. Note that in practice the hydraulic pressure will usually be measured at the ground surface, but the cell is situated at some distance below the ground surface, e.g., about 110 ft (33.5 m) for the Osterberg Cell<sup>®</sup> assembly shown in Figure 9-75. Therefore, the actual pressure at the level of the cell is the pressure that is measured plus the vertical distance from the pressure gauge to the middle of the cell times the unit weight of the cell fluid. This correction needs to be made before load versus movement is plotted. Movement can be measured at the top of the cell through telltales attached to the top of the cell that are monitored by movement sensors, e. g., dial gauges suspended from stable reference beams on the ground surface. Similarly, movement can be measured at the top of the test shaft by means of movement sensors suspended from stable reference beams. Movement of the bottom plate can be determined by measuring the movement of the top of the Osterberg Cell<sup>®</sup> with telltales and then measuring the relative movement between the upper and lower ends of the cell by means of sacrificial electronic movement sensors attached between the top and bottom plates.

The O-Cell<sup>®</sup> test has some limitations in that the total failure load of the foundation element cannot usually be measured; only the failure load of the friction above the cell or the resistance below the cell are measured.

The Osterberg Cell<sup>®</sup> has been used in a variety of soil and rock conditions. The cell has been used to determine the bond stress in rock sockets and in dense glacial tills. In addition, a variety of strain gage devices have been used in conjunction with the O-Cell<sup>®</sup> test to develop a distribution of resistance along the foundation element. Such measurements can also be obtained below an Osterberg Cell<sup>®</sup> installed at the mid-height of a shaft by extending instrumented rebar below the base of the cell.

The cost of a single O-cell<sup>®</sup> test, including the Osterberg Cell<sup>®</sup> itself, instrumentation and shaft construction, is often in the range of 50 to 60 per cent of the cost of performing a conventional static load test for situations, such as shafts of small capacity, in which conventional static load tests can be used, although the percentage varies considerably from site to site.

By using multiple Osterberg Cells<sup>®</sup> in a given shaft, it is possible to mobilize up to 25,000 tons of combined side and base resistance. The O-Cell<sup>®</sup> test has not been standardized by

AASHTO or ASTM as of 2006. Additional information on the O-Cell<sup>®</sup> test can be found at [www.loadtest.com](http://www.loadtest.com).

#### **9.15.8.2 The Statnamic<sup>®</sup> Test Method**

The Statnamic<sup>®</sup> test method is a proprietary method developed by the Birmingham Foundation Corporation ([www.birmingham.com](http://www.birmingham.com)). A new ASTM draft standard, entitled “Standard Test Method for Piles under Rapid Axial Compressive Load,” has been proposed but had not been approved as of 2006.

A Statnamic<sup>®</sup> loading test also can be performed without the need for an expensive reaction system. An advantage of this type of test relative to the O-Cell<sup>®</sup> test is that it does not require the loading device to be cast into the shaft. Therefore, the Statnamic<sup>®</sup> loading test can be performed on a drilled shaft for which a loading test was not originally planned.

The principle of the Statnamic<sup>®</sup> test is shown in Figure 9-76. Dead weights are placed upon the surface of the test shaft. Beneath the dead weights is a small volume of propellant and a load cell. The propellant is ignited and accelerates the masses upward. As this occurs a reaction force equal to the masses times their acceleration is produced against the head of the shaft, as indicated in Figure 9-76. This force, which increases with time up to one to two hundred milliseconds, causes the shaft to displace downward. As the ignition of the propellant stops, the reaction force rapidly decreases and the shaft rebounds. The displacement of the shaft head is measured by means of a laser beam from a source located some distance away from the test shaft. The laser beam is targeted on the shaft head. The load can be graphed against both time and displacement instantaneously.

For reasons of safety the reaction masses are contained within a metal sheath that is also filled with an energy absorbing material, such as dry gravel, that will cushion the impact of the masses as they fall back upon the head of the drilled shaft. A photograph of a Statnamic<sup>®</sup> test arrangement, with the gravel-filled sheath surrounding the reaction masses is shown in Figure 9-77 just after igniting the propellant.

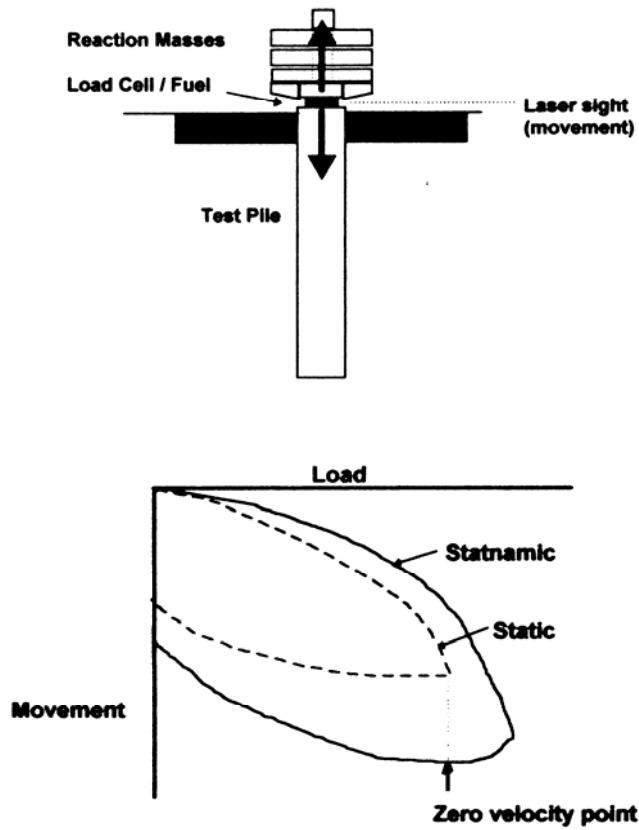


Figure 9-76. Schematic of Statnamic<sup>®</sup> test



Figure 9-77. Photograph of Statnamic<sup>®</sup> test arrangement showing masses being accelerated inside gravel-filled sheath.

Since there are dynamic components to the resistance of the drilled shaft, some interpretation of the data is necessary, as illustrated in the bottom part of Figure 9-76. Since the load produced at the head of the shaft by igniting the propellant is applied much more slowly than the load applied by the blow of a pile-driving hammer, it can usually be assumed that the length of the stress wave that is imparted to the drilled shaft is much longer than the length of the shaft itself and that the shaft is therefore penetrating into the soil or rock as a rigid body. It may not be possible to make this simplifying assumption if the test shaft is extremely long. However, if rigid body motion is assumed, the load acting on the head of the shaft can be reasoned to be the sum of (1) the total static soil resistance (base and sides), (2) damping forces produced by the relative velocity between the shaft and the soil/rock, and (3) the mass of the drilled shaft itself times its acceleration. In the Statnamic<sup>®</sup> test, if the load corresponding to a zero slope on the load-settlement relation measured near the beginning of rebound, as illustrated in Figure 9-76, is selected as the analysis point, then component (2), above, will be zero, since the velocity of the shaft will be zero, and the total static resistance of the drilled shaft,  $R_T$ , can be approximated by :

$$R_T = F_{so} - W_s \left( \frac{a_s}{g} \right) \quad 9-57$$

where,  $F_{so}$  = the force measured by the load cell at the point at which the slope of the rebound curve is zero, identified by the arrow in Figure 9-68

$W_s$  = total weight of the drilled shaft

$a_s$  = acceleration of the drilled shaft corresponding to  $F_{so}$ , which can be measured with an accelerometer at the head of the shaft

$g$  = acceleration of gravity.

Note that  $a_s$  will not be zero despite the fact that the velocity of the test shaft is momentarily zero at  $F_{so}$ . If the test shaft is long, a stress wave analysis may be necessary to obtain an accurate estimate of resistance.

Statnamic<sup>®</sup> devices have been constructed that are capable of applying head loads of up to approximately 3600 tons (32 MN). The cost of a Statnamic<sup>®</sup> test will usually be approximately the same as the cost of an O-Cell<sup>®</sup> test of the same magnitude.

Further technical information on the Statnamic<sup>®</sup> test method can be found in the *Proceedings of the First International Statnamic Seminar*, Vancouver, British Columbia, 1995. Copies

can be obtained from Berminghammer Foundation Equipment Company, Wellington Street Marine Terminal, Hamilton, Ontario L8L 4Z9, Canada. The reader is also referred to FHWA (2006a) for further information on the load test interpretation.

### **9.15.9 Limitations of Compression Load Tests**

Compression load tests can provide a wealth of information for design and construction of pile foundations and are the most accurate method of determining pile capacity. However, static load test results cannot be used to account for long-term settlement, downdrag from consolidating and settling soils, or to represent pile group action adequately. Other shortcomings of static load tests include cost, the time required to setup and complete a test, and the minimal information obtained on driving stresses or extent of potential pile damage. Static load test results can also be misleading on projects with highly variable soil conditions.

### **9.15.10 Axial Tension and Lateral Load Tests**

Load tests can also be performed such that uplift and lateral loading conditions are simulated. Such load tests are described in FHWA (1999) and FHWA (2006a).

[THIS PAGE INTENTIONALLY BLANK]

## CHAPTER 10.0

### EARTH RETAINING STRUCTURES

Earth retaining structures or systems are used to hold back earth and maintain a difference in the elevation of the ground surface as shown in Figure 10-1. The retaining wall is designed to withstand the forces exerted by the retained ground or “backfill” and other externally applied loads, and to transmit these forces safely to a foundation and/or to a portion of the restraining elements, if any, located beyond the failure surface.

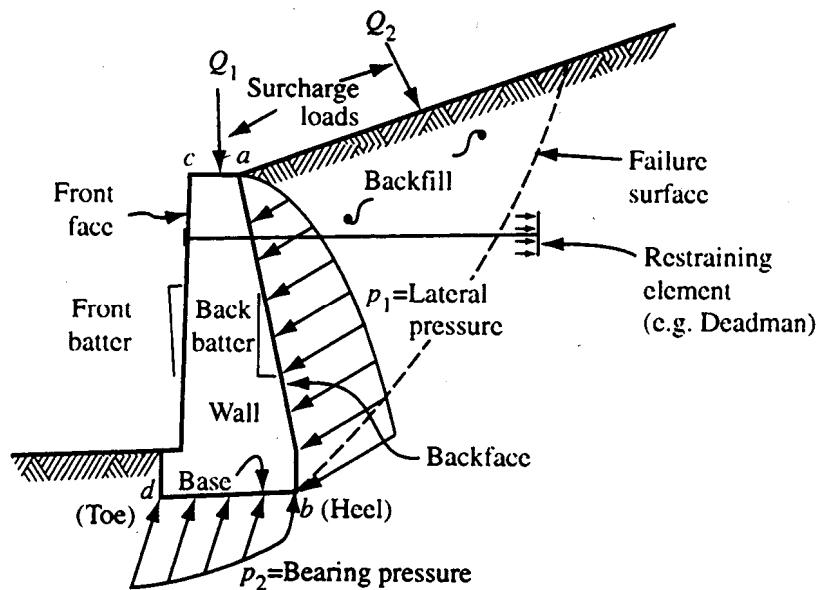


Figure 10-1. Schematic of a retaining wall and common terminology.

In general, the cost of constructing a retaining wall is usually high compared with the cost of forming a new slope. Therefore, the need for a retaining wall should be assessed carefully during preliminary design and an effort should be made to keep the retained height as low as possible.

In highway construction, retaining walls are used along cuts or fills where space is inadequate for construction of cut slopes or embankment slopes. Bridge abutments and foundation walls, which must support earth fills, are also designed as retaining walls.

Typical applications for earth retaining structures in highway construction include:

- new or widened highways in developed areas;
- new or widened highways at mountain or steep slopes;
- grade separation;
- bridge abutments, wing walls and approach embankments;

- culvert walls;
- tunnel portals and approaches;
- flood walls, bulkheads and waterfront structures;
- cofferdams for construction of bridge foundations;
- stabilization of new or existing slopes and protection against rockfalls; and
- groundwater cut-off barriers for excavations or depressed roadways.

Figure 10-2 provides schematic illustrations of several retaining wall systems traditionally used in highway applications. A great number of wall systems have been developed in the past two decades by specialty contractors who have been promoting either a special product or a specialized method of construction, or both. Due to the rapid development of these diversified systems and their many benefits, the design engineer is now faced with the difficult task of having to select the best possible system; design the structure; and ensure its proper construction.

An important breakthrough in the design of earth retaining structures (ERS) that occurred in this era was the recognition that the earth pressure acting on a wall is a function of the type of wall and the amount and distribution of wall movement. Classical earth pressure theories, which were developed by Coulomb (1776) and Rankine (1857), were formalized for use by Caquot and Kerisel (1948) and others. Sophisticated analyses of soil-structure interaction and wall/soil movements began in the 1960s with the development of finite difference and finite element analytical procedures. The simultaneous advancement of geotechnical instrumentation equipment and monitoring procedures made the “observational method” of design (Peck, 1969) popular and cost effective.

Since 1970 there has been a dramatic growth in the number of methods and products for retaining soil. O’Rourke and Jones (1990) describe two trends in particular that have emerged since 1970. First, there has been an increasing use of reinforcing elements, either by incremental burial to create reinforced soils (MSE walls), or by systematic in situ installation to reinforce natural soils or even existing fills (soil nailing); see Figure 10-2b. Mechanically stabilized earth and soil nailing have changed the ways we construct fill or cut walls, respectively, by providing economically attractive alternatives to traditional designs and construction methods. Second, there has been an increasing use of polymeric products to reinforce the soil and control drainage. Rapid developments in polymer manufacturing have supplied a wide array of geosynthetic materials. The use of these products in construction has encouraged a multitude of different earth retention schemes.

The rapid development of these new trends and the increased awareness of the impact of construction on the environment, have led to the emergence of the concept of “earth walls.”

In this concept, the soil supports itself or is incorporated into the structure and assumes a major structural or load carrying function. With this concept, structural member requirements of the system are reduced, or eliminated altogether. Examples of recently developed earth walls include the soil-reinforcement systems discussed above, as well as systems involving chemical treatment of the in-situ soil such as jet grouting or deep soil mixing.

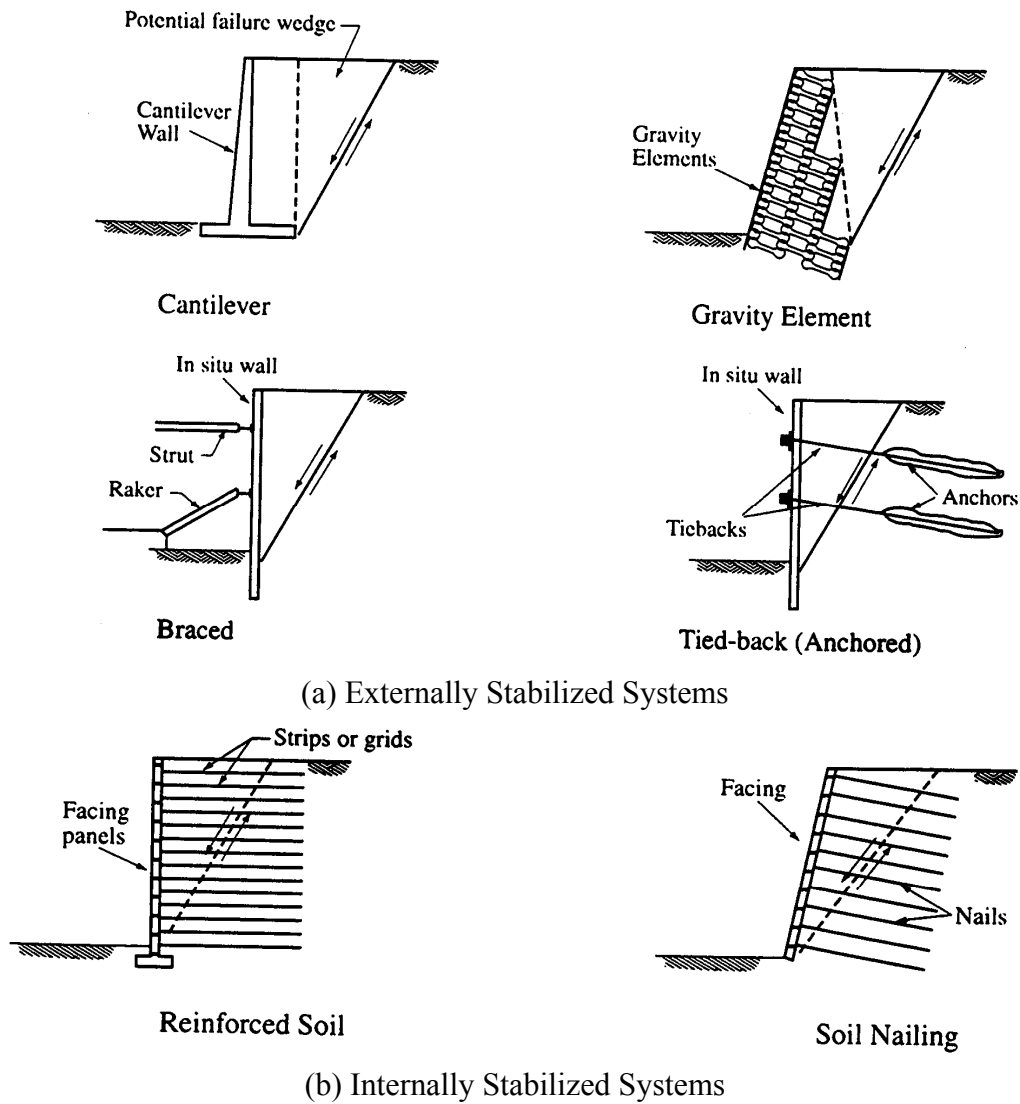


Figure 10-2. Variety of retaining walls (after O'Rourke and Jones, 1990)

## 10.01 Primary References:

The two primary references for earth retaining structures are:

FHWA (2005b). *Earth Retaining Structures - DRAFT*. Report No. FHWA-SA-05-046, Authors: Tanyu, B.F., Sabatini, P.J. and Berg, R.R., Federal Highway Administration, U.S. Department of Transportation.

AASHTO (2004 with 2006 Interims). *AASHTO LRFD Bridge Design Specifications*, 3rd Edition, American Association of State Highway and Transportation Officials, Washington, D.C.

## 10.1 CLASSIFICATION OF EARTH RETAINING STRUCTURES

Earth retaining systems may be classified according to:

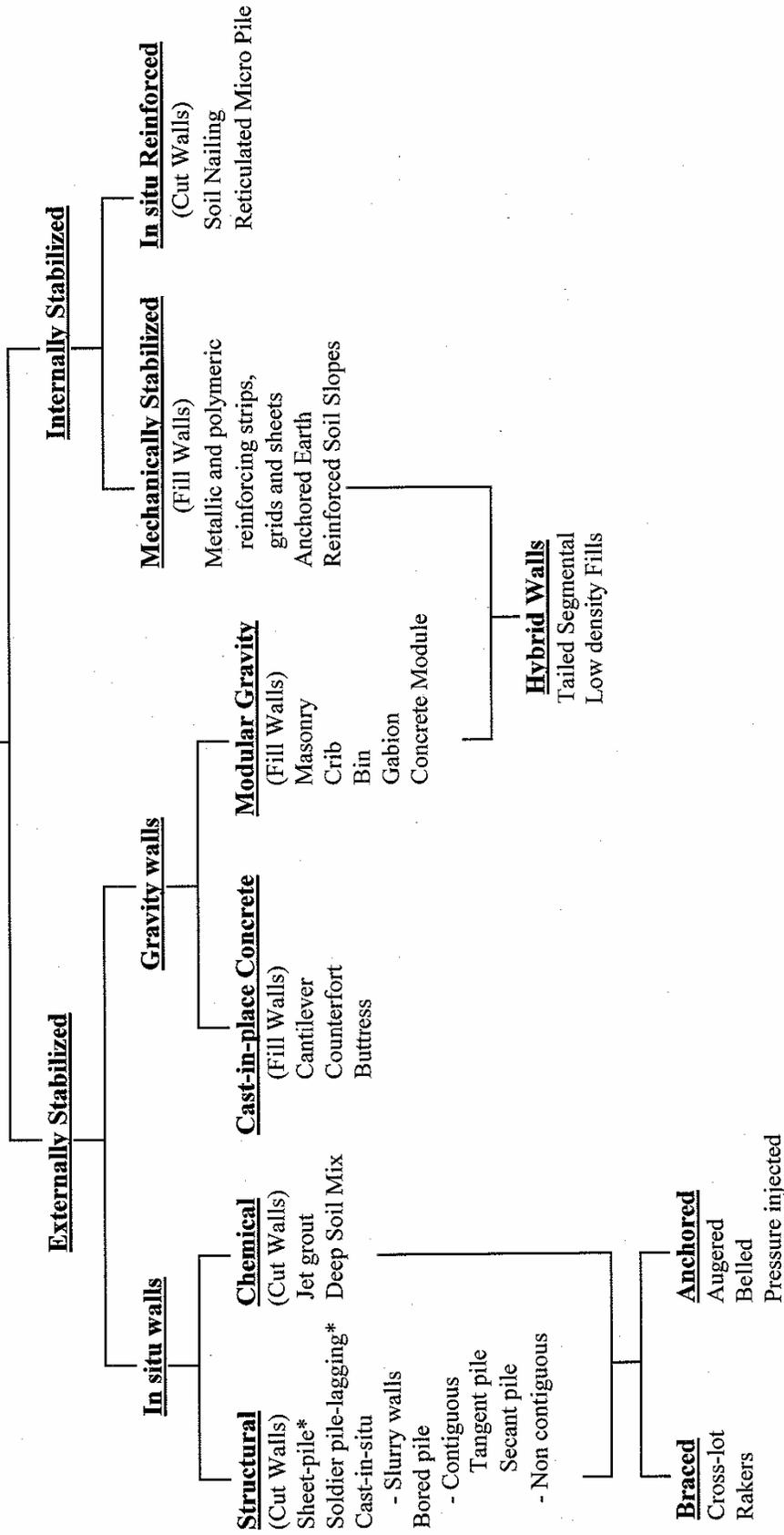
- load support mechanism, i.e., externally or internally stabilized walls;
- construction method, i.e., fill or cut walls; and
- system rigidity, i.e., rigid or flexible walls.

Every retaining wall can now be classified by using these three factors. For example, a sheet-pile wall would be classified as an **externally-stabilized cut** wall that is relatively **flexible**. A mechanically stabilized earth (MSE) wall is an **internally stabilized fill** wall that is relatively **flexible**. Further description of these classifications is provided subsequently.

### 10.1.1 Classification by Load Support Mechanism

The stability component of walls can be organized according to two principal categories: externally and internally stabilized systems (O'Rourke and Jones, 1990) as shown in Figure 10-3. An externally stabilized system uses an external structural wall against which stabilizing forces are mobilized. An internally stabilized system involves reinforcements installed within the retained soil mass and extending beyond the potential failure plane. Hybrid systems combine elements of both internally and externally supported walls.

# EARTH RETAINING STRUCTURES



\* can also be used in fill conditions

Figure 10-3. Classification of earth retaining systems (after O'Rourke and Jones, 1990).

Virtually all traditional types of walls may be regarded as externally stabilized systems (Refer to Figure 10-2a). Gravity walls, in the form of cantilever structures or gravity elements (e.g., bins, cribs and gabions), support the soil and, through their weight and stiffness, resist sliding, overturning, and shear. Bracing systems, such as cross-lot struts and rakers, provide temporary support for in situ structural and chemically stabilized walls. Ground anchors provide support through their pullout capacity in stable soils outside of the zone of potential failure.

It is in the area of internally stabilized systems that relatively new concepts have been introduced (Refer to Figure 10-2b). Shear transfer to mobilize the tensile capacity of closely spaced reinforcing elements embedded in the retained soil mass has enabled retaining structures to be constructed without an external structural wall element. The shear transfer mechanism allows a composite system of reinforcing elements and soil to serve as the primary structural entity. A facing is required on an internally stabilized system, however, its purpose is to prevent raveling and deterioration rather than to provide primary structural support.

### **10.1.2 Classification by Construction Method**

Earth retaining structures (ERS) can also be classified according to the method required for their construction, i.e., fill construction or cut construction. Fill wall construction refers to a wall system in which the wall is constructed from the base of the wall up to the top, i.e., “bottom-up” construction. Cut wall construction refers to a wall system in which the wall is constructed from the top of the wall down to the base concurrent with excavation operations, i.e., “top-down” construction. The classification of each wall system according to its construction method is also presented in Figure 10-3.

It is important to recognize that the “cut” and “fill” designations refer to how the wall is constructed, not necessarily the nature of the earthwork associated with the project. For example, a prefabricated modular gravity wall, which may be used to retain earth for a major highway cut, is considered a fill wall because its construction is not complete until the backfill has been placed from the “bottom-up” after the excavation for the cut has reached its final grade.

### **10.1.3 Classification by System Rigidity**

The rigidity or flexibility of a wall system is fundamental to the understanding of the development of earth pressures, discussed in Section 10.2. In simple terms, a wall is considered to be rigid if it moves as a unit in rigid body rotation and/or translation and does not experience bending deformations. Most gravity walls can be considered rigid walls. Flexible walls are those that undergo bending deformations in addition to rigid body motion. Such deformations result in a redistribution of lateral pressures from the more flexible to the stiffer portions of the system. Virtually all wall systems, except gravity walls, may be considered to be flexible.

### **10.1.4 Temporary and Permanent Wall Applications**

Permanent wall systems are generally considered to have a service life of 75 to 100 years. However, the ERS listed in Figure 10-3 are technically feasible for both temporary and permanent applications. In most cases, however, certain systems may not be cost-effective for temporary applications. Temporary walls generally have less restrictive requirements on material durability, design factors of safety, performance, and overall appearance than do permanent walls. Also, walls that can be constructed rapidly are often used for temporary applications. For example, MSE walls with segmental, precast facings are not typically used for temporary applications since the cost of the facing components and the select backfill may be more than 50 percent of the total cost of the wall.

The service life of temporary earth support systems is based on the time required to support the ground while the permanent systems are installed. This document has adopted the AASHTO guidance which considers temporary systems to be those that are removed upon completion of the permanent systems. The time period for temporary systems is commonly stated to be 18 to 36 months, but may be shorter or longer based on actual project conditions.

Temporary systems may be divided into “support of excavation” (SOE) temporary systems and “critical” temporary systems. In general the owner will determine which temporary systems are to be designated as critical. That decision is often based on the owner’s need to restrict lateral movement of the support system to minimize ground movements behind the support system. In general, specific components or design features for temporary systems may be designed to the same or similar criteria as used for permanent systems. Conversely, SOE systems are commonly designed to less restrictive criteria than permanent systems. The owner commonly assigns the responsibility for design and performance of SOE systems to the contractor. The design of SOE systems is often based more on system stability than on minimizing ground movements.

### 10.1.5 Wall Selection Considerations

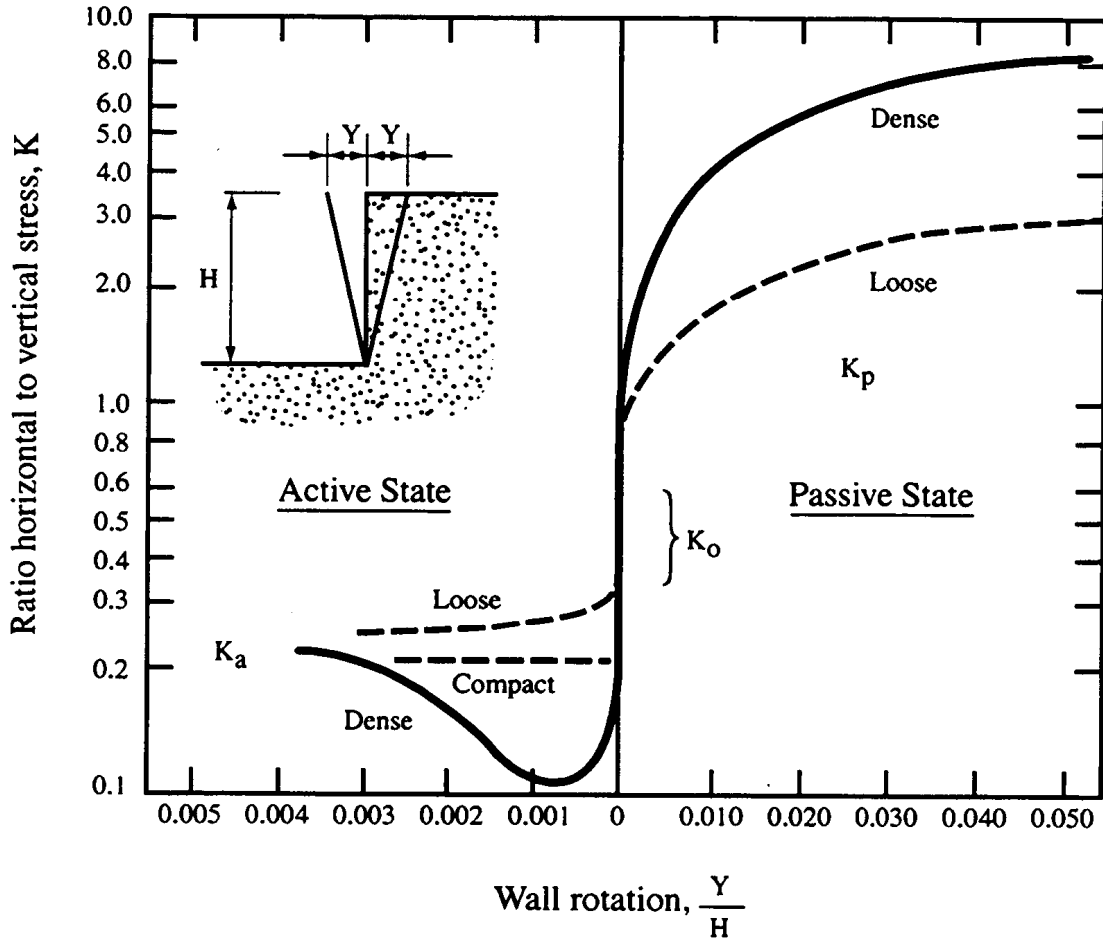
Given the wide variety of retaining walls as shown in Figure 10-3, it is important to select a wall that is most economical for the application being considered. The wall selection process should include consideration of various factors such as (1) ground type, (2) groundwater, (3) construction considerations, (4) speed of construction, (5) right of way, (6) aesthetics, (7) environmental concerns, (8) durability and maintenance, (9) tradition and (10) local contracting practices. A detailed discussion of these wall selection factors is outside the scope of this manual. The reader is referred to FHWA (2005b) where a systematic wall selection process considering these factors is described.

## 10.2 LATERAL EARTH PRESSURES

Some of the basic concepts of lateral earth and water pressures were discussed in Chapter 2. It is recommended that the reader should review Section 2.9 before proceeding further in this Chapter. Here the principles of lateral earth pressure are explained on the basis of deformation. A total lateral pressure diagram consistent with the assumed deformations is developed for use in assessing the forces acting on the wall from the backfill or retained ground. This section focuses primarily on theoretical earth pressure diagrams, which are most commonly used in the design of rigid gravity structures, nongravity cantilevered walls, MSE walls, and anchored walls with stiff structural facings such as diaphragm walls.

A wall system is designed to resist lateral earth pressures and water pressures that develop behind the wall. Earth pressures develop primarily as a result of loads induced by the weight of the backfill and/or retained in-situ soil, earthquake ground motions, and various surcharge loads. For purposes of earth retaining system design, three different types of lateral earth pressure are usually considered: (1) at-rest earth pressure; (2) active earth pressure; and (3) passive earth pressure. These conditions are shown in Figure 10-4 relative to lateral deformation of the walls. The conditions are defined as follows:

- At-rest earth pressure is defined as the lateral earth pressure that exists in level ground for a condition of no lateral deformation.
- Active earth pressure is developed as the wall moves away from the backfill or the retained soil. This movement results in a decrease in lateral pressure relative to the at-rest condition. A relatively small amount of lateral movement is necessary to reach the active condition.



Magnitude of Wall Rotation to Reach Failure

Soil type and condition	Rotation, $Y/H$	
	Active	Passive
Dense cohesionless	0.001	0.02
Loose cohesionless	0.004	0.06
Stiff cohesive	0.010	0.02
Soft cohesive	0.020	0.04

Figure 10-4. Effect of wall movement on wall pressures (after Canadian Geotechnical Society, 1992).

- Passive earth pressure is developed as the wall moves towards the backfill or the retained soil. This movement results in an increase in lateral pressure relative to the at-rest condition. The movements required to reach the passive condition are approximately ten times greater than those required to develop active earth pressure.

Each of these earth pressure conditions can be expressed in general form by:

$$p_h = Kp_o \quad 10-1$$

where  $p_h$  is the lateral earth pressure at a given depth behind the wall,  $p_o$ , is the vertical stress at the same depth, and  $K$  is the earth pressure coefficient that has a value related to the at-rest condition ( $K_o$ ), active conditions of movement, ( $K_a$ ), or passive conditions of movement, ( $K_p$ ).

As shown in Figure 10-4, the magnitudes of these earth pressure coefficients follow the relationship of  $K_p > K_o > K_a$ . The relationship between the magnitude of retaining wall movement, in this case rotation,  $Y/H$ , into or away from the retained material about its toe, and the horizontal pressure exerted by the soil is presented in Figure 10-4, with angular movement along the  $x$  axis and the mobilized coefficient of lateral earth pressure on the  $y$  axis. Figure 10-4 can also be used to estimate the state of stress for walls with uniform horizontal translation equal to  $Y$ . As illustrated in this figure, significantly larger lateral displacements are required to mobilize the passive resistance than those required to develop active pressures. The maximum values of  $K_a$  and  $K_p$  correspond to fully mobilized pressures that represent active and passive failure conditions, respectively.

**When the estimated wall movement is less than the value required to fully mobilize active or passive pressure, the earth pressure coefficient can be adjusted proportionally based on the graphical relationship presented in Figure 10-4.**

### 10.2.1 At-Rest Lateral Earth Pressure

The at-rest earth pressure represents the lateral effective stress that exists in a natural soil in its undisturbed state. For cut walls constructed in near normally consolidated soils, the at-rest earth pressure coefficient,  $K_o$ , can be approximated by the equation (Jaky, 1944):

$$K_o = 1 - \sin \phi' \quad 10-2$$

where  $\phi'$  is the effective (drained) friction angle of the soil. The magnitude of the at-rest earth pressure coefficient is primarily a function of soil shear strength and degree of

overconsolidation, which, as indicated in Chapter 7, may result from natural geologic processes for retained natural ground or from compaction effects for backfill soils.

In overconsolidated soils,  $K_o$  can be estimated as (Schmidt, 1966):

$$K_o = (1 - \sin \phi')(\text{OCR})^\Omega \quad 10-3$$

where  $\Omega$  is a dimensionless coefficient, which, for most soils, can be taken as  $\sin \phi'$  (Mayne and Kulhawy, 1982) and OCR is the overconsolidation ratio.

Usually, Equations 10-2 and 10-3 for the at-rest earth pressure coefficient are sufficiently accurate for normally to lightly overconsolidated soils provided the overconsolidation ratio has been evaluated from laboratory consolidation testing. For moderately to heavily overconsolidated clays, or where a more accurate assessment is required, laboratory triaxial tests on undisturbed samples and in-situ testing such as pressuremeter testing may be used.

For normally consolidated clay,  $K_o$  is typically in the range of 0.55 to 0.65; for sands, the typical range is 0.4 to 0.5. For lightly overconsolidated clays ( $\text{OCR} \leq 4$ ),  $K_o$  may reach a value up to 1; for heavily overconsolidated clays ( $\text{OCR} > 4$ ),  $K_o$  values may be greater than 2 (Brooker and Ireland, 1965). For heavily overconsolidated soils, values for  $K_o$  can be very large. A relatively stiff wall would be required to resist the large forces resulting from the lateral earth pressures in this case. For walls constructed in such soils, consideration should be given to performing pressuremeter tests, which provide a direct measure of lateral pressures in the ground.

In the context of wall designs consisting of steel soldier beams or sheet-pile wall elements, design earth pressures based on at-rest conditions are not typically used since at-rest earth pressures imply that the wall system undergoes no lateral deformation. This condition may be appropriate for heavily preloaded, stiff wall systems, but designing to a requirement of zero wall movement for flexible wall systems is not practical.

## 10.2.2 Active and Passive Lateral Earth Pressures

As discussed in Chapter 2, in stability analyses active and passive earth pressures are developed as a result of soil displacement within a failure zones developed behind the wall (active) or in front of the wall (passive) assuming that the wall displaces outward. For the purpose of illustration Figure 10-5 shows the two conditions with respect to wall movement relative to the backfill only. In one case the wall moves away from the backfill (active case) in the other case the wall moves into the backfill (passive case) As shown in the figure, the failure zone for both cases is typically bounded by the back face of the wall and a failure surface through the retained soil mass along which the soil has attained limiting equilibrium. In addition to the effect of lateral movements on the values of  $K_a$  and  $K_p$  shown in Figure 10-4, the magnitude of the active and passive earth pressure coefficients are functions of the soil shear strength, the backfill geometry, i.e., horizontal backfill surface or sloping ground surface above the wall, the orientation of the surface where the wall contacts the backfill or retained soil, i.e., vertical or inclined, and the friction and cohesive forces that develop on this surface as the wall moves relative to the retained ground.

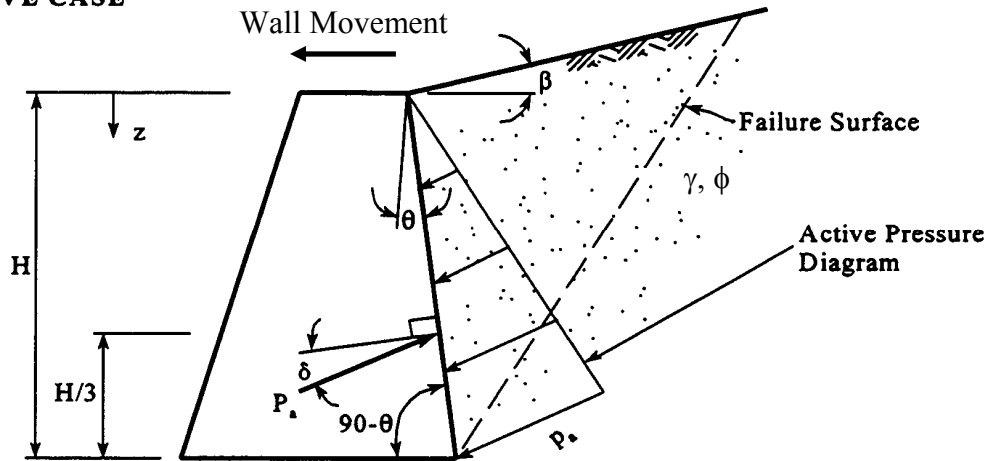
Active and passive earth pressure coefficients based on a plane wedge theory, which considers the effect of wall friction, sloping backfill and sloping wall face, was first proposed by Coulomb (1776) and are shown in Figure 10-5. The pressures calculated by using these coefficients are commonly known as the Coulomb earth pressures. Since Coulomb's method is based on limit equilibrium of a wedge of soil, only the magnitude and direction of the earth pressure is found. Pressure distributions and the location of the resultant are assumed to be triangular.

For simple cases involving vertical walls retaining homogeneous soil with a level ground surface, without friction between the soil and the wall face, and without the presence of groundwater, the formulas for computing the earth pressure coefficients can be simplified considerably by substituting,  $\delta = \theta = \beta = 0$  in Coulomb's equations, as shown in Figure 10-5. For such simplified cases,  $K_a$  and  $K_p$  can be expressed by Equations 10-4 and 10-5, respectively:

$$K_a = \frac{1 - \sin \phi'}{1 + \sin \phi'} = \tan^2(45 - \phi'/2) \quad 10-4$$

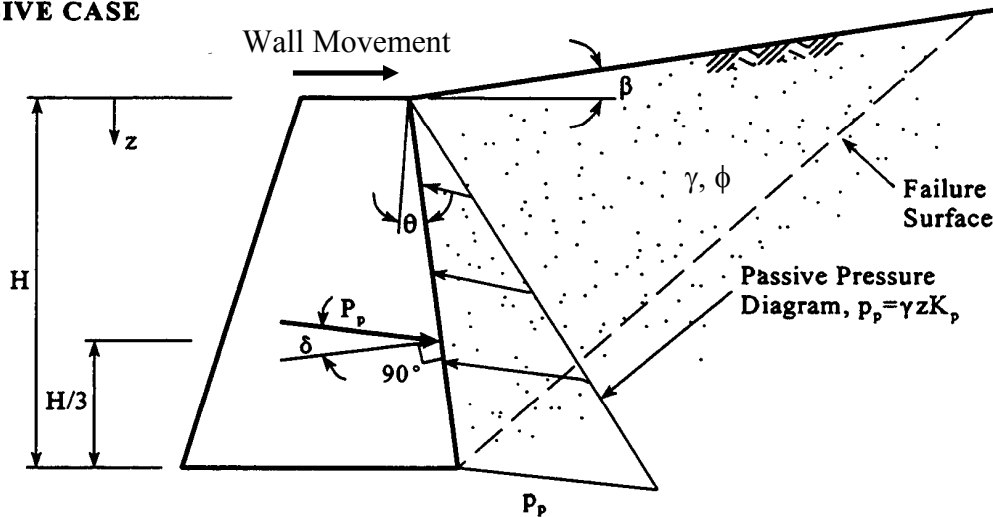
$$K_p = \frac{1 + \sin \phi'}{1 - \sin \phi'} = \tan^2(45 + \phi'/2) \quad 10-5$$

**ACTIVE CASE**



$$K_a = \frac{\cos^2(\phi - \theta)}{\cos^2 \theta \cos(\theta + \delta) \left[ 1 + \sqrt{\frac{\sin(\phi + \delta) \sin(\phi - \beta)}{\cos(\theta + \delta) \cos(\theta - \beta)}} \right]^2}$$

**PASSIVE CASE**



$$K_p = \frac{\cos^2(\theta + \phi)}{\cos^2 \theta \cos(\theta - \delta) \left[ 1 - \sqrt{\frac{\sin(\phi + \delta) \sin(\phi + \beta)}{\cos(\theta - \delta) \cos(\theta - \beta)}} \right]^2}$$

**Figure 10-5. Coulomb coefficients  $K_a$  and  $K_p$  for sloping wall with wall friction and sloping cohesionless backfill (after NAVFAC, 1986b).**

These simplified equations were also derived independently by Rankine (1857). Hence, the earth pressures computed by using these equations are commonly known as the Rankine earth pressures.

For a cohesionless soil with a groundwater table, the effective lateral earth pressure acting on the wall at any depth,  $z$ , below the surface is a function of the pore water pressure  $u$  as follows,

$$p_a' = K_a(\gamma z - u) \quad 10-6$$

$$p_p' = K_p(\gamma z - u) \quad 10-7$$

### 10.2.3 Effect of Cohesion on Lateral Earth Pressures

For a cohesive soil defined by effective stress strength parameters  $\phi'$  and  $c'$ , the active and passive earth pressure coefficients are:

$$K_a = \tan^2 (45 - \phi'/2) - \frac{2c'}{p_o'} \tan^2 (45 - \phi'/2) \quad 10-8$$

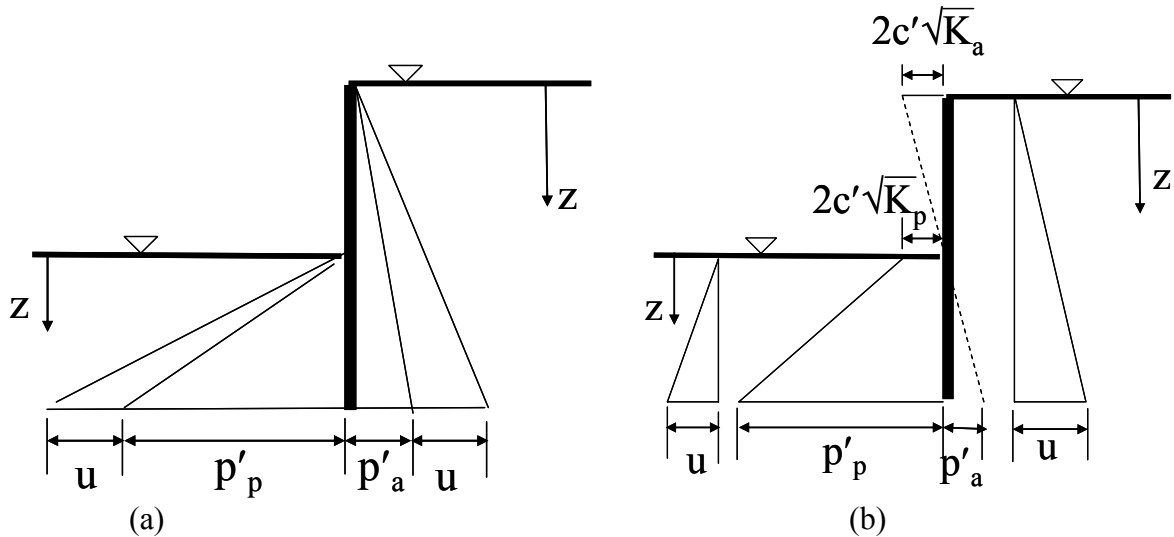
$$K_p = \tan^2 (45 + \phi'/2) + \frac{2c'}{p_o'} \tan^2 (45 + \phi'/2) \quad 10-9$$

Figure 10-6(a) presents active and passive pressure distributions for cohesionless soils ( $c' = 0$ ) while Figure 10-6(b) shows similar pressure distributions for  $c'$ - $\phi'$  soils.

For a  $c'$ - $\phi'$  soil with a groundwater table, the effective lateral earth pressure acting on the wall at any depth,  $z$ , below the surface is,

$$p_a' = K_a(\gamma z - u) - 2c'\sqrt{K_a} \quad 10-10$$

$$p_p' = K_p(\gamma z - u) + 2c'\sqrt{K_p} \quad 10-11$$



**Figure 10-6. (a) Wall pressures for a cohesionless soil, and (b) Wall pressures for soil with a cohesion intercept – with groundwater in both cases (after Padfield and Mair, 1984)**

Theoretically, in soils with cohesion, the active earth pressure behind the wall becomes negative from the ground surface to a critical depth  $z$  where  $\gamma z$  is less than  $2c'\sqrt{K_a}$ . This critical depth is referred to as the “tension crack.” The active earth pressure acting against the wall within the depth of the tension crack is assumed to be zero. Unless positive drainage measures are provided, water infiltration into the tension crack may result in hydrostatic pressure on the retaining structure.

Use of values of  $c'$  for the retained soil, greater than say, 100 psf (5 kPa), results in a significant depth of theoretical negative active earth pressure. Therefore, it is important either to:

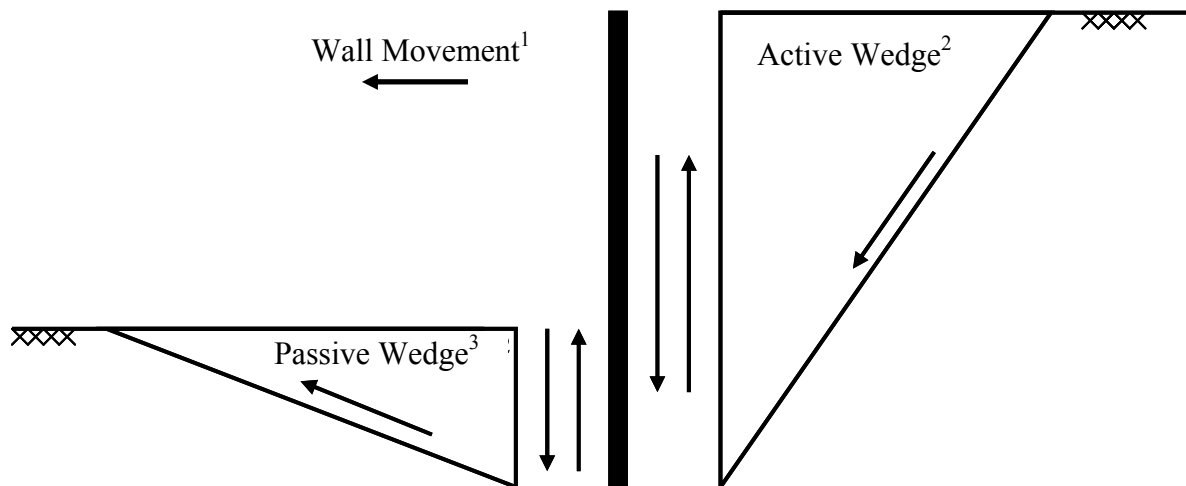
- reduce  $c'$  towards the surface, which may be realistic for many clays in view of weathering;
- or
- assume that the effective pressure on the wall at any depth should not be less than 30z psf where  $z$  = depth in ft ( $5z$  kN/m<sup>2</sup> ( $z$  = depth in m)).

**In all cases where water is present in the soil, full hydrostatic pressure is added to the lateral earth pressure computed by Equations 10-8 to 10-11 to obtain the total lateral pressure that will be experienced by a retaining wall.**

### 10.2.4 Effect of Wall Friction and Wall Adhesion on Lateral Earth Pressures

In practice, walls are not smooth. As indicated previously, wall friction and wall adhesion modify the stress distribution near a wall. Therefore, wall friction,  $\delta$ , and wall adhesion,  $c_w$ , should both be considered as proportions of  $\phi'$ , and  $c'$  or  $s_u$ , respectively. For a rigid wall moving away from the retained soil, the frictional forces exerted by the wall on the soil are in the sense shown in Figure 10-7. The active wedge moves down with respect to the wall, while the passive wedge moves upwards.

An important exception to this mechanism is when the wall acts as a significant load-bearing element, when large vertical loads are applied to the top of the wall, or when an inclined ground anchor is stressed to an appreciable load and the vertical component of the load acts downward. In such cases, the wall has to move down relative to the soil on both sides of the wall in order to mobilize the required skin friction to support the load. Therefore, the friction acts to increase the pressures on both the active and passive sides, because it acts on the soil wedges in a downward direction. This effect, however, is neglected because limiting or failure conditions are considered in calculation of overall stability and the directions in which the frictional forces act should be taken as shown in Figure 10-7.



- Note: (1) Assume wall moves as a rigid body to the left.  
(2) Active wedge moves downward relative to wall  
(3) Passive wedge moves upward relative to wall.

**Figure 10-7. Wall friction on soil wedges (after Padfield and Mair, 1984)**

Wall friction,  $\delta$ , and wall adhesion,  $c_w$ , have an important effect on soil pressures. Equations 10-10 and 10-11 can be written to account for those effects in a more general as follows:

$$p_a' = K_a(\gamma z - u) - K_{ac}c' \quad 10-12$$

$$p_p' = K_p(\gamma z - u) + K_{pc}c' \quad 10-13$$

where  $K_a$  and  $K_p$  depend on  $\delta$  and  $K_{ac}$  and  $K_{pc}$  depend on  $\delta$  and  $c_w$ , and  $p_a'$  and  $p_p'$  are the components of effective pressure normal to the wall. Where  $c'$  is incorporated into the soil strength characterization, approximate values of  $K_{ac}$  and  $K_{pc}$  should be calculated from the following expressions:

$$K_{ac} = 2 \sqrt{K_a (1 + c_w / c')} \quad 10-12a$$

$$K_{pc} = 2 \sqrt{K_p (1 + c_w / c')} \quad 10-13a$$

Different values of  $\delta$  are given by several sources. As shown in Table 10-1, values of  $\delta$  depend on soil type and the wall material. The maximum wall friction suggested for design is:

$$\text{Active: } \delta = 2/3 \phi'$$

$$\text{Passive: } \delta = 1/2 \phi'$$

Where a cohesion intercept is used as part of the characterization of strength in terms of effective stress, a maximum wall adhesion of  $c_w = 0.5c'$  could be used, but in view of the inevitable remolding of the clay close to the wall by any construction process, it is recommended that no wall adhesion be allowed in the design.

The values of wall friction provided above and in Table 10-1 are maximum values for design. These values can be adopted in most cases, but the design engineer should consider any circumstances where the values might be affected by the relative movement of the soil and the wall. For example, on the active side, reduced values should be used if there is a tendency for the wall to move downwards, e.g., for load-bearing walls or walls supported by prestressed ground anchors. For walls retaining soft cohesive soils or granular soils that will be subjected to significant vibration, e.g., walls near railway tracks or machine foundations,  $\delta$  should be assumed to be zero in the design.

**Table 10-1**  
**Wall friction and adhesion for dissimilar materials (after NAVFAC, 1986b)**

Interface Materials	Friction Factor, $\tan \delta$	Friction angle, $\delta$ degrees
<b>Mass concrete on the following foundation materials:</b>		
Clean sound rock	0.70	35
Clean gravel, gravel sand mixtures, coarse sand	0.55 to 0.60	29 to 31
Clean fine to medium sand, silty medium to coarse sand, silty or clayey gravel	0.45 to 0.55	24 to 29
Clean fine sand, silty or clayey fine to medium sand	0.35 to 0.45	19 to 24
Fine sandy silt, nonplastic silt	0.30 to 0.35	17 to 19
Very stiff and hard residual or preconsolidated clay	0.40 to 0.50	22 to 26
Medium stiff and stiff clay and silty clay (Masonry on foundation materials has same friction factor)	0.30 to 0.35	17 to 19
<b>Steel sheet piles against the following soils:</b>		
Clean gravel, gravel-sand mixtures, well-graded rock fill with spalls	0.40	22
Clean sand, silty sand-gravel mixtures, single size hard rock fill	0.30	17
Silty sand, gravel or sand mixed with silt or clay	0.25	14
Fine sandy silt, nonplastic silt	0.20	11
<b>Formed concrete or concrete sheet piling against the following soils:</b>		
Clean gravel, gravel-sand mixture, well-graded rock fill with spalls	0.40 to 0.50	22 to 26
Clean sand, silty sand-gravel mixture, single size hard rock fill	0.30 to 0.40	17 to 22
Silty sand, gravel or sand mixed with silt or clay	0.30	17
Fine sandy silt, nonplastic silt	0.25	14
<b>Various structural materials:</b>		
<b>Masonry on masonry, igneous and metamorphic rocks:</b>		
Dressed soft rock on dressed soft rock	0.70	35
Dressed hard rock on dressed soft rock	0.65	33
Dressed hard rock on dressed hard rock	0.55	29
Masonry on wood (cross grain)	0.50	26
Steel on steel at sheet pile interlocks	0.30	17
Interface Materials (Cohesion)	Adhesion $c_u$ (kPa)	
Very soft cohesive soil (0 - 12 kPa)	0 - 12	
Soft cohesive soil (12 - 24 kPa)	12 - 24	
Medium stiff cohesive soil (24 - 48 kPa)	24 - 36	
Stiff cohesive soil (48 - 96 kPa)	36 - 45	
Very stiff cohesive soil (96 - 192 kPa)	45 - 62	

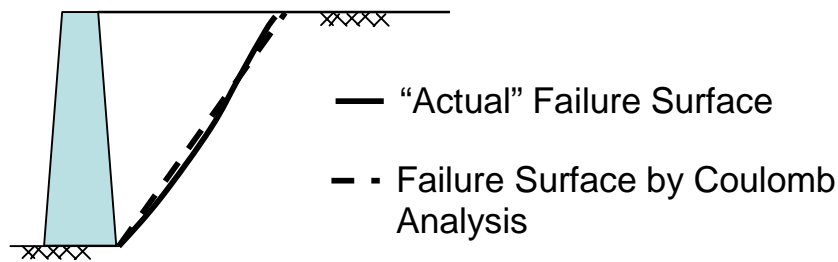
The effect of wall friction on the Rankine and Coulomb methods of earth pressure computation is as follows:

1. The Rankine method cannot take account of wall friction. Accordingly,  $K_a$  is overestimated slightly and  $K_p$  is under-estimated, thereby making the Rankine method conservative for most applications.
2. The Coulomb theory can take account of wall friction, but the results are unreliable for passive earth pressures for wall friction angle values greater than  $\phi'/3$  because the failure surface is assumed to be a plane. The failure wedges assumed in the Coulomb analysis take the form of straight lines as shown in Figure 10-8. This may be contrasted with the curved shapes of failure surface observed in model tests. The curvature results from the disturbing influence of wall friction on the stress field near the wall. The error in the Coulomb solutions results in  $K_a$  being underestimated slightly and  $K_p$  being overestimated very significantly for large values of  $\phi'$ .

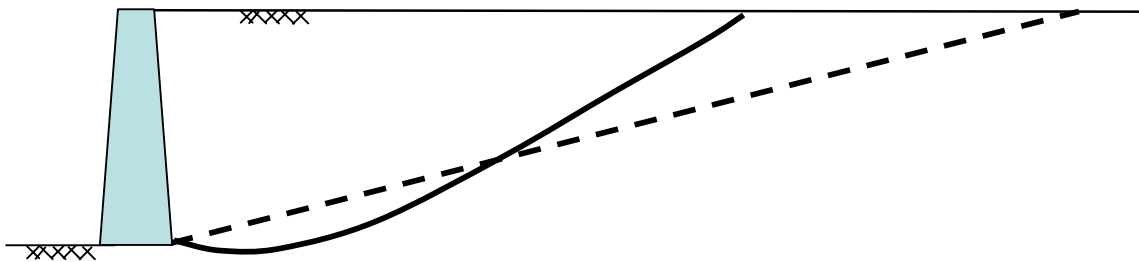
If the angle of wall friction  $\delta$  is small, the failure surface is almost linear. For large values of  $\delta$ , the failure surface is curved and can be approximated by a log-spiral. The deviation of the curved surface from a planar surface is minor for the active case but significant for the passive case as shown in Figure 10-8. For most applications, the effect of wall friction on active earth pressures is relatively small and is often neglected.

For the passive case, however, large values of  $\delta$  cause downward tangential shear forces to act on the passive wedge of soil adjacent to the wall, increasing its resistance to upward movement. This increased resistance to upward movement causes a curved failure surface to occur in the soil, as shown in Figure 10-8b. The soil fails on this curved surface of least resistance and not on the Coulomb plane, which would require greater lateral driving force. Hence, passive pressures computed on the basis of the plane wedge theory are always greater than those calculated on the basis of a log-spiral failure surface and may be on the unsafe side since passive earth pressure forces are generally resisting forces in stability analyses.

Based on the above discussions, it is recommended that the log-spiral theory be used for the determination of the passive earth pressure coefficients. Charts for two common wall configurations, sloping wall with level backfill and vertical wall with sloping backfill based on the log-spiral theory are presented in Figures 10-9 and 10-10 (Caquot and Kerisel, 1948; NAVFAC, 1986b). For walls that have a sloping backface and sloping backfill, the passive earth pressure coefficient can be calculated as indicated in Figure 10-5 by using  $\delta = \phi'/3$ .



(a) Active Case ( $\phi' = 30^\circ$ ,  $\delta = 30^\circ$ )



(b) Passive Case ( $\phi' = 30^\circ$ ,  $\delta = 30^\circ$ )

**Figure 10-8. Comparison of plane and log-spiral failure surfaces (a) Active case and (b) Passive case (after Sokolovski, 1954) – Note: Depiction of gravity wall is for illustration purpose only.**

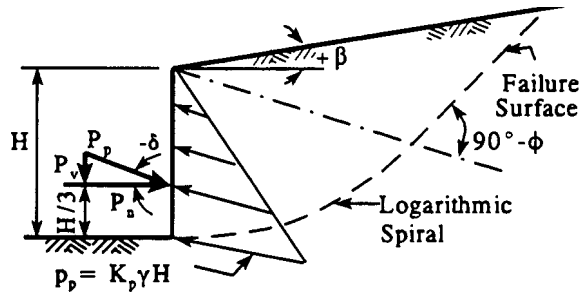
For the active case, the resultant load predicted by using coefficients based on the plane wedge theory is within 10 percent of that obtained with the more exact log-spiral theory. Hence, for the active case, Coulomb's theory can be used to calculate the earth pressure coefficient (Refer to Figure 10-5).

For some wall types, such as cantilever retaining walls and an MSE walls, the "interface" where the earth pressures are computed is within the retained soils along a vertical plane passing through the heel of the base slab. In such cases, there is soil-to-soil contact and the resultant may be oriented at the angle of mobilized friction. The angle of mobilized friction depends on the factor of safety used for the angle of internal friction. For these cases, it is generally conservative to assume that the earth pressure is parallel to the slope of the backfill.



REDUCTION FACTOR (R) OF $K_p$ FOR VARIOUS RATIOS OF $-\delta/\phi$									
$\phi$	$\delta/\phi$	-0.7	-0.6	-0.5	-0.4	-0.3	-0.2	-0.1	0.0
10		.978	.962	.946	.929	.912	.898	.881	.864
15		.961	.934	.907	.881	.854	.830	.803	.775
20		.939	.901	.862	.824	.787	.752	.716	.678
25		.912	.860	.808	.759	.711	.666	.620	.574
30		.878	.811	.746	.686	.627	.574	.520	.467
35		.836	.752	.674	.603	.536	.475	.417	.362
40		.783	.682	.592	.512	.439	.375	.316	.262
45		.718	.600	.500	.414	.339	.276	.221	.174

Note: Curves shown are for  $\delta/\phi = -1$



$$P_p = K_p \gamma H^2 / 2; P_n = P_p \cos \delta; P_v = P_p \sin \delta$$

Example:  $\phi = 25^\circ; \beta/\phi = -0.2; \delta/\phi = -0.3$

$$K_p = R(K_p \text{ for } \delta/\phi = -1) = (0.711)(3.62) = 2.58$$

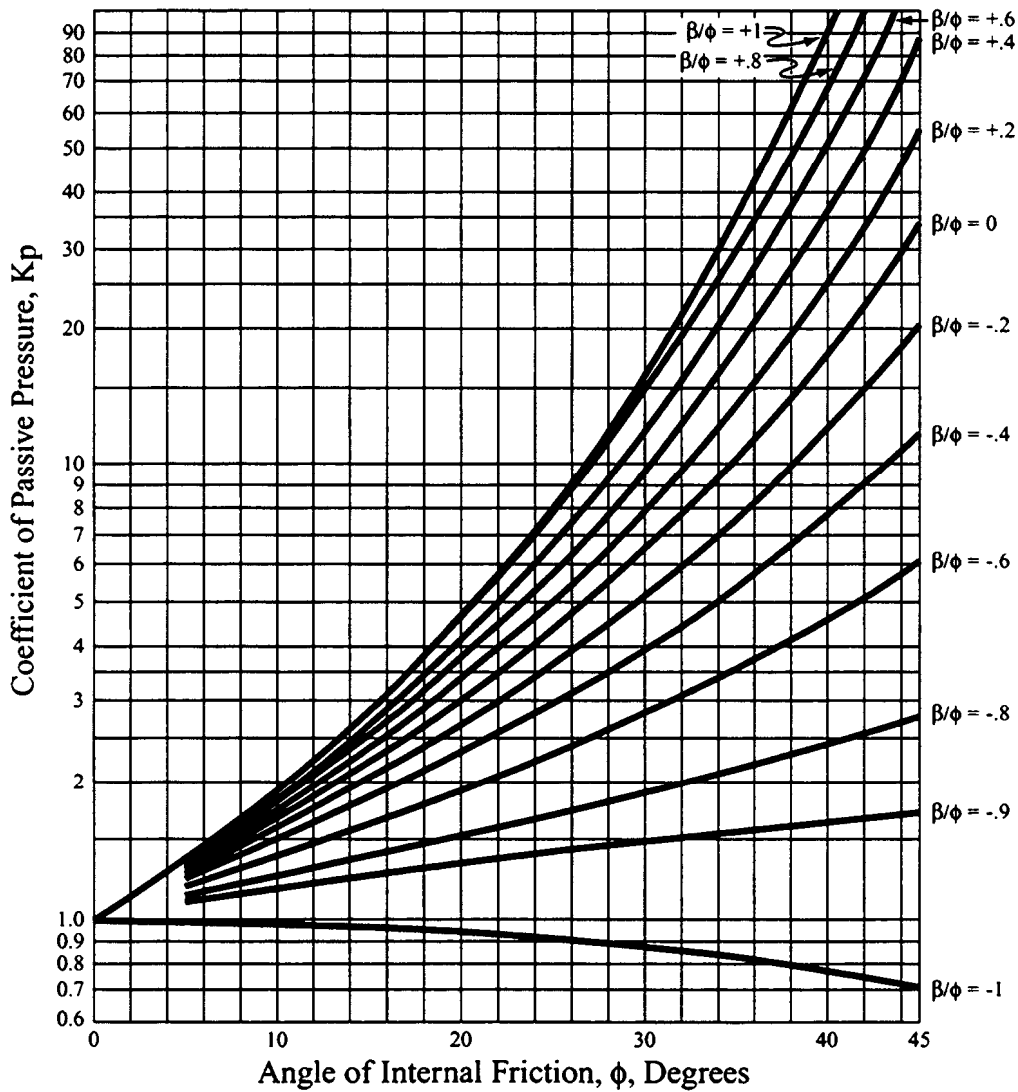
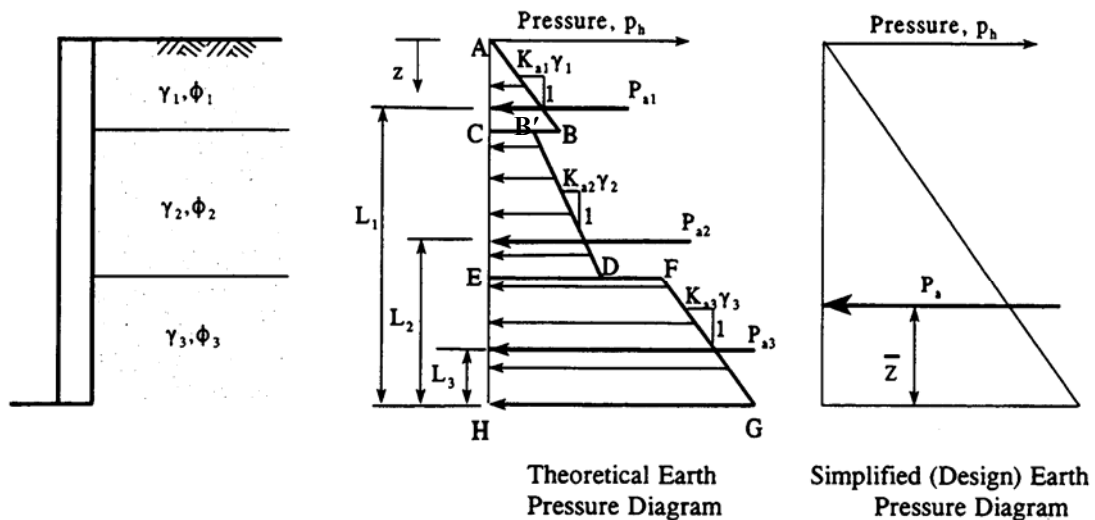


Figure 10-10: Passive coefficients for vertical wall with wall friction and sloping backfill (Caquot and Kerisel, 1948; NAVFAC, 1986b).

### 10.2.5 Theoretical Lateral Earth Pressures in Stratified Soils

For stratified or non-homogeneous soils, the theoretical earth pressures are assumed to be distributed as shown in Figure 10-11 where the discontinuities in the earth pressure diagram occur at the boundary between soil strata having different unit weights and shear strength parameters. Unless the computed earth pressures vary widely with depth, the total applied lateral force determined from the computed pressure diagram may be redistributed to a corresponding simplified equivalent triangular pressure diagram as indicated in Figure 10-11.

For complex cases such as layered soils, irregular backfill, irregular surcharges, wall friction, and sloping groundwater level, pressures can be determined by graphical solutions. Among the many graphical solutions are Culmann's method (1866) and the Trial Wedge method. These procedures can be found in Bowles (1996) or NAVFAC (1986b). The Trial Wedge method has the advantage of including cohesion as a soil parameter in the analysis.



The lateral force is equal to the area of the pressure diagram. Thus,

$$P_{a1} = \text{Area ABC} \quad P_{a2} = \text{Area CB'DE} \quad P_{a3} = \text{Area EFGH}$$

Resultant (total) active force per unit length,  $P_a = P_{a1} + P_{a2} + P_{a3}$

$$\text{Location of resultant from base of wall, } \bar{z} = \frac{P_{a1}L_1 + P_{a2}L_2 + P_{a3}L_3}{P_a}$$

- Use buoyant unit weight for soils below water table.
- Add water pressure as appropriate to obtain total lateral pressure.
- The simplified distribution may not be justified for all soil conditions. Use judgment to determine validity of such simplified distributions.

Figure 10-11. Pressure distribution for stratified soils.

### **10.2.6 Semi Empirical Lateral Earth Pressure Diagrams**

The earth pressure distributions discussed in the previous sections are strictly applicable to rigid wall systems, i.e., walls that translate and/or rotate as a unit and do not experience bending deformations. Most gravity walls can be considered rigid walls.

If a wall system undergoes bending deformations in addition to rigid body motion then such a wall system is considered flexible. Virtually all wall systems, except gravity walls, may be considered to be flexible. The bending deformations result in a redistribution of the lateral pressures from the more flexible to the stiffer portions of the system. Thus, in these walls the final distribution and magnitude of the lateral earth pressure may be considerably different from those used for rigid walls. For example, soldier-pile and lagging walls with multiple levels of support are usually designed by using empirical earth pressure distributions based on observed data. The shape of these empirical earth pressure distributions may vary from rectangular to trapezoidal. The magnitude of the pressures may also vary depending on the soil type.

Other factors that may influence the development of earth pressures are the type of construction, e.g., “bottom-up” or “top-down,” the wall support mechanism, e.g., tie-backs, struts, rakers, soil nails, reinforcing elements, single or multiple levels of support, etc., the geometry of the retained soil, e.g., silo pressure, the superimposed or surcharge loads, e.g., strip, line, concentrated, or equipment loads, and the type of analysis, e.g., static or seismic. In addition, for cases of soil reinforced by inclusions such as MSE walls or soil-nailed walls, different types of earth pressure distributions are used to evaluate the internal and external stability of the wall system. The empirical earth pressure distributions are generally related to the basic earth pressure coefficients  $K_a$ ,  $K_p$  and  $K_o$ , which, as indicated previously, are a function of the shear strength of the soil.

### **10.2.7 Lateral Earth Pressures in Cohesive Backfills**

Most DOTs involved in the design and procurement of fill wall systems, such as MSE walls, have well-defined backfill material requirements. In general, specifications for wall backfill require high-quality, granular, relatively free-draining backfills. However, in some cases a poorer quality on-site backfill material may be used, especially for temporary systems. These poorer quality backfills are generally more fine-grained and not free-draining. Methods to calculate earth pressures in clayey soils were described previously. In this section cautions are provided regarding the use of fine-grained cohesive backfill soils.

Lateral pressures can be caused by the volume expansion of ice in fine-grained soils such as fine sand, silt and clay. Lateral pressures due to volume expansion of the retained soil may achieve relatively high values that are difficult to predict. Since structures are usually not designed to withstand frost-generated stresses, provisions should be made so that frost-related stresses will not develop behind the structure or be kept to a minimum. The use of one or more of the following measures may be necessary:

- Isolate the backfill from underground sources of water either by providing a permeable drainage system or an impervious barrier;
- Use pervious backfill and provide weep holes in the structure;
- Provide an impervious soil layer near the ground surface, and grade the ground behind the wall to drain surface water away from the wall.

Expansive clays can cause very high lateral pressures on the back of a retaining structure and should therefore be avoided whenever possible. In cases where expansive clays are present behind a wall, swelling pressures should be evaluated based on laboratory tests so that the wall can be designed properly to withstand these swelling pressures, which can be significant. Alternatively, one of the following measures can be taken:

- A granular filter material can be provided between the clay backfill and the back of the wall. This material will drain the groundwater away from the expansive soil and, at the same time act as a buffer zone between the expansive soil and the structure.
- The expansive soil can be treated with lime to reduce or even eliminate its swelling potential, if the soil does not contain gypsum. Expansive soils that contain gypsum should not be treated with lime because the combination of the minerals in expansive soils with gypsum and water may lead to the formation of ettringite, which has a much higher swelling potential than the untreated expansive soils.

The following is noted by Duncan, *et al.* (1990) concerning the use of clayey soils as backfill for fill wall applications:

- Clayey backfills generally have lower drained shear strength than cohesionless soils. Low drained shear strength results in: (1) larger lateral earth pressures against the back of the wall; (2) lower frictional resistance along the reinforcement for MSE

walls that employ frictional reinforcement; and (3) lower bearing value for MSE walls that employ passive reinforcement.

- Clayey backfills are more plastic and contain more fines than cohesionless soils. Higher plasticity results in: (1) poor drainage and the potential for the development of water pressures behind the wall; (2) the potential for freezing of retained water and development of ice pressures on the back of the wall; and (3) greater potential for corrosion of metallic reinforcements for MSE walls.
- Clayey backfills have the potential to undergo creep deformations that can lead to higher earth pressures and greater wall face deformations than will occur with soils that do not exhibit significant creep potential. Earth pressures used for design of gravity walls employing clayey backfills should be based on past performance and field experience, as wall design methods do not consider the effects of creep.

Despite these problems, silts and clays may be used as backfill soils provided suitable design procedures are employed, including conservative estimates of lateral earth pressures, and construction control measures are incorporated into the contract documents. When silts and clays are used as backfills, walls may need to be designed for pressures between active and at-rest conditions. For soils that are deemed to have high swell potential, an earth-pressure coefficient as great as 1.0 may be used for design (Canadian Geotechnical Society, 1992). In all cases, water pressures and appropriate surcharge loads also need to be added to these earth pressures.

In general, any permanent fill wall system that incorporates silty or clayey backfills must have an appropriately designed subsurface and surface drainage system to minimize pore pressure build-up and soil saturation. Such wall systems should also include periodic measurements of wall face movements.

### 10.3 LATERAL PRESSURES DUE TO WATER

In retaining wall design, it is general practice to provide drainage paths, commonly known as “weep holes,” through the earth retaining structure, or use other methods to drain groundwater that may otherwise collect behind the structure. The purpose of these drainage features is to prevent the development of water pressure on the structure. Occasionally, however, it may not be feasible or desirable to drain the water from behind the structure. For example, maintenance of existing ground water levels may be desirable to safeguard against potential settlement of adjacent structures or to prevent contaminated groundwater from entering the excavation. In such instances, the earth retaining structure must be designed for both lateral earth pressure and water pressure.

Computation of active lateral earth pressures for the case of a uniform backfill and static groundwater is illustrated in Figure 10-12. In this case, the water pressure represents a hydrostatic condition since there is no seepage or flow of water through the soil. The lateral earth pressure below the water level is based on the effective vertical stress,  $p'_o$ , times the active lateral earth pressure coefficient. The lateral pressure due to the water is added to the active lateral earth pressure to obtain the total lateral pressure on the wall. By analogy to lateral earth pressure coefficients, the lateral water pressure coefficient = 1.0. The lateral pressure computations should consider the greatest unbalanced water head anticipated to act on the wall, since this generally results in the largest total lateral load.

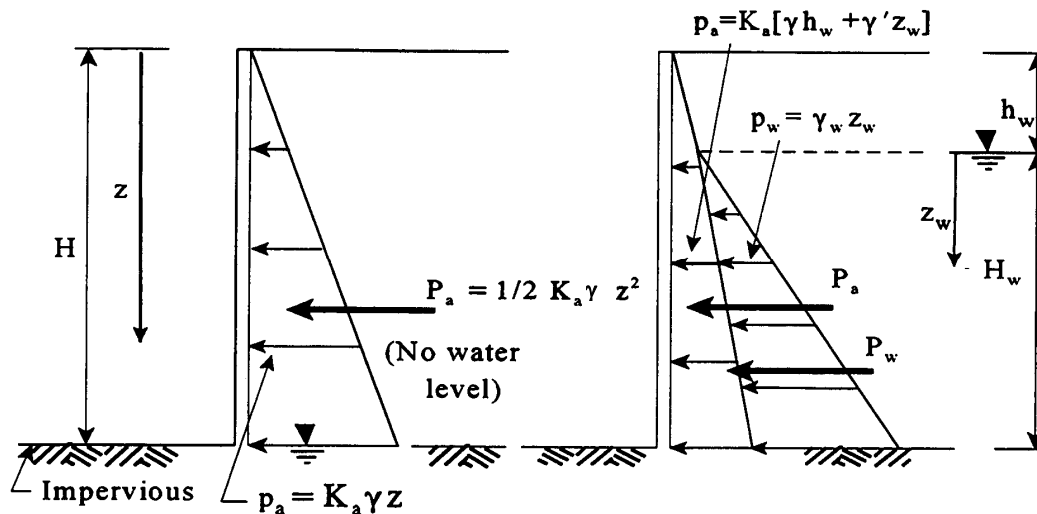
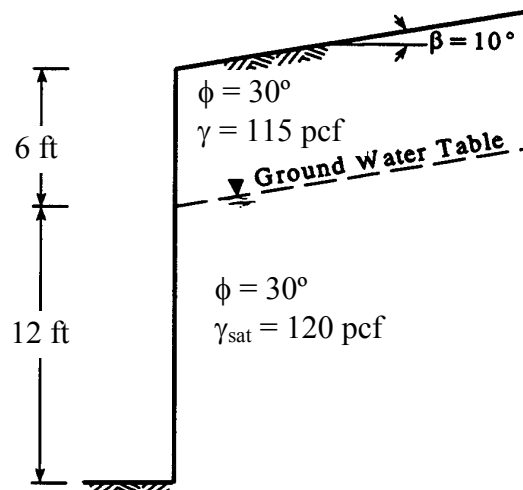


Figure 10-12. Computation of lateral pressures for static groundwater case.

For cases where seepage may occur through or beneath the earth retaining structure, the resulting seepage gradients will result in an increase or reduction in the water pressure depending on the direction of the seepage path. For such cases, flow net procedures can be used to compute the lateral pressure distribution due to water.

The concepts of lateral earth pressures and lateral pressures due to water are illustrated in Example 10-1.

**Example 10-1:** For the wall configuration shown below, construct the lateral pressure diagram. Assume the face of the wall to be smooth ( $\delta = 0$ ,  $c_w = 0$ ).



**Solution:**

Use the Coulomb method (Figure 10-5) for  $\phi = 30^\circ$ ,  $\beta = 10^\circ$ ,  $\theta = 0$ , and  $\delta = 0$ :

$$K_a = 0.374$$

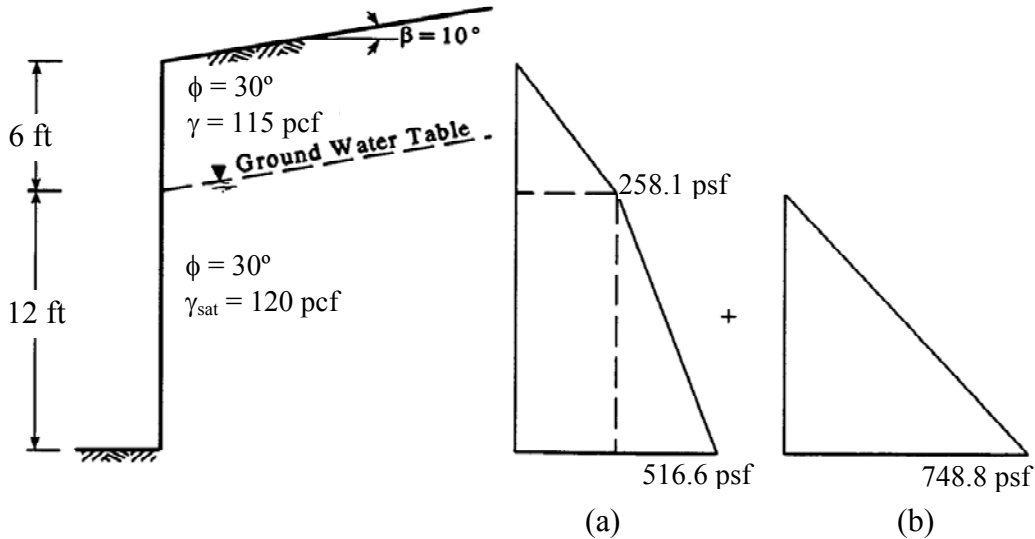
The pressures at various depths can then be calculated as shown in a tabular format as follows. Based on the values in the table, the lateral pressure diagrams due to earth and water can be constructed as shown below. The total lateral pressure diagram is the sum of the two lateral pressure diagrams shown in the figure accompanying this example.

**Effective Lateral Earth Pressures,  $p'_a$**

z, ft	$p_o$ , psf	$p_a = K_a p_o$ , psf
0	0	0
6	(115 pcf) (6 ft) = 690.0 psf	0.374(690.0 psf) = 258.1 psf
18	690 psf + (120 pcf - 62.4 pcf)(12 ft) = 1381.2 psf	0.374(1381.2 psf) = 516.6 psf

### Hydrostatic Pressure, $u = K_w u_w$

z, ft	$z_w$ , ft	$u_w = z_w \gamma_w$ , psf	Lateral water pressures, u psf
0	0	0	= 0
6	0	0	= 0
18	12	12 ft (62.4 pcf) = 748.8 psf	1.0(748.8 psf) = 748.8 psf



**(a) Lateral effective earth pressure diagram and (b) Lateral water pressure diagram.**

## 10.4 LATERAL PRESSURE FROM SURCHARGE LOADS

### 10.4.1 General

Surcharge loads on the backfill surface near an earth retaining structure also cause lateral pressures on the structure. Typical surcharge loadings may result from railroads, highways, sign/light structures, electric/telecommunications towers, buildings, construction equipment, and material stockpiles.

The loading cases of particular interest in the determination of lateral pressures are:

- uniform surcharge;
- point loads;
- line loads parallel to the wall; and
- strip loads parallel to the wall.

Figure 10-13 shows examples of retaining walls with surcharge loads.



(a)



(b)

**Figure 10-13: (a) Retaining wall with uniform surcharge load and (b) Retaining wall with line loads (railway tracks) and point loads (catenary support structure).**

### 10.4.2 Uniform Surcharge Loads

Surcharge loads are vertical loads applied at the ground surface, which are assumed to result in a uniform increase in lateral pressure over the entire height of the wall. The increase in lateral pressure for a uniform surcharge loading can be written as:

$$\Delta p_h = Kq_s \quad 10-14$$

where:  $\Delta p_h$  is the increase in lateral earth pressure due to the vertical surcharge load,  $q_s$ , applied at the ground surface, and  $K$  is an appropriate earth pressure coefficient. Examples of surcharge loads for highway wall system applications include: (1) dead load surcharges such as that resulting from the weight of a bridge approach slab or concrete pavement; (2) live load surcharges such as that due to traffic loadings; and (3) surcharges due to equipment or material storage during construction of the wall system.

When traffic is expected to come to within a distance from the wall face equivalent to one-half the wall height, the wall should be designed for a live load surcharge. For temporary walls that are not considered critical, actual surcharge loads may be evaluated and considered in the design instead of this prescriptive value. Both temporary and permanent wall designs should account for unusual surcharges such as large material stockpiles. Calculated lateral pressures resulting from these surcharges should be added explicitly to the design lateral earth pressure diagram. Surcharge loads from existing buildings need to be considered if they are within a horizontal distance from the wall equal to the wall height.

### 10.4.3 Point, Line, and Strip Loads

Point loads, line loads, and strip loads are vertical surface loadings that are applied over limited areas as compared to surcharge loads. As a result, the increase in lateral earth pressure used for wall system design is not constant with depth as is the case for uniform surcharge loadings. These loadings are typically calculated by using equations based on elasticity theory for lateral stress distribution with depth (Figure 10-14). Examples of such loads include heavy cranes (temporary) or walls (permanent). Lateral pressures resulting from these surcharges should be added explicitly to other lateral pressures.

A numerical problem solved by use of Figure 10-14 is presented in Example 10-2.

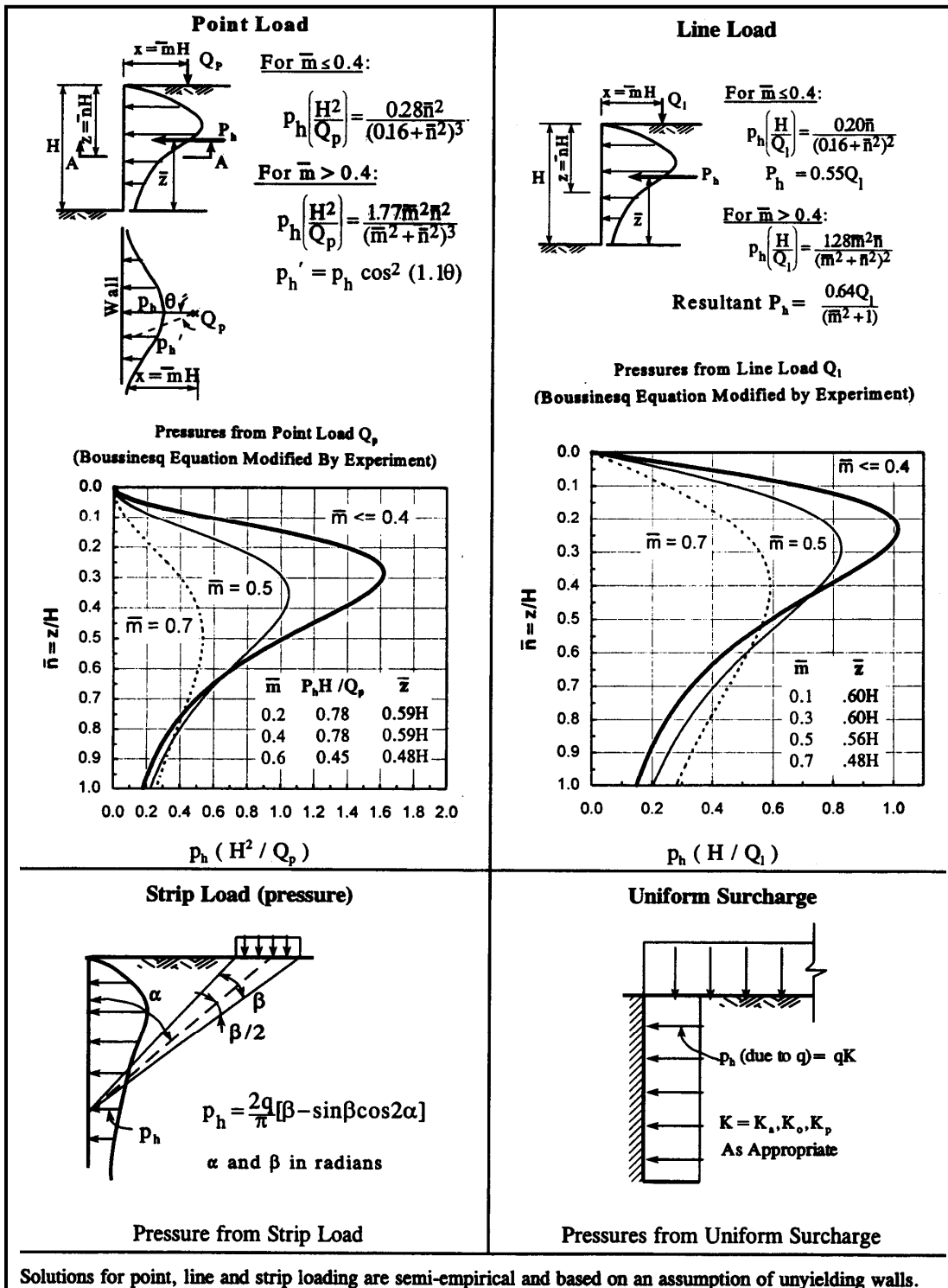
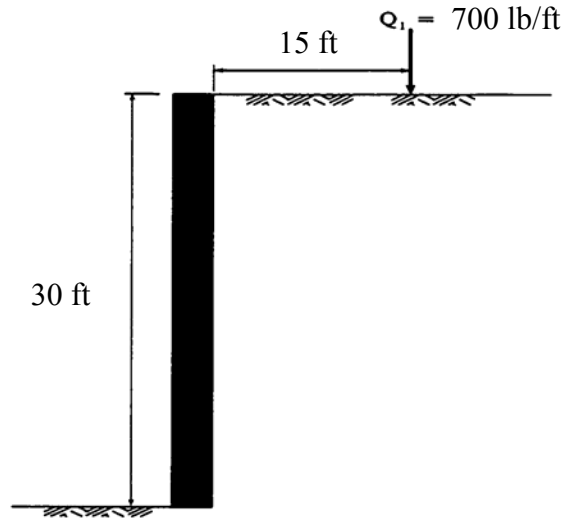


Figure 10-14. Lateral pressure due to surcharge loadings (after USS Steel, 1975)

**Example 10-2:** Construct the lateral pressure diagram due to a line load of 700 lb/ft located 15 ft behind the top of a 30 ft high unyielding wall shown below.



**Geometry of the Example Problem 10-2**

**Solution:**

The procedure to calculate the lateral pressures due to a line load is given in Figure 10-14. From this figure the lateral pressure can be found as follows:

$$\bar{m} = \frac{15 \text{ ft}}{30 \text{ ft}} = 0.5 > 0.4$$

For  $\bar{m} > 0.4$ , the lateral pressure is given by:

$$P_h = 1.28 \left( \frac{Q_1}{H} \right) \left[ \frac{\bar{m}^2 \bar{n}}{(\bar{m}^2 + \bar{n}^2)^2} \right]$$

For  $\bar{m} = 0.5$ ,  $Q_1 = 700 \text{ lb/ft}$  and  $H = 30 \text{ ft}$ , the lateral pressure is given by:

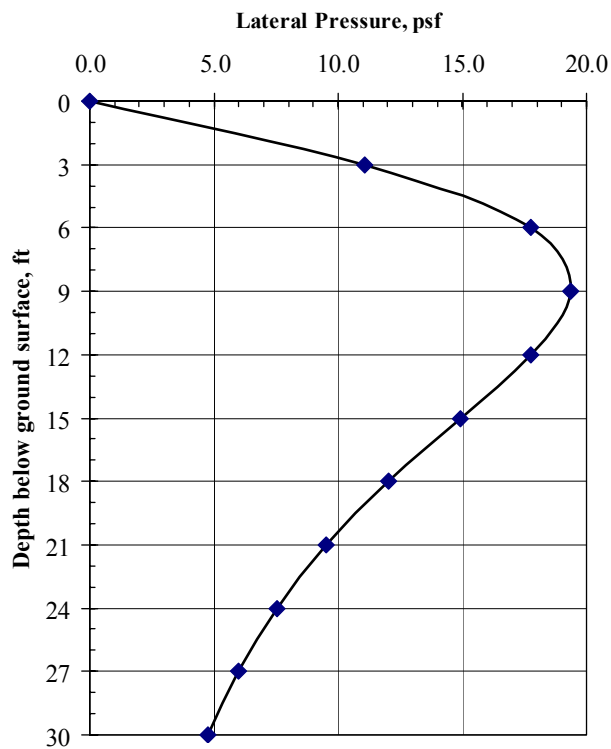
$$P_h = 1.28 \left( \frac{700 \text{ lb/ft}}{30 \text{ ft}} \right) \left[ \frac{0.5^2 \bar{n}}{(0.5^2 + \bar{n}^2)^2} \right] \rightarrow P_h = 29.9 \left[ \frac{0.25 \bar{n}}{(0.25 + \bar{n}^2)^2} \right]$$

Lateral pressures computed at various depths by using the above formula and the chart for line loads in Figure 10-14 are tabulated below.

**Computation of Lateral Earth Pressures Due To Line Load**

$\bar{n} = z/H$	Depth below top of wall (ft)	$P_h$ (psf)
0	0	0.00
0.1	3	11.0
0.2	6	17.8
0.3	9	19.4
0.4	12	17.8
0.5	15	14.9
0.6	18	12.0
0.7	21	9.5
0.8	24	7.5
0.9	27	6.0
1.0	30	4.8

The information in the table is used to construct the curve of depth vs. lateral pressure shown below.



## 10.5 WALL DESIGN

There are many different types of walls as shown in Figure 10-3. All walls have to be evaluated for stability with respect to different modes of deformation. There are four basic modes of instability from a geotechnical viewpoint. These are (a) sliding, (b) limiting eccentricity or overturning, (c) bearing capacity, and (d) global stability. The four modes of instability are shown in Figure 10-15. Since these modes of instability assume that the wall is intact, the evaluation of these modes is commonly referred to as the “external stability” analysis. All four modes may or may not be applicable to all wall types. Furthermore, depending on the wall type and its load support mechanism (refer to Section 10.1), there may be additional instability modes, such as pullout, tension breakage, bending and shear. The evaluation of these additional modes of instability are commonly referred to as “internal stability” analyses.

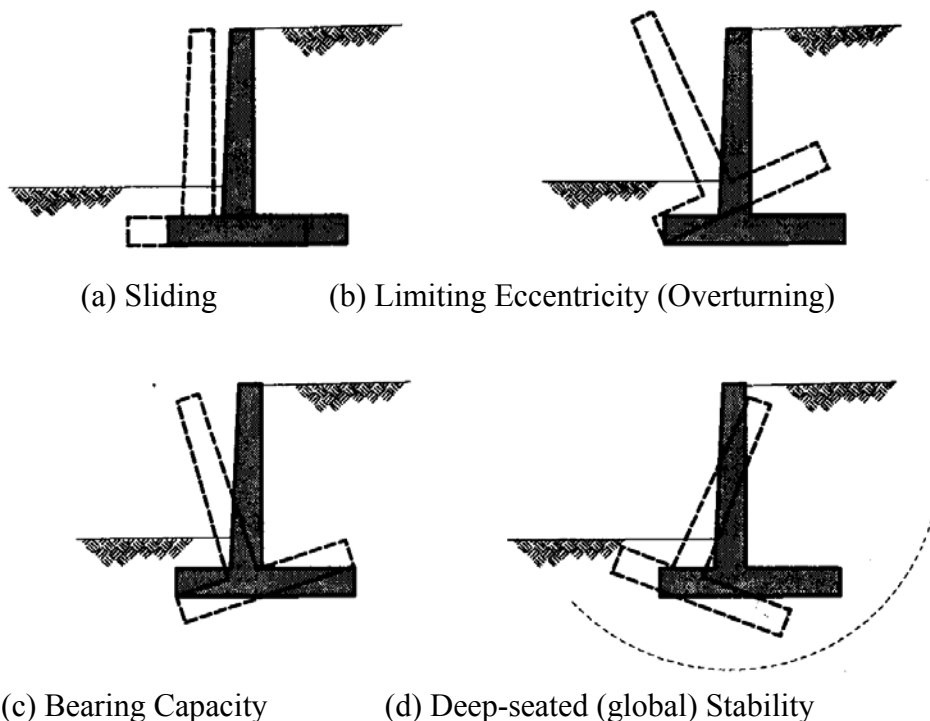


**Figure 10-15. Potential failure mechanisms for rigid gravity and semi-gravity walls.**

The external stability analysis is best illustrated by using the concept of gravity and semi-gravity walls. Table 10-2 summarizes the major design steps for cast-in-place concrete (CIP) gravity and semi-gravity walls.

**Table 10-2**  
**Design steps for gravity and semi-gravity walls**

Step 1.	Establish project requirements including all geometry, external loading conditions such as (temporary, permanent, and seismic, performance criteria, and construction constraints.
Step 2.	Evaluate site subsurface conditions and relevant properties of in situ soil and rock and wall backfill.
Step 3.	Evaluate soil and rock parameters for design and establish factors of safety.
Step 4.	Select initial base dimension of wall for evaluation of external stability.
Step 5.	Select lateral earth pressure distribution. Add appropriate water, surcharge, and seismic pressures and develop total lateral pressure diagram for design.
Step 6.	Evaluate bearing capacity.
Step 7.	Evaluate limiting eccentricity (overturning) and sliding.
Step 8.	Check overall stability and revise wall design if necessary.
Step 9.	Estimate maximum lateral wall movement, tilt, and wall settlement. Revise design if necessary.
Step 10.	Design wall drainage systems.

**10.5.1 Steps 1, 2, and 3 – Establish Project Requirements, Subsurface Conditions, Design Parameters**

It is assumed that Steps 1, 2 and 3 are completed and a CIP wall has been deemed appropriate. Soil and/or rock parameters for design have been established. In general, the required parameters for in situ soil and rock are the same as those required for a spread footing, in particular, foundation shear strength for bearing resistance and compression parameters of the foundation materials to allow for computations of wall settlement. For gravity walls that require deep foundation support, the soil/rock parameters are the same as those required for the design of a driven pile or drilled shaft foundation.

The drainage and shear strength characteristics of the wall backfill soil are assessed as part of Step 3. Guidelines for wall backfill material gradation and drainage behind gravity retaining walls can be found in the AASHTO (2002). Whenever possible, the backfill material should be free draining, nonexpansive, and noncorrosive. All backfill material should be free of organic material. The backfill gradation should follow the guidelines presented in Table 10-3.

**Table 10-3**  
**Suggested gradation for backfill for cantilever**  
**semi-gravity and gravity retaining walls**

Sieve Size	Percent Passing
3 in. (76.2 mm)	100
No. 4 (4.75 mm)	35 – 100
No. 30 (0.6 mm)	20 – 100
No. 200 (0.075 mm)	0 – 15

### 10.5.2 Step 4 – Select Base Dimension Based on Wall Height

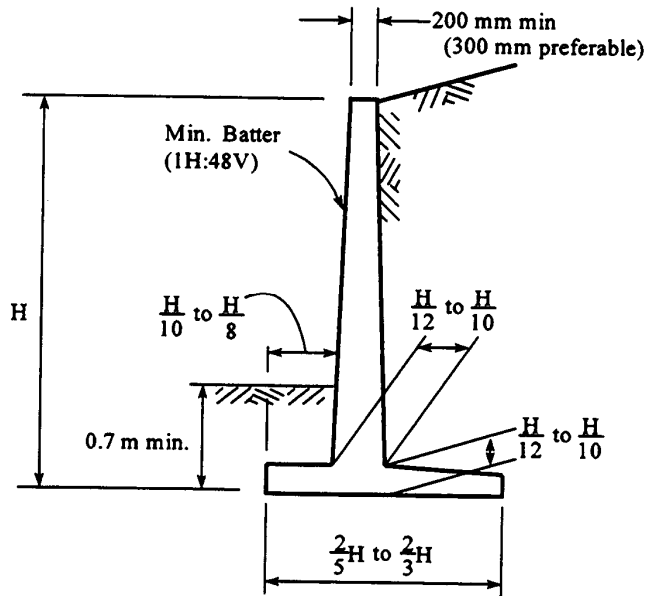
Figure 10-16 shows typical dimensions for a semi-gravity cantilever retaining wall and for a counterfort wall. These dimensions were developed based on a range of backfill properties, geometries, and stable foundation soils and can be used for preliminary design. However, the final external stability calculations should be performed based on the geometry requirements and specific conditions of the project, e.g., limited right-of-way. Similar guidelines exist for other wall types and can be found in FHWA (2005b).

### 10.5.3 Step 5 – Select Lateral Earth Pressure Distribution

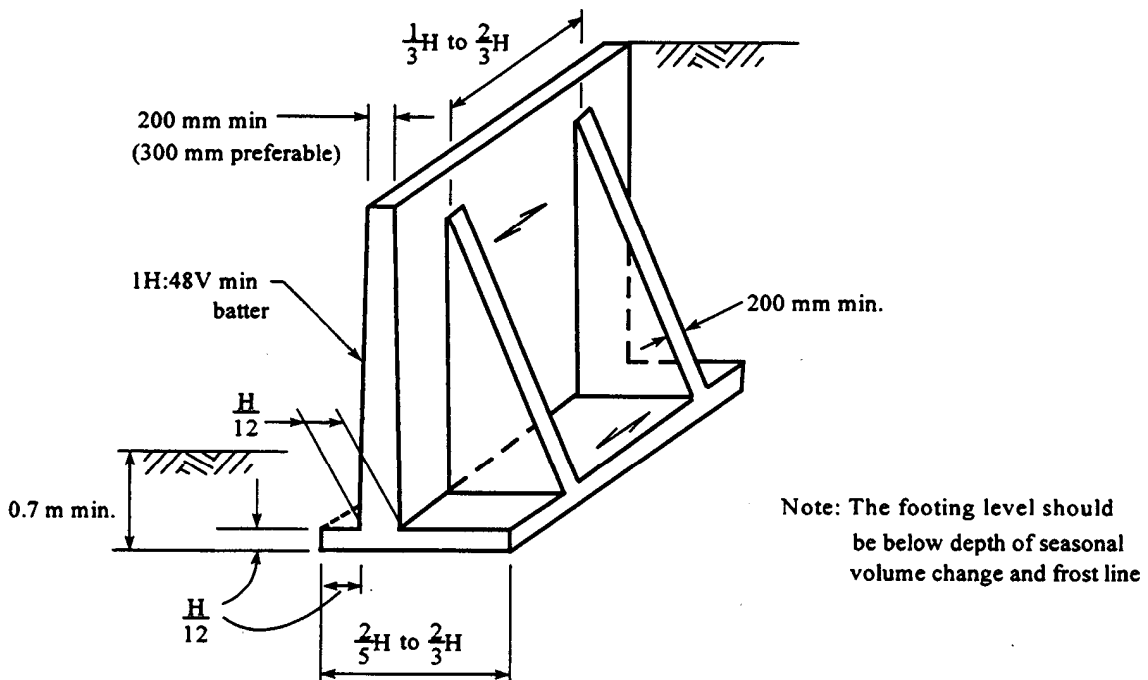
Lateral earth pressures for design of CIP walls are determined by using the procedures presented previously. Generally, Coulomb theory is used to compute earth pressures either directly on the back face of the wall, as is the case with a gravity wall, or on a vertical plane passing through the heel of the base slab, as is the case with a semi-gravity wall. Both of these concepts are illustrated in Figure 10-17.

The procedures described in Figure 10-17 are used to calculate the earth pressure loading for the wall subject to the following considerations:

- Use at-rest earth pressures for walls where rotation and displacement are restrained, e.g., rigid gravity retaining walls resting on rock or batter piles, unyielding walls such as culverts, tunnels and rigid abutment U-walls such as the CIP abutment with integral wingwalls shown in Figure 10-18.



(a)



(b)

**Figure 10-16. Typical dimensions (a) Cantilever wall, (b) Counterfort wall (Teng, 1962).**

[1 m = 3.28 ft; 25.4 mm = 1 in]

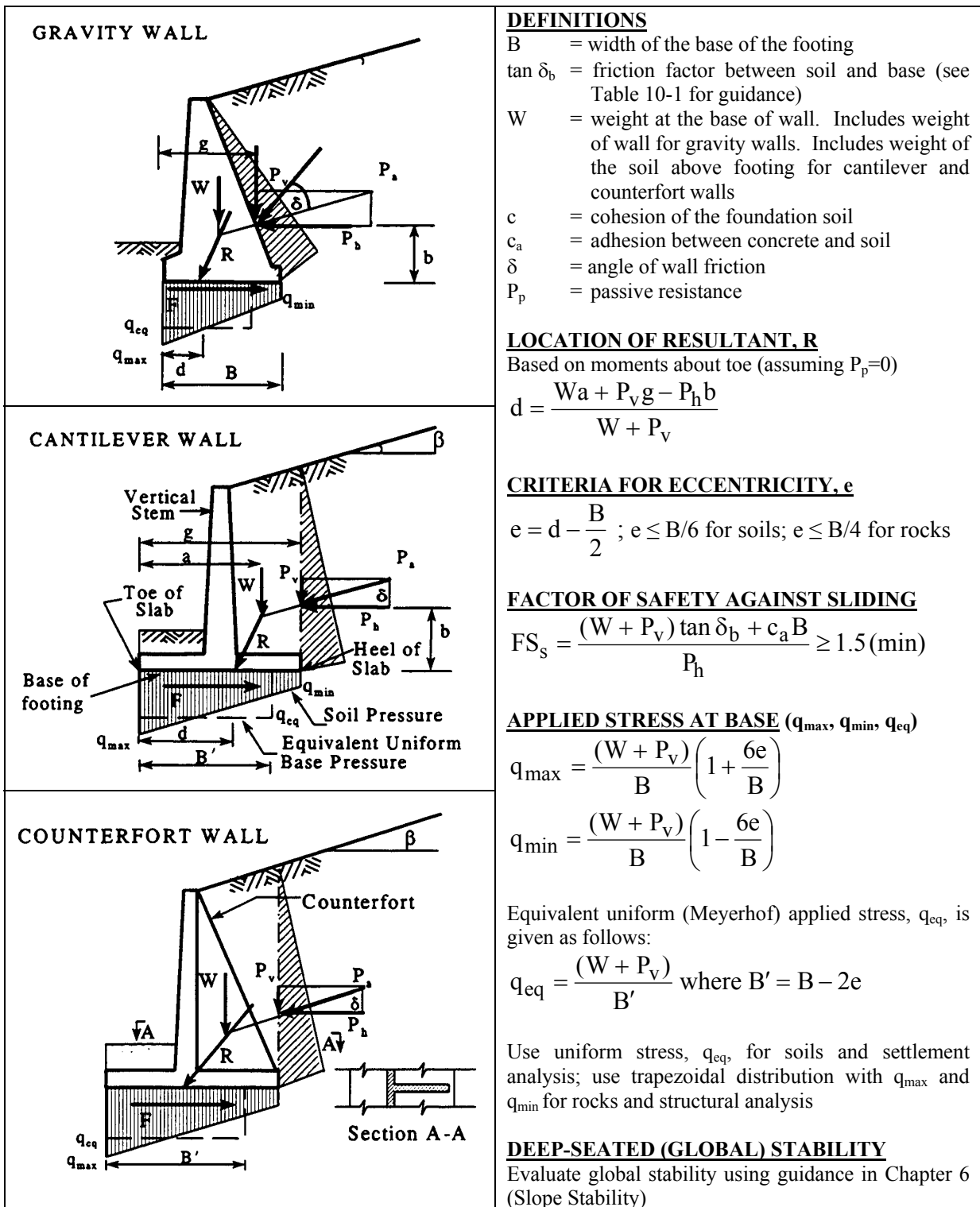


Figure 10-17. Design criteria for cast-in-place (CIP) Concrete retaining walls (after NAVFAC, 1986b).



**Figure 10-18. CIP abutment with integral wingwalls**

- Use the average of the at-rest and active earth pressures for CIP semi-gravity walls that are founded on rock or restrained from lateral movements, e.g., by the use of batter piles, and are less than 15 ft (5 m) in height.
- Use active earth pressures for CIP semi-gravity walls founded on rock or restrained from lateral movements that are greater than 15 ft (5 m) in height.
- Use the procedures described previously to compute pressure due to water and lateral earth pressures due to compaction and/or surcharges. Add these pressures to lateral earth pressure due to retained soil.
- Passive resistance in front of the wall should **not** be used in the analyses unless the wall extends well below the depth of frost penetration, scour or other types of disturbance such as a utility trench excavation in front of the wall. Development of the passive earth pressure in the soil in front of the wall requires a relatively large rotation or outward displacement of the wall; accordingly, the passive earth pressure

is neglected for walls with deep foundations and for other cases where the wall is restrained from rotation or displacement.

Figure 10-17 shows general loading diagrams for rigid gravity and semi-gravity walls. Loadings due to earth pressures behind the wall and for resultant vertical pressures at the base of the wall are shown.

If adequate drainage measures are provided, the hydrostatic pressure due to groundwater behind the wall generally need not be considered. However, hydrostatic pressure must be considered for portions of the wall below the level of the weep holes unless a deeper drainage system is provided behind the base of the wall. The wall must be designed for the full hydrostatic pressure when it is necessary to maintain the groundwater level behind the wall.

In addition to the lateral earth pressure, the wall must be designed for lateral pressure due to surcharge loads (see Section 10.4). For stability analyses of CIP gravity walls, the surcharge loads are generally assumed to be applied starting directly behind the top of the wall, unless specific conditions dictate otherwise. For CIP semi-gravity walls, the surcharge loads are generally assumed to be located behind the heel of the wall, and conservatively neglected within the width of the base slab since they contribute to overturning and sliding resistance. However, the surcharge loads within the width of the base slab are considered for the structural design of the wall stem.

## **10.5.4 Step 6 – Evaluate Bearing Capacity**

### **10.5.4.1 Shallow Foundations**

The computed vertical pressure at the base of the wall footing must be checked against the ultimate bearing capacity of the soil. The generalized distribution of the bearing pressure at the wall base is illustrated in Figure 10-17. Note that the bearing pressure at the toe is greater than that at the heel. The magnitude and distribution of these pressures are computed by using the applied loads shown in Figure 10-17. The equivalent uniform bearing pressure,  $q_{eq}$ , should be used for evaluating the factor of safety against bearing capacity failure. The procedures for determining the allowable bearing capacity of the foundation soils can be found in Chapter 8 (Spread Foundations) of this manual. Generally, a minimum factor of safety against bearing capacity failure of 3.0 is required for the spread footing foundation.

### 10.5.4.2 Deep Foundations

CIP walls founded on a deep foundation may be subject to potentially damaging ground and structural displacements at sites underlain by cohesive soils. Such damage may occur if the weight of the backfill material exceeds the bearing capacity of the cohesive subsoils causing plastic displacement of the ground beneath the retaining structure and heave of the ground surface in front of the wall. When the cohesive soil layer is located at or below the base of the wall, the factor of safety against this type of bearing capacity failure can be approximated by the following equation (Peck, *et al.*, 1974):

$$FS = \frac{5c}{(\gamma H + q)} \quad 10-15$$

where  $H$  is the height of the fill,  $\gamma$  is the unit weight of fill,  $c$  is the shear strength of the cohesive soil and  $q$  is the uniform surcharge load.

The computed factor of safety should not be less than 2.0 for the embankment loading. Below this value progressive lateral movements of the retaining structure are likely to occur (Peck, *et al.*, 1974). As the factor of safety decreases, the rate of movement will increase until failure occurs at a factor of safety of unity. For CIP walls founded on vertical piles or drilled shafts, this progressive ground movement would be reflected by an outward displacement of the wall. CIP walls founded on battered piles typically experience an outward displacement of the wall base and a backward tilt of the wall face (Figure 10-19).

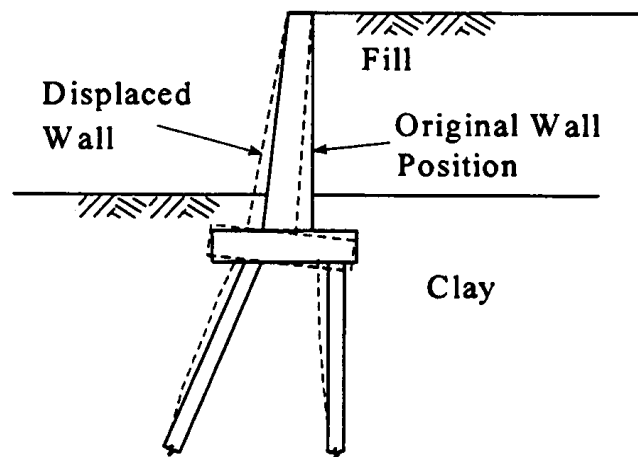


**Figure 10-19. Typical Movement of pile-supported cast-in-place (CIP) wall with soft foundation.**

### 10.5.5 Step 7 – Evaluate Overturning and Sliding

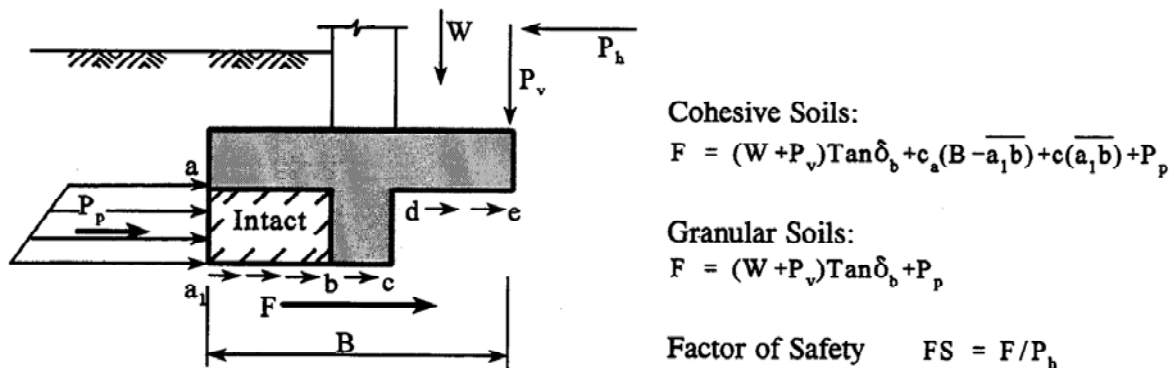
Figure 10-17 presents criteria for the design of CIP walls against sliding and eccentricity. The base dimensions of a CIP wall are determined by satisfying the following criteria:

- Sliding:  $FS \geq 1.5$

Sliding resistance along the base of the wall is evaluated by using the same procedures as for spread footing design (Refer to Chapter 8.0). Note that any passive resistance provided by soil at the toe of the wall by embedment is ignored due to the potential for the soil to be removed through natural or manmade processes during the service life of the structure. Also, the live load surcharge is not considered as a stabilizing force over the heel of the wall when sliding resistance is being checked.

If adequate sliding resistance cannot be achieved, design modifications may include: (1) increasing the width of the wall base; (2) using an inclined wall base or battering the wall to decrease the horizontal load; (3) incorporating deep foundation support; (4) constructing a shear key; and (5) embedding the wall base to a sufficient depth so that passive resistance can be relied upon.

If the wall is supported by rock, granular soils or stiff clay, a key may be installed below the foundation to provide additional resistance to sliding. The method for calculating the contribution of the key to sliding resistance is shown in Figure 10-20.



Note: See Figure 10-17 for list of symbol definitions.

**Figure 10-20. Resistance against sliding from keyed foundation.**

- Eccentricity,  $e$ , at base:  $\leq B/6$  in soil  
 $\leq B/4$  in rock

The eccentricity criterion essentially requires that the safety factor of the wall against overturning is approximately of 2.0 for soils and 1.5 for rocks. If the eccentricity is not within the required limits then it implies inadequate resistance to overturning and consideration should be given to either increasing the width of the wall base or providing a deep foundation.

### 10.5.6 Step 8 – Evaluate Global Stability

Where retaining walls are underlain by inadequate foundation materials, the overall stability of the soil mass must be checked with respect to the most critical failure surface. As shown in Figure 10-21, both circular and non-circular slip surfaces must be considered. A minimum factor of safety of 1.5 is desirable. If global stability is found to be a problem, deep foundations or the use of lightweight backfill may be considered. Alternatively, measures can be taken to improve the shear strength of the weak soil stratum. Other wall types, such as an anchored soldier pile and lagging wall or tangent or secant pile wall, should also be considered in this case.

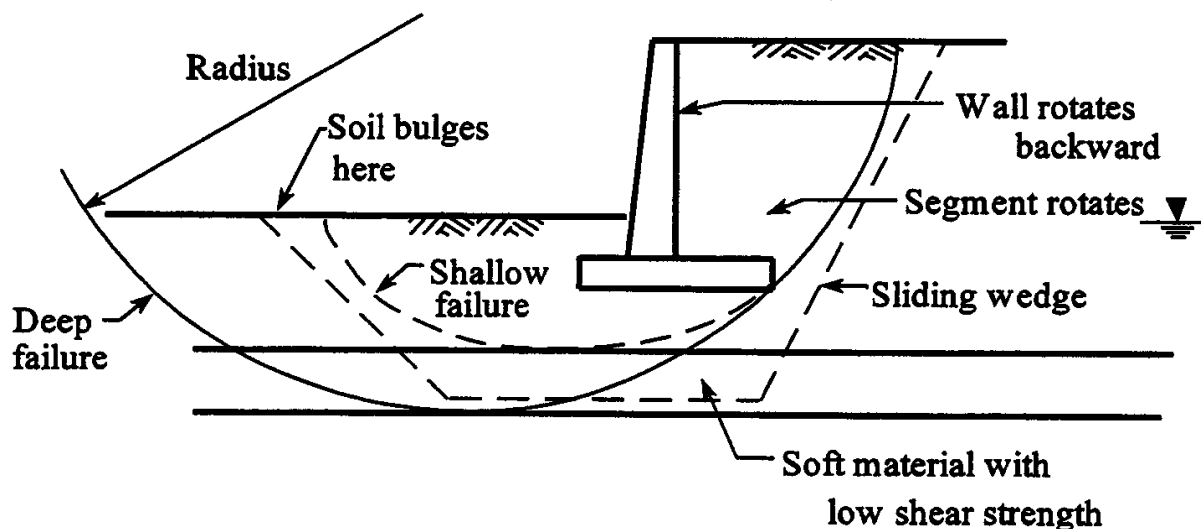


Figure 10-21. Typical modes of global stability (after Bowles, 1996)

### **10.5.7 Step 9 – Evaluate Settlement and Tilt**

Foundation settlement can be computed by the methods discussed in Chapter 8 (Spread Foundations). CIP walls can generally accommodate a differential settlement of up to about 1/500 measured as the ratio of differential settlement of two points along the wall to the horizontal distance between the points. In general, tolerable total settlements of CIP walls are limited to 1 inch as a means to control differential settlement. If the computed settlement and tilt exceed acceptable limits, the wall dimensions can be modified to shift the resultant force closer to the center of the base and thereby reduce the load eccentricity and differential settlement. In some cases, use of lightweight backfill material may solve the problem. The use of deep foundations can also be considered.

Unless CIP walls are provided with a deep foundation, a small amount of wall tilting should be anticipated. It is therefore advisable to provide the face of the wall with a small inward batter to compensate for the forward tilting. Otherwise, a small amount of forward tilting may give the illusion that the wall is unstable.

In cases where the foundation materials are stiffer or firmer at the toe of the base than at the heel, the resulting settlement may cause the wall to rotate backwards towards the retained soil. Such wall movements could substantially increase the lateral pressures on the wall since the wall is now pushing against the soil i.e., generating a passive pressure condition. Such wall movements can be avoided by reportioning the wall, supporting the wall on a deep foundation, or treating the foundation soils.

### **10.5.8 Step 10 – Design Wall Drainage Systems**

Water can have detrimental effects on earth retaining structures. Subsurface water and surface water can cause damage during and/or after construction of the wall. Control of water is a key component of the design of earth retaining structures.

A subsurface drainage system serves to prevent the accumulation of destabilizing hydrostatic pressures, which may develop as a result of groundwater seepage and/or infiltration of surface water. Subsurface drainage is addressed in Section 10.5.8.1. There may be several soil zones behind an earth retaining structure. Groundwater flow from one zone to another, and then to a drain and outlet feature, should be unimpeded. If impeded, water will backup at the interface of the two adjacent zones thereby increasing hydrostatic pressures and decreasing the stability of the wall structure. Soil filtration and permeability requirements must be met between the two adjacent zones of different soils to prevent impeded flow. Soil

and geotextile filter design and water collection components are discussed in Section 10.5.8.2.

Surface water runoff can destabilize a structure under construction by inundating the backfill. Surface water can also destabilize a completed structure by erosion or by infiltrating into the backfill. Design for surface water runoff is discussed in Section 10.5.8.3.

In most cases, and especially for fill walls, it is preferable to provide backfill drainage rather than design the wall for the large hydrostatic water pressure resulting from a saturated backfill. Saturation of the backfill may result from either a high static water table, from direct and/or indirect rainfall infiltrations, or from other wetting conditions, e.g., ruptured water lines, etc.

### 10.5.8.1 Subsurface Drainage

Potential sources of subsurface water are surface water infiltration and groundwater as illustrated in Figure 10-22. Groundwater present at an elevation above the base of the wall may have flowed into the backfill from an excavation backcut. Ground water may also be present beneath the bottom of the wall. A groundwater surface beneath a wall may rise into the structure, depending on the hydrogeology of the site. Surface water may infiltrate into the wall backfill from above, or from the front face of the wall for the case of flowing water in front of the structure (after Collin, *et al.*, 2002).

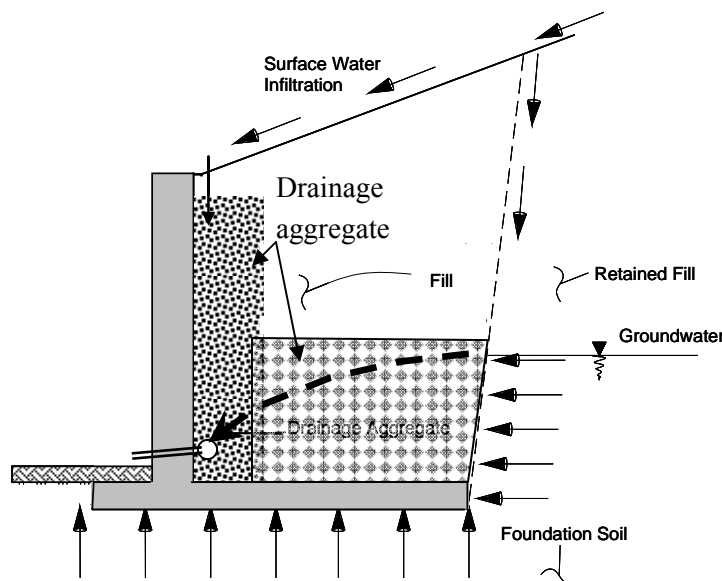
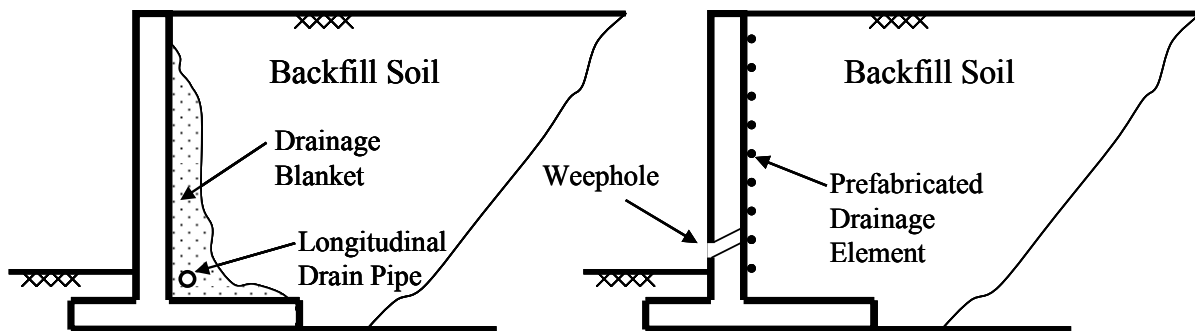


Figure 10-22. Potential sources of subsurface water.

Drainage system design depends on wall type, backfill and/or retained soil type, and groundwater conditions. Drainage system components such as granular soils, prefabricated drainage elements and filters, are usually sized and selected based on local experience, site geometry, and estimated flows, although detailed design is only occasionally performed. Drainage systems may be omitted if the wall is designed to resist full water pressure.

Drainage measures for fill wall systems, such as CIP walls, and cut wall systems typically consist of the use of a free-draining material at the back face of the wall, with “weep holes” and/or longitudinal collector drains along the back face as shown in Figure 10-23. The collector drains may be perforated pipes or gravel drains. This minimum amount of drainage should be sufficient if the wall backfill is relatively free-draining and allows the entire backfill to serve as a drain. It may be costly to fully backfill with free-draining or relatively free-draining material for some project applications therefore, it may be necessary to construct other types of drainage systems.

Fill wall drains may be placed (1) immediately behind the concrete facing or wall stem; (2) between wall backfill and embankment fill; (3) along a backcut; and (4) as a blanket drain beneath the wall. Examples of drains behind a wall stem are shown in Figure 10-24. The drainage system shown in the figure primarily serves to collect surface water that has infiltrated immediately behind the wall and transport it to an outlet. The system may also serve to drain the wall backfill, if the backfill soil is relatively free-draining.



**Figure 10-23. Typical retaining wall drainage alternatives.**

A drain behind the wall backfill should be used when the backfill is not relatively free-draining. Such a drain may be located as noted in (2) or (3) above, and as illustrated in Figure 10-24. A granular blanket drain with collection pipes and outlets should be used beneath fill wall structures where a high or seasonally high groundwater table exists.

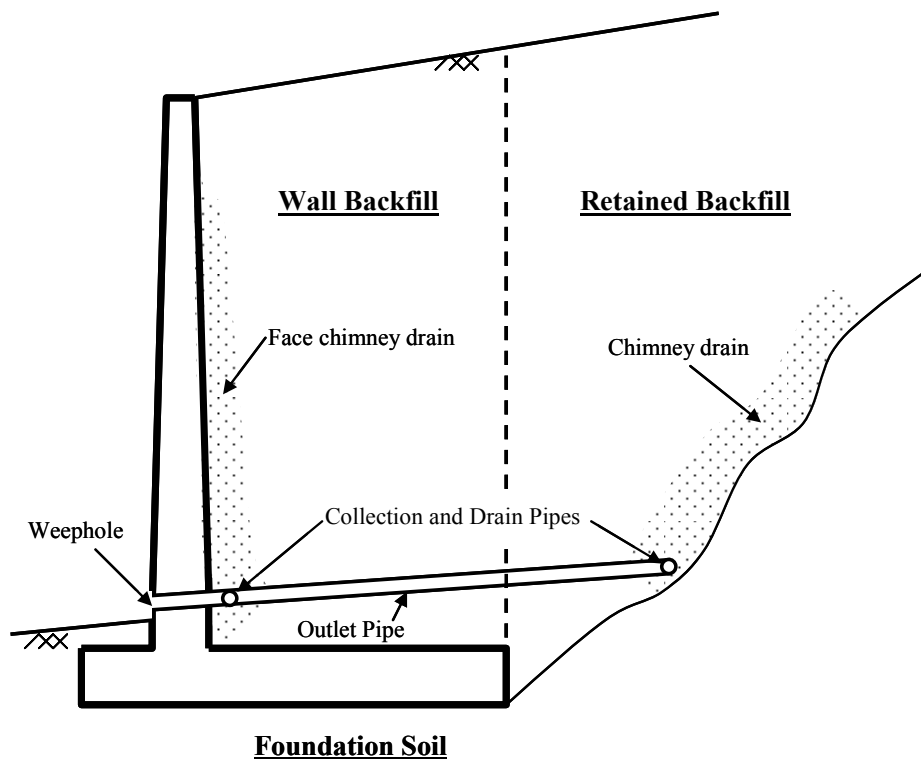


**Figure 10-24. Drains behind backfill in cantilever wall in a cut situation.**

### 10.5.8.2 Drainage System Components

Drainage systems for fill walls may include:

- column(s) or zone(s) of free-draining gravel or coarse sand to collect water seepage from the backfill;
- perforated pipe(s) to collect water in the granular column(s) or zone(s);
- conveyance piping;
- outlet(s); and
- filter(s) between backfill soil(s) and granular column(s) or zone(s).

Longitudinal pipes transport collected water to outlet pipes that discharge at appropriate points in front of and/or below the wall. Outlets may be via weep holes through the wall facing that discharge in front of the structure to grade; via conveyance piping to storm sewers as is common in urban applications, or via conveyance piping to a slope beneath the wall structure. Weep holes generally consist of 1½ - 3 in (40 - 75 mm) diameter holes that extend through the wall facing and are closely spaced horizontally along the wall, typically less than 10 ft (3 m) apart. If weep holes are used with a counterfort wall, at least one weep hole

should be located between counterforts. A screen and/or filter are used to prevent soil piping through a weep hole.

The collection and conveyance pipes need to be large enough and sufficiently sloped to effectively drain water by gravity flow from behind the wall while maintaining sufficient pipe flow velocity to prevent sediment buildup in the pipe. Use of 3 to 4 in (75 to 100 mm) diameter pipes is typical and practical. The diameter is usually much greater than that required for theoretical flow capacity. Procedures for the design of pipe perforations, such as holes or slots, is provided in Section 5.2 of Cedergren (1989). Pipe outlets to slope areas beneath wall structures should be detailed similar to pavement drain outlets. If the outlet is to a grass area, it should have a concrete apron, a vertical post marking its location (for maintenance), and a screen to prevent animal ingress.

Filters are required for water flowing between zones of different soils. A filter must prevent piping of the retained soil while providing sufficient permeability for unimpeded flow. The filter may be a soil or a geotextile. A geotextile is not required if the two adjacent soils meet certain soil filtration criteria. An open-graded aggregate will generally not allow the development of a soil filter at its interface with the backfill soil. In this case a geotextile filter will be required.

Geocomposite drains may be used in lieu of clean gravel or coarse sand and a geotextile. A geocomposite, or prefabricated, drain consists of a geotextile filter and a water collection and conveyance core. The cores convey the water and are generally made of plastic waffles, three-dimensional meshes or mats, extruded and fluted plastic sheets, or nets. A wide variety of geocomposites are readily available. However, the filtration and flow properties, detailing requirements, and installation recommendations vary and may be poorly defined for some products.

The flow capacity of geocomposite drains can be determined by using the procedures described in ASTM D 4716. Long-term compressive stresses and eccentric loadings on the geocomposite core should be considered during design and selection. The geotextile of the geocomposite should be designed to meet filter and permeability requirements.

Installation details, such as joining adjacent sections of the geocomposite and connections to outlets, are usually product-specific. Product-specific variances should be considered and addressed in the design, specification, detailing and construction phases of a project. Post installation examination of the drainage core/path with a camera scope should be considered for critical applications.

### 10.5.8.3 Surface Water Runoff

Surface drainage is an important aspect of ensuring wall performance and must be addressed during design. Appropriate measures to prevent surface water from infiltrating into the wall backfill should be included in the design of all earth retaining structures.

During construction of a fill wall, the backfill surface should be graded away from the wall face at the end of each day of construction to prevent water from ponding behind the wall and saturating the soil. Surface water running onto a partially completed backfill can carry fine-grained soils into the backfill work area and locally contaminate a free-draining granular backfill with fines. If a fine-grained soil is being utilized for the backfill, saturation can cause movements of the partially constructed wall facing.

Finish grading at the top of a wall structure should provide positive drainage away from the wall, when possible, to prevent or minimize infiltration of surface water into the backfill. If the area above the wall is paved, a curb and gutter is typically used to direct the flow away from the wall. Concrete-, asphalt- or vegetation-lined drainage swales may be used where a vegetated finished grade slopes to the wall. Water runoff over the top of a wall where the backfill slopes towards it can lead to erosion and undercutting of the wall and can cause staining of the wall face as soil is carried with the water. Construction of a collection swale close to the wall will help to prevent runoff from going over the top of the wall. Runoff flow will concentrate at grading low points behind the face. Ponding of runoff behind the wall leads to undesirable infiltration of water into the backfill.

Collection and conveyance swales should prevent overtopping of the wall for the design storm event. Extreme events (e.g., heavy rainfalls of short duration) have been known to cause substantial damage to earth retaining structures due to erosion and undercutting, flooding, and/or increased hydrostatic pressures both during and after construction. This is particularly true for sites where surface drainage flows toward the wall structure and where finer-grained backfills are used.

Site drainage features are designed for an assumed or prescribed design storm event, such as, the 25 year storm event. However, extreme events can occur that result in short duration flows, e.g., 1 to 3 hours, that significantly exceed the design capacity of the stormwater management system. When such events occur, site flooding can cause overtopping of the wall, erosion and undercutting, and an increase in hydrostatic forces within and behind the reinforced soil mass.

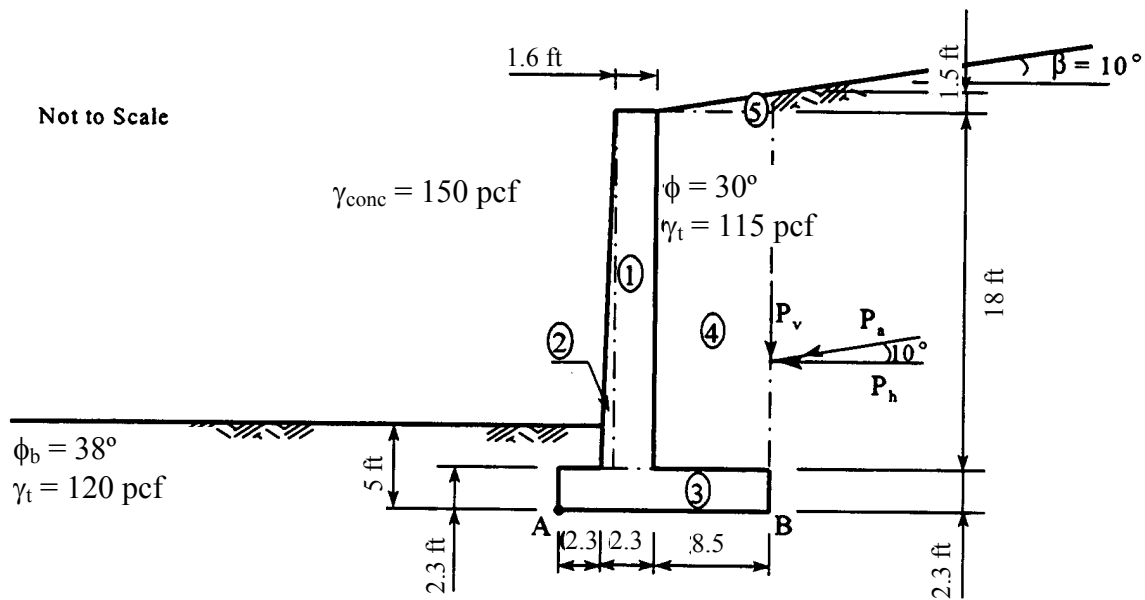
If surface water flows toward an earth retaining structure, the water is likely to be picked up in a gutter or other collection feature. Such features are often sized based upon the design storm event. The site layout and wall structure should include features for handling flows greater than the design event as is typically done in the design of an overflow spillway for a dam. The wall designer should address potential excess flows and coordinate work with other project designers. Consideration should be given to incorporating details of overflow features, such as a spillway, into the wall design for sites where surface water flows towards the wall structure.

## 10.6 EXTERNAL STABILITY ANALYSIS OF A CIP CANTILEVER WALL

The following example problem is used to illustrate the procedure for performing an external stability analysis of a CIP cantilever retaining wall.

### Example 10-3.

Analyze the CIP cantilever wall shown below for factors of safety against sliding, overturning and bearing capacity failure. The backfill and foundation soils consist of clean, fine to medium sand, and the groundwater table is well below the base of the wall.



Geometry and parameters for example problem.

### Solution

**Step 1:** Determine the total height of soil exerting pressure.

$$H = \text{thickness of base slab} + \text{height of stem} + (\text{width of heel slab}) \tan(\text{backslope angle})$$

$$\begin{aligned} H &= 2.3 \text{ ft} + 18 \text{ ft} + 8.5 \text{ ft} (\tan 10^\circ) \\ &= 21.8 \text{ ft} \end{aligned}$$

**Step 2:** Compute the coefficient of active earth pressure by using the equation of  $K_a$  in Figure 10-5 for a vertical backface ( $\theta=0$ ).

$$K_a = \frac{\cos^2 \phi}{\cos \delta \left[ 1 + \sqrt{\frac{\sin(\phi + \delta) \sin(\phi - \beta)}{\cos \delta \cos(-\beta)}} \right]^2}$$

where:

$\phi$  = internal friction angle of soil =  $30^\circ$

$\beta$  = angle of backfill slope =  $10^\circ$

$\delta$  = angle of wall friction =  $\beta = 10^\circ$

For the example problem:

$$K_a = \frac{\cos^2 30^\circ}{\cos 10^\circ \left[ 1 + \sqrt{\frac{\sin(30^\circ + 10^\circ) \sin(30^\circ - 10^\circ)}{\cos 10^\circ \cos(-10^\circ)}} \right]^2}$$

$$K_a = 0.35$$

**Step 3.** Compute the magnitude of the resultant of active pressure,  $P_a$ , per foot of wall into the plane of the paper.

$$\begin{aligned} P_a &= \frac{1}{2} K_a \gamma H^2 \\ &= \frac{1}{2} (0.35)(115 \text{ pcf})(21.8 \text{ ft})^2 = 9,564.2 \text{ lb/ft} \end{aligned}$$

**Step 4.** Resolve  $P_a$  into horizontal and vertical components:

$$\begin{aligned} P_h &= P_a \cos \beta & P_v &= P_a \sin \beta \\ &= (9,564.2 \text{ lb/ft}) \cos 10^\circ & &= (9,564.2 \text{ lb/ft}) \sin 10^\circ \\ &= 9,418.9 \text{ lb/ft} & &= 1,660.8 \text{ lb/ft} \end{aligned}$$

Moment arm of  $P_h$  about point A =  $(2.3 \text{ ft} + 18 \text{ ft} + 1.5 \text{ ft})/3 = 21.8/3 = 7.27 \text{ ft} = b$

Moment arm of  $P_v$  about point A =  $2.3 \text{ ft} + 2.3 \text{ ft} + 8.5 \text{ ft} = 13.1 \text{ ft} = g$

**Step 5:** Determine weights and sum moments about the toe of the wall (point A).

The weights of various areas and the moments due to the weights shown in the geometry of the example problem are set out in the following table. The unit weight of concrete is assumed to be 150 pcf and the weight of the soil above the footing toe is neglected.

Area	Weight, lb/ft	Moment arm about A, ft	Moment about A, lb.ft/ft
1	(1.6 ft) (18 ft) (150 pcf) = 4,320	2.3 ft+0.7 ft+(1.6/2) ft = 3.80	(4,320 lb) (3.80 ft) = 16,416.0
2	(0.5) (0.7 ft) (18 ft) (150 pcf) = 945	2.3 ft+ (2/3) (0.7) ft = 2.77	(945 lb) (2.77 ft) = 2,617.7
3	(13.1 ft) (2.3 ft) (150 pcf) = 4,519.5	13.1/2 ft = 6.55	(4,519.5 lb) (6.55 ft) = 29,602.7
4	(8.5 ft) (18 ft) (115 pcf) = 17,595	2.3 ft+ 2.3 ft+(8.5/2) ft = 8.85	(17,595 lb) (8.85 ft) = 155,715.8
5	(0.5) (8.5 ft) (1.5 ft) (115 pcf) = 733.1	2.3 ft+2.3 ft+(2/3)(8.5) ft = 10.27	(733.1lb) (10.27 ft) = 7,528.9
<b>Total</b>	<b>W = 28,112.6</b>		<b>M<sub>w</sub> = 211,881.1</b>

**Step 6:** Check factor of safety against sliding; neglect passive resistance of embedment depth soil (Refer to Figure 10-20)

$$FS_s = \frac{(W + P_V) \tan \delta_b}{P_h}$$

where:

W = weight of concrete and soil on the base of the wall footing AB

$\delta_b$  = friction angle between concrete base and foundation soil

Use  $\delta_b = (3/4) \phi_b = (3/4) (38^\circ) = 28.5^\circ$ , for friction angle between concrete and clean, fine to medium sand (see NAVFAC, 1986b). This value of  $\delta_b$  is within the range of values listed in Table 10-1 for clean fine to medium sand.

$$FS_s = \frac{(28,112.6 \text{ lb/ft} + 1,660.8 \text{ lb/ft}) \tan 28.5^\circ}{9,418.9 \text{ lb/ft}} = \frac{16,165.6 \text{ lb/ft}}{9,418.9 \text{ lb/ft}} = 1.72 \quad \text{O.K.}$$

**Step 7:** Check the limiting eccentricity and factor of safety against bearing failure.

**(1)** Compute the location of resultant at distance d from point A.

$$d = \frac{\sum M_R - \sum M_0}{\sum V}$$

$$d = \frac{M_W - P_h b + P_V g}{W + P_V}$$

$$d = \frac{21,1881.1 \text{ lb.ft/ft} + (1,660.8 \text{ lb/ft})(13.1 \text{ ft}) - (9,418.9 \text{ lb/ft})(7.27 \text{ ft})}{28,112.6 \text{ lb/ft} + 1,660.8 \text{ lb/ft}}$$

where:  $W + P_V = \sum V$

$$d = \frac{16,5162.2 \text{ lb.ft/ft}}{29,773.4 \text{ lb/ft}} = 5.55 \text{ ft}$$

(2) Compute the eccentricity of the load about the center of base.

$$e = \frac{B}{2} - d = \frac{13.1 \text{ ft}}{2} - 5.55 \text{ ft} = 1.0 \text{ ft}$$

$$e = 1.0 \text{ ft} < \frac{B}{6} = \frac{13.1 \text{ ft}}{6} = 2.18 \text{ ft} \quad \text{O.K.}$$

(3) Compute the maximum and minimum pressures under the wall footing.

$$\begin{aligned} q_{\max, \min} &= \frac{\sum V}{B} \left( 1 \pm \frac{6e}{B} \right) \\ &= \frac{29,773.4 \text{ lb/ft}}{13.1 \text{ ft}} \left( 1 \pm \frac{6(1.0 \text{ ft})}{13.1 \text{ ft}} \right) \\ &= 2,272.7 \text{ psf} \quad (1.46 \text{ or } 0.54) \end{aligned}$$

$$\begin{aligned} \text{i.e., } q_{\max} &= 3,318.1 \text{ psf} \\ q_{\min} &= 1,227.3 \text{ psf} \end{aligned}$$

(4) Estimate ultimate bearing capacity.

Use the procedures presented in Chapter 8 (Shallow Foundations). Assume that for a footing with eccentric and inclined loading the ultimate bearing capacity computed by the geotechnical specialist is:

$$q_{\text{ult}} = 20,000 \text{ psf}$$

(5) Check factor of safety against bearing capacity failure.

$$FS_{bc} = \frac{q_{\text{ult}}}{q_{\max}} = \frac{20,000 \text{ psf}}{3,318.1 \text{ psf}} = 6.03 > 3.0 \quad \text{O.K.}$$

## **SUMMARY**

Factor of safety against sliding	$FS_s$	= 1.72
Eccentricity	$e$	= 1.0 ft < B/6
Factor of safety against bearing failure	$FS_{bc}$	= 6.03

In addition, the factor of safety against global failure and wall settlement including tilting and lateral squeeze should be evaluated to complete the analysis.

### **10.7 CONSTRUCTION INSPECTION**

FHWA (2005b) discusses construction considerations for many of the walls presented in Figure 10-3. Construction considerations for CIP walls only are presented in this manual. In general, the construction inspection requirements for CIP walls are similar to those for other concrete structures. In some cases, state agencies may have inspector checklists for this type of construction. Table 10-4 provides a summary of typical construction inspection requirements for CIP retaining walls.

**Table 10-4**

**Inspector responsibilities for a typical CIP gravity and semi-gravity wall project**

<b>CONTRACTOR SET UP</b>
Review plans and specifications
Review the contractor's schedule
Review test results and certifications for preapproved materials, e.g., cement, coarse and fine aggregate.
Confirm that the contractor's stockpile and staging area are consistent with locations shown on the plans
Discuss anticipated ground conditions and potential problems with the contractor
Review the contractor's survey results against the plans
<b>EXCAVATION</b>
Verify that excavation slopes and/or structural excavation support is consistent with the plans
Confirm that limits of any required excavations are within right-of-way limits shown on plans
Confirm that all unsuitable materials, e.g., sod, snow, frost, topsoil, soft/muddy soil are removed to the limits and depths shown on the plans and that the excavation is backfilled with granular material and properly compacted
Confirm that leveling and proof-rolling of the foundation area is consistent with requirements of the specifications
Confirm that the contractor's excavation operations do not result in significant water ponding
Confirm that existing drainage features, utilities, and other features are protected
Identify areas not shown on the plans where unsuitable material exists and notify the engineer

<b>FOOTING</b>
Approve condition of footing foundation soil/rock before concrete is poured
Confirm reinforcement strength, size, and type consistent with the specifications
Confirm the consistency of the contractor's outline of the footing (footing size and bottom of footing depth) with the plans
Confirm the location and spacing of reinforcing steel consistent with the plans
Confirm water/cement ratio and concrete mix design consistent with the specifications
Record concrete volumes poured for the footing
Confirm appropriate concrete curing times and methods as provided in the specifications
Confirm that concrete is not placed on ice, snow, or otherwise unsuitable ground
Confirm that concrete is being placed in continuous horizontal layers and that the time between successive layers is consistent with the specifications
<b>STEM</b>
Confirm the placement of weep hole inserts (number, elevation, and specific locations) with the plans if weep holes are used,
Confirm that concrete is poured in section lengths consistent with the specifications
Record concrete volumes used to form the stem
Confirm that all wall face depressions, air pockets, gaps, rough spots, etc. are repaired
Confirm that storage of reinforcing bars is consistent with the specifications, e.g.-use of platform or supports.
Perform preliminary check of condition of epoxy-coated reinforcing bars
Confirm that forms are clean and appropriately braced during concrete pour operations
Confirm that all reinforcing bars are held securely in place and are being rigidly supported at the face of forms and in the bottom of wall footings
Confirm that construction joints are being made only at locations shown on the plans or otherwise at locations approved by the engineer
<b>DRAINAGE SYSTEMS AND BACKFILL</b>
Confirm that installation of the drainage system is consistent with the specifications and plans
Confirm that the backfill material being used is approved by the engineer
Confirm that placement of the backfill is performed in lifts consistent with the specifications
Confirm that minimum concrete strength is achieved before backfill is placed and compacted against back of wall
Confirm that the backfill placement method used by the contractor does not cause damage to prefabricated drainage material or drain pipes
Confirm that earth cover over drainage pipes is sufficient to prevent damage from heavy equipment. The minimum cover based on ground pressure from equipment should be provided in the specifications.
Perform required backfill density tests at the frequencies specified, especially for areas that are compacted with lightweight equipment, e.g., areas just behind the wall.
Check that the drainage backfill just behind weep holes is the correct gradation and that it is properly installed
<b>POST INSTALLATION</b>
Verify pay quantities

Note: Throughout the project, check submittals for completeness before transmitting them to the engineer.

[THIS PAGE INTENTIONALLY BLANK]

## **CHAPTER 11.0 GEOTECHNICAL REPORTS**

Upon completion of the subsurface exploration and laboratory testing program, the geotechnical specialist will compile, evaluate, and interpret the data and perform engineering analyses for the design of foundations, cut slopes, embankments, and other required facilities. Additionally, the geotechnical specialist will be responsible for producing a report that presents the subsurface information obtained from the site investigations and provides specific design and construction recommendations. The geotechnical analyses and design procedures to be implemented for the various types of highway facilities are addressed in various other FHWA publications. This chapter provides guidelines and recommendations for developing a geotechnical report.

### **11.01 Primary References**

FHWA (1988). *Checklist and Guidelines for Review of Geotechnical Reports and Preliminary Plans and Specifications*. Report No. FHWA ED-88-053, Federal Highway Administration, U.S. Department of Transportation, Revised 2003.

Geotechnical Engineering Notebook. *FHWA Geotechnical Guidelines GT1–GT16*.  
<http://www.fhwa.dot.gov/engineering/geotech/index.cfm>.

### **11.1 TYPES OF REPORTS**

Generally, one or more of three types of reports will be prepared: A geotechnical investigation report; a geotechnical design report and/ or a geoenvironmental report. Several disciplines within an agency may contribute to the development of the geotechnical report. The preparer and the choice of the report depends on the requirements of the highway agency (owner) and the agreement between the geotechnical specialist and the facility designer. The need for multiple types of reports on a single project depends on the project size, phasing and complexity. Regardless, all the typical sections of a report outlined herein must be included. All consultant produced work should be in conformance with the reporting guidelines for the agency.

### 11.1.1 Geotechnical Investigation Reports

Geotechnical investigation reports present site-specific data and have three major components:

- 1. Background Information:** The initial sections of the report summarize the geotechnical specialist's understanding of the facility for which the report is being prepared and the purposes of the subsurface exploration. This section includes information on loads, deformations and additional performance requirements. This section also presents a general description of site conditions, geology and geologic features, drainage, ground cover and accessibility, and any peculiarities of the site that may affect the design and construction.
- 2. Work Scope:** The second part of the investigation report documents the scope of the exploration program and the specific procedures used to perform this work. These sections identify the types of exploration methods used; the number, location and depths of borings, exploration pits and in-situ tests; the types and frequency of samples obtained; the dates of subsurface exploration; the subcontractors used to perform the work; the types and number of laboratory tests performed; the testing standards used; and any variations from conventional procedures.
- 3. Data Presentation:** This portion of the report, generally contained in appendices with a complementary narrative of explanation, presents the data obtained from the field and laboratory exploration program. The appendices typically include final logs of all borings, exploration pits, and piezometer or well installations, water level readings, data plots from each in-situ bore hole, summary tables and individual data sheets for all laboratory tests performed, rock core photographs, geologic mapping data sheets and summary plots, subsurface profiles developed from the field and laboratory test data, as well as statistical summaries. The geotechnical investigation report often includes copies of existing information such as boring logs or laboratory test data from previous investigations at the project site.

The intent of a geotechnical investigation report is to document the investigation performed and present the data obtained. The report should include a summary of the subsurface and lab data. Interpretations and recommendations on the index and design properties of soil and rock should also be included. The geotechnical investigation report typically does not include detailed design analyses and recommendations, but it should include a narrative that summarizes and provides an interpretation of the subsurface data. The geotechnical

investigation report is sometimes used when the subsurface explorations are subcontracted to a geotechnical consultant, but the data interpretation and design tasks are performed by the owner's or the prime consultant's in-house geotechnical staff. An example Table of Contents for a geotechnical investigation report is presented in Figure 11-1.

### **11.1.2 Geotechnical Design Reports**

A geotechnical design report typically provides an assessment of existing subsurface conditions at a project site, presents, describes and summarizes the procedures and findings of all geotechnical analyses performed, and provides appropriate recommendations for design and construction of foundations, earth retaining structures, embankments, cuts, and other required facilities. Unless a separate geotechnical investigation report was developed previously, the geotechnical design report will also include documentation of any subsurface explorations and laboratory investigations performed and a presentation of the results of those investigations as described in Section 11.1.1. An example Table of Contents for a geotechnical design report is presented in Figure 11-2.

Since the scope, site conditions, and design/construction requirements of each project are unique, the specific contents of a geotechnical design report must be tailored for each project. In order to develop this report, the author must possess detailed knowledge of the facility. In general, however, the geotechnical design report must address all the geotechnical issues that may be anticipated on a project. The report must identify each soil and rock unit of engineering significance, and must provide recommended design parameters for each of these units. To this end, all factual data must be synthesized and analyzed to justify the recommended index and design properties. Groundwater conditions are particularly important for both design and construction and, accordingly, they need to be carefully assessed and described. For every project, the subsurface conditions encountered in the site investigation need to be compared with the geologic setting in order to understand the nature of the deposits better and to predict the degree of variability between exploration locations.

Each geotechnical design issue must be addressed in accordance with the methodology described in the various chapters of this manual. The results of these studies need to be discussed concisely and clearly in the report. Of particular importance is an assessment of the impact of existing subsurface conditions on construction operations, phasing and timing. Properly addressing any construction issues in the report that are related to subsurface conditions can preclude change-of-conditions claims. Examples include but are not limited to:

1.0	INTRODUCTION
2.0	SCOPE OF WORK
3.0	SITE DESCRIPTION
4.0	SITE CONDITIONS, GEOLOGIC SETTING, AND TOPOGRAPHIC INFORMATION
5.0	FIELD INVESTIGATION PROGRAM AND IN-SITU TESTING
6.0	DISCUSSION OF LABORATORY TESTING
7.0	SUMMARY OF SUBSURFACE CONDITIONS AND SOIL PROFILES
8.0	DISCUSSION OF FINDINGS, CONCLUSIONS, AND RECOMMENDATIONS
8.1	GENERAL
8.1.1	Subgrade and Foundation Soil/Rock Types
8.1.2	Soil/Rock Properties
8.2	GROUND WATER CONDITIONS/ OBSERVATIONS
8.3	SPECIAL TOPICS (e.g., dynamic properties, seismicity, environmental).
8.4	CHEMICAL ANALYSIS
9.0	FIELD PERMEABILITY TESTS
10.0	REFERENCES
	LIST OF APPENDICES
Appendix A	- Boring Location Plan and Subsurface Profiles
Appendix B	- Test Boring Logs and Core Logs With Core Photographs
Appendix C	- Cone Penetration Test Soundings
Appendix D	- Flat Plate Dilatometer, Pressuremeter, Vane Shear Test Results
Appendix E	- Geophysical Survey Data
Appendix F	- Field Permeability Test Data and Pumping Test Results
Appendix G	- Laboratory Test Results
Appendix H	- Existing Information
	LIST OF FIGURES
	LIST OF TABLES

**Figure 11-1. Example Table of Contents for a Geotechnical Investigation Report.**

1.0	INTRODUCTION
1.1	Project Description (includes facility description, loads and performance requirements)
1.2	Scope of Work
2.0	GEOLOGY
2.1	Regional Geology
2.2	Site Geology
3.0	EXISTING GEOTECHNICAL INFORMATION
4.0	SUBSURFACE EXPLORATION PROGRAM
4.1	Subsurface Exploration Procedures
4.2	Laboratory Testing
5.0	SUBSURFACE CONDITIONS
5.1	Topography
5.2	Stratigraphy
5.3	Soil Properties
5.4	Groundwater Conditions
6.0	RECOMMENDATIONS FOR BRIDGE FOUNDATIONS
6.1	Design Alternatives
6.2	Group Effects
6.3	Foundation Settlement
6.4	Downdrag
6.5	Lateral Loading
6.6	Construction Considerations
6.7	Pile Testing
7.0	RECOMMENDATIONS FOR EARTH RETAINING STRUCTURES
7.1	Suitable Types
7.2	Design and Construction Considerations
8.0	ROADWAY RECOMMENDATIONS
8.1	Embankments and Embankment Foundations
8.2	Cuts
8.3	Pavement
9.0	SEISMIC CONSIDERATIONS
9.1	Seismicity
9.2	Seismic Hazard Criteria
9.3	Liquefaction Potential
10.0	CONSTRUCTION RECOMMENDATIONS
	LIST OF REFERENCES
	LIST OF FIGURES
	APPENDICES
	Appendix A Boring Logs
	Appendix B Laboratory Test Data
	Appendix C Existing Subsurface Information

**Figure 11-2. Example Table of Contents for a Geotechnical Design Report.**

- vertical and lateral limits for recommended excavation and replacement of any unsuitable shallow surface deposits such as peat, muck and top soil;
- excavation and cut requirements, i.e., safe slopes for open excavations or the need for sheeting or shoring;
- anticipated fluctuations of the groundwater table along with the consequences of a high groundwater table on excavations;
- effect of boulders on pile drivability or drilled shaft drilling, and rock hardness on rippability.

Recommendations should be provided for the solution of anticipated problems. The above issues are but a few of those that need to be addressed in a geotechnical design report. To aid engineers with a quantitative review of geotechnical reports, FHWA has prepared review checklists and technical guidelines (FHWA, 2003b). One of the primary purposes of the FHWA guidelines is to provide transportation agencies and consultants with minimum standards/criteria for the geotechnical information that FHWA recommends be included in geotechnical reports as well as plans and specification packages. Technical guidelines for “minimum” site investigation information common to all geotechnical reports for any type of geotechnical feature and basic information and recommendations for specific geotechnical features are provided in the checklists and technical guidelines (FHWA, 2003b). Checklists are presented in the form of a question and answer format for specific geotechnical features such as:

- centerline cuts and embankments;
- embankments over soft ground;
- landslide corrections;
- retaining walls;
- structural foundations such as spread footings, driven piles and drilled shafts;
- borrow material sites.

### **11.1.3 GeoEnvironmental Reports**

When the subsurface exploration indicates the presence of contaminants at the project site, the geotechnical specialist may be requested to prepare a geoenvironmental report in which the findings of the investigation are presented and discussed, and recommendations made for the remediation of the site.

The preparation of such a report usually requires the geotechnical specialist to work with a team of experts, since many aspects of the contamination or the remediation may be beyond his/her expertise. A representative team preparing a geoenvironmental report may be composed of chemists, geologists, hydrogeologists, environmental scientists, toxicologists, air quality and regulatory experts, as well as one or more geotechnical specialists. The report should contain all of the components of the geotechnical investigation report, as discussed above. Additionally, the geoenvironmental report will have a clear and concise discussion of the nature and extent of contamination, the risk factors involved, if applicable, a contaminant transport model, and the source of the contamination, if known, e.g., landfill, industrial waste water line, broken sanitary sewer, above-ground or underground storage tanks, overturned truck or train derailment, etc.

The team may also be required to present solutions to remediate the site. Depending upon the nature and amount of contaminant and its location within the geologic profile and its potential impact on the environment, remediation measures may include removal of the contaminated material, pumping and treatment of the contaminated groundwater, installation of slurry cut-off walls, abandonment of that portion of the right-of-way, deep soil mixing, bioremediation, and electrokinetics. The geoenvironmental report should also address the regulatory issues pertinent to the specific contaminants found and the proposed site remediation methods.

## **11.2 DATA PRESENTATION**

### **11.2.1 Boring Logs**

Boring logs, rock coring, soundings, and exploration logging should be prepared in accordance with the procedures and formats discussed in Chapters 3 through 5. Test boring logs and exploration test pit records can be prepared by using software capable of storing, manipulating, and presenting geotechnical data in simple one-dimensional profiles, or alternatively two-dimensional graphs of the subsurface profiles, or three-dimensional representations. These and other similar software allow for the orderly storage of project data for future reference. The website: <http://www.ggsd.com> lists over 40 separate software packages available for the preparation of soil boring logs.

Many new software programs offer a menu-based boring log drafting program. The computer-aided drafting tools let users create custom boring log formats that can include graphic logs, monitoring well details, and data plots. Custom designed legends explaining

graphic symbols and containing additional notes can be added to boring logs for greater clarity. These legends can include a library of soil types, sampler and well symbols as well as other nomenclature used on the boring logs. Geological profiles can be generated by the program and may be annotated with text and drawings.

Similarly, the results of various in-situ tests performed by using cones, pressuremeters and vanes, can be presented by the use of available commercial software. Links to many geotechnical software programs may be found at: <http://www.usucger.org>

Alternatively, it is convenient for the in-situ test data to be reduced directly and simply by using a spreadsheet format such as EXCEL and QUATTRO PRO. In many ways, the spreadsheet is a superior approach as it allows the engineer to tailor the interpretations individually to account for specific geologic settings and local formations. The spreadsheet also permits creativity and uniqueness in the graphical presentation of the results, thereby enhancing the abilities and resources available to the geotechnical personnel. Since soils and rocks are complex materials with enumerable variants and facets, a site-specific tailoring of the interpreted profiles and properties is prudent.

### **11.2.2 Boring Location Plans**

A boring location plan should be provided for reference on a regional or local scale. County or city street maps or USGS topographic quad maps are ideally suited for this purpose. Topographic information at 20 ft (6 m) contour line intervals is now downloadable from the internet (e.g., [www.usgs.gov](http://www.usgs.gov)). Topographic maps for the entire United States can also be purchased from commercial suppliers.

The locations of all field tests, sampling, and exploratory studies should be shown clearly on a scaled plan of the specific site under investigation. Preferably, the plan should be a topographic map with well-delineated elevation contours and a properly-established benchmark. The direction of magnetic or true north should be shown. Figure 11-3 shows an example of a boring location plan. The fence baseline defines the line along which a vertical profile of subsurface conditions will be developed based on information from adjacent boring logs. If multiple types of exploratory methods are used, the legend on the site test location plan should clearly show the different types of soundings.

A geographic information system (GIS) can be utilized on the project to locate the test locations with reference to existing facilities on the premises including any and all underground and above-ground utilities, as well as roadways, culverts, buildings, or other

structures. Recent advances have been made in portable measuring devices that utilize global positioning systems (GPS) to permit quick, approximate determinations of coordinates of test locations and installations.

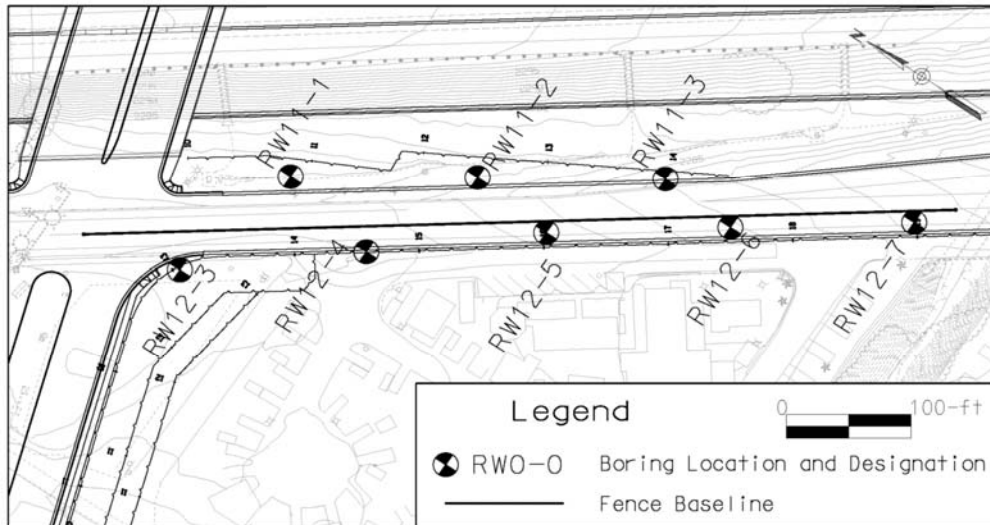


**Figure 11-3. Example boring location plan for retaining walls RW-11 and RW-12 retaining an on-ramp to a freeway.**

### 11.2.3 Subsurface Profiles

Geotechnical reports are normally accompanied by the presentation of subsurface profiles developed from the field and laboratory test data. Longitudinal profiles are typically developed along the roadway or bridge alignment, and a limited number of transverse profiles may be included for key locations such as at major bridge foundations, cut slopes or high embankments. Such profiles provide an effective means of summarizing pertinent subsurface information. The subsurface profiles, coupled with judgment and an understanding of the geologic setting, aid the geotechnical specialist in his/her interpretation of subsurface conditions between the investigation sites.

For the development of a two-dimensional subsurface profile, the profile baseline, typically the roadway centerline, needs to be defined on the boring location plan, and the relevant borings projected to this line. Figure 11-4 shows the subsurface profile along the “Fence Baseline” between retaining walls RW-11 and RW-12 shown in Figure 11-3. Judgment should be exercised in the selection of the borings since projection of the borings, even for short distances, may result in a misleading representation of the subsurface conditions in some situations. The subsurface profile should be presented at a scale appropriate to the depth and frequency of the borings and soundings and the overall length of the cross-section. An exaggerated scale of 1(V):10(H) or 1(V):20(H) is typically used.

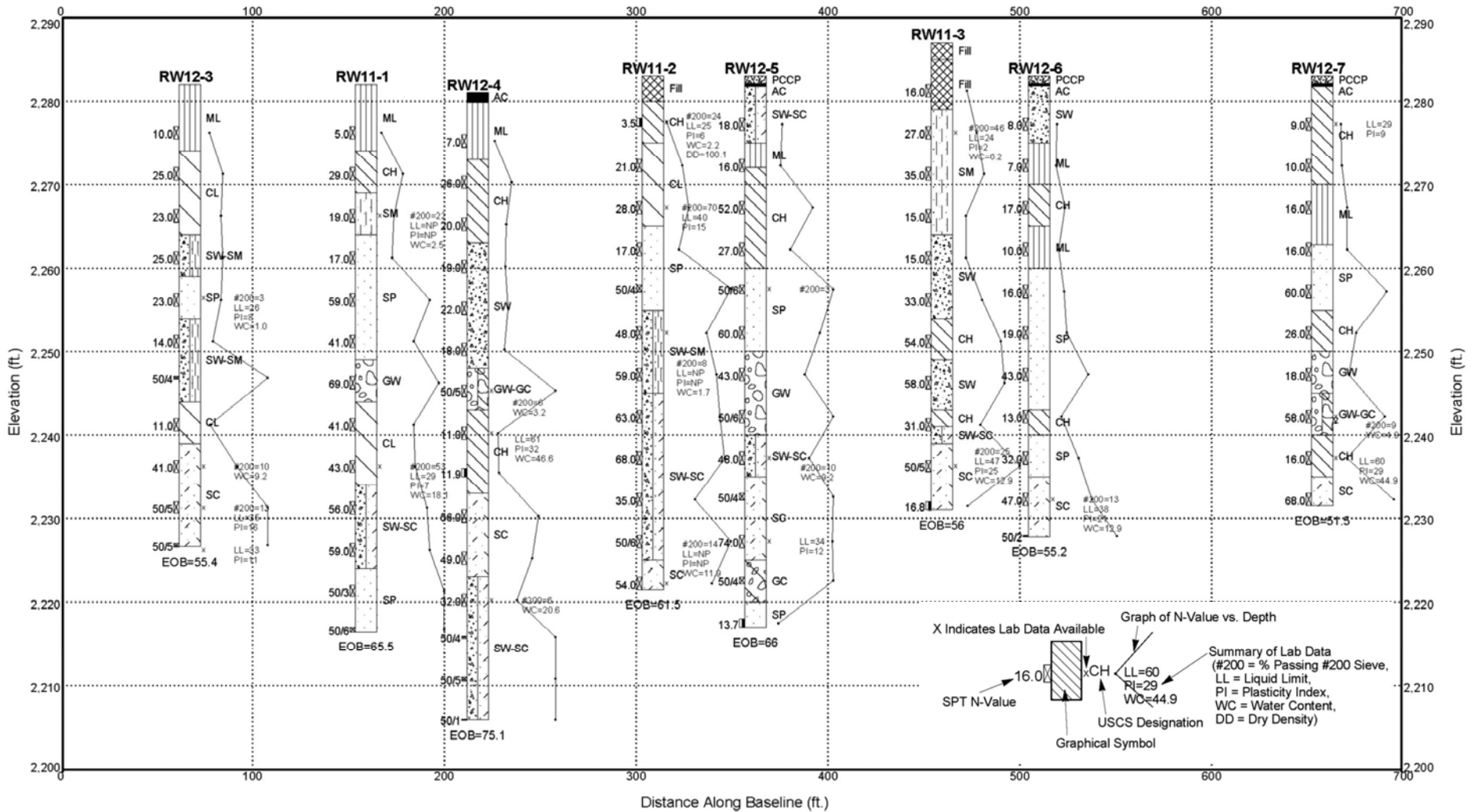


Figure 11-4. Subsurface profile along the baseline between retaining walls RW-11 and RW-12 shown in Figure 11-3.

The subsurface profile can be presented with reasonable accuracy and confidence at the locations of the borings. However, owners and designers generally expect the geotechnical specialist to present a continuous subsurface profile that shows an interpretation of the location, extent and nature of subsurface formations or deposits between borings. At a site where rock or soil profiles vary significantly between boring locations, the value of such presentations become questionable. The geotechnical specialist must be very cautious in presenting such data. Such presentations should include clear and simple caveats explaining that the profiles, as presented, cannot be relied upon fully to represent actual subsurface conditions between investigation locations. Should there be a need to provide more reliable continuous subsurface profiles, the geotechnical specialist should increase the frequency of borings and/or utilize geophysical methods to determine the continuity of subsurface conditions, or lack thereof.

### **11.3 TYPICAL SPECIAL CONTRACT NOTES**

The geotechnical specialist should include in the geotechnical design report any special notes that should be placed in the contract plans or special provisions. The purpose of such special notes is to bring the contractor's and/or project engineer's attention to certain special requirements of the design or construction. Example special notes relating to pile driving, drilled shaft, and embankment construction are as follows:

1. "Difficult driving of piles may be encountered and mechanical equipment may be necessary to remove consolidated material or boulders from the location of piles. This may be accomplished by various types of earth augers, well drilling equipment, or other devices to remove the consolidated material to permit piles to be driven to the desired depth or rated resistance without damage."
2. "If any obstructions to pile driving are encountered ten (10) feet or less from the bottom of the footing, the contractor shall, if so ordered by the engineer, pull the partially driven pile or piles, remove the obstruction, and backfill the hole with approved suitable material, which shall be thoroughly compacted to the satisfaction of the engineer. However, no partially driven pile shall be removed until the engineer is satisfied that the contractor has made every effort to drive the pile through the obstruction. Payment for excavation will be made at the unit price bid for the structure excavation item and for the temporary sheeting under Item \_\_\_\_\_ when sheeting is used. No other extra payment will be made for this work."

3. "The ordered length of pile shall be measured below the cut-off elevation shown on the plans. Any additional lengths of pile or splices above the cut-off elevation necessary to facilitate the contractor's operation shall be at his own expense."
4. "Piles for \_\_\_\_\_ are driven because of possible future scour of the stream bed and shall be driven to the minimum lengths shown on the plans regardless of the resistance to driving. The actual driving resistance is estimated to be \_\_\_\_ tons."
5. "Piles will be acceptable only when driven to pile driving criteria established by the Chief Bridge Engineer. Prerequisite to establishing these criteria, the contractor shall submit, to the Chief Bridge Engineer, and others as required, Form \_\_\_\_\_ 'Pile and Driving Equipment Data'. All information listed on Form \_\_\_\_\_ shall be provided within fourteen (14) days after the award of the contract. Each separate combination of pile and pile driving equipment proposed by the contractor will require the submission of a corresponding Form \_\_\_\_\_."
6. "Piles for the existing structure shall be removed where they interfere with the pile driving for the new structure."
7. "It shall be the contractor's responsibility to place the cofferdams for \_\_\_\_\_ so that they will not interfere with the driving of batter piles. Pay lines for the cofferdams shall be as shown on the plans."
8. "The general subsurface conditions at the site of this structure are as shown on Drawing No. \_\_\_\_\_."
9. "Pile driving will not be allowed at the abutments until fill settlement is complete. Estimated settlement time is \_\_\_\_\_ months after placement of the \_\_\_\_\_ foot surcharge."
10. "The bottom of all drilled shafts shall be cleaned with a mechanical cleanout bucket before the concrete is placed in the shaft. A minimum of \_\_\_\_\_ passes of the cleanout bucket is recommended. For dry shafts, the bottom of the shaft shall be cleaned such that no more than \_\_\_\_\_ inches of excavated spoil and no more than xxxxx inches of water remain at the bottom of the shaft prior to concreting. If wet (slurry) construction processes are used, then the sand content prior to concreting shall not be greater than \_\_\_\_\_ % by volume. In the event that wet (slurry) construction processes are used, the Engineer shall be contacted for further criteria."

11. "Temporary surface casing is recommended to aid in alignment of drilled shafts as well as to prevent surface sloughing or raveling and to ensure personnel safety. A minimum \_\_\_\_\_ ft long temporary surface casing with at least \_\_\_\_\_ ft stick-up above the ground surface is recommended. The diameter of the surface casing shall not be more than be \_\_\_\_\_ inches larger than the nominal diameter of the shaft.
12. "Poorly graded sands and gravels were encountered during the design stage investigations. These soils are prone to caving and may cause large fluid losses during slurry-assisted drilled shaft construction. Therefore, localized caving should be anticipated during drilled shaft construction. These local caving zones may be up to \_\_\_\_\_ ft thick and can occur at various depths."
13. "The contractor shall coordinate the project construction schedule to allow installation of embankment monitoring instrumentation by the Agency forces."  
"Instrumentation damaged by the contractor's personnel shall be repaired or replaced at the contractor's expense. All construction activity in the area of any damaged instrument shall cease until the damage has been corrected."
14. "The contractor's attention is directed to the soil sample gradation test results, which are shown on Drawing No.\_\_\_\_\_. Soil sample gradation test results have been furnished to assist the contractor in determining dewatering procedures, if necessary."
15. "The actual soil resistance to be overcome to reach estimated pile tip elevation is as shown below for each abutment and pier. The contractor shall size his pile driving equipment to install piles to the estimated length without damage."
16. "The south embankment shall be constructed to final grade and a month waiting period observed before pile driving begins. The actual length of the waiting period may be reduced by the Engineer based on an analysis of settlement platform and piezometer data."

## 11.4 SUBSURFACE INFORMATION MADE AVAILABLE TO BIDDERS

The finished boring logs and/or generalized soil profile should be made available to bidders and included with the contract plans. Other subsurface information, such as soil and rock samples and results of field and laboratory testing, should also be made available for inspection by bidders. The invitation for bids should indicate the type of information available and when and where it may be inspected. The highway agency should have a system for documenting what information each contractor inspects. Such documentation can be of major importance in the event of later claim actions.

The information developed during the subsurface exploration is very useful in the selection of effective construction procedures and for estimating construction costs. Such information is, therefore, of value to knowledgeable contractors bidding on the project. There has been much disagreement among owners and engineers as to what information should be made available to bidders, and how. The legal aspects are conflicting. In general, the owner's best interests are served by releasing pertinent information prior to the bid. Indeed, some courts have opined that failure to reveal information can weaken the owner's position in the event of dispute. On the other hand, some engineers are fearful that the release of information will imply guarantees on their part that the information is fully representative of the actual conditions that will be encountered.

One of the best surveys of the problem was prepared by Standing Subcommittee No. 4 of the U.S. National Committee on Tunneling Technology. The Subcommittee was composed of engineers and attorneys having experience dealing with owners, engineering firms, and contracting organizations.

The following is excerpted from their recommendations:

"In sum, all subsurface data obtained for a project, professional interpretations thereof, and the design considerations based on these data and interpretations should be included in the bidding documents or otherwise made readily available to prospective contractors. Fact and opinion should be clearly separated.

The bidder should be entitled to rely on the basic subsurface data, with no obligation to conduct his own subsurface survey.

It is considered, however, that specific disclaimers of responsibility for accuracy are appropriate, with respect to the following categories:

- Information obtained by others, perhaps at other times and for other purposes, which is being furnished prospective bidders in order to comply with the legal obligation to make full disclosure of all available data.
- Interpretations and opinions drawn from basic subsurface data, because equally competent professionals may reasonably draw different interpretations from the same basic data."

Additional information on this topic is included in *Geotechnical Guideline No. 15 – Geotechnical Differing Site Conditions* of FHWA's Geotechnical Engineering Notebook.

## **11.5 LIMITATIONS (DISCLAIMERS)**

Soil and rock exploration and testing have inherent uncertainties. Thus users of the data who are unfamiliar with the variability of natural and manmade deposits should be informed in the report of the limitations inherent in the extrapolation of the limited subsurface information obtained from the site investigation. This notification often takes the form of "Disclaimer" clauses. The validity that courts give disclaimer clauses varies from state to state. However, the courts generally give much more validity to "specific" versus "general" disclaimer clauses. "General" disclaimer clauses are the types that say, in effect - subsurface information was gathered for use in design. However, the contractor should not rely on this information in preparing his bid. It is no big surprise, therefore, that judges give little validity to such general disclaimer clauses since common sense dictates that if the subsurface information is good enough to base the design on, then the contractor should be able to place some reliance on the information in preparing his bid. Dr. Ralph Peck, a noted geotechnical specialist, put it succinctly when asked his opinion concerning general disclaimer of subsurface information on a recent large Interstate project. He stated, "If the state or engineers it has engaged to develop the contract documents have accepted certain information as the basis for those documents, that information should not be disclaimed."

As mentioned previously, the courts have generally upheld the use of "specific" disclaimer clauses. The use of specific disclaimer clauses is strongly recommended over the use of general disclaimer clauses. An example of a specific disclaimer would be a statement such

as – “the boring logs are representative of the conditions at the location where the boring was made but conditions may vary between borings.”

The following are examples of good "specific" disclaimer clauses used by one highway agency. These disclaimer clauses are placed on the interpreted soil profile that is included in the contract plans:

#### General Notes

1. The explorations were made between \_\_\_\_ and \_\_\_\_ by \_\_\_\_\_.
2. General soil and rock (where encountered) strata descriptions and indicated boundaries are based on an engineering interpretation of all available subsurface information by the Agency Name and may not necessarily reflect the actual variation in subsurface conditions between borings and samples. Data and field interpretation of conditions encountered in individual borings are shown on the subsurface exploration logs.
3. The observed water levels and/or conditions indicated on the subsurface profiles are as recorded at the time of exploration. These water levels and/or conditions may vary considerably, with time, according to the prevailing climate, rainfall or other factors and are otherwise dependent on the duration of and methods used in the explorations program.
4. Sound engineering judgment was exercised in preparing the subsurface information presented hereon. This information was prepared and is intended for State design and estimate purposes. Its presentation on the plans or elsewhere is for the purpose of providing intended users with access to the same information available to the State. This interpretation of subsurface information is presented in good faith and is not intended as a substitute for personal investigation, independent interpretations or judgment of the contractor.
5. All structural details shown hereon are for illustrative purposes only and may not be indicative of the final design conditions shown in the contract plans.
6. Footing elevations shown are as indicated at the time of this drawing's preparation.

Other examples of site-specific disclaimers are as follows:

- “The boring logs for BAF-1 through BAF-4 are representative of the conditions at the location where each boring was made, but conditions may vary between borings.”
- “Although boulders in large quantities were not encountered on this site, in the borings that are numbered BAF-1 through BAF-4, previous projects in this area have found large quantities of boulders. Therefore, the contractor should be expected to encounter substantial boulder quantities in excavations. The contractor should include any perceived extra costs for boulder removal in this area in his bid price for Item xxx.”

The reader is referred to a document entitled “*Important Information About Your Geotechnical Engineering Report*,” which is published by ASFE, The Association of Engineering Firms Practicing In The Geosciences ([www.asfe.org](http://www.asfe.org)). This document presents suggestions for writing a geotechnical report and observations to help reduce the geotechnical-related delays, cost overruns and other costly headaches that can occur during a construction project.

[THIS PAGE INTENTIONALLY BLANK]

## CHAPTER 12.0 REFERENCES

AASHTO (1988). *Manual on Subsurface Investigations*. American Association of State Highway and Transportation Officials, Washington, D.C.

AASHTO (1994). *AASHTO LRFD Bridge Design Specifications*, 1<sup>st</sup> Edition. American Association of State Highway and Transportation Officials, Washington, D.C.

AASHTO (1996). *Standard Specifications for Highway Bridges*. American Association of State Highway and Transportation Officials, Washington, D.C.

AASHTO (2002). *Standard Specifications for Highway Bridges*. American Association of State Highway and Transportation Officials, Washington, D.C.

AASHTO (2004 with 2006 Interims). *AASHTO LRFD Bridge Design Specifications*. 3<sup>rd</sup> Edition, American Association of State Highway and Transportation Officials, Washington, D.C.

AASHTO (2006). *Standard Specifications for Transportation Materials and Methods of Sampling and Testing, Parts I and II*. American Association of State Highway and Transportation Officials, Washington, DC.

ACI (1956). *Building Code Requirements for Reinforced Concrete, ACI 318-56*. American Concrete Institute, Detroit, MI.

ACI (1963). *Building Code Requirements for Reinforced Concrete, ACI 318-63*. American Concrete Institute, Detroit, MI.

ACI (1968). *Building Code Requirements for Reinforced Concrete, ACI 318-68*. American Concrete Institute, Detroit, MI.

ACI (2002). *Building Code Requirements for Structural Concrete, ACI 318-02*. American Concrete Institute, Detroit, MI.

API-RP-2A (1993). *Recommended Practice for Planning, Designing and Constructing Fixed Offshore Platforms - Load and Resistance Factor Design*. American Petroleum Institute – Recommended Practices.

- ASCE (1993). *Unsaturated Soils*, Editors: Houston, S. L. and Wray, W. K., Geotechnical Special Publication No. 39, American Society of Civil Engineers, Reston, VA.
- ASCE (1994). *Predicted and Measured Behavior of Five Spread Footings on Sand*. Editors: Briaud, J-L, and Gibbens, R. M. Geotechnical Special Publication No. 41, American Society of Civil Engineers (co-sponsored by the Federal Highway Administration).
- ASCE (1997). *Unsaturated Soil Engineering Practice*, Editors: Houston, S. L. and Fredlund, D. G., Geotechnical Special Publication No. 68, American Society of Civil Engineers, New York, NY.
- ASTM (1988). *Vane Shear Strength Testing in Soils: Field and Laboratory Studies*. American Society for Testing and Materials, Committee D-18 on Soil and Rock For Engineering Purposes, Philadelphia, PA.
- ASTM (2006). *Annual Book of ASTM Standards – Sections 4.02, 4.08, 4.09 and 4.13*. ASTM International, West Conshohocken, PA.
- Atterberg, A. (1911). "Über die Physikalische Bodenuntersuchung und über die Plastizität der Tone." *Internationale Mitteilungen Für Bodenkunde*, 1, 10-43.
- Bielefeld, M.W. and Middendorp, P. (1992). Improved Pile Driving Prediction for Impact and Vibratory Hammers, Proceedings of the 4th International Conference on the Application of Stresswave Theory to Piles, The Hague, A.A. Balkema Publishers.
- Bieniawski, Z. T. (1989). *Engineering Rock Mass Classification*. John Wiley & Sons, NY.
- Bishop, A. W. (1955). "The Use of the Slip Circle in the Stability Analysis of Slopes." *Geotechnique*, Vol. 5 (1), 7-17.
- Blendy, M.M. (1979). Rational Approach to Pile Foundations. Symposium on Deep Foundations, ASCE National Convention.
- Boussinesq, J. (1885). *Application des potentiels à l'étude de l'équilibre et du mouvement des solides élastiques: principalement au calcul des déformations et des pressions que produisent, dans ces solides, des efforts quelconques exercés sur une petite partie de leur surface ou de leur intérieur : mémoire suivi de notes étendues sur divers points de physique, mathématique et d'analyse*. Gauthier-Villars, Paris.

- Bowles, J. E. (1979). *Physical and Geotechnical Properties of Soils*. McGraw-Hill, New York.
- Bowles, J. E. (1996). *Foundation Analysis and Design*. 5<sup>th</sup> Edition, McGraw-Hill, New York.
- Brooker, E. W., and Ireland, H. O. (1965). "Earth Pressures at Rest Related to Stress History." *Canadian Geotechnical Journal*, Vol II, No. 1, 1-15.
- Burmister, D. M. (1970). "Suggested Methods for Identification of Soils." *Special Procedures for Testing Soil and Rock for Engineering Purposes*, American Society for Testing and Materials, Committee D-18 on Soil and Rock for Engineering Purposes, Philadelphia, PA, 311-323.
- Campanella, R. G. (1994). "Field Methods for Dynamic Geotechnical Testing: An Overview of Capabilities and Needs." *Dynamic Geotechnical Testing II*, Special Technical Publication No. 1213, American Society for Testing and Materials, Philadelphia, PA, 3-23.
- Canadian Geotechnical Society. (1992). *Canadian Foundation Engineering Manual*. 3rd, Canadian Geotechnical Society, Richmond, B.C.
- Caquot, A., and Kerisel, F. (1948). *Tables for the Calculation of Passive Pressure, Active Pressure and Bearing Capacity of Foundations*. Gautier-Villars, Paris.
- Carter, M., and Bentley, S. P. (1991). *Correlations of Soil Properties*. Pentech Press Limited, London, U.K.
- Casagrande, A. (1936). "The Determination of the Preconsolidation Load and its Practical Significance." *Discussion 34, Proceedings of the First International Conference on Soil Mechanics and Foundation Engineering*, (III), 60-64.
- Casagrande, A., and Fadum, R. E. (1940). "Notes on Soil Testing for Engineering Purposes." *Publication 268*, Graduate School of Engineering, Harvard University, Cambridge, MA.
- Casagrande, A. (1959). "Discussion of Requirements for the Practice of Applied Soil Mechanics." *Proceedings of the First Panamerican Conference on Soil Mechanics and Foundation Engineering*, Vol III, 1029-1037.

- Cedergren, H. R. (1989). *Seepage, Drainage, and Flow Nets*. 3<sup>rd</sup> Edition, John Wiley & Sons, New York.
- Cernica, J. N. (1982). *Geotechnical Engineering*. CBS College Publishing, Holt, Rinehart and Winston, New York.
- Chen, W., and McCarron, W. O. (1991). "Bearing Capacity of Shallow Foundations." *Foundation Engineering Handbook*, 2nd, Van Nostrand Reinhold, New York, 144-165.
- Clarke, B. G. (1995). *Pressuremeters in Geotechnical Design*. Blackie Academic & Professional, London.
- Collin, J. G., Berg, R. R., and Meyers, M. (2002). "Segmental Retaining Wall Drainage Manual." National Concrete Masonry Association, Herdon, Va.
- Cornell, C. A. (1969). "Probability-Based Structural Code." *American Concrete Institute Journal*, 66(12), 974-985.
- Coulomb, C. A. (1776). *Essai sur une application des règles de maximis & minimis à quelques problèmes de statique, relatifs à l'architecture*. De l'Imprimerie Royale, Paris.
- Culmann, K. (1866). *Die Graphische Statik*. Meyer & Zeller, Zürich.
- Daniel, C. R., Howie, J. A., and Sy, A. (2003). "A Method for Correlating Large Penetration Test (LPT) to Standard Penetration Test (SPT) Blow Counts." *Canadian Geotechnical Journal*, 40(1), 66-77.
- D'Appolonia, D. J., D'Appolonia, E. E., and Brissette, R. F. (1968). "Settlement of Spread Footings on Sand." American Society of Civil Engineers, *Journal of the Soil Mechanics and Foundations Division*, 94 (SM3), 735-760.
- D'Appolonia, D. J., D'Appolonia, E. E., and Brissette, R. F. (1970). Closure to discussions on "Settlement of Spread Footings on Sand." American Society of Civil Engineers, *Journal of the Soil Mechanics and Foundations Division*, 96 (SM2), 754-761.
- Das, B. M. (1990). *Principles of Geotechnical Engineering*. 2<sup>nd</sup> Edition, PWS-Kent Pub. Co, Boston, MA.

- Davisson, M.T. (1972). "High Capacity Piles." *Proceedings, Soil Mechanics Lecture Series on Innovations in Foundation Construction*. American Society of Civil Engineers, Illinois Section, Chicago, 81-112.
- Day, R. W. (1999). *Geotechnical and Foundation Engineering: Design and Construction*. McGraw-Hill, NY.
- Deere, D. U. (1963). "Technical Description of Rock Cores for Engineering Purposes." *Felsmechanik Und Ingenieurgeologie*, 1(1), 16-22.
- Deere, D. U., and Deere, D. W. (1989). "Rock Quality Designation (RQD) After Twenty Years." Report No. DACW39-86-M-4273, U.S. Army Corps of Engineers, Washington, D.C.
- Deere, D. U., and Patton, F. D. (1971). "Slope Stability in Residual Soils." *Proceedings 4th Panamerican Conference on Soil Mechanics and Foundation Engineering, June 1971*, San Juan, PR, 87-170.
- Duncan, J. M. (2000). "Factors of Safety and Reliability in Geotechnical Engineering." American Society of Civil Engineers, *Journal of Geotechnical and Geoenvironmental Engineering*, 126(4), 307-316.
- Duncan, J. M., and Buchignani, A. L. (1976). *An Engineering Manual for Settlement Studies*. University of California, Department of Civil Engineering, Berkeley, CA.
- Duncan, J. M., Clough, G. W., and Ebeling, R. M. (1990). "Behavior and Design of Gravity Earth Retaining Structures." American Society of Civil Engineers, *Geotechnical Special Publication No. 25*, 251-277.
- Duncan, J. M., and Tan, C. K. (1991). "Engineering Manual for Estimating Tolerable Movements of Bridges." *Manuals for the Design of Bridge Foundations: Shallow Foundations, Driven Piles, Retaining Walls and Abutments, Drilled Shafts, Estimating Tolerable Movements, Load Factor Design Specifications, and Commentary.*, NCHRP Report No. 343, Transportation Research Board, National Research Council, Washington, D.C., 219-225.
- Duncan, J. M., and Wright, S. G. (2005). *Soil Strength and Slope Stability*. John Wiley & Sons, New York.

- Dunnicliff, J. (1988). *Geotechnical Instrumentation for Monitoring Field Performance*. John Wiley & Sons, NY.
- Ellingwood, B., Galambos, T. V., MacGregor, J. G., and Cornell, C. A. (1980). *Development of a Probability Based Load Criterion for American National Standard A-58: Building Code Requirements for Minimum Design Loads in Buildings and Other Structures*. U.S. Department of Commerce, National Bureau of Standards, Washington, D.C.
- Fellenius, B. H. (1990). *Guidelines for the Interpretation and Analysis of the Static Loading Test*. Deep Foundation Institute, Sparta, NJ.
- Fellenius, B. H. (1991). *Guidelines for Static Pile Design: Unified Design of Piles and Pile Groups Considering Capacity, Settlement, and Negative Skin Friction*. Deep Foundations Institute, Sparta, NJ.
- Fellenius, B.H., Riker, R.E., O'Brien, A.J. and Tracy, G.R. (1989). "Dynamic and Static Testing in a Soil Exhibiting Set-up." American Society of Civil Engineers, *Journal of Geotechnical Engineering*, Vol. 115, No. 7, 984-1001.
- Fellenius, W. (1936). "Calculation of the Stability of Earth Dams." *Proceedings of the Second Congress of Large Dams*, Vol. 4, 445-463.
- FHWA (1978). *Design and Construction of Compacted Shale Embankments*. Report No. FHWA RD-78-141, Authors: Strohm, W. E., Bragg, G. H., Zeigler, T. W., Federal Highway Administration, U.S. Department of Transportation.
- FHWA (1982). *Performance of Highway Bridge Abutments on Spread Footings on Compacted Fill*. Report No. FHWA RD-81-184, Author: DiMillio, A. F., Federal Highway Administration, U.S. Department of Transportation.
- FHWA (1984). *Handbook on Piles and Drilled Shafts under Lateral Load*. Report No. FHWA IP-84-11, Federal Highway Administration, U.S. Department of Transportation.
- FHWA (1985). *Tolerable Movement Criteria for Highway Bridges*. Report No. FHWA RD-85-107, Authors: Moulton, L. K., GangaRao, H. V. S., Halvorsen, G. T., Federal Highway Administration, U.S. Department of Transportation.

- FHWA (1986). *Prefabricated Vertical Drains – Vol. I, Engineering Guidelines*. Report No. FHWA/RD-86/168, Authors: Rixner, J. J., Kraemer, S. R., and Smith, A. D., Federal Highway Administration, U.S. Department of Transportation.
- FHWA (1987). *Spread Footings for Highway Bridges*. Report No. FHWA RD-86-185, Author: Gifford, D. G., Kraemer, S. R., Wheeler, J. R., McKown, A. F., Federal Highway Administration, U.S. Department of Transportation.
- FHWA (1988). *Checklist and Guidelines for Review of Geotechnical Reports and Preliminary Plans and Specifications*. Report No. FHWA ED-88-053, Federal Highway Administration, U.S. Department of Transportation, Revised 2003.
- FHWA (1989a). *Geotechnical Differing Site Conditions*. Geotechnical Engineering Notebook GT-15, Federal Highway Administration, U.S. Department of Transportation.
- FHWA (1989b). *The Pressuremeter Test for Highway Applications*. Report No. FHWA IP-89-008, Authors: Briaud, J., Federal Highway Administration, U.S. Department of Transportation.
- FHWA (1992a). *The Cone Penetrometer Test*. Report No. FHWA NHI-91-043, Authors: Riaund J-L and Miran J., Federal Highway Administration, U.S. Department of Transportation.
- FHWA (1992b). *The Flat Dilatometer Test*. Report No. FHWA SA-91-044, Authors: Riaund, J. L., and Miran, J., Federal Highway Administration, U.S. Department of Transformation.
- FHWA (1992c). *Static Testing of Deep Foundations*. Report No. FHWA SA-91-042, Author: Kyfor, Z. G., Federal Highway Administration, U.S. Department of Transportation.
- FHWA (1996). *Determination of Pile Driveability and Capacity from Penetration Tests*. FHWA Contract No. DTFH61-91-C-00047, Authors: Rausche, F., Thendean, G., Aboumatar, H., Likins, G. and Goble, G., Federal Highway Administration, U.S. Department of Transportation.
- FHWA (1997). *Subsurface Investigations: Training Course in Geotechnical and Foundation Engineering*. Report No. FHWA HI-97-021, Authors: Arman, A., Samtani, N. C., and Castelli, R. J., Federal Highway Administration, U.S. Department of Transportation.

- FHWA (1998a). *Rock Slopes: Reference Manual*. Report No. FHWA HI-99-007, Authors: Wyllie, D. and Mah, C., Federal Highway Administration, U.S. Department of Transportation.
- FHWA (1998b). *DRIVEN 1.0: A Microsoft Windows™ Based Program For Determining Ultimate Vertical Static Pile Capacity*. Report No. FHWA SA-98-074, Authors: Mathias, D., and Cribbs, M., Federal Highway Administration, U.S. Department of Transportation.
- FHWA (1999). *Drilled Shafts: Construction Procedures and Design Methods*. Report No. FHWA IF-99-025, Authors: O'Neill, M. W., Reese, L. C., Federal Highway Administration, U.S. Department of Transportation.
- FHWA (2001a). *Soil Slope and Embankment Design Reference Manual*. Report No. FHWA NHI-01-026, Authors: Collin, J. G., Hung, J. C., Lee, W. S., Munfakh, G., Federal Highway Administration, U.S. Department of Transportation.
- FHWA (2001b). *Mechanically Stabilized Earth Walls and Reinforced Soil Slopes: Design and Construction Guidelines*. Report No. FHWA NHI-00-043, Authors: Elias, V., Ryan B., Federal Highway Administration, National Highway Institute, U.S. Department of Transportation.
- FHWA (2001c). *Evaluating Scour at Bridges*. Hydraulic Engineering Circular No. 18, Authors: Richardson, E. V. and Davis, S. R., Federal Highway Administration, U.S. Department of Transportation.
- FHWA (2002a). *Geotechnical Engineering Circular 5 (GEC5) - Evaluation of Soil and Rock Properties*. Report No FHWA-IF-02-034. Authors: Sabatini, P.J, Bachus, R.C, Mayne, P.W., Schneider, J.A., Zettler, T.E., Federal Highway Administration, U.S. Department of Transportation.
- FHWA (2002b). *Subsurface Investigations (Geotechnical Site Characterization)*. Report No. FHWA NHI-01-031, Authors: Mayne, P. W., Christopher, B. R., and DeJong, J., Federal Highway Administration, U.S. Department of Transportation.
- FHWA (2002c). *Geotechnical Engineering Circular 6, Shallow Foundations*. Report No. FHWA-SA-02-054, Author: Kimmerling, R.E. 2002, Federal Highway Administration, U.S. Department of Transportation.

FHWA (2002d). *Drilled Shaft Inspector's Qualification Course*. Report No. FHWA NHI-03-018, Authors: Willams, R., Burnett, D., and Savidge, J., Federal Highway Administration, U.S. Department of Transportation.

FHWA (2003). *Application of Geophysical Methods to Highway Related Problems*. Contract No. DTFH68-02-P-00083, Authors: Wightman, W. E., Jalinoos, F., Sirles, P., and Hanna, K., Federal Highway Administration, U.S. Department of Transportation.

FHWA (2005a). "Micropile Design and Construction," Report No. FHWA NHI-05-039, Authors: Sabatini, P.J., Tanyu, B., Armour, P., Groneck, P., and Keeley, J., National Highway Institute, Federal Highway Administration, U.S. Department of Transportation.

FHWA (2005b). *Earth Retaining Structures - DRAFT*. Report No. FHWA-SA-05-046, Authors: Tanyu, B.F., Sabatini, P.J. and Berg, R.R., Federal Highway Administration, U.S. Department of Transportation.

FHWA (2006a). *Design and Construction of Driven Pile Foundations - Vol. I and II*, Report No. FHWA-NHI-05-042 and FHWA-NHI-05-043, Authors: Hannigan, P.J., G.G. Goble, G. Thendean, G.E. Likins and F. Rausche., Federal Highway Administration, U.S. Department of Transportation.

FHWA (2006b). *Ground Improvement Methods*, FHWA NHI-06-019 (Vol. I) and FHWA NHI-06-020 (Vol. II) Authors: Elias, V., Welsh, J., Warren, J., Lukas, R., Collin, J.G. and Berg, R.R., Federal Highway Administration, U.S. Department of Transportation.

FHWA (2006c) *Geotechnical Engineering Circular No. 8, Continuous Flight Auger Piles*, Authors: Brown, D. and Dapp, S., Federal Highway Administration, U.S. Department of Transportation. (unpublished).

FoSSA (2003). ADAMA Engineering ([www.GeoPrograms.com](http://www.GeoPrograms.com)), Newark, DE.

Fredlund, D. G., and Rahardjo, H. (1993). *Soil Mechanics for Unsaturated Soils*. John Wiley & Sons, NY.

Geotechnical Engineering Notebook. *FHWA Geotechnical Guidelines GT1 –GT16*.  
<http://www.fhwa.dot.gov/engineering/geotech/index.cfm>.

- Glossop, R. (1968). "The Rise of Geotechnology and its Influence on Engineering Practice." Eighth Rankine Lecture, *Geotechnique*, Vol. 18 (2), 107-150.
- Goble, G. G. and Rausche, F. (1976). *Wave Equation Analysis of Pile Driving – WEAP Program*. Vol. I-IV, Federal Highway Administration, U.S. Department of Transportation.
- Goodman, R. E. (1989). *Introduction to Rock Mechanics*. 2<sup>nd</sup> Edition, John Wiley & Sons, NY.
- Goodman, R. E. (1993). *Engineering Geology: Rock in Engineering Construction*. John Wiley & Sons, NY.
- Hansen, J. B., and Inan, S. (1970). *A Revised and Extended Formula for Bearing Capacity*. Bulletin No. 28, Danish Geotechnical Institute, Copenhagen.
- Hazen, A. (1911). Discussion of "Dams on Sand Foundations." By A. C. Koenig, *Transactions*, ASCE, Vol. 73, 199-203.
- Hirsch, T.J., Carr, L. and Lowery, L.L. (1976). *Pile Driving Analysis*. TTI Program, U.S. Department of Transportation, Federal Highway Administration, Offices of Research and Development, IP-76-13, Washington, D.C., Volumes I-IV.
- Holloway, D.M. and Beddard, D.L. (1995). "Dynamic Testing Results Indicator Pile Test Program - I-880." *Proceedings of the 20th Annual Members Conference of the Deep Foundations Institute*.
- Holtz, R. D., and Kovacs, W. D. (1981). *An Introduction to Geotechnical Engineering*. Prentice-Hall, Englewood Cliffs, N.J.
- Holtz, W. C., and Hilf, J. W. (1961). "Settlement of Soil Foundations Due to Saturation." *Proceedings of the 5th International Conference on Soil Mechanics and Foundation Engineering*, Paris, France, 673-679.
- Horvath, R. G., and Kenney, T. C. (1979). "Shaft Resistance of Rock-Socketed Drilled Piers." *Proceedings of the Symposium on Deep Foundations*, American Society of Civil Engineers, Atlanta, GA, 182-214.

- Hough, B. K. (1957). *Basic Soils Engineering*. 2<sup>nd</sup> Edition, The Ronald Press Company, New York, NY.
- Hough, B. K. (1959). "Compressibility as Basis for Soil Bearing Value." American Society of Civil Engineers, *Journal of the Soil Mechanics and Foundations Division*, 85(SM4, Part 1), 11-39.
- Hussein, M.H., Likins, G.E. and Hannigan, P.J. (1993). "Pile Evaluation by Dynamic Testing During Restrike." *Eleventh Southeast Asian Geotechnical Conference, Singapore*.
- Hvorslev, M. J. (1948). *Subsurface Exploration and Sampling of Soils for Civil Engineering Purposes*. U.S. Army Corps of Engineers, Waterways Experiment Station, Vicksburg, MS.
- Ingles, O. G. (1962). "Bonding Forces in Soils, Part 3: A Theory of Tensile Strength for Stabilised and Naturally Coherent Soils." *Proceedings of the First Conference of the Australian Road Research Board*, Victoria, Australia, 1025-1047.
- ISRM. (1981). *Suggested Methods for the Quantitative Description of Discontinuities in Rock Masses*. International Society for Rock Mechanics, Committee on Field Tests, No. 4, Pergamon Press, UK.
- Jaky, J. (1944). "The Coefficient of Earth Pressure at Rest." *Journal of the Society of Hungarian Architects and Engineers*, Vol. 78, No. 22, 355-358.
- Janbu, N. (1954). "Applications of Composite Slip Surfaces for Stability Analysis." *Proceedings of the European Conference on the Stability of Earth Slopes*, Stockholm, Vol. 3, 39-43.
- Janbu, N. (1968). *Stability Analysis of Slopes with Dimensionless Parameters*. Harvard University, Cambridge, MA.
- Jumikis, A. R. (1962). *Soil Mechanics*. D. Van Nostrand Company, Princeton, N.J.
- Komurka, V. E., Wagner, A. B., and Edil, T. (2003). *Estimating Soil/Pile Set-Up*. Wisconsin Highway Research Program, Madison, WI.
- Krebs, R. D., and Walker, R. D. (1971). *Highway Materials*. McGraw-Hill, NY.

- Kulhawy, F. H., and Mayne, P. W. (1990). *Manual on Estimating Soil Properties for Foundation Design*. Report EL-6800, Electric Power Research Institute, Palo Alto, CA.
- Kulhawy, F.H. (1983). *Transmission Line Structure Foundations for Uplift and Compression Loading*, Report No. EL-2870, Electric Power Research Institute.
- Kulicki, J. M. (1998). *Development of Comprehensive Bridge Specifications and Commentary*. NCHRP Research Results Digest 198, Transportation Research Board, National Research Council, Washington, D.C.
- Lambe, P. C. (1996). "Residual Soils." *Landslides Investigation and Mitigation*, Special Report No. 247, Transportation Research Board, National Research Council, Washington, D.C., 507-524.
- Lambe, T. W., and Whitman, R. V. (1979). *Soil Mechanics: SI Version*. John Wiley & Sons, NY.
- Lee, K. L., and Singh, A. (1971). "Compaction of Granular Soils." *Proceedings of the 9th Annual Engineering Geology and Soils Engineering Symposium*, Idaho Department of Highways, Boise, ID, 161-174.
- Leshchinsky, D. and Perry, E. B. (1987). "A Design Procedure for Geotextile-Reinforced Walls." *Proceedings Geosynthetics '87 Conference.*, IFAI, Industrial Fabric Association International, New Orleans, 95-107.
- Lunne, T., Robertson, P. K., and Powell, J. J. M. (1997). *Cone Penetration Testing in Geotechnical Practice*. E & FN Spon, New York, NY.
- Mayne, P. W., and Kulhawy, F. H. (1982). "K<sub>o</sub>-OCR Relationships in Soil." American Society of Civil Engineers, *Journal of the Geotechnical Engineering Division*, 108(GT6), 851-872.
- Meyerhof, G. G. (1953). "The Bearing Capacity of Foundations under Eccentric and Inclined Loads." *Proceedings of the 3<sup>rd</sup> International Conference of Soil Mechanics and Foundation Engineering, Volume I* Zurich, 440-445.

- Meyerhof, G. G. (1957). "The Ultimate Bearing Capacity of Foundations on Slopes." *Proceedings of the 4th International Conference of Soil Mechanics and Foundation Engineering*, London, Paris, 384-386.
- Meyerhof, G. G. (1976). "Bearing Capacity and Settlement of Pile Foundations." American Society of Civil Engineers, *Journal of Geotechnical Engineering*, 102(No. GT3), 197-228.
- Mitchell, J. K. (1976). *Fundamentals of Soil Behavior*. John Wiley & Sons, NY.
- Murthy, V. N. S. (1989). *Soil Mechanics and Foundation Engineering*. Vol I - Soil Mechanics, 3<sup>rd</sup> Edition, Sai Kripa Technical Consultants, Bangalore.
- NAVFAC (1986a). *Design Manual 7.01 - Soil Mechanics*. Department of the Navy, Naval Facilities Engineering Command, Alexandria, VA.
- NAVFAC (1986b). *Design Manual 7.02 - Foundation and Earth Structures*. Department of the Navy, Naval Facilities Engineering Command, Alexandria, VA.
- NCHRP (1983). *Shallow Foundations for Highway Structures*. NCHRP Report 107, Author: Wahls, H. E., Transportation Research Board, National Research Council, Washington, D.C.
- NCHRP (1989). *Treatment of Problem Foundations for Highway Embankments*. NCHRP Report 147, Author: Holtz, R. D., Transportation Research Board, National Research Council, Washington, D.C.
- NCHRP (1990). *Design and Construction of Bridge Approaches*. NCHRP Report 159, Author: Wahls, H. E., Transportation Research Board, National Research Council, Washington, D.C.
- NCHRP (1991). *Manuals for the Design of Bridge Foundations : Shallow Foundations, Driven Piles, Retaining Walls and Abutments, Drilled Shafts, Estimating Tolerable Movements, Load Factor Design Specifications, and Commentary*. NCHRP Report 343, Authors: Barker, R.M., J.M. Duncan, K.B. Rojiani, P.S.K. Ooi, C.K. Tan and S.G. Kim, Transportation Research Board, National Research Council, Washington, D.C.

- NCHRP (1993). *Downdrag on Bitumen-Coated Piles*. NCHRP Report 24-5, Author: Briaud, J-L and Tucker, L. M., Transportation Research Board, National Research Council, Washington, D.C.
- NCHRP (1997). *Settlement of Bridge Approaches (The Bump at the End of the Bridge)*. NCHRP Report 234, Authors: Briaud, J-L, James, R. W., and Hoffman S. B., Transportation Research Board, National Research Council, Washington, D.C.
- Nicu, N. D., Antes, D. R., and Kessler, R. S. (1971). "Field Measurements on Instrumented Piles Under an Overpass Abutment." *Highway Research Record No. 354 - Bridges and Bridge Foundations*, Discussion by Seymour-Jones, Highway Research Board, National Research Council, Washington, D.C., 90-102.
- Nordlund, R. L. (1979). "Point Bearing and Shaft Friction of Piles in Sand." *5<sup>th</sup> Annual Fundamentals of Deep Foundation Design*.
- Nordlund, R. L. (1963). "Bearing Capacity of Piles in Cohesionless Soils." American Society of Civil Engineers, *Journal of the Soil Mechanics and Foundations Division*, 89(SM3), 1-35.
- NYSDOT. "Pressure Coefficients Beneath the End of a Fill." Drawing SM 1330, New York State Department of Transportation, Albany, NY.
- O'Neill, M. W. (1983). "Group Action in Offshore Piles." *Proceedings of the Conference on Geotechnical Practice in Offshore Engineering*, American Society of Civil Engineers, University of Texas at Austin, Austin, TX., 25-64.
- O'Neill, M. W., and Raines, R. D. (1991). "Load Transfer for Pipe Piles in Highly Pressured Dense Sand." American Society of Civil Engineers, *Journal of Geotechnical Engineering*, 117(8), 1208-1226.
- O'Rourke, T. D., and Jones, C. J. F. P. (1990). "Overview of Earth Retention Systems: 1970-1990." *Proceedings of Conference on Design and Performance of Earth Retaining Structures*, American Society of Civil Engineers, New York, NY, 22-51.
- Padfield, C. J., and Mair, R. J. (1984). *Design of Retaining Walls Embedded in Stiff Clay*. Report No. 104, Construction Industry Research and Information Association, London, England.

- Paikowsky, S. G., and Whitman, R. V. (1990). "Effects of Plugging on Pile Performance and Design." *Canadian Geotechnical Journal*, 27(4), 429-440.
- Peck, R. B. (1969). "Advantages and Limitations of the Observational Method in Applied Soil Mechanics." *Geotechnique*, Vol. 19 (2), 171-187.
- Peck, R. B., Hanson, W. E., and Thornburn, T. H. (1974). *Foundation Engineering*. 2<sup>nd</sup> Edition, John Wiley & Sons, NY.
- Perloff, W. H., and Baron, W. (1976). *Soil Mechanics: Principles and Applications*. John Wiley & Sons, NY.
- Pile Dynamics, Inc. (2005). GRLWEAP Procedures and Models, Version 2005. 4535 Renaissance Parkway, Cleveland, OH.
- Poulos, H. G., and Davis, E. H. (1974). *Elastic Solutions for Soil and Rock Mechanics*. John Wiley & Sons, NY.
- Powers, J. P. (1992). *Construction Dewatering: New Methods and Applications*. 2nd, John Wiley & Sons, NY.
- Raines, R. D., Ugaz, O. G., and O'Neill, M. W. (1992). "Driving Characteristics of Open-Toe Piles in Dense Sand." American Society of Civil Engineers, *Journal of Geotechnical Engineering*, 118 (No. 1), 72-88.
- Rankine, W. J. M. (1857). "On the Stability of Loose Earth." *Proceedings of the Royal Society of London*, London, 185-187.
- Rausche, F., Liang, L., Allin, R., and Rancman, D. (2004). "Applications and Correlations of the Wave Equation Analysis Program GRLWEAP." *Proceedings of the 7th International Conference on the Application of Stresswave Theory to Piles*, Petaling Jaya, Selangor, Malaysia, 2004.
- Reese, L. C., Isenhower, W. M., and Wang, S-T. (2006). *Analysis and Design of Shallow and Deep Foundations*. John Wiley & Sons, NY.
- ReSSA (2001). ADAMA Engineering ([www.GeoPrograms.com](http://www.GeoPrograms.com)), Newark, DE.

- Roberts, F.L., Kandhal, P.S., Brown, E.R., Lee, D.Y., and Kennedy, T.W. (1996). *Hot Mix Asphalt Materials, Mixture Design, and Construction*. National Asphalt Pavement Association Education Foundation. Lanham, MD.
- Robertson, P. K., Campanella, R. G., Gillespie, D., and Greig, J. (1986). "Use of Piezometer Cone Data." *Geotechnical Special Publication No. 6, Use of In-Situ Tests in Geotechnical Engineering*, American Society of Civil Engineers, New York, N.Y., 1263-1280.
- Robertson, P. K., and Campanella, R. G. (1983). "Interpretation of Cone Penetration Tests." *Canadian Geotechnical Journal*, 20(4), 718-754.
- Samtani, N.C., Jalinoos, F., and Poland, D. M. (2005). "Integrity Testing of Drilled Shafts – Existing and New Techniques." *Proceedings of the GEO<sup>3</sup> Conference*, ADSC, Dallas, TX.
- Schmertmann, G. R., Chouery-Curtis, V. E., Johnson, R. D., and Bonaparte, R. (1987). "Design Charts for Geogrid-Reinforced Soil Slopes." *Proceedings Geosynthetics '87 Conference*, IFAI, Industrial Fabric Association International, New Orleans, 108-120.
- Schmertmann, J. H. (1955). "The Undisturbed Consolidation Behavior of Clay." *Transactions*, ASCE, Vol. 120, 1201-1233.
- Schmertmann, J. H., Hartman, J. P., and Brown, P. R. (1978). "Improved Strain Influence Factor Diagrams." American Society of Civil Engineers, *Journal of the Geotechnical Engineering Division*, 104 (No. GT8), 1131-1135.
- Schmidt, B. (1966). "Discussion of, Earth Pressure At-Rest Related to Stress History." *Canadian Geotechnical Journal*, 3(4), 239-242.
- Schroeder, W. L. (1980). *Soils in Construction*. 2<sup>nd</sup> Edition, John Wiley & Sons, NY.
- Seed, H. B., Woodward, R. J., and Lundgren, R. (1962). "Prediction of Swelling Potential for Compacted Clays." American Society of Civil Engineers, *Journal of the Soil Mechanics and Foundations Division*, 88(SM3, Part 1), 53-87.
- Silvestri, V. (1983). "Bearing Capacity of Dykes and Fills Founded on Soft Soils of Limited Thickness." *Canadian Geotechnical Journal*, 20(3), 428-436.

- Skempton, A. W. (1953). "The Collodial Activity of Clays." *Proceedings 3rd International Conference on Soil Mechanics and Foundation Engineering*, 57-61.
- Skempton, A. W. (1957). "Discussion on the Planning and Design of the New Hong Kong Airport." *Proceedings of the Institution of Civil Engineering*, 7(3), 305-307
- Skempton, A. W. (1986). "Standard Penetration Test Procedures and the Effects in Sands of Overburden Pressure, Relative Density, Particle Size, Ageing, and Overconsolidation." *Geotechnique*, Vol. 3(1), 30-53.
- SLOPE/W (2004). Geo-SLOPE/W International Ltd., Calgary, Alberta, Canada.
- Smith, E.A.L. (1960). "Pile Driving Analysis by the Wave Equation." American Society of Civil Engineers, *Journal of the Soil Mechanics and Foundations Division*, 86(4), 35-61.
- Stevens, R.F. (1988). "The Effect of a Soil Plug on Pile Driveability in Clay." *Proceedings of the Third International Conference on the Application of Stress Wave Theory to Piles*, B.H. Fellenius, Editor, BiTech Publishers, Vancouver, 861-868.
- Soares, M., de Mello, J. and de Matos, S. (1984). "Pile Driveability Studies, Pile Driving Measurements." *Proceedings of the Second International Conference on the Application of Stress-Wave Theory to Piles*, Stockholm, 64-71.
- Sokolovski, V. V. (1954). *Statics of Soil Media*. Translated from Russian by D. H. Jones and A. N. Schoefield, Butterworths, London.
- Sowers, G. F. (1979). *Introductory Soil Mechanics and Foundations: Geotechnical Engineering*. 4<sup>th</sup> Edition, Macmillan, New York, NY.
- Spencer, E. (1967). "A Method of Analysis of Embankments assuming Parallel Interslice Forces." *Geotechnique*, Vol. 17 (1), 11-26.
- Taylor, D. W. (1948). *Fundamentals of Soil Mechanics*. John Wiley & Sons, New York, NY.
- Teng, W. (1962). *Foundation Design*. Prentice-Hall, Inc., Englewood Cliffs, NJ.
- Terzaghi, K. (1943). *Theoretical Soil Mechanics*. John Wiley & Sons, New York, NY.

- Terzaghi, K., and Peck, R. (1967). *Soil Mechanics in Engineering Practice*. 2<sup>nd</sup> Edition, John Wiley & Sons, New York, NY.
- Terzaghi, K., Peck, R. B., and Mesri, G. (1996). *Soil Mechanics in Engineering Practice*. 3<sup>rd</sup> Edition, John Wiley & Sons, New York, NY.
- Thompson, C. D., and Thompson, D. E. (1985). "Real and Apparent Relaxation of Driven Piles." American Society of Civil Engineers, *Journal of Geotechnical Engineering*, 111(2), 225-237.
- Thorburn, S. H. (1966). "Large Diameter Piles Founded in Bedrock." *Proceedings, Symposium on Large Bored Piles* (Institute for Civil Engineering, London), 95-103.
- Tomlinson, M. J. (1994). *Pile Design and Construction Practice*. 4<sup>th</sup> Edition, E & FN Spon, New York, NY.
- Tomlinson, M. J. (1980). *Foundation Design and Construction*. 4<sup>th</sup> Edition, Pitman, Boston, MA.
- Tomlinson, M. J. (1995). *Foundation Design and Construction*. 6<sup>th</sup> Edition, Pitman, Boston, MA.
- Tschebotarioff, G.P. (1951). *Soil Mechanics, Foundations and Earth Structures*, McGraw-Hill, New York.
- USACE (1994). *Settlement Analysis*. US Army Corps of Engineers, Washington, D.C.
- USBR (1960). *Design of Small Dams*. U.S. Bureau of Reclamation, Washington, D.C.
- USDA (1993). *Soil Survey Manual*. U.S. Department of Agriculture, Washington, D.C.
- USS Steel (1975). *USS Steel Sheet Piling Design Manual*. USS Steel, Pittsburg, PA.
- Utah DOT – Pavement Design and Management Manual (2005).
- Vaughan, P. R., Maccarini, M., and Mokhtar, S. M. (1988). "Indexing the Engineering Properties of Residual Soil." *Quarterly Journal of Engineering Geology & Hydrogeology*, 21(1), 69-84.

- Vesic, A. S. (1977). *Design of Pile Foundations*. NCHRP Report 42, Transportation Research Board, National Research Council, Washington, D.C.
- Vesic, A. S. (1975). "Bearing Capacity of Shallow Foundations." *Foundation Engineering Handbook*, 2nd, Van Nostrand Reinhold, New York, NY, 121-147.
- Westergaard, H. M. (1938). *A Problem of Elasticity Suggested by a Problem in Soil Mechanics: Soft Material Reinforced by Numerous Strong Horizontal Sheets*. Harvard University, Cambridge, MA.
- Winterkorn, H. F., and Fang, H. (1975). *Foundation Engineering Handbook*. 2<sup>nd</sup> Edition, Van Nostrand Reinhold, New York, NY.
- Woodward, R. J., Gardner, W. S., and Greer, D. M. (1972). *Drilled Pier Foundations*. McGraw-Hill, NY.
- Wright, S. G., Arcement, B., and Benson, C. H. (2003). "Comparison of Maximum Density of Cohesionless Soils Determined Using Vibratory and Impact Compaction Methods." *Soil and Rock America 2003, Proceeding of the 12<sup>th</sup> Panamerician Conference on Soil Mechanics and Geotechnical Engineering*, Cambridge, MA, 1709-1715.
- WSDOT (1988). Comparison of Methods for Estimating Pile Capacity. Report No. WA-RD 163.1, Authors: Fragasny, R. J., Higgins, J. D., and Argo, D. E., Washington State Department of Transportation, Olympia.
- Wyllie, D. C. (1999). *Foundations on Rock*. 2<sup>nd</sup> Edition, E & FN Spon, New York, NY.

[THIS PAGE INTENTIONALLY BLANK]

**APPENDIX A**

**APPLE FREEWAY PROJECT**

[THIS PAGE INTENTIONALLY BLANK]

**APPENDIX A**  
**APPLE FREEWAY PROJECT**  
**GENERAL NOTES**

This appendix presents the geotechnical engineering considerations and calculations for a fictitious bridge project from conception to completion in a serialized illustrative workshop design problem. The appendix is divided into several sections. Each section corresponds to a specific phase in the design and construction monitoring process. The section numbering system is as follows:

A.#

where A denotes appendix designation and # denotes the section number in the manual. Thus, Section A.2 relates to the second section in the appendix. Within each section, the numbering system for pages, figures, tables, etc. is in accordance with the following format:

A.# - \*

where # denotes the section number in the appendix and \* denotes the page number, figure number and so on in that section. Thus, for example, “Figure A.2-4” refers to the fourth figure in the second section, and “A.2-4” at the bottom of the page refers to the fourth page in the second section.

As an aid to following the design process, a summary of relevant concepts and/or procedures is presented at the beginning of each section with cross reference to the appropriate chapter(s) in the text of the manual. Equations used in the computations are also cross referenced to the equation number listed in the text of the manual.

To simplify hand calculations, the unit weight of water,  $\gamma_w$ , of 60 pcf has been used in some of the calculations. In actual calculations for any given project, the user should use the more common value of  $\gamma_w = 62.4$  pcf unless higher values are justified, e.g., in brackish water.

## **SECTION A.1 INTRODUCTION AND SCOPE OF WORK**

### **A.1-1 RELEVANT CONCEPTS AND PROCEDURES**

- Description of the project.
- Development of a scope of work

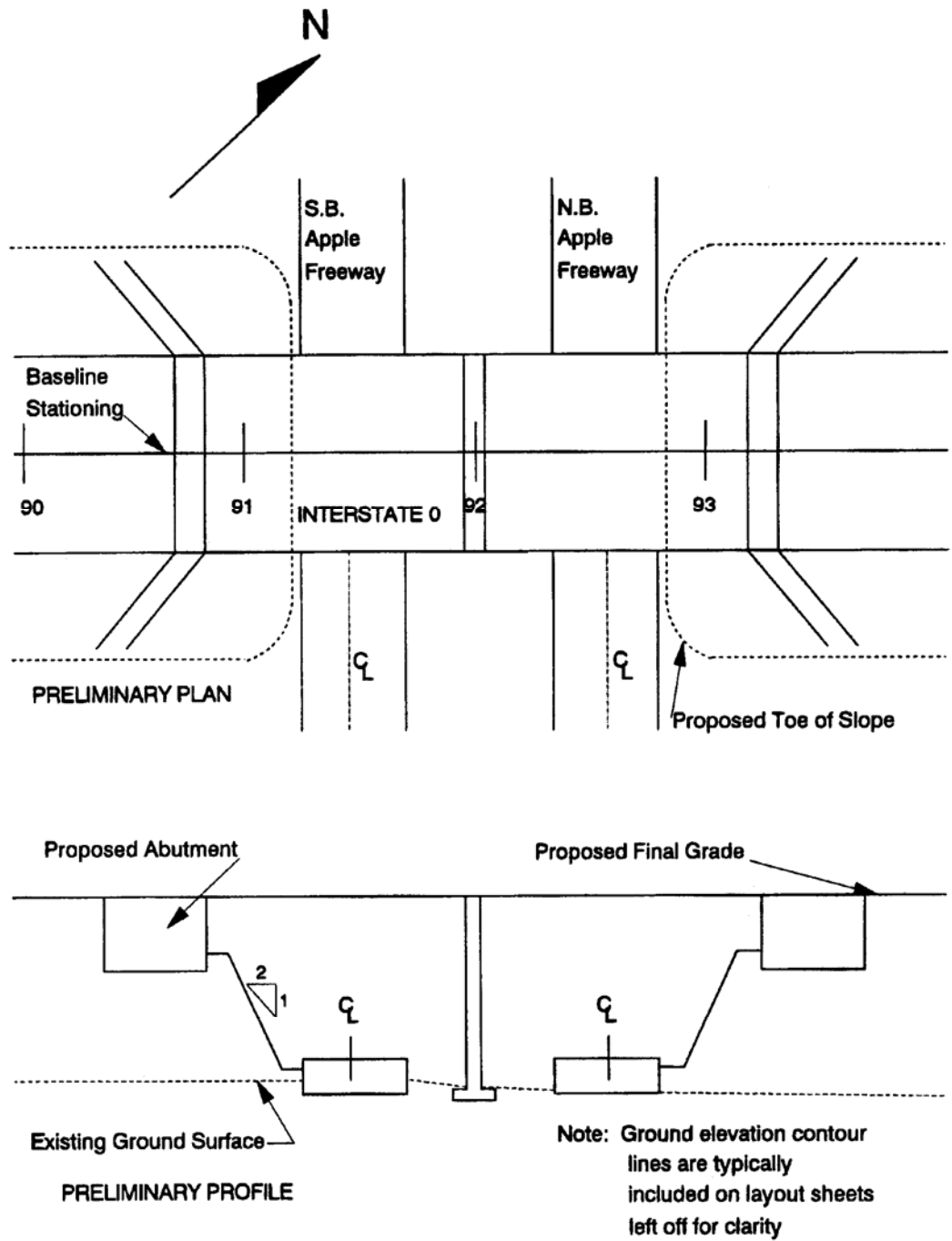
### **A.1-2 DESCRIPTION OF THE PROJECT**

Figure A.1-1 shows the layout of a two-span bridge that carries Interstate 0 (I-0) over the Apple Freeway, which is a divided freeway. The center pier of the I-0 bridge will be in the median between the northbound (NB) and southbound (SB) freeway. The approaches to the bridge will be constructed on embankment fills. The fills will have an end-slope spilling through the abutment locations at a grade of 2H:1V (H: Horizontal, V: Vertical) as shown in Figure A.1-1.

### **A.1-3 SCOPE OF WORK**

The scope of the work includes the following:

- Setup and perform the field investigations. The field investigations should include SPTs in drilled holes and CPTs to obtain continuous stratigraphic profiles. Develop idealized subsurface profile based on visual description of soils and information from CPT sounding profiles.
- Setup and perform laboratory investigations including consolidation and strength tests.
- Perform slope stability analyses for the 2H:1V end-slopes. Evaluate the end-slopes for both circular and block failure mechanisms.
- Perform immediate and consolidation settlement analyses and lateral squeeze computations for embankment fills. If warranted, perform ground improvement as necessary to mitigate large long-term settlements. Evaluate two alternatives (a) surcharging and (b) surcharging with wick-drains.
- Evaluate and analyze spread shallow foundations at both abutment and pier locations. Determine the allowable bearing capacity, anticipated settlement and settlement rates.
- Evaluate and analyze driven pile foundations at both abutments and pier locations. Evaluate driving resistance for pile foundation alternative. Estimate the possible abutment lateral movement due to lateral squeeze of soils.
- Perform wave equation analyses for pile foundations as part of construction monitoring and QA/QC.
- Prepare a memorandum report summarizing the above work.



**Figure A.1-1. Apple Freeway plan and section.**

[THIS PAGE INTENTIONALLY BLANK]

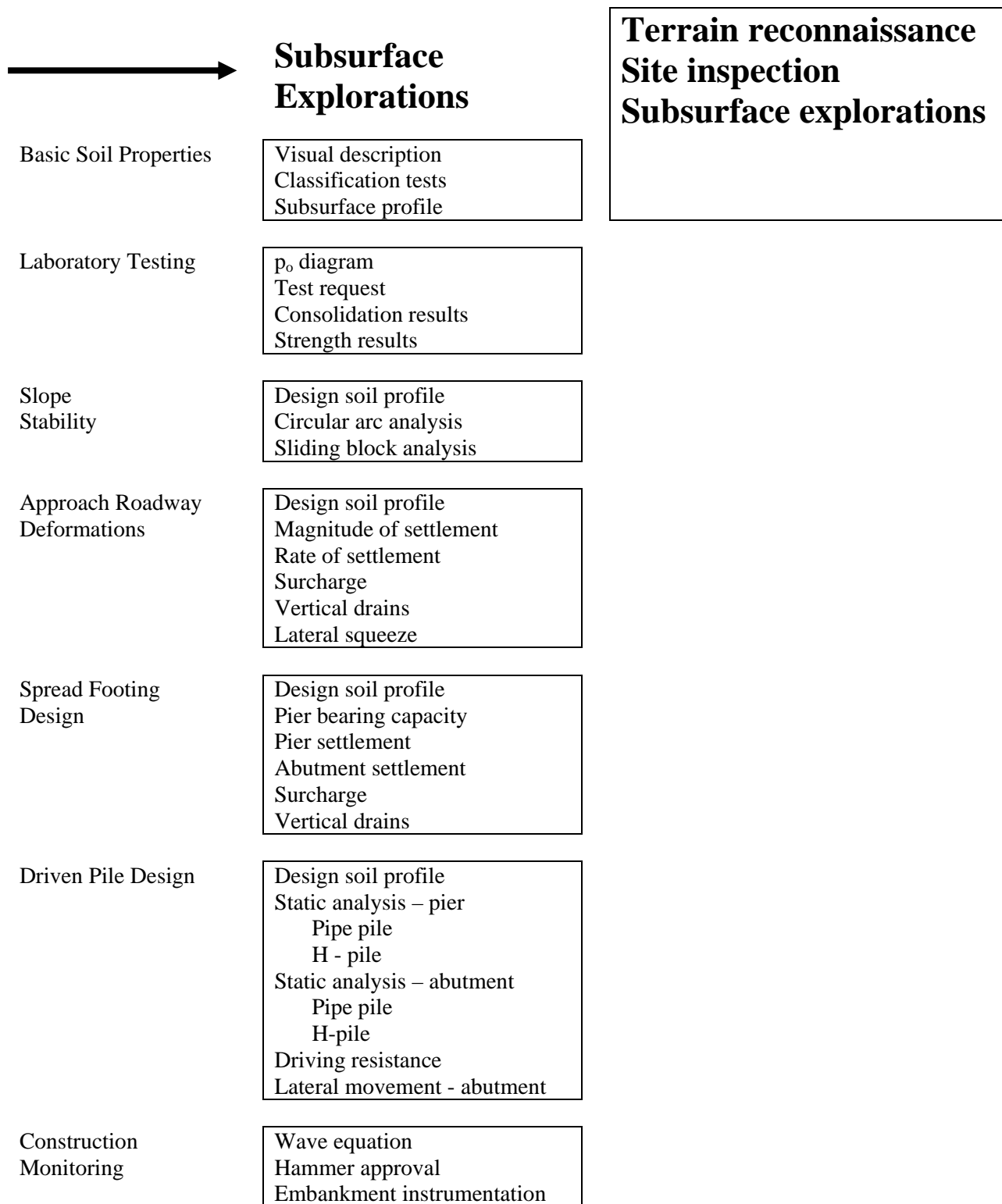


**Figure A.2-1. Overview of the geotechnical work to be performed.**

## SECTION A.2 SUBSURFACE EXPLORATIONS

### A.2-1 RELEVANT CONCEPTS AND PROCEDURES (Refer to Figure A.2-1)

- Terrain reconnaissance and site inspection – Chapter 3
- Preparation of a field exploration program – Chapter 3
- Subsurface borings for SPT sampling – Chapter 3
- Subsurface soundings for CPT logging – Chapter 3

### A.2-2 DETAILED PROCEDURES

**Given:** Examination of USGS topo and geology maps and USDA soil map showed structure to be located in a delta landform. Field inspection showed wet area with cattails in vicinity of east abutment.

**Required:** Plan subsurface exploration program and prepare boring request.

#### **Solution Procedure:**

#### **Step 1: Prepare terrain reconnaissance and site inspection**

- Locate structure on USGS topo map or other maps available from local agencies that show greater surface detail to obtain preliminary estimates of boring locations and site access by drilling equipment.
- Visit the site to verify conditions.

#### **Step 2: Prepare preliminary field exploration program (see Figure A.2-2)**

- Identify types of subsurface borings and establish location of each.
- Specify borings with disturbed SPT sampling (DH BAF) at each abutment and intermediate support
- Specify CPT soundings (CPT BAF) immediately next to the drill hole in which the SPTs were performed.
- Specify hand auger holes (EA) in wet area within east approach fill limits

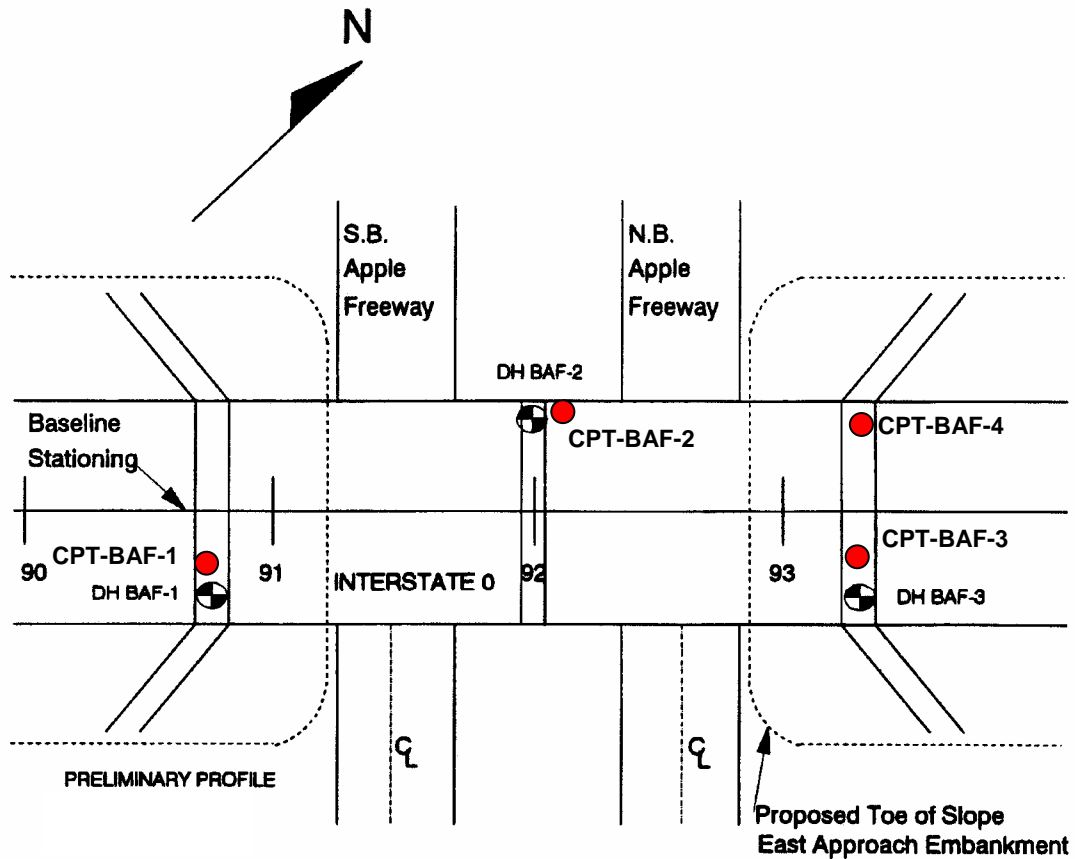


Figure A.2-2. Proposed site exploration – Preliminary.

**Step 3: Establish criteria for determining boring depth**

- SPT holes to depth where the minimum average SPT-N equals 20 for 20-ft depth or 10-ft into bedrock, whichever depth is less.
- Based on the observations from terrain reconnaissance, use a 20-ton CPT rig which should be sufficient to explore the soft and/or organic soils
- Hand auger holes to a maximum depth of 10-ft or at least 3-ft below bottom of unstable soils (soft and/or organic soils), whichever depth is less.

**Step 4: Establish sampling criteria**

- East and west abutments: disturbed SPT every 5-ft.
- Pier footing: continuous SPT samples to depth of 15-ft, then 5-ft intervals since spread footings may be considered
- Wet area: obtain representative samples from each auger hole.

- CPTs: perform with a piezocone to permit pore water pressure measurements

**Step 5: Identify and address other important considerations.**

- Since area is a delta landform, granular deposits overlying clay may be encountered. If so, an undisturbed drill hole (UDH) will be required. The location, depth, and sampling details will be selected based on the results of the three SPT boring. Notify the drillers of possibility of UDH and field vane shear so necessary equipment can be taken to site.
- Long-term water level reading should be taken in one hole.
- Obtain all required right-of-way (ROW) and entry permits. Consult with state and local departments of environmental quality for any environmental permits if required.
- Arrange for traffic control on Apple Freeway

**Step 6: Prepare preliminary field exploration request (see Figure A.2-3).**

**Step 7: Perform field exploration and prepare final field exploration layout (see Figure A.2-4)**

- Perform three (3) SPT drill hole (DH) borings (DH BAF-1, DH BAF-2, DH BAF-3)
- Perform four (4) CPT probes (CPT BAF-1, CPT BAF-2, CPT BAF-3 and CPT BAF-4)
- Perform one (1) undisturbed drill hole (UDH) borings (UDH BAF-4)
- Perform nine (9) hand-augured holes (EA1 to EA9) on a rectangular grid pattern at the east abutment site
- Logs of borings, CPT soundings and hand-augured holes are included herein.

SUBSURFACE EXPLORATION REQUEST

August 1, 2006

Subject: Request for Subsurface Exploration  
Interstate Structure over the Apple Freeway

From: Foundation Engineer

To: Regional Office

In accordance with project authorization from the Chief Engineer dated January 16, 2006, a subsurface exploration program has been prepared for the subject structure. We request that your office advance a 2½ - inch diameter cased drill hole and a CPT sounding at each of the following locations:

<u>Hole No.</u>	<u>Baseline Station</u>	<u>Offset (ft)</u>
DH-BAF-1	90 + 77	50' Rt
DH-BAF-2	92 + 00	50' Lt
DH-BAF-3	93 + 27	50' Rt

The locations may be field adjusted along the footing line shown on the attached drawing if necessary.

Each boring shall extend to a depth where the blow count per foot on the sample spoon exceeds 20 for a 20-foot depth. If rock is encountered above this depth, 10 feet of rock core shall be cored and extracted. Spoon samples shall be taken at intervals of 5-feet except for the top 15-feet of BAF-2 where continuous spoon samples are required. On completion of BAF-2 a perforated plastic pipe shall be inserted before extracting the casing to permit long-term water level observation. It is anticipated that soft clay soils may be encountered at this site. If so, an additional 4-inch diameter cased hole (UDH) may be required to extract undisturbed tube samples and/or perform in situ vane shear tests. Before the drill crew demobilizes, the driller should telephone the results of the first three SPT borings to the project engineer, Mr. Richard Cheney at 202-555-0355. At that time, a decision on the details of the UDH will be issued.

The CPT soundings shall be performed by using CPTu equipment that includes a piezocone to permit continuous pore water pressure measurements. The CPT truck should provide a minimum reaction of 20 tons. A CPT sounding shall be performed in the immediate vicinity of each of the drilled holes.

A wet area of potentially unstable soil (soft and/or organic soils) exists in the area of the proposed east approach embankment. Please define the depth of this deposit beneath the limits of the east approach embankment back to Baseline station 93 + 50 with hand auger exploration. Perform at least 9 hand auger holes in that area on a rectangular grid pattern and show the locations on the final exploration layout plan.

The present schedule for structure design requires that all samples and subsurface logs be received in the main office by November 1, 2006.

Attachment: Proposed preliminary site exploration plan (Figure A.2-2).

**Figure A.2-3. Typical preliminary exploration request.**

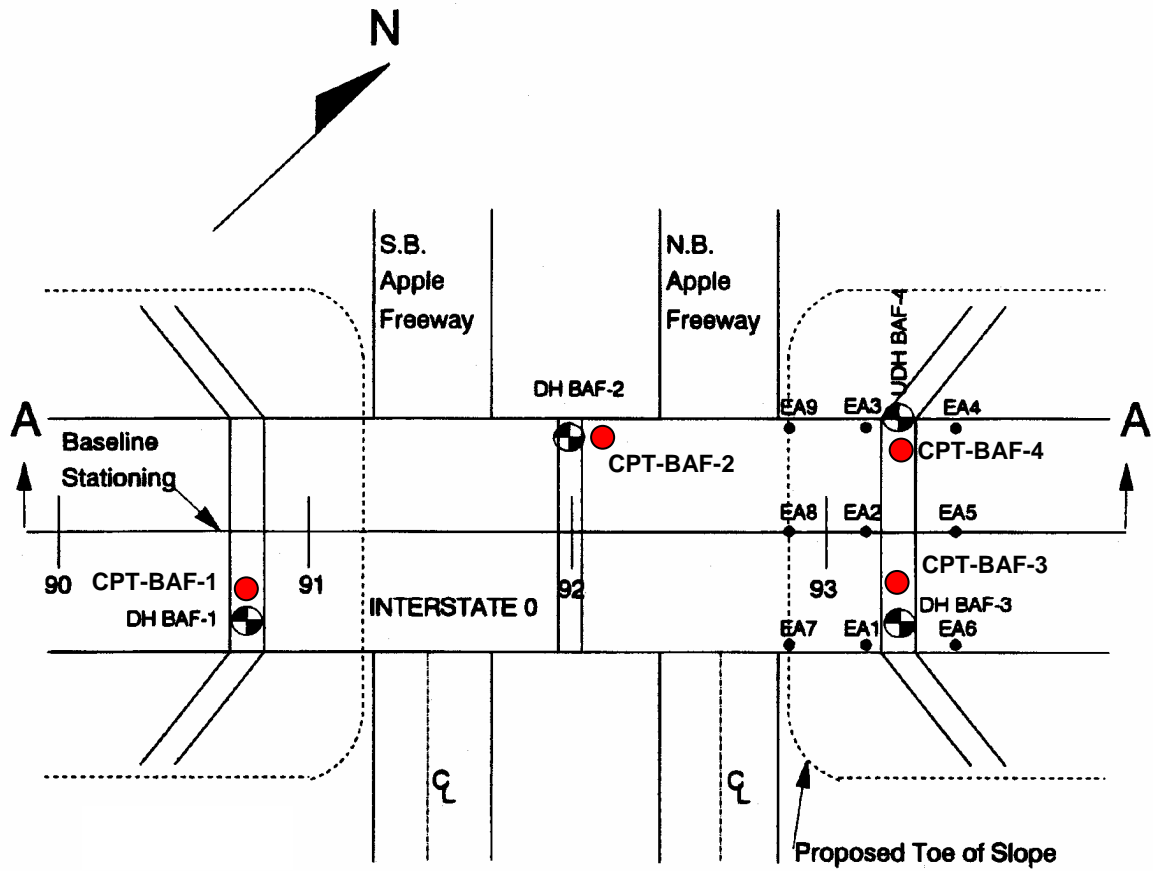


Figure A.2-4. Final field exploration layout.

## **A.2-3 SUMMARY OF THE SITE EXPLORATION PHASE FOR THE APPLE FREEWAY DESIGN PROBLEM**

### 1. Terrain Reconnaissance

- Delta landform - possible clay deposit buried

### 2. Site Inspection

- Unsuitable soils near east approach embankment
- Easy access for drilling equipment and CPT rig.

### 3. Subsurface Borings

- Hand auger holes define limits and depth of unsuitable organic deposit.
- SPT drill holes show sand over clay over gravel and rock.
- CPT soundings indicate that the clay layer may have thin silt seams in it (this would possibly help in reducing consolidation time)
- Undisturbed samples and vane shear tests taken in clay.

REGION 3 COUNTY <u>Orange</u> PROJECT <u>Interstate 0</u> DATE START <u>5/2/92</u> DATE FINISH <u>5/3/92</u> CASING O.D. <u>2 1/2"</u> I.D. <u>2 1/4"</u> SAMPLER O.D. <u>2"</u> I.D. <u>1-3/8"</u> RIG TYPE <u>Acker B-40</u> CORE BARREL <u>Double Tube</u>	<b>SUBSURFACE EXPLORATION LOG</b>  HAMMER FALL-CASING <u>18"</u> HAMMER FALL-SAMPLER <u>30"</u> WEIGHT OF HAMMER-CASING <u>300</u> LBS. WEIGHT OF HAMMER-SAMPLER <u>140</u> LBS.	HOLE <u>BAF-1</u> LINE <u>Baseline</u> STA. <u>90+77</u> OFFSET <u>50' Rt.</u> SURF. ELEV. <u>1001.1</u>  TIME <table border="1" style="display: inline-table; border-collapse: collapse;"> <tr> <td style="width:33%;">4:00 pm</td> <td style="width:33%;">8:00 am</td> <td style="width:33%;"></td> </tr> <tr> <td>DATE <u>5/2/92</u></td> <td><u>5/3/92</u></td> <td></td> </tr> <tr> <td>DEPTH TO WATER <u>15'</u></td> <td><u>15'</u></td> <td></td> </tr> </table>	4:00 pm	8:00 am		DATE <u>5/2/92</u>	<u>5/3/92</u>		DEPTH TO WATER <u>15'</u>	<u>15'</u>	
4:00 pm	8:00 am										
DATE <u>5/2/92</u>	<u>5/3/92</u>										
DEPTH TO WATER <u>15'</u>	<u>15'</u>										

DEPTH BELOW SURFACE	BLOWS ON CASING	SAMPLE NO.	BLOWS ON SAMPLER					RECOVER (ft)	DESCRIPTION OF SOIL AND ROCK	MOIST CONT %
			0	0.5	1.0	1.5	2.0			
0	4	J1	1	3	5		11		10	
16										
25										
16										
20										
30		J2	7	7	8		15		7	
21										
35										
38										
10										
51										
40		J3	10	21	20		18	GR. FINE TO COARSE SAND MOIST NON PLASTIC	6	
35										
52										
58										
61										
50		J4	10	18	21		12		6	
42										
65										
72										
20									20'	
76										
60		J5	3	6	6		12		31	
51										
72										
75										
81										
80		J6	3	6	7		18	GR. SILTY CLAY MOIST - PLASTIC	32	
71										
90										
83										
30										
84										
80		J7	2	4	4		10		36	
77										
83										
84										
86										

THE SUBSURFACE INFORMATION SHOWN HERE WAS OBTAINED FOR STATE DESIGN AND ESTIMATE PURPOSES. IT IS MADE AVAILABLE TO AUTHORIZED USERS ONLY THAT THEY MAY HAVE ACCESS TO THE SAME INFORMATION AVAILABLE TO THE STATE. IT IS PRESENTED IN GOOD FAITH, BUT IS NOT INTENDED AS A SUBSTITUTE FOR INVESTIGATION, INTERPRETATION OR JUDGMENT OF SUCH AUTHORIZED USERS.  CONTRACTOR <u>ACME Drilling, Inc. SM</u>	DRILL RIG OPERATOR <u>Klinedinst</u> SOIL & ROCK DESCRIP. <u>Chassie</u> REGIONAL SOILS ENGR. <u>Cheney</u> SHEET <u>1</u> OF <u>2</u> STRUCTURE NAME/NO. <u>Apple Freeway #2</u>  HOLE <u>BAF-1</u>
---	--

**Figure A.2-5. Field log for boring DH BAF-1 (0-35 ft).**



REGION <u>3</u>		<u>SUBSURFACE EXPLORATION LOG</u>				HOLE <u>BAF-2</u>													
COUNTY <u>Orange</u>						LINE <u>Baseline</u>													
PROJECT <u>Interstate 0</u>						STA. <u>92+00</u>													
DATE START <u>5/4/92</u>		HAMMER FALL-CASING <u>18"</u>				OFFSET <u>50' Lt</u>													
DATE FINISH <u>5/6/92</u>		HAMMER FALL-SAMPLER <u>30"</u>				SURF. ELEV. <u>996.2</u>													
CASING O.D. <u>2 1/2"</u> I.D. <u>2 1/4"</u>		WEIGHT OF HAMMER-CASING <u>300</u> LBS.				<table border="1" style="width:100%; border-collapse: collapse;"> <tr> <td>TIME</td> <td><u>4:00 pm</u></td> <td><u>8:00 am</u></td> <td></td> </tr> <tr> <td>DATE</td> <td><u>5/4/92</u></td> <td><u>5/6/92</u></td> <td></td> </tr> <tr> <td>DEPTH TO WATER</td> <td><u>10'</u></td> <td><u>10'</u></td> <td></td> </tr> </table>		TIME	<u>4:00 pm</u>	<u>8:00 am</u>		DATE	<u>5/4/92</u>	<u>5/6/92</u>		DEPTH TO WATER	<u>10'</u>	<u>10'</u>	
TIME	<u>4:00 pm</u>	<u>8:00 am</u>																	
DATE	<u>5/4/92</u>	<u>5/6/92</u>																	
DEPTH TO WATER	<u>10'</u>	<u>10'</u>																	
SAMPLER O.D. <u>2"</u> I.D. <u>1-3/8"</u>		WEIGHT OF HAMMER-SAMPLER <u>140</u> LBS.																	
RIG TYPE <u>Acker B-40</u>																			
CORE BARREL <u>Double Tube</u>																			

DEPTH BELOW SURFACE	BLOWS ON CASING	SAMPLE NO.	BLOWS ON SAMPLER					RECOVER (in)	DESCRIPTION OF SOIL AND ROCK	MOIST CONT %
			0-0.5	0.5-1.0	1.0-1.5	1.5-2.0	2.0-			
0	6	J1	1	2	2		5	GR. FINE TO COARSE SAND MOIST NON PLASTIC	12	
	19									
	27	J2	1	3	3		10		8	
	35									
	21	J3	2	5	6		17		7	
	30	J4	7	9	12		15		10	
	22									
	25	J5	8	7	15		18		6	
	24									
10	28	J6	14	20	20		16		7	
	27	J7	15	18	19					
	36									
	34	J8	13	16	17		17	7		
	37									
	39	J8	15	10	3		18	34		
	31									
	40									
	46									
	46									
20	45									
	41	J10	2	4	4		15	31		
	42									
	56									
	52									
	58									
	50	J11	2	3	3		14	36		
	56									
	52									
	49									
30	58									
	52	J12	1	2	3		18	37		
	56									
	61									
	63									
	65									

<p>THE SUBSURFACE INFORMATION SHOWN HERE WAS OBTAINED FOR STATE DESIGN AND ESTIMATE PURPOSES. IT IS MADE AVAILABLE TO AUTHORIZED USERS ONLY THAT THEY MAY HAVE ACCESS TO THE SAME INFORMATION AVAILABLE TO THE STATE. IT IS PRESENTED IN GOOD FAITH, BUT IS NOT INTENDED AS A SUBSTITUTE FOR INVESTIGATION, INTERPRETATION OR JUDGMENT OF SUCH AUTHORIZED USERS.</p> <p>CONTRACTOR <u>ACME Drilling, Inc. SM</u></p>	<p>DRILL RIG OPERATOR <u>Klinedinst</u></p> <p>SOIL &amp; ROCK DESCRIP. <u>Chassie</u></p> <p>REGIONAL SOILS ENGR. <u>Cheney</u></p> <p>SHEET <u>1</u> OF <u>2</u></p> <p>STRUCTURE NAME/NO. <u>Apple Freeway #2</u></p> <p style="text-align: right;">HOLE <u>BAF-2</u></p>
--	--

**Figure A.2-6. Field log for boring DH BAF-2 (0-35 ft).**

REGION <u>3</u>		<b>SUBSURFACE EXPLORATION LOG</b>				HOLE <u>BAF-2</u>	
COUNTY <u>Orange</u>						LINE <u>Baseline</u>	
PROJECT <u>Interstate 0</u>						STA. <u>92+00</u>	
DATE START <u>5/4/92</u>		HAMMER FALL-CASING <u>18"</u>				OFFSET <u>50' Lt</u>	
DATE FINISH <u>5/6/92</u>		HAMMER FALL-SAMPLER <u>30"</u>				SURF. ELEV. <u>996.2</u>	
CASING O.D. <u>2 1/2"</u> I.D. <u>2 1/4"</u>		WEIGHT OF HAMMER-CASING <u>300</u> LBS.					
SAMPLER O.D. <u>2"</u> I.D. <u>1-3/8"</u>		WEIGHT OF HAMMER-SAMPLER <u>140</u> LBS.				TIME <u>4:00 pm</u> <u>8:00 am</u>	
RIG TYPE <u>Acker B-40</u>						DATE <u>5/4/92</u> <u>5/6/92</u>	
CORE BARREL <u>Double Tube</u>		DEPTH TO WATER				<u>10'</u> <u>10'</u>	

DEPTH BELOW SURFACE	BLOWS ON CASING	SAMPLE NO.	BLOWS ON SAMPLER					RECOVER (ft)	DESCRIPTION OF SOIL AND ROCK	MOIST CONT %
			0-0.5	0.5-1.0	1.0-1.5	1.5-2.0	2.0			
62	J13	1	2	4			16	GR. SILTY CLAY MOIST - PLASTIC	34	
63										
72										
71										
40								GR SANDY GRAVEL MOIST - NON PLASTIC (Cored Boulder 42.5' to 45' recovered 12'-7' pieces: used boulder buster)		
89										
75		30	20	35						
81										
104										
120										
								HARD UNWEATHERED BASALT  Run 1 50 - 55' RQD = 80%	55'	
140										
110										
136										
166										
191										
50		482								
								HARD UNWEATHERED BASALT  Run 2 55 - 60' RQD = 75%	60'	
								END OF BORING 60'		
70										

<p>THE SUBSURFACE INFORMATION SHOWN HERE WAS OBTAINED FOR STATE DESIGN AND ESTIMATE PURPOSES. IT IS MADE AVAILABLE TO AUTHORIZED USERS ONLY THAT THEY MAY HAVE ACCESS TO THE SAME INFORMATION AVAILABLE TO THE STATE. IT IS PRESENTED IN GOOD FAITH, BUT IS NOT INTENDED AS A SUBSTITUTE FOR INVESTIGATION, INTERPRETATION OR JUDGMENT OF SUCH AUTHORIZED USERS.</p>	<p>DRILL RIG OPERATOR <u>Klinedinst</u>          SOIL &amp; ROCK DESCRIP. <u>Chassie</u>          REGIONAL SOILS ENGR. <u>Cheney</u>          SHEET <u>2</u> OF <u>2</u>          STRUCTURE NAME/NO. <u>Apple Freeway #2</u></p>
CONTRACTOR <u>ACME Drilling, Inc.</u> SM _____	HOLE <u>BAF-2</u>

**Figure A.2-6 (Continued). Field log for boring DH BAF-2 (35-60 ft).**

REGION 3		<b>SUBSURFACE EXPLORATION LOG</b>				HOLE BAF-3													
COUNTY <u>Orange</u>						LINE <u>Baseline</u>													
PROJECT <u>Interstate 0</u>						STA. <u>93+27</u>													
DATE START <u>5/8/92</u>		HAMMER FALL-CASING <u>18"</u>				OFFSET <u>50' Rt.</u>													
DATE FINISH <u>5/9/92</u>		HAMMER FALL-SAMPLER <u>30"</u>				SURF. ELEV. <u>990</u>													
CASING O.D. <u>2 1/2"</u> I.D. <u>2 1/4"</u>		WEIGHT OF HAMMER-CASING <u>300</u> LBS.				<table border="1" style="width:100%; border-collapse: collapse;"> <tr> <td>TIME</td> <td>4:00 pm</td> <td>8:00 am</td> <td></td> </tr> <tr> <td>DATE</td> <td>5/8/92</td> <td>5/9/92</td> <td></td> </tr> <tr> <td>DEPTH TO WATER</td> <td>6'</td> <td>6'</td> <td></td> </tr> </table>		TIME	4:00 pm	8:00 am		DATE	5/8/92	5/9/92		DEPTH TO WATER	6'	6'	
TIME	4:00 pm	8:00 am																	
DATE	5/8/92	5/9/92																	
DEPTH TO WATER	6'	6'																	
SAMPLER O.D. <u>2"</u> I.D. <u>1 1/2"</u>		WEIGHT OF HAMMER-SAMPLER <u>140</u> LBS.																	
RIG TYPE <u>Acker B-40</u>																			
CORE BARREL <u>Double Tube</u>																			

DEPTH BELOW SURFACE	BLOWS ON CASING	SAMPLE NO.	BLOWS ON SAMPLER					RECOVER (ft)	DESCRIPTION OF SOIL AND ROCK	MOIST CONT %
			0	0.5	1.0	1.5	2.0			
0	0	J1	1	0	1		12	BLACK MUCK WET - PLASTIC	115	
2										
11		J2	3	5	7		12		20	
25										
31										
40								GR. SAND W/ ROOTS AND FIBERS		
41								MOIST - NON PLASTIC		
56		J3	8	8	9		10		8	
71										
10										
83										
70		J4	6	5	5		12		29	
91										
93										
82										
93								GR-BR CLAYEY SILT		
81		J5	2	3	6		15	MOIST PLASTIC	31	
80										
87										
85										
20										
90										
82		J6	4	3	3		18		34	
86										
87										
85										
90										
73		J7	2	2	3		18		39	
72								GR SILTY CLAY		
83								MOIST - PLASTIC		
71										
30										
61										
81		J8	2	2	2		17		40	
83										
72										
76										
83										

<p>THE SUBSURFACE INFORMATION SHOWN HERE WAS OBTAINED FOR STATE DESIGN AND ESTIMATE PURPOSES. IT IS MADE AVAILABLE TO AUTHORIZED USERS ONLY THAT THEY MAY HAVE ACCESS TO THE SAME INFORMATION AVAILABLE TO THE STATE. IT IS PRESENTED IN GOOD FAITH, BUT IS NOT INTENDED AS A SUBSTITUTE FOR INVESTIGATION, INTERPRETATION OR JUDGMENT OF SUCH AUTHORIZED USERS.</p> <p>CONTRACTOR <u>ACME Drilling, Inc. SM</u></p>	<p>DRILL RIG OPERATOR <u>Klinedinst</u>          SOIL &amp; ROCK DESCRIP. <u>Chassie</u>          REGIONAL SOILS ENGR. <u>Cheney</u>          SHEET <u>1</u> OF <u>2</u>          STRUCTURE NAME/NO. <u>Apple Freeway #2</u></p> <p style="text-align: right;">HOLE BAF-3</p>
--	---

**Figure A.2-7. Field log for boring DH BAF-3 (0-35 ft).**

REGION 3		<b>SUBSURFACE EXPLORATION LOG</b>				HOLE BAF-3	
COUNTY Orange						LINE Baseline	
PROJECT Interstate 0						STA 93+27	
DATE START 5/8/92		HAMMER FALL-CASING 18"				OFFSET 50' Rt.	
DATE FINISH 5/9/92		HAMMER FALL-SAMPLER 30"				SURF. ELEV. 990	
CASING O.D. 2 1/2" I.D. 2 1/4"		WEIGHT OF HAMMER-CASING 300 LBS.				TIME 4:00 pm 8:00 am DATE 5/8/92 5/9/92	
SAMPLER O.D. 2" I.D. 1 1/2"		WEIGHT OF HAMMER-SAMPLER 140 LBS.					
RIG TYPE Acker B-40						DEPTH TO WATER	
CORE BARREL Double Tube						6' 6'	

DEPTH BELOW SURFACE	BLOWS ON CASING	SAMPLE NO.	BLOWS ON SAMPLER				RECOVER (ft)	DESCRIPTION OF SOIL AND ROCK	MOIST CONT %
			0-0.5	0.5-1.0	1.0-1.5	1.5-2.0			
71	J9	2	3	2		14	GR SILTY CLAY MOIST - PLASTIC	36	
79									
86									
83									
85									
40	J10	3	4	3		15		35	
81									
93									
91									
96								45'	
121	J11	20	21	35		13		10	
450									
391									
220									
50	J12	15	36	40		12	GR. SILTY GRAVEL MOIST - NON PLASTIC 52' to 53' CORED BOULDER RECOVERY 3" MANY FRAGMENTS	5	
200									
370									
400									
410									
380	J13	40	60	80		15		7	
60	J14	100				Refusal	TOP OF ROCK 60.5'		
							HARD UNWEATEHRED BASALT		
							Run 1 60.5 - 65'		
							RQD = 70%	65'	
							HARD UNWEATEHRED BASALT		
							Run 2 65 - 70.5'		
							RQD = 95%	69'	
70							END OF BORING 69'		

<p>THE SUBSURFACE INFORMATION SHOWN HERE WAS OBTAINED FOR STATE DESIGN AND ESTIMATE PURPOSES. IT IS MADE AVAILABLE TO AUTHORIZED USERS ONLY THAT THEY MAY HAVE ACCESS TO THE SAME INFORMATION AVAILABLE TO THE STATE. IT IS PRESENTED IN GOOD FAITH, BUT IS NOT INTENDED AS A SUBSTITUTE FOR INVESTIGATION, INTERPRETATION OR JUDGMENT OF SUCH AUTHORIZED USERS.</p>	<p>DRILL RIG OPERATOR <u>Klinedinst</u>          SOIL &amp; ROCK DESCRIP. <u>Chassie</u>          REGIONAL SOILS ENGR. <u>Cheney</u>          SHEET <u>2</u> OF <u>2</u>          STRUCTURE NAME/NO. <u>Apple Freeway #2</u></p>
CONTRACTOR <u>ACME Drilling, Inc. SM</u>	HOLE <u>BAF-3</u>

**Figure A.2-7 (Continued). Field log for boring DH BAF-3 (35-69 ft).**

REGION <u>3</u>		<b>SUBSURFACE EXPLORATION LOG</b>				HOLE <u>BAF-4</u>		
COUNTY <u>Orange</u>						LINE <u>Baseline</u>		
PROJECT <u>Interstate 0</u>						STA. <u>93+27</u>		
DATE START <u>5/10/92</u>		HAMMER FALL-CASING <u>18"</u>				OFFSET <u>50' Lt</u>		
DATE FINISH <u>5/12/92</u>		HAMMER FALL-SAMPLER <u>30"</u>				SURF. ELEV. <u>991</u>		
CASING O.D. <u>4"</u> I.D. <u>3½"</u>		WEIGHT OF HAMMER-CASING <u>300</u> LBS.				TIME		
SAMPLER O.D. <u>2"</u> I.D. <u>1-3/8"</u>		WEIGHT OF HAMMER-SAMPLER <u>140</u> LBS.				DATE		
RIG TYPE <u>Acker B-40</u>						4:00 pm    8:00 am    3:00 pm		
CORE BARREL <u>Double Tube</u>						5/10/92    5/12/92    5/20/93		
						DEPTH TO WATER		
						6'            6'            Dry		

DEPTH BELOW SURFACE	BLOWS ON CASING	SAMPLE NO.	BLOWS ON SAMPLER					RECOVER (ft)	DESCRIPTION OF SOIL AND ROCK	MOIST CONT %
			0	0.5	1.0	1.5	2.0			
0	0	J1	1	1	1		12	BLACK ORGANIC SILT WET - PLASTIC	120	
2										
11									3'	
25										
31										
40	J2		4	8	9		12	GR. SAND MOIST - NON PLASTIC	12	
41										
56										
71										
10	83								10'	
70	T3							(10' - 12' PUSHED TUBE)	33	
91										
93										
82		Vane						(13' VANE SHEAR TEST)		
93										
81	T4							(15' - 17' PUSHED TUBE)	35	
80										
87										
85		Vane						(18' VANE SHEAR TEST)		
20	90									
82	T5							(20' - 22' PUSHED TUBE)	31	
86										
87										
85		Vane						(23' VANE SHEAR TEST)		
75										
73	T6							(25' - 27' PUSHED TUBE)	36	
72										
83										
71	T							(28' - ' PUSHED TUBE)		
30	61									
81	T7							(30' - 32' PUSHED TUBE)	38	
83										
72										
76										
83										

<p>THE SUBSURFACE INFORMATION SHOWN HERE WAS OBTAINED FOR STATE DESIGN AND ESTIMATE PURPOSES. IT IS MADE AVAILABLE TO AUTHORIZED USERS ONLY THAT THEY MAY HAVE ACCESS TO THE SAME INFORMATION AVAILABLE TO THE STATE. IT IS PRESENTED IN GOOD FAITH, BUT IS NOT INTENDED AS A SUBSTITUTE FOR INVESTIGATION, INTERPRETATION OR JUDGMENT OF SUCH AUTHORIZED USERS.</p>	<p>DRILL RIG OPERATOR <u>Klinedinst</u>  SOIL &amp; ROCK DESCRIP. <u>Chassie</u>  REGIONAL SOILS ENGR. <u>Cheney</u>  SHEET <u>1</u> OF <u>2</u>  STRUCTURE NAME/NO. <u>Apple Freeway #2</u></p>
<p>CONTRACTOR <u>ACME Drilling, Inc. SM</u></p>	<p>HOLE <u>BAF-4</u></p>

**Figure A.2-8. Field log for boring DH BAF-4 (0-35 ft).**

REGION <u>3</u>		<b>SUBSURFACE EXPLORATION LOG</b>				HOLE <u>BAF-4</u>		
COUNTY <u>Orange</u>						LINE <u>Baseline</u>		
PROJECT <u>Interstate 0</u>						STA. <u>93+27</u>		
DATE START <u>5/10/92</u>		HAMMER FALL-CASING <u>18"</u>				OFFSET <u>50' Lt</u>		
DATE FINISH <u>5/12/92</u>		HAMMER FALL-SAMPLER <u>30"</u>				SURF. ELEV. <u>991</u>		
CASING O.D. <u>4"</u> I.D. <u>3½"</u>		WEIGHT OF HAMMER-CASING <u>300</u> LBS.				TIME		
SAMPLER O.D. <u>2"</u> I.D. <u>1-3/8"</u>		WEIGHT OF HAMMER-SAMPLER <u>140</u> LBS.				DATE		
RIG TYPE <u>Acker B-40</u>						4:00 pm    8:00 am    3:00 pm		
CORE BARREL <u>Double Tube</u>						5/10/92    5/12/92    5/20/93		
						DEPTH TO WATER		
						6'            6'            Dry		

DEPTH BELOW SURFACE	BLOWS ON CASING	SAMPLE NO.	BLOWS ON SAMPLER					RECOVER (ft)	DESCRIPTION OF SOIL AND ROCK	MOIST CONT %
			0	0.5	1.0	1.5	2.0			
71	J8		2	2	4		15		38	
79										
86		Vane						(37' VANE SHEAR TEST)		
83										
40										
85										
82	T9							(40' - 42' PUSHED TUBE)	37	
81										
93										
91										
96									45'	
121	J10		7	8	15		15			
450										
391										
220										
50										
230										
200	J11		40	100			12	GR. SANDY GRAVEL MOIST - NON PLASTIC		
370										
400										
410										
380										
								TOP OF ROCK	55'	
								HARD UNWEATHERED BASALT		
								Run 1 55 - 60' RQD = 90%	60'	
60								HARD UNWEATHERED BASALT		
								Run 2 60 - 65' RQD = 95%	65'	
								END OF BORING 65'		
70										

<p>THE SUBSURFACE INFORMATION SHOWN HERE WAS OBTAINED FOR STATE DESIGN AND ESTIMATE PURPOSES. IT IS MADE AVAILABLE TO AUTHORIZED USERS ONLY THAT THEY MAY HAVE ACCESS TO THE SAME INFORMATION AVAILABLE TO THE STATE. IT IS PRESENTED IN GOOD FAITH, BUT IS NOT INTENDED AS A SUBSTITUTE FOR INVESTIGATION, INTERPRETATION OR JUDGMENT OF SUCH AUTHORIZED USERS.</p> <p>CONTRACTOR <u>ACME Drilling, Inc. SM</u></p>	<p>DRILL RIG OPERATOR <u>Klinedinst</u></p> <p>SOIL &amp; ROCK DESCRIP. <u>Chassie</u></p> <p>REGIONAL SOILS ENGR. <u>Cheney</u></p> <p>SHEET <u>2</u> OF <u>2</u></p> <p>STRUCTURE NAME/NO. <u>Apple Freeway #2</u></p> <p style="text-align: right;">HOLE <u>BAF-4</u></p>
--	--

**Figure A.2-8 (Continued). Field log for boring DH BAF-4 (35-65 ft).**

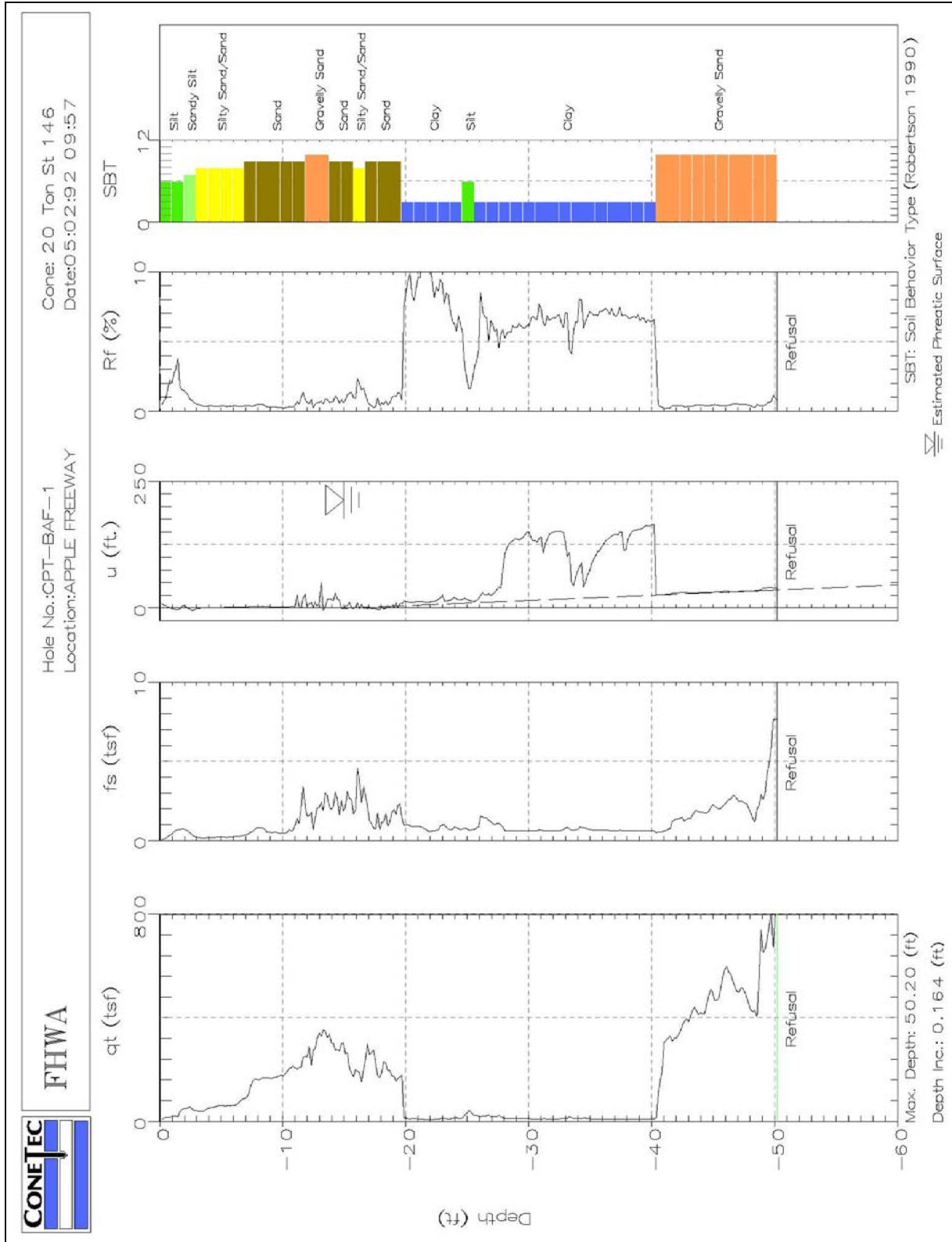


Figure A.2-9. CPT sounding from CPT-BAF-1 in vicinity of DH BAF-1.

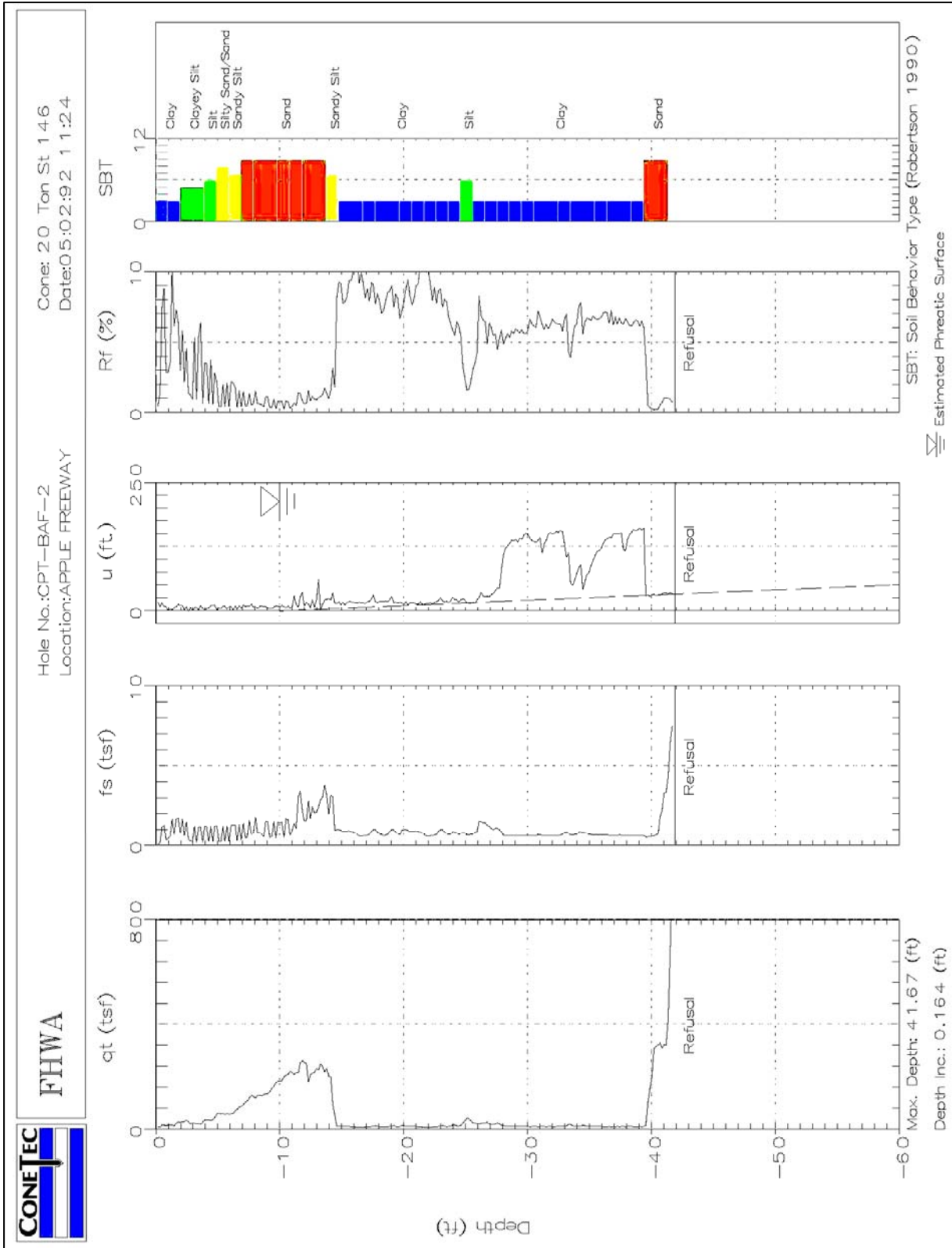
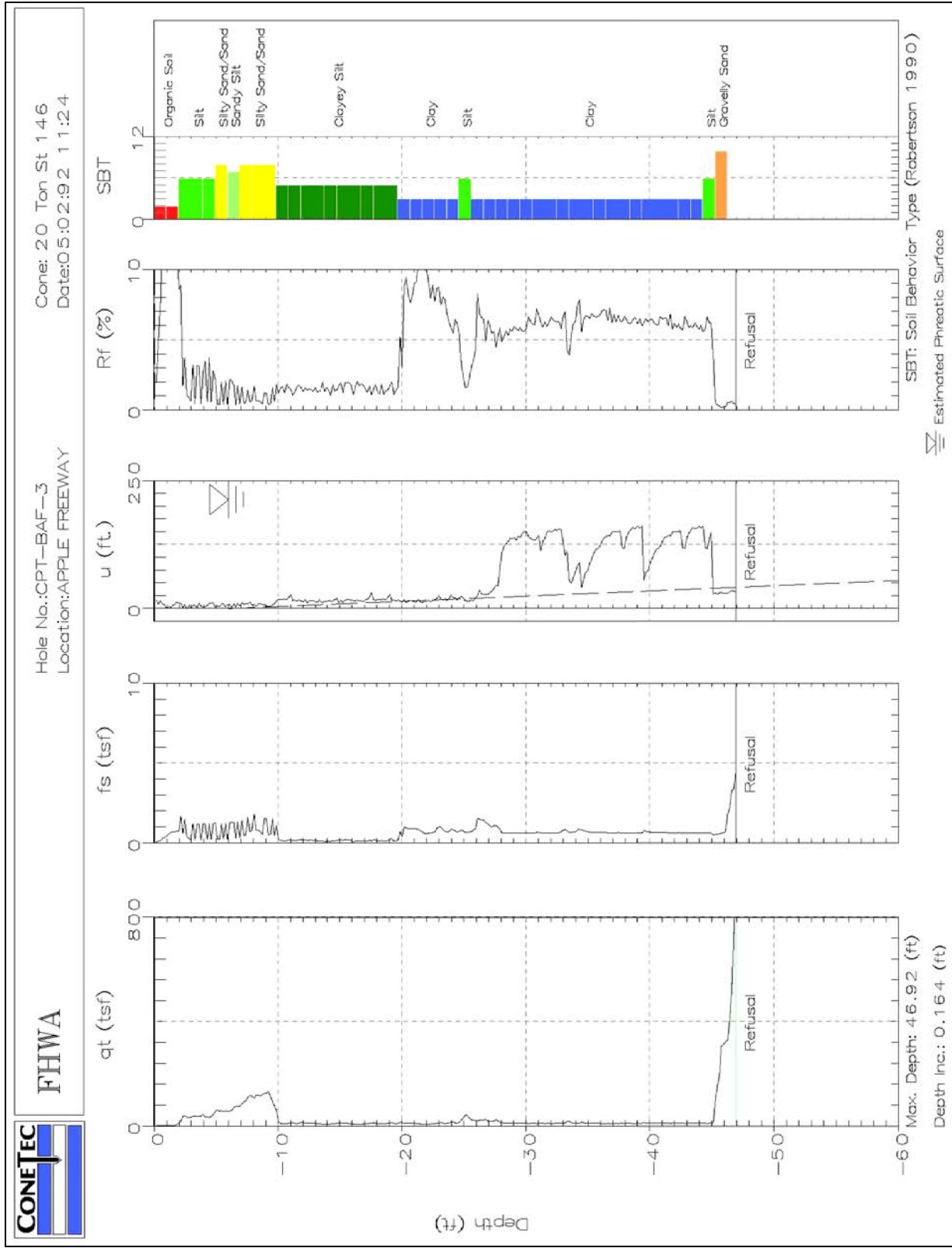


Figure A.2-10. CPT sounding from CPT-BAF-2 in vicinity of DH BAF-2.



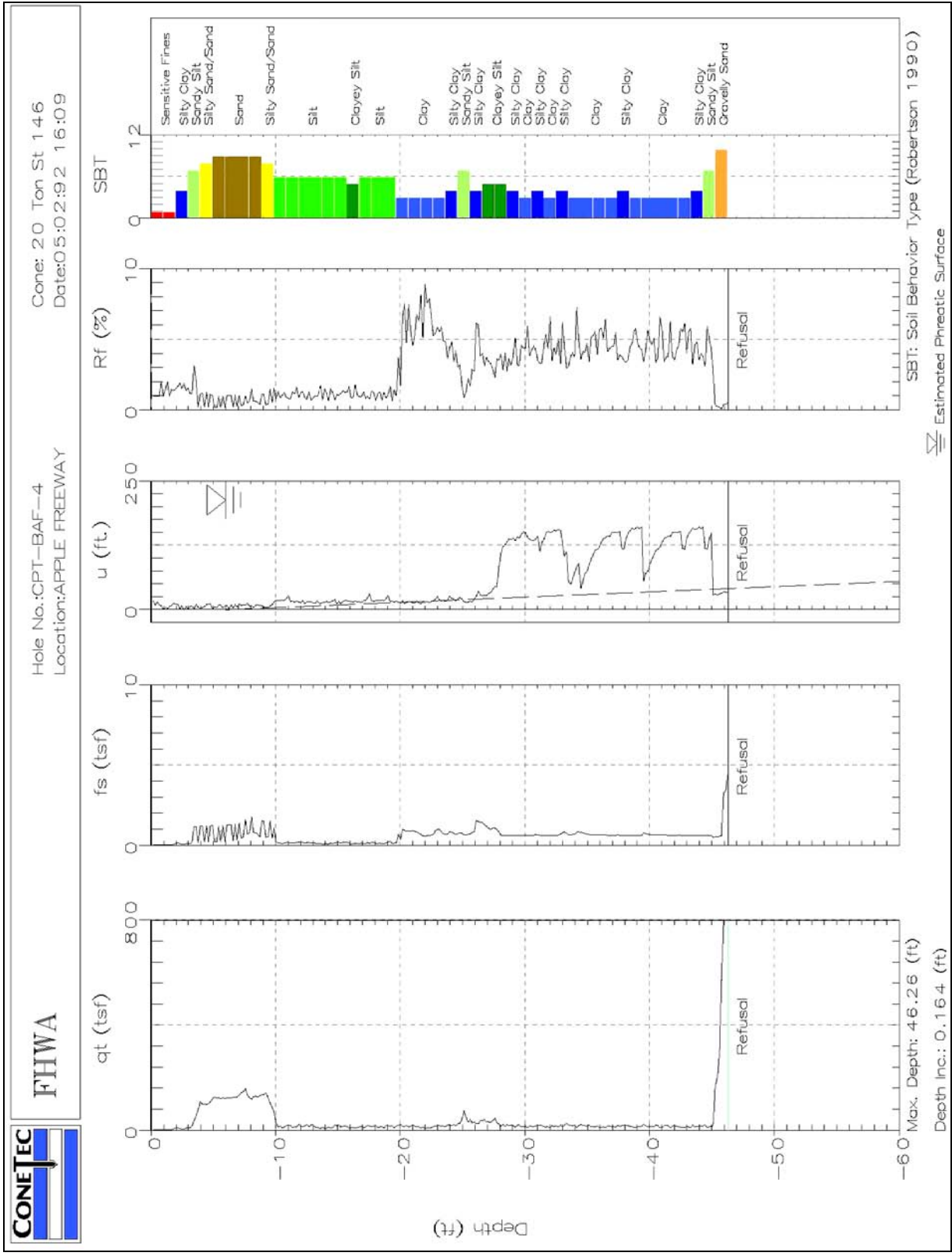


Figure A.2-12. CPT sounding from CPT-BAF-4 in vicinity of UDH BAF-4.

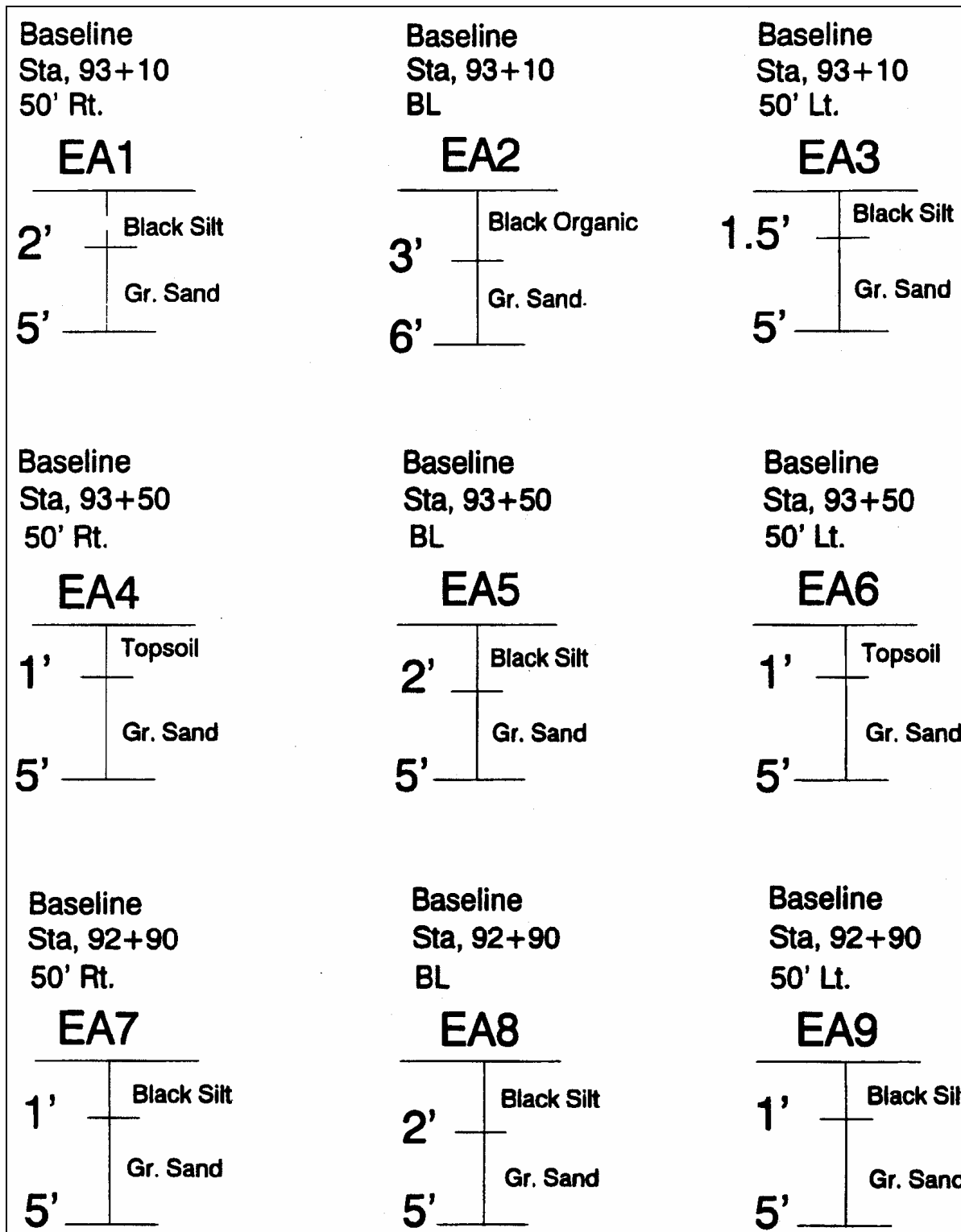
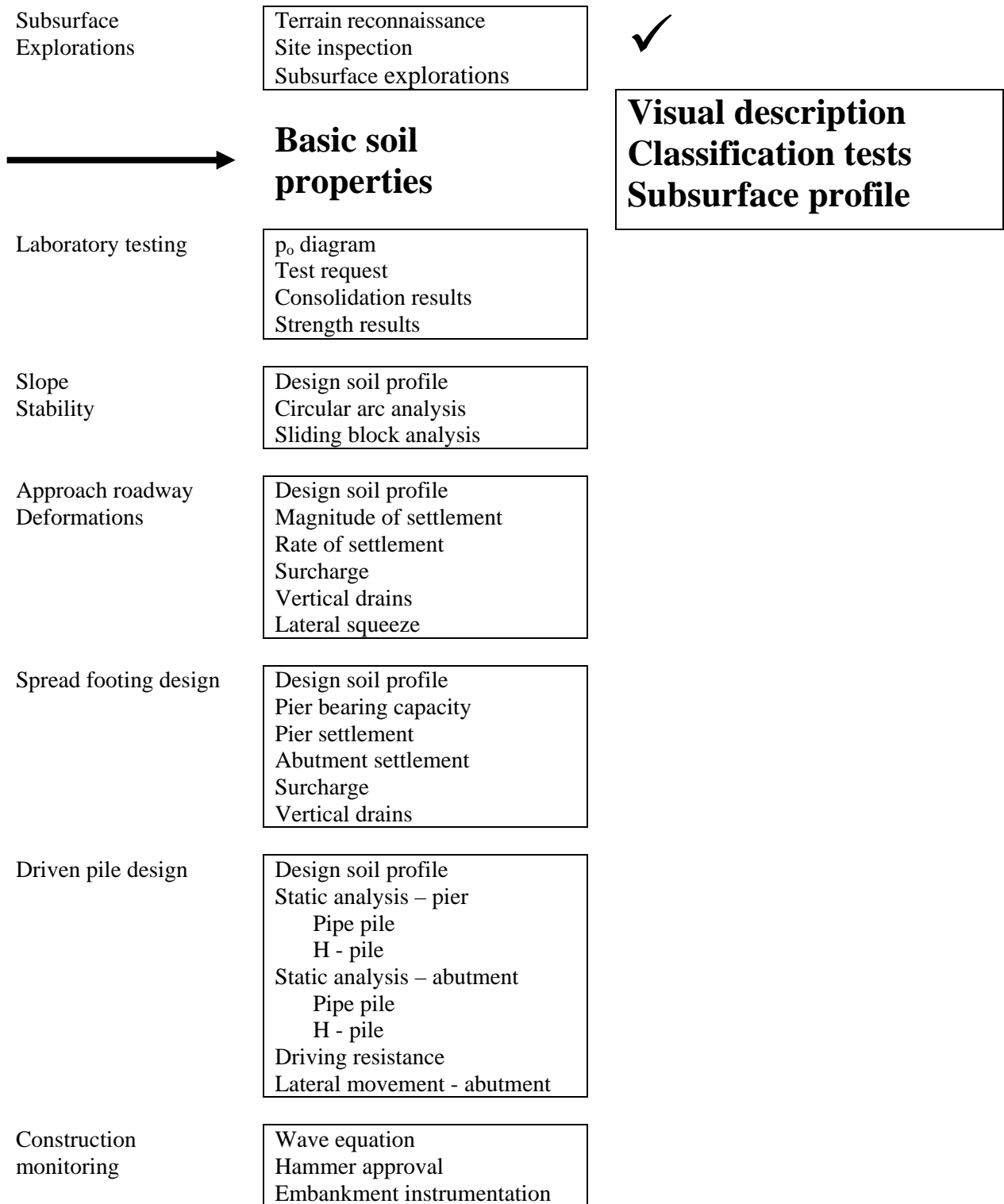


Figure A.2-13. Hand Auger Hole Logs - East Abutment Area.



**Figure A.3-1. Overview of the geotechnical work to be performed.**

## SECTION A.3 BASIC SOIL PROPERTIES

### A.3-1 RELEVANT CONCEPTS AND PROCEDURES (Refer to Figure A.3-1)

- Visual description of soils – Chapter 4.1
- Classification tests – Chapter 4.2
- Engineering characteristics of main soil types – Chapter 4.3
- Idealized soil profile – Chapter 4.7

In this section the process of estimating the engineering characteristics of the main soil types based on visual descriptions (logs) and classification tests (field and laboratory) is illustrated. The boring logs, CPT soundings and laboratory moisture content test data presented in Appendix A.2-1 are used to illustrate how an idealized soil profile is established for analysis and design. Note that the idealized profile is not suitable for bidding purposes

### A.3-2 DETAILED PROCEDURES

**Given:** Boring logs with SPT-N, logs of CPT soundings, and laboratory moisture content test data.

**Required:** Develop a preliminary idealized soil profile for analysis and design.

#### **Solution Procedure:**

**Step 1: Locate the borings in plan (Refer to Figure A.3-2).**

- Distinguish between SPT borings (target symbols), CPT soundings (large solid circles), and hand-auger borings (small solid circles).
- Use appropriate designations to identify each probe (Refer to Section A.2-2 – Step 2).

**Step 2: Show corresponding elevation view of borings, soundings and auger holes (Refer to Figure A.3-3).**

- Plot the variation of field SPT-N values and laboratory moisture content test data with depth.
- SPT values are boxed and designated by the symbol “N”.
- Corresponding moisture contents are listed to the right of the SPT-N values and are designated by the symbol “W.”
- Make sure the designation used to identify each probe is consistent with

that shown in Figure A.3-2.

- Plot the observed water levels in the borings and the date observed.

**Step 3: Develop a preliminary idealized soil profile by interpolating between borings to identify zones where soils may have similar characteristics.**

- Use SPT-N values and visual descriptions made by field personnel as the initial criteria for distinguishing between different types of soil.
- Include soil descriptions on the elevation drawings.
- Perform a preliminary classification of the soils according to the Unified Soil Classification System (USCS) or some other system commonly used in region. The preliminary classification according to visual-manual procedures (ASTM D2488) will be verified or changed based on the results of the laboratory testing phase of the geotechnical investigation. In lieu of the soil descriptions, USCS symbols may be included on the profile.
- Show the idealized profile on the elevation drawing in terms of zones, with the top and bottom of each zone clearly marked in each boring. The lines between borings are solely for the purpose of the design and should not be shown on bid documents since such well-defined boundaries may not exist in reality.
- Compare the preliminary idealized soil profile with CPT soundings and adjust as necessary.

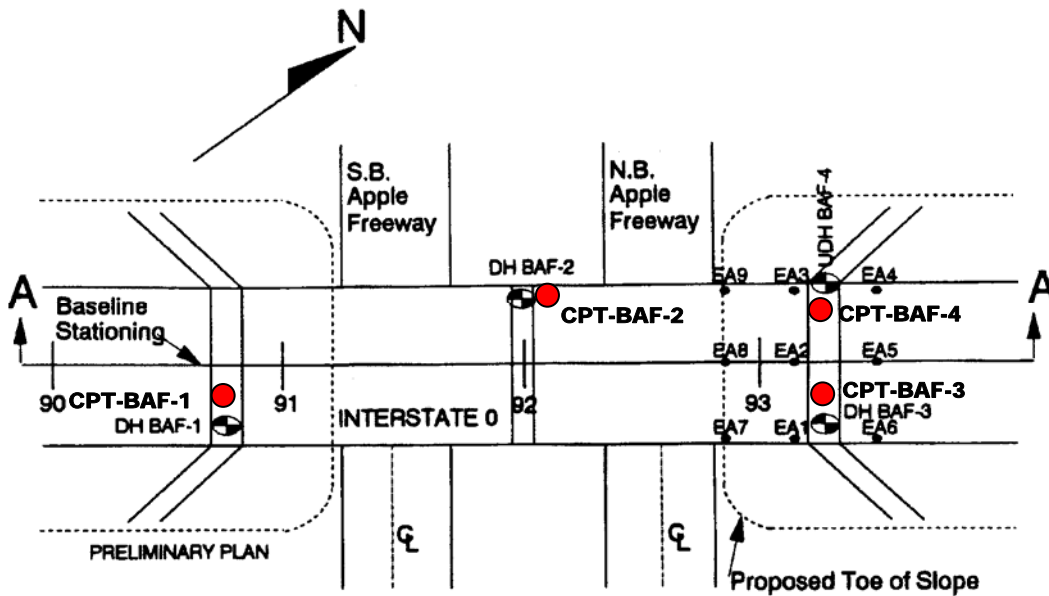


Figure A.3-2. Location Plan – SPT Borings, CPT Soundings and Hand-Auger Holes.

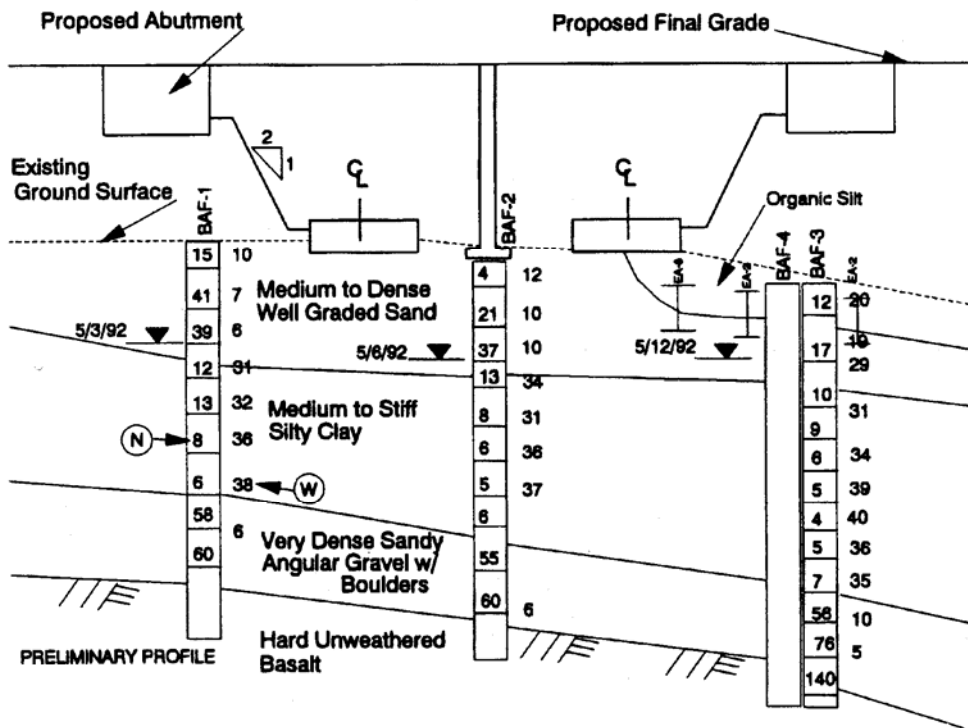
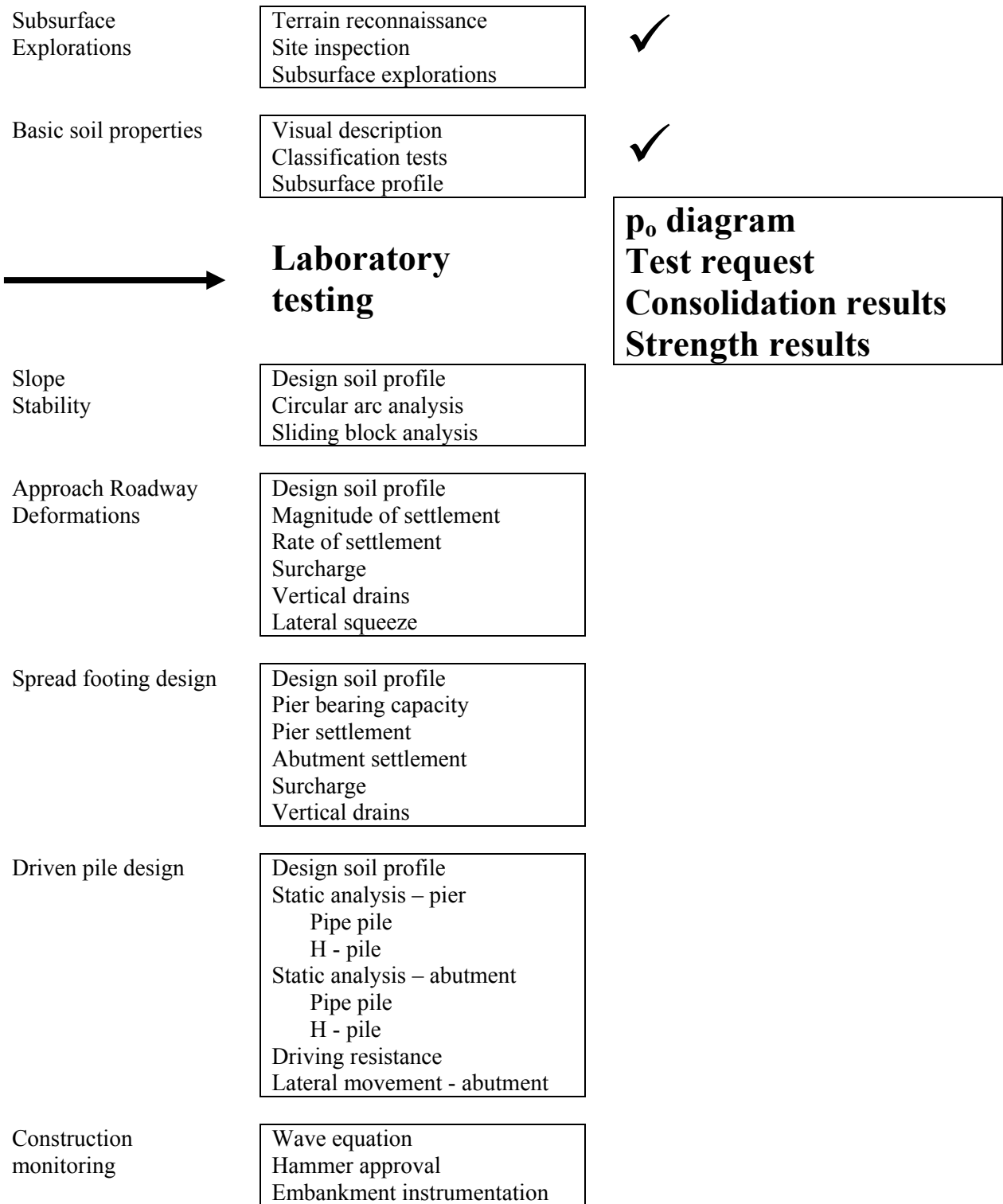


Figure A.3-3. Designer's interpretation of preliminary idealized soil profile through Section A-A.

### **A.3-3 SUMMARY OF SOIL CHARACTERISTICS FROM RESULTS OF FIELD INVESTIGATIONS AND THEIR USE IN DEVELOPING AN IDEALIZED SOIL PROFILE**

1. Boring location (plan and elevation) prepared by designer
  - SPT-N and depth to ground water table are shown on longitudinal and transverse sections cut through selected boring locations shown on plan.
2. Visual description of materials encountered during drilling performed by field personnel
  - Predominant soil types are sand, silty clay and sandy gravel.
  - Rock
3. Visual-manual procedures used by field personnel to classify soils
  - Preliminary classifications are sand (SW), silty clay (CL), and sandy gravel (GW) according to the Unified Soil Classification System
4. Moisture content determined in the laboratory.
  - Values of moisture content are shown on the sections next to SPT-N values.
5. Preliminary idealized soil profile developed based on information shown on the sections.
  - Subsurface variation of soil layers and ground water estimated between borings.
  - Idealized profile expressed in terms of zones with boundaries shown at boring locations only.
  - Profile may differ in transverse and longitudinal directions.
  - Preliminary profile compared to CPT soundings to refine characteristics of soils identified. For example, CPT soundings indicate that the silty clay layer may contain distinct seams of silt. The presence of such seams may help to reduce consolidation time.

[THIS PAGE INTENTIONALLY BLANK]



**Figure A.4-1. Status of geotechnical work.**

## SECTION A.4 LABORATORY TESTING

### A.4-1 RELEVANT CONCEPTS AND PROCEDURES (Refer to Figure A.4-1)

- Construction of the  $p_o$  diagram – Example 2-1.
- Preparation of a soil mechanics laboratory test request.
- Presentation of typical consolidation test results – Chapter 5.4.
- Presentation of typical strength test results – Chapter 5.5.

In this section the construction of a  $p_o$  diagram based on the Apple Freeway soil profile is demonstrated. A laboratory test request for consolidation and strength tests is presented. The numerical results of such tests are included in tabular form at the end of the chapter. The results are also presented in graphical form to show the variation of maximum past effective stress ( $p_c$ ) and undrained shear strength ( $s_u$ ) with depth.

### A.4-2 DETAILED PROCEDURES

**Given:** Preliminary idealized soil profile as determined in Section A.3 and total ( $\gamma_t$ ) and dry ( $\gamma_d$ ) unit weights of soils in the profile as determined from laboratory tests (Refer to Chapter 2)

**Required:**

- Construct the  $p_o$  diagram (Refer to Figure A.4-2). The  $p_o$  diagram represents the variation of the effective geostatic vertical stress ( $p_o$ ) with depth. Typically, the variation of the total geostatic vertical stress ( $p_t$ ) with depth is also shown on the  $p_o$  diagram to illustrate the effect of the groundwater table on the effective stress distribution. The difference between the two curves is the hydrostatic pore water pressure ( $p_w$ ) (Refer to Chapter 2)
- Prepare laboratory test request for consolidation and strength testing (Refer to Figure A.4-3).
- Superimpose on the  $p_o$  diagram a plot of the maximum past effective stress ( $p_c$ ) as determined from the results of consolidation tests (Refer to Figure A.4-4 and Table A.4-3).
- Prepare a plot of undrained shear strength ( $s_u$ ) with depth based on the results of vane shear tests, unconsolidated -undrained (UU) and consolidated-undrained (CU) triaxial tests (Refer to Figure A.4-5 and Table A.4-4)

**Solution:**

**Step 1: Construct the  $p_o$  diagram at boring UDH BAF – 4.**

- UDH BAF – 4 is the boring where the samples for strength and consolidation tests were obtained.
- Table A.4-1 shows the unit weights of the soils in the idealized profile as determined in the laboratory.
- The computations for  $p_o$ ,  $p_t$ , and  $p_w$  at soil layer and ground water table boundaries are shown in Table A.4-2. (Refer to Chapter 2 and Example 2-1)

**Step 2: Based on the effective geostatic vertical pressure ( $p_o$ ) at each depth specify test parameter for consolidation and strength tests.**

- Specify loads, test duration and loading pattern for consolidation tests (Refer to Figure A.4-3)
- Specify confining pressure for UU tests corresponding to total in situ geostatic vertical stress at the depth from which each sample was retrieved (Refer to Figure A.4-3)
- Specify three consolidation pressures for each CU test starting with  $p_o$  at the depth from which each sample was retrieved (Refer to Figure A.4-3).

**Step 3: Use the results laboratory tests to determine design parameters.**

- From consolidation test results determine the maximum past effective stress ( $p_c$ ), the compression index ( $C_c$ ), the recompression index ( $C_r$ ) and the coefficient of consolidation ( $c_v$ ) for samples retrieved at various depths (Refer to Table A.4-3).
- Plot the values of maximum past effective stress ( $p_c$ ) as estimated from the results of the consolidation tests on the  $p_o$  diagram to determine the stress history of the compressible layer (Refer to Figure A.4-4). Since the OCR ( $p_c/p_o$ )  $>1$ , the soil is overconsolidated (Refer to Chapter 5.4)
- From UU tests determine the undrained shear strength ( $s_u$ ) directly as one-half the undrained shear strength (Refer to Table A.4-4).
- From CU tests determine the undrained shear strength ( $s_u$ ) as one-half the undrained shear strength for each sample consolidated under a confining pressure equal to  $p_o$  at the depth from it was retrieved (Refer to Table A.4-4).
- From vane shear tests determine the undrained shear strength directly as one-half the measured undrained shear strength for both undisturbed and

remolded conditions (Refer to Table A.4-4).

- Plot the results of the vane shear tests (V), UU tests (U) and CU tests (C) versus depth in the clay layer (Refer to Figure A.4-5). Select 1,100 psf as the design value since it is (a) close to the middle of the consolidating clay layer and (b) it is a lower bound value.

### **A.4-3 Summary of Laboratory Testing and Illustration of the Use of Laboratory Test Results to Obtain Values for Geotechnical Design Parameters**

#### 1. Construct $p_v$ diagram

- Show increase of total and effective vertical geostatic pressures with depth
- Show effect of groundwater table and hydrostatic pore water pressure

#### 2. Prepare soil mechanics laboratory test request

- Assign consolidation test pressures and load times.
- Assign confining pressures for UU strength test to simulate variation of total geostatic pressures with depth.
- Assign range of consolidation pressures for CU test performed on samples retrieved from various depths to simulate effective stresses states ranging from initial value to final value due to the embankment.

#### 3. Consolidation test results

- Determine compression and recompression indices, maximum past effective stress, overconsolidation ratio (OCR), and coefficient of consolidation at various depths within the silty clay deposit.

#### 4. Strength test results

- Determine variation of undrained shear strength with depth (confining pressure) from results of vane shear tests.
- Determine variation of undrained shear strength with depth (confining pressure) from results of UU tests.
- Determine variation of undrained shear strength with depth (confining pressure) from results of CU tests.
- Compare differences of undrained shear strength obtained from the three tests and select a design value based on anticipated loading conditions.

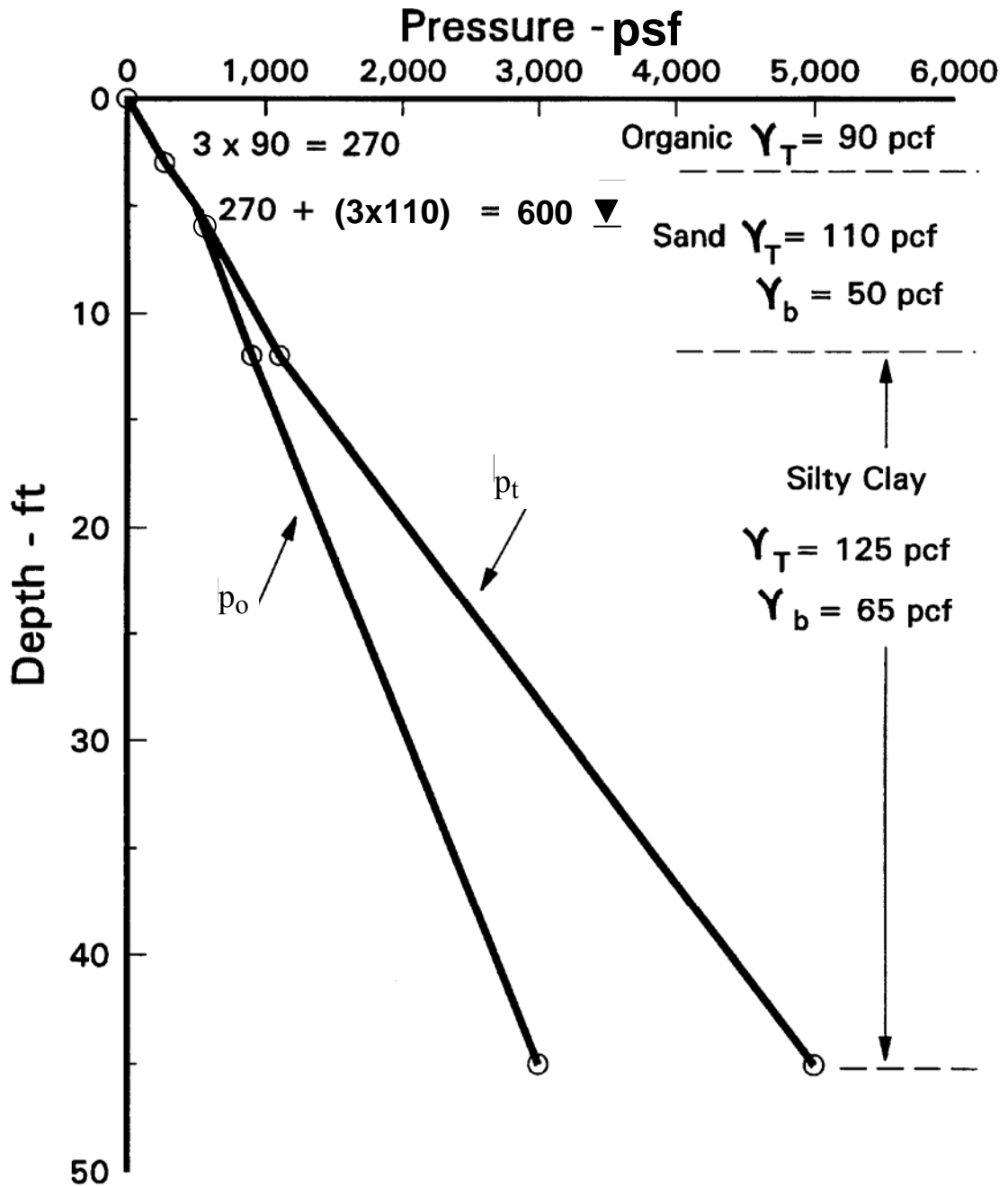


Figure A.4-2. The  $p_o$  diagram for boring UDH BAF – 4  
 (Note: Ground water was encountered at a depth of 6 ft in UDH BAF-4).



**Table A.4-1**  
**Unit weights of soils in idealized profile (Boring UDH BAF-4)**  
 (Assume unit weight of water = 60 pcf)

Soil stratum	Inclusive Depth (ft.)	Total unit weight ( $\gamma_t$ ) pcf	Saturated unit weight ( $\gamma_{sat}$ ) pcf	Buoyant unit weight ( $\gamma_b$ ) pcf
Organics	0 - 3	90	-	-
Sand	3 - 10	110	110	50
Silty clay	10 - 45	125	125	65

**Table A.4-2**  
**Computations for construction of  $p_o$  diagram (Boring UDH BAF-4)**  
 (The ground water table [GWT] is located at a depth of 6-ft below the surface)

Depth (ft) to a boundary	Total ( $p_t$ ) geostatic vertical pressure (psf)	Effective ( $p_o$ ) geostatic vertical pressure (psf)	Hydrostatic ( $p_w$ ) pore water pressure (psf)
3	3-ft x 90 pcf = 270 psf	3-ft x 90 pcf = 270 psf	$p_t - p_o = 0$ (above GWT)
6	270 psf + 3 ft x 110 pcf = 600 psf	270 psf + 3 ft x 110 pcf = 600 psf	$p_t - p_o = 0$ (at GWT)
10	600 psf + 4 ft x 110 pcf = 1,040 psf	600 psf + 4 ft x 50 pcf = 800 psf	1,040 psf – 800 psf = 240 psf or 4 ft x 60 pcf = 240 psf
45	1,040 psf + 35 ft x 125 pcf = 5,415 psf	800 psf + 35-ft x 65 pcf = 3,075 psf	5,415 psf – 3,075 psf = 2,340 psf or 39-ft x 60 pcf = 2,340 psf

**Table A.4-3**  
**Consolidation test results summary (Boring UDH BAF-4)**

Depth, ft	Tube No.	w %	$p_o$ , psf	$e_o$	$p_c$ , psf	$C_r$	$C_c$	$c_v$ ft <sup>2</sup> /day
11	T3	33	800	0.91	6,500	0.033	0.35	0.6
16	T4	35	1150	0.89	6,000	0.031	0.32	0.4
21	T5	31	1450	0.96	4,800	0.040	0.36	0.8
26	T6	36	1790	1.01	4,200	0.035	0.34	0.6
31	T7	38	2130	0.98	3,400	0.037	0.34	0.8
40	T9	37	2720	1.02	3,800	0.032	0.35	0.4

**Table A.4-4  
Shear strength test results summary (Boring UDH BAF-4)**

<b>Undrained Shear Strength – psf</b>						
<b>Depth, ft</b>	<b>Tube No.</b>	<b>w %</b>	<b>s<sub>u</sub> from UU tests (U)</b>	<b>s<sub>u</sub> @ p<sub>o</sub> from CU tests (C)</b>	<b>s<sub>u</sub> from vane shear tests (V)</b>	
					<b>Undisturbed</b>	<b>Remolded</b>
13		34			1,150	550
16	T4	34	1,050	1,150		
18		36			1,100	600
21	T5	35	950	1,250		
23		38			1,050	500
26	T6	39	975	1,200		
28		37			1,125	550
31	T7	40	1,000	1,250		
37		35			1,250	600
40	T9	38	800	1,300		

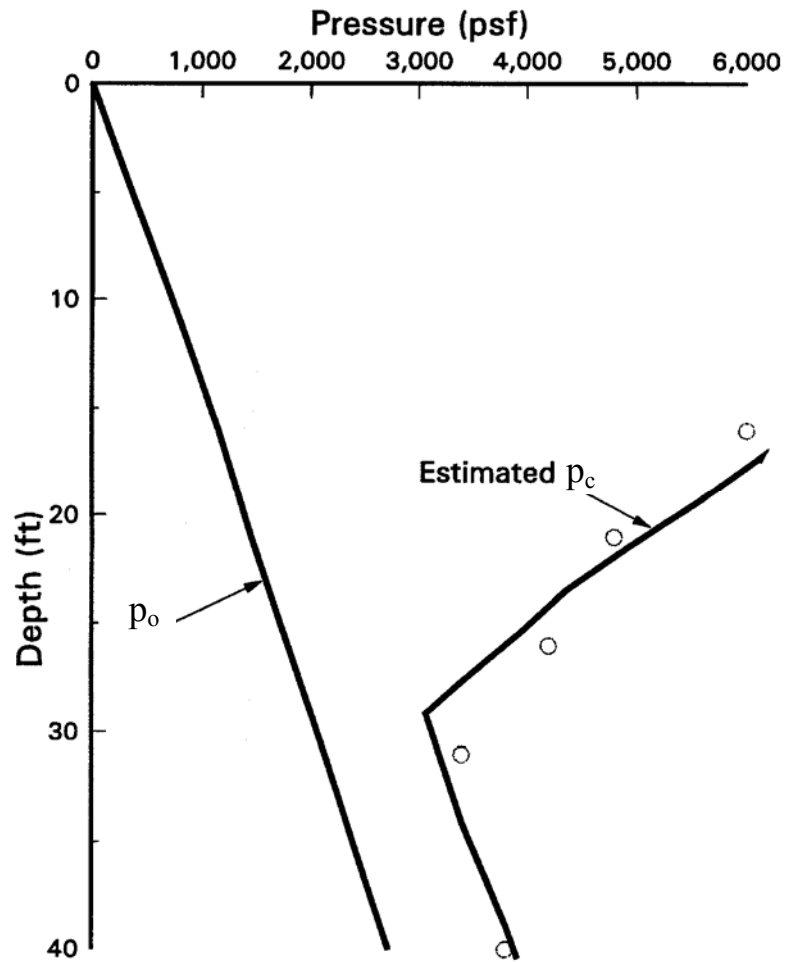
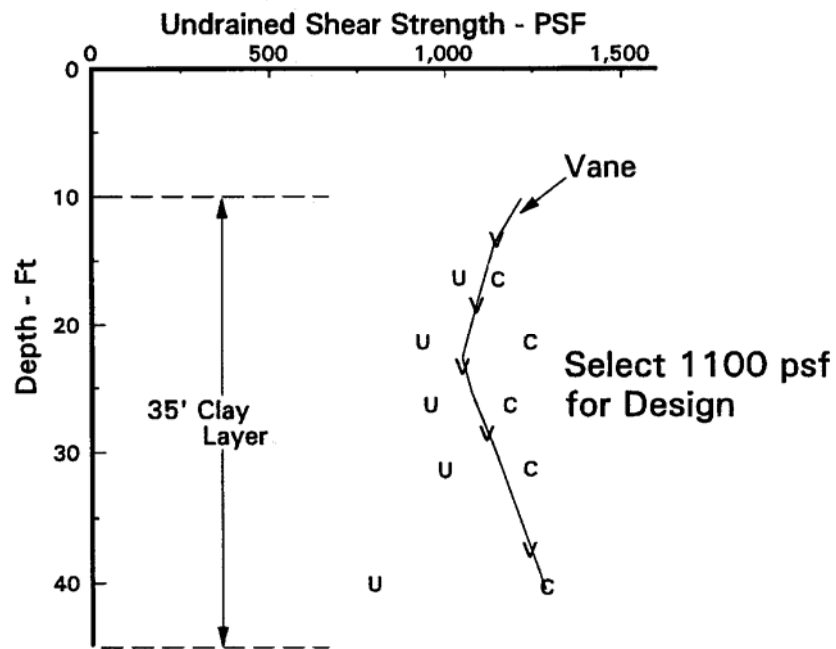


Figure A.4-4. Plot of estimated preconsolidation pressure,  $p_c$ , on a  $p_o$  plot.



**Figure A.4-5. Plot of variation of undrained shear strength with depth determined by various test methods (U = UU Test, C = CU Test, V = Undisturbed Vane Shear Test).**

Subsurface Explorations	Terrain reconnaissance Site inspection Subsurface explorations	✓
Basic Soil Properties	Visual description Classification tests Subsurface Profile	✓
Laboratory Testing	p <sub>o</sub> diagram Test request Consolidation results Strength results	✓
	<b>Slope Stability</b>	<b>Design soil profile</b> <b>Circular arc analysis</b> <b>Sliding block analysis</b>
Approach Roadway Deformations	Design soil profile Magnitude of settlement Rate of settlement Surcharge Vertical drains Lateral squeeze	
Spread Footing Design	Design soil profile Pier bearing capacity Pier settlement Abutment settlement Surcharge Vertical drains	
Driven Pile Design	Design soil profile Static analysis – pier Pipe pile H – pile Static analysis – abutment Pipe pile H – pile Driving resistance Lateral movement - abutment	
Construction Monitoring	Wave equation Hammer approval Embankment instrumentation	

**Figure A.5-1. Status of geotechnical work.**

## SECTION A.5 SLOPE STABILITY

### A.5-1 RELEVANT CONCEPTS AND PROCEDURES (Refer to Figure A.5-1)

- Design factor of safety (FS) - Chapter 6.2.
- Ordinary Method of Slices – hand solution - Chapter 6.4.3.
- Bishop’s Method – computer solution - Chapter 6.4.4; Table 6-1.
- Sliding (Rankine) Block Method – hand solution - Chapter 6.7.

In this section the analysis and design of an embankment with respect to global stability considerations are illustrated. The Ordinary Method of Slices is used to perform a stability analysis of the I-0 embankment. The results of hand calculations are compared to the results of computer-generated solutions based on the Ordinary Method of Slices and Bishop’s Simplified Method. A sliding block analysis is performed and the possibility of lateral squeeze is examined.

### A.5-2 DETAILED PROCEDURES

**Given:** The proposed embankment geometry as shown in Figure A.5-2 and the embankment and foundation soil properties at the east approach as provided in Table A.5-1. Assume that the shallow ( $\approx 3'$ ) surface layer of organic material shown in the idealized soil profile (Figure A.4-2) has been removed and replaced with select material having the same properties as the embankment fill.

**Required:**

- Perform hand calculations based on the Ordinary Method of Slices to compute the minimum factor of safety of the I-0 approach embankment at the east abutment.
- Compare the minimum factor of safety obtained from the hand calculations with the minimum factors of safety obtained from computer analyses based on the Ordinary Method of Slices and Bishop’s Method.
- Perform hand calculations based on the sliding (Rankine) block method to compute the minimum factor of safety of the I-0 approach embankment at the east abutment and compare the result with the results obtained from the two circular arc type failure analyses. Determine critical failure mode.
- Perform hand calculations to assess the potential for lateral squeeze of the embankment foundation soils at this location.

**Table A.5-1**  
**Geotechnical engineering properties of embankment and foundation soils**  
**East Abutment - (Boring BAF-4)**

Soil Type	Cohesion (c) - psf	Friction angle ( $\phi'$ )	$\gamma_t$ (pcf)	$\gamma_{sat}$ (pcf)	$\gamma_b$ (pcf)
Embankment fill	0	40°	130		
Sand	0	36°	110	110	50
Silty clay	1,100	0	125	125	65
Gravel	0	43°	130	130	70

**Solution:**

**Step 1:** As illustrated in Figure A.5-2, construct an idealized design profile to scale including the embankment and accounting for the assumption listed above.

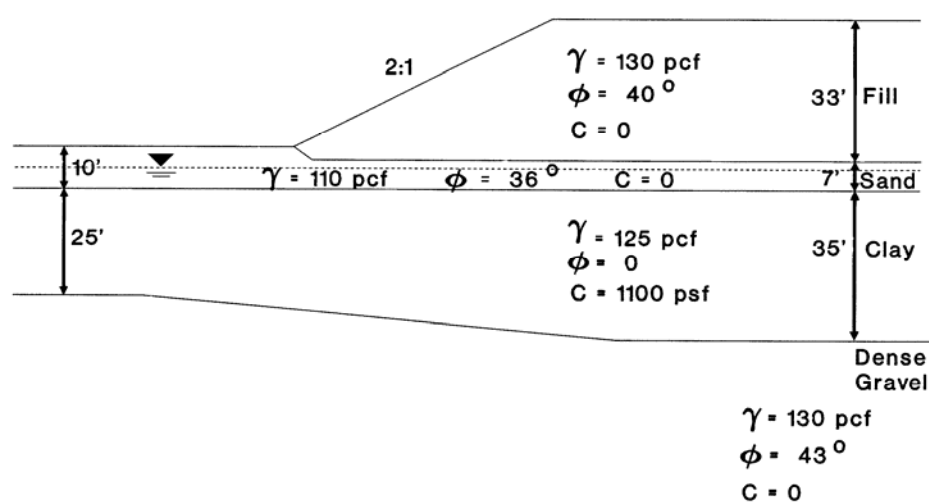


**Figure A.5-2. Idealized design soil profile – East Abutment.**

**Step 2:** Compute the FS against circular arc failure by a hand solution based on the Ordinary Method of Slices.

- Chose a trial failure circle, i.e., select a center (Point O) of a circle having radius (R) that will subtend a failure arc through the soils shown in Figure A.5-3. Depending upon the soil profile, the critical circle may be “deep seated”, i.e., be tangent to a relatively strong stratum underlying a much weaker layer, or it may be a “toe circle”, i.e., the arc passes through the toe of the slope when the soil profile is virtually homogeneous.

- For a complete hand solution many trial failure circles must be chosen to determine the minimum factor of safety. The circles typically cover a range of center points and radii.

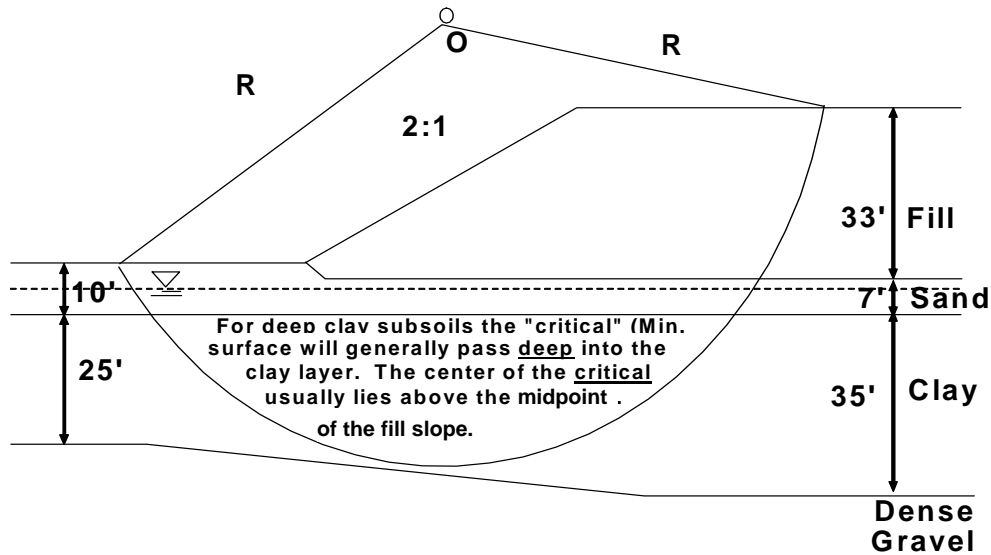


**Figure A.5-3. Trial failure circle – Embankment fill - East Abutment.**

- For the purpose of illustrating the hand procedure here and for comparison with the computer solution later on, the coordinates of the Point O chosen in this example correspond to the coordinates for the circle yielding the minimum factor of safety as determined by the computer solution based on Bishop's Method.
- Depending upon the geometry of the cross section and the number of soil layers intersected by the failure arc, divide the soil mass above the arc of the failure circle into at least 10 and no more than 20 vertical slices. For this example there are 16 slices selected as shown in Figure A.5-4.
- As shown in Figure A.5-5, determine the  $\alpha$  – angles for each vertical slice, where  $\alpha$  = the angle, as measured at Point O, between a vertical line through Point O and the radius that intersects the middle of the failure arc segment for a given slice.



- Once the geometry and  $\alpha$  – angle for each vertical slice have been determined, compute the resisting and driving forces for all slices by use of the following procedure as illustrated for Slice 7. Figure A.5-6 shows the geometry of the slice and the relevant soil properties. (Refer to equations 6-14 to 6-20).

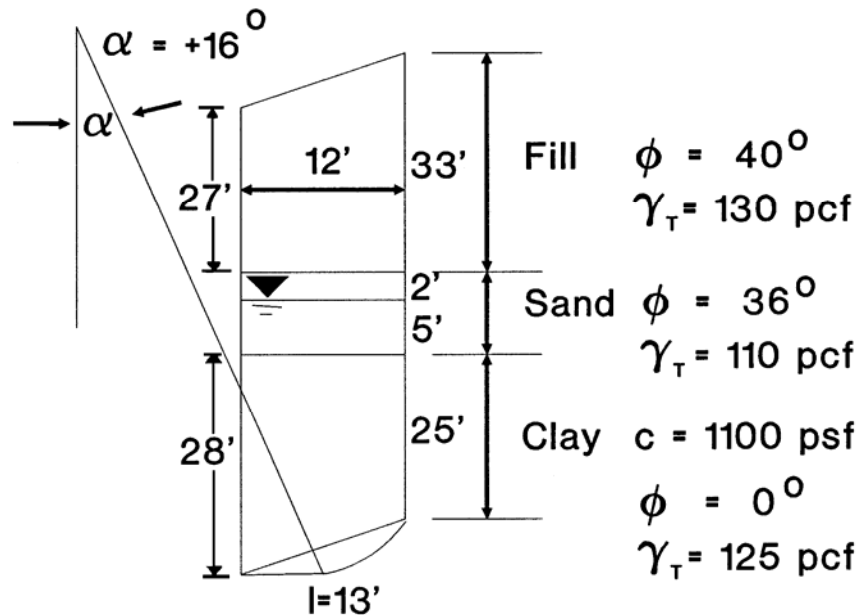


**Figure A.5-6. Geometry and relevant soil properties for slice 7 (Not-to-scale).**

- Calculate the total weight of the slice for a unit thickness into the plane of the paper by summing the contributions of the various soil strata lying above the failure arc.

$$W_T = (1\text{ft})(12\text{ft})\left(\frac{27\text{ft} + 33\text{ft}}{2}\right)(130\text{pcf}) + (1\text{ft})(12\text{ft})(7\text{ft})(110\text{pcf}) + (1\text{ft})(12\text{ft})\left(\frac{28\text{ft} + 25\text{ft}}{2}\right)(125\text{pcf}) = 95,790\text{lbs}$$

- Calculate the tangential driving force, which is the component of the weight of the slice acting perpendicular to the radius (R).

$$T = W_T \sin \alpha = 95,790 \text{ lbs} (\sin 16^\circ) = 26,403 \text{ lbs}$$

- Calculate the shearing resistance along the length of arc subtended by the failure surface. Use the length of the chord (l) to approximate the arc length. In general, the shearing resistance consists of a frictional component and a cohesion component. For a unit thickness into the plane of the paper, the frictional component is given by:  $N' \tan \phi = (W_T \cos \alpha - ul) \tan \phi$ , where  $u$  = the average

pore water pressure acting along the chord length,  $l$  (Refer to Eq. 6-18). The cohesion component is given by  $cl$  where  $c$  = the cohesion for drained conditions and the undrained shear strength ( $s_u$ ) for undrained conditions. Since undrained conditions are usually critical, the undrained shear strength ( $s_u$ ) is generally used in the calculation.

Since the bottom of Slice 7 is in clay where  $\phi = 0$ ,  $N \tan \phi = 0$ . Therefore, the total shearing resistance for a unit thickness into the plane of the paper is given by the cohesion component as follows:

$$c l = (1,100 \text{ psf})(13 \text{ ft})(1 \text{ ft}) = 14,300 \text{ lbs}$$

Therefore for Slice 7:

$$\text{Driving Force} = T = 26,403 \text{ lbs}$$

$$\text{Resisting Force} = c l = 14,300 \text{ lbs}$$

- Slice 7 was used to illustrate the case where the failure surface passed through a purely cohesive material below the ground water table. Slice 15 is used to illustrate the procedure when the failure surface passes through a purely frictional material below the ground water table. Figure A.5-7 shows the geometry of Slice 15 and the relevant soil properties.

- As before, calculate the total weight of the slice for a unit thickness into the plane of the paper

$$W_T = (1 \text{ ft})(4 \text{ ft}) \left( \frac{10 \text{ ft} + 5 \text{ ft}}{2} \right) (110 \text{ pcf}) = 3,300 \text{ lbs}$$

- As before, calculate the tangential driving force

$$T = W_T \sin \alpha = 3,300 \text{ lbs} (\sin (-49^\circ)) = - 2,491 \text{ lbs}$$

Note:  $T$  is negative for this slice since the weight tends to RESIST sliding.

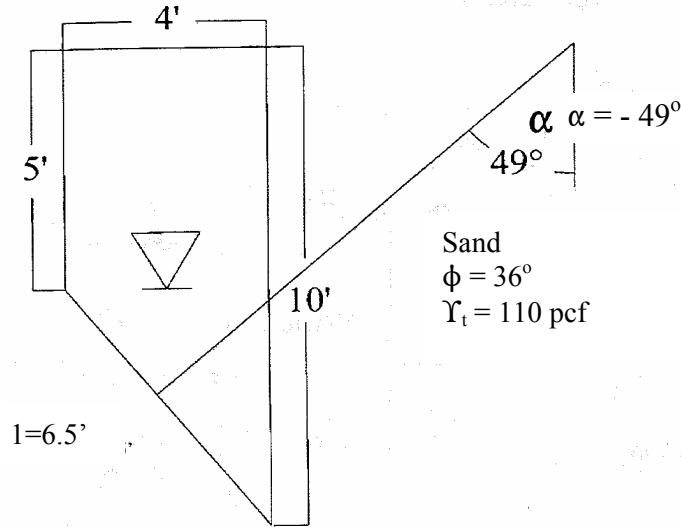


**Figure A.5-7. Geometry and relevant soil properties for slice 15 (Not-to-scale).**

- As before, calculate the shearing resistance along the length of arc subtended by the failure surface. Use the length of the chord (l) to approximate the arc length.

Since the bottom of Slice 15 is in sand where  $c = 0$ ,  $c_l = 0$ . Therefore, the total shearing resistance for a unit thickness into the plane of the paper is given by the frictional component based on  $\phi = 36^\circ$  as follows:

$$N = W_t \cos \alpha - ul$$

$$N = (3,300 \text{ lbs})(\cos (-49^\circ)) - (1 \text{ ft})(5 \text{ ft}/2) (6.5 \text{ ft}) (60 \text{ pcf})$$

$$N = 2,165 \text{ lbs} - 975 \text{ lbs} = 1,190 \text{ lbs}$$

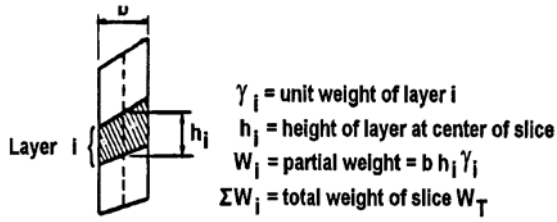
$$N \tan \phi = 1,190 \text{ lbs} (\tan 36^\circ) = 865 \text{ lbs}$$

Therefore, for Slice 15:  
 Driving Force =  $T = -2,491 \text{ lbs}$   
 Resisting Force =  $865 \text{ lbs}$

- Follow the procedures described above to calculate weights for each slice. For ease in computation use the tabular format illustrated in Table A.5-2.

**Table A.5-2**

**Tabular form for computing total weights of slices for a unit thickness into the plane of the paper**



Slice No.	B (ft)	$h_i$ (ft)	$\gamma_i$ (pcf)	$W_i$ (lbs/ft)	$\Sigma W_i = W_T$ (lbs)
1	15	33/2	130	32,175	32,175
2	2	33	130	8,580	
		2/2	110	220	8,800
3	4	33	130	17,160	
		(7+2)/2	110	1,980	19,140
4	12	33	130	51,480	
		7	110	9,240	
		12/2	125	9,000	69,720
5	12	33	130	51,480	
		7	110	9,240	
		(19+12)/2	125	23,250	83,970
6	12	33	130	51,480	
		7	110	9,240	
		(19+25)/2	125	33,000	93,720
7	12	(27+33)/2	130	46,800	
		7	110	9,240	
		(25+28)/2	125	39,750	95,790
8	12	(20+27)/2	130	36,660	
		7	110	9,240	
		(30+28)/2	125	43,500	89,400
9	12	(14+20)/2	130	26,520	
		7	110	9,240	
		30	125	45,000	80,760
10	12	(9+14)/2	130	17,940	
		7	110	9,240	
		(28+30)/2	125	43,500	70,680
11	12	(9+3)/2	130	9,360	
		7	110	9,240	
		(25+28)/2	125	39,750	58,350
12	13	10	110	14,300	
		(19+25)/2	125	35,750	50,050
13	12	10	110	13,200	
		(12+19)/2	125	23,250	36,450
14	12	10	110	13,200	
		12/2	125	9,000	22,200
15	4	(5+10)/2	110	3,300	3,300
16	4	5/2	110	1,100	1,100

- Follow the computational procedures described above and record the relevant soil and geometric properties and the calculated values of driving and resisting forces for each slice in a table. For ease in computation of the global factor of safety, use the tabular format illustrated in Table A.5-3.
- Calculate the global factor of safety by using the equations shown in Table A.5-3.
- Summarize the results of the Ordinary Method of Slices based on hand calculations by showing the critical failure circle and its associated minimum factor of safety graphically (Refer to Figure A.5-8).

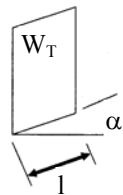
**Step 3: Compute the FS against circular arc failure by computer solutions based on the Ordinary Method of Slices and the Bishop Simplified Method.**

- Summarize the results of the Ordinary Method of Slices (OMS) and Bishop's Simplified Method based on a computer solution by showing the critical failure circle and its associated minimum factor of safety graphically (Refer to Figure A.5-9). Note that for the purpose of illustrating the difference between the FS for the two computer solutions, the coordinates of Point O and the radius of the failure arc, R, for the Ordinary Method of Slices computer solution correspond to those of the circle yielding the minimum factor of safety as determined by the computer solution based on Bishop's Method. As noted previously, the same geometry was used for the Ordinary Method of Slices solution by hand calculations.
- Figure A.5-10 illustrates the search routine used by the computer program to obtain the minimum FS. Contours of equal FS are shown with the minimum FS being the point at the center of the contours. The contours represent the results of many computer runs in which the center and radius of the failure circle were varied in a systematic way until the minimum FS was reached. The efficiency of the computer solution over the hand solution in terms of time and accuracy is obvious.

**Table A.5-3**  
**Tabular form for computing factor of safety by Ordinary Method of Slices**

Slice No.	$W_T$ (from Table A.5-2) (lbs)	$l$ (ft)	$\alpha$ (deg)	$c$ (psf)	$\phi$ (deg)	$u$ (psf)	$ul$ (lbs)	$W_T \cos \alpha$ (lbs)	$N' = W_T \cos \alpha - ul$ (lbs)	$N' \tan \phi$ (lbs)	$cl$ (lbs)	$T = W_T \sin \alpha$ (lbs)
1	32,175	36	60	0	40	0	0	16,088	16,088	13,499	0	27,864
2	8,800	3	54	0	36	0	0	5,173	5,173	3,758	0	7,119
3	19,140	7	51	0	36	150	1,050	12,045	10,995	7,988	0	14,875
4	69,720	17	43	1,100	0	-	-	-	-	0	18,700	47,549
5	83,970	15	34	1,100	0	-	-	-	-	0	16,500	46,955
6	93,720	15	25	1,100	0	-	-	-	-	0	16,500	39,608
7	95,790	13	16	1,100	0	-	-	-	-	0	14,300	26,403
8	89,400	13	9	1,100	0	-	-	-	-	0	14,300	13,985
9	80,760	12	1	1,100	0	-	-	-	-	0	13,200	1,409
10	70,680	12	-7	1,100	0	-	-	-	-	0	13,200	-8,614
11	58,350	13	-15	1,100	0	-	-	-	-	0	14,300	-15,102
12	50,050	14	-24	1,100	0	-	-	-	-	0	15,400	-20,357
13	36,450	14	-32	1,100	0	-	-	-	-	0	15,400	-19,316
14	22,200	16	-42	1,100	0	-	-	-	-	0	17,600	-14,855
15	3,300	6.5	-49	0	36	150	975	2,165	1,190	865	0	-2,491
16	1,100	6.5	-53	0	36	0	0	662	662	481	0	-878
									$\Sigma$	26,591	169,400	144,154

$$FS = \frac{\Sigma (W_T \cos \alpha - ul) \tan \phi + \Sigma cl}{\Sigma W_T \sin \alpha} = \frac{\Sigma N' \tan \phi + \Sigma cl}{\Sigma W_T \sin \alpha} = \frac{26,591 \text{ lbs} + 169,400 \text{ lbs}}{144,154 \text{ lbs}} = 1.36$$



Legend: Refer to Figure 6-10 for definition of various slice quantities

- $W_T$  = Total weight of Slice (soil + water)
- $l$  = Base length of the slice
- $c$  = Cohesion at base of slice
- $\phi$  = angle of internal friction
- $u$  = pore water pressure at base of slice

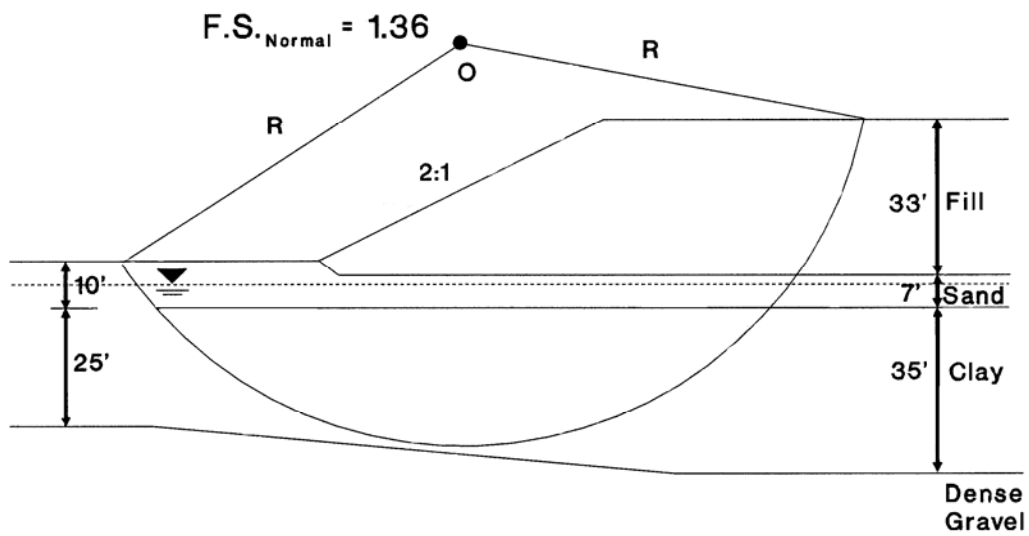


Figure A.5-8. Graphical representation of solution for minimum Factor of Safety by Ordinary Method of Slices/Hand computation – East Abutment.

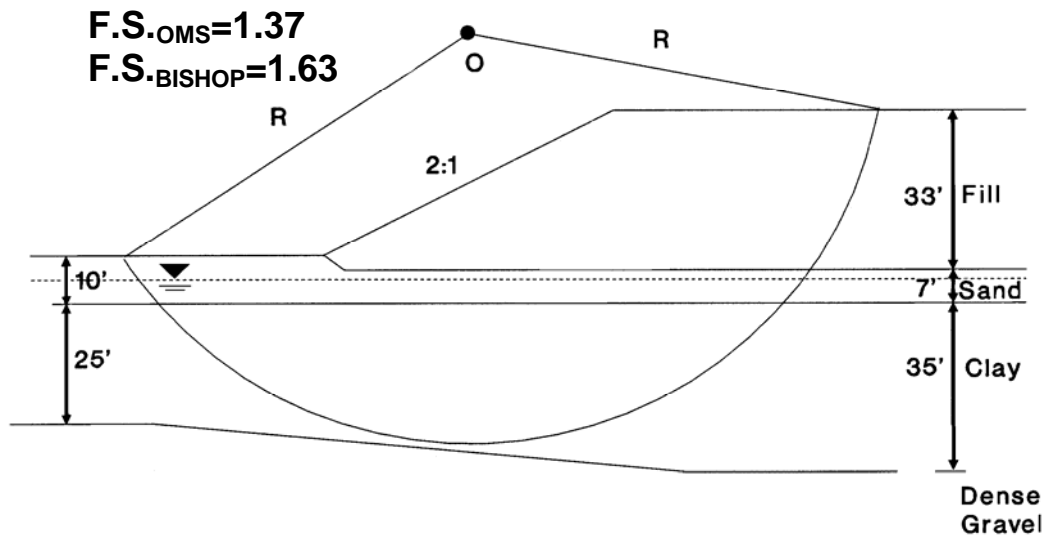


Figure A.5-9. Graphical representation of solution for minimum Factor of Safety by Ordinary Method of Slices (OMS)/Computer solution and Bishop's Method – East Abutment.

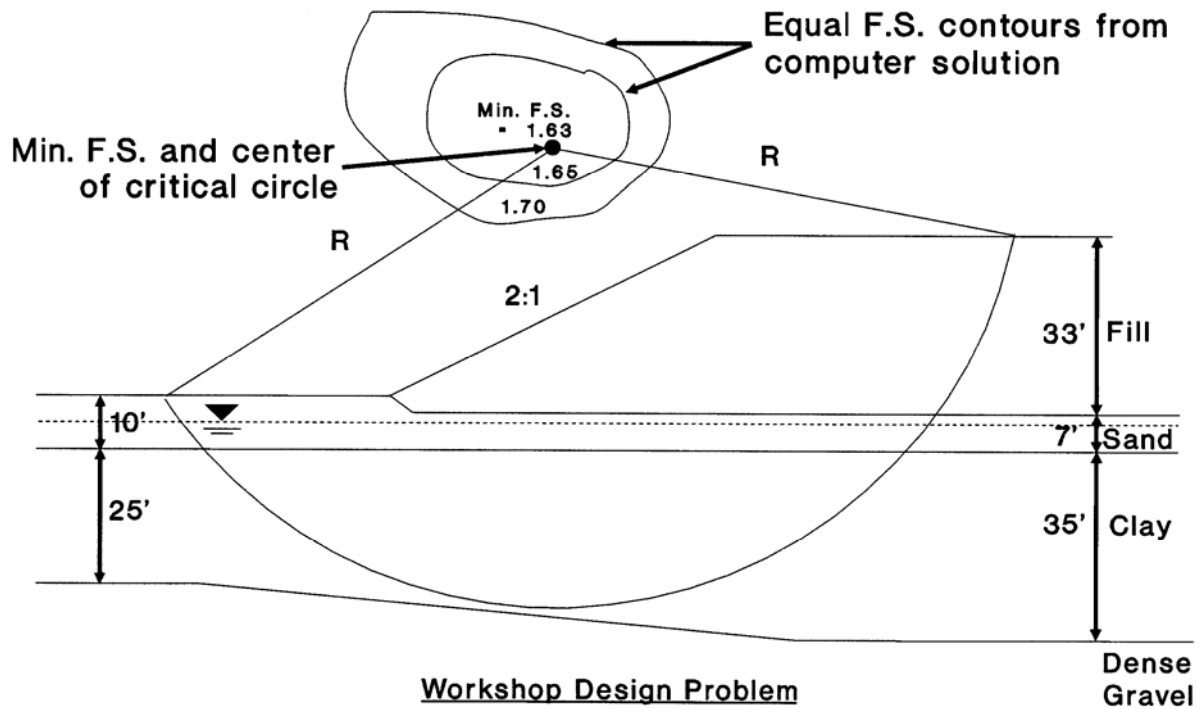


Figure A.5-10

Illustration of search routine used by computer program to develop contours of equal FS that converge on the point of minimum FS and center of critical circle.

**Step 4: Compare the FS against circular arc failure computed by each of the three methods and select a design FS.**

F.S. = 1.36 - Ordinary Method of Slices: Hand Solution  
 F.S. = 1.37 - Ordinary Method of Slices: Computer Solution  
 F.S. = 1.63 - Bishop's Simplified Method: Computer Solution

Use a minimum factor of safety for design F.S. (Bishop) = 1.63

**Step 5: Calculate FS against a Sliding Block Type Failure by Using Rankine Wedges and Sliding Block Analysis**

- Choose a trial block type failure surface along the top of clay layer as shown in Figure A.5-11.



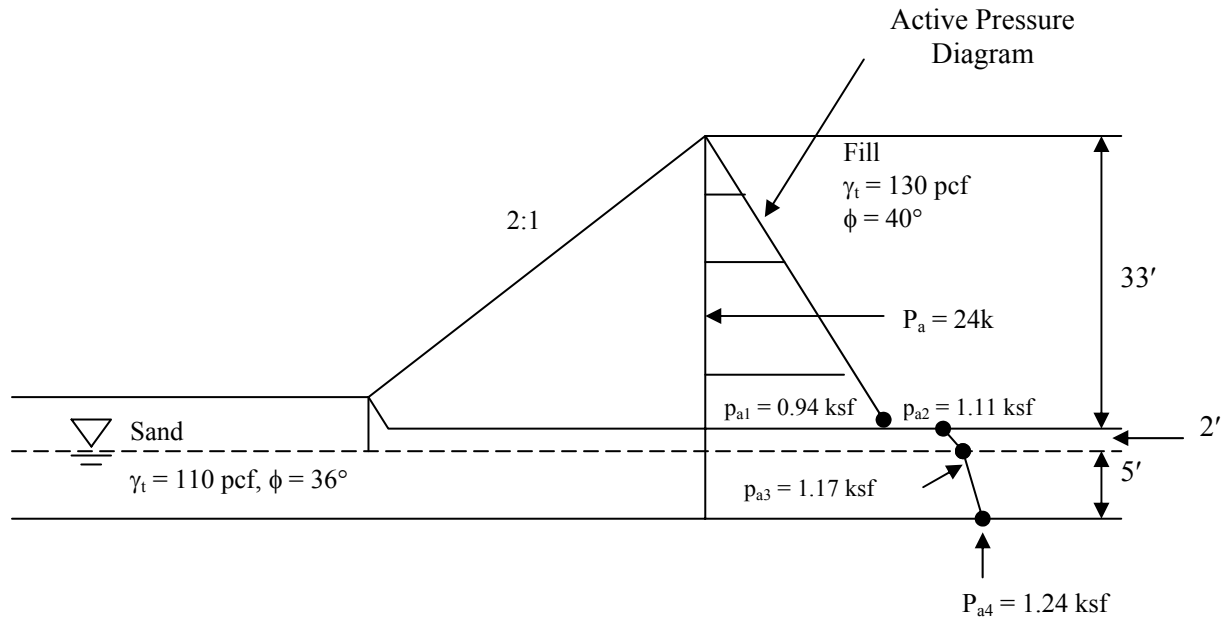


**Figure A.5-12**  
**Active earth pressure diagram and resultant active Rankine force**

- Calculate passive Rankine coefficient of lateral earth pressure ( $K_p$ )
  - For sand
 
$$K_p = \tan^2 (45^\circ + 36^\circ/2) = \tan^2 (63^\circ) = 3.85$$
- Calculate passive lateral earth pressure ( $p_p$ )
  - At 5-ft below top of sand layer (i.e. at water table elevation)
 
$$p_{p1} = (0.110 \text{ kcf})(5 \text{ ft})(3.85) = 2.1 \text{ ksf}$$
  - At base of sand layer
 
$$p_{p2} = 2.1 \text{ ksf} + (0.050 \text{ kcf}^*)(5 \text{ ft})(3.85) = 3.1 \text{ ksf}$$
 (\*buoyant unit weight below water table)
- Calculate passive Rankine force ( $P_p$ ) for a unit thickness into the plane of the paper and plot force and passive lateral earth pressure diagram as shown in Figure A.5-13
  - $$P_p = (2.1 \text{ ksf})(5 \text{ ft})(1/2)(1 \text{ ft}) + ((2.1 \text{ ksf} + 3.1 \text{ ksf})/2)(5 \text{ ft})(1 \text{ ft}) = 5.3 \text{ k} + 13 \text{ k} \approx 18 \text{ k}$$
- Calculate the resisting force of the central block for assumed failure plane along the top of the clay layer and the plot the force system as shown on Figure A.5-14.
  - $c = 1,100 \text{ psf} = 1.1 \text{ ksf}$
  - $L = 60 \text{ ft}$
  - $cL = (1.1 \text{ ksf})(60 \text{ ft})(1 \text{ ft}) = 66^{\text{k}}$

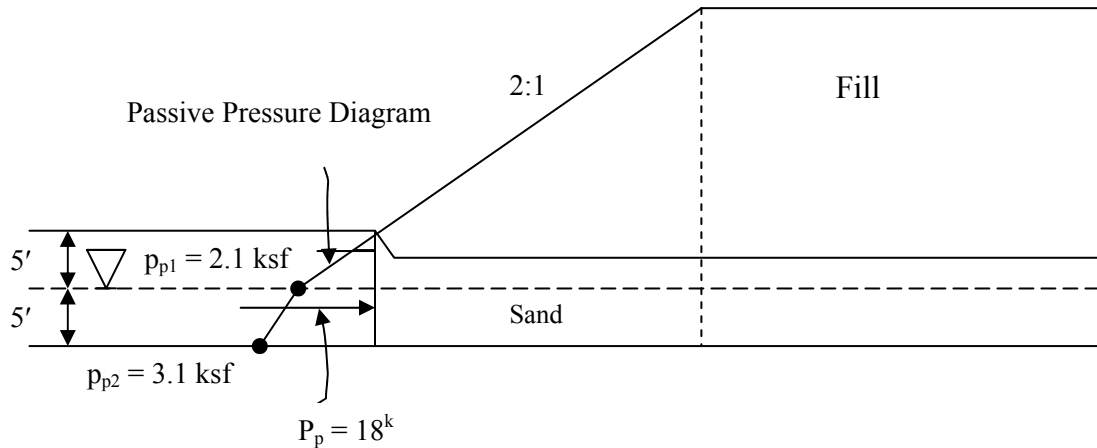


**Figure A.5-13. Passive earth pressure diagram and resultant passive Rankine force.**

- Calculate the FS against sliding failure

$$F.S. = \frac{\text{Horizontal Resisting Forces}}{\text{Horizontal Driving Forces}} = \frac{P_p + CL}{P_A}$$

$$= \frac{18^k + 66^k}{24^k} = \frac{84^k}{24^k} = 3.5$$

- Compare FS against sliding failure (3.5) vs. minimum FS against circular arc failure (1.63).
- Conclusion: circular arc failure is more critical and governs the design.

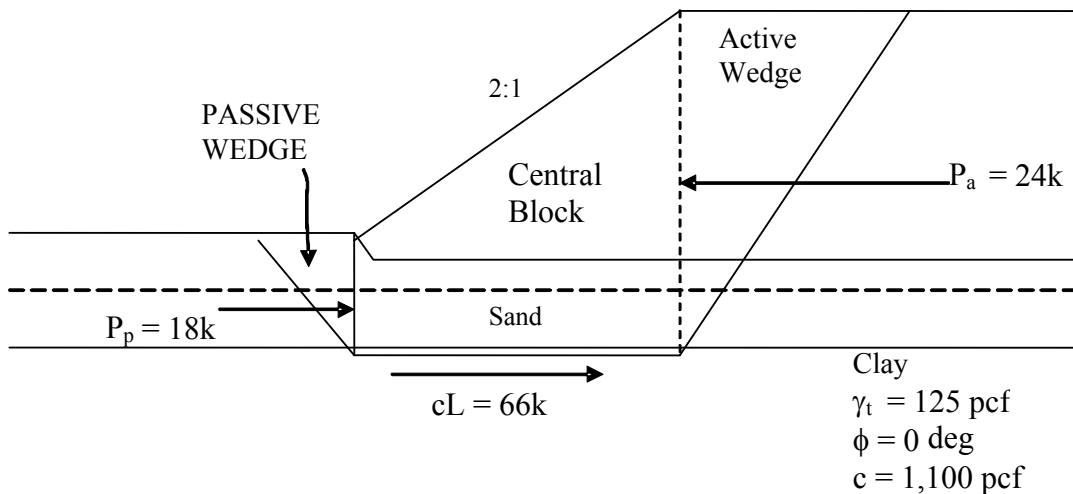


**Figure A.5-14. Force system acting on central block.**

**A.5-3 SUMMARY OF THE APPROACH USED TO DETERMINE EMBANKMENT STABILITY FOR THE APPLE FREEWAY DESIGN PROBLEM**

1. Construct an idealized design profile to scale.
  - Use idealized soil profile from Boring UDH BAF-4
  - Include 33-ft high embankment at east abutment.
  - Estimate geotechnical properties of soil layers from results of field and laboratory tests.
  
2. Perform hand calculations to determine FS against circular arc failure by using the Ordinary Method of Slices.
  - For illustration use center and radius of circle from computer solution that provided minimum FS by Bishop Simplified Method
  - Divide the soil mass above the arc of the failure circle into at least 10 and no more than 20 vertical slices.
  - Set up a table to aid in the performance of the calculations.
  - Fill the table with soil properties and geometric data for each slice.
  - Illustrate calculations performed for Slice 7 – arc segment in clay.
  - Illustrate calculations performed for Slice 15 – arc segment in sand.
  - Calculate the FS for the assumed center and radius.
  
3. Compute the FS against a circular arc failure by using computer solutions based on the Ordinary Method of Slices and the Bishop Simplified Method.
  
4. Compare the FS against a circular arc failure computed by each of the three methods and select the minimum FS.
  - Note that only the computer solution by Bishop’s Modified Method provides a minimum FS against circular arc failure. The values obtained from the Ordinary Method of Slices hand calculations and computer solution may not be the minima for that method since the center and radius of the circle used here to illustrate the method are those that provided the minimum FS by Bishop Simplified Method computer solution.
  
5. Calculate the FS against a sliding block type failure by using Rankine wedges and sliding block analysis.
  1. Calculate the active and passive coefficients of lateral earth pressure for each soil layer by using Rankine equations.

2. Calculate the active and passive lateral earth pressure distributions taking into account changes in soil layering and the presence of ground water.
3. Calculate the active (driving) and passive (resisting) forces due to the Rankine wedges.
4. Assume that sliding occurs along the top of the clay layer and calculate the resisting force of the central block.
5. Calculate the FS against a sliding block type failure and compare it to the minimum FS against a circular arc failure. Select the lower of the two as the design FS.

Subsurface Explorations	Terrain reconnaissance Site inspection Subsurface explorations	✓
Basic Soil Properties	Visual description Classification tests Subsurface profile	✓
Laboratory Testing	p <sub>o</sub> diagram Test request Consolidation results Strength results	✓
Slope Stability	Design soil profile Circular arc analysis Sliding block analysis	✓
 <b>Approach Roadway Deformations</b>		<b>Design soil profile Magnitude and rate of settlement Surcharge Vertical drains Lateral Squeeze</b>
Spread Footing Design	Design soil profile Pier bearing capacity Pier settlement Abutment settlement Surcharge Vertical drains	
Driven Pile Design	Design soil profile Static analysis – pier Pipe pile H - pile Static analysis – abutment Pipe pile H - pile Driving resistance Lateral movement - abutment	
Construction Monitoring	Wave equation Hammer approval Embankment instrumentation	

**Figure A.6-1. Status of geotechnical work.**

## SECTION A.6 APPROACH ROADWAY DEFORMATIONS

### A.6-1 RELEVANT CONCEPTS AND PROCEDURES (Refer to Figure A.6-1)

- General procedure to determine pressure distribution with depth due to approach embankment; Chapter 7.3
- Immediate settlement – computation of magnitude; Chapter 7.4.
- Consolidation settlement – computation of magnitude; Chapter 7.5.
- Consolidation settlement – computation of time rate; Chapter 7.5.3.
- Treatment by surcharging to accelerate consolidation settlement and reduce time; Chapter 7.7
- Treatment by Wick Drains without surcharge to accelerate consolidation settlement and reduce time; Chapter 7.7
- Estimating horizontal movement due to lateral squeeze of embankment foundation soils; Chapter 7.6

In this section the computation of the magnitude of immediate settlement of a sand layer and the magnitudes and rates of consolidation settlement of an organic layer and a clay layer due to the construction of an embankment fill are illustrated. The options of surcharging and vertical drains with and without surcharge are also examined as a means of treatment to accelerate consolidation settlement and reduce time.

### A.6-2 DETAILED PROCEDURES

#### Given:

- The subsurface profile and soil properties shown in Figure A.6-2 for the east abutment embankment of the Apple Freeway Bridge.
- The consolidation test results presented in Table A.6-1.
- Assume that N-values in the profile are  $N_{60}$  values.

#### Required:

- Perform hand calculations to compute the pressure distribution with depth due to the embankment fill.
- Perform hand calculations to compute the magnitude of the anticipated consolidation settlement due to the embankment fill.
- Perform hand calculations to compute the time required for the settlement to occur without treatment by surcharging or vertical drains and plot the time vs. settlement

curve.

- Evaluate the stability of the 30 ft embankment fill with the addition of 10 ft of surcharge treatment.
- Examine the effect of treatment by surcharging on settlement and time (including cost analysis).
- Examine the effect of treatment by vertical wick drains without surcharge on settlement and time (including cost analysis).
- Estimate the amount of horizontal deformation due to lateral squeeze of the embankment foundation soils

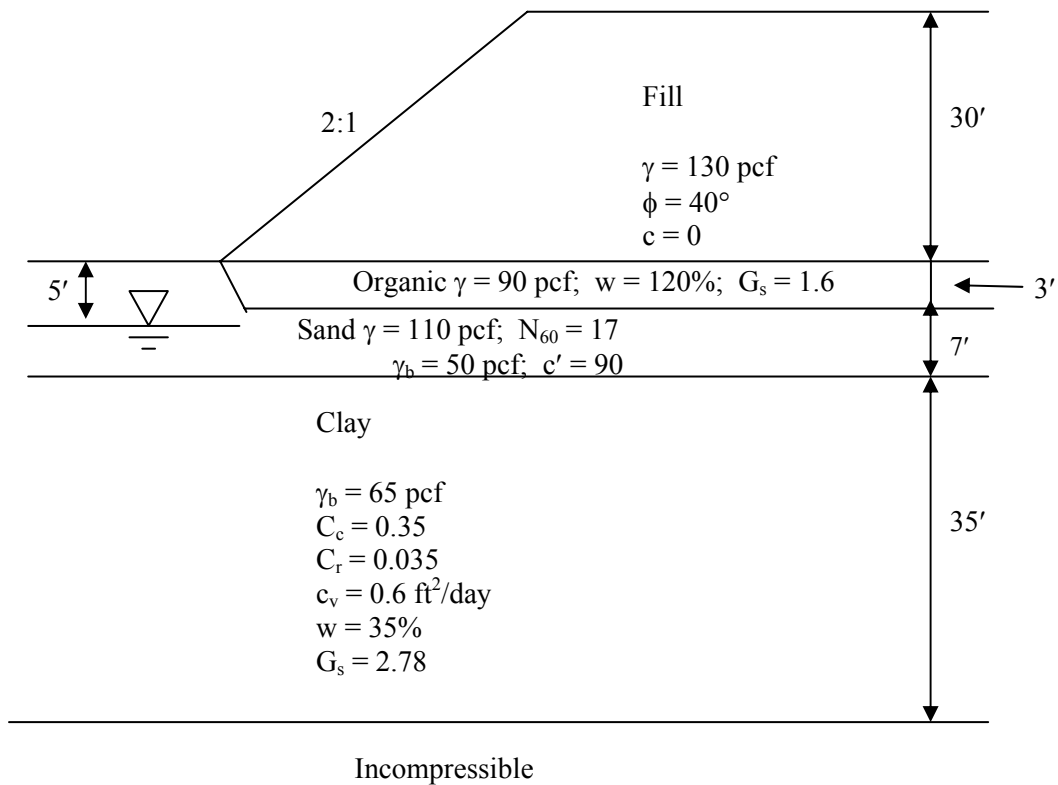


**Figure A.6-2. Design subsurface profile and soil properties at east embankment location.**

### A.6-3 SOLUTION TO DETERMINE THE MAGNITUDE OF AND TIME FOR THE ANTICIPATED SETTLEMENT DUE TO THE EMBANKMENT FILL

**Step 1: Obtain soil consolidation characteristics (from laboratory tests).**

**Table A.6-1  
Consolidation test results summary (Hole BAF-4)**

Depth	Tube	$p_c$ (psf)	$C_c$	$C_r$	$c_v$ (ft <sup>2</sup> /day)
11	T3	6,500	0.35	0.033	0.6
16	T4	6,000	0.32	0.031	0.4
21	T5	4,800	0.36	0.040	0.8
26	T6	4,200	0.34	0.035	0.6
31	T7	3,400	0.34	0.037	0.8
40	T9	3,800	0.35	0.032	0.4

$e_o$  (average) = 0.97

**Step 2: Plot overburden pressure (Figure A.4-2) and preconsolidation pressure (Table A.6-1) with Depth as shown in Figure A.6-3.**

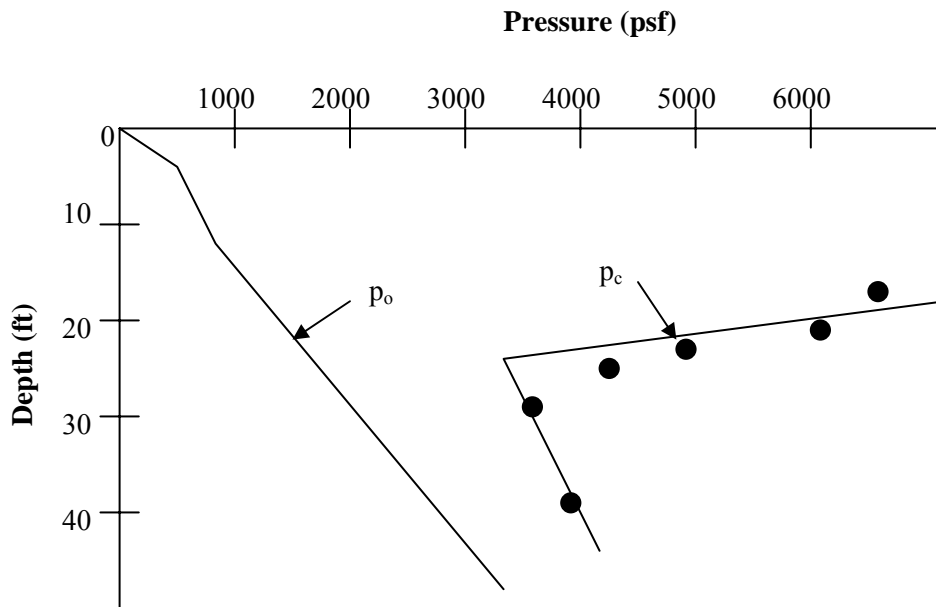


**Figure A.6-3. Variation of overburden pressure and preconsolidation pressure with depth.**

**Step 3: Determine the distribution of pressure increase with depth due to the embankment pressure ( $p_f$ ) at end of construction:**

- Obtain embankment geometry. Use the same geometry (plan and section) from Example 7-1 in Chapter 7.
- Embankment top width = 100 ft
- Side and end slopes = 1V on 2H
- Top of end slope from toe = 60 ft
- Embankment height = 30 ft
- Embankment load (at longitudinal centerline) =  $H_{emb} \times \gamma_{emb} = 30 \text{ ft} \times 130 \text{ pcf} = 3,900 \text{ psf}$
- Use Figure A.6-4 to obtain pressure coefficient K (left ordinate) for  $b = \left( \frac{100 \text{ ft}}{2} + \frac{60 \text{ ft}}{2} \right) = 80 \text{ ft}$  and a distance from midpoint of end slope =  $0.375b$ .
- Abutment center located 30 ft from midpoint of end slope  $\rightarrow \frac{30 \text{ ft}}{80 \text{ ft}} (b) = 0.375b$
- Use a series of charts corresponding to different depths expressed as a percentage of  $b_f$  (right ordinate) to obtain a distribution of pressure coefficients with depth.
- Compute pressure change  $\Delta p = K \times \text{embankment load}$  at various depths expressed as a percentage of  $b_f$ . The results of these computations are presented in Table A.6-2.

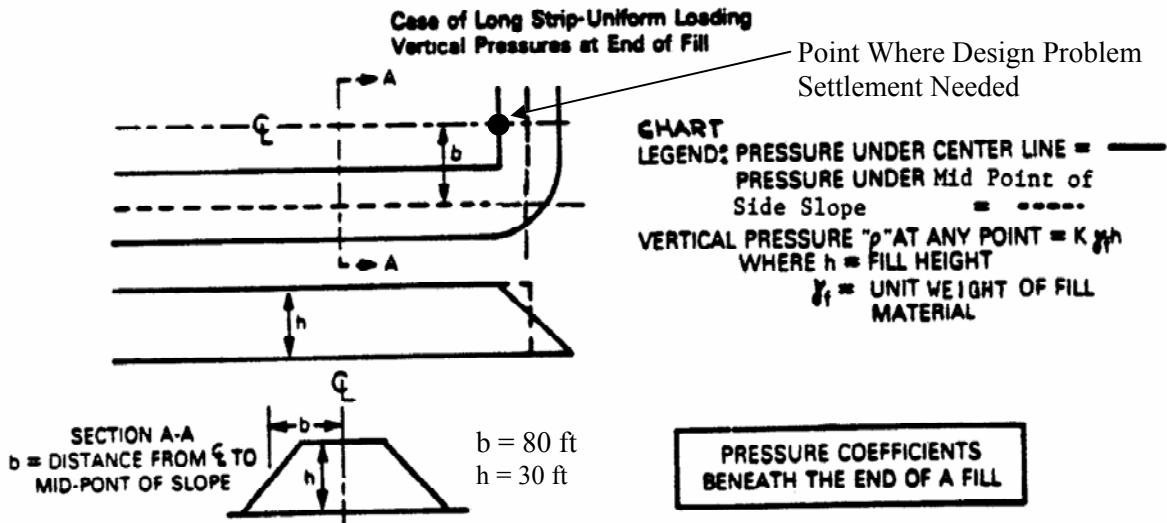
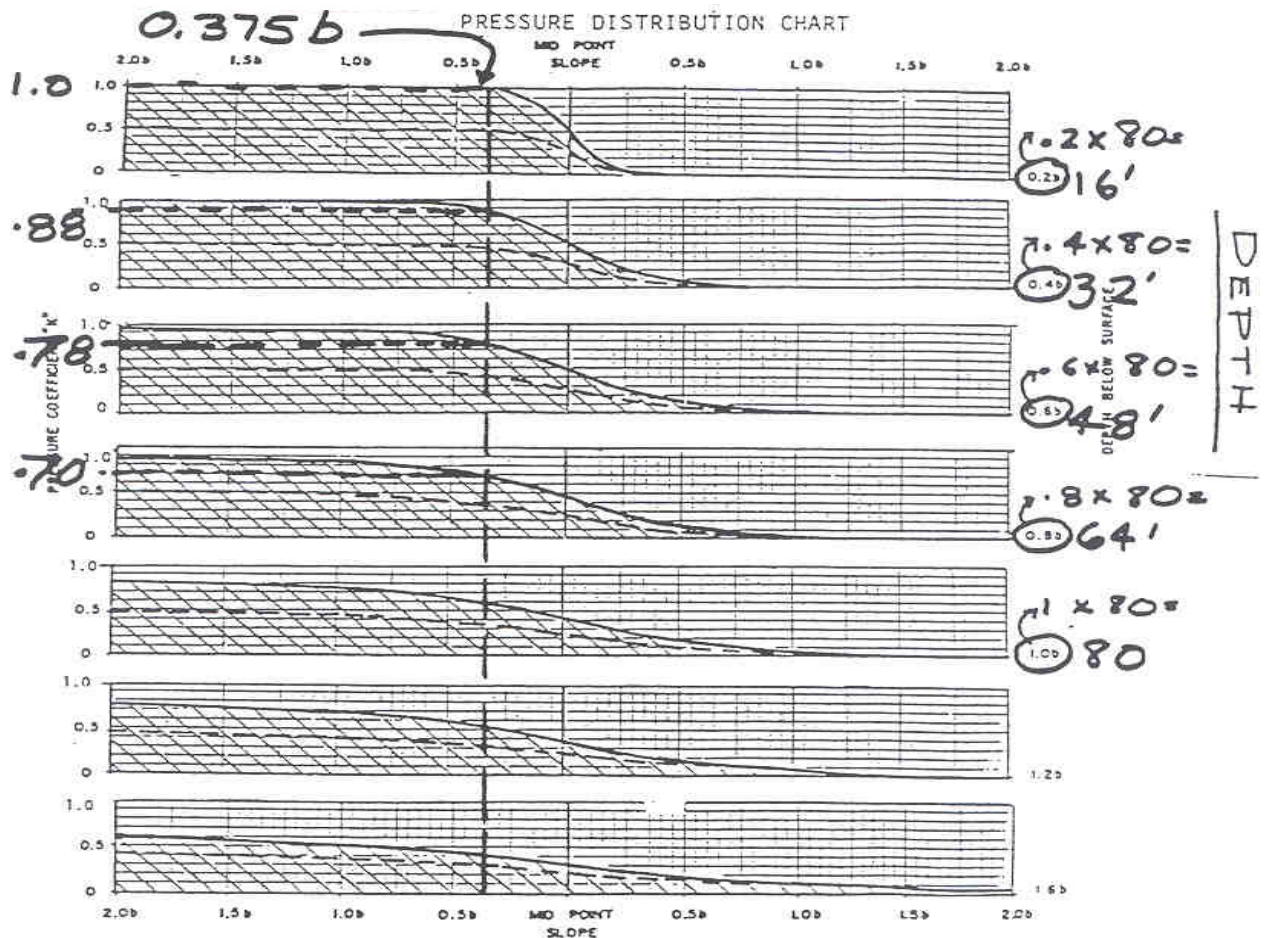
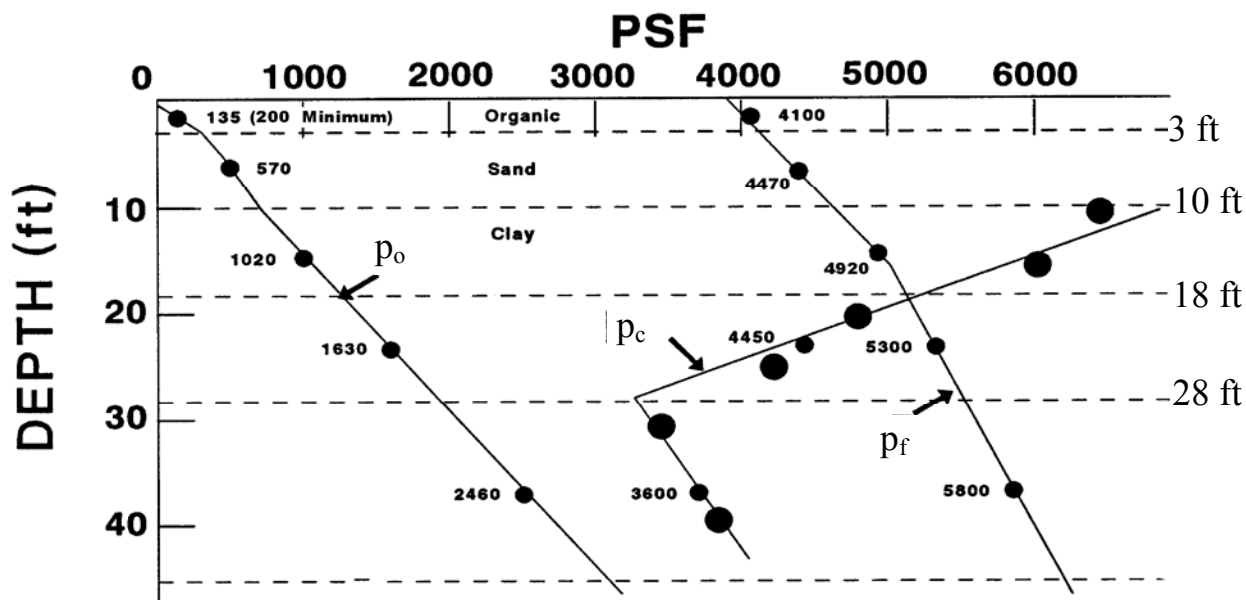


Figure A.6-4. Pressure distribution chart used to estimate the change in pressure at depths below the end of an embankment fill.

**Table A.6-2**  
**Summary of pressure increments at various depths due to embankment fill**

Depth (ft)	"K" - from Figure A.6-4	$\Delta p = "K" \times 3,900$ psf Distributed pressure (psf)
0.2 $b_f = 16$ ft	1.00	3,900
0.4 $b_f = 32$ ft	0.88	3,432
0.6 $b_f = 48$ ft	0.78	3,042
0.8 $b_f = 64$ ft	0.70	2,730
1.0 $b_f = 80$ ft	0.60	2,340

**Step 4:** Calculate the final pressure ( $p_f = p_o + \Delta p$ ) at various depths and plot the overburden pressure ( $p_o$ ), preconsolidation pressure ( $p_c$ ), and  $p_f$  with depth as shown in Figure A.6-5

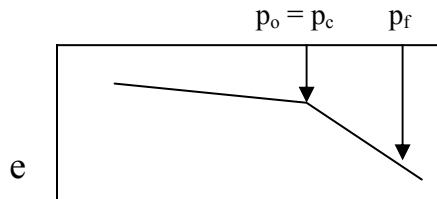


**Figure A.6-5. Variation of overburden pressure ( $p_o$ ), preconsolidation pressure ( $p_c$ ) and final pressure due to embankment ( $p_f$ ) with depth.**

In settlement analyses, use pressures measured at the center of a layer or a partial layer. Thick layers should be subdivided (i.e., if a layer is 20 ft thick compute settlement in 10 ft increments) unless the slope of  $p_o$ ,  $p_c$ , or  $p_f$  are slowly converging straight lines. Dashed horizontal lines in Figure A.6-5 show the increments selected here for analysis.

**Step 5: Compute settlement in each layer (or partial layer).**

- Layer 1 – Organic (0 ft to 3 ft)** – use equation for consolidation settlement (Refer to Chapter 7.5). As indicated in the logs of Borings BAF-3 and BAF-4 where this material was encountered, no tube samples were obtained for consolidation testing. Therefore, the stress history of the layer cannot be determined from test results. However, based on the description of the material given in the boring logs and from experience with surface and near-surface organic soils, the organic layer is assumed to be normally consolidated for the computation presented here as shown in the sketch of the generic consolidation curve below. As is generally the case with these soils in practice, for the Apple Freeway Bridge the organic layer will be removed and replaced with compacted select material before the embankment fill is constructed. Settlement of 3-ft of compacted select material is considered to be negligible. The situation presented here illustrates the importance of sampling and testing all soils that have the potential to cause problems during and after construction.



$$\Delta H = H \frac{C_c}{1 + e_o} \log \frac{p_f}{p_o}$$

$$H = 3 \text{ ft} - 0 \text{ ft} = 3 \text{ ft}$$

$$\text{The mid-thickness depth of the Organic Layer is } \frac{3 \text{ ft}}{2} = 1.5 \text{ ft}$$

$$C_c = 0.0115 w = 0.0115 (120) = 1.38 \text{ - (Refer to Table 5-5 of Chapter 5)}$$

From Figure 5-9 of Chapter 5,  $C_c \approx 1.0$

Therefore use  $C_c$  (average) = 1.2

$$e_0 = \frac{w \times G_s}{\% \text{Sat.}} = \frac{120 \times 1.6}{100} = 1.9$$

$$\Delta H = 3 \text{ ft} \left( \frac{1.2}{1 + 1.9} \right) \log \frac{4,100 \text{ psf}}{200 \text{ psf}} \quad * \text{ Remember } (p_o \geq 200 \text{ psf})$$

$$\Delta H = 1.63 \text{ ft} = 19.54 \text{ in}$$

This enormous amount of settlement corresponds to more than 50% of the original thickness of the organic layer, which is one of the reasons why such materials, when located at or close to the surface, should be removed and replaced with compacted select material.

- **Layer 2 – Sand (3 ft to 10 ft)** – use equation for immediate settlement (Refer to Chapter 7.4).

$$\Delta H = H \frac{1}{C'} \log \frac{p_f}{p_o}$$

$$H = 10 \text{ ft} - 3 \text{ ft} = 7 \text{ ft}$$

$$\text{The mid-thickness depth of the Sand Layer is } 3 \text{ ft} + \frac{7 \text{ ft}}{2} = 6.5 \text{ ft}$$

To find  $C'$  use  $N_{60} = 17$  (Refer to Boring BAF-3 at depth = 7 ft)

$$\frac{N_{160}}{N_{60}} = 2 @ p_o = 500 \text{ psf} \quad (\text{Refer to Eq. 3-3 in Chapter 3})$$

$$\text{Therefore } N_{160} = 34$$

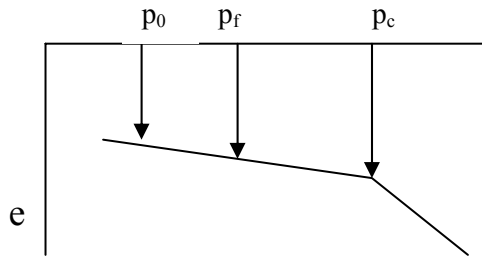
$C' = 90$  (Refer to Figure 7-7 in Chapter 7 – interpolate between silty sand & fine to coarse sand)

$$\Delta H = (7 \text{ ft}) \left( \frac{1}{90} \right) \log \frac{4470 \text{ psf}}{570 \text{ psf}}$$

$$\Delta H = 0.069 \text{ ft} = 0.83 \text{ in}$$

- **Layer 3 – Clay – Sub-layer 1 (10 ft to 18 ft)** – use equation for consolidation settlement (Refer to Chapter 7.5). As shown in Figure A.6-5, the clay layer is over-consolidated since  $p_c > p_o$  and remains so during application of the entire load increment within this depth range as shown in the sketch of the generic

consolidation curve below, i.e.,  $p_f < p_c$ . (Refer to Chapter 7.5.2)



$$\Delta H = H \frac{C_c}{1 + e_o} \log \frac{p_f}{p_o}$$

$$H = 18 \text{ ft} - 10 \text{ ft} = 8 \text{ ft}$$

$$\text{The mid-thickness depth of Clay Sub-layer 1 is } 10 \text{ ft} + \frac{8 \text{ ft}}{2} = 14 \text{ ft}$$

From consolidation test data:

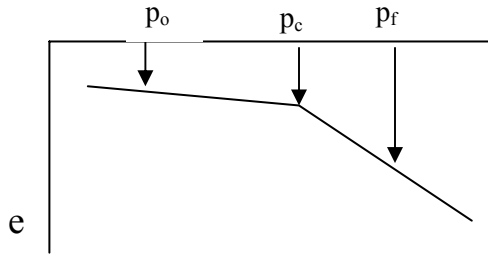
$$C_r \text{ (average)} = 0.035$$

$$e_o \text{ (average)} = 0.97$$

$$\Delta H = (8 \text{ ft}) \left( \frac{0.035}{1 + 0.97} \right) \log \frac{4,920 \text{ psf}}{1,020 \text{ psf}}$$

$$\Delta H = 0.097 \text{ ft} = 1.17 \text{ in}$$

- Layer 3 – Clay - Sub-layer 2 (18 ft to 28 ft)** - use equation for consolidation settlement (Refer to Chapter 7.5). The thickness of this sub-layer of the clay stratum was chosen because of the sharp break in the slope of the  $p_c$  vs. depth curve at 28-ft (Refer to Figure A.6-5). As shown in Figure A.6-5, the clay layer is over-consolidated within this depth range since  $p_c > p_o$ , but at the mid-depth the load increment causes  $p_f > p_c$ . Therefore the settlement for this sub-layer must be calculated in two steps as shown in the following sketch of the generic consolidation curve, one step for the pressure increment from  $p_o$  to  $p_c$  for which  $C_r$  applies, and the other for the pressure increment from  $p_c$  to  $p_f$  for which  $C_c$  applies. (Refer to Chapter 7.5)



$$\Delta H = H \frac{C_r}{1 + e_o} \log \frac{p_c}{p_o} + H \frac{C_c}{1 + e_o} \log \frac{p_f}{p_c}$$

$$H = 28 \text{ ft} - 18 \text{ ft} = 10 \text{ ft}$$

$$\text{Mid-thickness depth of Clay Sub-layer 2 is at } 18 \text{ ft} + \frac{10 \text{ ft}}{2} = 23 \text{ ft}$$

From consolidation test data:

$$C_r (\text{avg.}) = 0.035$$

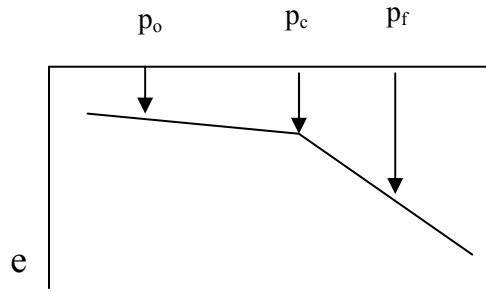
$$C_c (\text{avg.}) = 0.35$$

$$e_o (\text{avg.}) = 0.97$$

$$\Delta H = (10 \text{ ft}) \left( \frac{0.035}{1 + 0.97} \right) \log \frac{4,450 \text{ psf}}{1,630 \text{ psf}} + 10 \text{ ft} \left( \frac{0.35}{1 + 0.97} \right) \log \frac{5,300 \text{ psf}}{4,450 \text{ psf}}$$

$$\Delta H = 0.077 \text{ ft} + 0.135 \text{ ft} = 0.93 \text{ in} + 1.62 \text{ in} = 2.55 \text{ in}$$

- Layer 3 – Clay - Sub-layer 3 (28 ft to 45 ft)** - use equation for consolidation settlement (Refer to Chapter 7.5). The thickness of this sub-layer of the clay stratum represents the depth from the sharp peak in the  $p_c$  vs. depth curve at 28-ft to the bottom of the clay stratum (Refer to Figure A.6-5). As shown in Figure A.6-5, the clay layer is over-consolidated within this depth range since  $p_c > p_o$ , but at the mid-depth the load increment causes  $p_f > p_c$ . Therefore the settlement for this sub-layer, as was the case for Sub-layer 2, must be calculated in two steps as shown in the following sketch of the generic consolidation curve, step one for the pressure increment from  $p_o$  to  $p_c$  for which  $C_r$  applies, and the other for the pressure increment from  $p_c$  to  $p_f$  for which  $C_c$  applies. (Refer to Chapter 7.5)



$$\Delta H = H \frac{C_r}{1 + e_o} \log \frac{p_c}{p_o} + H \frac{C_c}{1 + e_o} \log \frac{p_f}{p_c}$$

$$H = 45 \text{ ft} - 28 \text{ ft} = 17 \text{ ft}$$

The mid-thickness depth of Clay Sub-layer 3 is  $28 \text{ ft} + \frac{17 \text{ ft}}{2} = 36.5 \text{ ft}$

From consolidation test data:

$$C_r \text{ (average)} = 0.035$$

$$C_c \text{ (average)} = 0.35$$

$$e_o \text{ (average)} = 0.97$$

$$\Delta H = (17 \text{ ft}) \left( \frac{0.035}{1 + 0.97} \right) \log \frac{3,600 \text{ psf}}{2,460 \text{ psf}} + (17 \text{ ft}) \left( \frac{0.35}{1 + 0.97} \right) \log \frac{5,800 \text{ psf}}{3,600 \text{ psf}}$$

$$\Delta H = 0.050 \text{ ft} + 0.63 \text{ ft} = 0.60 \text{ in} + 7.51 \text{ in} = 8.11 \text{ in}$$

**Table A.6-3**  
**Summary of layer and sub-layer settlements due to embankment fill**  
**and computation of total settlement**

Layer	Settlement (in)
Layer 1 – Organic (0 ft to 3 ft) - replaced with compacted select material	≈ 0
Layer 2 – Sand (3 ft to 10 ft)	0.83 in
Layer 3 – Clay (10 ft to 45 ft)	
Sub-layer 1 - (10 ft to 18 ft)	1.17 in
Sub-layer 2 - (18 ft to 28 ft)	2.55 in
Sub-layer 3 - (28 ft to 45 ft)	8.11 in
$\Delta H_{\text{Total}}$	12.66 in

**Step 6: Compute Time for Settlement to Occur in Clay (Layer 3)**

- Layer 1 – Select backfill material no settlement expected.
- Layer 2 – 0.83 inch settlement occurs immediately in sand.
- Layer 3 –  $\Delta H_{\text{Total}}$  (Layer 3) = 1.17 in + 2.55 in + 8.11 in = 11.83 in

Time required for a specified percentage of total settlement to occur is computed

from:  $t = \frac{T_v H_d^2}{c_v}$  where:

$H_d$  = longest drainage path (ft) =  $\frac{1}{2}$  thickness of clay layer since permeable layers exist above and below. Therefore, for the clay layer

$$H_d = \frac{35 \text{ ft}}{2} = 17.5 \text{ ft}$$

$$c_v = 0.6 \text{ ft}^2/\text{day}$$

$T_v$  = time factor corresponding to a specified average percent consolidation (U) - (Refer to Table 7-4 in Chapter 7 or calculate by using Equation 7-8 in the Chapter 7)

Table A.6-4 provides a convenient template for performing computations to obtain settlement vs. time values for arbitrarily chosen values of average percent consolidation.

**Table A.6-4**  
**Template to compute values of consolidation settlement ( $\Delta H$ ) in clay layer at various times (t) after application of embankment load**

Average % Consol. (U)	$\Delta H$ (in) = (U)( $\Delta H_{\text{Total}}$ (Layer 3))	Time Factor (T) From Table 7-4	$\frac{H_d^2}{c_v}$	t (days)
20	2.4	0.031	510.4	16
50	5.9	0.197		101
70	8.3	0.403		206
90	10.6	0.848	↓	432

The time-settlement plot can now be constructed for all soil layers. Remember to include 0.83 inch sand settlement, which occurs immediately as load is applied. Therefore  $\Delta H_{\text{Total}} = 12.66$  in

**Step 7: Plot Settlement vs. Time Curve – (include  $\Delta H$  Sand = 0.83 in)**

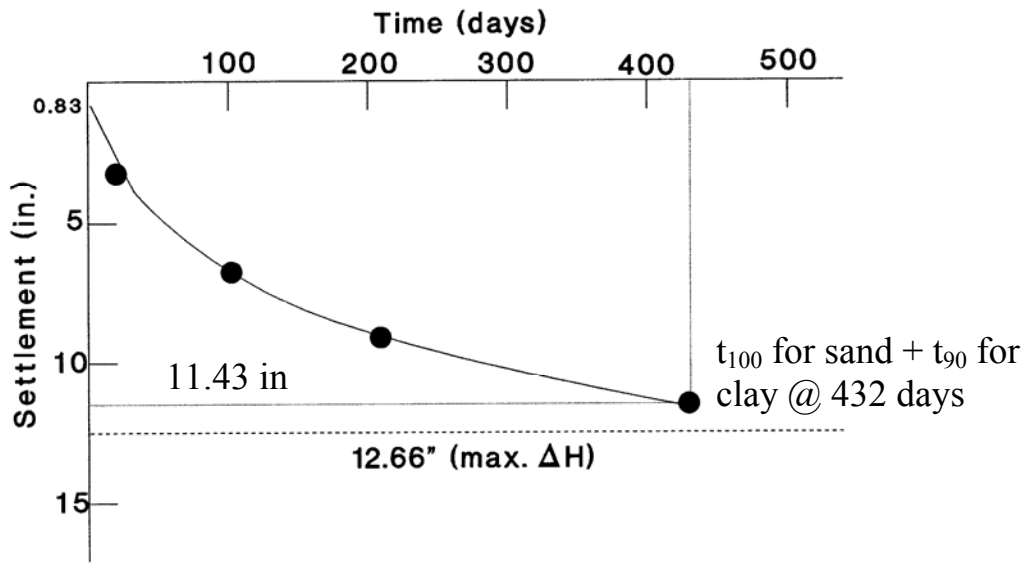


**Figure A.6-6. Settlement vs. Time after construction of 30-ft embankment fill.**

The designer must insure that 90% consolidation is achieved before construction of the abutment foundation begins. If the waiting period is too long, as it is in this case for the Apple Freeway (432 days  $\approx$  14 months), the choices of treatment are:

1. Surcharge.
2. Vertical drains

It should be noted that the decision on the choice of treatments will be made before construction of the embankment fill begins. That decision will influence the construction procedure, e.g., if surcharging is chosen, the surcharge will be placed as part of the embankment fill and removed afterward.

**A.6-4 CONSIDERATION OF SURCHARGE OPTION TO ACCELERATE CONSOLIDATION SETTLEMENT AND REDUCE TIME REQUIRED FOR SETTLEMENT DUE TO THE EMBANKMENT FILL**

**Assume:**

- 10-ft high compacted surcharged ( $\gamma = 130$  pcf). Therefore, the total change in pressure ( $\Delta p_{total}$ ) at the surface is now due to the embankment fill ( $\Delta p_{fill}$ ) plus the surcharge ( $\Delta p_s$ ) = (30-ft)(130 pcf) + (10-ft)(130 pcf) = 5,200 psf.
- The pressure increase at various depths below the surface is calculated as before, but with the value of the change in pressure at the surface = 5,200 psf. Since the dimensions of the embankment, except for the height, are the same as before, the values of “K” are unchanged. The results of these computations are presented in

Table A.6-5.

- Additional immediate settlement of sand due to the surcharge is negligible.
- $e_o$  remains 0.97 although the actual value is less due to compression under the previous load.

**Step 1: Obtain pressure increase with depth (use previous “K” value)**

**Table A.6-5**  
**Pressure increments at various depths due to embankment fill + surcharge**

Depth (ft)	"K" - from Figure A.6-4	$\Delta p_{total} = "K" \times 5,200$ psf Distributed pressure (psf)
0.2b = 16 ft	1.00	5,200
0.4b = 32 ft	0.88	4,580
0.6b = 48 ft	0.78	4,060

**Step 2: Calculate the new final pressure ( $p_f + p_s = p_o + \Delta p_{total}$ ) at various depths and plot the overburden pressure ( $p_o$ ), preconsolidation pressure ( $p_c$ ), and the new final pressure due to the embankment plus the surcharge ( $p_f + p_s$ ) with depth.**

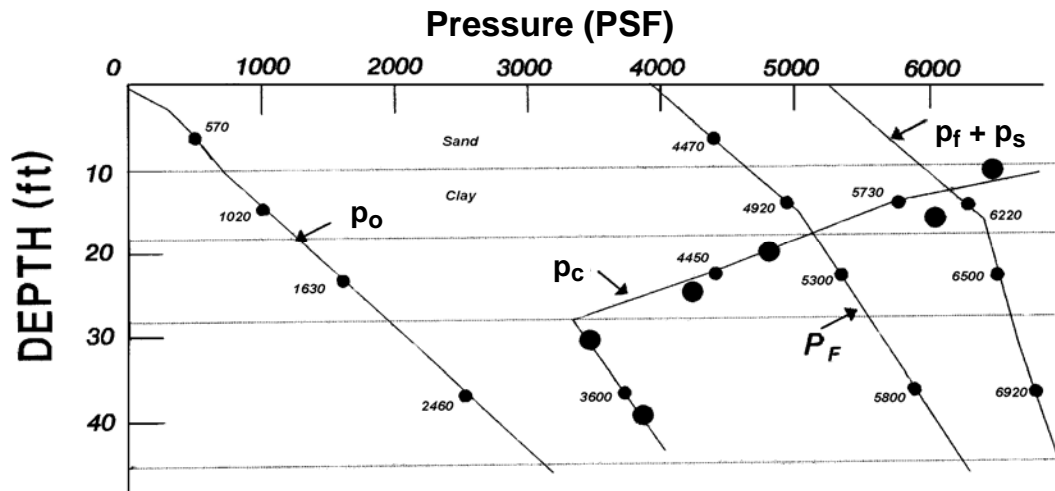
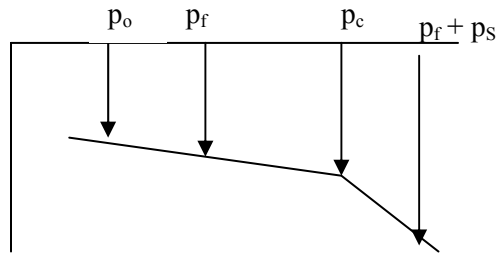


**Figure A.6-7. Variation of overburden pressure ( $p_o$ ), preconsolidation pressure ( $p_c$ ) and final pressure due to embankment + surcharge ( $p_f + p_s$ ) with depth.**

### Step 3: Compute Settlement in Layer 3

The Layer 1 organics were replaced by compacted select fill, therefore any settlement of this layer will be negligible even with the 10 ft surcharge. As indicated previously, additional settlement of Layer 2 due to an additional 10 ft of surcharge fill will also be negligible. Therefore, Layer 3 is the only layer that will settle more than originally calculated due to the additional 10 ft of surcharge. As was done originally, subdivide Layer 3 into three partial layers or sub-layers for computational purposes.

- Layer 3 – Clay – Sub-layer 1 (10 ft to 18 ft)** – use equation for consolidation settlement (Refer to Chapter 7.5). As shown in Figure A.6-5, the clay layer is over-consolidated since  $p_c > p_o$ , but at the mid-depth the load increment due to the additional 10 ft of surcharge causes  $p_f + p_s > p_c$ . Therefore the settlement for this sub-layer must now be calculated in two steps as shown in the following sketch of the generic consolidation curve, one step for the pressure increment from  $p_o$  to  $p_c$  for which  $C_r$  applies, and the other for the pressure increment from  $p_c$  to  $(p_f + p_s)$  for which  $C_c$  applies. (Refer to Chapter 7.5)



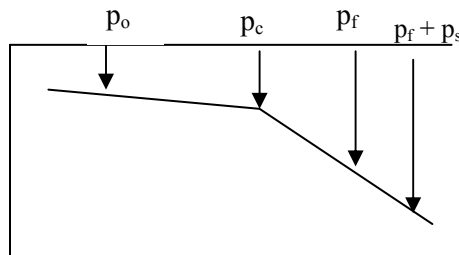
$$\Delta H = H \frac{C_r}{1 + e_o} \log \frac{p_c}{p_o} + H \frac{C_c}{1 + e_o} \log \frac{p_f + p_s}{p_c}$$

$$\Delta H = (8 \text{ ft}) \left( \frac{0.035}{1 + 0.97} \right) \log \frac{5,730 \text{ psf}}{1,020 \text{ psf}} + (8 \text{ ft}) \left( \frac{0.35}{1 + 0.97} \right) \log \frac{6,220 \text{ psf}}{5,730 \text{ psf}}$$

$$\Delta H = 0.11 \text{ ft} + 0.05 \text{ ft} = 0.16 \text{ ft}$$

$$\Delta H = 1.32 \text{ in} + 0.61 \text{ in} = 1.93 \text{ in}$$

- Layer 3 – Clay - Sub-layer 2 (18 ft to 28 ft)** - use equation for consolidation settlement (Refer to Chapter 7.5). The thickness of this sub-layer of the clay stratum was chosen because of the sharp break in the slope of  $p_c$  vs depth curve at 28-ft (Refer to Figure A.6-5). As shown in Figure A.6-5, the clay layer is over-consolidated within this depth range since  $p_c > p_o$ , but at the mid-depth the load increment including the 10-ft surcharge causes  $p_f + p_s > p_c$ . Therefore the settlement for this sub-layer must be calculated in two steps as shown in the following sketch of the generic consolidation curve, one step for the pressure increment from  $p_o$  to  $p_c$  for which  $C_r$  applies, and the other for the pressure increment from  $p_c$  to  $(p_f + p_s)$  for which  $C_c$  applies. (Refer to Chapter 7.5)



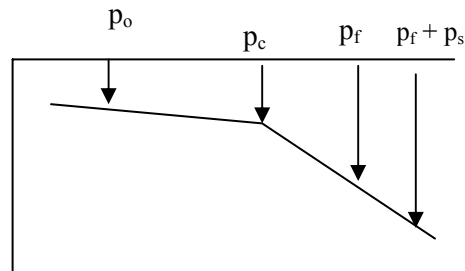
$$\Delta H = H \frac{C_r}{1 + e_o} \log \frac{p_c}{p_o} + H \frac{C_c}{1 + e_o} \log \frac{p_f + p_s}{p_c}$$

$$\Delta H = (10 \text{ ft}) \left( \frac{0.035}{1 + 0.97} \right) \log \frac{4,450 \text{ psf}}{1,630 \text{ psf}} + 10 \text{ ft} \left( \frac{0.35}{1 + 0.97} \right) \log \frac{6,500 \text{ psf}}{4,450 \text{ psf}}$$

$$\Delta H = 0.08 \text{ ft} + 0.29 \text{ ft} = 0.37 \text{ ft}$$

$$\Delta H = 0.93 \text{ in} + 3.51 \text{ in} = 4.44 \text{ in}$$

- Layer 3 – Clay - Sub-layer 3 (28 ft to 45 ft)** - use equation for consolidation settlement (Refer to Chapter 7.5). The thickness of this sub-layer represents the depth from the sharp break in the  $p_c$  vs. depth curve at 28-ft to the bottom of the clay stratum (Refer to Figure A.6-5). As shown in Figure A.6-5, the clay layer is over-consolidated within this depth range since  $p_c > p_o$ , but at the mid-depth the load increment including the 10-ft surcharge causes  $p_f + p_s > p_c$ . Therefore the settlement for this sub-layer, must also be calculated in two steps as shown in the following sketch of the generic consolidation curve, step one for the pressure increment from  $p_o$  to  $p_c$  for which  $C_r$  applies, and the other for the pressure increment from  $p_c$  to  $(p_f + p_s)$  for which  $C_c$  applies. (Refer to Chapter 7.5).



$$\Delta H = H \frac{C_r}{1 + e_o} \log \frac{p_c}{p_o} + H \frac{C_c}{1 + e_o} \log \frac{p_f + p_s}{p_c}$$

$$\Delta H = (17 \text{ ft}) \left( \frac{0.035}{1 + 0.97} \right) \log \frac{3,600 \text{ psf}}{2,460 \text{ psf}} + (17 \text{ ft}) \left( \frac{0.35}{1 + 0.97} \right) \log \frac{6,920 \text{ psf}}{3,600 \text{ psf}}$$

$$\Delta H = 0.05 \text{ ft} + 0.86 \text{ ft} = 0.91 \text{ ft}$$

$$\Delta H = 0.60 \text{ in} + 10.32 \text{ in} = 10.89 \text{ in}$$

**Table A.6-6**

**Summary of sub-layer settlements in clay due to embankment fill + surcharge and computation of total settlement of clay - Layer 3**

Layer	Embankment Only	Embankment + Surcharge	Surcharge
10 ft to 18 ft	1.17 in	1.93 in	0.76 in
18 ft to 28 ft	2.55 in	4.44 in	1.89 in
28 ft to 45 ft	8.11 in	10.89 in	2.78 in
Total $\Delta H =$	11.83 in	17.26 in	5.43 in

**Step 4: Obtain Time-Settlement Relationship:**  $t = \frac{T_v H_d^2}{c_v}$

**Table A.6-7**

**Template to compute values of consolidation settlement ( $\Delta H$ ) in clay layer at various times (t) after application of embankment and surcharge loads**

Average % Consol. (U)	$\Delta H$ (in) = (U)( $\Delta H_{\text{Total}} - \text{Layer 3}$ )	Time Factor (T) From Table 6-3	$\frac{H_d^2}{c_v}$	t (days)
20	3.5 in	0.031	510.4	16
50	8.6 in	0.197		101
70	12.1 in	0.403		206
90	15.5 in	0.848	▼	432

**Step 5: Plot Settlement vs. Time Curve – (include  $\Delta H$  Sand = 0.83 in)**

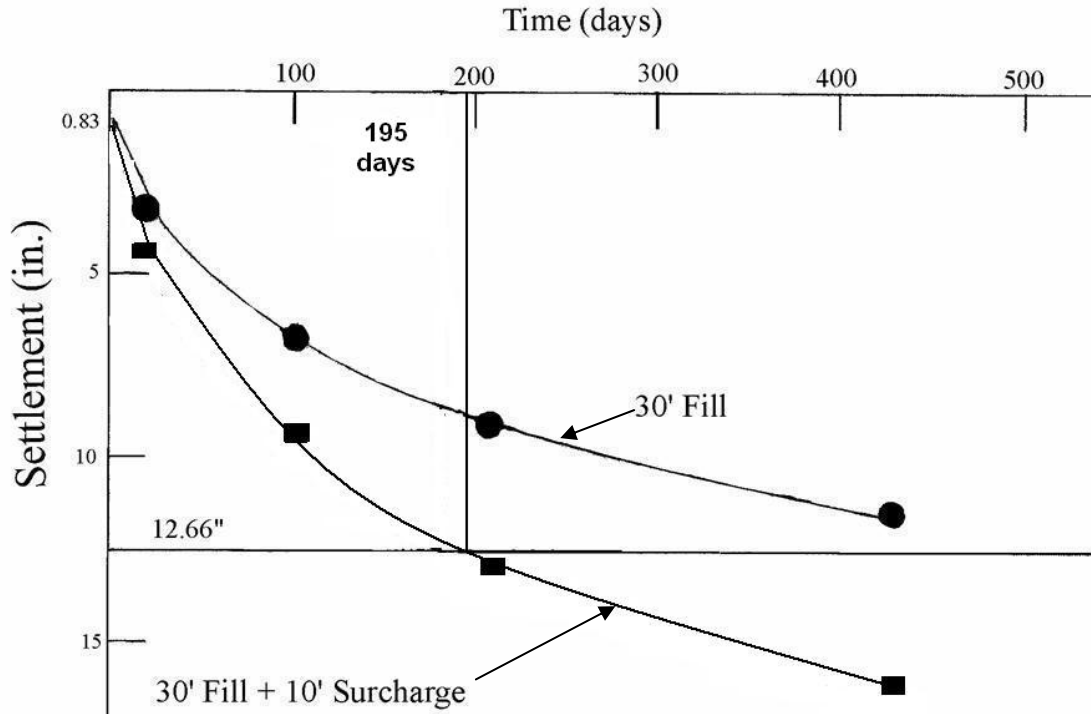


**Figure A.6-8. Settlement vs. Time after construction of 30 ft embankment fill with and without surcharge.**

**Step 6: Determine time of waiting period with surcharge to obtain equivalent settlement to that of proposed embankment.**

Enter the settlement vs. time plot for 30 ft fill with 10 ft surcharge with 12.66 inches (total [immediate + consolidation] settlement expected for 30 ft fill). Extend the line across to the “30’ Fill + 10’ Surcharge” curve and read the waiting period time in days on the time axis, i.e. 195 days or 6.5 months.

**Step 7: Recommend instrumentation for monitoring settlement and pore water pressures – (Table A.6-8)**

**Table A.6-8  
Recommend instrumentation for monitoring settlement and excess pore water pressures at East Abutment**

Instrument	Station	Depth Below Ground
Settlement plate	90 + 00	At ground surface
Settlement plate	93 + 50	At ground surface
Settlement plate	96 + 50	At ground surface
Piezometers	93 + 50	20 ft, 28 ft, 36 ft
Piezometers	96 + 50	20 ft, 28 ft, 36 ft

**Step 8: Recheck stability of 30 ft fill with 10 ft surcharge – Refer to procedure in Section A.5**

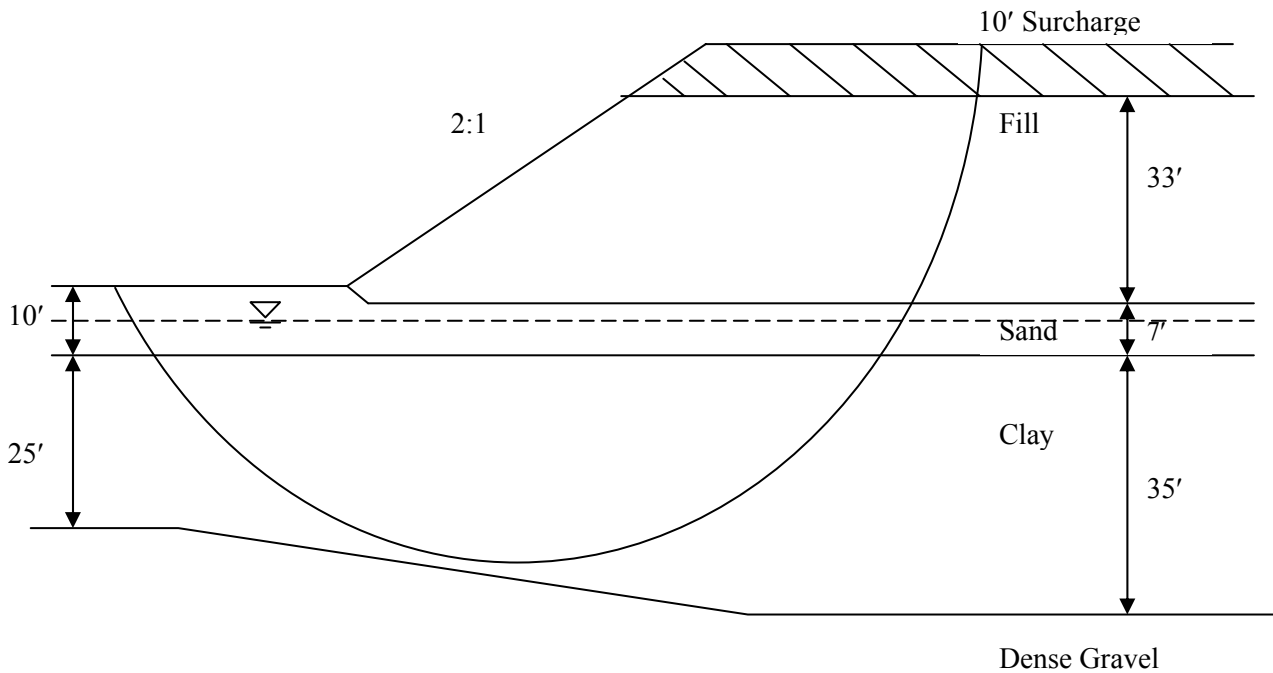


**Figure A.6-9. Trial failure circle – embankment fill + surcharge - East Abutment.**

Safety Factor with surcharge = 1.33.

Safety Factor without surcharge = 1.63.

Conclusion: the safety factor in both cases is greater than 1.30, which is minimum recommended for bridge approach stability for the temporary case of surcharge.

**Step 9: Prepare cost estimate for surcharge**

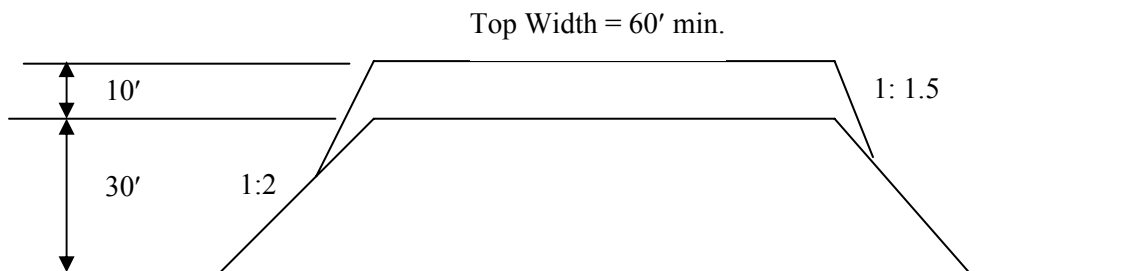


**Figure A.6-10. Idealized cross section of embankment fill + surcharge.**

- Assume 500 linear feet behind top of end slope to be surcharged at each approach, therefore total length of surcharge = 1,000 feet.
- Assume average width of surcharge = 80 feet including side slopes.
- Calculate surcharge quantity ( $V_{sur}$ ) as:

$$80 \text{ ft} \times 10 \text{ ft} \times \frac{1,000 \text{ ft}}{27 \text{ ft}^3 / \text{yd}^3} = 29,630 \text{ yd}^3$$

- Unit cost to place and remove surcharge = \$4.00 /yd<sup>3</sup>, therefore total cost is as follows:

$$\text{Total cost} = 29,630 \text{ yd}^3 \times \$4.00 / \text{yd}^3 \approx \$120,000$$

**[THIS IS AN EXAMPLE. ALWAYS CHECK THE LOCAL UNIT PRICES]**

#### **A.6-5 CONSIDERATION OF WICK DRAIN OPTION (NO SURCHARGE) TO ACCELERATE CONSOLIDATION SETTLEMENT AND REDUCE TIME REQUIRED FOR SETTLEMENT DUE TO THE EMBANKMENT FILL**

**Step 1: Choose reasonable spacing of wick drains – assume equivalent wick drain diameter of 0.5 ft and try 7.5-ft center to center triangular spacing.**

- Recent designs for wick drains have used equivalent diameters of 0.5 ft, i.e.,  $d_w = 0.5 \text{ ft}$
- For triangular spacing:  
 $d_e = 1.05 \times s = 1.05 \times 7.5 \text{ ft} = 7.875 \text{ ft}$   
 $\eta = d_e / d_w = 7.875 \text{ ft} / 0.5 \text{ ft} = 15.75 \text{ ft} \approx 16 \text{ ft}$

**Step 2: Compute settlement-time-relationship**

- $c_v = c_r = 0.6 \text{ ft}^2/\text{day}$
- Arbitrarily select a reasonable range of values of time (days) and calculate the corresponding time factors for vertical ( $T_v$ ) and radial ( $T_r$ ) drainage as follows:

$$T_r = t c_h / d_e^2 = t (\text{days}) 0.6 \text{ ft}^2/\text{day} / (7.875 \text{ ft})^2$$

$$T_v = t c_v / H_d^2 = t (\text{days}) 0.6 \text{ ft}^2/\text{day} / (17.5 \text{ ft})^2$$

$$H_d = \frac{1}{2} H = 17.5 \text{ ft} \text{ (Refer to previous calculation for vertical drainage only)}$$

- Calculate the values of average percent consolidation ( $U_v$ ) corresponding to the calculated values of time factor ( $T_v$ ) by:

$$U_v = (4 T_v / \pi)^{1/2}$$

- Estimate the values of average percent consolidation ( $U_r$ ) corresponding to the calculated values of time factor ( $T_r$ ) for  $\eta = 16$  from the curves in Figure 4 in FHWA (1986).

- Calculate average percent consolidation for combined drainage ( $U_c$ ) by:

$$U_c = 1 - [(1 - U_r)(1 - U_v)]$$

where  $U_r$  and  $U_v$  are in decimals.

- Calculate values of consolidation settlement  $\Delta H$  (inches) in clay Layer 3 due to combined vertical and radial drainage corresponding to the arbitrarily assumed values of time –use template shown in Table A.6-10 to aid in the calculation.

**Table A.6-10**

**Template to compute values of consolidation settlement ( $\Delta H$ ) in clay -Layer 3 at various times (t) after application of embankment load (wick drains with no surcharge) due to combined vertical and radial drainage**

Time after loading t (days)	Time factor- $T_v$	Average % Consolidation $U_v$	Time factor- $T_r$	Average % Consolidation $U_r$	Combined Average % Consolidation $U_c\%$	Layer 3 $\Delta H$ (in)
10	0.020	16	0.097	34	44	5.2
20	0.039	22	0.193	57	66	7.8
30	0.059	27	0.290	71	79	9.3
40	0.078	32	0.387	81	87	10.3
50	0.098	35	0.484	85	90	10.6
60	0.118	39	0.580	92	95	11.2
70	0.137	42	0.677	94	97	11.4
80	0.157	45	0.774	97	98	11.6
90	01.76	47	0.871	99	99	11.8

**Step 3: Plot settlement-time-curve for wick drains – Refer to Figure A.6-11.**

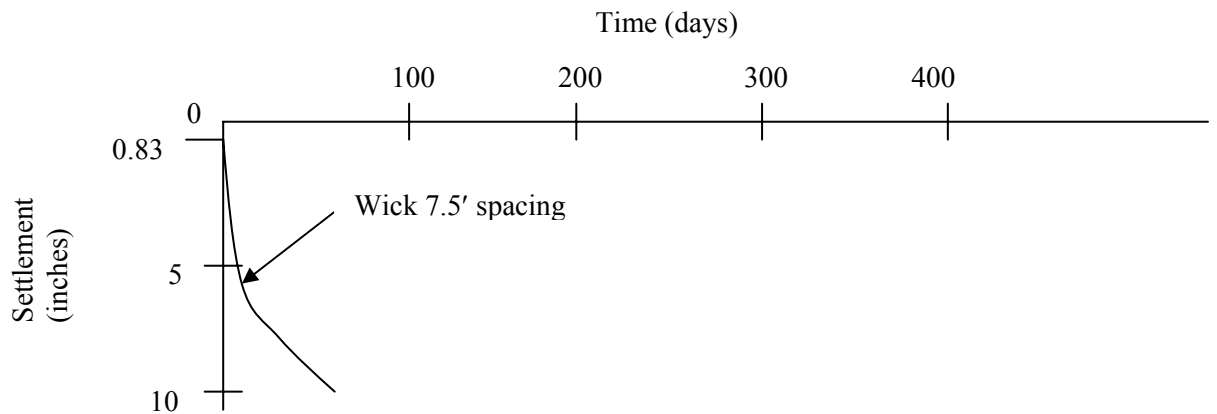


**Figure A.6-11. Time versus settlement after completion of embankment fill for wick drain treatment without surcharge.**

**Step 4: Prepare cost estimate for wick drains**

- Assume:
  1. 500 linear feet of drains at both approaches, therefore total length = 1,000 linear feet.
  2. Width of drain treatment midslope to midslope = 160 linear ft
  3. Length of each drain = 45 ft
  4. Unit cost per wick drain: \$1.00/ft (**THE USER SHOULD CALL THE LOCAL CONTRACTORS FOR LATEST COSTS**)
- Consider Wick Drains - 7.5 ft center to center.
 

Treated area/drain =  $0.866 S^2 = 0.866(7.5 \text{ ft})^2 = 49 \text{ ft}^2/\text{drain}$

No. of drains =  $(160 \text{ ft})(1,000 \text{ ft})/49 \text{ ft}^2/\text{drain} = 3,265 \text{ drains}$

Linear feet of drain =  $(3,265 \text{ drains}) 45 \text{ ft/drain} = 146,925 \text{ ft}$

Cost =  $(146,925 \text{ ft})(\$1.00/\text{ft}) + \$25,000 \text{ (Mobilization)} = \$172,000$

**Step 5: Prepare settlement–time curves for (a) 30-ft embankment fill, (b) 30-ft embankment fill with 10-ft surcharge (c) 30-ft fill embankment with vertical drains (wick) without surcharge (Refer to Figure A.6-12)**

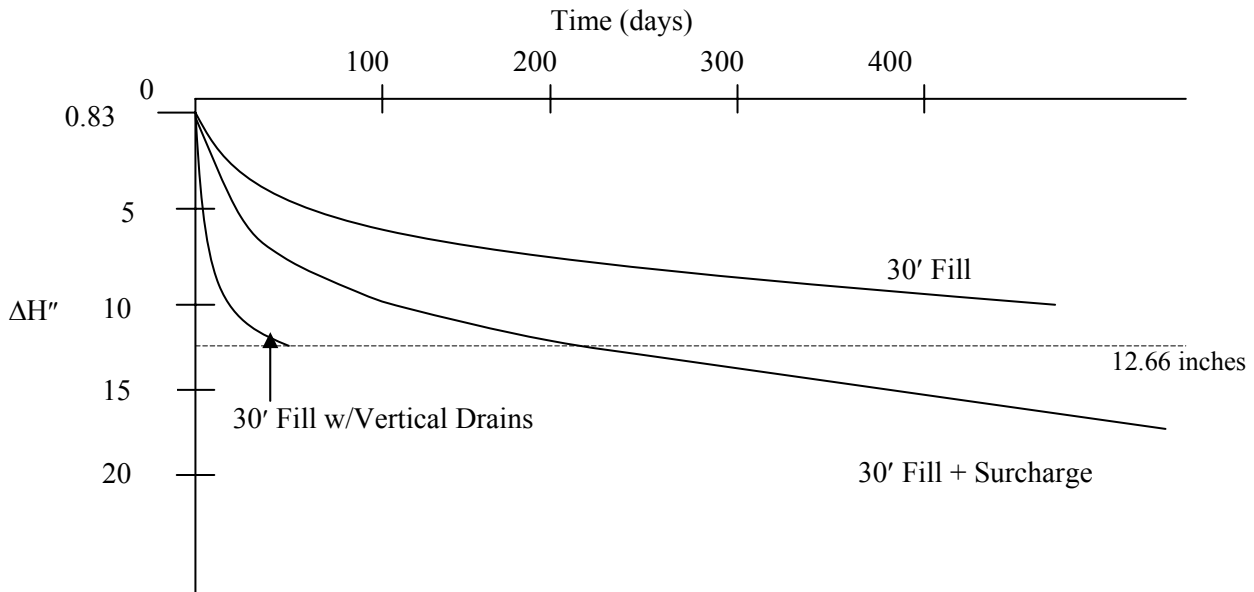


**Figure A.6-12. Summary of time-settlement curves for baseline case (30-ft embankment fill) and various treatment options.**

**Step 6: Prepare table showing summary of results for base-line case (embankment fill only) and various treatment options in terms of waiting period and extra costs of treatment. Refer to Table A.6-12**

**Table A.6-12  
Summary of results for base-line case (embankment fill only) and various treatment options**

<b>Treatment</b>	<b>Time for at Least 90% Consolidation (Months)</b>	<b>Extra Cost</b>
Fill only	14	Base line
Fill with 10-ft of surcharge	6.5	\$120,000
Fill with Wick Drains	2	\$172,000

## A.6-6 CHECK FOR LATERAL SQUEEZE OF CLAY

### Step 1 Determine whether or not lateral squeeze will occur.

Lateral squeeze causes pile supported abutments to rotate into embankment or spread footing abutments to move laterally. Lateral squeeze occurs if (see Chapter 7.6):

$$\gamma_{\text{fill}} H_{\text{fill}} > 3 \times \text{cohesion}$$

For East Abutment:

$$\gamma_{\text{fill}} H_{\text{fill}} = 130 \text{ pcf} \times 30 \text{ ft} > 3 \times 1,100 \text{ psf}$$

3,900 psf > 3,300 psf, therefore:

- lateral squeeze may occur.
- consider waiting period to dissipate settlement of fill.
- do not construct abutments until settlement dissipates, i.e. until the average percent consolidation ( $U$ )  $\geq 90\%$ .

### Step 2 Estimate amount of horizontal movement of abutment due to lateral squeeze of clay - Layer 3.

Assume baseline case – 30-ft embankment fill only

Rule of thumb:

$$\begin{aligned} \text{Horizontal Movement} &= 0.25 \Delta H \text{ of embankment (in clay)} \\ &= 0.25 \times 11.83 \text{ in} \end{aligned}$$

$$\text{Horizontal Movement} = 3 \text{ in}$$

Recommend no spread footing construction or pile driving until settlement is at least 90% complete, i.e., at time =  $t_{90}$ .

#### **A.6-7 SUMMARY OF THE APPROACH ROADWAY STABILITY – FOR DETAILS REFER TO SECTION A.5-4 OF PREVIOUS PROBLEM**

1. Develop a design soil profile
  - Soil layer unit weights and strength estimated.
2. Circular Arc Analysis
  - Approach embankment safety factor 1.63 against circular failure.
3. Sliding and Block Analysis
  - Approach embankment safety factor 3.5 against sliding failure.
4. Lateral Squeeze
  - Possible abutment rotation problem.

#### **A.6-8 SUMMARY OF EMBANKMENT SETTLEMENT ANALYSES AT EAST ABUTMENT**

1. Construct an idealized design profile to scale.
  - Use idealized soil profile from Boring UDH BAF-4
  - Include 30-ft high embankment at east abutment (assume 3 ft organic layer at the surface is replaced by compacted select material).
  - Estimate consolidation properties of clay layer from results of field and laboratory tests.
2. Determine overburden pressure ( $p_o$ ), change in pressure due to embankment fill ( $\Delta p$ ), and maximum past pressure ( $p_c$ ), all as a function of depth.
  - Plot pressure distributions with depth and determine stress history of impacted layers.
3. Calculate settlement of each layer impacted by 30-ft embankment fill
  - Compacted select fill (Layer 1 organic replacement material ) - negligible settlement
  - Sand (Layer 2) - 0.8 inches of immediate settlement
  - Clay (Layer 1) - 11.83 inches of consolidation settlement.
  - Total of 12.6 inches of settlement predicted.

4. Calculate time required for 90% of primary consolidation to occur and plot settlement vs. time curve including immediate settlement of sand layer.
  - $t_{90} = 432$  days. (organic material replaced)
  
5. Consider surcharge option to accelerate consolidation settlement and reduce time required for settlement due to the embankment fill.
  - Calculate the new final pressure due to the embankment plus the surcharge ( $p_f + p_s$ ) and plot values of ( $p_f + p_s$ ), the overburden pressure ( $p_o$ ), and the preconsolidation pressure ( $p_c$ ) with depth.
  - Calculate settlement in Layer 3.
  - Calculate and plot settlement-time relationship.
  - Determine waiting time with 10-ft of surcharge to obtain settlement equivalent to that of proposed embankment.
  - $t_{90} = 432$  days. (organic material replaced)
  - Recheck stability of 30 ft fill with 10 ft surcharge – FS = 1.33.
  - Prepare cost estimate for surcharge - cost = \$120,000.
  
6. Consideration of vertical drain option (wick drains - no surcharge) to accelerate consolidation settlement and reduce time required for settlement due to the embankment fill.
  - Choose reasonable spacing of drains.
  - Calculate and plot settlement-time-curve for combined vertical and radial drainage.
  - Determine waiting times to obtain settlement equivalent that of proposed embankment.
  - $t_{90} \approx 50$  days for wick drains (organic material replaced).
  - Prepare cost estimate for vertical drains - cost = \$172,000 (wick drains).

[THIS PAGE INTENTIONALLY BLANK]

Subsurface Explorations	Terrain reconnaissance Site inspection Subsurface explorations	✓
Basic Soil Properties	Visual description Classification tests Subsurface profile	✓
Laboratory Testing	p <sub>o</sub> diagram Test request Consolidation results Strength results	✓
Slope Stability	Design soil profile Circular arc analysis Sliding block analysis	✓
Approach Roadway Deformations	Design soil profile Magnitude and rate of settlement Surcharge Vertical drains Lateral Squeeze	✓
<b>→ Spread Footing Design</b>		<b>Design soil profile</b> <b>Pier bearing capacity</b> <b>Pier settlement</b> <b>Abutment settlement</b> <b>Surcharge</b> <b>Vertical drains</b>
Driven Pile Design	Design soil profile Static analysis – pier Pipe pile H - pile Static analysis – abutment Pipe pile H - pile Driving resistance Lateral movement - abutment	
Construction Monitoring	Wave equation Hammer approval Embankment instrumentation	

**Figure A.7-1. Status of geotechnical work.**

## **SECTION A.7**

### **GEOTECHNICAL DESIGN OF SPREAD FOOTING**

#### **A.7-1 RELEVANT CONCEPTS AND PROCEDURES (Refer to Figure A.7-1)**

- General procedure to calculate ultimate bearing capacity of a rectangular footing in a layered subsurface profile; Chapter 8
- Procedure based on 2:1 geometric attenuation of applied pressure with depth to determine pressure distribution with depth due to rectangular footing; Chapter 2.
- Immediate and consolidation settlement of rectangular footing – computation of magnitude; Chapter 7 and Chapter 8
- Consolidation settlement - rectangular footing – computation of time rate; Chapter 7.
- Effect of pre-construction treatment by surcharging or vertical drains on consolidation settlement of rectangular footing; Chapter 7.

In this section the geotechnical design process for spread footings for the pier and abutment foundations is illustrated. The computation procedures for the evaluation of ultimate bearing capacity are presented. The assessment of allowable bearing capacity is discussed with the context of settlement criteria. Settlement analysis for both immediate and consolidation settlement are performed to illustrate the effect of footing geometry on the magnitude of those settlements. The effect of pre-treatment by surcharging or vertical drains on both the magnitude of settlement and time required for full consolidation settlement is illustrated.

#### **A.7-2 DETAILED PROCEDURES**

**Given:**

- The footing geometry and subsurface conditions shown in Figure A.7-2 for the center pier of the Apple Freeway Bridge.
- The results of Standard Penetration tests (SPT-N blow counts) performed in Boring BAF – 2 as shown in Figure A.7-2.
- The footing geometry and subsurface conditions shown in Figure A.6-2 for the east embankment of the Apple Freeway Bridge.
- Values of relevant soil as provided in the previous example (Refer to Section A.6)

**Required:**

- Compute the ultimate bearing capacity of a rectangular footing at the pier location and apply an appropriate factor of safety to obtain the allowable bearing pressure.
- Compute the pressure transmitted to the underlying clay layer by the footing and compare that pressure to the allowable clay bearing capacity.
- Compute the magnitudes of the anticipated immediate and consolidation settlement due to the rectangular footing at the pier location.
- Compute the ultimate bearing capacity of a rectangular footing founded within the embankment at the East Abutment and apply an appropriate factor of safety to obtain the allowable bearing pressure
- Compute the magnitudes of the anticipated immediate and consolidation settlement due to the rectangular footing founded within the embankment at the East Abutment. Taking into account pretreatment by wick drains (Refer to Section A.6-5).
- Compute the time required for the settlement of the footing to occur. Take into account pretreatment by wick drains and continuing consolidation due to the embankment fill.
- Plot settlement-time curves for both the pier and embankment footings.

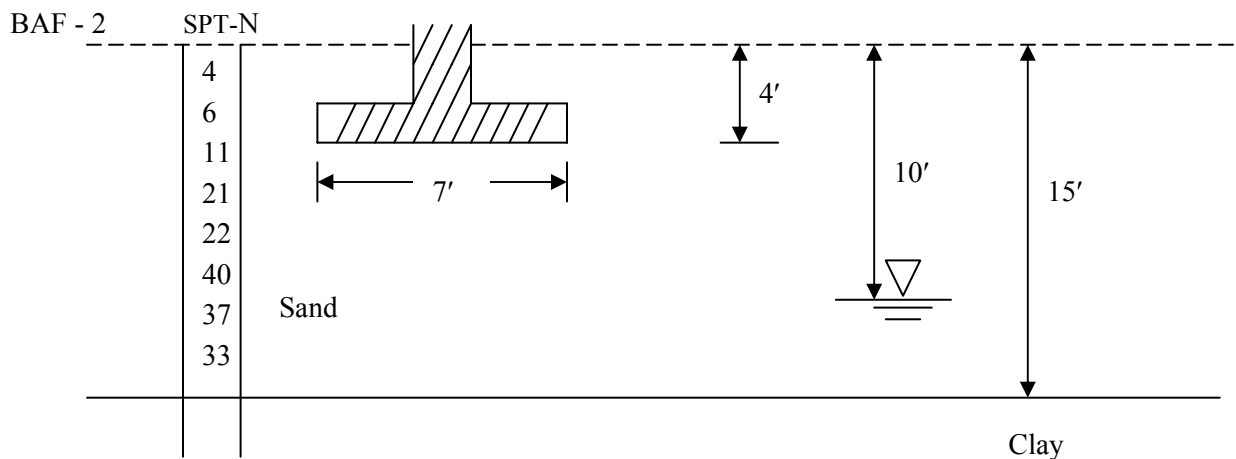


**Figure A7-2. Footing geometry and subsurface conditions for center pier of the Apple Freeway Bridge including SPT-N blow counts from Boring BAF-2.**

### A.7-3 COMPUTE ULTIMATE AND ALLOWABLE BEARING CAPACITY OF PIER FOOTING

- **Define geometry of the problem.**
  - Footing embedment below final grade ( $D_f$ ) = 4 feet.
  - Footing width ( $B_f$ ) = 1/3 pier height = 7 feet
  - Footing length ( $L_f$ ) = 100 feet
  - Depth to ground water below base of footing ( $D_w$ ) = 6 feet.
  
- **Identify characteristics of geometry that are relevant to solution.**
  - $L_f / B_f = 100 \text{ ft} / 7 \text{ ft} > 10$ , therefore consider the footing to be continuous.
  - If ( $D_w < 1.5B_f + D_f$ ), the effect of ground water table must be considered. Check:  $6 \text{ ft} < 1.5 (7 \text{ ft})$ , therefore ground water table must be considered.
  - Use SPT-N values to estimate internal friction angle ( $\phi$ ) of the sand.

**Step 1: Find average corrected SPT-N blow count ( $N_{160}$ ) below footing (Refer to Section 3-7 of text) and estimate internal friction angle ( $\phi$ ) of soil.**

**Table A-7.1**

**Determination of SPT-N values corrected for hammer energy and depth**

Depth (ft)	$p_o$ (psf)	$p_o$ (tsf)	N (bpf)	Hammer Efficiency ( $E_f$ )	$E_f / 60$	$N_{60}$ (bpf)	$C_N$	$N_{160}$ (bpf)
5	550	0.275	11	65	1.083	12	1.43	17
7	770	0.385	21	65	1.083	23	1.32	30
8	880	0.440	22	65	1.083	24	1.28	31
10	1100	0.550	40	65	1.083	43	1.20	52
12	1195	0.598	37	65	1.083	40	1.17	47
14	1290	0.645	33	65	1.083	36	1.15	41
<b>Average corrected blow count =</b>								<b>36</b>

- For average corrected blow count assume internal friction angle of sand  $\phi \approx 36^\circ$  (Refer to Table 8-3 in Chapter 8)

**Step 2: Determine ultimate capacity ( $q_{ult}$ ).**

- Equation 8-6 in the text can be re-written as follows since cohesion = 0.

$$q_{ult} = c N_c s_c b_c + q N_q C_{wq} s_q b_q d_q + 0.5 \gamma B_f N_\gamma C_{w\gamma} s_\gamma b_\gamma$$



- By using the appropriate equations in Table 8-4 of the text the shape factors are:  
 $s_q = 1.05$   
 $s_\gamma = 0.97$
- Since the base of the footing is horizontal, the base inclination factors  $b_q$  and  $b_\gamma$  both = 1.0
- The surcharge parameter  $q = \gamma_t D_f = 110 \text{ pcf} (4 \text{ ft}) = 440 \text{ psf}$
- By using the Table 8-5 in the text, the groundwater correction factors are:  
 $C_{wq} = 1.0$  (i.e., the groundwater level is below the base of the footing)  
 $C_{w\gamma} = 0.786$  (i.e., the groundwater level is within  $1.5B_f$  of the bottom of the footing.)
- From Table 8-6 in the text, the depth correction factor for  $D_f / B_f = 4 \text{ ft} / 7 \text{ ft} = 0.57$  is estimated as:  
 $d_q \approx 1.15$
- The bearing capacity factors for  $\phi = 36^\circ$  are estimated from Table 8-1 in the text as:  
 $N_q = 37.8$   
 $N_\gamma = 56.3$

Therefore, the ultimate bearing capacity of the pier footing in sand is calculated as:

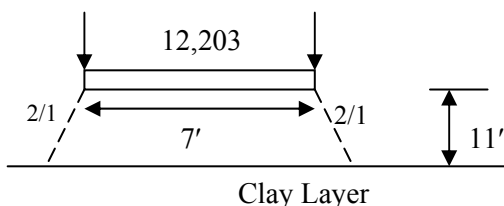
$$q_{ult} = (440 \text{ psf})(37.8)(1.0)(1.05)(1.0)(1.15) + 0.5(110 \text{ pcf})(7 \text{ ft})(56.3)(0.786)(0.97)(1.0)$$

$$q_{ult} = 20,083 \text{ psf} + 16,526 \text{ psf} = 36,609 \text{ psf}$$

**Step 3: Determine allowable bearing capacity (use FS = 3)**

$$q_{all} = \frac{36,609 \text{ psf}}{3} = 12,203 \text{ psf} = 6.1 \text{ tsf} \approx 6 \text{ tsf}$$

**A7-4 CHECK PRESSURE TRANSMITTED TO CLAY LAYER AND COMPARE IT TO THE ALLOWABLE BEARING CAPACITY OF THE CLAY**



**Step 1 Determine pressure on clay layer (Refer to Section A.6-3 of text)**

- Footing pressure transmitted to clay surface ( $p_{\text{clay}}$ ) =  $\left(\frac{7 \text{ ft}}{7 \text{ ft} + 11 \text{ ft}}\right)(12,203 \text{ psf}) = 4,746$  psf

**Step 2 Check bearing capacity of virtual footing on top of clay layer**

For the virtual (transferred) footing:

- Footing embedment below final grade ( $D_{\text{tf}}$ ) = 4 ft + 11 ft = 15 ft
- Footing width ( $B_{\text{tf}}$ ) = 7 ft + 11 ft = 18 ft
- Footing length ( $L_{\text{tf}}$ ) = 100 ft + 11 ft = 111 ft
- Ground water is 5 ft above the base of virtual footing

Equation 8-6 in the text can be re-written as follows for a purely cohesive soil ( $\phi = 0$ ) for which  $N_\gamma = 0$ .

$$q_{\text{ult clay}} = c N_c s_c b_c + q N_q C_{Wq} s_q b_q d_q + 0.5 \gamma B_{\text{tf}} N_\gamma C_{W\gamma} s_\gamma b_\gamma$$


- By using the appropriate equations in Table 8-4 of the text the shape factors are:  
 $s_q = 1.00$   
 $s_c = 1.03$
- Since the base of the footing is horizontal, the base inclination factors  $b_q$  and  $b_\gamma$  both = 1.0
- The surcharge parameter  $q = 110 \text{ pcf}(10 \text{ ft}) + 50 \text{ pcf}(5 \text{ ft}) = 1,350 \text{ psf}$
- By Table 8-5 in the text, the groundwater correction factors are:  
 $C_{Wq} = 0.5$  (i.e., the groundwater level is at or above the footing base).
- From Table 8-6 in the text, the depth correction factor for  $D_{\text{tf}} / B_{\text{tf}} = 15 \text{ ft} / 18 \text{ ft} = 0.83$  is estimated as:  
 $d_q \approx 1.18$
- The bearing capacity factors for  $\phi = 0^\circ$  are estimated from Table 8-1 in the text as:  
 $N_q = 1.0$   
 $N_c = 5.14$

Therefore, the ultimate bearing capacity of the virtual footing on clay is calculated as:

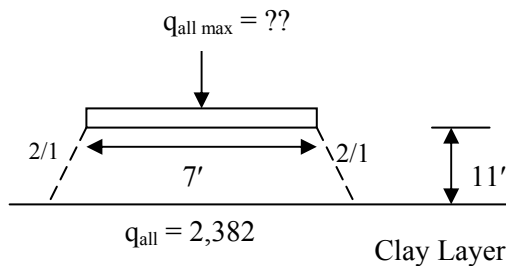
$$q_{\text{ult.clay}} = (1,100 \text{ psf})(5.14)(1.03)(1.0) + (1,350) \text{ psf}(1.0)(0.83)(1.0)(1.0)(1.18) =$$
$$q_{\text{ult.clay}} = 5,824 \text{ psf} + 1,322 \text{ psf} = 7,146 \text{ psf}$$

**Step 3: Determine allowable bearing capacity of virtual footing on clay (use FS = 3)**

$$q_{\text{all clay}} = \frac{7,146 \text{ psf}}{3} = 2,382 \text{ psf}$$

Since  $q_{\text{all clay}} < p_{\text{clay}}$ , the actual footing pressure needs to be reduced since  $q_{\text{all clay}}$  controls bearing capacity of pier footing founded on the layered system.

**Step 4: Transfer  $q_{\text{all clay}}$  up to the base of the pier footing to determine the limiting allowable bearing capacity  $q_{\text{all max}}$  of the pier footing founded on sand.**



$$q_{\text{all max}} = q_{\text{all clay}} \left( \frac{7 \text{ ft} + 11 \text{ ft}}{7 \text{ ft}} \right)$$

$$q_{\text{all max}} = 2,382 \text{ psf} \left( \frac{18 \text{ ft}}{7 \text{ ft}} \right) = 6,125 \text{ psf}$$

$$q_{\text{all max}} \approx 6,125 \text{ psf} \approx 3.1 \text{ tsf}$$

- Check with bridge designer to see if 3.1 tsf is a realistic pressure.
- Designer estimates a maximum un-factored structural load of 2,200 tons, and a minimum footing width of 7 ft
- The estimated maximum footing pressure ( $q_{\text{fts}}$ ) =  $\frac{2,200 \text{ tons}}{7 \text{ ft} \times 100 \text{ ft}} = 3.14 \text{ tsf}$
- Since the estimated maximum footing pressure is virtually identical to the estimate allowable bearing capacity, the footing size is acceptable for the load and use applied pressure ( $q$ ) = 3 tsf for settlement analysis.

**A7-5 CALCULATE SETTLEMENT OF PIER FOOTING FOUNDED WITHIN A TWO-LAYER SYSTEM**

**Step 1: Find pressure distribution by 2 on 1 construction (Refer to Chapter A.6-3 of text for procedure and Table A.7-2 below for results)**

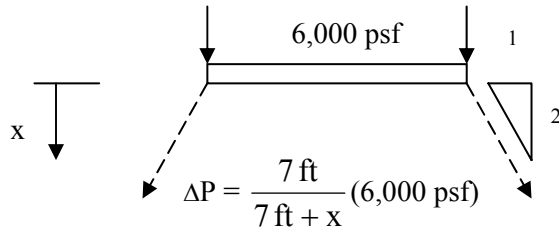


**Table A.7-2  
Computation of pressure change at various depths due to pressure applied by footing**

Depth $x$ (feet)	$k = \frac{7 \text{ ft}}{7 \text{ ft} + x}$	$\Delta p = k (6,000 \text{ psf})$ (psf)
3.5	0.67	4,000
7	0.50	3,000
10.5	0.40	2,400
14	0.33	2,000
21	0.25	1,500
28	0.20	1,200
35	0.17	1,000

**Step 2: Calculate the final pressure ( $p_f = p_o + \Delta p$ ) at various depths and plot the overburden pressure ( $p_o$ ), preconsolidation pressure ( $p_c$ ), and  $p_f$  with depth as shown in Figure A.7-3**

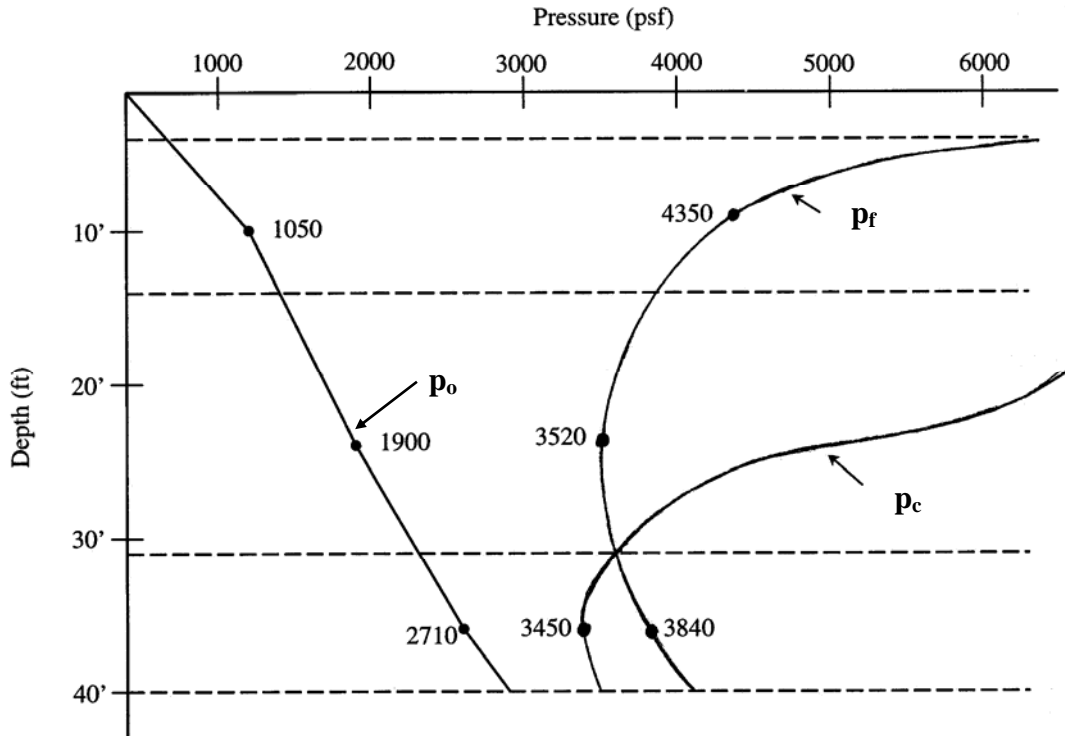


**Figure A.7-3. Variation of overburden pressure ( $p_o$ ), preconsolidation pressure ( $p_c$ ) and final pressure due to pier footing ( $p_f$ ) with depth.**

**Step 3: Calculate immediate settlement of the pier due to compression of the sand layer from 4 ft to 15 ft**

**Settlement computation by Hough's Method**

- Thickness of sand layer beneath pier footing = 15 ft - 4 ft = 11 ft
- Calculate immediate settlement (Refer to Chapter 7.4.1 in text)

$$\Delta H = H \frac{1}{C'} \log \frac{p_f}{p_o}$$

- For ( $N_{160}$ ) average = 36,  $C' = 90$  (Refer to Figure 7-7 of text –use curve for “well-graded fine to medium silty sand”).
- Calculate settlement for  $p_o = 1,050$  psf and  $p_f = 4,350$  psf.

$$\Delta H = 11 \text{ ft} \left( \frac{1}{90} \right) \log \frac{4,350 \text{ psf}}{1,050 \text{ psf}} \left( \frac{12 \text{ in}}{\text{ft}} \right)$$

$$\Delta H = 0.90 \text{ in}$$

### Settlement Computation by Schmertmann's method (Chapter 8.5 in the text)

- Begin by drawing the strain influence diagram. The  $L_f/B_f$  ratio for the footing is:  
 $100 \text{ ft}/7 \text{ ft} = 14.3$

Determine the value of the strain influence factor at the base of the footing,  $I_{ZB}$ , as follows:

$$I_{ZB} = 0.2 \text{ for plane strain case} \quad (L_f/B_f \geq 10)$$

- Determine the maximum depth of influence,  $D_I$ , as follows:

$$D_I = 4B_f \quad \text{for } L_f/B_f > 10$$

$$D_I = 4 \times 7 \text{ ft} = 28 \text{ ft}$$

- Determine the depth to the peak strain influence factor,  $D_{IP}$ , as follows:

$$D_{IP} = B_f \quad \text{for } L_f/B_f > 10$$

$$D_{IP} = 7 \text{ ft}$$

- Determine the value of the maximum strain influence factor,  $I_{ZP}$ , as follows:

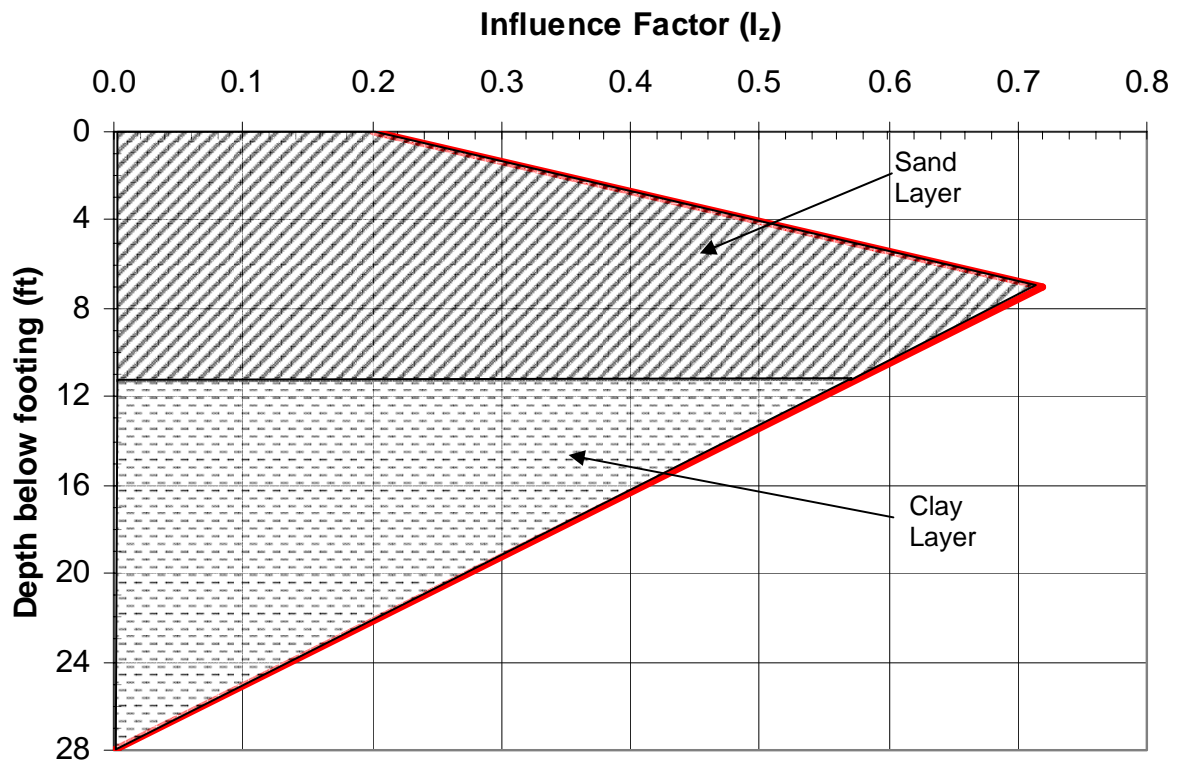
$$I_{ZP} = 0.5 + 0.1 \left( \frac{\Delta p}{p_{op}} \right)^{0.5}$$

$$\Delta p = 6,000 \text{ psf} - 4 \text{ ft}(110 \text{ pcf}) = 5,560 \text{ psf} = 5.56 \text{ ksf}$$

$$p_{op} = 10 \text{ ft}(110 \text{ pcf}) + 1 \text{ ft}(110 \text{ pcf} - 62.4 \text{ pcf}) = 1,147.6 \text{ psf} = 1.15 \text{ ksf}$$

$$I_{ZP} = 0.5 + 0.1 \sqrt{\frac{5,560 \text{ psf}}{1,147.6 \text{ psf}}} = 0.72$$

- Draw the  $I_Z$  vs. depth diagram as shown below. The hatched portions show portions of the strain influence diagram within the sand layer and the clay layer. The immediate settlement will occur only in the sand layer. Therefore, the portion of the strain influence diagram in the clay layer will not be considered in the computation of the immediate settlement.



- Determine value of elastic modulus  $E_s$  from Table 5-16 in Chapter 5.

For “clean fine to medium sands with slightly silty sands”  $E_s = 7N_{160}$  tsf. Since the elastic modulus  $E_s$  is based on correlations with  $N_{160}$ -values obtained from Table 5-16, calculate the X multiplication factor as follows:

$$X = 1.75 \quad \text{for } L_f/B_f \geq 10$$

$$\text{Thus, } XE_s = 1.75 (7) (36) = 441 \text{ tsf.}$$

- Divide the sand layer into convenient sublayers using the guidelines in Chapter 8.5.1.2. Using those guidelines, the sand layer below the footing is divided into 1 ft and 2 ft sublayers. Using the sublayers determine the settlement by setting up a table as follows:

Layer	H <sub>c</sub> (inches)	N <sub>160</sub>	E <sub>s</sub> (tsf)	XE <sub>s</sub> (tsf)	Z <sub>1</sub> (ft)	I <sub>Z</sub> at Z <sub>i</sub>	H <sub>i</sub> = $\frac{I_Z}{XE_s} H_c$ (in/tsf)
1	12	36	252	441	0.5	0.237	0.00645
2	24	36	252	441	2.0	0.349	0.01897
3	12	36	252	441	3.5	0.460	0.01252
4	24	36	252	441	5.0	0.571	0.03110
5	24	36	252	441	7.0	0.720	0.03918
6	24	36	252	441	9.0	0.651	0.03543
7	12	36	252	441	10.5	0.600	0.01633
Σ H <sub>i</sub> =							<b>0.15998</b>

- Determine embedment factor (C<sub>1</sub>) and creep factor (C<sub>2</sub>) as follows:

- Embedment factor

$$C_1 = 1 - 0.5 \left( \frac{p_o}{\Delta p} \right) = 1 - 0.5 \left( \frac{4 \text{ ft} \times 110 \text{ pcf}}{5,560 \text{ psf}} \right) = 0.960$$

- Creep Factor

$$C_2 = 1 + 0.2 \log_{10} \left( \frac{t(\text{years})}{0.1} \right)$$

For end of construction t(yrs) = 0.1 yr (1.2 months)

$$C_2 = 1 + 0.2 \log_{10} \left( \frac{0.1}{0.1} \right) = 1.0$$

- Determine the settlement at end of construction as follows:

$$S_i = C_1 C_2 \Delta p \sum H_i$$

$$S_i = (0.960)(1.0) \left( \frac{5,560 \text{ psf}}{2,000 \text{ psf/tsf}} \right) \left( 0.15998 \frac{\text{in}}{\text{tsf}} \right)$$

$$S_i = 0.43 \text{ inches}$$

**Note:** The settlement computed by Hough's method was 0.90 inches which is approximately 2 times more than that computed above by Schmertmann's method. This difference is similar to that found by FHWA (1987) and discussed in Chapter 8.5.1 in the text.

**Step 4: Calculate settlement of the pier due to consolidation of the clay layer. Use equation for consolidation settlement (Refer to Chapter 7.5) and consider two sublayers; sublayer 1 from 15 ft to 32 ft and sublayer 2 from 32 ft to 40 ft**

- Thickness of clay Sub-layer 1 = 32 ft - 15 ft = 17 ft
  - As shown in Figure A.7-3, the clay in Sub-layer 1 is over-consolidated since  $p_o < p_c$  and the load increment results in  $p_f$  which is also less than  $p_c$  within this depth range. Therefore, calculate settlement for the pressure increment from  $p_o = 1,900$  psf to  $p_f = 3,520$  psf and use the recompression index  $C_r$ .

$$\Delta H = H \frac{C_r}{1 + e_o} \log \frac{p_f}{p_o}$$

$$\Delta H = 17 \text{ ft} \frac{0.035}{1 + 0.97} \log \frac{3,520 \text{ psf}}{1,900 \text{ psf}} \left( \frac{12 \text{ in}}{\text{ft}} \right)$$

$$\Delta H = 0.97 \text{ in}$$

- Thickness of clay Sub-layer 2 = 40 ft - 32 ft = 8 ft
  - As shown in Figure A.7-3, the clay in Sub-layer 2 is over-consolidated within this depth range since  $p_c > p_o$ , but at the mid-depth the load increment causes  $p_f > p_c$ . Therefore the settlement for this sub-layer must be calculated in two steps, one step for the pressure increment from  $p_o$  to  $p_c$  for which  $C_r$  applies, and the other for the pressure increment from  $p_c$  to  $p_f$  for which  $C_c$  applies. (Refer to Chapter 7.5.2)
  - Calculate settlement of clay Sub-layer 2 for the pressure increment from  $p_o = 2,710$  psf to  $p_c = 3,450$  psf.

$$\Delta H = H \frac{C_r}{1 + e_o} \log \frac{p_c}{p_o}$$

$$\Delta H = 8 \text{ ft} \frac{0.035}{1 + 0.97} \log \frac{3,450 \text{ psf}}{2,710 \text{ psf}} \left( \frac{12 \text{ in}}{\text{ft}} \right)$$

$$\Delta H = 0.18 \text{ in}$$

- Calculate settlement of clay Sub-layer 2 for the pressure increment from  $p_c = 3,450$  psf to  $p_f = 3,840$  psf.

$$\Delta H = H \frac{C_c}{1 + e_o} \log \frac{p_f}{p_c}$$

$$\Delta H = 8 \text{ ft} \frac{0.35}{1 + 0.97} \log \frac{3,840 \text{ psf}}{3,450 \text{ psf}} \left( \frac{12 \text{ in}}{\text{ft}} \right)$$

$$\Delta H = 0.80 \text{ in}$$

**Step 5: Summarize settlement contributions from sand and clay layers (Refer to Table A.7-3)**

**Table A.7-3  
Summary of settlement of pier footing**

Layer	Settlement (in)
Sand (4 ft to 15 ft)	0.90 in
Clay – Sub-layer 1 (15 ft to 32 ft)	0.97 in
Clay – Sub-layer 2 (32 ft to 40 ft)	0.98 in
Total settlement =	2.85 in
Total settlement of clay layer =	1.95 in

**Step 6: Compute time for settlement due to pier footing to occur in clay layer**

- Obtain time for various percentages of settlement as shown in Table A.7-4 by using Table 7-4 in Chapter 7.5.3.1 in the text and the following equations

- $H_d = \frac{1}{2} H = \frac{1}{2} (40 \text{ ft} - 15 \text{ ft}) = 12.5 \text{ ft}$

- $c_v = 0.6 \text{ ft}^2/\text{day}$

- $(H_d)^2/c_v = (12.5 \text{ ft})^2 / (0.6 \text{ ft}^2/\text{day}) = 260 \text{ days}$

- For time (t) use Equation 7-8 of text

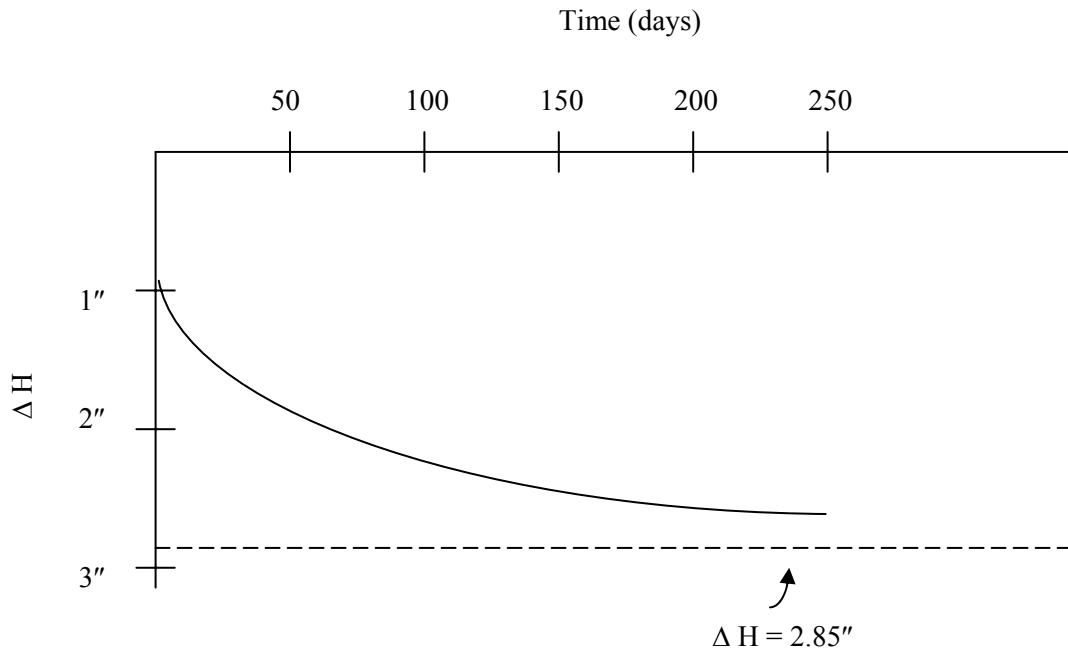
$$t = \frac{T H_d^2}{c_v}$$

Table A.7-4 provides a convenient template for performing computations to obtain settlement vs. time values for arbitrarily chosen values of average percent consolidation.

**Table A.7-4**  
**Template to compute values of consolidation settlement ( $\Delta H$ ) in clay layer at various times**  
**(t) after application of pier footing load (refer to section A.6)**

Average % Consol. (U)	$\Delta H$ (in) = (U)( $\Delta H_{\text{Total Clay}}$ Layer)	Time Factor (T) (from Table 7-4 in text)	$\frac{H_d^2}{c_v}$	t (days)
20	0.39	0.031	260	8
50	0.98	0.197		51
70	1.37	0.403		104
90	1.76	0.848	↓	220

**Step 7: Plot settlement-time curve for the pier including immediate settlement of sand as shown in Figure A.7-4.**



**Figure A.7-4. Settlement-time curve for pier including immediate settlement of sand.**

### A.7-6 CALCULATE SETTLEMENT OF EAST ABUTMENT FOOTING FOUNDED WITHIN A TWO-LAYER SYSTEM

- **Define geometry of the problem and state relevant assumptions.**
  - Footing embedment below final grade of embankment fill ( $D_f$ ) = 10 ft
  - Footing width ( $B_f$ ) = 1/3 pier height = 7 ft
  - Footing length ( $L_f$ ) = 100 ft
  - Depth to ground water below base of footing ( $D_w$ ) = 25 ft
  - Internal consolidation of embankment fill under its own weight is negligible.
  - Organic layer is excavated and replaced with 3-feet of compacted select fill.

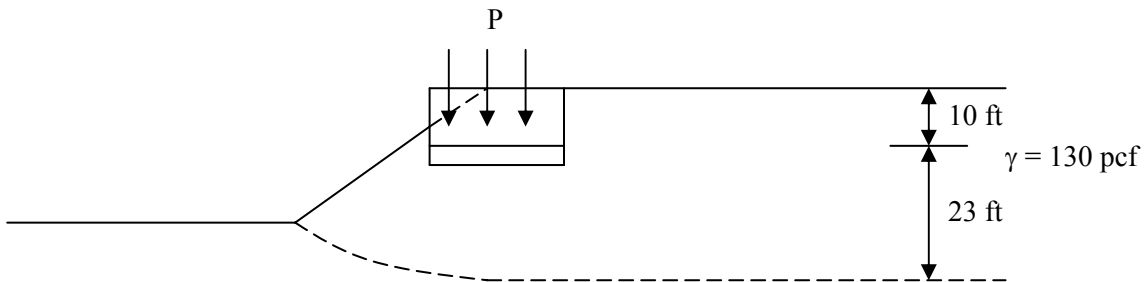
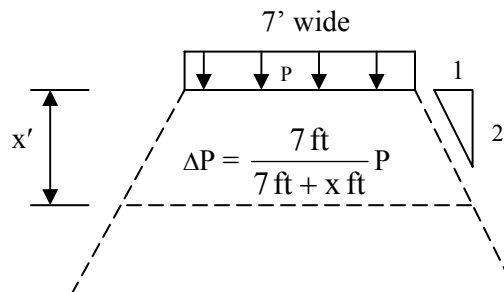


Figure A.7-5. Footing geometry for embankment footing.

**Step 1: Determine net footing pressure at footing embedment depth due to soil removal for footing excavation.**

- $p$  = the net pressure applied at the footing level. Assume that the abutment will be constructed after the embankment fill is in place.
- $p = 6,300 \text{ psf} - (10 \text{ ft})130 \text{ pcf} = 5,000 \text{ psf}$

**Step 2: Calculate change in pressure due to embankment footing by 2:1 construction. Consider layer mid-depths corresponding to those considered in calculation of  $p_o$  and  $p_f$  in Section 6 for embankment settlement. (Refer to Figure A.6-5 Refer to Table A.7-5 below for results)**



- $p_{\text{abut}} = p_f + \Delta p_{\text{abut}}$  where  
 $p_f = p_o + \text{change in pressure due to embankment load}$  (Refer to Table A.6-2)

**Table A.7-5**  
**Computation of pressure change due to pressure applied by abutment footing and  $p_{abut}$**   
**at various depths the embankment**

Layer	Thickness (feet)	Depth x from top of sand to layer mid-point (ft)	Depth z to midpoint (feet)	$k = \frac{7 \text{ ft}}{7 \text{ ft} + x}$	$\Delta p_{abut} = k (5,000 \text{ psf})$ (psf)	$p_f$ (psf)	$p_{abut}$ (psf)
Sand	7	3.5	26.5	0.21	1,050	4,470	5,520
Clay Sub-layer 1	8	11.0	34.0	0.17	850	4,920	5,770
Clay Sub-layer 2	27	28.5	51.5	0.12	600	5,650	6,250

**Step 3:** Plot the pressure distributions with depth of the overburden pressure ( $p_o$ ), preconsolidation pressure ( $p_c$ ), final pressure due to embankment fill only ( $p_f$ ), and the final pressure due to embankment fill plus abutment footing ( $p_{abut}$ ) as shown in Figure A.7-6

**Step 4:** Calculate immediate settlement of the abutment footing due to compression of the sand layer (3 ft to 10 ft).

- Thickness of sand layer beneath pier footing = 10 ft - 3 ft = 7 ft
- Calculate immediate settlement (Refer to Chapter 7)

$$\Delta H = H \frac{1}{C'} \log \frac{p_{abut}}{p_f}$$

$$\Delta H = 7 \text{ ft} \left( \frac{1}{90} \right) \log \frac{5,520 \text{ psf}}{4,470 \text{ psf}}$$

$$\Delta H = 0.0071 \text{ ft} \sim 0.09 \text{ in}$$

Note: Schmertmann's method can also be used. This was demonstrated earlier.

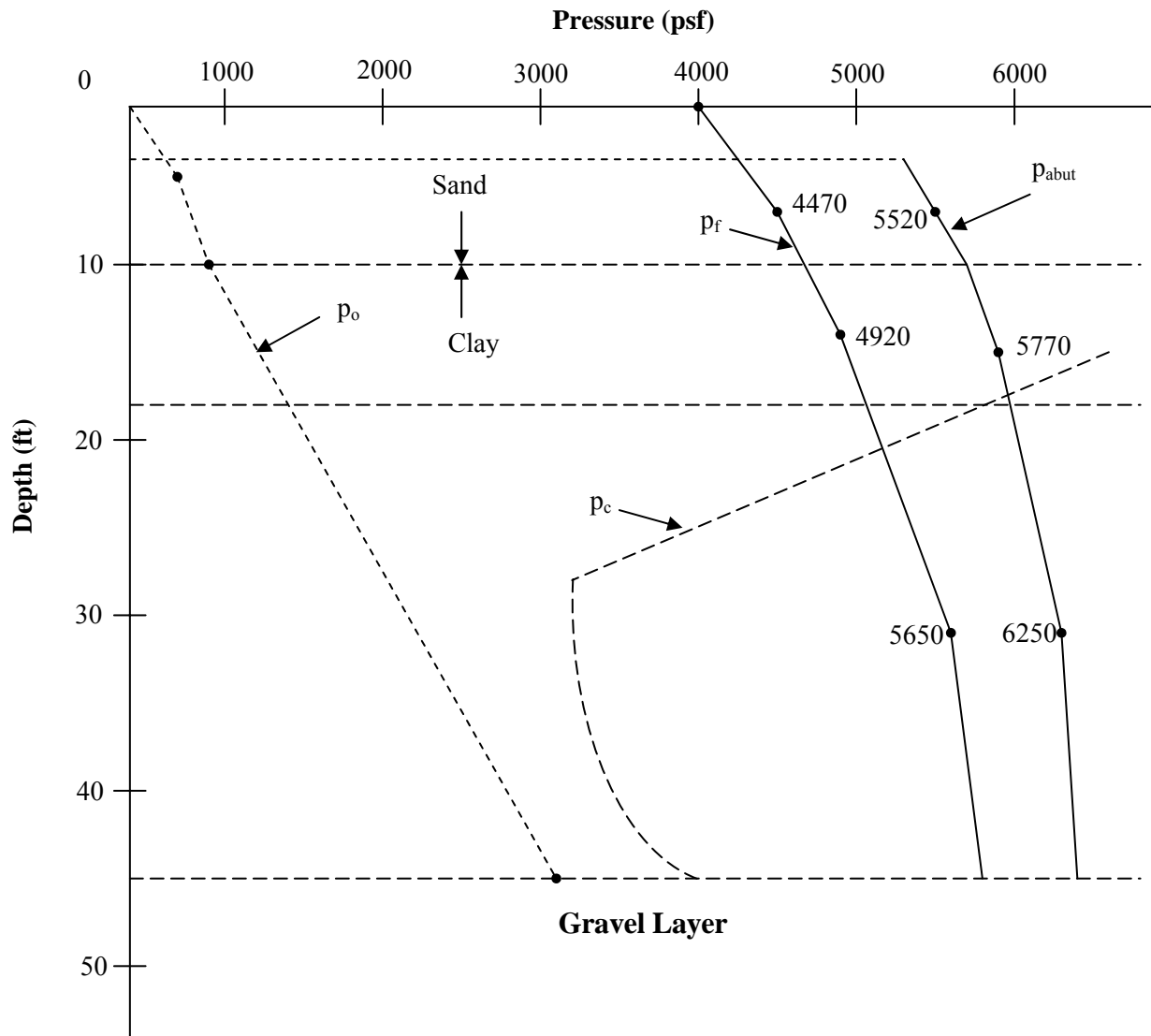


**Figure A.7-6. Pressure distributions with depth at East Abutment for the overburden pressure ( $p_o$ ), preconsolidation pressure ( $p_c$ ), final pressure due to embankment fill only ( $p_f$ ), and the final pressure due to embankment fill plus abutment footing ( $p_{abut}$ ).**

**Step 5: Calculate settlement of the abutment footing due to consolidation of the clay layer. Use equation for consolidation settlement (Refer to Chapter 7.5) and consider two partial layers, Sub-layer 1 from 10 ft to 18 ft and Sub-layer 2 from 18 ft to 45 ft.**

- Thickness of clay Sub-layer 1 = 18 ft - 10 ft = 8 ft
  - As shown in Figure A.7-6, the clay in Sub-layer 1 was over-consolidated prior to the construction of the embankment fill since  $p_o < p_c$  and remained so during and after consolidation under the embankment fill since  $p_f$  is also  $< p_c$ . Figure A.7-6 further shows that Sub-layer 1 will continue to be over-consolidated during and after consolidation under the abutment footing, i.e.,  $p_{abut}$  is also  $< p_c$  within this depth range. Therefore, calculate settlement due to the abutment footing for the pressure increment from  $p_f = 4,920$  psf to  $p_{abut} = 5,770$  psf and use the recompression index  $C_r = 0.035$ .

$$\Delta H = H \frac{C_r}{1 + e_o} \log \frac{p_{abut}}{p_f}$$

$$\Delta H = 8 \text{ ft} \frac{0.035}{1 + 0.97} \log \frac{5,770 \text{ psf}}{4,920 \text{ psf}}$$

$$\Delta H = 0.0098 \text{ ft} \sim 0.12 \text{ in}$$

- Thickness of clay Sub-layer 2 = 45 ft - 18 ft = 27 ft
  - As shown in Figure A.7-6, the clay in Sub-layer 2 was also over-consolidated prior to the construction of the embankment fill since  $p_o < p_c$ . However, during consolidation under the embankment fill, the pressure increment at every depth in Sub-layer 2 caused the final pressure  $p_f$  to become  $> p_c$ . It was for this reason that the total consolidation settlement for this Sub-layer under the embankment fill had to be calculated by the use of a two-step procedure. In the first step the settlement was calculated as the pressure increased from  $p_o$  to  $p_c$ ; in the second step the settlement was calculated as the pressure increased from  $p_c$  to  $p_f$ . As described in Step 5 of Section A.6-3,  $C_r$  was used in the first step and  $C_c$  in the second. Therefore, unless the abutment footing is built after 100% consolidation of the clay layer under the embankment load has occurred, the clay will be under-consolidated at the time of construction of the footing, i.e., settlement due to the abutment footing will be accompanied by continued settlement due to the embankment. Therefore, calculate settlement due to the abutment footing for the

pressure increment from  $p_f = 5,650$  psf to  $p_{abut} = 6,250$  psf and use the compression index  $C_c = 0.35$ .

$$\Delta H = H \frac{C_c}{1 + e_o} \log \frac{p_{abut}}{p_f}$$

$$\Delta H = 27 \text{ ft} \frac{0.35}{1 + 0.97} \log \frac{6,250 \text{ psf}}{5,650 \text{ psf}}$$

$$\Delta H = 0.21 \text{ ft} \sim 2.50 \text{ in}$$

**Step 6: Summarize contributions to settlement under abutment footing loads from sand and clay layers (Refer to Table A-7.6)**

**Table A.7-6  
Summary of settlement of pier footing**

Layer	Settlement (in)
Sand (3 ft to 10 ft)	0.09 in
Clay – Sub-layer 1 (10 ft to 17 ft)	0.12 in
Clay – Sub-layer 2 (17 ft to 45 ft)	2.50 in
Total settlement due to abutment footing=	2.71 in
Total settlement of clay layer due to abutment footing=	2.62 in

**Step 7: Compute Time for Settlement Due to Abutment Footing to Occur in Clay Layer**

- Obtain time for various percentages of settlement as shown in Table A.7-4 by using Table 7-4 in Chapter 7.5.3.1 in the text and the following equations

➤  $H_d = \frac{1}{2} H = \frac{1}{2} (45 \text{ ft} - 10 \text{ ft}) = 17.5 \text{ ft}$

➤  $c_v = 0.6 \text{ ft}^2/\text{day}$

➤  $(H_d)^2/c_v = (17.5 \text{ ft})^2 / (0.6 \text{ ft}^2/\text{day}) = 510 \text{ days}$

➤ For time (t) use Equation 7-8 of text

$$t = \frac{T H_d^2}{c_v}$$

Table A.7-7 provides a convenient template for performing computations to obtain settlement vs. time values for arbitrarily chosen values of average percent consolidation.

**Table A.7-7**

**Template to compute values of consolidation settlement ( $\Delta H$ ) in clay layer at various times ( $t$ ) after application of abutment footing load (refer to section A.6)**

Average % Consol. (U)	$\Delta H$ (in) = (U)( $\Delta H_{\text{Total Clay Layer}}$ )	Time Factor (T)	$\frac{H_d^2}{c_v}$	t (days)
20	0.52	0.031	510	16
50	1.31	0.197		100
70	1.83	0.403		206
90	2.36	0.848	↓	432

**Step 9: Plot settlement-time curve for the pier including immediate settlement of sand as shown in Figure A.7-7.**

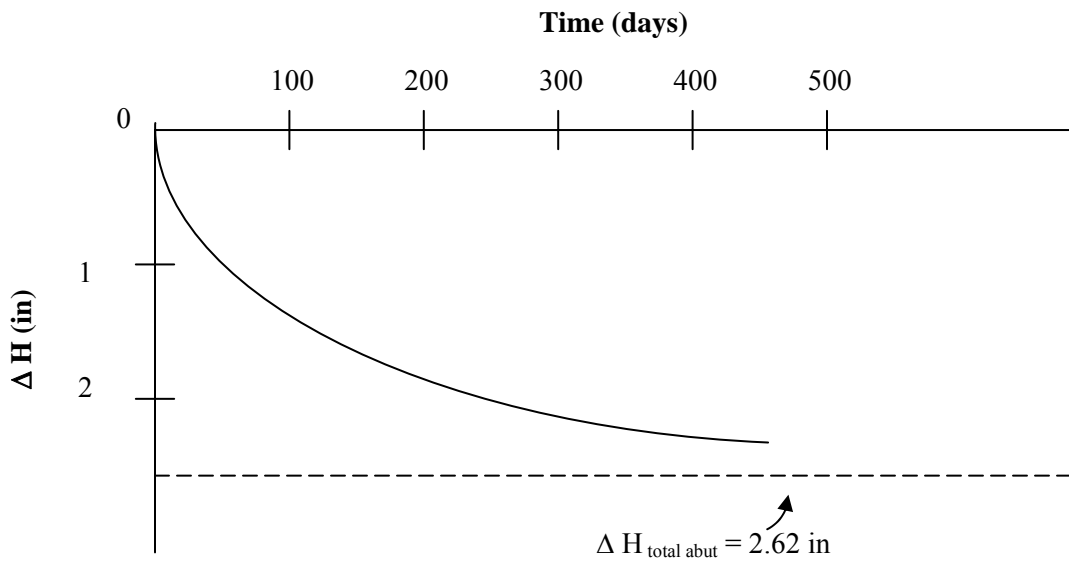


**Figure A.7-7. Settlement-Time curve for abutment footing.**

### A.7-7 EVALUATE THE EFFECT OF PRE-TREATMENT ON THE SETTLEMENT OF EAST ABUTMENT FOOTING

- As indicated in Step 6 of Section A.7-6 above, the settlement due to the abutment footing will occur while the settlement remaining due to embankment load continues. Therefore the actual settlement of is the sum of these two components of settlement. For example, if the abutment footing were built immediately after placement of the embankment fill ( $t = 0$ ) without pre-treatment by surcharging and/or vertical drains, the total consolidation settlement of the abutment footing would be:

$$\Delta H_{\text{total (emb + abut)}} = \Delta H_{\text{total emb}} + \Delta H_{\text{total abut}} = 12.66 \text{ in} + 2.62 \text{ in} = 15.28 \text{ in}$$

- However, pretreatment by surcharges and/or vertical drains can be used to accelerate consolidation of the clay layer under the embankment load so that when the abutment footing is built at a later time, e.g., at a time when the  $t_{90}$  for the embankment fill without treatment is reached, the total settlement due to the abutment footing ( $\Delta H_{\text{total (emb + abut)}}$ ) will be only slightly larger than the settlement due to the abutment footing alone ( $\Delta H_{\text{total abut}}$ ).
- For the case of pre-treatment by wick drains, Figure A.7-8 shows that the  $t_{90}$  settlement of 11.43 inches due to the 30 ft of embankment fill without treatment is reached after approximately 50 days. If the abutment footing is constructed at that time, only about 1.23 inches of settlement due to the embankment alone remains. Therefore, the abutment footing will undergo a total settlement of 1.23 in + 2.62 in = 3.85 in as compared to 15.28 in it would have undergone had the pre-treatment not been used and the abutment footing built immediately after construction of the embankment.

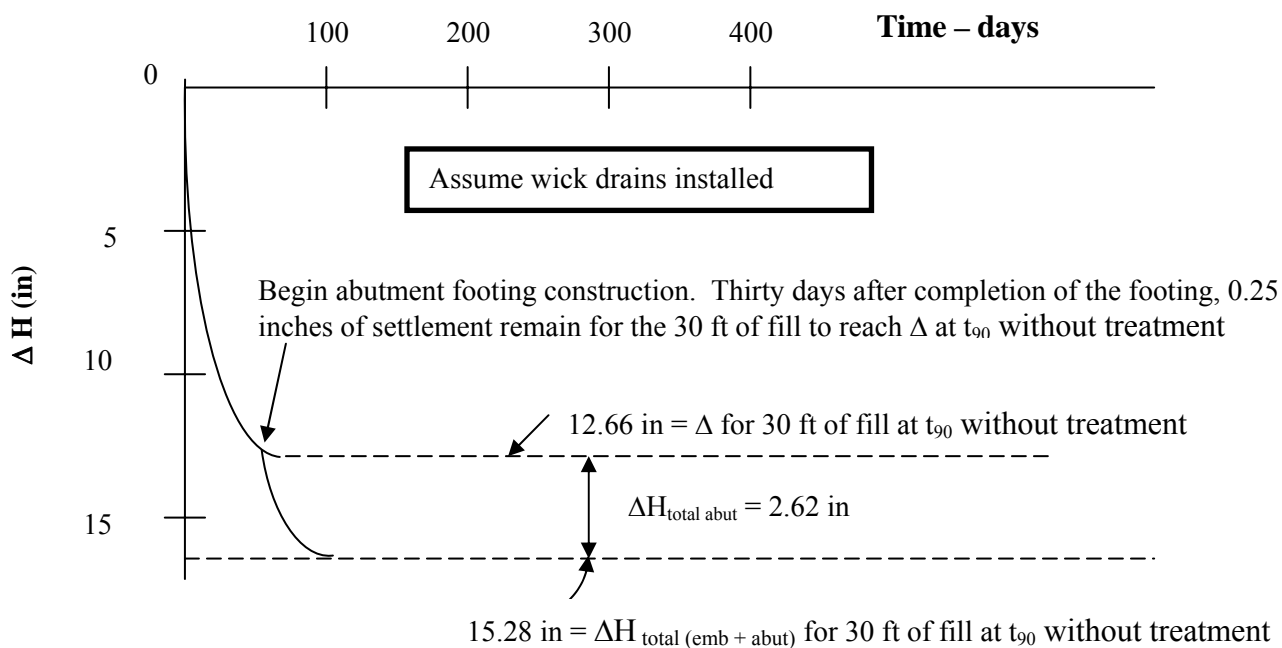


**Figure A.7-8. Settlement –Time curve for abutment footing built 6 months after completion of embankment fill with vertical drain pre-treatment.**

- For the case of pre-treatment by 10 ft of surcharge, Figure A.7-9 shows that the  $t_{90}$  settlement of 13.7 inches due to 30 ft of embankment fill plus surcharge is reached after approximately 240 days.

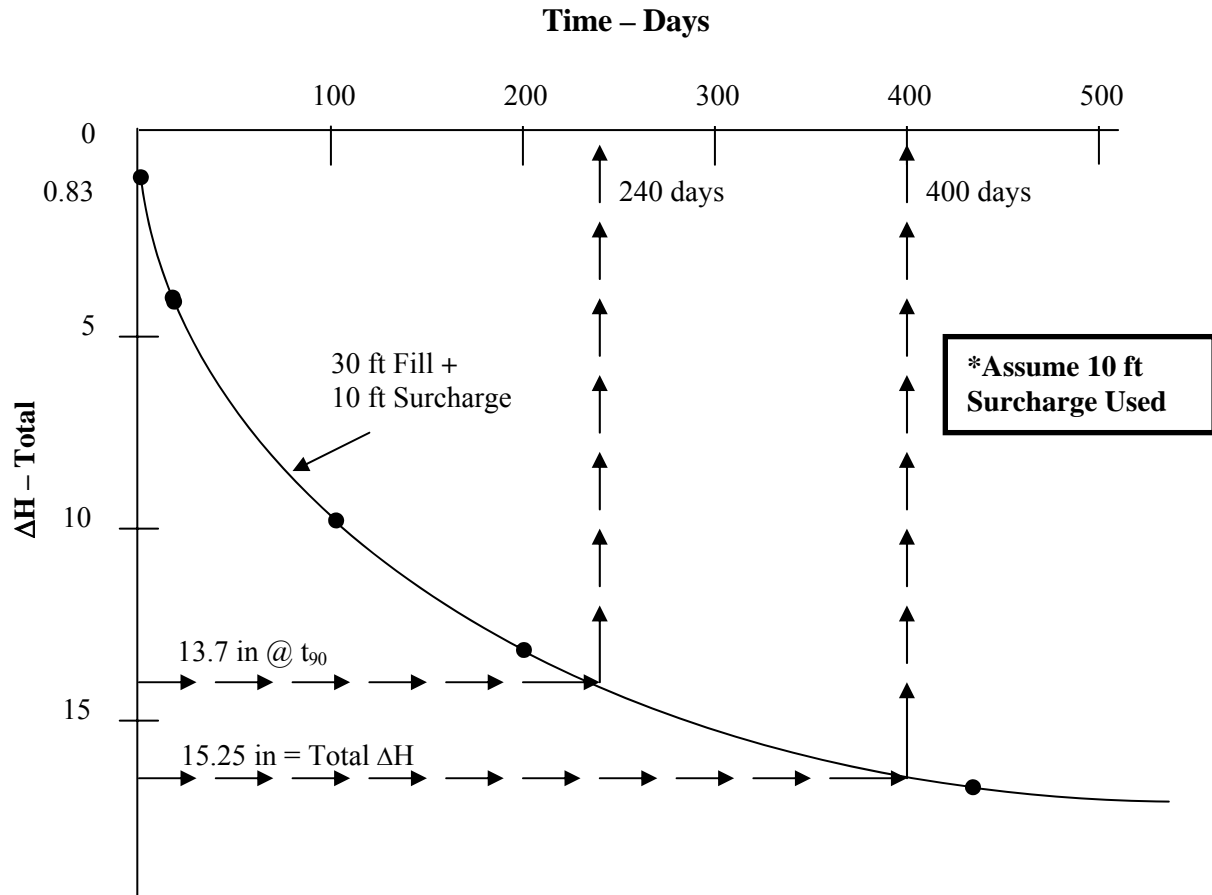


**Figure A.7-9. Settlement –Time curve for 30 ft of embankment fill plus 10 ft surcharge.**

\* Surcharge must be left in place for 13 months to dissipate all embankment and abutment  $\Delta H$

### Summary of the Spread Footing Design Phase for Apple Freeway Design Problem

- Design Soil Profile

Strength and consolidation values selected for all soil layers. Footing elevation and width chosen.

- Pier Bearing Capacity

$$Q_{\text{allowable}} = 3 \text{ tsf}$$

- Pier Settlement

Settlement = 2.67 in,  $t_{90}$  = 220 days.

- Abutment Settlement

Settlement = 2.7 in,  $t_{90}$  = 432 days.

- Vertical Drains

$t_{90}$  = 60 days - could reduce settlement to 0.25 in after abutment constructed and loaded.

- Surcharge

10 ft surcharge:  $t_{90}$  = 240 days  
before abutment constructed.

### **A.7-7 SUMMARY OF GEOTECHNICAL DESIGN OF PIER AND ABUTMENT SPREAD FOOTINGS**

1. Construct idealized design profile with footing geometry shown.

- Use logs of appropriate borings
- Include 30 ft high embankment at East abutment (assume 3 ft organic layer at the surface is replaced by compacted select material).
- Estimate consolidation properties of clay layer at each location from results of field and laboratory tests.
- Estimate internal friction angle of sand from SPT-N corrected blow counts ( $\phi \approx 36^\circ$ )

2. Determine overburden pressure at each location, change in pressure due to pier footing, change in pressure due to embankment fill at East abutment, change in pressure due to abutment footing, and maximum past pressure at each location, all as a function of depth.

- Plot pressure distributions with depth and determine stress history of impacted layers at each location.

3. Calculate ultimate and allowable bearing capacity of pier footing

- Footing width = 7 ft
- Footing length = 100 ft
- Depth of embedment = 4 ft
- $q_{ult} = 33,000$  psf
- $q_{all} = 11,000$  psf

4. Check pressure transmitted to clay layer and compare it to the allowable bearing capacity of the clay
  - $q_{\text{all max}} \approx 3.1 \text{ tsf}$ – use 3 tsf for settlement analysis
  
5. Calculate settlement of pier footing founded within a two-layer system and plot settlement time relationship
  - Sand (4–15 ft) = 0.91 in
  - Clay (15–32 ft) = 0.97 in
  - Clay (32-40 ft) = 0.98 in
  - Total settlement = 2.85 in due to clay plus sand
  - Total settlement = 1.95 in due to clay alone
  - $t_{90}$  = 220 days
  
6. Calculate settlement of East abutment footing founded within the embankment and underlain by a two-layer system. Plot settlement time relationship
  - Sand (3-10 ft) = 0.09 in
  - Clay (10-17 ft) = 0.12 in
  - Clay (17-45 ft) = 2.50 in
  - Total settlement = 2.71 in - footing due to clay plus sand
  - Total settlement = 2.62 in - footing due to clay alone
  - Total settlement = 15.28 in - footing plus embankment due to clay plus sand
  - $t_{90}$  = 433 days for embankment alone without pre-treatment
  
7. Evaluate the effect of pre-treatment on the settlement-time relationship of the East abutment footing and embankment fill.
  - $t_{90}$  = 60 days for embankment alone pre- treated with vertical drains.
  - Total settlement = 0.25 in remaining due to embankment.
  - Abutment footing constructed at this time.
  - Total settlement = 0.25 in + 2.60 in = 2.85 in – footing plus embankment due to clay alone after abutment footing constructed and loaded.

Subsurface Explorations	Terrain Reconnaissance Site Inspection Subsurface Explorations	✓
Basic Soil Properties	Visual Description Classification Tests Subsurface Profile	✓
Laboratory Testing	p <sub>o</sub> Diagram Test Request Consolidation Results Strength Results	✓
Slope Stability	Design Soil Profile Circular Arc Analysis Sliding Block Analysis	✓
Approach Roadway Deformations	Design Soil Profile Settlement Time – Rate Surcharge Vertical Drains Lateral Squeeze	✓
Spread Footing Design	Design Soil Profile Pier Bearing Capacity Pier Settlement Abutment Settlement Surcharge Vertical Drains	✓
→	<b>Driven Pile Design</b>	Design Soil Profile Static Analysis – Pier Pipe Pile H – Pile Static Analysis – abutment Pipe Pile H – Pile Driving Resistance Abutment Lateral Movement
Construction Monitoring	Wave Equation Hammer Approval Embankment Instrumentation	

**Figure A.8-1. Status of geotechnical work.**

## SECTION A.8 DRIVEN PILE DESIGN

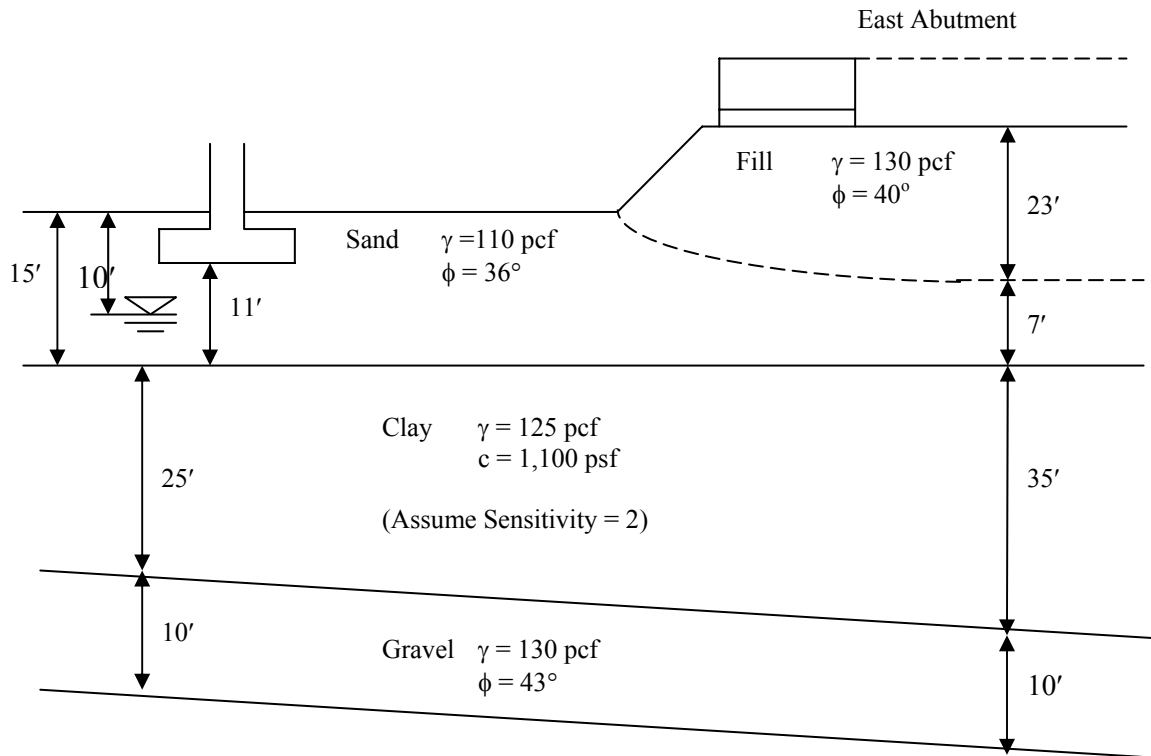
### A.8-1 RELEVANT CONCEPTS AND PROCEDURES (Refer to Figure A.8-1)

- Refer to Chapter 9 for driven pile design

In this Section, the Apple Freeway is used to illustrate the pile design for support of the pier and abutment. **Although drilled shafts may also be a feasible deep foundation design alternate for this structure, only driven piles are discussed herein because they involve a lot more detail in design and construction.** The computation process for static analysis to determine pile capacity by Nordlund Method is presented along with the computation of pile driving resistance.

**Given:** The subsurface profile and soil properties shown below.

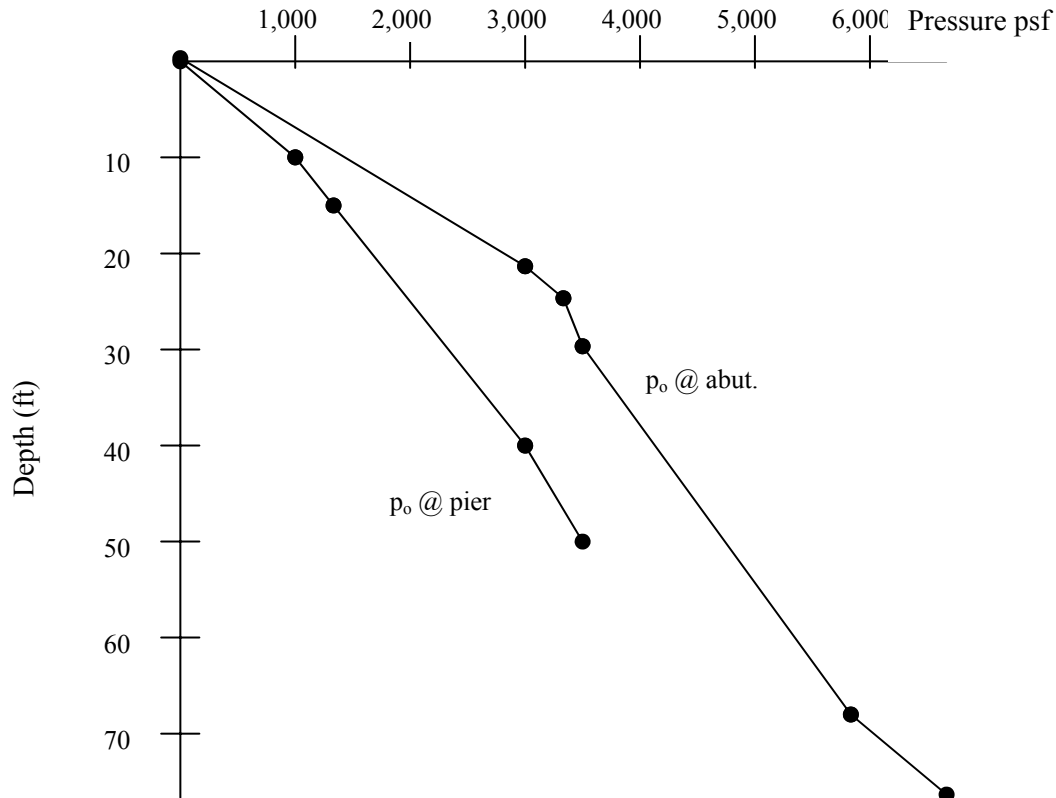
**Required:** Determine the allowable pile capacity using static analysis.



## A.8-2 CONSIDERATION FOR PILE TYPE SELECTION

- Spread footings would be feasible at both the pier and abutment except for settlements due to consolidation of the clay deposit. To eliminate these settlements any pile type selected must achieve capacity below the bottom of the clay deposit.
- End bearing will provide most of the ultimate resistance at either the pier or abutment location due to the minimal thickness of the gravel layer.
- The maximum estimated design structural load of 2,200 tons can be supported by either the gravel or the rock layer. However pile driveability appears to be an issue in design.
- Required loads, end bearing support, and difficult driving concerns would favor a straight-sided steel pile over either a timber or concrete or tapered pile.
- Static analyses will be used to determine if a displacement pile with an end plate or a non-displacement pile will provide the best choice for both bearing and driveability. The designer selected a 12 inch diameter closed end pipe pile and a 12 inch H-pile for alternate evaluation at this site. The project's structural engineer usually designs the pipe pile for a 70-ton design load and the H-pile for a 120-ton design load.

### Step 1: Plot $p_o$ diagram.



### A.8-3 STATIC PILE ANALYSIS – PIER

#### A. For 12 inch diameter pipe pile (closed end, 70 ton design)

##### Step 2A: Compute shaft resistance.

- Sand Layer (4 ft – 15 ft - Use Nordlund Method – Chapter 9.5.1.1)

$$D = 15 \text{ ft} - 4 \text{ ft} = 11 \text{ ft}$$

$$\begin{aligned} V &= \frac{\text{pile vol.}}{\text{foot}} \\ &= \frac{\pi d^2}{4} = 0.785 \text{ ft}^3/\text{ft} \end{aligned}$$

$$\frac{\delta}{\phi} = 0.6 \text{ (for closed end pipe pile from Figure 9-7 in Chapter 9)}$$

$$\delta = (0.6)(36^\circ) = 21.6^\circ$$

$$K_\delta = 1.92 \text{ (for } \phi = 36^\circ \text{ from Table 9-6(a) in Chapter 9)}$$

$$\text{Correction Factor, } C_F = 0.75 \text{ (from Figure 9-12 in Chapter 9)}$$

$$C_d = \pi d = \pi (1 \text{ ft}) = 3.14 \text{ ft}$$

$$p_d \text{ Avg. @ } \frac{4 \text{ ft} + 15 \text{ ft}}{2} = 9.5 \text{ ft is } 1,050 \text{ psf}$$

$$\begin{aligned} R_{s(\text{sand})} &= K_\delta (C_F)(p_d)(C_d)(\sin \delta)D \quad \text{(Equation 9-6 in Chapter 9)} \\ &= (1.92)(0.75)(1,050 \text{ psf})(3.14 \text{ ft})(\sin 21.6^\circ)(11 \text{ ft}) \end{aligned}$$

$$R_{s(\text{sand})} = 19,225 \text{ lbs} = 9.6 \text{ tons}$$

- Clay Layer (15 ft – 40 ft)

$$R_{s(\text{clay})} = c_a C_d D$$

$$c_a \text{ (Adhesion)} \cong 1,100 \text{ psf (assume adhesion } \approx \text{ cohesion, i.e., } \alpha \approx 1.0)$$

$$R_{s(\text{clay})} = 1,100 \text{ psf} (3.14 \text{ ft}) 25 \text{ ft} = 86,350 \text{ lbs} = 43.1 \text{ tons}$$

- \*Gravel Layer (Try 4 ft Embedment i.e.. 40 ft – 44 ft)

\*Remember to reduce  $\phi$  of  $43^\circ$  to maximum  $36^\circ$  value for hard, angular gravel skin friction.

$$R_s = (K_\delta)(C_F)(p_d)(C_d)(\sin \delta)D$$

$$\frac{\delta}{\phi} = 0.6$$

$$\delta = (0.6)(36^\circ) = 21.6^\circ$$

$$K_\delta = 1.92 \text{ (for } \phi = 36^\circ \text{ from Table 9-6(a) in Chapter 9)}$$

$$C_F = 0.7 \text{ (from Figure 9-12 in Chapter 9)}$$

$$p_o = 3,200 \text{ psf}$$

$$R_{s(\text{gravel})} = (1.92)(0.7)(3,200 \text{ psf})(3.14 \text{ ft})(\sin 21.6^\circ)4 \text{ ft}$$

$$R_{s(\text{gravel})} = 19,885 \text{ lbs} = 9.9 \text{ tons}$$

**Step 3A: Compute toe resistance.**

- Gravel Layer

For  $\phi = 43^\circ$ ,  $\alpha \approx 0.75$  from Figure 9-13(a) in Chapter 9

For  $\phi = 43^\circ$ ,  $N'_q = 300$  from Figure 9-13(b) in Chapter 9

$$\begin{aligned} \text{a. } R_t &= A_p \alpha_t p_t N'_q && \text{(Equation 9-7a in Chapter 9)} \\ &= (0.785 \text{ ft}^2)(0.75)(3,000 \text{ psf})(300) \\ R_t &= 529,875 \text{ lbs} = 265 \text{ tons} \end{aligned}$$

$$\begin{aligned} \text{b. } R_t(\text{max}) &= q_L \times A_p && \text{(Equation 9-7b in Chapter 9)} \\ &= (680 \text{ ksf})(0.785 \text{ ft}^2) && (q_L=680 \text{ ksf for } \phi = 43^\circ \text{ from Figure 9-14 in Chapter 9)} \end{aligned}$$

$$R_t(\text{max}) = 533.8 \text{ kips} = 267 \text{ tons}$$

$$\therefore R_t = 265 \text{ tons}$$

It is obvious that any embedment in gravel layer will produce capacities  $> 200$  tons. Therefore, estimate pile length to top of gravel.

**Step 4A: Determine soil resistance to driving SRD for 70 ton load with SF = 2.**

$$\text{SRD} = R_{s(\text{sand})} + \frac{R_{s(\text{clay})}}{\text{sensitivity}} + (70 \text{ tons} \times 2)$$

$$= 9.6 \text{ tons} + \frac{43.1 \text{ tons}}{2} + 140 \text{ tons}$$

(note sensitivity = 2 is given in problem statement)

$$\text{SRD} = 171.1 \text{ tons}$$

**B. For 12 inch H-Pile\* (120 ton design load)**  
**\*Assume HP 12x84 pile section**

**Step 2B: Compute Shaft Resistance**

(References to Figures and Tables are as in Step 2A above)

Sand Layer (4 ft - 15 ft)

$$V = \frac{24.6}{144} = 0.17 \text{ ft}^3/\text{ft}$$

$$\frac{\delta}{\phi} = 0.80$$

$$\delta = (0.80)(36^\circ) = 28.8^\circ$$

$$K_\delta = 1.30$$

$$C_F = 0.92$$

$$C_d = 4 \text{ ft}$$

$$p_d \text{ Avg. @ } \frac{4 \text{ ft} + 15 \text{ ft}}{2} = 9.5 \text{ ft is } 1,050 \text{ psf}$$

$$R_{s(\text{sand})} = (1.30)(0.92)(1,050 \text{ psf})(4 \text{ ft})(\sin 28.8^\circ) (11 \text{ ft})$$

$$R_{s(\text{sand})} = 26,619 \text{ lbs} \approx 13.0 \text{ tons}$$

Clay Layer (15 ft - 40 ft)

$$R_{s(\text{clay})} = c_a C_d D$$

$$c_a \text{ (Adhesion)} \cong 1,100 \text{ psf (assume adhesion} \approx \text{cohesion, i.e., } \alpha \approx 1.0)$$

$$R_{s(\text{clay})} = 1,100 \text{ psf (4 ft) } 25 \text{ ft} = 110,000 \text{ lbs} = 55 \text{ tons}$$

- \*Gravel Layer (Try 4 ft Embedment, ie. 40 ft – 44 ft)

\*Use  $\phi_{\text{Max}} = 36^\circ$

$$q_s = (K_\delta)(C_F)(P_0)(C_d)(\text{Sin } \delta)D$$

$$V = \frac{24.6}{144} = 0.17 \text{ CF/Ft.}$$

$$\frac{\delta}{\phi} = 0.80$$

$$\delta = (0.80)(36^\circ) = 28.8^\circ$$

$$K_\delta = 1.30$$

$$C_F = 0.92$$

$$C_d = 4 \text{ ft}$$

$$p_d = 3,200 \text{ psf}$$

$$R_{s(\text{gravel})} = (1.30)(0.92)(3,200 \text{ psf})(4 \text{ ft})(\text{sin } 28.8^\circ)(4 \text{ ft})$$

$$R_{s(\text{gravel})} = 29,500 \text{ lbs} \approx 14.7 \text{ tons}$$

**Step 3B:**      **Compute toe resistance** (Use  $\phi = 43^\circ$ ) at 44 ft

(References to Figures and Tables are as in Step 3A above)

- Gravel Layer

For  $\phi = 43^\circ$ ,  $\alpha_t \approx 0.75$  from Figure 9-13(a) in Chapter 9

For  $\phi = 43^\circ$ ,  $N'_q = 300$  from Figure 9-13(b) in Chapter 9

$$\begin{aligned} \text{c. } R_t &= A_p \alpha_t p_t N'_q && \text{(Equation 9-7a in Chapter 9)} \\ &= \frac{24.6 \text{ in}^2}{144 \text{ in}^2 / \text{ft}^2} (0.75)(3,000 \text{ psf})(300) \end{aligned}$$

$$R_t = 115,313 \text{ lbs} \approx 57.7 \text{ tons}$$

$$\begin{aligned}
 \text{d. } R_t(\text{max}) &= q_L \times A_p && \text{(Equation 9-7b in Chapter 9)} \\
 &= (680 \text{ksf}) \frac{24.6 \text{in}^2}{144 \text{in}^2 / \text{ft}^2} && (q_L = 680 \text{ksf for } \phi = 43^\circ \text{ from Figure 9-14 in Chapter 9)}
 \end{aligned}$$

$$R_t(\text{max}) = 116.2 \text{ kips} = 58.1 \text{ tons} > 57.7 \text{ tons}$$

$$\therefore R_t = 57.7 \text{ tons}$$

- Total useable soil capacity below clay is = 14.7 tons + 57.7 tons = 72.4 tons
- Total Required capacity is 240 Tons
- Extending pile to 50 ft only increases  $R_s$  to 37 tons

Conclusion: Pile must bear on rock to develop 240 tons capacity below clay layer.  
Therefore estimate pile length to rock.

**Step 4B: Determine soil resistance to driving SRD for 120 ton load with SF = 2.**

$$\begin{aligned}
 \text{SRD} &= R_{s(\text{sand})} + \frac{R_{s(\text{clay})}}{\text{sensitivity}} + (120 \text{ tons} \times 2) \\
 &= 13.0 \text{ tons} + \frac{55 \text{ tons}}{2} + 240 \text{ tons} && \text{(note sensitivity = 2 is given in problem statement)}
 \end{aligned}$$

$$\text{SRD} = 280.5 \text{ tons}$$

\* Composed of 37 tons skin friction in the gravel and 203 tons in end bearing on rock.

## STATIC PILE ANALYSIS - ABUTMENT @ STA 93 + 50

### A. For 12 inch Diameter Pipe Pile

**Step 2A & 3A:** Based on computation at the pier, the pipe pile will develop the 140 ton ultimate load at the top of the gravel layer, ie. an estimated length of 65 ft. However the driving resistance will increase.

**Step 4A:** Compute driving resistance.

- Fill (Use  $\phi_{\max} = 36^\circ$ )

$$q_s = (K_\delta)(C_F)(p_o)(C_d)(\sin \delta) C_d D$$

$$V = 0.785 \text{ ft}^3/\text{ft.}$$

$$\frac{\delta}{\phi} = 0.6 \text{ (for closed end pipe pile from Figure 9-7 in Chapter 9)}$$

$$\delta = (0.6)(36^\circ) = 21.6^\circ$$

$$K_\delta = 1.92 \text{ (for } \phi = 36^\circ \text{ from Table 9-6(a) in Chapter 9)}$$

$$\text{Correction Factor, } C_F = 0.75 \text{ (from Figure 9-12 in Chapter 9)}$$

$$C_d = \pi d = \pi (1 \text{ ft}) = 3.14 \text{ ft}$$

$$p_d = 1,650 \text{ psf}$$

$$\begin{aligned} R_{s(\text{fill})} &= K_\delta (C_F)(p_d)(C_d)(\sin \delta)D \text{ (Equation 9-6 in Chapter 9)} \\ &= (1.92)(0.75)(1,650 \text{ psf})(3.14 \text{ ft})(\sin 21.6^\circ)(23 \text{ ft}) \\ R_{s(\text{fill})} &= 63,168 \text{ lbs} \approx 31.6 \text{ tons} \end{aligned}$$

- Sand

$$\begin{aligned} R_{s(\text{sand})} &= (1.92)(0.75)(3,330 \text{ psf})(3.14 \text{ ft})(\sin 21.6^\circ) (7 \text{ ft}) \\ R_{s(\text{sand})} &= 38,800 \text{ lbs} \approx 19.4 \text{ tons} \end{aligned}$$

- Clay

$$R_{s(\text{clay})} = \frac{c_a C_d D}{\text{sensitivity}}$$

$$R_{s(\text{clay})} = \frac{(1,100 \text{ psf})(3.14)(1 \text{ ft})(35 \text{ ft})}{2} = 60,445 \text{ lbs} \approx 30.2 \text{ tons}$$

Soil Resistance to driving, SRD @ top of gravel= 31.6 tons + 19.4 tons +30.2 tons + 140 tons  
 = 221.2 tons

**Step 5A: Check driving resistance in embankment.**

Assume pile tip embedded 23 ft

$$R_{s(\text{fill})} = 31.6 \text{ tons (from Step 4A)}$$

$$R_t = A_p \alpha_t p_{d \text{ at } 23'} N'q$$

$$= (0.785 \text{ ft}^2) (0.74) (2,990 \text{ psf}) 170$$

$$R_t = 147.6 \text{ tons} < R_t (\text{max}) = 200 (0.785) = 157 \text{ tons}$$

$$\text{SRD}(\text{fill}) = 31.6 \text{ tons} + 147.6 \text{ tons} = 179.2 \text{ tons}$$

To overcome this SRD, pre-augering may be required through the fill

**B. 12 inch H – Pile (120 ton design) – assume HP 12×84 section**

Steps 2B & 2C: Estimate length to rock i.e., 75 ft, as pier computation showed H-pile must bear on rock to achieve designed ultimate capacity.

**Step 4B: Compute driving resistance.**

- Fill

$$V = 0.17 \text{ CF/Ft.}$$

$$\frac{\delta}{\phi} = 0.80$$

$$\delta = (0.80)(36^\circ) = 28.8^\circ$$



$$K_\delta = 1.30$$

$$C_F = 0.92$$

$$R_{s(\text{fill})} = (1.30)(0.92)(1,495 \text{ psf})(4 \text{ ft})(\sin 28.8^\circ)(23 \text{ ft})$$

$$R_{s(\text{fill})} = 79,247 \text{ lbs} \approx 39.6 \text{ tons}$$

- Sand

$$R_{s(\text{sand})} = (1.30)(0.92)(3,303 \text{ psf})(4 \text{ ft})(\sin 28.8^\circ)(7 \text{ ft})$$

$$R_{s(\text{sand})} = 53,287 \text{ lbs} \approx 26.6 \text{ tons}$$

- Clay

$$R_{s(\text{clay})} = \frac{c_a C_d D}{\text{sensitivity}}$$

$$R_{s(\text{clay})} = \frac{(1,100 \text{ psf})(4 \text{ ft})(35 \text{ ft})}{2} = 77,000 \text{ lbs} = 38.5 \text{ tons}$$

- Gravel

$$R_{s(\text{gravel})} = (1.30)(0.92)(5,600 \text{ psf})(4 \text{ ft})(\sin 28.8^\circ)(10 \text{ ft})$$

$$R_{s(\text{gravel})} = 129,063 \text{ lbs} \approx 64.5 \text{ tons}$$

$$\text{Total } R_s = R_{s(\text{fill})} + R_{s(\text{sand})} + R_{s(\text{clay})} = R_{s(\text{gravel})}$$

$$\text{Total } R_s = 39.6 \text{ tons} + 26.6 \text{ tons} + 38.5 \text{ tons} + 64.5 \text{ tons}$$

$$\text{Total } R_s = 169.2 \text{ tons} = 338.4 \text{ kips}$$

$$\text{SRD} = 39.6 \text{ tons} + 26.6 \text{ tons} + 38.5 \text{ tons} + \underbrace{[64.5 \text{ tons} + 175.5 \text{ tons}]}_{240 \text{ tons}}$$

$$\text{SRD} = 344.7 \text{ tons} = 689.4 \text{ kips}$$

$$\therefore (\text{Total } R_s) / \text{SRD} = 338.4 \text{ kips} / 689.4 \text{ kips} = 0.49 \text{ or } 49\%$$

### Step 5B: Check H – Pile driving resistance in embankment

Assume pile tip embedded 23 ft

$$R_{s(\text{fill})} = 39.6 \text{ tons (from Step 4B)}$$

$$R_t = A_p \alpha_t p_{d \text{ at } 23'} N' q$$

$$R_t = \frac{24.6 \text{ in}^2}{144 \text{ in}^2 / \text{ft}^2} (0.74)(2,990 \text{ psf}) 170$$

$$R_t = 64,257 \text{ lbs} \approx 32.1 \text{ tons} < q_{\text{lim}} = (200)(0.17) = 34 \text{ tons} > 32.1 \text{ tons (use 32.1 tons)}$$

$$\text{SRD (fill)} = 39.6 \text{ tons} + 32.1 \text{ tons} = 71.7 \text{ tons}$$

To overcome this SRD, pre-augering may be required through the fill

## Summary of the Pile Design Phase for the Apple Freeway Design Problem

- Design Soil Profile

Strength value selected for all layers.

- Static Analysis - Pier

12 inch closed end pipe pile - 70 ton – 36 ft length required  
12 inch HP 12x84 - 120 ton – 46 ft length required.

- Static Analysis Abutment

12 inch closed end pipe pile- 70 ton – 65 ft length required  
12 inch HP 12 x 84- 120 ton – 75 ft length required.

- Soil Driving Resistance

Driving Resistances computed for both pipe and H-piles to permit design check of pile section overstress.

Pipe pile will require pre-augering through embankment.

- Abutment Lateral Movement

From Step 2 in Section A.6-6, 3 inch possible horizontal movement even with a pile foundation unless recommended waiting period observed prior to pile driving.

Subsurface Explorations	Terrain Reconnaissance Site Inspection Subsurface explorations	✓
Basic Soil Properties	Visual Description Classification Tests Subsurface Profile	✓
Laboratory Testing	p <sub>o</sub> Diagram Test Request Consolidation Results Strength Results	✓
Slope Stability	Design Soil Profile Circular Arc Sliding Block Analysis	✓
Approach Roadway Settlement	Design Soil Profile Settlement Time – Rate Surcharge Vertical Drains Lateral Squeeze	✓
Spread Footing Design	Design Soil Profile Pier Bearing Capacity Pier Settlement Abutment Settlement Vertical Drains Surface	✓
Driven Pile Design	Design Soil Profile Static Analysis – Pier Pipe Pile H – Pile Static Analysis – abutment Pipe Pile H – Pile Driving Resistance Abutment Lateral Movement	✓
		✓
→	<b>Construction Monitoring</b>	Wave Equation Hammer Approval Embankment Instrumentation

**Figure A.9-1. Status of geotechnical work.**

## SECTION A.9 CONSTRUCTION MONITORING OF DRIVEN PILES

In this Section the Apple Freeway Design Example is used to illustrate the wave equation analysis using a wave equation analysis program. The use of wave equation analysis for pile driveability analysis, checking suitability of contractors driving system, and determining pile driving criteria is addressed. A commonly used wave equation analysis program is the GRLWEAP. Other similar products such as TNOWave are also available as noted in Chapter 9. Herein, the program GRLWEAP will be used for the example problem. The use of GRLWEAP does not constitute an endorsement of the product by FHWA.

**Given:** Using the soil profile and pile driving resistance previously computed (Section A.8)

**Required:** Complete wave equation analyses using the GRLWEAP program for the following:

- Driveability of the proposed design pile section
- Acceptance of contractors driving system
- Production pile driving criteria

**Solution:**

### Driveability of Proposed Design Pile Section

Proposed pile section is a HP 12 × 84. The maximum driving resistance determined from static analyses is at the east abutment where the total driving resistance including embankment penetration is 689.4 kips. Perform wave equation analysis for the proposed pile section using the maximum driving resistances.

**Step 1: Prepare Wave Equation Input:**

1. Select hammer (IHAMR)

- Hammer size selected from Figure 9-44 in Chapter 9 using maximum driving resistance of 689.4 kips (345 tons). Minimum hammer energy = 57,000 ft-lbs.
- Using GRLWEAP help screen, scan hammer library for hammers with sufficient energies. Select Delmag 30 – 13 hammer which has slightly more energy than required (66,000 ft-lbs) to insure efficient driving.

2. Select uniform or non-uniform pile cross-section along the entire pile (NCROSS)

Select non-uniform option (1) because pile point will be used. Pile cross-section described on input screen NCROSS =1 as shown on “page 7” of the GRLINP input printoutogram.

3. Select percent pile skin friction (IPERC)

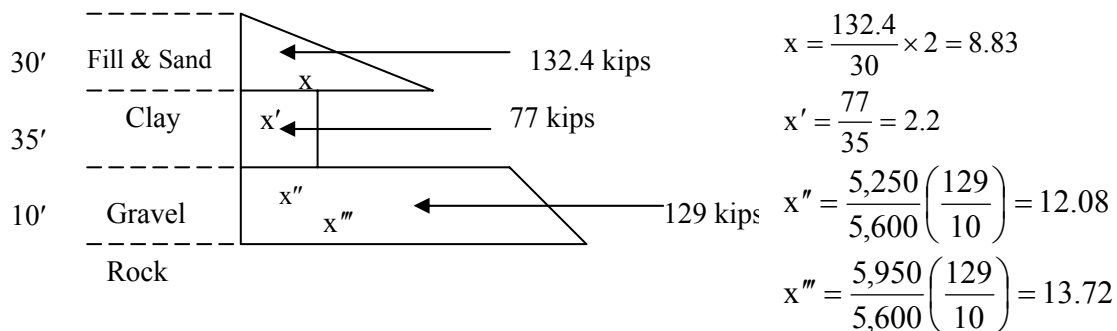
- From static analysis, (skin friction resistance/total driving resistance) =  $(338/689)(100) = 49\%$ .

4. Select skin friction distribution (ITYS)

- Use the actual skin friction distribution determined in the static analysis ultimate driving resistance computation (ITYS = 0). An analysis using the actual skin friction distribution is more realistic and accurate. From static analyses (see next page).

5. Select helmet and hammer cushion information (helmet weight, hammer cushion area, elastic modulus and thickness).

- Using GRLWEAP help screen, scan hammer library for Delmag Hammers using the proposed pile section.



6. Select Pile Top Information (length, x-section area, elastic modulus, specific weight, coefficient of restitution).

- Using GRLWEAP help screen, obtain the x-sectional area and weight for the proposed HP12×84.

7. Select soil parameters (quake and damping).

- Using GRLWEAP help screen, select appropriate soil parameters.

8. Select ultimate driving capacities to be analyzed.

- Input a range of ultimate driving capacities around and including the maximum soil driving resistance (SRD) calculated from static analyses (689.4 kips). A range of capacities highlights trends within the graphical plots.

GRLINP Input Screens for HP 12x84 Driven through the Embankment Material –  
 Ultimate Resistance 689.4 kips.

Title: APPLE FREEWAY H-PILE @ ABUTMENT Page: 1

ANALYSIS OPTIONS  
 IOUT IJJ IHAMR IOSTR IFUEL IPEL  
 . . 13. . . .

ANALYSIS OPTIONS  
 N ISPL NCROSS IBEDAM IPERCS ISMITH DMPEXP  
 . . 1. . 49. . .0

ANALYSIS OPTIONS  
 ITYS IPHI IRSAO ITER IDAHA IMAXT  
 . . . . .

HELMET AND HAMMER CUSHION INFORMATION

Helmet Weight	Area	ElasMod	Thickness	Hammer C.O.R.	Cushion RoundOut	Stiffness
2.15	283.50	280.0	2.000	.800	.0100	.0

Title: APPLE FREEWAY H-PILE @ ABUT FULL EMBEDMT Page: 2

PILE CUSHION INFORMATION

Area	Elastic Modulus	Thickness	C.o.R.	Round Out	Stiffness
.00	.0	.000	.500	.0100	.0

PILE TOP INFORMATION

Total Length	X-Sectn Area	Elastic Modulus	Specific Weight	C.o.R.	Round Out	D.O.A.1 Slick P2	D.O.A.2 Stiff P2
75.00	24.60	30000.0	492.00	.850	.0100	.00	.00

HAMMER OVERRIDE VALUES

Stroke	Efcy	Pressure	Reaction Weight	ComDelay Ign Vol	Comb Exp Coeff	Stroke Conv Crit
.00	.000	.0	.000	.000	.00	.00

SOIL PARAMETERS

Quake		Damping		Toe No. 2		Depth
Skin	Toe	Skin	Toe	Quake	Damping	Fraction
.100	.100	.050	.150	.000	.000	.000

Title: APPLE FREEWAY H-PILE @ ABUTMENT Page: 3

ULTIMATE CAPACITIES  
 Give up to 10 Capacities (5 on first line)

350.00	550.00	631.80	689.40	740.00
--------	--------	--------	--------	--------

ULTIMATE CAPACITIES (Continued)  
 (5 on the second line)

.00	.00	.00	.00	.00
-----	-----	-----	-----	-----

**CONTINUE GRLINP INPUT SCREENS FOR HP12x84 (689.4 kips).**

Title: APPLE FREEWAY H-PILE @ ABUTMENT Page: 7  
 NCROSS=1: NON-UNIFORM PROFILE, 1ST PILE \*\* PILE LENGTH: 75.00

Depth	Area	Elastic Modulus	Specific Weight
.00	24.60	30000.0	492.00
74.60	24.60	30000.0	492.00
74.60	42.50	30000.0	492.00
75.00	42.50	30000.0	492.00

75500 PILE POINT (12" H)  
 AREA = 42.5 in<sup>2</sup>  
 HEIGHT = 4.8 in

Title: APPLE FREEWAY H-PILE @ ABUTMENT Page: 8  
 ITYS=-1, 0: SKIN FRICTION DISTRIBUTION, 1ST PILE \*\* PILE LENGTH: 75.00

Depth	Relative Distribn
.00	.000
30.00	8.830
30.00	2.200
65.00	2.200
65.00	12.080
75.00	13.720

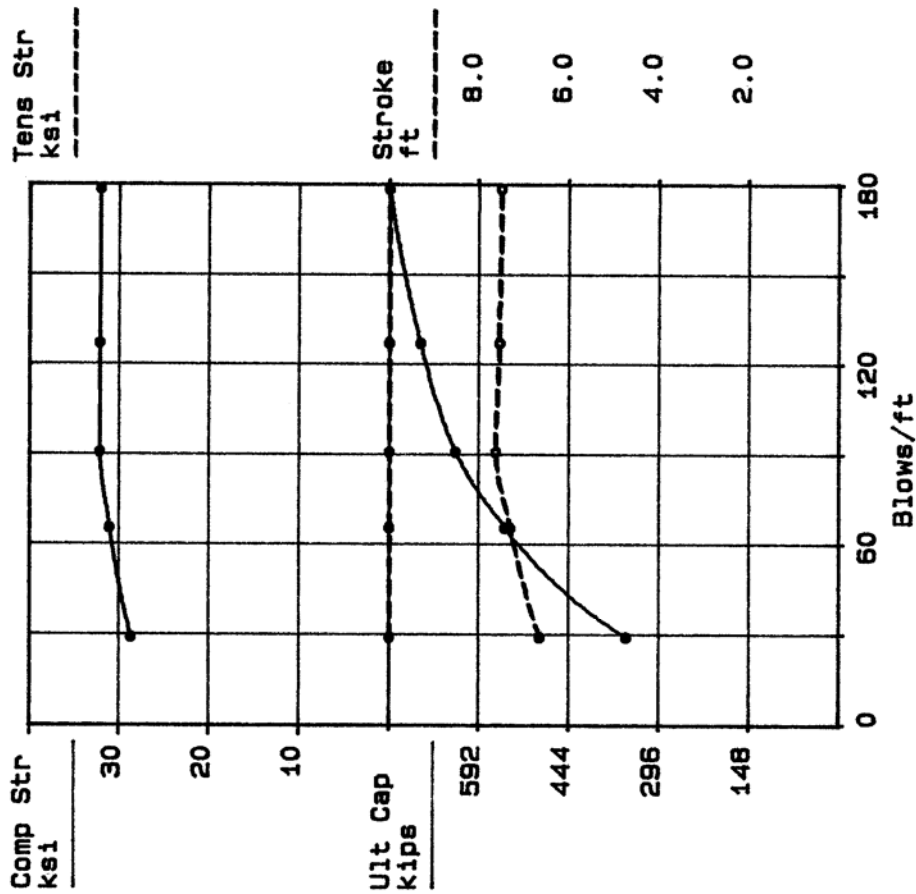
**SUMMARY OF GRLWEAP RESULTS FOR HP12X84 (DELMAG 30-13)**

Rut (kips)	Bl Ct (bpf)	Stroke down (ft)	Stroke up (ft)	min Str (ksi)	max Str (ksi)	ENTHRU (kip-ft)	Bl Rt (b/min)
350.0	32.9	6.83	6.70	.00(	29.09(	25.9	45.3
550.0	79.6	7.38	7.32	.00(	31.53(	26.3	43.5
631.8	114.8	7.66	7.44	.00(	32.67(	26.9	42.9
689.4	170.6	7.51	7.47	.00(	32.46(	26.3	43.1
740.0	256.7	7.44	7.49	.00(	32.19(	25.9	43.2

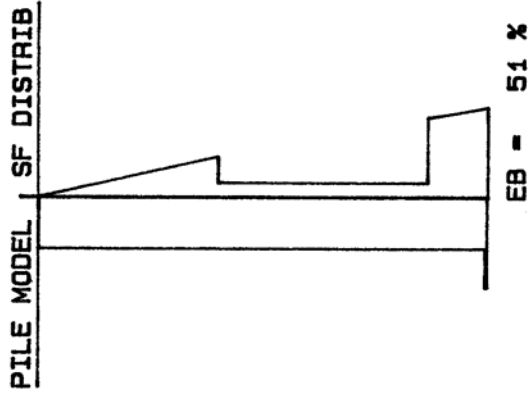
G R L W E A P - Federal Highway Adm.

APPLE FREEWAY H-PILE @ ABUTMENT

05/10/93



DELMAG D 30-13  
 Efficiency .720  
 Helmet 2.15 kips  
 H Cushion 39690 k/in  
  
 G = .100 .100 in  
 J = .050 .100 s/ft  
  
 Pile Length 75.00 ft  
 P-Top Area 24.60 in<sup>2</sup>



APPLE FREEWAY - HP12X84 DRIVEN THROUGH EMBANKMENT MATERIAL

**SUMMARY OF DRIVEABILITY ANALYSES FOR HP12X84**

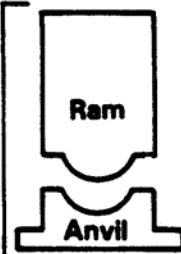
Pile section is adequate for the hardest driving conditions encountered at the east abutment. Driving stresses are below the maximum allowable driving stress of 32.4 ksi. Stresses are insensitive to the blow count and therefore, the pile won't be damaged when seated into the rock.

HP12X84 pile section is acceptable ✓

**ACCEPTANCE OF CONTRACTORS DRIVING SYSTEM**

Contractor has submitted a ICE 70-S driving system. The pile and driving equipment data sheet is shown below.

**Hammer Components:**



**Ram**

**Anvil**

**Hammer**

Manufacturer: ICE Model: 70S

Type: OED Serial No.: 123

Rated Energy: 79,000 lb-ft at 10 ft Length of Stroke

Modifications: \_\_\_\_\_

Material: Micarta

Thickness: 2 in Area: 398 in<sup>2</sup>

Modulus of Elasticity - E: 280,000 psi (P.S.I.)

Coefficient of Restitution - e: 0.8



**Hammer Cushion**

**Drive Head**

Helmet  
Bonnet  
Anvil Block  
Pile Cap

Weight: 2.44 kips

Cushion Material: N/A

Thickness: \_\_\_\_\_ Area: \_\_\_\_\_

Modulus of Elasticity - E: \_\_\_\_\_ (P.S.I.)

Coefficient of Restitution: \_\_\_\_\_



**Pile**

Pile Type: HP12X84

Length (in-Lead): 75'

Weight/ft.: 498 lb/ft<sup>3</sup>

Wall Thickness: \_\_\_\_\_ Taper: No

Cross Sectional Area: 24.6 in<sup>2</sup> in<sup>2</sup>

Design Pile Capacity: 120 (Tons)

Description of Splice: \_\_\_\_\_

Tip Treatment Description: \_\_\_\_\_

† Driving Resistance: 280.5 tons @ Pier  
344.7 tons @ Embankments

Perform wave equation analysis for the submitted driving system.

- Modify hammer data in the GRLWEAP input file previously used to analyze the HP 12x84 pile section. Use the submitted driving system data, and the GRLWEAP driveability option.

**GRLINP Input Screens for GRLWEAP Driveability option. Screens not Shown Below are Unchanged from the Pile Section Analysis.**

```

Title:  FULL EMBEDMT - DRIVABILITY OPTION                               Page:    1

ANALYSIS OPTIONS
  IOUT      IJJ      IHAMR      IOSTR      IFUEL      IPEL
  -100.      .        129.      .          .          .

ANALYSIS OPTIONS
  N         ISPL      NCROSS      IBEDAM      IPERCS      ISMITH      DMPEXP
  .         .         1.         .          .          .          .0

ANALYSIS OPTIONS
  ITYS      IPHI      IRSAO      ITER      IDAHA      IMAXT
  .         .         .         .         .         .

HELMET AND HAMMER CUSHION INFORMATION
Helmet      Area      ElasMod      Thickness      Hammer      Cushion      RoundOut      Stiffness
Weight      C.O.R.
  2.44      398.00      280.0      2.000      .800      .0100      .0
  
```

**Continue GRLINP Input Screens for GRLWEAP Driveability Options Analysis of Ice 70S Driving System.**

```

Title:  FULL EMBEDMT - DRIVABILITY OPTION                               Page:    3

IPERCS = 0: Friction Loss/Gain Factors
Give up to 10 Friction Loss/Gain Factors (5 on first line)
  .90      1.00      1.10      .00      .00

IPERCS = 0: Friction Loss/Gain Factors
(5 on the second line)
  .00      .00      .00      .00      .00
  
```

Title: FULL EMBEDMT - DRIVABILITY OPTION

Page: 6

IPERCS=0: DEPTHS & DRIVING SYSTEMS MODIFICATIONS \*\* PILE LENGTH: 75.00

Analysis	Stroke	IFUEL	Efficiency	Stiffn. Factor	Cushion	CoR
20.00	.00	.0	.00	.00	.00	.00
30.00	.00	.0	.00	.00	.00	.00
45.00	.00	.0	.00	.00	.00	.00
65.00	.00	.0	.00	.00	.00	.00
74.00	.00	.0	.00	.00	.00	.00
74.50	.00	.0	.00	.00	.00	.00
74.88	.00	.0	.00	.00	.00	.00
75.00	.00	.0	.00	.00	.00	.00
.00	.00	.0	.00	.00	.00	.00

Title: FULL EMBEDMT - DRIVABILITY OPTION

Page: 8

IPERCS = 0: SOIL PARAMETERS VS DEPTH \*\* PILE LENGTH: 75.00

Depth	Friction	Bearing	Quake	Toe Quake	Toe Skin Damping	Toe Damping	Sens.
.00	.000	5.000	.100	.100	.050	.150	.000
30.00	8.830	58.000	.100	.100	.050	.150	.000
30.00	2.200	5.000	.100	.100	.200	.150	.000
65.00	2.200	5.000	.100	.100	.200	.150	.000
65.00	12.080	96.000	.100	.100	.050	.150	.000
75.00	13.720	351.000	.100	.100	.050	.150	.000

### SUMMARY RESULTS OVER DEPTH FOR ICE 70S HAMMER

FRICITION LOSS/GAIN FACTOR: .900

Depth (ft)	Rut (kips)	Frictn (kips)	End Bg (kips)	Bl Ct (bpf)	max Str (ksi)	min Str (ksi)	Bl Rte (b/min)	ENTHRU (kip-ft)
20.0	83.7	48.4	35.3	4.1	15.493	.000	45.4	34.8
30.0	170.1	114.4	55.7	8.5	25.056	-.032	40.8	35.0
45.0	148.1	143.3	4.8	7.2	23.653	-4.327	41.7	33.6
65.0	189.3	184.5	4.9	10.9	27.935	-7.017	39.9	31.3
74.0	384.7	289.6	95.1	31.3	31.664	-.150	37.2	29.3
74.5	390.8	295.7	95.1	31.6	31.888	-.148	37.1	29.7
74.9	395.5	300.4	95.1	32.1	31.942	-.154	37.1	29.7
75.0	651.9	302.9	349.0	128.3	31.664	.000	36.8	30.0

Total Driving Time 15.72 min;

Total No. of Blows 631

FRICION LOSS/GAIN FACTOR: 1.000

Depth (ft)	Rut (kips)	Frictn (kips)	End Bg (kips)	Bl Ct (bpf)	max Str (ksi)	min Str (ksi)	Bl Rte (b/min)	ENTHRU (kip-ft)
20.0	89.6	54.1	35.5	4.3	15.098	.000	45.3	34.0
30.0	183.3	127.5	55.8	9.7	24.582	-.135	40.9	32.0
45.0	164.6	159.8	4.8	8.4	24.303	-4.221	41.2	32.5
65.0	210.3	205.4	4.9	12.8	28.075	-6.177	39.5	30.2
74.0	417.1	322.0	95.1	35.1	32.602	-.115	37.0	29.5
74.5	423.9	328.8	95.2	36.1	32.693	-.069	37.0	29.4
74.9	429.1	334.0	95.2	36.8	32.740	-.052	37.0	29.4
75.0	685.8	336.7	349.1	158.6	32.103	.000	37.3	29.6

Total Driving Time 18.08 min;

Total No. of Blows 720

FRICION LOSS/GAIN FACTOR: 1.100

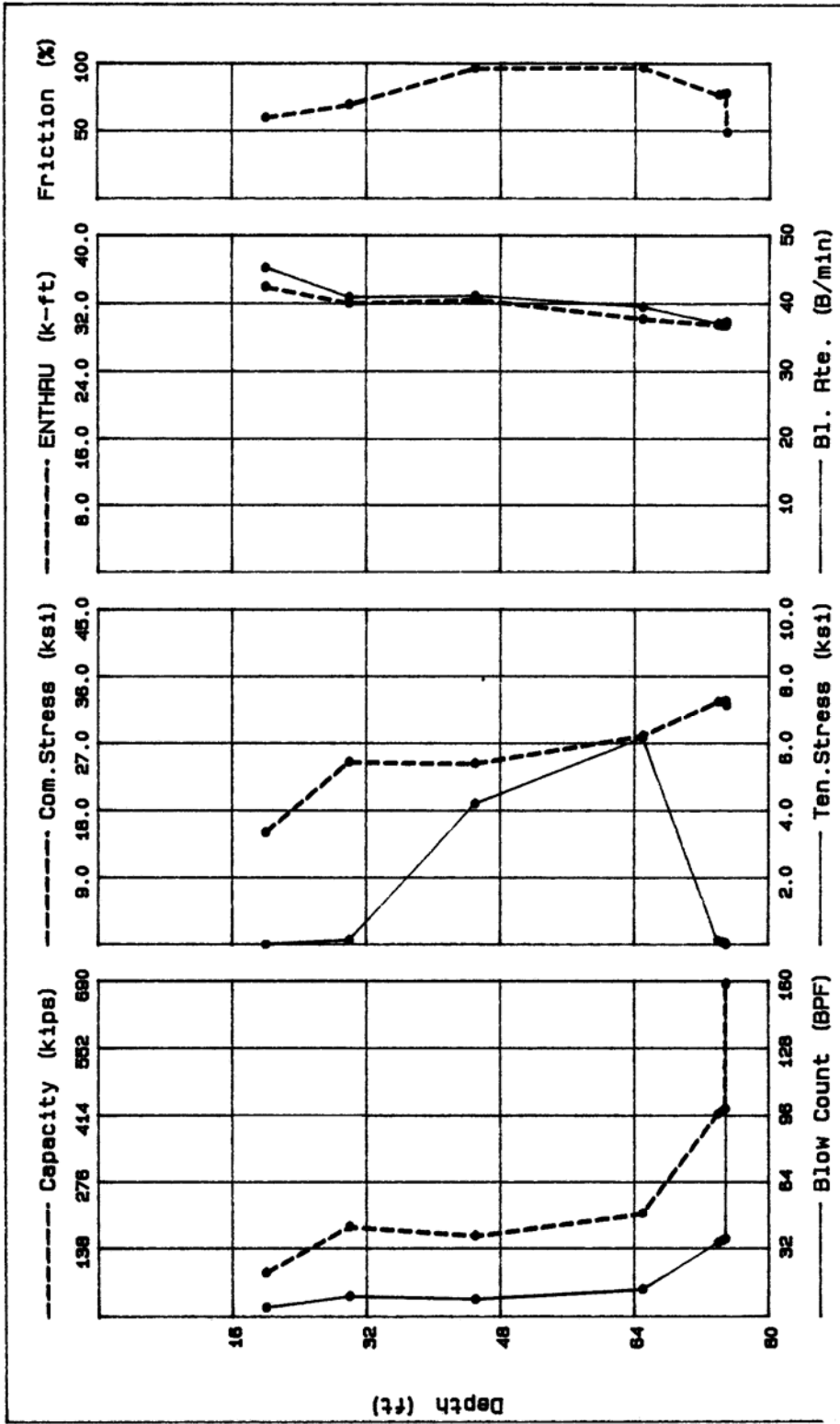
Depth (ft)	Rut (kips)	Frictn (kips)	End Bg (kips)	Bl Ct (bpf)	max Str (ksi)	min Str (ksi)	Bl Rte (b/min)	ENTHRU (kip-ft)
20.0	95.5	59.8	35.7	4.5	16.319	.000	44.9	34.6
30.0	196.6	140.6	56.0	10.2	25.761	-.978	40.6	32.9
45.0	181.2	176.3	4.8	9.3	26.005	-4.863	40.7	32.7
65.0	231.2	226.3	4.9	14.3	29.119	-5.837	39.0	30.6
74.0	449.6	354.4	95.2	40.4	33.106	-.338	37.4	29.2
74.5	457.1	361.9	95.2	41.6	33.171	-.348	37.4	29.2
74.9	462.8	367.6	95.2	42.5	33.191	-.350	37.4	29.1
75.0	719.6	370.5	349.2	204.9	32.518	-.066	37.3	29.2

Total Driving Time 20.19 min;

Total No. of Blows 799

G R L W E A P - F e d e r a l H i g h w a y A d m .

FULL EMBEDMT - DRIVABILITY OPTION Friction Factor=1.000 05/12/93



APPLE FREEWAY - DRIVEABILITY ANALYSIS FOR ICE 70S HAMMER

## SUMMARY OF DRIVEABILITY ANALYSES FOR ICE 70S

Driving Stresses: 32.7  $\approx$  32.4 ksi ✓ OKAY

Driving stresses vary between 31.66 ksi (0.9 friction reduction) to 33.19 ksi (1.1 friction reduction), well below the yield strength of 36 ksi. Since, the maximum stresses occur when the pile has penetrated the rock and is at near refusal conditions, the piles should be capable of being seated into the rock without damage.

Blow Count: 159 bpf  $\approx$  144 bpf ✓ OKAY

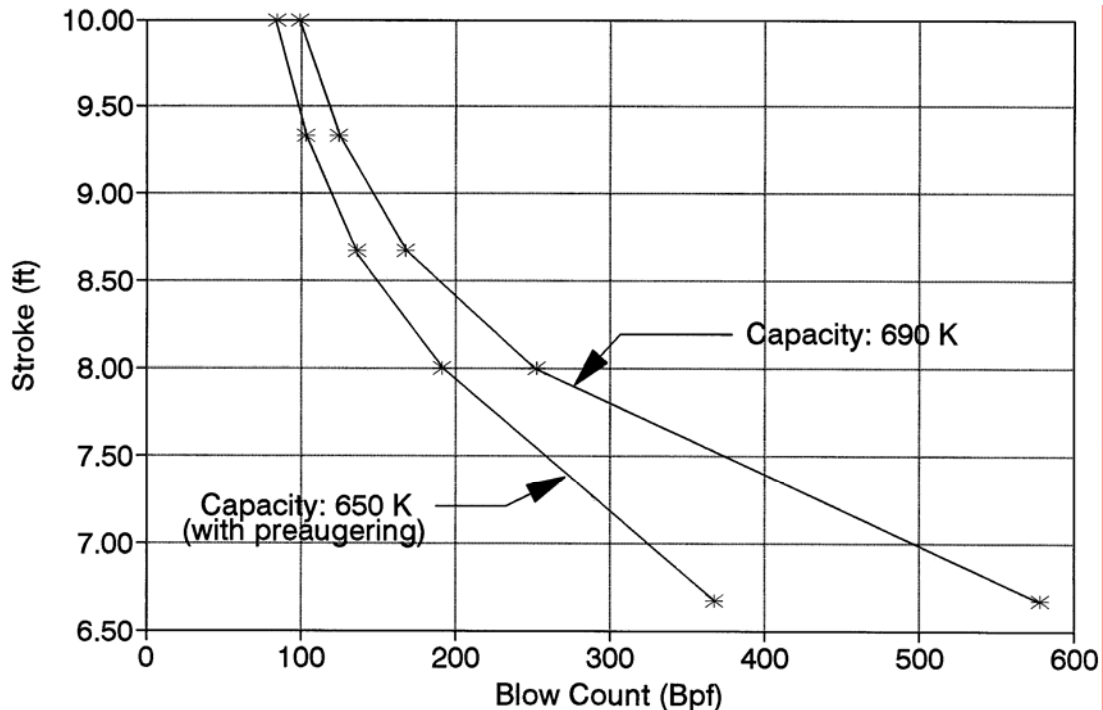
The blow count is approximately 35 bpf at just above the rock line, and near refusal 150 - 220 bpf in the rock layer. Therefore, the hammer should (if operating properly) penetrate quickly through the embankment and into the rock.

**HAMMER APPROVED ✓**

### **PRODUCTION PILE DRIVING CRITERIA FOR ICE 70S DRIVING SYSTEM**

Drive HP12x84 pile through the embankment material and into the rock. Pile driving shall be terminated when the combination of stroke and blow count indicates a driving capacity of 690 kips. If pre-augering is used the driving capacity of 650 kips should be attained.

Stroke Vs. Blow Count Plot



## **CONSTRUCTION CONTROL**

- Pile Driveability

Driveability of HP 12 x 84 pile

Section verified for most difficult driving condition.

- Driveability versus Depth

Driveability of HP 12 x 84 computed for full 75 feet depth.

Pile installation time expected to vary between 16 and 20 minutes (no pre- augering).



**SECTION A.10**  
**GEOTECHNICAL DESIGN SUMMARY REPORT**

A typical example of a Geotechnical Design Summary Report is presented in the following section with reference to the Apple Freeway Design Example. The report illustrates the inclusion of various items discussed in the preceding sections of this chapter and summarize the pertinent results and conclusions obtained from the various analysis/design stages in the preceding chapters.

# WORKSHOP DESIGN PROBLEM - GEOTECHNICAL DESIGN SUMMARY REPORT

December 15, 2006  
Geotechnical Design Summary Report

To: Mr. A. J. Jones  
Chief Engineer

From: Mr. A. B. Smith  
Chief Foundation Engineer

Subject: Interstate 0 Structure over the Apple Freeway

---

The Geotechnical Section has completed an analysis of the foundation conditions at the site of the subject structure. Our analysis is based on the following information:

1. A 1-inch equals 20 feet plan and profile prepared by the Bridge Division and received in this office October 1, 2006.
2. An interpretation of the boring logs and analysis of soil samples from three drill holes numbered BAF-1 thru 3, nine auger holes numbered EA-1 thru 9, one drill hole numbered BAF-4 from which undisturbed samples were taken, and four Cone Penetration Test (CPT) soundings numbered CPT BAF-1 through 4.
3. Laboratory testing on undisturbed samples from BAF-4.

## Subsurface Conditions:

The general subsurface conditions are shown on Drawing No. 5 GS 331.

## Foundation Recommendations:

1. Elevation Assumptions

The foundation recommendations are based on the following bottom of footing elevations:

West Abutment	1011
Pier	992
East Abutment	1012

Changes to footing elevations may affect the foundation recommendations and should be discussed with this office.

## 2. Embankment Construction

### A. Unsuitable Subexcavation

An approximate 1 to 3-foot thick organic layer exists between approximate stations 92+70 to 94+00 in the area of the east approach embankment. This organic layer should be removed and replaced with granular embankment material in accordance with Bridge Design Data Sheet 80-1.

### B. Embankment Material and Placement

The approach embankment shall be constructed of materials placed in accordance with Bridge Design Data Sheet 80-1.

### C. Embankment Settlement

An estimated 12 inches of fill settlement will occur due to consolidation of the 35-foot thick clay layer underlying the proposed 30-foot high east approach embankment. Estimated settlement time for 90 percent primary settlement is 14 months. Settlement time can be reduced to, (1) 6 months by use of a 10-foot surcharge fill or (2) 2 months with wick drains at 7.5 foot center to center spacing. Estimated cost for each of these treatments is:

<b>Treatment</b>	<b>Estimated Settlement Time</b>	<b>Estimated Extra Cost</b>
Fill only	14 months	\$ ---
Fill w/10 foot surcharge	6 months	120,000
Fill w/wick drains	2 months	172,000

It is understood the construction schedule will not allow a 14-month waiting period but will allow up to an 8-month waiting period, therefore, the 10-foot surcharge treatment is recommended as the most cost-effective method to reduce settlement time. The surcharge should be placed full height for a length of 500 feet back of the bridge ends on both the east and west approach and sloped at 1 vertical to 1.5 horizontal down to the embankment grade.

#### D. Embankment Stability

The estimated immediate end of construction factor of safety for the proposed 30' high east approach embankment is 1.63. The estimated immediate end-of-construction factor of safety for the proposed 30-foot fill plus 10 foot temporary surcharge is 1.33. Both factors of safety are adequate and no special approach embankment treatment is necessary. Long-term factor of safety will increase as consolidation of the foundation soils occur. The factor of safety for the west approach embankment will be higher as the fill height is 10' less. An analysis of highway borings confirms that no stability problems will occur due to the 500' extension of the surcharge.

#### E. Embankment Monitoring

Fill settlement is recommended to be monitored with settlement plates and piezometers. Settlement plates should be installed at existing ground elevation at centerline stations 90+00, 93 + 50, and 96 + 50. Piezometers to monitor excess pore pressure buildup and dissipation in the clay subsoil are recommended at centerline stations 93 + 50 and 96 + 50. A total of three piezometers should be installed at each location - one each at 20, 28, and 36 foot depths. Instrumentation will be installed by State forces.

### 3. Abutment Foundation

#### A. Spread Footings

The abutments may be supported on spread footings placed on compacted select material with a maximum allowable bearing capacity of 3 tons per square foot assuming a footing width of 7 feet is used. Changes to the footing width affect both bearing capacity and settlement and should be discussed with this office. The total settlement of the east and west abutments respectively will be 2.6 and 1.9

inches which occurs over respective time periods of 14 months and 7 months. About 60 percent of the settlement will occur in 2 months after structure construction. This settlement may be reduced by extending the surcharge period. For 90 percent consolidation the surcharge should remain in place a total of 8 months; 2 months longer than required for embankment considerations. If vertical drains are installed during embankment construction, these drains will reduce the time for abutment settlement such that only ¼” will remain 30 days after all abutment loads have been placed

## B. Piles

Two pile types were analyzed at the abutment; a displacement pile (12" diameter closed end pipe) and a non-displacement pile (HP 12 x 84 pile). Displacement type piles are not recommended due to their inability to be driven through the fill and the uncertainty of obtaining penetration in the dense gravel stratum. Non-displacement H-piles are recommended. However, to insure that the pile can be driven to rock without damage, the section should not be less than a HP 12 x 84 pile. A HP 12 x 84 pile driven to rock may be designed for a maximum load of 120 tons. Tip reinforcement, such as APF 75500, should be used to prevent tip damage by boulders in the gravel stratum and to insure penetration to rock. Estimated pile lengths are 60 feet at the west abutment and 75 feet at the east abutment.

At the abutments, negative skin friction may be expected if the piles are installed before fill settlement is complete. In addition lateral squeeze of the clay subsoil will occur as the clay consolidates. Therefore, to prevent increased vertical downdrag pile loads, bending of abutment piles and rotation of the abutment toward the fill, the abutment piling should not be installed until embankment settlement is complete.

The actual driving resistance estimated to develop the design load for the H-pile at the estimated length is 345 tons at the east abutment and 290 tons at the west abutment. The contractor should size his equipment to achieve this resistance without damaging the pile.

#### 4. Pier Foundation

##### A. Spread Footings

The pier may be supported on spread footings placed 4 feet below ground on natural undisturbed soil and designed for a maximum allowable bearing capacity of 3 tons per square foot assuming a footing width of 7' is used. Changes in footing width should be discussed with this office. Approximately 2.8 inches of settlement is expected at this location over about 7 months with 1 inch occurring immediately and 2 inches occurring in less than 2 months. If a spread footing foundation is chosen, consideration should be given to increasing the structure clearance over the Apple Freeway to account for these settlements. Settlement along the footing axes will be uniform. However a short term differential settlement of 1.5" can be expected between the abutment and pier footings if spread footings are used.

##### B. Piles

A 12" diameter closed end pipe pile and a HP 12 x 84 pile were analyzed at the pier. The closed end pipe may be designed for 70 tons with a safety factor of 2 if driven into the dense gravel layer. The estimated length is 36 feet. However a minimum wall thickness of 0.375 inches should be used to prevent overstress during driving. A driving resistance of 170 tons is estimated to reach the estimated length. A conical reinforced point should be used to prevent tip damage due to boulders. The cost per ton on a per foot basis equals \$11.

A HP 12 x 84 pile may be designed for 120 tons with a safety factor of 2 if driven to rock. The estimated length is 46 feet. A driving resistance of 280 tons is estimated to obtain design resistance at the estimated length. A reinforced tip similar to APF 75500 should be used to prevent tip damage due to boulders. The cost per ton on a per foot basis equals \$8.

We recommend that H-piles be chosen if piles are used because of cost advantages and installation advantages.

## 5. Special Notes

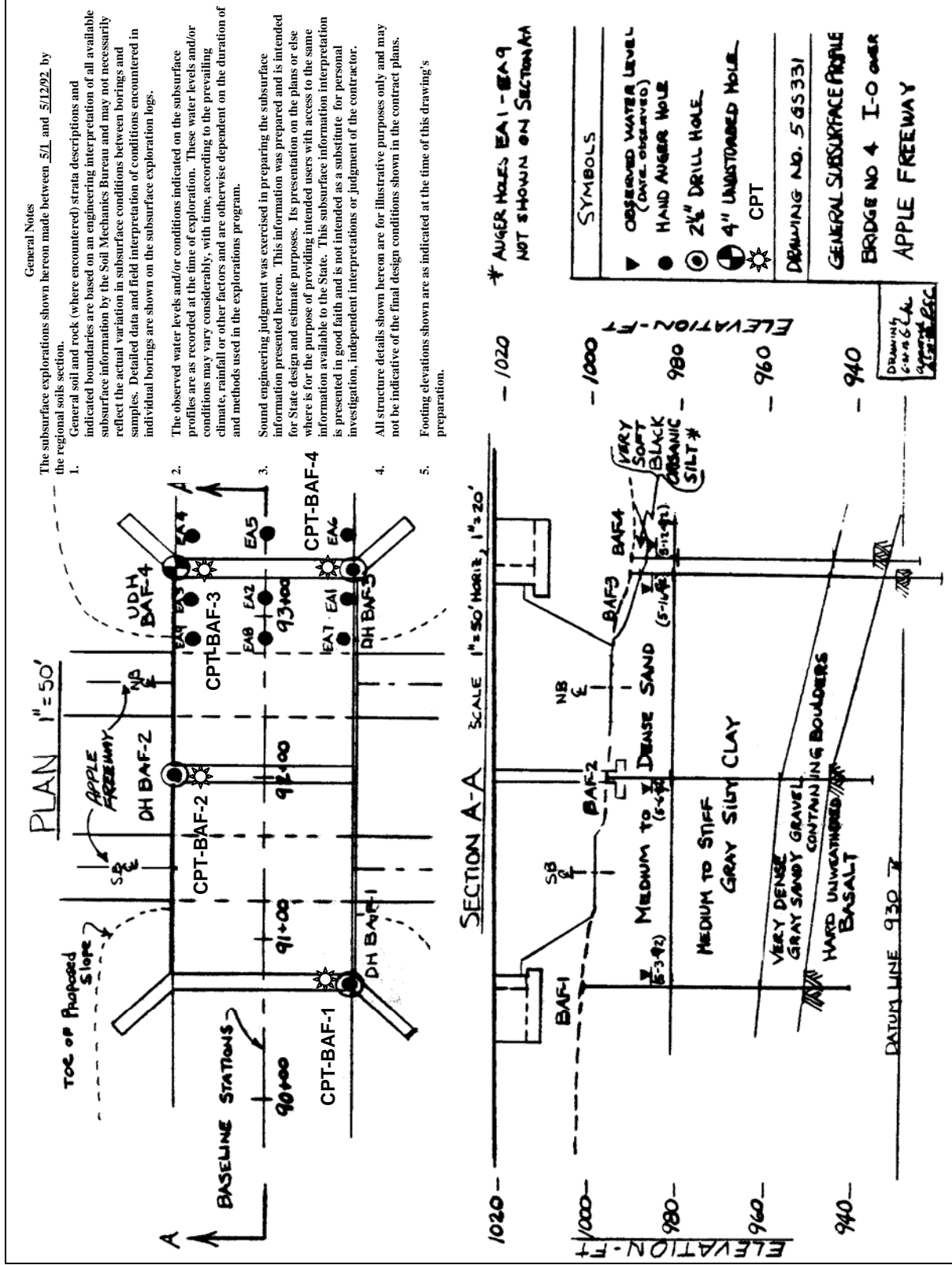
The following special notes are recommended to be included in the contract documents.

1. The general subsurface conditions at this site are shown on Drawing No. 5 GS 331.
2. A 6-month waiting period will be imposed between completion of the 10-foot surcharge on the east embankment. The actual length of the waiting period may be reduced by the Engineer based on an analysis of settlement platform and piezometer readings.
3. The contractor shall coordinate his construction schedule to allow installation of instrumentation by State forces.
4. Instrumentation damaged by contractor personnel shall be repaired or replaced at the contractor's expense. All construction activity in the area of any damaged instrument shall cease until the damage has been corrected.

If piles are used the additional special notes should be provided.

5. Pile driving will not be allowed at the abutments until fill settlement is complete. Estimated maximum settlement time is 6 months after placement of the 10-foot surcharge. This time may be reduced based on interpretation by the State of settlement plate readings.
6. Piles will be acceptable only when driven to pile driving criteria established by the Deputy Chief Engineer (Structures). Prerequisite to establishing these criteria, the contractor shall submit, to the Deputy Chief Engineer (Structures) and others as required, Form entitled, "Pile and Driving Equipment Data." All information listed on the Form shall be provided within 14 days after the award of the contract. Each separate combination of pile and pile driving equipment proposed by the contractor will require the submission of a corresponding Form.

The actual driving resistance to install the 12 x 84 H-piles to the estimated lengths shown on the plans is estimated to be 280 tons at the pier, 345 tons at the east abutment and 290 tons at the west abutment. The contractor's equipment shall be capable of overcoming these resistances without inflicting pile damage.



**APPENDIX B**

**MOHR'S CIRCLE AND ITS  
APPLICATIONS IN GEOTECHNICAL  
ENGINEERING**

[THIS PAGE INTENTIONALLY BLANK]

## APPENDIX B MOHR'S CIRCLE AND ITS APPLICATIONS IN GEOTECHNICAL ENGINEERING

The relationship between the normal and shear stress acting on any plane within a solid mass (continuum) may be represented graphically by an extremely useful device known as *Mohr's Circle for Stress*. It is named after the German engineer Otto Mohr who devised it in 1882.

### B.1 BASIC CONVENTIONS FOR PLOTTING A MOHR'S CIRCLE

The basic conventions for plotting a Mohr's circle are as follows:

1. The *normal* stresses ( $\sigma$ ) are plotted on the abscissa. In conventional solid mechanics, *tensile* stresses are considered positive (plotted to the right of the origin) and *compressive* stresses are considered negative (plotted to the left of the origin).
2. The *shear* stresses ( $\tau$ ) are plotted on the ordinate. In both conventional solid mechanics and soil mechanics, positive shear stresses are plotted above the origin while negative shear stresses are plotted below the origin. This sign convention for plotting the shear stresses should not be confused with the sign convention for the shear stresses themselves. Although sign conventions for the shear stresses themselves vary from one text to another, in general positive shear causes clockwise rotation of the stress element and negative shear causes counterclockwise rotation of the stress element (as discussed in Section B.2).
3. Positive angles on the circle are measured in the counterclockwise sense; negative angles are obtained in the clockwise sense. An angle of  $2\theta$  on the circle corresponds to an angle of  $\theta$  on the element, where  $\theta$  is defined as the angle between any two planes within the soil element (as discussed in Section B.2).

### B.2 MOHR'S CIRCLE CONSTRUCTION FOR GENERAL STRESS CONDITIONS

Figure B-1(a) shows a solid element subjected to a normal stress ( $\sigma$ ) and a shear stress ( $\tau$ ) on each of its four planes. The element can be considered to consist of a set of two mutually perpendicular planes – one horizontal, e.g., Plane Q, the other vertical, e.g., Plane P. Table B-1 presents a summary of the stresses acting on the four planes shown in Figure B-1(a) and their directions (sign) according to the conventions discussed in Section B.1.

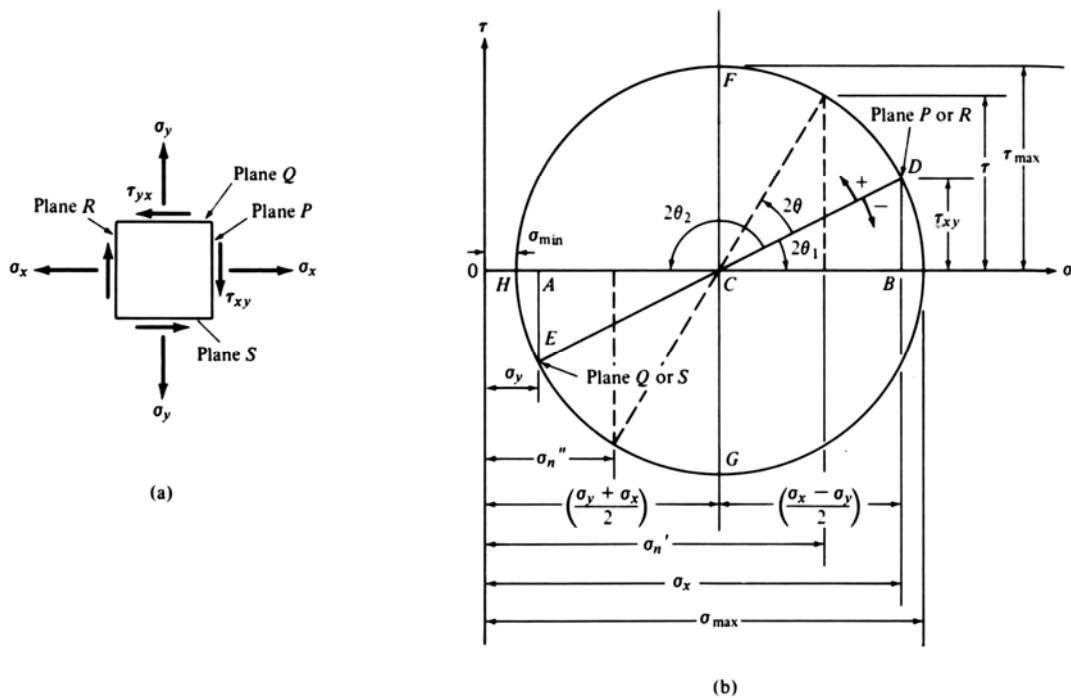


Figure B-1. Mohr's circle for general stress conditions (Cernica, 1982).

Table B-1

Summary of stresses acting on the four planes shown in Figure B-1(a)

Plane	Normal Stress	Sign	Shear Stress	Sign
P	$\sigma_x$	+	$\tau_{xy}$	+
Q	$\sigma_y$	+	$\tau_{yx}$	-
R	$\sigma_x$	+	$\tau_{yx}$	+
S	$\sigma_y$	+	$\tau_{xy}$	-

Note: In this table and Figure B-1, the sign convention is according to that commonly used in solid mechanics, i.e., tensile (normal) stresses are considered positive and are plotted to the right of the origin. In soil mechanics it is customary to indicate *compressive* stresses as positive because soil cannot sustain tensile stresses since it has virtually no strength in tension. The use of the soil mechanics convention will be illustrated in Sections B.3 and B.4.

The following convention is used for the subscripts in Figure B-1:

- For normal stresses, the subscript denotes the orientation of the stress with respect to an x-y coordinate system centered on the element where x is the horizontal axis and y is the vertical axis. Thus  $\sigma_y$  acts in the vertical direction on planes Q and S, both of which are horizontal planes. Since the element is in static equilibrium, the normal stresses acting on the two horizontal planes must be equal. The same logic applies to  $\sigma_x$ , which acts horizontally on vertical planes R and P.
- For shear stress, there are two letters in the subscript. The first letter refers to the subscript of the normal stress acting on the same plane as the shear stress. The second letter refers to the direction in which the shear stress itself is acting. Thus,  $\tau_{yx}$  acts on Plane Q where the normal stress is  $\sigma_y$  and it acts horizontally (x-direction). Since  $\tau_{yx}$  causes counterclockwise rotation of the element, it is considered to be negative as per the sign convention discussed previously. Although it is not shown on the figure, the shear stress acting on Plane S is also  $\tau_{yx}$  and it also causes counterclockwise rotation of the element. Since moment equilibrium must exist for the element to be in static equilibrium,  $\tau_{xy} = \tau_{yx}$  but the signs must be opposite. This can be verified by reference to Table B-1, which was derived from Figure B-1(a).

For the purpose of illustration, assume  $\sigma_x > \sigma_y > 0$ . The Mohr circle for the stress element shown in Figure B-1(a) is then plotted as follows (Recall that Mohr's circle is plotted on shear stress ( $\tau$ ) vs. normal stress ( $\sigma$ ) coordinates where ( $\tau$ ) is the ordinate and ( $\sigma$ ) is the abscissa.):

1. Find the planes having the larger normal stress and determine its sign. In this case,  $\sigma_x$  acts on planes P and R and its sign is positive (tension). Determine the magnitude and sign of the shear stress acting on those planes;  $\tau_{xy}$  is of known magnitude and it causes clockwise rotation of the element, therefore it is positive. Refer to Table B.1 for confirmation. The normal and shear stresses on plane P (or R) represent a point on the  $\tau$ - $\sigma$  axis shown in Figure B-1(b).
2. Plot the normal and shear stress values on plane P (or R) at the coordinate point D shown in Figure B-1(b). The reason the stresses on these two planes plot at the same point is that one plane is oriented 180-degrees from the other on the stress element, i.e., refer to Figure B-1(a) and rotate vertical plane P and its normal and shear stresses by 180-degrees to obtain vertical Plane R that has the same magnitude and direction

(sign) of normal and shear stresses as plane P. Since an angle between two planes on the stress element ( $\theta$ ) plots as twice the angle on the Mohr's circle ( $2\theta$ ), point D represents the stress conditions on both planes P and R since  $2\theta = 360$ -degrees. The same holds true for the stress conditions on planes S and Q. Note that the point plots in the first quadrant since both  $\sigma_x$  and  $\tau_{xy}$  are positive as per the sign convention discussed previously.

3. Find the planes perpendicular to planes P and R; those are planes Q and S. The lesser normal stress,  $\sigma_y$ , acts on those planes and it too is positive (tension). Determine the magnitude and sign of the shear stress acting on those planes;  $\tau_{yx}$  is of known magnitude and it causes counterclockwise rotation of the element, therefore it is negative. Refer to Table B-1 for confirmation. The normal and shear stresses on plane Q (or S) represent a point on the  $\tau$ - $\sigma$  axis shown in Figure B-1(b).
4. As in Step 2, plot the normal and shear stress values on plane Q (or S) at the coordinate point E shown in Figure B-1(b). The reason that both planes plot at the same point was explained previously in #2. Note that the point plots in the fourth quadrant since both  $\sigma_x$  is positive but and  $\tau_{yx}$  is negative as per the sign convention discussed previously.
5. The line ED represents the diameter of the Mohr's circle. The center of the circle lies on the  $\sigma$  axis at point C, which is simply the average value of the normal stresses  $\sigma_x$  and  $\sigma_y$ . Use the center of the circle and the diameter to draw the full circle.

A number of important stress conditions can be determined once the full Mohr's circle is drawn. For example, the values of the major and minor principal stresses can be read directly from the circle. By definition, **the major and minor principal stresses are normal stresses that occur on planes where the shear stress equals zero.** The major principal stress is shown as  $\sigma_{\max}$  and the minor principal stress as  $\sigma_{\min}$  (point H) on Figure B-1(b). In soil mechanics, the major and minor principal stresses are called  $\sigma_1$  and  $\sigma_3$ , respectively.

Also, **the magnitude of the maximum shear stress ( $\tau_{\max}$ ), which is equal to the radius of the circle,** can be read directly from the circle at points F (or G) on Figure B-1(b). Alternatively, the radius of the circle can be calculated from triangle ACE shown in the figure. The orientation of the maximum shear stress with respect to the original plane can either be measured directly on the Mohr's circle or easily calculated with the help of trigonometry.

In general, the normal and shear stresses on any plane oriented at an angle  $\theta$  from a plane of known stress conditions ( $2\theta$  on the Mohr's circle), e.g., planes P, Q, R, S, can either be read directly from the Mohr's circle or easily calculated with the help of trigonometry.

### B.3 BASIC RELATIONSHIPS DERIVED FROM THE MOHR'S CIRCLE

Figure B-2 shows a simplified version of Figure B-1(b). A number of basic relationships between stresses can be obtained from a Mohr's circle. The following relationships can be observed directly from Figure B-2:

1. As indicated previously, **the maximum shear stress ( $\tau_{\max}$ ) is equal to the radius of the circle.** Furthermore, since  $\tau_{\max}$  is oriented at  $+ \text{ or } - 90^\circ$  ( $2\theta$ ) from a principle stress on the Mohr's circle, the maximum shear stress in the stress element acts on planes that make an angle ( $\theta$ ) of  $+ \text{ or } - 45^\circ$  with the principal stress planes.
2. For the stress conditions ( $\sigma$ ,  $\tau$ ) at a point S on the circle, which correspond to the stress conditions on some plane in the soil element, the resultant stress (OS) has a magnitude of  $\sqrt{\sigma^2 + \tau^2}$  as shown in Figure B-2. Furthermore, the angle of obliquity ( $\alpha$ ) of the resultant is equal to  $\tan^{-1}(\tau/\sigma)$ . **The angle of obliquity is the angle formed between the  $\sigma$ -axis and the line drawn from the point on the  $\sigma$ -axis where  $\tau = 0$  to any point on the Mohr's circle.**
3. **The maximum angle of obliquity ( $\alpha_f$ ) is constructed by passing a line through the origin that is also tangent to the Mohr circle**, such as line OT in Figure B-2. The normal and shear stresses that correspond to point T on the circle represent the stresses on the plane of maximum obliquity. Note that the shear stress on this plane is less than  $\tau_{\max}$  and that slippage occurs at the point of maximum obliquity and not at the angle where  $\tau_{\max}$  occurs. Therefore  $\alpha_f$  assumes the more prominent position regarding slip failure.

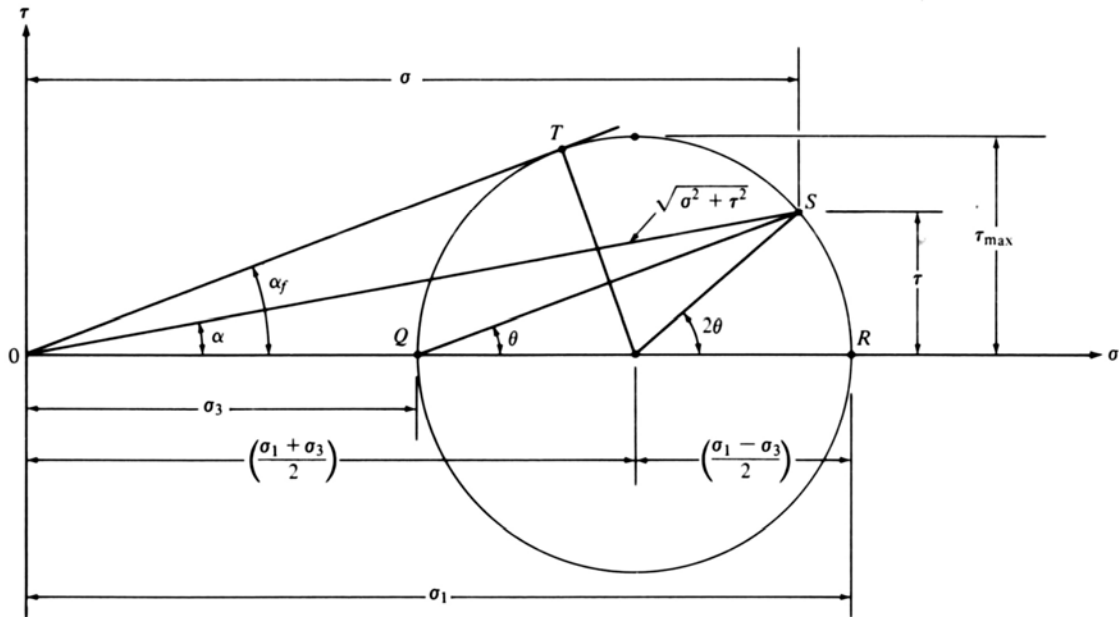


**Figure B-2. Simplified version of Figure B-1(b) showing some basic relationships and characteristics of the Mohr's Circle (Cernica, 1982).**

#### **B.4 MOHR'S THEORY OF FAILURE – APPLICATION TO SOILS**

The following concise description of Mohr's theory of failure is provided by Cernica (1982).

*“The shear strength of soil is generally regarded as the resistance to deformation by continuous shear displacement of soil particles along surfaces or rupture. That is, the shear strength of the soil is not regarded solely in terms of its ability to resist peak stresses, but it must be viewed in the context of deformation which may govern its performance. In that light, therefore, shear failure is necessarily viewed as the state of deformation when the functional performance of the soil mass is impaired.*”

*There are a number of different theories as to the nature and extent of the state of stress and deformation at the time of failure. Failure of a soil mass, particularly cohesionless soil which develops its strength primarily from solid frictional resistance between and interlocking of grains, appears to be best explained by Mohr's rupture theory. According to Mohr's theory, the shear stress in the plane of slip reaches, at the limit a maximum value which depends on the normal stress acting in the same planes and the properties of the material. This represents the combination of normal*

and shear stresses which results in a maximum angle of obliquity  $\alpha_f$ .” (see Figure B-2).”

The combination of normal and shear stresses that results in the line inclined at the maximum angle of obliquity  $\alpha_f$  represents the stress conditions on the failure plane within the soil mass. **The Mohr’s circle corresponding to failure conditions is called the “Mohr failure circle” and the straight line inclined at the maximum angle of obliquity  $\alpha_f$  is called the “Mohr failure envelope.”** The combination of stresses at any other point on the Mohr’s circle defined by an obliquity angle smaller than  $\alpha_f$  represents stress conditions on a plane where failure has not occurred even though the soil mass has failed. Thus, for example, failure does not occur on the plane where the shear stress equals  $\tau_{max}$ .

In reality, the relationship between normal stress and shear stress in soils is usually non-linear, as shown in Figure B-3(a). In addition, depending upon the type of soil and the conditions of loading, a soil might exhibit shear strength when the normal stress = 0, as is also illustrated in Figure B-3(a). Fortunately, the curvature of the Mohr failure envelope is relatively small for most practical problems where the stress range of interest is fairly narrow. Thus, it is mathematically convenient to represent the Mohr envelope by a straight line, sloped at an angle  $\phi$ , that intersects the  $\tau$ -axis at a value of shear stress =  $c$ . This is shown in Figure B-3(b) where  $\phi$  represents the internal friction angle of the soil and  $c$  represents its “cohesion.” The cohesion and friction angle are called the shear strength parameters of the soils.

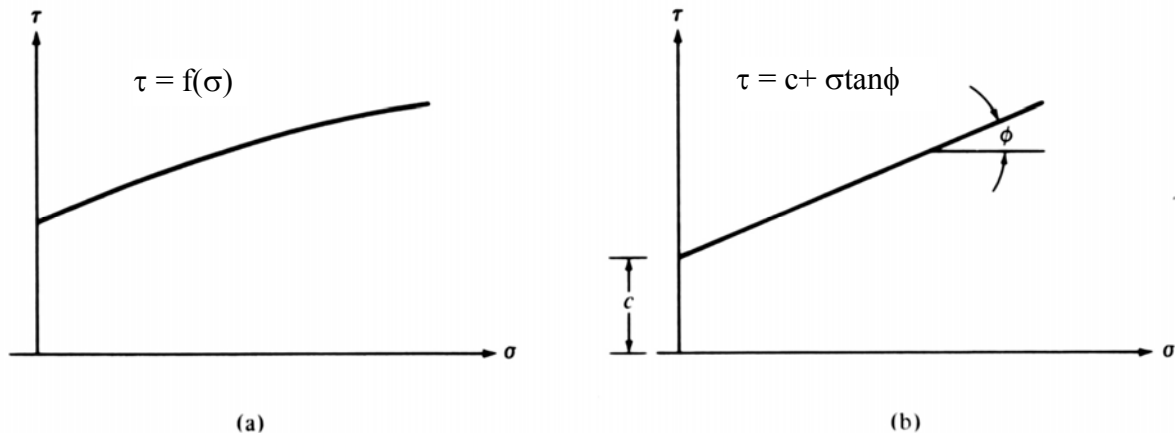


**Figure B-3. Shear strength according to Mohr (a) and Coulomb (b) (Cernica, 1982).**

The linear approximation was first proposed by Coulomb in 1776 in connection with his investigations of retaining walls. Therefore, the linear approximation to the Mohr failure envelope is called the “Mohr-Coulomb failure envelope” and constitutes the Mohr-Coulomb failure criterion. As shown in Figure B-3(b), the Mohr-Coulomb failure criterion can be expressed as:

$$\tau = c + \sigma \tan \phi \quad \text{B-2a}$$

Equation B-2a is a general expression of the Mohr-Coulomb failure criterion that is applicable to all soils and conditions of loading. It can be easily modified to account of those cases. For example:

- For cohesionless soils ( $c = 0$ )

$$\tau = \sigma \tan \phi \quad \text{B-2b}$$

- For purely cohesive soils ( $\phi = 0$ )

$$\tau = c \quad \text{B-2c}$$

- For use with effective stress parameters ( $c = c'$  ,  $\phi = \phi'$ )

$$\tau' = c' + \sigma' \tan \phi' \quad \text{B-2d}$$

Since many applications of soil mechanics to problems in practice involve knowledge of the principal stresses in the soil (e.g. lateral earth pressure theory and use of triaxial test results for slope stability analyses), it is useful to express the Mohr Coulomb failure criterion in terms of principal stresses rather than in the formats used in Equations B-2a to B-2d. Figure B-4 shows the Mohr coulomb strength envelope for one Mohr circle at failure. The principal stresses contain a subscript “f” to indicate that they are the principal stress acting at failure on the stress element shown in the insert.

The following relationships can be derived from Figure B-4.

$$\sin \phi = \frac{R}{D} \quad \text{B-3a}$$

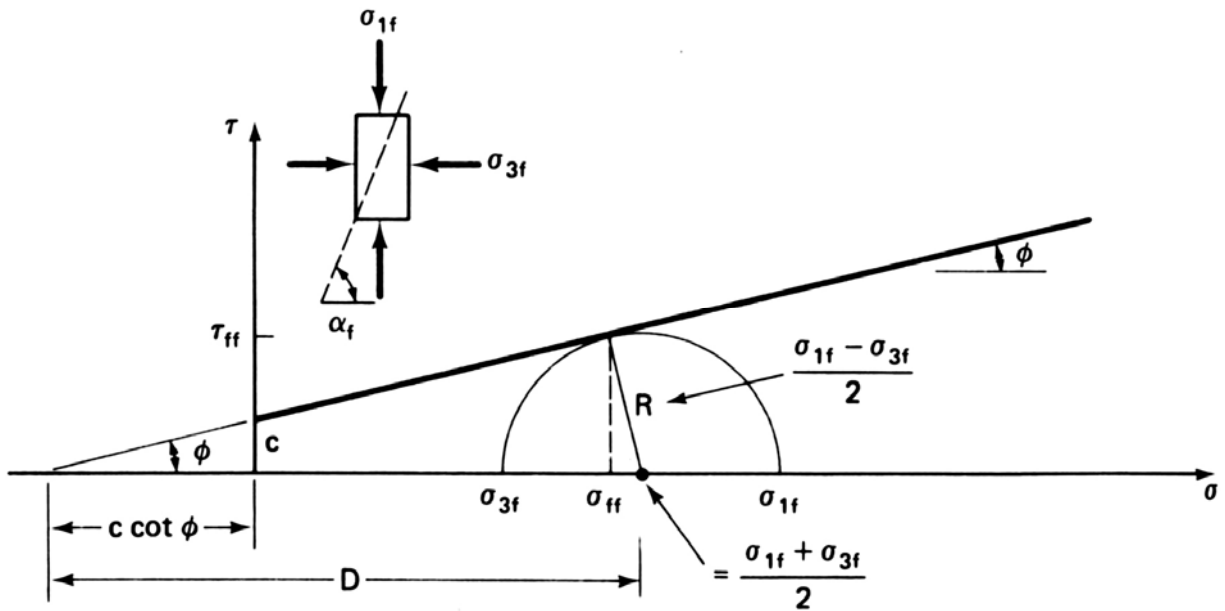


**Figure B-4. Mohr coulomb failure envelope with one Mohr failure circle (Holtz and Kovacs, 1981).**

Substitution of the stresses corresponding to R and D into Eq. B-3a yields:

$$\sin \phi = \frac{\frac{\sigma_{1f} - \sigma_{3f}}{2}}{\frac{\sigma_{1f} + \sigma_{3f}}{2} + c \cot \phi} \quad \text{B-3b}$$

Rearrangement of terms in Eq. B-3b and substitution of trigonometric identities yields:

$$(\sigma_{1f} - \sigma_{3f}) = (\sigma_{1f} + \sigma_{3f}) \sin \phi + 2c \cos \phi \quad \text{B-3c}$$

Solving Eq. B-3c for  $\sigma_{1f}$  yields:

$$\sigma_{1f} = \sigma_{3f} \left[ \frac{(1 + \sin \phi)}{(1 - \sin \phi)} \right] + \left[ \frac{2c \cos \phi}{(1 - \sin \phi)} \right] \quad \text{B-3d}$$

Substitution of the identity  $\cos \phi = (1 - \sin^2 \phi)^{1/2}$  into Eq. B-3d yields:

$$\sigma_{1f} = \sigma_{3f} \left[ \frac{(1 + \sin \phi)}{(1 - \sin \phi)} \right] + \left[ \frac{2c \sqrt{(1 + \sin \phi)}}{\sqrt{(1 - \sin \phi)}} \right] \quad \text{B-3e}$$

Equation B-3e represents the general relationship between the major ( $\sigma_1$ ) and minor ( $\sigma_3$ ) principal stresses in terms of the soil strength parameters  $c$  and  $\phi$ .

For cohesionless soils ( $c = 0$ ), Eq. B-3e reduces to:

$$\frac{\sigma_{1f}}{\sigma_{3f}} = \frac{(1 + \sin \phi)}{(1 - \sin \phi)} \quad \text{B-3f}$$

The reciprocal of Eq. B-3f yields:

$$\frac{\sigma_{3f}}{\sigma_{13f}} = \frac{(1 - \sin \phi)}{(1 + \sin \phi)} \quad \text{B-3g}$$

By the use of trigonometric identities Eq. B-3f can be re-written as:

$$\frac{\sigma_{1f}}{\sigma_{3f}} = \tan^2 \left( 45^\circ + \frac{\phi}{2} \right) \quad \text{B-3h}$$

Similarly, Eq. B-3g can be re-written as:

$$\frac{\sigma_{3f}}{\sigma_{1f}} = \tan^2 \left( 45^\circ - \frac{\phi}{2} \right) \quad \text{B-3h}$$

Equation B-3h gives the coefficient of passive earth pressure,  $K_p$ , while Equation B-3i gives the coefficient of active earth pressure,  $K_a$  that were introduced in Chapter 2. Many concepts in geotechnical engineering can be similarly explained by used of Mohr's circle. The most common use of Mohr's circle is for interpretation of the results of shear strength tests discussed in Chapter 5. For use of Mohr's circle in interpretation of shear strength tests, the reader is referred to well-known text books such as Holtz and Kovacs (1981) and Lambe and Whitman (1979).

**APPENDIX C**

**LOAD AND RESISTANCE  
FACTOR DESIGN (LRFD)**

[THIS PAGE INTENTIONALLY BLANK]

## **APPENDIX C**

### **LOAD AND RESISTANCE FACTOR DESIGN (LRFD)**

#### **C.1 INTRODUCTION**

In 1994, the AASHTO Subcommittee on Bridges adopted a Bridge Design Specification based on the use of the Load and Resistance Factor (LRFD) method (AASHTO, 1994). The geotechnical parts of the new specification had been developed by an NCHRP Research Project (NCHRP, 1991). The most recent version of the LRFD specifications is the 2004 version of AASHTO. Most states are now in the process of implementing the LRFD specifications.

The geotechnical portion of the LRFD specification has proven to be one of the most difficult to implement. This includes shallow and deep foundations, and earth retaining systems. In fact, the Section 10 of the LRFD specification, was significantly updated in 2006 Interims. In this Appendix, basic concepts of LRFD will be presented including a brief discussion on comparison of LRFD with allowable stress design (ASD) approach. The purpose here is to provide the necessary basis for preparing the geotechnical specialist to use this new method. The material presented in this Appendix has been adapted from similar material included in the FHWA (2006a) manual on driven pile foundations.

##### **C.1.1 Primary References**

The primary references for this Appendix are as follows:

AASHTO (2002). *Standard Specifications for Highway Bridges*. 17<sup>th</sup> Edition, American Association of State Highway and Transportation Officials, Washington, D.C.

AASHTO (2004 with 2006 Interims). *AASHTO LRFD Bridge Design Specifications*, 3rd Edition, American Association of State Highway and Transportation Officials, Washington, D.C.

## C.2 CONCEPTS OF ASD AND LRFD

To understand and appreciate LRFD approach, it is necessary to first briefly summarize the fundamental basis for allowable stress design (ASD) and then to review the history of the development of the LRFD and its early implementation.

Allowable Stress Design (ASD) evolved from the development of methods of structural analysis during the nineteenth century. Prior to these developments, structures were designed based entirely on experience and of rules-of-thumb. The methods of structural analyses were developed based on the assumption that the structure behaved elastically and that they produced a rational evaluation of structural behavior that satisfied both equilibrium and compatibility. But, the analyses only explained structural behavior. It was desirable that a rational design approach be developed and it was logical to limit the calculated stresses in a structure to some fraction of the structural material strength. Gradually, structural loads appropriate for design were defined and then codified. So, if member stresses could be calculated it was logical to limit those stresses and values of allowable stresses were gradually accepted based on the experience that the structure did not fail. These limiting stress values became known “**design stresses**” or “**allowable stresses.**” For instance, the allowable stresses in steel beams in bending have been limited to between about 0.4 and 0.66 times the steel yield strength.

But, linear elastic behavior is not universally observed in all structural elements. For example, the failure strength of a column is related the slenderness ratio of the member and methods are available to confidently calculate the failure load. Similar considerations affect the design of other structural elements. The approach that came to be used in some applications during the development of ASD was to apply a “**factor of safety**” to the calculated ultimate member capacity.

Once the structural analysis was performed based on linear elastic theory and an appropriate factor of safety, the forces at the foundation element were obtained. At this stage, it was realized that the foundation element is embedded in geomaterials (i.e., soils and rocks) which are inherently inelastic and use of linear elastic theory will not represent the strength of a soil structure. Therefore, to account for inherent uncertainties in the characterization of geomaterials, the use of the concept of factor of safety was extended to geomaterials as well and has become universal in geotechnical design. Rather than use of two factors of safety, one for structural analysis and one for geotechnical analysis, a single combined factor of safety was applied to account for all uncertainties and this was commonly applied in the geotechnical analysis.

The combined factors of safety were selected so that failures were very unlikely, based on experience, but the magnitudes of the factors of safety were based only on experience. The geotechnical engineer should understand that he/she does not “own” all of the factor of safety. It must be adequate to deal with the variability of the loads and the inadequacy of the analysis in addition to the strength variability.

Until 1956, the analysis of a concrete section subject to bending was performed assuming that the compression stress in the concrete was linearly distributed on the cross section with the further assumption that concrete could carry no tension. Designs were limited by placing limits on the calculated stress in both the concrete in compression and in the steel in both tension and compression (if compression steel was present). In other words, the element strength was treated as if the materials were elastic and, to perform the analysis, the steel was then “transformed” into concrete based on the relative moduli of the two materials. The result of these assumptions produced quite conservative results, particularly if compression reinforcement was present as is always the case with columns. The time dependent deformation of concrete subjected to compression causes its effective modulus to be time dependent. Extensive research was performed in the first half of the twentieth century to understand what the actual stress distribution was and how it could be used in design.

These fundamental problems with the use of ASD caused the American Concrete Institute (ACI) in 1956 to adopt a new edition of their Building Code for the design of concrete structures and in that code an Appendix was included that used a **strength design** approach (ACI 1956) to replace the allowable stress method described above. The ultimate strength of the element in bending was calculated using a prescribed, nonlinear concrete stress distribution on the section at failure. The computational procedure was quite simple and the result was element strength not stress. The Appendix of ACI 318-56 achieved little use.

The ACI Committee that prepared this method then took another major step. Instead of selecting a factor of safety for particular failure modes they broke the factor of safety into parts. They realized that the limiting value of ultimate load should depend on the variability of the particular load types. So they specified different “**load factors**” for the various types of loads and, indirectly, they applied an additional multiplier to provide structural safety for the strength variability of member types and failure modes.

ACI 318-63, adopted in 1963, made extensive changes from the 1956 Code and the result had the form that we now know as LRFD (ACI 1963).

$$\sum \gamma_{ij} Q_{ij} \leq \phi_k R_{nk} \quad \text{C-1}$$

Where,  $\gamma$  is the **load factor**,  $Q$  is the **load effect** (this refers the element load calculated from the applied loads by a linear elastic structural analysis.) The subscripts  $i$  and  $j$  refer to the load condition (dead, live, wind, etc.) and the load combination, respectively.  $\phi$  is the **resistance factor** for a given **limit state** (failure mode),  $R_{nk}$  is the **nominal resistance** in the  $k^{\text{th}}$  limit state. The term nominal resistance was adopted to define the element strength determined by some specified method. **(It should be noted that in the AASHTO LRFD Code the term nominal resistance is used instead of nominal strength.)** The summation on the left side of Equation (1) is known as the **factored load**. A generally used name for the right side of the expression has not been accepted. The term **factored resistance** will be used here.

The version of Equation (1) used in the AASHTO LRFD Design Specification is somewhat different. It has the following form:

$$\sum \eta \gamma_{ij} Q_{ij} \leq \phi_k R_{nk} \quad \text{C-2}$$

where  $\eta$  is a factor related to the ductility, redundancy and operational importance.

When ACI 318-63 was adopted, the load and resistance factors were generated based on judgment followed by extensive comparative designs. By 1965, the designers of concrete structures in the private sector had almost universally adopted the ACI LRFD Code. There were a few minor changes in the load factors in the next edition of the Code in 1968 (ACI 1968) and the ASD section was dropped completely. The ACI LRFD Building Code was then essentially unchanged until 2002 (ACI 2002) when extensive changes were made primarily to the load and resistance factors. During this entire development period the design method was known as “**Ultimate Strength Design.**”

The LRFD procedure adopted by ACI 318-63 was applicable to structural concrete elements for buildings only. It did not apply to the geotechnical aspects of foundation design. This produced a considerable anomaly for reinforced concrete building designers. For example, in the design process the geotechnical engineer recommended an allowable bearing pressure for a spread footing. The structural designer then had to size the footing using allowable loads – and that implied the use of a different set of loads - but perform the structural design of the reinforced concrete footing with factored loads.

Driven pile cap design was even more absurd. The geotechnical engineer selected an ultimate pile capacity based on subsurface conditions. Most of the methods that are used to establish pile capacity produce ultimate capacity. As discussed in Chapter 9, those methods include wave equation analysis, dynamic testing or static load testing. The one exception is

the use of a dynamic formula and most formulas usually give allowable loads. The Gates Formula is an exception in that it produces a predicted ultimate load. The geotechnical engineer then selected a factor of safety to arrive at an allowable load. Again, the structural engineer had to use allowable loads to do the pile group selection and layout but then use factored loads to design the pile cap. Private sector designers have been dealing with this inconsistency for forty years.

In 1969, Cornell published a paper in the ACI Journal (Cornell, 1969) showing that the load and resistance factors could be determined rationally using a probabilistic analysis. As input to that analysis the variability of both the loads and the resistance was required. The National Bureau of Standards (NBS) completed a research project to collect the necessary information for buildings and they generated the associated factors (Ellingwood, *et al.*, 1980). At that time the only LRFD Design Code in use was the ACI Code and the NBS factors were quite different than those contained in the ACI Code. These differences continued until 2002.

Today, LRFD design specifications are available for both steel and concrete buildings. Beginning with the 2002 ACI Building Code the load factors for both steel and concrete structures became the same. All concrete buildings are designed using LRFD but in the case of steel buildings the implementation of LRFD is not complete and an ASD design specification is still available and widely used for steel structures.

### **C.3 CALIBRATION OF PROBABILITY BASED LRFD**

The original work of Cornell (1969) produced a major research effort to develop a probabilistic approach to structural design based on the load and resistance factor concept. The fundamental concept held that, since neither the loads nor the resistance are deterministic, it is appropriate to treat both load and resistance as random variables and to develop an approach to the design of structures based on probability theory. The concept is illustrated in Figure C-1 where **probability density functions** (PDFs) are shown for both the load effect,  $Q$ , and the resistance,  $R$ . The area under the resistance curve between  $a$  and  $b$  represents the probability of the resistance being between  $a$  and  $b$ . The region where the two curves overlap represents cases of “**failure.**” Probability-based design is founded on the concept that the design be selected so that the probability of failure is equal to, or less than, some prescribed value. The limiting failure probability was originally established from laboratory test data on structural elements.

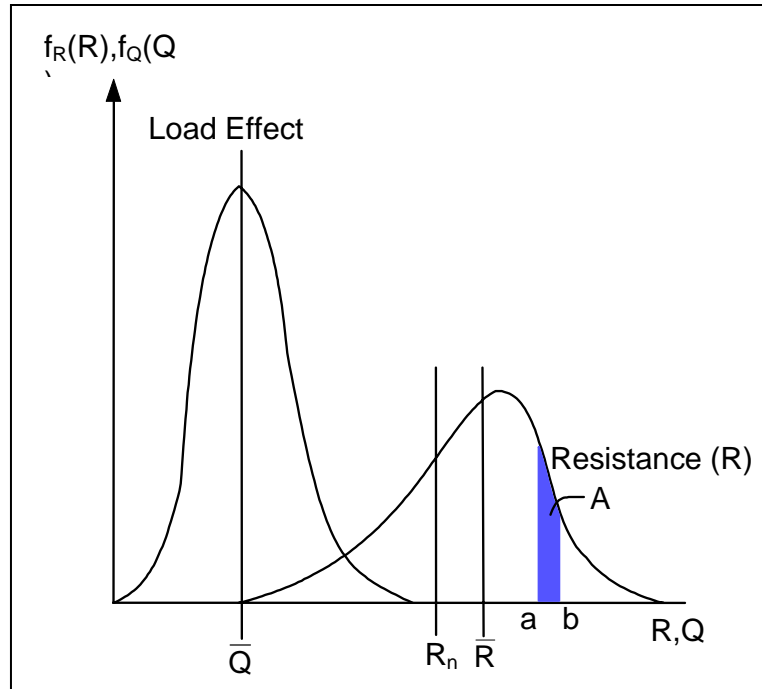


**Figure C-1. Example of Probability Density Functions for both Load and Resistance.**

The load effect in Figure C-1 has been shown much narrower than the resistance for illustrative purposes, indicating that, in this case, the load has less variability than the resistance. The variability is defined by the standard deviation of the distribution. (The standard deviations are not shown in Figure C-1.) In Figure C-1, the mean values are denoted by  $\bar{Q}$  and  $\bar{R}$ . The **nominal resistance,  $R_n$**  is not necessarily the same as the **mean resistance** as illustrated in Figure C-1, but is the resistance that would be determined by the specified analysis method.

If distributions are available for both the load effect and the resistance, then the probability of failure can be determined. One approach that has been used is to consider the combined probability density function for  $R-Q$  and this is illustrated in Figure C-2. **Failure is defined when  $R-Q$  is less than zero and the region is shaded in Figure C-2.** The probability of failure is the area of the shaded portion under the curve. The basis for design is to require that the mean of that distribution,  $\overline{R - Q}$ , be greater than the value of  $R-Q = 0$ . The distance of that mean above zero is taken as a multiple,  $\beta$ , of the standard deviation of the distribution.  $\beta$  is known as the **safety index** or **reliability index**. There are other approaches to establishing a measure of safety. A more detailed discussion of probabilistic code calibration has been presented by Kulicki (1998).

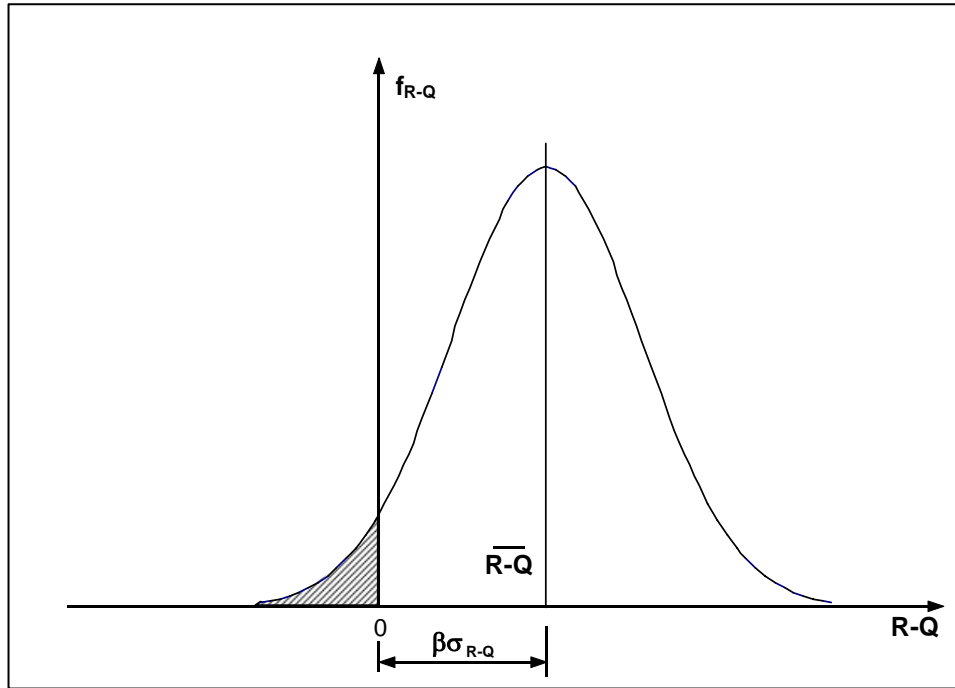


**Figure C-2. Probability Density Function for R-Q.**

Existing structures that have performed satisfactorily have been analyzed to determine safety indices and from these analyses recommended values have been determined. Then, with knowledge of the load and the strength variabilities it is possible to select load and resistance factors to produce the required safety index. Structural engineers have established load factors for the various load types in the AASHTO Bridge Code and most of these values are probably not subject to change today. So the geotechnical resistance factors must be selected to achieve the required appropriate safety index.

Geotechnical strength measurement is very difficult to describe statistically due to the lack of standardized procedures for material characterization of soils. But, load and resistance factors can be calibrated based on a direct comparison with existing design practice. Load factors have been selected for the AASHTO LRFD Bridge Code so resistance factors can be directly determined to produce designs similar to those obtained in current ASD practice. For example, the AASHTO Strength I case is considered since it is commonly critical in design. The equality condition is used to obtain a unique and limiting expression. The expression can be stated in a simplified fashion as

$$\gamma_D Q_D + \gamma_L Q_L = \phi_k R_{nk} \quad \text{C-3}$$

where the subscript D refers to dead load and L refers to live load. Values are available for the dead and live load factors for Strength I in the AASHTO LRFD Bridge Code and Equation C-3 becomes

$$1.25 Q_D + 1.75 Q_L = \phi_k R_{nk} \quad \text{C-4}$$

The equivalent ASD relationship can be stated

$$(Q_D + Q_L) FS = R_{nk} \quad \text{C-5}$$

where FS is the ASD factor of safety. For the equality condition,  $R_{nk}$  can be eliminated from Equations C-4 and C-5 and this results in a single relationship for  $\phi_k$ , in terms of FS and the  $Q_L/Q_D$  ratio.

$$\phi_k = \frac{FS(1 + Q_L / Q_D)}{(1.25 + 1.75 Q_L / Q_D)} \quad \text{C-6}$$

Figure C-3 shows resistance factors for various factors of safety as a function of  $Q_L/Q_D$  ratio for the AASHTO LRFD Code. From Equation C-6 and Figure C-2, the importance of live-dead load ratio becomes clear. For short span bridges the live load may be much larger than the dead load while for very long spans structures the live loads can be almost inconsequential. Regardless of the source of resistance factors they must be checked against existing ASD practice. For example, if the probability analysis produced smaller resistance factors than the equivalent ASD factors of safety this would imply an unnecessary increase in conservatism in the design.

The factor  $\eta$  in Equation C-2 has been ignored in the above discussion. The primary concern with  $\eta$  in foundation design comes when only a very few deep foundation elements are used so that the foundation is non-redundant. While it is not so clear how redundancy can be determined since it is to some degree controlled by the superstructure geometry it can be critical and must be evaluated. Certainly a single deep foundation element will be non-redundant. Of course, most driven pile foundations will have enough piles to be redundant.

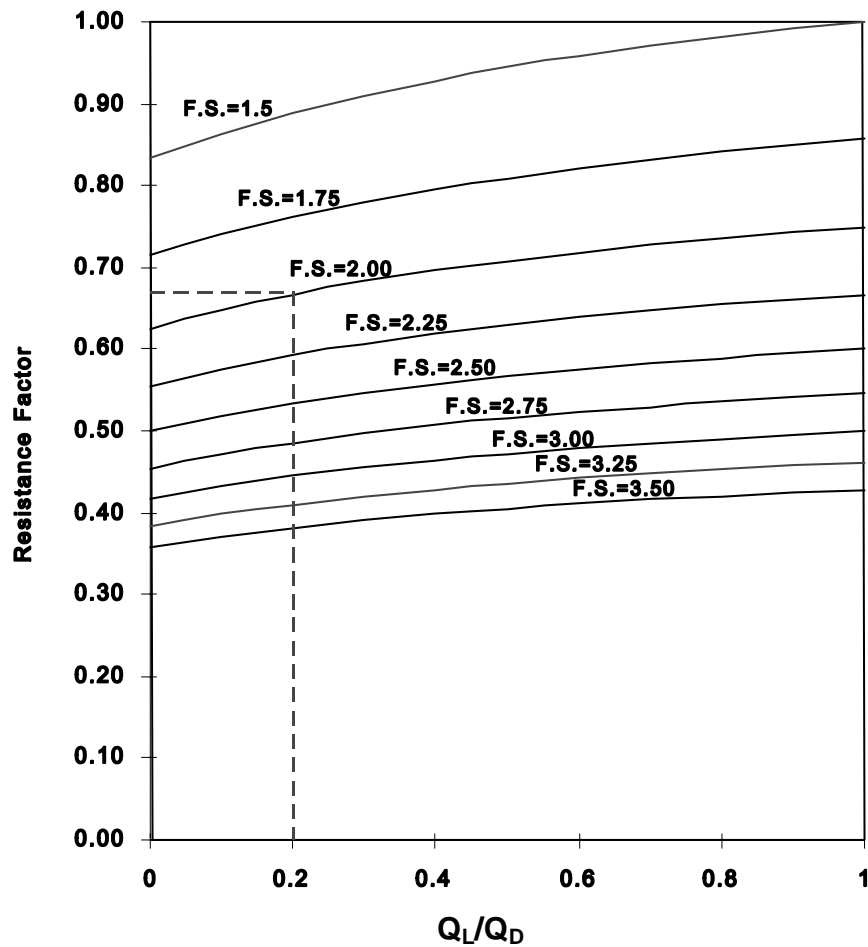


**Figure C-3. Resistance factor as a function of  $Q_L/Q_D$  for various factors of safety for the AASHTO LRFD Bridge Code.**

#### **C.4 LRFD DETAILS**

The issue of the verification of the safety of an LRFD-based design is now discussed. The question that will be considered is, “Does the structural element (pile) have adequate axial strength.” To answer this question it is best to consider some details. First, consider the determination of the loads that would be used in bridge design. There are five strength limit states, two extreme event limit states, four serviceability limit states and one fatigue limit state given in Table 3.4.1-1 of the AASHTO LRFD Bridge Code (AASHTO 2004 with 2006 Interims). Here only the strength limit states will be considered for illustration purposes. The factored loads for those five cases are as shown in Table C-1. These load combinations have been somewhat simplified for this discussion.

**Table C-1**

<b>Strength Limit State</b>	<b>Load Combination</b>
I	$\gamma_p D + 1.75 L + 1.0 WA + 1.0 FR$
II	$\gamma_p D + 1.35 L + 1.0 WA + 1.0 FR$
III	$\gamma_p D + 1.0 WA + 1.4 WS + 1.0 FR$
IV	$\gamma_p D + 1.0 WA + 1.0 FR$ (but for dead load due to structural components only 1.5 D)
V	$\gamma_p D + 1.35 L + 1.0 WA + 0.4 WS + 1.0 WL + 1.0 FR$
<u>Notations:</u>	
$\gamma_p$ – load factor for the various types of dead load. For the superstructure dead load $\gamma_p$ is 1.25, but other values are specified for other types of dead load. D – dead load. L – live load WA – water and stream load FR – friction load WS – wind load on the structure WL – wind load on the live load	

Since the load combinations have been somewhat simplified, the reader is encouraged to review Section 3 of the AASHTO LRFD Bridge Design Specifications (AASHTO 2004 with 2006 Interims). Probably geotechnical engineers that are responsible for foundation design will not be required to determine the factored loads, but a general understanding of those loads provides a better understanding of the entire design process. While the above loads and load combinations have differences from that of previous AASHTO Specifications the general structure of the loads is unchanged. Since there may be several different sets of loads (for instance, maximum and minimum) for each of the strength limit states the final set of factored loads will usually be larger than the five given above and sometimes much larger, particularly if extreme event conditions must be considered.

At this stage of the foundation design process, the factored loads will have been determined by the structural designer and with the exception of the downdrag case it is unlikely that these loads or load combinations will change in future AASHTO Codes. Therefore, the left side of Equation C-2 has now been determined.

The right side of Equation C-2 is of greater concern for the geotechnical foundation designer who must determine values of  $\phi_k$ , the **resistance factor**, and  $R_{nk}$ , the **nominal strength**. Values for  $\phi_k$  must be defined by code. It has often been implied that resistance factors may be determined in the design process using a probability analysis. This is not realistic and

certainly not necessary for deep foundation design. At the present, the resistance factors are prescribed in AASHTO (2004 with 2006 Interims) and are not always unique. The reader is referred to Sections 10 and 11 of AASHTO 2006 Interims for selection of appropriate resistance factors and methods to determine the nominal strength,  $R_{nk}$ .

## **C.5 THE DESIGN PROCESS**

The design process for LRFD will now be reviewed. The flow chart for LRFD-based design is given in Figure C-4. In Blocks 1 to 5, project requirements must be determined and the subsurface must be explored and evaluated to obtain the necessary geotechnical design quantities. In Blocks 6 and 7, an appropriate foundation type is selected. For illustration purposes herein, a driven pile type is selected. Then in Block 8 the factored loads are determined. After determining whether the pile is driven in soil or to rock (see Blocks 9 or 11), the designer selects the resistance factor in Blocks 10 or 12 based on the capacity verification procedure and the quality control method that has been selected. In the ASD method, a factor of safety is selected based on the information in Table 4.5.6.2.1A of AASHTO (2002). The resistance factor for LRFD is given in the Tables 10.5.5.2.3-1, 10.5.5.2.3-2 of AASHTO (2004 with 2006 Interims). Selection of the proper value for resistance factor from the LRFD Specification will not be discussed here.

The rest of the flow chart is similar to the one for ASD. It can be seen that there is little difference in the design process for LRFD compared to ASD.

## **C.6 A SIMPLE EXAMPLE**

A very simple numerical design example will be solved to illustrate the differences between ASD and LRFD. Only strength will be considered since those limitations are the only ones that are different for the two methods. The soil is a medium dense sand with an adjusted  $N_{160}$ -value of 20 and a friction angle of 33 degrees. The site has some variability and in terms of low, medium and high variability, the site can be characterized as having medium variability. In this trial design, a closed end steel pile having a length of 66 ft (20 m) and a cross section 14 in x 5/16 in (356 mm x 8 mm) has been selected and a geotechnical analysis indicates a nominal axial resistance of 330 kips (1470 kN). The working load on the foundation will be taken as 500 kips (2,225 kN) dead load and 800 kips (3,560 kN) live load including impact. Assume one (1) static load test will be performed.



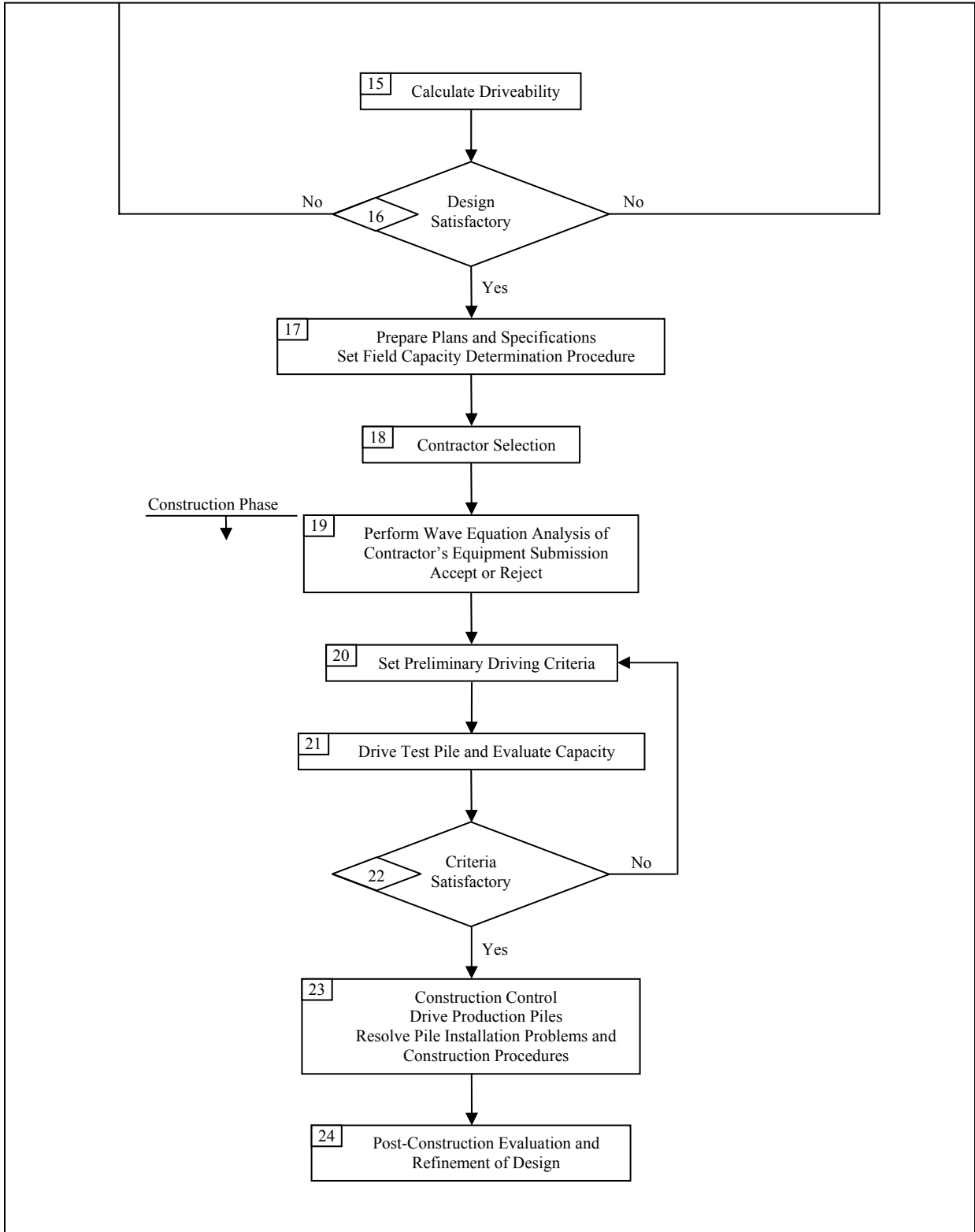


**Figure C-4. Driven pile design and construction process by LRFD (FHWA, 2006a)  
(Continued).**

### C.6.1 ASD

According to Table 3.22.1A of AASHTO (2002) for the service load Case I, the design load is

$$500 \text{ kips} + 800 \text{ kips} = 1,300 \text{ kips (5,785 kN)}$$

First, assume that a static load test will be used in addition to a drivability analysis by wave equation with subsurface exploration and static analysis to verify the driving criteria. Therefore, the factor of safety specified in Table 4.5.6.2A of AASHTO (2002) is 2.0 and the required nominal axial resistance is 2,600 kips (11,570 kN). Now if the pile nominal resistance is 330 kips (1,470 kN), then the total required number of piles will be

$$2,600 \text{ kips} / 330 \text{ kips} = 7.8 \text{ piles, say 8 piles}$$

If dynamic measurement and analysis is used the specified factor of safety is 2.25 per AASHTO (2002), giving a required ultimate axial resistance of  $1,300 \text{ kips} \times 2.25 = 2,925 \text{ kips}$  (13,016 kN). In this case the required number of piles will be

$$2,925 \text{ kips} / 330 \text{ kips} = 8.9 \text{ piles, say 9 piles}$$

### C.6.2 LRFD

First, determine the factored load. In this very simple example, only Strength I of Table 3.4.1-1 of the AASHTO LRFD Bridge Code (AASHTO 2004 with 2006 Interims) will be considered.

$$1.25 \times 500 + 1.75 \times 800 = 2,025 \text{ kips (9,007 kN)}$$

As per Table 10.5.5.2.3-2 of AASHTO (2004 with 2006 Interims), the specified resistance factor to be used for the case of one (1) on a site with medium variability is 0.70. Based on this resistance factor, the required nominal resistance is as follows:

$$2,025 \text{ kips} / 0.70 = 2,893 \text{ kips (12,868 kN)}$$

The required number of piles is

$$2,892 \text{ kips} / 330 \text{ kips} = 8.8 \text{ piles, say 9.0 piles}$$

### **C.6.3 Comments**

This very simple example illustrates the difference between ASD and LRFD. Of course, only one failure mode limit state was considered. In a real design problem, several load combinations would be included, the loads would include overturning loads and all aspects of the problem would be much more complex. This simple example illustrates the difference between ASD and LRFD clearly and simply. No conclusions should be made regarding the fact that the LRFD design for this simple example was virtually the same as the ASD design. For other load combination, the design may be different. (In the latter case, Strength IV load combination would become critical and fewer piles would be required.)

[THIS PAGE INTENTIONALLY BLANK]

**APPENDIX D**

**USE OF THE COMPUTER PROGRAM**

**ReSSA**

[THIS PAGE INTENTIONALLY BLANK]

## APPENDIX D USE OF THE COMPUTER PROGRAM ReSSA

### D.1 INTRODUCTION

The computer program Reinforced Slope Stability Analysis (ReSSA), version 2.0 was developed by ADAMA Engineering, Inc. (ADAMA), Newark, Delaware under contract to FHWA. The following description of the program is provided by ADAMA:

*“ReSSA(2.0) is an interactive program for analyzing rotational and translational stability of slopes. It was developed to allow for convenient integration of horizontally placed reinforcement, thus also enabling the analysis of mechanically stabilized earth slopes. The sole purpose of the ReSSA software is to assist experienced engineers in the analysis of reinforced and unreinforced earth slopes.”*

ReSSA(1.0), the first released version, is a user-friendly, Windows-based program that is provided free-of-charge (but in a limited number of licenses) to each state DOT for use on reinforced and slope stability analysis applications. ReSSA(2.0) has additional features that were added in response to users comments. For rotational (i.e., circular) failure modes, the program addresses moment equilibrium utilizing the Modified Bishop method of analysis. For translational (i.e., sliding) failure modes, the program addresses moment and force equilibrium utilizing the Spencer’s method of analysis. For reinforced soil slopes (RSS) in fill, the program incorporates the AASHTO/FHWA method of analysis (FHWA, 2001b). In these regards, it is recognized that ReSSA is not a comprehensive slope stability software package because it does not deal with general-shape slip surface. This limitation notwithstanding, ReSSA is an extremely powerful design and analysis software package that can address complex subsurface stratigraphic conditions and slope configurations. Given the potential application of ReSSA to DOT projects and to provide an introduction to the course participants regarding the utility of computer programs that have been developed to address slope stability problems, a summary of the use and capabilities of ReSSA is provided herein as part of the Soils and Foundations course.

This appendix was prepared to provide a narrative summary of some of the specific features of ReSSA, as most of these capabilities are also included in other readily available commercial computer programs that are used for assessing slope stability. It is recognized that this document is provided in lieu of a hands-on demonstration of the program capabilities as part of the course. The instructor is available to demonstrate ReSSA if there is interest among individual participants. It is important to note, however, that this summary

was never intended to serve as or replace the Users Manual and the supporting technical documentation provided with the ReSSA program by ADAMA.

The remainder of this appendix is organized to provide several screen shots from ReSSA and will demonstrate the use of the program to assess the calculated factor of safety of a 30 ft deep cut slope in a uniform deposit of clay. This problem was originally presented in the Reference Manual in Chapter 6 and was explicitly selected because the solution (i.e., the calculated factors of safety) was presented as an example problem in the Reference Manual to demonstrate the use of chart solutions.

## **D.2 PREPARING FOR INPUT TO THE COMPUTER PROGRAM**

Before any slope stability analysis can be performed using a computer, it is essential that the user/designer prepare a hand sketch using an “unexaggerated” x-y scale (i.e., the same scale in the x and y directions). This sketch should show the geometry of slope, the subsurface stratigraphy, and the location of the water table. It will be necessary to assign coordinates to the various points on this sketch so that information regarding the geometry can be input to the computer. Remember that the computer will only solve the problem that the user asks it to solve, so the user needs to be sure that the geometry developed in the hand sketch matches the geometry presented on the computer screen. Once the hand sketch is developed, it is possible to now enter the information into the computer. This initial step of developing a hand sketch is absolutely essential, particularly for complex subsurface conditions. If the subsurface conditions change across the actual project site, it is necessary to develop multiple cross-sections for analysis so that the most critical cross-section can be identified and reported.

## **D.3 WORKING WITH ReSSA**

When ReSSA is executed, an introductory screen is provided, identifying the copyright information. This is followed by a screen that flashes the ReSSA startup screen (Figure D-1). Most important here is the “File” button on the taskbar. From here the user can start a new analysis or retrieve a previous project; this latter capability of being able to retrieve previous problems is one of the biggest advantages of computer programs. For our example, the Example 6-1 in Chapter 6 will be launched from this menu. What follows next is the Main Menu for ReSSA (Figure D-2), where the user will sequentially develop the problem and perform the stability analysis.

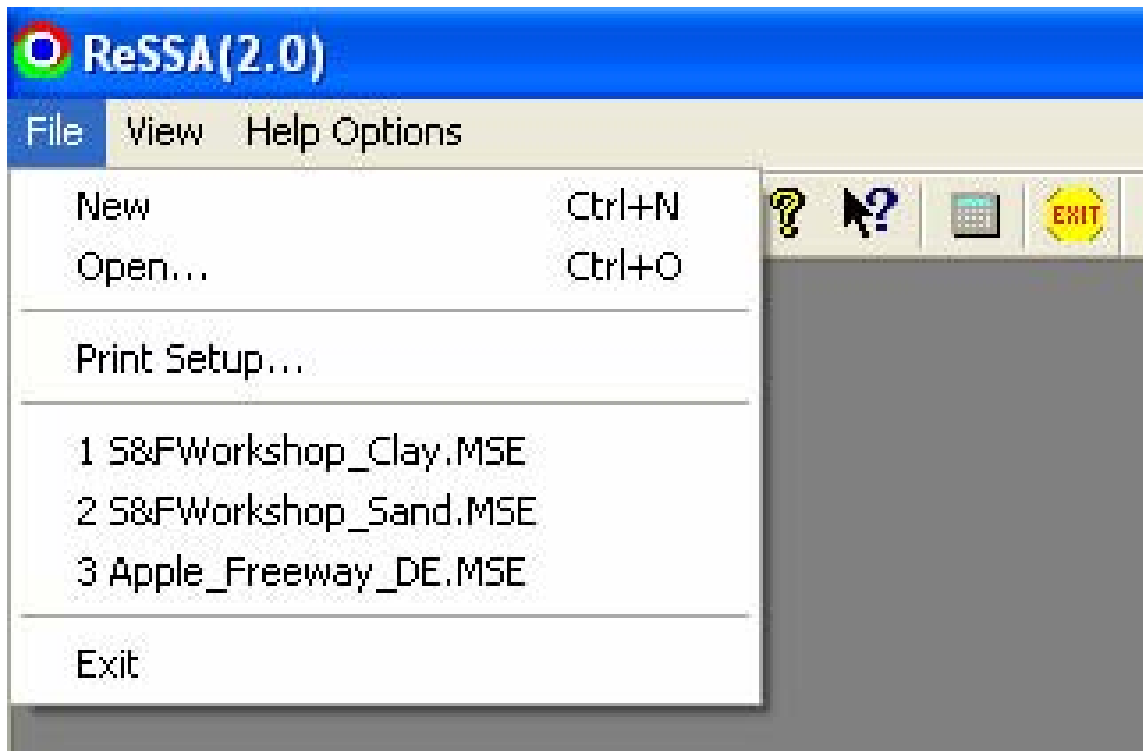


**Figure D-1. ReSSA startup screen.**

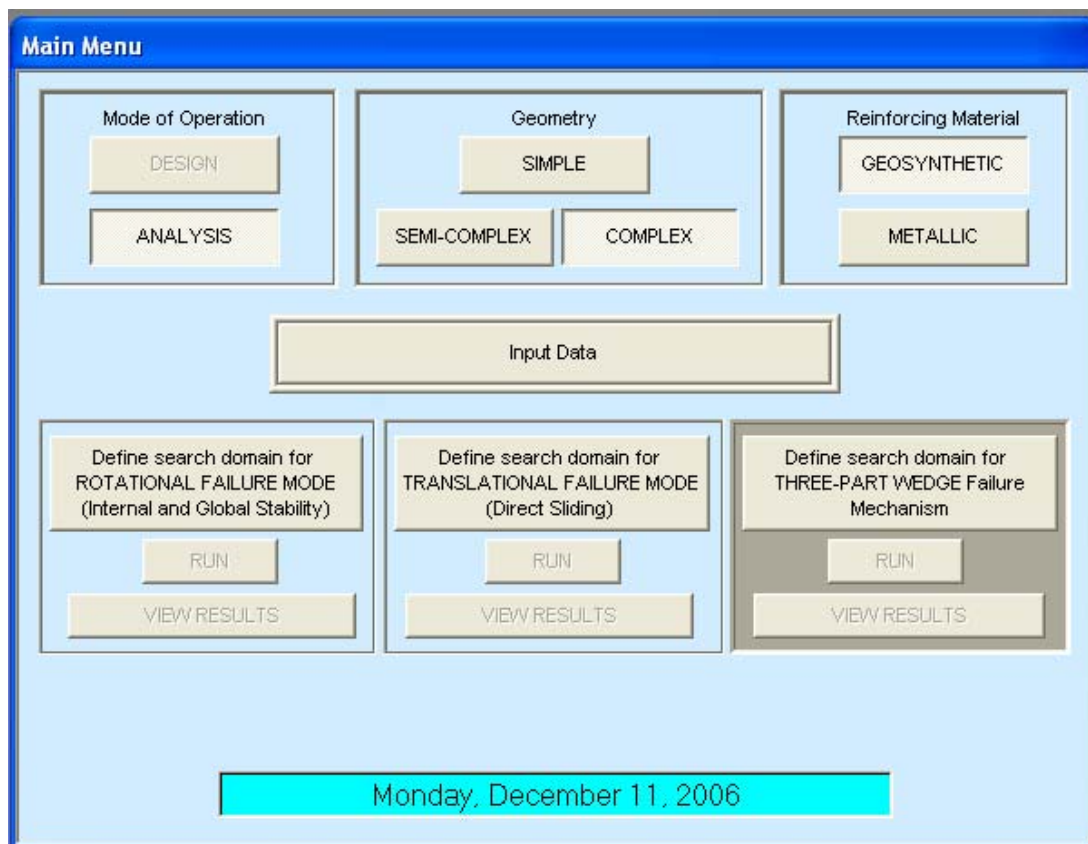


**Figure D-2. ReSSA main menu.**

In ReSSA, the user has the following options:

- **Mode of Operation:** User selects whether a “design” or “analysis” will be performed. For slope stability, we select “analysis.” For MSE slopes, the user can either use the “design” or “analysis” mode. In “design” mode, ReSSA determines the length of the reinforcement based on target factors of safety; this option is limited to simple slopes and should be used only as a first step. The user can switch from “design” to “analysis” and find the actual factors of safety corresponding to the computer generated reinforcement layout or any other layout specified by the user.
- **Geometry:** User can select several different inputs modes in ReSSA. In general, the “simple” and “semi-complex” modes are used when performing parametric analyses to assess relative sensitivity of parameter (i.e., slope angle, strength, etc.) selection. For the vast majority of slope stability analyses, it is recommended (and often required) to select the “complex” method of data entry.
- **Reinforcement:** ReSSA can perform an MSE slope analysis using either geosynthetic or metallic reinforcement. For unreinforced slope stability calculations, no reinforcement is used. At this step, the user selects one of the two reinforcement types and will later have the opportunity to overwrite this selection. This select/overwrite requirement is simply a procedural detail in ReSSA.

The next step is to select the “Input Data” tab (Figure D-3), where the user has the opportunity to set up the slope stability analysis project and essentially convert the handwritten slope geometry to an electronic record. Importantly, if a previous version of the project is selected, it is possible to change select parameters from the previous selection and then proceed with analysis. Data are input using the following screens:

- **Units:** User selects whether the input data are provided in English or SI units. It is important to recognize the specific units that are used and to be consistent throughout the analysis.
- **General Information:** This screen (Figure D-4) allows user to input information about the specific analysis and can help distinguish between various computer runs.

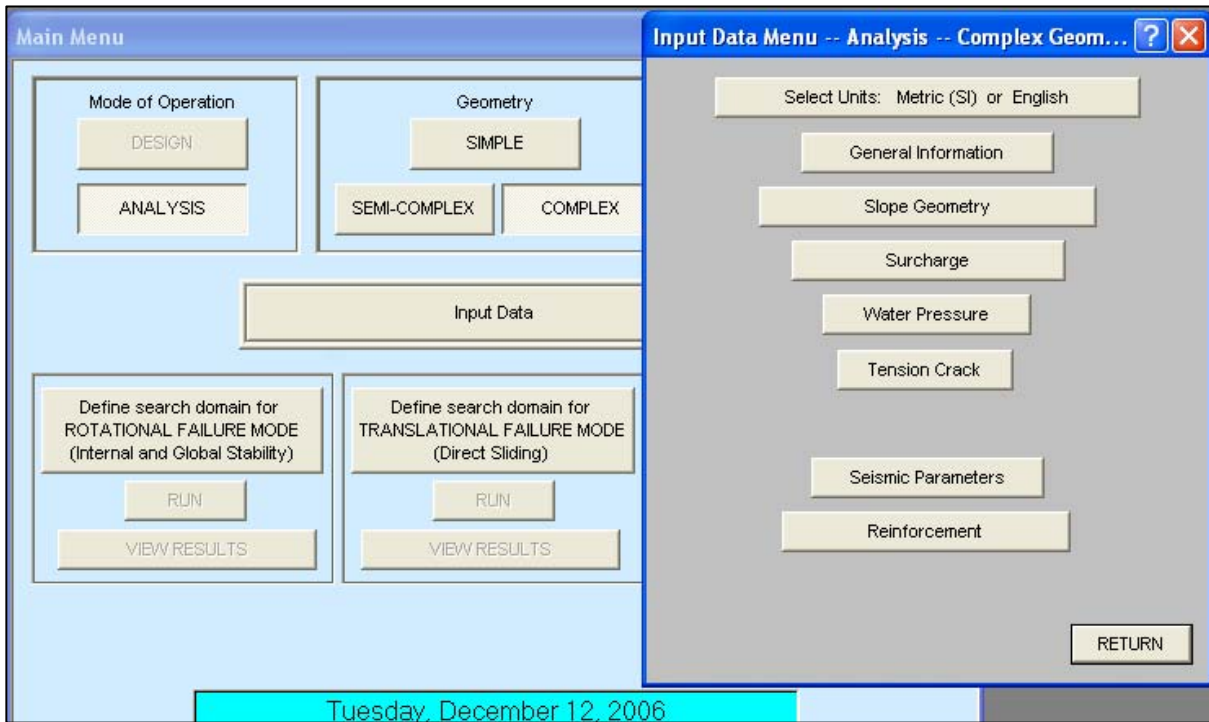


**Figure D-3. Data input screen from main menu.**

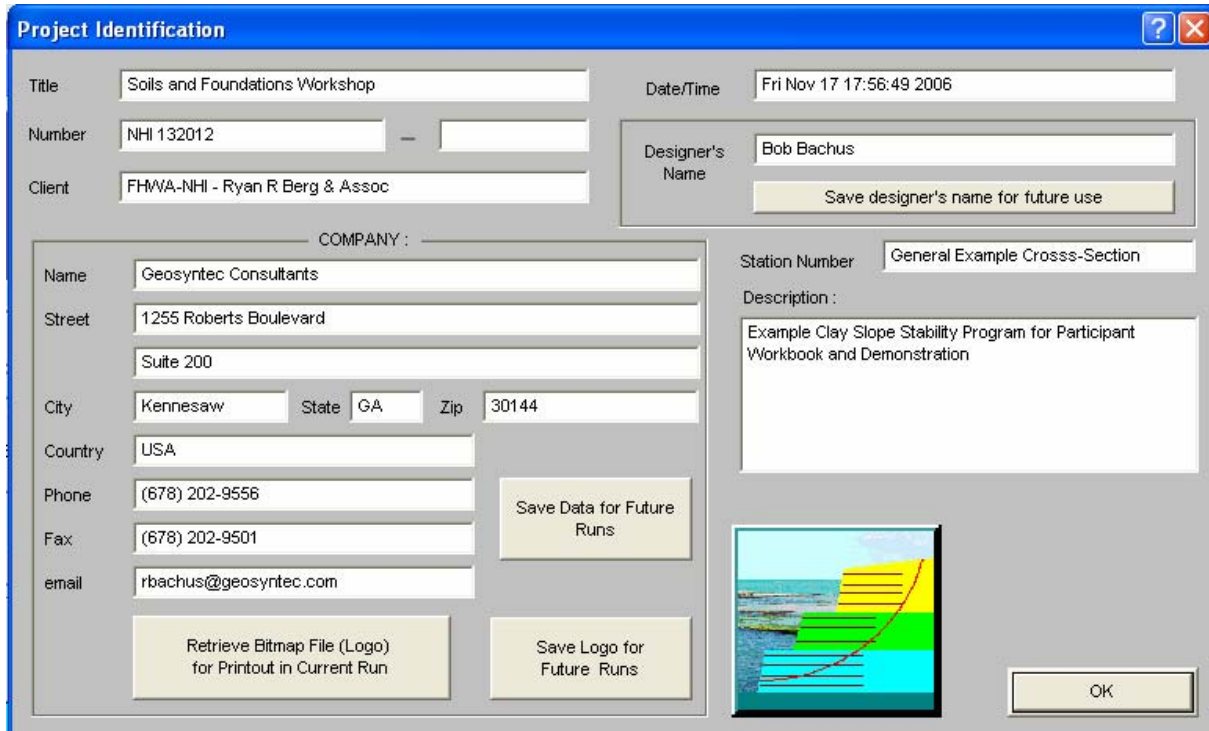


**Figure D-4. General information screen.**

- **Slope Geometry:** When the user selects the “Slope Geometry” tab, they are given the opportunity select the technique used to input the slope and subsurface geometry (Figure D-5). ReSSA also provides a “tip” to help the user in the data input process. Other computer programs have similar nuances that were incorporated by the developer to facilitate data input. The user next selects the number of input soil layers that will be used and then the “Define Geometry of Layers” tab. For the selected problem, Figure D-6 shows an example of the slope and subsurface profile that was previously input. The following information is presented on this figure:
  - Layer Number: For each layer, commencing at the ground surface, the user defines the geometry of the layer and the properties of the soils beneath the layer. When the geometry of a layer is entered, the user selects the next layer and repeats the geometry/properties data input. Once the geometry for the entire problem is entered, the user can return to these tabs and rapidly assess and modify any of the information.
  - Unit Weight: The total unit weight of the soil within the selected layer.
  - Friction Angle: The angle of internal friction for the soils within the selected layer.
  - Cohesion: The cohesion for the soils within the selected layer.
  - Table of X and Y Coordinates: Using the hand sketch as a guide, the user sequentially enters the coordinates of selected problem. At this stage, the user can observe the slope geometry being constructed.
  
- **Surcharge:** The user has the opportunity to place point loads or line loads as surcharges anywhere on the top surface. The loads can be vertical or inclined with respect to the vertical.
  
- **Water Level:** A single water table (or phreatic surface) can be considered in ReSSA. This surface can be horizontal or “sloped”, where the attitude of the surface is controlled by a series of line segments defined by their x and y coordinates. On this screen the user also has the opportunity to select whether a total or effective stress analysis will be performed. Guidelines for selection of the analysis type is beyond the scope of the course.
  
- **Tension Crack:** ReSSA gives the opportunity for the user to select a tension crack at the ground surface. The user can indicate the location and depth of the crack, as well as whether water will be considered to act on the crack. For purposes of analysis, the shear strength of this zone is not considered.

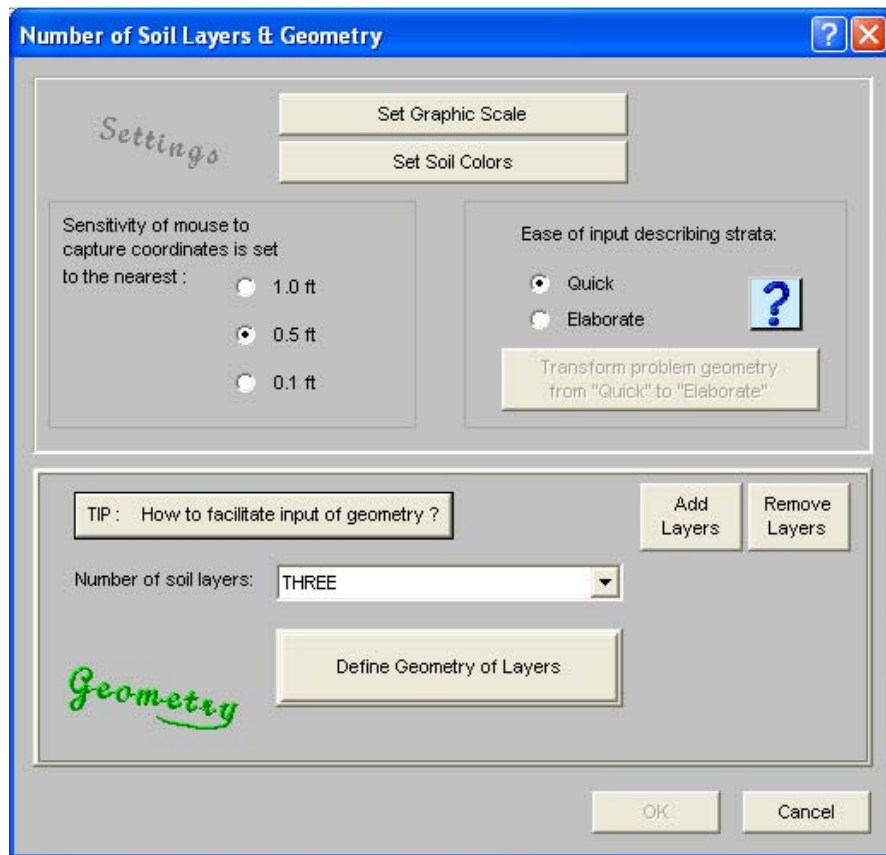


Figure D-5. Screen used to define soil layer geometry.

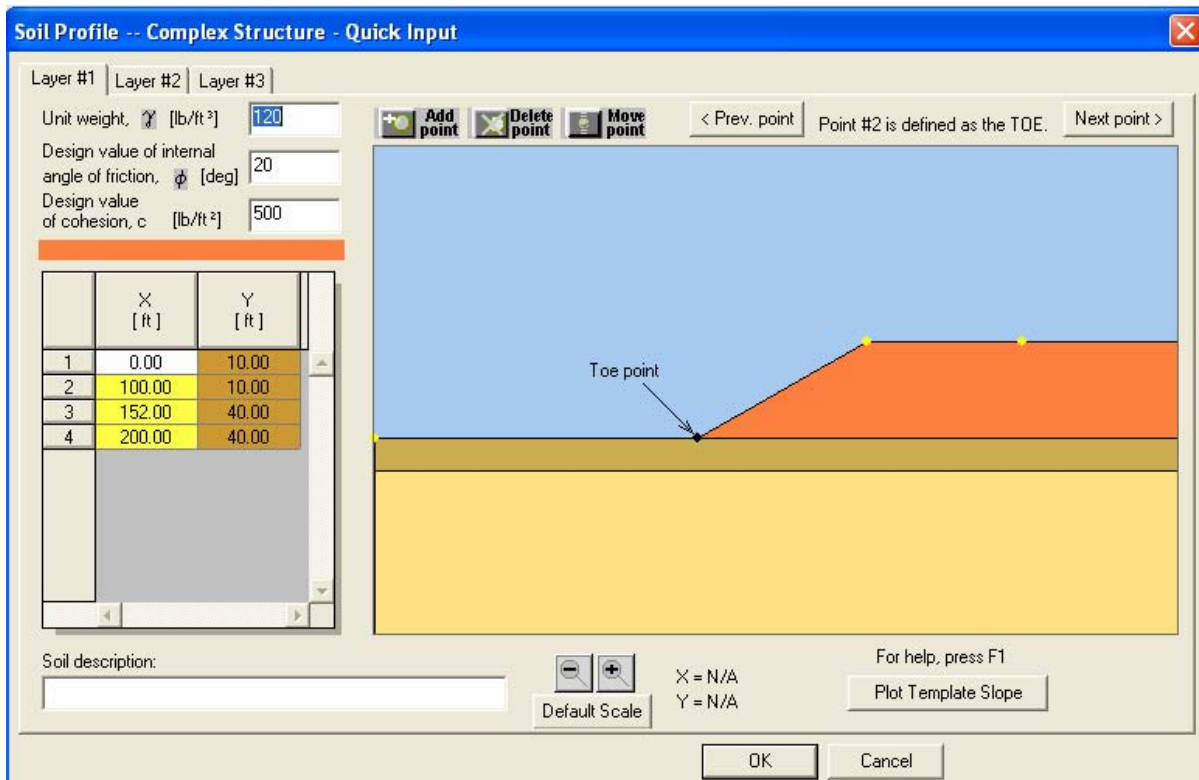


Figure D-6. Screen used to establish soil profile.

- **Seismic Parameters:** If a pseudo-static analysis is considered, the user can select the horizontal ground acceleration coefficient,  $A_0$ , as a specific percentage of the gravitational acceleration “g”. Procedures and guidelines for selecting an appropriate value of  $A_0$  is beyond the scope of this course.
- **Reinforcement:** Finally, the type of reinforcement considered in the analysis is selected. The user will note that the option “No Reinforcement Used” is selected to overwrite the previous selection when unreinforced slopes are considered.

At this point, the problem is ready to solve. It is recommended to double check all of the input screens to assure that the appropriate values and options are selected. Once this has been completed, the user will note that ReSSA offers the following three analysis options:

- **Rotational Failure Mode:** This option is selected when performing a circular or rotational analysis in assessing global slope stability. Additional discussion follows.
- **Translational Failure Mode:** This failure mode is limited to reinforced slopes and will not be used for general slope stability of unreinforced slopes. No additional discussion is presented in this document.
- **Three-Part Wedge Failure Mechanism:** This option is selected to assess the potential for sliding along the base, also referenced as a “block sliding” mode. Additional discussion follows.

Before an analysis can be performed, the user needs to select one of the two options. Regardless of the option selected, this first step of the analysis allows the user to select the controls that will be used to assess either rotational or sliding failure modes. For each of these, the user selects the “locations” where the analyses will be conducted. For the rotational failure mode, ReSSA accomplishes this by selecting a range of “Start” points at the top of the slope, the “Exit” points at the bottom of the slope, and the number of start and exit points within the selected range (Figure D-7). ReSSA makes it very easy for the user to select and modify the selected points by use of either: (i) coordinate selection; or (ii) drag and click using the mouse. For the three-part wedge failure mechanism, the user selects “boxes” in the subsurface where the base of the wedge will pass through (Figure D-8). Like the rotational failure mode, the box location can be selected using specific coordinates or by dragging the corners of the boxes using the mouse. The user can select a fairly wide range of potential surfaces in the initial runs and then “fine tune” the selection after preliminary review of the analysis results.

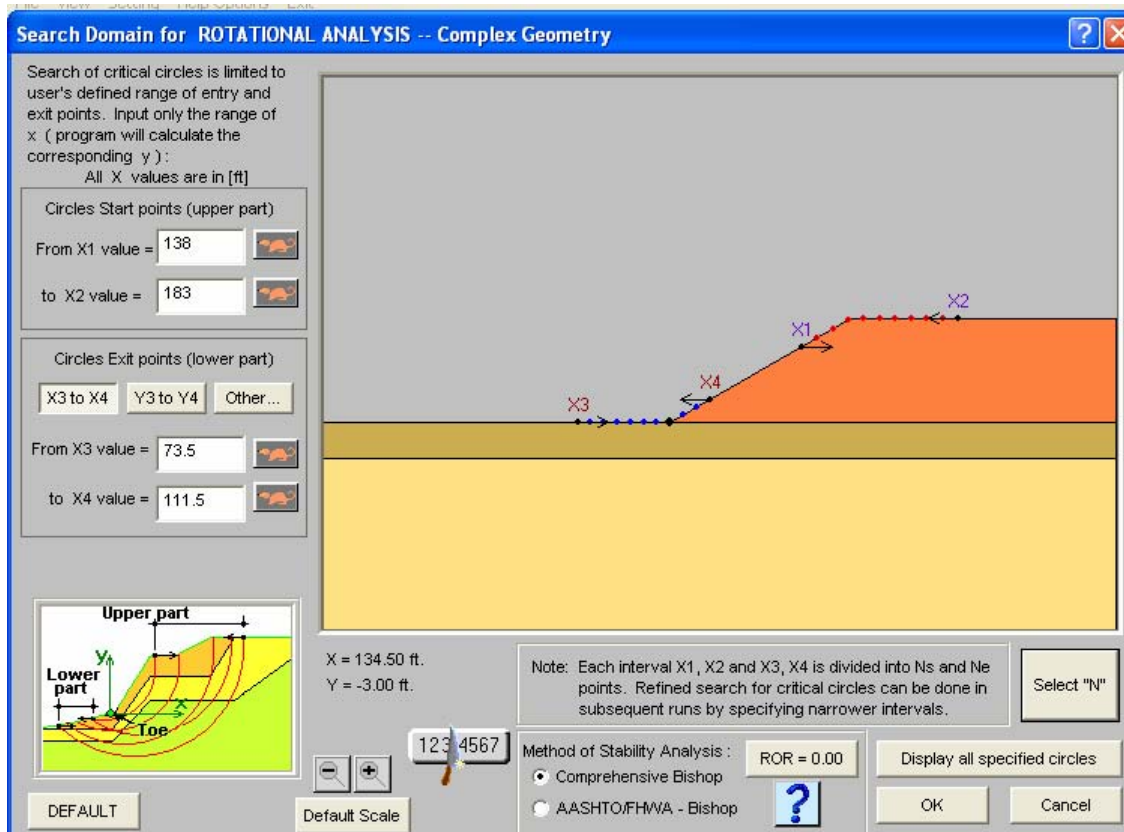


**Figure D-7. Selection of Start and Exit analysis points (Rotational failure mode).**

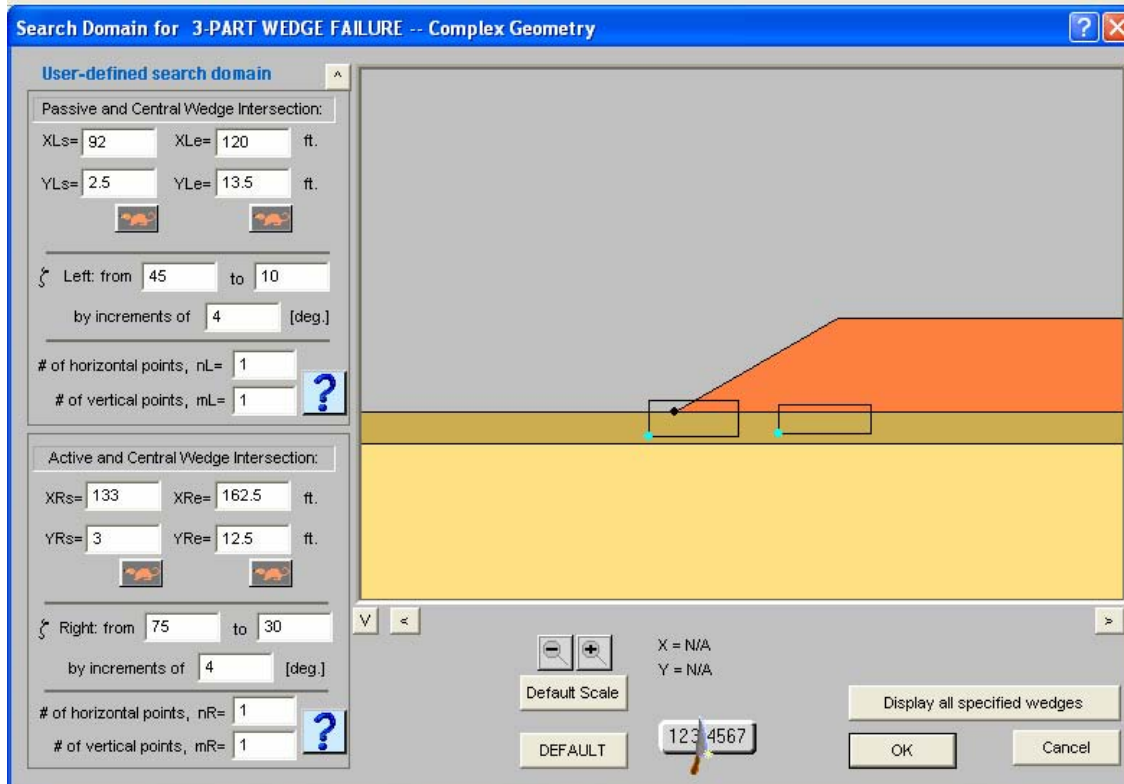


**Figure D-8. Selection of Boxes for Three-Part Wedge (Sliding Block analysis).**

After all of this preliminary work has been completed, it is now possible to actually conduct the analysis. This is accomplished by simply hitting the “Run” button. In a few seconds, the calculated lowest factor of safety, the most critical failure surface, and the center of the critical circle for the specific user-selected controls are displayed (Figure D-9). At this point, the user can perform additional analyses by narrowing the selection windows, as displayed in Figures D-7 and D-8 to assure that the computer is converging on the correct critical surface. With regards to the rotational failure mode, ReSSA provides the user with several useful options to help assess the calculated results. The following three options presented in Figure D-10 are particularly helpful and can be accessed using the “Results” tab on the toolbar.

- **Display 10 Most Critical Circles:** Although the program returns the analysis results for the single most critical calculation result, there is an option to display the surfaces that exhibit the 10 most critical (i.e., lowest calculated FS) surfaces. This option allows the user to assess whether there may be additional failure surfaces that need to be investigated.
- **FS Distribution:** This option is particularly helpful and is displayed at the top of Figure D-10. It shows the lowest calculated factor of safety at each of the “Start” and “Exit” points selected by the user. As shown on this figure, the selected range of start and exit points should result in a local minimum calculated factor of safety (FS). If the distribution indicates multiple local low values or low values at the edge of one of the start/exit points, it is recommended that the user “fine tune” the analysis to assure that the most critical condition(s) are identified and assessed.
- **Display Safety Map:** This option allows the user to observe all of the surfaces that were analyzed by the computer. Furthermore, using a user selected sensitivity scale bar, the calculation results are essentially “color coded” to indicate the relative sensitivity of the calculated FS. The safety map is a diagnostic tool that can indicate how efficient the reinforcement is utilized considering both its strength and length.

Using other options of the taskbar the user can observe the number of slices used in the analysis and assess the orientation of calculated forces, etc. on each slice. Importantly, a tabulated summary of results can be obtained for review by the user. Finally, a summary report can be presented. It is recommended that once an analysis has been completed, the user print a hard copy of the report for the project files and to assure that the problem solved by the computer is, in fact, the one desired by the user.

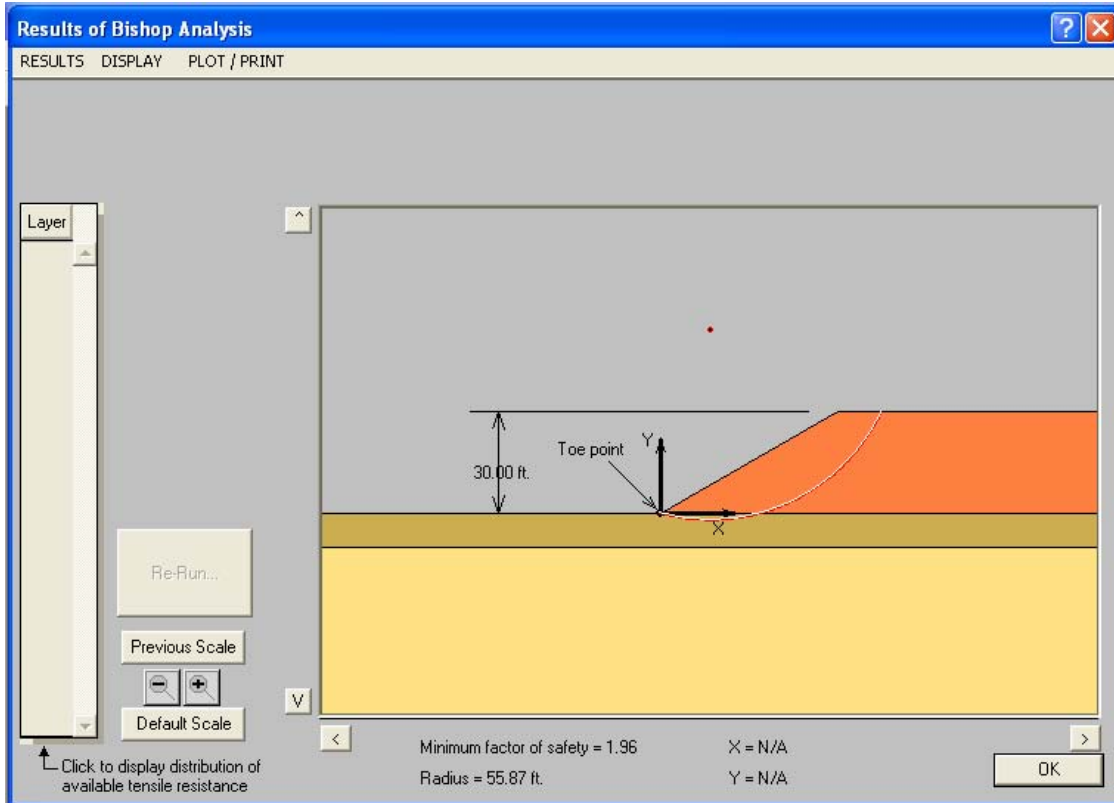


Figure D-9. Critical failure surface (Rotational analysis).

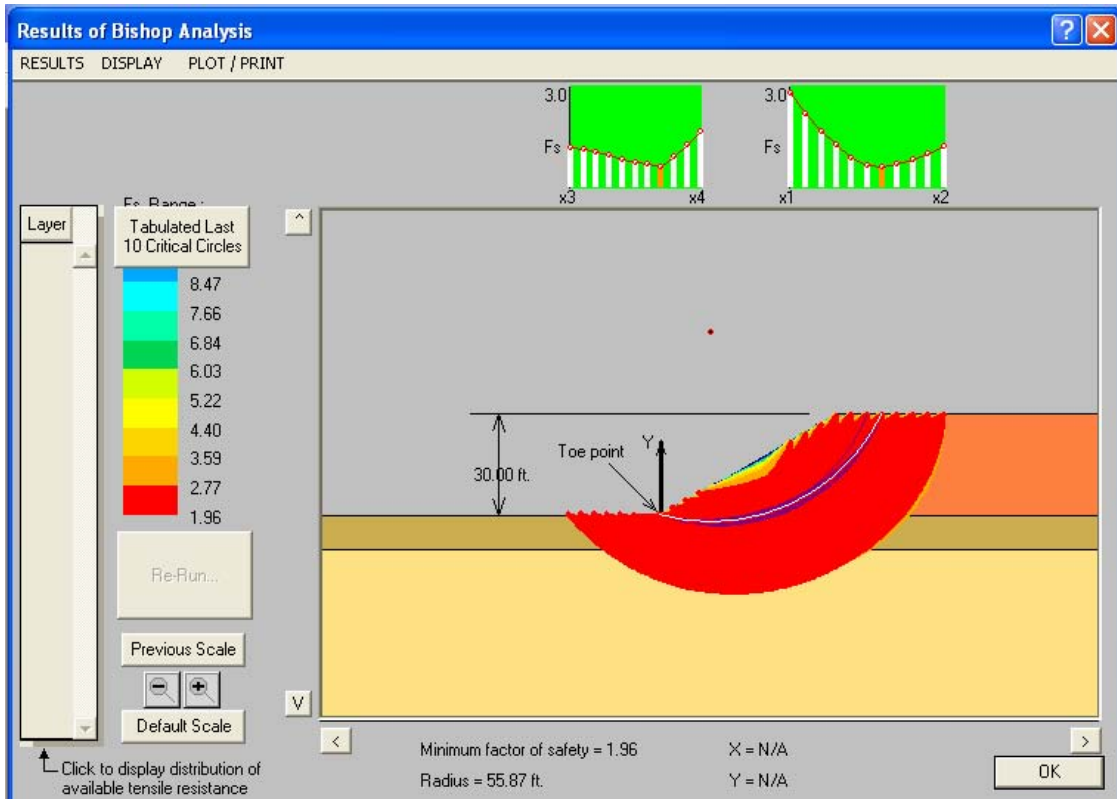


Figure D-10. Factor of safety distribution and Safety Map.

As can be seen in this narrative summary and the selected screen shots, ReSSA is a powerful analysis tool that can greatly aid the geotechnical specialist in assessing slope stability. One of the biggest advantages of ReSSA (and other computer programs) is that the “learning curve” for the program is not very steep, implying that users can be “up and running” fairly quickly. Most commercial programs are user-friendly and provide analysis/display options to help the user perform several “what-if” sensitivity analyses, which can be tremendously beneficial for a given project. In term of advice to the user, the authors recommend that they refer to the example programs provided by the software developers and try to re-create the published solutions. Most commercial slope stability software programs have extremely helpful example programs, Help Screens, and Users Manuals to help the user increase competence and confidence in assessing slope stability.

**Finally, it is always recommended that a selected solution be verified or validated using independent resources (i.e., other computer codes, chart solutions, etc.) and that final results be reviewed by an experienced peer and senior reviewer.**

**APPENDIX E**

**USE OF THE COMPUTER PROGRAM**

**FoSSA**

[THIS PAGE INTENTIONALLY BLANK]

## APPENDIX E USE OF THE COMPUTER PROGRAM FoSSA

### E.1 INTRODUCTION

The computer program Foundation Stress and Settlement Analysis (FoSSA), version 2.0 was developed by ADAMA Engineering, Inc. (ADAMA), Newark, Delaware under contract to FHWA. The following description of the program is provided by ADAMA:

*“FoSSA(2.0) is an interactive program for computing the stress and settlement resulting from an embankment loading. It can consider the effects of staged construction and PVD’s.”*

FoSSA(1.0), the first released version, is a user-friendly, Windows-based program that is provided free-of-charge (but in a limited number of licenses) to each state DOT for their use to assess stress distribution and to calculate settlements beneath embankments. FoSSA(2.0) has additional features that were added in response to users comments. As indicated in the above description, FoSSA can also address partial consolidation under staged loading conditions and the beneficial effects of prefabricated vertical drains (PVDs). There is also a provision in FoSSA to address the stress distribution and settlement beneath multiple footings. As FoSSA is used in the Soils and Foundations course primarily to assess and understand the stress distribution beneath embankments, this narrative focuses on this component of the program. The other components (i.e., staged loading, PVDs, multiple footings) are considered beyond the scope of the course and will not be addressed. An excellent introduction regarding the program capabilities related to these other topics is provided on the opening screen taskbar titled ‘Help Topics’ (Figure E-1).

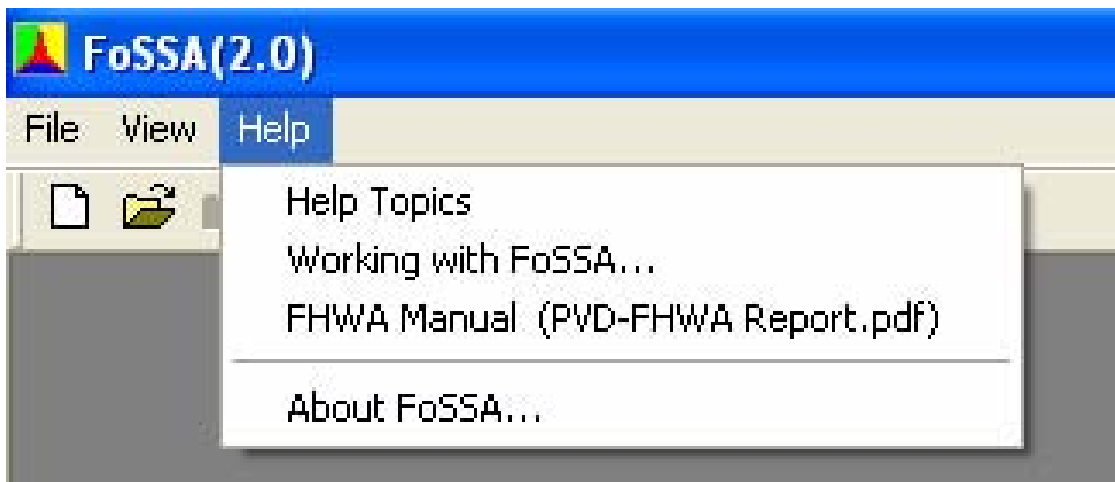


**Figure E-1. Opening screen to learn capabilities of the program (Help Topics).**

With regards to embankment stress distribution and settlement, FoSSA represents an advancement of the DOS-based program titled EMBANK (version 2.00), a program developed for FHWA by Prototype Engineering, Inc. in 1991. FoSSA can also be used to confirm the validity of the chart solutions regarding stress distribution beneath embankments attributed to the New York State DOT as presented in Figure 7-6 in the Reference Manual.

This appendix was prepared to provide a narrative summary of some of the specific features of FoSSA. It is recognized that this document is provided in lieu of a hands-on demonstration of the program capabilities as part of the course. The instructor can demonstrate FoSSA if there is interest among individual participants. It is important to note, however, that this summary was never intended to serve as or replace the Users Manual and the supporting technical documentation provided with the FoSSA program by ADAMA. The remainder of this appendix is organized to provide several screen shots from FoSSA and will demonstrate the use of the program for the case of an embankment on clay deposit.

## **E.2 PREPARING FOR INPUT TO THE COMPUTER PROGRAM**

Before the analysis can be performed using a computer, it is essential that the user/designer prepare a hand sketch using an “unexaggerated” x-y scale (i.e., the same scale in the x and y directions). This sketch should show the geometry of embankment, geometry of the loads, the subsurface stratigraphy, and the location of the water table. It will be necessary to assign coordinates to the various points on this sketch so that information regarding the geometry can be input to the computer. Remember that the computer will only solve the problem that the user asks it to solve, so the user needs to be sure that the geometry developed in the hand sketch matches the geometry presented on the computer screen. Once the hand sketch is developed, it is possible to now enter the information into the computer. This initial step of developing a hand sketch is absolutely essential, particularly for complex embankment geometries and subsurface conditions. If the subsurface conditions change across the actual project site, it is necessary to develop multiple cross-sections for analysis so that the most critical cross-section can be identified and reported.

## **E.3 WORKING WITH FoSSA**

The opening screens for FoSSA are similar to the opening screens for the program ReSSA presented previously in Appendix D. Under the “File” tab on the initial screen, the user opens an existing file or selects “New.” At this step, the user has the option to: (i) re-run the program using an existing file; (ii) modify the input of an existing file and re-run the program; or (iii) establish a new program. For whichever option is selected, the next screen (Figure E-2) allows the user to select: (i) 2D geometry represented by a long rectangular

embankment of uniform cross section (i.e., plane strain); (ii) 3D geometry for representing relatively square embankment or footing loadings; or (iii) multiple foundations to simulate the interaction of foundation loading. Only the 2D case is discussed for the course. When the user selects “2D” and “Input Data,” Figure E-3 is presented. The user can “Select Units” and provide “General Information” in a manner similar to that used previously for ReSSA.

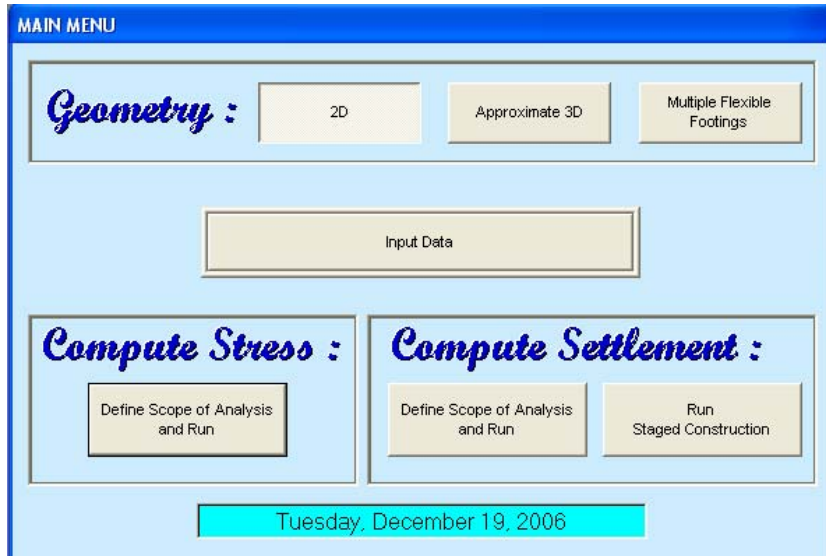


**Figure E-2. Launch screen for computing stress and settlement.**

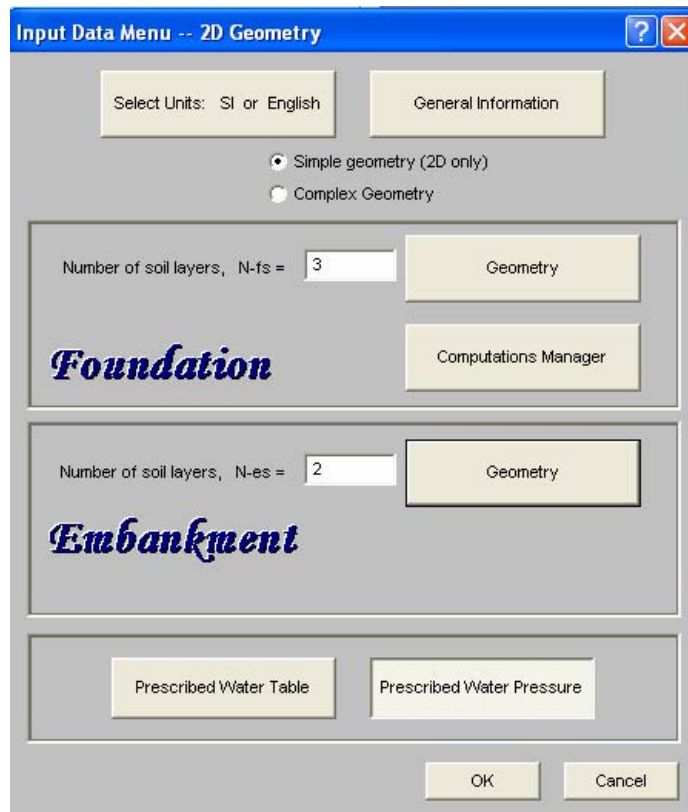


**Figure E-3. Input Data Menu (2D Geometry).**

After the initial general information is provided, the problem geometry is ready to be input to the computer. As mentioned in Section E.2 earlier, it is imperative that the user first sketch the analysis cross-section by hand and assign coordinates to all of the relevant foundation and embankments layers. For this example problem, Figure E-3 indicates that the user can select an option to consider a “Simple” (i.e., horizontal subsurface stratigraphy that will be used herein) or a “Complex” 3D geometry (i.e., plane strain geometry assuming soil layers of non-uniform thickness in the cross-section). For the purpose of this demonstration, select “Simple Geometry” which will then give the opportunity to develop the profile by selecting the “Foundation” and “Embankment” tabs. An example of a “Simple” stratigraphy is presented in Figure E-4, while an example of a “Complex” stratigraphy is provided in Figure E-5. Note that for the Simple stratigraphy, only the vertical elevation is required, while for the Complex model data for the subsurface are entered as lines exhibiting x-y coordinates similar to the procedure used in ReSSA (Appendix D).

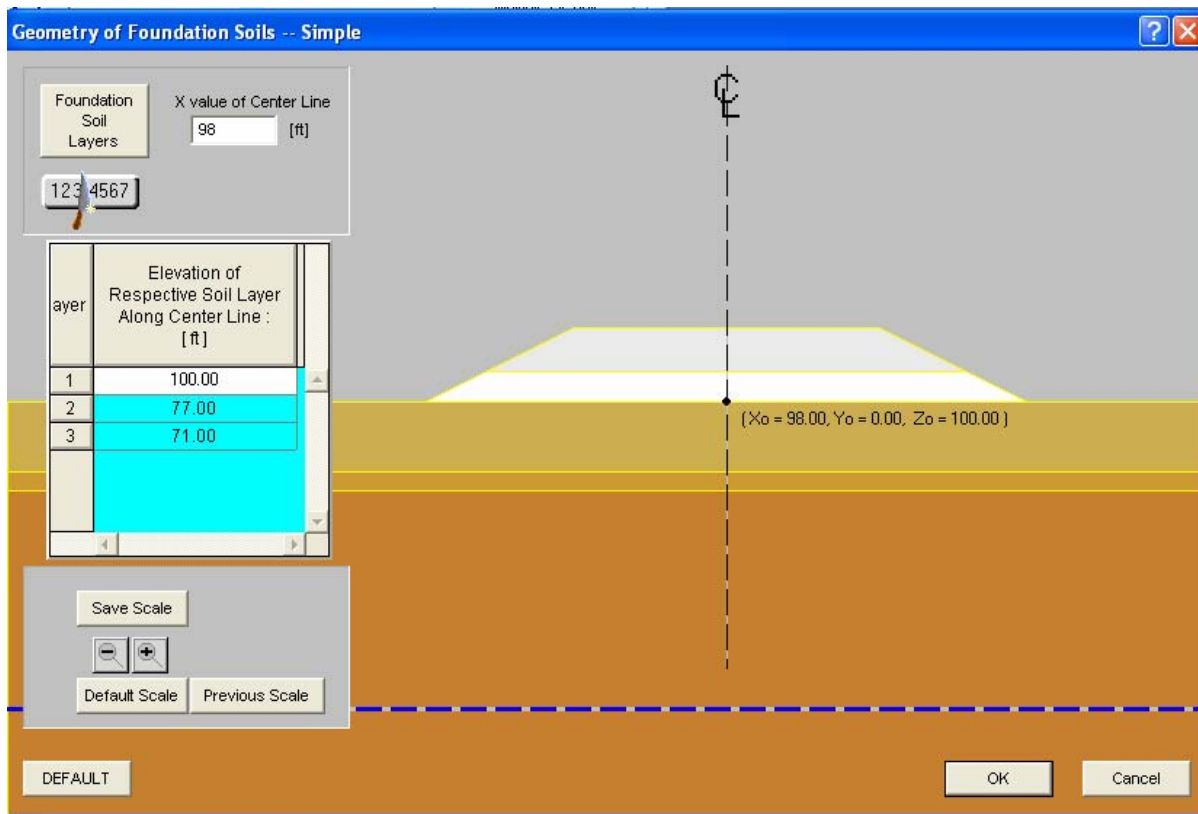


**Figure E-4. Example problem with “Simple” horizontal geometry.**

From Figure E-4 the user provides information regarding the geometry of the Foundation soils and the Embankment soils by accessing the relevant “Geometry” tabs. For the “Foundation” layer, there is a tab designated “Computations Manager” where input regarding the analysis are provided (Figure E-6). At this tab, the user can identify the following analysis conditions: (i) primary consolidation; (ii) effects of PVDs; (iii) calculation of increased shear strength due to consolidation; (iv) secondary consolidation; and (v) elastic or immediate settlement.

By accessing the “Modify Input” button on this screen, the user is provided the opportunity to input the consolidation (and time rate of consolidation) properties of the foundation soils (Figure E-7). With regards to the “Embankment” layer, the “Geometry” tab allows the user to provide information regarding the geometry and properties of the embankment (Figure E-8). In FoSSA, it is assumed that the embankment provides the loading for the foundation soils. Internal settlement of the embankment is explicitly not considered. From the “Input Data” button shown in Figure E-2, the user can also locate the water table using x and y coordinates (Figure E-9).

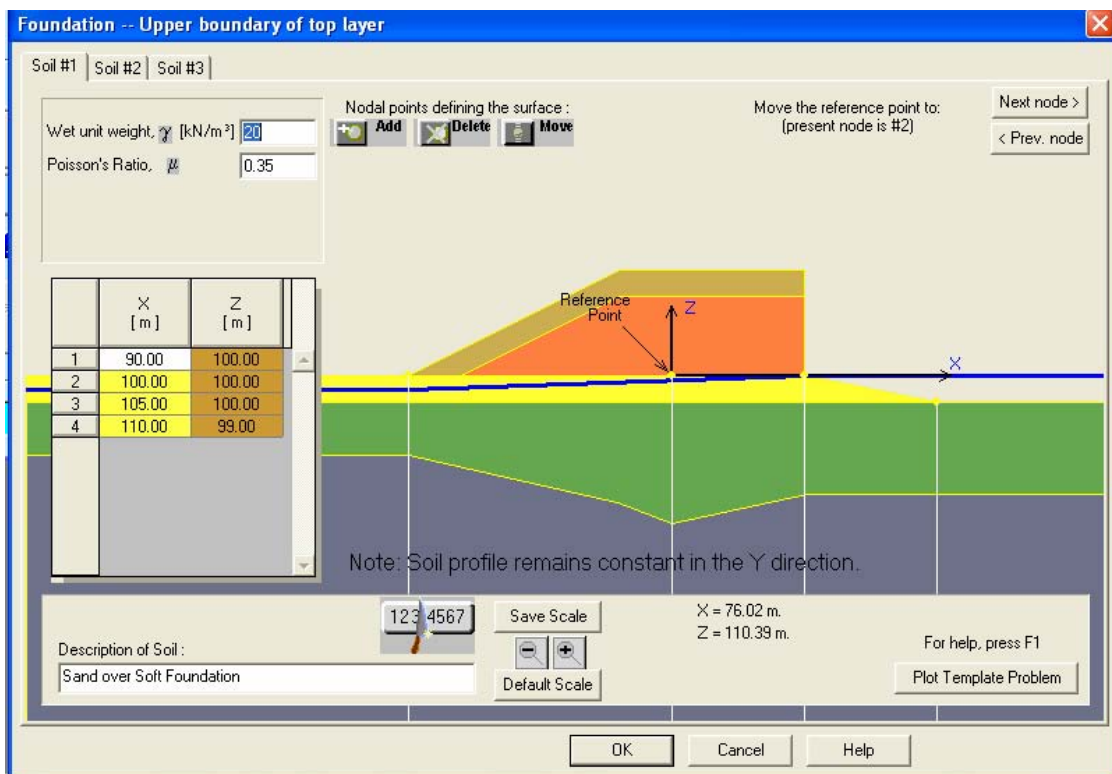


**Figure E-5. Example of 2D “Complex” subsurface stratigraphy.**

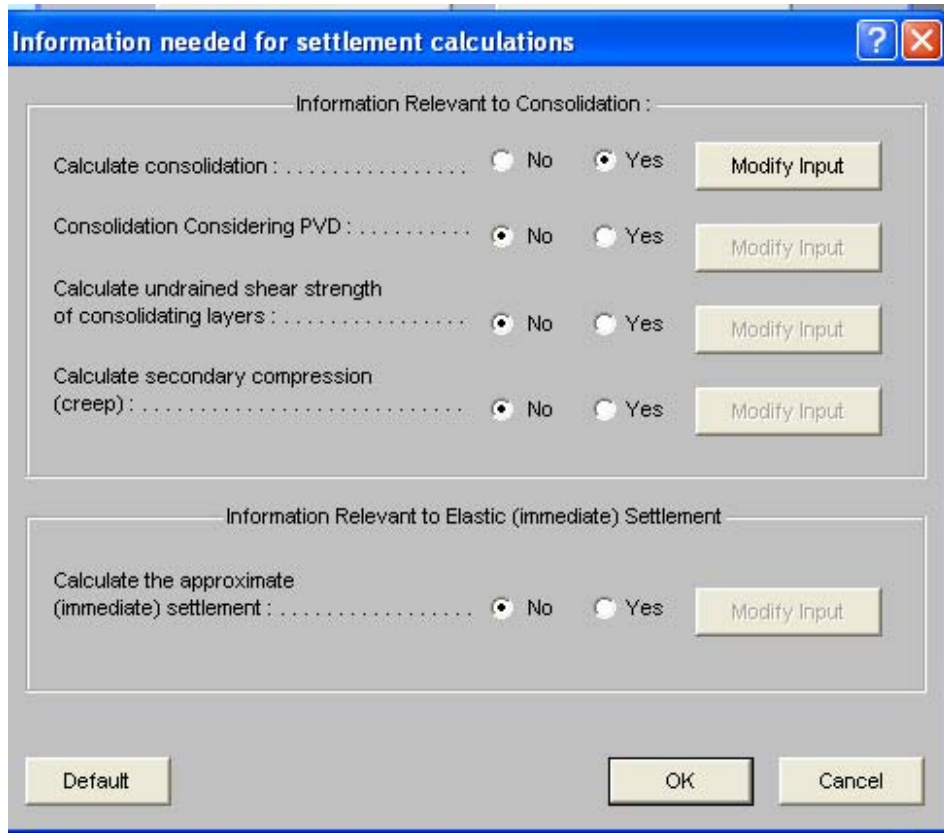


Figure E-6. Computation Manager Tab for defining the analysis case.

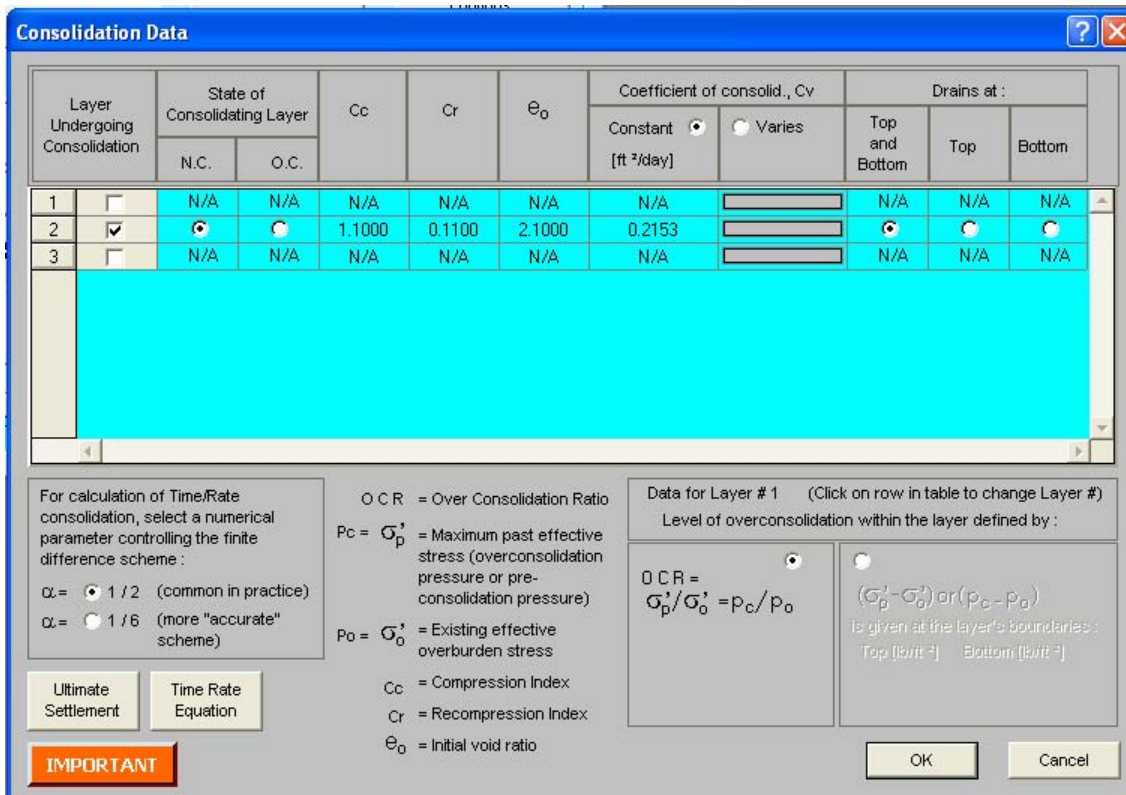


Figure E-7. Screen to provide foundation soil properties.

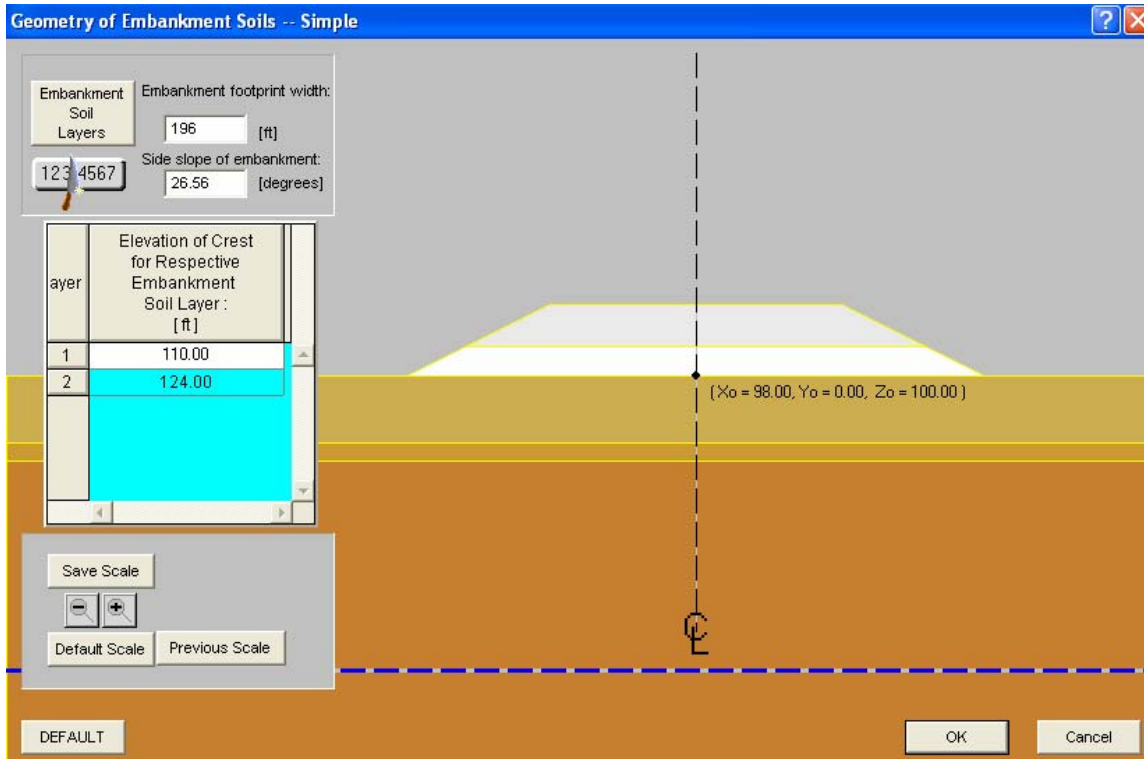


Figure E-8. Screen for embankment properties and geometry.

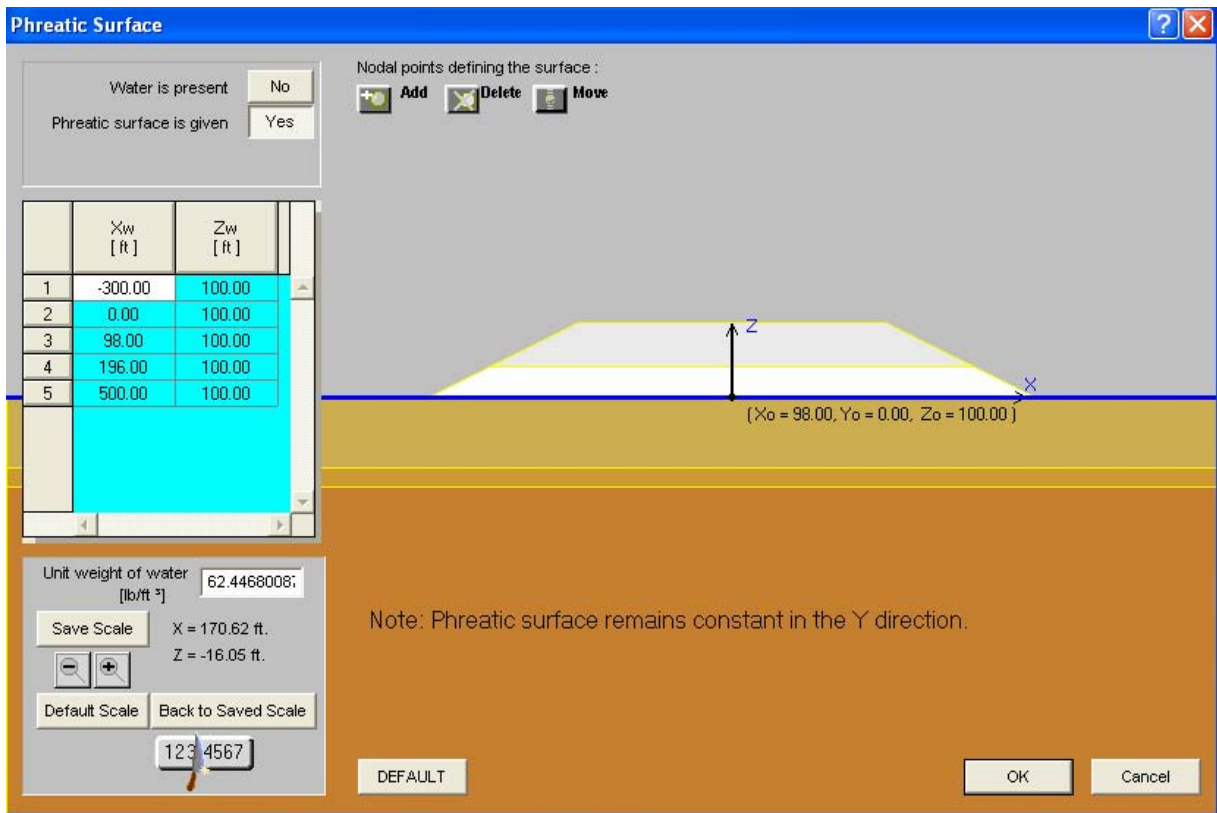


Figure E-9. Input of water table.

At this point, the program goes back to the screen (Figure E-2) and is ready to “Compute Stress” or “Compute Settlement” that would be induced in the foundation soils by the overlying embankment. Under each computation section is the launch tab titled “Define Scope and Analysis of Run.” For the “Compute Stress” analysis, the user is directed to the taskbar, where there are several options to define the analysis limits and the results display format (Figure E-10). Of major importance are the “Define” task and the “Define Domain” option under this task (Figure E-11). At this screen, the user can select whether the analysis results (and display) will be presented along vertical or horizontal profiles, at a single point, or at selected grid points. The user selects the number of analysis and display points. Example outputs are presented in: (i) Figure E-12 for the vertical incremental stress distribution at 50 different depths beneath the centerline of the embankment to a depth of 400 ft below the embankment; and (ii) Figure E-13 for the contour of vertical incremental stresses using an analysis grid. Figure E-14 shows the analysis grid used for the contours presented in Figure E-13. As shown in the lower right hand corner of Figures E-10 through E-14, the user has the option to display the incremental vertical, horizontal and/or shear stresses on the display. Finally, by selecting the “Results” tab on the Taskbar after a specific analysis is complete, a tabulated summary of results is produced for export to Excel. This tabulated summary can include the vertical overburden stress or all of the incremental stress calculation results not just the displayed results (Figure E-15).

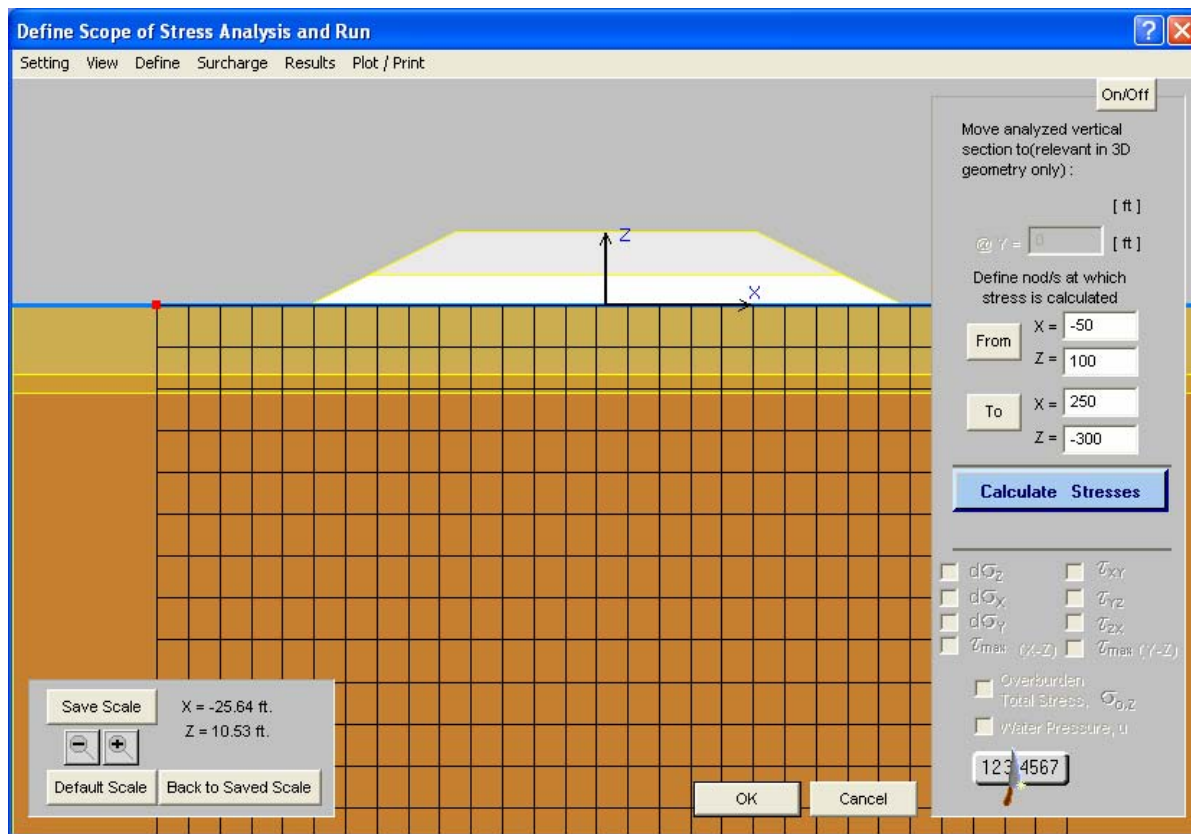
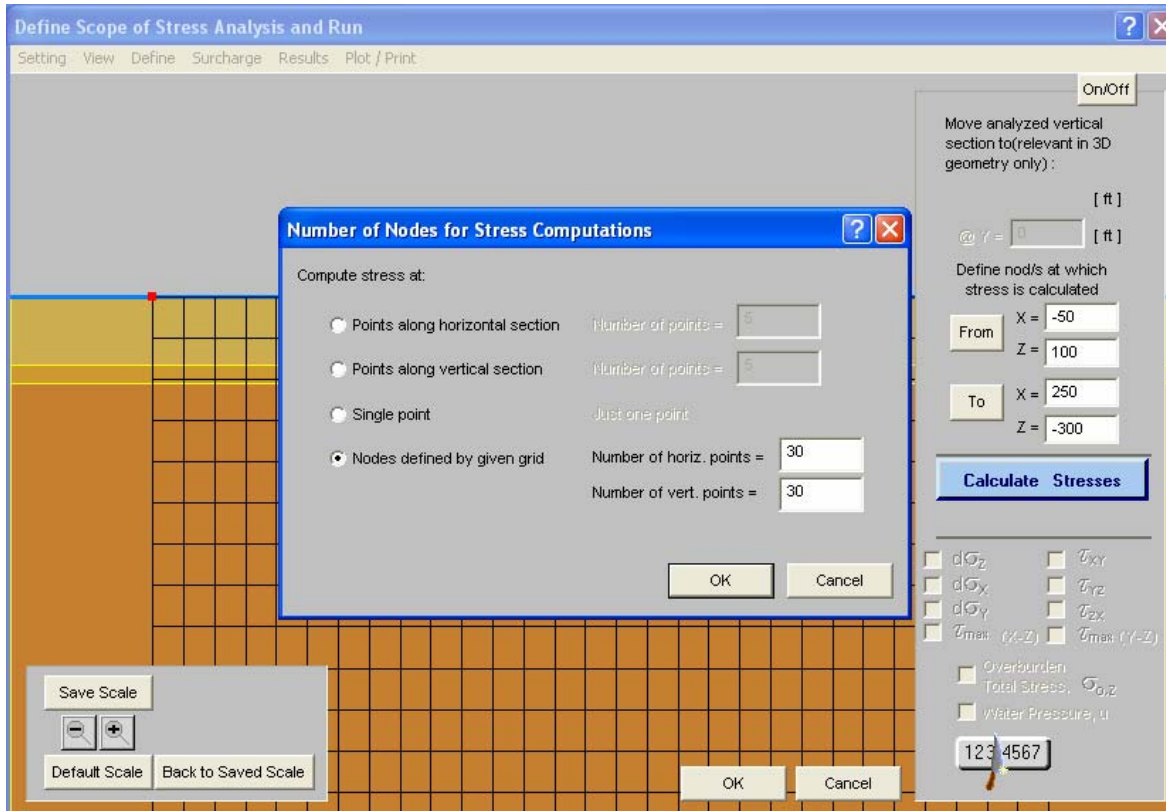
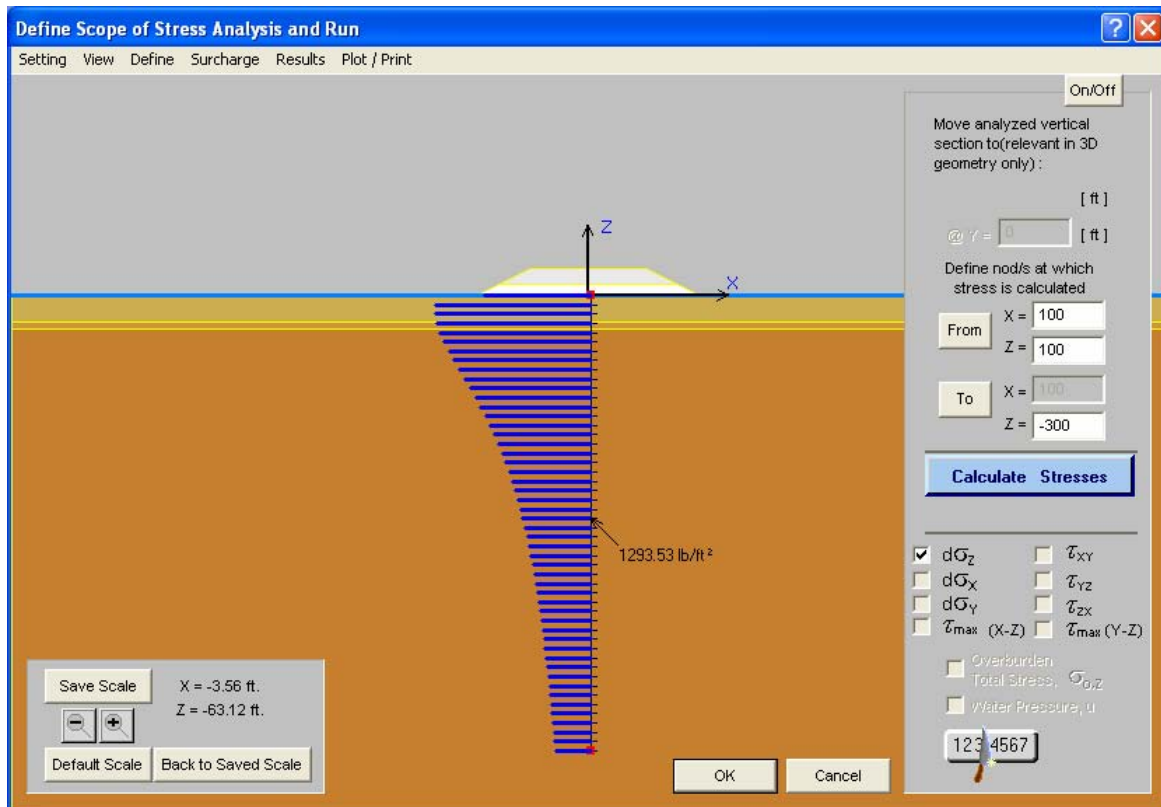


Figure E-10. Defining scope of stress analysis



**Figure E-11. Defining scope of stress analysis using Define Domain on Taskbar.**



**Figure E-12. Example output for vertical stress profile beneath centerline.**

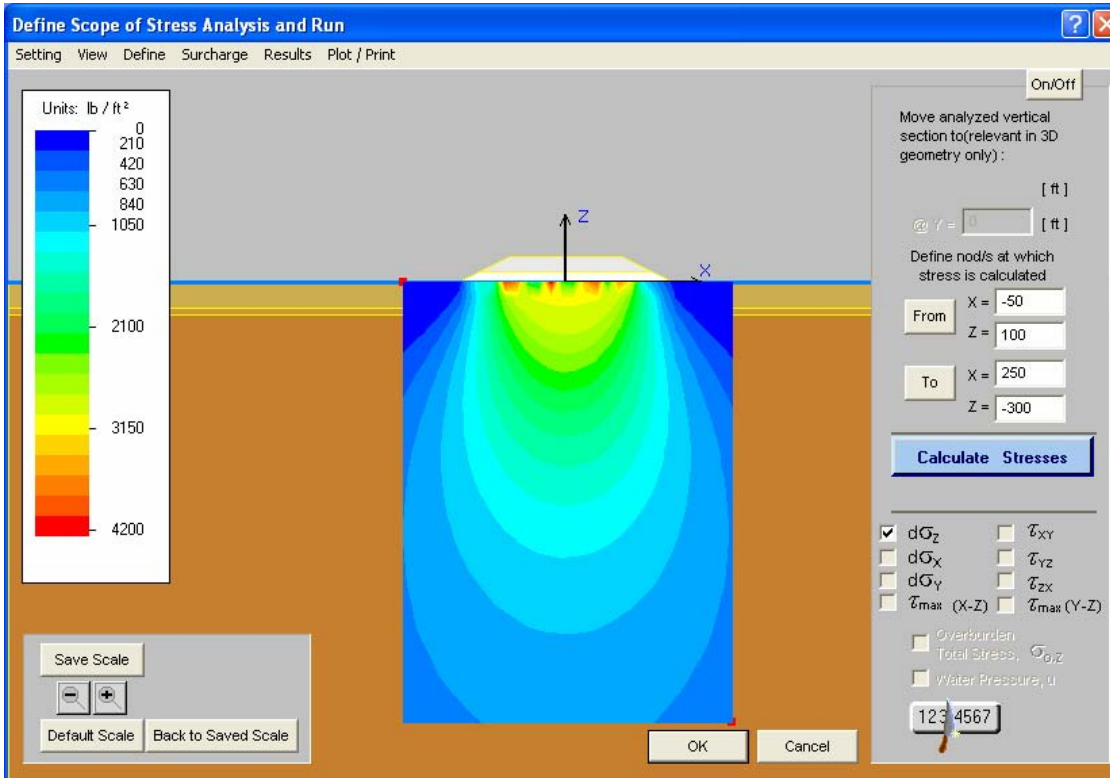


Figure E-13. Example contour plot of incremental vertical stress increase.

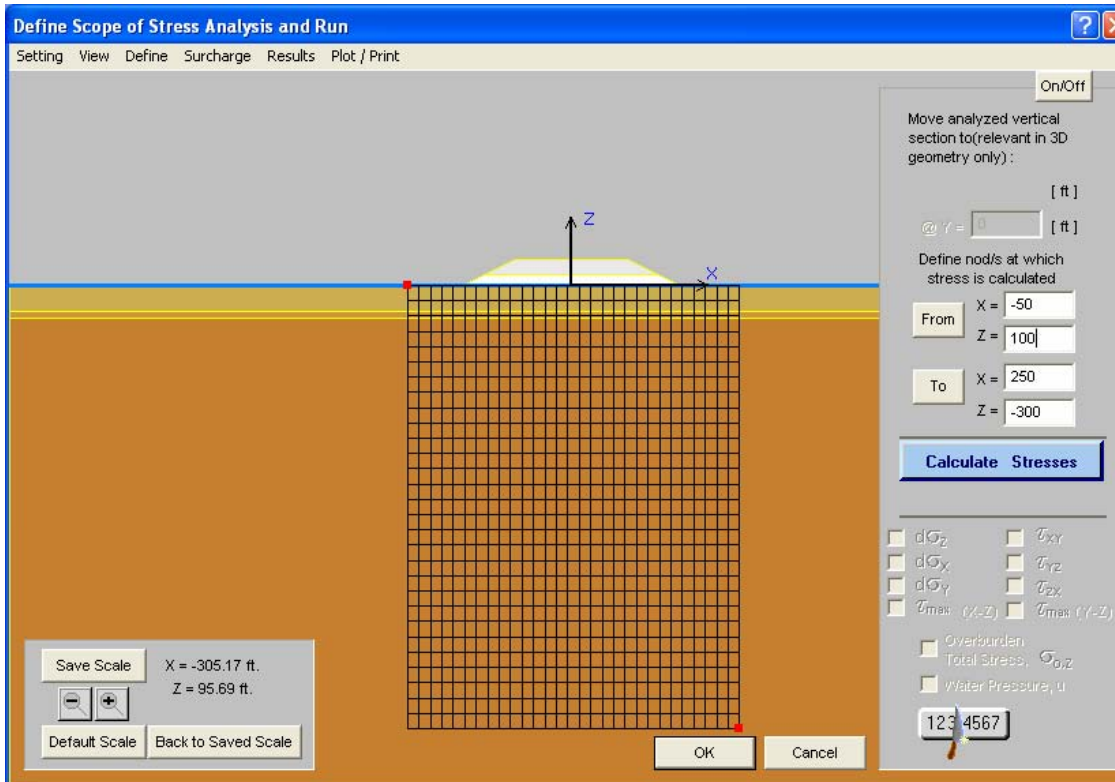


Figure E-14. Example of analysis grid used to produce Figure E-13.

View Computed Stresses

STRESS DUE TO SURCHARGE:

#	Elevation, -----			Normal Stress -----			Shear Stress -----			$\tau_{max}$ (X--Z)	$\tau_{max}$ (Y--Z)
	Z [ ft ]	X [ ft ]	Y [ ft ]	$d\sigma_z$ [ lb/ft <sup>2</sup> ]	$d\sigma_x$ [ lb/ft <sup>2</sup> ]	$d\sigma_y$ [ lb/ft <sup>2</sup> ]	$\tau_{xy}$ [ lb/ft <sup>2</sup> ]	$\tau_{yz}$ [ lb/ft <sup>2</sup> ]	$\tau_{zx}$ [ lb/ft <sup>2</sup> ]		
1	100.00	-50.00	0.00	0.00	-0.00	0.00	0.00	0.00	0.00	0.00	0.00
2	100.00	-39.66	0.00	0.00	-0.00	0.00	0.00	0.00	0.00	0.00	0.00
3	100.00	-29.31	0.00	0.00	-0.00	0.00	0.00	0.00	0.00	0.00	0.00
4	100.00	-18.97	0.00	0.00	-0.00	0.00	0.00	0.00	0.00	0.00	0.00
5	100.00	-8.62	0.00	0.00	-0.00	0.00	0.00	0.00	0.00	0.00	0.00
6	100.00	1.72	0.00	108.39	70.13	72.89	0.00	0.00	-34.06	39.07	17.75
7	100.00	12.07	0.00	891.39	448.80	553.34	0.00	0.00	-218.38	310.90	169.03
8	100.00	22.41	0.00	1397.64	986.82	1006.89	0.00	0.00	-445.99	491.02	195.37
9	100.00	32.76	0.00	1387.68	1788.84	1394.82	0.00	0.00	387.55	436.38	3.57

View results for points at elevation 100.00 ft.

Back << >> Next

Tabulated results:

Export to Excel Print / Save as Text

RETURN

**Figure E-15. Examples of results in a tabulated output format.**

With regards to settlement calculations, the user can launch the “Compute Settlement” analysis independent of the stress calculations on the screen shown in Figure E-9. The resulting display from the launch is shown on Figure E-16. Calculated settlements at the base of the embankment are calculated. The user has the option to define the horizontal limits of the presented results and the number of analysis points that will be displayed. After launching “Calculate Ultimate Settlement,” the user has the option to display results on a true axis or on an exaggerated vertical axis (Figure E-17). By accessing the “Results” option on the taskbar, a tabulated summary of results is presented in an Excel format similar to that previously shown in Figure E-15. Time rate of settlement calculations can also be performed, but are limited to a single horizontal location. After selecting the analysis location and performing an ultimate settlement calculation, the user launches the “Time Rate of Consolidation” button. The user selects either the time of the percent consolidation criteria for controlling the analysis, as displayed in the upper right hand corner, and then launches the analysis by selecting “Calculate” on the displayed screen. Results are presented as isochrones (Figure E-18). Results can also be presented in a tabulated format by selecting the “Tabulated Results for approximately “x days,” where x was previously selected by the user (Figure E-19).

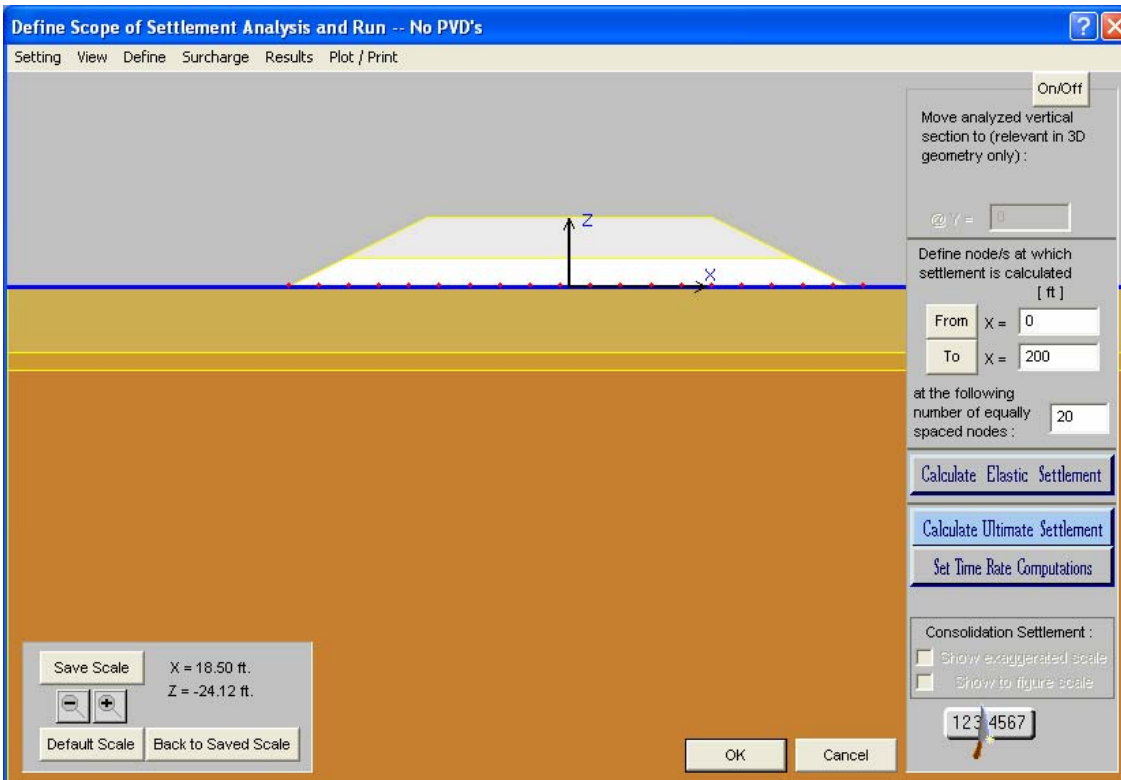


**Figure E-16. Resulting screen from Launch to compute settlement.**

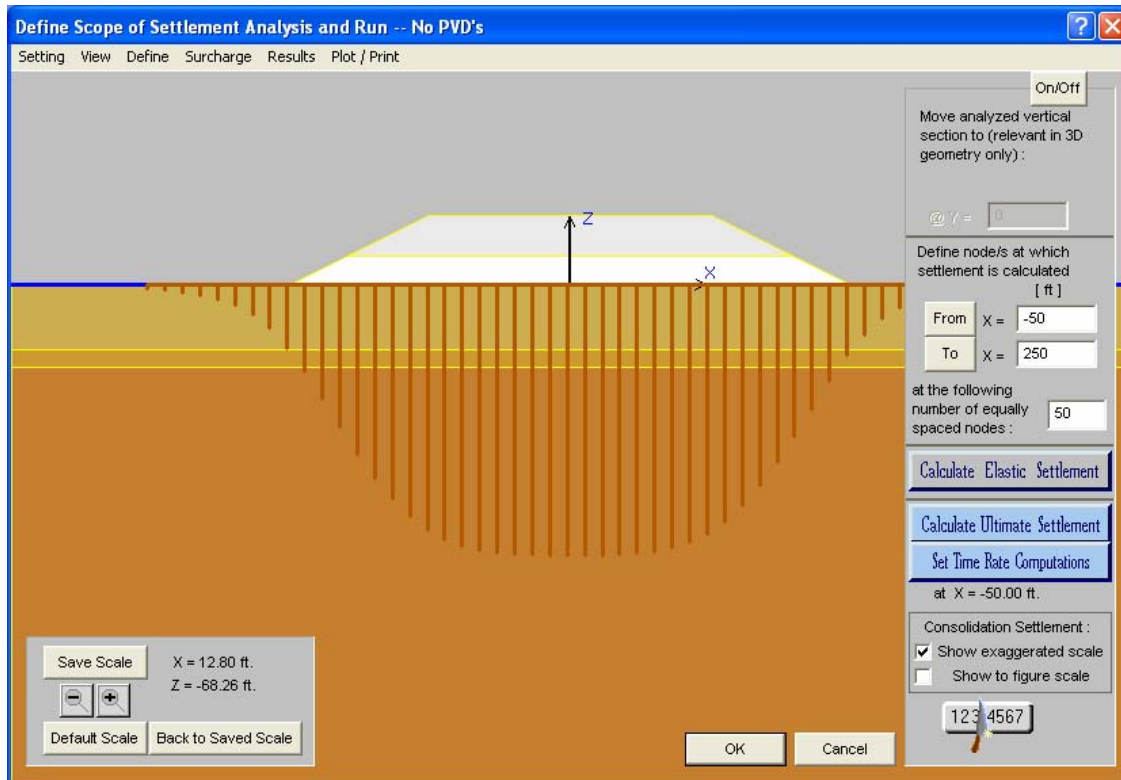


**Figure E-17. Settlement results presented on exaggerated vertical axis.**

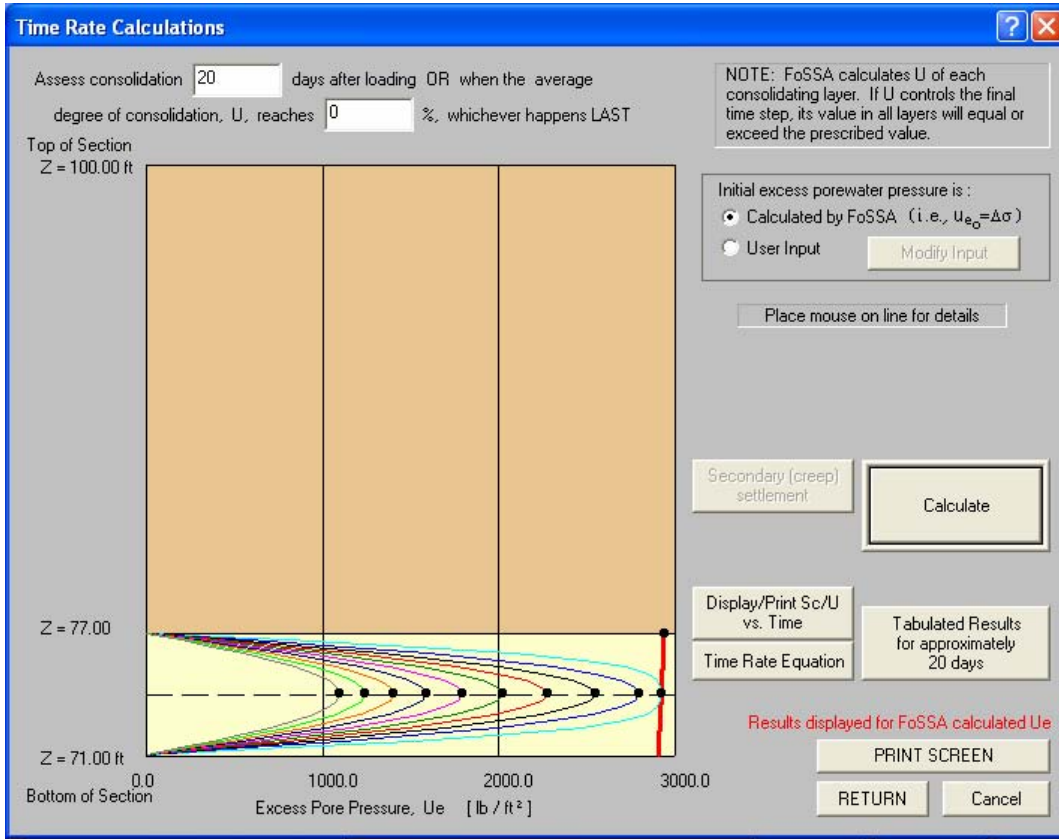


Figure E-18. Example of time rate of consolidation results.

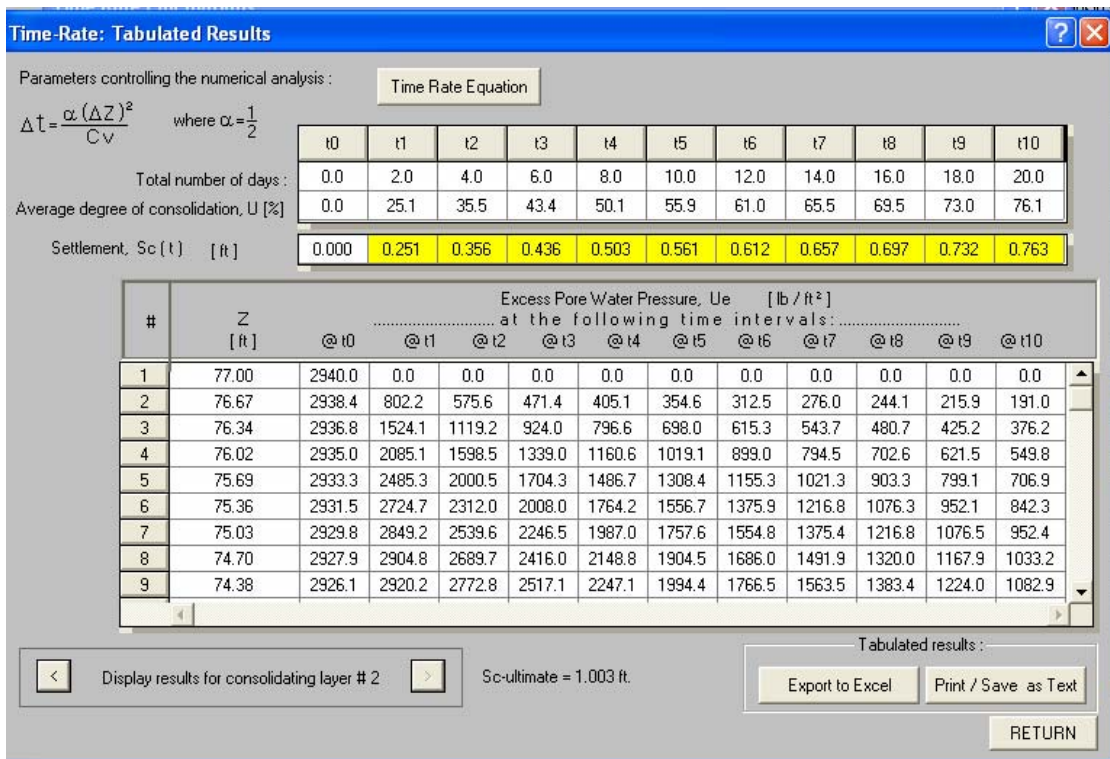


Figure E-19. Tabulated time rate of consolidation results.

FoSSA provides a significant advancement in capabilities relative to its predecessor (i.e., the DOS program EMBANK). As can be seen in this narrative summary and the selected screen shots, FoSSA is a powerful analysis tool that can greatly aid the geotechnical specialist in assessing stress distribution and settlement induced in foundation soils subjected to embankment loading. Like its sister program, ReSSA, the computer program FoSSA enjoys a fairly modest “learning curve,” in that the user can be “up and running” fairly quickly. FoSSA is user-friendly and provides analysis/display options to help the user perform several “what-if” sensitivity analyses, which can be tremendously beneficial for a given project. In term of advice to the user, the authors recommend that they refer to the example programs provided by the software developers and try to re-create the published solutions. FoSSA has an extremely helpful range of example problems, Help Screens, and Users Manual to help the user increase competence and confidence in using and understanding the program.

**Finally, it is always recommended that a selected solution be verified or validated using independent resources (i.e., hand calculations for approximate stress distribution and settlement or chart solutions) and that final results be reviewed by an experienced peer and senior reviewer.**